INTERNATIONAL MINERALOGICAL ASSOCIATION

A COMPENDIUM OF IMA-APPROVED MINERAL NOMENCLATURE

H.-P. Schertl, S.J. Mills, W.V. Maresch (Eds.)

XXII GENERAL MEETING OF THE INTERNATIONAL MINERALOGICAL ASSOCIATION

MELBOURNE, AUSTRALIA, AUGUST 2018

The XXII Meeting of the International Mineralogical Association (IMA2018), 13–17 August 2018 is hosted by

ISBN 978-3-510-65428-4
US-ISBN 1-59326-270-1

Information on this title: www.schweizerbart.com/9783510654284

e-ISBN: 978-3-510-65429-1

Publisher: E. Schweizerbart'sche Verlagsbuchhandlung (Nägele u. Obermiller)
Johannesstr. 3A, 70176 Stuttgart, Germany
mail@schweizerbart.de
www.schweizerbart.com

Printed by Printforce Nederland B.V., Culemborg

Table of contents

PREAMBLE

It was exactly 20 years ago that Robert F. Martin, then editor of *The Canadian Mineralogist*, proposed to the Mineralogical Association of Canada that a compilation of published IMA recommendations on mineral nomenclature could be a worthwhile project. This booklet was distributed during the 17th General Meeting of the International Mineralogical Association (IMA) in Toronto in 1998 and became a great success. Over the years it has graced the shelves of many colleagues. A digital version became available on the IMA web-site. This quick and handy reference guide was of great help to authors and editors alike.

The source of IMA nomenclature recommendations can be traced back to the diligent work of the Commission on New Minerals and Mineral Names (CNMMN), which was established in 1959 for the purpose of supervising the introduction of new minerals and mineral names, and of rationalizing mineral nomenclature. The Commission on Classification of Minerals (CCM) was created to review existing systems of mineral classification and to provide advice on the classification of minerals to the mineralogical community. Both Commissions were merged into the Commission on New Minerals, Nomenclature and Classification (CNMNC) in 2006. The CNMNC consists of representatives appointed from the 39 national mineralogical societies of IMA and thus represents the combined expert opinions of the world's most eminent and active mineralogists. The work of this Commission has been documented in many international publications (see the CNMNC link at "https://www.ima-mineralogy.org/CNMNC_Strategy.htm").

It must be stressed here that the goal of the CNMNC is not to impose an arbitrary set of rigid rules on the mineralogical community, but rather to provide a set of coherent guidelines for the introduction of new minerals and to provide internally consistent nomenclature schemes for mineral groups with complex solid-solutions that are sufficiently proactive to allow integration of new mineral species as they are found and described.

Since the first compendium in 1998, nomenclature protocols have been honed and improved. Many rational, internally consistent nomenclature schemes have been worked out for the most complex mineral supergroups. All of these results are published, but are scattered in the literature. They can also be looked up on-line on the CNMNC web-site, but the path to this trove of knowledge is not a standard one for many authors and editors. The goal of this compendium is therefore to provide a quick and handy reference guide. We have concentrated on some of the most significant and common rock-forming minerals, but have also included examples of technical and economic interest. There are of course numerous additional mineral groups that have been processed by the CNMNC, but not all of them could be included; examples are the eudialyte, arrojadite, lovozerite, dumortierite and sapphirine groups. The work of the CNMNC will always be a work in progress. At this time there is no IMA-approved nomenclature for the chlorite or mica groups that incorporates recent developments. We have also included the paper by Whitney and Evans (2010), who revised the older version of Kretz (1983), to provide an expanded, systematic list of abbreviations for rock-forming minerals and mineral components.

The printing of this booklet would not have been possible without the support and permission of various scientific journals and mineralogical associations. Many thanks are due

- J. Alexander Speer from *American Mineralogist* (http://www.minsocam.org/msa/AmMin/AmMineral.html; Mineralogical Society of America),
- Jodi J. Rosso (Elements; http://elementsmagazine.org/),

- Lee Groat from *The Canadian Mineralogist* (https://canminportal.wordpress.com/; Mineralogical Association of Canada),
- Kevin Murphy from *Mineralogical Magazine* (https://www.cambridge.org/core/journals/mineralogical-magazine; The Mineralogical Society of Great Britain & Ireland),
- Christian Chopin and Schweizerbart´sche Verlagsbuchhandlung from *European Journal of Mineralogy* (https://www.schweizerbart.de/papers/ejm/list?l=EN),
- IMA Council, who provided mental and financial support and made the printing of this nomenclature compendium possible.

Finally, we would like to address an important point concerning so-called varietal names. As noted by Nickel and Grice (1998), these do not fall under the direct jurisdiction of the CNMNC, so that designations such as 'kunzite', 'amethyst' or 'ruby' are IMA-unregulated. Similarly, designations for transitional phases observed experimentally in minerals at non-ambient conditions also do not fall under CNMNC jurisdiction. Problems arise when the *dominant-constituent-rule* (Hatert and Burke, 2008) is imposed and the names of intermediate solid-solution members become redundant in terms of nomenclature. Very often some of these classical names, such as 'bronzite', 'labradorite', 'hornblende', etc. are extremely helpful to petrologists and provide important compositional information simply on the basis of optical appearance or other physical characteristics. In keeping with the statement above, *i.e.* that the goal of the CNMNC is not to impose an arbitrary set of rigid rules but rather to provide a set of coherent guidelines, it should be stressed that such varietal names may be used as long as their informal character is made clear and their names do not conflict with regulated CNMNC nomenclature.

Hans-Peter Schertl (IMA Secretary)

Stuart J. Mills (IMA 2nd Vice-President; CNMNC secretary)

Walter V. Maresch (IMA President 2012-2014)

References cited:

Hatert, F. and Burke, E.A.J. (2008) Canadian Mineralogist, v. 46, 717-728.
Kretz, R. (1983) American Mineralogist, v. 68, 277-279.
Nickel, E.-H. and Grice, J. (1998) Canadian Mineralogist, v. 36, 913-926.
Whitney, D.L. and Evans, B.W. (2010) American Mineralogist, v. 95, 185-187.

SOCIETY NEWS

International Mineralogical Association

www.ima-mineralogy.org

HOW TO DEFINE, REDEFINE OR DISCREDIT A MINERAL SPECIES?

The Commission on New Minerals, Nomenclature and Classification (CNMNC) was created by the International Mineralogical Association (IMA) in 2006 by merging the Commission on New Minerals and Mineral Names (established in 1959) with the Commission on Classification of Minerals (established in the 1980s). The CNMNC is one of the most active commissions within the IMA because it is in charge of all aspects of mineral species definition, naming, nomenclature, and classification. It is constituted by four officers and 34 members, representing the countries affiliated to the IMA. The national representatives are designated by the national mineralogical societies; their nominations are independent of the CNMNC itself. However, when a member is not active, or does not follow the CNMNC rules, the IMA officers may contact the corresponding national society to ask for a replacement of the member.

To define a new species, it is necessary, prior to publication, to pass a new mineral proposal through the CNMNC. A new mineral checklist is available on the CNMNC website (http://nrmima.nrm.se/), comprising a template in which all key data on the potential new species have to be reported: occurrence, appearance, physical and optical properties, chemical data, X-ray powder diffraction data, unit-cell parameters and space group, crystal structure and relationship to other species. Proposals are handled by the chairman, who carefully checks the data before assigning an official IMA number to the proposal. It is then forwarded to the CNMNC members for direct voting, with a two-month deadline. The members have to vote separately on the validity of the mineral, and on its name. A two-thirds voting majority is required for the acceptance of both.

Nomenclature proposals have to be submitted to the 1st Vice-Chairman, in a free publication-type format. These proposals mainly concern name modifications, species discreditations, revalidations or redefinitions, as well as type/neotype sample (re)definitions. To change a mineral name, good scientific arguments are necessary: a name cannot be modified for personal conflicts of interest. The CNMNC guidelines require authors to preserve historical and well-established mineral names (Hatert et al. 2013). For species revalidations or discreditations, it is recommended that the original type specimens, if available, be investigated in detail. If the type samples are missing, historical samples from the type locality, and/or investigations by the original authors of the mineral, may also be used. The redefinition of chemical formulae must pass through the CNMNC when some significant modifications occur, as for example when a new chemical element is added to or subtracted from the formula. However, if new data just show slight modifications of atomic ratios in the formula, as for example when the number of water molecules is revised, it is generally not necessary to submit a nomenclature proposal. In such cases, the data may be published without CNMNC approval, though we encourage authors to send a copy of the paper to the CNMNC 2nd Vice-Chairman in order to update the CNMNC official mineral list (http://ima-cnmnc.nrm.se/imalist.htm). Such modifications are then noted in the *CNMNC Newsletter* (Mills, 2010).

The procedure to handle nomenclature proposals depends on the complexity of the proposal. When the proposal is quite simple and straightforward, a direct voting procedure is applied, with a maximum deadline of two months. However, if the proposal is more complex, a two-step procedure is applied, with a first round of comments, and a second round for voting. The comments of the CNMNC members are sent to the authors after the first round, and the new proposal, which takes these comments into account, is sent to the members for voting. This long procedure may take approximately four months.

Group nomenclature and classification proposals are handled by the Secretary. The guidelines for the classification of mineral groups were published by the CNMNC in 2009 (Mills et al. 2009). The establishment of an official CNMNC list of mineral (super)groups is in progress.

The commission's website is handled by the Chairman, and contains the new mineral checklist, all CNMNC published nomenclature and groups proposals, a list of unnamed mineral species, an official mineral list, and the *CNMNC Newsletter*. This newsletter presents recently accepted new minerals and changes to nomenclature, and it is published on a bimonthly basis in the *Mineralogical Magazine* and *European Journal of Mineralogy*. Its editor is the 2nd Vice-Chairman, who also updates the official IMA-CNMNC mineral list at the same time. We encourage all members of the mineralogical community to visit our website (http://nrmima.nrm.se/), where all documents are freely available.

Finally, we would like to underline the involvement of the CNMNC members, who work on a volunteer basis for the commission: thank you so much! This represents a huge task: nowadays, no less than 120 new mineral, ten nomenclature and two group proposals are handled each year. The work of the CNMNC can be compared to a classical review process in scientific journals. The main difference is that the proposals are evaluated by up to 34 reviewers, thus ensuring a good reliability of the CNMNC evaluation process. All authors are encouraged to submit their proposals to the CNMNC. They will be forwarded to the members if they are scientifically grounded and follow our guidelines. However, as in all scientific publications, it may appear that some mineralogists do not agree with our decisions; this is particularly sensitive when mineral species are discredited or renamed. In that case, the authors are free to submit a proposal to revalidate or rename the species; if it is scientifically grounded, the CNMNC may modify its decision. Neither the IMA, the CNMNC, nor its individual members and officers may be considered as legally responsible for any decision. We all act as volunteers to ensure a consistent mineral nomenclature, in order to facilitate the progress of mineral science.

Frédéric Hatert (1st Vice-Chairman, CNMNC)[1]
Marco Pasero (2nd Vice-Chairman, CNMNC)[2]
Stuart J. Mills (Secretary, CNMNC)[3]
Ulf Hålenius (Chairman, CNMNC)[4]

REFERENCES

Hatert F, Mills SJ, Pasero M, Williams PA (2013) CNMNC guidelines for the use of suffixes and prefixes in mineral nomenclature, and for the preservation of historical names. European Journal of Mineralogy 25: 113-115

Mills SJ (2010) The early publication of new mineral names: new procedures for the release of new mineral names and publication. CNMNC Newsletter 1. Mineralogical Magazine 74: 179-182

Mills SJ, Hatert F, Nickel EH, Ferraris G (2009) The standardization of mineral group hierarchies: application to recent nomenclature proposals. European Journal of Mineralogy 21: 1073-1080

1 Laboratoire de Minéralogie, Université de Liège, B-4000 Liège, Belgium – fhatert@ulg.ac.be

2 Dipartimento di Scienzedella Terra, Università di Pisa, Via Santa Maria 53, I-56126 Pisa, Italy – marco.pasero@unipi.it

3 Geosciences, Museum Victoria, PO Box 666, Melbourne, Victoria 3001, Australia – smills@museum.vic.gov.au

4 Department of Geosciences, NaturhistoriskaRiksmuseet, Box 50007, SE-104 05 Stockholm, Sweden – ulf.halenius@nrm.se

The Canadian Mineralogist
Vol. 46, pp. 717-728 (2008)
DOI: 10.3749/canmin.46.3.717

THE IMA–CNMNC DOMINANT-CONSTITUENT RULE REVISITED AND EXTENDED

FRÉDÉRIC HATERT[§]

Vice-Chairman, Commission on New Minerals, Nomenclature and Classification (CNMNC) of the International Mineralogical Association (IMA), Laboratory of Mineralogy, University of Liège, Bâtiment B-18, B–4000 Liège, Belgium

ERNST A.J. BURKE

Chairman, Commission on New Minerals, Nomenclature and Classification (CNMNC) of the International Mineralogical Association (IMA), Faculty of Earth and Life Sciences, Vrije Universiteit Amsterdam, De Boelelaan 1085, NL–1081 HV, Amsterdam, The Netherlands

ABSTRACT

Mineralogical nomenclature in solid-solution series follows a system that has been called the 50% rule, more correctly the 100%/*n* rule or the dominant-constituent rule, in which the constituents are atoms (cations or anions), molecular groups, or vacancies. Recently developed systems of nomenclature for the arrojadite and epidote groups have shown that a group of atoms with the same valency state must also be considered as a single constituent to avoid the creation of impossible end-member formulae. The extension with this dominant-valency rule is imposed by all cases of coupled heterovalent–homovalent substitutions. End members with a valency-imposed double site-occupancy may result from single-site heterovalent substitutions and from coupled heterovalent substitutions at two sites where there is a disparity in the number of these two sites.

Keywords: mineral nomenclature, solid-solution series, dominant-constituent rule, dominant-valency rule, IMA–CNMNC.

SOMMAIRE

La nomenclature minéralogique au sein des solutions solides suit une règle généralement connue sous le nom de "règle des 50%", mais qui devrait plus exactement s'appeler "règle des 100%/*n*" ou "règle du constituant dominant". Le terme "constituant" peut désigner des atomes (cations ou anions), des groupements moléculaires ou des lacunes. Récemment, les révisions de nomenclature au sein des groupes de l'arrojadite et de l'épidote ont démontré que des groupes d'atomes homovalents devaient également être considérés comme un seul et unique constituant, de manière à éviter l'apparition de formules chimiques aberrantes pour les termes extrêmes. Cette extension vers une "règle de valence dominante" est absolument nécessaire lorsque des substitutions couplées homovalentes et hétérovalentes sont impliquées. Des termes extrêmes présentant une occupation double de sites cristallographiques peuvent résulter soit d'une substitution hétérovalente affectant un seul site, soit de substitutions hétérovalentes couplées affectant deux sites, lorsqu'il existe une différence de multiplicité entre ces deux sites.

Mots-clés: nomenclature des minéraux, solutions solides, règle du constituant dominant, règle de valence dominante, IMA–CNMNC.

INTRODUCTION

The Commission on New Minerals, Nomenclature and Classification (CNMNC) of the International Mineralogical Association (IMA) has defined the nature of minerals (Nickel 1995). The IMA–CNMNC considers the terms "mineral species" and "mineral" to be identical (Dunn & Mandarino 1987, Nickel & Grice 1998). The criteria for the definition of a new mineral (species) currently used by the IMA–CNMNC (Nickel 1992, Nickel & Grice 1998) involve what should now be called the ***rule of the dominant constituent***: a mineral is a distinct species if the set of dominant constituents at the sites in the crystal structure is distinct from that of any other mineral with the same structural arrangement. Nickel (1992) called this rule for the sake of brevity the ***50% rule***, a name that unfortunately is a source of confusion, as this name can of course only be applied in binary systems: the predominant occupancy of a site in multicomponent (three and higher) systems is of course

§ *E-mail address*: fhatert@ulg.ac.be

much lower than 50%. Wenk & Bulakh (2004) proposed, therefore, to use the name ***100%/n rule*** (with *n* being the number of components). But it is recommended to use the more descriptive name ***dominant-constituent rule***, in which the term "constituent" may designate atoms (cations or anions), molecular groups, or vacancies.

The earlier guidelines for mineral nomenclature recommended by the then Commission on New Minerals and Mineral Names (CNMMN) of the IMA, as published by Nickel & Mandarino (1987), did not cover the nomenclature problems related to solid-solution series. There was only a general guideline for compositional criteria: "***At least one major structural site*** should be occupied by a different chemical component than that which occurs in the equivalent site in an existing mineral."

Nickel (1992) published the current CNMMN–CNMNC guidelines for mineral nomenclature within three categories of solid-solution series (complete solid solutions without structural order, solid solutions with structural order and partial solid solutions). These guidelines focused mainly on the general influence of compositional ranges, not on the occupancies of individual crystallographic sites.

In the more recent CNMMN procedures and guidelines on mineral nomenclature, Nickel & Grice (1998) broadened the general guideline for compositional criteria by omitting the word "major" from the previous ones: "***At least one structural site*** in the potential new mineral should be predominantly occupied by a different chemical component than that which occurs in the equivalent site in an existing mineral species." Nickel & Grice (1998) also regarded site vacancies as a component in the dominant-constituent rule, prescribed crystal-structure analysis to apply this rule for sites in minerals with complex structures, and suggested the grouping of sites in such structures.

The current dominant-constituent rule is applied in most approved new-mineral proposals. On the one hand, this rule has in some instances been applied rigorously, thus leading to some (substantiated) proliferation of new mineral species as, *e.g.*, in the complex labuntsovite and eudialyte groups (Chukanov *et al.* 2002, Johnsen *et al.* 2003). However, on the other hand, besides the well-known problems in the nomenclature system in the complex amphibole group (Hawthorne & Oberti 2006), new nomenclature systems for minerals of the arrojadite and epidote groups have recently been approved by the CNMNC that do not follow the current definition of the dominant-constituent rule (Cámara *et al.* 2006, Chopin *et al.* 2006, Armbruster *et al.* 2006). ***In these systems, the dominant-constituent rule has been extended by considering "a group of atoms with the same valency state" as a single constituent.***

Moreover, Hawthorne (2002, and pers. commun.) had already pointed out several problems in the nomenclature of certain end-members in complex mineral groups (*e.g.*, tourmaline and milarite).

Our aim in this paper is to clarify, revise and extend the dominant-constituent rule, taking into account the recent problems encumbering or prohibiting a strict application of the rule. Mineralogists wishing to define members of known solid-solution series are required to follow the recommendations set out in this paper. However, mineral names previously accepted by the IMA–CNMMN–CNMNC that contravene the recommendations should not be changed without a formal vote of members of the CNMNC.

Complete Solid-Solutions without Structural Order

Homovalent substitutions at a single site

The simplest binary case is where an atom B^{n+} replaces the atom A^{n+} at a defined crystallographic *M* site, according to the substitution mechanism $A^{n+}{}_M \leftrightarrow B^{n+}{}_M$. Such a solid-solution series, which involves mutual substitution of only two kinds of atoms, leads to two different mineral names for each compositional range from the end members to the 50 mol.% mark (Fig. 1a).

Example 1: Mg ↔ Fe^{2+} in the series diopside–hedenbergite, $CaMgSi_2O_6 \leftrightarrow CaFeSi_2O_6$.

Example 2: As ↔ Sb in the series luzonite–famatinite, $Cu_3AsS_4 \leftrightarrow Cu_3SbS_4$.

The example usually given for this type of solid solution, $Mg_2SiO_4 \leftrightarrow Fe_2SiO_4$ (forsterite–fayalite in the olivine series), is not appropriate, as the substitution takes place at two different crystallographic sites (see below).

Where more than two kinds of homovalent atoms occur at a single crystallographic site, the predominant atom has to be considered in defining the mineral species. Consequently, the 50% mark is not applicable any longer, and instead the limit becomes 33.3% (three atoms, Fig. 1b), 25% (four atoms) or 20% (five atoms) marks in the dominant-constituent rule.

Example 1: In the preisingerite group, mutual substitution of the anionic groups (AsO_4), (VO_4) and (PO_4) leads to three fields in the composition triangle, with the end-members preisingerite, $Bi_3(AsO_4)_2OOH$, schumacherite, $Bi_3(VO_4)_2OOH$, and petitjeanite, $Bi_3(PO_4)_2OOH$.

Example 2: In the structure of schoenfliesite-group minerals, with formula $XSn(OH)_6$, one octahedral site can be dominated by six different homovalent cations, whereby *X* = Mg is dominant in schoenfliesite, Fe^{2+} in natanite, Mn^{2+} in wickmanite, Cu^{2+} in mushistonite, Zn in vismirnovite, and Ca in burtite.

Independent homovalent substitutions at several sites

The simple binary case (Fig. 1a) of homovalent substitution can take place at more than one site in a crystal structure.

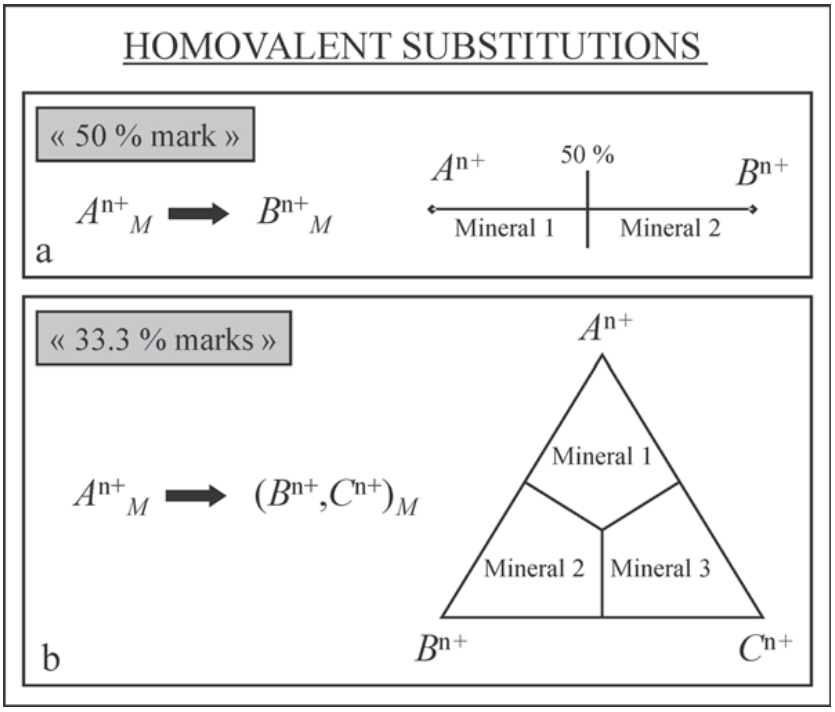

FIG. 1. Diagrammatic representations of homovalent substitutions. a. Complete binary solid-solution series. b. Complete ternary solid-solution series.

Example: The substitutions $Mn^{2+} \leftrightarrow Fe^{2+}$ at the *A* site and $Nb^{5+} \leftrightarrow Ta^{5+}$ at the *B* site in the columbite group lead to four end members (using the new nomenclature: Burke 2008): columbite-(Fe) ($FeNb_2O_6$), tantalite-(Fe) ($FeTa_2O_6$), columbite-(Mn) ($MnNb_2O_6$), and tantalite-(Mn) ($MnTa_2O_6$).

Coupled heterovalent substitutions at a single site

In a coupled heterovalent substitution at a single crystallographic site (Fig. 2), the A^{n+} atom, located at an *M* site, is progressively replaced by an equal amount of $B^{(n+1)+}$ and $C^{(n-1)+}$, according to the substitution mechanism $A^{n+}{}_M \leftrightarrow 0.5\ B^{(n+1)+}{}_M + 0.5\ C^{(n-1)+}{}_M$. The composition of one end member contains only A^{n+} at the *M* site, but the other end member contains an equal amount of $B^{(n+1)+}$ and $C^{(n-1)+}$ at this site. The dominant-constituent rule in such a series leads to the boundary mark $[A^{n+}{}_{0.5}B^{(n+1)+}{}_{0.25}C^{(n-1)+}{}_{0.25}]^{n+}{}_M$ between the two end members.

Example 1: The substitution $Ce^{3+} \rightarrow 0.5\ Ca^{2+} + 0.5\ Th^{4+}$ in monazite-(Ce), $Ce(PO_4)$, leads to the end member cheralite (formerly called "brabantite"), $(Ca^{2+}{}_{0.5}Th^{4+}{}_{0.5})(PO_4)$ (Linthout 2007).

Example 2: The substitution $Fe^{2+} \rightarrow 0.5\ Li^{1+} + 0.5\ Al^{3+}$ at the *Y* sites of the tourmaline mineral schorl, $NaFe^{2+}{}_3Al_6(Si_6O_{18})(BO_3)_3(OH)_4$, leads to the end member elbaite, $Na(Li_{1.5}Al_{1.5})Al_6(Si_6O_{18})(BO_3)_3(OH)_4$.

Single-site heterovalent substitutions lead thus to end members with (disordered) sites occupied by two constituents, imposed by the differences in valency of the two constituents: this is ***valency-imposed double site-occupancy***.

Coupled heterovalent substitutions at two sites

Where a heterovalent substitution occurs at a given crystallographic site, the charge balance can also be maintained by coupling this substitution to another heterovalent substitution at a different site (Fig. 3a). At the *M* site, the atom A^{n+} is progressively replaced by $B^{(n+1)+}$, and to maintain charge balance, the atom $C^{(n+1)+}$ is progressively replaced by D^{n+} at the *N* site. The substitution mechanism is $A^{n+}{}_M + C^{(n+1)+}{}_N \leftrightarrow B^{(n+1)+}{}_M + D^{n+}{}_N$, and the boundary site-occupancies between the two members of the series are $[A^{n+}{}_{0.5}B^{(n+1)+}{}_{0.5}]_M$ $[C^{(n+1)+}{}_{0.5}D^{n+}{}_{0.5}]_N$.

Example 1: The two-site coupled substitution $Na^{1+} + Si^{4+} \leftrightarrow Ca^{2+} + Al^{3+}$ leads to the end members albite, $Na(AlSi_3O_8)$, and anorthite, $Ca(Al_2Si_2O_8)$, in the plagioclase series.

Example 2: The two-site coupled substitution $Cu^{1+} + As^{5+} \leftrightarrow Zn^{2+} + Ge^{4+}$ leads to the compositional

variation $Cu_{11}GeAsFe_4S_{16} \leftrightarrow Cu_{10}ZnGe_2Fe_4S_{16}$ in the mineral renierite (for which no separate names for the end members have been used or proposed).

Example 3: The two-site coupled substitution $Mn^{2+}_A + Sn^{4+}_B \leftrightarrow Li^{1+}_A + Ta^{5+}_B$ leads to the end members wodginite, $MnSnTa_2O_8$, and lithiowodginite, $LiTaTa_2O_8$.

Coupled heterovalent substitutions at two sites lead to end members with ***valency-imposed double site-occupancy*** (see above) where there is a disparity in the multiplicity of these two sites.

Example 1: The substitution $\square_A + Ca^{2+}_B \leftrightarrow Na^{1+}_A + Na^{1+}_B$ in the amphibole mineral tremolite, $\square Ca_2Mg_5(Si_8O_{22})(OH)_2$, leads to a valency-imposed double occupancy of the *B* site in the end member richterite, $Na(CaNa)Mg_5(Si_8O_{22})(OH)_2$ (Hawthorne & Oberti 2006) because there are two atoms at the *B* site, but only one at the *A* site.

Example 2: The substitution $Ti^{4+}_Z + Ca^{2+}_X \rightarrow Al^{3+}_Z + REE^{3+}_X$ in the hellandite-group mineral tadzhikite-(Ce), $Ca_4Ce_2Ti\square_2(Si_4B_4O_{22})(OH)_2$, leads to a valency-imposed double occupancy of the *X* sites in hellandite-(Ce), $(Ca_3REE)_{\Sigma 4}Ce_2Al\square_2(Si_4B_4O_{22})(OH)_2$ (Oberti *et al.* 2002) because there are four atoms at the *X* sites, but only one at the *Z* site. The hellandite group has more examples of such heterovalent pairs at a single site.

Hawthorne (2002) has extensively discussed such valency-imposed double site-occupancy for some end members, notably in the milarite group.

Example: The end-member formula of milarite (omitting H_2O for simplicity) is $Ca_2K[(Be_2Al)Si_{12}O_{30}]$. The coupled substitution $Ca^{2+} + Al^{3+} \rightarrow Sc^{3+} + Be^{2+}$ leads to the end member $(ScCa)K[Be_3Si_{12}O_{30}]$ in which the *A* site must have a double occupancy (ScCa) because there is only one Al that can be replaced by Be at the *T*2 site. This end member is to be named oftedalite. On the basis of the strict application of the current dominant-constituent rule, however, the IMA–CNMNC approved in 2004 the mineral oftedalite as being Sc-dominant at the *A* site with the formula $(Sc,Ca,Mn)_2K[(Be,Al)_3Si_{12}O_{30}]$ (Cooper *et al.* 2006). But milarite can only become Sc-dominant (and thus be named oftedalite, according to the rules valid in 2004) if some Ca is partly replaced by a third cation at that site; otherwise Ca will usually have more than 50% occupancy, and such specimens are then simply Sc-rich milarite. The adoption of the new dominant-valency rule, however, causes additional problems about the current definition of oftedalite (see below).

Remark: Spinel-group (AB_2O_4) and thiospinel-group (AB_2S_4) minerals occur in "normal" and "inverse" spinel structures. End-member magnesiochromite has a normal spinel site-occupancy, $Mg^{2+}Cr^{3+}{}_2O_4$; end-member magnetite has an inverse spinel site-occupancy, $Fe^{3+}(Fe^{2+}Fe^{3+})O_4$. There is a complete solid-solution series between magnesiochromite and magnetite, but without certainty about the cation distribution in the intermediate members. For the sake of nomenclatural simplicity, divalent and trivalent cations are kept separate in (thio-)spinels, regardless of their (double) site occupancies, as these are not imposed by valency considerations.

Coupled heterovalent–homovalent substitutions

Coupled heterovalent substitutions, at a single site or at two sites, become more complex if an additional homovalent substitution takes place. In the case of a coupled heterovalent substitution at two sites, a homovalent substitution at one of these sites causes the following problem (Fig. 3b). Starting from a composi-

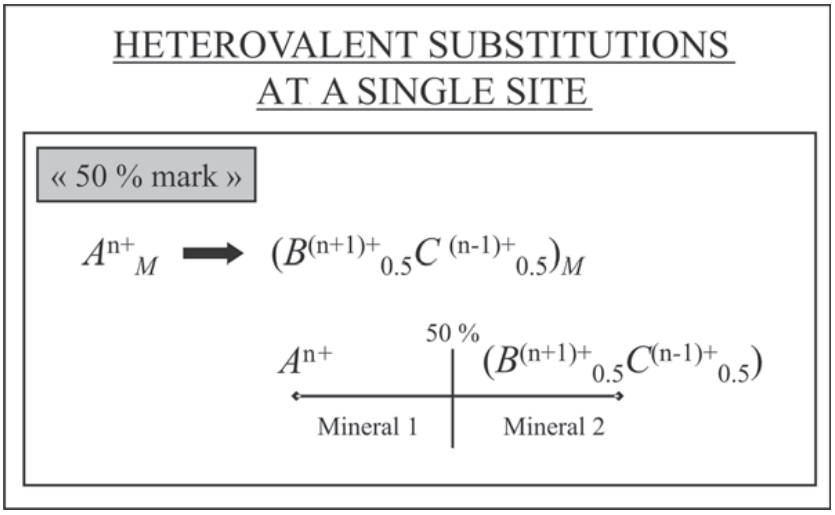

FIG. 2. Diagrammatic representation of heterovalent substitution at a single site.

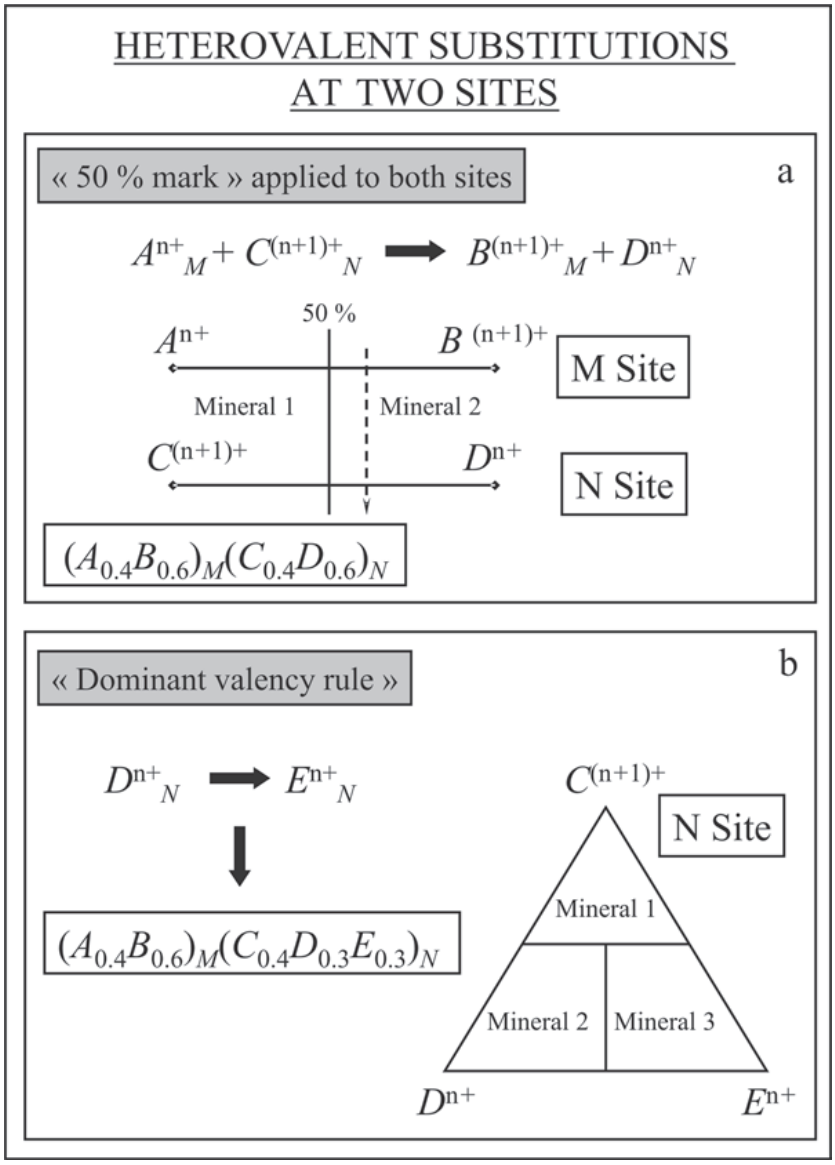

FIG. 3. Diagrammatic representations of heterovalent substitutions involving two sites. a. Coupled heterovalent substitution at two sites. b. Coupled heterovalent–homovalent substitution, leading to the dominant-valency rule.

tion $[A^{n+}_{0.4}B^{(n+1)+}_{0.6}]_M[C^{(n+1)+}_{0.4}D^{n+}_{0.6}]_N$, the homovalent substitution $E^{n+}_N \rightarrow D^{n+}_N$ could progressively take place, leading to an eventual composition $[A^{n+}_{0.4}B^{(n+1)+}_{0.6}]_M$ $[C^{(n+1)+}_{0.4}D^{n+}_{0.3}E^{n+}_{0.3}]_N$. The strict application of the dominant-constituent rule would indicate that this composition corresponds to a new species, with $C^{(n+1)+}$ instead of D^{n+} as the dominant constituent at the *N* site. However, the end-member formula for this supposedly new species, $[B^{(n+1)+}]_M[C^{(n+1)+}]_N$, is impossible because it is not charge-balanced.

This valency-nomenclatural problem can be solved by considering the elements of the homovalent substitution $E^{n+}_N \rightarrow D^{n+}_N$ as a whole, so that the group of cations with n^+ valency are still dominant at the *N* site, in spite of the majority of $C^{(n+1)}$. Consequently, species with such coupled heterovalent–homovalent substitutions must be defined by the most abundant amongst the cations with the same valency state at this site, here n^+. This rule is called the ***dominant-valency rule***, as it is necessary to preserve charge balance in any end-member formula. ***This rule is thus an extension of the***

current dominant-constituent rule, brought about by considering a group of atoms with the same valency state as a single constituent.

An important implication of this valency rule becomes evident if compositions of such minerals are plotted in a triangular diagram. As shown in Figure 3b, the usual boundaries crossing at the center of the diagram (33.3% of each component, Fig. 1b) are significantly displaced, and atom *C* needs dominance over the group (*D* + *E*) at the *N* site to allow the definition of a new species.

This dominant-valency rule is not new, as it was already applied (albeit without this specific name) by the CNMMN for rare-earth minerals (Nickel & Grice 1998): "An example of a situation that may arise is one in which a mineral with a particular structural site is occupied by both Ca and REE, and the sum of the REE elements (in molar proportions) is greater than that of Ca, but individual REE elements are subordinate to that of Ca. In such a case, the mineral is regarded as a rare-earth mineral, with a Levinson modifier specifying the predominant REE."

The dominant-valency rule should also be applied to minerals with coupled heterovalent–homovalent substitutions at a *single site*.

Example: The *Y*-site composition ($Fe^{2+}_{1.5}Li_{0.75}Al_{0.75}$) is the boundary between schorl and elbaite series in their solid-solution series (see above). A composition ($Fe^{2+}_{1.60}Li_{0.70}Al_{0.70}$) represents thus schorl, but what about the composition ($Fe^{2+}_{0.60}Mg_{0.50}Mn_{0.50}Li_{0.70}Al_{0.70}$) caused by a multiple homovalent substitution? Application of the current dominant-constituent rule would lead to the name elbaite (as Li and Al are now the dominant elements at the site). But this is erroneous: the divalent ions (Fe + Mg + Mn) are still dominant (Σ = 1.60), with Fe^{2+} as the dominant ion, and the composition corresponds to schorl.

A number of examples illustrate the application of the dominant-valency rule to coupled heterovalent–homovalent substitutions at *two sites*.

Example 1: A simple case is given by the plagioclase feldspars. Albite, $NaAlSi_3O_8$, is related to anorthite, $CaAlSi_2O_8$, by the substitution mechanism $Na^{1+} + Si^{4+} \rightarrow Ca^{2+} + Al^{3+}$. This coupled heterovalent substitution at two sites of the feldspar structure may lead to an empirical composition $(Na_{0.6}Ca_{0.4})Al_{1.4}Si_{2.6}O_8$, which is clearly albite. A second, homovalent substitution $Na^{1+} \rightarrow K^{1+}$ may lead to a (high-temperature) composition $(Ca_{0.4}Na_{0.35}K_{0.25})Al_{1.4}Si_{2.6}O_8$. According to the current dominant-constituent rule, this mineral is Ca-dominant and would thus be anorthite. But its idealized end-member formula, $CaAlSi_3O_8$, is not charge-balanced! Application of the dominant-valency rule, however, clearly shows that the monovalent cations are dominant at the large crystallographic site, not Ca. Amongst these monovalent cations, Na is the dominant one, and this sample is thus simply a Ca- and K-rich albite.

More complex examples of minerals for which this dominant-valency rule has to be applied have recently been provided by Cámara *et al*. (2006) and Chopin *et al*. (2006) in the arrojadite group. The application of this dominant-valency rule has been approved by the CNMNC.

Example 2: On considering a solution for the nomenclature problems in the arrojadite group, the dominant-constituent rule is implemented as follows: in a relevant site, the *dominant cation of the dominant valency state* is considered for nomenclature. Note that in case of multiple occupancy of a site involved in a heterovalent–homovalent exchange, the dominant cation of the dominant valency state may not be the site-predominant cation.

An arrojadite-group mineral has a formula: $A1A2B_2CaNa_{2+x}M_{13}Al(PO_4)_{11}(PO_3OH)_{1-x}W_2$. The mineral arrojadite-(KNa) is thus $KNaNa_2CaNa_2Fe_{13}Al(PO_4)_{11}(PO_3OH)(OH)_2$. Substitutions at the *A*1 site lead to $(Ba_{0.40}K_{0.35}Na_{0.25})(Na_{0.6}\square_{0.4})Na_2CaNa_2Fe_{13}Al(PO_4)_{11}(PO_3OH)(OH)_2$. This specimen does not receive the name arrojadite-(BaNa), but remains arrojadite-(KNa) because K is the dominant cation of the dominant valency at site *A*1.

Also, the many coupled heterovalent–homovalent substitutions in the epidote-group minerals require the application of the dominant-valency rule in the solid-solution series. This is necessary because strict adherence to the rule based on the dominant ionic species leads to inconsistencies and unbalanced formulae (Armbruster *et al*. 2006). The application of this dominant-valency rule has been approved by the CNMNC.

Example 3: In the clinozoisite subgroup, the dominant trivalent cation at the *M*3 site determines the name, whereas the cation at the *A*2 site appearing in the suffix has to be selected from among the divalent cations. An epidote-group mineral has the generic formula: $A1A2M1M2M3(T_2O_7)(TO_4)(O,F)(OH,O)$. Following this sequence, clinozoisite is $CaCaAlAlAl(Si_2O_7)(SiO_4)O(OH)$. Consider now the *A*2 occupancy ($Ce_{0.35}La_{0.05}Ca_{0.30}Sr_{0.20}Pb_{0.10}$). Because $(REE)^{3+} < 0.5$, the mineral belongs to the clinozoisite subgroup. Although Ce is the dominant cation at *A*2, the critical cation is Ca, the dominant divalent cation. No suffix is needed because a suffix is only added for a dominant *A*2 cation other than Ca. The *A*2 occupancy ($Ce_{0.35}La_{0.05}Sr_{0.30}Ca_{0.20}Pb_{0.10}$) would thus lead to the name clinozoisite-(Sr). Similarly, with the *M*3 occupancy ($Mg_{0.40}Al_{0.35}Fe^{3+}_{0.25}$), the dominant M^{3+} ion (*i.e*., Al, not Mg) is decisive for the root name of the species, again clinozoisite (with Ca dominant in *A*2). The *M*3 occupancy ($Mg_{0.40}Fe^{3+}_{0.35}Al_{0.25}$) would thus lead to the name epidote.

Example 4: In the allanite and dollaseite subgroups, for the sites involved in the charge compensation of a heterovalent–homovalent substitution involving *A*2 and *O*4 (*i.e*., *M*3 in the allanite subgroup; *M*3 and also

*M*1 in the dollaseite subgroup), identification of the relevant end-member formula must take into account *the dominant divalent charge-compensating octahedral cation* (M^{2+}) and not the dominant cation at these sites (Armbruster *et al*. 2006).

An epidote-group mineral has the generic formula: *A*1*A*2*M*1*M*2*M*3(T_2O_7)(*T*O_4)(O,F)(OH,O).

Following this sequence, allanite-(Ce) is $CaCe^{3+}AlAlFe^{2+}(Si_2O_7)(SiO_4)O(OH)$. For an allanite-subgroup mineral where *M*3 is not dominated by a single divalent cation but by several, so that a trivalent cation is the most abundant one, *e.g*., $Ca(Ce_{0.6}Ca_{0.4})AlAl(Al_{0.4}Fe^{2+}_{0.3}Mg_{0.2}\ Mn^{2+}_{0.1})(Si_2O_7)(SiO_4)O(OH)$, Fe^{2+} is dominant among the M^{2+} cations, *i.e*., Fe^{2+} is the dominant *charge-compensating* cation. Thus the mineral would properly be named allanite-(Ce). The *M*3 occupancy ($Al_{0.4}Mg_{0.3}Fe^{2+}_{0.2}Mn^{2+}_{0.1}$) leads to the name dissakisite-(Ce).

The dominant-valency rule is also valid for anionic sites.

Example 1: Oxidation of iron in annite, $KFe^{2+}_3(AlSi_3O_{10})(OH)_2$, evolves along the reaction $Fe^{2+} + (OH)^- \rightarrow Fe^{3+} + O^{2-}$ (Dercourt *et al*. 2001). Partial oxidation of iron and some substitution of (OH) by F could lead to a composition $K(Fe^{2+}_{2.2}Fe^{3+}_{0.8})(AlSi_3O_{10})[O_{0.8}(OH)_{0.7}F_{0.5})]$. In spite of oxygen dominance at the anion *A* site, this specimen cannot be called "oxyannite", as the sum of monovalent anions at the *A* site is higher than the oxygen occupancy. The name is thus still annite or, using some modifiers of Bayliss *et al*. (2005), iron(3+)-enriched F-bearing annite. On the other hand, using the same dominant-valency rule for the composition $K(Fe^{2+}_{2.2}Fe^{3+}_{0.8})(AlSi_3O_{10})[O_{0.8}F_{0.7}(OH)_{0.5}]$ would result in the name fluorannite. The end-member formula of "oxyannite" is $K(Fe^{3+}_2Fe^{2+})AlSi_3O_{10}O_2$, an example of "valency-imposed double site-occupancy".

Example 2: The end-member formula of staněkite is $Mn^{2+}Fe^{3+}(PO_4)O$, and that of triploidite is $Mn^{2+}_2(PO_4)(OH)$. The composition $(Mn^{2+}_{1.60}Fe^{3+}_{0.40})(PO_4)[O_{0.40}(OH)_{0.35}F_{0.25}]$ has oxygen as the dominant constituent at the additional anion site. Nevertheless, the specimen does not get a new mineral name ("oxytriploidite"); it is simply triploidite because the sum of the monovalent additional anions is higher than that of the divalent ones. The end-member formula of staněkite is also an example of "valency-imposed double site-occupancy".

The adoption of the extension of the dominant-constituent rule with the dominant-valency rule for the description of new minerals in the future has possible implications for minerals that have been approved in the past on the basis of the old dominant-constituent rule.

Example 1: The pumpellyite series consists of five end members [pumpellyite-(Mg), pumpellyite-(Fe^{2+}), pumpellyite-(Mn^{2+}), pumpellyite-(Fe^{3+}) and pumpellyite-(Al)], based on the dominant cation at the *M*1 site. The dominant presence of trivalent ions at that site is balanced by the replacement of the H_2O molecule by (OH), *e.g*., $Ca_2AlAl_2(SiO_4)(Si_2O_7)(OH)_3$. The empirical formula of the IMA–CNMNC-approved pumpellyite-(Al) is $(Ca_{1.99}Na_{0.01})_{\Sigma 2.00}(Al_{0.42}Fe^{2+}_{0.33}Mg_{0.24}Mn_{0.01})_{\Sigma 1.00}Al_{2.00}(SiO_4)(Si_2O_7)(OH)_{2.42}\bullet 0.58H_2O$ (Hatert *et al*. 2007). Aluminum as a single element is dominant at the *M*1 site (0.42 *apfu* Al), but the sum of the divalent ions (Fe + Mg + Mn) is greater (0.58 *apfu*). If the dominant-valency rule is applied, the name of this mineral is not pumpellyite-(Al) but pumpellyite-(Fe^{2+}), because Fe^{2+} is the dominant cation of the dominant valency at that site. Crystal-structure refinement of the same pumpellyite-(Al) specimen showed, however, that the occupancy of the *M*1 site is 75% Al, 12.5% Mg and 12.5% Fe^{2+}. A similar discrepancy between chemical and crystal-structure-derived *M*1 site occupancies has been described for a sample of pumpellyite by Yoshiasha & Matsumoto (1985), $(Al_{0.47}Mg_{0.33}Fe^{2+}_{0.23})_{\Sigma 1.03}$ and (80% Al, 20% Fe^{2+}), respectively; on the basis of its chemical composition, this specimen would now be named pumpellyite-(Mg). Several chemical compositions of pumpellyite-group minerals (*e.g*., Passaglia & Gottardi 1973), however, show Al to be dominant at the *M*1 site; these are examples of real pumpellyite-(Al) specimens.

Example 2: Ganterite has been approved as the Ba-dominant analogue of muscovite (Graeser *et al*. 2003). The empirical formula is $(Ba_{0.44}K_{0.28}Na_{0.27})_{\Sigma 0.99}(Al_{1.84}Mg_{0.09}Fe^{2+}_{0.04}Ti_{0.04})_{\Sigma 2.01}[Si_{2.72}Al_{1.28}O_{10}](OH)_{1.89}$. Barium is indeed the dominant constituent at the *I* site (0.44 *apfu*), but the sum of the monovalent ions (K + Na) is greater (0.55 *apfu*). Application of the dominant-valency rule in the scheme of mica nomenclature would not lead to a new mineral, but its name would be a Ba-rich muscovite, although the amount of ^{IV}Si and ^{VI}Al in *apfu* fall outside the range indicated for muscovite by Rieder *et al*. (1998).

As stated in the introduction, it is not our aim in this paper to automatically change mineral names previously accepted by the IMA–CNMNC, even where this new dominant-valency rule is to be applied in the future. There is even an example where the old dominant-constituent rule is to be maintained because application of the dominant-valency rule would make the existence of the mineral almost impossible.

Example: This very special case is oftedalite. It is unique, perhaps with the exception of the hypothetical Y-dominant analogue of milarite and oftedalite, which may also exist in nature (Hawthorne 2002). It has been stated (see above) that milarite can only become Sc-dominant at the *A* site (and thus be named oftedalite following the old dominant-constituent rule) if some Ca is replaced by a third cation at that site, otherwise Ca will usually have more than 50% occupancy, such specimens are then simply milarite. But if that third cation also is divalent, then the application of the dominant-valency rule changes oftedalite back to milarite! The empirical formula of oftedalite is $(Sc_{0.96}Ca_{0.79}Mn^{2+}_{0.18}Fe^{2+}_{0.04}Y_{0.03})_{\Sigma 2.00}K_{0.98}(Be_{2.91}Al_{0.09})_{\Sigma 3.00}$

$Si_{11.98}O_{30}$ (Cooper *et al*. 2006). It is true that Sc is dominant as a single element at the *A* site, but the sum of divalent ions (Ca+Mn+Fe) is greater (1.01 *apfu*) than the sum of the trivalent ions (Sc+Y = 0.99 *apfu*). The new valency-dominant rule implies that in oftedalite Sc must be the dominant cation of the dominant valency at the *A* site (except for the end member, which has a valency-imposed double site-occupancy; see above). Current samples of "oftedalite", as previously defined by the old constituent rule, are thus simply Sc-rich milarite as defined by the new constituent rule. It is of course possible, however, that Ca is replaced by a monovalent ion, *e.g*. Na^{1+}, so that Sc is the dominant cation of the then dominant trivalent ions, in that case producing an oftedalite specimen that obeys both the dominant-constituent and the dominant-valency rules.

Grouping of crystallographic sites

It is frequently observed that a group of similar cations or anions can occupy more than one crystallographically distinct site. Such sites with similar crystal-chemical roles may be considered as a whole in nomenclature proposals.

Example 1: The olivine structure has two octahedral sites, *M*1 and *M*2, which in the forsterite–fayalite series are occupied by Mg and Fe^{2+}, in a not completely disordered way. However, recognition of only two species is deemed to be appropriate, as the two intermediate compositions and their implied arrangements are not approached in nature (Hawthorne 2002).

Example 2: In the structure of wiluite, a vesuvianite-group mineral, there are four *T*1 sites and one *T*2 site. Ideally, only one of these sites needs to be more than half-occupied by boron to give rise to a new mineral species; thus there are four potential end-members involving the *T* sites. However, some of the resulting species can only be identified *via* crystal-structure refinement to derive B occupancies at the *T*1 and *T*2 sites. This is obviously not practical, and therefore wiluite was defined as containing > 2.5 B *apfu*, such that the *T*1 and *T*2 sites have an aggregate occupancy of greater than 0.5 (Groat *et al*. 1998).

Example 3: The nomenclature of the amphibole group is based on the formula $AB_2C_5T_8O_{22}W_2$, where *C* represents the group of five *apfu* in the three *M*(1), *M*(2) and *M*(3) crystallographic sites (Leake *et al*. 1997). Grouping these sites had to be done to avoid an unnecessary proliferation of mineral species in this complex group, which would have been caused by the strict application of the dominant-constituent rule to each crystallographic site. The 1997 amphibole nomenclature is based on the *A*, *B* and *T* groups of sites. Hawthorne & Oberti (2006) argued that a nomenclature based on the *A*, *B* and *C* groups of sites is to be preferred, as it is in these groups that the maximum variation in chemical composition occurs, and this scheme would thus also be more in accord with the IMA-sanctioned dominant-constituent principle. In their proposed scheme, Hawthorne & Oberti (2006) deviate considerably from the end-member rules of Hawthorne (2002), as most of their proposed amphibole end-members need more than one type of cation at more than one group of sites, even up to three groups of sites, *e.g*., $Na(CaNa)(Fe^{2+}{}_4Al)(Si_7Al)O_{22}(OH)_2$ for katophorite. The *C*-site group may have four different cations in the end-member formula, *e.g*., $NaNa_2(MgMn^{3+}{}_2LiTi^{4+})Si_8O_{22}O_2$ for dellaventuraite; for valency reasons, this end-member formula must have $Mn^{3+}{}_2$ although the empirical formula has only 0.85 *apfu* Mn^{3+} (Tait *et al*. 2005). The amphibole subcommittee of the CNMNC is working to establish an acceptable scheme of nomenclature for this important, but very complex group of minerals.

According to the current CNMNC rules (Nickel 1992, Nickel & Grice 1998), all crystallographically distinct sites, even minor ones, may play a role in mineral nomenclature. It might be a matter of discussion whether it is desirable to return to the restriction in the Nickel & Mandarino (1987) guidelines of using only "major" structural sites. Meanwhile, there are examples of both views in our nomenclature systems.

Example 1: The mineral stornesite-(Y) has recently been described by Grew *et al*. (2006). This mineral belongs to the fillowite group of phosphates, characterized by the general formula $(M^{2+},Y,REE,Na)(Na,K,\square)_2(Na,K)_6(M^{2+},Na,K)_8(M^{2+},M^{3+})_{43}(PO_4)_{36}$. Depending on the dominant divalent cation at the 43 *M* sites, the three minerals fillowite ($M^{2+} = Mn^{2+}$), johnsomervilleite ($M^{2+} = Fe^{2+}$), and chladniite ($M^{2+} = Mg^{2+}$) are defined. The main difference between chladniite and stornesite-(Y) is the presence, in the latter, of small amounts of Y and Yb occurring at the (0,0,0) position. This position has a multiplicity of 3, whereas the other *M* sites have generally multiplicities between 6 and 18. As a consequence, the amount of Y is 0.460–0.870 *apfu* or 0.97–1.85 wt.% Y_2O_3, and the amount of Yb is 0.056–0.105 *apfu* or 0.20–0.39% Yb_2O_3. A better knowledge of the crystal chemistry of the fillowite group is now required to confirm that the substitution of divalent cations by Y and REE at the (0,0,0) position really plays a significant role.

Example 2: In order to restrict the number of species in the eudialyte group, it was decided to ignore the *X* anion sites in nomenclature as a rule. To assist in the evaluation of future proposals of these complicated eudialyte-group minerals, however, it was recommended that refined site-scattering data and a table of site assignments for all sites relevant to the space group in question should be submitted with the proposal.

Example 3: The fundamental structural formula for arrojadite-group minerals is $A_2B_2CaNa_{2+x}M_{13}Al(PO_4)_{11}(PO_3OH)_{1-x}W_2$. If the content of each site is considered for nomenclature, the number of independent cation sites in the formula unit has the potential to yield a wealth of mineral names in the arrojadite group. Regardless of whether or not such proliferation would

be a service to Mineralogy, the mixed occupancy of most sites (by Fe, Mn, Mg, and Li in the *M* sites; by Ca, Na, Fe, and vacancies in the *A*, *B*, Ca and Na sites) makes a unique assignment of site population impossible in most instances, even if individual site-scattering values are known through crystal-structure refinement. Therefore, some sites were grouped, and in others, the dominant-constituent rule was adapted to a dominant-valency rule, as above.

There are thus divergent tendencies in establishing systems of nomenclature for mineral groups, especially in complex ones. On the one hand, crystal-structure refinement allows in principle to determine occupancies of all sites, and thus to use all of these in a system of nomenclature. On the other hand, there is a definite need for practical systems of nomenclature, *i.e.*, systems that can be applied on the basis of chemical data (usually obtained by electron microprobe) or X-ray powder diffraction alone, without having to resort to structure refinement (which, as shown by the arrojadite-group example, is not unequivocal in every case). To assist the mineralogical community in its work, nomenclature systems enabling mineral identifications with relatively simple methods are certainly to be preferred.

Partial Solid-Solution Without Structural Order

Binary partial solid-solution series

The case of partial solid-solution series has already been addressed in detail by Nickel (1992), and only an overview of the issue will be given here. If there is limited solid-solution in the vicinity of one or both end-members, and the solid solution does not extend to the 50% boundary (in a binary system), then the dominant-constituent rule is generally applied (Fig. 4a). For purposes of nomenclature, it does not matter whether or not both end-members are isostructural.

Example: Solid solution in the system hematite–ilmenite, $Fe^{3+}{}_2O_3$ – $Fe^{2+}Ti^{4+}O_3$, at low temperatures is limited to small ranges near the end members.

If the miscibility gap in a binary solid-solution series between non-isostructural phases is to one side of the 50% mark, the composition of one of the two members will extend beyond the 50% mark (Fig. 4b). Nickel (1992) made a distinction in these ranges beyond 50% between a "small" one and a "substantial" one, the dividing line between these being "about 10 mol. %, although each situation should be regarded on its own merits". Only "substantial" ranges would merit a separate name. A new name, however, should be given to any range beyond the 50% mark if it can be satisfactorily demonstrated that a given composition exceeds the 50% mark. There is, after all, not such a 10% "no-name-land" for members around the 50% mark in complete solid-solution series.

Example: The system ZnS (sphalerite) – FeS is a partial solid-solution series, with solution of FeS in ZnS ending at 66 mol.% FeS. The Fe-dominant phase with a sphalerite-type structure and compositions between $Zn_{0.5}Fe_{0.5}S$ and $Zn_{0.34}Fe_{0.66}S$ has been approved as the mineral rudashevskyite.

A different approach to nomenclature has to be considered if the known compositions in a binary partial solid-solution series cluster around the 50% mark, but do not appear to extend to either end-member (Fig. 4c). In principle, only one name should be given to such a limited compositional range because the situation also applies to small deviations from the fixed 1:1 ratio in valency-imposed double site-occupancies (see above). The distinction in these cluster ranges made by Nickel (1992), now between "small" and "large", for the eventual use of separate names might have to be used if the range is shown to extend beyond the cluster conception.

Example: In pentlandite, $Fe(Fe,Ni)_8S_8$, Fe and Ni substitute for each other to a limited extent, with compositions centered around Fe:Ni = 1:1; compositions near the Fe and Ni end members are not known. It has not been found necessary to divide pentlandite into two species.

Ternary partial solid-solution series

Similar considerations should be applied to ternary or higher-order partial solid-solution series (Figs. 5a, b). It is evident that analysis of new mineral specimens may enlarge the compositional range within a partial solid-solution series, thus bringing a mineral from the left side to the right side of Figure 5 (or from the upper to lower level in Fig. 4c), and eventually necessitating a change in nomenclature.

Solid Solutions with Structural Order

If there is structural order involving the ions that define the end members within an otherwise disordered solid-solution series, the ordered phase is to be given a mineral name different from those of the end members. Where structural ordering occurs, at least one crystallographic site is split in two distinct positions, thus leading to a change of symmetry and also commonly to a doubling of some unit-cell parameters. A somewhat artificial ordering of cations, without a specific table of site occupancies, but with a concurrent artificial lowering of symmetry, should be avoided as the key point in new-mineral proposals.

Example 1: Ordering of Ca and Mg ions in dolomite, $CaMg(CO_3)_2$, results in a crystal structure distinct from those of the end members calcite, $CaCO_3$, and magnesite, $MgCO_3$ of the $(Ca,Mg)CO_3$ series.

Example 2: At temperatures below 700°C, Mg and Al atoms are disordered in the diopside, $CaMgSi_2O_6$, and jadeite, $NaAlSi_2O_6$, end members with *C*2/*c* space

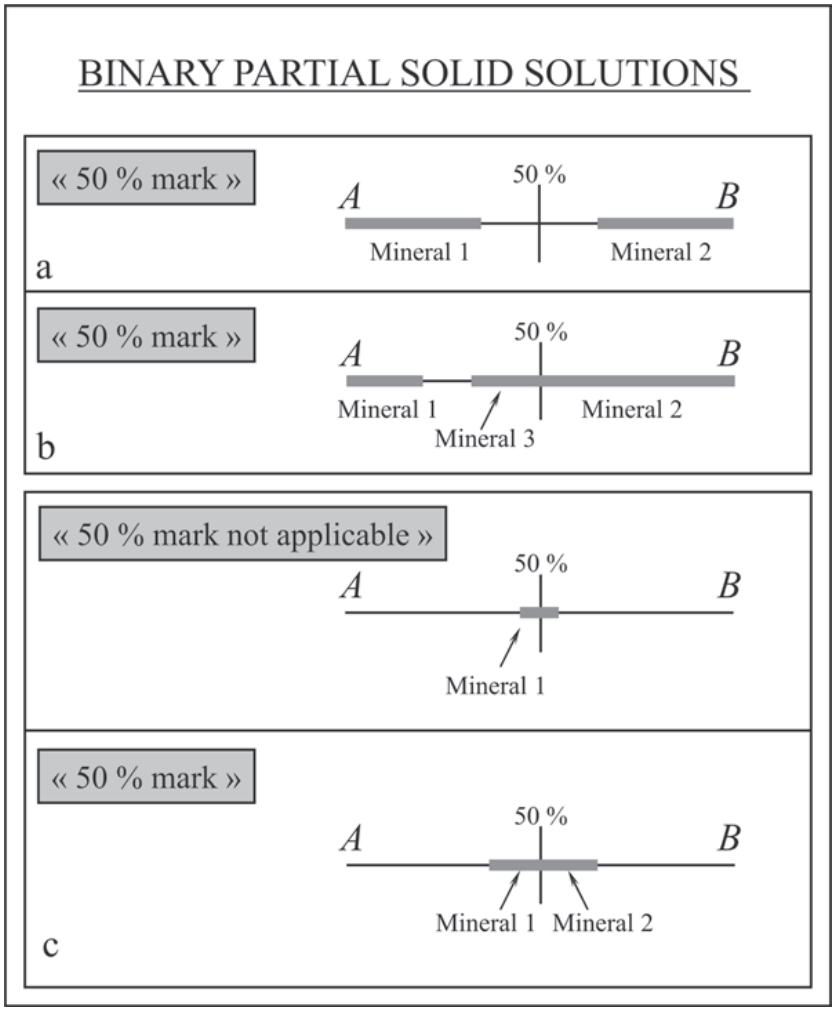

FIG. 4. Diagrammatic representations of partial binary solid-solution series. a. Series with a miscibility gap. b. Series with a miscibility gap, but with one member encompassing the midpoint. c. Series with members limited around the midpoint.

group, but ordered in the intermediate member omphacite, ideally $(Ca_{0.5}Na_{0.5})(Mg_{0.5}Al_{0.5})Si_2O_6$, with $P2/n$ space group.

Both are examples of so-called "non-convergent order" in thermodynamics.

CONCLUSIONS

The nomenclature of members in complete solid-solution series remains in principle determined by the application of the dominant-constituent rule, but the rule has been extended with the dominant-valency rule by considering a group of atoms with the same valency state as a single constituent. The old dominant-constituent rule (with only atoms, molecular groups or vacancies as constituents) can only be applied without problems or errors to solid-solution series involving homovalent substitutions or singular coupled heterovalent substitutions. The extension with the dominant-valency rule is imposed by all cases of coupled heterovalent–homovalent substitutions. The application of the old dominant-constituent rule in such systems is a possible source of problems or errors, as illustrated by examples given in this paper. The extension with the dominant-valency rule is necessary to establish charge-balanced end-member formulae for solid-solution series with complex mechanisms of substitution.

Although these general guidelines are recommended, a certain degree of flexibility might be necessary in the cases of conflicting dominant-constituent and dominant-valency rules, and in partial solid-solution series. Proposals for mineral names in this category will be judged by the CNMNC on the merits of each particular case.

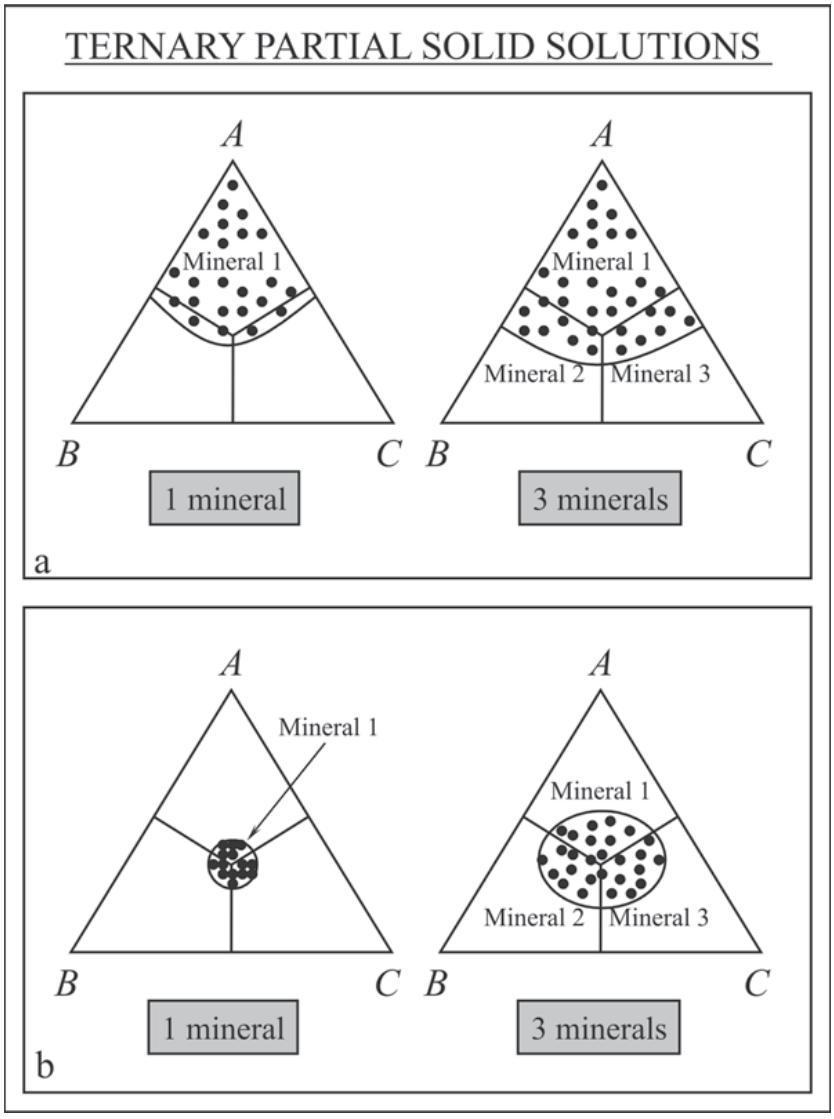

FIG. 5. Diagrammatic representations of partial ternary solid-solution series. a. Series with members encompassing geometrical boundaries. b. Series with members having compositions about the geometric midpoint.

ACKNOWLEDGEMENTS

We thank Frank Hawthorne, Christian Chopin and Thomas Armbruster for starting the discussion on the application of the dominant-constituent rule, and for providing examples showing that it should be revised urgently. Several CNMNC members helped to improve the text of this revision, especially Gunnar Raade, Paul Keller and André-Mathieu Fransolet on the oftedalite problem. F.H. acknowledges the FNRS–FRS (Belgium) for a position of "Chercheur qualifié". Robert F. Martin edited this report.

REFERENCES

ARMBRUSTER, T., BONAZZI, P., AKASAKA, M., BERMANEC, V., CHOPIN, C., GIERÉ, R., HEUSS- ASSBICHLER, S., LIEBSCHER, A., MENCHETTI, S., PAN, YUANMING & PASERO, M. (2006): Recommended nomenclature of epidote-group minerals. *Eur. J. Mineral.* **18**, 551-567.

BAYLISS, P., KAESZ, H.D. & NICKEL, E.H. (2005): The use of chemical-element adjectival modifiers in mineral nomenclature. *Can. Mineral.* **43**, 1429-1433.

BURKE, E.A.J. (2008): Tidying up mineral names: an IMA–CNMNC scheme for suffixes, hyphens and diacritical marks. *Mineral. Rec.* **39**, 131-135.

CÁMARA, F., OBERTI, R., CHOPIN, C. & MEDENBACH, O. (2006): The arrojadite enigma. I. A new formula and a new model for the arrojadite structure. *Am. Mineral.* **91**, 1249-1259.

CHOPIN, C., OBERTI, R. & CÁMARA, F. (2006): The arrojadite enigma. II. Compositional space, new members, and nomenclature of the group. *Am. Mineral.* **91**, 1260-1270.

CHUKANOV, N.V., PEKOV, I.V. & KHOMYAKOV, A.P. (2002): Recommended nomenclature for labuntsovite-group minerals. *Eur. J. Mineral.* **14**, 165-173.

COOPER, M.A., HAWTHORNE, F.C., BALL, N.A., ČERNÝ, P. & KRISTIANSEN, R. (2006): Oftedalite, $(Sc,Ca,Mn^{2+})_2K(Be,Al)_3Si_{12}O_{30}$, a new member of the milarite group from the Heftetjern pegmatite, Tørdal, Norway: description and crystal structure. *Can. Mineral.* **44**, 943-949.

DERCOURT, D.G., MERCIER, P.H.J., CHERNIAK, D.J., DESGRENIERS, S., KODAMA, H., ROBERT, J.-L. & MURAD, E. (2001): Mechanisms and crystal chemistry of oxidation in annite: resolving the hydrogen-loss and vacancy reactions. *Clays Clay Minerals* **49**, 455-491.

DUNN, P.J. & MANDARINO, J.A. (1987): Formal definitions of type mineral specimens. *Can. Mineral.* **25**, 571-572.

GRAESER, S., HETHERINGTON, C.J. & GIERÉ, R. (2003): Ganterite, a new barium-dominant analogue of muscovite from the Berisal Complex, Simplon Region, Switzerland. *Can. Mineral.* **41**, 1271-1280.

GREW, E.S., ARMBRUSTER, T., MEDENBACH, O., YATES, M.G. & CARSON, C.J. (2006): Stornesite-(Y), $(Y,Ca)_2Na_6(Ca,Na)_8(Mg,Fe)_{43}(PO_4)_{36}$, the first terrestrial Mg-dominant member of the fillowite group, from granulite-facies paragenesis in the Larsemann Hills, Prydz Bay, East Antarctica. *Am. Mineral.* **91**, 1412-1424.

GROAT, L.A., HAWTHORNE, F.C., ERCIT, T.S. & GRICE, J.D. (1998): Wiluite, $Ca_{19}(Al,Mg,Fe,Ti)_{13}(B,Al,\square)_5Si_{18}O_{68}(O,OH)_2$, a new mineral species isostructural with vesuvianite, from the Sakha Republic, Russian Federation. *Can. Mineral.* **36**, 1301-1304.

HATERT, F., PASERO, M., PERCHIAZZI, N. & THEYE, T. (2007): Pumpellyite-(Al), a new mineral from Bertrix, Belgian Ardennes. *Eur. J. Mineral.* **19**, 247-253.

HAWTHORNE, F.C. (2002): The use of end-member charge-arrangements in defining new mineral species and heterovalent substitutions in complex minerals. *Can. Mineral.* **40**, 699-710.

HAWTHORNE, F.C. & OBERTI, R. (2006): On the classification of amphiboles. *Can. Mineral.* **44**, 1-21.

JOHNSEN, O., FERRARIS, G., GAULT, R.A., GRICE, J., KAMPF, A.R. & PEKOV, I.V. (2003): The nomenclature of eudialyte-group minerals. *Can. Mineral.* **41**, 785-794.

LEAKE, B., WOOLLEY, A.R., ARPS, C.E.S., BIRCH, W.D., GILBERT, M.C., GRICE, J.D., HAWTHORNE, F.C., KATO, A., KISCH, H.J., KRIVOVICHEV, V.G., LINTHOUT, K., LAIRD, J., MANDARINO, J.A., MARESCH, W.V., NICKEL, E.H., ROCK, N.M.S., SCHUMACHER, J.C., SMITH, D.C., STEPHENSON, N.C.N., UNGARETTI, L., WHITTAKER, E.J.W. & GUO YOUZHI (1997): Nomenclature of amphiboles: report of the subcommittee on amphiboles of the International Mineralogical Association, Commission on New Minerals and Mineral Names. *Can. Mineral.* **35**, 219-246.

LINTHOUT, K. (2007): Tripartite division of the system $2REEPO_4 – CaTh(PO_4)_2 – 2ThSiO_4$, discreditation of brabantite, and recognition of cheralite as name for members dominated by $CaTh(PO_4)_2$. *Can. Mineral.* **45**, 503-508.

NICKEL, E.H. (1992): Solid solutions in mineral nomenclature. *Can. Mineral.* **30**, 231-234.

NICKEL, E.H. (1995): The definition of a mineral. *Can. Mineral.* **33**, 689-690.

NICKEL, E.H. & GRICE, J.D. (1998): The IMA Commission on New Minerals and Mineral Names: procedures and guidelines on mineral nomenclature, 1998. *Can. Mineral.* **36**, 913-926.

NICKEL, E.H. & MANDARINO, J.A. (1987): Procedures involving the IMA Commission on New Minerals and Mineral Names, and guidelines on mineral nomenclature. *Can. Mineral.* **25**, 353-377.

OBERTI, R., DELLA VENTURA, G., OTTOLINI, L., HAWTHORNE, F.C. & BONAZZI, P. (2002): Re-definition, nomenclature and crystal-chemistry of the hellandite group. *Am. Mineral.* **87**, 745-752.

PASSAGLIA, E. & GOTTARDI, G. (1973): Crystal chemistry and nomenclature of pumpellyites and julgoldites. *Can. Mineral.* **12**, 219-223.

RIEDER, M., CAVAZZINI, G., D'YAKONOV, YU., FRANK-KAMENETSKII, V.A., GUGGENHEIM, S., KOVAL, P.V., MÜLLER, G., NEIVA, A.M.R., RADOSLOVICH, E.W., ROBERT, J.-L., SASSI, F.P., TAKEDA, H., WEISS, Z. & WONES, D.R. (1998): Nomenclature of the micas. *Can. Mineral.* **36**, 905-912.

TAIT, K.T., HAWTHORNE, F.C., GRICE, J.D., OTTOLINI, L. & NAYAK, V.K. (2005): Dellaventuraite, $NaNa_2(MgMn^{3+}_2Ti^{4+}Li)Si_8O_{22}O_2$, a new anhydrous amphibole from the Kajlidongri manganese mine, Jhabua District, Madhya Pradesh, India. *Am. Mineral.* **90**, 304-309.

WENK, H.-R. & BULAKH, A.G. (2004): *Minerals: their Constitution and Origin.* Cambridge University Press, Cambridge, U.K.

YOSHIASHA, A. & MATSUMOTO, T. (1985): Crystal structure refinement and crystal chemistry of pumpellyite. *Am. Mineral.* **70**, 1011-1019.

Received June 17, 2008.

Eur. J. Mineral.
2013, **25**, 113–115
Published online December 2012

CNMNC guidelines for the use of suffixes and prefixes in mineral nomenclature, and for the preservation of historical names

FRÉDÉRIC HATERT[1,*], STUART J. MILLS[2], MARCO PASERO[3] and PETER A. WILLIAMS[4]

[1] Laboratoire de Minéralogie, Université de Liège, B-4000 Liège, Belgium
*Corresponding author, e-mail: fhatert@ulg.ac.be
[2] Geosciences, Museum Victoria, GPO Box 666, Melbourne 3001, Victoria, Australia
[3] Dipartimento di Scienze della Terra, Università degli Studi di Pisa, Via Santa Maria 53, I-56126 Pisa, Italy
[4] School of Science and Health, University of Western Sydney, Locked Bag 1797, Penrith, NSW 2751, Australia

Abstract: New CNMNC guidelines are established, in order to standardize the use of prefixes and suffixes in mineral nomenclature, and to preserve historical names. The recommendations for the use of suffixes are: (I) chemical suffixes have to be in parentheses, except for extra-framework cations; (II) a maximum of three chemical suffixes is allowed; (III) cations and anions should never be used together in the parentheses. For the use of prefixes, the following guidelines were adopted: (I) for common names, prefix-type nomenclature is preferred to facilitate the pronunciation; (II) an unnecessary proliferation of prefixes must be avoided, and a maximum of three chemical prefixes is recommended; (III) it is allowed to use a combination of chemical, structural or other descriptive prefixes; (IV) when Levinson modifiers are used as suffix for REE, then other cations or anions have to be placed as a prefix; (V) in case of polytypes and topologically similar polymorphs, a chemical prefix-type nomenclature is preferred, since the polytype and polymorph symbols have to be suffixes. When possible, the CNMNC recommends to avoid changing names, especially for grandfathered species. Well-established mineral names or names dedicated to localities or persons have to be preserved, except if the species is shown to be not valid. Historical names cannot be changed in order to standardize the nomenclature of a group or supergroup, since mixed nomenclature systems are now accepted by the CNMNC.

Key-words: IMA-CNMNC, new guidelines, prefixes, suffixes, mineral nomenclature, historical mineral names.

1. Introduction

Mineralogical nomenclature is a particularly complex matter, because the procedures to define mineral species have become more elaborate since the development of chemistry in the 18th century, and of X-ray diffraction in the 20th century. During Antiquity, minerals were already observed and described by scientists, but their definitions were exclusively based on some physical properties like colour, streak, lustre, hardness, density, or morphology, for example. A mineral is essentially defined as a naturally occurring solid that has been formed by geological processes, with a well-defined chemical composition and crystallographic properties, and which merits a unique name (Nickel & Grice, 1998).

Mineral names are chosen by authors of new mineral species, according to the guidelines established by Nickel & Grice (1998), and are then voted on by the Commission on New Minerals, Nomenclature and Classification (CNMNC). These names may reflect the morphology of minerals (*e.g.* anatase, axinite, auriacusite, fibroferrite, pyromorphite, staurolite or tetrahedrite), their colour (*e.g.* albite, azurite, chlorite, crocoite, erythrite, euchroite, hematite, lazulite, leucite, orpiment, purpurite or rutile), their chemical composition (*e.g.* anhydrite, arsenopyrite, chalcocite, cobaltite, cuprite, cavansite, fluorapatite, pharmacolite, rutheniridosmine, siderite, sodalite or uraninite), their physical properties (*e.g.* barite, euclase, orthoclase, periclase or scorodite), their use (*e.g.* fluorite, graphite, muscovite, pyrite or pyrolusite), similarity to biological objects (*e.g.* garnet, malachite or oursinite) or some of their structural features (*e.g.* clinoenstatite, clinomimetite, orthoserpierite or parahopeite); they are also frequently given to remember the type locality, geographical or administrative name (*e.g.* andalusite, atacamite, brazilianite, ettringite, ilmenite, lakebogaite, lovozerite, montebrasite, tyrolite or vesuvianite), to honour outstanding scientists by first or family name, or both (*e.g.* bobfergusonite, breithauptite, eskolaite, goethite, haüyne, hurlbutite, mandarinoite, melonjosephite, millerite, moissanite, nielsbohrite, sillimanite or wollastonite) or companies, societies, journals and institutions (*e.g.* afmite, imgreite, minrecordite, museumite, nimite, philolithite or tsumcorite), as well as related to mythology (*e.g.* aegirine, atheneite or neptunite) (*e.g.* Mitchell, 1979). Besides these descriptive

DOI: 10.1127/0935-1221/2013/0025-2267
0935-1221/13/0025-2267 $ 1.35

names, recent CNMNC guidelines allowed one to use chemical prefixes and suffixes in mineral names (Nickel & Grice, 1998; Burke, 2008), thus leading to a hybrid mineralogical nomenclature in which descriptive names, prefixes, and suffixes coexist.

In an attempt to rationalize mineralogical nomenclature, the CNMNC has suggested, in 2008, to progressively evolve towards a suffix-based nomenclature (Burke, 2008), in order to better reflect the chemical complexity occurring in some mineral groups like the labuntsovite group (Chukanov *et al*. 2002), the epidote supergroup (Armbruster *et al*. 2006; Mills *et al*. 2009), or the arrojadite group (Cámara *et al*. 2006; Chopin *et al*. 2006). However, strict applications of these new guidelines have sometimes been negatively understood by the mineralogical community, particularly when historical or well-established names were modified, as for example when hancockite was renamed epidote-(Pb) (Armbruster *et al*. 2006), or when the nomenclature of the apatite-supergroup minerals was modified (Burke, 2008). The latter was revisited in considerable detail for this and several other reasons as outlined by Pasero *et al*. (2010).

During the IMA2010 meeting in Budapest, a discussion was initiated among the CNMNC members, in order to establish firm nomenclature guidelines which will guide the mineralogical community into the appropriate uses of prefix- and suffix-based nomenclature, whilst promoting the preservation of historical and well-established names. Authors of nomenclature or new mineral species proposals are asked to follow these recommendations, but retroactivity will not be applied. Every change in nomenclature has to go through the CNMNC, and is examined on its own merit.

2. General guidelines

In mineral groups or supergroups (see Mills *et al*. 2009), flexibility is allowed by the CNMNC when choosing between suffix- and prefix-based nomenclature systems. The CNMNC has no preference about this choice, and the authors can choose according to the nomenclature of pre-existing mineral species in the group/supergroup, and according to the recommendations given below. Mixed nomenclature systems are allowed, even within mineral groups or supergroups; however, authors should provide strong arguments to support such mixed systems. For new mineral proposals, it is recommended to follow the established nomenclature scheme.

Example: A mixed nomenclature system exists in the jahnsite supergroup, in which jahnsite-(CaMnFe) and whiteite-(CaMnMg) coexist with rittmannite and keckite (Kampf *et al*. 2008).

3. Recommendations for the use of suffixes

The following recommendations have to be applied for the use of chemical suffixes in mineralogical nomenclature:

(I) Chemical suffixes have to be in parentheses, except for extra-framework cations. Extra-framework cations and framework cations cannot be mixed in the suffixes, and if such a situation would occur, we would recommend to use a suffix for the extra-framework cations, and a prefix for the framework cations.
Example: Na and Ca are extra-framework cations in chabazite-Na and chabazite-Ca, whereas they occur in the framework of arrojadite-(KNa) (Chopin *et al*. 2006) and of jahnsite-(CaMnMn) (Grice *et al*. 1990).

(II) A maximum of three chemical suffixes is allowed. The chemical suffixes must appear in the same order as in the chemical formula; generally, they must be classified by decreasing ionic radii.
Example: The nomenclature of the whiteite-jahnsite group is based on a root name followed by parentheses containing three chemical suffixes: whiteite-(CaMnMg), jahnsite-(CaMnMg), and jahnsite-(CaMnMn) are valid names (Kampf *et al*. 2008).

(III) Cations and anions should never be used together in the parentheses. In the case where both anions and cations have to appear in the name, then the anions have to be placed as a prefix.
Example: In the apatite supergroup, the names ''apatite-(CaCl)'' and ''apatite-(CaF)'' were introduced by Burke (2008), but the recent report of the apatite subcommittee has re-validated the previous names chlorapatite and fluorapatite, in which the anions occur as prefixes (Pasero *et al*. 2010). Fluorbritholite-(Y) and fluorbritholite-(Ce) are also valid names of minerals in the apatite supergroup.

Remark: In the apophyllite group, Burke (2008) replaced the names ''fluorapophyllite'', ''hydroxyapophyllite'', and ''natroapophyllite'' by apophyllite-(KF), apophyllite-(KOH), and apophyllite-(NaF), in which cations and anions are grouped in the suffix. We propose here, for the sake of consistency, to re-name these minerals fluorapophyllite-(K), hydroxyapophyllite-(K), and fluorapophyllite-(Na).

4. Recommendations for the use of prefixes

The following recommendations have to be applied for the use of chemical prefixes in mineralogical nomenclature.

(I) For common names, prefix-type nomenclature is preferred to facilitate the pronunciation.
Example: The names ''apatite-(CaOH)'' and ''apatite-(CaF)'' are more difficult to pronounce than the approved names hydroxylapatite and fluorapatite.

(II) An unnecessary proliferation of prefixes must be avoided, and a maximum of three chemical prefixes is recommended. Hyphenated names may be chosen to assist in deciphering the name.
Example: Chromo-alumino-povondraite (Henry *et al*. 2011), fluorphosphohedyphane (Pasero *et al*.

2010), oxycalciopyrochlore, and oxystibiomicrolite (Atencio *et al*. 2010) are valid mineral names.

(III) It is allowed to use a combination of chemical, structural or other descriptive prefixes.
Example: Clinoferroholmquistite (Leake *et al*. 2003), hydroxylclinohumite, strontio-orthojoaquinite, bario-orthojoaquinite, and para-alumohydrocalcite are valid mineral names.

(IV) When Levinson modifiers are used as suffix for REE, then other cations or anions have to be placed as a prefix. A new root-name can also be used.
Example: Manganiandrosite-(Ce), vanadoandrosite-(Ce) (Armbruster *et al*. 2006), fluorbritholite-(Y), fluorbritholite-(Ce) (Pasero *et al*. 2010), arsenoflorencite-(Ce) and arsenoflorencite-(La) (Bayliss *et al*. 2010; Mills *et al*. 2010), calcioancylite-(Ce), hydroxylbastnäsite-(Nd), and nioboaeschynite-(Ce) are valid mineral names.

(V) In case of polytypes and topologically similar polymorphs, a chemical prefix-type nomenclature is preferred, since the polytype and polymorph symbols have to be suffixes. It must be remembered, however, that polytypes and topologically similar polymorphs are not considered as separate mineral species (Nickel & Grice, 1998).
Example: In the apatite supergroup, prefixes are preferred, since the polytypes chlorapatite-*M* and hydroxylapatite-*M* have been reported (Pasero *et al*. 2010). In the alunite supergroup, a prefix-type nomenclature is applied for natroalunite, since the polymorphs natroalunite-1*c* and natroalunite-2*c* exist (Bayliss *et al*. 2010).

5. Preservation of historical and well-established names

When possible, the CNMNC recommends to avoid changing names, especially for grandfathered species. Well-established mineral names or names dedicated to localities or persons have to be preserved, except if the species is shown to be not valid. In this case, a renaming, redefinition or discreditation procedure has to be submitted to the CNMNC. Historical names cannot be changed in order to standardize the nomenclature of a group or supergroup, since mixed nomenclature systems are accepted by the CNMNC (see above). However, modern reorganisation of a group or supergroup may require re-examination of incompletely or ambiguously characterised type material, so that its associated historical name can be redefined to fit with a particular species composition field in the new classification scheme. If this cannot be done, then the name may need to be discredited as a species name, although it may be retained as a group name.

Acknowledgements: Many thanks are due to the CNMNC members for their support to this proposal. F.H. thanks the FRS-F.N.R.S. (Belgium) for a position of ''Chercheur qualifié''.

References

Armbruster, T., Bonazzi, P., Akasaka, M., Bermanec, V., Chopin, C., Gieré, R., Heuss-Assbichler, S., Liebscher, A., Menchetti, S., Pan, Y., Pasero, M. (2006): Recommended nomenclature of epidote-group minerals. *Eur. J. Mineral*., **18**, 551–567.

Atencio, D., Andrade, M.B., Christy, A.G., Gieré, R., Kartashov, P.M. (2010): The pyrochlore supergroup of minerals: nomenclature. *Can. Mineral*., **48**, 673–698.

Bayliss, P., Kolitsch, U., Nickel, E.H., Pring, A. (2010): Alunite supergroup: recommended nomenclature. *Mineral. Mag*., **74**(5), 919–927.

Burke, E.A.J. (2008): Tidying up mineral names: an IMA-CNMNC scheme for suffixes, hyphens and diacritical marks. *Mineral. Rec*., **39**, 131–135.

Cámara, F., Oberti, R., Chopin, C., Medenbach, O. (2006): The arrojadite enigma: I. A new formula and a new model for the arrojadite structure. *Am. Mineral*., **91**, 1249–1259.

Chopin, C., Oberti, R., Cámara, F. (2006): The arrojadite enigma: II. Compositional space, new members, and nomenclature of the group. *Am. Mineral*., **91**, 1260–1270.

Chukanov, N.V., Pekov, I.V., Khomyakov, A.P. (2002): Recommended nomenclature for labuntsovite-group minerals. *Eur. J. Mineral*., **14**, 165–173.

Grice, J.D., Dunn, P.J., Ramik, R.A. (1990): Jahnsite-(CaMnMn), a new member of the whiteite group from Mangualde, Beira, Portugal. *Am. Mineral*., **75**, 401–404.

Henry, D.J., Novák, M., Hawthorne, F.C., Ertl, A., Dutrow, B.L., Uher, P., Pezzota, F. (2011): Nomenclature of the tourmaline-supergroup minerals. *Am. Mineral*., **96**, 895–913.

Kampf, A.R., Steele, I.M., Loomis, T.A. (2008): Jahnsite-(NaFeMg), a new mineral from the Tip Top mine, Custer County, South Dakota: description and crystal structure. *Am. Mineral*., **93**, 940–945.

Leake, B.E., Woolley, A.R., Birch, W.D., Burke, E.A.J., Ferraris, G., Grice, J.D., Hawthorne, F.C., Kisch, H.J., Krivovichev, V.G., Schumacher, J.C., Stephenson, N.C.N., Whittaker, E.J.W. (2003): Nomenclature of amphiboles: additions and revisions to the International Mineralogical Association's 1997 recommendations. *Can. Mineral*., **41**, 1355–1362.

Mills, S.J., Hatert, F., Nickel, E.H., Ferraris, G. (2009): The standardisation of mineral group hierarchies: application to recent nomenclature proposals. *Eur. J. Mineral*., **21**, 1073–1080.

Mills, S.J., Kartashov, P.M., Kampf, A.R., Raudsepp, M. (2010): Arsenoflorencite-(La), a new mineral from the Komi Republic, Russian Federation: description and crystal structure. *Eur. J. Mineral*., **22**, 613–621.

Mitchell, R.S. (1979): Mineral names. What do they mean? Van Nostrand Reinhold Company, New York, xv, 229 p.

Nickel, E.H. & Grice, J.D. (1998): The IMA Commission on New Minerals and Mineral Names: procedures and guidelines on mineral nomenclature, 1998. *Can. Mineral*., **36**, 913–926.

Pasero, M., Kampf, A.R., Ferraris, C., Pekov, I.V., Rakovan, J., White, T.J. (2010): Nomenclature of the apatite supergroup minerals. *Eur. J. Mineral*., **22**, 163–179.

Received 25 October 2012
Modified version received 6 November 2012
Accepted 12 November 2012

Eur. J. Mineral.
2009, **21**, 1073–1080
Published online October 2009

The standardisation of mineral group hierarchies: application to recent nomenclature proposals

STUART J. MILLS[1,*], FRÉDÉRIC HATERT[2], ERNEST H. NICKEL[3,**] and GIOVANNI FERRARIS[4]

[1] Department of Earth and Ocean Sciences, University of British Columbia, Vancouver, BC, V6T 1Z4, Canada
Commission on New Minerals, Nomenclature and Classification, of the International Mineralogical Association (IMA–CNMNC), Secretary
*Corresponding author, e-mail: smills@eos.ubc.ca
[2] Laboratoire de Minéralogie et de Cristallochimie, B-18, Université de Liège, 4000 Liège, Belgium
IMA–CNMNC, Vice-Chairman
[3] CSIRO, Private Bag 5, Wembley, Western Australia 6913, Australia
[4] Dipartimento di Scienze Mineralogiche e Petrologiche, Università di Torino, Via Valperga Caluso 35, 10125, Torino, Italy

Abstract: A simplified definition of a mineral group is given on the basis of structural and compositional aspects. Then a hierarchical scheme for group nomenclature and mineral classification is introduced and applied to recent nomenclature proposals. A new procedure has been put in place in order to facilitate the future proposal and naming of new mineral groups within the IMA–CNMNC framework.

Key-words: mineral group, supergroup, nomenclature, mineral classification, IMA–CNMNC.

Introduction

There are many ways which are in current use to help with the classification of minerals, such as: *Dana's New Mineralogy* (Gaines *et al.*, 1997), the *Strunz classification* (Strunz & Nickel, 2001), *A Systematic Classification of Minerals* (Ferraiolo, 2003) and the various volumes of Deer, Howie and Zussman (*Rock-forming Minerals* series), which use combinations of mineral structure and chemical composition to classify minerals. There is also *Fleischer's Glossary of Minerals* (Mandarino, 1999; Back & Mandarino, 2008) which lists 'groups' of minerals in the back section of the glossary. All are useful aids, however, there has been no systematic approach to mineral group naming or a definite hierarchical system put in place. There is also no system for the proposal and approval of mineral groups and group names.

In the past, some mineral groups have been referred to by different names and some mineral species have been proposed as members of more than one group. This proposal aims to standardise group nomenclature by introducing a hierarchy in which to classify mineral species (applied to recent nomenclature proposals) and to introduce a new procedure for the approval of new mineral groups. The following proposal has been approved by the IMA Commission on New Minerals and Mineral Names prior to publication (Voting Proposal 09–A).

** Deceased, July 18, 2009.

History

From time to time, the issue of how the names of groups have been applied and its consistency has been discussed by both the CNMMN/CNMNC and the Commission on Classification of Minerals (CCM)[1]. In 2004, a proposal was prepared by Drs Pushcharovsky, Pasero, Nickel and Ferraris which set out some definitions and criteria for establishing a standard set of group names. This document was circulated for comment at that time; however, there were many competing views. A revised version of this document was commented on by the CNMNC in 2008 and the definition of a mineral group in this scheme has been incorporated from that document.

Definition of a mineral group

Mineral species can be grouped in a number of different ways, on the basis of chemistry, crystal structure, occurrence, association, genetic history, or resource, for example, depending on the purpose to be served by the classification. However, if the classification is to adequately meet

[1] The Commission on New Minerals, Nomenclature and Classification (CNMNC) was formed in July 2006 by a merger between the Commission on New Minerals and Mineral Names (CNMMN) and the Commission on Classification of Minerals (CCM), at the request of both commissions (Burke, 2006).

DOI: 10.1127/0935-1221/2009/0021-1994
0935-1221/09/0021-1994 $ 3.60

the needs of the CNMNC, it is proposed that the grouping be based on chemical composition and crystal structure, as these are the two essential components in the characterisation of a mineral species. Consequently, the simplified definition of a mineral group is:

> *A mineral group consists of two or more minerals with the same or essentially the same structure, and composed of chemically similar elements.*

Structural aspects of a mineral group

The expression "the same structure" means isotypic structures, *i.e.*, structures belonging to one structural type. Crystal structures regarded as being 'essentially the same' can be encompassed by the term 'homeotypic'. As defined by the IUCr, "two structures are considered as homeotypic if all essential features of topology are preserved between them" (Lima-de-Faria *et al.*, 1990). In particular, homeotypic structures do not necessarily have the same space group. Therefore crystallographic variants such as superstructures, substructures and differences in the ordering of atoms that may give rise to multiple cells and/or different space groups, are considered to be homeotypic (*e.g.*, as in the recently defined labuntsovite (Chukanov *et al.*, 2002) and eudialyte (Johnsen *et al.*, 2003) groups). Some polymorphs, such as triclinic and monoclinic feldspars, can be regarded as homeotypic and can therefore be included in a group; others, such as the carbon polymorphs diamond and graphite, are topologically too dissimilar (*i.e.*, they are not homeotypic) and should not belong to the same group.

Homologous series (*e.g.*, lillianite and pavonite series), polysomatic series (*e.g.*, biopyriboles, heterophyllosilicates) and other structural categories that comprise modular structures (Ferraris *et al.*, 2008) go beyond the strict definition of a homeotype, and therefore are not to be regarded as groups. However, some mineral species in these categories may belong to groups if they meet the necessary criteria.

Polytypic variations within mineral species, as defined in Guinier *et al.* (1984), are not regarded as comprising groups.

Compositional aspects of a mineral group

"Chemically similar elements" is taken to mean elements that have similar crystal-chemical behaviour. Thus, isoconfigurational minerals composed of elements with dissimilar crystal-chemical behaviour, such as galena, periclase and halite, are not to be regarded as belonging to the same group. Unoccupied structural sites are to be treated in the same way as chemical elements for the purpose of group placement.

A hierarchical scheme for group nomenclature

The hierarchical scheme draws on the strengths of the various publications mentioned above. We have subdivided the scheme into six levels, however, because some of these levels are described differently in various texts, we provide the following definitions:

1. Mineral class.
2. Mineral subclass.
3. Mineral family.
4. Mineral supergroup.
5. Mineral group(s).
6. Mineral subgroup or mineral series[2].

Definitions of the group levels

1. At the highest level, mineral species can be classified primarily on the main *anion* (O^{2-}, S^{2-} etc.), *anionic complex* (OH^{-}, SO_4^{2-}, CO_2^{2-}, PO_4^{3-}, $B_xO_y^{Z-}$, $Si_xO_y^{Z-}$ etc.) or lack of an anion (native elements) to form classes. The most common mineral classes are: native elements, sulphides, sulphosalts, halides, oxides, hydroxides, arsenites (including antimonites, bismuthites, sulphites, selenites and tellurites), carbonates, nitrates, borates, sulphates, chromates, molybdates, tungstates, phosphates, arsenates, vanadates, silicates and organic compounds.
2. Mineral subclasses apply to the *borate* and *silicate classes*, where the configuration and bonding of tetrahedra are used to group structurally similar minerals. The subclasses are: neso-, soro-, cyclo-, ino-, phyllo- and tectosilicates(borates). Traditionally the borates are divided into monoborates, diborates, triborates, tetraborates etc. (*e.g.* Strunz & Nickel, 2001), however, enough structural data is known to base classification of borates on the polymerisation of the borate anion.
3. Mineral families apply to groups and/or supergroups having similar structural and/or chemical features that make them unique. A mineral family can also consist of two or more supergroups. An example of a mineral family established on the basis of structural criteria is the zeolite family, where all members are characterised by their framework structures containing cavities, but individual minerals themselves may also belong to different groups (and supergroups). The feldspathoid family also belongs to this type of 'structural' family. Other families are defined on the basis of chemical features, as for example the pyrite–marcasite family (which would consist of the pyrite and marcasite supergroups).
4. A mineral supergroup consists of *two or more* groups which have essentially the same structure and composed of chemically similar elements. Generally, a supergroup will contain members from the same mineral class (*e.g.* the epidote supergroup, Table 1c), however in rare cases a supergroup may also contain groups belonging to different classes, as for example in the alunite supergroup (Table 1a). A supergroup may also contain isolated mineral species which do not belong to any mineral group, as for example vanadinite, which is the only vanadate in the apatite supergroup.

[2] Due to the definition of a group as containing two or more minerals, it negates the need for a lower level classification. A mineral subgroup/series must also contain two or more members.

Table 1a. Group nomenclature for the alunite supergroup.

Alunite supergroup[1]			
Alunite group	**Beudantite group**	**Dussertite group**	**Plumbogummite group**
Alunite	Beudantite	Arsenocrandallite	Benauite
Ammonioalunite	Corkite	Arsenoflorencite-(Ce)	Crandallite
Ammoniojarosite	Gallobeudantite	Arsenogorceixite	Eylettersite
Argentojarosite	Hidalgoite	Arsenogoyazite	Florencite-(Ce)
Beaverite-(Cu)	Hinsdalite	Dussertite	Florencite-(La)
Beaverite-(Zn)	Kemmlitzite	Graulichite-(Ce)	Florencite-(Nd)
Dorallcharite	Svanbergite	Philipsbornite	Gorceixite
Huangite	Weilerite	Segnitite	Goyazite
Hydroniumjarosite	Woodhouseite		Kintoreite
Jarosite			Plumbogummite
Natroalunite			Springcreekite
Natroalunite-2R			Waylandite
Natrojarosite			Zaïrite
Osarizawaite			
Plumbojarosite			
Schlossmacherite			
Walthierite			

[1] References: Scott (1987), Birch *et al.* (1992), Jambor (1999), Scott (2000), Back & Mandarino (2008), Sato *et al.* (2008); Bayliss *et al.* (2009).

Table 1b. Group nomenclature for the astrophyllite group.

Astrophyllite group[2]
Astrophyllite
Magnesioastrophyllite
Hydroastrophyllite
Niobophyllite
Zircophyllite
Kupletskite
Kupletskite-(Cs)
Niobokupletskite

[2] Reference: Piilonen *et al.* (2003).

5. A mineral group consists of *two or more* minerals with the same or essentially the same structure and composed of chemically similar elements (see above).
6. A mineral subgroup or mineral series should be used for minerals of a homologous series (*e.g.*, the lillianite and pavonite series and other sulphosalt series, Moëlo *et al.*, 2008) or polysomatic series (*e.g.*, biopyriboles and heterophyllosilicates, Ferraris *et al.*, 2008), where they do not meet the strict definition of a mineral group.

The naming of the group and supergroup levels

It is desirable that the group name be that of the first mineral to have been adequately characterised. This will generally require full structural characterisation. However, in some cases it may be preferable to name a group by a particular chemical or structural attribute (*e.g.*, sodic-calcic amphiboles, Leake *et al.*, 2003) rather than by a specific species name. The historical name should be used as the group name wherever possible.

The supergroup name should also be taken from the first mineral to have been adequately characterised (*i.e.* the first group name) or a historically significant name which no longer defines a single mineral species, such as tourmaline.

In a few cases, a group or a supergroup name can be selected contrary to the precedence rule because the name of this group (supergroup) is very firmly established in the literature. For example, it would be confusing to refer to the alunite supergroup as the "plumbogummite supergroup", even though plumbogummite was described in 1819 and has precedence over alunite which was described in 1824.

Procedure for the introduction of mineral groups and supergroups

A mineral group (or supergroup) can be introduced in the following different ways:

1. If an author (or group of authors) is submitting a new mineral proposal to the CNMNC Chairman, whereby the new mineral would either become the second mineral of a new group, or a group has not been validated previously (and has more than two members), the author(s) can submit at the same time as the new mineral proposal, a proposal for the creation of a new group.
2. During a nomenclature report by a CNMNC subcommittee handled by the CNMNC Secretary.
3. In a proposal by an author (or group of authors) to the CNMNC Vice-Chairman (responsible for changes to

Table 1c. Group nomenclature for the epidote supergroup.

Epidote supergroup[3]		
Epidote group	**Allanite group**	**Dollaseite group**
Clinozoisite	Allanite-(Ce)	Dollaseite-(Ce)
Epidote	Allanite-(La)	Khristovite-(Ce)
Epidote-(Pb)	Allanite-(Y)	
Mukhinite	Dissakisite-(Ce)	
Clinozoisite-(Sr)	Dissakisite-(La)	
Piemontite	Ferriallanite-(Ce)	
Piemontite-(Sr)	Manganiandrosite-(Ce)	
Manganipiemontite-(Sr)	Manganiandrosite-(La)	
	Vanadoandrosite-(Ce)	

[3] Reference: Armbruster *et al*. (2006).

Table 1d. Group nomenclature for the eudialyte group.

Eudialyte group[4]
Carbokentbrooksite
Eudialyte
Feklichevite
Ferrokentbrooksite
Georgbarsanovite
Golyshevite
Ikranite
Johnsenite-(Ce)
Kentbrooksite
Khomyakovite
Manganokhomyakovite
Mogovidite
Oneillite
Raslakite
Rastsvetaevite
Taseqite
Zirsilite-(Ce)
Alluaivite
Andrianovite
Aqualite
Dualite
Labyrinthite

[4] References: Johnsen *et al*. (2003), Nickel & Nichols (2007), Back & Mandarino (2008).

Table 1e. Group nomenclature for the arrojadite group.

Arrojadite group[5]
Arrojadite-(KFe)
Arrojadite-(KNa)
Arrojadite-(PbFe)
Arrojadite-(SrFe)
Arrojadite-(BaFe)
Dickinsonite-(KMnNa)
Fluorarrojadite-(BaFe)
Fluorarrojadite-(BaNa)

[5] Reference: Chopin *et al*. (2006).

Table 1f. Group nomenclature for the joaquinite group.

Joaquinite group[7]
Bario-orthojoaquinite
Byelorussite-(Ce)
Joaquinite-(Ce)
Orthojoaquinite-(Ce)
Orthojoaquinite-(La)
Strontiojoaquinite
Strontio-orthojoaquinite

[7] Reference: Matsubara *et al.* (2001).

existing nomenclature) to create a new mineral group (or supergroup) based on data collected by those author(s).

Subgroup *vs.* Group in previous publications

The term ‘subgroup’ has been used in a number of different nomenclature proposals (*e.g.* the epidote nomenclature report, Armbruster *et al.*, 2006), which is the equivalent of ‘level 5 mineral group’ in the hierarchical system described above. The term ‘subgroup’ is often applied where ‘group’ has been used as the equivalent of ‘level 4 mineral supergroup’. Thus, there is a simple transformation between this style of mineral group naming and the one described here.

Family *vs.* Supergroup *vs.* Group in previous publications

The terms ‘family’, ‘supergroup’ and ‘group’ have been used interchangeably in several different schemes; in particular when referring to the alunite (jarosite) supergroup, which has been called the alunitejarosite family, alunite and jarosite supergroups, alunite–jarosite supergroup or the

Table 1g. Group nomenclature for the amphibole supergroup.

Amphibole supergroup				
Mg-Fe-Mn-Li group	**Calcic group**	**Sodic-calcic group**	**Sodic group**	**Na-Ca-Mg-Fe-Mn-Li group**
Anthophyllite	Actinolite	Aluminobarroisite	Arfvedsonite	Ferri-ottoliniite
Clinoferroholmquistite	Alumino-ferrotschermakite	Alumino-magnesiotaramite	Dellaventuraite	Ferriwhittakerite
Cummingtonite	Alumino-magnesiosadanagaite	Aluminotaramite	Eckermannite	Ottoliniite
Ferri-clinoferroholmquistite	Aluminotschermakite	Barroisite	Ferric-ferronybøite	Whittakerite
Ferri-clinoholmquistite	Cannilloite	Ferribarroisite	Ferricnybøite	
Ferripedrizite	Chloro-potassichastingsite	Ferrikatophorite	Ferro-eckermannite	
Ferro-anthophyllite	Chloro-potassicpargasite	Ferri-ferrobarroisite	Ferroglaucophane	
Ferrogedrite	Edenite	Ferri-magnesiotaramite	Fluoro-ferroleakeite	
Ferroholmquistite	Ferri-ferrotschermakite	Ferritaramite	Fluoro-magnesio-arfvedsonite	
Ferropedrizite	Ferritschermakite	Ferriwinchite	Fluoronybøite	
Fluoro-sodic-pedrizite	Ferro-actinolite	Ferrobarroisite	Fluoro-potassic-magnesio-arfvedsonite	
Gedrite	Ferro-edenite	Ferrorichterite	Glaucophane	
Grunerite	Ferrohornblende	Ferrowinchite	Kornite	
Holmquistite	Ferrokaersutite	Fluoro-alumino-magnesiotaramite	Kôzulite	
Manganocummingtonite	Ferropargasite	Fluoro-potassic-richterite	Leakeite	
Manganogrunerite	Ferrotschermakite	Fluororichterite	Magnesio-arfvedsonite	
Proto-anthophyllite	Ferrocannilloite	Katophorite	Magnesioriebeckite	
Protoferro-anthophyllite	Fluoro-edenite	Magnesiokatophorite	Nybøite	
Protomangano-ferro-anthophyllite	Fluoro-magnesiohastingsite	Magnesiotaramite	Obertiite	
Sodicanthophyllite	Fluoropargasite	Parvowinchite	Potassicarfvedsonite	
Sodic-ferri-clinoferroholmquistite	Fluoro-potassichastingsite	Potassic-fluororichterite	Potassicleakeite	
Socdic-ferri-ferropedrizite	Hastingsite	Richterite	Potassic-magnesio-arfvedsonite	
Sodic-ferripedrizite	Joesmithite	Taramite	Riebeckite	
Sodic-ferro-anthophyllite	Kaersutite	Winchite	Ungarettiite	
Sodic-ferrogedrite	Magnesiohastingsite			
Sodicgedrite	Magnesiohornblende			
	Magnesiosadanagaite			
	Pargasite			
	Parvo-mangano-edenite			
	Parvo-manganotremolite			
	potassic-aluminosadanagaite			
	Potassic-ferrisadanagaite			
	Potassic-ferropargasite			
	Potassic-hastingsite			
	Potassic-magnesiohastingsite			
	Potassic-magnesiosadanagaite			
	Potassicpargasite			
	Potassicsadanagaite			
	Sadanagaite			
	Tremolite			
	Tschermakite			

[8] References: Leake *et al.* (1997, 2003), Nickel & Nichols (2007), Back & Mandarino (2008). Only amphiboles found in nature are reported.

Table 1h. Group nomenclature for the labuntsovite supergroup.

Labuntsovite supergroup[9]				
Nenadkevichite group	**Vuoriyarvite group**	**Paratsepinite group**	**Lemmleinite group**	**Labuntsovite group**
Korobitsynite	Tsepinite-Ca	Paratsepinite-Ba	Lemmleinite-Ba	Labuntsovite-Fe
Nenadkevichite	Tsepinite-K	Paratsepinite-Na	Lemmleinite-K	Labuntsovite-Mg
	Tsepinite-Na			Labuntsovite-Mn
	Tsepinite-Sr			
	Vuoriyarvite-K			
Gutkovaite group	**Kuzmenkoite group**	**Organovaite group**	**Unassigned member of the labuntsovite supergroup**	
Alsakharovite-Zn	Gjerdingenite-Ca	Organovaite-Mn	Paralabuntsovite-Mg	
Gutkovaite-Mn	Gjerdingenite-Fe	Organovaite-Zn		
Neskevaaraite-Fe	Gjerdingenite-Mn	Parakuzmenkoite-Fe		
	Gjerdingenite-Na			
	Karupmøllerite-Ca			
	Kuzmenkoite-Mn			
	Kuzmenkoite-Zn			
	Lepkhenelmite-Zn			

[9] References: Chukanov *et al.* (2002) , Raade *et al.* (2004), Back & Mandarino (2008).

Table 1i. Group nomenclature for the sapphirine supergroup.

Sapphirine supergroup[10]			
Sapphirine group	**Aenigmatite group**	**Rhönite group**	**Unassigned member of the sapphirine supergroup**
Khmaralite	Aenigmatite	Dorrite	Surinamite
Sapphirine	Krinovite	Høgtuvaite	
	Wilkinsonite	Makarochkinite	
		Rhönite	
		Serendibite	
		Welshite	

[10] References: Grew *et al*. (2008).

Table 1j. Group nomenclature for the högbomite supergroup.

Högbomite supergroup[11]		
Högbomite group	**Nigerite group**	**Taaffeite group**
Ferrohögbomite-2*N*2*S*	Ferronigerite-6*N*6*S*	Magnesiotaaffeite-6*N*'3*S*
Magnesiohögbomite-2*N*2*S*	Magnesionigerite-6*N*6*S*	Ferrotaaffeite-6*N*'3*S*
Magnesiohögbomite-2*N*3*S*	Ferronigerite-2*N*1*S*	Magnesiotaaffeite-2*N*'2*S*
Magnesiohögbomite-6*N*6*S*	Magnesionigerite-2*N*1*S*	
Zincohögbomite-2*N*2*S*		
Zincohögbomite-2*N*6*S*		

[11] References: Armbruster (2002), Back & Mandarino (2008).

alunite supergroup. There have also been many different allocations of minerals into various groups within the 'supergroup' (Mills, 2007). In this case, the terms family and supergroup are equivalent to 'level 3 mineral supergroup' in the hierarchical scheme described above. The new scheme provides a way of simplifying large mineral groups so that confusing and inconsistent terms cannot be used to indicate the same thing.

Application of mineral group hierarchies to recent nomenclature proposals

As a test that the new hierarchical scheme can classify all minerals, we have applied it to recent nomenclature proposals (Table 1a to 1j). Here, we have created new groups and supergroups where they were previously 'subgroups' and

'groups', such as the new högbomite, labuntsovite, epidote and sapphirine supergroups.

In the case of the högbomite supergroup, the 'subgroups' that were established on the basis of Mg^{2+}, Fe^{2+} or Zn^{2+} by Armbruster (2002) have been combined so that they fall within the högbomite, nigerite or taaffeite groups. Likewise, the alunite supergroup has been simplified (from Scott, 1987; Birch *et al.*, 1992; Bayliss *et al.*, 2009), so that all members fall within the alunite (SO_4-dominant), dussertite (AsO_4-dominant), plumbogummite (PO_4-dominant), or beudantite (mixed SO_4-PO_4 and SO_4-AsO_4) groups.

In the sapphirine supergroup, surinamite is an unassigned member because there is no other member to allow a group to be established. Paralabuntsovite is also an unassigned member of the labuntsovite supergroup, for the same reason.

Conclusion

The new hierarchical scheme has been successfully applied to recent nomenclature reports in order to standardise the way in which minerals are organised into groups. A new procedure has been put in place in order to facilitate the future proposal and naming of new mineral groups within the IMA–CNMNC framework.

The next step is to apply the hierarchical scheme to all known minerals (via a CNMNC subcommittee) and to compile a list of mineral groups, supergroups, *etc*., which should be published in an appropriate mineralogical journal and on the CNMNC website.

References

Armbruster, T. (2002): Revised nomenclature of högbomite, nigerite, and taaffeite minerals. *Eur. J. Mineral.*, **14**, 389–395.

Armbruster, T., Bonazzi, P., Akasaka, M., Beremanec, V., Chopin, C., Gieré, R., Heuss-Assbichler, S., Liebscher, A., Menchetti, S., Pan, Y., Pasero, M. (2006): Recommended nomenclature of epidote-group minerals. *Eur. J. Mineral.*, **18**, 551–567.

Back, M. & Mandarino, J.A. (2008): Fleischer's Glossary of Mineral Species 2008. Mineralogical Record Inc., Tuscon, 346 p.

Bayliss, P., Kolitsch, U., Nickel, E.H., Pring, A., Scott, K. (2009): Recommended nomenclature of the alunite supergroup. CNMNC proposal 07–D.

Birch, W.D., Pring, A., Gatehouse, B.M. (1992): Segnitite, $PbFe_3H(AsO_4)_2(OH)_6$, a new mineral in the lusingite group, from Broken Hill, New South Wales. *Am. Mineral.*, **77**, 656–659.

Burke, E.A.J. (2006): The end of CNMMN and CCM—LONG LIVE THE CNMNC! *Elements*, **2**, 388.

Chopin, C., Oberti, R., Cámara, F. (2006): The arrojadite enigma: II. Compositional space, new members, and nomenclature of the group. *Am. Mineral.*, **91**, 1260–1270.

Chukanov, N.V., Pekov, I.V., Khomyakov, A.P. (2002): Recommended nomenclature for labuntsovite-group minerals. *Eur. J. Mineral.*, **14**, 165–173.

Ferraiolo, J.A. (2003): A Systematic Classification of Minerals. 2206 Harwood Lane, Bowie, Maryland 20716–1107, U.S.A., 441 p.

Ferraris, G., Makovicky, E., Merlino, S. (2008): Crystallography of Modular Materials. Oxford University Press, 370 p.

Gaines, R.V., Skinner, H.C., Foord, E.E., Mason, B., Rosenzweig, A. (1997): Dana's new mineralogy. Wiley & Sons, New York, 1819 p.

Grew, E., Hålenius, U., Pasero, M., Barbier, J. (2008): Recommended nomenclature for the sapphirine and surinamite groups (sapphirine supergroup). *Mineral. Mag.*, **72**, 839–876.

Guinier, A., Bokij, G.B., Boll-Dornberger, K., Cowley, J.M., Ďurovič, S., Jagodzinski, H., Krishna, P., de Wolff, P.M., Zvyagin, B.B., Cox, D.E., Goodman, P., Hahn, T., Kuchitsu, K., Abrahams, S.C. (1984): Nomenclature of polytype structures. *Acta Crystallogr. A*, **40**, 399–404.

Jambor, J.L. (1999): Nomenclature of the alunite supergroup. *Can. Mineral.*, **37**, 1323–1341.

Johnsen, O., Ferraris, G., Gault, R.A., Grice, J., Kampf, A. R., Pekov, I.V. (2003): The nomenclature of eudialyte-group minerals. *Can. Mineral.*, **41**, 785–794.

Leake, B., Woolley, A.R., Arps, C.E.S., Birch, W.D., Gilbert, M.C., Grice, J.D., Hawthorne, F.C., Kato, A., Kisch, H.J., Krivovichev, V.G., Linthout, K., Laird, J., Mandarino, J.A., Maresch, W.V., Nickel, E.H., Rock, N.M.S., Schumacher, J.C., Smith, D.C., Stephenson, N.C.N., Ungaretti, L., Whittaker, E.J.W., Youzhi, G. (1997): Nomenclature of amphiboles: report of the subcommittee on amphiboles of the International Mineralogical Association, Commission on New Minerals and Mineral Names. *Eur. J. Mineral.*, **9**, 623–651.

Leake, B.E., Woolley, A.R., Birch, W.D., Burke, E.A.J., Ferraris, G., Grice, J.D., Hawthorne, F.C., Kisch, H.J., Krivovichev, V.G., Schumacher, J.C., Stephenson, N.C.N., Whittaker, E.J.W. (2003): Nomenclature of amphiboles: Additions and revisions to the International Mineralogical Association's 1997 recommendations. *Can. Mineral.*, **41**, 1355–1362.

Lima-de-Faria, J., Hellner, E., Liebau, F., Makovicky, E., Parthé, E. (1990): Nomenclature of inorganic structure types. Report of the International Union of Crystallography Commission on Crystallographic Nomenclature, Sub-Committee on the Nomenclature of Inorganic Structure Types. *Acta Crystallogr. A*, **46**, 1–11.

Mandarino, J.A. (1999): Fleischer's Glossary of Mineral Species 1999. Mineralogical Record Inc., Tuscon, 226 p.

Matsubara, S., Mandarino, J.A., Semenov, E.I. (2001): Redefinition of a mineral in the joaquinite group: Orthojoaquinite-(La). *Can. Mineral.*, **39**, 757–760.

Mills, S.J. (2007): The crystal chemistry and geochronology of secondary minerals from the Broken Hill deposit, New South Wales. Ph.D. thesis, University of Melbourne, Melbourne, Australia, 249 p.

Moëlo, Y., Makovicky, E., Mozgova, N.N., Jambor, J.L., Cook, N., Pring, A., Paar, W., Nickel, E.H., Graeser, S., Karup-Møller, S., Balic-Žunic, T., Mumme, W.G., Vurro, F., Topa, D., Bindi, L., Bente, K., Shimizu, M. (2008): Sulfosalts systematics: a review. Report of the sulfosalt sub-committee of the IMA Commission on Ore Mineralogy. *Eur. J. Mineral.*, **20**, 7–46.

Nickel, E.H. & Nichols, M. (2007): Minerals Database. MDI Minerals Data. California, USA.

Oberti, R., Della Ventura, G., Ottolini, L., Hawthorne, F.C., Bonazzi, P. (2002): Re-definition, nomenclature and crystal-chemistry of the hellandite group. *Am. Mineral.*, **87**, 745–752.

Piilonen, P.C., Lalonde, A.E., McDonald, A.M., Gault, R.A., Larsen, A.O. (2003): Insights into astrophyllite-group minerals. I. Nomenclature, composition and development of a general standard formula. *Can. Mineral.*, **41**, 1–26.

Raade, G., Chukanov, N.V., Kolitsch, U., Möckel, S., Zadov, A.E., Pekov, I.V. (2004): Gjerdingenite-Mn from Norway – a new mineral species in the labuntsovite group: descriptive data and crystal structure. *Eur. J. Mineral.*, **16**, 979–987.

Sato, E., Nakai, I., Terada, Y., Tstusumi, Y., Yokoyama, K., Miyawaki, R., Mastubara, S. (2008): Study of Zn-bearing beaverite $Pb(Fe_2Zn)(SO_4)_2(OH)_6$ obtained from Mikawa mine, Niigata Prefecture, Japan. *J. Mineral. Petrol. Sci.*, **103**, 141–144.

Scott, K.M. (1987): Solid solution in, and classification of, gossan-derived members of the alunite–jarosite family, northwest Queensland, Australia. *Am. Mineral.*, **72**, 178–187.

— (2000): Nomenclature of the alunite supergroup: discussion. *Can. Mineral.*, **38**, 1295–1297.

Strunz, H. & Nickel, E.H. (2001): Strunz mineralogical tables. Schweizerbart, Stuttgart, 869 p.

Received 6 October 2009
Accepted 6 October 2009

American Mineralogist, Volume 95, pages 185–187, 2010

Abbreviations for names of rock-forming minerals

Donna L. Whitney[1,*] and Bernard W. Evans[2]

[1]Department of Geology and Geophysics, University of Minnesota, Minneapolis, Minnesota 55455, U.S.A.
[2]Department of Earth and Space Sciences, Box 351310, University of Washington, Seattle, Washington 98185, U.S.A.

Nearly 30 years have elapsed since Kretz (1983) provided the mineralogical community with a systematized list of abbreviations for rock-forming minerals and mineral components. Its logic and simplicity have led to broad acceptance among authors and editors who were eager to adopt a widely recognized set of mineral symbols to save space in text, tables, and figures.

Few of the nearly 5000 known mineral species occur in nature with a frequency sufficient to earn repeated mention in the geoscience literature and thus qualify for the designation "rock-forming mineral," but a reasonable selection of the most common and useful rock-forming minerals likely numbers in the several hundreds. The original list by Kretz (1983) contained abbreviations for 193 of these.

We propose an expansion to the list initiated by Kretz (1983) (see next page). Modest expansions and revisions were made by Spear (1993), Holland and Powell (1998), the Mineralogical Association of Canada, and Siivola and Schmid (2007). Our revised list of abbreviations has 371 entries. Significant numbers of the new entries are the result of three decades of research in high- and ultrahigh-pressure metamorphic terrains, the explicit inclusion of Mg and Fe end-members of solid-solution series (as in the amphiboles), recent work on extraterrestrial samples, and the increased relevance to petrology of numerous accessory minerals.

The two systems of abbreviations currently most in use—Kretz (1983), including modifications; and Holland and Powell (1998)—differ in terms of style and concept. Kretz abbreviations are 2–3 letters and use uppercase first letters for minerals and lower case letters throughout for mineral components (e.g., the almandine component of garnet); the Holland and Powell system varies from 1–5 letters and uses lowercase throughout. The Kretz system provides abbreviations for selected intermediates in solid-solution mineral series. The Holland and Powell system is restricted to abbreviations for end-members for which there are available thermodynamic data that have been included in the Holland and Powell database. The two systems have the same abbreviations for some minerals (other than capitalization), but in many cases use different symbols for the same mineral, for example, "Crn" (Kretz) and "cor" (H&P).

The selection of minerals to include in a list of abbreviations is subjective, but we have tried to err on the side of being inclusive, listing some minerals for which the status is questionable according to the International Mineralogical Association. For example, we accommodate alternative choices such as titanite (Ttn) and sphene (Spn); hypersthene (Hyp), enstatite (En), and orthopyroxene (Opx); glaucophane (Gln), crossite (Crt), and riebeckite (Rbk); and albite (Ab) and anorthite (An) as well as plagioclase (Pl), recognizing that some petrologists have uses for these mineral names. In addition, although our focus is on rock-forming minerals, some hypothetical and/or synthetic phases are included in our list, as well as an abbreviation for "liquid" (Liq). We have also included some abbreviations for mineral groups, e.g., aluminosilicates (Als, the Al_2SiO_5 polymorphs), and other descriptive terms (e.g., opaque minerals). The choice of abbreviations attempts as much as possible to make the identity of the mineral instantly obvious and unambiguous.

Updated list of mineral abbreviations

In this contribution, abbreviations from Kretz (with some modifications) and new abbreviations are listed (Table 1, next page). The following format was used for assigning abbreviations:

(1) The first letter is capitalized; the other letter(s) are lower case, with the exception of Phase A, abbreviated as PhA.

(2) The first letter of the abbreviation is the first letter of the mineral name; subsequent letters are selected from the mineral name.

(3) Most abbreviations consist of 2 or 3 letters, but a 4-letter abbreviation is used when the addition of F for ferro- or M for magnesio- resulted in ambiguity in the 3-letter version (e.g., Mcar for magnesiocarpholite).

(4) Mineral abbreviations were selected so as not to correspond to abbreviations for elements. Note that rule 4 was violated by a few of the original Kretz abbreviations (Mo for molybdenite; Ne for nepheline), so some original Kretz abbreviations have been changed to follow this rule. Others have been modified to avoid ambiguity with minerals added to the list.

Acknowledgment

We thank Marc Hirschmann and Howard Day for input on the updated abbreviation system.

References cited

Kretz, R. (1983) Symbols of rock-forming minerals. American Mineralogist, 68, 277–279.

Holland, T.J.B. and Powell, R. (1998) An internally-consistent thermodynamic data set for phases of petrologic interest. Journal of Metamorphic Geology, 16, 309–343.

Siivola, J. and Schmid, R. (2007) Recommendations by the IUGS Subcommission on the Systematics of Metamorphic Rocks: List of mineral abbreviations. Web version 01.02.07. (http://www.bgs.ac.uk/scmr/docs/papers/paper_12.pdf) IUGS Commission on the Systematics in Petrology.

Spear, F.S. (1993) Metamorphic Phase Equilibria and Pressure-Temperature-Time Paths. Monograph 1, Mineralogical Society of America, Chantilly, Virginia.

Manuscript received August 11, 2009
Manuscript accepted August 13, 2009
Manuscript handled by Bryan Chakoumakos

* E-mail: dwhitney@umn.edu

TABLE 1. Updated list of abbreviations

Symbol	Mineral Name	IMA status*
Acm	acmite	D
Act	actinolite	A
Adl	adularia	I
Aeg	aegirine	A
Ak	åkermanite	G
Ab	albite	G
Afs	alkali feldspar	GROUP
Aln	allanite	A
Alm	almandine	G
Als	aluminosilicate (Al_2SiO_5 polymorphs)	GROUP
Alu	alunite	Rd
Amk	amakinite	Rd
Ame	amesite	G
Amp	amphibole	GROUP
Anl	analcime (analcite)	A
Ant	anatase	A
And	andalusite	G
Adr	andradite	G
Ang	anglesite	G
Anh	anhydrite	G
Ank	ankerite	G
Ann	annite	A
An	anorthite	G
Ano	anorthoclase	I
Ath	anthophyllite	Rd
Atg	antigorite	Rn
Ap	apatite	GROUP
Apo	apophyllite	GROUP
Arg	aragonite	G
Arf	arfvedsonite	A
Arm	armalcolite	Rd
Apy	arsenopyrite	A
Aug	augite	A
Awr	awaruite	G
Ax	axinite	GROUP
Bab	babingtonite	G
Bdy	baddeleyite	G
Brt	barite (baryte)	A
Brs	barroisite	Rd
Bei	beidellite	G
Brl	beryl	G
Bt	biotite	GROUP
Bxb	bixbyite	G
Bhm	böhmite (boehmite)	G
Bn	bornite	A
Brk	brookite	G
Brc	brucite	G
Bst	bustamite	G
Cal	calcite	G
Ccn	cancrinite	G
Cnl	cannilloite	H
Cb	carbonate mineral	GROUP
Car	carpholite	G
Cst	cassiterite	G
Cel	celadonite	A
Clt	celestine	A
Cls	celsian	G
Cer	cerussite	G
Cbz	chabazite	A
Cct	chalcocite	G
Ccp	chalcopyrite	G
Chm	chamosite	G
Chs	chesterite	A
Chl	chlorite	GROUP
Cld	chloritoid	G
Chn	chondrodite	G
Chr	chromite	G
Ccl	chrysocolla	A
Ctl	chrysotile	Rd
Cin	cinnabar	G
Cam	clinoamphibole	GROUP
Clc	clinochlore	G
Cen	clinoenstatite	A
Cfs	clinoferrosilite	A
Chu	clinohumite	G
Cpt	clinoptilolite	A
Cpx	clinopyroxene	GROUP
Czo	clinozoisite	G
Cln	clintonite	A
Coe	coesite	A
Coh	cohenite	G
Crd	cordierite	G
Crr	corrensite	G
Crn	corundum	G
Cv	covellite	G
Crs	cristobalite	G
Crt	crossite	D
Crl	cryolite	G
Cbn	cubanite	G
Cum	cummingtonite	Rd
Cpr	cuprite	G
Csp	cuspidine	G
Dph	daphnite	not listed
Dat	datolite	G
Dbr	daubreelite	G
Dee	deerite	A
Dia	diamond	G
Dsp	diaspore	G
Dck	dickite	G
Dg	digenite	A
Di	diopside	A
Dpt	dioptase	G
Dol	dolomite	G
Drv	dravite	G
Dum	dumortierite	G
Eas	eastonite	Rd
Ec	ecandrewsite	A
Eck	eckermannite	A
Ed	edenite	A
Elb	elbaite	G
Ell	ellenbergerite	A
Eng	enargite	G
En	enstatite (ortho-)	A
Ep	epidote	GROUP
Eri	erionite	A
Esk	eskolaite	G
Ess	esseneite	A
Eud	eudialite	A
Fas	fassaite	D
Fa	fayalite	G
Fsp	feldspar	GROUP
Fac	ferro-actinolite	Rd
Fath	ferro-anthophyllite	Rd
Fbrs	ferrobarroisite	A
Fcar	ferrocarpholite	A
Fcel	ferroceladonite	A
Fec	ferro-eckermannite	Rd
Fed	ferro-edenite	Rd
Fgd	ferrogedrite	Rd
Fgl	ferroglaucophane	Rd
Fkrs	ferrokaersutite	A
Fny	ferronyboite	H
Fprg	ferropargasite	Rd
Frct	ferrorichterite	A
Fs	ferrosilite	Rn
Fts	ferrotschermakite	Rd
Fwn	ferrowinchite	Rd
Fi	fibrolite (fibrous sillimanite)	informal
Fl	fluorite	G
Fo	forsterite	G
Fos	foshagite	G
Frk	franklinite	G
Ful	fullerite	N
Ghn	gahnite	G
Glx	galaxite	G
Gn	galena	G
Grt	garnet	GROUP
Ged	gedrite	Rd
Gh	gehlenite	G
Gk	geikielite	G
Gbs	gibbsite	A
Gis	gismondine	A
Glt	glauconite	GROUP
Gln	glaucophane	Rd
Gme	gmelinite	A
Gth	goethite	A
Gdd	grandidierite	G
Gr	graphite	G
Gre	greenalite	G
Grs	grossular	A
Gru	grunerite	Rd
Gp	gypsum	G
Hl	halite	G
Hrm	harmotome	A
Hst	hastingsite	Rd
Hsm	hausmannite	G
Hyn	haüyne	G
Hzl	heazlewoodite	G
Hd	hedenbergite	A
Hem	hematite	A
Hc	hercynite	G
Hul	heulandite	A
Hbn	hibonite	G
Hbs	hibschite	Rn
Hgb	högbomite	D
Hol	hollandite	G
Hlm	holmquistite	Rd
Hbl	hornblende	GROUP
Hw	howieite	A
Hu	humite	G
Hgr	hydrogrossular	GROUP
Hyp	hypersthene	D
Ilt	illite	GROUP
Ilm	ilmenite	G
Ilv	ilvaite	G
Jd	jadeite	A
Jrs	jarosite	Rd
Jim	jimthompsonite	A
Jhn	johannsenite	A
Krs	kaersutite	Rd
Kls	kalsilite	G
Kam	kamacite (α-FeNi)	D
Kln	kaolinite	A
Ktp	katophorite	Rd
Kfs	K-feldspar	informal
Khl	K-hollandite	H
Kir	kirschsteinite	G
Krn	kornerupine	G
Kos	kosmochlor	A
Kut	kutnohorite (kutnahorite)	G
Ky	kyanite	A
Lrn	larnite	G
Lmt	laumontite	A
Lws	lawsonite	G
Lzl	lazulite	A
Lzr	lazurite	G
Lpd	lepidolite	GROUP
Lct	leucite	G
Lm	limonite	not listed
Liq	liquid	
Lz	lizardite	G
Lo	löllingite (loellingite)	G
Mgh	maghemite	G
Marf	magnesio-arfvedsonite	Rd
Mcar	magnesiocarpholite	A
Mfr	magnesioferrite	G
Mhs	magnesiohastingsite	Rd
Mhb	magnesiohornblende	Rd
Mkt	magnesiokatophorite	Rd

Symbol	Mineral Name	IMA status*
Mrbk	magnesioriebeckite	Rd
Msdg	magnesiosadanagite	Rd
Mst	magnesiostaurolite	A
Mtm	magnesiotaramite	Rn
Mws	magnesiowustite	not listed
Mgs	magnesite	A
Mag	magnetite	G
Maj	majorite	A
Mlc	malachite	G
Mng	manganosite	G
Mrc	marcasite	G
Mrg	margarite	A
Mar	marialite	G
Mei	meionite	G
Mll	melilite	GROUP
Mw	merwinite	G
Mes	mesolite	A
Mc	microcline	G
Mlr	millerite	G
Mns	minnesotaite	G
Mog	moganite	A
Mol	molybdenite	G
Mnz	monazite	A
Mtc	monticellite	G
Mnt	montmorillonite	G
Mor	mordenite	A
Mul	mullite	G
Ms	muscovite	A
Ntr	natrolite	A
Nph	nepheline	G
Nrb	norbergite	G
Nsn	nosean	G
Nyb	nyböite	Rd
Ol	olivine	GROUP
Omp	omphacite	A
Opl	opal	G
Opq	opaque mineral	informal
Orp	orpiment	G
Oam	orthoamphibole	GROUP
Or	orthoclase	A
Oen	orthoenstatite	D
Opx	orthopyroxene	GROUP
Osm	osumilite	G
Plg	palygorskite	G
Pg	paragonite	A
Prg	pargasite	Rd
Pct	pectolite	G
Pn	pentlandite	G
Per	periclase	G
Prv	perovskite	G
Ptl	petalite	G
PhA	phase A	not listed
Ph	phengite	G
Php	phillipsite	A
Phl	phlogopite	A
Pmt	piemontite	A

Symbol	Mineral Name	IMA status*
Pgt	pigeonite	A
Pl	plagioclase	GROUP
Prh	prehnite	G
Prm	prismatine	Rd
Psb	pseudobrookite	Rd
Pmp	pumpellyite-(Al)	A
Py	pyrite	G
Pcl	pyrochlore	A
Prp	pyrope	G
Pph	pyrophanite	G
Prl	pyrophyllite	G
Pxf	pyroxferroite	A
Pxm	pyroxmangite	G
Po	pyrrhotite	G
Qnd	qandilite	A
Qz	quartz	A
Rnk	rankinite	G
Rlg	realgar	G
Rds	rhodochrosite	A
Rdn	rhodonite	A
Rct	richterite	A
Rbk	riebeckite	Rd
Rwd	ringwoodite	A
Rdr	roedderite	A
Rsm	rossmanite	A
Rt	rutile	G
Sdg	sadanagaite	Rd
Sa	sanidine	G
Sap	saponite	G
Spr	sapphirine	G
Scp	scapolite	GROUP
Sch	scheelite	G
Srl	schorl	G
Scb	schreibersite	G
Sep	sepiolite	G
Ser	sericite	D
Srp	serpentine	GROUP
Sd	siderite	G
Sil	sillimanite	G
Sme	smectite	GROUP
Sdl	sodalite	G
Sps	spessartine	A
Sp	sphalerite	A
Spn	sphene (titanite)	D
Spl	spinel	G
Spd	spodumene	A
Spu	spurrite	G
St	staurolite	G
Stv	stevensite	Q
Stb	stilbite	A
Stp	stilpnomelane	A
Sti	stishovite	A
Str	strontianite	G
Sud	sudoite	Rd
Syl	sylvite	G

Symbol	Mineral Name	IMA status*
Tae	taenite (γ-Fe, Ni)	G
Tlc	talc	G
Trm	taramite	Rd
Tnt	tennantite	G
Tnr	tenorite	A
Tep	tephroite	G
Ttr	tetrahedrite	A
Thm	thomsonite	A
Thr	thorite	G
Tly	tilleyite	G
Ttn	titanite (sphene)	A
Tpz	topaz	G
Tur	tourmaline	GROUP
Tr	tremolite	Rd
Trd	tridymite	G
Tro	troilite	G
Ts	tschermakite	Rd
Usp	ulvöspinel	G
Urn	uraninite	G
Uv	uvarovite	A
Vtr	vaterite	A
Vrm	vermiculite	G
Ves	vesuvianite	A
Wds	wadsleyite	A
Wag	wagnerite	Rd
Wrk	wairakite	A
Wav	wavellite	A
Wht	whitlockite	G
Wlm	willmenite	G
Wnc	winchite	Rd
Wth	witherite	G
Wo	wollastonite	A
Wur	wurtzite	G
Wus	wüstite	G
Xtm	xenotime	A
Xon	xonotlite	G
Yug	yugawaralite	A
Zeo	zeolite	GROUP
Znw	zinnwaldite	GROUP
Zrn	zircon	G
Zo	zoisite	G

* International Mineralogical Association (IMA) abbreviations: A = Approved; D = Discredited; G = Grandfathered (generally regarded as valid mineral name); GROUP = Name designates a group of mineral species; H = hypothetical (e.g., synthetic); I = intermediate in a solid-solution series; Q = questionable; Rd = Redefinition approved by IMA Commission on New Minerals, Nomenclature and Classification (CNMNC); Rn = Renamed with approval of the CNMNC.

American Mineralogist, Volume 98, pages 785–811, 2013

IMA Report

Nomenclature of the garnet supergroup

Edward S. Grew,[1,*] Andrew J. Locock,[2] Stuart J. Mills,[3,†] Irina O. Galuskina,[4] Evgeny V. Galuskin,[4] and Ulf Hålenius[5]

[1]School of Earth and Climate Sciences, University of Maine, Orono, Maine 04469, U.S.A.
[2]Department of Earth and Atmospheric Sciences, University of Alberta, Edmonton, Alberta T6G 2E3, Canada
[3]Geosciences, Museum Victoria, GPO Box 666, Melbourne 3001, Victoria, Australia
[4]Faculty of Earth Sciences, Department of Geochemistry, Mineralogy and Petrography, University of Silesia, Będzińska 60, 41-200 Sosnowiec, Poland
[5]Swedish Museum of Natural History, Department of Mineralogy, P.O. Box 50 007, 104 05 Stockholm, Sweden

Abstract

The garnet supergroup includes all minerals isostructural with garnet regardless of what elements occupy the four atomic sites, i.e., the supergroup includes several chemical classes. There are presently 32 approved species, with an additional 5 possible species needing further study to be approved. The general formula for the garnet supergroup minerals is $\{X_3\}[Y_2](Z_3)\varphi_{12}$, where *X*, *Y*, and *Z* refer to dodecahedral, octahedral, and tetrahedral sites, respectively, and φ is O, OH, or F. Most garnets are cubic, space group $Ia\bar{3}d$ (no. 230), but two OH-bearing species (henritermierite and holtstamite) have tetragonal symmetry, space group, $I4_1/acd$ (no. 142), and their *X*, *Z*, and φ sites are split into more symmetrically unique atomic positions. Total charge at the *Z* site and symmetry are criteria for distinguishing groups, whereas the dominant-constituent and dominant-valency rules are critical in identifying species. Twenty-nine species belong to one of five groups: the tetragonal henritermierite group and the isometric bitikleite, schorlomite, garnet, and berzeliite groups with a total charge at *Z* of 8 (silicate), 9 (oxide), 10 (silicate), 12 (silicate), and 15 (vanadate, arsenate), respectively. Three species are single representatives of potential groups in which *Z* is vacant or occupied by monovalent (halide, hydroxide) or divalent cations (oxide). We recommend that suffixes (other than Levinson modifiers) not be used in naming minerals in the garnet supergroup. Existing names with suffixes have been replaced with new root names where necessary: bitikleite-(SnAl) to bitikleite, bitikleite-(SnFe) to dzhuluite, bitikleite-(ZrFe) to usturite, and elbrusite-(Zr) to elbrusite. The name hibschite has been discredited in favor of grossular as Si is the dominant cation at the *Z* site. Twenty-one end-members have been reported as subordinate components in minerals of the garnet supergroup of which six have been reported in amounts up to 20 mol% or more, and, thus, there is potential for more species to be discovered in the garnet supergroup. The nomenclature outlined in this report has been approved by the Commission on New Minerals, Nomenclature and Classification of the International Mineralogical Association (Voting Proposal 11-D).

Keywords: Garnet group, schorlomite group, bitikleite group, berzeliite group, henritermierite group, katoite, nomenclature, crystal chemistry

Introduction

The garnets pose somewhat different nomenclature problems than other mineral supergroups recently considered for nomenclature review, i.e., sapphirine (Grew et al. 2008), apatite (Pasero et al. 2010), pyrochlore (Atencio et al. 2010), tourmaline (Henry et al. 2011), and amphibole (Hawthorne et al. 2012), where a supergroup is defined as "consisting of two or more groups that have essentially the same structure and composed of chemically similar elements" (Mills et al. 2009). Compared to the structures of the minerals in these groups, the archetypal garnet structure, cubic space group $Ia\bar{3}d$ (no. 230) has few sites: only three cationic and one anionic (e.g., Menzer 1928; Novak and Gibbs 1971; Merli et al. 1995; Geiger 2008), and the most common garnets have relatively simple chemical compositions. However, the garnet structure is remarkably flexible in a chemical sense: 53 elements were reported in the Inorganic Crystal Structure Database (Allmann and Hinek 2007) and five more are reported in synthetic garnets (Geller 1967; Ronniger and Mill' 1973; Yudintsev 2003; Yudintsev et al. 2002; Utsunomiya et al. 2005). In the period 2009–2010, 10 new species of garnet, with constituents such as Sc, Y, Sn, Sb, and U, which have not been previously reported in significant quantities in natural garnet, were approved by the Commission on New Minerals, Nomenclature and Classification (CNMNC) of the International Mineralogical Association (IMA), resulting in a nearly 50% increase in the number of accepted species with the garnet structure. There are four more possible species, bringing to 26 the number of elements essential to defining existing and possible mineral species with the garnet structure.

In view of this situation, it seemed an opportune time to convene a subcommittee to review the nomenclature of garnets. The garnet group traditionally included only silicate minerals (e.g.,

* Chair, E-mail: esgrew@maine.edu
† Vice-Chair.

0003-004X/13/0004–785$05.00/DOI: http://dx.doi.org/10.2138/am.2013.4201

Yakovlevskaya 1972; Strunz and Nickel 2001; Back and Mandarino 2008). However, there are minerals from other classes, such as arsenates, vanadates, oxides, and even fluorides that are isostructural with the silicate garnets, and whose major constituents show chemical similarities with constituents in silicate garnets, i.e., these minerals meet the criteria for inclusion in a broader entity, the garnet supergroup (Mills et al. 2009). McConnell (1942) introduced the term "garnetoid" to "designate those substances which are not primarily silicates but have structures similar to that of true garnets," such as "hydrogarnet," berzeliite and the phosphate griphite (Headden 1891). It does not appear that garnetoid was discredited as a group name (Clark 1993), but our preference is to use the term garnet for the supergroup. Rinaldi (1978) showed that griphite is not isostructural with garnet, although he found that there are some structural features in common, which were also discussed by Sokolova and Hawthorne (2002), and thus griphite is not considered to be a garnet. In addition, the silicate mineral wadalite had been thought to be related to garnet because of similarities in cell dimensions and diffraction intensities (Feng et al. 1988; Tsukimura et al. 1993; Glasser 1995). Although wadalite lacks a center of symmetry, so that the single tetrahedral site found in grossular is split in wadalite into two sites, one of which is vacant, it still can be considered a derivative of grossular, but Glasser (1995) emphasized the much closer relationship of wadalite to mayenite. Recent crystal structure refinements make no mention of a relationship of wadalite or mayenite to garnet (Boysen et al. 2007; Iwata et al. 2008; Ma et al. 2011), and the structural relationship between garnet and wadalite (or mayenite) is sufficiently distant that these minerals are not included in the garnet supergroup. The so-called "tetragonal almandine-pyrope phase" (TAPP) has the stoichiometry, but not the structure of garnet (Harris et al. 1997; Finger and Conrad 2000), i.e., TAPP has edges shared between tetrahedra and octahedra, a feature not found in garnet (see below) and thus is not considered further in this report. Similarly, although some natural and synthetic arsenates of the alluaudite group, e.g., caryinite, are approximately polymorphous with the garnet supergroup mineral manganberzeliite (Ercit 1993; Khorari et al. 1995, 1997), the structures of alluaudite-group compounds are too different from garnet to warrant further consideration of the alluaudite group in this report.

Twenty-nine of the thirty-two approved species of the garnet supergroup are divided here into five groups on the basis of the total charge of cations at the tetrahedral site, leaving three ungrouped species (Table 1); four potential new species can be accommodated in two of these groups (see below). One group is also distinguished on the basis of symmetry: the tetragonal henritermierite group (Fig. 1a). The classification in Table 1 keeps the number of groups at a practical level that still reflects crystal-chemical relationships. Table 1 also gives the class for the five groups and ungrouped species to emphasize that the garnet supergroup comprises not only silicates (Figs. 1a, 1c, 1d, and 1e), but also a halide (Fig. 1b), hydroxides, oxides, vanadates, and arsenates (Fig. 1g). The groups are listed in order of increasing charge of cations that occupy the *Z* site of the end-members. Species within each group are listed as end-members with increasing atomic number of the *Z* site, followed by increasing atomic number of the *Y* site and last, by increasing atomic number of the *X* site, whereas species with joint occupancies at the *Y* site are placed last. Table 2 lists the 32 species as end-members in the same order and compares formulas given in the 2009 list (updated in 2012) of minerals approved by the CNMNC with the end-member formulas approved with the classification presented here.

Subdivision of the groups into mineral subgroups or mineral series is not recommended, as these terms should be reserved for homologous or polysomatic series (Mills et al. 2009). This restriction constitutes another rationale for discouraging the traditional division of the garnet group into the "pyralspite" and "ugrandite" species (Winchell 1933) or series (Strunz and Nickel 2001), although there could be some fundamental structural differences that limit solid solution between the two groupings (e.g., Ungaretti et al. 1995; Boiocchi et al. 2012; cf. Geiger 2008).

Our procedure for distinguishing species relies heavily on the dominant-valency rule, which is an extension of the dominant-constituent rule (Hatert and Burke 2008). The latter rule states that species designation is based on the dominant constituent at a given crystallographic site, which works well when all constituents have the same valence. However, when ions at a given crystallographic site have different valences, it is essential that the dominant valence be determined first, and then species and group designation is determined by the dominant ion having this valence. Traditionally, identifying a garnet species has

Table 1. A classification of the 32 approved species in the garnet supergroup

Z charge	GROUP or species name	Class	*X*	*Y*	*Z*	φ
0	Katoite	Hydroxide	Ca_3	Al_2	□	$(OH)_{12}$
3	Cryolithionite	Halide	Na_3	Al_2	Li_3	F_{12}
6	Yafsoanite	Oxide	Ca_3	Te^{6+}_2	Zn_3	O_{12}
8	HENRITERMIERITE	Silicate				
	Holtstamite		Ca_3	Al_2	Si_2 | □	$O_8(OH)_4$
	Henritermierite		Ca_3	Mn^{3+}_2	Si_2 | □	$O_8(OH)_4$
9	BITIKLEITE	Oxide				
	Bitikleite		Ca_3	$Sb^{5+}Sn^{4+}$	Al_3	O_{12}
	Usturite		Ca_3	$Sb^{5+}Zr$	Fe^{3+}_3	O_{12}
	Dzhuluite		Ca_3	$Sb^{5+}Sn^{4+}$	Fe^{3+}_3	O_{12}
	Elbrusite		Ca_3	$U^{6+}_{0.5}Zr_{1.5}$	Fe^{3+}_3	O_{12}
10	SCHORLOMITE	Silicate				
	Kimzeyite		Ca_3	Zr_2	$SiAl_2$	O_{12}
	Irinarassite		Ca_3	Sn^{4+}_2	$SiAl_2$	O_{12}
	Schorlomite		Ca_3	Ti_2	$SiFe^{3+}_2$	O_{12}
	Kerimasite		Ca_3	Zr_2	$SiFe^{3+}_2$	O_{12}
	Toturite		Ca_3	Sn^{4+}_2	$SiFe^{3+}_2$	O_{12}
12	GARNET	Silicate				
	Menzerite-(Y)		Y_2Ca	Mg_2	Si_3	O_{12}
	Pyrope		Mg_3	Al_2	Si_3	O_{12}
	Grossular		Ca_3	Al_2	Si_3	O_{12}
	Spessartine		Mn^{2+}_3	Al_2	Si_3	O_{12}
	Almandine		Fe^{2+}_3	Al_2	Si_3	O_{12}
	Eringaite		Ca_3	Sc_2	Si_3	O_{12}
	Goldmanite		Ca_3	V^{3+}_2	Si_3	O_{12}
	Momoiite		Mn^{2+}_3	V^{3+}_2	Si_3	O_{12}
	Knorringite		Mg_3	Cr^{3+}_2	Si_3	O_{12}
	Uvarovite		Ca_3	Cr^{3+}_2	Si_3	O_{12}
	Andradite		Ca_3	Fe^{3+}_2	Si_3	O_{12}
	Calderite		Mn^{2+}_3	Fe^{3+}_2	Si_3	O_{12}
	Majorite		Mg_3	SiMg	Si_3	O_{12}
	Morimotoite		Ca_3	$TiFe^{2+}$	Si_3	O_{12}
15	BERZELIITE	Vanadate, arsenate				
	Schäferite		Ca_2Na	Mg_2	V^{5+}_3	O_{12}
	Palenzonaite		Ca_2Na	Mn^{2+}_2	V^{5+}_3	O_{12}
	Berzeliite		Ca_2Na	Mg_2	As^{5+}_3	O_{12}
	Manganberzeliite		Ca_2Na	Mn^{2+}_2	As^{5+}_3	O_{12}

Notes: Formulas are given in the form $\{X_3\}[Y_2](Z_3)\varphi_{12}$. Group names are given in capitals.

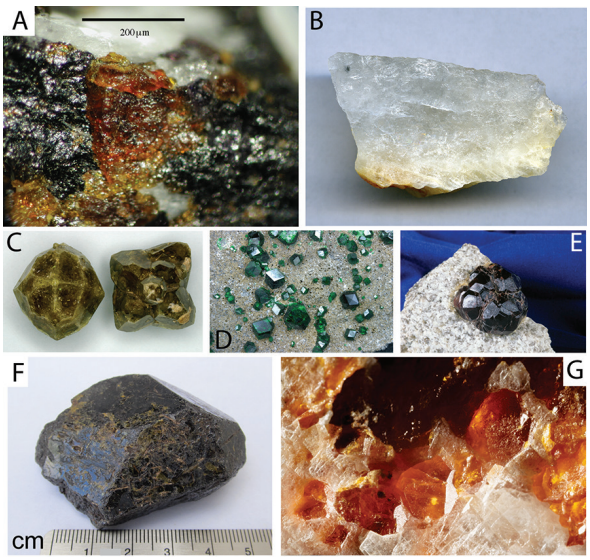

FIGURE 1. Photographs of representative garnet supergroup minerals illustrating the diversity in appearance exhibited by the supergroup. (**a**) Holtstamite, formula $\{Ca_3\}[Al,Mn^{3+}_2](Si_2)(\square)O_8(OH)_4$, as a yellow brown crystal between grains of Mn- and Cu-rich vesuvianite (purplish black) and calcite (white) in the holotype specimen from Wessels Mine, South Africa. Swedish Museum of Natural History specimen no. 19960380. Photo by U. Hålenius. (**b**) Cryolithionite, end-member formula $\{Na_3\}[Al_2](Li_3)F_{12}$: a transparent, colorless single grain in yellowish-white fine-grained cryolite. Specimen size is 4.5 × 2 × 1.7 cm. From the type locality, Ivigtut Cryolite deposit, Ivittuut (Ivigtut), Kitaa, Greenland. Pavel M. Kartashov collection and photograph. (**c**) Grossular, end-member formula $\{Ca_3\}[Al_2](Si_3)O_{12}$: a trapezohedron {211}, 3.5 cm across on the left and crystals in a cyclic intergrowth on the right, from the type locality, Wiluy River, Sakha-Yakutia Republic, Russia. The distinctive brown color is due a 30–50 µm zone of brown andradite a short distance under the crystal faces. Evgeny and Irina Galuskin collection and Evgeny Galuskin photograph. (**d**) Uvarovite, end-member formula $\{Ca_3\}[Cr^{3+}_2](Si_3)O_{12}$: green dodecahedral crystals on chromite, from the type locality, Saranovskii Mine, Permskaya Oblast, Middle Urals, Russia. Largest crystal is 4 mm across. Museum of the Faculty of Earth Sciences, University of Silesia, no. WNoZ/M/9/19. Evgeny Galuskin photograph. (**e**) Almandine, end-member formula $\{Fe_3\}[Al_2](Si_3)O_{12}$: a crystal group 2.5 cm across on granite, Mount Lady Franklin, Barnawartha, Victoria, Australia. Museum Victoria registration no. M34200. Frank Coffa photograph. (**f**) Schorlomite, end-member formula $\{Ca_3\}[Ti_2](SiFe^{3+}_2)O_{12}$: an incomplete crystal from the type locality, Magnet Cove, Hot Spring County, Arkansas. E.S. Grew collection and photograph. (**g**) Manganberzeliite, end-member formula $\{Ca_2Na\}[Mn^{2+}_2](As^{5+}_3)O_{12}$, from the type locality, Långban, Sweden. The largest crystals are 3 mm across. Swedish Museum of Natural History specimen no. 19170722. M. Cooper photograph.

relied heavily on the proportion of end-member components, and therefore depended on a specific sequence of calculating end-member proportions: garnet end-member proportions constitute an underdetermined system from the point of view of linear algebra: there are more end-members than oxides (e.g., Rickwood 1968; Locock 2008).

The purpose of this report is to present the essential elements of garnet nomenclature, to define concepts that are central to garnet classification, and to provide practical guidelines for application of the nomenclature in distinguishing species. The nomenclature outlined in this report has been approved by the CNMNC (Voting proposal 11-D, April 3, 2012).

TABLE 2. Former formulas and end-member formulas approved in the present report

Name	Former formula	Approved end-member formula
Katoite	$Ca_3Al_2(SiO_4)_{3-x}(OH)_{4x}$ (x = 1.5–3.0)	$\{Ca_3\}[Al_2](\square_3)(OH)_{12}$
Cryolithionite	$Na_3Al_2(LiF_4)_3$	$\{Na_3\}[Al_2](Li_3)F_{12}$
Yafsoanite	$Ca_3Te^{6+}_2Zn_3O_{12}$	$\{Ca_3\}[Te^{6+}_2](Zn_3)O_{12}$
Holtstamite	$Ca_3Al_2(SiO_4)_2(OH)_4$	$\{Ca_3\}[Al_2](Si_2)(\square)O_8(OH)_4$
Henritermierite	$Ca_3(Mn^{3+})_2(SiO_4)_2(OH)_4$	$\{Ca_3\}[Mn^{3+}_2](Si_2)(\square)O_8(OH)_4$
Bitikleite*	$Ca_3SbSnAl_3O_{12}$	$\{Ca_3\}[Sb^{5+}Sn^{4+}](Al_3)O_{12}$
Usturite*	$Ca_3SbZrFe_3O_{12}$	$\{Ca_3\}[Sb^{5+}Zr](Fe^{3+}_3)O_{12}$
Dzhuluite*	$Ca_3(SnSb^{5+})Fe^{3+}_3O_{12}$	$\{Ca_3\}[Sb^{5+}Sn^{4+}](Fe^{3+}_3)O_{12}$
Elbrusite*	$Ca_3(U^{6+}Zr)(Fe^{3+}Fe^{2+})O_{12}$	$\{Ca_3\}[U^{6+}_{0.5}Zr_{1.5}](Fe^{3+}_3)O_{12}$
Kimzeyite	$Ca_3(Zr,Ti)_2(Si,Al,Fe^{3+})_3O_{12}$	$\{Ca_3\}[Zr_2](SiAl_2)O_{12}$
Irinarassite	$Ca_3Sn_2Al_2SiO_{12}$	$\{Ca_3\}[Sn^{4+}](SiAl_2)O_{12}$
Schorlomite	$Ca_3(Ti,Fe^{3+})_2[(Si,Fe)O_4]_3O_{12}$	$\{Ca_3\}[Ti_2](SiFe^{3+}_2)O_{12}$
Kerimasite	$Ca_3Zr_2(Fe^{3+}_2Si)O_{12}$	$\{Ca_3\}[Zr_2](SiFe^{3+}_2)O_{12}$
Toturite	$Ca_3Sn_2Fe_2SiO_{12}$	$\{Ca_3\}[Sn^{4+}](SiFe^{3+}_2)O_{12}$
Menzerite-(Y)	$\{CaY_2\}[Mg_2](Si_3)O_{12}$	$\{Y_2Ca\}[Mg_2](Si_3)O_{12}$
Pyrope	$Mg_3Al_2(SiO_4)_3$	$\{Mg_3\}[Al_2](Si_3)O_{12}$
Grossular	$Ca_3Al_2(SiO_4)_3$	$\{Ca_3\}[Al_2](Si_3)O_{12}$
Spessartine	$(Mn^{2+})_3Al_2(SiO_4)_3$	$\{Mn^{2+}_3\}[Al_2](Si_3)O_{12}$
Almandine	$(Fe^{2+})_3Al_2(SiO_4)_3$	$\{Fe^{2+}_3\}[Al_2](Si_3)O_{12}$
Eringaite	$Ca_3Sc_2(SiO_4)_3$	$\{Ca_3\}[Sc_2](Si_3)O_{12}$
Goldmanite	$Ca_3(V^{3+})_2(SiO_4)_3$	$\{Ca_3\}[V^{3+}_2](Si_3)O_{12}$
Momoiite	$(Mn^{2+},Ca)_3(V^{3+},Al)_2Si_3O_{12}$	$\{Mn^{2+}_3\}[V^{3+}_2](Si_3)O_{12}$
Knorringite	$Mg_3Cr_2(SiO_4)_3$	$\{Mg_3\}[Cr^{3+}_2](Si_3)O_{12}$
Uvarovite	$Ca_3Cr_2(SiO_4)_3$	$\{Ca_3\}[Cr^{3+}_2](Si_3)O_{12}$
Andradite	$Ca_3(Fe^{3+})_2(SiO_4)_3$	$\{Ca_3\}[Fe^{3+}_2](Si_3)O_{12}$
Calderite	$(Mn^{2+})_3(Fe^{3+})_2(SiO_4)_3$	$\{Mn^{2+}_3\}[Fe^{3+}_2](Si_3)O_{12}$
Majorite	$Mg_3(Fe^{2+},Si)_2(SiO_4)_3$	$\{Mg_3\}[SiMg](Si_3)O_{12}$
Morimotoite	$Ca_3(Ti,Fe^{2+},Fe^{3+})_2(Si,Fe^{3+})_3O_{12}$	$\{Ca_3\}[TiFe^{2+}](Si_3)O_{12}$
Schäferite	$NaCa_2Mg_2(VO_4)_3$	$\{Ca_2Na\}[Mg_2](V^{5+}_3)O_{12}$
Palenzonaite	$NaCa_2(Mn^{2+})_2(VO_4)_3$	$\{Ca_2Na\}[Mn^{2+}_2](V^{5+}_3)O_{12}$
Berzeliite	$NaCa_2Mg_2(AsO_4)_3$	$\{Ca_2Na\}[Mg_2](As^{5+}_3)O_{12}$
Manganberzeliite	$NaCa_2(Mn^{2+})_2(AsO_4)_3$	$\{Ca_2Na\}[Mn^{2+}_2](As^{5+}_3)O_{12}$

Note: Former names from IMA-CNMNC List of Mineral Names compiled in March 2009 by E.H. Nickel and M.C. Nichols and from the Official IMA list of mineral names (updated from March 2009 list) at http://pubsites.uws.edu.au/ima-cnmnc/. Names of minerals approved after the list was published are taken from the original description.
* Table 5 lists the names under which these four minerals were originally described.

CRYSTALLOGRAPHIC AND CRYSTAL-CHEMICAL ASPECTS OF GARNET-SUPERGROUP MINERALS

In the structure of cubic garnets (e.g., Menzer 1928; Novak and Gibbs 1971; Hawthorne 1981; Merli et al. 1995; Geiger 2008), space group $Ia\bar{3}d$ (no. 230), there are only four symmetrically unique atomic sites (not including hydrogen): dodecahedral $\{X\}$, octahedral $[Y]$, and tetrahedral (Z) cation sites, as well as an anionic site designated φ to indicate O, OH, and F, giving a generalized chemical formula for the garnet supergroup, $\{X_3\}[Y_2](Z_3)\varphi_{12}$ (modified after Geller 1967). The three cation sites are at special positions fixed by symmetry, with the Wyckoff positions 24*c*, 16*a*, and 24*d*, respectively, whereas the anion site is located at a general position, 96*h*. The structure consists of alternating $Z\varphi_4$ tetrahedra and $Y\varphi_6$ octahedra, which share corners to form a three-dimensional framework (Fig. 2). Cavities enclosed in this framework have the form of triangular dodecahedra surrounding the *X* site (Novak and Gibbs 1971). Each anion is coordinated by one *Z*, one *Y*, and two *X* cations, resulting in a high percentage of shared edges between the dodecahedra on the one hand and the octahedra and tetrahedra on the other. However, the octahedra

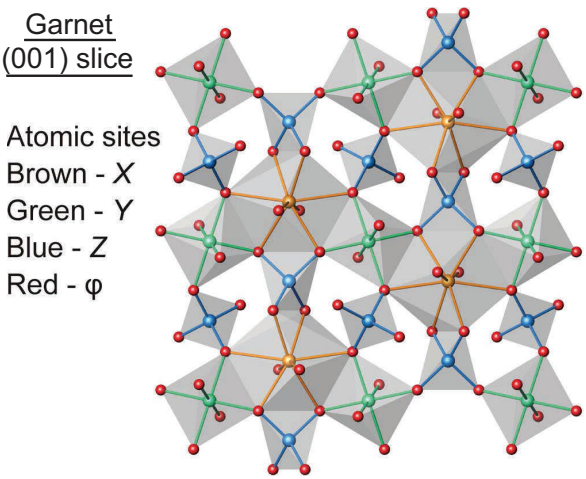

FIGURE 2. Portion of the garnet structure projected along [001].

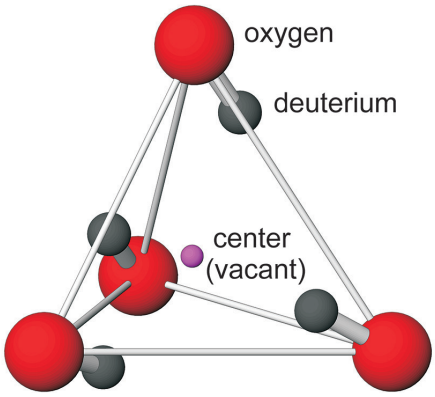

FIGURE 3. Local coordination environment of the tetrahedral position from the low-*T* (200 K) refinement of synthetic deuterated katoite (Lager et al. 1987) showing that the deuterium ions are approximately on the faces of the O tetrahedron and ~1.3 Å from the ideal tetrahedral cation position, which is vacant. O-O distances shown as thin rods, O-D bonds as thick rods.

and tetrahedra do not share edges with each other (cf. TAPP: Harris et al. 1997; Finger and Conrad 2000).

In hydrous garnets, the major mechanism of hydroxyl incorporation is by the coupled substitution $4H^{+Z}\square \rightarrow \square^{+Z}Si$, i.e., the hydrogen ions occupy a separate site of general symmetry (Wyckoff position 96*h*) coordinated to O defining the tetrahedral site, which is vacant (e.g., Ferro et al. 2003; Lager et al. 1987, 1989). The hydrogen ions lie approximately on the faces of the tetrahedron of O around a vacant center, as do the deuterium ions shown in Figure 3. The O-H and O-D distances reported for minerals or their synthetic analogues range from 0.65 Å in synthetic deuterium katoite (X-ray diffraction, Lager et al. 1987) and 0.68 Å in natural katoite (X-ray diffraction, Sacerdoti and Passaglia 1985) to 0.75 Å in henritermierite (X-ray diffraction, Armbruster et al. 2001) to 0.904–0.95 Å in synthetic katoite (neutron diffraction, Lager et al. 1987; Cohen-Addad et al. 1967). Allowing that O-H and O-D distances obtained by X-ray diffraction are shorter than those obtained by neutron diffraction, Lager et al. (1987) concluded that the reported distances are consistent with isolated OH groups (lacking H-bonding) and assumed that the residual density located near oxygen can be attributed to the displaced (bonding) electron between O and H and not to the hydrogen itself.

However, compositional data, nuclear magnetic resonance (NMR) spectra, and infrared (IR) spectra have been cited as evidence for multiple H occupancy in grossular and garnets in the hydrogrossular series. Cation vacancies at the *X* and *Y* sites calculated from electron microprobe analyses without direct determination of H_2O have been cited as evidence for the presence of H in these polyhedra, either without crystallographic data (Birkett and Trzcienski 1984), or in conjunction with single-crystal refinements of Ca, Al, Fe, and Si, whereas H could be located only in a few of the crystals studied and not quantified (Basso et al. 1984a, 1984b; Basso and Cabella 1990). Kalinichenko et al. (1987) interpreted NMR spectra obtained on a grossular to indicate 2H in the octahedra and 1H in the tetrahedra. In a comprehensive IR study of the hydrogrossular series, Rossman and Aines (1991) reported that samples containing substantial H (>11.7 wt% H_2O equivalent to >5.43 OH per formula unit) gave spectra consistent with the substitution $4H^{+Z}\square \rightarrow \square^{+Z}Si$, whereas samples with much less H (<3.6 wt% H_2O, mostly <0.5 wt%) gave 7 different types of IR spectra, suggesting OH groups were present in multiple site environments, an inference supported by NMR spectra on three grossular samples (Cho and Rossman 1993). On the basis of Fourier-transform IR spectra, Eeckhout et al. (2002) concluded that there is no evidence for a multisite OH substitution in spessartine-almandine garnets from Brazilian pegmatites, leaving the hydrogarnet substitution as the only proposed mechanism for the incorporation of H. In summary, garnet samples in which concentrations of H are too low to be studied by conventional X-ray and neutron diffraction techniques give conflicting and equivocal results, whereas H-rich samples in which H can be determined by these techniques give data consistent with $4H^{+Z}\square \rightarrow \square^{+Z}Si$. Consequently, for nomenclature purposes, we have assumed that H is incorporated exclusively by $4H^{+Z}\square \rightarrow \square^{+Z}Si$.

The symmetry of garnet is predominantly isometric, space group $Ia\bar{3}d$ (no. 230) but the two species in the henritermierite group have tetragonal symmetry $I4_1/acd$ (no. 142), and the *X*, *Z*, and φ sites are split into more symmetrically unique sites, without altering the topology such that the idealized formula becomes $\{Ca1_2\}\{Ca2\}[R^{3+}_2](Si1_2)(\square 2)O1_4O2_4(O3H)_4$, where R^{3+} = Mn or Al. Armbruster et al. (2001) concluded that Jahn-Teller distortion resulting from Mn^{3+} occupancy of *Y* and the arrangement of the hydroxyl tetrahedra are coupled, and together are responsible for the lowering to tetragonal symmetry in henritermierite. Moreover, stabilization of the Al-dominant analog holtstamite has been thought to require a minimum Mn^{3+} content, which is estimated to be at least 0.2 Mn^{3+} per formula unit (pfu), the amount reported in an isometric andradite (Armbruster 1995) and no more than 0.64 Mn^{3+} pfu, the lowest amount found in holtstamite, i.e., between 10 and 32% of the henritermierite end-member must be present to stabilize the tetragonal form (Hålenius 2004; Hålenius et al. 2005). However, these arguments are not supported by a Si-deficient spessartine containing no Mn^{3+}, but showing $I4_1/acd$ symmetry attributed to $(OH,F)_4$ groups (Boiocchi et al. 2012),

implying symmetry lowering could have more than one cause.

In addition, there are numerous reports of natural garnets having orthorhombic, monoclinic, or triclinic symmetry, which have been attributed to crystal growth phenomena, multiple diffraction, strain, and/or cation ordering (e.g., Griffen et al. 1992; McAloon and Hofmeister 1993; Armbruster and Geiger 1993; Rossmanith and Armbruster 1995; Hofmeister et al. 1998; Wildner and Andrut 2001; Shtukenberg et al. 2005; Frank-Kamenetskaya et al. 2007). As these structures have essentially the same topology, they are not regarded as separate species (Nickel and Grice 1998).

Table 3 gives the relative abundance of the generalized cations (R^{n+} with n = 1–6) and anions (φ^{1-}, φ^{2-}) at each of the sites reported in the $Ia\bar{3}d$ structure, and presents the major reported cation and anion substituents in natural garnets for each of the valence states of the ions. Table 4 summarizes significant heterovalent substitutions in natural garnet, as well as some chemical relations among species.

Specific nomenclature issues in the garnet supergroup

Historical information on the 32 approved species of the garnet supergroup is summarized in Appendix 1. A more complete list of 715 synonyms, varietal, obsolete, and discredited names applied to minerals in the garnet supergroup since antiquity has been compiled in Appendix 2[1]. This list includes the synonyms of current names that have been used in the mineralogical and gemological literature. In the following section, we discuss only those species in which there were problems or difficulties in their original characterization or where the name or formula has had to be significantly modified since the original description.

Table 3. Relative site abundances of cations and anions in garnet-supergroup minerals

Site	Relative abundance of ions	Cations and anions at each site in order of relative abundance
X	$R^{2+} >> R^{3+} >> R^{1+} >> R^{4+}$	R^{2+}: **Fe** ~ **Mn** ~ **Ca** > **Mg** >> Pb R^{3+}: Y > HREE > LREE R^{1+}: Na R^{4+}: Th
Y	$R^{3+} > R^{4+} > R^{2+} > R^{5+} > R^{6+}$	R^{3+}: **Al** ~ **Fe** > V, Cr, Mn > Sc >> Ga R^{4+}: **Ti** > **Zr** > Si, Sn R^{2+}: Mg > Fe, Mn R^{5+}: Sb, Nb R^{6+}: Te, U
Z	$R^{4+} > R^{3+} > R^{5+} \sim \square$ (vacancy) > R^{2+}, R^{1+}	R^{4+}: **Si** >> Ti > Ge R^{3+}: **Fe** ~ **Al** R^{5+}: As > V > P R^{2+}: Zn, Fe R^{1+}: Li
φ	$\varphi^{2-} >> \varphi^{1-}$	φ^{2-}: **O** φ^{1-}: **OH** > F

Notes: The cations and anions shown in bold type represent the most common ions at these sites. HREE and LREE are heavy and light rare-earth elements, respectively, excluding Y.

[1] Deposit item AM-13-036, Appendixes 2–4. Deposit items are available two ways: For a paper copy contact the Business Office of the Mineralogical Society of America (see inside front cover of recent issue) for price information. For an electronic copy visit the MSA web site at http://www.minsocam.org, go to the *American Mineralogist* Contents, find the table of contents for the specific volume/issue wanted, and then click on the deposit link there.

Table 5. Former names, new names and approved end-member formulas for renamed/discredited minerals listed in this report

Former name	New name (approved by CNMNC)	Formula (approved by CNMNC)
Bitikleite-(SnAl)	Bitikleite	$\{Ca_3\}[Sb^{5+}Sn^{4+}](Al_3)O_{12}$
Bitikleite-(SnFe)	Dzhuluite	$\{Ca_3\}[Sb^{5+}Sn^{4+}](Fe^{3+}_3)O_{12}$
Bitikleite-(ZrFe)	Usturite	$\{Ca_3\}[Sb^{5+}Zr](Fe^{3+}_3)O_{12}$
Elbrusite-(Zr)	Elbrusite	$\{Ca_3\}[U^{6+}_{0.5}Zr_{1.5}](Fe^{3+}_3)O_{12}$
Hibschite*	Grossular	$\{Ca_3\}[Al_2](Si_{3-x}\square_x)O_{12-4x}(OH)_{4x}$ where x < 1.5†

* Former formula: $Ca_3Al_2(SiO_4)_{3-x}(OH)_{4x}$, where x = 0.2–1.5.
† Includes OH-bearing grossular. Ideal anhydrous grossular has the formula: $\{Ca_3\}[Al_2](Si_3)O_{12}$.

Table 4. Significant garnet coupled heterovalent substitutions

Generalized coupled substitution	Relationship
$^{Z}\square + 4\varphi^{1-} \rightarrow {}^{Z}Si^{4+} + 4O^{2-}$	relates katoite, henritermierite and holtstamite to OH-free minerals in the garnet group
$^{Y}R^{2+} + {}^{Y}R^{4+} \rightarrow 2{}^{Y}R^{3+}$	relates morimotoite ($^{[6]}$Ti) and majorite ($^{[6]}$Si) to other garnet-group minerals
$^{Z}R^{4+} + {}^{Y}R^{3+} \rightarrow {}^{Z}R^{3+} + {}^{Y}R^{4+}$	relates the schorlomite group to the garnet group
$^{X}(Y, REE)^{3+} + {}^{Z}R^{3+} \rightarrow {}^{X}R^{2+} + {}^{Z}R^{4+}$	introduces Y + REE as a YAG, $\{Y_3\}[Al_2](Al_3)O_{12}$-type component
$^{X}(Y, REE)^{3+} + {}^{X}Na^{1+} \rightarrow 2{}^{X}R^{2+}$	introduces Y + REE into garnet-group minerals
$^{X}(Y, REE)^{3+} + {}^{Y}R^{2+} \rightarrow {}^{X}R^{2+} + {}^{Y}R^{3+}$	relates menzerite-(Y) to other garnet-group minerals
$^{Y}R^{5+} + {}^{Z}R^{3+} \rightarrow {}^{Y}R^{4+} + {}^{Z}R^{4+}$	relates bitikleite, dzhuluite and usturite with schorlomite-group minerals
$^{Y}0.5R^{6+} + {}^{Z}R^{3+} \rightarrow {}^{Y}0.5R^{4+} + {}^{Z}R^{4+}$	relates elbrusite with schorlomite-group minerals
$^{Y}U^{6+} + {}^{Z}R^{2+} \rightarrow {}^{Y}R^{4+} + {}^{Z}R^{4+}$	observed relationship between elbrusite and schorlomite group minerals (Fig. 4)
$0.5{}^{X}Th^{4+} + {}^{Z}R^{3} \rightarrow 0.5{}^{X}R^{2+} + {}^{Z}R^{4+}$	introduces Th into minerals of the bitikleite and schorlomite groups
$^{Y}R^{4+} + 0.5{}^{Z}V^{5+} \rightarrow 0.5{}^{Z}R^{3+} + {}^{Y}Sb^{5+}$	introduces V into bitikleite
$^{Y}R^{4+} + {}^{Z}V^{5+} \rightarrow {}^{Y}U^{6+} + {}^{Z}R^{3+}$	introduces V into elbrusite
$^{X}Na^{1+} + {}^{Y}R^{4+} \rightarrow {}^{X}R^{2+} + {}^{Y}R^{3+}$	introduces Na and $^{[6]}$Si or $^{[6]}$Ti into the garnet group
$^{X}Na^{1+} + {}^{Z}R^{5+} \rightarrow {}^{X}R^{2+} + {}^{Z}R^{4+}$	relates the berzeliite group to the garnet group

Note: *R* represents generalized cations (see Table 3).

Suffixes

With the exception of manganberzeliite (see below), up until 2009, garnets have been given new root names, without prefixes or suffixes. However, since 2009 five new names with suffixes have been approved by the CNMNC. For one of these, menzerite-(Y), the suffix is a Levinson modifier for the rare earth elements (Levinson 1966), whereas the suffixes for the other four garnets identified the dominant tetravalent cation at the *Y* site, i.e., Sn vs. Zr in two bitikleite species [formerly bitikleite-(SnFe) and bitikleite-(ZrFe)] and elbrusite [formerly elbrusite-(Zr)], and the dominant trivalent cation at the *Z* site, i.e., Al vs. Fe [formerly bitikleite-(SnAl) and bitikleite-(ZrFe), Table 5]. In the present report we restrict the term "rare earth elements" to the elements from La to Lu (atomic numbers 57–71) and Y (atomic number 39) as defined by Levinson (1966), rather than calling La-Lu "lanthanoids" and including Sc as well as Y in the rare earth elements as recommended by the International Union of Pure and Applied Chemistry. With the exception of the Levinson modifiers for the rare earth elements, e.g., menzerite-(Y), the application of suffixes results in unnecessary complexity in the nomenclature and could lead to confusion as further new spe-

cies are discovered. Consequently, we recommend that suffixes (except Levinson modifiers for the REE) not be used for names of minerals in the garnet supergroup. Moreover, as the four garnets with suffixes, which are not Levinson modifiers, have only recently been described and are not entrenched in the literature, we have given these garnets new names without suffixes. This renaming has been approved by the CNMNC as part of the overall nomenclature (Table 5). The etymology of the new names can also be found in Appendix 1.

"Hydrogarnets"

The nomenclature of naturally occurring garnet containing substantial amounts of the hydroxyl ion has had a complex history (e.g., Pertlik 2003). Many of these garnets have compositions intermediate between grossular (x = 0) and katoite (x = 3), i.e., $\{Ca_3\}[Al_2](Si_{3-x}\square_x)O_{12-4x}(OH)_{4x}$ where $0 < x < 3$ and $\square$ is vacancy. For the majority of these garnets, $x < 1.5$ (e.g., Passaglia and Rinaldi 1984). "Hibschite" was approved by the then Commission on New Minerals and Mineral Names (CNMMN, the predecessor of the CNMNC) as a name for OH-bearing grossular with $x < 1.5$ (Dunn et al. 1985) because "hibschite" had priority (Cornu 1905, 1906) over "plazolite" (Foshag 1920) and "hydrogrossular" (Hutton 1943). However, "hibschite" is not distinct from grossular according to the dominant-constituent rule, i.e., Si > $\square$ at the *Z* site, therefore "hibschite" is discredited in favor of grossular (Table 5). Dunn et al. (1985) allowed that "the name hydrogrossular may still be applied to members of the series with appreciable OH content but undetermined $SiO_4/(OH)_4$ ratio."

Several names have also been used describe the OH-bearing garnets considered together, including the "grossularoid group" (Belyankin and Petrov 1941) and the "hydrogarnet series" (Flint et al. 1941). Dunn et al. (1985) implied that the term "hydrogrossular group" and "hydrogrossular series" would be acceptable for compositions along the grossular katoite join, but in our classification the binary would no longer qualify as a group, whereas the term "series" has a more restrictive meaning than a simple binary solid solution (Mills et al. 2009; see above).

The tetragonal hydroxyl-bearing garnets henritermierite and holtstamite (Fig. 1a) are considered to constitute a distinct group because of their lower symmetry and because one tetrahedral site is largely vacant, i.e., $\square$ > Si at one of the two sites corresponding to *Z* in the archetypal garnet structure (Aubry et al. 1969; Armbruster et al. 2001; Hålenius et al. 2005). Optical determinations are sufficient to distinguish this group from members of the garnet group, and crystal structure determinations are not necessary. Holtstamite is uniaxial and shows a high (0.030) birefringence. In contrast birefringent grossular garnets are normally biaxial (as a consequence of symmetry lowering to orthorhombic, monoclinic, or triclinic symmetries) and show low to moderate (0.001–0.010) birefringence (Shtukenberg et al. 2001, 2005), although birefringence as high as 0.015 has been observed for compositions with considerable andradite component. In addition, the powder XRD pattern for holtstamite and grossular are distinct because they show different *d*-spacings for their respective 5 strongest reflections. Henritermierite and holtstamite are distinguished from each other on the basis of the dominant cation at the *Y* site, respectively Mn^{3+} and Al.

Elbrusite

Elbrusite was originally described as "elbrusite-(Zr)" with the formula $\{Ca_3\}[U^{6+}Zr](Fe_2^{3+}Fe^{2+})O_{12}$ (Table 2 from Galuskina et al. 2010a). Determination of the site occupancies and valence states were hampered by its metamict state, which was nearly complete in elbrusite containing 24 wt% UO_3 (0.62 U per formula unit) and well advanced in U-rich kerimasite (Fe-dominant analog of kimzeyite in the original description) (15–17 wt% UO_3, 0.37–0.42 U pfu); single-crystal X-ray diffraction was only practical for kerimasite containing 9 wt% UO_3 (0.21 U pfu) (Galuskina et al. 2010a). The authors noted that a Raman band below 700 cm^{-1} could indicate the presence of some Fe^{2+} in elbrusite, but the only evidence for U being hexavalent is the association with vorlanite, $CaU^{+6}O_4$, for which the hexavalent state of U could be determined (Galuskin et al. 2011a).

The composition $\{Ca_3\}[U^{6+}Zr](Fe_2^{3+}Fe^{2+})O_{12}$ is not a valid end-member because more than one site has two occupants (Hawthorne 2002). Instead, it can be considered as the sum of two valid end-members, $\frac{2}{3}\{Ca_3\}[U_{0.5}^{6+}Zr_{1.5}](Fe_3^{3+})O_{12} + \frac{1}{3}\{Ca_3\}[U_2^{6+}](Fe_3^{2+})O_{12}$ (Fig. 4). Compositions of elbrusite and U-rich kerimasite plot in a linear trend in terms of U and the sum of tetravalent cations between the composition representing kerimasite, $\{Ca_3\}[R_2^{4+}](R^{4+}R_2^{3+})O_{12}$, and $\{Ca_3\}[U^{6+}R^{4+}](R_2^{3+}R^{2+})O_{12}$ (Fig. 4). The trend is very close to the substitution mechanism $U^{6+}+R^{2+} = 2R^{4+}$, and thus is consistent with the interpretation by Galuskina et al. (2010a) that U is hexavalent and Fe^{2+} is present. Moreover, the compositions that Galuskina et al. (2010a) identified as elbrusite and kerimasite plot in the fields for $\{Ca_3\}[U^{6+}R^{4+}](R_2^{3+}R^{2+})O_{12}$ and $\{Ca_3\}[R_2^{4+}](R^{4+}R_2^{3+})O_{12}$, respectively, requiring no revision of their species identifications if $\{Ca_3\}[U_{0.5}^{6+}Zr_{1.5}](Fe_3^{3+})O_{12}$ is considered to be the end-member of elbrusite. Therefore $\{Ca_3\}[U_{0.5}^{6+}Zr_{1.5}](Fe_3^{3+})O_{12}$ should now be used as the elbrusite end-member formula.

Yudintsev (2001) and Yudintsev et al. (2002) reported a U-rich garnet, one of three compounds synthesized in corundum crucibles from a $(Ca_{2.5}U_{0.5})Zr_2Fe_3O_{12}$ bulk composition at 1400 °C in air: $\{Ca_{2.64}U_{0.36}\}[Zr_{1.66}Fe_{0.30}U_{0.04}](Fe_{1.85}Al_{1.15})O_{12}$, whereas Utsunomiya et al. (2002) reported synthesis of a U-rich garnet with a slightly different composition, $\{Ca_{2.93}U_{0.07}\}[Zr_{1.52}U_{0.47}Fe_{0.01}](Fe_{1.83}Al_{1.17})O_{12}$, under unspecified conditions, but presumably similar. Uranium is largely tetravalent in the starting material, and despite having been heated in a relatively oxidizing environment, was assumed by Yudintsev (2001) to have remained mostly tetravalent in the garnet because of its association with cubic oxide with the fluorite structure typical of U^{4+}. However, charge balance requires that 72–81% of the U be hexavalent in the two synthetic garnets. If U is assumed to be tetravalent at the *X* site and hexavalent at the *Y* site, a distribution consistent with the relative sizes of the two U ions, the two formulas give 11.754 and 12.030 positive charges, respectively. The formula of the garnet synthesized by Utsunomiya et al. 2002) is very close to the proposed elbrusite end-member (Fig. 4), and thus provides support for use of this end-member for elbrusite.

Ti-rich garnets: Schorlomite and morimotoite

The site occupancies of Ti-rich garnets have been the subject of considerable controversy despite being extensively studied using a diverse arsenal of spectroscopic techniques as well

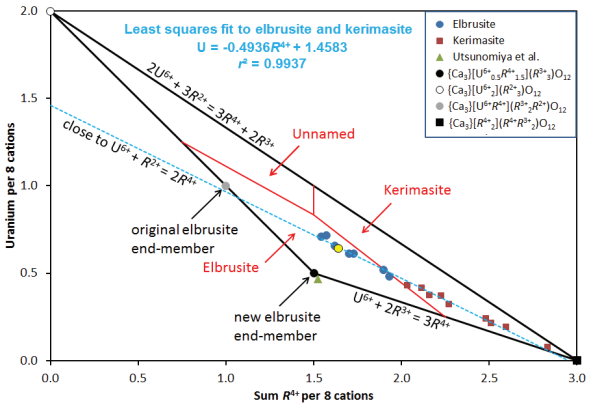

FIGURE 4. Compositions of U-rich garnets from the Upper Chegem caldera, Northern Caucasus, Russia (Galuskina et al. 2010a; Utsunomiya et al. 2002). The red lines mark the boundaries between elbrusite, kerimasite and an unnamed species based on the relative proportions of the kerimasite end-member, new elbrusite end-member and the unnamed $\{Ca_3\}[U_2^{6+}](R_3^{2+})O_{12}$ end-member. Yellow circle indicates the Sn-dominant analog of elbrusite, which was included in the least-squares fit.

as X-ray diffraction (e.g., Chakhmouradian and McCammon 2005). The two species currently accepted by the CNMNC are schorlomite, $Ca_3(Ti,Fe^{3+})_2(Si,Fe)_3O_{12}$, and morimotoite, $Ca_3(Ti,Fe^{2+},Fe^{3+})_2(Si,Fe^{3+})_3O_{12}$ (Table 2). These formulas, which are listed as approved by the CNMNC, are too generalized to indicate what the distinction is between the two species, and clearly new formulas based on end-members are needed.

Schorlomite (Fig. 1f) was first described and named by Shepard (1846), who reported it to be a hydrous silicate containing Y, Fe, and possibly Th from Magnet Cove, Arkansas, U.S.A. However, Whitney (1849) and Rammelsberg (1850a, 1850b) showed schorlomite to be a silicate of Ca, Fe, and Ti, reporting compositions approaching those obtained by modern techniques. Chemical data obtained subsequently of Ti-bearing andradite, often called by the varietal name "melanite," showed that TiO_2 content ranged continuously from 0 to 19 wt%, whereas Labotka (1995) reported immiscibility at one locality. Grapes et al. (1979) and Laverne et al. (2006) reported up to 30 wt% TiO_2 in garnets having anomalous compositions, which will be discussed separately below. Chakhmouradian and McCammon (2005) summarized the criteria proposed by various authors for distinguishing schorlomite from Ti-bearing andradite; among the most frequently used have been ${}^{Y}Ti > {}^{Y}Fe^{3+}$ (Ito and Frondel 1967a; Deer et al. 1982), approximately the same as $TiO_2 > 15$ wt% (Zedlitz 1933) and about twice the minimum Ti content suggested by Howie and Woolley (1968). Chakhmouradian and McCammon (2005) recommended that the proportion of schorlomite be determined as the amount of ${}^{Y}Ti$, balanced by substitutions at the *Z* site, relative to the total occupancy in the *Y* site, $({}^{Y}Ti–{}^{Y}Fe^{2+}–{}^{Y}Mg–{}^{X}Na)/2$, i.e., deducting a morimotoite component (see below) together with a contribution from a hypothetical $\{Na_2Ca\}[Ti_2](Si_3)O_{12}$ component. Several end-member formulas have been proposed for schorlomite, e.g., $\{Ca_3\}[Ti_2](Fe_2^{3+}Si)O_{12}$ (Ito and Frondel 1967a) and $\{Ca_3\}[Ti_2](Fe_2^{3+}Ti)O_{12}$ (Rickwood 1968), whereas Chakhmouradian and McCammon (2005) argued that the crystal chemistry was too complex to be represented by a single end-member, and proposed a generalized formula instead, $\{Ca_3\}[Ti_2](Si_{3-x})(Fe^{3+},Al,Fe^{2+})_xO_{12}$.

Morimotoite was introduced by Henmi et al. (1995) with an end-member formula $Ca_3TiFe^{2+}Si_3O_{12}$, based entirely on electron-microprobe data of garnet containing nearly 20 wt% TiO_2 from Fuka, Okayama Prefecture, Japan. Formulas that we recalculated assuming 8 cations and 12 O anions from three analyses in Henmi et al. (1995), including the one designated as type, gave 1–8% andradite, $\{Ca_3\}[Fe_2^{3+}](Si_3)O_{12}$, 27–34% $\{Ca_3\}[Ti_2](Fe_2^{3+}Si)O_{12}$, and 58–71% $\{Ca_3\}[TiFe^{2+}](Si_3)O_{12}$ with minor Zr, Mg, Mn, and Al included with Ti, Fe^{2+}, Ca, and Fe^{3+} according to valence. Garnets synthesized by Henmi et al. (1995) under reducing conditions (iron-wüstite buffer) have compositions very similar to the natural material; end-member morimotoite could not be synthesized. However, no structural or spectroscopic data were obtained to confirm the assumed site occupancies and calculated Fe valence, and thus the report raised objections. Fehr and Amthauer (1996) and Rass (1997) questioned the assumption that Ti was all Ti^{4+}. The latter authors also dismissed the infrared evidence that Henmi et al. (1995) used to justify their conclusion that OH was absent, and cited experiments by Kühberger et al. (1989) that OH is likely to be present in morimotoite. Their conclusion is supported by the report by Armbruster et al. (1998) that the morimotoite substitution, $Fe^{2+}+Ti^{4+} \rightarrow 2Fe^{3+}$ at the *Y* site is coupled with $4OH^- \rightarrow SiO_4^{4-}$ at the tetrahedral site in Ti-bearing andradite.

Despite the variety of methods deployed to locate cations in the structure of Ti-rich garnets, authors have yet to reach a consensus, which reflects not only differing interpretations of the spectroscopic and structural data, but probably also variation between samples. Nonetheless, the question confronting us is whether we can still propose a meaningful classification based on formulas calculated from a full electron microprobe analysis assuming 8 cations and 12 oxygen anions. There is little disagreement on the occupancy of the *X* site, which with rare exception contains at least 2.7 (Ca+Na) atoms per formula unit (apfu), to which are added sufficient Mn and Mg to bring total *X* site occupancy to 3, but fewer authors (e.g., Chakhmouradian and McCammon 2005) would also place Fe^{2+} at the *X* site. Problematic issues include the valence and location of Ti and Fe, as well as the location of Al. Locock (2008) reviewed the literature on Ti^{3+} in garnet and concluded that the oxygen fugacities required for this valence were far too low to be found in most geologic environments. This conclusion is consistent with most spectroscopic studies, for example, X-ray absorption near-edge structure spectroscopy (XANES) has revealed little or no Ti^{3+} in natural garnet (Waychunas 1987; Locock et al. 1995), whereas electron spin resonance spectroscopy revealed that Ti^{3+} is much subordinate to Ti^{4+} in pyrope synthesized under relatively reducing conditions (Rager et al. 2003; Geiger 2004). In contrast, Malitesta et al. (1995) and Schingaro et al. (2004) reported significant Ti^{3+} in Ti-bearing garnet by X-ray photoelectron spectroscopy (XPS). Since XPS examines the near-surface of a solid, i.e., to a depth of a few tens of angstroms (Hochella 1988), the discrepancy between the XPS and XANES results could be due to differences at the mineral surface not detected by XANES, and consequently we are inclined to accept the conclu-

sion that Ti^{3+} plays a negligible role in natural terrestrial garnet, although it could be significant constituent in some meteoritic garnet (e.g., Ma 2012).

As regards the location of Ti, Armbruster et al. (1998) located Ti at *Z* as well as *Y*, but most authors place Ti only at *Y*, which seems reasonable in the relatively Si-rich and Ti-rich garnets (Si > 2 apfu) because of the rarity of Si = Ti substitution at tetrahedral sites (Hartman 1969). Nonetheless, combined low pressure and high temperature could favor Ti substitution for Si at a tetrahedral site as it does in lamproitic richterite (Oberti et al. 1992). The most robust element-specific technique, XANES, yields results consistent with the bulk of Ti occupying the octahedral site in most natural garnets (Waychunas 1987; Locock et al. 1995). Significant Ti may occupy the *Z* site in Si-poor garnets such as elbrusite and bitikleite (e.g., Galuskina et al. 2010a, 2010b), and its presence has been demonstrated in Si-free synthetic garnets (Povarennykh and Shabilin 1983; Cartie et al. 1992; Yamane and Kawano 2011). Another question is the possible presence of tetrahedrally coordinated Fe^{2+}. Some studies reported Mössbauer spectroscopic evidence for significant Fe^{2+} at the *Z* site (e.g., Locock et al. 1995; Koritnig et al. 1978), but the spectroscopic data do not always give unequivocal site assignments (Chakhmouradian and McCammon 2005). Last, there is the role of the hydroxyl ion; ignoring hydroxyl results in an underestimate of Fe^{2+} in the formulas calculated by the method of Droop (1987). However, the effect would be serious only if >0.4 wt% H_2O were present, in which case at least 0.1 Fe^{2+} per formula unit would not show up in the calculated formula unless OH were included in the formula calculation, i.e., $(OH)+O = 12$ and $\Sigma\{X\}+\Sigma[Y]+\Sigma(Z)+{}^{Z}\square_{(OH)/4} = 8$, or if F present, $O+(OH)+F = 12$ and $\Sigma\{X\}+\Sigma[Y]+\Sigma(Z)+{}^{Z}\square_{(OH)/4}+{}^{Z}\square_{F/4} = 8$. The few analyses available in the recent comprehensive studies give 0.02–0.21 wt% H_2O for natural Ti-rich garnets with >12 wt% TiO_2 (Kühberger et al. 1989; Locock et al. 1995; Amthauer and Rossman 1998; Chakhmouradian and McCammon 2005). An exception is "hydroschorlomite" with 5 wt% H_2O (Galuskin 2005); such H_2O-rich garnets cannot be treated in the approach discussed below.

To identify end-member formulas for the two Ti-rich garnet species schorlomite and morimotoite, we should compare the results from as many studies as possible, which necessitate our relying on chemical data. Few authors have supplemented chemical data with structure refinements using X-ray diffraction and with spectroscopic methods to determine site occupancy, and thus we think that reliance on chemical data is the most consistent approach for treating compositional data from different studies. In addition, we have made the following assumptions in treating the chemical data.

(1) Ti is Ti^{4+} and preferentially occupies the *Y* site, which rules out the end-member $\{Ca_3\}[Ti_2](TiFe^{3+}_2)O_{12}$ proposed by Rickwood (1968).

(2) H_2O content is ≤0.2 wt%.

(3) Site occupancies are estimated using formulas calculated for 8 cations and 12 oxygen anions and the procedure outlined in the next section (see below).

Figure 5 is a plot of *Y*-site compositions for garnets containing >12 wt% TiO_2 and Ti > Zr apfu in terms of the following generalized end-members $\{Ca_3\}[R^{3+}_2](Si_3)O_{12}$, $\{Ca_3\}[R^{4+}_2](SiR^{3+}_2)O_{12}$, and $\{Ca_3\}[R^{4+}R^{2+}](Si_3)O_{12}$. For R^{4+} = Ti, $R^{3+} = Fe^{3+}$, and $R^{2+} = Fe^{2+}$, these generalized end-members correspond, respectively, to andradite, the schorlomite end-member of Ito and Frondel (1967a), and the morimotoite end-member of Henmi et al. (1995), i.e., the same components plotted by Henmi et al. (1995, their Fig. 1). It turns out that 15 wt% TiO_2, which Zedlitz (1933) suggested as a cutoff for schorlomite, is a good estimate of the minimum TiO_2 content of compositions plotting in the morimotoite and schorlomite fields unless significant Zr is present.

Three reports of garnets reported to contain over 20 wt% TiO_2 have not been plotted in Figure 5 either because of their high-H_2O content or because of their questionable identity as garnet. Galuskina and Galuskin (unpublished data) were able to confirm the identity of an OH-bearing schorlomite in a xenolith from the upper Chegem caldera, northern Caucasus by Raman spectroscopy. Analyses of the cores of two honey-colored crystals about 30 μm across enclosed in grossular-katoite give 12.61–13.75 wt% SiO_2, 25.42–25.86 wt% TiO_2, 0.41–0.49 wt% SnO_2, 2.20–2.28 wt% Al_2O_3, 24.86–26.09 wt% Fe as Fe_2O_3, 31.03–31.71 wt% CaO, ≤ 0.03 wt% MgO, and 0.27 to 1.2 wt% H_2O (calculated); Mn, Cr, Zr, Nb, V, Ce, La, Na, F, and Cl were below the detection limit. These data correspond approximately to 73–76% $\{Ca_3\}[Ti^{4+}_2](SiFe^{3+}_2)O_{12}$, the highest proportion of the schorlomite end-member reported in a natural garnet, 12–13% $\{Ca_3\}[Ti^{4+}_2](SiAl_2)O_{12}$ and 12–14% andradite plus its OH analog. Grapes et al. (1979) reported an electron microprobe analysis of a garnet from Morotu, Sakhalin Island, Russia, containing 27.38 wt% TiO_2 and 33.50 wt% Fe as FeO, but deficient in Si and Ca with the formula: $\{Ca_{1.53}Fe^{2+}_{1.46}Mn_{0.01}\}[Ti_{1.28}Fe^{2+}_{0.71}Mg_{0.01}](Si_{1.84}Ti_{0.60}Fe^{3+}_{0.38}Al_{0.18})O_{12}$, i.e., a morimotoite from site occupancies, but anomalous because so much Ti (or Fe^{2+}) is forced by the formula calculation onto the *Z* site. A possible explanation for the high-Fe and Ti contents is X-ray fluorescence from contiguous phases (Chakhmouradian and McCammon 2005). In a study of altered basalt from the equatorial east Pacific, Laverne et al. (2006) described a "hydroschorlomite" with 22.0–28.6 wt% TiO_2, 6.2–12.9 wt% Fe as FeO and 22.5–26.5% wt% CaO. Laverne et al. (2006) tried to correct for celadonite impurities, which were manifested by the presence of ~1 wt% K_2O in the analyses. The study included SEM and TEM, as well as micro-Raman spectra, but none provided corroborative evidence that the mineral was indeed a garnet; the reported compositions suggest the mineral could be titanite.

Three analyses, including the holotype, from the type locality of morimotoite in Fuka, Japan, plot in the morimotoite field and show that Ti and Fe^{2+} are the dominant R^{4+} and R^{2+} cations at *Y* if we assume that Ti and Fe^{2+} do not occupy the *Z* site, whereas four of the five analyses of garnet from the type locality of schorlomite at Magnet Cove, U.S.A., plot in the schorlomite field and show that Ti is the dominant R^{4+} cation, and Fe^{3+} is the dominant ${}^{Z}R^{3+}$ cation. The latter situation holds even if Al is assumed to preferentially occupy the *Z* site (e.g., Chakhmouradian and McCammon 2005), which is not supported by all studies (e.g., Locock et al. 1995; Armbruster et al. 1998). Thus, we recommend that $\{Ca_3\}[Ti^{4+}Fe^{2+}](Si_3)O_{12}$ and $\{Ca_3\}[Ti^{4+}_2](SiFe^{3+}_2)O_{12}$ be the end-member formulas for morimotoite and schorlomite, respectively. Despite the assumptions and simplifications discussed above,

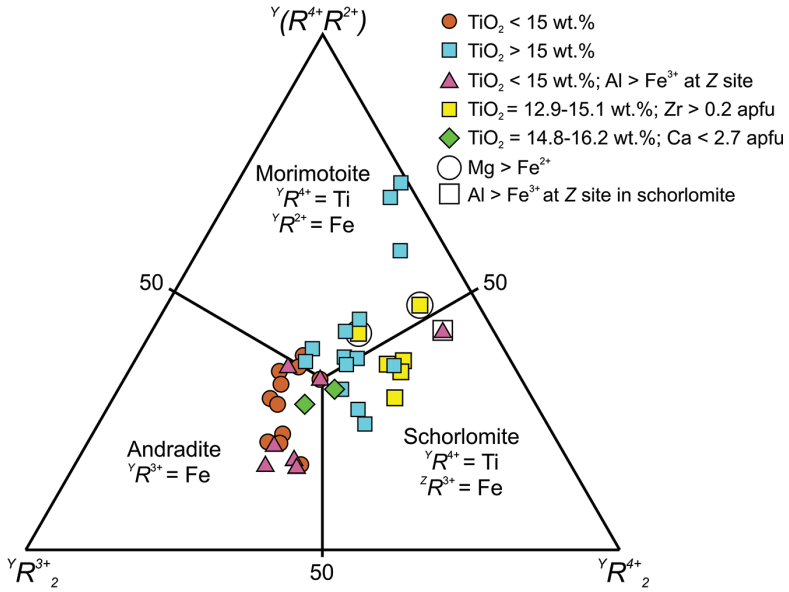

Figure 5. Plot of the *Y*-site contents of 40 natural garnets with TiO_2 > 12 wt% based on formulas normalized to 8 cations and 12 O anions (excluding H); BaO and ZnO not included. *Y*-site contents were calculated from the relative proportions of (1) Ti+Zr (=R^{3+} at *Z*), (2) remaining Ti+Zr as $R^{4+}R^{2+}$, and (3) R^{3+}, which correspond to schorlomite, morimotoite and andradite, respectively. Sources of data: Zedlitz (1935); Lehijärvi (1960); Gnevushev and Fedorova (1964); Howie and Woolley (1968); Dowty (1971); von Eckermann (1974); Amthauer et al. (1977); Huggins et al. (1977); Koritnig et al. (1978); Platt and Mitchell (1979); Flohr and Ross (1989); Lupini et al. (1992); Henmi et al. (1995); Labotka (1995); Locock et al. (1995); Chakhmouradian and McCammon (2005); Marks et al. (2008); Melluso et al. (2010); Saha et al. (2010). Circles for Mg > Fe^{2+} (total for analysis) have been added only for compositions plotting in the morimotoite field. The square enclosing a triangle indicates the schorlomite in which $^{Z}Al > {}^{Z}Fe^{3+}$ and 0.55 Zr pfu reported by Koritnig et al. (1978); it is a possible new species, the Al-dominant analog of schorlomite. Compositions are plotted under the assumption that Al preferentially is incorporated at the *Z* site (except from Fuka, see text).

we believe that Figure 5 can be used to distinguish schorlomite and morimotoite in the absence of structural and spectroscopic studies if allowance is made for the uncertainties in attempting to identify borderline cases.

Figure 5 shows that many garnets reported as schorlomite plot in the morimotoite and andradite fields; garnets plotting in the schorlomite field other than those from Magnet Cove are from Ardnamurchan, Scotland (Huggins et al. 1977), the Tamazeght complex, Morocco (Marks et al. 2008), the Polino carbonatite, Italy (Lupini et al. 1992), and Alnö Island, Sweden (von Eckermann 1974). The dominant $^{Z}R^{3+}$ cation in these garnets is Fe^{3+}, even if Al is assumed to preferentially occupy the *Z* site. Using the above assumptions, garnets plotting in the morimotoite field (with Fe^{2+} > Mg at the *Y* site) are from Iivaara, Finland (Zedlitz 1935), Afrikanda, Russia (Chakhmouradian and McCammon 2005), Ice River, Canada (Locock et al. 1995; Peterson et al. 1995), Sung Valley, India (Melluso et al. 2010), and Rusing Island, Kenya (Howie and Woolley 1968). However, Mössbauer spectroscopy of the Ice River garnet indicates that a significant proportion of the Fe^{2+} is located at the *Z* site and dominance of $[(Ti,Zr)_2]$ over $[(Ti,Zr)R^{2+}]$ at *Y*, so Locock et al. (1995) and Peterson et al. (1995) had reason to call this garnet schorlomite. Two relatively Zr-rich garnets from the Marathon Dikes, Ontario, Canada (Platt and Mitchell 1979), also plot in the morimotoite field, but are unique in that total Mg > Fe^{2+}_{total} (circled in Fig. 5) suggesting the possibility of a Mg-dominant analog of morimotoite (see the section on Possible new species and compositional variations in natural garnet).

All the analyses plotted in Figure 5 have Si > 2 and total charge at *Z* > 11, i.e., all the garnets would be classed as garnet group, including compositions of schorlomite from the type locality (e.g., Appendix 3[1]). This contradiction arises because the compositions include more garnet-group components, largely andradite, $\{Ca_3\}[R^{3+}_2](Si_3)O_{12}$, and morimotoite, $\{Ca_3\}[R^{4+}R^{2+}](Si_3)O_{12}$, than schorlomite-group components, largely, $\{Ca_3\}[R^{4+}_2](SiR^{3+}_2)O_{12}$.

Menzerite-(Y)

The validity of menzerite-(Y) has been questioned because the end-member formula proposed for menzerite-(Y), $\{Y_2Ca\}[Mg_2](Si_3)O_{12}$, is quite far from the measured compositions of the type and only known material, which averages much closer to $\{Y(Ca,Fe^{2+})_2\}[(Mg,Fe^{2+})(Fe^{3+},Al)](Si_3)O_{12}$, an empirical formula that can be simplified to $\{YCa_2\}[MgFe^{3+}](Si_3)O_{12}$. This simplified formula is not a valid end-member because it has two sites with two occupants (Hawthorne 2002). Instead, it can be resolved into an equal mixture of $\{Y_2Ca\}[Mg_2](Si_3)O_{12}$ [menzerite-(Y)] and $\{Ca_3\}[Fe^{3+}_2](Si_3)O_{12}$ (andradite). Type menzerite-(Y) compositions are close to the midpoint between these two end-members, but in two grains divalent cations are dominant at the *Y* site and Mg is the dominant divalent cation at this site (e.g., Appendices 3 and 4), confirming that menzerite-(Y) is a valid species (Grew et al. 2010). Of course, this approach depends on the accuracy of the electron microprobe analyses and calculation of Fe^{3+}/Fe^{2+}

ratio from stoichiometry (Droop 1987). The calculated Fe^{3+}/Fe^{2+} ratios are consistent with single-crystal X-ray diffraction data although not with preliminary micro-X-ray absorption near-edge spectroscopy (Grew et al. 2010).

A second argument forwarded to challenge the validity of menzerite-(Y) is that trivalent cations, i.e., Y+REE, are not dominant at the *X* site in any of the analyzed menzerite-(Y) grains, the maximum being 1.1 Y + REE per formula unit. Simple application of the dominant-valency rule gives $\{Ca_3\}[Mg_2](Si_3)O_{12}$, which is not balanced in charge. Charge balance allows only 2 (Y+REE) per formula unit, i.e., the menzerite end-member should be $\{Y_2Ca\}[Mg_2](Si_3)O_{12}$. The presence of >1 (Y+REE) means that $[(Y,REE)_2Ca]$ exceeds 50% of the maximum possible consistent with valency-imposed double site-occupancy.

Rates of diffusion of Y and REE in garnet provide evidence for the importance of the menzerite component in garnet, i.e., mobility of Y and REE at the *X* site is closely linked to mobility of Al at the *Y* site (Carlson 2012).

Majorite

The current list of CNMNC approved minerals (http://pubsites.uws.edu.au/ima-cnmnc/) gives the formula for majorite as $Mg_3(Fe^{2+},Si)(SiO_4)_3$ (Table 2), equivalent to $\{Mg_3\}[SiFe^{2+}](Si_3)O_{12}$, which indeed is a good approximation of the empirical formula of the type material reported by Smith and Mason (1970), $(Mg,Na)_3(Fe,Si,Al,Cr)_2Si_3O_{12}$. It was assumed that Fe occupied the *Y* site, but the valence and distribution of the Fe were not determined. Recalculating a formula for 8 cations and 12 oxygen anions from the published analysis and listing cations at a given site in order of decreasing abundance gives: $\{Mg_{2.91}Na_{0.09}\}[(Si_{0.71}Fe^{2+}_{0.60}Fe^{3+}_{0.41}Al_{0.22}Cr_{0.04}\ Mg_{0.02}](Si_3)O_{12}$.

However, the assumption regarding Fe^{2+} occupancy is not supported by Mössbauer spectroscopic data on synthetic majorite (Geiger et al. 1991a, 1991b; O'Neill et al. 1993a, 1993b; McCammon and Ross 2003). In a study that included samples that Geiger et al. (1991a, 1991b) and O'Neill et al. (1993a, 1993b) had investigated, McCammon and Ross (2003) reported that $^{X}Fe^{2+}/\Sigma Fe^{2+}$ = 0.89–0.95, and $Fe^{2+}/(Fe^{2+}+Mg)$ at *X* (0.05–0.22) is three to seven times $Fe^{2+}/(Fe^{2+}+Mg)$ at *Y* (0.01–0.08) in 15 synthetic tetragonal majorite samples, and $^{X}Fe^{2+}/\Sigma Fe^{2+}$ = 1.0 in one isometric synthetic sample, demonstrating that Fe^{2+} is strongly fractionated onto the *X* site. Because the compositions of the type specimen and these synthetic samples are similar, we think it is reasonable to assume that Fe distribution is the same in synthetic and natural majorite, and the partial ordering at the *X* and *Y* sites in tetragonal samples does not significantly affect the Fe distribution. Assuming that Fe^{2+} occupies only the *X* site, the formula of the type material becomes $\{Mg_{2.31}Fe^{2+}_{0.60}Na_{0.09}\}[(Si_{0.71}Mg_{0.62}Fe^{3+}_{0.41}Al_{0.22}Cr_{0.04}](Si_3)O_{12}$, i.e., the dominant component is $\{Mg_3\}[SiMg](Si_3)O_{12}$. Consequently, we recommend that $\{Mg_3\}[SiMg](Si_3)O_{12}$ be used as the end-member formula for majorite. A natural $^{X}Fe^{2+}$ analog has not been reported, and as far as we are aware, it has not been synthesized (e.g., Kato 1986).

Although synthetic majorite has tetragonal symmetry (space group $I4_1/a$, no. 88) resulting from a high degree of ordering of Mg and Si at the two symmetrically unique octahedral sites (e.g., Angel et al. 1989), no naturally occurring tetragonal majorite has been reported. Apparently, majorite in shocked meteorites was quenched with sufficient rapidity to preserve cubic symmetry (Tomioka et al. 2002). The problem of preserving cubic symmetry on cooling would probably not arise in terrestrial majorite, which contains substantial Al, because incorporation of Al at the *Y* site is thought to stabilize the cubic structure (Hatch and Ghose 1989). Moore and Gurney (1985) confirmed isometric symmetry for garnet from the Monastery Mine kimberlite pipe, South Africa, one of which we calculated to contain 36% of a generalized majorite component, $\{R^{2+}_3\}[MgSi](Si_3)O_{12}$.

The term "majoritic" has found wide use in the literature on garnets included in diamond (e.g., Harte 2010; Collerson et al. 2010), i.e., garnet is described as "majoritic" if Si is incorporated at the *Y* site through the "majorite" substitution $^{Y}R^{2+}+{}^{Y}Si \rightarrow 2\,{}^{Y}Al$ (Table 4). Collerson et al. (2010) also include the contribution from the generalized component $\{R^{2+}Na_2\}[R^{4+}_2](Si_3)O_{12}$ in their majorite substitution parameter, $X^{cat}Mj$. In contrast to majorite reported from shocked meteorites, in which the majorite component is clearly dominant (Collerson et al. 2010), none of the "majoritic" garnets occurring in diamonds are properly majorite, i.e., the majorite component $\{Mg_3\}[SiMg](Si_3)O_{12}$ or $(R^{2+}+R^{4+}) > 2R^{3+}$ at the *Y* site, is not dominant, even in sample JF-22 from the Jagersfontein kimberlite, South Africa (Tappert et al. 2005; Harte 2010), which has the highest content of Si at the *Y* site among terrestrial garnet as far as we are aware: a maximum 47.2% $\{R^{2+}_3\}[R^{4+}Mg](Si_3)O_{12}$ or 44.9% $\{R^{2+}_3\}[SiMg](Si_3)O_{12}$ (Appendix 3[1], example 5). The "Ca-rich majorite" in shock veins of crustal rocks from the Ries impact crater, Germany (Stähle et al. 2011), is not majorite because $({}^{Y}Si+{}^{Y}Ti) < ({}^{Y}Al+{}^{Y}Fe^{3+}+{}^{Y}Cr)$; instead, the three average compositions comprise about 58–71% pyrope-grossular-almandine, 17–33% $\{R^{2+}_3\}[R^{4+}Mg](Si_3)O_{12}$ (generalized majorite), and 10–13% $\{R^{2+}(Na,K)_2\}[R^{4+}_2](Si_3)O_{12}$, where $^{Y}R^{4+}$ = 90–93% Si.

Manganberzeliite

Manganberzeliite, $\{Ca_2Na\}[Mn^{2+}_2](As^{5+}_3)O_{12}$ (Fig. 1g) has a complicated history revolving around the use of its name, which is briefly described below. Over 40 yr after the original description of berzeliite from Långban, Filipstad district, Sweden (Kühn 1840), Igelström (1886) described a Sb-bearing, Mn-rich berzeliite-like mineral from the nearby Sjögruvan mine, and named it "pyrrhoarsenite." On the basis of a new chemical analysis giving 28.38 wt% MnO, Igelström (1894) concluded that "pyrrhoarsenite" is a manganese-dominant variety of berzeliite and could also be referred to as "Mangan-Berzeliit."

In summarizing his discussion of the mineral, Hintze (1922) wrote that Igelström (1894) had found no antimony and had concluded from his studies that "pyrrhoarsenite" is just a Mn-rich variety of berzeliite. Hintze (1922) cited Igelström's (1894) conclusion that the mineral containing 28% MnO can be referred to as "Manganberzeliit," but Hintze (1922) wrote the name in bold type and unhyphenated.

Landergren (1930) used the terms "Mg-berzeliit" and "Mn-berzeliit" for the end-members of the series. These names were later used by other mineralogists studying this series, e.g., Blix and Wickman (1959).

Moore (1972) reported powder XRD data for the type specimen of "pyrrhoarsenite" studied by Igelström (specimen NRM18870324 at the Swedish Museum of Natural History)

from Sjögruvan. He concluded that "pyrrhoarsenite" = berzeliite. However, recent energy-dispersive spectroscopic analyses (Hålenius, unpublished data) of fragments of the mineral from this specimen, as well as cell parameter refinement (Locock, unpublished data) of Moore's powder X-ray diffraction data, show that it is in fact Mn-dominant berzeliite, i.e., manganberzeliite (or "pyrrhoarsenite"). Prior to publication, Moore in 1971 submitted to the CNMMN a proposal to discredit several of the minerals outlined in his 1972 paper. After Moore published his paper, it was subsequently abstracted by Fleischer (1973), who noted that these minerals were discredited by the CNMMN and that "pyrrhoarsenite" was equivalent to berzeliite. However, the discreditation of pyrrhoarsenite was actually not included in Moore's proposal to the CNMMN. Therefore, the report by Fleischer (1973), which was then carried forward by Nickel and Mandarino (1987), was in error.

This raises the question whether "pyrrhoarsenite" has priority over manganberzeliite and should be reinstated, although manganberzeliite has been the preferred name since 1894 (e.g., Hintze 1922; Palache et al. 1951). Given that Igelström's original description of the mineral was poor even by the standards of the late 19th century, e.g., he did not detect the appreciable sodium content, in contrast to his contemporary Sjögren (1894), we conclude that priority does not justify reviving "pyrrhoarsenite" at the present time and manganberzeliite should remain the name for the Mn analog of berzeliite.

Applying the nomenclature of the garnet supergroup

Assumed cation occupancies

A major objective of the classification is to provide a basis for identifying the species of an analyzed garnet from its chemical composition. As is the case for the tourmaline supergroup (Henry et al. 2011), chemical analyses of garnet establish which elements are present, but provide no information on which site(s) they occupy in the structure. Proper site allocation requires single-crystal or Rietveld structure refinement using X-ray or neutron diffraction methods, and spectroscopic data are often also needed for unambiguous site assignment, particularly when constituents could be present in more than one valence state, which is not rare in garnet. However, most investigators have only electron microprobe analyses, which provide no direct evidence of valence state. An added difficulty is that as a result of charge balance requirements, several garnet end-members have one site with mixed occupancy, the so-called valency-imposed double site-occupancy of Hatert and Burke (2008).

For all garnet-supergroup minerals we recommend that cations be allocated from a chemical analysis with the procedure given in the next section. This procedure is analogous to that proposed in connection with the nomenclature recommended for the tourmaline supergroup of Henry et al. (2011). It includes only constituents found in known end-members (Table 1) or some potential end-members (Tables 6–7). Examples illustrating our recommended procedure are given in Appendix 3[1], and a spreadsheet is given in Appendix 4[1].

As in the case of many mineral groups, some reasonable assumptions can be made concerning site assignments of specific cations on the basis of relative abundance (Table 3). Lithium and hydrogen are the only light elements (atomic number < 8) that have been reported in major amounts in garnet supergroup minerals, e.g., cryolithionite and katoite, respectively. When common silicate garnet species are checked for light elements, generally very little is found, i.e., Li contents are reported to not exceed 121 ppm, and Be and B contents, not to exceed 20 ppm (e.g., Grew et al. 1990; Grew 2002a, 2002b; Steppan 2003; Marschall 2005). An exception are the 259–1113 ppm Li in almandine from leucocratic granulite at Horní Bory, Czech Republic, corresponding to 0.019–0.079 Li pfu, determined by laser ablation-inductively coupled plasma-mass spectroscopy (Cempírek et al. 2010 and unpublished data). According to Cempírek et al. (2010), Li could occupy either the *X* site as it does in synthetic $\{Li_2Mg\}[Si_2](Si_3)O_{12}$ (Yang et al. 2009) or sites occupied by Li in synthetic garnets. The majority of synthetic Li garnets are compounds of Li with REE, Ta, Nb, Te, Zr, and Ba that are valued for their high-ionic conductivity (e.g., Cussen 2006, 2010; O'Callaghan and Cussen 2007; Wang and Lai 2012). Lithium occupies not only the Z site, but also octahedral sites that are vacant in natural garnet, resulting in Li contents up to 6.8 apfu and cation totals up 11.8 apfu. Other exceptions involving light elements are the reports of 4.40 wt% B_2O_3 determined by electron microprobe analysis (EMPA) in andradite (Galuskin et al. 1995) and 0.45–2.09 wt% B_2O_3 by EMPA in OH-bearing grossular (Galuskina et al. 1998, 2001) from the Wiluy River, Yakutia, Russia. Pending studies of Li and B in silicate and hydroxyl garnet, it would be best to assume Li and B, as well as S^{6+} (up to 2.27 wt% SO_3, equivalent to 0.11 S pfu, Passaglia and Rinaldi 1984; Galuskina et al. 2001), are located at the *Z* site.

Calcium has been assumed to occupy only the *X* site in natural garnet; even in synthetic garnets there are very few reports of Ca at the *Y* site and none can be considered unequivocal (Geller 1967; Lobanov et al. 1989). Nonetheless, it should be noted that Huggins et al. (1977) and Pieper et al. (1983) concluded that a small excess of cations at *X* and a correspondingly small deficit at *Y* could be explained in some cases by small amounts of Ca at *Y*, 0.024–0.055 apfu in andradite and 0.04 apfu in grossular, respectively. Gadas et al. (2012) reported up to 3.15 Ca pfu in grossular from pegmatite at Ruda nad Moravou, Czech Republic.

Scandium is assumed to occupy only the *Y* site as in eringaite, although its role could depend on the occupancy of *X* if synthetic garnets are any guide, where Sc preferentially occupies *Y* only in andradite, whereas in pyrope, *X* is favored and in grossular, a more even distribution (Oberti et al. 2006; Quartieri et al. 2006). Titanium is assumed to be tetravalent, and V, either pentavalent or trivalent. The last assumption received validation from Bordage et al. (2010), who reported that V was entirely V^{3+} in a grossular (variety "tsavorite" containing 0.14 V pfu) based on the *K*-edge X-ray absorption near-edge structure (XANES) spectra obtained with high-energy resolution fluorescence-detected X-ray absorption spectroscopy. In contrast, Righter et al. (2011) reported mixed valences also based on the *K*-edge X-ray absorption near-edge structure in other garnets, viz. 2.46–2.55 ±0.15 in pyrope of mantle origin and 2.56–2.67 (±0.15) for V valence in a goldmanite from the Czech Republic, i.e., 40% of the V in the goldmanite is V^{2+}, the remainder V^{3+}. However, this conclusion is in contrast to the structural and chemical data reported by these authors.

TABLE 6. Components and end-members reported in the literature, but not yet found to be dominant in natural garnet

Name	*X*	*Y*	*Z*	φ	Syn?	Occurrence in natural garnet	Source
			"Kenogarnet" group				
Fe^{3+} analog of katoite	Ca_3	Fe^{3+}_2	$\square_3$	$(OH)_{12}$	Yes	≤35 mol% in andradite	(1)
F analog of katoite	Ca_3	Al_2	$\square_3$	F_{12}	No	≤11 mol% in OH-bearing grossular	(2)
Mn^{2+}, F analog of katoite	Mn^{2+}_3	Al_2	$\square_3$	F_{12}	–	≤8 mol% in spessartine	(3)
			Unnamed group				
Pb^{2+} analog of yafsoanite	Pb_3	Te^{6+}_2	Zn_3	O_{12}	–	9 mol% in yafsoanite	(4)
unnamed	Ca_3	U^{6+}_2	Fe^{2+}_3	O_{12}	–	≤24 mol% in elbrusite	(5)
			Henritermierite group				
Mn^{2+} analog of holtstamite	Mn^{2+}_3	Al_2	$Si_2 \mid \square$	$O_8(OH)_4$	–	28 mol% in spessartine	(6)
Mn^{2+}, F analog of holtstamite	Mn^{2+}_3	Al_2	$Si_2 \mid \square$	O_8F_4	–	20 mol% in spessartine	(6)
			Bitikleite group				
unnamed	$Th_{0.5}Ca_{2.5}$	R^{4+}_2	R^{3+}	O_{12}	Yes	≤20 mol% in kerimasite	(7)
			Unnamed group				
$Y_3Al_5O_{12}$, $Y_3Fe_5O_{12}$	$(Y,REE)^{3+}_3$	R^{3+}_2	R^{3+}	O_{12}	Yes	≤8 mol% in menzerite-(Y), spessartine, andradite	(8)
			Garnet group				
"Blythite" in part	R^{2+}_3	Mn^{3+}_2	Si_3	O_{12}	Yes	≤9 mol% in calderite-andradite±spessartine	(9)
Fe analog of menzerite-(Y)	Y_2Ca	Fe^{2+}_2	Si_3	O_{12}	–	≤20 mol% in menzerite (Y)	(10)
unnamed	$(Y,Yb)_{1.5}Na_{1.5}$	R^{3+}_2	Si_3	O_{12}	–	≤7 mol% in almandine, spessartine, grossular	(11)
unnamed	$R^{2+}Na_2$	Si_2	Si_3	O_{12}	Yes	≤12 mol% in pyrope-grossular	(12)
			Berzeliite group				
unnamed	Na_3	Al_2	P_3	O_{12}	Yes	<1 mol% in almandine and pyrope	(13)
unnamed	Ca_2Na	Fe^{2+}_2	As^{5+}_3	O_{12}	No	<6 mol% in berzeliite	(14)

Note: Syn? = has compound been synthesized? Yes: synthesis in which component is dominant as well as syntheses in which component constitutes 100%. No: synthesis attempted but failed. Sources for contents in natural garnets and syntheses of end-members:
(1) Armbruster (1995); Cohen-Addad (1970).
(2) Chakhmouradian et al. (2008); Takamori et al. (1987).
(3) Smyth et al. (1990).
(4) Mills et al. (2010).
(5) Galuskina et al. (2010a).
(6) Si and □ are not fully ordered at *Z*1 and *Z*2. Boiocchi et al. (2012).
(7) Ito and Frondel (1967a); Yudintsev (2003); Galuskina et al. (2010e and unpublished).
(8) Yoder and Keith (1951); Geller (1967); Jaffe (1951); Kasowski and Hogarth (1968); Grew et al. (2010).
(9) Fursenko (1982); Nishizawa and Koizuma (1975); Bühn et al. (1995); Amthauer et al. (1989); Arlt et al. (1998).
(10) Grew et al. (2010).
(11) Enami et al. (1995); Røhr et al. (2007).
(12) Ringwood and Major (1971); Stähle et al. (2011).
(13) Bishop et al. (1978); Ye et al. (2000); Breiter et al. (2005); Brunet et al. (2006).
(14) Nagashima and Armbruster (2012); Ito (1968).

Site allocation of cations

The assumed occupancies, most importantly, ^{Z}Li, ^{X}Ca, ^{Y}Sc, Ti^{4+}, $^{Y}V^{3+}$, and $^{Z}V^{5+}$ in conjunction with Table 3, lead to the following procedure for recasting chemical data into idealized site occupancies for purposes of classification.

(1) Calculate formulas from the chemical analysis assuming 8 cations and 12 anions and apportion Fe^{2+} and Fe^{3+} or Mn^{2+} and Mn^{3+} if calculations give negative values for Fe^{2+} (method of Droop 1987). If quantitative F or H data are available, assume $^{Z}\square = ¼F + ¼H$. In this case, the basis for formula calculation becomes O+(OH)+F = 12 and $\Sigma\{X\}+\Sigma[Y]+\Sigma(Z)+{}^{Z}\square_{(OH)/4}+{}^{Z}\square_{F/4} = 8$.

(2) Li, Zn, P, As^{5+}, and V^{5+} to *Z*. If Li < ¼F, assume sufficient vacancies to make up the deficit (see step 1).

(3) Si and Ge: First to *Z* to a maximum of 3 apfu, including □, overflow to *Y*.

(4) Al: First to *Z* to bring total to 3 apfu, then *Y*.

(5) Fe^{3+}: First to *Z* to bring total to 3 apfu, then *Y*.

(6) Ca, Na, K, Y, REE, Th, Pb to *X*.

(7) Al (remainder after deducting Al at *Z*), Sc^{3+}, Ti^{4+}, V^{3+}, Cr^{3+}, Mn^{3+}, Fe^{3+} (remainder after deducting Fe^{3+} at *Z*), Ga, Zr^{4+}, Hf^{4+}, Nb^{5+}, Sn^{4+}, Sb^{5+}, Te^{6+}, and U^{6+} to *Y*. If *Z* is still <3 apfu, then add Fe^{2+} to bring *Z* total to 3 apfu. If the content of *Y* exceeds 2 apfu, and *Z* is <3 apfu, then move Ti to *Z* to bring *Z* total to 3 apfu.

(8) Mg: First to *Y* to bring total to 2 apfu, then to *X*.

(9) Fe^{2+} (remainder after deducting Fe^{2+} at *Z*): First to *Y* to bring total to 2 apfu, then to *X*.

(10) Mn^{2+}: First to *Y* to bring total to 2 apfu, then to *X*. This should bring total X to 3 apfu, if calculations were done correctly.

If H is suspected, but no quantitative data are available, as is the case with electron microprobe analyses, then either its content must be assumed so that Fe^{2+}/Fe^{3+} ratio can be calculated, or the Fe^{2+}/Fe^{3+} ratio must be assumed so that H content can be calculated. In garnets containing significant Si, it is reasonable to assume that H is incorporated at the expense of Si, that is, $H = 4*({}^{Z}\square)$.

The site allocation procedure above, based solely on chemical data, fails to differentiate holtstamite from grossular, which would require additional information such as optical properties or crystallographic data, although henritermierite is uniquely determined because there is no report as yet of an isometric garnet having the composition $\{Ca_3\}[Mn^{3+}_2](Si^{4+}_2\square)O_8(OH)_4$.

We have also prepared an Excel spreadsheet (Appendix 4[1]) to perform the above cation allocation, species and group determination, but have omitted several elements that rarely exceed 1 wt% in natural garnets: B, S, K, Ni, Sr; or which occur in significant amounts but whose occurrence is rare: Ga, Ge, and Pb (Tables 6 and 8).

Identifying a garnet species

Once the cations have been allocated, then the dominant valence is determined for each site by summing the ions for each valence, e.g., Ca+Mg+Mn at the *X* site, and then the dominant

cation identified. As species are defined in terms charge-balanced end-members (Hawthorne 2002), the possibility of valency-imposed double site-occupancy (Hatert and Burke 2008) must be considered. The dominant ion for each valence determines the species (e.g., bitikleite group, Fig. 6). Six examples are given in Appendix 3[1], and a calculation procedure for species and group determination in Appendix 4[1]. Our discussion below is limited to the schorlomite and garnet groups because these are most likely to cause difficulties in identifying species.

Applying the nomenclature to the schorlomite group

Characteristic of the end-member formulas in this group is Si = 1 apfu; there are no divalent and trivalent cations at the *Y* site and no divalent or pentavalent cations at the *Z* site. However, in most analyses of Ti-, Zr-, or Sn-rich garnets containing minor Sb^{5+}, Nb^{5+}, or U^{6+}, Si commonly exceeds 1 apfu, e.g., all the analyses plotting in the schorlomite field in Figure 5 have Si >2 apfu and total charge at the *Z* site >11, because all contain substantial proportions of garnet group components (see above).

The primary criterion for a composition to belong to the schorlomite group is that the generalized schorlomite component $\{R^{2+}_3\}[R^{4+}_2](R^{4+}R^{3+}_2)O_{12}$ be the most abundant (Fig. 7); i.e., the spreadsheet gives this as the most abundant component possible. In the worked example of schorlomite from the type locality, Magnet Cove, Arkansas (Example 2), the schorlomite component is dominant, with $R^{4+} > R^{3+} > R^{2+}$ at the *Y* site in the empirical formula (Example 2), whereas in the garnet-group mineral morimotoite, the generalized morimotoite component, $\{R^{2+}_3\}[R^{4+}R^{2+}](R^{4+}_3)O_{12}$, is dominant with $R^{4+} > R^{2+} > R^{3+}$ at the *Y* site in the empirical formula (Example 5). Homovalent substitutions at the *Y* and *Z* sites distinguish species within the schorlomite group (Figs. 7 and 8), whereas the *X* site remains occupied exclusively by Ca in all end-members (Table 1).

Applying the nomenclature to the garnet group

In contrast to the schorlomite group, heterovalent substitutions relating species within the garnet group involve only the *Y* site, or the *X* and *Y* sites. Figure 9 illustrates the division of the garnet group in terms of valence of the *Y* site cations: R^{2+} = menzerite-(Y), R^{3+} = the familiar silicate garnets, and $R^{2+}R^{4+}$ = majorite, morimotoite, which results from valency-imposed double site-occupancy.

Figure 10 illustrates one approach to identification of species in complex garnet-group minerals. It is the same as Figure 9, but adapted specifically for compositions of menzerite-(Y) reported by Grew et al. (2010), i.e., R^{4+} = Ti, R^{3+} = Fe^{3+}, Al,

TABLE 7. Summary of specific components potentially significant in natural garnets

Name	Synthesis	Formula
–	62 to 90%	$\{Fe^{2+}_3\}[Al_2](\square_3)(OH)_{12}$
–	No	$\{Ca_3\}[Al_2](\square_3)F_{12}$
–	–	$\{Mn^{2+}_3\}[Al_2](\square_3)F_{12}$
–	–	$\{Fe^{2+}_3\}[Al_2](\square_3)F_{12}$
–	–	$\{Pb^{2+}_3\}[Te^{6+}](Zn_3)O_{12}$
–	–	$\{Ca_3\}[U^{6+}_2](Fe^{2+}_3)O_{12}$
–	–	$\{Mn^{2+}_3\}[Al_2](Si_2)(\square)O_8(OH)_4$
–	–	$\{Mn^{2+}_3\}[Al_2](Si_2)(\square)O_8F_4$
–	100%	$\{Th_{0.5}Ca_{2.5}\}[Zr_2](Fe^{2+}_2)O_{12}$
YIG	100%	$\{Y_3\}[Al_2](Al_3)O_{12}$
YAG	100%	$\{Y_3\}[Fe^{3+}_2](Fe^{3+}_3)O_{12}$
"Blythite"	100%	$\{Mn^{2+}_3\}[Mn^{2+}](Si_3)O_{12}$
–	100%	$\{Ca_3\}[Mn^{3+}_2](Si_3)O_{12}$
"Khoharite"	100%	$\{Mg_3\}[Fe^{3+}_2](Si_3)O_{12}$
"Skiagite"	100%	$\{Fe^{2+}_3\}[Fe^{3+}_2](Si_3)O_{12}$
–	–	$\{Y_2Ca\}[Fe^{2+}_2](Si_3)O_{12}$
–	–	$\{Y_{1.5}Na_{1.5}\}[Al_2](Si_3)O_{12}$
–	100%	$\{CaNa_2\}[Si_2](Si_3)O_{12}$
–	100%	$\{CaNa_2\}[Ti_2](Si_3)O_{12}$
–	100%	$\{Na_3\}[Al_2](P_3)O_{12}$
–	No	$\{Ca_2Na\}[Fe^{2+}_2](As^{5+}_3)O_{12}$

Note: Syntheses: percentage gives the amount of the component reported in the synthesis; no = synthesis attempted but without success, dash = synthesis has not been not attempted. Sources are given in the text and Table 6.

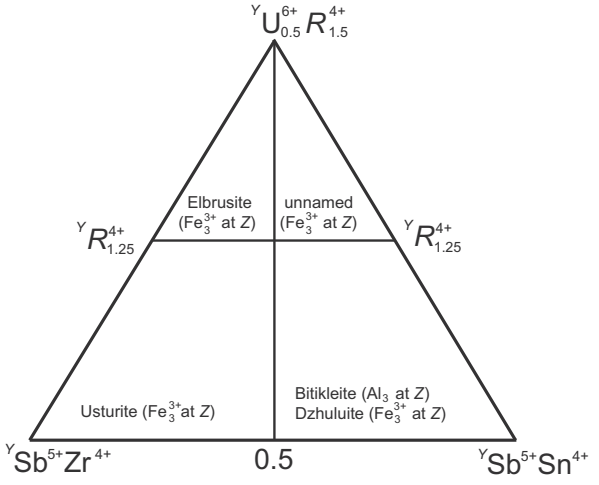

FIGURE 6. *Y*-site occupancy in species of the bitikleite group, including the possible unnamed Sn-dominant analog of elbrusite. Placement of the divisions is indicated.

TABLE 8. Possible new species in the garnet supergroup

Relationship to known species	UM no.	End-member formula	Criteria	Source
		Bitikleite group		
Sn analog of elbrusite		$\{Ca_3\}[U^{6+}_{0.5}Sn^{4+}_{1.5}](Fe^{3+}_3)O_{12}$	Sn/(Sn + Zr) = 0.93	(1)
Nb analog of usturite		$\{Ca_3\}[NbZr](Fe^{3+}_3)O_{12}$	1.33 Zr, 0.05 Ti, 0.48 Nb pfu at *Y* site	(2)
		Schorlomite group		
Al analog of schorlomite (Ti analog of kimzeyite)		$\{Ca_3\}[Ti_2](SiAl_2)O_{12}$	$Al/(Al+Fe^{3+}) = 0.65$	(3)
		Garnet group		
Mg analog of morimotoite		$\{Ca_3\}[TiMg](Si_3)O_{12}$	$Mg/(Mg + Fe^{2+}) = 0.63–0.64$	(4)
Ga–Ge analog of grossular	UM1986-19	$\{Ca_3\}[Ga_2](Ge_3)O_{12}$	$^{Z}Ge > {}^{Z}Si$; $^{Y}Ga > {}^{Y}Fe^{3+}$, ^{Y}Al	(5)
Ge analog of grossular	UM1986-20	$\{Ca_3\}[Al_2](Ge_3)O_{12}$	Criterion of $^{Z}Ge > {}^{Z}Si$ not met.	(5)

Note: UM no. refers to the list of valid unnamed minerals, update 2011-01 (Smith and Nickel 2007). Sources: (1) Galuskina et al. (2010a); (2) Zaitsev et al. (2010); (3) Koritnig et al. (1978); (4) Platt and Mitchell (1979); (5) Johan and Oudin (1986); Jambor et al. (1988b).

and R^{2+} = Mg, Fe^{2+}, and differs from Figure 7a of Grew et al. (2010) in that the Ti corner is now TiR^{2+}, representing a component in garnet, morimotoite. However, menzerite-(Y) is a four component system because of the substitution of R^{3+} for Si at the *Z* site, and compositions must be projected from four-component space onto the three-component plane shown in Figure 10. Appendix 3[1] (Example 3) gives the five possible generalized components in menzerite-(Y), of which only four are independent. We have selected the $\{Y_3\}[Al_2](Al_3)O_{12}$-type component to project menzerite-(Y) compositions. The $\{Y_3\}[Al_2](Al_3)O_{12}$-type component comprises 4–8% of the analyzed menzerite-(Y) grains. Despite the differences between Figure 10 and Figure 7a of Grew et al. (2010), the disposition of the points is very similar.

The most widespread garnet-group minerals are related by homovalent substitutions at the *X* and *Y* sites, i.e., $\{R^{2+}_3\}[R^{3+}_2](Si^{4+}_3)O_{12}$. Since only four constituents occupy the *X* site, the compositions can be plotted in a tetrahedron with Ca, Mg, Mn^{2+}, and Fe^{2+} as vertices (Fig. 11a). Garnets with one of these cations dominant at the *X* site fill a volume whose edges inside the Ca-Mg-Mn^{2+}-Fe^{2+} tetrahedron are shown as lines inside this tetrahedron. Figures 11b and 11c show compositions projected from the Mn and Ca vertices of the tetrahedron, respectively. These two faces of the tetrahedron suffice to illustrate the dispositions of the species. Final characterization will depend on the dominant occupancy of the *Y* site.

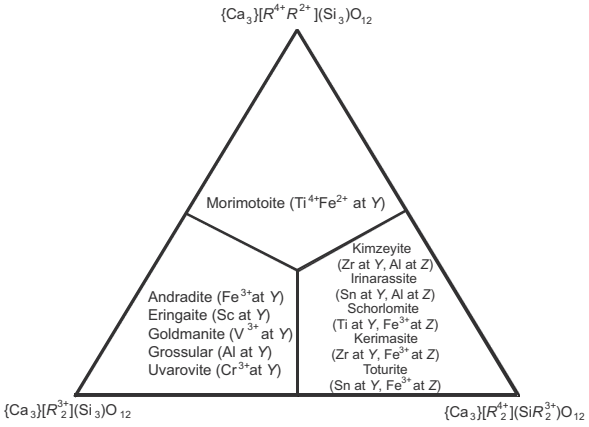

Figure 7. Diagram for discriminating the five species of the schorlomite group from Ca species in the garnet group.

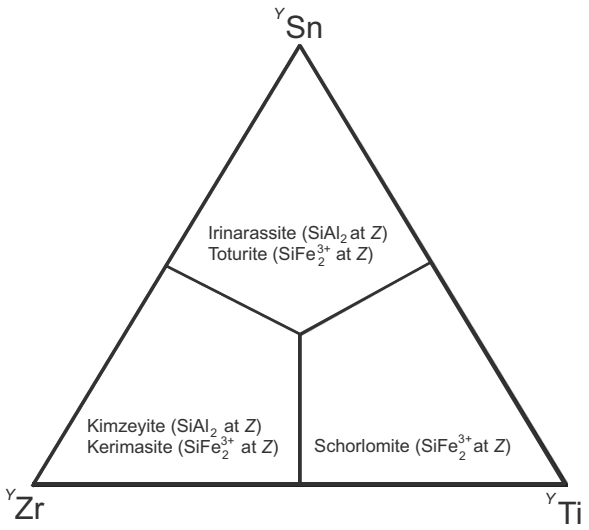

Figure 8. *Y*-site occupancy in species of the schorlomite group.

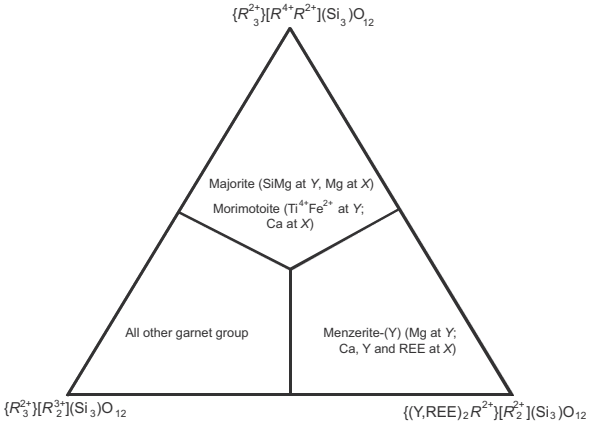

Figure 9. Diagram distinguishing menzerite-(Y) from species within the garnet group.

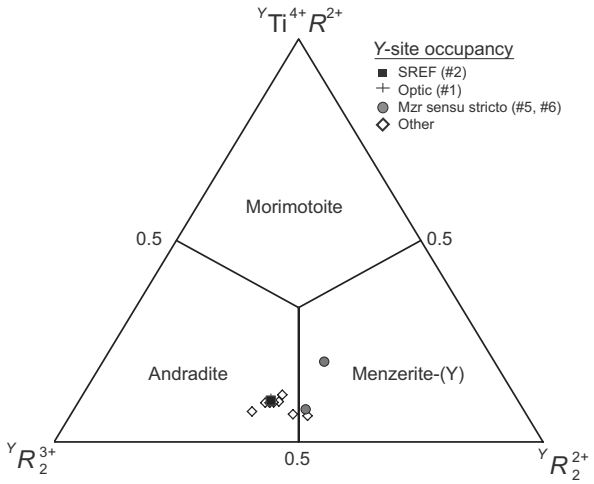

Figure 10. Plot of menzerite-(Y) compositions at the *Y* site projected from $\{Y_3\}[R^{3+}_3](R^{3+}_3)O_{12}$ onto the plane defined by the components $\{Ca_3\}[Ti^{4+}R^{2+}](Si^{4+}_3)O_{12}$, $\{Ca_3\}[R^{3+}_2](Si^{4+}_3)O_{12}$, and $\{(REE)_2Ca\}[R^{2+}_2](Si^{4+}_3)O_{12}$ (cf. Fig. 7a, Grew et al. 2010). R^{2+} = Fe in morimotoite, Mg in menzerite-(Y); R^{3+} = Fe in andradite. Numbers refer to grains used for the crystal-structure refinement (SREF), optical measurements, and menzerite-(Y) sensu stricto (Mzr), including grain no. 5 used as the holotype to characterize the mineral. The points for SREF and Optic are superimposed. Open diamonds indicate the other nine grains analyzed (data from Grew et al. 2010).

Possible new species and compositional variations in natural garnet

The compositional variations found in the 32 approved species by no means exhaust the compositional variations observed in natural garnet, which is greatly exceeded by the very extensive variations in synthetic garnet. In the present section we will consider these variations, note compositions containing components that could be new species if they were present in larger amounts (Tables 6 and 7), and briefly describe possible new species (Table 8). Synthetic garnets will be considered only in so far that they relate to natural garnets. The components are discussed under the group to which they would belong.

Vacancy-dominant garnets—A "kenogarnet" group?

Vacancy-dominant garnets are distinguished by φ being a monovalent anion such as OH or F, as well as low content of cations at the *Z* site. Katoite is the only known garnet that is vacancy-dominant. However, there is considerable potential to discover more species, and thus a group could be recognized following the procedures outlined in Mills et al. (2009). In anticipation, we suggest the name "kenogarnet" from the Greek *kenos*, meaning "empty," a term introduced as a prefix in pyrochlore supergroup nomenclature (Atencio et al. 2010).

The most abundant vacancy-dominant garnets are the so-called "hydrogarnets," an informal term (Appendix 2) introduced by Flint et al. (1941) and generally used for any garnet containing OH incorporated by the substitution of (O_4H_4) tetrahedra for (SiO_4) tetrahedra (Fig. 3). Significant incorporation of OH by this substitution is largely limited to garnet in which the *X* site is occupied by Ca, e.g., katoite, henritermierite, and holtstamite. Up to 10 wt% H_2O has also been reported in andradite (Peters 1965; Lager et al. 1989; Armbruster 1995; Amthauer and Rossman 1998), leading to compositions with up to 35% of the Fe^{3+} analog of katoite (Table 6) and 4.5% of its Mn^{3+} analog (H content calculated by difference from Si occupancy determined by single-crystal refinement, Armbruster 1995). Galuskina and Galuskin (2003) and Galuskin (2005) calculated OH contents of 2.6–2.9 apfu (equivalent to 4.8–5.1 wt% H_2O) from charge balance in "hydroschorlomite" containing 13.5–14.5 wt% TiO_2 from the Wiluy River, Yakutia, Russia, the highest reported in Ti-rich garnets (cf. Chegem caldera schorlomite discussed above). In contrast, H_2O contents in pyrope, almandine, and uvarovite are reported not to exceed 0.3 wt%, and, in spessartine, not above 0.64 wt% (e.g., Aines and Rossman 1984; Rossman et al. 1988; Smyth et al. 1990; Andrut and Wildner 2001; Maldener et al. 2003; Beran and Libowitzky 2006; Johnson 2006). Wilkins and Sabine (1973) reported 2.5 wt% H_2O in spessartine,

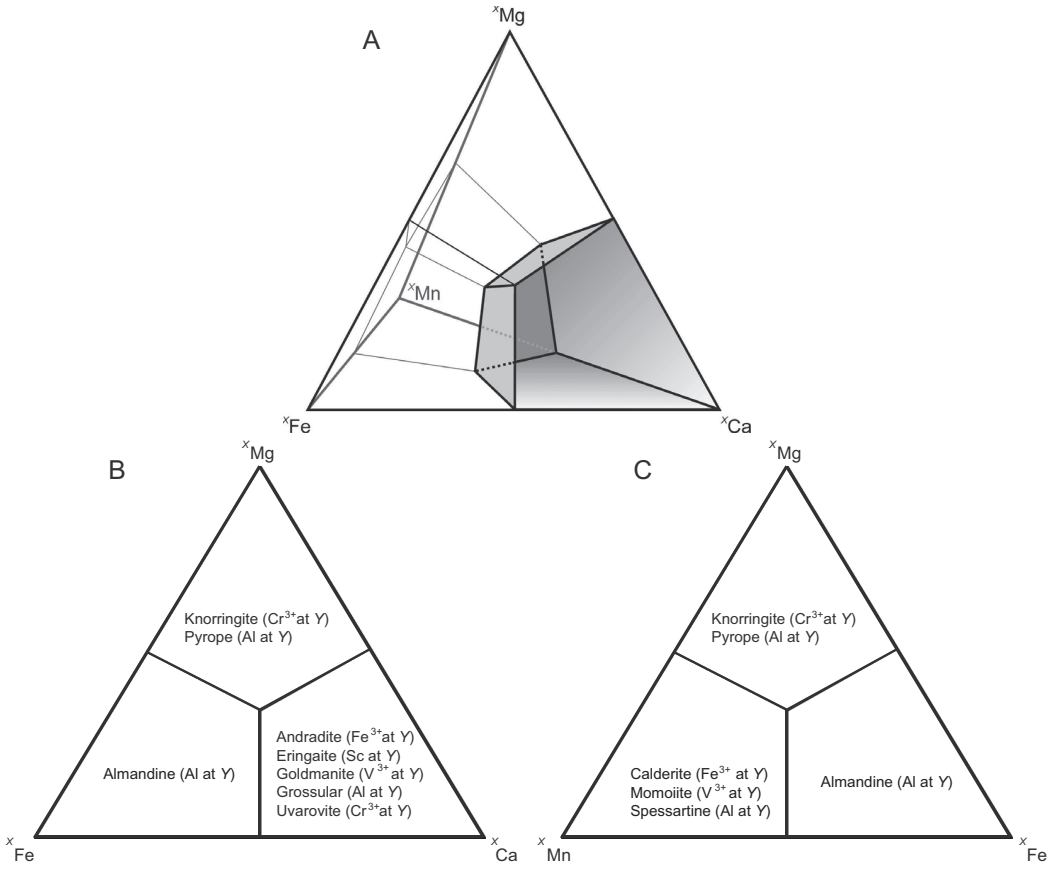

Figure 11. (**a**) Tetrahedron illustrating divisions in the garnet group based on occupancy of the *X* site. One compositional volume is shown with shading. (**b**) Projection from the Mn vertex onto front face of the tetrahedron to distinguish species. (**c**) Projection from the Ca vertex onto left face of the tetrahedron to distinguish species.

but this high content is anomalous and needs confirmation.

Only "hydrogarnets" with the large cations Ca and Sr (Ito and Frondel 1967b; Ivanov-Emin et al. 1982a, 1982b) at the *X* site have been synthesized, including katoite (Flint et al. 1941; Cohen-Addad et al. 1967). Syntheses of the hydroxyl-dominant analogues of uvarovite (Morán-Miguélez et al. 1986) and eringaite (Ivanov-Emin et al. 1982a); as well as of $\{Ca_3\}[Mn_2^{3+}](\square_3)(OH)_{12}$ (Ivanov-Emin et al. 1982b), $\{Ca_3\}[TiFe^{3+}](Fe^{3+}\square_2)(OH)_8O_4$ (Ito and Frondel 1967b), and $\{Ca_3\}[ZrFe^{3+}](Fe^{3+}\square_2)(OH)_8O_4$ (Ito and Frondel 1967b) have been reported. However, attempts to synthesize the end-member $\{Ca_3\}[Fe_2^{3+}](\square_3)(OH)_{12}$ failed, although a garnet with about 90% $\{Ca_3\}[Fe_2^{3+}](\square_3)(OH)_{12}$ and 10% andradite could be synthesized (Flint et al. 1941; Ito and Frondel 1967b). The reported compositions are based on starting materials; only the compositions of katoite and a hydroxyl-dominant analog of andradite, $\{Ca_3\}[Fe_2^{3+}](Si_{1.15}\square_{1.85})(OH)_{7.4}O_{4.6}$, have been confirmed independently (e.g., by structure refinement, Cohen-Addad 1970; Cohen-Addad et al. 1967). In summary, the H_2O contents of natural and synthetic garnets are consistent with the conclusion reached by Lager et al. (1989) that the extent of OH substitution in garnets appears to be structurally controlled, i.e., it is greater, when the effective ionic radius (Shannon 1976) of the *X*-site cation exceeds 1.0 Å and the shared octahedral edge is longer than the unshared edge, which is the case for natural and synthetic garnets with Ca dominant at the *X* site (Novak and Gibbs 1971; Quartieri et al. 2006).

Fluorine contents up to 6 wt% F, equivalent to about 11 mol% of a $\{R_3^{2+}\}[R_2^{3+}](\square_3)F_{12}$, have been reported in grossular, spessartine, and andradite (Valley et al. 1983; Flohr and Ross 1989; Manning and Bird 1990; Smyth et al. 1990; Barbanson and Bastos Neto 1992; Visser 1993; Włodyka and Karwowski 2006; Chakhmouradian et al. 2008). Only Smyth et al. (1990) measured H_2O content, reporting 0.64 wt% in the F-bearing spessartine (Table 6), equivalent to 3% $\{R_3^{2+}\}[R_2^{3+}](\square_3)(OH)_{12}$, but Flohr and Ross (1989) and Chakhmouradian et al. (2008) reported evidence for H_2O in the infrared and Raman spectra. Attempts to synthesize an F-dominant analog of katoite have not been successful (Takamori et al. 1987).

Chlorine was sought in four of the studies of F-bearing garnet cited above, but no more than 0.01 wt% Cl was reported. Up to 0.2 wt% Cl was reported in OH-bearing grossular from the Wiluy River, Yakutia, Russia (Galuskina et al. 2001). Chesnokov (1996), Chesnokov and Bushmakin (1995), and Chesnokov et al. (1994, 2008) described "igumnovite," ideally $\{Ca_3\}[Al_2](Si_2\square)O_8Cl_4$, and "chlorhibschite," ideally, $\{Ca_3\}[Al_2](Si_{3-x}\square_x)O_8Cl_{4-x}$, from burned material in the Chelyabinsk coal basin, Urals, Russia, but these compounds are not considered to be naturally formed, and thus do not qualify as minerals (e.g., "igumnovite," Jambor et al. 1997). The reported cell parameter of 12.008 Å for "igumnovite" is smaller than expected for a Cl-rich garnet from the relationship of Langley and Sturgeon (1979). Although the measured composition for "igumnovite," $Ca_{3.04}Al_{1.72}Fe_{0.13}Mg_{0.01}Si_{2.07}F_{0.03}O_{7.90}Cl_{4.07}$ approaches ideal garnet stoichiometry, it is doubtful that either "igumnovite" or "chlorhibschite" are garnets. More likely, "igumnovite" is related to mayenite, wadalite, and the new mineral eltyubyuite (Galuskin et al. 2011b), whereas "chlorhibschite" could be a mixture of grossular, wadalite, and, perhaps, chlorides.

Yafsoanite

The 9% proportion of the component $\{Pb_3^{2+}\}[Te_2^{6+}](Zn_3)O_{12}$ listed in Tables 6 and 7 is based on the single-crystal structure refinement of material from the type locality (Mills et al. 2010; cf. Jarosch and Zemann 1989). Electron microprobe analyses reported in the original description gave 11–16% of the Pb analog (Kim et al. 1982), but the formulas deviate from ideal stoichiometry, possibly as a result of using sulfides, a silicate and a native element for standards. Ronniger and Mill' (1973) reported synthesis of several Pb^{2+}-bearing vanadate garnets (berzeliite group) with Pb at the *X* site, and Mill' (1970) reported synthesis of yafsoanite and other Te-bearing garnets, but neither reported attempts to synthesize the Pb^{2+} analog of yafsoanite.

The unnamed end-member $\{Ca_3^{2+}\}[U_2^{6+}](Fe_3^{2+})O_{12}$ is calculated to be major constituent of elbrusite (Fig. 4; Table 6) and dzhuluite (Appendix 3[1]), but has not yet been synthesized.

Henritermierite group

Boiocchi et al. (2012) reported nearly end-member spessartine containing 0.09 Fe and 0.04 Ca pfu, but only 2.52 Si pfu, the deficiency being made up by OH and F in nearly equal proportions (Table 6). The $I4_1/acd$ symmetry indicates that the mineral is more closely analogous to holtstamite rather than katoite. The spessartine is the first example of a garnet showing $I4_1/acd$ symmetry but containing no Mn^{3+}, and thus Boiocchi et al. (2012) attribute the lower symmetry to $(OH, F)_4$ groups. Si is partially ordered, preferentially occupying the *Z*1 site (93.0%) vs. the *Z*2 site (73.8%).

Bitikleite group

Given the large number of elements found in analyses of garnets of the bitikleite group, the potential for new species is great. For example, analysis 10 of elbrusite in Table 2 of Galuskina et al. (2010a) corresponds to the Sn-dominant analog of elbrusite (Fig. 4), and is possibly a new species (Table 8). Zaitsev et al. (2010) reported a zone with up to 10.1 wt% Nb_2O_5 in a kerimasite crystal, this amount corresponds to 0.48 Nb per formula unit, or nearly 50% of a $\{Ca_3\}[NbZr](R_3^{3+})O_{12}$ component, which implies the possibility of new species for R^{3+} = Fe and Al, the Nb analog of usturite (Table 8).

Up to 4 wt% ThO_2 (0.1 Th pfu) has been reported in bitikleite and schorlomite-group minerals (Lupini et al. 1992; Galuskina et al. 2010a, 2010e), which would correspond to 20 mol% of a $\{Th_{0.5}Ca_{2.5}\}[R_2^{4+}](R_3^{3+})O_{12}$ component. The end-member with Zr and Fe, i.e., $\{Th_{0.5}Ca_{2.5}\}[Zr_2^{4+}](Fe_3^{3+})O_{12}$, has been synthesized (Ito and Frondel 1967a; Yudintsev 2003; Utsunomiya et al. 2005).

Yttrium-aluminum (YAG) and yttrium-iron (YIG) garnets

The rare earth elements can form a large number of synthetic compounds having general formulas of the type $\{R_3^{3+}\}[R_2^{3+}](R_3^{3+})O_{12}$ and isostructural with garnet (e.g., Yoder and Keith 1951; Geller 1967), of which $\{Y_3\}[Al_2](Al_3)O_{12}$ (yttrium aluminum garnet or YAG) and $\{Y_3\}[Fe_2^{3+}](Fe_3^{3+})O_{12}$ (yttrium iron garnet or YIG) are the most relevant to minerals (Tables 6 and 7). Although the total charge at *Z* is 9, the garnet end-members YAG and YIG have not been placed in the bitikleite group because of the very different occupancies at *Y* and *X*. Up to 5 mol% of the YAG component has been reported in spessartine and almandine (e.g.,

Jaffe 1951; Røhr et al. 2007), and 5 mol% of the YIG component has been reported in andradite (Kasowski and Hogarth 1968), but the maximum proportion of a generalized $\{(Y,REE)_3\}[(Fe^{3+},Al)_2](Al_3)O_{12}$ component in a natural garnet is 8% in menzerite-(Y)-andradite solid solution (Grew et al. 2010).

Schorlomite group

Koritnig et al. (1978) reported Zr-rich schorlomite from calc-silicate inclusions in gabbro of Radautal, Harz Mountains, Germany. Analyses of three samples gave 6.2–6.8 wt% Al_2O_3 and 23.1–25.6 wt% SiO_2 contents; the sample giving the highest ZrO_2 content (Zr = 0.55 apfu) is plotted in Figure 5. Our calculations for this sample give 48.9–49.0% $\{Ca_3\}[R^{4+}_2](SiR^{3+}_2)O_{12}$ with Ti > Zr at *Y* and Al > Fe^{3+} at Z, i.e., a possible Al analog of schorlomite or Ti analog of kimzeyite. Using Mössbauer spectroscopic data, Koritnig et al. (1978) gave the Z site composition as $(Si_{2.00}Al_{0.56}Fe^{2+}_{0.24}Ti_{0.16}Fe^{3+}_{0.03})$. Ito and Frondel (1967a) synthesized end-member schorlomite and kimzeyite, but we are not aware of a successful synthesis of the end-member $\{Ca_3\}[Ti_2](SiAl_2)O_{12}$.

Garnet group

Formulas calculated from the two analyses richest in Ti from garnets of the Marathon dikes, Ontario (Platt and Mitchell 1979), plot in the morimotoite field (Fig. 5) and have total Mg/(Mg+Fe^{2+}) = 0.63–0.64, i.e., the end-member $\{Ca_3\}[TiMg](Si_3)O_{12}$, the Mg analog of morimotoite, is dominant (Table 8). However, the Marathon dike compositions plot close to the boundary with schorlomite and calculation of Fe^{2+}/Fe^{3+} ratio from stoichiometry has a large uncertainty (Giaramita and Day 1990); thus a clear dominance of $\{Ca_3\}[TiMg](Si_3)O_{12}$ in a natural garnet remains to be demonstrated.

Gallium and germanium can form a large number of synthetic compounds isostructural with garnet (Geller 1967), but only $\{Ca_3\}[Ga_2](Ge_3)O_{12}$ might have a natural analog. Johan and Oudin (1986) reported from the Pyrenees of France equant, six-sided crystals up to 10 μm across of a Ca-Ga-Ge mineral having compositions consistent with garnet stoichiometry (abstract in Jambor et al. 1988b). Cores of the highly zoned grains are close to $\{Ca_3\}[Ga_2](Ge_3)O_{12}$ in composition, whereas the rims have compositions approximately intermediate between this composition and grossular. The list of valid unnamed minerals (Smith and Nickel 2007) also gave $\{Ca_3\}[Al_2](Ge_3)O_{12}$ as a possible new species (Table 8), but our recalculation of formulas from the two compositions closest to this end-member (Johan and Oudin 1986) gave Si > Ge at the *Z* site and minor Ge at the *Y* site assuming Si is preferentially incorporated at the *Z* site. The crystals were too small to confirm the identification as a garnet by the technologies available at the time.

Fermor (1926, 1938) introduced three hypothetical garnet end-members (Tables 6–7; Appendix 2): "blythite," $\{Mn^{2+}_3\}[Mn^{3+}_2](Si_3)O_{12}$, as a subordinate component in a garnet from Cargoan, Nagpur, India; "khoharite," $\{Mg^{2+}_3\}[Fe^{3+}_2](Si_3)O_{12}$, as the precursor to enstatitic chondrules in the Khohar meteorite and as a subordinate component in a pyrope from a "garnet-diopside" xenolith (eclogite?) in kimberlite from South Africa; and "skiagite," $\{Fe^{2+}_3\}[Fe^{3+}_2](Si_3)O_{12}$, as a component in almandine from Glen Skiag, Scotland. Although later studies have reported up to nearly 9 mol% "blythite" based on measurement or stoichiometric calculation of Mn^{3+} in andradite from manganese formations, Otjosondu, Namibia (Amthauer et al. 1989; Bühn et al. 1995), "khoharite" and "skiagite" have been elusive, e.g., Virgo and Yoder (1974) failed to find "skiagite" in spessartine-almandine from the type locality at Glen Skiag, Scotland. The main problem in identifying these components in complex natural garnets is that the calculation depends on the sequence of calculation (Rickwood 1968; Locock 2008), i.e., Fe^{3+} is first assumed to be present as the andradite component; only leftover Fe^{3+} would be combined with Fe^{2+} or Mg in the "skiagite" or "khoharite" components, respectively, and Mn^{3+} could be present as $\{Ca_3\}[Mn^{3+}_2](Si_3)O_{12}$ as well as $\{Mn^{2+}_3\}[Mn^{3+}_2](Si_3)O_{12}$ in the Otjosondu garnet (Table 6). Garnets containing a significant proportion of the $\{Ca_3\}[Mn^{3+}_2](Si_3)O_{12}$,"blythite," "khoharite," and "skiagite" end-members have been synthesized at relatively high pressures, i.e., above 30 kbar (Coes 1955; Nishizawa and Koizumi 1975; Karpinskaya et al. 1982; Fursenko 1983; Woodland and O'Neill 1993, 1995; Arlt et al. 1998), and could become more abundant under mantle pressures.

Rudashevskii and Mochalov (1984) reported a Mn-Cr-Si mineral thought be a garnet in heavy concentrates from eluvium of Pt-bearing serpentinite in the Far East of Russia (summary in Jambor et al. 1988a). The mineral forms highly zoned grains 1–30 μm across enclosed in Cr-Ni-bearing γ-Fe. The formula (with cations grouped by valence) for the analysis with the highest Cr content is $\{Mn^{2+}_{2.99}\}[(Cr^{3+}_{1.14}Mn^{3+}_{0.51})Ti_{0.35}]\{(Si_{2.22}Ti_{0.35})(Al_{0.28}Fe^{3+}_{0.08})\}O_{12}$, i.e., a $\{Mn^{2+}_3\}[Cr^{3+}_2](Si_3)O_{12}$ component can be considered dominant, whereas that for the lowest Cr content is $\{Mn^{2+}_3\}[(Mn^{3+}_{0.79}Cr^{3+}_{0.60}Al_{0.09}Fe^{3+}_{0.08})Ti_{0.22}Mn^{2+}_{0.22}](Si_{3.01})O_{12}$, i.e., with "blythite" dominant. The presence of significant Mn^{3+} in association with Fe^0 is unexpected, as is the preservation of metallic Fe in eluvium. In the absence of X-ray or electron diffraction patterns and clearer evidence for the natural origin of the concentrates, the natural occurrence of a $\{Mn^{2+}_3\}[Cr^{3+}_2](Si_3)O_{12}$-dominant or $\{Mn^{2+}_3\}[Mn^{3+}_2](Si_3)O_{12}$-dominant garnet remains to be demonstrated.

Three components have been proposed for incorporation of Na in garnet-group minerals (Tables 4 and 6), all of which have been inferred to be favored by increasing pressure, $^{X}Na+^{X}(Y, Yb) = 2^{X}R^{2+}$ (Enami et al. 1995; Røhr et al. 2007) and $^{X}Na+^{Y}Si = {}^{X}R^{2+}+{}^{Y}Al$ or $^{X}Na+^{Y}Ti = {}^{X}R^{2+}+{}^{Y}Al$ (Ringwood and Major 1971; Sobolev and Lavrent'ev 1971; Bobrov et al. 2008; Harte 2010; Collerson et al. 2010).

Berzeliite group

Phosphorus contents generally do not exceed 1 wt% P_2O_5 in pyrope, almandine, and spessartine, both in wet chemical (e.g., Koritnig 1965; Deer et al. 1982) and in electron microprobe analyses (e.g., Bishop et al. 1978; Hiroi et al. 1997; Breiter et al. 2005; Kawakami and Hokada 2010). Mason and Berggren (1942) reported 4.1 wt% P_2O_5 in spessartine from Wodgina, Australia (sample no. NRM 884695, Swedish Museum of Natural History), but Breiter et al. (2005) found only 0.24–0.27 wt% with the electron microprobe. An energy-dispersive spectroscopic analysis of the spessartine in this specimen (normalized to 100%) with an SEM gave P contents closer to the amounts reported by Breiter et al. (2005): SiO_2 35.78, Al_2O_3 20.52 FeO 3.91, MnO 39.15, CaO 0.20, P_2O_5 0.42 (±0.12) (Hålenius, unpublished data). The spessartine grains are cut by microfissures ranging

from <1 μm to ca. 10 μm thick filled with Ca-Mn-phosphates. In some grains, the microfissures are sufficiently abundant to form networks, whereas in other grains they occurred singly up to 100 μm apart. It would have been nearly impossible to obtain a pure spessartine concentrate suitable for wet chemical analyses from this specimen.

Thompson (1975) reported experimental evidence for increased incorporation of P and Na with increasing pressure, a relationship consistent with the presence of up to 0.25 wt% P_2O_5 in pyrope associated with coesite at Dora Maira, Italy (Brunet and Lecocq 1999), exsolved apatite in garnet from mantle eclogite (Haggerty et al. 1994) and with the synthesis of $\{Na_3\}[Al_2](P_3)O_{12}$ at 150–170 kbar by Brunet et al. (2006). Thilo (1941) reported synthesis of $\{Na_3\}[Al_2](P_3)O_{12}$ at atmospheric pressure, but subsequent attempts to reproduce such syntheses failed (Schwarz and Schmidt 1971). On the basis of a large number of analyses yielding up to 1.21 wt% P_2O_5 (equivalent to 0.086 P pfu) in almandine and spessartine from granitic rocks, Breiter et al. (2005) showed that: (1) P content varies inversely with Si; (2) Na/P ratio to be approximately 1/5; and (3) Al is relatively constant, consistent with the substitutions $^X\square+2^Z\mathrm{P} = {}^X\!R^{2+}+2^Z\mathrm{Si}$ and much subordinate $^X\mathrm{Na}+^Z\mathrm{P} = {}^X\!R^{2+}+{}^Z\mathrm{Si}$. There was no evidence in their data for the substitution $^Z(\mathrm{Al,Fe^{3+}})+^Z\mathrm{P} = 2^Z\mathrm{Si}$ reported in an almandine-spessartine containing up to 2.1 wt% P_2O_5 from rhyolite, Tanzawa Mountainland, Japan (Arima and Yamashita 1994). Breiter et al. (2005) also concluded that the main control on incorporation of P seems to be the P contents in melt or post-magmatic fluid instead of pressure.

The maximum FeO content reported in a berzeliite-group mineral is 1.52 wt% in berzeliite from Montaldo mine, Italy, equivalent to 6% of the $\{Ca_2Na\}[Fe_2^{2+}](As_3^{5+})O_{12}$ end-member (Nagashima and Armbruster 2012). Attempts to synthesize the Fe^{2+} analog of berzeliite have not been successful (Ito 1968; Schwarz and Schmidt 1971).

Summary of conclusions, actions, and recommendations

- The garnet supergroup comprises 32 approved species, with an additional 5 possible species needing further study to be approved.
- The supergroup includes all minerals isostructural with garnet regardless of what elements occupy specific cation or anion sites.
- We have subdivided the supergroup into groups based on symmetry and total charge at the tetrahedral *Z* site. Twenty-nine species belong to one of five groups, one tetragonal (henritermierite), and four isometric—bitikleite, schorlomite, garnet, and berzeliite, in which the total *Z* charge is 8, 9, 10, 12, and 15, respectively. Three species are single representatives of potential groups in which total charge at *Z* is 0 (katoite), 3 (cryolithionite), and 6 (yafsoanite).
- Species are identified on the basis of the dominant-constituent and dominant-valency rules, and in some cases, by valency-imposed double site-occupancy.
- We recommend that suffixes (other than Levinson modifiers) not be used in naming minerals in the garnet supergroup. We have discredited existing names that have suffixes and replaced them with new root names where necessary, specifically, bitikleite-(SnAl) with bitikleite, bitikleite-(SnFe) with dzhuluite, bitikleite-(ZrFe) with usturite, and elbrusite-(Zr) with elbrusite.
- We have discredited the name hibschite in favor of grossular, as Si is the dominant cation at the *Z* site.
- Twenty-one end-members have been reported as subordinate components in minerals of the garnet supergroup of which six have been reported in amounts up to 20 mol% or more, whereas several others have been synthesized, which implies the potential for more species in the garnet supergroup.

Acknowledgments

We thank Thomas Armbruster, Anton Chakhmouradian, Anastasia Chopelas, and Anatoly Zaitsev for their assistance during preparation of these recommendations. Members of the CNMNC and Roberta Oberti commented on the version voted on by the CNMNC; Fernando Colombo, Darrell Henry, and Milan Novák commented on the version submitted to *American Mineralogist*—we are grateful to all for their constructive reviews, which resulted in substantial improvement of the manuscript. Makoto Arima is thanked for a translation of Arima and Yamashita (1994) and Pavel Kartashov for permission to publish his photograph of cryolithionite (Fig. 1b). We thank Carol Stockton for her assistance with Appendix 2. Jan Cempírek is thanked for sharing unpublished EMPA and LA-ICP-MS data on Li-bearing garnet from Horní Bory, Czech Republic. E.S.G. is supported by U.S. National Science Foundation Grant EAR 0837980 to the University of Maine.

References cited

Agricola, G. (1546) De natura fossilium. Translated by M.C. Bandy and J.A. Bandy (1955) Textbook of Mineralogy, Geological Society of America Special Paper 63.

Aines, R.D. and Rossman, G.R. (1984) The hydrous component in garnets: pyralspites. American Mineralogist, 69, 1116–1126.

Allmann, R. and Hinek, R. (2007) The introduction of structure types into the inorganic crystal structure database ICSD. Acta Crystallographica, A63, 412–417.

Amthauer, G. and Rossman, G.R. (1998) The hydrous component in andradite garnet. American Mineralogist, 83, 835–840.

Amthauer, G., Annersten, H., and Hafner, S.S. (1977) The Mössbauer spectrum of ^{57}Fe in titanium-bearing andradites. Physics and Chemistry of Minerals, 1, 399–413.

Amthauer, G., Katz-Lehnert, K., Lattard, D., Okrusch, M., and Woermann, E. (1989) Crystal chemistry of natural Mn^{3+}-bearing calderite-andradite garnets from Otjosondu, SWA/Namibia. Zeitschrift für Kristallographie, 189, 43–56.

Andrut, M. and Wildner, M. (2001) The crystal chemistry of birefringent natural uvarovites: Part I. Optical investigations and UV-VIS-IR absorption spectroscopy. American Mineralogist, 86, 1219–1230.

Angel, R.J., Finger, L.W., Hazen, R.M., Kanzaki, M., Weidner, D.J., Liebermann, R.C., and Veblen, D.R. (1989) Structure and twinning of single-crystal $MgSiO_3$ garnet synthesized at 17 GPa and 1800 °C. American Mineralogist, 74, 509–512.

Arima, M. and Yamashita, H. (1994) P_2O_5-rich garnet from Hosokawa-dani, Tanzawa Mountainland. Journal of Mineralogy, Petrology and Economic Geology, 89, 166 (Abstract, in Japanese).

Arlt, T., Armbruster, T., Miletich, R., Ulmer, P., and Peters, T. (1998) High pressure single-crystal synthesis, structure and compressibility of the garnet $Mn_3^{2+}Mn_2^{3+}[SiO_4]_3$. Physics and Chemistry of Minerals, 26, 100–106.

Armbruster, T. (1995) Structure refinement of hydrous andradite, $Ca_3Fe_{1.54}Mn_{0.20}Al_{0.26}(SiO_4)_{1.65}(O_4H_4)_{1.35}$, from the Wessels mine, Kalahari manganese field, South Africa. European Journal of Mineralogy, 7, 1221–1225.

Armbruster, T. and Geiger, C.A. (1993) Andradite crystal chemistry, dynamic X-site disorder and structural strain in silicate garnets. European Journal of Mineralogy, 5, 59–71.

Armbruster, T., Geiger, C.A., and Lager, G.A. (1992) Single-crystal X-ray structure study of synthetic pyrope almandine garnets at 100 and 293 K. American Mineralogist, 77, 512–521.

Armbruster, T., Birrer, J., Libowitzky, E., and Beran, A. (1998) Crystal chemistry of Ti-bearing andradites. European Journal of Mineralogy, 10, 907–921.

Armbruster, T., Kohler, T., Libowitzky, E., Friedrich, A., Miletich, R., Kunz, M., Medenbach, O., and Gutzmer, J. (2001) Structure, compressibility, hydrogen bonding, and dehydration of the tetragonal Mn^{3+} hydrogarnet, henritermierite. American Mineralogist, 86, 147–158.

Atencio, D., Andrade, M.B., Christy, A.G., Gieré, R., and Kartashov, P.M. (2010) The pyrochlore supergroup of minerals: Nomenclature. Canadian Mineralogist, 48, 673–698.

Aubry, A., Dusausoy, Y., Laffaille, A., and Protas, J. (1969) Détermination et

étude de la structure cristalline de l'henritermiérite, hydrogrenat de symétrie quadratique. Bulletin de la Société Française de Minéralogie et de Cristallographie, 92, 126–133.
Back, M.E. and Mandarino, J.A. (2008) Fleischer's Glossary of Mineral Species 2008. The Mineralogical Record, Inc., Tucson, Arizona.
Barbanson, L. and Bastos Neto, A.C. (1992) Hydroandradite titanifère fluorée et grenat ($Spe_{39}Gro_{31}Alm_{23}And_6$) fluoré des granitoïdes du district à fluorine de Santa Catarina (Brésil): Description minéralogique, mécanisme d'incorporation du fluor, signification pétrologique et métallogénique. Comptes Rendus de l'Académie des Sciences, Série, 2, 314, 63–69.
Basso, R. (1987) The crystal structure of palenzonaite, a new vanadate garnet from Val Graveglia (Northern Apennines, Italy). Neues Jahrbuch für Mineralogie Monatshefte, 1987, 136–144.
Basso, R. and Cabella, R. (1990) Crystal chemical study of garnets from metarodingites in the Voltri Group metaophiolites (Ligurian Alps, Italy). Neues Jahrbuch für Mineralogie Monatshefte, 1990, 127–136.
Basso, R., Cimmino, F., and Messiga, B. (1984a) Crystal chemistry of hydrogarnets from three different microstructural sites of a basaltic metarodingite from the Voltri Massif (Western Liguria, Italy). Neues Jahrbuch für Mineralogie Abhandlungen, 148, 246–258.
——— (1984b) Crystal chemical and petrological study of hydrogarnets from a Fe-gabbro metarodingite (Gruppo di Voltri, Western Liguria, Italy). Neues Jahrbuch für Mineralogie Abhandlungen, 150, 247–258.
Belyankin, D.S. and Petrov, V.P. (1941) The grossularoid group (hibschite, plazolite). American Mineralogist, 26, 450–453.
Beran, A. and Libowitzky, E. (2006) Water in natural mantle minerals II: Olivine, garnet and accessory minerals. In H. Keppler and J.R. Smyth, Eds., Water in nominally anhydrous minerals, 62, 169–191. Reviews in Mineralogy and Geochemistry, Mineralogical Society of America, Chantilly, Virginia.
Beudant, F.S. (1832) Spessartine. Traité Élémentaire de Minéralogie, Second edition, volume 2, Paris, 52–55.
Birkett, T.C. and Trzcienski, W.E. Jr. (1984) Hydrogarnet: multi-site hydrogen occupancy in the garnet structure. Canadian Mineralogist, 22, 675–680.
Bishop, F.C., Smith, J.V., and Dawson, J.B. (1978) Na, K, P and Ti in garnet, pyroxene and olivine from peridotite and eclogite xenoliths from African kimberlites. Lithos, 11, 155–173.
Blix, R. and Wickman, F.E. (1959) A contribution to the knowledge of the mineral berzeliite. Arkiv för Mineralogi och Geologi, 2, 417–424.
Bobrov, A.V., Litvin, Yu.A., Bindi, L., and Dymshits, A.M. (2008) Phase relations and formation of sodium-rich majoritic garnet in the system $Mg_3Al_2Si_3O_{12}$-$Na_2MgSi_5O_{12}$ at 7.0 and 8.5 GPa. Contributions to Mineralogy and Petrology, 156, 243–257.
Boiocchi, M., Bellatreccia, F., Della Ventura, G., and Oberti, R. (2012) On the symmetry and atomic ordering in (OH,F)-rich spessartine: towards a new hydrogarnet end-member. Zeitschrift für Kristallographie, 227, 385–395, DOI: 10.1524/zkri.2012.1487.
Bordage, A., Brouder, C., Balan, E., Cabaret, D., Juhin, A., Arrio, M.-A., Sainctavit, P., Calas, G., and Glatzel, P. (2010) Electronic structure and local environment of substitutional V^{3+} in grossular garnet $Ca_3Al_2(SiO_4)_3$: *K*-edge X-ray absorption spectroscopy and first-principles modeling. American Mineralogist, 95, 1161–1171.
Boysen, H., Lerch, M., Stys, A., and Senyshyn, A. (2007) Structure and oxygen mobility in mayenite ($Ca_{12}Al_{14}O_{33}$): A high-temperature neutron powder diffraction study. Acta Crystallographica, B63, 675–682.
Breiter, K., Novák, M., Koller, F., and Cempírek, J. (2005) Phosphorus – an omnipresent minor element in garnet of diverse textural types from leucocratic granitic rocks. Mineralogy and Petrology, 85, 205–221.
Brunet, F. and Lecocq, D. (1999) Phosphorus incorporation in garnet: natural and experimental data. European Journal of Mineralogy, 11, 43 (abstract).
Brunet, F., Bonneau, V., and Irifune, T. (2006) Complete solid-solution between $Na_3Al_2(PO_4)_3$ and $Mg_3Al_2(SiO_4)_3$ garnets at high pressure. American Mineralogist, 91, 211–215.
Bubeck, W. and Machatschki, F. (1935) Die Kristallstruktur des Berzeliit $(Ca,Na)_3(Mg,Mn)_2[AsO_4]_3$. Zeitschrift für Kristallographie, 90, 44–50.
Bühn, B., Okrusch, M., Woermann, E., Lehnert, K., and Hoernes, S. (1995) Metamorphic evolution of Neoproterozoic manganese formations and their country rocks at Otjosondu, Namibia. Journal of Petrology, 36, 463–496.
Carlson, W.D. (2012) Rates and mechanism of Y, REE, and Cr diffusion in garnet. American Mineralogist, 97, 1598–1618.
Cartie, B., Archaimbault, F., Choisnet, J., Rulmont, A., Tarte, P., and Abs-Wurmbach, I. (1992) About the occurrence of tetrahedrally co-ordinated Sn^{4+} and Ti^{4+} in the new synthetic garnet-type solid solution $Ca_3Sn_{3-x}Ti_xFe_2O_{12}$ ($0.25 \leq x \leq 1.50$). Journal of Materials Science Letters, 11, 1163–1166.
Cempírek, J., Novák, M., Dolníček, Z., Kotková, J., and Škoda, R. (2010) Crystal chemistry and origin of grandidierite, ominelite, boralsilite, and werdingite from the Bory Granulite Massif, Czech Republic. American Mineralogist, 95, 1533–1547.
Chakhmouradian, A.R. and McCammon, C.A. (2005) Schorlomite: a discussion of the crystal chemistry, formula, and inter-species boundaries. Physics and Chemistry of Minerals, 32, 277–289.
Chakhmouradian, A.R., Cooper, M.A., Medici, L., Hawthorne, F.C., and Adar, F. (2008) Fluorine-rich hibschite from silicocarbonatite, Afrikanda complex, Russia: Crystal chemistry and conditions of crystallization. Canadian Mineralogist, 46, 1033–1042.
Chesnokov, B.V. (1996) High-temperature chlorosilicate in burned-out mine spoil heaps in the Chelyabinsk coal basin. Transactions of the Russian Academy of Science, Earth Sciences Section, 345, 104–106.
Chesnokov, B.V. and Bushmakin, A.F. (1995) New minerals from the burnt dumps of the Chelyabinsk coal basin, (eighth communication). Ural'skii Mineralogischeskii Sbornik, 5, 3–22 (in Russian).
Chesnokov, B.V., Vilisov, V.A., Bushmakin, A.F., Kotlyarov, V.A., and Belogub, Ye.V. (1994) New minerals from the burnt dumps of the Chelyabinsk coal basin, (sixth communication). Ural'skii Mineralogischeskii Sbornik, 3, 3–34 (in Russian).
Chesnokov, B.V., Shcherbakova, Ye.P., and Nishanbayev, T.P. (2008) Minerals from the Burnt Dumps of the Chelyabinsk Coal Basin. Miass, Russian Academy of Sciences, Urals Division, Institute of Mineralogy (in Russian).
Cho, H. and Rossman, G.R. (1993) Single-crystal NMR studies of low-concentration hydrous species in minerals: Grossular garnet. American Mineralogist, 78, 1149–1164.
Clark, A.M. (1993) Hey's mineral index. Mineral species, varieties and synonyms, third edition. Chapman and Hall, London.
Coes, L. Jr. (1955) High pressure minerals. Journal of the American Ceramic Society, 38, 298.
Cohen-Addad, C. (1970) Etude du composé $Ca_3Fe_2(SiO_4)_{1.15}(OH)_{7.4}$ par absorption infrarouge et diffraction des rayons X et des neutrons. Acta Crystallographica, A26, 68–70.
Cohen-Addad, C., Ducros, P., and Bertaut, E.F. (1967) Étude de la substitution du groupement SiO_4 par $(OH)_4$ dans les composés $Al_2Ca_3(OH)_{12}$ et $Al_2Ca_3(SiO_4)_{2.16}(OH)_{3.36}$ de type grenat. Acta Crystallographica, 23, 220–230.
Collerson, K.D., Williams, Q., Kamber, B.S., Omori, S., Arai, H., and Ohtani, E. (2010) Majoritic garnet: A new approach to pressure estimation of shock events in meteorites and the encapsulation of sub-lithospheric inclusions in diamond. Geochimica et Cosmochimica Acta, 74, 5939–5957.
Cornu, F. (1905) Neues Kontaktmineral "Hibschit." Tschermaks Mineralogische und Petrographische Mitteilungen, 24, 327–328.
——— (1906) Beiträge zur Petrographie des Böhmischen Mittelgebirges. I. Hibschit, ein neues Kontaktmineral. Tschermaks Mineralogische und Petrographische Mitteilungen, 25, 249–268.
Cussen, E.J. (2006) The structure of lithium garnets: cation disorder and clustering in a new family of fast Li^+ conductors. Chemical Communications, 2006, 412–413, DOI: 10.1039/b514640b.
——— (2010) Structure and ionic conductivity in lithium garnets. Journal of Materials Chemistry, 20, 5167–5173, DOI: 10.1039/b925553b.
Dana, J.D. (1837) A System of Mineralogy. Durrie and Peck and Herrick and Noyes, New Haven.
Dana, E.S. (1892) System of Mineralogy, Sixth edition. Wiley, New York.
Deer, W.A., Howie R.A., and Zussman J. (1982) Rock-forming minerals, Vol. 1A, Orthosilicates, Second edition. Longman, London.
Dowty, E. (1971) Crystal chemistry of titanian and zirconian garnet: I. Review and spectral studies. American Mineralogist, 56, 1983–2009.
Droop, G.T.R. (1987) A general equation for estimating Fe^{3+} concentrations in ferromagnesian silicates and oxides from microprobe analyses, using stoichiometric criteria. Mineralogical Magazine, 51, 431–435.
Dunn, P.J., Fleischer, M., Langley, R.H., Shigley, J.E., and Zilczer, J.A. (1985) New mineral names. American Mineralogist, 70, 871–881.
Eeckhout, S.G., Castañeda, C., Ferreira, A.C.M., Sabioni, A.C.S., de Grave, E., and Vasconcelos, D.C.L. (2002) Spectroscopic studies of spessartine from Brazilian pegmatites. American Mineralogist, 87, 1297–1306.
Enami, M., Cong, B., Yoshida, T., and Kawabe, I. (1995) A mechanism for Na incorporation in garnet: An example from garnet in orthogneiss from the Su-Lu terrane, eastern China. American Mineralogist, 80, 475–482.
Ercit, T.S. (1993) Caryinite revisited. Mineralogical Magazine, 57, 721–727.
Fehr, K.T. and Amthauer, G. (1996) Comment on "Morimotoite, $Ca_3TiFe^{2+}Si_3O_{12}$, a new titanian garnet from Fuka, Okayama Prefecture, Japan" by Henmi et al. Mineralogical Magazine, 60:842-845, 1995.
Feng, Q.L., Glasser, F.P., Howie, R.A., and Lachowski, E.E. (1988) Chlorosilicate with the 12CaO. $7Al_2O_3$ structure and its relationship to garnet. Acta Crystallographica, C44, 589–592.
Fermor, L.L. (1909) The manganese-ore deposits of India. Calderite, in Chapter 6, Memoirs of the Geological Society of India, 37, 182–186.
——— (1926) On the composition of some Indian garnets. Records of the Geological Society of India, 59(2), 191–207.
——— (1938) On khoharite, a new garnet and on the nomenclature of garnets. Records of the Geological Survey of India, 73(1), 145–156.
Ferro, O., Galli, E., Papp, G., Quartieri, S., Szakáll, S., and Vezzalini, G. (2003) A new occurrence of katoite and re-examination of the hydrogrossular group.

European Journal of Mineralogy, 15, 419–426.
Finger, L.W. and Conrad, P.G. (2000) The crystal structure of "tetragonal almandine-pyrope phase" (TAPP): A reexamination. American Mineralogist, 85, 1804–1807.
Fleischer, M. (1965) New mineral names. American Mineralogist, 50, 805–813.
——— (1973) New mineral names. American Mineralogist, 58, 560–562.
Flint, E.P., McMurdie, H.F., and Wells, L.S. (1941) Hydrothermal and X-ray studies of the garnet-hydrogarnet series and the relationship of the series to hydration products of portland cement. Journal of Research of the National Bureau of Standards, 26, 13–33.
Flohr, M.J.K. and Ross, M. (1989) Alkaline igneous rocks of Magnet Cove, Arkansas: Metasomatized ijolite xenoliths from Diamond Jo quarry. American Mineralogist, 74, 113–131.
Foshag, W.F. (1920) Plazolite, a new mineral. American Mineralogist, 5, 183–185.
Frank-Kamenetskaya, O.V., Rozhdestvenskaya, L.V., Shtukenberg, A.G., Bannova, I.I., and Skalkina, Yu.A. (2007) Dissymmetrization of crystal structures of grossular-andradite garnets $Ca_3(Al, Fe)_2(SiO_4)_3$. Structural Chemistry, 18, 493–503.
Fursenko, B.A. (1983) Synthesis of new high-pressure silicate garnets $Mn_3M_2Si_3O_{12}$ (M = V, Mn, Ga). Doklady Akademii Nauk SSSR, 268, 421–424 (in Russian).
Gadas, P., Novák, M., Talla, D., and Vašinová Galiová, M. (2012) Compositional evolution of grossular garnet from leucotonalitic pegmatite at Ruda nad Moravou, Czech Republic; a complex EMPA, LA-ICP-MS, IR and CL study. Mineralogy and Petrology, in press, DOI: 10.1007/s00710-012-0232-8.
Galuskin, E.V. (2005) Minerals of the vesuvianite group from the achtarandite rocks (Wiluy River, Yakutia), 191 p. University of Silesia Publishing House, Katowice, Poland (in Polish).
Galuskin, E.V., Galuskina, I.O., and Winiarska, A. (1995) Epitaxy of achtarandite on grossular - the key to the problem of achtarandite. Neues Jahrbuch für Mineralogie Monatshefte, 1995(7), 306–320.
Galuskin, E.V., Armbruster, T., Galuskina, I.O., Lazic, B., Winiarski, A., Gazeev, V.M., Dzierżanowski, P., Zadov, A.E., Pertsev, N.N., Wrzalik, R., Gurbanov, A.G., and Janeczek, J. (2011a) Vorlanite ($CaU^{6+}O_4$): A new mineral from the Upper Chegem caldera, Kabardino-Balkaria, Northern Caucasus, Russia. American Mineralogist, 96, 188–196.
Galuskin, E.V., Bailau, R., Galuskina, I.O., Prusik, A.K., Gazeev, V.M., Zadov, A.E., Pertsev, N.N., Jeżak, L., Gurbanov, A.G., and Dubrovinsky, L. (2011b) Eltyubyuite, IMA 2011-022. CNMNC Newsletter No. 10, October 2011, page 2553; Mineralogical Magazine, 75, 2549–2561.
Galuskina, I.O. and Galuskin, E.V. (2003) Garnets of the hydrogrossular – "hydroandradite" – "hydroschorlomite" series. Special Papers of the Mineralogical Society of Poland, 22, 54–57.
Galuskina, I.O., Galuskin, E.V., and Sitarz, M. (1998) Atoll hydrogarnets and mechanism of the formation of achtarandite pseudomorphs. Neues Jahrbuch für Mineralogie, Monatshefte, 49–62.
——— (2001) Evolution of morphology and composition of hibschite, Wiluy River, Yakutia. Neues Jahrbuch für Mineralogie Monatshefte, 49–66.
Galuskina, I.O., Galuskin, E.V., Dzierżanowski, P., Armbruster, T., and Kozanecki, M. (2005) A natural scandian garnet. American Mineralogist, 90, 1688–1692.
Galuskina, I.O., Galuskin, E.V., Armbruster, T., Lazic, B., Kusz, J., Dzierżanowski, P., Gazeev, V.M., Pertsev, N.N., Prusik, K., Zadov, A.E., Winiarski, A., Wrzalik, R., and Gurbanov, A.G. (2010a) Elbrusite-(Zr) — a new uranian garnet from the Upper Chegem caldera, Kabardino-Balkaria, Northern Caucasus, Russia. American Mineralogist, 95, 1172–1181.
Galuskina, I.O., Galuskin, E.V., Armbruster, T., Lazic, B., Dzierżanowski, P., Gazeev, V.M., Prusik, K., Pertsev, N.N., Winiarski, A., Zadov, A.E., Wrzalik, R., and Gurbanov, A.G. (2010b) Bitikleite-(SnAl) and bitikleite-(ZrFe): New garnets from xenoliths of the Upper Chegem volcanic structure, Kabardino-Balkaria, Northern Caucasus, Russia. American Mineralogist, 95, 959–967.
Galuskina, I.O., Galuskin, E.V., Dzierżanowski, P., Gazeev, V.M., Prusik, K., Pertsev, N.N., Winiarski, A., Zadov, A.E., and Wrzalik, R. (2010c) Toturite $Ca_3Sn_2Fe_2SiO_{12}$ — A new mineral species of the garnet group. American Mineralogist, 95, 1305–1311.
Galuskina, I.O., Galuskin, E.V., Lazic, B., Armbruster, T., Dzierżanowski, P., Prusik, K., and Wrzalik, R. (2010d) Eringaite, $Ca_3Sc_2(SiO_4)_3$, a new mineral of the garnet group. Mineralogical Magazine, 74, 365–373.
Galuskina, I.O., Galuskin, E.V., Gazeev, V.M., and Pertsev, N.N. (2010e) Natural uranian and thorian garnets. In Modern mineralogy: from theory to practice, Proceedings of the XI Russian Mineralogical Society General Meeting and the Fedorov Session 2010, no. 2010-1-169-0, p. 77–79 (in Russian, abstract), http://www.minsoc.ru/2010-1-169-0.
Galuskina, I.O., Galuskin, E.V., Kusz, J., Dzierżanowski, P., Prusik, K., Gazeev, V.M., Pertsev, N.N., and Dubrovinsky, L. (2011a) Bitikleite-(SnFe), IMA 2010-064. CNMNC Newsletter No. 8, April 2011, p. 290; Mineralogical Magazine, 75, 289–294.
Galuskina, I.O., Galuskin, E.V., Prusik, K., Gazeev, V.M., Pertsev, N.N., and Dzierżanowski, P. (2011b) Irinarassite, IMA 2010-073. CNMNC Newsletter No. 8, April 2011, p. 292; Mineralogical Magazine, 75, 289–294.
Gaudefroy, C., Orliac, M., Permingeat, F., and Parfenoff, E. (1969) L'henritermiérite, une nouvelle espèce minérale. Bulletin de la Société Française de Minéralogie et de Cristallographie, 92, 185–190.
Geiger, C.A. (2004) An introduction to spectroscopic methods in the mineral sciences and geochemistry. In A. Beran and E. Libowitzky, Eds., Spectroscopic Methods in Mineralogy, 6, 1–42. European Mineralogical Union Notes in Mineralogy, Eötvös Press, Budapest.
——— (2008) Silicate garnet: A micro to macroscopic (re)view. American Mineralogist, 93, 360–372.
Geiger, C.A. and Armbruster, T. (1997) $Mn_3Al_2Si_3O_{12}$ spessartine and $Ca_3Al_2Si_3O_{12}$ grossular garnet: Structural dynamic and thermodynamic properties. American Mineralogist, 82, 740–747.
Geiger, C.A., Rubie, D.C., Ross, C.R. II, and Seifert, F. (1991a) Synthesis and ^{57}Fe Mössbauer study of $(Mg,Fe)SiO_3$ garnet. Terra Abstracts, 3, 63 (abstract).
——— (1991b) A cation partitioning study of $(Mg,Fe)SiO_3$ garnet using ^{57}Fe Mössbauer spectroscopy. American Geophysical Union Eos Transactions, 72, 564–565 (abstract).
Geller, S. (1967) Crystal chemistry of the garnets. Zeitschrift für Kristallographie, 125, 1–47.
——— (1971) Refinement of the crystal structure of cryolithionite, $\{Na_3\}[Al_2](Li_3)F_{12}$. American Mineralogist, 56, 18–23.
Giaramita, M.J. and Day, H.W. (1990) Error propagation in calculations of structural formulas. American Mineralogist, 75, 170–182.
Glasser, F.P. (1995) Comments on wadalite, $Ca_6Al_5SiO_{16}Cl_3$, and the structures of garnet, mayenite and calcium chlorosilicate. Addendum. Acta Crystallographica, C51, 340.
Gnevushev, M.A. and Fedorova, L.G. (1964) Effect of isomorphous replacement on the infrared spectra of garnets. Doklady of the Academy of Sciences of the U.S.S.R. Earth Sciences Sections, 146, 115–117.
Grapes, R., Yagi, K., and Okumura, K. (1979) Aenigmatite, sodic pyroxene, arfvedsonite and associated minerals in syenites from Morotu, Sakhalin. Contributions to Mineralogy and Petrology, 69, 97–103.
Grew, E.S. (2002a) Borosilicates (exclusive of tourmaline) and boron in rock-forming minerals in metamorphic environments. L.M. Anovitz and E.S. Grew, Eds., In Boron: Mineralogy, Petrology, and Geochemistry, 33, 387–502. Reviews in Mineralogy, Mineralogical Society of America, Chantilly, Virginia.
——— (2002b) Beryllium in metamorphic environments (emphasis on aluminous compositions). In E.S. Grew, Ed., Beryllium: Mineralogy, petrology, and geochemistry, 50, 487–549. Reviews in Mineralogy and Geochemistry, Mineralogical Society of America, Chantilly, Virginia.
Grew, E.S., Chernosky, J.V., Werding, G., Abraham, K., Marquez, N., and Hinthorne, J.R. (1990) Chemistry of kornerupine and associated minerals, a wet chemical, ion microprobe, and X-ray study emphasizing Li, Be, B and F contents. Journal of Petrology, 31, 1025–1070.
Grew, E.S., Hålenius, U., Pasero, M., and Barbier, J. (2008) Recommended nomenclature for the sapphirine and surinamite groups (sapphirine supergroup). Mineralogical Magazine, 72, 839–876.
Grew, E.S., Marsh, J.H., Yates, M.G., Lazic, B., Armbruster, T., Locock, A., Bell, S.W., Dyar, M.D., Bernhardt, H.-J., and Medenbach, O. (2010) Menzerite-(Y), a new garnet species, $\{(Y, REE)(Ca, Fe^{2+})_2\}[(Mg,Fe^{2+})(Fe^{3+},Al)](Si_3)O_{12}$, from a felsic granulite, Parry Sound, Ontario, and a new garnet end-member, $\{Y_2Ca\}[Mg_2](Si_3)O_{12}$. Canadian Mineralogist, 48, 1171–1193.
Griffen, D.T., Hatch, D.M., Phillips, W.R., and Kulaksiz, S. (1992) Crystal chemistry and symmetry of a birefringent tetragonal pyralspite$_{75}$-grandite$_{25}$ garnet. American Mineralogist, 77, 399–406.
Haggerty, S.E., Fung, A.T., and Burt, D.M. (1994) Apatite, phosphorus and titanium in eclogitic garnet from the upper mantle. Geophysical Research Letters, 21, 1699–1702.
Hålenius, U. (2004) Stabilization of trivalent Mn in natural tetragonal hydrogarnets on the join "hydrogrossular"-henritermierite, $Ca_3Mn^{3+}_2[SiO_4]_2(H_4O_4)$. Mineralogical Magazine, 68, 335–341.
Hålenius, U., Häussermann, U., and Harryson, H. (2005) Holtstamite, $Ca_3(Al,Mn^{3+})_2(SiO_4)_{3-x}(H_4O_4)_x$, a new tetragonal hydrogarnet from Wessels Mine, South Africa. European Journal of Mineralogy, 17, 375–382.
Harris, J., Hutchison, M.T., Hursthouse, M., Light, M., and Harte, B. (1997) A new tetragonal silicate mineral occurring as inclusions in lower-mantle diamonds. Nature, 387, 486–488.
Harte, B. (2010) Diamond formation in the deep mantle: the record of mineral inclusions and their distribution in relation to mantle dehydration zones. Mineralogical Magazine, 74, 189–215.
Hartman, P. (1969) Can Ti^{+4} replace Si^{4+} in silicates? Mineralogical Magazine, 37, 366–369.
Hatch, D.M. and Ghose, S. (1989) Symmetry analysis of the phase transition and twinning in $MgSiO_3$ garnet: Implications to mantle mineralogy. American Mineralogist, 74, 1221–1224.
Hatert, F. and Burke, E.A.J. (2008) The IMA–CNMNC dominant-constituent rule revisited and extended. Canadian Mineralogist, 46, 717–728.
Hawthorne, F.C. (1976) Refinement of the crystal structure of berzeliite. Acta

Crystallographica, B32, 1581–1583.
——— (1981) Some systematics of the garnet structure. Journal of Solid State Chemistry, 37, 157–164.
——— (2002) The use of end-member charge-arrangements in defining new mineral species and heterovalent substitutions in complex minerals. Canadian Mineralogist, 40, 699–710.
Hawthorne, F.C., Oberti, R., Harlow, G.E., Maresch, W.V., Martin, R.F., Schumacher, J.C., and Welch, M.D. (2012) Nomenclature of the amphibole-supergroup. American Mineralogist, 97, 2031–2048.
Hazen, R.M., Downs, R.T., Finger, L.W., Conrad, P.G., and Gasparik, T. (1994) Crystal chemistry of calcium-bearing majorite. American Mineralogist, 79, 581–584.
Headden, W.P. (1891) A new phosphate from the Black Hills of South Dakota. American Journal of Science, 141, 415–417.
Henmi, C., Kusachi, I., and Henmi, K. (1995) Morimotoite, $Ca_3TiFe^{2+}Si_3O_{12}$, a new titanian garnet from Fuka, Okayama Prefecture, Japan. Mineralogical Magazine, 59, 115–120.
Henry, D.J., Novák, M., Hawthorne, F.C., Ertl, A., Dutrow, B.L., Uher, P., and Pezzotta, F. (2011) Nomenclature of the tourmaline-supergroup minerals. American Mineralogist, 96, 895–913.
Hess, H. (1832) Ueber den Uwarowit, eine neue Mineralspecies. Annalen der Physik und Chemie, 24, 388–389.
Hintze, C.A.F. (1922) Handbuch der Mineralogie, volume 1, part 4:1, 213. Veit and Company, Leipzig.
Hiroi, Y., Motoyoshi, Y., Ellis, D. J., Shiraishi, K., and Kondo, Y. (1997) The significance of phosphorus zonation in garnet from high grade pelitic rocks: A new indicator of partial melting. In C.A. Ricci, Ed., The Antarctic Region: Geological evolution and processes, 73–77. Terra Antartica Publication, Siena, Italy.
Hochella, M.F. Jr. (1988) Auger electron and X-ray photoelectron spectroscopies. In F.C. Hawthorne, Ed., Spectroscopic Methods in Mineralogy and Geology, 18, 573–637. Reviews in Mineralogy, Mineralogical Society of America, Chantilly, Virginia.
Hofmeister, A.M., Schaal, R.B., Campbell, K.R., Berry, S.L., and Fagan, T.J. (1998) Prevalence and origin of birefringence in 48 garnets from the pyrope-almandine-grossularite-spessartine quaternary. American Mineralogist, 83, 1293–1301.
Howie, R.A. and Woolley, A.R. (1968) The role of titanium and the effect of TiO_2 on the cell-size, refractive index, and specific gravity in the andradite-melanite-schorlomite series. Mineralogical Magazine, 36, 775–790.
Huggins, F.E., Virgo, D., and Huckenholz, H.G. (1977) Titanium-containing silicate garnets. II. The crystal chemistry of melanites and schorlomites. American Mineralogist, 62, 646–665.
Hutton, C.O. (1943) Hydrogrossular, a new mineral of the garnet-hydrogarnet series. Royal Society of New Zealand Transactions and Proceedings, 73, 174–180.
Igelström, L.J. (1886) Pyrrhoarsénit, nouveau minéral de Sjœgrufvan, paroisse de Grythyttan, gouvernement d'Œrebro, Suède. Bulletin de la Société Française de Minéralogie, 9, 218–220.
——— (1894) Mineralogische Notizen. 1. Lindesit. 2. Pyrrhoarsenit. Zeitschrift für Kristallographie, Mineralogie und Petrographie, 23, 590–593.
Ito, J. (1968) Synthesis of the berzeliite ($Ca_2NaMg_2As_3O_{22}$)—manganese berzeliite ($Ca_2NaMn_2As_3O_{12}$) series (arsenate garnet). American Mineralogist, 53, 316–319.
Ito, J. and Frondel, C. (1967a) Synthetic zirconium and titanium garnets. American Mineralogist, 52, 773–781.
——— (1967b) New synthetic hydrogarnets. American Mineralogist, 52, 1105–1109.
Ivanov-Emin, B.N., Nevskaya, N.A., Zaitsev, B.E., and Tsirel'nikov, V.I. (1982a) Hydroxoscandiates of calcium and strontium. Zhurnal Neorganicheskoi Khimii, 27, 2228–2230 (in Russian).
Ivanov-Emin, B.N., Nevskaya, N.A., Zaitsev, B.E., and Ivanova, T.M. (1982b) Synthesis and properties of calcium and strontium hydroxomanganates (III). Zhurnal Neorganicheskoi Khimii, 27, 3101–3104 (in Russian).
Iwata, T., Haniuda, M., and Fukuda, K. (2008) Crystal structure of $Ca_{12}Al_{14}O_{32}Cl_2$ and luminescence properties of $Ca_{12}Al_{14}O_{32}Cl_2$:Eu^{2+}. Journal of Solid State Chemistry, 181, 51–55.
Jaffe, H.W. (1951) The role of yttrium and other minor elements in the garnet group. American Mineralogist, 36, 133–155.
Jambor, J.L., Grew, E.S., Puziewicz, J., and Vanko, D.A. (1988a) New mineral names. American Mineralogist, 73, 439–445.
Jambor, J.L., Bladh, K.W., Ercit, T.S., Grice, J.D., and Grew, E.S. (1988b) New mineral names. American Mineralogist, 73, 927–935.
Jambor, J.L., Pertsev, N.N., and Roberts, A.C. (1997) New mineral names. American Mineralogist, 82, 1038–1041.
Jarosch, D. and Zemann, J. (1989) Yafsoanite: a garnet type calcium-tellurium(VI)-zinc oxide. Mineralogy and Petrology, 40, 111–116.
Johan, Z. and Oudin, E. (1986) Présence de grenats, $Ca_3Ga_2(GeO_4)_3$, $Ca_3Al_2[(Ge, Si)O_4]_3$ et d'un équivalent ferrifère, germanifère et gallifère de la sapphirine, $Fe_4(Ga, Sn, Fe)_4(Ga, Ge)_6O_{20}$, dans la blende des gisements de la zone axiale pyrénéenne. Conditions de formation des phases germanifères et gallifère. Compte Rendus de l'Académie des Sciences, 303, Series II, 811–816.
Johnson, E.A. (2006) Water in nominally anhydrous crustal minerals: Speciation, concentration, and geologic significance. In H. Keppler and J.R. Smyth, Eds., Water in nominally anhydrous minerals, 62, 117–154. Reviews in Mineralogy and Geochemistry, Mineralogical Society of America, Chantilly, Virginia.
Juhin, A., Morin, G., Elkaïm, E., Frost, D.J., Fialin, M., Juillot, F., and Calas, G. (2010) Structure refinement of a synthetic knorringite, $Mg_3(Cr_{0.8}Mg_{0.1}Si_{0.1})_2(SiO_4)_3$. American Mineralogist, 95, 59–63.
Kalinichenko, A.M., Proshko, V.Ya., Matyash, I.V., Pavlishin, V.I., and Gamarnik, M.Ya. (1987) NMR Data on crystallochemical features of hydrogrossular. Geochemistry International, 24, 132–135.
Karpinskaya, T.B., Ostrovskiy, I.A., and Yevstigneyeva, T.L. (1982) Synthetic pure iron garnet skiagite. Izvestiya Akademii Nauk SSSR. Seriya Geologicheskaya 1982, Issue 9, 128–129 (in Russian).
Kasowski, M.A. and Hogarth, D.D. (1968) Yttrian andradite from the Gatineau Park, Quebec. Canadian Mineralogist, 9, 552–558.
Kato, T. (1986) Stability relation of $(Mg,Fe)SiO_3$ garnets, major constituents in the Earth's interior. Earth and Planetary Science Letters, 77, 399–408.
Kawakami, T. and Hokada, T. (2010) Linking *P-T* path with development of discontinuous phosphorus zoning in garnet during high-temperature metamorphism – An example from Lützow-Holm Complex, East Antarctica. Journal of Mineralogical and Petrological Sciences, 105, 175–186.
Khorari, S., Rulmont, A., Cahay, R., and Tarte, P. (1995) Structures of the complex arsenates $NaCa_2M^{2+}_2(AsO_4)_3$ (M^{2+} = Mg, Ni, Co): First experimental evidence of a garnet-alluaudite reversible polymorphism. Journal of Solid State Chemistry, 118, 267–273.
Khorari, S., Rulmont, A., and Tarte, P. (1997) The arsenates $NaCa_2M^{2+}_2(AsO_4)_3$ (M^{2+} = Mg, Ni, Co): Influence of cationic substitutions on the garnet-alluaudite polymorphism. Journal of Solid State Chemistry, 131, 290–297.
Kim, A.A., Zayakina, N.V., and Lavrent'yev, Yu.G. (1982) Yafsoanite $(Zn_{1.38}Ca_{1.36}Pb_{0.26})_3Te_1O_6$ – a new mineral of tellurium. Zapiski Vsesoyuznogo Mineralogicheskogo Obshchestva, 111, 118–121 (in Russian; English translation: International Geology Review, 24, 1295–1298).
Klaproth, M.H. (1797) Beiträge zur chemischen Kenntniss der Mineralkörper, Volume 2, Posen and Berlin.
Koritnig, S. (1965) Geochemistry of phosphorus—I. The replacement of Si^{4+} by P^{5+} in rock-forming silicate minerals. Geochimica et Cosmochimica Acta, 29, 361–371.
Koritnig, S., Rösch, H., Schneider, A., and Seifert, F. (1978) Der Titan-Zirkon-Granat aus den Kalksilikatfels-Einschlüssen des Gabbro im Radautal, Harz, Bundesrepublik Deutschland. Tschermaks Mineralogische und Petrographische Mitteilungen, 25, 305–313.
Krause, W., Blaß, G., and Effenberger, H. (1999) Schäferite, a new vanadium garnet from the Bellberg volcano, Eifel, Germany. Neues Jahrbuch für Mineralogie Monatshefte, 123–134.
Kühberger, A., Fehr, T., Huckenholz, H.G., and Amthauer, G. (1989) Crystal chemistry of a natural schorlomite and Ti-andradites synthesized at different oxygen fugacities. Physics and Chemistry of Minerals, 16, 734–740.
Kühn, O.B. (1840) Neues Mineral von Langbanshytta bei Fahlun. Annalen der Chemie und Pharmacie, 34, 211–218.
Labotka, T.C. (1995) Evidence for immiscibility in Ti-rich garnet in a calc-silicate hornfels from northeastern Minnesota. American Mineralogist, 80, 1026–1030.
Lager, G.A., Armbruster, T., and Faber, J. (1987) Neutron and X-ray diffraction study of hydrogarnet $Ca_3Al_2(O_4H_4)_3$. American Mineralogist, 72, 756–765.
Lager, G.A., Armbruster, T., Rotella, F.J., and Rossman, G.R. (1989) OH substitution in garnets: X-ray and neutron diffraction, infrared, and geometric-modeling studies. American Mineralogist, 74, 840–851.
Landergren, S. (1930) Studier över berzeliitgruppens mineral. Geologiska Föreningens i Stockholm Förhandlingar, 52, 123–133 (in Swedish).
Langley, R.H. and Sturgeon, G.D. (1979) Lattice parameters and ionic radii of the oxide and fluoride garnets. Journal of Solid State Chemistry, 30, 79–82.
Laverne, C., Grauby, O., Alt, J.C., and Bohn, M. (2006) Hydroschorlomite in altered basalts from Hole 1256D, ODP Leg 206: The transition from low-temperature to hydrothermal alteration. Geochemistry Geophysics Geosystems, 7(10), Q10O03, DOI: 10.1029/2005GC001180.
Lehijärvi, M. (1960) The alkaline district of Iivaara, Kuusamo, Finland. Bulletin de la Commission Géologique de Finlande, 185, 1–62.
Levinson, A.A. (1966) A system of nomenclature for rare-earth minerals. American Mineralogist, 51, 152–158.
Lobanov, N.N., Butman, L.A., and Tsirel'son, V.G. (1989) Precision X-ray diffraction study of the garnets. $Na_3Sc_2V_3O_{12}$ and $Na_{0.90}Ca_{2.38}Mn_{1.72}V_3O_{12}$. Journal of Structural Chemistry, 30, 96–104.
Locock, A.J. (2008) An Excel spreadsheet to recast analyses of garnet into end-member components, and a synopsis of the crystal chemistry of natural silicate garnets. Computers and Geosciences, 34, 1769–1780.
Locock, A.J., Luth, R.W., Cavell, R.G., Smith, D.G.W., and Duke, M.J.M. (1995) Spectroscopy of the cation distribution in the schorlomite species of garnet.

American Mineralogist, 80, 27–38.
Lupini, L., Williams, C.T., and Woolley, A.R. (1992) Zr-rich garnet and Zr- and Th-rich perovskite from the Polino carbonatite, Italy. Mineralogical Magazine, 56, 581–586.
Ma, C. (2012) Discovery of meteoritic eringaite, $Ca_3(Sc,Y,Ti)_2Si_3O_{12}$, the first solar garnet. Meteoritics and Planetary Science, 47, Supplement S1, Abstract 5015.
Ma, C., Connolly, H.C. Jr., Beckett, J.R., Tschauner, O., Rossman, G.R., Kampf, A.R., Zega, T.J., Sweeney Smith, S.A., and Schrader, D.L. (2011) Brearleyite, $Ca_{12}Al_{14}O_{32}Cl_2$, a new alteration mineral from the NWA 1934 meteorite. American Mineralogist, 96, 1199–1206.
Maldener, J., Hösch, A., Langer, K., and Rauch, F. (2003) Hydrogen in some natural garnets studied by nuclear reaction analysis and vibrational spectroscopy. Physics and Chemistry of Minerals, 30, 337–344.
Malitesta, C., Losito, I., Scordari, F., and Schingaro, E. (1995) XPS investigation of titanium in melanites from Monte Vulture (Italy). European Journal of Mineralogy, 7, 847–858.
Manning, C.E. and Bird, D.K. (1990) Fluorian garnets from the host rocks of the Skaergaard intrusion: Implications for metamorphic fluid composition. American Mineralogist, 75, 859–873.
Marks, M.A.W., Schilling, J., Coulson, I.M., Wenzel, T., and Markl, G. (2008) The alkaline-peralkaline Tamazeght Complex, High Atlas Mountains, Morocco: Mineral chemistry and petrological constraints for derivation from a compositionally heterogeneous mantle source. Journal of Petrology, 49, 1097–1131.
Marschall, H.R. (2005) Lithium, beryllium and boron in high-pressure metamorphic rocks from Syros (Greece). Unpublished Inaugural-Dissertation, Ruprecht-Karls-Unitversität Heidelberg, Germany.
Mason, B. and Berggren, T. (1942) A phosphate-bearing spessartite garnet from Wodgina, Western Australia. Geologiska Föreningens i Stockholm Förhandlingar, 63, 413–418.
McAloon, B.P. and Hofmeister, A.M. (1993) Single-crystal absorption and reflection infrared spectroscopy of birefringent grossular-andradite garnets. American Mineralogist, 78, 957–967.
McCammon, C.A. and Ross, N.L. (2003) Crystal chemistry of ferric iron in $(Mg,Fe)(Si,Al)O_3$ majorite with implications for the transition zone. Physics and Chemistry of Minerals, 30, 206–216.
McConnell, D. (1942) Griphite, a hydrophosphate garnetoid. American Mineralogist, 27, 452–461.
Melluso, L., Srivastava, R.K., Guarino, V., Zanetti, A., and Sinha, A.K. (2010) Mineral compositions and petrogenetic evolution of the ultramafic-alkaline – carbonatitic complex of Sung Valley, northeastern India. Canadian Mineralogist, 48, 205–229.
Menzer, G. (1928) Die Kristallstruktur der Granate. Zeitschrift für Kristallographie, 69, 300–396.
Merli, M., Callegari, A., Cannillo, E., Caucia, F., Leona, M., Oberti, R., and Ungaretti, L. (1995) Crystal-chemical complexity in natural garnets: structural constraints on chemical variability. European Journal of Mineralogy, 7, 1239–1249.
Mill', B.V. (1970) New series of Te^{6+}-containing garnets. Doklady Akademii Nauk SSSR, 191, 86-88 (in Russian).
Mill', B.V., Belokoneva, E.L., Simonov, M.A., and Belov, N.V. (1977) Refined crystal structures of the scandium garnets $Ca_3Sc_2Si_3O_{12}$, $Ca_3Sc_2Ge_3O_{12}$, and $Cd_3Sc_2Ge_3O_{12}$. Journal of Structural Chemistry, 18, 321–323.
Mills, S.J., Hatert, F., Nickel, E.H., and Ferraris, G. (2009) The standardisation of mineral group hierarchies: application to recent nomenclature proposals. European Journal of Mineralogy, 21, 1073–1080.
Mills, S.J., Kampf, A.R., Kolitsch, U., Housley, R.H., and Raudsepp, M. (2010) The crystal chemistry and crystal structure of kuksite, $Pb_3Zn_3Te^{6+}P_2O_{14}$, and a note on the crystal structure of yafsoanite, $(Ca,Pb)_3Zn(TeO_6)_2$. American Mineralogist, 95, 933–938.
Milton, C. and Blade, L.V. (1958) Preliminary note on kimzeyite, a new zirconium garnet. Science, 127, 1343.
Milton, C., Ingram, B.L., and Blade, L.V. (1961) Kimzeyite, a zirconium garnet from Magnet Cove, Arkansas. American Mineralogist, 46, 533–548.
Moench, R.H. and Meyrowitz, R. (1964) Goldmanite, a vanadium garnet from Laguna, New Mexico. American Mineralogist, 49, 644–655.
Momoi, H. (1964) A new vanadium garnet, $(Mn, Ca)_3V_2Si_3O_{12}$, from Yamato mine, Amami Islands, Japan. Memoirs of the Faculty of Science, Kyushu University, Series D, Geology, 15, 73–78.
Moore, P.B. (1972) Contributions to the mineralogy of Sweden. III. On Igelström's manganese arsenates and antimonates from the Sjö Mine, Grythyttan, Örebro County, Sweden. Geologiska Föreningens i Stockholm Förhandlingar, 94, 423–434.
Moore, R.O. and Gurney, J.J. (1985) Pyroxene solid solution in garnets included in diamond. Nature, 318, 553–555.
Morán-Miguélez, E., Alario-Franco, M.A., and Joubert, J.C. (1986) Hydrothermal synthesis and field of existence of silicon-free garnets. Materials Research Bulletin, 21, 107–113.
Munno, R., Rossi, G., and Tadini, C. (1980) Crystal chemistry of kimzeyite from Stromboli, Aeolian Islands, Italy. American Mineralogist, 65, 188–191.
Nagashima, M. and Armbruster, T. (2012) Palenzonaite, berzeliite, and manganberzeliite: $(As^{5+},V^{5+},Si^{4+})O_4$ tetrahedra in garnet structures. Mineralogical Magazine, 76, 1081–1097.
Nickel, E.H. and Grice, J.D. (1998) The IMA Commission on New Minerals and Mineral Names: procedures and guidelines on mineral nomenclature. Canadian Mineralogist, 36, 913–926.
Nickel, E.H. and Mandarino, J.A. (1987) Procedures involving the IMA Commission on New Minerals and Mineral Names and guidelines on mineral nomenclature. American Mineralogist, 72, 1031–1042.
Nishizawa, H. and Koizumi, M. (1975) Synthesis and infrared spectra of $Ca_3Mn_2Si_3O_{12}$ and $Cd_3B_2Si_3O_{12}$ (B: Al, Ga, Cr, V, Fe, Mn) garnets. American Mineralogist, 60, 84–87.
Nixon, P.H. and Hornung, G. (1968) A new chromium garnet end member, knorringite, from kimberlite. American Mineralogist, 53, 1833–1840.
Novak, G.A. and Gibbs, G.V. (1971) The crystal chemistry of the silicate garnets. American Mineralogist, 56, 791–825.
Oberti, R., Ungaretti, L., Cannillo, E., and Hawthorne, F.C. (1992) The behaviour of Ti in amphiboles: I. Four- and six-coordinate Ti in richterite. European Journal of Mineralogy, 4, 425–439.
Oberti, R. Quartieri, S., Dalconi, C.M., Boscherini, F., Iezzi, G., Boiocchi, M., and Eeckout, S.G. (2006) Site preference and local geometry of Sc in garnets: Part I. Multifarious mechanisms in the pyrope-grossular join. American Mineralogist, 91, 1230–1239.
O'Callaghan, M.P. and Cussen, E.J. (2007) Lithium dimer formation in the Li-conducting garnets $Li_{5+x}Ba_xLa_{3-x}Ta_2O_{12}$ ($0 < x \leq 1.6$). Chemical Communications 2007, 2048–2050, DOI: 10.1039/b700369b.
O'Neill, H.St.C., McCammon, C.A., Canil, D., Rubie, D.C., Ross, C.R. II, and Seifert, F. (1993a) Mössbauer spectroscopy of mantle transition zone phases and determination of minimum Fe^{3+} content. American Mineralogist, 78, 456–460.
O'Neill, H.St.C., Rubie, D.C., Canil, D., Geiger, C.A., Ross, C.R. II, Seifert, F., and Woodland, A.B. (1993b) Ferric iron in the upper mantle and in transition zone assemblages: Implications for relative oxygen fugacities in the mantle. In E. Takahashi, R. Jeanloz, and D.C. Rubie, Eds., Evolution of the Earth and Planets, Geophysical Monograph, 74, 73–88. American Geophysical Union, Washington, D.C.
Ottonello, G., Bokreta, M., and Sciuto, P.F. (1996) Parameterization of energy and interactions in garnets: End-member properties. American Mineralogist, 81, 429–447.
Palache, C., Berman, H., and Frondel, C. (1951) The system of mineralogy of James Dwight Dana and Edward Salisbury Dana, Yale University, 1837-1892, Seventh edition. Wiley, New York.
Pasero, M., Kampf, A.R., Ferraris, C., Pekov, I.V., Rakovan, J., and White, T.J. (2010) Nomenclature of the apatite supergroup minerals. European Journal of Mineralogy, 22, 163–179.
Passaglia, E. and Rinaldi, R. (1984) Katoite, a new member of the $Ca_3Al_2(SiO_4)_3$-$Ca_3Al_2(OH)_{12}$ series and a new nomenclature for the hydrogrossular group of minerals. Bulletin de la Société Française de Minéralogie et de Cristallographie, 107, 605–618.
Pekov, I.V. (1998) Minerals first discovered on the territory of the former Soviet Union. Ocean Pictures, Moscow.
Pertlik, F. (2003) Bibliography of hibschite, a hydrogarnet of grossular type. GeoLines, 15, 113–119.
Peters, Tj. (1965) A water-bearing andradite from the Totalp serpentine (Davos, Switzerland). American Mineralogist, 50, 1482–1486.
Peterson, R.C., Locock, A.J., and Luth, R.W. (1995) Positional disorder of oxygen in garnet: The crystal-structure refinement of schorlomite. Canadian Mineralogist, 33, 627–631.
Piddington, H. (1850) On calderite, an undescribed siliceo-iron-and-manganese rock, from the district of Burdwan. Journal of the Asiatic Society of Bengal, 19, 145–148.
Pieper, G., Fuess, H., Töpel-Schadt, J., and Amthauer, G. (1983) Die Bestimmung der Kationenverteilung in den natürlichen Granatan Pyrop und Hessonit durch Neutronenbeugung. Neues Jahrbuch für Mineralogie Abhandlungen, 147, 147–159.
Platt, R.G. and Mitchell, R.G. (1979) The Marathon Dikes. I: Zirconium-rich titanian garnets and manganoan magnesian ulvöspinel-magnetite spinels. American Mineralogist, 64, 546–550.
Povarennykh, A.S. and Shabilin, B.G. (1983) Structural role of titanium and iron in synthetic zirconium- and titanium-containing garnets. Geologicheskiy Zhurnal, 43, 45–50 (in Russian).
Quartieri, S., Oberti, R., Boiocchi, M., Dalconi, M.C., Boscherini, F., Safonova, O., and Woodland, A.B. (2006) Site preference and local geometry of Sc in garnets: Part II. The crystal-chemistry of octahedral Sc in the andradite-$Ca_3Sc_2Si_3O_{12}$ join. American Mineralogist, 91, 1240–1248.
Rager, H., Geiger, C.A., and Stahl, A. (2003) Ti(III) in synthetic pyrope: A single-crystal electron paramagnetic resonance study. European Journal of Mineralogy, 15, 697–699.
Rammelsberg, K.F.A. (1850a) V. Mineralogical Notices. Schorlamite $2(3RO+2SiO^3)+3(2RO+TiO^2)$. Philosophical Magazine and Journal of Science, 36, 21.

Rammelsberg, K.F. (1850b) Analysis of the schorlomite of Shepard. American Journal of Science and Arts, 9, 429.
Rass, I.T. (1997) Morimotoite, a new titanian garnet? — Discussion. Mineralogical Magazine, 61, 728–730.
Rickwood, P.C. (1968) On recasting analyses of garnet into end-member molecules. Contributions to Mineralogy and Petrology, 18, 175–198.
Righter, K., Sutton, S., Danielson, L., Pando, K., Schmidt, G., Yang, H., Berthet, S., Newville, M., Choi, Y., Downs, R.T., and Malavergne, V. (2011) The effect of f_{O_2} on the partitioning and valence of V and Cr in garnet/melt pairs and the relation to terrestrial mantle V and Cr content. American Mineralogist, 96, 1278–1290.
Rinaldi, R. (1978) The crystal structure of griphite, a complex phosphate, not a garnetoid. Bulletin de Minéralogie, 101, 543–547.
Ringwood, A.E. and Major, A. (1971) Synthesis of majorite and other high pressure garnets and perovskites. Earth and Planetary Science Letters, 12, 411–418.
Røhr, T.S., Austrheim, H., and Erambert, S. (2007) Stress-induced redistribution of yttrium and heavy rare-earth elements (HREE) in garnet during high-grade polymetamorphism. American Mineralogist, 92, 1276–1287.
Ronniger, G. and Mill', B.V. (1973) New ions in the garnet structure. Kristallografiya, 18, 539–543 (in Russian).
Rossman, G.R. and Aines, R.D. (1991) The hydrous components in garnets: Grossular-hydrogrossular. American Mineralogist, 76, 1153–1164.
Rossman, G.R., Rauch, F., Livi, R., Tombrello, T.A., Shi, C.R., and Zhou, Z.Y. (1988) Nuclear reaction analysis of hydrogen in almandine, pyrope and spessartite garnets. Neues Jahrbuch für Mineralogie Monatshefte, 1988(4), 172–178.
Rossmanith, E. and Armbruster, T. (1995) The intensity of forbidden reflections of pyrope: Umweganregung or symmetry reduction? Zeitschrift für Kristallographie, 210, 645–649.
Rudashevskii, N.S. and Mochalov, A.G. (1984) New associations of native elements in ultrabasites. Geologiya i Geofizika, 25, 38–44 (English translation: Soviet Geology and Geophysics, 25, 35–41).
Sacerdoti, M. and Passaglia, E. (1985) The crystal structure of katoite and implications within the hydrogrossular group of minerals. Bulletin de Minéralogie, 108, 1–8.
Saha, A., Ganguly, S., Ray, J., and Chatterjee, N. (2010) Evaluation of phase chemistry and petrochemical aspects of Samchampi–Samteran differentiated alkaline complex of Mikir Hills, northeastern India. Journal of Earth System Science, 119, 675–699.
Schingaro, E., Scordari, F., Capitanio, F., Parodi, G., Smith, D.C., and Mottana, A. (2001) Crystal chemistry of kimzeyite from Anguillara, Mts. Sabatini, Italy. European Journal of Mineralogy, 13, 749–759.
Schingaro, E., Scordari, F., Pedrazzi, G., and Malitesta, C. (2004) Ti and Fe speciation by X-ray photoelectron spectroscopy (XPS) and Mössbauer spectroscopy for a full chemical characterization of Ti-garnets from Colli Albani (Italy). Annali di Chimica, 94, 185–196.
Schwarz, H. and Schmidt, L. (1971) Arsenate des Typs $\{NaCa_2\}[M^{II}_2](As_3)O_{12}$. Zeitschrift für anorganische und allgemeine Chemie, 382, 257–269.
Shannon, R.D. (1976) Revised effective ionic radii and systematic studies of interatomic distances in halides and chalcogenides. Acta Crystallographica, A32, 751–767.
Shepard, C.U. (1846) On three new mineral species from Arkansas, and the discovery of the diamond in North Carolina. American Journal of Science, 2, 249–254.
Shtukenberg, A.G., Punin, Yu.O., Frank-Kamenetskaya, O.V., Kovalev, O.G., and Sokolov, P.B. (2001) On the origin of anomalous birefringence in grandite garnets. Mineralogical Magazine, 65, 445–459.
Shtukenberg, A.G., Popov, D. Yu., and Punin, Yu.O. (2005) Growth ordering and anomalous birefringence in ugrandite garnets. Mineralogical Magazine, 69, 537–550.
Sjögren, S.A.H. (1894) Contributions to Swedish mineralogy - 17. On soda berzeliite from Långban. Bulletin of the Geological Institution of the University of Uppsala, 2, 92–95.
Smith, J.V. and Mason, B. (1970) Pyroxene-garnet transformation in Coorara meteorite. Science, 168, 832–833.
Smith, D.G.W. and Nickel, E.H. (2007) A system of codification for unnamed minerals: Report of the Subcommittee for Unnamed Minerals of the IMA Commission on New Minerals, Nomenclature and Classification. Canadian Mineralogist, 45, 983–1055.
Smyth, J.R., Madel, R.E., McCormick, T.C., Munoz, J.L., and Rossman, G.R. (1990) Crystal-structure refinement of a F-bearing spessartine garnet. American Mineralogist, 75, 314–318.
Sobolev, N.V. Jr. and Lavrent'ev, Ju.G. (1971) Isomorphic sodium admixture in garnets formed at high pressures. Contributions to Mineralogy and Petrology, 31, 1–12.
Sokolova, E. and Hawthorne, F.C. (2002) Reconsideration of the crystal structure of paranatisite and the crystal chemistry of $[^{[6]}M_2^{[4]}T_2\varphi_{12}]$ sheets. Canadian Mineralogist, 40, 947–960.
Stähle, V., Altherr, R., Nasdala, L., and Ludwig, T. (2011) Ca-rich majorite derived from high-temperature melt and thermally stressed hornblende in shock veins of crustal rocks from the Ries impact crater (Germany). Contributions to Mineralogy and Petrology, 161, 275–291.
Steppan, N. (2003) Li, Be und B in Mineralen metapelitischer Gesteine: Fallstudien auf der Insel Ikaria, im Künischen Gebirge und den Schweizer Alpen. Unpublished Inaugural-Dissertation, Ruprecht-Karls-Universität, Heidelberg, Germany.
Strunz, H. and Nickel, E.H. (2001) Strunz mineralogical tables. Chemical-Structural Mineral Classification System, Ninth edition, 870 p. E. Schweizerbart'sche Verlagsbuchhandlung, Stuttgart.
Takamori, T., Shafer, M.W., Cooper, E.I., and Figat, R.A. (1987) Partial fluoridation of hydrogarnet. Journal of Materials Science Letters, 6, 60–62.
Tanaka, H., Endo, S., Minakawa, T., Enami, M., Nishio-Hamane, D., Miura, H., and Hagiwara, A. (2010) Momoiite, $(Mn^{2+},Ca)_3(V^{3+},Al)_2Si_3O_{12}$, a new manganese vanadium garnet from Japan. Journal of Mineralogical and Petrological Sciences, 105, 92–96.
Tappert, R., Stachel, T., Harris, J.W., Muehlenbachs, K., Ludwig, T., and Brey, G.P. (2005) Subducting oceanic crust: The source of deep diamonds. Geology, 33, 565–568.
Thilo, E. (1941) Über die Isotypie zwischen Phosphaten der allgemeinen Zusammensetzung $(Me_1)_3(Me_2)_2[PO_4]_3$ und den Silikaten der Granatgruppe. Naturwissenschaften, 29, 239.
Thompson, R.N. (1975) Is upper-mantle phosphorus contained in sodic garnet? Earth and Planetary Science Letters, 26, 417–424.
Tomioka, N., Fujino, K., Ito, E., Katsura, T., Sharp, T., and Kato, K. (2002) Microstructures and structural phase transition in $(Mg,Fe)SiO_3$ majorite. European Journal of Mineralogy, 14, 7–14.
Tsukimura, K., Kanazawa, Y., Aoki, M., and Bunno, M. (1993) Structure of wadalite $Ca_6Al_5Si_2O_{16}Cl_3$. Acta Crystallographica, C49, 205–207.
Ungaretti, L., Leona, M., Merli, M., and Oberti, R. (1995) Non-ideal solid-solution in garnet: Crystal-structure evidence and modelling. European Journal of Mineralogy, 7, 1299–1312.
Ussing, N.V. (1904) Sur la cryolithionite, espèce minérale nouvelle. Oversigt over det Kongelige Danske Videnskabernes Selskabs Forhandlinger, 1, 3–12.
Utsunomiya, S., Wang, L.M., Yudintsev, S., and Ewing, R.C. (2002) Ion irradiation-induced amorphization and nano-crystal formation in garnets. Journal of Nuclear Materials, 303, 177–187.
Utsunomiya, S., Yudintsev, S., and Ewing, R.C. (2005) Radiation effects in ferrate garnet. Journal of Nuclear Materials, 336, 251–260.
Valley, J.W., Essene, E.J., and Peacor, D.R. (1983) Fluorine-bearing garnets in Adirondack calc-silicates. American Mineralogist, 68, 444–448.
Virgo, D. and Yoder, H.S. Jr. (1974) The alleged skiagite molecule in garnet from two type localities in Scotland. Year Book - Carnegie Institution of Washington, 73, 433–436.
Visser, D. (1993) Fluorine-bearing hydrogarnets from Blengsvatn, Bamble Sector, South Norway. Mineralogy and Petrology, 47, 209–218.
von Eckermann, H. von. (1974) The chemistry and optical properties of some minerals of the Alnö alkaline rocks. Arkiv för Mineralogi och Geologi, 5, 93–210.
Wang, Y. and Lai, W. (2012) High ionic conductivity lithium garnet oxides of $Li_{7-x}La_3Zr_{2-x}Ta_xO_{12}$ compositions. Electrochemical and Solid-State Letters, 15 (5), A68–A71.
Waychunas, G.A. (1987) Synchrotron radiation xanes spectroscopy of Ti in minerals: Effects of Ti bonding distances, Ti valence, and site geometry on absorption edge structure. American Mineralogist, 72, 89–101.
Whitney, J.D. (1849) Examination of three new mineralogical species proposed by Professor C. U. Shepard. Journal of Natural History, Boston, 6, 42–48.
Whittle, K.R., Lumpkin, G.R., Berry, F.J., Oates, G., Smith, K.L., Yudintsev, S., and Zaluzec, N.J. (2007) The structure and ordering of zirconium and hafnium containing garnets studied by electron channeling, neutron diffraction, and Mössbauer spectroscopy. Journal of Solid State Chemistry, 180, 785–791.
Wildner, M. and Andrut, M. (2001) The crystal chemistry of birefringent natural uvarovites: Part II. Single-crystal X-ray structures. American Mineralogist, 86, 1231–1251.
Wilkins, R.W.T. and Sabine, W. (1973) Water content of some nominally anhydrous silicates. American Mineralogist, 58, 508–516.
Winchell, A.N. (1933) Elements of optical mineralogy. An introduction to microscopic petrography. Part II Descriptions of Minerals, Third edition, 459 p. Wiley, New York.
Włodyka, R. and Karwowski, Ł. (2006) Fluorine-bearing garnets from the teschenite sill in the Polish Western Carpathians. Acta Mineralogica-Petrographica Abstract Series, 5, 131.
Woodland, A.B. and O'Neill, H.St.C. (1993) Synthesis and stability of $Fe_3^{2+}Fe_2^{3+}Si_3O_{12}$ garnet and phase relations with $Fe_3Al_2Si_3O_{12}$ - $Fe_3^{2+}Fe_2^{3+}Si_3O_{12}$ solutions. American Mineralogist, 78, 1002–1015.
——— (1995) Phase relations between $Ca_3Fe_2^{3+}Si_3O_{12}$-$Fe_3^{2+}Fe_2^{3+}Si_3O_{12}$ garnet and $CaFeSi_2O_6$-$Fe_2Si_2O_6$ pyroxene solid solutions. Contributions to Mineralogy and Petrology, 121, 87–98.
Yakovlevskaya, T.A. (1972) Garnet group. In F.V. Chukhrov, Ed., Minerals Handbook, 17–95. Volume III. Part I. Moscow, Nauka (in Russian).
Yamane, H. and Kawano, T. (2011) Preparation, crystal structure and photoluminescence of garnet-type calcium tin titanium aluminates. Journal of Solid State

Chemistry, 184, 965–970.
Yang, H., Konzett, J., Downs, R.T., and Frost, D.J. (2009) Crystal structure and Raman spectrum of a high-pressure Li-rich majoritic garnet, $(Li_2Mg)Si_2(SiO_4)_3$. American Mineralogist, 94, 630–633.
Ye, K., Cong, B., and Ye, D. (2000) The possible subduction of continental material to depths greater than 200 km. Nature, 407, 734–736.
Yoder, H.S. and Keith, M.L. (1951) Complete substitution of aluminum for silicon: The system $3MnO{\cdot}Al_2O_3{\cdot}3SiO_2 - 3Y_2O_3{\cdot}5Al_2O_3$. American Mineralogist, 36, 519–533.
Yudintsev, S.V. (2001) Incorporation of U, Th, Zr and Gd into the garnet-structured host. Proceedings of ICEM'01, 8th International Conference Environment Management, Bruges, Belgium, September 30–October, 4, 2001, 20–23.
——— (2003) A structural-chemical approach to selecting crystalline matrices for actinide immobilization. Geology of Ore Deposits, 45, 151–165.
Yudintsev, S.V., Lapina, M.I., Ptashkin, A.G., Ioudintseva, T.S., Utsunomiya, S., Wang, L.M., and Ewing, R.C. (2002) Accommodation of uranium into the garnet structure. In B.P. McGrail and G.A. Cragnolino, Eds., Scientific Basis for Nuclear Waste Management XXV, 713, 477–480. Materials Research Society Symposium Proceedings.
Zaitsev, A.N., Williams, C.T., Britvin, S.N., Kuznetsova, I.V., Spratt, J., Petrov, S.V., and Keller, J. (2010) Kerimasite, $Ca_3Zr_2(Fe^{3+}Si)O_{12}$, a new garnet from carbonatites of Kerimasi volcano and surrounding explosion craters, northern Tanzania. Mineralogical Magazine, 74, 803–820.
Zedlitz, O. (1933) über titanhaltige Kalkeisengranate. Zentralblatt für Mineralogie, Geologie und Paläontologie, Abteilung A: Mineralogie und Petrographie, 225–239.
——— (1935) über titanhaltige Kalkeisengranate. II. Zentralblatt für Mineralogie, Geologie und Paläontologie, Abteilung A: Mineralogie und Petrographie, 68–78.

Manuscript received April 18, 2012
Manuscript accepted November 16, 2012
Manuscript handled by Fernando Colombo

Appendix 1. List of garnet species, end-member formulas, modifications, etymology, type localities; crystal structure refinements

The following garnet species either have been previously accepted by the IMA-CNMNC or have been modified by the current garnet subcommittee. Modifications to the original garnet species descriptions are noted except for grandfathered species. One or two references are given for the crystal structure, either of natural material (when available) or of synthetic material, or both.

Almandine

End-member formula: $\{Fe^{2+}_3\}[Al_2](Si_3)O_{12}$
Group: Garnet
IMA number: Grandfathered
Modifications: None
Etymology: The "Alabandic carbuncles" of Pliny were so named as they were cut and polished in Alabanda (Dana 1837, 1892), an ancient city in what is presently Aydin Province, Turkey.
Type locality: Not known
Crystal system, space group and structure refinement: Isometric, *Ia*$\bar{3}$*d*. Novak and Gibbs (1971); synthetic material: Armbruster et al. (1992).
Original or oldest description: Known in ancient times. Name first used by D.L.G. Karsten in 1800 (Dana 1892).

Andradite

End-member formula: $\{Ca_3\}[Fe^{3+}_2](Si_3)O_{12}$
Group: Garnet
IMA number: Grandfathered
Modifications: None
Etymology: For José Bonifácio de Andrada e Silva (1763–1838), the Brazilian mineralogist who described a variety under the name "allochroite" in 1800 (Dana 1892; Clark 1993).
Type locality: Not known
Crystal system, space group and structure refinement: Isometric, *Ia*$\bar{3}$*d*. Armbruster and Geiger (1993). Original or oldest description: "allochroite" of de Andrada in 1800 and "melanite" of Werner in 1800 (Dana 1892).

Berzeliite

End-member formula: $\{Ca_2Na\}[Mg_2](As^{5+}_3)O_{12}$
Group: Berzeliite
IMA number: Grandfathered
Modifications: None
Etymology: For Jacob Berzelius (1799–1848), a Swedish chemist.
Type locality: Långban, Filipstad district, Värmland, Sweden.
Crystal system and structure refinement: Isometric, *Ia*$\bar{3}$*d*. Hawthorne (1976); Nagashima and Armbruster (2012).
Original or oldest description: Kühn (1840)

Bitikleite

End-member formula: $\{Ca_3\}[Sb^{5+}Sn^{4+}](Al_3)O_{12}$
Group: Bitikleite
IMA number: 2009-052
Modifications: Originally described as bitikleite-(SnAl) with the same formula.
Etymology: From Bitikle, the name of an old fortification near the type locality.
Type locality: Upper Chegem caldera, Kabardino-Balkaria, North Caucasus, Russia.
Crystal system, space group and structure refinement: Isometric, *Ia*$\bar{3}$*d*. Galuskina et al. (2010b)
Original or oldest description: Galuskina et al. (2010b)

Calderite

End-member formula: $\{Mn^{2+}_3\}[Fe^{3+}_2](Si_3)O_{12}$
Group: Garnet
IMA number: Grandfathered
Modifications: None
Etymology: For James Calder, a member of the Asiatic Society of Bengal, originally applied to the rock containing the mineral (Piddington 1850).
Type locality: Either in Burdwan (Bardhaman) district, West Bengal State, or near Hazaribagh, Jharkhand State, India.
Crystal system, space group and structure report: Isometric, *Ia*$\bar{3}$*d*. No structure refinement; structure optimization by distance least-squares refinement (Ottonello et al. 1996).
Original or oldest description: Fermor (1909, 1926)

Cryolithionite

End-member formula: $\{Na_3\}[Al_2](Li_3)F_{12}$
Group: ungrouped
IMA number: Grandfathered
Modifications: None
Etymology: From the presence of Li and its relation to cryolite
Type locality: The Ivigtut cryolite deposit, Ivittuut (Ivigtut), Arsuk, Kitaa Province, Greenland.
Crystal system, space group and structure refinement: Isometric, *Ia*$\bar{3}$*d*. Geller (1971).
Original or oldest description: Ussing (1904)

Dzhuluite

End-member formula: $\{Ca_3\}[Sb^{5+}Sn^{4+}](Fe^{3+}_3)O_{12}$
Group: Bitikleite
IMA number: 2010-64
Modifications: Originally described as bitikleite-(SnFe) with the same formula.
Etymology: After Dzhulu Mountain near the type locality.
Type locality: Upper Chegem caldera, Kabardino-Balkaria, North Caucasus, Russia.
Crystal system and space group: Isometric, *Ia*$\bar{3}$*d*. Structure not yet refined.
Original or oldest description: Galuskina et al. (2011a)

Elbrusite

End-member formula: $\{Ca_3\}[U^{6+}_{0.5}Zr_{1.5}](Fe^{3+}_3)O_{12}$
Group: Bitikleite
IMA number: 2009-051
Modifications: Originally described as elbrusite-(Zr) with a formula $\{Ca_3\}[U^{6+}Zr](Fe^{3+}_2Fe^{2+})O_{12}$.
Etymology: From the highest peak in Europe - Mount Elbrus (5642 m).
Type locality: Upper Chegem caldera, Kabardino-Balkaria, North Caucasus, Russia.
Crystal system, space group and structure refinement: Isometric, *Ia*$\bar{3}$*d*. The structure of elbrusite has not yet been refined, but that of U-rich kerimasite has been refined [under the name "Fe-dominant analog of kimzeyite", Galuskina et al. (2010a)].
Original or oldest description: Galuskina et al. (2010a)

Eringaite

End-member formula: $\{Ca_3\}[Sc_2](Si_3)O_{12}$
Group: Garnet
IMA number: 2009-054
Modifications: None
Etymology: From the Eringa River, a tributary of the Wiluy River.
Type locality: Wiluy River, Sakha-Yakutia Republic, Russia. (63.0°N, 112.3°E).
Crystal system, space group and structure refinement: Isometric, *Ia*$\bar{3}$*d*.
Synthetic material: Mill' et al. (1977), Quartieri et al. (2006)
Original or oldest description: Galuskina et al. (2010d)

Goldmanite

End-member formula: $\{Ca_3\}[V^{3+}_2](Si_3)O_{12}$

Group: Garnet
IMA number: 1963-003
Modifications: None
Etymology: For Marcus I. Goldman (1881–1965), a sedimentary petrologist with the U.S. Geological Survey.
Type locality: Sandy (or South Laguna) mine area, Laguna, New Mexico, U.S.A.
Crystal system, space group and structure refinement: Isometric, *Ia3d*. Novak and Gibbs (1971); Righter et al. (2011).
Original or oldest description: Moench and Meyrowitz (1964)

Grossular

End-member formula: $\{Ca_3\}[Al_2](Si_3)O_{12}$
Group: Garnet
IMA number: Grandfathered
Modifications: None
Etymology: From the color resembling gooseberry, *Ribes grossularia* (Dana 1892; Clark 1993).
Type locality: Wiluy River, Sakha-Yakutia Republic, Russia.
Crystal system, space group and structure refinement: Isometric, *Ia3d*. Novak and Gibbs (1971).
Synthetic material: Geiger and Armbruster (1997).
Original or oldest description: A.G. Werner in 1808–1809. However, grossular was described earlier under other names, viz. as "Cinnamon Stone" (Kanelstein) from Sri Lanka by Werner in 1803–1804 and as "Granat" by Pallas in 1793 (Dana (1892).

Henritermierite

End-member formula: $\{Ca_3\}[Mn^{3+}_2](Si_2)(\square)O_8(OH)_4$
Group: Henritermierite
IMA number: 1968-029
Modifications: None
Etymology: For Henri-François-Émile Termier (1897–1989), a French geologist.
Type locality: Tachgagalt mine, Morocco.
Crystal system, space group and structure refinement: Tetragonal, $I4_1/acd$. Armbruster et al. (2001).
Original or oldest description: Gaudefroy et al. (1969)

Holtstamite

Formula: $\{Ca_3\}[Al,Mn^{3+}_2](Si_2)(\square)O_8(OH)_4$
Group: Henritermierite
IMA number: 2003-047
Modifications: None
Etymology: For Dan Holtstam (b. 1963), a Swedish mineralogist.
Type locality: Wessels Mine, Kalahari manganese field, South Africa.
Crystal system, space group and structure refinement: Tetragonal, $I4_1/acd$. Hålenius et al. (2005)
Original or oldest description: Hålenius (2004), Hålenius et al. (2005)

Irinarassite

End-member formula: $\{Ca_3\}[Sn^{4+}_2](SiAl_2)O_{12}$
Group: Schorlomite
IMA number: 2010-73
Modifications: None
Etymology: For Irina Rass (b. 1940), a Russian mineralogist.
Type locality: Upper Chegem caldera, Kabardino-Balkaria, North Caucasus, Russia.
Crystal system and space group: Isometric, *Ia3d*. Structure not yet refined.
Original or oldest description: Galuskina et al. (2011b)

Katoite

End-member formula: $\{Ca_3\}[Al_2](\square_3)(OH)_{12}$
Group: ungrouped
IMA number: 1982-080
Modifications: None
Etymology: For Akira Kato (b. 1931), a Japanese mineralogist.
Type locality: Campomorto quarry, Pietra Massa, Viterbo, Lazio, Italy.
Crystal system, space group and structure refinement: Isometric, *Ia3d*. Sacerdoti and Passaglia (1985); synthetic material (Lager et al. 1987).
Original or oldest description: Passaglia and Rinaldi (1984)

Kerimasite

End-member formula: $\{Ca_3\}[Zr_2](SiFe^{3+}_2)O_{12}$
Group: Schorlomite
IMA number: 2009-29
Modifications: None
Etymology: For the Kerimasi volcano.
Type locality: Kerimasi volcano, Gregory Rift, northern Tanzania.
Crystal system, space group and structure refinement: Isometric, *Ia3d*. Zaitsev et al. (2010), and under the name kimzeyite, Schingaro et al. (2001); synthetic material under the name kimzeyite (Whittle et al. 2007).
Original or oldest description: Zaitsev et al. (2010). Under the name kimzeyite: Schingaro et al. (2001) and Galuskina et al. (2005); under the name "Fe-dominant analog of kimzeyite" (Galuskina et al. 2010a, 2010b, 2010c).

Kimzeyite

End-member formula: $\{Ca_3\}[Zr_2](SiAl_2)O_{12}$
Group: Schorlomite
IMA number: Not recorded
Modifications: None
Etymology: For members of the Kimzey family, who were instrumental in obtaining and preserving mineral specimens from Magnet Cove.
Type locality: Kimzey quarry, Magnet Cove, Arkansas, U.S.A.
Crystal system, space group and structure refinement: Isometric, *Ia3d*. Munno et al. (1980)
Original or oldest description: Milton and Blade (1958), Milton et al. (1961)

Knorringite

End-member formula: $\{Mg_3\}[Cr^{3+}_2](Si_3)O_{12}$
Group: Garnet
IMA number: 1968-010
Modifications: None
Etymology: For Oleg von Knorring (1915–1994), a Russian mineralogist who worked in Finland and the United Kingdom.
Type locality: Kao kimberlite pipe, Butha-Buthe, Lesotho.
Crystal system, space group and structure refinement: Isometric, *Ia3d*. Synthetic material: Juhin et al. (2010).
Original or oldest description: Nixon and Hornung (1968)

Majorite

End-member formula: $\{Mg_3\}[SiMg](Si_3)O_{12}$
Group: Garnet
IMA number: 1969-018. Modifications: Formula originally given as $\{(Mg,Na)_3\}[(Fe,Si,Al,Cr)_2](Si_3)O_{12}$.
Etymology: For Alan Major, who assisted A.E. Ringwood in experiments.
Type locality: Coorara L6 chondrite (recovered in Western Australia).
Crystal system, space group and structure refinement: Isometric, *Ia3d*.
Synthetic material: Hazen et al. (1994)
Original or oldest description: Smith and Mason (1970)

Manganberzeliite

End-member formula: $\{Ca_2Na\}[Mn^{2+}_2](As^{5+}_3)O_{12}$
Group: Berzeliite
IMA number: Grandfathered
Modifications: See text.
Etymology: The manganese analog of berzeliite.
Type locality: Långban, Filipstad district, Värmland, Sweden.
Crystal system, space group and structure refinement: Isometric, *Ia3d*.
Qualitative description of the structure: Bubeck and Machatschki (1935); Nagashima and Armbruster (2012)
Original or oldest description: Igelström (1886, 1894)

Menzerite-(Y)

End-member formula: $\{Y_2Ca\}[Mg_2](Si_3)O_{12}$
Group: Garnet
IMA number: 2009-050
Modifications: None
Etymology: For Georg Menzer (1897–1989), the German crystallographer who was the first to solve the structure of garnet (Menzer 1928); the suffix Y is a Levinson modifier that indicates that Y is dominant among the sum of Y and the rare-earth elements.
Type locality: Bonnet Island in Georgian Bay, near Parry Sound, Ontario, Canada.
Crystal system, space group and structure refinement: Isometric, *Ia3d*. Grew et al. (2010)
Original or oldest description: Grew et al. (2010)

Momoiite

End-member formula: $\{Mn^{2+}_3\}[V^{3+}_2](Si_3)O_{12}$
Group: Garnet
IMA number: 2009-026.
Modifications: None; see the "yamatoite" of Momoi (1964), which was not approved because this component was not dominant in the material that they investigated (Fleischer 1965).
Etymology: For Hitoshi Momoi (1930–2002), the Japanese mineralogist who was the first to recognize $\{Mn^{2+}_3\}[V^{3+}_2](Si_3)O_{12}$ as a component in garnet.
Type locality: Kurase mine, Ehime Prefecture, Japan.
Crystal system and space group: Isometric, *Ia3d*. Structure not yet refined, but the atomic coordinates were predicted by Novak and Gibbs (1971).
Original or oldest description: Tanaka et al. (2010)

Morimotoite

End-member formula: $\{Ca_3\}[TiFe^{2+}](Si_3)O_{12}$
Group: Garnet
IMA number: 1992-017
Modifications: None
Etymology: For Nobuo Morimoto (b. 1925), a Japanese mineralogist.
Type locality: Fuku, Bitchu-Cho, Okayama Prefecture, Japan.
Crystal system and space group: Isometric, *Ia*$\bar{3}$*d*. Structure not yet refined.
Original or oldest description: Henmi et al. (1995)

Palenzonaite

End-member formula: $\{Ca_2Na\}[Mn^{2+}_2](V^{5+}_3)O_{12}$
Group: Berzeliite
IMA number: 1986-011
Modifications: None
Etymology: For Andrea Palenzona (b. 1935), an Italian chemist.
Type locality: Molinello mine, Ne, Val Graveglia, Liguria, Italy.
Crystal system, space group and structure refinement: Isometric, *Ia*$\bar{3}$*d*. Basso (1987); Nagashima and Armbruster (2012)
Original or oldest description: Basso (1987)

Pyrope

End-member formula: $\{Mg_3\}[Al_2](Si_3)O_{12}$
Group: Garnet
IMA number: Grandfathered
Modifications: None
Etymology: From the Greek πυρωπός (pyropos) – firelike for its deep-red color.
Type locality: Bohemia (Czech Republic).
Crystal system, space group and structure refinement: Isometric, *Ia*$\bar{3}$*d*. Novak and Gibbs (1971)
Synthetic material: Armbruster et al. (1992)
Original or oldest description: Recognized by Georgius Agricola (1546), but the name pyrope was introduced by A.G. Werner in 1800 (Dana 1892; Clark 1993).

Schäferite

End-member formula: $\{Ca_2Na\}[Mg_2](V^{5+}_3)O_{12}$
Group: Berzeliite
IMA number: 1997-048
Modifications: None
Etymology: For Helmut Schäfer (b. 1931), an amateur German mineralogist who discovered the mineral.
Type locality: Bellberg volcano near Mayen, Eifel, Germany.
Crystal system, space group and structure refinement: Isometric, *Ia*$\bar{3}$*d*. Krause et al. (1999)
Original or oldest description: Krause et al. (1999)

Schorlomite

End-member formula: $\{Ca_3\}[Ti_2](SiFe^{3+}_2)O_{12}$
Group: Schorlomite
IMA number: Grandfathered
Modifications: Extensive; see main text.
Etymology: For its resemblance to schorl.
Type locality: Magnet Cove, Hot Springs County, Arkansas, U.S.A.
Crystal system, space group and structure refinement: Isometric, *Ia*$\bar{3}$*d*. Chakhmouradian and McCammon (2005)
Original or oldest description: Shepard (1846), Whitney (1849), and Rammelsberg (1850a, 1850b)

Spessartine

End-member formula: $\{Mn^{2+}_3\}[Al_2](Si_3)O_{12}$
Group: Garnet
IMA number: Grandfathered
Modifications: None
Etymology: From the Spessart Mountains, Germany.
Type locality: Sommer quarry, Wendelberg Mt., Spessart Mountains, Bavaria, Germany.
Crystal system, space group and structure refinement: Isometric, *Ia*$\bar{3}$*d*. Novak and Gibbs (1971); for F-bearing, Smyth et al. (1990).
Synthetic material: Geiger and Armbruster (1997)
Original or oldest description: Recognized by M.H. Klaproth (1797), but the name spessartine was introduced by F.S. Beudant (1832) according to Dana (1892) and Clark (1993).

Toturite

End-member formula: $\{Ca_3\}[Sn^{4+}_2](SiFe^{3+}_2)O_{12}$
Group: Schorlomite
IMA number: 2009-033
Modifications: None
Etymology: From both the Totur River situated in Eltyubyu village near the type locality and the name of a Balkarian deity and ancient warrior.
Type locality: Upper Chegem caldera, Kabardino-Balkaria, North Caucasus, Russia.
Crystal system and space group: Isometric, *Ia*$\bar{3}$*d*. Structure not yet refined.
Original or oldest description: Galuskina et al. (2010c)

Usturite

End-member formula: $\{Ca_3\}[Sb^{5+}Zr](Fe^{3+}_2)O_{12}$
Group: Bitikleite
IMA number: 2009-053
Modifications: Originally described as bitikleite-(ZrFe) with the same formula.
Etymology: From the Ustur Mountain near the type locality.
Type locality: Upper Chegem caldera, Kabardino-Balkaria, North Caucasus, Russia.
Crystal system and space group: Isometric, *Ia*$\bar{3}$*d*. Structure not yet refined.
Original or oldest description: Galuskina et al. (2010b)

Uvarovite

End-member formula: $\{Ca_3\}[Cr^{3+}_2](Si_3)O_{12}$
Group: Garnet
IMA number: Grandfathered
Modifications: None
Etymology: For Count Sergei Semenovich Uvarov (1786–1855), a Russian historian.
Type locality: Saranovskiy mine Biserskoye chromite deposit, Perm district, Urals, Russia (Pekov 1998).
Crystal system, space group and structure refinement: Isometric, *Ia*$\bar{3}$*d*. Novak and Gibbs (1971)
For birefringent uvarovite: Wildner and Andrut (2001)
Original or oldest description: Hess (1832)

Yafsoanite

End-member formula: $\{Ca_3\}[Te^{6+}_2](Zn_3)O_{12}$
Group: ungrouped
IMA number: 1981-022
Modifications: Introduced with the idealized formula $(Zn_{1.38}Ca_{1.36}Pb_{0.26})_{\Sigma=3.00}TeO_6$; current formula from Jarosch and Zemann (1989) and Mills et al. (2010).
Etymology: From the acronym *Ya*kytskii *F*ilial *S*ibirskogo *O*tdeleniya *A*kademii *N*auk (Yakyt Filial of the Siberian Branch of the Academy of Sciences).
Type locality: Kuranakh gold deposit, near Aldan, Yakutia, Russia (Pekov 1998).
Crystal system, space group and structure refinement: Isometric, *Ia*$\bar{3}$*d*. Mills et al. (2010)
Original or oldest description: Kim et al. (1982)

Eur. J. Mineral.
2006, **18**, 551-567

Recommended nomenclature of epidote-group minerals

THOMAS ARMBRUSTER[1,*] (Chairman), PAOLA BONAZZI[2] (Vice-chairman), MASAHIDE AKASAKA[3], VLADIMIR BERMANEC[4], CHRISTIAN CHOPIN[5], RETO GIERÉ[6], SORAYA HEUSS-ASSBICHLER[7], AXEL LIEBSCHER[8], SILVIO MENCHETTI[2], YUANMING PAN[9] and MARCO PASERO[10]

[1]Laboratorium für chemische und mineralogische Kristallographie, Universität Bern, Freiestr. 3, CH-3012 Bern, Switzerland
[2]Dipartimento di Scienze della Terra dell'Università di Firenze, Via La Pira 4, I-50121 Firenze, Italy
[3]Department of Geoscience, Faculty of Science and Engineering, Shimane University, 1060 Nishikawatsu, Matsue 690, Japan
[4]Geoloski odsjek, Mineralosko petrografski zavod PMF-a, University of Zagreb, Horvatovac bb, HR-1000 Zagreb, Croatia
[5]Laboratoire de Géologie, UMR 8538 du CNRS, Ecole Normale Supérieure, 24 rue Lhomond, F-75005 Paris, France
[6]Mineralogisch-Geochemisches Institut, Albert-Ludwigs-Universität, Albertstrasse 23b, D-79104 Freiburg, Germany
[7]Department für Geo- und Umweltwissenschaften, Sektion Mineralogie, Petrologie und Geochemie, Ludwig-Maximilians-Universität, Theresienstraße 41/III,D-80333 München, Germany
[8]Department 4 Chemistry of the Earth, GeoForschungsZentrum Potsdam, Telegrafenberg, D-14473 Potsdam, Germany
[9]Department of Geological Sciences, University of Saskatchewan, Saskatoon, SK S7N 5E2, Canada
[10]Dipartimento di Scienze della Terra, Università di Pisa, Via S. Maria 53, I-56126 Pisa, Italy

Abstract: Epidote-group minerals are monoclinic in symmetry and have topology consistent with space group $P2_1/m$ and the general formula $A_2M_3[T_2O_7][TO_4](O,F)(OH,O)$. Zoisite is an orthorhombic polymorph of clinozoisite $Ca_2Al_3[Si_2O_7][SiO_4]O(OH)$ and is thus not considered a member of the epidote-group. Epidote-group minerals are divided into three subgroups. (1) Members of the **clinozoisite subgroup** are derived from the mineral clinozoisite $Ca_2Al_3[Si_2O_7][SiO_4]O(OH)$ by homovalent substitutions only. The key cation- and anion-sites are A1 = M^{2+}, A2 = M^{2+}, M1 = M^{3+}, M2 = M^{3+}, M3 = M^{3+}, O4 = O^{2-}, O10 = $(OH)^-$. In other words, the dominant valence as listed above must be maintained. (2) Members of the **allanite subgroup** are REE-rich minerals typified by the eponymous mineral "allanite". This subgroup may be derived from clinozoisite by homovalent substitutions and **one** coupled heterovalent substitution of the type $^{A2}(REE)^{3+} + {}^{M3}M^{2+} \rightarrow {}^{A2}Ca^{2+} + {}^{M3}M^{3+}$. Thus the valences on the key sites are: A1 = M^{2+}, **A2 = M^{3+}**, M1 = M^{3+}, M2 = M^{3+}, **M3 = M^{2+}**, O4 = O^{2-}, O10 = $(OH)^-$. (3) Members of the **dollaseite subgroup** are REE-rich minerals typified by the eponymous mineral "dollaseite". This subgroup may be derived from clinozoisite by homovalent substitutions and **two** coupled heterovalent substitutions of the type $^{A2}(REE)^{3+} + {}^{M3}M^{2+} \rightarrow {}^{A2}Ca^{2+} + {}^{M3}M^{3+}$ and $^{M1}M^{2+} + {}^{O4}F^- \rightarrow {}^{M1}M^{3+} + {}^{O4}O^{-2}$. Thus the valences on the key sites are: A1 = M^{2+}, **A2 = M^{3+}, M1 = M^{2+}**, M2 = M^{3+}, **M3 = M^{2+}**, **O4 = F^-**, O10 = $(OH)^-$.

The key cation-sites M3 and A1 (and, in principle, M2) determine the root name. In both clinozoisite and allanite subgroups no prefix is added to the root name if M1 = Al. The prefixes ferri, mangani, chromo, and vanado indicate dominant Fe^{3+}, Mn^{3+}, Cr^{3+}, and V^{3+} on M1, respectively. In the dollaseite subgroup no prefix is added to the root name if M1 = Mg. Otherwise a proper prefix must be attached; the prefixes ferro and mangano indicate dominant Fe^{2+} and Mn^{2+} at M1, respectively. The dominant cation on A2 (other than Ca) is treated according to the *Extended Levinson* suffix designation. This simple nomenclature requires renaming of the following approved species: Niigataite (old) = **clinozoisite-(Sr) (new)**, hancockite (old) = **epidote-(Pb) (new)**, tweddillite (old) = **manganipiemontite-(Sr) (new)**. Minor modifications are necessary for the following species: Strontiopiemontite (old) = **piemontite-(Sr) (new)**, androsite-(La) (old) = **manganiandrosite-(La) (new)**. Before a mineral name can be assigned, the proper subgroup has to be determined. The determination of a proper subgroup is made by the dominating valence at M3, M1, and A2 expressed as M^{2+} and or M^{3+}, not by a single, dominant ion (*i.e.*, Fe^{2+}, or Mg, or Al). In addition, the dominant valence on O4: X^- or X^{2-} must be ascertained. $[M^{2+}]_{A2} > 0.50$, $[M^{3+}]_{M3} > 0.50 \rightarrow$ clinozoisite subgroup, $[M^{3+}+ M^{4+}]_{A2} > 0.50$, $[M^{2+}]_{M3} > 0.50 \rightarrow$ allanite subgroup, $\{[M^{2+}]_{M3+M1} - [M^{3+}+ M^{4+}]_{A2}\} > 0.50$ **and** $[X^-]_{O4} > 0.5 \rightarrow$ dollaseite subgroup. Coupled heterovalent substitutions in epidote-group minerals require a special application of the so-called 50 % rule in solid-solution series. (1) Clinozoisite subgroup: The dominant **trivalent** cation on M3 determines the name, whereas the A2 cation appearing in the suffix has to be selected from among the **divalent** cations. (2) Allanite and dollaseite subgroups: For the sites involved in the charge compensation of a heterovalent substitution in A2 and O4 (*i.e.* M3 in the allanite subgroup; M3 and M1 in the dollaseite subgroup), identification of the relevant end-member formula must take into account the **dominant divalent charge-compensating octahedral cation (M^{2+})** and not the dominant cation in these sites.

Formal guidelines and examples are provided in order to determine a mineral "working name" from electron-microprobe analytical data.

Key-words: Nomenclature, epidote-group minerals, clinozoisite, allanite, dollaseite.

*E-mail: Thomas.Armbruster@krist.unibe.ch

0935-1221/06/0018-0551 $ 7.65
DOI: 10.1127/0935-1221/2006/0018-0551

1. Introduction

1.1. Some obvious problems

Deer *et al.* (1986) concluded in their Rock-forming Minerals: "There is no universally accepted nomenclature of the monoclinic Fe–Al members of the epidote group. Some earlier names, e.g. fouquéite for compositions containing up to about 10 mol. % of the $Ca_2Fe_3Si_3O_{12}(OH)$[1] component, have fallen into disuse and clinozoisite is now used to describe those members of the series that are optically positive, corresponding with approximately 15 mol.% $Ca_2Fe_3Si_3O_{12}(OH)$. For the more iron-rich, optically negative members, the name pistacite is used by some authors; the majority, however, describe those members with between 15 and 33 mol.% $Ca_2Fe_3Si_3O_{12}(OH)$ as epidote. This common use of the name is preferred in spite of its use to designate the group as a whole. The optical distinction of members of the clinozoisite-epidote series around the 15 mol.% composition is difficult, and in the absence of a chemical analysis is generally based on color and pleochroism. Where the composition is known it is usually expressed in terms of the theoretical pistacite end-member, $p_s = 100 \times Fe^{3+}/(Fe^{3+} + Al)$."

The nomenclature problems discussed by Deer *et al.* (1986) were only partly solved after publication of the criteria for new mineral names (Nickel & Mandarino, 1987). Are these "rules" only applicable to new minerals (the corresponding paragraph was entitled "criteria for new mineral names")? What about the "grandfathered" mineral names epidote and clinozoisite described in the past and generally believed to represent valid species names? How are the boundaries between epidote and clinozoisite defined?

Of the 22 "piemontite" analytical data reported by Deer *et al.* (1986) only seven meet the minimum criterion of Fe < Mn > 0.5 required to satisfy the rule given by Nickel & Mandarino (1987): "At least one major structural site is occupied by a different chemical component."

Ercit (2002), in his article "The mess that is allanite", asks the provocative question: What is "allanite"? He states that the name "allanite" is often incorrectly used to describe any REE-bearing epidote. Investigators were additionally confused by introduction of new mineral names for REE-bearing epidote-group minerals such as dissakisite-(Ce), dollaseite-(Ce), khristovite-(Ce), and androsite-(La). Until 1988, the mineralogy of REE-rich epidote-group minerals was very simple because there was only the one official root name allanite with the end-member formula $CaREEAl_2Fe^{2+}[Si_2O_7][SiO_4]O(OH)$. An additional source of confusion (Ercit, 2002) is that cations in the formula of REE-rich epidote-group minerals are commonly grouped rather than assigned to specific sites. However, specific site assignments determine the species. In the absence of appropriate guidelines, Ercit (2002) discusses several approaches for using electron-microprobe analytical data to calculate formulae of REE-bearing epidote-group minerals. Then he uses analytical data from the literature to obtain a simplified end-member formula corresponding to a mineral name. There are two major criticisms to his approach: (1) Analytical data from the literature that had been obtained on metamict materials were used, which do not fulfill the criterion that a mineral be crystalline; (2) Standard guidelines for mineral nomenclature (Nickel & Grice, 1998) were uncritically applied, resulting in end-member formulae [*e.g.*, $CaLaAl_2V^{3+}[Si_2O_7][SiO_4]O(OH)$] that are not charge-balanced and thus meaningless.

1.2. Objectives

The Commission on New Minerals and Mineral Names (CNMMN) of the International Mineralogical Association (IMA) established at the beginning of 2003 the Subcommittee on Epidote-Group Mineral Nomenclature. This subcommittee defined following aims: (1) Development of a consistent nomenclature system to minimize proliferation of unrelated mineral names; (2) to explain appropriate use of existing and new names within this mineral group by defining simple rules for nomenclature based on chemistry and ion (cation and anion) order; (3) to provide a simple but powerful scheme to derive a "working name" of an epidote-group mineral based on electron-microprobe analytical data.

Finally, this report supplies an Appendix with specifically selected chemical data of epidote-group minerals representing either borderline cases, or incomplete or erroneous analytical data, or data originating from partly metamict minerals. These examples have been chosen to demonstrate naming of epidote-group minerals in non-trivial cases.

It is not the intent of this nomenclature recommendation to provide a complete view of chemical variations reported for epidote-group minerals. For additional references on this subject we refer to Liebscher & Franz (2004).

2. Historical synopsis

2.1. Epidote and clinozoisite

Epidote, a monoclinic mineral with the idealized formula $Ca_2Al_2Fe^{3+}[Si_2O_7][SiO_4]O(OH)$, was named by Haüy (1801). The type locality is Bourg d'Oisans, Dauphiné, France. The name comes from the Greek *epi* over plus *dotós* given (verbid of *didóni), i.e.*, given besides, "increased". A related noun is epidosis, *i.e.* "increase". This refers to Haüy's observation that the base of the mineral's prism has one side longer than the other. The rationale for the name epidote may appear quaint to us today, but it has to be understood in the context of criteria for distinguishing minerals at the beginning of the 19th century (mainly crystal forms, density, and optical properties, as well as chemical composition). Dana (1896) stated that Haüy set aside several older names: Thallite, derived from the Greek noun *thallos* meaning young twig (alluding to the green color), was rejected because of color variation; delphinite,

[1]Given as $Ca_2FeAl_2Si_3O_{12}(OH)$ in the text by Deer *et al.* (1986). However, it is clear from the molar percentage values (15 -33) cited by these authors for the epidote (*sensu stricto*) compositional range that they are actually referring to a $Ca_2Fe_3Si_3O_{12}(OH)$ component.

and arendalite (also named akanticone) were rejected because they were derived from specific localities. A synonym for epidote, pistacite, comes from the Greek for pistachio nut, a reference to the distinctive yellowish-green color of some epidote. The name pistacite was introduced by Ludwig (1803-1804), who extended the systematic nomenclature of Abraham Gottlob Werner (1750-1817). This timing gives epidote precedence. Pistacite is not listed among accepted mineral names (in spite of its frequent use) by Hey (1955) but referenced as synonym of epidote. Other obsolete names (Dana, 1896) are oisanite, puschkinite (six other spellings have also been used, *e.g.*, pushklinite in Dufrénoy, 1856), achmatite, beustite and escherite. Withamite was used for a strongly pleochroic deep crimson and straw yellow epidote-group mineral from Glen Coe, Strathclyde (Argyllshire), Scotland, UK and sometimes referred to as piemontite. However, chemical analyses gave only 0.24 wt.% MnO – equivalent to 0.27 wt. % Mn_2O_3 – (Dana, 1896). Thus this low Mn^{3+} content is already sufficient for piemontite-like pleochroism. Subsequent chemical analyses of "withamite" (Hutton, 1938) clearly suggest its identity with epidote. Withamite from the Yamanaka mine (Japan) described by Yoshimura & Momoi (1964) is manganian clinozoisite.

Weiss (1820) presented the first complete indexing of crystal faces of monoclinic epidote, which may be considered the beginning of systematic crystallographic work on this mineral group. Dufrénoy (1856) used epidote as the group name and distinguished thallite (green iron-bearing epidote) and zoisite on the basis of different cleavage and habit. Ito (1950) and Ito *et al.* (1954) first deduced the correct atomic arrangement in epidote, which they showed to contain both single SiO_4 tetrahedra and double-tetrahedral Si_2O_7 groups (*cf.* Ito, 1947). Systematic structural studies by Dollase (1968, 1969, 1971) clarified the crystal-chemical relationships of the epidote group.

The name **clinozoisite** was given by Weinschenk (1896) to Fe-poor epidote from Prägratten, Tyrol, Austria. The name is for the polymorphism with zoisite, $Ca_2Al_3[Si_2O_7][SiO_4]O(OH)$ (see below). However, Lacroix (1889) was probably the first to describe this mineral under the name fouquéite. We quote Dana (1896): "Composition like zoisite from which it differs in form; it appears to be an epidote essentially, containing but little iron… Occurs in anorthite-gneiss at Salem, and less often at Kandy, Ceylon. The rock also contains ordinary epidote (but not immediately associated with fouquéite)… Named for M. Fouqué." The analysis reported by Lacroix (1889) is given in Table 1.

According to the structural studies of Ito *et al.* (1954) and Dollase (1968, 1969, 1971) monoclinic members of the epidote group have three distinct octahedral sites (M1, M2, M3), each contributing with the same multiplicity to the formula. If one of these sites in an unnamed mineral were found to be dominantly occupied by a chemical component that is not dominant at the equivalent site in an existing mineral, then the unnamed would be a new mineral species with its own name (Nickel & Mandarino, 1987). Application of this rule requires detailed crystal-chemical knowledge of the various mineral groups and particularly of the cation site-preference. In the epidote group, if by chance ferric iron did not order onto the largest and most distorted octahedral site M3, but were randomly distributed over the three available sites, the composition $Ca_2Al_2Fe^{3+}[Si_2O_7][SiO_4]O(OH)$ could not be given an independent mineral name. Instead, it would have to be called ferrian clinozoisite because Al would be dominant at all three octahedral sites (M1, M2, M3). However, structure refinements and spectroscopic investigations of epidote-group minerals have consistently shown a strong preference of Fe^{3+} for M3 (*e.g.*, Ito *et al.*, 1954; Dollase, 1971, 1973). Thus, the old name epidote is retained.

Table 1. Historical chemical data (wt.%) of epidote (Laspeyres, 1879), fouquéite (Lacroix, 1889), and piemontite (Rammelsberg, 1875), all data cited from Dana (1896).

Sample	Epidote (Bourg d'Oisans)	Fouquéite = Clinozoisite (Sri Lanka)	Piemontite (St. Marcel)
SiO_2	36.49	38.6	38.64
Al_2O_3	22.45	32.5	15.03
Fe_2O_3	14.93	2.1	8.38
Mn_2O_3	0.03		15.00
CaO	23.52	23.9	22.19
LOI	1.91	2.7	1.78
Sum	99.35	99.8	101.02
Si	2.94	2.97	3.16
Al	2.13	2.94	1.45
Fe	0.91	0.12	0.52
Mn	0.00		0.93
Ca	2.02	1.97	1.94
O(calc.)	12.45	12.50	12.61

Formula normalized on 8 cations. LOI – loss on ignition.

2.2. Zoisite

Originally this mineral was named saualpite for the locality Saualpe in Carinthia, Austria, where it occurs in eclogites. The name zoisite was chosen by A.G. Werner in 1805 to honor Siegmund Zois, Baron von Edelstein (1747-1819), the Austrian mineral collector from whom Werner obtained the holotype specimen from Saualpe (Dana, 1896). **Zoisite** is the orthorhombic polymorph of clinozoisite. Other obsolete names or synonyms cited by Dana (1896) are: Illuderite, lime-epidote, thulite, unionite. Hey (1955) also cited chrome-zoisite and manganese-zoisite. Tanzanite is a gem name for vanadium-bearing zoisite from Tanzania, which turns from brown into blue upon heat-treatment at 400-500°C. A dense green chromium-bearing zoisite in a zoisite amphibolite associated with mostly non-transparent ruby also from Tanzania was named "anyolite" meaning green in the language of the Massai (Eppler, 1984). Ito (1950) first proposed a structural model for zoisite, which was subsequently confirmed by Fesenko *et al.* (1955) and Dollase (1968). Zoisite is the only orthorhombic mineral species originally assigned to the epidote group.

2.3. Piemontite, strontiopiemontite, and tweddillite

A Mn-rich, epidote-related mineral from Praborna mine, St. Marcel, Aosta Valley, in the Italian Western Alps, was named **piemontite** (originally "*Piemontit*") by Kenngott (1853). The English spelling of the Italian word Piemonte is Piedmont, and Dana (1896) arbitrarily anglicized the mineral name to piedmontite. However, the Italian region of the type locality, St. Marcel, was called Piemonte when the mineral was first described, and for this reason the name piemontite is correct. Today, St. Marcel belongs to Valle d'Aosta, which was established as an autonomous region in 1945. Dufrénoy (1856) stated that the "variété manganésifère" from Piemonte is named "piemonite". Hey (1955) considered both piedmontite and manganepidote to be synonyms of piemontite.

Dollase (1969) demonstrated by single-crystal X-ray structure refinement that Mn^{3+} in piemontite, ideally $Ca_2Al_2Mn^{3+}[Si_2O_7][SiO_4]O(OH)$, is preferentially ordered on the octahedral M3 site, thus confirming the interpretation of spectroscopic data by Burns & Strens (1967). Nonetheless, there seems to be a general problem

with the assignment of the name piemontite (Catti *et al.*, 1989). Dana (1896) included under the name piemontite monoclinic, dark-red epidote-group minerals with characteristic red – pink to amethyst – orange to yellow pleochroism, even if the molar Mn_2O_3 content was less than Fe_2O_3 content. Mottana & Griffin (1986) showed that piemontite from the type locality (the Praborna manganese mine) is rather heterogeneous. Nonetheless, the compositions of most samples fall in the vicinity of Al:Mn = 2:1 with a general trend of some excess Mn extending to Al:Mn = 1.3:1. In addition, Mottana & Griffin (1986) found that piemontite from St. Marcel is frequently strontian piemontite with up to 0.47 Sr pfu. Catti *et al.* (1989) and Ferraris *et al.* (1989) reported structural data on this strontian piemontite.

Strontiopiemontite, ideally $CaSrAl_2Mn^{3+}[Si_2O_7][SiO_4]O(OH)$, is the analogue of piemontite with Sr dominant in the structural site A2, as shown by X-ray single-crystal structure refinement (Bonazzi *et al.*, 1990). It is a low-temperature metamorphic product and occurs in the manganese ore at Molinello and Cassagna mines of Val Graveglia, Northern Apennines, Italy.

Tweddillite, $CaSrMn^{3+}AlMn^{3+}[Si_2O_7][SiO_4]O(OH)$, is a mineral related to strontiopiemontite (Armbruster *et al.*, 2002). It is found as a hydrothermal alteration product of primary manganese ore in the Wessels mine of the Kalahari manganese field, Republic of South Africa. It was named tweddillite in honor of S. M. Tweddill, the first curator (from 1897 to 1916) of the Museum of the Geological Survey at Pretoria, RSA. Definition of this new mineral species was justified, as shown by structure refinement, because Mn^{3+} dominates both octahedral M1 and M3 sites, different from just M3 in strontiopiemontite and piemontite.

2.4. "Tawmawite" and mukhinite

The name "**tawmawite"** was introduced by Bleeck (1907) in his description of jadeite deposits in Upper Burma (now Myanmar). Tawmaw was a major jadeite mining-district in this area at the beginning of the 20th century. Bleeck (1907) described "tawmawite" as an emerald green, chromium-rich epidote mineral. However, the chemical analysis did not correspond to epidote-group stoichiometry, mainly due to contamination with chromite. The existence of a mineral with idealized composition $Ca_2Al_2Cr^{3+}[Si_2O_7][SiO_4]O(OH)$ has been shown by electron-microprobe analyses of epidote-group minerals occurring as inclusions in calcic plagioclase in a kyanite amphibolite from Southern Alps, New Zealand (Grapes, 1981), and in a quartzite from Outokumpu, Finland (Treloar, 1987). Chromium-rich epidote-group minerals are commonly zoned on a very fine scale (oscillatory zoning) so that determination of specific site preference of Cr using crystal-structure refinement has not been possible to date. Burns & Strens (1967) provided spectroscopic evidence that Fe^{3+}, and Mn^{3+} in epidote-group minerals order preferentially on M3, but assumed that Cr^{3+} orders preferentially on M1. However, Liebscher (2004) concluded that the derived Δ_{oct} with the position of ν_{II} (Burns & Strens, 1967) results in a Racah parameter *B* that is higher than that of the free Cr^{3+} ion and therefore physically meaningless. The interpretation of the spectra by Burn & Strens (1967) is thus open to question. Armbruster & Lahti (in prep.) have recently performed a combined electron microprobe - crystal-structure study on V^{3+}-rich "tawmawite" from Outokumpu, Finland, first described by Eskola (1933). Preliminary results indicate that Cr is disordered over M3 and M1 (with a slight preference for M3), which cast doubts on the species character of "tawmawite" if the Cr content is below 1 Cr pfu. To our knowledge the highest Cr content in chromian clinozoisite was reported as 15.37 wt.% Cr_2O_3 (Treloar, 1987), corresponding to 0.98 Cr pfu, which is still slightly below the limit required for highly disordered partition of Cr between M1 and M3. On the basis of available data "tawmawite" cannot be considered a valid species. Such samples have to be described as chromian (or better Cr^{3+}-rich) clinozoisite until new evidence is presented.

Mukhinite, $Ca_2Al_2V^{3+}[Si_2O_7][SiO_4]O(OH)$, was described by Shepel & Karpenko (1969) from marbles (Gornaya Shoriya, Kemerovo Oblast, Siberia, Russia). The name is for the geologist A.S. Mukhin of the West Siberian Geological Survey. In the absence of crystallographic data ordering of V^{3+} on M3 may be assumed by analogy with Fe^{3+}. Structural data including cation site-distributions are highly desirable for mukhinite.

2.5. Hancockite and niigataite

Hancockite is another old name. Penfield & Warren (1899) named a Pb-rich monoclinic epidote-group mineral discovered at Franklin, N.J., USA after Elwood P. Hancock (1836-1916) of Burlington, N.J., a collector of Franklin minerals. At the type locality the mineral contains appreciable amounts of Sr, and of Mn^{3+}, the latter being responsible for the strong red color (Dunn, 1985). Holtstam & Langhof (1994) reported a second occurrence of this very rare species from Jakobsberg, Filipstad, Sweden (skarn enclosed in dolomitic marble). Hancockite, $CaPbAl_2Fe^{3+}[Si_2O_7][SiO_4]O(OH)$, may be considered an epidote (*sensu stricto*) with Ca on A2 substituted by Pb.

Niigataite, $CaSrAl_3[Si_2O_7][SiO_4]O(OH)$, is related to clinozoisite but with Ca on the A2 site substituted by Sr (shown by single-crystal X-ray structure refinement). The name is for the Japanese prefecture where the mineral was discovered. Niigataite was found in a boulder of prehnite rock, where the mineral occurs interstitially with diaspore and chlorite in close association with strontian clinozoisite (Miyajima *et al.*, 2003).

2.6. REE-rich epidote-group minerals

In the following text REE represents the lanthanides (elements 57 to 71) and Y because of its chemical similarity to the lanthanides.

Historically, "allanite" (Thomson, 1810) is the second monoclinic mineral of the epidote group with a name that is still in use. The name is for Thomas Allan (1777-1833), a Scottish mineralogist who discovered the mineral. The type material is allegedly from Iglorsoit, East Greenland. However, studies of Giesecke's diaries from 1806 suggest that the type locality is most likely Qaqarssuatsiaq, Aluk, East Greenland (Petersen & Johnsen, 2005). Dana (1896) listed following synonyms or varieties of "allanite": Cerine, bucklandite, tautolite, uralorthite, bagrationite, orthite, xanthorthite, pyrorthite, and wasite. Those names describe partly altered "allanites" or solid-solution members between "allanite" and epidote from specific localities with more or less characteristic crystal forms. In addition, the Y-rich minerals muromontite (5.52 % BeO) and bodenite were considered varieties of "allanite" (Dana, 1896). The latter two names are nowadays no longer listed among minerals and their relation to "allanite" is also under question [for a discussion on muromontite and Be in "allanite" *cf.* Grew (2002)]. Nagatelite is supposedly a phosphatian "allanite" (Iimori *et al.*, 1931). However, X-ray diffraction data are mandatory to confirm this relationship. Hey (1955) referenced also treanorite as synonym for "allanite" and additionally the following "allanite" varieties: Cerepidote, cerorthite, yttrio-orthite, magnesium-orthite, and mangan-orthite. The "orthite" vs. "allanite" controversy was resolved in 1986 by the Commission on New Minerals and Mineral Names, IMA, in favor of "allanite". Taking into account Levison's

nomenclature (1966) for rare-earth minerals, the mineral from Greenland originally described by Thomson (1810) is actually **allanite-(Ce)** and, citing that priority, the CNMMN formally approved the name allanite-(Ce) (Nickel & Mandarino, 1987). Cerium is the dominant REE in most "allanite". However, chemical data are available in the literature for La- and Y-dominant "allanite", which should be properly considered as distinct mineral species. Their status has not until recently been formally approved, although the corresponding mineral names allanite-(La) and allanite-(Y) have been in circulation (Levinson, 1966) and are included in the IMA list of minerals. With the aim of securing official status for such unapproved epidote-group minerals, Orlandi & Pasero (2006) recently defined the "new" mineral **allanite-(La),** which has now the status of an IMA-approved species (proposal # 2003-065).

Lombaardite was first described by Nels *et al.* (1949) from the Zaaiplaats tin mine, central Transvaal, and re-examined by Neumann & Nilssen (1962) reporting *ca*. 10 -15wt.% $(REE)_2O_3$. Neumann & Nilssen (1962) suggested that lombaardite is very similar or even identical to a Y_2O_3 dominant "allanite" (with 22.16 wt.% $(REE)_2O_3$ including 5.39 wt.% Y_2O_3) from a pegmatite at Åskagen, Värmland, Sweden. Thus the Åskagen, Värmland, sample represents **allanite-(Y)**.

"Allanite" is characterized by one coupled heterovalent substitution where the higher charge of $(REE)^{3+}$ replacing Ca on the A2 site (Dollase, 1971) is compensated by ferrous iron occupying the octahedral M3 site. Peacor & Dunn (1988) restudied material first investigated by Geijer (1927), which was originally named "magnesium orthite" and therefore considered the Mg-dominant analogue of "allanite". However, chemical analyses accompanied by crystal-structure refinement showed that the true composition of this material is close to $CaREEMgAlMg[Si_2O_7][SiO_4]F(OH)$, an epidote-group mineral characterized by two different types of coupled heterovalent substitutions: (1) $^{A2}(REE)^{3+} + {}^{M3}Mg \rightarrow {}^{A2}Ca + {}^{M3}Al$ and (2) $^{M1}Mg + {}^{O4}F^- \rightarrow {}^{M1}Al + {}^{O4}O^{2-}$. This new type of REE-rich epidote-group mineral was given the root name dollaseite in honor of Wayne Dollase for his crystal chemical research on epidote-group minerals. The type material for **dollaseite-(Ce)** is from the Östanmossa mine, Norberg district, Sweden, originally studied by Geijer (1927).

However, Geijer (1927) also analyzed Mg-rich material with F < 0.5 apfu, which seemed close to the Mg analogue of "allanite". Subsequently, in a literature review Grew *et al.* (1991) found several reports of "allanite" analogues with $Mg > Fe^{2+}$ and compositionally distinct from "dollaseite". The corresponding mineral with the end-member formula $CaCeAl_2Mg^{2+}[Si_2O_7][SiO_4]O(OH)$ was named **dissakisite-(Ce)** from the Greek *dissakis* = "twice over" in reference to the Mg equivalent of "allanite" being described twice. The type material was found in marble from Balchen Mountain in the eastern Sør Rondane Mountains, Queen Maud Land, Antarctica. The type material of the newly discovered **dissakisite-(La)** is from a peridotite body of the Ulten zone, Austroalpine domain, Eastern Alps (Tumiati *et al.*, 2005).

Sokolova *et al.* (1991) described the structure of a Ce-rich epidote-group mineral from the Inyl´chek Massif, Kyrgyzstan (former Kirghiz SSR), which was also F-rich and thus closely related to "dollaseite" but with the octahedral M3 site dominated by Mn^{2+}. Pautov *et al.* (1993) later defined this mineral as a new species, **khristovite-(Ce)**, $CaCeMgAlMn^{2+}[Si_2O_7][SiO_4]F(OH)$, which was named after the Russian geologist Evgenia Vladimirovicha Khristova.

It has been known for a long time that piemontite may incorporate significant amounts of REE (for a literature review see Bonazzi *et al.*, 1992). Bonazzi *et al.* (1996) defined a new end-member from Andros Island, Cyclades, Greece named **androsite-(La)** with the end-member composition $Mn^{2+}LaMn^{3+}AlMn^{2+}[Si_2O_7][SiO_4]O(OH)$. This REE-rich epidote-group mineral with La on A2 has the smaller of the two A sites (A1) occupied by Mn^{2+} and the largest octahedral site (M3) also occupied by Mn^{2+}, whereas the M1 octahedron is dominated by Mn^{3+}. In addition, epidote-group minerals with compositions corresponding to **vanadoandrosite-(Ce)** and **(mangani)androsite-(Ce)** (Cenki-Tok *et al.*, 2006) have been approved by CNMMN (IMA 2004-015 and IMA 2002-049).

Ferriallanite-(Ce), ideally, $CaCeFe^{3+}AlFe^{2+}[Si_2O_7][SiO_4]O(OH)$, is the analogue of allanite-(Ce) with Fe^{3+} dominant in the octahedral M1 site. It is of metasomatic origin and occurs in an alkaline granitic pegmatite of Mount Ulyn Khuren in the Altai Range, Mongolia (Kartashov *et al.*, 2002). Furthermore, ferriallanite-(Ce), previously reported as "cerine" or iron-rich "allanite" is the most common lanthanide mineral next to cerite-(Ce) at the Bastnäs Fe-Cu-REE deposit, Skinnskatteberg, Västmanland, Sweden (Holtstam *et al.*, 2003).

2.7. Epidote modules in polysomatic series

As exemplified by the minerals gatelite-(Ce) (Bonazzi *et al.*, 2003) and västmanlandite-(Ce) (Holtstam *et al.*, 2005) the epidote-type structure (*E*) easily matches with that of törnebohmite, $(REE)_2Al[SiO_4]_2(OH)$, (*T*) to form a polysomatic series (*E*, *ET*, *T*). Sequences in addition to *ET* are to be expected because *E* and *T* modules fit together in any order and the *E*-*T* interface does not require significant structural distortions. Both gatelite-(Ce) and västmanlandite-(Ce) represent iso-topological *ET* type polysomes distinct by space-group symmetry and composition of the epidote-type module. The *E* module in gatelite-(Ce) is of dissakisite-(Ce) composition whereas the *E* module in västmanlandite-(Ce) is of dollaseite-(Ce) composition. To clarify the structural relationship between *E* and *T* modules Bonazzi *et al.* (2003) have chosen a unit-cell setting for gatelite-(Ce) where $\mathbf{a}_{gat.} \approx 2\mathbf{a}_{epi.} \approx [201]_{tör.}$; $\mathbf{b}_{gat.} \approx \mathbf{b}_{epi.} \approx \mathbf{b}_{tör.}$; $\mathbf{c}_{gat.} \approx (\mathbf{c}_{epi.} + \mathbf{c}_{tör.})$; $\beta_{gat.} \approx \beta_{epi.}$. Unfortunately, a corresponding setting was not used for västmanlandite-(Ce) by Holtstam *et al.* (2005). Their original setting, $a = 8.939$, $b = 5.706$, $c = 15.855$ Å, $\beta = 94.58°$, space group $P2_1/m$ may be transformed by the matrix [-100 | 010 | 101] to obtain a setting in space group $P2_1/m$ with $a = 8.939$, $b = 5.706$, $c = 17.568$ Å, $\beta = 115.90°$ corresponding to gatelite-(Ce) with $a = 17.770$, $b = 5.651$, $c = 17.458$ Å, $\beta = 116.18°$ (space group $P2_1/a$).

3. Recommended nomenclature

3.1 Definition of an epidote-group mineral

The oldest, still accepted mineral name of the mineral group under review is epidote (Haüy, 1801). For this reason the name epidote is used to not only describe a mineral species of idealized $Ca_2Al_2Fe^{3+}[Si_2O_7][SiO_4]O(OH)$ composition but also to designate the entire group. The subcommittee discussed the point whether zoisite should be regarded a member of the epidote group (*e.g.*, Franz & Liebscher, 2004). However, given that *ca.* 20 mineral species are presently recognized as isostructural with epidote but zoisite stands alone, the subcommittee decided to limit the epidote group to closely related species having monoclinic symmetry so as to avoid having to mention repeatedly the one exception having orthorhombic symmetry. Exclusion of zoisite from the epidote group has

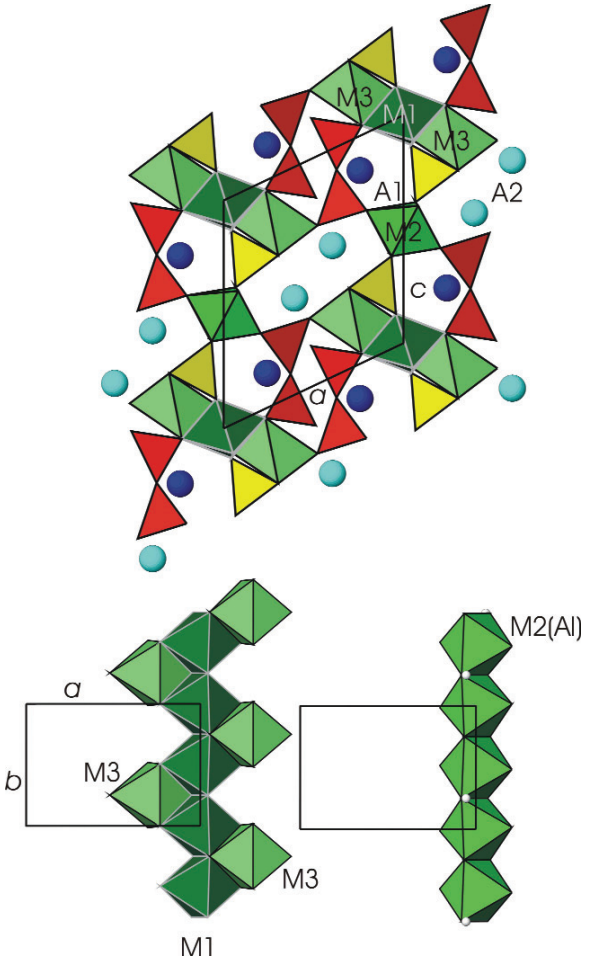

Fig.1, Top: Polyhedral model of the clinozoisite structure (space group $P2_1/m$) projected along the **b**-axis. TO_4 tetrahedra are in yellow, T_2O_7 groups are in red, octahedra in green, A sites are shown as blue spheres (A1 dark blue, A2 light blue); Bottom: Linkage of octahedral sites forming chains parallel to the **b**-axis. H atoms on the chain formed by M2 octahedra are shown as small white spheres.

a historical precedent (Tschermak, 1905) and was followed in the most recent edition of Strunz Mineralogical Tables (Strunz & Nickel, 2001).

Definition

An epidote-group mineral is described with the generic formula $A_2M_3[T_2O_7][TO_4](O,F)(OH,O)$. The monoclinic crystal structure is composed of T_2O_7 (usually Si_2O_7) and TO_4 (usually SiO_4) units linked to two kinds of chains (parallel to the *b*-axis) built by edge-sharing octahedra (Fig. 1). One chain consists of M2 octahedra while the other chain is formed by M1 octahedra with M3 octahedra attached on alternate sides along its length. M octahedra are mainly occupied by trivalent ions such as Al, Fe^{3+}, Mn^{3+}, Cr^{3+}, V^{3+}. Divalent cations (*e.g.*, Mg, Fe^{2+}, Mn^{2+}) may occupy M sites (preferentially M3) if various heterovalent substitutions come into play. M2 has a strong preference for Al whereas the occupancy of M1 and M3 depends on competing ions. Usually an OH group is bonded to the M2 cation. The overall structural arrangement gives rise to two types of cavities, a smaller one named A1, usually occupied by Ca or Mn^{2+} and a larger one named A2, usually occupied by Ca, Sr, Pb, and REE. The resulting connectivity (topology) is consistent with space group $P2_1/m$.

The $P2_1/m$ structure of epidote-group minerals displays ten symmetry independent anion sites, commonly labelled O1 – O10. In natural samples the site O10 represents O bonded to H (hydroxyl group) whereas the O4 site may be occupied by O^{2-} (clinozoisite and allanite subgroups) or by F^- (dollaseite subgroup).

Annotation

Zoisite is a polymorph of clinozoisite $Ca_2Al_3[Si_2O_7][SiO_4]O(OH)$ of orthorhombic symmetry (space group *Pnma*) with only one type of edge-sharing octahedral chain and M3 octahedra attached only on one side along its length. Alternatively, zoisite and clinozoisite may even be interpreted to have polytypic relations (Ito, 1950; Merlino, 1990).

3.2. Definition of subgroups

For better and easier distinction of epidote-group minerals we introduce three subgroups based on the existing accepted mineral species. Additional subgroups may be defined if new species are not accommodated in the following three.

Members of the **clinozoisite subgroup** are derived from the mineral clinozoisite $Ca_2Al_3[Si_2O_7][SiO_4]O(OH)$ solely by homovalent substitutions. The key cation and anion sites are A1 = M^{2+}, A2 = M^{2+}, M1 = M^{3+}, M2 = M^{3+}, M3 = M^{3+}, O4 = O^{2-}, O10 = $(OH)^-$. In other words, the dominant valence as listed above must be maintained.

Members of the **allanite subgroup** are REE-rich minerals typified by the eponymous mineral "allanite". This subgroup is derived from clinozoisite by homovalent substitutions and **one** coupled heterovalent substitution of the type $^{A2}(REE)^{3+} + {}^{M3}M^{2+} \rightarrow {}^{A2}Ca^{2+} + {}^{M3}M^{3+}$. Thus the valences on the key sites are: A1 = M^{2+}, **A2 = M^{3+}**, M1 = M^{3+}, M2 = M^{3+}, **M3 = M^{2+}**, O4 = O^{2-}, O10 = $(OH)^-$.

Members of the **dollaseite subgroup** are REE-rich minerals typified by the eponymous mineral "dollaseite". This subgroup is derived from clinozoisite by homovalent substitutions and **two** coupled heterovalent substitutions of the type $^{A2}(REE)^{3+} + {}^{M3}M^{2+} \rightarrow {}^{A2}Ca^{2+} + {}^{M3}M^{3+}$ and $^{M1}M^{2+} + {}^{O4}F^- \rightarrow {}^{M1}M^{3+} + {}^{O4}O^{-2}$. Thus the valences on the key sites are: A1 = M^{2+}, **A2 = M^{3+}**, **M1 = M^{2+}**, M2 = M^{3+}, **M3 = M^{2+}**, **O4 = F^-**, O10 = $(OH)^-$.

3.3. Role of U^{4+} and Th^{4+} in the allanite and dollaseite subgroups

Gieré & Sorensen (2004) reviewed Th^{4+} and U^{4+} contents in "allanite". According to their literature review

the maximum reported ThO_2 content is 4.9 wt.% corresponding to *ca*. 0.07 Th pfu. The maximum UO_2 content is 0.82 wt.% in a crystal containing additionally 1.09 wt.% ThO_2, corresponding to 0.02 apfu each. Thus, Th and U are minor constituents of the actinides (ACT) group of elements. The recommended chemical criterion to assign minerals to the allanite and dollaseite subgroups is REE +ACT > 0.5 pfu. The major argument for adding U and Th to REE is that the coupled heterovalent substitution mechanism is presumably: $^{A2}(Th^{4+},U^{4+}) + 2\ ^{M3}M^{2+} \rightarrow {}^{A2}Ca + 2\ ^{M3}M^{3+}$. *Comment:* The IMA CNMMN guidelines for new minerals also list Sc^{3+} together with Y^{3+} and lanthanides as candidates for which the Levinson extension should be used. However, Sc^{3+} has also a strong preference for octahedral sites (*E.g*., bazzite is a beryl analogue where Sc replaces Al). For this reason a special treatment of Sc-rich epidote-group minerals seems necessary, and, if such compositions were found in nature, the Sc distribution will have to be studied.

3.4. Derivation of mineral names

Considering members of the clinozoisite subgroup, most frequent are homovalent substitutions on M3 by Fe^{3+}, V^{3+}, Cr^{3+}, and Mn^{3+} (replacing Al) as well as on A2 by Sr, Pb^{2+}, and less commonly, Ba (replacing Ca). These substitutions, in principle, yield 20 combinations each corresponding to a distinct mineral species. If we further consider that homovalent substitutions may also occur on M1 as exemplified by the mineral tweddillite (Armbruster *et al.*, 2002) and that Mn^{2+} can also substitute for Ca on A1, the number of potential species increases further. For this reason we believe that the free choice of a mineral name needs to be restricted in order to avoid proliferation of unrelated mineral names. Relationships among minerals should be evident in the names. For example, the chemical relation between piemontite and strontiopiemontite is obvious, whereas the name tweddillite obscures its relation to strontiopiemontite.

In the recommended new nomenclature the key cation-sites M3 and A1 (and, in principle, M2) determine the root name. If the dominant cations at A1, M3 (and M2) exactly match those of an approved species, **the same root name must be given**. If at one of these sites the dominant cation is different a new root name may be suggested.

In both clinozoisite and allanite subgroups no prefix is added to the root name if M1 = Al. In the dollaseite subgroup no prefix is added to the root name if M1 = Mg. Otherwise a proper prefix derived from the name of a chemical element must be attached. The prefixes ferri, mangani, chromo, and vanado indicate dominant Fe^{3+}, Mn^{3+}, Cr^{3+}, and V^{3+} on M1, respectively (clinozoisite and allanite subgroups). The prefixes ferro and mangano indicate dominant Fe^{2+} and Mn^{2+} at M1, respectively (dollaseite subgroup). The dominant cation on A2 in the clinozoisite subgroup (other than Ca) is defined as *extended Levinson suffix* (Levinson, 1966; Bayliss & Levinson, 1988). Note that A2 in the allanite and dollaseite subgroups is occupied by REE. Thus for those minerals Levinson suffixes *per se* apply to the dominant REE. This simple nomenclature requires complete renaming of following species:

Table 2. Clinozoisite subgroup: accepted mineral species (in bold) along with selected examples of recommended names for possible new members of epidote-group minerals.

Name	Old name	A1	A2	M1	M2	M3	O4	O10
Clinozoisite		Ca	Ca	Al	Al	Al	O	OH
Clinozoisite-(Sr)*	*Niigataite*	Ca	Sr	Al	Al	Al	O	OH
Clinozoisite-(Pb)		Ca	Pb	Al	Al	Al	O	OH
Epidote		Ca	Ca	Al	Al	Fe^{3+}	O	OH
Epidote-(Pb)*	*Hancockite*	Ca	Pb	Al	Al	Fe^{3+}	O	OH
Epidote-(Sr)		Ca	Sr	Al	Al	Fe^{3+}	O	OH
Ferriepidote		Ca	Ca	Fe^{3+}	Al	Fe^{3+}	O	OH
Ferriepidote-(Sr)		Ca	Sr	Fe^{3+}	Al	Fe^{3+}	O	OH
Ferriepidote-(Pb)		Ca	Pb	Fe^{3+}	Al	Fe^{3+}	O	OH
Vanadoepidote		Ca	Ca	V^{3+}	Al	Fe^{3+}	O	OH
Vanadoepidote-(Sr)		Ca	Sr	V^{3+}	Al	Fe^{3+}	O	OH
Vanadoepidote-(Pb)		Ca	Pb	V^{3+}	Al	Fe^{3+}	O	OH
Mukhinite		Ca	Ca	Al	Al	V^{3+}	O	OH
Mukhinite-(Sr)		Ca	Sr	Al	Al	V^{3+}	O	OH
Mukhinite-(Pb)		Ca	Pb	Al	Al	V^{3+}	O	OH
Tawmawite #		Ca	Ca	Al	Al	Cr^{3+}	O	OH
Chromotawmawite		Ca	Ca	Cr^{3+}	Al	Cr^{3+}	O	OH
Piemontite		Ca	Ca	Al	Al	Mn^{3+}	O	OH
Piemontite-(Sr)*	*Strontiopiemontite*	Ca	Sr	Al	Al	Mn^{3+}	O	OH
Piemontite-(Pb)		Ca	Pb	Al	Al	Mn^{3+}	O	OH
Manganipiemontite		Ca	Ca	Mn^{3+}	Al	Mn^{3+}	O	OH
Manganipiemontite-(Sr)*	*Tweddillite*	Ca	Sr	Mn^{3+}	Al	Mn^{3+}	O	OH
new root name		Mn^{2+}	Ca	Mn^{3+}	Al	Mn^{3+}	O	OH

Notes: * recommended new mineral names for accepted species; # not a valid species until clear evidence for Cr > 0.5 pfu on M1or M3 is presented.

Niigataite (old) = **clinozoisite-(Sr) (new)**,
hancockite (old) = **epidote-(Pb) (new)**,
tweddillite (old) = **manganipiemontite-(Sr) (new)**.

Fortunately, two of these species were very recently described and all three species are rare, so that the mineralogical community is not familiar with the original names. Minor modifications are necessary for following species:

Strontiopiemontite (old) = **piemontite-(Sr) (new)**,
androsite-(La) (old) = **manganiandrosite-(La) (new)**.

Comments: "Androsite" is an example for a root name derived from the occupancy of two key sites A1 (Mn^{2+}) and M3 (Mn^{2+}). Additional root names are required for corresponding compositions with either A1 occupied by Ca or M3 occupied by any other divalent cation.

Kartashov *et al.* (2002) list analytical data for a mineral of idealized composition $CaCeFe^{3+}{}_2Fe^{2+}$ $[Si_2O_7][SiO_4]O(OH)$ but the available data were not considered sufficient for naming a new species. On the one hand, such a hypothetical mineral would qualify for a new root name due to its unique occupancy of M3 and M2. The strong relation to ferriallanite-(Ce) could also be expressed by the possible name "ferriferriallanite-(Ce)" where the dominant occupancy on M2 is expressed by a second prefix. If the two prefixes are identical an alternate choice could be the name "diferriallanite-(Ce)". Because there are yet no accepted examples for such species with M2 ≠ Al we defer the naming decision to the authors proposing the new species and to the CNMMN members reviewing the proposal. We believe that awkward doubly prefixed names should be the exception rather than the rule in epidote-group minerals.

Table 3. Allanite subgroup: accepted mineral species (in bold) along with selected examples of recommended names for possible new members of epidote-group minerals.

Name	Old name	A1	A2	M1	M2	M3	O4	O10
Allanite-(Ce), -(La), -(Y)		Ca	$(REE)^{3+}$	Al	Al	Fe^{2+}	O	OH
Ferriallanite-(Ce)		Ca	Ce^{3+}	Fe^{3+}	Al	Fe^{2+}	O	OH
Vanadoallanite-(REE)		Ca	$(REE)^{3+}$	V^{3+}	Al	Fe^{2+}	O	OH
Chromoallanite-(REE)		Ca	$(REE)^{3+}$	Cr^{3+}	Al	Fe^{2+}	O	OH
Dissakisite-(Ce),-(La)		Ca	$(REE)^{3+}$	Al	Al	Mg	O	OH
Ferridissakisite-(REE)		Ca	$(REE)^{3+}$	Fe^{3+}	Al	Mg	O	OH
Vanadodissakisite-(REE)		Ca	$(REE)^{3+}$	V^{3+}	Al	Mg	O	OH
Manganidissakisite-(REE)		Ca	$(REE)^{3+}$	Mn^{3+}	Al	Mg	O	OH
Chromodissakisite-(REE)		Ca	$(REE)^{3+}$	Cr^{3+}	Al	Mg	O	OH
Androsite-(REE) (new def.)		Mn^{2+}	$(REE)^{3+}$	Al	Al	Mn^{2+}	O	OH
Manganiandrosite-(La)*, -(Ce)■	*androsite*	Mn^{2+}	$(REE)^{3+}$	Mn^{3+}	Al	Mn^{2+}	O	OH
Ferriandrosite-(REE)		Mn^{2+}	$(REE)^{3+}$	Fe^{3+}	Al	Mn^{2+}	O	OH
Vanadoandrosite-(Ce) ■		Mn^{2+}	Ce^{3+}	V^{3+}	Al	Mn^{2+}	O	OH
Chromoandrosite-(REE)		Mn^{2+}	$(REE)^{3+}$	Cr^{3+}	Al	Mn^{2+}	O	OH
New root names		Ca	$(REE)^{3+}$	Al	Al	Mn^{2+}	O	OH
		Ca	$(REE)^{3+}$	Fe^{3+}	Fe^{3+}	Fe^{2+}	O	OH
		Mn^{2+}	$(REE)^{3+}$	Al	Al	Mg^{2+}	O	OH
		Mn^{2+}	$(REE)^{3+}$	Al	Al	Fe^{2+}	O	OH

Notes: * recommended new mineral names for accepted species; ■ approved by CNMMN (Cenki-Tok *et al*., 2006); vanadoandrosite-(Ce) has originally been approved as vanadio-androsite-(Ce).

Table 4. Dollaseite subgroup: accepted mineral species (in bold) along with selected examples of recommended names for possible new members of epidote-group minerals.

Name	A1	A2	M1	M2	M3	O4	O10
Dollaseite-(Ce)	Ca	Ce^{3+}	Mg	Al	Mg	F	OH
Khristovite-(Ce)	Ca	Ce^{3+}	Mg	Al	Mn^{2+}	F	OH
Ferrokhristovite-(REE)	Ca	$(REE)^{3+}$	Fe^{2+}	Al	Mn^{2+}	F	OH
Manganokhristovite-(REE)	Ca	$(REE)^{3+}$	Mn^{2+}	Al	Mn^{2+}	F	OH
New root name	Ca	$(REE)^{3+}$	Mg	Al	Fe^{2+}	F	OH
New root name	Mn^{2+}	$(REE)^{3+}$	Mg	Al	Mn^{2+}	F	OH

Occupancy of the *key sites* and recommended names for all hitherto defined epidote-group minerals and for some examples of possible compositions not yet found are summarized in Tables 2-4. In addition, cell dimensions of approved species are given in Table 5.

Comment: In particular, our subcommittee discussed the use of proper prefixes for V^{3+} and Cr^{3+}. The ending for both prefixes should be –o because V^{3+} and Cr^{3+} are the predominant low valences of V and Cr in mineral formulas (V^{2+}, although reported in minerals, is not considered a potential constituent because it is so rare). We have chosen the prefix "chromo" for Cr^{3+} by analogy with

Table 5. Cell dimensions of epidote-group minerals (space group $P2_1/m$).

Name	*a* (Å)	*b* (Å)	*c* (Å)	β (°)	***V*** **(Å³)**	Ref.
Clinozoisite	8.861	5.5830	10.141	115.46	453.0	Pawley *et al.* 1996
Clinozoisite-(Sr)	8.890	5.5878	10.211	115.12	459.3	Miyajima *et al.* 2003
Epidote	8.908	5.663	10.175	115.35	463.9	Bonazzi & Menchetti 1995
Epidote-(Pb)	8.958	5.665	10.304	114.4	476.2	Dollase 1971
Mukhinite	8.90	5.61	10.15	115.5	457	Shepel & Karpenko 1969
Piemontite	8.844	5.577	10.167	115.54	460.6	Langer *et al.* 2002
Piemontite-(Sr)	8.870	5.681	10.209	114.88	466.7	Bonazzi *et al.* 1990
Manganipiemontite-(Sr)	8.932	5.698	10.310	114.56	477.3	Armbruster *et al.* 2002
Allanite-(Ce)	8.927	5.761	10.150	114.77	474.0	Dollase 1971
Allanite-(La)	8.914	5.726	10.132	114.87	469.1	Orlandi & Pasero 2006
Allanite-(Y) [$]	-	-	-	-	-	
Ferriallanite-(Ce)	8.962	5.836	10.182	115.02	482.6	Kartashov *et al.* 2002
Manganiandrosite-(La)	8.896	5.706	10.083	113.88	468.0	Bonazzi *et al.* 1996
Manganiandrosite-(Ce)	8.901	5.738	10.068	113.43	471.8	Cenki-Tok *et al.*, 2006
Vanadoandrosite-(Ce)	8.856	5.729	10.038	113.09	468.5	Cenki-Tok *et al.*, 2006
Dissakisite-(Ce)	8.905	5.684	10.113	114.62	465.3	Rouse & Peacor 1993
Dissakisite-(La)	8.962	5.727	10.235	115.19	475.3	Tumiati *et al.* 2005
Dollaseite-(Ce)	8.934	5.721	10.176	114.31	474.0	Peacor & Dunn 1988
Khristovite-(Ce)	8.903	5.748	10.107	113.41	474.6	Pautov *et al.* 1993

[$]refined cell dimensions for allanite-(Y) are not available. However, Neumann & Nilssen (1962) published an X-ray powder pattern, indicating that the cell dimensions of allanite-(Y) are similar to other "allanites". All mineral names are according to the new nomenclature suggested in this paper.

the common use of this Greek root meaning color in scientific terms (chromophore, chromosome, *etc.*). For V^{3+} we have agreed on "vanado" although we were aware that the element name is derived from the goddess Vanadis in Norse mythology. "Vanado" was preferred over "vanadio" because this prefix implies "vanadii" would be the prefix for V^{4+}. Both prefixes would lead to awkward mineral names, in particular if the root name begins with a vowel. We also discussed the possibility of hyphenation between prefix and root name for certain epidote-group mineral names and concluded that hyphenation should be avoided. Nevertheless, we concur with the IMA CNMMN guidelines (Nickel & Grice, 1998) and recommend that a hyphen be used if an unhyphenated name is awkward and the hyphen assists in deciphering the name.

3.5. Definition of new species of epidote-group minerals

The definition of mineral species of the epidote-group of minerals depends on the preferred occupancy of various structural sites. Therefore, submission of any new species to CNMMN **must** be accompanied by crystal-structure refinement and/or spectroscopic experiments indicating the extent of order of a chemical species on a given structural site. Exceptions are permissible only for new species distinguished by REE cation, or for simple compositions where the cation distribution is unambiguous from the chemical composition alone. In such cases high-quality chemical data would be considered sufficient. Given the role of F in the dollaseite subgroup, a fluorine analysis is mandatory for epidote-group minerals.

It is emphasized that all new species, for which names (*e.g.*, "clinozoisite-(Pb)", "epidote-(Sr)", for additional examples see Tables 2-4) are already defined in this recommended nomenclature, require approval of a formal new-mineral proposal submitted to IMA CNMMN.

3.6. Assigning subgroups and mineral names to solid-solution members

3.6.1. Assigning subgroups

In order to name an epidote-group mineral, priority should be given to the choice of subgroup, then root name, and last the specific name. The starting point will be a table reporting the cations on A1, A2, M1, M2 and M3 and the anions on O4 and O10 (*key sites*).

For a proper subgroup assignment one has to determine the dominant valence at M3, M1 and A2 expressed as M^{2+} and M^{3+}, **not** just specify a single dominant ion (*i.e.*, Fe^{2+} or Mg or Al). In addition, the dominant valence on O4: X^- or X^{2-} must be evaluated.

$[M^{2+}]_{A2} > 0.50$, $[M^{3+}]_{M3} > 0.50 \rightarrow$ clinozoisite subgroup,

$[M^{3+} + M^{4+}]_{A2} > 0.50$, $[M^{2+}]_{M3} > 0.50 \rightarrow$ allanite subgroup,

$\{[M^{2+}]_{M3+M1} - [M^{3+} + M^{4+}]_{A2}\} > 0.50$ **and** $[X^-]_{O4} > 0.5 \rightarrow$ dollaseite subgroup.

Comment: The structural refinement of both dollaseite-(Ce) and kristovite-(Ce) convincingly showed F^- to be ordered at the O4 site. Thus, the presence of more than 0.5 F per formula unit corresponds to the dollaseite subgroup. Assigning F to O4 and not to O10 has major implications; substitution of F^- for O^{2-} reduces total negative charge and thus must be balanced by decreasing the M^{3+}: M^{2+} value.

The above definition of the dollaseite subgroup may at first glance appear unduly complex. A simpler scheme based solely on cation occupancy would be:

$[M^{2+}]_{A2} > 0.5$, $[M^{3+}]_{M1} > 0.5$, $[M^{3+}]_{M3} > 0.5 \rightarrow$ clinozoisite subgroup (with $[X^-]_{O4} < 0.5$ implicit),

$[M^{3+} + M^{4+}]_{A2} > 0.5$, $[M^{3+}]_{M1} > 0.5$, $[M^{2+}]_{M3} > 0.5 \rightarrow$ allanite subgroup (with $[X^-]_{O4} < 0.5$ implicit),

$[M^{3+} + M^{4+}]_{A2} > 0.5$, $[M^{2+}]_{M1} > 0.5$, $[M^{2+}]_{M3} > 0.5 \rightarrow$ dollaseite subgroup (with $[X^-]_{O4} > 0.5$ implicit).

The above alternate scheme is not recommended although it is correct for ideal end-members. For members with $0.5 < (REE)^{3+} << 1.0$ the scheme might fail. There are only two structure refinements addressing cation order on M1 and M3 in dollaseite subgroup minerals (Peacor & Dunn, 1988; Sokolova *et al.*, 1991). These are not sufficient for us to provide a more rigorous definition of the dollaseite subgroup.

3.6.2. Assigning mineral names

As mentioned in the introduction, the traditional distinction between clinozoisite and epidote is based on their optical character. Clinozoisite was defined as optically positive whereas epidote was shown to be optically negative. The change over occurs at ~ 40 % epidote component ($Ca_2Al_2Fe^{3+}[Si_2O_7][SiO_4]O(OH)$). In a similar way, the name piemontite has been commonly assigned to monoclinic, Mn-bearing epidote-group minerals exhibiting the characteristic pleochroism, even if the molar Mn_2O_3 content is less than Fe_2O_3 content.

There is a wealth of optical data on epidote-group minerals, recently summarized by Franz & Liebscher (2004). Crystal optics is a fundamental tool in analyzing and describing rocks and minerals, and good optical data may be used in some cases to identify a species or even to quantify a solid-solution member. Nevertheless, binary behaviour should not be assumed *a priori* for complex systems such as the epidote-group minerals. If the chemical composition becomes too complex optical data are ambiguous and have their limitations in mineral identification. As an example, different species of the allanite and dollaseite subgroups are very difficult to distinguish on optical grounds. For a proper evaluation of capabilities and limitations of optical methods for the identification of epidote-group minerals comparative studies are necessary.

The subcommittee, therefore, strongly recommends that optical criteria alone not be used for distinguishing epidote-group minerals. Although optical tests (*e.g.*, determination of the optical sign, optical orientation or pleochroism) are useful for preliminary species identification, we recommend that electron-microprobe analytical data be used to determine a mineral name of a solid-solution member. The dominant cation at *key structural sites*, with the restriction described below, determines the name (*e.g.*, Nickel & Grice, 1998; Nickel, 1992).

3.6.2.1. Clinozoisite subgroup

If only homovalent substitutions take place, the dominant cation at *key structural sites* simply determines the name. Coupled heterovalent substitutions in epidote-group minerals require a special treatment of the so-called 50 %

rule in a solid-solution series. Even for the REE-bearing minerals, the A2 cation appearing in the suffix has to be selected from among the divalent cations in order to name a species belonging to the clinozoisite group. The root name depends on the dominant trivalent cation on M3.

Example:

Consider the A2 occupancy (0.35 Ce, 0.05 La, 0.30 Ca, 0.20 Sr, 0.10 Pb). Because $(REE)^{3+} < 0.5$ the mineral belongs to the clinozoisite subgroup. Although Ce is the dominant cation on A2, the critical cation is Ca, the dominant divalent cation. No suffix is needed in this case because a suffix is only added for a dominant A2 cation other than Ca.

The above hypothetical mineral might have the M3 site occupied by 0.4 Mg, 0.25 Fe^{3+}, 0.35 Al. Because this mineral is a member of the clinozoisite subgroup the dominant M^{3+} ion (*i.e*. Al, not Mg) is decisive for the root name of the species. Formal derivation of the proper name gives clinozoisite. The adjectival modifiers cerian and magnesian (Schaller, 1930; Bayliss *et al.*, 2005) may be added to emphasize the high Ce and Mg contents.

This deviation from the common procedure of naming minerals is necessary because strict adherence to the rule based on the dominant ionic species leads to inconsistencies and unbalanced formulas. For example, the above mineral would have the idealized formula $CaCeAl_2Mg[Si_2O_7][SiO_4]O(OH)$, which is the same as the formula for dissakisite-(Ce), a member of the allanite subgroup. If 0.1 Fe^{2+} were to replace 0.1 Mg, M3 composition becomes 0.3 Mg, 0.1 Fe^{2+}, 0.25 Fe^{3+}, 0.35 Al, and the idealized formula becomes $CaCeAl_3[Si_2O_7][SiO_4]O(OH)$. The latter formula is not charge balanced and thus nonsensical. Furthermore, the requirement to name clinozoisite-subgroup minerals on the basis of dominant M^{2+} on A2 and dominant M^{3+} on M3 reduces proliferation of unwanted mineral names.

3.6.2.2. Allanite and dollaseite subgroups

For the sites involved in the charge compensation of a heterovalent substitution in A2 (*i.e.* M3 in the allanite subgroup, and also M1 in the dollaseite subgroup), the identification of the relevant end-member formula **must** take into account the dominant *charge-compensating* octahedral cation (M^{2+}) and **not** the dominant cation in these sites.

Example:

An allanite-subgroup mineral where M3 is not dominated by a single divalent cation but by several, so that a trivalent cation is the most abundant one: *e.g*., $Ca(La_{0.6}Ca_{0.4})Al_2(Fe^{2+}_{0.3}Mg_{0.2}Mn^{2+}_{0.1}Al_{0.4})[Si_2O_7][SiO_4]O(OH)$ *[One might be tempted to write a meaningless, non-charge-balanced end-member* $CaLaAl_3[Si_2O_7][SiO_4]O(OH)$*]*.

Within the framework proposed above, the correct way to proceed is: First assign the mineral to the allanite subgroup ($[M^{3+}]_{A2} > 0.5$, $[M^{2+}]_{M3} > 0.5$, $[F^-]_{O4} < 0.5$). Thus the end-member formula is: $CaLaAl_2M^{2+}[Si_2O_7][SiO_4]O(OH)$. Fe^{2+} is dominant among the M^{2+} cations (*i.e*. Fe^{2+} is the dominant *charge-compensating* cation). Thus the mineral would properly be named allanite-(La). Likewise, another allanite-subgroup mineral with the same formula except for 0.4 Al replaced by 0.4 Cr must be given the same name, *i.e.* allanite-(La). The adjectival modifier Cr-rich (chromian) may be added to distinguish this mineral from Cr-poor allanite-(La).

4. Deriving a mineral name from electron-microprobe analytical data

One of the pitfalls in epidote-group mineralogy has been the derivation of a mineral name from chemical data. There are four major problems. (1) Rules of finding a proper root name depend on the subgroup because of interference between homovalent and coupled heterovalent substitutions (discussed above). Thus, before a mineral name can be assigned, the subgroup has to be determined. (2) Epidote-group minerals are frequently mixed-valence Fe and/or Mn compounds and the charge of the respective cations has to be calculated on the basis of assumed negative charges. (3) Frequent oscillatory zoning may be masked if the zoning is perpendicular to the incident electron beam. (4) Minerals of the allanite and dollaseite subgroups are commonly metamict, in some cases with complete loss of crystallinity (for a review, see Gieré & Sorensen, 2004). Strongly metamict materials significantly deviate in composition and stoichiometry from their non-metamict equivalents. Metamictization is accompanied with hydration, swelling, and selective leaching. The transition from an ideal crystal to amorphous material during metamictization is continuous. The question of crystal quality remains open if electron-microprobe analytical data are applied without accompanying diffraction experiment.

A central question intimately associated with the problem of metamictization concerns the existence of significant vacancies, in particular on the A sites. This issue becomes important when discussing how the mineral formula should be normalized. Ercit (2002) states two arguments in favor of A-site vacancies: (1) the structure refinement of Sokolova *et al.* (1991) and (2) the electron-microprobe analyses by Peterson & MacFarlane (1993) and Chesner & Ettlinger (1989).

Ad (1). We believe that the structure refinement by Sokolova *et al.* (1991) on a very Mn-rich sample does not unambiguously demonstrate the presence of vacancies on A sites if the cation distribution is critically scrutinized. Normalization of the corresponding electron-microprobe analysis to Si = 3 leads to an excess of M-type cations. Coordination of the A1 site, for which vacancies are assumed, is approximately six-fold, which is characteristic of Mn^{2+} on A1 (Bonazzi & Menchetti, 2004). Furthermore, the determined scattering power at A1 is 23 electrons, which is intermediate between Ca (20 electrons) and Mn (25 electrons).

Ad (2). Allanites from granitic pegmatites and uraniferous calcite veins in the Grenville Province of the Canadian Shield (Peterson & MacFarlane, 1993) contain up to 4.16 wt. % ThO_2 and are mostly metamict. Thus the analyzed deficit of A-site cations might be associated with partial metamictization. Interestingly, significant A-site vacancies were also calculated from electron-microprobe analytical data (Chesner & Ettlinger, 1989) on young (75 000 y. to 1.2 m.y) volcanic allanites (ThO_2 up to 2.17 wt.%). These allanites appear optically rather fresh and metamictization is certainly not advanced. Thus the A-site substitution vector $(REE)^{3+}_{2/3} + Vac_{1/3} \leftrightarrow Ca$ should not be ignored.

4.1. Formula normalization

We recommend normalization of electron-microprobe analytical data on the basis of $\Sigma(A+M+T) = 8$. This method,

however, is inadequate whenever **A-site vacancies** are present or if not all elements have been analyzed. In either case, the assumption Σ cations = 8.0 leads to Si > 3.00 apfu. If Si becomes > 3.05 apfu, the formula may be renormalized on Si = 3. One should be aware that normalization to 3 Si transfers all errors of the Si determination to the other cations in the formula, resulting in larger absolute errors on the number of cations (Ercit, 2002). We discourage normalization on Σ (M+T) = 6 because Mn^{2+} and probably also Fe^{2+} (to a lesser extent) may occupy M1, M3, and A1 (Bonazzi *et al.*, 1996)

4.2. Determination of negative charges

Because refinement of the dollaseite-(Ce) and kristovite-(Ce) structures convincingly showed F^- to be ordered at the O4 site, the total sum of negative charge should be assumed as follows: Σ (anion charge) = 2 (12 – x) + x + 1, where x = F + Cl (apfu).

Comment: Significant amounts of Cl have been rarely reported, except for Cl up to 0.86 wt.% (0.126 apfu) in the halogen-bearing "allanite" from the Hemlo area, Ontario (Pan & Fleet, 1990). We have no knowledge about the role of Cl in the epidote structure. By analogy with F, we recommend the simplest scheme: Assign Cl to the O4 site.

4.3. Charge-balance of the empirical formula

The Fe^{2+}/Fe^{3+} and Mn^{2+}/Mn^{3+} values are varied until Σ (cation charge) equals Σ (anion charge), oxidizing first Fe^{2+}, then Mn^{2+}, in order to account for their different redox potentials. The assignment of all Mg to the M sites also contributes to the balancing of excess positive charge in the REE-bearing members. One must be aware that this step introduces considerable errors if not all cations have been analyzed (one possible indicator is Si > 3.05 apfu). Furthermore, this step assumes that there is no "oxyallanite" component.

4.4. Assignment of ionic species to the various key sites

i) All Si is assigned to the T sites. If Si < 3.00 apfu (or $Si^{4+}+P^{5+}+Be^{2+}+B^{3+}$ < 3.00 apfu), $^{[IV]}Al$ is calculated as 3 – Si. However, if Si is *significantly*[2] below 3.00, the analysis is probably not reliable.

ii) If there is sufficient Al after step i), the M2 site is fully occupied by Al. Otherwise, any deficit (1 – Al) is to be compensated by Fe^{3+}.

iii) Any excess (oct – 2) of octahedral cations (oct = Al, Fe^{3+}, Mn^{3+}, V^{3+}, Cr^{3+}, Ti^{4+}, Sn^{4+}, Fe^{2+}, Mn^{2+}, Mg, Cu^{2+},….) is to be assigned to A1. Priority must be given to Mn^{2+}. If the amount of Mn^{2+} is not sufficient preference should be given to Fe^{2+} or other available cations with large ionic radii.

iv) The A1 site is filled with Ca to sum up to 1.0 apfu. (minor Na will also be assigned to A1). Exception: If Σ(REE+ACT+Ba+Sr+Pb^{2+}) > 1.0, excess cations may be assigned to A1 (preferentially those with the smaller ionic radii).

v) All $(REE)^{3+}$ (together with Th^{4+} and U^{4+}) are assigned to A2. Larger divalent cations such as Sr, Pb^{2+}, Ba, and K are also added to this site. Remaining Ca is added to A2.

Comment: In the absence of knowledge on octahedral REE in allanite and dollaseite-subgroub minerals we ignore this possibility in this simplified procedure. Cressey & Steel (1988), on the basis of L_{III} edge extended X-ray absorption fine structure (EXAFS), suggested that Lu in synthetic dissakisite-(La) is located at the M3 site and that Gd and Er reside at the A2 and A1 sites, respectively. These results, while interesting, require confirmation.

vi) If any, F and Cl must be assigned to the O4 site.

vii) The remaining 2.00 octahedral cations are assigned to M3 and M1. In the lack of structural information, a sequence based on **decreasing ionic radii** could be written to fill first M3 and then M1. Octahedral ionic radii according to Shannon (1976) are listed in Table 6.

Comment: In particular, we do not know how M^{2+} is ordered between M1 and M3 if O4 is partly occupied by F. Because M1 has two bonds to O4 whereas M3 has only one, we would expect that M1 would have a rather strong selectivity for M^{2+} if O4 = F. The method must be certainly refined if additional information on cation order in minerals of this subgroup is available.

Table 6. Effective octahedral ionic radii in Å (Shannon, 1976).

Ion	Octahedral radius (Å)
Al^{3+}	0.535
Ti^{4+}	0.605
Cr^{3+}	0.615
V^{3+}	0.640
Fe^{3+}	0.645[1] (high spin)
Mn^{3+}	0.645[1] (high spin)
Sn^{4+}	0.690
Mg	0.720
Cu^{2+}	0.730
Zn	0.740
Fe^{2+}	0.780 (high spin)
Mn^{2+}	0.830 (high spin)

[1]to avoid ambiguity Mn^{3+} (Jahn-Teller distortion) should be regarded larger than Fe^{3+} although the average ionic radii are equal.

4.5. Subgroup and root name

Before a name can be given to a mineral species the subgroup has to be determined (see above). In case of dollaseite-subgroup minerals, assigning an individual name may fail for compositions 0.5 < REE + ACT << 1 and 1 >> (F on O4) > 0.5. This shortcoming results from our

[2]A good and complete electron-microprobe analysis of an epidote-group mineral should reproduce the stoichiometric constrains within 1 % relative, *i.e.* Si = 2.97 to 3.03 pfu. Thus, analyses yielding < 2.97 Si pfu may indicate T-site substitution. However, Si values below 2.9 pfu should be regarded as anomalous and probably erroneous. Si values > 3.03 pfu may indicate either A-site vacancies (partial metamictization?) or incomplete analyses.

limited knowledge about order of M^{2+} between M1 and M3 for this subgroup. In the Appendix several examples are presented to illustrate how a "working name" can be derived from an electron-microprobe analysis. The term "working name" is used to emphasize that a strongly simplified scheme for the naming procedure was applied. The "working name" may be used in any mineralogical or petrological investigation as long as the derived mineral name agrees with the recommendations of this IMA CNMMN subcommittee. No quotation marks are needed in case the name is already that of an approved species; otherwise they are mandatory. Of course, the "working name" procedure is not sufficient to define a new species of the epidote-group minerals.

4.6. Usage of the term "pistacite"

The term "pistacite" is not an accepted mineral name and should therefore not be used as a synonym for epidote. There is a tradition among petrologists to name the hypothetical composition $Ca_2Fe^{3+}{}_3[Si_2O_7][SiO_4]O(OH)$ "pistacite" component in clinozoisite – epidote solid solutions. If the term "pistacite" is used in this sense it should be written in quotation marks accompanied by the word *component* to indicate its theoretical meaning ["pistacite" component]. We firmly discourage from using "pistacite" component and recommend an alternative, less confusing expression $X_{Fe} = Fe^{3+}/(Fe^{3+} + Al)$ to quantify a solid-solution member.

4.7. Usage of the term "oxyallanite"

It has been shown by several investigators (e.g., Dollase, 1973; Bonazzi & Menchetti, 1994) that "allanite" dehydroxylates in air between ca. 600 and 700°C where charge balance is maintained by oxidation of ferrous to ferric iron according to: $^{M3}Fe^{2+} + {}^{O10}OH^- \rightarrow {}^{M3}Fe^{3+} + {}^{O10}O^{2-} + {}^1/_2\ H_2$. This substitution has been achieved experimentally, but it has not yet been demonstrated to occur in nature. The term "oxyallanite" may be used for the theoretical end-member $CaREEAl_2Fe^{3+}[Si_2O_7][SiO_4]O_2$. If the term "oxyallanite" is used in this sense it should be written in quotation marks accompanied by the word *component* to indicate its theoretical meaning ["oxyallanite" component]. A recommended more descriptive term is oxidized or dehydroxylated allanite-(REE).

5. Metamictization

Metamictization is a major problem in assigning a proper species name, in particular for REE-bearing epidote-group minerals. Metamict samples tend to be more reactive than well-crystallized minerals (for a review see Gieré & Sorensen, 2004) and exhibit anion- and cation-exchange properties (*e.g.*, possibly leading to vacancies on A sites). There is no sharp borderline between a completely X-ray amorphous substance (due to metamictization) and a mineral with a well-ordered crystal lattice. Subsequent heat-treatment under inert conditions to reestablish an ordered crystal lattice seems to be questionable if the resulting "mineral" adopts a composition that is characteristic of a partly ion-exchanged poorly crystalline (metastable) substance, but not of the original mineral. There is at least some suspicion that such "mineral" compositions are influenced by the experimenter and are not an unaltered product of nature. These problems are not specific of epidote-group minerals but are much more prominent in other mineral groups with higher concentrations of radioisotopes. For this reason the issue of metamictization is out of the scope of this subcommittee and should be treated in a general way by a different working group. We recommend exercising caution with compositions of "partly" metamict epidote-group minerals in naming new species, even if the "faulty" lattice has been mended by subsequent heat treatment.

6. Appendix

Some selected electron-microprobe analytical data cited from the literature are summarized in Table 7. Those data have been selected because they represent either borderline compositions (approximately intermediate between two species), or the data are incomplete and/or erroneous, or they originate from partly metamict samples. The aim of this appendix and the data in Table 7 is to demonstrate how a mineral name (Table 8) can be derived in non-trivial cases, based on the formal ion assignment to the *key sites* as discussed in Chapter 4.

The selected analytical data by Chessner & Ettlinger (1989) and Treloar & Charnley (1987) had to be normalized to Si = 3 because normalization on Σ (A + M + Z) yielded Si > 3.05. The Chessner & Ettlinger (1989) data suggest either A-site vacancies or incomplete analyses of A-site cations, whereas the Treloar & Charnley (1987) analytical data on dissakisite-(Ce) (originally described as allanite) from Outokumpu (Finland) indicate significant M-site vacancies, which are most probably related to incomplete analyses. In particular, the presence of V in the Outokumpu deposit suggests that V^{3+} could have been incorporated in the epidote-group minerals, but Treloar & Charnley (1987) did not analyze V. Another indication of missing cations in the analytical data of Treloar & Charnley (1987) is the sum of positive charges, which is insufficient to balance 25 negative charges even if all iron is calculated as ferric. A less likely alternative is significant F replacing O on O4 and thus lowering the sum of negative charges. F on O4, however, would not explain the low sum of M cations. There is also a deficit of positive charges (with all Fe as ferric) in some analytical data of "epidote-(Sr)" reported by Ahijado *et al.* (2005) (*e.g.*, analysis Nr. 8). Furthermore, analysis ACNF-8 (Table 7) gives only 2.847 Si pfu, which is anomalously low and probably is an analytical artifact.

What to do if subgroup and/or mineral name assignment fails?

(1) Poor or incomplete analyses or analyses from metamict materials are not expected to lead to the correct species name. There are several indicators for questionable analytical data such as Si > 3.0 or Si < 2.9, vacancies on M sites, or unbalanced charge (Δ charge).

(2a) Border-line case (REE + ACT > 0.5, close to 0.5 apfu): It may happen that, due to small amounts of Na, and/or vacancies on the A sites, and/or minor amounts of tetrahedral Al, the charge balance of the formula requires $^{M3}[M^{3+}]$ to slightly exceed $^{M3}[M^{2+}]$ even if $^{A2}[REE + ACT] > 0.5$. In other words, the dominant valence on M3 is not in agreement with the definition of the allanite subgroup (example: Analysis PF6 in Tables 7 and 8).

Solution. Priority must be given to the A2 key site. Because $^{A2}[REE + ACT] > 0.5$ and $^{O4}F < 0.5$ the mineral is assigned to the allanite

Table 7. Formula calculation based on electron-microprobe analytical data.

Analysis	PF1[1]	PF2[1]	PF6[1]	PF8[1]	PF11[1]	ACNF-2[2]	ACNF-8[2]
SiO_2	34.38	33.62	33.52	32.14	31.23	34.76	32.80
TiO_2	0.49	0.31	0.44	0.21	0.34	0.00	0.06
Al_2O_3	13.93	16.88	18.16	15.61	18.33	19.35	17.79
Cr_2O_3	0.71	0.70	0.82	0.40	0.42		
V_2O_3	8.89	8.06	6.78	8.46	0.97		
Fe_2O_3						15.42	18.42
FeO*	11.42	6.55	4.39	8.34	9.58		
MgO	0.09	1.25	0.62	0.4	0.14	0.00	0.05
MnO	1.90	1.40	1.14	1.26	1.21	0.14	0.44
CaO	17.78	14.24	14.82	11.76	10.99	15.91	16.13
SrO						10.76	11.64
BaO						0.10	0.04
Na_2O	0.06	0.12	0.06	0.17	0.14	0.00	0.01
K_2O						0.01	0.01
La_2O_3	3.88	6.74	7.48	4.23	4.95		
Ce_2O_3	3.54	5.56	6.78	8.76	12.18		
Pr_2O_3	0.20	0.33	0.38	1.43	1.06		
Nd_2O_3	0.50	1.00	0.78	3.95	4.32		
Sm_2O_3	0.10	0.21	0.21	0.57	0.61		
Gd_2O_3				0.28	0.52		
Dy_2O_3				0.30	0.34		
Y_2O_3	0.11	0.14	0.17	0.12	0.12		
F	nd	0.31	0.28	nd	0.19		
O=F	0	0.13	0.12	0	0.08		
Total	97.98	97.29	96.71	98.39	97.56	96.45	97.39
Norm.	Σ = 8	Σ = 8	Σ = 8	Σ = 8	Σ = 8	Σ = 8	Σ = 8
Si	2.977	2.997	3.023	2.972	2.965	3.003	2.847
Al	0.023	0.003	0	0.028	0.035	0	0.153
Σ Z	3	3	3.023	3	3	3.003	3
Ti	0.032	0.021	0.030	0.015	0.024	0.00	0.004
Al	1.399	1.770	1.930	1.673	2.016	1.970	1.667
Cr	0.049	0.049	0.059	0.029	0.032		
V	0.617	0.576	0.490	0.627	0.074		
Fe^{3+}	0.636	0.045		0.040	0.004	1.002	1.203
Fe^{2+}	0.191	0.373	0.331	0.561	0.757		
Mg	0.012	0.166	0.083	0.055	0.020		0.006
Mn^{2+}	0.064	0	0.077	0	0.073		
Mn^{3+}						0.010	0.032
Σ M	3	3	3	3	3	2.982	2.912
Mn^{2+}	0.075	0.106	0.010	0.099	0.024		
Fe^{2+}		0.070		0.044			
Ca	1.650	1.360	1.432	1.165	1.118	1.472	1.500
Sr						0.539	0.585
Ba						0.003	0.001
Na	0.01	0.015	0.011	0.030	0.026		0.001
K						0.001	0.001
REE	0.265	0.449	0.525	0.662	0.832		
Σ A	2.000	2.000	1.978	2.000	2.000	2.015	2.088
F	0	0.087	0.080	0	0.057		
Σcat.charge	25	24.91	25.10	25	24.94	24.99	24.75
Σan.charge	25	24.91	24.92	25	24.94	25	25
Δ charge	0	0	+0.18	0	0	-0.01	-0.25

Analysis	BAOZ-11[3]	BAOZ-C3-7[3]	OTT 16-1[4]	MTT 8-1[4]	YTT 51A5-2[4]	TC3[5]	TC9[5]
SiO_2	31.81	30.77	32.61	31.40	31.21	34.39	34.90
TiO_2	0.03	0.04	0.89	0.78	0.90		
Al_2O_3	14.34	13.41	13.99	13.70	13.15	18.55	18.89
Cr_2O_3						4.91	4.95
Fe_2O_3	7.52	7.62					
Mn_2O_3	13.93	13.27					
FeO*			15.57	16.10	15.48	2.84	2.70
MgO	0.56	0.54	0.84	0.41	0.90	3.01	2.92
MnO			0.66	0.67	0.99		
ZnO	0.74	0.69					
CaO	12.08	11.16	9.95	9.13	9.54	13.95	14.19
PbO	6.08	9.86					
Na_2O	0.19	0.13					
K_2O	0.02	0.00					
La_2O_3	3.88	4.55	5.77	4.80	5.95	9.24	9.21
Ce_2O_3	3.11	1.20	11.25	10.81	11.76	9.43	9.08
Pr_2O_3			1.09	1.21	1.17		
Nd_2O_3	1.57	1.07	3.61	4.51	3.83	1.29	1.31
Sm_2O_3			0.47	0.80	0.46	0.24	0.24
Dy_2O_3							
Y_2O_3			0.29	0.48	0.43	0.14	0.16
ThO_2			1.75	2.17	1.83		
Total	95.86	94.31	98.74	96.97	97.60	97.99	98.55
Norm.	Σ = 8	Σ = 8	Si = 3	Si = 3	Si = 3	Si = 3	Si = 3
Si	3.012	3.035	3.0	3.0	3.0	3.0	3.0
Ti	0.002	0.003	0.062	0.056	0.065		
Al	1.600	1.559	1.518	1.543	1.491	1.907	1.914
Cr						0.339	0.336
Fe^{3+}	0.536	0.566	1.080	0.912	0.735	0.207	0.194
Fe^{2+}			0.117	0.375	0.509		
Mg	0.079	0.079	0.115	0.058	0.129	0.391	0.374
Mn^{3+}	0.576	0.579					
Mn^{2+}	0.155	0.164	0.051	0.054	0.081		
Zn	0.052	0.050					
Σ M	3.000	3.000	2.943	2.998	3.010	2.844	2.818
Mn^{2+}	0.273	0.253					
Ca	1.226	1.179	0.981	0.935	0.982	1.304	1.307
Pb	0.155	0.262					
Na	0.035	0.025					
REE	0.299	0.246	0.761	0.793	0.835	0.651	0.632
Th			0.037	0.047	0.040		
REE+Th	0.299	0.246	0.798	0.840	0.875	0.651	0.632
Σ A	1.988	1.965	1.779	1.775	1.857	1.955	1.939
Σcat.charge	25	25	25	25	25	24.70	24.59
Σan.charge	25	25	25	25	25	25	25
Δ charge	0	0	0	0	0	-0.30	-0.41

[1]Pan & Fleet (1991) ; [2]Ahijado *et al.* (2005); [3]Bermanec *et al.* (1994); [4]Chesner & Ettlinger (1989); [5]Treloar & Charnley (1987); * total iron content given as FeO. All calculations were done for three decimals to reduce rounding errors (although only two decimals may be significant).

Table 8. Distribution of ions on key sites and derivation of mineral name based on electron-microprobe analytical data listed in Table 7.

	A1	A2	M1	M2	M3	O4	*subgroup* mineral name
PF1[1]	2+	2+	3+	3+	3+	2-	*clinozoisite*
	0.075 Mn^{2+} 0.010 Na 0.925 Ca	0.726 Ca 0.265 REE	0.520 V^{3+} 0.049 Cr 0.032 Ti 0.399 Al	Al	0.064 Mn^{2+} 0.191 Fe^{2+} 0.012 Mg 0.636 Fe^{3+} 0.097 V^{3+}	0.000 F	vanadoepidote*
PF2[1]	2+	2+	3+	3+	2+ !!	2-	*clinozoisite*[$]
	0.106 Mn^{2+} 0.070 Fe^{2+} 0.015 Na 0.809 Ca	0.551 Ca 0.449 REE	0.160 V^{3+} 0.049 Cr 0.021 Ti 0.770 Al	Al	0.373 Fe^{2+} 0.166 Mg 0.045 Fe^{3+} 0.416 V^{3+}	0.087 F	mukhinite[$]
PF6[1]	2+	3+	3+	3+	3+ !!	2-	*allanite*[$]
	0.010 Mn^{2+} 0.011 Na 0.979 Ca	0.453 Ca 0.525 REE 0.022 #	0.040 Cr 0.030 Ti 0.930 Al	Al	0.077 Mn^{2+} 0.331 Fe^{2+} 0.083 Mg 0.490 V^{3+} 0.019 Cr	0.080 F	(V^{3+}-rich) allanite-(La)[$]
PF8[1]	2+	3+	3+	3+	2+	2-	*allanite*
	0.099 Mn^{2+} 0.044 Fe^{2+} 0.030 Na 0.827 Ca	0.338 Ca 0.662 REE	0.283 V^{3+} 0.029 Cr 0.015 Ti 0.673 Al	Al	0.561 Fe^{2+} 0.055 Mg 0.040 Fe^{3+} 0.344 V^{3+}	0.000 F	(V^{3+}-rich) allanite-(Ce)
PF11[1]	2+	3+	3+	3+	2+	2-	*allanite*
	0.024 Mn^{2+} 0.026 Na 0.950 Ca	0.168 Ca 0.832 REE	1.000 Al	Al	0.073 Mn^{2+} 0.757 Fe^{2+} 0.020 Mg 0.004 Fe^{3+} 0.074 V^{3+} 0.032 Cr 0.024 Ti 0.016 Al	0.057 F	allanite-(Ce)
ACNF-2[2]	2+	2+	3+	3+	3+	2-	*clinozoisite*
	0.001 Na 0.999 Ca	0.473 Ca 0.539 Sr 0.003 Ba 0.001 K	0.012 Fe^{3+} 0.970 Al 0.018 #	Al	0.010 Mn^{3+} 0.990 Fe^{3+}	0.000 F	epidote-(Sr)*
ACNF-8[2]	2+	2+	3+	3+	3+	2-	*clinozoisite*
	0.001 Na 0.999 Ca	0.501Ca 0.585 Sr 0.001Ba 0.001K	0.241Fe^{3+} 0.667Al 0.004 Ti 0.088 #	Al	0.006 Mg 0.032 Mn^{3+} 0.962 Fe^{3+}	0.000 F	epidote-(Sr)*
BAOZ-11[3]	2+	2+	3+	3+	3+	2-	*clinozoisite*
	0.273 Mn^{2+} 0.035 Na 0.692 Ca	0.534 Ca 0.299 REE 0.155 Pb 0.012 #	0.398 Fe^{3+} 0.002 Ti 0.600 Al	Al	0.155 Mn^{2+} 0.576 Mn^{3+} 0.052 Zn 0.079 Mg 0.138 Fe^{3}	0.000 F	piemontite
BAOZ-C3-7[3]	2+	2+	3+	3+	3+	2-	*clinozoisite*
	0.253 Mn^{2+} 0.025 Na 0.722 Ca	0.457 Ca 0.246 REE 0.262 Pb 0.035 #	0.438 Fe^{3+} 0.559 Al	Al	0.164 Mn^{2+} 0.579 Mn^{3+} 0.050 Zn 0.079 Mg 0.128 Fe^{3+}	0.000 F	piemontite
OTT16-1[4]	2+	3+	3+	3+	3+!!	2-	*allanite*[$]
	0.981 Ca 0.019 #	0.798 REE + Th 0.202 #	0.363 Fe^{3+} 0.062 Ti 0.518 Al 0.057 #	Al	0.051 Mn^{2+} 0.117 Fe^{2+} 0.115 Mg 0.717 Fe^{3+}	0.000 F	allanite-(Ce)[$]

Table 8. (continued)

	A1	A2	M1	M2	M3	O4	*subgroup* mineral name
MTT8-1[4]	2+ 0.935 Ca 0.065 #	3+ 0.840 REE + Th 0.160 #	3+ 0.399 Fe^{3+} 0.056 Ti 0.543 Al 0.002 #	3+ Al	3+!! 0.054 Mn^{2+} 0.375 Fe^{2+} 0.058 Mg 0.513 Fe^{3+}	2- 0.000 F	*allanite*[$] allanite-(Ce)[$]
YTT51A5-2[4]	2+ 0.982 Ca 0.018 #	3+ 0.875 REE + Th 0.125 #	3+ 0.454 Fe^{3+} 0.065 Ti 0.491 Al	3+ Al	2+ 0.081 Mn^{2+} 0.509 Fe^{2+} 0.129 Mg 0.281 Fe^{3+}	2- 0.000 F	*allanite* allanite-(Ce)
TC-3[5]	2+ 1.000 Ca	3+ 0.304 Ca 0.651 REE 0.045 #	3+ 0.844 Al 0.156 #	3+ Al	3+ !! 0.391 Mg 0.207 Fe^{3+} 0.339 Cr 0.063 Al	2- 0.000 F	*allanite*[$] dissakisite-(Ce)[$]
TC-9[5]	2+ 1.000 Ca	3+ 0.307 Ca 0.632 REE 0.061 #	3+ 0.818 Al 0.182 #	3+ Al	3+ !! 0.374 Mg 0.194 Fe^{3+} 0.336 Cr 0.096 Al	2- 	*allanite*[$] dissakisite-(La)[$]

Note: * Recommended names: However, these names are not acceptable without corresponding new mineral approval by IMA CNMMN ; [$]subgroup and/or name assignment fails with the standard procedure (for solution see appendix).
[1]Pan & Fleet (1991); [2]Ahijado *et al.* (2005); [3]Bermanec *et al.* (1994); [4]Chesner & Ettlinger (1989); [5]Treloar & Charnley (1987).

subgroup and the species name is determined by the dominant M^{2+} on M3.
(2b) Border-line case (REE + ACT < 0.5, close to 0.5 apfu); it may happen that, due to small amounts of Th^{4+} on the A2 site, and/or Si slightly exceeding 3.00, and/or minor amounts of octahedral Ti^{4+}, Sn^{4+}, and/or significant F on O4, the charge balance of the formula requires $^{M3}[M^{2+}]$ to slightly exceed $^{M3}[M^{3+}]$ even if $^{A2}[REE^{3+}] < 0.5$ (example: Analysis PF2 in Tables 7 and 8).
Solution. Priority must be given to the A2 key site. Because ^{A2}[REE +ACT] < 0.5 the mineral is assigned to the clinozoisite subgroup and the species name is determined by the dominant M^{3+} on M3.
(3) ^{A2}[REE +ACT] partly charge-balanced by vacancies: We may suspect a certain degree of metamictization (examples OTT16-1 and MTT8-1 in Tables 7 and 8).
Solution: In analogy to (2a).

Acknowledgement: We are highly indebted to E.S. Grew (Orono, Maine) for improving the English. Former members of this subcommittee are thanked for their contributions. The revised report benefited from comments and corrections by the members of IMA CNMMN. We highly appreciate the supporting comments by Stefano Merlino on the draft version of this report.

References

Ahijado, A., Casillas, R., Nagy, G., Fernández, C. (2005): Sr-rich minerals in a carbonatite skarn, Fuerteventura, Canary Islands (Spain). *Mineral. Petrol.*, **84**, 107–127

Armbruster, T., Gnos, E., Dixon, R., Gutzmer, J., Hejny, C., Döbelin, N., Medenbach, O. (2002): Manganvesuvianite and tweddillite, two new Mn^{3+} minerals from the Kalahari manganese fields, South Africa. *Mineral. Mag.*, **66**, 137-150.

Bayliss, P. & Levinson, A.A. (1988): A system of nomenclature for rare-earth mineral species: revision and extension. *Am. Mineral.*, **73**, 422-423.

Bayliss, P., Kaesz, H.D., Nickel, E.H. (2005): The use of chemical-element adjectival modifiers in mineral nomenclature. *Can. Mineral.*, **43**, 1429-1433.

Bleeck, A.W.G. (1907): Die Jadeitlagerstätten in Upper Burma. *Z. Prakt.Geol.*, **1907**, 341-365.

Bermanec, V., Armbruster, T., Oberhänsli, R., Zebec, V. (1994): Crystal chemistry of Pb- and REE-rich piemontite from Nezilovo, Macedonia. *Schweiz. Mineral. Petrogr. Mitt.*, **74**, 321-328.

Bonazzi, P. & Menchetti, S. (1994:) Structural variations induced by heat treatment in allanite and REE-bearing piemontite. *Am. Mineral.*, **79**, 1176-1184

—,— (1995): Monoclinic members of the epidote group: Effects of the Al ↔ Fe^{3+} ↔ Fe^{2+} substitution and the entry of REE^{3+}. *Mineral. Petrol.*, **53**, 133-153.

—,— (2004): Manganese in monoclinic members of the epidote group: Piemontite and related minerals. *In*: "Reviews in Mineralogy & Geochemistry", Vol. **56**, Mineralogical Society of America, 495-552.

Bonazzi, P., Menchetti, S., Palenzona, A. (1990): Strontiopiemontite, a new member of the epidote group from Val Graveglia, Liguria, Italy. *Eur. J. Mineral.*, **2**, 519-523.

Bonazzi, P., Garbarino, C. Menchetti, S. (1992): Crystal chemistry of piemontites: REE-bearing piemontite from Monte Brugiana, Alpi Apuane, Italy. *Eur. J. Mineral.*, **4**, 23-33.

Bonazzi, P., Menchetti, S., Reinecke, T. (1996): Solid solution between piemontite and androsite-(La), a new mineral of the epidote group from Andros Island, Greece. *Am. Mineral.*, **81**, 735-742.

Bonazzi, P., Bindi, L., Parodi, G. (2003): Gatelite-(Ce), a new REE-bearing mineral from Trimouns, French Pyrenees: Crystal

structure and polysomatic relationships with epidote and törnebohmite-(Ce). *Am. Mineral.*, **88**, 223-228.

Burns, R.G & Strens, R.G. (1967): Structural interpretation of polarized absorption spectra of the Al-Fe-Mn-Cr-epidotes. *Mineral. Mag.*, **36**, 204-226.

Catti, M., Ferraris, G, Ivaldi, G. (1989): On the crystal chemistry of strontian piemontite with some remarks on the nomenclature of the epidote group. *N. Jahrb. Mineral. Mh.*, **1989**, 357-366.

Cenki-Tok, B., Ragu, A., Armbruster, T., Chopin, C., Medenbach, O. (2006): Mn- and rare-earth-rich epidote-group minerals in metacherts: manganiandrosite-(Ce) and vanadoandrosite-(Ce). *Eur. J. Mineral.*, **18**, 569-582.

Chesner, C.A. & Ettlinger, A.D. (1989): Composition of volcanic allanite from the Toba Tuffs, Sumatra, Indonesia. *Am. Mineral.*, **74**, 750-758.

Cressey, G. & Steel, A.T. (1988): An EXAFS study of Gd, Er and Lu site location in the epidote structure. *Phys. Chem. Minerals*, **15**, 304-312.

Dana, E.S. (1896): «The System of Mineralogy of James Dwight Dana 1837-1868»: Descriptive Mineralogy, 6th Edition, John Wiley & Sons, New York, p. 513-525 and supplement p. 1035.

Deer, W.A., Howie, R.A., Zussman, J. (1986): «Rock-forming Minerals», Vol. **1b**, 2. Edition, Disilicates and Ring Silicates, Longman Group U.K., 629 p.

Dollase, W.A. (1968): Refinement and comparison of the structure of zoisite and clinozoisite. *Am. Mineral.*, **53**, 1882-1898.

— (1969): Crystal structure and cation ordering of piemontite. *Am. Mineral.*, **54**, 710-717.

— (1971): Refinement of the crystal structures of epidote, allanite and hancockite. *Am. Mineral.*, **56**, 447-464.

— (1973): Mössbauer spectra and iron distribution in the epidote-group minerals. *Z. Kristallogr.*, **138**, 41-63.

Dufrénoy, A. (1856): «Traité de Minéralogie», second Edition, Victor Dalmont, Paris, Vol. **3**, p. 624-643.

Dunn, P. J. (1985): The lead silicates from Franklin, New Jersey: occurrence and composition. *Mineral. Mag.*, **49**, 721-727.

Eppler, W.F. (1984): «Praktische Gemmologie», 2nd Ed., Rühle-Diebener-Verlag, Stuttgart, 504 p.

Ercit, T. S. (2002): The mess that is allanite. *Can. Mineral.*, **40**, 1411-1419.

Eskola, P. (1933): On the chrome minerals of Outokumpu. *Bull. Commiss. Geol. Finlande*, **103**, 26-44.

Ferraris, G., Ivaldi, G., Fuess, H., Gregson, D. (1989): Manganese/iron distribution in a strontian piemontite by neutron diffraction. *Z. Kristallogr.*, **187**, 145-151.

Fesenko, E.G., Rumanova, I.M., Belov, N.V. (1955): The crystal structure of zoisite. *Dokl. Acad. Sci. USSR*, **102**, 275-278.

Franz, G. & Liebscher, A. (2004): Physical and chemical properties of the epidote minerals – An introduction. *In* «Reviews in Mineralogy and Geochemistry», Vol. **56**, Epidotes, Mineralogical Society of America, Washington. 1-82.

Geijer, P. (1927): Some mineral associations from the Norberg district. Sveriges Geologiska Undersökning. *Avhandlingar och Uppsatser*, series **C 343**, 32 p.

Gieré, R. & Sorensen, S.S. (2004): Allanite and other REE-rich epidote-group minerals. *In «*Reviews in Mineralogy and Geochemistry», Vol. **56**, Epidotes, Mineralogical Society of America, Washington. 431-493.

Grapes, R.H. (1981): Chromian epidote and zoisite in kyanite amphibolite, Southern Alps, New Zealand. *Am. Mineral.*, **66**, 974-975.

Grew, E.S. (2002): Mineralogy, petrology and geochemistry of beryllium: An introduction and list of beryllium minerals. *In* «Reviews in Mineralogy and Geochemistry», Vol. **50**, - Beryllium – Mineralogy, Petrology, and Geochemistry, Mineralogical Society of America, Washington. 1-76.

Grew, E.S., Essene, E.J., Peacor, D.R., Su, S.C., Asami, M. (1991): Dissakisite-(Ce), a new member of the epidote group and the Mg analogue of allanite-(Ce), from Antarctica. *Am. Mineral.*, **76**, 1990-1997.

Haüy, R.J. (1801): «Traité de Minéralogie», Vol. **3**, chez Louis libraire, Paris, p. 102-113.

Hey, M.H. (1955): «An Index of Mineral Species & Varieties», second revised Ed., British Museum, 728 p.

Holtstam, D. & Langhof, J. (1994): Hancockite from Jakobsberg, Filipstad, Sweden: The second world occurrence. *Mineral. Mag.*, **58**, 172-174.

Holtstam, D., Andersson, U.B., Mansfeld, J. (2003): Ferriallanite-(Ce) from the Bastnäs deposit, Västmanland, Sweden. *Can. Mineral.*, **41**, 1233-1240.

Holtstam, D., Kolitsch, U., Andersson, U.B. (2005): Västmanlandite-(Ce) – a new lanthanide – and F-bearing sorosilicate mineral from Västmanland, Sweden: description, crystal structure, and relation to gatelite-(Ce). *Eur. J. Mineral.*, **17**, 129-141.

Hutton, C.O. (1938): On the nature of withamite from Glen Coe, Scotland. *Min. Mag.*, **25**, 119-124.

Iimori, T., Yoshimora, J., Hata, S. (1931): A new radioactive mineral found in Japan. *Sci. Pap. Inst. Phys. Chem. Res. Tokyo*, **15**, 83-88.

Ito, T. (1947): The structure of epidote ($HCa_2(Al,Fe)Al_2Si_3O_{12}$) *Am. Mineral.*, **32**, 309-321.

— (1950): «X-ray studies on polymorphism», chapter 5. Maruzen Company, Tokyo.

Ito, T., Morimoto, N., Sadanaga, R. (1954): On the structure of epidote. *Acta Cryst.*, **7**, 53-59.

Kartashov, P.M., Ferraris, G., Ivaldi, G., Sokolova, E., McCammon, C.A. (2002): Ferriallanite-(Ce), $CaCeFe^{3+}AlFe^{2+}[SiO_4][Si_2O_7]O(OH)$, a new member of the epidote group: Description, X-ray and Mössbauer study. *Can. Mineral.*, **40**, 1641-1648.

Kenngott, G.A. (1853): Das Mohs'sche Mineralsystem, Wien, p. 75.

Lacroix, A. (1889): *Bull. Soc. Min.*, **12**, 327; not consulted; cited in Dana (1896).

Langer, K., Tillmanns, E., Kersten, M, Almen, H., Arni, R.K. (2002): The crystal chemistry of Mn^{3+} in the clino- and orthozoisite structure types, $Ca_2M^{3+}{}_3[OH/O/SiO_4/Si_2O_7]$: A structural and spectroscopic study of some natural piemontites and «thulites» and their synthetic equivalents. *Z. Kristallogr.*, **217**, 563-580.

Laspeyres, H. (1879): *Z. Krystallogr. Mineral.*, **3**, 561; not consulted, cited in Dana (1896).

Levinson, A.A. (1966): A system of nomenclature for rare-earth minerals. *Am. Mineral.*, **51**, 152-158.

Liebscher, A. (2004): Spectroscopy of epidote minerals. *In* «Reviews in Mineralogy and Geochemistry», Vol. **56**, Epidotes, Mineralogical Society of America, Washington. 125-170.

Liebscher, A. & Franz, G. (2004): «Reviews in Mineralogy and Geochemistry», Vol. **56**, Epidotes, Mineralogical Society of America, Washington. 628 p.

Ludwig, C.F. (1803-1804): «Handbuch der Mineralogie nach A.G. Werner», Vol. **2**, p. 209.

Merlino, S. (1990): OD structures in mineralogy. *Period. Mineral.*, **59**, 69-92.

Miyajima, H., Matsubara, S., Miyawaki, R., Hirokawa, K. (2003): Niigataite, $CaSrAl_3[Si_2O_7][SiO_4]O(OH)$: Sr-analogue of clinozoisite a new member of the epidote group from Itoigawa-Ohmi

district, Niigata Prefecture, central Japan. *J. Mineral. Petrol. Sci.*, **98**, 118-129.

Mottana, A. & Griffin, W.L. (1986): The crystal chemistry of piemontite from the type-locality (St. Marcel, Val d'Aosta, Italy); *in* «Crystal Chemistry of Minerals», Proc. of the 13th Gen. Meet. of IMA, Varna, Sept. 19th-25th 1982, Bulgarian Academy of Science, Sofia, p. 635-640.

Nels, H.J., Straus, C.A., Wickmann, F. (1949): Lombaardite, a new mineral from the Zaaiplaats tin mine, central Transvaal. Union S. Africa. *Dept. Mines Mem. Geol. Surv.*, **43**, 45-57.

Neumann, H. & Nilssen, B. (1962): Lombaardite, a rare earth silicate, identical with, or very closely related to allanite. *Norsk. Geol. Tidsskrift*, **42**, 277-286.

Nickel, E.H. (1992): Solid solutions in mineral nomenclature. *Can. Mineral.*, **30**, 231-234.

Nickel, E.H. & Grice, J.D (1998): The IMA Commission on New Minerals and Mineral Names: Procedures and guidelines on mineral nomenclature. *Can. Mineral.*, **36**, 913-926.

Nickel, E.H. & Mandarino, J.A. (1987): Procedures involving the IMA commission on New Minerals and Mineral Names, and guidelines on mineral nomenclature. *Can. Mineral.*, **25**, 353-377.

Orlandi, P. & Pasero, M. (2006): Allanite-(La) from Buca della Vena mine, Apuan Alps, Italy, an epidote group mineral. *Can. Mineral.*, **44**, 173-178.

Pan, Y. & Fleet, M.E. (1990): Halogen-bearing allanite from the White River gold occurrence, Hemlo area, Ontario. *Can. Mineral.*, **28**, 67-75.

—,— (1991): Vanadian allanite-(La) and vanadian allanite-(Ce) from the Hemlo gold deposit, Ontario, Canada. *Mineral. Mag.*, **55**, 497-507.

Pautov, L.A., Khvorov, P.V., Ignatenko, K.I., Sokolova, E.V, Nadezhina, T.N. (1993): Khristovite-(Ce) (Ca, REE)REE (Mg,Fe)$MnAlSi_3O_{11}$(OH)(F,O). *Proc. Russ. Mineral. Soc.*, **122** (3), 103-111.

Pawley, A.R., Redfern, S.A.T., Holland, T.J.B. (1996): Volume behavior of hydrous minerals at high pressure and temperature: I. Thermal expansion of lawsonite, zoisite, clinozoisite, and diaspore. *Am. Mineral.*, **81**, 335-340.

Peacor D.R. & Dunn, P.J. (1988): Dollaseite-(Ce) (magnesium orthite redefined): Structural refinement and implications for F + M^{2+} substitutions in epidote-group minerals. *Am. Mineral.*, **73**, 838-842.

Penfield, S.L. & Warren, C.H. (1899): Some new minerals from the zinc mines at Franklin, N.J., and note concerning the chemical composition of ganomalite. *Am. J. Sci.*, **8**, 339-353.

Petersen, O. & Johnsen, O. (2005): Mineral Species First Discovered from Greenland. *Can. Mineral. Spec. Publ.*, **8**, 184 p.

Peterson, R.C. & MacFarlane, D.B. (1993): The Rare-Earth-Element chemistry of allanite from the Grenville Province. *Can. Mineral.*, **31**, 159-166.

Rammelsberg (1875): *Min. Ch.*, 595; not consulted; cited in Dana (1896).

Rouse, R.C. & Peacor, D.R. (1993): The crystal structure of dissakisite-(Ce), the Mg analogue of allanite-(Ce). *Can. Mineral.*, **31**, 153-157.

Schaller, W.T. (1930): Adjectival ending of chemical elements used as modifiers to mineral names. *Am. Mineral.*, **15**, 567-574.

Shannon, R.D. (1976): Revised effective ionic radii and systematic studies of interatomic distances in halides and chalcogenides. *Acta Cryst.*, **A32**, 751-767.

Shepel, A.V. & Karpenko, M.V. (1969): Mukhinite, a new vanadium species of epidote. *Dokl. Acad. Nauk SSSR*, **185**, 1342-1345 (in Russian).

Sokolova, E.V., Nadezhina, T.N., Pautov, L.A. (1991): Crystal structure of a new natural silicate of manganese from the epidote group. *Kristallografiya*, **36**, 330-333.

Strunz, H. & Nickel, E.H. (2001): «Strunz Mineralogical Tables», 9th Edition, E. Schweizerbart'sche Verlagsbuchhandlung, Stuttgart, 870 p.

Thomson, T. (1810): Experiments on allanite, a new mineral from Greenland. *Trans. Royal Soc. Edinburgh*, **8**, 371-386.

Treloar, P.J. (1987): Chromian muscovites and epidotes from Outokumpu, Finland. *Mineral. Mag.*, **51**, 593-599.

Treloar, P.J. & Charnley, N.R. (1987): Chromian allanite from Outokumpu, Finland. *Can. Mineral.*, **25**, 413-418.

Tschermak, G. (1905): «Lehrbuch der Mineralogie», 6th Edition, A. Hölder, Wien, 682 p.

Tumiati, S., Godard, G., Martin, S., Nimis, P., Mair, V., Boyer, B. (2005): Dissakisite-(La) from the Ulten zone peridotite (Italian Eastern Alps): A new end-member of the epidote group**.** *Am. Mineral.*, **90**, 1177-1185.

Weinschenk, E. (1896): Über Epidot und Zoisit. *Z. Krystallogr. Mineral.*, **26**, 154-177.

Weiss, C.S. (1820): Über die Theorie des Epidotsystems. *Abh. k. Akad. Wiss. Berlin*, 242-269.

Yoshimura, T. & Momoi, H. (1964): [Withamite from the Yamanaka mine, Hyogo Prefecture. *Sci. Rept. Kyushu Univ. Geol.*, **6**, 201-206]. (English abstract) *Mineral. Abst.*, **17**, 299.

Received 24 May 2006
Accepted 5 June 2006

American Mineralogist, Volume 96, pages 895–913, 2011

Nomenclature of the tourmaline-supergroup minerals

Darrell J. Henry,[1,*] Milan Novák (chairman),[2] Frank C. Hawthorne,[3] Andreas Ertl,[4] Barbara L. Dutrow,[1] Pavel Uher,[5] and Federico Pezzotta[6]

[1]Department of Geology and Geophysics, Louisiana Street University, Baton Rouge, Louisiana 70803, U.S.A.
[2]Chairman of the Subcommittee on Tourmaline Nomenclature, Department of Geological Sciences, Petrology and Geochemistry, Masaryk University, Kotlářská 2, CZ-611 37 Brno, Czech Republic
[3]Department of Geological Sciences, University of Manitoba, Winnipeg, Manitoba R3T 2N2, Canada
[4]Institut für Mineralogie und Kristallographie Geozentrum, Universität Wien, Althanstrasse 14, 1090 Wien, Austria
[5]Department of Mineral Deposits, Faculty of Natural Sciences, Department of Mineralogy and Petrology, Comenius University in Bratislava, Mlynská dolina, 842 15 Bratislava, Slovak Republic
[6]Mineralogy Department, Museo di Storia Naturale di Milano, Corso Venezia 55, I-20121 Milan, Italy

Abstract

A nomenclature for tourmaline-supergroup minerals is based on chemical systematics using the generalized tourmaline structural formula: $XY_3Z_6(T_6O_{18})(BO_3)_3V_3W$, where the most common ions (or vacancy) at each site are X = Na^{1+}, Ca^{2+}, K^{1+}, and vacancy; Y = Fe^{2+}, Mg^{2+}, Mn^{2+}, Al^{3+}, Li^{1+}, Fe^{3+}, and Cr^{3+}; Z = Al^{3+}, Fe^{3+}, Mg^{2+}, and Cr^{3+}; T = Si^{4+}, Al^{3+}, and B^{3+}; B = B^{3+}; V = OH^{1-} and O^{2-}; and W = OH^{1-}, F^{1-}, and O^{2-}. Most compositional variability occurs at the X, Y, Z, W, and V sites. Tourmaline species are defined in accordance with the dominant-valency rule such that in a relevant site the dominant ion of the dominant valence state is used for the basis of nomenclature. Tourmaline can be divided into several groups and subgroups. The primary groups are based on occupancy of the X site, which yields alkali, calcic, or X-vacant groups. Because each of these groups involves cations (or vacancy) with a different charge, coupled substitutions are required to relate the compositions of the groups. Within each group, there are several subgroups related by heterovalent coupled substitutions. If there is more than one tourmaline species within a subgroup, they are related by homovalent substitutions. Additionally, the following considerations are made. (1) In tourmaline-supergroup minerals dominated by either OH^{1-} or F^{1-} at the W site, the OH^{1-}-dominant species is considered the reference root composition for that root name: e.g., dravite. (2) For a tourmaline composition that has most of the chemical characteristics of a root composition, but is dominated by other cations or anions at one or more sites, the mineral species is designated by the root name plus prefix modifiers, e.g., fluor-dravite. (3) If there are multiple prefixes, they should be arranged in the order occurring in the structural formula, e.g., "potassium-fluor-dravite."

Keywords: Tourmaline, mineral chemistry, nomenclature, substitutions, order-disorder

Introduction

The Subcommittee on Tourmaline Nomenclature (STN) of the International Mineralogical Association's Commission on New Minerals, Nomenclature and Classification (IMA-CNMNC) has reconsidered the nomenclature of tourmaline-supergroup[1] minerals. This was prompted by the general ambiguity in the assignment of mineral names to specific tourmaline compositions. There are several reasons for this uncertainty (Hawthorne and Henry 1999). (1) Formal descriptions of tourmaline minerals often specify the ideal end-member compositions, but do not specify the limits for the use of the name. (2) Some of the formal descriptions of tourmaline minerals specify the general composition, but do not specify the end-member composition. (3) Tourmaline is commonly incompletely chemically characterized, with critical light elements (H, Li, F, and B) and the oxidation states of transition elements (Fe, Mn) often being undetermined. (4) Site assignments can be equivocal in the absence of crystal-structure refinements. (5) Current graphical representations of tourmaline compositional variations are inadequate to express the actual substitutional nature of tourmaline. These considerations motivated Hawthorne and Henry (1999) and the STN to re-examine and, where necessary, redefine end-members and potential new end-members and species, which led to the development of several compositional diagrams that aid in classification of the tourmaline-supergroup minerals. The proposal for systematic classification of the tourmaline-supergroup miner-

[1] Tourmaline is considered to be a supergroup in terms of nomenclature procedures because it "consists of two or more mineral groups, which have essentially the same structure and composed of chemically similar elements" (Mills et al. 2009).

* E-mail: glhenr@lsu.edu

0003-004X/11/0506–895$05.00/DOI: 10.2138/am.2011.3636

als submitted by the STN was accepted by the IMA-CNMNC (Novák et al. 2009).

The purpose of this paper is to present the essential elements of tourmaline nomenclature, to define concepts that are central to tourmaline classification, and to provide practical guidelines for application of the nomenclature.

Crystallographic and crystal-chemical aspects of tourmaline-supergroup minerals

Tourmaline is a crystallographically acentric borosilicate mineral with the generalized chemical formula $XY_3Z_6(T_6O_{18})(BO_3)_3V_3W$ (Hawthorne and Henry 1999). This general formula makes no assumptions about site occupancy, besides those sites known to be occupied exclusively by O^{2-}. Consequently, as knowledge of site occupancy in tourmaline progresses, it will be unnecessary to change the general formula. Only the assignment of the cations and anions to the letters of the general formula will be changed. The symmetry of tourmaline is predominantly rhombohedral in the *R*3*m* space group. However, there are some reports of tourmalines, or sectors within tourmaline crystals, having orthorhombic, monoclinic, or triclinic symmetry (e.g., Akizuki et al. 2001; Shtukenberg et al. 2007; Williams et al. 2010; IMA no. 2009-46).

Table 1 gives the relative abundance of the generalized cations (R^{1+}, R^{2+}, R^{3+}, R^{4+}) and anions (S^{1-}, S^{2-}) at each of these sites, and presents the most common cation and anion substituents for each of the valence states of the ions. Although tourmaline can accommodate a great variety of cations in minor or trace amounts, all current tourmaline species are, and most prospective species will likely be, represented by combinations of the cations, anions, or vacancies listed in Table 1.

In addition to the ionic size and charge of the cations and anions, two related factors influence the content and location of these ions in the tourmaline structure: short-range bond-valence requirements and order-disorder reactions. (1) In the Y site, the incident bond-valence requirements at the W site mandate that only certain short-range configurations are stable (Hawthorne 1996). Table 2 gives the possible stable local cation configurations at the Y site for generalized Li-free and Li-bearing tourmalines. For a given Y-site bulk composition, the tourmaline can have a single local Y-site cation configuration or a mixture of possible local cation configurations. For example, the chemical composition of end-member liddicoatite has the stable Y-site configuration of Li_2Al, whereas end-member elbaite, with a Y-site bulk composition of $Al_{1.5}Li_{1.5}$, will have equal proportions of Al_2Li and $AlLi_2$ clusters at the Y site (Hawthorne 1996). These relatively few local cation configurations will constrain the number and type of potential stable end-members possible in tourmaline. (2) Order-disorder reactions control the actual location of ions in the tourmaline structure. When O^{2-} is located at the W site, disordering tends to develop at the Y and Z sites (Hawthorne and Henry 1999). For example, Hawthorne (1996) showed that in Li-free tourmaline the occurrence of Mg at the Z site and Al at the Y site is commonly due to disorder reactions associated with the occurrence of O^{2-} at the W site, and this can be expressed as $^{Y}Mg^{2+} + {}^{Z}Al^{3+} + {}^{W}(OH)^{1-} \leftrightarrow {}^{Y}Al^{3+} + {}^{Z}Mg^{2+} + {}^{W}O^{2-}$. For the $3R^{3+}$ Y-site configuration in Li-free tourmaline the disorder relation is $3^{Y}Mg^{2+} + 2^{Z}Al^{3+} + {}^{W}(OH)^{1-} \leftrightarrow 3^{Y}Al^{3+} + 2^{Z}Mg^{2+} + {}^{W}O^{2-}$. Effectively, the disordering substitution enhances the amount of Mg that is located at the Z site and Al at the Y site with the maximal amount being 2 Mg atoms per formula unit (apfu) at the Z site (e.g., Bosi and Lucchesi 2007). Similar arguments have been put forward for the disordering of Fe^{2+} to the Z site (Bosi 2008).

In terms of a classification scheme, most of the compositional variability occurs at the X, Y, Z, W and, to a lesser extent, V sites. The T site is typically dominated by Si and the B site exclusively contains B, such that the cationic occupancies at these sites do not serve as primary parameters for classification, except in some unusual tourmaline species. The atomic ordering in the structure will be confidently established only with crystal-structure refinement data and information from allied techniques such as Mössbauer and NMR spectroscopy. The influence of W-site O^{2-} appears to require disordering reactions to occur such that, in this paper, the recognized or prospective W-site O^{2-}-tourmaline species are presented in their disordered form—their most likely actual cation distribution. However, when oxy-tourmalines are considered *for classification purposes*, they are recast in their

Table 2. Stable local short-range Y-site cation configurations for anions of different charge at the W site

General chemical type of tourmaline	W-site anion	Y-site stable short-range configurations
Li-free tourmaline	$(OH)^{1-}$ or F^{1-}	$3R^{2+}$ or $R^{3+} + 2R^{2+}$
Li-free tourmaline	O^{2-}	$3R^{3+}$ or $2R^{3+} + R^{2+}$
Li-bearing tourmaline	$(OH)^{1-}$ or F^{1-}	$2Al^{3+} + Li^{1+}$ or $Al^{3+} + 2Li^{1+}$
Li-bearing tourmaline	O^{2-}	$3Al^{3+}$ and $Al^{3+} + 2Li^{1+}$

Note: R is a generalized divalent cation (R^{2+}) or trivalent cation (R^{3+}).

Table 1. Relative site abundances of cations and anions in tourmaline-supergroup minerals

Site	Relative abundance of ions with different valence states	Common cations and anions at each site in order of relative abundance
X	$R^{1+} > R^{2+} > \square$ (vacancy)	R^{1+}: **Na^{1+}**>>K^{1+}
		R^{2+}: **Ca^{2+}**
Y	$R^{2+} > R^{3+} > R^{1+} > R^{4+}$	R^{2+}: **Fe^{2+}** ~ **Mg^{2+}** > **Mn^{2+}** >>> Zn^{2+} , Ni^{2+} , Co^{2+}, Cu^{2+}
		R^{3+}: **Al^{3+}** >> **Fe^{3+}** > Cr^{3+} >> V^{3+}
		R^{1+}: **Li^{1+}**
		R^{4+}: **Ti^{4+}**
Z	$R^{3+} >> R^{2+}$	R^{3+}: **Al^{3+}** >> **Fe^{3+}** > Cr^{3+} > V^{3+}
		R^{2+}: **Mg^{2+}** > Fe^{2+}
T	$R^{4+} >> R^{3+}$	R^{4+}: **Si^{4+}**
		R^{3+}: **Al^{3+}** > B^{3+}
B	R^{3+}	R^{3+}: **B^{3+}**
V	$S^{1-} >> S^{2-}$	S^{1-}: **OH^{1-}**
		S^{2-}: **O^{2-}**
W	$S^{1-} \sim S^{2-}$	S^{1-}: **OH^{1-} ~ F^{1-}**
		S^{2-}: **O^{2-}**

Note: The bolded cations and anions represent the most common ions at these sites.

ordered form. Tourmaline species that contain OH^{1-} and F^{1-} at the W site are also presented in their ordered form.

Definitions and classification principles

There are several terms associated with mineral classification schemes that should be elucidated. *Mineral species (minerals)* are defined on the basis of their unique chemical and crystallographic properties (Nickel and Grice 1998). In most cases tourmaline-supergroup minerals are isostructural (space group *R*3*m*), with the exceptions previously noted. Consequently, the primary criterion for classification is such that most tourmaline species are defined in terms of chemical composition, with the dominance of a chemical constituent of the dominant valency state at a given crystallographic site being the primary criterion for classification. A "chemical constituent" designates a specific cation or anion, group of atoms with the same valency state, molecular group, or vacancies. This dominance criterion is a statement of the *dominant-constituent rule* (Hatert and Burke 2008). Tourmaline solid solutions involve both homovalent substitutions at a given site and heterovalent coupled substitutions over single or multiple sites. An extension of the dominant-constituent rule is the *dominant-valency rule* that states that in a relevant site, the dominant ion of the dominant valence state is considered for nomenclature (Hatert and Burke 2008). Additional complexity is encountered where heterovalent coupled substitutions occur on single or multiple sites such that end-members are produced in which two constituent ions occupy a single site: this is termed the *valency-imposed double-site occupancy* (Hatert and Burke 2008). For example, in the case of the chemical substitution that occurs from schorl to elbaite, there is a single-site coupled substitution that involves the incorporation of Li^{1+} and Al^{3+} in equal amounts for Fe^{2+} to produce an end-member with two cations at the Y site of elbaite, i.e., $^{Y}(Al_{1.5}Li_{1.5})$. In the case of two-site coupled substitution, dravite can be transformed to uvite by the substitution of Ca^{2+} for Na^{1+} at the X site, coupled with the substitution of Mg^{2+} for Al^{3+} at the Z site, resulting in multiple-cation occupancy of the Z site as $^{Z}(MgAl_5)$ for the uvite end-member.

An *end-member* is an algebraic and chemical construct[2] that is irreducible and is conformable with the crystal structure under consideration (Hawthorne 2002; see also Appendix 1 for more details). For example, the dravite end-member $[NaMg_3Al_6(Si_6O_{18})(BO_3)_3(OH)_3OH]$ is irreducible in that it cannot be expressed as a combination of other tourmaline end-members. In the case in which a tourmaline is determined to have *dominant* cation and anion occupancies of the crystallographic sites in accordance with this end-member, it is given the *root name* dravite and is, by implication, considered to be the dravite *mineral species*.

In determining the systematics of tourmaline-supergroup mineral species, the STN recommends the following general procedure be considered:

(1) In tourmaline-supergroup minerals that are dominated by S^{1-} anions (OH^{1-} and F^{1-}) in the W site, it is recommended that the OH^{1-} species be the reference *root composition* for that root name. As such, this OH^{1-} species becomes the root name without a "hydroxyl-" prefix e.g., dravite.

(2) For a tourmaline composition that has most of the chemical characteristics of a root composition, but is dominated by other cations or anions at one or more sites, the mineral species is designated by the root name *plus* the appropriate prefix modifiers. For example, a tourmaline with a composition that is generally consistent with dravite, but that contains F^{1-} as the most prevalent S^{1-} anion where S^{1-} anions are dominant over S^{2-} anions at the W site, the mineral species is termed fluor-dravite. To take advantage of search capabilities, it is recommended that any modifiers to tourmaline root names be separated by hyphens. Hyphens are considered important to clarify the components of the species name.

(3) If there are multiple prefix modifiers, the modifiers should be arranged in the order in which it occurs in the structural formula i.e., X-site modifier, Y-site modifier, Z-site modifier, T-site modifier, and then W-site modifier. This has the advantage of ordering the modifiers in a consistent and intuitive manner. For example, a composition that is generally consistent with dravite, but with K^{1+} being the most prevalent R^{1+} cation for R^{1+}-dominant X-site occupancy and F^{1-} being the most prevalent S^{1-} anion for S^{1-}-dominant W-site occupancy, the hypothetical mineral species would be termed "potassium-fluor-dravite."

(4) Consistent with the IMA-CNMNC and the International Union of Crystallography procedures, any deviation from the reference rhombohedral space group *R*3*m* symmetry is accommodated in the nomenclature by adding a suffix to the root name that indicates any atypical symmetry i.e., orthorhombic (-O), monoclinic (-M), or triclinic (-T) (Bailey 1977). For example, an elbaite exhibiting triclinic symmetry would be termed "elbaite-T."

The cationic and anionic occupancy of the X and W sites serve as particularly convenient and petrologically meaningful ways to define the primary tourmaline groups and a subset of general series of tourmaline species.

Primary tourmaline groups: X-site occupancy

Tourmaline can be classified into primary groups based on the dominant occupancy of the X site. Tourmalines have been described that contain dominant Na^{1+}, Ca^{2+}, $^{X}\square$, and, rarely, K^{1+}. However, because of the relatively rare occurrence of K-rich tourmalines, it is practical to combine the cations with like charges, Na^{1+} and K^{1+}, into an alkali group. This results in primary groups that are termed the alkali-, calcic-, and X-vacant-tourmaline groups. This general grouping makes petrologic sense because X-site occupancy generally reflects the paragenesis of the rock in which these tourmalines crystallize, analogous to similar general groupings in the amphibole- and pyroxene-supergroup minerals. The alkali-, calcic-, X-vacant ternary system for X-site occupancy can be plotted on the simple ternary diagram illustrated in Figure 1. Arithmetically, the primary X-site groups are defined as follows: *alkali* if $(Na^{1+}+K^{1+}) \geq Ca^{2+}$ and $(Na^{1+}+K^{1+}) \geq {}^{X}\square$; *calcic* if $Ca^{2+} > (Na^{1+}+K^{1+})$ and $Ca^{2+} > {}^{X}\square$; and *X-vacant* if $^{X}\square > (Na^{1+}+K^{1+})$ and $^{X}\square > Ca^{2+}$. The dominance of Na^{1+} or K^{1+} in alkali-group tourmaline is an example of the dominant-valency rule. In the uncommon case,

[2] End-members are important in a thermodynamic sense because the thermodynamic properties of end-members can be determined, regardless of whether they exist as stable minerals. Thermodynamic properties are essential for modeling the behavior of solid solutions in petrological and geochemical processes.

in which tourmaline is classified as an alkali-group tourmaline *and* K^{1+} dominates over Na^{1+}, it is considered a "potassium-" tourmaline. In this case, the root name should be prefixed by "potassium-" e.g., "potassium-povondraite." Arithmetically, to be considered a "potassium-"tourmaline the following conditions must be satisfied: $(Na^{1+}+K^{1+}) \geq Ca^{2+}$, $(Na^{1+}+K^{1+}) \geq {}^{X}\square$, *and* $K^{1+} > Na^{1+}$. If there are other cations with relatively large ion ionic radii that are found in significant amounts at the X site (e.g., Pb^{2+}), they should be included with the cations of the same charge to establish the dominance of the valency at the X site

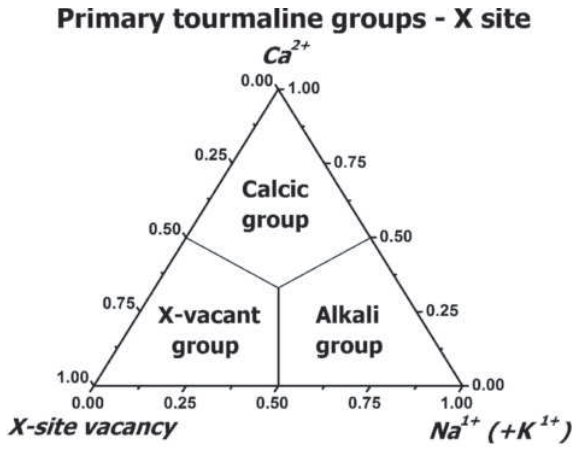

Figure 1. Ternary system for the primary tourmaline groups based on the dominant occupancy of the X site.

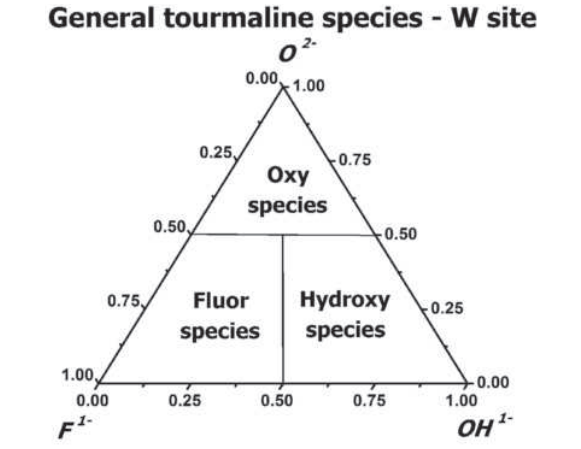

Figure 2. Ternary system for a general series of tourmaline species based on the anion occupancy of the W site.

in accordance with the dominant-valency rule. Consequently, X-site occupancy as it relates to tourmaline nomenclature can be extended as needed.

General series of tourmaline species: W-site occupancy

Three distinct anions (OH^{1-}, F^{1-}, and O^{2-}) can occur at the W site, and the occupancy of the W site forms the basis for a general series of tourmaline species: hydroxy-, fluor- and oxy-species (Fig. 2). These are defined as follows: *hydroxy* if $OH^{1-} + F^{1-} \geq O^{2-}$ *and* $OH^{1-} \geq F^{1-}$; *fluor* if $OH^{1-} + F^{1-} \geq O^{2-}$ *and* $F^{1-} > OH^{1-}$; and *oxy* if $O^{2-} > OH^{1-} + F^{1-}$. The appearance of the general series of tourmaline species based on W-site occupancy differs from the X-site grouping shown in Figure 1 because it involves two anions with a common 1^- charge (OH^{1-} and F^{1-}) and a single anion with a 2^- charge (O^{2-}). Consequently, for O^{2-} to be the dominant anion of the W site, there must be >50% O^{2-} (cf. Nickel 1992; Chopin 2006). Despite the difficulty of measuring H content in tourmaline, H must be considered in the tourmaline nomenclature because its content does vary, and it can result in oxy-tourmaline species. In the case of an oxy-species, a coupled substitution involving another site is required, and a new root name is typically warranted rather than placing a modifying prefix on the root name.

Specific tourmaline species

At the time of the revision of this paper, the IMA-CNMNC has recognized 18 tourmaline species with an additional species having a different structure (Appendix 2). Hawthorne and Henry (1999) and the STN re-examined the compositions of the holotype material of these species and, in some cases, redefined the end-member formulas and mineral species in accordance with guidelines suggested by Hawthorne and Henry (1999), Hawthorne (2002), and this paper (Appendix 2). In addition to the IMA-CNMNC-accepted tourmaline species, several varietal names based on the color of tourmaline in hand sample have been used in describing tourmaline, but these were not considered as part of the IMA-CNMNC classification scheme (see Appendix 3). Furthermore, there are a series of names that have been used for tourmaline that are obsolete or have been discredited (Appendix 4).

Tourmaline can be broken into several groups and subgroups that are useful for classification purposes. The primary tourmaline groups are based on occupancy of the X site, which serves as a convenient division into the alkali-tourmaline group, calcic-tourmaline group or the X-vacant-tourmaline group (Fig. 1). Because each of these groups involves a cation or vacancy with a different charge, coupled substitutions are required to compositionally shift among the groups (Tables 3–6). Within

Table 3. Significant tourmaline heterovalent coupled substitutions and associated exchange vectors

	Generalized coupled substitutions	Corresponding exchange vector	Resulting actions
(1)	${}^{X}R^{1+} + R^{2+} \leftrightarrow {}^{X}\square + R^{3+}$	$({}^{X}\square R^{3+})(R^{1+} R^{2+})_{-1}$	relates alkali-vacant groups
(2)	${}^{X}R^{1+} + R^{3+} \leftrightarrow {}^{X}Ca + R^{2+}$	$(CaR^{2+})(R^{1+} R^{3+})_{-1}$	relates alkali-calcic groups
(3)	$2\,{}^{Y}R^{2+} \leftrightarrow {}^{Y}Li^{1+} + {}^{Y}Al^{3+}$	$(Li\,Al)\,(2R^{2+})_{-1}$	relates incorporation of Li in all groups
(4)	$R^{2+} + OH^{1-} \leftrightarrow R^{3+} + O^{2-}$	$(R^{3+} O^{2-})(R^{2+} (OH^{1-}))_{-1}$	relates deprotonation in all groups
(5)	$0.5Li^{1+} + OH^{1-} \leftrightarrow 0.5\,{}^{Y}Al + O^{2-}$	$(Al_{0.5}O)(Li_{0.5}(OH))_{-1}$	relates deprotonation in Li species
(6)	$R^{2+} + {}^{T}Si^{4+} \leftrightarrow R^{3+} + {}^{T}R^{3+}$	$(R^{3+} R^{3+})(R^{2+} Si^{4+})_{-1}$	relates Tschermak-like tetrahedral-octahedral substitution in all groups

Note: R represents generalized cations such that ${}^{X}R^{1+} = Na^{1+}, K^{1+}$; $R^{2+} = Mg^{2+}, Fe^{2+}, Mn^{2+}, Co^{2+}, Ni^{2+}, Zn^{2+}$; $R^{3+} = Al^{3+}, Fe^{3+}, Cr^{3+}, V^{3+}, B^{3+}$ (T site); and no site designation reflects possibilities involving multiple sites.

TABLE 4. Generalized structural formula types for recognized or prospective tourmaline species listed by X-site alkali-group tourmaline

General formula	(X)	(Y_3)	(Z_6)	T_6O_{18}	$(BO_3)_3$	V_3	W
Alkali-subgroup 1	R^{1+}	R_3^{2+}	R_6^{3+}	$R_6^{4+}O_{18}$	$(BO_3)_3$	S_3^{1-}	S^{1-}
Dravite*	Na	Mg_3	Al_6	Si_6O_{18}	$(BO_3)_3$	$(OH)_3$	(OH)
Schorl*	Na	Fe_3^{2+}	Al_6	Si_6O_{18}	$(BO_3)_3$	$(OH)_3$	(OH)
Chromium-dravite*	Na	Mg_3	Cr_6	Si_6O_{18}	$(BO_3)_3$	$(OH)_3$	(OH)
Vanadium-dravite*	Na	Mg_3	V_6	Si_6O_{18}	$(BO_3)_3$	$(OH)_3$	(OH)
Fluor-dravite*	Na	Mg_3	Al_6	Si_6O_{18}	$(BO_3)_3$	$(OH)_3$	F
Fluor-schorl*	Na	Fe_3^{2+}	Al_6	Si_6O_{18}	$(BO_3)_3$	$(OH)_3$	F
"Potassium-dravite"†	K	Mg_3	Al_6	Si_6O_{18}	$(BO_3)_3$	$(OH)_3$	(OH)
"Tsilaisite"‡	Na	Mn_3^{2+}	Al_6	Si_6O_{18}	$(BO_3)_3$	$(OH)_3$	(OH)
Alkali-subgroup 2	R^{1+}	$R_{1.5}^{1+}R_{1.5}^{3+}$	R_6^{3+}	$R_6^{4+}O_{18}$	$(BO_3)_3$	S_3^{1-}	S^{1-}
Elbaite*	Na	$Li_{1.5}^{1+}Al_{1.5}^{3+}$	Al_6	Si_6O_{18}	$(BO_3)_3$	$(OH)_3$	(OH)
"Fluor-elbaite"†	Na	$Li_{1.5}^{1+}Al_{1.5}^{3+}$	Al_6	Si_6O_{18}	$(BO_3)_3$	$(OH)_3$	F
Alkali-subgroup 3	R^{1+}	R_3^{3+}	$R_4^{3+}R_2^{2+}$§	$R_6^{4+}O_{18}$	$(BO_3)_3$	S_3^{1-}	S^{2-}
Povondraite*	Na	Fe_3^{3+}	$Fe_4^{3+}Mg_2$	Si_6O_{18}	$(BO_3)_3$	$(OH)_3$	O
Chromo-alumino-povondraite*	Na	Cr_3	Al_4Mg_2	Si_6O_{18}	$(BO_3)_3$	$(OH)_3$	O
"Oxy-dravite"†‖	Na	Al_3	Al_4Mg_2	Si_6O_{18}	$(BO_3)_3$	$(OH)_3$	O
"Oxy-schorl"†‖	Na	Al_3	$Al_4Fe_2^{2+}$	Si_6O_{18}	$(BO_3)_3$	$(OH)_3$	O
"Na-Cr-O root name"†	Na	Cr_3	Cr_4Mg_2	Si_6O_{18}	$(BO_3)_3$	$(OH)_3$	O
"Potassium-povondraite"†	K	Fe_3^{3+}	$Fe_4^{3+}Mg_2$	Si_6O_{18}	$(BO_3)_3$	$(OH)_3$	O
Alkali-subgroup 4	R^{1+}	$R_1^{1+}R_2^{3+}$	R_6^{3+}	$R_6^{4+}O_{18}$	$(BO_3)_3$	S_3^{1-}	S^{2-}
"Na-Li-O root name "†	Na	Li_1Al_2	Al_6	Si_6O_{18}	$(BO_3)_3$	$(OH)_3$	O
Alkali-subgroup 5	R^{1+}	R_3^{3+}	R_6^{3+}	$R_6^{3+}O_{18}$	$(BO_3)_3$	S_3^{2-}	S^{1-}
Fluor-buergerite*	Na	Fe_3^{3+}	Al_6	Si_6O_{18}	$(BO_3)_3$	$(O)_3$	F
Olenite*	Na	Al_3	Al_6	Si_6O_{18}	$(BO_3)_3$	$(O)_3$	(OH)
"Buergerite"‡	Na	Fe_3^{3+}	Al_6	Si_6O_{18}	$(BO_3)_3$	$(O)_3$	(OH)
"Fluor-olenite"‡	Na	Al_3	Al_6	Si_6O_{18}	$(BO_3)_3$	$(O)_3$	F
Alkali-subgroup 6	R^{1+}	R_3^{3+}	R_6^{3+}	$R_3^{3+}R_3^{4+}O_{18}$	$(BO_3)_3$	S_3^{1-}	S^{1-}
"Na-Al-Al-Al root name"‡	Na	Al_3	Al_6	$Al_3Si_3O_{18}$	$(BO_3)_3$	$(OH)_3$	(OH)
"Na-Al-Al-B root name"‡	Na	Al_3	Al_6	$B_3Si_3O_{18}$	$(BO_3)_3$	$(OH)_3$	(OH)
"Fluor-Na-Al-Al-Al root name"‡	Na	Al_3	Al_6	$Al_3Si_3O_{18}$	$(BO_3)_3$	$(OH)_3$	F
"Fluor-Na-Al-Al-B root name"‡	Na	Al_3	Al_6	$B_3Si_3O_{18}$	$(BO_3)_3$	$(OH)_3$	F

* Tourmaline species currently recognized by the IMA-CNMNC in the original or modified form (Appendix 2).
† Tourmaline species with compositions found in natural settings, but, as of the time of manuscript revision, not currently recognized by the IMA-CNMNC. Examples of reported compositions consistent with prospective tourmaline species include: "potassium-dravite" (Ota et al. 2008), "fluor-elbaite" (Lussier et al. 2009), "oxy-dravite" (Žáček et al. 2000), "oxy-schorl" (Novák et al. 2004), "Na-Cr-O root name" (Bosi and Lucchesi 2007) and "potassium-povondraite" (Grice et al. 1993), and "Na-Li-O root name" (Quensel and Gabrielson 1939).
‡ Tourmaline species produced experimentally (e.g., Schreyer et al. 2000; Marler et al. 2002) or found in natural settings in which the tourmalines show a tendency for development of these compositions, and not recognized by the IMA CNMNC.
§ For the oxy-tourmaline species the formula is given as the disordered form, consistent with the Y- and Z-site occupancy demonstrated for povondraite, and implied by the short-range disordering effects of O^{2-} at the W site. However, for the verification of each prospective oxy-tourmaline species the disordering on the Z site should be demonstrated for the proper determination of the structural formula.
‖ Although a new root name is appropriate, because the species names "oxy-dravite" and "oxy-schorl" have been used relatively commonly in the literature (e.g., Žáček al. 2000; Novák et al. 2004; Henry et al. 2008), it is recommended that these names be formally accepted as the species names for these end-members.

TABLE 5. Generalized structural formula types for recognized or prospective tourmaline species listed by X-site calcic-group tourmaline

General formula	(X)	(Y_3)	(Z_6)	T_6O_{18}	$(BO_3)_3$	V_3	W
Calcic-subgroup 1	Ca^{2+}	R_3^{2+}	$R^{2+}R_5^{3+}$	$R_6^{4+}O_{18}$	$(BO_3)_3$	S_3^{1-}	S^{1-}
Fluor-uvite*	Ca	Mg_3	$MgAl_5$	Si_6O_{18}	$(BO_3)_3$	$(OH)_3$	F
Feruvite*	Ca	Fe_3^{2+}	$MgAl_5$	Si_6O_{18}	$(BO_3)_3$	$(OH)_3$	(OH)
Uvite*	Ca	Mg_3	$MgAl_5$	Si_6O_{18}	$(BO_3)_3$	$(OH)_3$	(OH)
"Fluor-feruvite"†	Ca	Fe_3^{2+}	$MgAl_5$	Si_6O_{18}	$(BO_3)_3$	$(OH)_3$	F
Calcic-subgroup 2	Ca^{2+}	$R_2^{1+}R_2^{3+}$	R_6^{3+}	$R_6^{4+}O_{18}$	$(BO_3)_3$	S_3^{1-}	S^{1-}
Fluor-liddicoatite*	Ca	$Li_2^{1+}Al^{3+}$	Al_6	Si_6O_{18}	$(BO_3)_3$	$(OH)_3$	F
"Liddicoatite"†	Ca	$Li_2^{1+}Al^{3+}$	Al_6	Si_6O_{18}	$(BO_3)_3$	$(OH)_3$	(OH)
Calcic-subgroup 3	Ca^{2+}	R_3^{2+}	R_6^{3+}	$R_6^{4+}O_{18}$	$(BO_3)_3$	S_3^{1-}	S^{2-}
"Ca-Mg-O root name"‡	Ca	Mg_3	Al_6	Si_6O_{18}	$(BO_3)_3$	$(OH)_3$	O
"Ca-Fe-O root name"‡	Ca	Fe_3^{2+}	Al_6	Si_6O_{18}	$(BO_3)_3$	$(OH)_3$	O
Calcic-subgroup 4	Ca^{2+}	$R_{1.5}^{1+}R_{1.5}^{3+}$	R_6^{3+}	$R_6^{4+}O_{18}$	$(BO_3)_3$	S_3^{1-}	S^{2-}
"Ca-Li-O root name "‡	Ca	$Li_{1.5}Al_{1.5}$	Al_6	Si_6O_{18}	$(BO_3)_3$	$(OH)_3$	O

* Tourmaline species currently recognized by the IMA-CNMNC in the original or modified form (Appendix 2).
† Tourmaline species with compositions found in natural settings, but, as of the time of manuscript revision, not currently recognized by the IMA-CNMNC. Examples of reported compositions consistent with prospective tourmaline species include: "fluor-feruvite" (Breaks et al. 2008) and "liddicoatite" (Breaks et al. 2008).
‡ Tourmaline species produced experimentally or found in natural settings in which the tourmalines show a tendency for development of these compositions, and not recognized by the IMA-CNMNC.

each group there is a fundamental subgroup, subgroup 1, from which additional subgroups can be generated. Incorporation of Li^{1+} via coupled substitution (3) of Table 3 can result in additional Li-bearing subgroups, which will warrant new root names (e.g., elbaite in alkali-subgroup 2 of Table 4). Likewise, the coupled substitution (4) of Table 3 can result in deprotonated tourmaline species (e.g., alkali-subgroups 3 and 4 of Table 4), and these species should, by analogy, have distinct root names. Coupled substitution (6) of Table 3 could yield species with trivalent cations in up to 50% of the T site. Although such species have not been reported from natural settings, experimental syntheses (e.g., Schreyer et al. 2000; Marler et al. 2002) or compositional tendencies in natural tourmaline warrant their inclusion as prospective species. Within a given tourmaline subgroup there can be several homovalent substitutions that result in extensive or complete solid solution, but it does not change the fundamental character of a tourmaline subgroup (e.g., Fe^{2+} for Mg^{2+} substitution that relates schorl and dravite in alkali-subgroup 1 tourmaline). Within each group, subgroup 1 generally has the most species. For instance, alkali-subgroup 1 contains 8 possible species, mostly variants with dravite or schorl root names. Table 7 presents several additional considerations associated with various substitutions in the tourmaline-supergroup minerals. This approach of identifying subgroups based on operation of general heterovalent coupled substitutions is similar to that used for the epidote-group nomenclature (Armbruster et al. 2006).

The hypothetical tourmaline species in Tables 4–6 (in quotation marks) are considered to be species likely to be found naturally with many published tourmaline analyses being consistent with these species (see footnotes of Tables 4–6). The hydroxy- and fluor-species are written in the ordered form at the Y and Z sites. The oxy-species are written in the disordered form, with the understanding that disorder over the Y and Z sites is likely (e.g., Hawthorne 1996). Additional end-members that have other cations dominant at one or more sites are likely, and these can be added as new tourmaline species when/if they are discovered and characterized. This proposed scheme is therefore, readily expandable. Whenever possible or reasonable, new tourmaline species should be named using currently recognized root names with appropriate prefix modifiers concatenated to the existing root name. For example, the IMA-CNMNC-accepted Mg-equivalent of foitite is magnesio-foitite (Table 6). Tourmaline compositions generated through heterovalent coupled substitutions of existing root compositions will generally mandate the introduction of new root names. *All proposed mineral species must be submitted to the IMA-CNMNC and fulfill the requirements for new mineral*

TABLE 6. Generalized structural formula types for recognized or prospective tourmaline species listed by X-site vacant-group tourmaline

General formula	(X)	(Y_3)	(Z_6)	T_6O_{18}	$(BO_3)_3$	V_3	W
Vacant-subgroup 1	□	$R^{2+}_2 R^{3+}$	R^{3+}_6	$R^{4+}_6O_{18}$	$(BO_3)_3$	S^{1-}_3	S^{1-}
Foitite*	□	Fe^{2+}_2Al	Al_6	Si_6O_{18}	$(BO_3)_3$	$(OH)_3$	(OH)
Magnesio-foitite*	□	Mg_2Al	Al_6	Si_6O_{18}	$(BO_3)_3$	$(OH)_3$	(OH)
Vacant-subgroup 2	□	$R^{1+}_1 R^{3+}_2$	R^{3+}_6	$R^{4+}_6O_{18}$	$(BO_3)_3$	S^{1-}_3	S^{1-}
Rossmanite*	□	$Li^{1+}Al^{3+}_2$	Al_6	Si_6O_{18}	$(BO_3)_3$	$(OH)_3$	(OH)
Vacant-subgroup 3	□	$R^{2+}_1 R^{3+}_2$	R^{3+}_6	$R^{4+}_6O_{18}$	$(BO_3)_3$	S^{1-}_3	S^{2-}
"□-Mg-O root name"‡	□	$MgAl_2$	Al_6	Si_6O_{18}	$(BO_3)_3$	$(OH)_3$	O
"□-Fe-O root name"†	□	$Fe^{2+}Al_2$	Al_6	Si_6O_{18}	$(BO_3)_3$	$(OH)_3$	O
Vacant-subgroup 4	□	$R^{1+}_{0.5} R^{3+}_{2.5}$	R^{3+}_6	$R^{4+}_6O_{18}$	$(BO_3)_3$	S^{1-}_3	S^{2-}
"□-Li-O root name"†	□	$Li_{0.5}Al_{2.5}$	Al_6	Si_6O_{18}	$(BO_3)_3$	$(OH)_3$	O

* Tourmaline species currently recognized by the IMA-CNMNC in the original or modified form (Appendix 2).
† Tourmaline species with compositions found in natural settings, but, as of the time of manuscript revision, not currently recognized by the IMA-CNMNC. Examples of reported compositions generally consistent with prospective tourmaline species include: "□-Fe-O root name" (Medaris et al. 2003) and "□-Li-O root name" (Ertl et al. 2005).
‡ Tourmaline species produced experimentally or found in natural settings in which the tourmalines show a tendency for development of these compositions, and not recognized by the IMA-CNMNC.

TABLE 7. Additional considerations associated with homovalent and heterovalent substitutions in tourmaline-supergroup minerals

(a) The most common R^{1+} *homovalent substitution* in the **X-site** is $Na^{1+} \leftrightarrow K^{1+}$. The tourmaline is considered to be a member of the *alkali* group if $(Na^{1+}+K^{1+}) \geq Ca^{2+}$ and $(Na^{1+}+K^{1+}) \geq {}^{X}\square$. In the uncommon case in which tourmaline is classified as an alkali-group tourmaline and $K^{1+} > Na^{1+}$, it is considered a "potassium-tourmaline". The tourmaline is considered part of the calcic group if $Ca^{2+} > (Na^{1+}+K^{1+})$ and $Ca^{2+} > {}^{X}\square$. The tourmaline is considered part of the X-site vacancy group if ${}^{X}\square > (Na^{1+}+K^{1+})$ and ${}^{X}\square > Ca^{2+}$.

(b) R^{2+} *homovalent substitutions* involve a number of divalent cations such as Mg^{2+}, Fe^{2+}, Mn^{2+}, Co^{2+}, Ni^{2+}, and Zn^{2+}. For example, the most common substitution is probably $Mg^{2+} \leftrightarrow Fe^{2+}$. In this case the complicating factor is that Mg^{2+} and possibly Fe^{2+} are generally the primary $\mathbf{R^{2+}}$ cations that can be significantly accommodated on the **Z site** at concentrations up to 2 apfu, most commonly associated with disordering related to incorporation of O^{2-} on the W site. Within a divalent group of elements on a given site, the dominant $\mathbf{R^{2+}}$ cations lead to a different modifier/root names. For classification purposes the tourmaline formula should be cast in its ordered form.

(c) R^{3+} *homovalent substitutions* occur on both the Y and Z sites and include trivalent cations such as Al^{3+}, Fe^{3+}, Cr^{3+}, and V^{3+}. For example, a common substitution is $Fe^{3+} \leftrightarrow Al^{3+}$. The $\mathbf{R^{3+}}$ cations are most commonly found on the Z site, but the Y site and T site can contain up to 3 apfu $\mathbf{R^{3+}}$ cations. If there is O^{2-} on the W site, there is likely to be a disordering resulting in the displacement of the $\mathbf{R^{3+}}$ to the Y site with a concomitant substitution of Mg^{2+} on the Z site. For classification purposes the tourmaline formula should be cast in its ordered form.

(d) If there is **Li** in the tourmaline it is typically introduced via *heterovalent substitution* (3) ${}^{Y}2R^{2+} \leftrightarrow {}^{Y}Li^{1+} + {}^{Y}Al^{3+}$. Note that for each **Li** that is introduced there is 2 R^{2+} displaced. That means that plotting parameters in the ternary elbaite-schorl-dravite subsystem are 2Li-Fe^{2+}-Mg.

(e) The introduction of O^{2-} in the W or V site can take place via the *heterovalent-deprotonation substitution* (4) $R^{2+} + OH^{1-} \leftrightarrow R^{3+} + O^{2-}$. Note that for each O^{2-} there must be the introduction of an R^{3+} at the expense of R^{2+}.

(f) The introduction of R^{3+} (typically Al or B) into the tetrahedral site can take place via a Tschermak type of *heterovalent substitution* (5) $R^{2+} + {}^{T}Si^{4+} \leftrightarrow R^{3+} + {}^{T}R^{3+}$.

species prior to IMA-CNMNC approval as a new mineral species.

For classification, it is recommended that a tourmaline be named for the dominant species in the dominant subgroup, i.e., consistent with the dominant constituent of the dominant-valency state (the last adapted from Hatert and Burke 2008). For example, if there is a mixture of 40% elbaite, 35% schorl, and 25% dravite, the resulting subgroups would be 100% alkali-group tourmaline. However, within this group 60% will be alkali-subgroup 1 tourmaline species and 40% alkali-subgroup 2 species. Alkali-subgroup 1 is the dominant subgroup and schorl is the dominant species within this dominant subgroup such that the tourmaline should be considered a schorl. In this case, these relations for this ternary subsystem can be graphically illustrated (Fig. 3). The addition of other cations beyond the three shown graphically will complicate the application of these subsystem diagrams, but the grouping of common valency components can extend the generality of this approach and allow determination of the proper tourmaline species.

For identification of the wider range of possible natural and synthetic tourmaline species there are general procedures that should be followed. After the primary X-site group is established, the appropriate subgroup should be determined within each of the primary groups. This can be done graphically or by considering the numerical thresholds that serve to separate the subgroups. Identification of the appropriate subgroup 1–4 within each of the primary X-site group tourmalines can be established with a series of diagrams that use the X-site occupancy and $^{YZ}R^{2+}/(^{YZ}R^{2+} + 2Li^{1+})$ ratio as the primary discriminating factor, with the W-site occupancy as a further discriminator, which will further refine the species within the subgroup (Fig. 4). An alternative diagram of $^{YZ}R^{2+}/(^{YZ}R^{2+} + 2Li^{1+})$ vs. $^{W}O^{2-}/(^{W}O^{2-} + {}^{W}OH^{1-} + F^{1-})$ results in a comparable discrimination diagram (Fig. 5). Significant variability of T-site and V-site occupancy can result in other relatively uncommon tourmaline species or prospective species. For tourmalines in which the V site contains more than 50% O^{2-}, tourmaline in the alkali group will fall in alkali subgroup 5 and

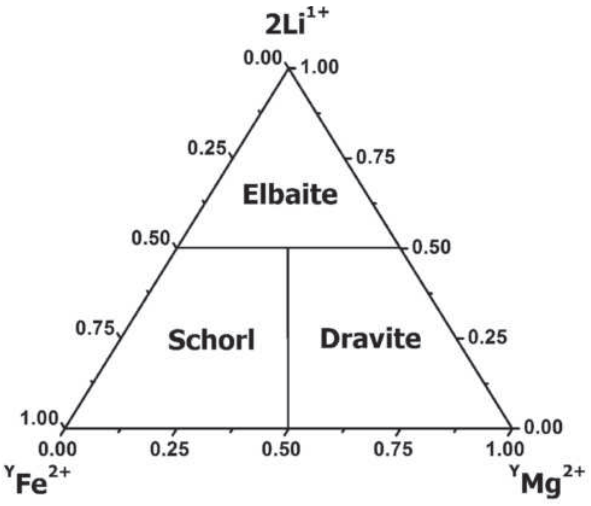

Figure 3. Ternary dravite-schorl-elbaite subsystem. Note that dravite and schorl are species within alkali-subgroup 1 and elbaite is a species within alkali-subgroup 2.

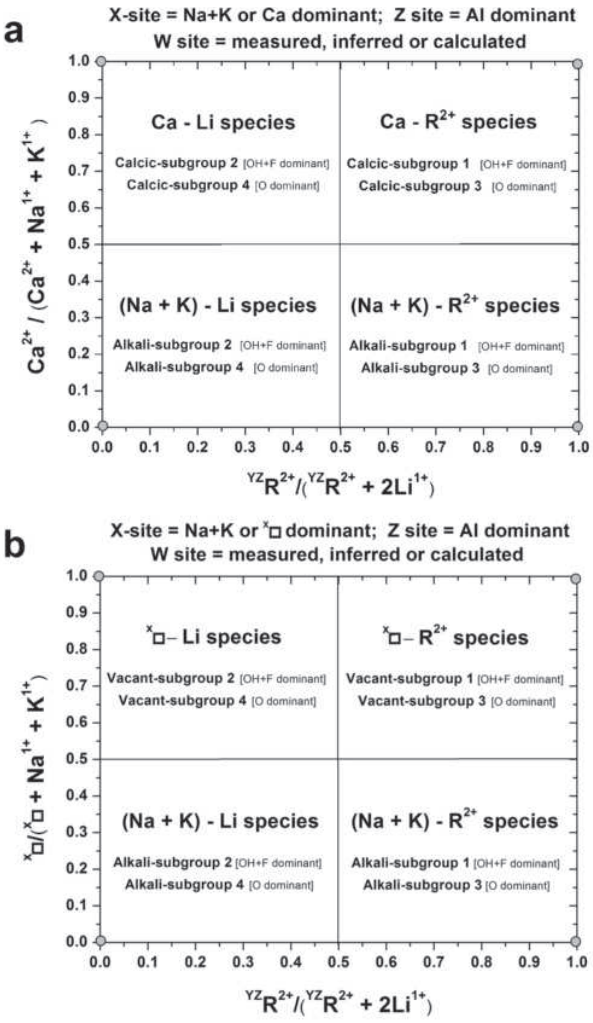

Figure 4. Diagrams useful for establishing the appropriate tourmaline subgroups within the alkali, calcic, and vacant groups. (**a**) Determination of subgroups 1–4 for alkali- and calcic-group tourmalines use parameters $^{YZ}R^{2+}/(^{YZ}R^{2+} + 2Li^{1+})$ vs. $Ca^{2+}/(Ca^{2+} + Na^{1+} + K^{1+})$ together with the dominant valency anion(s) in the W site i.e., $(OH^{1-} + F^{1-})$ vs. O^{2-}. $^{YZ}R^{2+}$ represents the total number of divalent cations in the Y and Z site. (**b**) Determination of subgroups 1–4 for alkali- and X-vacant-group tourmalines use parameters $^{YZ}R^{2+}/(^{YZ}R^{2+} + 2Li^{1+})$ vs. $^{X}\square/(^{X}\square + Na^{1+} + K^{1+})$ together with the dominant valency anion(s) in the W site i.e., $(OH^{1-} + F^{1-})$ vs. O^{2-}.

species such as fluor-buergerite and olenite can be recognized. In the alkali-group tourmalines, up to 3 apfu $(Al^{3+} + B^{3+})$ can substitute for Si assuming Y and Z are fully occupied by trivalent cations and W and V sites, by monovalent cations. Thus, the criterion for distinguishing alkali subgroup 6 is $Si^{4+} < 4.5$ apfu. In this case, the dominant tetrahedral trivalent cation (Al^{3+} or B^{3+}) becomes the basis for discriminating the species (Table 4). Once the subgroup is determined, the appropriate species name is given as the dominant species within that subgroup (Tables 4–6). Uncertainties arise when the tourmalines are incompletely analyzed and procedures for dealing with this possibility are addressed in the discussion below.

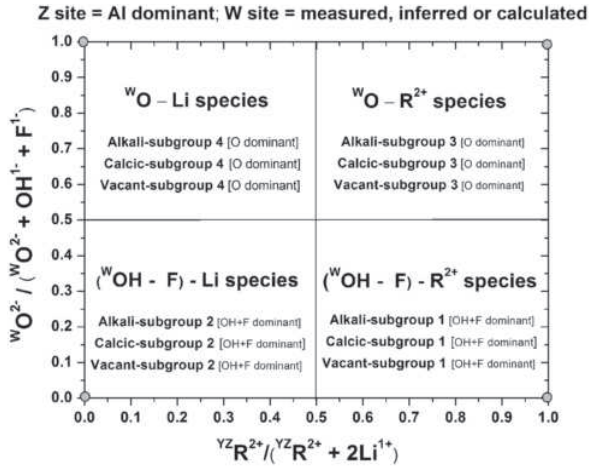

FIGURE 5. Alternative diagram useful for establishing the appropriate tourmaline subgroups within the alkali-, calcic- and vacant groups. The determination of subgroups 1–4 for alkali-, calcic- and vacant-group tourmalines use parameters $^{YZ}R^{2+}/(^{YZ}R^{2+} + 2Li^{1+})$ vs. $^{W}O^{2-}/(^{W}O^{2-} + OH^{1-} + F^{1-})$ together with the dominant cation in the X-site and dominant valency anion(s) in the W site, i.e., $(OH^{1-} + F^{1-})$ vs. O^{2-}.

Additional adjectival modifiers

Although not required, tourmaline species can be further modified with various adjectives that precede the species names (Tables 4–6). In the past, the IMA-CNMNC recommended use of the "Schaller modifiers" in which the valency of the substituent ion is indicated by the suffix "-oan" (for the lower valency cation) and "-ian" (for the higher valency cation). However, this scheme has several shortcomings that have prompted the approval of alternative chemical-element adjectival modifiers in place of the Schaller-type modifiers (Bayliss et al. 2005). In the most general case, it is recommended that adjectival modifier such as "-rich" or "-bearing" be used together with the specific element(s) and, where known, an indication of the oxidation state of the cation and/or the site it occupies, e.g., "Fe^{2+}-rich," "K-bearing," or "^{T}Al-rich." The chemical-element adjectival modifiers are not part of the name of the tourmaline species, and, consequently, authors are free to use chemical-element modifiers that are chemically correct and meet the needs of the author in expressing significant chemical information about the mineral species (Bayliss et al. 2005). However, it is recommended that the authors define the magnitude of the compositional parameters implied by these adjectival modifier terms. Multiple modifiers are possible, and the order of the modifiers should be such that the modifier with the greatest percentage of site occupancy is next to the mineral-species name, the modifier with the second most percentage preceding that one, etc. For example, a hypothetical tourmaline solid solution with 60% dravite-schorl, 40% uvite-feruvite and 2/1 ratio of Mg-Fe^{2+} at the Y site, has a structural formula of $(Na_{0.6}Ca_{0.4})(Mg_2Fe^{2+})(Mg_{0.4}Al_{5.6})(Si_6O_{18})(BO_3)_3(OH)_3(OH)$ and the appropriate name could be expressed as Fe^{2+}-,Ca-rich dravite i.e., reflecting 33% Fe^{2+} at the Y site and 40% Ca at the X site.

SITE ALLOCATION OF CATIONS AND ANIONS

Hawthorne (1996) notes that chemical analyses of tourmaline merely establish which elements are present, but do not determine where they are located in the structure. Structural refinement and site assignment based on crystallographic evidence is required for accurate site allocation. Furthermore, tourmaline site occupancies can be modeled with appropriate optimization procedures (e.g., Wright et al. 2000). In the absence of site assignments directly established by crystal structure refinements, it is possible to make some "reasonable" assumptions concerning site assignments of specific cations and anions (Table 1). With this basic information, it is recommended that cations and anions in tourmaline be allocated with the following procedure:

(1) Based on the type of analytical techniques and data generated, the most appropriate normalization scheme is used and any significant unanalyzed cations or anions are calculated whenever possible (see procedures in Appendix 5).

(2) Only B^{3+} is allocated to the B site. With compelling chemical, crystallographic, or spectroscopic evidence, excess B^{3+} ($B^{3+} > 3.0$ apfu) may be assumed to be in the T site. Compelling evidence includes NMR spectra indicating tetrahedral B^{3+}, structural refinements with tetrahedral bond length determinations and well-constrained analytical evidence that demonstrate $B^{3+} > 3.0$ apfu (e.g., Tagg et al. 1999; Hughes et al. 2000; Schreyer et al. 2002; Ertl et al. 2006a; Lussier et al. 2009).

(3) Na^{1+}, Ca^{2+}, and K^{1+} are assigned to the X site with any site deficiency assumed to represent X-site vacancy ($^{X}\square$). Additional large cations, such as Pb^{2+}, are likely located in the X site and should be assigned to that site.

(4) Si^{4+} is assumed to be exclusively located in the T site with any deficiency made up by Al^{3+} (MacDonald and Hawthorne 1995). If there is compelling chemical, crystallographic, or spectroscopic evidence for tetrahedral B^{3+}, this tetrahedral B^{3+} should be assigned to the T site prior to the assignment of the tetrahedral Al^{3+} (e.g., Lussier et al. 2009).

(5) The relative distribution of anions in the V and W sites is reasonably well established. F^{1-} is exclusively contained in the W site and O^{2-} tends to be preferentially contained in this site (Grice and Ercit 1993). Consequently, it is appropriate that all F^{1-} be assigned to the W site, and then O^{2-}. Any excess O^{2-} is assigned to the V site. To date, evidence from bond angle distortion of the ZO_6 octahedron and Y-O distances and bond-valence sums at the V site indicate that most of the tourmaline species (except buergerite and some olenitic tourmalines) have ~ $3(OH^{1-})$ at the V site (Ertl et al. 2002; Cempírek et al. 2006; Bosi and Lucchesi 2007).

(6) The Y and Z site assignments can be more ambiguous. The least problematic assignment is the exclusive allocation of Li^{1+}, Mn^{2+}, Zn^{2+}, Ni^{2+}, Co^{2+}, Cu^{2+}, and Ti^{4+} to the Y site. However, the smaller cation allocation between the Y and Z sites can be more uncertain. Based on crystallographic and mineral chemical information, it is considered that, with the presence of O^{2-} at the W site, Mg^{2+} and possibly Fe^{2+} may be disordered into the Z site and trivalent cations (especially Al^{3+} and Fe^{3+}) may be disordered into the Y site (Henry and Dutrow 1990, 2001; Hawthorne et al. 1993; Taylor et al. 1995; Ertl et al. 2003a; Bosi et al. 2004). Consequently, actual tourmaline structures can exhibit a significant amount of disordering.

For the purposes of classification of tourmaline species only, the ordered form of the tourmaline is assumed for all tourmaline species including the oxy-tourmaline. Consequently, the proce-

dure that is recommended for classification involves allocation of the small cations among the Z and Y sites as follows: Initially assign the most abundant R^{3+} cations to the Z site (not including any Al^{3+} and B^{3+} assigned to the tetrahedral site). Next, the remainder of the R^{3+} cations should be assigned in accordance with their abundance. If there is an excess of R^{3+} cations on the Z site, the excess R^{3+} cations go into the Y site. If there is a deficiency in the Z site after assigning all of the R^{3+} to that site (i.e., <6.0 cations), assign Mg^{2+} and then Fe^{2+} to the Z site up to 2 apfu (Bosi and Lucchesi 2007).

Tourmaline classification procedure: A hierarchical approach

Tourmaline investigations generally have varying levels of information available. The tourmaline information may range from complete analytical and crystal structural data to incomplete chemical data. However, it is important that a hierarchical classification procedure be used to accommodate the levels of information that are accessible.

Level 1—complete analytical and structural data

This level considers those tourmalines in which all elements are measured, including the oxidation states of transition elements, and the specific cation and anion site occupancies are established by crystal-structure refinement. Note that an ordered structural formula is assumed for classification purposes only, and proper site occupancies should be included in the ultimate tourmaline structural formula, whenever possible (e.g., Ertl et al. 2003a; Bosi and Lucchesi 2004). *This level of complete characterization of tourmaline is the optimal situation, but one which is currently relatively uncommon.*

Level 2—complete analytical data

This level implies direct knowledge of all elements (light elements and oxidation states of transition elements), but generally with assumed site assignments. Because an ordered structural formula is assumed, the site allocation procedure in the previous section can be used and is appropriate for classification purposes.

Recommended classification procedure for tourmaline with Level 1 and Level 2 data. With complete analytical data, the following procedure for systematically naming tourmaline species is suggested:

(1) Cast the structural formula in an ordered form consistent with the site allocation procedures given above.

(2) Determine the dominant X-site cation or vacancy to establish the primary tourmaline group (Fig. 1).

(3) Establish the dominant anion (OH^{1-}, F^{1-}, or O^{2-}) at the W site (Fig. 2).

(4) Ascertain the dominant anion (OH^{1-} or O^{2-}) at the V site. The current state of knowledge is that most tourmalines are dominated by OH^{1-} at the V site. The exceptions are buergerite and some olenitic tourmalines (Ertl et al. 2005; Cempírek et al. 2006; Bosi and Lucchesi 2007).

(5) Determine whether $Si^{4+} < 4.5$ apfu with the remainder of the tetrahedral site being occupied by $^{T}Al^{3+}$ and $^{T}B^{3+}$. Although, natural tourmalines with these characteristics have not been identified, tourmalines with these characterizations have been synthesized (Schreyer et al. 2000; Marler et al. 2002).

(6) Establish the dominant Z-site cation (Al^{3+}, Cr^{3+}, Fe^{3+}, or V^{3+}). This can be done simply by inspection or calculation, or can be illustrated graphically. For example, in tourmaline with low amounts of Fe^{3+} at the Z site of the ordered formula, the Al-V-Cr ternary can be used to graphically display the Z-site dominant cation (Fig. 6). The most common Z-site dominant cation is Al^{3+}, and a procedure for graphically classifying 24 possible ^{Z}Al-dominant tourmaline species is given in Figures 7 to 9. There are only a few Cr^{3+}-, Fe^{3+}-, V^{3+}- end-members that have been described at this time (e.g., chromium-dravite, povondraite, and vanadium-dravite) so comparable diagrams were not generated for these chemical systems. The Fe^{3+}-dominant end-member povondraite is commonly in solid solution with the "oxy-dravite" and dravite and the distinction between these species can be evaluated by examining the dominant $^{YZ}R^{3+}$ cation i.e., Fe^{3+} or Al^{3+} (Henry et al. 1999, 2008; Žáček et al. 2000).

(7) Determine the Y-site cation occupancy, recalling that an ordered form of the structural formula is used for classification purposes only. The dominant subgroup (subgroup1–4 of each of the three groups) can be established graphically from Figures 4 and 5.

(8) Once the dominant subgroup is determined, the dominant species in that subgroup defines the species name. In many instances, this can be done simply by comparing the structural formula with the possible species found within the appropriate subgroup (Tables 4–6). If tourmaline compositions fall within the appropriate subsystems, the species can also be generally established through the use of compositional diagrams such as Figures 7–9. A more inclusive approach is to calculate the dominant cation or anion of the dominant valency on given sites to directly establish subgroup and species. An Excel spreadsheet program (TourmalineSpecies-Henry1-1) is available[3] for these calculations and species determinations.

[3] Deposit item AM-11-036, Excel spreadsheet program. Deposit items are available two ways: For a paper copy contact the Business Office of the Mineralogical Society of America (see inside front cover) for price information. Online, visit the MSA web site at http://www.minsocam.org, go to the *American Mineralogist* Contents, find the table of contents for the specific volume/issue wanted, and then click on the deposit link there.

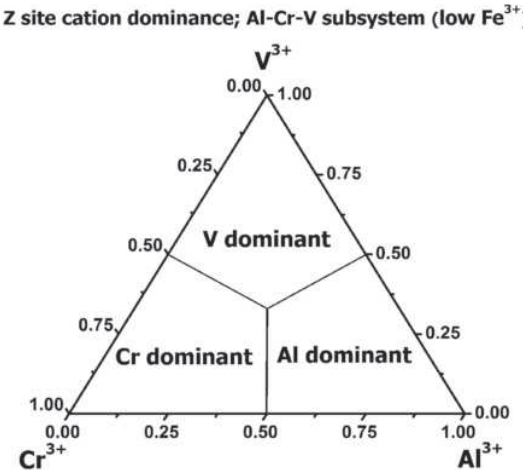

Figure 6. Ternary diagram for the Al-V-Cr subsystem of the Al-Fe-V-Cr quaternary system used for illustrating the dominant occupancy of the Z site for tourmaline, assuming minor Fe^{3+} on the Z site.

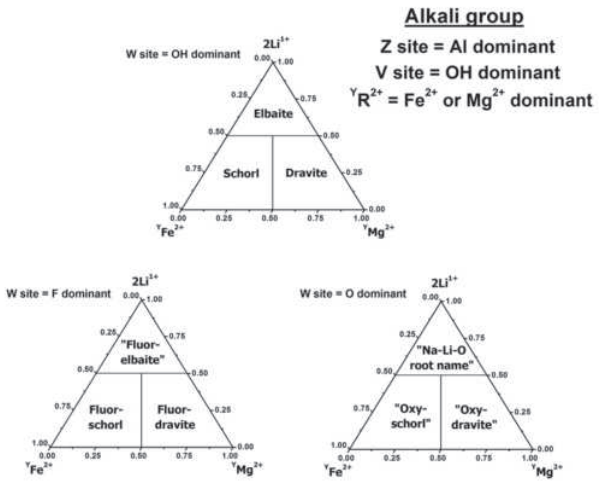

Figure 7. Ternary diagrams useful for plotting and classifying alkali-group tourmaline species with Al^{3+} dominance at the Z site and OH^{1-} dominance at the V site. The three ternary subsystems represent dominance of OH^{1-}, F^{1-}, or O^{2-} at the W site, respectively. Determination of the species is made by plotting Y-site cations on the appropriate ternary. The Y site occupancy is determined by an ordered structural formula. Significant deviation from this chemical subsystem will result in greater uncertainty of species designation.

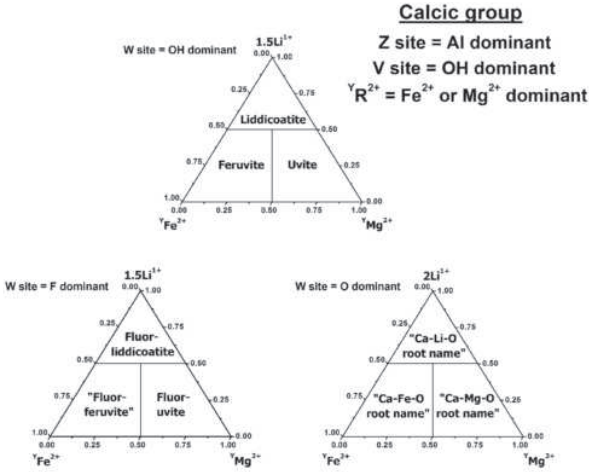

Figure 8. Ternary diagrams useful for plotting and classifying calcic-group tourmaline species with Al^{3+} dominance at the Z site and OH^{1-} dominance at the V site. The three ternary subsystems represent dominance of OH^{1-}, F^{1-}, or O^{2-} at the W site. Determination of the species is made by plotting Y-site cations on the appropriate ternary. The Y site occupancy is determined by an ordered structural formula. Significant deviation from this chemical subsystem will result in greater uncertainty of species designation.

In addition, a table of representative tourmaline analyses with diagnostic parameters for identification of tourmaline species is given in Appendix 6.

Level 3—Partial tourmaline compositional data without direct measurement of B, H, Li, and the oxidation states of transition elements

This is the most common situation, typical of tourmalines analyzed only by the electron microprobe. The procedures outlined in Appendix 5 allow estimation of some of the unmeasured cations and anions found in tourmaline. However, there can be considerable uncertainty associated with these procedures. As noted earlier, an ordered structural formula is assumed and the cations allocated accordingly.

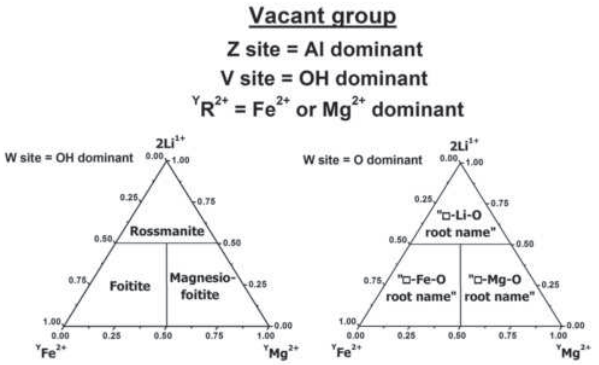

Figure 9. Ternary diagrams useful for plotting and classifying vacant-group tourmaline species with Al^{3+} dominance at the Z site and OH^{1-} dominance at the V site. The two ternary subsystems represent dominance of OH^{1-} or O^{2-} at the W site. F^{1-} is likely not a dominant anion at the W site. Determination of the species is made by plotting Y-site cations on the appropriate ternary. The Y-site occupancy is determined by an ordered structural formula. Significant deviation from this chemical subsystem will result in greater uncertainty of species designation.

Recommended classification procedure for tourmaline with Level 3 data. With the appropriate analytical data, estimation of unanalyzed elements and assumed site occupancies, the following procedure for systematically naming tourmaline species is suggested:

(1) Cast the structural formula in an ordered form consistent with the site allocation procedures outlined above.

(2) Determine the dominant X-site cation or vacancy to establish the principal tourmaline subgroup (Fig. 1). This data are readily accessible from a good-quality electron microprobe analysis.

(3) Establish the dominant anion (OH^{1-}, F^{1-}, or O^{2-}) at the W site (Fig. 2). In the absence of direct measurement of H, the uncertainty associated with estimating H can be large, and the resultant $^{W}O^{2-}$ estimate inaccurate. In contrast, F^{1-} can be accurately measured with the electron microprobe if proper care is taken in the analytical procedure. If H is undetermined (measured or calculated), it is recommended that the criterion $F^{1-} > 0.5$ apfu, be met for the tourmaline to be considered a fluor-species.

(4) Estimate the dominant anion (OH^{1-} or O^{2-}) at the V site. The current state of knowledge is that most tourmalines are greatly dominated by OH^{1-} at the V site. Consequently, the assumption of $^{V}(OH)^{1-} = 3$ is generally correct. The exceptions are buergerite and some olenitic tourmalines (Ertl et al. 2002; Cempírek et al. 2006; Bosi and Lucchesi 2007).

(5) Determine whether $Si^{4+} < 4.5$ apfu with the rest of the tetrahedral site being occupied by $^{T}Al^{3+}$ and $^{T}B^{3+}$. Although, natural tourmalines with these characteristics have not been identified, tourmalines with these characterizations have been synthesized (Schreyer et al. 2000; Marler et al. 2002).

(6) Establish the dominant Z-site cation (Al^{3+}, Cr^{3+}, Fe^{3+}, or

TABLE 8. Recommended names for incompletely or inadequately determined tourmalines

General formula	(X)	(Y_3)	(Z_6)	V_3 (likely)*	W (unknown)†
Alkali-group tourmaline					
Elbaitic tourmaline	Na	Li and Al	Al	(OH^{1-})	unknown
Schorlitic tourmaline	Na	Fe^{2+}	Al	(OH^{1-})	unknown
Dravitic tourmaline	Na	Mg	Al	(OH^{1-})	unknown
Buergeritic tourmaline	Na	Fe^{3+}	Al	(O^{2-})	unknown
Olenitic tourmaline	Na	Al	Al	(OH^{1-})	unknown
Povondraitic tourmaline	Na	Fe^{3+}	Fe^{3+}	(OH^{1-})	unknown
Chromium-dravitic tourmaline	Na	Mg	Cr	(OH^{1-})	unknown
Vanadium-dravitic tourmaline	Na	Mg	V	(OH^{1-})	unknown
Calcic-group tourmaline					
Liddicoatitic tourmaline	Ca	Li and Al	Al	(OH^{1-})	unknown
Uvitic tourmaline	Ca	Mg	Al	(OH^{1-})	unknown
Feruvitic tourmaline	Ca	Fe^{2+}	Al	(OH^{1-})	unknown
Vacant-group tourmaline					
Rossmanitic tourmaline	□	Li and Al	Al	(OH^{1-})	unknown
Foititic tourmaline	□	Fe^{2+}	Al	(OH^{1-})	unknown
Magnesio-foititic tourmaline	□	Mg	Al	(OH^{1-})	unknown

* Anion presumed to occupy the V site.
† Unknown amounts of OH^{1-} and O^{2-}. However, F^{1-} >0.5 apfu will signify a fluor-species, and earlier species-designation procedures are warranted.

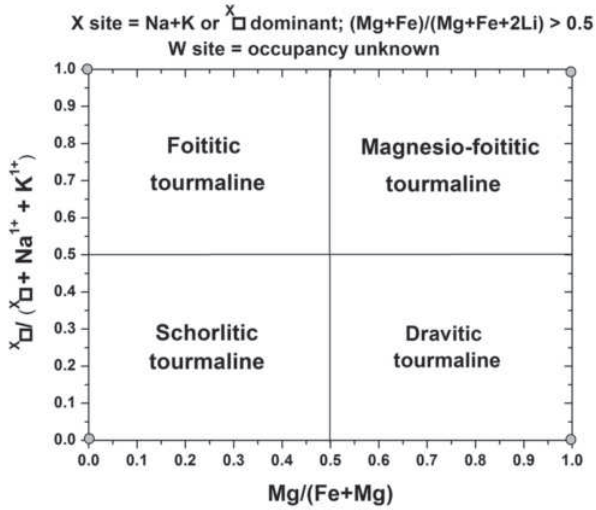

FIGURE 10. Example of a diagram that can be used to illustrate the generalized tourmaline species based on Mg/(Mg + Fe) vs. $^{X}\square/(^{X}\square + Na^{1+} + K^{1+})$ ratios.

V^{3+}). This can be done simply by inspection or calculation, or can be illustrated graphically. For tourmaline with low amounts of Fe^{3+} at the Z site of the ordered formula, the Al-V-Cr ternary can be used to graphically establish this Z-site subgroup (Fig. 6). The most common Z-site dominant cation is Al^{3+}, and a graphical approach for classifying 24 possible ^{Z}Al-dominant tourmaline species is given in Figures 7 to 9. The Fe^{3+}-dominant end-member povondraite is commonly in solid solution with the "oxy-dravite" and dravite species (Henry et al. 1999, 2008; Žáček et al. 2000).

(7) Determine the Y-site cation occupancy, recalling that an ordered form of the structural formula is used for classification purposes only. The dominant subgroup (subgroup 1–4 of each of the three subgroups) can be roughly established graphically from Figures 4 and 5.

(8) With the determination of the dominant subgroup, the dominant species in that subgroup can be identified with the same procedure given in the previous section.

The user must decide whether the results of the assumptions used in calculating unmeasured elements are accurate enough to adequately characterize the tourmaline composition. If the user considers the calculated unanalyzed elements inadequate, it is recommended that a more generalized name be used (Table 8, Fig. 10). However, if $F^{1-} > 0.5$ apfu the tourmaline will necessarily be a "fluor-tourmaline" species and the earlier classification procedures can be followed.

ACKNOWLEDGMENTS

The authors thank Alfonso Pesquera and Ferdinando Bosi for very detailed, insightful, and instructive reviews. Ed Grew, *American Mineralogist* Associate Editor, provided very important input into the final version of the paper. Scores of interested individuals helped keep this process vital and dynamic. This work was supported in part by the Austrian Science Fund (FWF) project no. P20509-N10 to A. Ertl; Grant Agency of Czech Republic, GAČR P210/10/0743 to M. Novák; and NSF grant EAR-9405747 to D. Henry.

REFERENCES CITED

Akizuki, M., Kuribayashi, T., Nagase, T., and Kitakaze, A. (2001) Triclinic liddicoatite and elbaite in growth sectors of tourmaline from Madagascar. American Mineralogist, 86, 364–369.

Andreozzi, G.B., Bosi, F., and Longo, M. (2008) Linking Mössbauer and structural parameters in elbaite-schorl-dravite tourmalines. American Mineralogist, 93, 658–666.

Anthony, J.W., Bideaux, R.A., Bladh, K.W., and Nichols, M.C. (1995) Handbook of Mineralogy. Volume II Silica, Silicates, Part 1 and 2. Mineral Data Publishing, Tucson, Arizona.

Armbruster, T., Bonazzi, P., Akasaka, M., Bermanec, V., Chopin, C., Gieré, R., Heuss-Assbichler, S., Liebscher, A., Menchetti, S., Pan, Y., and Pasero, M. (2006) Recommended nomenclature of epidote-group minerals. European Journal of Mineralogy, 18, 551–567.

Aurisicchio, C., Demartin, F., Ottolini, L., and Pezzotta, F. (1999) Homogeneous liddicoatite from Madagascar: a possible reference material? First EMPA, SIMS and SREF data. European Journal of Mineralogy, 11, 237–242.

Bailey, S.W. (1977) Report of I.M.A-I.U. Cr. Joint Committee on Nomenclature. American Mineralogist, 62, 411–415.

Barton, R. Jr. (1969) Refinement of the crystal structure of buergerite and the absolute orientation of tourmalines. Acta Crystallographica, B25, 1524–1533.

Bastin, G.F. and Heijligers, H.J.M. (2000) Quantitative electron probe microanalysis of boron. Journal of Solid State Chemistry, 154, 177–187.

Bayliss, P. (2000) Glossary of Obsolete Mineral Names, 235 pp. Mineralogical Record, Tucson, Arizona.

Bayliss, P., Kaesz, H.D., and Nickel, E.H. (2005) The use of chemical-element adjectival modifiers in mineral nomenclature. Canadian Mineralogist, 43, 1429–1433.

Bosi, F. (2008) Disordering of Fe^{2+} over octahedrally coordinated sites of tourmaline. American Mineralogist, 93, 1647–1653.

Bosi, F. and Lucchesi, S. (2004) Crystal chemistry of the schorl-dravite series. European Journal of Mineralogy, 16, 335–344.

——— (2007) Crystal chemical relationships in the tourmaline group: Structural constraints on chemical variability. American Mineralogist, 92, 1054–1063.

Bosi, F., Lucchesi, S., and Reznitskii, L. (2004) Crystal chemistry of the dravite-chromdravite series. European Journal of Mineralogy, 16, 345–352.

Breaks, F.W., Tindle, A.G., and Selway, J.B. (2008) Electron microprobe and bulk rock and mineral compositions from rare-element pegmatites and peraluminous, S-type granitic rocks from the Fort Hope pegmatite field, north-central Superior Province of Ontario. Ontario Geological Survey, Miscellaneous Release Data, 235.

Burns, P.C., MacDonald, D.J., and Hawthorne, F.C. (1994) The crystal-chemistry of manganese-bearing elbaite. Canadian Mineralogist, 32, 31–41.

Cámara, F., Ottolini, L., and Hawthorne, F.C. (2002) Crystal chemistry of three tourmalines by SREF, EMPA, and SIMS. American Mineralogist, 87, 1437–1442.

Cempírek, J., Novák, M., Ertl, A., Hughes, J.M., Rossman, G.R., and Dyar, M.D. (2006) Fe-bearing olenite with tetrahedrally coordinated Al from an abyssal pegmatite at Kutná Hora, Czech Republic: structure, crystal chemistry, optical spectra and XANES spectra. Canadian Mineralogist, 44, 23–30.

Chopin, C. (2006) Heterovalent substitutions in mineral nomenclature: the dominant-ion rule revisited. Abstracts and Programs of the 19th General Meeting of the International Mineralogical Association, 300.

Chukhrov, F.V., Ed. (1981) Minerals: A Handbook. 3(3), Silicates with Multiple Chains of Si-O Tetrahedra. Nauka, Moscow, Russia (in Russian).

Clark, C.M. (2007) Tourmaline: Structural formula calculations. Canadian Mineralogist, 45, 229–238.

Dietrich, R.V. (1985) The Tourmaline Group. Van Nostrand Reinhold Company, New York, 300 p.

Donnay, G. and Barton, R. Jr. (1972) Refinement of the crystal structure of elbaite and the mechanism of tourmaline solid solution. Tschermaks Mineralogische und Petrographische Mitteilungen, 18, 273–286.
Donnay, G., Ingamells, C.O., and Mason, B.H. (1966) Buergerite, a new species of tourmaline. American Mineralogist, 50, 198–199.
Dunn, P.J. (1977) Chromium in dravite. Mineralogical Magazine, 41, 408–410.
Dunn, P.J., Appleman, D., Nelen, J.A., and Norberg, J. (1977a) Uvite, a new (old) common member of the tourmaline group and its implications to collectors. Mineralogical Record, 8, 100–108.
Dunn, P.J., Appleman, D.E., and Nelen, J.E. (1977b) Liddicoatite, a new calcium end-member of tourmaline group. American Mineralogist, 62, 1121–1124.
Dutrow, B.L. and Henry, D.J. (2000) Complexly zoned fibrous tourmaline, Cruzeiro mine, Minas Gerais, Brazil: A record of evolving magmatic and hydrothermal fluids. Canadian Mineralogist, 38, 131–143.
Dyar, M.D., Taylor, M.E., Lutz, T.M., Francis, C.A., Guidotti, C.V., and Wise, M. (1998) Inclusive chemical characterization of tourmaline: Mössbauer study of Fe valence and site occupancy. American Mineralogist, 83, 848–864.
Dyar, M.D., Lowe, E.W., Guidotti, C.V., and Delaney, J.S. (2002) Fe^{3+} and Fe^{2+} partitioning among silicates in metapelites: a synchrotron micro-XANES study. American Mineralogist, 87, 514–522.
Ertl, A. (2006) Über die Etymologie und die Typlokalitäten des Minerals Schörl (About the etymology and the type localities of schorl). Mitteilungen der Österreichischen Mineralogischen Gesellschaft, 152, 7–16.
——— (2007) Über die Typlokalität und die Nomenklatur des Minerals Dravit (About the type locality and the nomenclature of dravite). Mitteilungen der Österreichischen Mineralogischen Gesellschaft, 153, 23–29.
——— (2008) About the nomenclature and the type locality of elbaite: A historical review. Mitteilungen der Österreichischen Mineralogischen Gesellschaft, 154, 35–44.
Ertl, A., Pertlik, F., and Bernhardt, H.-J. (1997) Investigations on olenite with excess boron from the Koralpe, Styria, Austria. Österreichische Akademie der Wissenschaften, Mathematisch-Naturwissenschaftliche Klasse, Abteilung I, Anzeiger, 134, 3–10.
Ertl, A., Hughes, J.M., Pertlik, F., Foit, F.F. Jr., Wright, S.E., Brandstätter, F., and Marler, B. (2002) Polyhedron distortions in tourmaline. Canadian Mineralogist, 40, 153–162.
Ertl, A., Hughes, J.M., Brandstätter, F., Dyar, M.D., and Prasad, P.S.R. (2003a) Disordered Mg-bearing olenite from a granitic pegmatite at Goslarn, Austria: A chemical, structural, and infrared spectroscopic study. Canadian Mineralogist, 41, 1363–1370.
Ertl, A., Hughes, J.M., Prowatke, S., Rossman, G.R., London, D., and Fritz, E.A. (2003b) Mn-rich tourmaline from Austria: structure, chemistry, optical spectra, and relations to synthetic solid solutions. American Mineralogist, 88, 1369–1376.
Ertl, A., Rossman, G.R., Hughes, J.M., Prowatke, S., and Ludwig, T. (2005) Mn-bearing "oxy-rossmanite" with tetrahedrally coordinated Al and B from Austria: Structure, chemistry, and infrared and optical spectroscopic study. American Mineralogist, 90, 481–487.
Ertl, A., Hughes, J.M., Prowatke, S., Ludwig, T., Prasad, P.S.R., Brandstätter,F., Körner, W., Schuster, R., Pertlik, F., and Marschall, H. (2006a) Tetrahedrally coordinated boron in tourmalines from the liddicoatite-elbaite series from Madagascar: structure, chemistry, and infrared spectroscopc studies. American Mineralogist, 91, 1847–1856.
Ertl, A., Kolitsch, U., Prowatke, S., Dyar, M.D., and Henry, D.J. (2006b) The F-analogue of schorl from Grasstein, Trentino South Tyrol, Italy: crystal structure and chemistry. European Journal of Mineralogy, 18, 583–588.
Ferrow, E.A. (1994) Mössbauer-effect study of the crystal chemistry of tourmaline. Hyperfine Interactions, 91, 689–695.
Ferrow, E.A., Annersten, H., and Gunawardane, R.P. (1988) Mössbauer-effect study on the mixed-valence state of iron in tourmaline. Mineralogical Magazine, 52, 221–228.
Fleischer, M. (1969) New mineral names. American Mineralogist, 54, 326–330.
Foit, F.F. (1989) Crystal chemistry of alkali-deficient schorl and tourmaline structural relationships. American Mineralogist, 74, 422–431.
Fortier, S., and Donnay, G. (1975) Schorl refinement showing composition dependence of the tourmaline structure. Canadian Mineralogist, 13, Part, 2, 173.
Gorelikova, N.V., Perfil'yev, Y.D., and Bubeshkin, A.M. (1978) Mössbauer data on distribution of Fe ions in tourmaline. International Geology Review, 20, 982–990.
Grew, E.S., Chernosky, J.V., Werding, G., Abraham, K., Marquez, N., and Hinthorne, J.R. (1990) Chemistry of kornerupine and associated minerals, a wet chemical, ion microprobe, and X-ray study emphasizing Li-contents, Be-contents, B-contents and F-contents. Journal of Petrology, 31, 1025–1070.
Grice, J.D. and Ercit, T.S. (1993) Ordering of Fe and Mg in the tourmaline crystal structure—the correct formula. Neues Jahrbuch für Mineralogie, Abhandlungen, 165, 245–266.
Grice, J.D. and Robinson, G.W. (1989) Feruvite, a new member of the tourmaline group, and its crystal structure. Canadian Mineralogist, 27, 199–203.
Grice, J.D., Ercit, T.S., and Hawthorne, F.C. (1993) Povondraite, a redefinition of the tourmaline ferridravite. American Mineralogist, 78, 433–436.
Harris, N.B.W., Gravestock, P., and Inger, S. (1992) Ion-microprobe determinations of trace-element concentrations in garnets from anatectic assemblages. Chemical Geology, 100, 41–49.
Hatert, F. and Burke, E.A.J. (2008) The IMA-CNMNC dominant-constituent rule revisited and extended. Canadian Mineralogist, 46, 717–728.
Hawthorne, F.C. (1996) Structural mechanisms for light-element variations in tourmaline. Canadian Mineralogist, 34, 123–132.
——— (2002) The use of end-member charge-arrangements in defining new mineral species and heterovalent substitutions in complex minerals. Canadian Mineralogist, 40, 699–710.
Hawthorne, F.C. and Grice, J.D. (1990) Crystal structure analysis as a chemical analytical method—application to light-elements. Canadian Mineralogist, 28, 693–702.
Hawthorne, F.C. and Henry, D.J. (1999) Classification of the minerals of the tourmaline group. European Journal of Mineralogy, 11, 201–215.
Hawthorne, F.C., MacDonald, D.J., and Burns, P.C. (1993) Reassignment of cation site occupancies in tourmaline—Al-Mg disorder in the crystal-structure of dravite. American Mineralogist, 78, 265–270.
Hawthorne, F.C., Cooper, M., Bottazzi, P., Ottolini, L., Ercit, T.S., and Grew, E.S. (1995) Microanalysis of Minerals for Boron by SREF, SIMS and EMPA—a comparative study. Canadian Mineralogist, 33, 389–397.
Hawthorne, F.C., Selway, J.B., Kato, A., Matsubara, S., Shimizu, M., Grice, J.D., and Vajdak, J. (1999) Magnesiofoitite, □ (Mg_2Al) Al_6 (Si_6O_{18}) $(BO_3)_3$ $(OH)_4$, a new alkali-deficient tourmaline. Canadian Mineralogist, 37, 1439–1443.
Henry, D.J. and Dutrow, B.L. (1990) Ca substitution in Li-poor aluminous tourmaline. Canadian Mineralogist, 28, 111–124.
——— (1996) Metamorphic tourmaline and its petrologic applications. In L.M. Anovitz and E.S. Grew, Eds., Boron: Mineralogy, Petrology and Geochemistry, 33, p. 503–557. Reviews in Mineralogy, Mineralogical Society of America, Chantilly, Virginia.
——— (2001) Compositional zoning and element partitioning in nickeloan tourmaline from a metamorphosed karstbauxite from Samos, Greece. American Mineralogist, 86, 1130–1142.
Henry, D.J., Kirkland, B.L., and Kirkland, D.W. (1999) Sector-zoned tourmaline from the cap rock of a salt dome. European Journal of Mineralogy, 11, 263–280.
Henry, D.J., Viator, D., and Dutrow, B.L. (2002) Estimation of light element concentrations in tourmaline: How accurate can it be? Programme with Abstracts of the 18th International Mineralogical Association, 209.
Henry, D.J., Sun, H., Slack, J., and Dutrow, B.L. (2008) Tourmaline in meta-evaporites and highly magnesian rocks: perspectives from Namibian tourmalinites. European Journal of Mineralogy, 20, 889–904.
Hermon, E., Sankin, D.J., Donnay, G., and Muir, W.B. (1973) The distribution of Fe^{2+} and Fe^{3+} in iron-bearing tourmalines: a Mössbauer study. Tschermaks Mineralogische und Petrographische Mitteilungen, 19, 124–132.
Hughes, J.M., Ertl, A., Dyar, M.D., Grew, E.S., Shearer, C.K., Yates, M.G., and Guidotti, C.V. (2000) Tetrahedrally coordinated boron in a tourmaline: Boron-rich olenite from Stoffhutte, Koralpe, Austria. Canadian Mineralogist, 38, 861–868.
Hughes, J.M., Ertl, A., Dyar, M.D., Grew, E.S., Wiedenbeck, M., and Brandstätter, F. (2004) Structural and chemical response to varying B-[4] content in zoned Fe-bearing olenite from Koralpe, Austria. American Mineralogist, 89, 447–454.
Jarosowich, E. (1966) Chemical analyses of ten stony meteorites. Geochimica et Cosmochimica Acta, 30, 1261–1265.
Kantipuly, C.J., Longerich, H.P., and Strong, D.F. (1988) Application of inductively coupled argon plasma mass-spectrometry (ICAP-MS) for the determination of uranium and thorium in tourmalines. Chemical Geology, 69, 171–176.
King, R.W., Kerrich, R.W., and Daddar, R. (1988) REE distributions in tourmaline—an INAA technique involving pretreatment by B-volatilization. American Mineralogist, 73, 424–431.
Kunitz, W. (1929) Die Mischungsreihen in der Turmalingruppe und die genetischen Beziehungen zwischen Turmalinen und Glimmern. Chemie der Erde, 4, 208–251.
Lussier, A.J., Aguiar, P.M., Michaelis, V.K., Kroeker, S., and Hawthorne, F.C. (2009) The occurrence of tetrahedrally coordinated Al and B in tourmaline: An ^{11}B and ^{27}Al MAS NMR study. American Mineralogist, 94, 785–792.
MacDonald, D.J. and Hawthorne, F.C. (1995) The crystal chemistry of Si = Al substitution in tourmaline. Canadian Mineralogist, 33, 849–858.
MacDonald, D.J., Hawthorne, F.C., and Grice, J.D. (1993) Foitite, □ $[Fe^{2+}_2(Al,Fe^{3+})]$ Al_6 Si_6O_{18} $(BO_3)_3$ $(OH)_4$, a new alkali-deficient tourmaline—description and crystal structure, American Mineralogist, 78, 1299–1303.
Marler, B., Borowski, M., Wodara, U., and Schreyer, W. (2002) Synthetic tourmaline (olenite) with excess boron replacing silicon in the tetrahedral site. II Structural analysis. European Journal of Mineralogy, 14, 763–772.
Mathesij, J. (1562) Sarepta oder Bergpostill sampt der Jochimßthalischen kurtzen Chroniken, 233 pp. Gedruckt zu Nürnberg, durch Johann vom Berg und Ulrich Newber.
McGee, J.J. and Anovitz, L.M. (1996) Electron probe microanalysis of geologic materials for boron. In L.M. Anovitz and E.S. Grew, Eds., Boron: Mineralogy, Petrology and Geochemistry, 33, p. 771–788. Reviews in Mineralogy, Mineralogical Society of America, Chantilly, Virginia.
Medaris, L.G., Fournelle, J.H., and Henry, D.J. (2003) Tourmaline-bearing quartz veins in the Baraboo Quartzite, Wisconsin: Occurrence and significance of foitite and "oxy-foitite." Canadian Mineralogist, 41, 749–758.
Mills, S.J., Hatert, F., Nickel, E.H., and Ferraris, G. (2009) The standardisation

of mineral group hierarchies: application to recent nomenclature proposals. European Journal of Mineralogy, 21, 1073–1080.
Nickel, E.H. (1992) Nomenclature for mineral solid solutions. American Mineralogist, 77, 660–662.
Nickel, E.H. and Grice, J.D. (1998) The IMA commission on new minerals and mineral names: Procedures and guidelines on mineral nomenclature. Canadian Mineralogist, 36, 913–926.
Novák, M., and Taylor, M.C. (2000) Foitite: Formation during late stages of evolution of complex granitic pegmatites at Dobra Voda, Czech Republic, and Pala, California, USA. Canadian Mineralogist, 38, 1399–1408.
Novák, M., Selway, J.B., Černý, P., Hawthorne, F.C., and Ottolini, L. (1999) Tourmaline of the elbaite-dravite series from an elbaite-subtype pegmatite at Blizna, southern Bohemia, Czech Republic. European Journal of Mineralogy, 11, 557–568.
Novák, M., Povondra, P., and Selway, J.B. (2004) Schorl-oxy-schorl to dravite-oxy-dravite tourmaline from granitic pegmatites; examples from the Moldanubicum, Czech Republic. European Journal of Mineralogy, 16, 323–333
Novák, M., Henry, D., Hawthorne F.C., Ertl, A., Uher, P., Dutrow, B., and Pezzotta, F. (2009) Nomenclature of the tourmaline-group minerals. Report of the Subcommittee on Tourmaline Nomenclature to the International Mineralogical Association's Commission on New Minerals, Nomenclature and Classification.
Nuber, B. and Schmetzer, K. (1981) Strukturverfeinernng von Liddicoatit. Neues Jahrbuch für Mineralogie, Monatshefte, 5, 215–219.
Ota, T., Kobayashi, K., Kunihiro, T., and Nakamura, E. (2008) Boron cycling by subducted lithosphere; insights from diamondiferous tourmaline from the Kokchetav ultrahigh-pressure metamorphic belt. Geochimica et Cosmochimica Acta, 72, 3531–3541.
Peck, L.C. (1964) Systematic analysis of silicates. Bulletin of the U.S. Geological Survey 1170.
Pezzotta, F., Hawthorne, F.C., Cooper, M.A., and Teerstra, D.K. (1996) Fibrous foitite from San Piedro. Canadian Mineralogist, 34, 741–744.
Povondra, P. (1981) The crystal chemistry of tourmalines of the schorl-dravite series. Acta Universitatis Carolinae, Geologica, 223–264.
Povondra, P. and Čech, F. (1976) A method for the chemical analysis of tourmaline. Acta Universitatis Carolinae, Geologica, 209–218.
Povondra, P. and Novák, M. (1986) Tourmalines in metamorphosed carbonate rocks from western Moravia, Czechoslovakia. Neues Jahrbuch für Mineralogie, Monatshefte, 273–282.
Povondra, P., Lang, M., Pivec, E., and Ulrych, J. (1998) Tourmaline from the Přibyslavice peraluminous granite, Czech Republic. Journal of the Czech Geological Society, 43, 3–8.
Prowatke, S., Ertl, A., and Hughes, J.M. (2003) Tetrahedrally coordinated Al in Mn-rich, Li- and Fe-bearing olenite from Eibenstein an der Thaya, Lower Austria: A chemical and structural investigation. Neues Jahrbuch für Mineralogie, Abhandlungen, 385–395.
Quensel, P. and Gabrielson, O. (1939) Minerals of the Varutrask pegmatite. XIV. The tourmaline group. Geologiska Föreningens Stockholm Förhandlingar, 61, 63–90.
Reznitsky, L.Z., Sklyarov, E.V., Ushchapovskaya, Z.V., Nartova, N.V., Kashaev, A.A., Karmanov, N.S., Kanakin, S.V., Smolin, A.S., and Nekrosova, E.A. (2001) Vanadiumdravite, $NaMg_3V_6[Si_6O_{18}][BO_3]_3(OH)_4$, and new mineral of the tourmaline group. Zapiski Vsesoyuznogo Mineralogicheskogo Obshchestva, 130, 59–72 (in Russian).
Roda, E., Pesquera, A., and Velasco, F. (1995) Tourmaline in granitic pegmatites and their country rocks, Fregeneda area, Salamanca, Spain. Canadian Mineralogist, 33, 835–848.
Romé de l'Isle, J.-B.L. (1772) Essai de Cristallographie ou Description des Figures Géométriques, Propres à Differents Corps du Regne, 427 pp. Didot jeune, Paris.
Rumyantseva, F.V. (1983) Chromdravite, a new mineral. Zapiski Vsesoyuznogo Mineralogicheskogo Obshchestva, 112, 222–226 (English summary in American Mineralogist, 69, 210).
Saegusa, N., Price, D.C., and Smith, G. (1979) Analysis of the Mössbauer spectra of several iron-rich tourmalines (schorls). Journal of Physics (Paris), 40C, 456–459.
Schmetzer, K., Nuber, B., and Abraham, K. (1979) Crystal chemistry of magnesium-rich tourmalines. Neues Jahrbuch für Mineralogie Abhandlungen, 136, 93–112.
Schreyer, W., Wodara, U., Marler, B., van Aken, P.A., Seifert, F., and Robert, J.L. (2000) Synthetic tourmaline (olenite) with excess boron replacing silicon in the tetrahedral site: I. Synthesis conditions, chemical and spectroscopic evidence. European Journal of Mineralogy, 12, 529–541.
Schreyer, W., Hughes, J.M., Bernhardt, H.J., Kalt, A., Prowatke, S., and Ertl, A. (2002) Reexamination of olenite from the type locality: detection of boron in tetrahedral coordination. European Journal of Mineralogy, 14, 935–942.
Selway, J.B., Černy, P., and Hawthorne, F.C. (1998a) Feruvite from lepidolite pegmatites at Red Cross Lake, Manitoba. Canadian Mineralogist, 36, 433–440.
Selway, J.B., Novák, M., Hawthorne, F.C., Černý, P., Ottolini, L., and Kyser, T.K. (1998b) Rossmanite, $(LiAl_2)Al_6(Si_6O_{18})(BO_3)_3(OH)_4$, a new alkali-deficient tourmaline: Description and crystal structure. American Mineralogist, 83, 896–900.
Shearer, C.K. and Papike, J.J. (1986) Distribution of boron in the Tip Top Pegmatite, Black Hills, South-Dakota. Geology, 14, 119–123.
Shtukenberg, A., Rozhdestvenskaya, I., Frank-Kamenetskaya, O., Bronzova, J., Euler, H., Kirfel, A., Bannova, I., and Zolotarev, A. (2007) Symmetry and crystal structure of biaxial elbaite-liddicoatite tourmaline from the Transbaikalia region, Russia. American Mineralogist, 92, 675–686.
Smith, D.G.W. and Nickel, E.H. (2007) A system of codification for unnamed minerals: Report of the subcommittee for unnamed minerals of the IMA commission on new minerals, nomenclature and classification. Canadian Mineralogist, 45, 983–990.
Sokolov, P.B., Gorskaya, M.G., Gordienko, V.V., Petrova, M.G., Kretser, Yu.l., and Frank-Kamentskii, V.A. (1986) Olenite, $Na_{1-x}Al_3Al_6B_3Si_6O_{27}(O,OH)_4$—novyy vysokoglinozemistyy mineral iz gruppy turmalinov. Zapiski Vsesoyuznogo Mineralogicheskogo Obshchestva, 115, 119–123 (Russian). [Translated title: "Olenite Na_{1-x} $Al_3Al_6B_3Si_6O_{27}(O,OH)_4$—a new high-alumina mineral of the tourmaline group" in American Mineralogist, 73, 441, "New Mineral Names."]
Tagg, S.L., Cho, H., Dyar, M.D., and Grew, E.S. (1999) Tetrahedral boron in naturally occurring tourmaline. American Mineralogist, 84, 1451–1455.
Taylor, M.C., Cooper, M.A., and Hawthorne, F.C. (1995) Local charge-compensation in hydroxyl-deficient uvite. Canadian Mineralogist, 33, 1215–1221.
Tippe, A. and Hamilton, W.C. (1971) Neutron-diffraction study of ferric tourmaline, buergerite. American Mineralogist, 56, 101–113.
Tschermak, G. (1884) Lehrbuch der Mineralogie. IX, 589 pp., 700 Abb., 2 Farbtafeln, Hölder, Wien.
Vernadsky, W. (1913) Über die chemische Formel der Turmaline. Zeitschrift für Kristallographie, Kristallogeometrie Kristallphysik, Kristallchemie, 53, 273–288.
Walenta, K. and Dunn, P.J. (1979) Ferridravite, a new mineral of the tourmaline group from Bolivia. American Mineralogist, 64, 945–948.
Wallerius, J.G. (1747) Mineralogy, and mineral kingdom, 479 pp. Printed by Lorentz Ludwig Grefing, Stockholm. (In Swedish)
Wang, H. and Hsu, H. (1966) A new variety of dravite and its significance in mineralogy. Kexue Tangbao, 17, 91–96 [English summary in American Mineralogist (1967), 52, 562–563].
Werner, A.G. (1780) Constedt's Versuch einer Mineralogie, vol. 1, part 1. Übersetzt und Vermehrt, Leipzig.
Williams, P.A., Hatert, F., Pasero, M., and Mills, S. (2010) New minerals, nomenclature modifications approved in 2010. Mineralogical Magazine, 74, 375–377.
Wilson, G.C. and Long, J.V.P. (1983) The distribution of lithium in some Cornish minerals—Ion microprobe measurements. Mineralogical Magazine, 47, 191–199.
Wright, S.E., Foley, J.A., and Hughes, J.M. (2000) Optimization of site occupancies in minerals using quadratic programming. American Mineralogist, 85, 524–531.
Žáček, V., Frýda, J., Petrov, A., and Hyršl, J. (2000) Tourmalines of the povondraite—(oxy)dravite series from the caps rocks of meta-evaporite in Alto Chapare, Cochamba, Bolivia. Journal of the Czech Geological Society, 45, 3–12.

Manuscript received June 24, 2010
Manuscript accepted January 28, 2011
Manuscript handled by Edward Grew

Appendix 1. Tourmaline end-members: general characteristics

There are inconsistencies in the earlier definitions of several of the tourmaline end-member formulas that prompt redefining some of these end-members (Hawthorne and Henry 1999). In defining end-member compositions there are several characteristics that should be considered (Hawthorne 2002).

(1) *An end-member composition must be fixed*. Consequently, formulas expressed with variable cations or anions on a given site, such as (Al^{3+}, Fe^{3+}) on the Y site or (F^-, OH^-) at the W site, can be factored into two or more end-member components of fixed composition. For example, in the case of the original end-member definition of foitite, the composition was expressed as $\square$ [Fe^{2+}_2 (Al, Fe^{3+})] Al_6 (Si_6O_{18}) (BO_3)$_3$ (OH)$_4$ (MacDonald et al. 1993). However, this definition is incorrect because the composition is variable and can be factored into the two fixed compositions: $\square$ [Fe^{2+}_2 Al] Al_6 (Si_6O_{18}) (BO_3)$_3$ (OH)$_4$ and $\square$ [Fe^{2+}_2 Fe^{3+}] Al_6 (Si_6O_{18}) (BO_3)$_3$ (OH)$_4$.

(2) An end-member may have more than a single cation or anion at a single given site if it is necessary to attain electroneutrality in the crystal structure. Electroneutrality in crystal structures mandate that, in some instances, two cations or anions may be required for charge balance on a single site. One of the best examples is the tourmaline end-member elbaite: Na [$Li_{1.5}$ $Al_{1.5}$] Al_6

(Si_6O_{18}) $(BO_3)_3$ $(OH)_3$ (OH). The X, Z, T, B, V, and W sites are completely ordered (occupied by only one type of cation or anion) such that the aggregate charge is 6^-. This requires that cations on the Y site have a total charge of 6^+. In the case of elbaite, with a mix of Li^+ and Al^{3+}, the aggregate charge is only met with the Y-site composition of $[Li_{1.5}\ Al_{1.5}]$.

(3) Anions are critical in defining end-members, and similar anions can occupy more than one crystallographically distinct site in a crystal structure. Anions such as OH^-, F^-, and O^{2-} can define distinct end-members. Anions sites can have crystallographic distinctions that mandate preferences of certain anions for specific anion sites. For example, in the tourmaline structure the V site can be occupied by O^{2-} and OH^-, but the W site can be occupied by F^-, O^{2-}, and/or OH^-. In the case of homovalent anion substitution of F^- for OH^-, tourmaline will range from $(OH)_3(OH)$ to $(OH)_3(F)$, thus defining the OH (hydroxy) and F (fluor) end-members. In the case of heterovalent anion substitution of O^{2-} for OH^- or F^-, coupled substitutions must involve other cations in the crystal structure to define an "oxy" end-member.

Appendix 2: Tourmaline species, end-member formulas, modifications, etymology, type localities, and representative cell dimensions

The following tourmaline species have either been previously accepted by the IMA-CNMNC or have been modified by the STN for internal consistency among the tourmaline species. Modifications to the original tourmaline species descriptions are noted.

Chromium-dravite

Structural formula: Na Mg_3 Cr_6 (Si_6O_{18}) $(BO_3)_3$ $(OH)_3$ OH
IMA number: IMA 82-055. Original name: chromdravite.
Modifications: Due to its distinction in the tourmaline structure, the structural formula is written to designate two OH-bearing sites (the V and W sites). This contrasts with the earlier formula that combined these two sites into a single "OH" site with four possible OH^{1-} anionic groups. The full term "chromium" is used as a prefix for consistency among species.
Etymology: Named for its relationship to dravite and chemical composition.
Type locality: Velikaya Guba uranium occurrence, Zaonezhskiy Peninsula, Karelia, Russia.
Crystal system: Trigonal; *R*3*m*
Representative cell dimensions (type material): a = 16.11 Å, c = 7.27 Å, V = 1634 Å^3
Selected references: Rumyantseva (1983)

Chromo-alumino-povondraite

Structural formula: Na Cr_3 $(Al_4Mg_2)(Si_6O_{18})$ $(BO_3)_3$ $(OH)_3$ O
IMA number: IMA 2009-088
Modifications: none
Etymology: Named for its chemical composition and its relationship to povondraite.
Type locality: Chromite deposits of Nausahi, Keonjhar District, Orissa, India.
Crystal system: Trigonal; *R*3*m*
Representative cell dimensions (type material): a = 16.036 Å, c = 7.319 Å, V = 1589.9 Å^3
Selected references: Williams et al. (2010)

Dravite

Structural formula: Na Mg_3 Al_6 (Si_6O_{18}) $(BO_3)_3$ $(OH)_3$ OH
IMA number: First described prior the establishment of IMA in 1958—Grandfathered status.
Modifications: Due to its distinction in the tourmaline structure, the structural formula is written to designate two OH-bearing sites (the V and W sites). This contrasts with the earlier formula that combined these two sites into a single "OH" site with four possible OH^{1-} anionic groups.
Etymology: Named in 1884 by Tschermak for the Drava river area, the location of a Mg- and Na-rich tourmaline. The Drava river area, which is the district along the Drava River (in German: Drau; in Latin: Drave) is in Austria and Slovenia (Ertl 2007).
Type locality: Unterdrauburg, Carinthia, Austria (today Dobrava pri Dravogradu, Slovenia); Ertl (2007).
Crystal system: Trigonal; *R*3*m*
Representative cell dimensions (type material): a = 15.96 Å, c = 7.21 Å, V = 1590 Å^3
Selected references: Tschermak (1884), Kunitz (1929), and Dunn (1977)

Elbaite

Structural formula: Na $(Li_{1.5}Al_{1.5})$ Al_6 (Si_6O_{18}) $(BO_3)_3$ $(OH)_3$ OH
IMA number: First described prior the establishment of IMA in 1958—Grandfathered status.
Modifications: Due to its distinction in the tourmaline structure, the structural formula is written to designate two OH-bearing sites (the V and W sites). This contrasts with the earlier formula that combined these two sites into a single "OH" site with four possible OH^{1-} anionic groups.
Etymology: Named after the type locality, on the island of Elba, Tuscany, Italy
Type locality: San Piero in Campo, Campo nell'Elba, Elba Island, Livorno Province, Tuscany, Italy.
Crystal system: Trigonal; *R*3*m*
Representative cell dimensions (type material): a = 15.85Å, c = 7.11 Å, V = 1546.9 Å^3
Selected references: Vernadsky (1913), Donnay and Barton (1972), Novák et al. (1999), and Ertl (2008)

Feruvite

Structural formula: Ca Fe^{2+}_3 (Al_5Mg) (Si_6O_{18}) $(BO_3)_3$ $(OH)_3$ OH
IMA number: IMA 87-057
Modifications of the end-member definition: The original formula for feruvite is Ca Fe_3 $(Al,Mg)_6$ (Si_6O_{18}) $(BO_3)_3$ $(OH)_4$ (Grice and Robinson 1989). This is not considered to be an appropriate end-member and it does not specify the valence state of Fe. The Z site was determined to be $(Al_{4.72}Fe^{3+}_{0.34}Mg_{0.82}Fe^{2+}_{0.12})$, which is close to an (Al_5Mg) end-member.
Etymology: Named for its relationship to uvite and chemical composition.
Crystal system: Trigonal; *R*3*m*
Type locality: Repanga Island (Cuvier Island), Waikato, North Island, New Zealand.
Representative cell dimensions (type material): a = 16.01 Å, c = 7.25 Å, V = 1609 Å^3
Selected references: Grice and Robinson (1989) and Selway et al. (1998a)

Fluor-buergerite

Structural formula: Na Fe^{3+}_3 Al_6 (Si_6O_{18}) $(BO_3)_3$ O_3 F
IMA number: IMA 65-005. Original name: buergerite
Etymology: Named for Martin Julian Buerger (1903–1986), a professor of mineralogy at the Massachusetts Institute of Technology and a pioneer of crystal structure analysis.
Modifications: For consistency among tourmaline species, the STN advocates that hydroxy species becomes the root name of a species. For those tourmalines in which the W site exhibits dominance of S^{1-} relative to S^{2-} anions and dominance F^{1-} relative to OH^{1-}, the species becomes the fluor-species equivalent.
Type locality: Mexquitic, San Luis Potosí, Mexico.
Crystal system: Trigonal; *R*3*m*
Representative cell dimensions (type material): a = 15.87 Å, c = 7.19 Å, V = 1568 Å^3
Selected references: Donnay et al. (1966), Barton (1969), and Tippe and Hamilton (1971)

Fluor-dravite

Structural formula: Na Mg_3 Al_6 (Si_6O_{18}) $(BO_3)_3$ $(OH)_3$ F
IMA number: 2009-089
Modifications: For consistency among tourmaline species, the STN advocates that hydroxy species becomes the root name of a species. For those tourmalines in which the W site exhibits dominance of S^{1-} relative to S^{2-} anions and dominance F^{1-} relative to OH^{1-}, the species becomes the fluor-species equivalent.
Etymology: Named for its relationship to dravite and chemical composition.
Type locality: Crabtree Emerald mine, Mitchell County, North Carolina, U.S.A.
Crystal system: Trigonal; *R*3*m*
Representative cell dimensions (type material): a = 15.955 Å, c = 7.153 Å, V = 1576.9 Å^3
Selected references: Williams et al. (2010)

Fluor-liddicoatite

Structural formula: Ca (Li_2Al) Al_6 (Si_6O_{18}) $(BO_3)_3$ $(OH)_3$ F
IMA number: IMA 76-041. Original name: liddicoatite
Modifications of the end-member definition: Dunn et al. (1977b) gave the structural formula for the holotype liddicoatite material as $(Ca_{0.72}Na_{0.27})$ $(Li_{1.59}Al_{1.13}$ $Fe_{0.11}Ti_{0.05}Mn_{0.04}Mg_{0.04})$ $Al_{6.00}$ Si_6O_{18} $(BO_3)_3$ $[(OH)_{2.73}O_{0.27}]$ $[F_{0.87}(OH)_{0.13}]$. Based on this composition and the structural analogy with elbaite, they extrapolated the end-member composition of liddicoatite as Ca $(Li_{1.74}Al_{1.26})$ Al_6 (Si_6O_{18}) $(BO_3)_3$ $[(OH)_{2.48}O_{0.52}]$ (F,OH), but stipulated that this is not a "pure end-member." Fur-

thermore, they gave the "ideal" composition of liddicoatite as Ca $(Li,Al)_3$ Al_6 (Si_6O_{18}) $(BO_3)_3$ $(O,OH)_3$ (OH,F). Several aspects of this formula warrant modification of the end-member structural formula to the one given here. (1) Because F partitions exclusively in the W site, the holotype material is an F-dominant species. (2) Any oxygen at the W and V sites should be assigned to the W site in the holotype material structural formula (Hawthorne 1996). (3) The divalent charge of Ca requires an adjustment of the Li:Al ratio so the Y-site is (Li_2Al).

Etymology: Named for Richard T. Liddicoat (1918–2002), gemologist and president of the Gemological Institute of America.

Type locality: Pegmatitic area southwest of the towns of Antsirabé and Betafo, Vakinankaratra region, Antananarivo Province, Madagascar.

Crystal system: Trigonal; *R*3*m*

Representative cell dimensions (type material): a = 15.87 Å, c = 7.14 Å, V = 1557 Å^3

Selected references: Dunn et al. (1977b), Nuber and Schmetzer (1981), and Aurisicchio et al. (1999)

Fluor-schorl

Structural formula: Na Fe^{2+}_3 Al_6 (Si_6O_{18}) $(BO_3)_3$ $(OH)_3$ F

IMA number: 2010-067

Modifications: For consistency among tourmaline species, the STN advocates that hydroxy species becomes the root name of a species. For those tourmalines in which the W site exhibits dominance of S^{1-} relative to S^{2-} anions and dominance F^{1-} relative to OH^{1-}, the species becomes the fluor-species equivalent.

Etymology: Named for its relationship to schorl and chemical composition.

Type locality: Area near Zschorlau, Erzgebirge, Saxony, Germany and area near Grasstein, Trentino, South Tyrol, Italy.

Crystal system: Trigonal; *R*3*m*

Representative cell dimensions (type material): a = 15.996 Å, c = 7.186 Å, V = 1576.9 Å^3

Selected references: Ertl et al. (2006)

Fluor-uvite

Structural formula: Ca Mg_3 (Al_5Mg) (Si_6O_{18}) $(BO_3)_3$ $(OH)_3$ F

IMA number: First described prior the establishment of IMA in 1958—Grandfathered status. Original name: uvite.

Modifications of the end-member definition: Uvite, originally defined by Kunitz (1929), was considered to have an ideal formula of Ca Mg_3 (Al_5Mg) (Si_6O_{18}) $(BO_3)_3$ $(OH)_4$. This formula was based on the examination of tourmalines from Uva (Sri Lanka), De Kalb (New York), and Gouverneur (New York) with OH contents of approximately 4 apfu. However, all other analyses from these localities contain F in the 0.5–1.0 apfu range. Dunn et al. (1977a) designated a sample of uvite from Uva, Sri Lanka as a neotype, and this sample has an anion content of $(OH_{2.90}F_{0.76}O_{0.34})$. This anion content would mandate that the W site would be dominated by F and that uvite should be an F-end-member.

Etymology: Named for the type locality area, Uva Province, Sri Lanka.

Type locality: Uva Province, Sri Lanka.

Crystal system: Trigonal; *R*3*m*

Representative cell dimensions (type material): a = 15.97 Å, c = 7.21 Å, V = 1592 Å^3

Selected references: Kunitz (1929), Schmetzer et al. (1979), and Dunn et al. (1977a)

Foitite

Structural formula: □ (Fe^{2+}_2Al) Al_6 (Si_6O_{18}) $(BO_3)_3$ $(OH)_3$ OH

IMA number: IMA 92-034

Modifications of the end-member definition: The original end-member composition of foitite was given with a variable cation occupancy at the Y site i.e., Y_3 = $[Fe^{2+}_2(Al,Fe^{3+})]$ (MacDonald et al. 1993). Because Al is dominant relative to Fe^{3+} in the holotype material, the Y-site composition of the end-member is considered Fe^{2+}_2Al.

Etymology: Named for Franklin F. Foit Jr. (1942-), mineralogist at Washington State University, Pullman, in recognition of his work on tourmaline-supergroup minerals.

Type locality: Found as museum specimens designated only as from "southern California", U.S.A., probably from White Queen mine, Pala district, San Diego County, California, U.S.A. (Anthony et al. 1995; Novák and Taylor 2000).

Crystal system: Trigonal; *R*3*m*

Representative cell dimensions (type material): a = 15.97 Å, c = 7.13 Å, V = 1575 Å^3

Selected references: MacDonald et al. (1993) and Pezzotta et al. (1996)

Magnesio-foitite

Structural formula: □ (Mg_2Al) Al_6 (Si_6O_{18}) $(BO_3)_3$ $(OH)_3$ OH

IMA number: IMA 98-037

Modifications: Due to its distinction in the tourmaline structure, the structural formula is written to designate two OH-bearing sites (the V and W sites). This contrasts with the earlier formula that combined these two sites into a single "OH" site with four possible OH^{1-} anionic groups.

Etymology: Named for its relationship to foitite and chemical composition.

Type locality: Kyonosawa, Mitomi-mura, Yamanashi Prefecture, Chubu region, Honshu Island, Japan.

Crystal system: Trigonal; *R*3*m*

Representative cell dimensions (type material): a = 15.88 Å, c = 7.18 Å, V = 1568 Å^3

Selected references: Hawthorne et al. (1999)

Olenite

Structural formula: Na Al_3 Al_6 (Si_6O_{18}) $(BO_3)_3$ (O_3) OH

IMA number: IMA 85-006

Modifications of the end-member definition: Sokolov et al. (1986) gave the formula for the type olenite as Na_{1-x} Al_3 Al_6 B_3 Si_6 O_{27} $(O,OH)_4$. To create an end-member formula with the ideal occupancy of one Na at the X site, three Al at the Y site, and where the T site is completely occupied by Si, the V and W site can only be occupied by $[O_3(OH)]$. To create an ordered formula, the (OH) is eventually assigned to the W site, while O_3 is assigned to the V site.

Etymology: Named for the type locality area, Olenek River basin, Russia.

Type locality: Olenek River basin, Olenii (Oleny) Range, Voron'i Tundry, Kola Peninsula, Murmansk Oblast region, Russia.

Crystal system: Trigonal; *R*3*m*

Representative cell dimensions (type material): a = 15.80 Å, c = 7.09 Å, V = 1533 Å^3

Selected references: Sokolov et al. (1986), Ertl et al. (1997), Hughes et al. (2000 2004), Schreyer et al. (2002), and Cempírek et al. (2006)

Povondraite

Structural formula: Na Fe^{3+}_3 $(Fe^{3+}_4Mg_2)$ (Si_6O_{18}) $(BO_3)_3$ $(OH)_3$ O

IMA number: Renamed/redefined by IMA 90-E

Modifications of the end-member definition: Povondraite was redefined from the original "ferridravite" (Walenta and Dunn 1979) because the initially assumed site assignments were incorrect and did not correspond to the Fe^{3+}-equivalent of dravite (Grice et al. 1993). Hawthorne and Henry (1999) suggested that Mg is ordered at the Z site and should be part of the end-member formula.

Etymology: Named for Pavel Povondra (1924-), mineralogist and chemist at the Charles University, Prague, Czech Republic, for his extensive work on the tourmaline supergroup.

Type locality: Alto Chapare district, Chapare Province, Cochabamba Department, Bolivia.

Crystal system: Trigonal; *R*3*m*

Representative cell dimensions (type material): a = 16.19 Å, c = 7.44 Å, V = 1689 Å^3

Selected references: Walenta and Dunn (1979), Grice et al. (1993), and Žácek et al. (2000)

Rossmanite

Structural formula: □ $(LiAl_2)$ Al_6 (Si_6O_{18}) $(BO_3)_3$ $(OH)_3$ OH

IMA number: IMA 96-018

Modifications: Due to its distinction in the tourmaline structure, the structural formula is written to designate two OH-bearing sites (the V and W sites). This contrasts with the earlier formula that combined these two sites into a single "OH" site with four possible OH^{1-} anionic groups.

Etymology: Named after George R. Rossman (1945-), California Institute of Technology, Pasadena, California, U.S.A., in recognition for his work on the spectroscopy of the tourmaline-supergroup minerals.

Type locality: Hradisko quarry, Rožná, Morava (Moravia), Czech Republic.

Crystal system: Trigonal; *R*3*m*

Representative cell dimensions (type material): a = 15.77 Å, c = 7.09 Å, V = 1527 Å^3

Selected references: Selway et al. (1998b)

Schorl

Structural formula: Na Fe^{2+}_3 Al_6 (Si_6O_{18}) $(BO_3)_3$ $(OH)_3$ OH

IMA number: First described prior the establishment of IMA in 1958—Grandfathered status.

Modifications: Due to its distinction in the tourmaline structure, the structural formula is written to designate two OH-bearing sites (the V and W sites). This contrasts with the earlier formula that combined these two sites into a single "OH" site with four possible OH^{1-} anionic groups.

Etymology: Name probably derived from the early German mining term "Schor" (mud) or after the name of the former village "Schorl" (today: Zschorlau) in Saxony, Germany. The first relatively detailed description of schorl with the name "schürl" and its occurrence (various tin mines in the Saxony Ore Mountains) was written by Johannes Mathesius (1504–1565) in 1562 under the title "Sarepta oder Bergpostill" (Ertl 2006).

Type locality: Saxony Ore Mountains, Germany.

Crystal system: Trigonal; *R*3*m*

Representative cell dimensions: a = 15.98 Å, c = 7.16 Å, V = 1583 Å^3.
Selected references: First described in 1562 by Mathesius (Mathesij 1562) as reported in Wallerius (1747), Romé de l'Isle (1772), Werner (1780), Fortier and Donnay (1975), Foit (1989), and Ertl (2006)

Uvite

Structural formula: Ca Mg_3 (Al_5Mg) (Si_6O_{18}) (BO_3)$_3$ (OH)$_3$ OH
IMA number: IMA 2000-030a
Modifications of the end-member definition: Uvite, originally defined by Kunitz (1929), was considered to have an ideal formula of Ca Mg_3 (Al_5Mg) (Si_6O_{18}) (BO_3)$_3$ (OH)$_4$. This formula was based on the examination of tourmalines from Uva (Sri Lanka), De Kalb (New York) and Gouverneur (New York) with OH contents of approximately 4 apfu. However, all other analyses from these localities contain F in the 0.5–1.0 apfu range. Dunn et al. (1977a) designated a sample of uvite from Uva, Sri Lanka as a neotype, and this sample has an anion content of ($OH_{2.90}F_{0.76}O_{0.34}$). This anion content would mandate that the W site would be dominated by F and that the type uvite should most properly be termed fluor-uvite. More recently, uvitic species with OH dominant on the W site were described by Christine M. Clark, Frank C. Hawthorne and Joel D. Grice from the Brumado mine, Brazil locality.
Etymology: Named for the type locality area of the currently defined fluor-uvite, Uva Province, Sri Lanka. Uvite is redefined as the hydroxy equivalent to fluor-uvite.
Type locality: Brumado mine, Bahia, Brazil.
Type material: deposited in the Royal Ontario Museum (Toronto, Canada), specimen number M55101.
Crystal system: Trigonal; *R*3*m*
Representative cell dimensions (type material): a = 15.954 Å, c = 7.214 Å, V = 1590.2 Å^3
Selected references: Williams et al. (2010)

Vanadium-dravite

Structural formula: Na Mg_3 V_6^{3+} (Si_6O_{18}) (BO_3)$_3$ (OH)$_3$ OH
IMA number: IMA 1999-050
Modifications: Due to its distinction in the tourmaline structure, the structural formula is written to designate two OH-bearing sites (the V and W sites). This contrasts with the earlier formula that combined these two sites into a single "OH" site with four possible OH^{1-} anionic groups.
Etymology: Named for its relationship to dravite and chemical composition.
Type locality: Slyudyanka complex, Lake Baikal region, Siberia, Russia.
Crystal system: Trigonal; *R*3*m*
Representative cell dimensions (type material): a = 16.12 Å, c = 7.39 Å, V = 1663 Å^3
Selected references: Reznitsky et al. (2001)

Additional Potential, but Unnamed, Tourmaline Species

At the time of the manuscript revision the following tourmalines are described either in a proposal to IMA or via the codification for unnamed minerals (Smith and Nickel 2007) and further expanded in the IMA-CNMNC website (http://pubsites.uws.edu.au/ima-cnmnc/).

IMA No. 2009-046

Proposed structural formula: (Na,□)(Fe^{2+}, Mg)$_3$$Al_6$($BO_3$)$_3$$Si_6O_{18}$($OH$)$_4$
Localities: Cleveland tin mine, Luina, Waratah, Tasmania, Australia (41°28′57″S, 145°23′7″E; type locality); Mount Bendoc, Victoria, Australia (37°7′60″S, 148°54′0″E); Mount Bischoff, Tasmania, Australia (41°25′S, 145°31′E); Blue Mountain Saddle (Bald Hornet Claim), North Bend, King County, Washington, U.S.A. (47°31′N, 121°43′W).
Crystal system: Monoclinic: *Cm*; structure determined.
Representative cell dimensions (type material): a = 10.408(3), b = 15.991(5), c = 7.189(2) Å, β 117.44(2)°, V = 1061.88 Å^3

UM2000-//-SiO:AlBFLiNa (invalid list)

Proposed structural formula: Na(Al,Li)$_3$ Al_6 (BO_3)$_3$ Si_6 O_{18} (F,OH)$_4$
Comment: This is the fluorine-dominant analog of elbaite (e.g., Lussier et al. 2009). The suggested name "fluor-elbaite" has not yet been approved by the IMA-CNMNC.

UM2000-64-SiO:BFeHKMg

Proposed structural formula: (K,Na) (Fe^{3+})$_3$ (Fe^{3+},Mg)$_6$ (BO_3)$_3$ Si_6 O_{18} (OH,O)$_4$
Comment: This is a K-dominant tourmaline (Žáček et al. 2000).

Appendix 3. Color-based tourmaline varietal names

Although mineral varietal names are not under the jurisdiction of the IMA-CNMNC, the STN acknowledges the use of the color-based tourmaline varietal names. Appendix Table 1 is a listing of some of the varietal names that have been used, with possible tourmaline species associations.

Appendix 4. Obsolete or discredited tourmaline names

Throughout the history of tourmaline investigations several names have been used for tourmaline or minerals that were considered to be tourmaline. A list of former tourmaline names that are considered obsolete or have been discredited are presented in Appendix Table 2.

Appendix 5. Analytical considerations and normalization procedures

The crystal chemistry of tourmaline can be evaluated utilizing various analytical procedures, each with strengths and weaknesses that should be carefully considered when assessing the results and classifying a given tourmaline. Several of the techniques used specifically for tourmaline analysis are briefly mentioned below. Special attention is given to normalization procedures used for the electron microprobe data of tourmaline.

Bulk tourmaline analysis techniques

Several "bulk" sample techniques have been used to analyze tourmaline. The general disadvantage of these techniques is the averaging effect of "bulk" samples in which chemical zonation may be masked, and mineral and fluid inclusions may introduce contamination. (1) Wet chemical analysis was the standard procedure for analysis of materials prior to the widespread use of the electron microprobe (e.g., Peck 1964; Jarosowich 1966; Povondra and Čech 1976). The chief advantages were that light elements could be analyzed and oxidation states of transition elements were determined. (2) Inductively coupled plasma-atomic emission spectroscopy (ICP-AES) has commonly been used to supplement electron microprobe analysis by determining light element concentrations as well as trace element levels in tourmaline (e.g., Shearer and Papike 1986; Kantipuly et al. 1988). Sample amounts as small as 200–300 mg have been analyzed. (3) Induced neutron activation analysis (INAA) has been successfully used to determine REE in tourmaline (e.g., King et al. 1988; Roda et al. 1995).

Tourmaline structural refinement and spectroscopic analysis techniques

Single crystal refinement and spectroscopic techniques provide valuable information about the local environments of specific cations, trace elements and oxidation states of transition elements. (1) Crystal structure refinement is an electron-counting technique that, in combination with chemical analysis, helps determine the site assignments through definition of stereochemical relationships and refined site-scattering values (e.g., Hawthorne and Grice 1990; Hawthorne et al. 1995; Cámara et al. 2002). This technique exhibits spatial resolution that will work on well-constrained analytical problems such as those encountered in elbaite (Burns

Appendix Table 1. Color-based tourmaline varietal names

Varietal name	Description
Achroite	colorless tourmaline, probably elbaite or rossmanite
Aphrizite	dark gray schorl
Brazilian chrysolite	yellow-green tourmaline resembling chrysolite
Brazilian emerald	green and transparent tourmaline resembling emerald
Brazilian peridot	honey-brown to green tourmaline resembling peridot
Brazilian ruby	transparent red tourmaline resembling ruby
Brazilian sapphire	transparent blue tourmaline resembling sapphire
Canary tourmaline	bright yellow tourmaline
Cat's eye tourmaline	chatoyant tourmaline in a variety of colors
Ceylon chrysolite	yellow-green tourmaline resembling chrysolite
Ceylon peridot	honey yellow tourmaline resembling peridot
Chameleonite	alexandrite-like tourmaline; color changes under different lighting conditions
Cromolite	green tourmaline, originally considered Cr-bearing tourmaline
Deuterolite	alexandrite-like tourmaline, probably a Cr-bearing dravite; color changes under different lighting conditions
Emeralite	emerald-green tourmaline
Indicolite	blue tourmaline, probably elbaite-schorl series
Iochroite	violet tourmaline
Moor's Head tourmaline	light-colored tourmaline with black top
Paraibaíte	blue-green (neon blue) Cu-bearing elbaite, originally described from the Paraíba State of Brazil
Rubellite	pink or red tourmaline, probably elbaite
Siberian ruby	red tourmaline resembling ruby
Siberite	purple rubellite, probably elbaite
Verdelite	green tourmaline, probably elbaite-schorl series
Watermelon tourmaline	color-zoned tourmaline with pink interiors and green rims, generally elbaite

Note: Source of terms: Dietrich (1985).

Appendix Table 2. Obsolete, discredited, or misidentified tourmaline species

Name	Additional information
Aluminobuergerite	Term for suggested end-member $Na_{1-x}Al_3Al_6(BO_3)_3O_{3-x}(OH)_{1-x}$ or synthetic $NaAl_3Al_6(BO_3)_3O_3(OH)$
Alumoelbaite	Elbaite
Chrome tourmaline	Green Cr-bearing tourmaline or chromdravite
Cockle	Schorl
Coronite	Dravite
Eicotourmaline	Tourmaline-like mineral without boron
Ferridravite	Povondraite
Ferroelbaite	Schorl
Ferroschorlite	Schorl
Gouverneurite	Dravite
Iochroite	Tourmaline
Jochroit	Tourmaline
Lithia tourmaline	Elbaite
Magnesioschorlite	Dravite
Magnodravite	Extremely Mg-rich uvite-like tourmaline
Mineral H	Ti-rich tourmaline from pegmatites
Oxytourmaline	Tourmaline with noteworthy replacement of O for (OH,F)
Pierrepontite	Schorl
Schirl	Schorl
Schorlite	Schorl
Schorlomite	Name mistakenly used for schorl; schorlomite is an accepted garnet group mineral
Taltalite	Mixture of tourmaline with Cu-ore or green tourmaline
Titanschorl (schörl)	Rutile
Titantourmaline	Ti-rich tourmaline
Titanturmaline	Ti-rich tourmaline
Tsilaisite	Mn-rich tourmaline, mostly in solid solution with elbaite
Zeuxite	Acicular tourmaline, Fe^{3+}-rich tourmaline, green tourmaline

Note: Sources of terms: Wang and Hsu (1966); Fleischer (1969); Chukhrov (1981); Dietrich (1985); Bayliss (2000).

et al. 1994). (2) Secondary ion microprobe spectroscopy has provided information on spatial distribution of light elements as well as trace and minor elements in tourmaline (e.g., Wilson and Long 1983; Grew et al. 1990; Harris et al. 1992; Hawthorne et al. 1995). (3) Mössbauer spectroscopy has been used to evaluate Fe^{3+}/Fe^{2+} ratios as well as the locations of Fe^{2+} and Fe^{3+} in the tourmaline structure (e.g., Hermon et al. 1973; Gorelikova et al. 1978; Saegusa et al. 1979; Ferrow et al. 1988; Ferrow 1994; Dyar et al. 1998; Andreozzi et al. 2008), but this approach is also a bulk technique. (4) Proton-induced γ-ray emission has also been used for light-element analysis in tourmaline (e.g., Dyar et al. 1998).

Tourmaline electron microprobe analytical techniques

The electron microprobe is currently the most commonly used analytical tool for tourmaline analysis. However, there are several analytical limitations that must be considered when calculating a structural formula from electron microprobe data. Although it is possible to analyze most of the major elements in tourmaline, Li and H as well as the valence states of transition elements, cannot be directly measured. In addition, a critical constituent of tourmaline is the light element B. Boron has been analyzed with the electron microprobe (e.g., Bastin and Heijligers 2000; McGee and Anovitz 1996; Hawthorne et al. 1995), but the analytical accuracy and precision remain unsatisfactory for confident structural formula calculations. These shortcomings require that the normalization procedure for tourmaline be carefully considered to minimize the limitations of electron microprobe analysis. Because of a greatly improved understanding of tourmaline's crystal structure and chemistry as well as the constraints imposed by geochemical settings of tourmaline, estimation techniques for unanalyzed light elements and oxidation states are possible.

Normalization procedures, and light element and ferric Fe estimation

A variety of tourmaline normalization procedures have been used. Each procedure has strengths and weaknesses. However, the most appropriate procedure depends on the completeness of the tourmaline analysis, the quality of the analysis, the assumptions for unanalyzed elements and the petrologic environment in which the tourmalines develop.

Normalization of tourmaline with complete chemical characterization.

Ultimately, the best approach for determination of the structural formula of tourmaline is to analyze tourmaline as completely as possible and by using as many techniques as possible. With a complete analysis, normalization can be properly done on a 31 anion basis (Henry and Dutrow 1996; Clark 2007). The most accurate site assignments are made by means of crystal structure refinements with a combination of site-scattering and mean bond-length information and structural formula optimization procedure (e.g., Hawthorne and Grice 1990; Hawthorne et al. 1993; Taylor et al. 1995; Hawthorne 1996; Ertl et al. 2003a, 2003b; Bosi and Lucchesi 2004).

Normalization of electron microprobe data and estimation of light elements and oxidation states of elements.

Most widespread tourmaline normalization procedures make assumptions concerning the anionic and cationic assignments. In the absence of accurate analyses of B, O, H, Li and the oxidation states of transition elements, several procedures can be used to calculate a structural formula. Each of these procedures, in turn, can provide the basis for estimation of light elements and oxidation states of transition elements.

Normalization procedure 1—fixed number of O atoms. Assume OH fills the four V+W sites after accounting for F and Cl. In essence, this implies normalization of the cations on the basis of 31 anions (O + F + OH), 29 oxygen atoms (both normalization assuming B is calculated by stoichiometry, B = 3 apfu) or 24.5 oxygen atoms (without B calculation). Generally, this approach provides a good first approximation (Clark 2007). However, if there is significant O^{2-} substitution for OH^{1-}, the oxygen normalization factor will be underestimated as will be the number of cations. In fact, significant amounts O^{2-} substitution for OH^{-1} have been demonstrated in uvite (Taylor et al. 1995) and in several other tourmaline compositions (e.g., Povondra 1981; Povondra and Novák 1986; Dyar et al. 1998). Consequently, this approach should be used with those tourmalines in which it is reasonably assured that OH+F+Cl~4 (e.g., Burns et al. 1994).

Normalization procedure 2—fixed Y+Z+T cations. Normalize the sum of the T+Z+Y cations to 15. *This is the recommended normalization approach for tourmaline with low Li contents and minor B in the tetrahedral site.* It assumes that there are no vacancies in the Y, Z and T sites, a valid assumption based on a majority of crystal structure refinement data. It also assumes that the amount of tetrahedral B is not significant. However, some recent refinement results indicate small numbers of vacancies in Y and Z sites (<0.22 apfu; Ertl et al. 1997, 2003b; Prowatke et al. 2003). To the extent that all of the significant cations on these sites are accurately analyzed, the structural formula can be calculated without having to rely on estimates of the OH content or valence states of transition elements. Fortunately, those tourmaline containing even a moderate amount of Mg (>0.02 apfu) and that coexist with minerals such as biotite, muscovite and staurolite typically have minor-to-insignificant amounts of Li due to the preferential partitioning of Li into these coexisting minerals (Henry and Dutrow 1996). This normalization procedure will be appropriate for almost all metamorphic and most igneous tourmalines.

Normalization procedure 3—fixed Si. Normalize on the basis of Si = 6. This procedure is useful for normalization of tourmalines with significant amounts of unanalyzed elements, particularly Li. It assumes that there is no significant tetrahedral Al or B. For many Li-rich tourmalines this general assumption is probably reasonable (e.g., Dutrow and Henry 2000). However, many low-Li tourmalines are known to contain significant amounts of tetrahedral Al and B, so that this procedure should be used with care in these instances (e.g., Hawthorne et al. 1993; Lussier et al. 2009).

Estimation of B. Based on the total B found in a series of high-quality wet-chemical analyses of tourmaline from various lithologies, Henry et al. (2002) indicate that the assumption that B fully occupies the triangular B site and can be calculated using stoichiometric constraints (i.e., B = 3) is likely to be valid for most petrologic occurrences of tourmaline (see also Clark 2007). Furthermore, crystal structure refinements and bond valence calculations indicate that there are essentially 3 B apfu in those tourmalines that have been determined to date (Hawthorne 1996). However, there are a few uncommon instances involving Al-rich tourmaline (e.g., olenite) in which some B may also be tetrahedral (Ertl et al. 1997, 2006a; Tagg et al. 1999; Hughes et al. 2000). This feature indicates that the assumption of 3 B may not be valid in all cases, but is likely to be reasonable for most tourmalines.

Estimation of Li. Li can be approximated by assuming that Li fills any cation deficiency in the Y site. However, this requires that the formula be calculated either on a fixed cation basis (e.g., Si = 6, see Dutrow and Henry 2000) or that Li be iteratively calculated using a fixed number of oxygens and assuming OH+F = 4 (e.g., Burns et al. 1994; Clark 2007). (1) The Si = 6 approach appears to work well for some Li-rich tourmaline (Li >0.7 apfu), but tends to underestimate the Li contents (Henry et al. 2002). The underestimate of Li is likely due to the existence of tetrahedral Al substituting for Si will result in calculated Li being too low. Henry et al. (2002) indicate that this procedure should be within 0.1–0.3 apfu of the correct Li values. (2) The Li by iteration and OH+F = 4.0 approach tends to result in high estimates of Li (Henry et al. 2002). For tourmalines with high values of Li (>0.7 apfu) this generally results in an overestimate of 0.1–0.3 Li apfu. This is a more significant problem in low-Li tourmalines, and generally appears to indicate that these tourmalines contain significant amounts of Li. The Li overestimates are a consequence of substantial amounts of substitution of O for OH+F in the W and V sites in many tourmalines or can result because of the occurrence of significant vacancies at the Y site in Al-rich tourmalines. Nonetheless, this procedure is very useful for tourmaline developed in Li-enriched environments (e.g., highly fractionated granitic pegmatites).

Estimation of H. H contents can be determined by charge balance if oxidation states can be measured or inferred, and Li contents can be estimated or inferred. Putative oxidation state evidence can be derived from tourmaline optical properties or by mineral assemblages, particularly graphite-bearing assemblages (Dyar et al. 1998). Minimal Li contents can be generally inferred by presence of significant Mg in tourmaline, which is a function of coexisting mineral assemblages that tend to efficiently partition Li (Henry and Dutrow 1996). Charge-balance estimates of H are subject to significant amounts of uncertainty, and likely result in minimum values of H. Despite the larger amounts of uncertainty, useful information on H contents can be derived using electron microprobe data (e.g., Henry et al. 2002).

Estimation of Fe oxidation states. Fe^{3+} contents can be determined by charge balance if H contents can be measured or inferred, and Li contents can be estimated or inferred. Despite the larger amounts of uncertainty, useful information on Fe^{3+} contents can be derived using electron microprobe data (e.g., Henry et al. 1999). However, all these procedures can have relatively large errors. The best way would be to employ techniques such as Mössbauer spectroscopy to determine the Fe^{2+}/Fe^{3+} ratio (e.g., Dyar et al. 1998). In some instances, the Fe^{2+}/Fe^{3+} ratio can be inferred for tourmalines found in certain mineral assemblages. For example, Dyar et al. (2002) found that tourmaline from graphite-bearing metapelites contained 20–34% of the total Fe as Fe^{3+}.

Appendix 6. Representative tourmaline analyses with diagnostic parameters for classification

To illustrate the manner in which various parameters are determined for use in the tourmaline nomenclature scheme, several tourmaline analyses from the literature are given in Appendix Table 3. These represent a range of tourmaline species and demonstrate the manner in which an ordered tourmaline is written and presents some of the important chemical parameters used for classification.

Appendix Table 3. Examples of complete tourmaline analyses with ordered structural formula and important parameters used for classification

Data source	Grice and Ercit (1993)						Povondra et al. (1998)
Sample no.	144478	49356	43293	43167	43873	55224	PAFG - Pr1
			Oxides				
B_2O_3	9.17	10.36	10.14	10.83	10.33	11.56	10.18
SiO_2	30.74	33.58	32.92	34.04	35.27	36.50	34.88
Al_2O_3	1.40	30.62	30.70	27.33	26.69	40.07	32.31
TiO_2		1.63	0.54	0.39	0.52		0.67
V_2O_3	0.04						
Fe_2O_3	43.89	0.86	12.37	7.63	5.46		1.20
FeO	2.69	12.65	5.98	4.91	2.20	0.22	12.66
MnO		0.06	0.11			3.07	0.21
MgO	6.45	2.69	0.16	7.34	10.77		1.60
Li_2O		0.03		0.01	0.00	1.61	0.06
CaO			0.20	0.99	1.67	0.20	0.41
Na_2O	2.12	2.84	2.49	2.35	2.15	2.15	2.24
K_2O	1.04	0.06	0.07		0.05		0.23
F		0.34	1.32		0.79	1.24	0.61
H_2O	2.56	2.96	1.15	3.18	2.92	3.13	2.57
Subtotal	100.10	98.68	98.15	99.00	98.82	99.75	99.83
O=F		0.14	0.56		0.33	0.52	0.26
Total	100.10	98.54	97.59	99.00	98.49	99.22	99.57
			31 O atoms normalization				
Total B	3.059	3.089	3.099	3.173	3.001	3.181	3.007
B site: B	3.000	3.000	3.000	3.000	3.000	3.000	3.000
T site: Si	5.941	5.801	5.829	5.778	5.935	5.818	5.969
B	0.059	0.089	0.099	0.173	0.001	0.181	0.007
Al	0.000	0.110	0.072	0.049	0.064	0.001	0.025
T-site Total	6.000	6.000	6.000	6.000	6.000	6.000	6.000
Al (Total)	0.319	6.234	6.407	5.467	5.294	7.528	6.516
Z site: Al	0.319	6.000	6.000	5.418	5.230	6.000	6.000
V^{3+}	0.006						
Fe^{3+}	5.675			0.582	0.691		
Mg^{2+}					0.079		
Z-site Total	6.000	6.000	6.000	6.000	6.000	6.000	6.000
Y site: Al		0.125	0.335			1.526	0.491
Ti		0.212	0.072	0.050	0.066		0.086
Fe^{3+}	0.707	0.112	1.648	0.392			0.155
Fe^{2+}	0.435	1.828	0.886	0.697	0.310	0.029	1.812
Mn^{2+}		0.009	0.016			0.414	0.030
Mg	1.858	0.693	0.042	1.857	2.623		0.408
Li		0.022		0.003	0.002	1.030	0.041
Y-site Total	3.000	3.000	3.000	3.000	3.001	3.000	3.024
Ca			0.038	0.180	0.301	0.034	0.075
Na	0.794	0.951	0.855	0.773	0.702	0.664	0.743
K	0.256	0.013	0.016		0.011		0.050
X-site vacancy		0.036	0.091	0.047		0.301	0.131
X-site Total	1.051	1.000	1.000	1.000	1.013	1.000	1.000
V+W site: OH	3.300	3.411	1.358	3.600	3.278	3.328	2.933
V site: OH	3.000	3.000	1.358	3.000	3.000	3.000	2.933
V site: O			1.642				0.067
W site OH	0.300	0.411		0.600	0.278	0.328	
W site: F		0.186	0.739		0.420	0.625	0.330
W site O	0.700	0.403	0.261	0.400	0.302	0.047	0.670
V,W-site Total	4.000	4.000	4.000	4.000	4.000	4.000	4.000
X-site primary group:	Alkali	Alkali	Alkali	Alkali	Alkali	Alkali	Alkali
W-site species series:	Oxy-	Hydroxy-	Fluor-	Hydroxy-	Fluor-	Fluor-	Oxy-
V-site dominant anion:	OH	OH	O	OH	OH	OH	OH
Y-site dominant divalent cation:	Mg^{2+}	Fe^{2+}	Fe^{2+}	Mg^{2+}	Mg^{2+}	Mn^{2+}	Fe^{2+}
Y-site dominant trivalent cation:	Fe^{3+}	Al^{3+}	Fe^{3+}	Fe^{3+}		Al^{3+}	Al^{3+}
Z-site dominant trivalent cation:	Fe^{3+}	Al^{3+}	Al^{3+}	Al^{3+}	Al^{3+}	Al^{3+}	Al^{3+}
Plotting parameters							
$R^{2+}/(R^{2+} + 2Li)$	1.000	0.983	1.000	0.997	0.999	0.177	0.965
Ca/(Ca+Na+K)			0.042	0.189	0.297	0.049	0.087
Vac/(Na+K+Vac)		0.036	0.095	0.057		0.312	0.142
W site O/(O+OH+F)	0.700	0.403	0.261	0.400	0.302	0.047	0.670
			Alkali group				
Subgroup	subgroup 3	subgroup 1	subgroup 5	subgroup 1	subgroup 1	subgroup 2	subgroup 3
Tourmaline species	Povondraite	Schorl	Fluor-buergerite	Dravite	Fluor-dravite	"Fluor-elbaite"	"Oxy-schorl"

American Mineralogist, Volume 73, pages 1123–1133, 1988

Nomenclature of pyroxenes

Subcommittee on Pyroxenes
Commission on New Minerals and Mineral Names
International Mineralogical Association

N. Morimoto, Chairman
Department of Geology and Mineralogy, Kyoto University, Kyoto 606, Japan

Subcommittee Members
J. Fabries (France), **A. K. Ferguson** (Australia) **I. V. Ginzburg** (USSR), **M. Ross** (U.S.A.), **F. A. Seifert** (Germany), **J. Zussman** (U.K.)

Nonvoting Members
K. Aoki (Japan), **G. Gottardi** (Italy)

Abstract

This is the final report on the nomenclature of pyroxenes by the Subcommittee on Pyroxenes established by the Commission on New Minerals and Mineral Names of the International Mineralogical Association. The recommendations of the Subcommittee as put forward in this report have been formally accepted by the Commission. Accepted and widely used names have been chemically defined, by combining new and conventional methods, to agree as far as possible with the consensus of present use. Twenty names are formally accepted, among which thirteen are used to represent the end members of definite chemical compositions. In common binary solid-solution series, species names are given to the two end members by the "50% rule." Adjectival modifiers for pyroxene mineral names are defined to indicate unusual amounts of chemical constituents. This report includes a list of 105 previously used pyroxene names that have been formally discarded by the Commission.

Introduction

The Subcommittee on Pyroxenes has, after a thorough evaluation of the group of pyroxene minerals, presented its recommendations for a new classification and nomenclature to the Commission on New Minerals and Mineral Names (hereafter abbreviated as CNMMN). These recommendations have been approved by the Commission by a formal vote (May 20, 1987).

The classification and nomenclature of the pyroxenes have been largely based on their crystal chemistry. In practice the chemical content of the pyroxene formula unit calculated to six oxygens, or to four cations (Vieten and Hamm, 1978), is essential for the classification. This formula unit corresponds to one-quarter of the unit cell for the monoclinic pyroxenes and to one-eighth of the unit cell for the orthorhombic pyroxenes. The basic principle adopted for amphibole nomenclature (Leake and Winchell, 1978) is to denote principal stoichiometries by generally well-established names, with adjectival modifiers to indicate the presence of substantial substitutions that are not essential constituents of the end members; this principle has been followed as far as possible in the pyroxene nomenclature.

No new names have been introduced in the proposed nomenclature. Accepted and widely used names have been chemically defined by combining new and conventional methods to agree as far as possible with the consensus of present use. Two kinds of adjectival modifiers are used: one to specify a part of the compositional range shown by a mineral that forms a wide solid solution [e.g., magnesium-rich (or Mg-rich) augite and iron-rich (or Fe-rich) augite]; the other to specify elemental substitutions that are not essential constituents (e.g., titanian augite). The CNMMN has formally discredited 105 previously used pyroxene names—mostly synonyms, obsolete or almost unused, or recommended for rejection.

General publications dealing with the pyroxene group include *Rock-Forming Minerals* (Deer et al., 1978), Mineralogical Society of America Special Paper 2 (Papike, 1969) and MSA *Reviews in Mineralogy,* volume 7 (Prewitt, 1980), which provide references to the voluminous literature.

Crystal chemistry of the pyroxenes

Pyroxenes are silicates that, in their simplest form, contain single SiO_3 chains of linked SiO_4 tetrahedra. Generally, small amounts of Si are replaced by Al and other small cations. The repeat along the chain (*c* axis) comprises two tetrahedra and is approximately 0.52 nm in length. The general chemical formula (formula unit) for all pyroxenes[1] is $M2M1T_2O_6$, where M2 refers to cations

[1] In omphacite-*P2/n*, the M1 and M2 sites are further divided into M1a and M1b (for M1) and M2a and M2b (for M2).

0003–004X/88/0910–1123$02.00

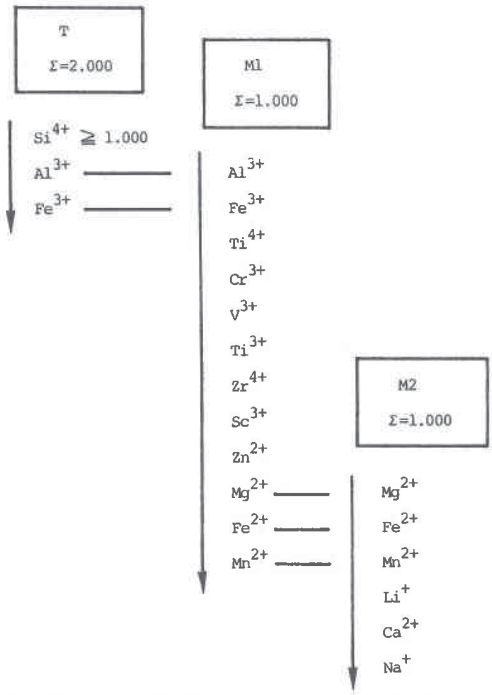

Fig. 1. Flow chart for ideal site occupancy of cations between the T, M1, and M2 sites of pyroxenes. Only representative cations are included. Arrows indicate order of filling of sites. Real site occupancy is usually slightly different from the ideal site occupancy.

in a generally distorted octahedral coordination, M1 to cations in a regular octahedral coordination, and T to tetrahedrally coordinated cations.

Any pyroxene belongs to either the orthorhombic or the monoclinic crystal system. There are two orthorhombic pyroxene types: orthopyroxene (*Pbca*) and orthopyroxene (*Pbcn*).[2] Only the former has been found in nature. Monoclinic pyroxenes are called clinopyroxenes. Their space groups are $C2/c$, $P2_1/c$, and $P2/n$, depending on their chemical composition and petrogenetic history.

Throughout this report, the standard pyroxene formula is used with superscripted arabic numerals (e.g., Fe^{2+}) referring to charges and subscripted numerals (e.g., Mg_2) referring to numbers of atoms.

In order to derive a pyroxene formula from a chemical analysis, the calculation should be based on six oxygen atoms when Fe^{2+} and Fe^{3+} are both determined. In microprobe analyses, only total Fe is determined, and the option of calculating to four cations should at least be permitted if not actually preferred. Vieten and Hamm (1978) have shown that calculation to four cations will be more reliable for microprobe analyses of the majority of pyroxenes. Therefore, for microprobe analyses, it is recommended that the components be totaled to six oxygens and four cations by adjusting the ratios Fe^{2+}/Fe^{3+}, Ti^{4+}/Ti^{3+}, etc.

The standard pyroxene formula $M2M1T_2O_6$ contains two tetrahedral sites. In the allocation of the cations to obtain a pyroxene formula, the following procedure is recommended:

1. Sum T to 2.000 using Si^{4+}, then Al^{3+}, and then Fe^{3+}.
2. Sum M1 to 1.000 using all Al^{3+} and Fe^{3+} in excess of that used to fill the T sites. If there is insufficient Al^{3+} and Fe^{3+} to sum to 1.000, then add Ti^{4+}, Cr^{3+}, V^{3+}, Ti^{3+}, Zr^{4+}, Sc^{3+}, Zn^{2+}, Mg^{2+}, Fe^{2+}, and finally Mn^{2+} until the sum is 1.000.
3. Sum M2 using all Mg^{2+}, Fe^{2+}, and Mn^{2+} in excess of that used to fill the M1 sites. Then add Li^+, Ca^{2+}, and Na^+ so that the sum becomes 1.000 or close to it. If the sum is far from 1.000, one must be suspicious about the results of the analysis.

A flow chart (Fig. 1) gives a diagrammatic representation of the site allocation of the principal cations in pyroxenes. However, because the distribution of cations among the M1, M2, and T sites in a given pyroxene is partly a function of temperature, the accurate site occupancy must be determined by structure determination. The site occupancy given in Figure 1 is called ideal site occupancy to distinguish it from real occupancy. A method for classifying pyroxenes by their ideal site occupancies has been proposed by Bokij and Ginzburg (1985). In the present classification of pyroxenes, the M1 and M2 sites are considered together as a single M site in order to avoid the difference between the real and ideal site occupancies.

Starting from the most common pyroxene formula, $M2(R^{2+})M1(R^{2+})T_2(2R^{4+})O_6$, four coupled substitutions are possible if one assumes more than one R^{4+} in the T site. They are listed in Table 1, where the elements in parentheses are coupled substitutions.

Substitution 1 encompasses the end members jadeite ($NaAlSi_2O_6$), aegirine[3] ($NaFe^{3+}Si_2O_6$), kosmochlor[4] ($NaCr^{3+}Si_2O_6$, Ko), and jervisite ($NaScSi_2O_6$, Je). Substitution 2 results in components such as $NaFe^{2+}_{0.5}Ti^{4+}_{0.5}Si_2O_6$, but is less important than the other substitutions.

In substitution 3, the Al-Al couple is often referred to as "Tschermak's component"; $CaAlAlSiO_6$, in particular, is called "calcium Tschermak's component." Substitution in esseneite,[5] $CaFe^{3+}AlSiO_6$, is obtained by this type of substitution. This substitution is also important in

[2] Orthopyroxene (*Pbcn*) is stable only at elevated temperatures for a limited composition near $MgSiO_3$.

[3] "Aegirine" is used in preference to "acmite" in this report. "Aegirine" is in common usage in the literature and is consistent with the almost universal use of "aegirine-augite" for minerals of intermediate compositions, though "acmite" has priority by 14 years (Dana, 1892). Common practice in experimental petrology has been to use the abbreviation Ac for $NaFe^{3+}Si_2O_6$; Ae should now be used instead.

[4] The CNMMN, IMA, has recently voted in favor of the name "kosmochlor" instead of "ureyite" for the pyroxene of generalized composition $NaCrSi_2O_6$.

[5] Esseneite is a new pyroxene with the composition $CaFe^{3+}AlSiO_6$ (Table 2, no. 13).

TABLE 1. Four coupled substitutions* of pyroxenes in the standard chemical formula $R^{2+}R^{2+}R^{4+}_2O_6$

	Substitution site			
	M2	M1	T	Examples
Standard occupancy	R^{2+}	R^{2+}	$2R^{4+}$	
Substitution 1	(R^{+})	(R^{3+})	$2R^{4+}$	Na-Al Na-Fe^{3+} Na-Cr^{3+} Na-Sc^{3+}
Substitution 2	(R^{+})	$R^{2+}_{0.5}(R^{4+}_{0.5})$	$2R^{4+}$	Na-(Ti^{4+}/2)
Substitution 3	R^{2+}	(R^{3+})	(R^{3+})R^{4+}	Al-Al Fe^{3+}-Al Cr^{3+}-Al
Substitution 4	R^{2+}	$R^{2+}_{0.5}(R^{4+}_{0.5})$	(R^{3+})R^{4+}	(Ti^{4+}/2)-Al

* Shown by parentheses.

"fassaite."[6] Substitution resulting in $CaTi^{3+}AlSiO_6$ was reported by Dowty and Clark (1973) and Mason (1974) in pyroxenes from the Allende meteorite (Table 3, no. 4). In substitution 4, the component $CaMg_{0.5}Ti^{4+}_{0.5}AlSiO_6$ is found in some pyroxenes. There are a few instances of the component of substitution 2 or 4 amounting to nearly 50%, as described later (Table 3). However, no particular names are given for the end-member components of substitutions 2 and 4.

[6] "Fassaite" has the general formula $Ca(Mg,Fe^{3+},Al)(Si,Al)_2O_6$. This name has been rejected as a formal name in this report.

MINERAL NAMES OF THE PYROXENES

Twenty (20) mineral names and their grouping

The pyroxenes form extensive solid solutions by various types of ionic substitutions, some of which are described above. To cope with the problem of pyroxene nomenclature, it is necessary to subdivide the solid-solution series into ranges with specified compositions and names. Whenever there is a complete solid-solution series between two end members, it is customary in mineral nomenclature to use only two names, and the division between them should be at $A_{50}B_{50}$ (the "50% rule"). However, this "50% rule" cannot be applied rigorously to the large groups of pyroxenes that show wide ranges of coupled substitutions. This is particularly so when the minerals concerned are abundant and widespread and have a historically established nomenclature in mineralogical and petrological circles. Taking this situation into consideration, 20 accepted and widely used names have been adopted as mineral species names of the pyroxenes (Table 2).

The definition of the pyroxene species has been based on 13 end members, or chemical components (given in

TABLE 2. Accepted pyroxene mineral names and their chemical subdivisons

Mineral names	Composition as end member	Main composition as solid solution	Space group
A. Mg-Fe pyroxenes			
1. **enstatite (En)**	$Mg_2Si_2O_6$	$(Mg,Fe)_2Si_2O_6$	*Pbca*
2. **ferrosilite (Fs)**	$Fe^{2+}_2Si_2O_6$		
3. clinoenstatite		$(Mg,Fe)_2Si_2O_6$	$P2_1/c$
4. clinoferrosilite			
5. pigeonite		$(Mg,Fe,Ca)_2Si_2O_6$	$P2_1/c$
B. Mn-Mg pyroxenes			
6. donpeacorite		$(Mn,Mg)MgSi_2O_6$	*Pbca*
7. **kanoite (Ka)**	$MnMgSi_2O_6$	$(Mn,Mg)MgSi_2O_6$	$P2_1/c$
C. Ca pyroxenes			
8. **diopside (Di)**	$CaMgSi_2O_6$	$Ca(Mg,Fe)Si_2O_6$	$C2/c$
9. **hedenbergite (Hd)**	$CaFe^{2+}Si_2O_6$		
10. augite		$(Ca,Mg,Fe)_2Si_2O_6$	$C2/c$
11. **johannsenite (Jo)**	$CaMnSi_2O_6$		$C2/c$
12. **petedunnite (Pe)***	$CaZnSi_2O_6$		$C2/c$
13. **esseneite (Es)****	$CaFe^{3+}AlSiO_6$		$C2/c$
D. Ca-Na pyroxenes			
14. omphacite		$(Ca,Na)(R^{2+},Al)Si_2O_6$	$C2/c$, $P2/n$
15. aegirine-augite		$(Ca,Na)(R^{2+},Fe^{3+})Si_2O_6$	$C2/c$
E. Na pyroxenes			
16. **jadeite (Jd)**	$NaAlSi_2O_6$	$Na(Al,Fe^{3+})Si_2O_6$	$C2/c$
17. **aegirine (Ae)**	$NaFe^{3+}Si_2O_6$		
18. **kosmochlor (Ko)**	$NaCr^{3+}Si_2O_6$		$C2/c$
19. **jervisite (Je)**†	$NaSc^{3+}Si_2O_6$		$C2/c$
F. Li pyroxene			
20. **spodumene (Sp)**	$LiAlSi_2O_6$		$C2/c$

Note: Name, abbreviation, and composition are given for any pyroxene that is used as an end member of a pyroxene solid solution; such end members are printed in boldface type. Main compositions are given for solid solutions. Space groups are also given.

* Petedunnite has been determined by Essene and Peacor (1987) to have the composition $(Ca_{0.92}Na_{0.06}Mn_{0.02})(Zn_{0.37}Mn_{0.19}Fe^{2+}_{0.19}Fe^{3+}_{0.12}Mg_{0.14})(Si_{1.94}Al_{0.06})O_6$ by means of an electron microprobe. This mineral was approved as a valid species by the CNMMN, IMA, in 1983.

** Esseneite has been determined by Cosca and Peacor (1987) to have the composition $(Ca_{1.01}Na_{0.01})(Fe^{3+}_{0.72}Mg_{0.16}Al_{0.04}Ti_{0.03}Fe^{2+}_{0.02})(Si_{1.19}Al_{0.81})O_{6.00}$ by means of an electron microprobe. This mineral was approved as a valid species by the CNMMN, IMA, in 1985.

† Jervisite has been determined by M. Mellini et al. (1982) to have the composition $(Na_{0.43}Ca_{0.31}Fe^{2+}_{0.14}\square_{0.12})(Sc_{0.66}Fe^{2+}_{0.15}Mg_{0.19})Si_2O_6$ by means of an electron microprobe. This mineral was approved as a valid species by the CNMMN, IMA, in 1982.

bold face in Table 2) and the component $Ca_2Si_2O_6$ (Wo).[7] These end members are given the names of the minerals whose compositions they most closely approximate. The 20 pyroxene species are grouped into six chemical subdivisions on the basis of the cation occupancy of the M2 sites and crystal-chemical similarity. This classification is a slight modification of the widely used scheme proposed by Deer et al. (1978).

For the precise classification of the pyroxenes into 20 mineral species, however, the following characteristics of the pyroxenes must be considered. First of all, the Mg-Fe pyroxenes and some of the Ca pyroxenes are the most common rock-forming pyroxenes and form wide solid solutions that cover the pyroxene quadrilateral of the ternary $Ca_2Si_2O_6$ (Wo)–$Mg_2Si_2O_6$ (En)–$Fe_2Si_6O_6$ (Fs) system. Therefore, these pyroxenes are better treated together as the Ca-Mg-Fe or "quadrilateral" pyroxenes. Second, Na pyroxenes form continuous solid-solution series with the Ca-Mg-Fe pyroxenes, forming the Na-Ca pyroxenes. Third, donpeacorite and kanoite in the Mn-Mg pyroxenes, johannsenite, petedunnite, and esseneite in the Ca pyroxenes, and spodumene are rare in occurrence and unique in chemistry. For simplicity they are treated together as "other" pyroxenes.[8]

All the pyroxenes are thus divided into four chemical groups for the purpose of broad classification: Ca-Mg-Fe pyroxenes (**Quad**, 8), Ca-Na pyroxenes (**Ca-Na**, 2), Na pyroxenes (**Na**, 4) and other pyroxenes (**Others**, 6). The abbreviations of the groups and the numbers of the accepted species are given in parentheses. **Quad** represents "quadrilateral" for the Ca-Mg-Fe pyroxenes. The four chemical groups are further divided into 20 mineral species by using 12 components (the Wo component is used for the Di and Hd components). The composition ranges for the accepted names will be given later in this report.

The pyroxene names may be qualified by one or more adjectival modifiers according to definite rules described later in this report to specify important (though relatively minor) departures from the composition ranges. When the composition range of the mineral species is large, as in augite, one or more adjectival modifiers are used to specify the composition more clearly (e.g., subcalcic augite, Fe-rich augite).

Application of 50% rule

The 50% rule has been applied to complete solid-solution series between two end members as far as possible. They are the Mg-Fe pyroxene series (enstatite-ferrosilite and clinoenstatite-clinoferrosilite series), Ca pyroxene series (diopside-hedenbergite series) and Na pyroxene series (jadeite-aegirine series). Subdivision names of the intermediate solid-solution ranges, such as bronzite, hypersthene, and eulite of the enstatite-ferrosilite series and salite and ferrosalite of the diopside-hedenbergite series, have been discarded. However, the 50% rule was not applied rigorously to the Ca-Mg-Fe pyroxenes and Na-Ca pyroxenes. The widely accepted terms such as augite, pigeonite, omphacite, and aegirine-augite[9] have been retained.

Gem names of spodumene

Two names, "hiddenite" and "kunzite," are often used for (pale) emerald-green– and lilac–colored spodumene of gem quality, respectively. They are not accepted as formal pyroxene names, but can be used as varietal gem names.

Relationships with the pyroxenoids

Pyroxenoids are closely related to pyroxenes in that they have a similar type of chemical composition and a structure that also consists of SiO_3 single chains. However, the repeat of the chains, which is two SiO_4 tetrahedra in the pyroxenes, is three or more SiO_4 tetrahedra in the pyroxenoids. Although the tetrahedral sites in both the pyroxenes and the pyroxenoids are mostly occupied by Si ions, the large cations in the pyroxenoids are mostly Ca, Mn, and Fe^{2+} ions. The classification and nomenclature of the pyroxenoids are beyond the scope of this report. However, the following two points may be noted. First, there is a polymorphic relationship with some pyroxenes such as ferrosilite, hedenbergite, and johannsenite. These show pyroxenoid structures at high temperatures or pressures. Second, the wollastonite chemical component ($Ca_2Si_2O_6$) is used to express the composition of the Ca-Mg-Fe pyroxenes, though wollastonite belongs to the pyroxenoid structural group.

Classification and nomenclature of the pyroxenes

Preliminary classifications: Construction of the *Q-J* diagram and application of pyroxene data

Before classifying the pyroxenes into the 20 mineral species listed in Table 2, the following procedure is recommended to divide them into four chemical groups: Ca-Mg-Fe pyroxenes (**Quad**), Na-Ca pyroxenes (**Na-Ca**), Na pyroxenes (**Na**), and other pyroxenes (**Others**) (Morimoto and Kitamura, 1983).

In this procedure the pyroxenes are classified by using the total numbers of specified cations at the M (M1 and M2) sites on the basis of six oxygens. The M1 and M2 sites are considered together as M sites, without considering the site preference of atoms between the two sites.

The numbers of Ca, Mg, Fe^{2+}, and Na cations in the M sites are plotted in the *Q-J* diagram (Fig. 2) as Q = Ca + Mg + Fe^{2+} and J = 2Na. The lines representing the

[7] $Ca_2Si_2O_6$ exists as wollastonite in nature, which belongs not to the pyroxenes but to the pyroxenoids. To represent the compositions of the Ca-Mg-Fe pyroxenes, the ternary $Ca_2Si_2O_6$ (Wo)–$Mg_2Si_2O_6$ (En)–$Fe_2Si_2O_6$ (Fs) system has been used, e.g., $En_{20}Fs_{38}Wo_{42}$.

[8] Definition of the "Other pyroxenes" is different from that given by Cameron and Papike (1981).

[9] The name "aegirine-augite" appears to be in more common usage than "aegirineaugite," and "acmite-augite."

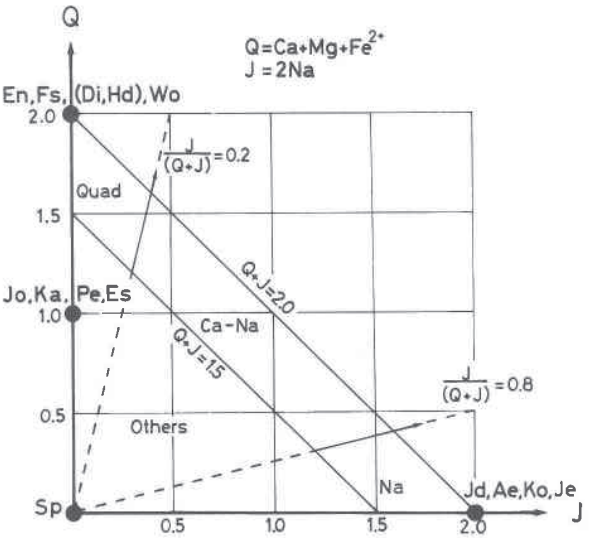

Fig. 2. *Q-J* diagram for the pyroxenes, on which the positions of the 13 accepted end members have been indicated. Abbreviations and compositions of the end members are listed in Table 2.

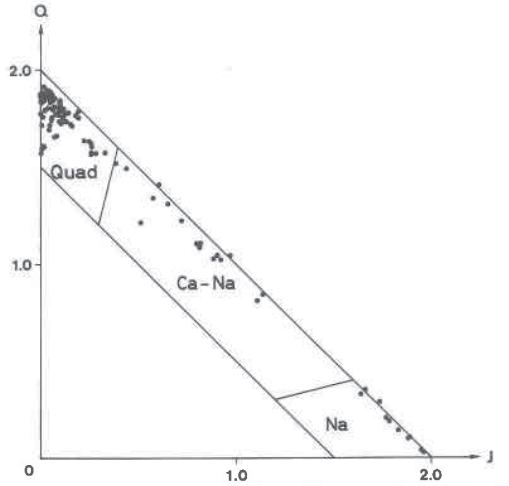

Fig. 3. The 103 pyroxenes from Deer et al. (1978) selected by Cameron and Papike (1981) plotted on the *Q-J* diagram. For these pyroxenes, the *Q* values are less than 1.90, and Mn is less than 0.08 atoms per formula unit.

following equations are used to subdivide the *Q-J* diagram:

$$Q + J = 2.0 \quad (1)$$
$$Q + J = 1.5 \quad (2)$$
$$J/(Q + J) = 0.2 \quad (3)$$
$$J/(Q + J) = 0.8. \quad (4)$$

The areas corresponding to the Ca-Mg-Fe pyroxenes, Ca-Na pyroxenes, Na pyroxenes, and other pyroxenes are labeled (Fig. 2) **Quad**, **Ca-Na**, **Na**, and **Others**, respectively.

In this diagram, *J* is meant to include the total number of Na and R^{3+}, usually Al, Fe^{3+}, Cr^{3+}, and Sc^{3+}, that couple with Na in substitution 1 mentioned in Table 1. When the coupled substitution in the pyroxene is not of type 1 but of type 2 or 3, the *J* value apparently does not represent the real numbers of Na and R^{3+} at the M sites. However, substitution 3 (e.g., Al-Al) works to move the *J* and *Q* values closer to the origin of the *Q-J* diagram, and substitution 2 (e.g., Na-Ti^{4+}) to move the *J* value farther away from the *Q* axis of ordinates. Therefore, the effects of substitutions 2 and 3 tend to cancel each other out in and near the area of the Na pyroxenes. Thus the *J* (= 2Na) values in the Na-rich pyroxenes represent, to a good approximation, the total number of Na and R^{3+} (Al, Fe^{3+}, Cr^{3+}, and Sc^{3+}) at the M sites.

The boundary $Q + J = 2.0$ represents the upper limit of $Q + J$ at the M sites. The boundary $Q + J = 1.5$ represents the limit below which more than half of the M1 or M2 sites may be occupied by ions other than *Q* and *J* ions. In this case, the pyroxenes are considered as belonging to Others, which include the Mn-Mg and Li pyroxenes, johannsenite, petedunnite, and esseneite. Equations 3 and 4 represent the lines dividing the area limited by the two above-mentioned $Q + J$ lines into Ca + Mg + Fe (Quad), Ca-Na, and Na pyroxenes. The boundaries defined by $J/(Q + J) = 0.2$ and 0.8 are used by Deer et al. (1978) and Cameron and Papike (1981).

Because the Mn-Mg pyroxenes and johannsenite (Table 2) have Mn ions occupying more than half of the M2 and M1 sites, respectively, they have *Q* values between 1.0 and 1.5 in the *Q-J* diagram. Similarly, petedunnite and esseneite plot along the *Q* axis with *Q* values between 1.0 and 1.5. Spodumene plots at the origin of the *Q-J* diagram because both *Q* and *J* are zero. Thus, the thirteen end members (Table 2) and Wo are located in the *Q-J* diagram (Fig. 2).

Application of this classification procedure to 406 pyroxene analyses presented in Deer et al. (1978) has shown that most of the analyses, except those of johannsenite and spodumene, are included in the area between the lines $Q + J = 2.0$ and $Q + J = 1.5$. The 103 Deer et al. (1978) pyroxenes selected by Cameron and Papike (1981), for which the *Q* values are less than 1.90 and Mn is less than 0.08 atoms per formula units, are plotted in the *Q-J* diagram of Figure 3. The "CaMgTAL" pyroxene (Cameron and Papike, 1981) is included in the Quad area as described later in this report (Table 3, no. 1). Only 20 analyses among 406 plot slightly over the line $Q + J = 2.0$, and most of these show unusual total numbers of cations. The results of the classification of the pyroxenes into the four chemical groups by this procedure are in almost complete agreement with the results obtained by Deer et al. (1978) and by Cameron and Papike (1981). A few unusual pyroxenes with Mn less than 0.08 atoms for the chemical formula unit have been found to lie outside the area between the lines $Q + J = 2.0$ and $Q + J = 1.5$ in the *Q-J* diagram. The classification of these unusual pyroxenes will be discussed later in this report.

The pyroxenes that plot in the area between $Q + J = 2.0$ and $Q + J = 1.5$ have components than *Q* and *J* ions at less than 25% of the M sites. Therefore, we can classify

TABLE 3. Chemical composition and classification of eight unusual pyroxenes

	A. Ca-rich group related to S3 and S4				B. Na-rich group related to S2			
	1: 320-8 (406-16)	2: 403-3	3: D and S*	4: T and R**	5: 488-9	6: 491-14	7: 492-19 C and G‡	8: C and G‡
Si	1.443 2.00	1.506 2.00	1.434 2.00	1.196 2.00	1.994 2.00	2.024 2.02	2.026 2.03	2.009 2.01
Al	0.577	0.494	0.566	0.804	0.032	0.000	0.000	0.000
Al	0.091	0.171	0.306	0.186	0.000	0.021	0.098	0.348
Ti^{4+}	0.165	0.065	0.022	0.111	0.265	0.023	0.227	0.104
Ti^{3+}				0.394				
Fe^{3+}	0.128	0.159	0.218		0.458	0.728	0.192	0.031
Mg	0.385	0.570	0.408	0.289	0.150	0.070	0.070	0.168
Fe^{2+}	0.229 2.00	0.063 2.02	0.060 2.00	2.00	0.107 2.00	0.113 2.00	0.420 1.98	0.356 2.00
Mn	0.005	0.007	0.005		0.003	0.006	0.021	0.011
Ca	0.992	0.975	0.979	1.021	0.083	0.155	0.152	0.361
Na	0.006	0.007	0.002		0.933	0.872	0.794	0.610
K	0.000	0.001	—		—	0.009	—	0.006
Q	1.61	1.61	1.45	1.31	0.34	0.34	0.64	0.89
J	0.01	0.01	0.00	0.00	1.87	1.74	1.59	1.22
Mineral names	subsilicic titanian ferrian diopside	subsilicic aluminian ferrian diopside	subsilicic aluminian ferrian diopside	subsilicic titanoan aluminian pyroxene	titanian magnesian ferroan aegirine	calcian ferroan aegirine	titanian aegirine-augite	titanian ferroan omphacite
Names in literature	titanaugite (320-8) titanium fassaite (406-16) CaMgTAL (C and P)†	fassaite	fassaite	titanaugite	titanian aegirine	aegirine-augite	titanian aegirine-augite (492-19) titanian aegirine (C and G)‡	titanian ferro-omphacite

Note: Numbers such as 320-8, etc. represent pages and analysis number in Deer et al. (1978). Other references are in text. With the exception of 320-8 (= 406-16), all the Deer et al. (1978) analyses in this table were not included in the 103 selected analyses of Cameron and Papike (1981). All pyroxenes in the table are shown with their numbers in the *Q-J* diagram (Fig. 7). S2, S3, and S4 represent the following components of substitutions 2, 3, and 4, respectively: S2 = $NaR^{2+}_{0.5}Ti^{4+}_{0.5}Si_2O_6$, S3 = $CaR^{3+}AlSiO_6$, and S4 = $CaR^{2+}_{0.5}Ti^{4+}_{0.5}AlSiO_6$. To indicate R ions explicitly in these components, the notation S(R), such as S2(Mg) and S3(Al), is used. S3(Fe) is a new pyroxene, esseneite (Es). Component ratios for the eight samples are as follows: (1) $(Wo_{22}En_{12}Fs_{10})_{44}S4(Mg)_{18}S4(Fe)_{16}Es_{13}S3(Al)_9$, (2) $(Wo_{26}En_{25}Fs_2)_{53}S3(Al)_{17}Es_{16}S4(Mg)_{12}S4(Fe)_2$, (3) $(Wo_{22}En_{20}Fs_2)_{44}S3(Al)_{31}Es_{21}S4(Mg)_4$, (4) $S3(Ti)_{39}S4(Mg)_{22}(Wo_{11}Fs_9)_{20}S3(Al)_{19}$, (5) $Ae_{46}S2(Mg)_{28}S2(Fe)_{20}\triangle_6$, (6) $(Ae_{73}Jd_2Wo_8Fs_6En_3)_{92}S2_4\triangle_4$, (7) $(Ae_{19}Jd_{10}Fs_{12}Wo_8En_2)_{51}S2(Fe)_{42}S2(Mg)_4\triangle_3$, (8) $(Jd_{35}Ae_3Wo_{18}Fs_{15}En_7)_{78}S2(Fe)_{14}S2(Mg)_8\triangle_2$. The symbol △ represents minor components, some of which have unusual metal ratios for the pyroxene structure.

* Devine and Sigurdsson (1980), Table 1 for fassaite.

** Tracy and Robinson (1977), Table 3, analysis I for pyroxene from the Allende meteorite (Mason, 1974).

† Cameron and Papike (1981), Table A3, analysis 320-8 and 406-16.

‡ Curtis and Gittins (1979), Table 2, analysis 5 for no. 7 and Table 5, analysis 5 for no. 8.

such pyroxenes on the basis of the normalized *Q* and *J* components, thereby neglecting the effects of the other components. The following procedures are adopted for further classification: (1) The pyroxenes in the Quad area are classified on the pyroxene quadrilateral Wo-En-Fs diagram with normalized Ca, Mg, and ΣFe (= Fe^{2+} + Fe^{3+} + Mn) atoms. (2) The pyroxenes in the Na area are jadeite, aegirine, kosmochlor, and jervisite. Because kosmochlor and jervisite show little or no solid solution toward other end members, they play no role in the classification. Jadeite and aegirine are classified on the Quad-Jd-Ae diagram together with the Ca-Na pyroxenes, aegirine-augite and omphacite.

Classification of the Ca-Mg-Fe "quadrilateral" pyroxenes

The common rock-forming pyroxenes form wide ranges of solid solutions of the Ca-Mg-Fe pyroxenes and can be expressed by the pyroxene quadrilateral of the $Mg_2Si_2O_6$ (En)–$Fe^{2+}_2Si_2O_6$ (Fs)–$CaMgSi_2O_6$ (Di)–$CaFe^{2+}Si_2O_6$ (Hd) system. The Ca-Mg-Fe pyroxenes include varieties that have orthorhombic symmetry. These orthopyroxenes consist essentially of a simple chemical series $(Mg,Fe)_2Si_2O_6$ and thus contrast with the Ca-Mg-Fe clinopyroxenes, which have wide ranges of chemical composition. Therefore, the Ca-Mg-Fe pyroxenes are defined on the basis of symmetry and relative amounts of $Ca_2Si_2O_6$ (Wo), $Mg_2Si_2O_6$ (En), and $Fe^{2+}_2Si_2O_6$ (Fs). The composition ranges of the clinopyroxenes and orthopyroxenes are indicated in Figures 4 and 5, respectively, where the composition is normalized to Ca + Mg + ΣFe = 100 with ΣFe = Fe^{2+} + Fe^{3+} + Mn^{2+}.[10]

[10] For the nomenclature of the Ca-Mg-Fe pyroxenes, normalization must be made to Ca + Mg + ΣFe = 100, where ΣFe = Fe^{2+} + Fe^{3+} + Mn. Hereafter the mole percent of the end member components is always used without remark and is represented simply by %. If the mole percents of quadrilateral components are calculated by the atomic percent of Ca to the total cations at the M sites, no pyroxenes should contain more than 50% $Ca_2Si_2O_6$. However, if Ca, Mg, and Fe are normalized, or calculated as 100Ca/(Ca + Mg + ΣFe), 100 Mg/(Ca + Mg + ΣFe), and 100 ΣFe/(Ca + Mg + ΣFe), respectively, then some augites will plot on a Wo-En-Fs triangular diagram above the 50% $Ca_2Si_2O_6$ line. Especially when the plot in the *Q-J* diagram is very close to or outside of the boundary $Q + J = 1.5$, the effect of johannsenite and petedunnite components must be considered. If the effect is negligible, the pyroxene must be considered to have an unusual composition and must be referred to the section of unusual pyroxenes.

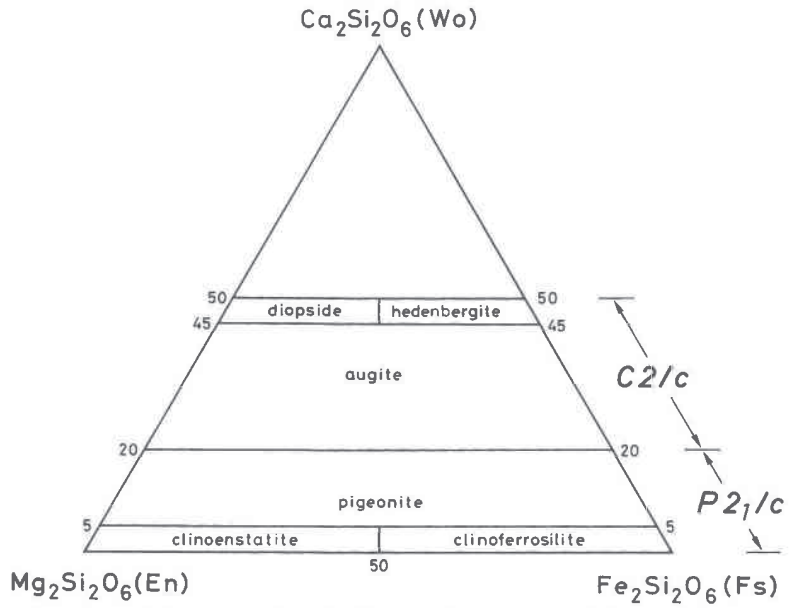

Fig. 4. Composition ranges of the Ca-Mg-Fe clinopyroxenes with accepted names.

The distinction between augite and pigeonite in the Ca-Mg-Fe pyroxenes is primarily structural, their space groups being $C2/c$ and $P2_1/c$, respectively. There is a miscibility gap between augite and pigeonite, and many pyroxenes with 15–25% Wo have proved to be mixtures of the two. Augite with less than about 25% Wo is often called subcalcic augite. On heating, pigeonite undergoes a rapid displacive transformation to a $C2/c$ structure, which cannot be quenched. Augite does not show this type of transformation.

The most Ca-rich orthopyroxene contains approximately 5% Wo. The high-temperature form of enstatite has the space group *Pbcn* and can be expressed as "enstatite-*Pbcn*." This form is not quenchable and has not been found in nature. "Protoenstatite" has been used conventionally to describe this form, but this name is not adopted as a mineral name. The Wo value of "enstatite-*Pbcn*" does not exceed 2%, and the En value commonly exceeds 90%. Thus the composition field of "enstatite-*Pbcn*" is different from that of enstatite-*Pbca*.

Classification of the Na and Ca-Na pyroxenes

The Na pyroxenes, jadeite and aegirine, commonly contain more than 90% of the $NaAlSi_2O_6$ or $NaFe^{3+}Si_2O_6$ component, respectively, but contain neither the Ko nor the Je component. Because kosmochlor is a rare accessory constituent of some iron meteorites and only one terrestrial locality is known for each of kosmochlor and jervisite, these two species are separately treated in the classification of the Na pyroxenes. Both jadeite and aegirine, however, show extensive solid solution with the Ca-Mg-Fe pyroxenes, especially with the diopside-hedenbergite series and augite, leading to the Ca-Na pyroxenes. The Na and Ca-Na pyroxenes are classified on the Quad-Jd-Ae diagram (Fig. 6) with normalized Q (Wo + En + Fs), Jd, and Ae components.[11] The arbitrary divi-

[11] To normalize Q, Jd, and Ae components, the sum of Ca + Mg + Fe^{2+} + 2Na at the M sites must be made to total 100%. Then the normalized percentage of 2Na must be divided into the ratio of Al/Fe^{3+} to give the ratio of Jd/Ae. Thus Q + Jd + Ae must always give 100%. When the plot in the Q-J diagram is significantly outside the boundary $Q + J = 2.0$, the effect of substitution 2 must be considered, as in the section of unusual pyroxenes.

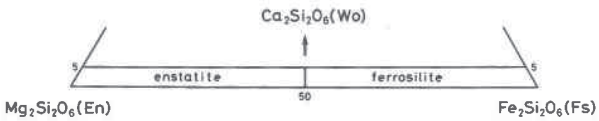

Fig. 5. Composition ranges of orthopyroxenes with accepted names.

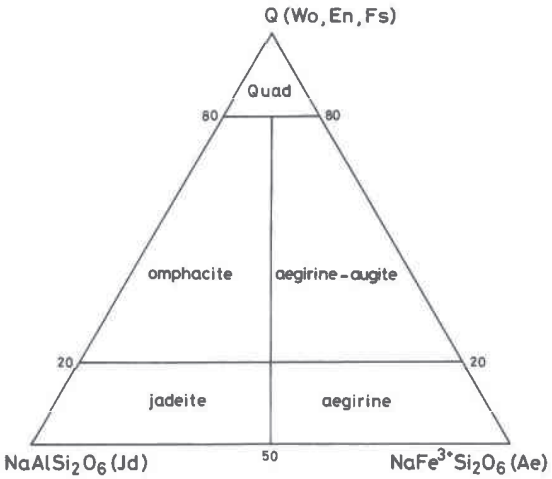

Fig. 6. Ca-Mg-Fe and Na pyroxenes with accepted names. Quad represents the Ca-Mg-Fe pyroxene area (see Fig. 4).

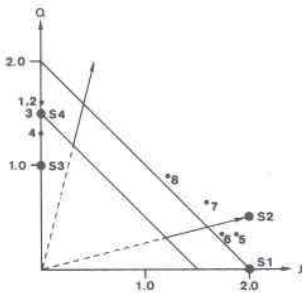

Fig. 7. Q-J diagram for eight unusual pyroxenes with Q value less than 1.62 and Mn less than 0.08 atoms per formula unit (Table 3). The components formed by the substitutions 1 to 4, as indicated in Table 1, are plotted in the diagram. They represent the following compositions: S1 = $NaR^{3+}Si_2O_6$, S2 = $NaR^{2+}_{0.5}Ti^{4+}_{0.5}Si_2O_6$, S3 = $CaR^{3+}AlSiO_6$, and S4 = $CaR^{2+}_{0.5}Ti^{4+}_{0.5}AlSiO_6$.

sions between the Ca-Mg-Fe pyroxenes, Na-Ca pyroxenes, and Na pyroxenes are defined at 20% and 80% of Q. Omphacite displays a $C2/c \rightleftharpoons P2/n$ polymorphic transition, and both high-temperature $C2/c$ and low-temperature $P2/n$ polymorphs appear in nature. Omphacite can thus be divided into two subspecies: omphacite-$C2/c$ and omphacite-$P2/n$. Because omphacite-$P2/n$ shows a unique crystal structure different from that of jadeite and augite, it is accepted as an independent pyroxene species. Aegirine-augite is also accepted as an independent species to keep balance with omphacite, though it is not known to occur with the $P2/n$ structure. The classification of the Ca-Na pyroxenes by Essene and Fyfe (1967) is not followed in this report.

TABLE 4. Extreme chemical compositions of pyroxenes in Deer et al. (1978)

	Mg-Fe pyroxenes	Ca pyroxenes	Na pyroxenes
Si	**1.76** (42-9)	**1.44** (320-8)[A]	**1.94** (488-9)
Al^{3+}	0.24 (42-9)	0.56 (320-8)	0.07 (488-8)
Fe^{3+}	0.04 (49-8)	0.09 (320-11)	0.02 (488-9)
Al^{3+}	0.15 (49-6)	0.35 (320-11)	**0.98** (464-1)
Ti^{4+}	0.04 (40-30)	0.17 (320-8)[B]	0.27 (488-9)[C]
Fe^{3+}	0.12 (170-8)	0.37 (321-5)[D]	**0.97** (487-1)
Mg^{2+}	**1.99** (41-1)	**1.27** (208-4)	0.15 (488-9)
Fe^{2+}	**1.72** (47-33)[E]	**1.09** (220-13)	0.11 (488-9)
Mn^{2+}	0.27 (45-21)[F]	0.36 (217-5)[G]	0.03 (487-4)
Cr^{2+}	0.02 (36-9)	0.06 (207-11)	—[H]
Ni^{2+}	—	0.003 (317-1)	—
Zn^{2+}	—	0.21 (216-11)[I]	—
Ca^{2+}	0.26 (169-2)	**1.03** (202-4)	0.16 (466-14)
Na^{+}	0.10 (169-2)	0.31 (323-7)	**0.98** (464-1)

Note: Given are the number of cations per formula unit, minimum values for Si, and maximum values for other cations. Bold numbers are for the main constituent elements. Numbers in the parentheses such as 42-9, etc., indicate pages and analysis numbers in Deer et al. (1978). Other references are in text.

[A] Table 3, no. 1; Table 3, no. 4: Pyroxene from the Allende meteorite 1.20 (Mason, 1974; Tracy and Robinson, 1977).

[B] Probe analyses 0.252 and 0.282, half of $CaR^{2+}_{0.5}Ti^{4+}_{0.5}AlSiO_6$ (S4) (Tracy and Robinson, 1977; Robinson, 1980).

[C] Table 3, no. 5. Half of $NaR^{2+}_{0.5}Ti^{4+}_{0.5}Si_2O_6$ (S2).

[D] 406-15 0.67, omitted because of possible errors in chemical analysis.

[E] Probe analysis 1.880 (Jaffe et al., 1978).

[F] Probe analysis 0.301 (Robinson, 1980), kanoite 1.04 (Kobayashi, 1977).

[G] Johannsenite 0.963 (417-2).

[H] Kosmochlor 0.90 (522-1).

[I] Petedunnite 0.37 (Table 2, footnote with asterisk).

TABLE 5. List of adjectival modifiers to be used for pyroxene mineral names

Cation	Content*	Name
Al^{3+}	>0.10	aluminian
Ca^{2+}	>0.10	calcian
Cr^{3+}	>0.01	chromian
Fe^{2+}	>0.10	ferroan
Fe^{3+}	>0.10	ferrian
Li^{+}	>0.01	lithian
Mg^{2+}	>0.10	magnesian
Mn^{2+}	>0.10	manganoan
Mn^{3+}	>0.01	manganian
Na^{+}	>0.10	sodian
Ni^{2+}	>0.01	nickeloan
Si^{4+}	<1.75	subsilicic
Ti^{3+}	>0.01	titanoan
Ti^{4+}	>0.10	titanian
Zn^{2+}	>0.01	zincian

Note: The limit of the content is based on the values listed in Table 4.

* Number of cations per formula unit $M2M1T_2O_6$. If the mineral name itself implies the presence of certain cations, adjectival modifiers for these cations should not be used ("subsilicic" is an exception).

Classification of other pyroxenes

Most naturally occurring pyroxenes in the Others area are johannsenite ($CaMnSi_2O_6$), petedunnite ($CaZnSi_2O_6$), and spodumene ($LiAlSi_2O_6$) (Fig. 2). Recent investigations of natural Mn-bearing pyroxenes have yielded two new minerals, kanoite and its dimorph donpeacorite, $(Mn,Mg)MgSi_2O_6$, which seem to form a solid solution with En (Peterson et al., 1984). They too occur in the Others area. These results suggest a possible Mn-Mg-Fe pyroxene quadrilateral. Esseneite ($CaFe^{3+}AlSiO_6$) is the first pyroxene with the substitution 3 as described in Table 1.

Classification of unusual pyroxenes

Several pyroxenes with unusual chemical compositions (Table 3) appear outside the area between the lines $Q + J = 2.0$ and $Q + J = 1.5$ in the Q-J diagram, though they do not belong in the area of Other pyroxenes mentioned above (Fig. 7). They contain large amounts of chemical components involved in substitutions 2, 3, and 4 mentioned in Table 1.

These pyroxenes can be divided into two groups: first, Ca-rich pyroxenes with $CaR^{3+}AlSiO_6$ (S3, Fig. 7) and $CaR^{2+}_{0.5}Ti^{4+}_{0.5}AlSiO_6$ (S4, Fig. 7) components representing substitutions 3 and 4, respectively, and second, Na-rich pyroxenes with the $NaR^{2+}_{0.5}Ti^{4+}_{0.5}Si_2O_6$ component representing substitution 2 (S2, Fig. 7). The former shows a significant deficiency of Si atoms such as $Si < 1.60$ in the standard formula resulting in the Q value close to or less than 1.5 (S4, Fig. 7). The latter appears outside the line $Q + J = 2.0$ approaching point S2 in Figure 7. All these unusual pyroxenes are classified by using the accepted pyroxene names and the adjectival modifiers mentioned

TABLE 6. Obsolete pyroxene names

acmite = *aegirine*
aegirite (aegyrite) = *aegirine*
aegerine-hedenbergite = *augite*
agalite = probably *enstatite* partly altered to talc
aglaite = altered *spodumene*
alalite = *diopside*
alkali augite = *aegirine-augite*
amblystegite = *enstatite*
anthochroite = *augite*
asteroite = iron-rich (or Fe-rich) *augite*
baikalite = *diopside*
bastite = *enstatite* that has altered to serpentine, talc, or perhaps anthophyllite
blanfordite = manganoan *aegirine-augite*
bronzite = *enstatite*
calc-clinobronzite = *pigeonite*
calc-clinoenstatite = *pigeonite*
calc-clinohypersthene = *pigeonite*
calc-pigeonite = subcalcic *augite*
canaanite = *diopside*
chladnite = *enstatite*
chloromelanite = *omphacite* or *aegirine-augite*
chrome-acmite = chromian *aegirine*
chromejadeite = chromian *jadeite*
clinohypersthene = *clinoenstatite* or *clinoferrosilite*
coccolite (kokkolith) = iron-rich (or Fe-rich) *augite*
cymatolite = altered *spodumene*
diaclasite = altered *enstatite*
diallage = *diopside* that has altered or that has good (100) parting; also used for alteration products of other pyroxenes
diopsidjadeite = *omphacite*
endiopside = magnesium-rich (or Mg-rich) *augite*
enstatite-diopside = magnesium-rich (or Mg-rich) *augite*
eulite = *ferrosilite*
eulysite = *ferrosilite*
fassaite = ferrian aluminian *diopside* or *augite*
fedorovite = *diopside*
ferroaugite = *augite*
ferrohedenbergite = *augite*
ferrohypersthene = *ferrosilite*
ferro-johannsenite = iron-rich (or Fe-rich) *johannsenite*
ferropigeonite = iron-rich (or Fe-rich) *pigeonite*
ferrosalite = *hedenbergite*
ficinite = *enstatite*
funkite = *hedenbergite*
germarite = altered *enstatite*
hiddenite = *spodumene*
hudsonite = *hedenbergite*
hypersthene = *enstatite* or *ferrosilite*
jadeite-aegirine (jadeite-aegirite) = *jadeite* or *aegirine*
jeffersonite = zincian manganoan *diopside* or *augite*
killinite = altered *spodumene*
korea-augite = *augite*
kunzite = *spodumene*
lavroffite = *diopside*
lavrovite = *diopside*
lawrowite = *diopside*
leucaugite = *diopside*
lime-bronzite = probably *pigeonite* or *enstatite* plus *augite* ("inverted" *pigeonite*)
loganite = *diopside* + actinolite + talc
lotalite = *hedenbergite*
malacolite = *diopside* with good (001) parting, also *diopside* from Sala, Sweden
mansjoite = *augite* or *diopside* or *hedenbergite*
mayaite = *omphacite*
mellcrite = *orthopyroxene*
mondradite = probably an altered *pyroxene*
mussite = *dipside*
orthobronzite = *enstatite*
orthoenstatite = *enstatite*
orthoeulite = *ferrosilite*
orthoferrosilite = *ferrosilite*
orthohypersthene = *enstatite* or *ferrosilite*
paulite = *enstatite*
peckhamite = *enstatite*
phastine = altered *enstatite*

TABLE 6—*Continued*

picrophyll = altered *pyroxene*?
pigeonite-augite = probably subcalcic *augite*
pitkarantite = *pyroxene*?
potash-aegirine = synthetic product, probably not properly characterized
protheite = *augite*
protobastite = *enstatite*
pyrallolite = altered *pyroxene*?, talc?
pyrgom = *pyroxene*
sahlite = *diopside*
salite = *diopside*
schefferite = manganoan *diopside*
schillerspar (schillerspat) = *enstatite* that is altered to serpentine, talc, or anthophyllite
shepardite = *enstatite*
soda-spodumene = sodian *spodumene*
strakonitzite = altered *pyroxene*, steatite?
szaboite = partly altered *enstatite*
titanaugite = titanian *augite*
titandiopside = titanian *diopside*
titanpigeonite = titanian *pigeonite*
trachyaugite = *augite*
traversellite = *diopside*
triphane = *spodumene*
tuxtlite = *omphacite*
uralite = pseudomorph of amphibole after pyroxenes
urbanite = iron-rich (or Fe-rich) *augite* or *aegirine-augite*
ureyite = *kosmochlor*
vanadinaugite = vanadium-bearing (or V-bearing) *augite*
vanadinbronzite = vanadium-bearing (or V-bearing) *enstatite*
vargasite = altered *pyroxene*?
victorite = *enstatite*
violaite = *augite*
violan = magnesium-rich (or Mg-rich) *augite* or *dipside*

Note: The above pyroxene mineral names, or names that refer to altered pyroxenes, have been formally discarded by the CNMMN. The correct names are italicized. The original form of this table was compiled by Malcolm Ross using the following references: Dana (1892); Tschermak (1897); Chester (1886); Ford (1932); Winchell and Winchell (1951); Deer et al. (1963, 1978); Strunz (1970); and the unpublished Thesaurus of Mineralogical Terms of the International Mineralogical Association, which has been available since August 1974.

below, except the Allende pyroxene (Table 3, no. 4), which is called subsilicic titanoan aluminian pyroxene.

The Allende pyroxene (no. 4) contains 39% of the S3(Ti) (for notation, see note in Table 3) component $CaR^{3+}AlSiO_6$, where R^{3+} = Ti, and can be considered as a new mineral. However, we have decided only to use the accepted names in this report and if a species has not yet been approved, we use "pyroxene" as for no. 4 in Table 3. The names used in literature for the unusual pyroxenes are listed in Table 3 in comparison with those in this report. The "CaMgTAL" pyroxene (no. 1) is "diopside" in this classification.

ADJECTIVAL MODIFIERS

Adjectival modifiers for mineral names are used to indicate unusual amounts of chemical constituents. In order to define the unusual amounts for the pyroxene mineral group quantitatively, extreme compositions of pyroxenes have been listed in Table 4, where the values for the main cations are shown as well as those for the accessory cations. Deer et al. (1978) and Robinson's (1980) table were mainly used in constructing Table 4.

An element specified as a modifier should be present as a general rule in a quantity larger than 0.1 atoms (or

0.01 for less abundant elements) in the standard chemical formula of 6 oxygens or 4 metal atoms (Table 5) depending on the maximum content in Table 4.

The suffixes are those proposed by Schaller (1930) and adapted by CNMMN (Nickel and Mandarino, 1987). The suffix "-ian" is used for the higher valence state (e.g., ferrian) or for an element with a nonvariable state (e.g., lithian). The suffix "-oan" implies the lower valence state (e.g., ferroan). It is recommended that such modifiers never be used for main cations normally contained in the named mineral, for example, in terms like "calcian augite," "aluminian omphacite," and "sodian aegirine-augite," in which the modifiers are obviously superfluous.

If there is less than the amount necessary for the assignment of the modifiers such as "aluminian" in Table 5, or <0.1 Al, but if the increased content of the element must be stressed, a modifier "Al-bearing" may be used. This second type of modifier should be used also (1) if only an incomplete analysis is available, preventing the calculation of a full chemical formula, or (2) for pyroxenes where the valence state of a cation is unknown. With regard to the Si content in pyroxenes, it is suggested that Si < 1.75 is a suitable limit for use of the term "subsilicic," though one should bear in mind that the limit of Si < 5.75 for "subsilicic" in amphiboles corresponds to Si < 1.5 for pyroxenes.

In certain cases, particularly for the augite series, it is convenient to use the following adjectival modifiers: Fe-rich, Mg-rich, and subcalcic. A prefix actually attached or hyphenated to a mineral name, however, is incorrect and should be avoided (Nickel and Mandarino, 1987), because it would cause the mineral to be indexed alphabetically under the prefix rather than under the proper mineral name. This is why such terms as "ferropigeonite," "ferro-augite," etc., should not be used as mineral names.

It is often useful to give the space group of the mineral, particularly when it can occur in two or more forms. For example, we could distinguish between the two forms of omphacite by adding the space-group symbol., i.e., omphacite-*C*2/*c* vs. omphacite-*P*2/*n*, or by adding the lattice-type symbol, i.e., omphacite-*C* vs. omphacite-*P* (Bailey, 1977).

Obsolete pyroxene names

The names of 105 pyroxenes or altered pyroxenes listed in Table 6 have formally been discarded by the CNMMN and are therefore obsolete. The preferred name is italicized in the same table.

Acknowledgments

We are thankful to Professor J.H.D. Donnay, McGill University, Montreal, who contributed greatly to the improvement of the report by his careful review. We also appreciate criticisms and comments by Dr. A. Kato, National Science Museum, Tokyo, Dr. M. Kitamura, Kyoto University, Kyoto, and the members of the Commission on New Minerals and Mineral Names, IMA.

References cited

Bailey, S.W. (1977) Report of the IMA-IUCr joint committee on nomenclature. American Mineralogist, 62, 411–415.

Bokij, G.B., and Ginzburg, J.V. (1985) The systematics of mineral species in pyroxene family. Trudy Instituta Geologii i Geofiziki (Novosibirsk), 610, 12–35.

Cameron, M. and Papike, J.J. (1981) Structural and chemical variations in pyroxenes. American Mineralogist, 66, 1–50.

Chester, A.H. (1886) Catalogue of minerals. John Wiley and Sons, N.Y.

Cosca, M.A., and Peacor, D.R. (1987) Chemistry and structure of esseneite ($CaFe^{3+}AlSiO_6$), a new pyroxene produced by pyrometamorphism. American Mineralogist, 72, 148–156.

Curtis, L.W., and Gittins, J. (1979) Aluminous and titaniferous clinopyroxenes from regionally metamorphosed agpaitic rocks in central Labrador. Journal of Petrology, 20, 165–186.

Dana, E.S. (1892) The system of mineralogy (6th edition). Wiley, New York.

Deer, W.A., Howie, R.A., and Zussman, J. (1963) Rock-forming minerals, vol. 2, Single-chain silicates (first edition). Longman, Green and Co. Ltd., London.

——— (1978) Rock-forming minerals, vol. 2A, Single-chain silicates (2nd edition). Longman, U.K. and Wiley, New York.

DeVine, J.D., and Sigurdsson, H. (1980) Garnet-fassaite calc-silicate nodule from La Soufriere, St. Vincent. American Mineralogist, 65, 302–305.

Dowty, E. and Clark, J.R. (1973) Crystal structure refinement and optical properties of a Ti^{3+} fassaite from the Allende meteorite. American Mineralogist, 58, 230–240.

Essene, E.J., and Fyfe, W.S. (1967) Omphacite in California metamorphic rocks. Contributions to Mineralogy and Petrology, 15, 1–23.

Essene, E.J., and Peacor, D.R. (1987) Petedunnite ($CaZnSi_2O_6$), a new zinc clinopyroxene from Franklin, New Jersey, and phase equilibria for zincian pyroxenes. American Mineralogist, 72, 157–166.

Ford, W.E. (1932) A textbook of mineralogy. Wiley, New York.

Jaffe, H.W., Jaffe, E.B., and Tracy, R.J. (1978) Orthoferrosilite and other iron-rich pyroxenes in microperthite gneiss of the Mount Marcy area, Adirondack Mountains. American Mineralogist, 63, 116–136.

Kobayashi, H. (1977) Kanoite, $(Mn^{2+}Mg)_2[Si_2O_6]$, a new clinopyroxene in the metamorphic rock from Tatehira, Oshima Peninsula, Hokkaido, Japan. Journal of the Geological Society of Japan, 83, 537–542.

Leake, B.E., and Winchell, H. (1978) Nomenclature of amphiboles. American Mineralogist, 63, 1023–1052.

Mason, B. (1974) Aluminum-titanium–rich pyroxenes, with special reference to the Allende meteorite. American Mineralogist, 59, 1198–1202.

Mellini, M., Merlino, S., Orlandi, P., and Rinaldi, R. (1982) Cascadite and jervisite, two new scandium silicates from Baveno, Italy. American Mineralogist, 67, 599–603.

Morimoto, N., and Kitamura, M. (1983) *Q-J* diagram for classification of pyroxenes. Journal of the Japanese Association of Mineralogists, Petrologists and Economic Geologists, 78, 141 (in Japanese).

Nickel, E.H., and Mandarino, J.A. (1987) Procedures involving the IMA Commission on New Minerals and Mineral Names and guidelines on mineral nomenclature. Canadian Mineralogist, 25, 353–377; American Mineralogist, 72, 1031–1042.

Papike, J.J., Ed. (1969) Pyroxenes and amphiboles: Crystal chemistry and phase petrology. Mineralogical Society of America Special Paper 2.

Peterson, E.U., Anovitz, L.M., and Essene, E.J. (1984) Donpeacorite, $(Mn,Mg)MgSi_2O_6$, a new orthopyroxene and its proposed phase relations in the system $MnSiO_3$-$MgSiO_3$-$FeSiO_3$. American Mineralogist, 69, 472–480.

Prewitt, C.T., Ed. (1980) Reviews in mineralogy, vol. 7. Pyroxenes. Mineralogical Society of America, Washington, D.C.

Robinson, P. (1980) The composition space of terrestrial pyroxenes—Internal and external limits. Mineralogical Society of America Reviews in Mineralogy, 7, 419–494.

Schaller, W.T. (1930) Adjectival endings of chemical elements used as modifiers to mineral names. American Mineralogist, 15, 566–574.

Strunz, H. (1970) Mineralogische Tabellen, 5 Auflage. Akademische Verlagsgesellschaft Geest and Portig K.-G., Leipzig.

Tracy, R.J., and Robinson, P. (1977) Zonal titanian augite in alkali olivine basalt from Tahiti and the nature of titanium substitutions in augite. American Mineralogist, 62, 634–645.

Tschermak, G. (1897) Lehrbuch der Mineralogie. Alfred Holder, Wien.

Vieten, K. and Hamm, H.M. (1978) Additional notes "On the calculation of the crystal chemical formula of clinopyroxenes and their contents of Fe^{3+} from microprobe analyses. Neues Jahrbuch für Mineralogie Monatshefte, 71–83.

Winchell, A.N., and Winchell, H. (1951) Elements of optical mineralogy. Wiley, New York.

Manuscript received March 7, 1988
Manuscript accepted May 6, 1988

American Mineralogist, Volume 97, pages 2031–2048, 2012

IMA Report

Nomenclature of the amphibole supergroup

Frank C. Hawthorne,[1,*,†] Roberta Oberti,[2,*,†] George E. Harlow,[3] Walter V. Maresch,[4] Robert F. Martin,[5] John C. Schumacher,[6] and Mark D. Welch[7]

[1]Geological Sciences, University of Manitoba, Winnipeg, Manitoba R3T 2N2, Canada
[2]CNR-Istituto di Geoscienze e Georisorse, unità di Pavia, via Ferrata 1, I-27100 Pavia, Italy
[3]Department of Earth and Planetary Sciences, American Museum of Natural History, Central Park West at 79th Street, New York, New York 10024, U.S.A.
[4]Institute of Mineralogy, Geology and Geophysics, Ruhr-University, D-44780 Bochum, Germany
[5]Department of Earth and Planetary Sciences, McGill University, 3450 University Street, Montreal, Quebec H3A 2A7, Canada
[6]Department of Earth Sciences, Wills Memorial Building, University of Bristol, Bristol BS8 1RJ, U.K.
[7]Department of Mineralogy, The Natural History Museum, Cromwell Road, London SW7 5BD, U.K.

Abstract

A new classification and nomenclature scheme for the amphibole-supergroup minerals is described, based on the general formula $AB_2C_5T_8O_{22}W_2$, where A = □, Na, K, Ca, Pb, Li; B = Na, Ca, Mn^{2+}, Fe^{2+}, Mg, Li; C = Mg, Fe^{2+}, Mn^{2+}, Al, Fe^{3+}, Mn^{3+}, Ti^{4+}, Li; T = Si, Al, Ti^{4+}, Be; W = (OH), F, Cl, O^{2-}. Distinct arrangements of formal charges at the sites (or groups of sites) in the amphibole structure warrant distinct *root names*, and are, by implication, distinct species; for a specific root name, different homovalent cations (e.g., Mg vs. Fe^{2+}) or anions (e.g., OH vs. F) are indicated by prefixes (e.g., ferro-, fluoro-). The classification is based on the A, B, and C groups of cations and the W group of anions, as these groups show the maximum compositional variability in the amphibole structure. The amphibole supergroup is divided into two groups according to the dominant W species: *^{W}(OH,F,Cl)-dominant amphiboles* and *^{W}O-dominant amphiboles (oxo-amphiboles)*. Amphiboles with (OH, F, Cl) dominant at W are divided into eight subgroups according to the dominant charge-arrangements and type of B-group cations: magnesium-iron-manganese amphiboles, calcium amphiboles, sodium-calcium amphiboles, sodium amphiboles, lithium amphiboles, sodium-(magnesium-iron-manganese) amphiboles, lithium-(magnesium-iron-manganese) amphiboles and lithium-calcium amphiboles. Within each of these subgroups, the A- and C-group cations are used to assign specific names to specific compositional ranges and root compositions. Root names are assigned to distinct arrangements of formal charges at the sites, and prefixes are assigned to describe homovalent variation in the dominant ion of the root composition. For amphiboles with O dominant at W, distinct root-compositions are currently known for four (calcium and sodium) amphiboles, and homovalent variation in the dominant cation is handled as for the ^{W}(OH,F,Cl)-dominant amphiboles. With this classification, we attempt to recognize the concerns of each constituent community interested in amphiboles and incorporate these into this classification scheme. Where such concerns conflict, we have attempted to act in accord with the more important concerns of each community.

Keywords: Amphibole, nomenclature, classification, chemical composition, crystal chemistry

Introduction

Leake (1968) presented a classification for calcic amphiboles, and this was expanded into the International Mineralogical Association (IMA) classification of Leake (1978), henceforth referred to as IMA1978. An IMA Subcommittee on Amphibole Classification was formed, and Leake et al. (1997), henceforth referred to as IMA1997, presented the current classification, as modified by Leake et al. (2003), henceforth referred to as IMA2003, to incorporate new discoveries in amphibole compositions in the intervening years. However, these schemes of classification do not adequately address subsequent discoveries of new compositional types of amphibole (e.g., Oberti et al. 2000, 2003, 2004, 2006; Caballero et al. 2002). Moreover, increasing appreciation of the crystal-chemical and petrological importance of compositional variables not incorporated into the previous schemes [e.g., Fe^{3+}, Fe^{2+}, Li, and $^{W}O^{2-}$ contents] forced reconsideration of the basis of amphibole classification. To focus on the classification and nomenclature, any extensive discussion of specific points is given in a series of Appendices.

General statement

Any classification scheme, particularly one involving a supergroup of minerals as complicated as the amphiboles, is of necessity a compromise: simplicity commonly conflicts with

* E-mail: frank_hawthorne@umanitoba.ca; oberti@crystal.unipv.it
† Co-Chairs IMA Subcommittee on Amphibole Classification.

0003-004X/12/1112–2031$05.00/DOI: http://dx.doi.org/10.2138/am.2012.4276

convenience of use. Moreover, crystallographers, mineralogists, and petrologists will generally have different expectations of a classification. Crystallographers will want a classification that encompasses all aspects of the crystal chemistry of the amphiboles in as concise a way as possible, whereas petrologists will be more concerned with utility and convenience of use from a petrological perspective. We have attempted to recognize the concerns of each constituent community interested in amphiboles and incorporate these into this new classification scheme. Where such concerns conflict, we have attempted to act in accord with the more important concerns of each community.

The new classification

The new classification presented here is based on the chemical formula of an amphibole measured by electron microprobe or wet-chemical techniques, possibly augmented by additional analytical, structural and spectroscopic data. It does *not* address classification or nomenclature of amphiboles characterized solely in hand specimen or in thin section; these issues need to be addressed in separate classifications.

This new classification scheme is based on the concept of dominance, and hence:

(1) All distinct arrangements of integral charges over the amphibole formula are considered as *root charge arrangements*.

(2) Specific ions [Na^{+}, Mg^{2+}, Al^{3+}, Si^{4+}, $(OH)^{-}$] of appropriate charge are associated with sites in the structure, and each distinct chemical composition is a *root composition*. These compositions are assigned trivial[1] names.

(3) Where another homovalent ion is dominant at a site (or group of sites) in the structure, a prefix (see Table 1) is used in conjunction with the root name to indicate the composition (except where well-established names of common species, e.g., grunerite, riebeckite, are involved).

(4) The approach described in 1–3 was applied to the amphiboles by Hawthorne and Oberti (2006), and has since been adopted by the IMA as being broadly applicable (Hatert and Burke 2008).

[1] The word *trivial* is defined by the International Union of Pure and Applied Chemistry to denote a non-scientific name that does not follow directly from the systematics of composition, and it is used thus in this report.

Amphibole classification by chemical formula

The general chemical formula of the minerals of the amphibole supergroup can be written as $A\ B_2\ C_5\ T_8\ O_{22}\ W_2$, where

A = □, Na, K, Ca, Pb, Li;
B = Na, Ca, Mn^{2+}, Fe^{2+}, Mg, Li;
C = Mg, Fe^{2+}, Mn^{2+}, Al, Fe^{3+}, Mn^{3+}, Cr^{3+}, Ti^{4+}, Li;
T = Si, Al, Ti^{4+}, Be;
W = (OH), F, Cl, O^{2-}.

In addition, minor elements such as Zn, Ni^{2+}, Co^{2+}, V^{3+}, Sc, and Zr are also observed as C cations. Note that we use non-italicized letters to represent groups of cations in the general formula, thus distinguishing between groups of cations and crystallographic sites (which are denoted by italicized letters). The monoclinic *C*2/*m* amphibole structure is illustrated in Appendix I. In minerals as chemically complicated as the amphiboles, particularly where not all constituents are determined (e.g., H, Li, Fe^{3+}), there is the significant problem of how to calculate the chemical formula from the chemical composition; this issue has been addressed by Hawthorne (1983) and Schumacher (1991, 1997, 2007), and is also discussed in Appendices II and III.

Significant issues involved in the classification of amphiboles

Root names

Compositional variation may involve cations of the same valence [homovalent variation] or cations of different valence [heterovalent variation]. Previous classifications are based on the premise that distinct arrangements of formal charges at the sites (or groups of sites) in the amphibole structure warrant distinct *root names*, and are, by implication, distinct species; for a specific root name, different homovalent cations (e.g., Mg vs. Fe^{2+}) or anions (e.g., OH vs. F) are indicated by prefixes. The definition that only distinct arrangements of formal charges for each amphibole group warrant distinct root names implicitly applied only to the A, B, and T cations in IMA1978 and IMA1997, and it explicitly applies only to the A, B, and C cations in the present classification.

Table 1. Prefixes to be used in naming amphiboles

Prefix	Meaning (apfu)	Not applicable to
Chloro	Cl > OH, F	Oxo-amphiboles
Chromio	$^{C}Cr > {}^{C}Al, {}^{C}Fe^{3+}, {}^{C}Mn^{3+}$	Amphiboles which do not contain trivalent cations in their root formulae*
Ferri †	$^{C}Fe^{3+} > {}^{C}Al, {}^{C}Cr, {}^{C}Mn^{3+}$	Amphiboles which do not contain trivalent cations in their root formulae*, plus riebeckite, arfvedsonite, hastingsite
Ferro	$^{C}Fe^{2+} > {}^{C}Mg, {}^{C}Mn^{2+}$	Any amphibole whose ferro-end-member has a trivial name: tremolite, cummingtonite, grunerite, hastingsite, riebeckite, arfvedsonite, rootname 16
Fluoro	F > OH, Cl	Oxo-amphiboles
Magnesio	$^{C}Mg > {}^{C}Fe^{2+}, {}^{C}Mn^{2+}$	All amphiboles except riebeckite, arfvedsonite, hastingsite, hornblende
Mangano	$^{C}Mn^{2+} > {}^{C}Mg, {}^{C}Fe^{2+}$	
Mangani	$^{C}Mn^{3+} > {}^{C}Al, {}^{C}Cr, {}^{C}Fe^{3+}$	Amphiboles that do not contain trivalent cations in their root formulae*
Oxo	$^{W}O^{2-} > OH + F + Cl$	Oxo-amphiboles where Ti = 1 *apfu* in the root formula‡, plus ungarettiite
Potassic	$^{A}K > {}^{A}Na, {}^{A}Ca, {}^{A}□$	Amphiboles that do not contain A-site cations in their root formulae§
Zinco	$^{C}Zn > {}^{C}Mg, {}^{C}Fe^{2+}$	

* Tremolite, actinolite, edenite, richterite, anthophyllite, rootnames 1 and 3, cummingtonite, grunerite.
† Where it is known that Fe^{3+} is involved in dehydrogenation via the oxo-component ($^{W}O^{2-}$), the prefix ferri- is assigned on the basis of $[{}^{C}Fe^{3+} - {}^{M(1,3)}Fe^{3+}]$ if $^{M(1,3)}Fe^{3+}$ is known. If the oxo-component is not known, *ferri-* is assigned on the basis of $^{C}Fe^{3+}$.
‡ Obertiite, dellaventuraite, kaersutite.
§ Tremolite, actinolite, magnesio-hornblende, tschermakite, winchite, barroisite, glaucophane, riebeckite, clino-holmquistite, cummingtonite, grunerite, rootname 3, anthophyllite, gedrite, holmquistite.

It would be good to have consistent use of prefixes in amphibole names. Most root names apply to the Mg-Al-dominant species, e.g., tremolite, pargasite, glaucophane. However, (1) some amphiboles were originally described as the ferro- and/or ferri- equivalent of the Mg-Al-containing species, and (2) some amphiboles are presently defined without specifying the dominant trivalent cation [e.g., winchite = $\square$(NaCa)$Mg_4(AlFe^{3+})Si_8O_{22}(OH)_2$]. We could define all root names as referring to the Mg-Al-dominant compositions; thus, for example, leakeite, currently $NaNa_2(Mg_2Fe^{3+}_2Li)Si_8O_{22}(OH)_2$, becomes $NaNa_2(Mg_2Al_2Li)Si_8O_{22}(OH)_2$, and winchite becomes $\square(NaCa)(Mg_4Al)Si_8O_{22}(OH)_2$. If this were done, we could dispense with the prefixes *magnesio* and *alumino*. However, such a course of action would result in the loss of some common and petrologically important names (e.g., riebeckite would become "ferro-ferri-glaucophane" and arfvedsonite would become "ferro-ferri-eckermannite", and a riebeckite-arfvedsonite granite would become…). On the other hand, uncommon amphiboles may be redefined without hardship (e.g., alumino-leakeite becomes leakeite, and sodic-kornite becomes mangani-leakeite). Thus except for some common amphiboles of major petrological significance (e.g., riebeckite, arfvedsonite, actinolite, hastingsite), we define all root names as the equivalent Mg-Al-dominant species.

Prefixes

The topic of prefixes and adjectival modifiers has generated much discussion since IMA1978 formalized their use for amphiboles. First, it must be noted that *the use of prefixes has nothing to do with the number of species*; the number of species is dictated (1) by the details of the classification criteria, and (2) by Nature herself. The issue here is what kind of names are preferable. There are two strategies that we may use: (1) each distinct species is a trivial name; (2) we may identify root names corresponding to distinct charge arrangements, and indicate homovalent variants by prefixes. In the amphibole classifications of IMA1978 and IMA1997, the authors chose the second option and discredited 220 trivial names for amphiboles. Few would wish to return to a situation where there are several hundred trivial names for amphiboles. Here, we use root names plus indicators of homovalent variants.

Prefixes are listed in Table 1; note that we have attempted to make the use of prefixes more homogeneous among the groups and subgroups. Burke and Leake (2004) specified in which order prefixes (where more than one is used) must be attached to the root name. We use a different sequence, which follows the order of the amphibole formula itself: A B_2 C_5 T_8 O_{22} W_2; hence, *potassic-ferro-ferri-fluoro-* followed by the root name. The one exception is the prefix *oxo-*, which is put first because this involves the primary division between the two amphibole groups: amphiboles with (OH, F, Cl) dominant at W and amphiboles with O^{2-} dominant at W. The prefix *proto-* is used to denote orthorhombic amphiboles with $a \sim 9.8$ Å and the space group *Pnmn*, and should precede all chemical adjectival modifiers. All prefixes must be followed by a hyphen (thus root names are easily identified in the complete name and can be found by computer search).

Adjectival modifiers

Although their suggested ranges were specified by adjectival modifiers, these modifiers were *not* part of previous classifications of amphiboles (IMA1978, IMA1997, IMA2003); their use was optional, and they are used to provide more information about an amphibole composition than is present in its formal name. For example, the presence of 0.54 Cl apfu (atoms per formula unit) in an amphibole is obviously of considerable crystal-chemical and petrological interest, but is not represented in the name of the amphibole; in the interest of propagating this information (particularly in this age of databases and keywords), the use of the adjectival modifier is a useful option both for an author and for a reader interested in Cl in amphiboles. However, a recent International Mineralogical Association Commission on New Minerals and Mineral Names (IMA-CNMMN) decision (voting proposal 03A; Bayliss et al. 2005) discredited the use of Schaller modifiers, and recommended using expressions of the type Cl-rich or Cl-bearing preceding the amphibole name (including the valence state of the species where appropriate and where known, e.g., Fe^{3+}-rich). Use of such descriptors is at an author's discretion.

Named amphiboles

The IMA-CNMMN introduced a new category of amphibole: *named amphiboles* (Burke and Leake 2004). These are names that are in accord with the current IMA-approved nomenclature scheme (i.e., involve no new root names) but have not been formally approved as accredited mineral species by the IMA-CNMMN or its successor, International Mineralogical Association Commission on New Minerals Nomenclature and Classification (IMA-CNMNC). The use of these names is thus allowed, but formal description for official recognition is desirable.

Synthetic amphiboles

There are many recent studies focusing on the synthesis and characterization of amphibole compositions, which are important in understanding such issues as (1) stability, (2) symmetry, (3) thermodynamics, and (4) short-range order. Some of these studies have produced compositions that have not (as yet) been observed in nature, either because the chemical systems in which they occur are enriched in geochemically rare elements or because the synthetic system is chemically simpler than is usual in geological systems. As a result, there is need for a way to name synthetic amphiboles. Bayliss et al. (2005) stated that any synthetic species that is still unknown in Nature should be named with the mineral name followed by a suffix indicating the exotic substitution, and that the whole name must be given within quotation marks, e.g., "topaz-(OH)". In the case of the amphiboles, the situation is more complicated, as new root compositions may occur only in synthesis experiments. Obviously, it is inappropriate to designate a new name for such compositions (until or unless they are discovered as minerals). It seems appropriate to designate such compositions by their chemical formula, possibly preceded by the word *synthetic* to distinguish it from hypothetical compositions (such as end-members) or suggested formulas. Where the natural analogue of the root composition of a synthetic amphibole does exist, the approach of Bayliss et al. (2005) seems appropriate.

However, the use of suffixes is not compatible with the use of prefixes in the current classification, and we recommend the use of chemical symbols denoting the substitution [e.g., Na(NaCa) $Ni_5Si_8O_{22}(OH)_2$ = synthetic Ni-richterite]. Note that the use of element symbols as a prefix to the name is not allowed for minerals (as distinct from synthetic materials).

Other issues

Issues such as the role of Li, justification for the existence of the sodium-calcium subgroup, and the role of the oxo-component [^{W}O], are discussed at length in Appendix II; recommendations for the calculation of the chemical formula, OH content and $Fe^{3+}/(Fe^{2+}+Fe^{3+})$ values are given in Appendix III.

The principal variables used in the classification procedure

The total variation in amphibole composition can be described by the quinary system A–B–C–T–W. However, authors of previous IMA classifications of amphiboles did not explicitly define the meanings of A, B, C, T, and W. Inspection of the general formula given above shows that each of these symbols represents several compositional variables, and we must be clear which of these variables we use to represent A, B, C, T, and W. The authors of IMA1997 used Si apfu to represent T, but used (Na + K) to represent A and (Ca + Na) to represent B. The latter two examples make it clear that in IMA1997, the *aggregate charges* at A, B, C, T, and W are used as classification variables (as T contains only Si and Al, plus very rarely Ti^{4+}, the Si content proxies as the aggregate charge). Here, we follow the same practice, and use aggregate charges as classification parameters. The variation of these parameters is constrained by the electroneutrality principle, and hence only four parameters are needed to formally represent this variation. In IMA1978 and IMA1997, variations in A, B, T, and W are the primary classification parameters. Here, we use variations in A, B, C, and W as our primary classification parameters; the reasons for this are discussed in Appendix IV, and the major differences between this classification and IMA1997 and IMA2003 are outlined in Appendix V. The classification diagrams introduced below involve the A and C cations, and we write the aggregate charges in the following way:

$A^{+} = {}^{A}(Na + K + 2Ca)$
$C^{+} = {}^{C}(Al + Fe^{3+} + 2Ti^{4+})$†

where the cations are expressed in apfu. Thus the axes of the diagrams involve amounts of cations in apfu and are convenient for plotting amphibole formulas. *Note that in all diagrams, amphibole names are for Na as the dominant monovalent A-cation and Al as the dominant trivalent C-cation. These diagrams provide the root name, and homovalent analogues are named by addition of the appropriate prefixes* (except where trivial names of petrological significance have been retained, e.g., riebeckite, hastingsite, see Appendix VI[2] for details).

A new scheme for the classification of amphiboles[3]

First, the amphibole supergroup is divided into two groups according to the dominant W species. This scheme is consistent with the CNMNC guidelines (Mills et al. 2009) for mineral groups. The groups are:

(1) ^{W}(OH, F, Cl)-dominant amphiboles;
(2) ^{W}O-dominant amphiboles (oxo-amphiboles).

Amphiboles with (OH, F, Cl) dominant at W

We use the symbols of Kretz (1983) for the amphiboles, and introduce new symbols for amphiboles not included in the original list of symbols. The full list of symbols used here for amphiboles is given as Appendix VII.

Amphiboles with (OH, F, Cl) dominant at W are divided into subgroups according to the dominant charge-arrangements and type of B-group cations. To make the notation simpler, let us write the sum of the small divalent cations at B as $^{B}\Sigma M^{2+} = {}^{B}Mg + {}^{B}Fe^{2+} + {}^{B}Mn^{2+}$, and the sum of the B cations as $\Sigma B = {}^{B}Li + {}^{B}Na + {}^{B}\Sigma M^{2+} + {}^{B}Ca$ (which generally is equal to 2.00 apfu). End-member (root) compositions may involve monovalent cations (Na, Li), divalent cations (Ca, ΣM^{2+}), and both monovalent and divalent cations in 1:1 proportion (e.g., Na + Ca, Li + $^{B}\Sigma M^{2+}$). The necessity for end-member compositions involving cations of different charge at one site is discussed in Appendix IV. There are eight subgroups, the first four of which comprise the most common rock-forming amphiboles:

Magnesium-iron-manganese amphiboles
Calcium amphiboles
Sodium-calcium amphiboles
Sodium amphiboles
Lithium amphiboles
Sodium-(magnesium-iron-manganese) amphiboles
Lithium-(magnesium-iron-manganese) amphiboles
Lithium-calcium amphiboles.

The dominant B constituents may be represented as follows:

Magnesium-iron-manganese $^{B}\Sigma M^{2+}$
Calcium ^{B}(Ca + Na)
Sodium-calcium ^{B}(Ca + Na)
Sodium ^{B}(Ca + Na)
Lithium ^{B}Li
Sodium-(magnesium-iron-manganese) ^{B}Na + $^{B}\Sigma M^{2+}$
Lithium-(magnesium-iron-manganese) ^{B}Li + $^{B}\Sigma M^{2+}$
Lithium-calcium ^{B}Li + ^{B}Ca.

The dominant constituent (or group of constituents) defines the subgroup. For example, ^{B}(Ca + Na) defines only the dominance of the calcium, sodium-calcium, and sodium subgroups

† This expression for C is somewhat simplified here; a more detailed discussion of its definition is given in Appendix IV.
[2] Deposit item AM-12-091, Appendix VI. Deposit items are available two ways: For a paper copy contact the Business Office of the Mineralogical Society of America (see inside front cover of recent issue) for price information. For an electronic copy visit the MSA web site at http://www.minsocam.org, go to the *American Mineralogist* Contents, find the table of contents for the specific volume/issue wanted, and then click on the deposit link there.
[3] A program for assigning amphibole names, using the content of the formula as input, is available at http://www_crystal.unipv.it/labcris/AMPH2012.zip.

collectively. Once the dominance of a collective group of constituents is established, which amphibole subgroup occurs is defined by the ratio of the constituents as indicated below for $^{B}Ca/^{B}(Ca + Na)$:

Calcium $^{B}Ca/^{B}(Ca + Na) \geq 0.75$
Sodium-calcium $0.75 > {}^{B}Ca/^{B}(Ca + Na) > 0.25$
Sodium $0.25 \geq {}^{B}Ca/^{B}(Ca + Na)$.

Boundaries at 0.25 and 0.75 apfu separate root compositions at 0.0, 0.5, and 1.0 according to the dominant cation or group of cations.

The magnesium-iron-manganese amphiboles

Defined by

$^{B}(Ca + \Sigma M^{2+})/\Sigma B \geq 0.75$, $^{B}\Sigma M^{2+}/\Sigma B > {}^{B}Ca/\Sigma B$

Amphiboles of this subgroup may be orthorhombic (space groups *Pnma* or *Pnmn*) or monoclinic (space groups *C*2/*m* or *P*2$_1$/*m*). Although we distinguish between the B and C cations in amphiboles in general, we cannot identify accurately the relative amounts of Mg and Fe^{2+} in the B- and C-cation groups in the magnesium-iron-manganese amphiboles without crystal-structure refinement or Mössbauer spectroscopy. Hence for this subgroup, we treat the divisions between Mg-Fe^{2+} homovalent analogues in terms of the sum of the B and C cations. However, Mn^{2+} has a significant preference for the *M*(4) site, and hence distinct species are recognized with Mn^{2+} assigned as the dominant B-cation (where direct experimental data are available, they take precedence over such an assignment).

Orthorhombic magnesium-iron-manganese amphiboles. The space group *Pnma* is assumed, and the space group *Pnmn* (where determined) is indicated by the prefix *proto*. There are four root compositions with Mg dominant at C (Table 2). The composition $NaMg_2Mg_5(Si_7Al)O_{22}(OH)_2$ was named sodicanthophyllite in IMA1997. However, this composition has a different charge arrangement from other root compositions for orthorhombic amphiboles and hence warrants a new root name, rootname 1. The composition Na Mg_2 (Mg_3 Al_2) (Si_5 Al_3) O_{22} $(OH)_2$ is introduced as a new root composition, rootname 2, replacing sodicgedrite, $NaMg_2(Mg_4Al)(Si_6Al_2)O_{22}(OH)_2$ in IMA1997. There are four homovalent analogues involving Fe^{2+} dominant at (B + C). The compositional ranges of the orthorhombic magnesium-iron-manganese amphiboles are shown in Figure 1.

Monoclinic magnesium-iron-manganese amphiboles. The space group *C*2/*m* is assumed, the space group *P*2$_1$/*m* (where determined) is indicated by the hyphenated suffix *P*2$_1$/*m*. There is one root composition with Mg dominant at (B + C), one analogue involving Fe^{2+} instead of Mg dominant at (B + C), and two additional analogues with Mn^{2+} dominant at (B + C) and at B only. IMA1997 designated the Mn^{2+} analogues by the prefix *mangano*. However, it is not consistent to apply the prefix *mangano* to the composition $\square Mn_2^{2+}Mg_5Si_8O_{22}(OH)_2$ as all other prefixes are used to indicate compositions of the A and C cations. Thus the composition $\square Mn_2^{2+}Mg_5Si_8O_{22}(OH)_2$ warrants a new root name: rootname 3, $\square Mn_2^{2+}Fe_5^{2+}Si_8O_{22}(OH)_2$ is ferro-rootname 3, and $\square Mn_2^{2+}Mn_5^{2+}Si_8O_{22}(OH)_2$ is mangano-rootname 3; note that the prefix *mangano* is used only where $^{C}Mn^{2+}$ is dominant.

Table 2. End-member compositions in magnesium-iron-manganese amphiboles

End-member formula	Name
Orthorhombic	
$\square Mg_2Mg_5Si_8O_{22}(OH)_2$	Anthophyllite
$NaMg_2Mg_5(Si_7Al)O_{22}(OH)_2$	Rootname 1
$\square Mg_2(Mg_3Al_2)(Si_6Al_2)O_{22}(OH)_2$	Gedrite
$NaMg_2(Mg_3Al_2)(Si_5Al_3)O_{22}(OH)_2$	Rootname 2
$\square Fe_2^{2+}Fe_5^{2+}Si_8O_{22}(OH)_2$	Ferro-anthophyllite
$NaFe_2^{2+}Fe_5^{2+}(Si_7Al)O_{22}(OH)_2$	Ferro-rootname 1
$\square Fe_2^{2+}(Fe_3^{3+}Al_2)(Si_6Al_2)O_{22}(OH)_2$	Ferro-gedrite
$NaFe_2^{2+}(Fe_5^{3+}Al_2)(Si_5Al_3)O_{22}(OH)_2$	Ferro-rootname 2
Monoclinic	
$\square Mg_2Mg_5Si_8O_{22}(OH)_2$	Cummingtonite
$\square Fe_2^{2+}Fe_5^{2+}Si_8O_{22}(OH)_2$	Grunerite
$\square Mn_2^{2+}Mg_5Si_8O_{22}(OH)_2$	Rootname 3
$\square Mn_2^{2+}Fe_5^{2+}Si_8O_{22}(OH)_2$	Ferro-rootname 3
$\square Mn_2^{2+}Mn_5^{2+}Si_8O_{22}(OH)_2$	Mangano-rootname 3

The compositional ranges of the monoclinic magnesium-iron-manganese amphiboles are shown in Figure 2, and end-member compositions are given in Table 2.

The calcium amphiboles

Defined by

$^{B}(Ca + \Sigma M^{2+})/\Sigma B \geq 0.75$, $^{B}Ca/\Sigma B \geq {}^{B}\Sigma M^{2+}/\Sigma B$

The eight root compositions are given in Table 3, and six of them are shown in Figure 3. Rootname 4, Na Ca_2 (Mg_4 Ti) (Si_5 Al_3) O_{22} $(OH)_2$, is discussed in Appendix IV in the section on amphiboles with Ti >0.50 apfu. Note that the name *hornblende* is never used without a prefix, as was the case in IMA1997, as hornblende is routinely used as a term when working in the field. Also, kaersutite is no longer considered as an ^{W}(OH, F, Cl)-dominant calcium amphibole; it is classified as an $^{W}O^{2-}$-dominant amphibole. Ferrous-iron and ferric-iron analogues are generally named by the prefixes *ferro*- and *ferri*- (Table 1), although some compositions retain their traditional name (e.g., hastingsite, magnesio-hastingsite) because of the petrological

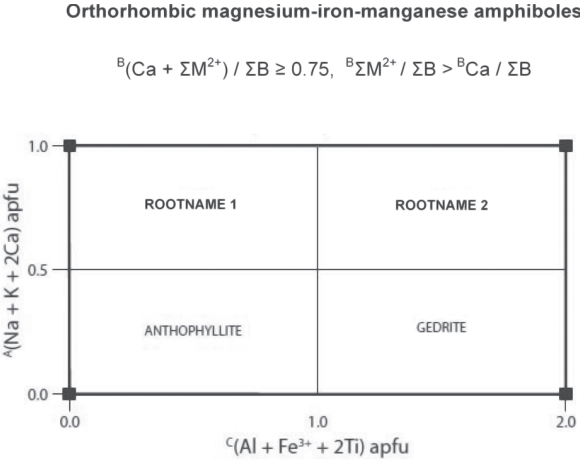

Figure 1. Orthorhombic magnesium-iron-manganese amphiboles and their compositional boundaries. Filled black squares are the locations of named and unnamed Mg end-members.

importance of these names.

Note that the IMA1997 definition of actinolite is retained for petrological reasons. In the tremolite–ferro-actinolite series, $\square Ca_2Mg_5Si_8O_{22}(OH)_2$ – $\square Ca_2Fe^{2+}_5Si_8O_{22}(OH)_2$, the compositional range of tremolite extends from $\square Ca_2Mg_5Si_8O_{22}(OH)_2$ to $\square Ca_2Mg_{4.5}Fe^{2+}_{0.5}Si_8O_{22}(OH)_2$, actinolite extends from $\square Ca_2Mg_{<4.5}Fe^{2+}_{>0.5}Si_8O_{22}(OH)_2$ to $\square Ca_2\ Mg_{2.5}Fe^{2+}_{2.5}Si_8O_{22}(OH)_2$, and ferro-actinolite extends from $\square Ca_2Mg_{<2.5}Fe^{2+}_{>2.5}\ Si_8\ O_{22}(OH)_2$ to $\square Ca_2Fe^{2+}_5Si_8O_{22}\ (OH)_2$.

Monoclinic magnesium-iron-manganese amphiboles

$^{B}(Ca + \Sigma M^{2+}) / \Sigma B \geq 0.75,\ ^{B}\Sigma M^{2+} / \Sigma B > {}^{B}Ca/{}^{B}\Sigma B$

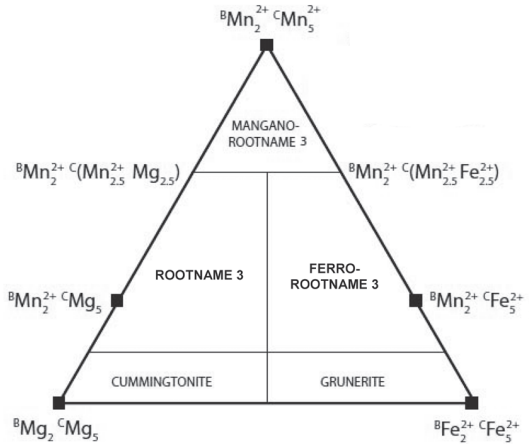

Figure 2. Monoclinic magnesium-iron-manganese amphiboles and their compositional boundaries. Filled black squares are the locations of named and unnamed Mg-Fe^{2+}-Mn end-member compositions.

Table 3. End-member compositions in calcium amphiboles

End-member formula	Name
$\square Ca_2Mg_5Si_8O_{22}(OH)_2$	Tremolite
$\square Ca_2(Mg_4Al)(Si_7Al)O_{22}(OH)_2$	Magnesio-hornblende
$\square Ca_2(Mg_3Al_2)(Si_6Al_2)O_{22}(OH)_2$	Tschermakite
$NaCa_2Mg_5(Si_7Al)O_{22}(OH)_2$	Edenite
$NaCa_2(Mg_4Al)(Si_6Al_2)O_{22}(OH)_2$	Pargasite
$NaCa_2(Mg_3Al_2)(Si_5Al_3)O_{22}(OH)_2$	Sadanagaite
$CaCa_2(Mg_4Al)(Si_5Al_3)O_{22}(OH)_2$	Cannilloite
$NaCa_2(Mg_4Ti)(Si_5Al_3)O_{22}(OH)_2$	Rootname 4
$Pb^{2+}Ca_2(Mg_3Fe^{3+}_2)(Si_6Be_2)O_{22}(OH)_2$	Joesmithite
$\square Ca_2Fe^{2+}_5Si_8O_{22}(OH)_2$	Ferro-actinolite
$\square Ca_2(Fe^{2+}_4Al)(Si_7Al)O_{22}(OH)_2$	Ferro-hornblende
$\square Ca_2(Fe^{3+}_2Al_2)(Si_6Al_2)O_{22}(OH)_2$	Ferro-tschermakite
$NaCa_2Fe^{2+}_5(Si_7Al)O_{22}(OH)_2$	Ferro-edenite
$NaCa_2(Fe^{2+}_4Al)(Si_6Al_2)O_{22}(OH)_2$	Ferro-pargasite
$NaCa_2(Fe^{3+}_2Al_2)(Si_5Al_3)O_{22}(OH)_2$	Ferro-sadanagaite
$CaCa_2(Fe^{2+}_4Al)(Si_5Al_3)O_{22}(OH)_2$	Ferro-cannilloite
$NaCa_2(Fe^{2+}_4Ti)(Si_5Al_3)O_{22}(OH)_2$	Ferro-rootname 4
$\square Ca_2(Mg_4Fe^{3+})(Si_7Al)O_{22}(OH)_2$	Magnesio-ferri-hornblende
$\square Ca_2(Mg_3Fe^{3+}_2)(Si_6Al_2)O_{22}(OH)_2$	Ferri-tschermakite
$NaCa_2(Mg_4Fe^{3+})(Si_6Al_2)O_{22}(OH)_2$	Magnesio-hastingsite
$NaCa_2(Mg_3Fe^{3+}_2)(Si_5Al_3)O_{22}(OH)_2$	Ferri-sadanagaite
$CaCa_2(Mg_4Fe^{3+})(Si_5Al_3)O_{22}(OH)_2$	Ferri-cannilloite
$\square Ca_2(Fe^{2+}_4Fe^{3+})(Si_7Al)O_{22}(OH)_2$	Ferro-ferri-hornblende
$\square Ca_2(Fe^{2+}_3Fe^{3+}_2)(Si_6Al_2)O_{22}(OH)_2$	Ferro-ferri-tschermakite
$NaCa_2(Fe^{2+}_4Fe^{3+})(Si_6Al_2)O_{22}(OH)_2$	Hastingsite
$NaCa_2(Fe^{2+}_3Fe^{3+}_2)(Si_5Al_3)O_{22}(OH)_2$	Ferro-ferri-sadanagaite
$CaCa_2(Fe^{2+}_4Fe^{3+})(Si_5Al_3)O_{22}(OH)_2$	Ferro-ferri-cannilloite

Joesmithite is an amphibole of unusual composition, ideally $Pb^{2+}Ca_2(Mg_3Fe^{3+}_2)(Si_6\ Be_2)O_{22}(OH)_2$, and space group $P2/a$ (Moore et al. 1993). It is a calcium amphibole but, because of the presence of Be as a T-group cation, it does not fit the compositional diagrams used here for calcium-amphibole classification; however, it is included in Table 3. It has been found only at one locality (Långban, Värmland, Sweden), and there is no information as to the extent of any solid solution.

Cannilloite, ideally $CaCa_2(Mg_4Al)(Si_5Al_3)O_{22}(OH)_2$ (Hawthorne et al. 1996), is also an unusual composition with Ca as the A cation and hence with 3 Al apfu as T cations. It does not fit the compositional diagrams used here for amphibole classification; however, it is included in Table 3. Its fluoro- counterpart has been found only at one locality (Pargas, Finland).

The sodium-calcium amphiboles

Defined by

$$0.75 > {}^{B}(Ca + \Sigma M^{2+})/\Sigma B > 0.25,\ {}^{B}Ca/\Sigma B \geq {}^{B}\Sigma M^{2+}/\Sigma B$$

and

$$0.75 > {}^{B}(Na + Li)/\Sigma B > 0.25,\ {}^{B}Na/\Sigma B \geq {}^{B}Li/\Sigma B.$$

There are five root compositions with Mg and Al dominant at C, together with their ferrous-iron, ferric-iron, and ferrous-ferric-iron analogues (Table 4). The compositional ranges of the root sodium-calcium amphiboles are shown in Figure 4.

The sodium amphiboles

Defined by

$$^{B}(Na + Li)/\Sigma B \geq 0.75,\ {}^{B}Na/\Sigma B \geq {}^{B}Li/\Sigma B.$$

Three root compositions are shown in Figure 5, and all end-member compositions are listed in Table 5. Leakeite, ideally,

Calcium amphiboles

$^{B}(Ca + \Sigma M^{2+}) / \Sigma B \geq 0.75,\ {}^{B}Ca / \Sigma B \geq {}^{B}\Sigma M^{2+} / \Sigma B$

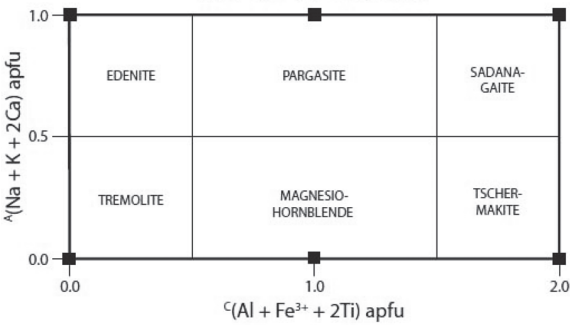

Figure 3. Calcium amphiboles and their compositional boundaries. The heavy solid black line is a two-dimensional section of amphibole compositional space (see Appendix Fig. 3) at $^{B}Ca/^{B}(Ca + Na) = 1.0$ that contains the calcium end-member compositions.

$NaNa_2(Mg_2Al_2Li)Si_8O_{22}(OH)_2$, occupies the same compositional space as eckermannite, ideally $NaNa_2(Mg_4Al)Si_8O_{22}(OH)_2$, in the compositional diagrams used here for amphibole classification [after subtracting from $^{C}(Al,Fe)^{3+}$ the same amount as ^{C}Li; cf. Appendix IV for more detail]. Riebeckite and arfvedsonite retain their traditional names because of their petrological importance.

The lithium amphiboles

Defined by

$^{B}(Na + Li)/\Sigma B \geq 0.75$, $^{B}Li/\Sigma B > {}^{B}Na/\Sigma B$

Amphiboles of this subgroup may be orthorhombic (space group *Pnma*) or monoclinic (space group *C*2/*m*).

Table 4. End-member compositions in sodium-calcium amphiboles

End-member formula	Name
$\square(NaCa)(Mg_4Al)Si_8O_{22}(OH)_2$	Winchite
$\square(NaCa)(Mg_3Al_2)(Si_7Al)O_{22}(OH)_2$	Barroisite
$Na(NaCa)Mg_5Si_8O_{22}(OH)_2$	Richterite
$Na(NaCa)(Mg_4Al)(Si_7Al)O_{22}(OH)_2$	Katophorite
$Na(NaCa)(Mg_3Al_2)(Si_6Al_2)O_{22}(OH)_2$	Taramite
$\square(NaCa)(Fe^{2+}_4Al)Si_8O_{22}(OH)_2$	Ferro-winchite
$\square(NaCa)(Fe^{2+}_3Al_2)(Si_7Al)O_{22}(OH)_2$	Ferro-barroisite
$Na(NaCa)Fe^{2+}_5Si_8O_{22}(OH)_2$	Ferro-richterite
$Na(NaCa)(Fe^{2+}_4Al)(Si_7Al)O_{22}(OH)_2$	Ferro-katophorite
$Na(NaCa)(Fe^{2+}_3Al_2)(Si_6Al_2)O_{22}(OH)_2$	Ferro-taramite
$\square(NaCa)(Mg_4Fe^{3+})Si_8O_{22}(OH)_2$	Ferri-winchite
$\square(NaCa)(Mg_3Fe^{3+}_2)(Si_7Al)O_{22}(OH)_2$	Ferri-barroisite
$Na(NaCa)(Mg_4Fe^{3+})(Si_7Al)O_{22}(OH)_2$	Ferri-katophorite
$Na(NaCa)(Mg_3Fe^{3+}_2)(Si_6Al_2)O_{22}(OH)_2$	Ferri-taramite
$\square(NaCa)(Fe^{2+}_4Fe^{3+})Si_8O_{22}(OH)_2$	Ferro-ferri-winchite
$\square(NaCa)(Fe^{2+}_3Fe^{3+}_2)(Si_7Al)O_{22}(OH)_2$	Ferro-ferri-barroisite
$Na(NaCa)(Fe^{2+}_4Fe^{3+})(Si_7Al)O_{22}(OH)_2$	Ferro-ferri-katophorite
$Na(NaCa)(Fe^{2+}_3Fe^{3+}_2)(Si_6Al_2)O_{22}(OH)_2$	Ferro-ferri-taramite

Sodium-calcium amphiboles

$0.75 > {}^{B}(Ca + \Sigma M^{2+}) / \Sigma B > 0.25$, $^{B}Ca / \Sigma B \geq {}^{B}\Sigma M^{2+} / \Sigma B$

and

$0.75 > {}^{B}(Na + Li) / \Sigma B > 0.25$, $^{B}Na / \Sigma B \geq {}^{B}Li / \Sigma B$

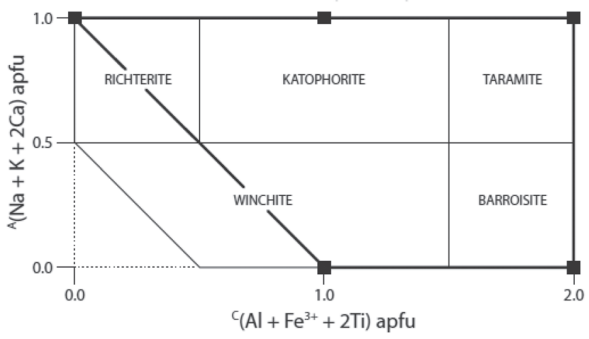

Figure 4. Sodium-calcium amphiboles and their compositional boundaries. The heavy solid black line is a two-dimensional section of amphibole composition space (see Appendix Fig. 3) at $^{B}Ca/^{B}(Ca + Na) = 0.5$ that contains the sodium-calcium end-member compositions. The thick solid lines show the possible range of amphibole compositions at $^{B}Ca/^{B}(Ca + Na) = 0.5$ and the solid lines to the left of the diagonal heavy solid black line show the possible range of amphibole compositions at $^{B}Ca/^{B}(Ca + Na) = 0.75$, the boundary between the sodium-calcium amphiboles and the calcium amphiboles.

Orthorhombic lithium amphiboles. There is one root composition plus its ferro-, ferri-, and ferro-ferri- analogues (Table 6).

Monoclinic lithium amphiboles. There are two root compositions plus their ferro-, ferri- and ferro-ferri- analogues (Table 6, Fig. 6). Note that "clinoholmquistite" has recently been discredited (Oberti et al. 2005); also, current knowledge and comparison with cummingtonite suggest that compositions close to that of the end-member clinoholmquistite formula (if stable) should have the space group $P2_1/m$. The composition $NaLi_2(Mg_4Al)Si_8O_{22}(OH)_2$ has not yet been described as a mineral; it is a root composition and warrants a new rootname: rootname 5.

The sodium-(magnesium-iron-manganese) amphiboles

Defined by

$0.75 > {}^{B}(Ca + \Sigma M^{2+})/\Sigma B > 0.25$, $^{B}\Sigma M^{2+}/\Sigma B > {}^{B}Ca/\Sigma B$

and

$0.75 > {}^{B}(Na + Li)/\Sigma B > 0.25$, $^{B}Na/\Sigma B \geq {}^{B}Li/\Sigma B$.

Table 5. End-member compositions in sodium amphiboles

End-member formula	Name
$\square Na_2(Mg_3Al_2)Si_8O_{22}(OH)_2$	Glaucophane
$NaNa_2(Mg_4Al)Si_8O_{22}(OH)_2$	Eckermannite
$NaNa_2(Mg_3Al_2)(Si_7Al)O_{22}(OH)_2$	Nybøite
$NaNa_2(Mg_2Al_2Li)Si_8O_{22}(OH)_2$	Leakeite
$\square Na_2(Fe^{2+}_3Al_2)Si_8O_{22}(OH)_2$	Ferro-glaucophane
$NaNa_2(Fe^{2+}_4Al)Si_8O_{22}(OH)_2$	Ferro-eckermannite
$NaNa_2(Fe^{2+}_3Al_2)(Si_7Al)O_{22}(OH)_2$	Ferro-nybøite
$NaNa_2(Fe^{2+}_4Al_2Li)Si_8O_{22}(OH)_2$	Ferro-leakeite
$\square Na_2(Mg_3Fe^{3+}_2)Si_8O_{22}(OH)_2$	Magnesio-riebeckite
$NaNa_2(Mg_4Fe^{3+})Si_8O_{22}(OH)_2$	Magnesio-arfvedsonite
$NaNa_2(Mg_3Fe^{3+}_2)(Si_7Al)O_{22}(OH)_2$	Ferri-nybøite
$NaNa_2(Mg_2Fe^{3+}_2Li)Si_8O_{22}(OH)_2$	Ferri-leakeite
$\square Na_2(Fe^{2+}_3Fe^{3+}_2)Si_8O_{22}(OH)_2$	Riebeckite
$NaNa_2(Fe^{2+}_4Fe^{3+})Si_8O_{22}(OH)_2$	Arfvedsonite
$NaNa_2(Fe^{2+}_3Fe^{3+}_2)(Si_7Al)O_{22}(OH)_2$	Ferro-ferri-nybøite
$NaNa_2(Fe^{2+}_2Fe^{3+}_2Li)Si_8O_{22}(OH)_2$	Ferro-ferri-leakeite

Sodium amphiboles

$^{B}(Na + Li) / \Sigma B \geq 0.75$, $^{B}Na / \Sigma B > {}^{B}Li / \Sigma B$

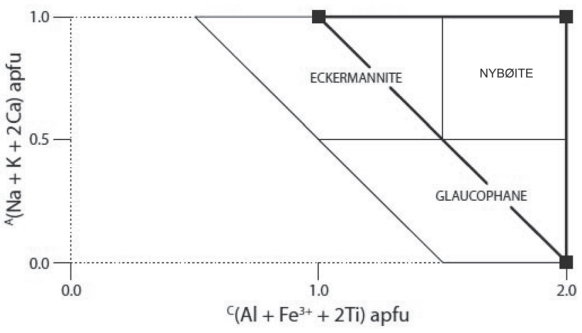

Figure 5. Sodium amphiboles and their compositional boundaries. The heavy solid black line is a two-dimensional section of amphibole compositional space (Appendix Fig. 3) at $^{B}Ca/^{B}(Ca + Na) = 0.0$ that contains sodium end-member compositions. The thick solid lines show the possible range of amphibole compositions at $^{B}Ca/^{B}(Ca + Na) = 0.0$ and the solid lines to the left of the diagonal heavy solid black line show the possible range of amphibole compositions at $^{B}Ca/^{B}(Ca + Na) = 0.25$, the boundary between the sodium amphiboles and the sodium-calcium amphiboles.

TABLE 6. End-member compositions in lithium amphiboles

End-member formula	Name
Orthorhombic	
$\square Li_2(Mg_3Al_2)Si_8O_{22}(OH)_2$	Holmquistite
$\square Li_2(Fe^{2+}_3Al_2)Si_8O_{22}(OH)_2$	Ferro-holmquistite
$\square Li_2(Mg_3Fe^{3+}_2)Si_8O_{22}(OH)_2$	Ferri-holmquistite
$\square Li_2(Fe^{2+}_3Fe^{3+}_2)Si_8O_{22}(OH)_2$	Ferro-ferri-holmquistite
Monoclinic	
$\square Li_2(Mg_3Al_2)Si_8O_{22}(OH)_2$	Clino-holmquistite
$NaLi_2(Mg_2Al_2Li)Si_8O_{22}(OH)_2$	Pedrizite
$NaLi_2(Mg_4Al)Si_8O_{22}(OH)_2$	Rootname 5
$\square Li_2(Fe^{2+}_3Al_2)Si_8O_{22}(OH)_2$	Clino-ferro-holmquistite
$NaLi_2(Fe^{2+}_2Al_2Li)Si_8O_{22}(OH)_2$	Ferro-pedrizite
$\square Li_2(Mg_3Fe^{3+}_2)Si_8O_{22}(OH)_2$	Clino-ferri-holmquistite
$NaLi_2(Mg_2Fe^{3+}_2Li)Si_8O_{22}(OH)_2$	Ferri-pedrizite
$\square Li_2(Fe^{2+}_3Fe^{3+}_2)Si_8O_{22}(OH)_2$	Clino-ferro-ferri-holmquistite
$NaLi_2(Fe^{2+}_2Fe^{3+}_2Li)Si_8O_{22}(OH)_2$	Ferro-ferri-pedrizite

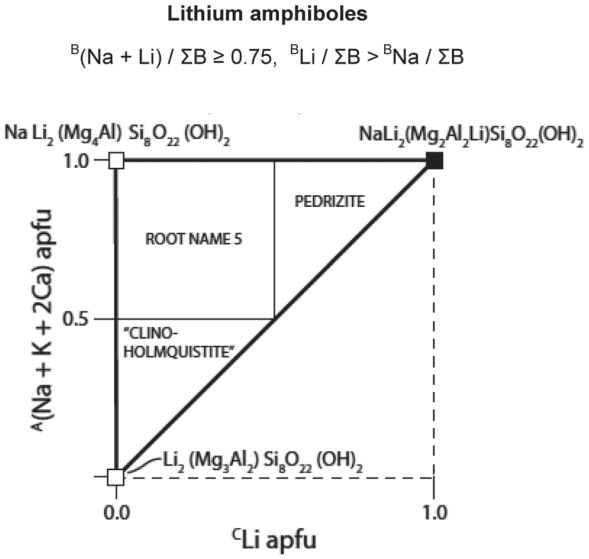

FIGURE 6. Monoclinic lithium amphiboles and their compositional boundaries. The filled black square is the location of a named end-member composition, white squares are as-yet un-named end-member compositions, and the solid black lines show the ranges of possible amphibole compositions. Note that "clino-holmquistite" is currently not an accredited species.

These amphiboles are the (Mg-Fe-Mn) analogues of the sodium-calcium amphiboles, where Ca is replaced by (Mg, Fe, Mn). The root compositions and compositional ranges are given in Table 7. Where possible, we recognize the dominant divalent B-cation: Mg, Fe^{2+}, or Mn^{2+}. The ^{B}(Na Mg) root compositions (Table 7) are labeled rootnames 6–10 and are shown in Figure 7; note that rootname 8 is the ^{B}Mg analogue of richterite (Table 4); note that its synthetic analogue has $P2_1/m$ symmetry (Cámara et al. 2003). ^{B}Mn analogues of the ^{B}Mg root compositions may be recognized from electron-microprobe data as Mn^{2+} orders very strongly at $M(4)$ (where the B cations reside) relative to Mg or Fe^{2+}. Note that this requires another set of root names as the prefix *mangano-* refers to the ^{C}Mn analogue of a ^{C}Mg root composition (rootnames 11–15, Table 7). However, we cannot recognize $^{B}Fe^{2+}$ analogues of ^{B}Mg root compositions from a chemical analysis as we are unable to assign Fe^{2+} as a B or C cation; crystal-structure refinement or Mössbauer spectroscopy

TABLE 7. End-member compositions in the sodium-(magnesium-iron-manganese) amphiboles

End-member formula	Name
$\square(NaMg)(Mg_4Al)Si_8O_{22}(OH)_2$	Rootname 6
$\square(NaMg)(Mg_3Al_2)(Si_7Al)O_{22}(OH)_2$	Rootname 7
$Na(NaMg)Mg_5Si_8O_{22}(OH)_2$	Rootname 8
$Na(NaMg)(Mg_4Al)(Si_7Al)O_{22}(OH)_2$	Rootname 9
$Na(NaMg)(Mg_3Al_2)(Si_6Al_2)O_{22}(OH)_2$	Rootname 10
$\square(NaMn^{2+})(Mg_4Al)Si_8O_{22}(OH)_2$	Rootname 11
$\square(NaMn^{2+})(Mg_3Al_2)(Si_7Al)O_{22}(OH)_2$	Rootname 12
$Na(NaMn^{2+})Mg_5Si_8O_{22}(OH)_2$	Rootname 13
$Na(NaMn^{2+})(Mg_4Al)(Si_7Al)O_{22}(OH)_2$	Rootname 14
$Na(NaMn^{2+})(Mg_3Al_2)(Si_6Al_2)O_{22}(OH)_2$	Rootname 15
$\square(NaFe^{2+})(Fe^{2+}_4Al)Si_8O_{22}(OH)_2$	Rootname 16

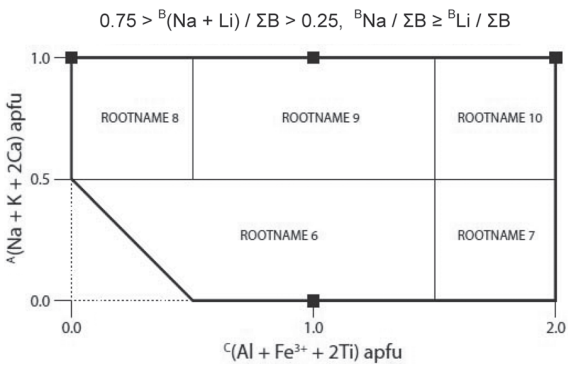

FIGURE 7. Sodium-(magnesium-iron-manganese) amphiboles and their compositional boundaries. Filled black squares are the locations of presently unnamed end-member compositions. The thick solid line refers to end-member compositions at $^{B}Na/^{B}(Na + \Sigma M^{2+}) = 0.5$. The solid lines to the left of the diagonal thick solid line show the possible range of amphibole compositions at $^{B}Na/^{B}(Na + \Sigma M^{2+}) = 0.25$, the boundary between the sodium-(magnesium-iron-manganese) amphiboles and the magnesium-iron-manganese amphiboles.

is necessary. Should $^{B}(Na\ Fe^{2+})$ compositions be detected, they would deserve new rootnames. Moreover, intermediate compositions can be named only using crystal-structure refinement or Mössbauer spectroscopy. The one exception is the root composition $\square(NaFe^{2+})(Fe^{2+}_4Al)Si_8O_{22}(OH)_2$ as Fe^{2+} is the only divalent B- and C-cation present (rootname 16, Table 7).

At the moment, there is only one known amphibole in this group, and that is close to the root composition, $\square(NaMn^{2+})(Mg_4Fe^{3+})Si_8O_{22}(OH)_2$ (Oberti and Ghose 1993). A new name for this amphibole must be assigned via submission to IMA: rootname 11. The analogues with Fe^{2+} at C will be named by the prefix *ferro-*, and the sample of Oberti and Ghose (1993) with Fe^{3+} dominant at C should be named with the prefix *ferri-*.

The lithium-(magnesium-iron-manganese) amphiboles

Defined by

$$0.75 > {}^{B}(Ca + \Sigma M^{2+})/\Sigma B > 0.25,\ {}^{B}\Sigma M^{2+}/\Sigma B > {}^{B}Ca/\Sigma B$$

and

$$0.75 > {}^{B}(Na + Li)/\Sigma B > 0.25,\ {}^{B}Li/\Sigma B > {}^{B}Na/\Sigma B.$$

These amphiboles are the lithium analogues of the sodium-(magnesium-iron-manganese) amphiboles, where Na is replaced by Li. The root compositions and compositional ranges are given in Table 8 and Figure 8. As these amphiboles are only known as synthetic phases (Iezzi et al. 2006), only the ^{B}(Li Mg) root compositions are listed and are labeled rootnames 17–21; note that rootname 19 is the ^{B}(Li Mg) analogue of richterite (Table 4).

The lithium-calcium amphiboles

Defined by

$$0.75 > {}^{B}(Ca + \Sigma M^{2+})/\Sigma B > 0.25,\ {}^{B}Ca/\Sigma B \geq {}^{B}\Sigma M^{2+}/\Sigma B$$

and

$$0.75 > {}^{B}(Na + Li)/\Sigma B > 0.25,\ {}^{B}Li/\Sigma B > {}^{B}Na/\Sigma B.$$

These amphiboles are the lithium analogues of the sodium-calcium amphiboles, where Na is replaced by Li. The root compositions and compositional ranges are given in Table 9 and Figure 9. The ^{B}(Li Ca) root compositions (Table 9) are labeled rootnames 22–26; note that rootname 24 is the ^{B}(Li Ca) analogue of richterite (Table 4).

Amphiboles with O^{2-} dominant at W

Dominance of W by O^{2-} is accompanied by the occurrence of additional high-charge ($\geq 3^{+}$) C-cations ordered at the *M*(1) and/or *M*(3) sites; the aggregate charge at C may thus exceed 12^{+}. There are four distinct root-compositions currently known for calcium and sodium amphiboles (Table 10), and Fe^{2+} and Fe^{3+} analogues can be indicated by the prefixes *ferro-* and *ferri-*.

Three of these amphiboles (root names obertiite, ungarettiite, and dellaventuraite) are rare, and analysis for H to characterize these species should not be regarded as unduly onerous. However, this is not the case for kaersutite, which is a reasonably common and petrologically important amphibole. Thus a different criterion would be convenient for the classification of kaersutite; this can be done on the basis of the Ti content. Although Ti is not completely related to the oxo component in amphibole, it is a useful indicator. Consequently, we use Ti content as a proxy for the oxo component in pargasite, and define kaersutite as having ^{C}Ti >0.50 apfu ($\approx O^{2-} > 1.00$ apfu). However, if the O^{2-} content is known from chemical or crystal-chemical analysis, it takes precedence over use of the Ti content as a proxy (see Appendix II).

Table 8. End-member compositions in the lithium-(magnesium-iron-manganese) amphiboles

End-member formula	Name
$\square(LiMg)(Mg_4Al)Si_8O_{22}(OH)_2$	Rootname 17
$\square(LiMg)(Mg_3Al_2)(Si_7Al)O_{22}(OH)_2$	Rootname 18
$Na(LiMg)Mg_5Si_8O_{22}(OH)_2$	Rootname 19
$Na(LiMg)(Mg_4Al)(Si_7Al)O_{22}(OH)_2$	Rootname 20
$Na(LiMg)(Mg_3Al_2)(Si_6Al_2)O_{22}(OH)_2$	Rootname 21

Table 9. End-member compositions in the lithium-calcium amphiboles

End-member formula	Name
$\square(LiCa)(Mg_4Al)Si_8O_{22}(OH)_2$	Rootname 22
$\square(LiCa)(Mg_3Al_2)(Si_7Al)O_{22}(OH)_2$	Rootname 23
$Na(LiCa)Mg_5Si_8O_{22}(OH)_2$	Rootname 24
$Na(LiCa)(Mg_4Al)(Si_7Al)O_{22}(OH)_2$	Rootname 25
$Na(LiCa)(Mg_3Al_2)(Si_6Al_2)O_{22}(OH)_2$	Rootname 26

Amphiboles with O^{2-} dominant at W are commonly characterized by Ti as the dominant high-charge C-cation. However, Fe^{3+} may also be the principal high-charge C-cation related to the presence of $^{W}O^{2-}$, and we need to recognize such amphiboles. In oxo-amphiboles, Fe^{3+} balancing $^{W}O^{2-}$ is ordered at the *M*(1) [and less commonly at the *M*(3)] site, so that the sum of high-charge cations does exceed 2.0 apfu and may reach 4.0 apfu. The

Lithium-(magnesium-iron-manganese) amphiboles

$$0.75 > {}^{B}(Ca + \Sigma M^{2+}) / \Sigma B > 0.25,\ {}^{B}\Sigma M^{2+}/\Sigma B > {}^{B}Ca / \Sigma B$$

and

$$0.75 > {}^{B}(Na + Li) / \Sigma B > 0.25,\ {}^{B}Li / \Sigma B > {}^{B}Na / \Sigma B$$

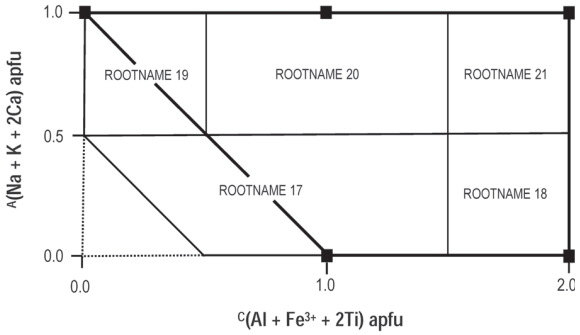

Figure 8. Lithium-(magnesium-iron-manganese) amphiboles and their compositional boundaries. Filled black squares are the locations of presently unnamed end-member compositions. The thick solid line refers to end-member compositions at $^{B}Li/^{B}(Li + \Sigma M^{2+}) = 0.5$. The solid lines to the left of the diagonal thick solid line show the possible range of amphibole compositions at $^{B}Li/^{B}(Li + \Sigma M^{2+}) = 0.75$, the boundary between the lithium-(magnesium-iron-manganese) amphiboles and the magnesium-iron-manganese amphiboles.

Lithium-calcium amphiboles

$$0.75 > {}^{B}(Ca + \Sigma M^{2+}) / \Sigma B > 0.25,\ {}^{B}Ca / \Sigma B \geq {}^{B}\Sigma M^{2+} / \Sigma B$$

and

$$0.75 > {}^{B}(Na + Li) / \Sigma B > 0.25,\ {}^{B}Li / \Sigma B > {}^{B}Na / \Sigma B$$

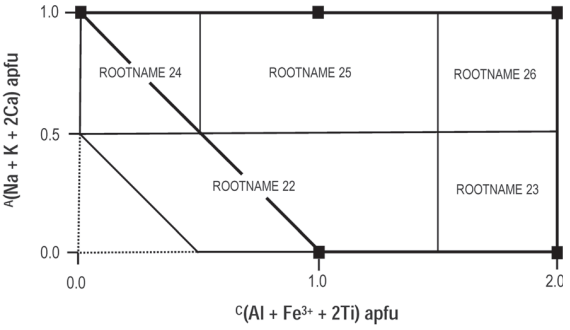

Figure 9. Lithium-calcium amphiboles and their compositional boundaries. Filled black squares are the locations of presently unnamed end-member compositions. The thick solid line refers to end-member compositions at $^{B}Li/^{B}(Li + Ca) = 0.5$. The solid lines to the left of the diagonal thick solid line show the possible range of amphibole compositions at $^{B}Li/^{B}(Li + Ca) = 0.75$, the boundary between the lithium-calcium amphiboles and the calcium amphiboles

TABLE 10. End-member compositions in oxo amphiboles

End-member formula	Name
$NaNa_2(Mg_3Fe^{3+}Ti^{4+})Si_8O_{22}O_2$	Ferri-obertiite
$NaNa_2(MgMn^{3+}_2Ti^{4+}Li)Si_8O_{22}O_2$	Mangani-dellaventuraite
$NaNa_2(Mn^{2+}_2Mn^{3+}_3)Si_8O_{22}O_2$	Mangano-mangani-ungarettiite
$NaCa_2(Mg_3Ti^{4+}Al)(Si_6Al_2)O_{22}O_2$	Kaersutite
$NaCa_2(Fe^{2+}_3Ti^{4+}Al)(Si_6Al_2)O_{22}O_2$	Ferro-kaersutite
$NaCa_2(Fe^{2+}_3Ti^{4+}Fe^{3+})(Si_6Al_2)O_{22}O_2$	Ferro-ferri-kaersutite
$NaCa_2(Mg_3Ti^{4+}Fe^{3+})(Si_6Al_2)O_{22}O_2$	Ferri-kaersutite

site preference of the C cations is not relevant for classification purposes. However, the prefix *ferri-* cannot be used to deal with Fe^{3+} related to the presence of $^{W}O^{2-}$. This is done by using the prefix *oxo-* with the appropriate rootname, e.g., Na(NaCa)$(Fe^{2+}_3Fe^{3+}_2)Si_8O_{22}O_2$: oxo-ferro-richterite; □$Ca_2(Mg_2Fe^{3+}_3)(Si_7Al)O_{22}O_2$: oxo-magnesio-ferri-hornblende; Na(NaCa)$(Mg_2Fe^{3+}_2Al)(Si_7Al)O_{22}O_2$: oxo-katophorite; $NaNa_2(Fe^{2+}Fe^{3+}_2Al_2)(Si_7Al)O_{22}O_2$: oxo-ferro-nybøite.

CODA

The amphiboles are chemically and structurally complicated, petrologically important, and they are the subject of extensive ongoing scientific attention. The classification and nomenclature of the amphiboles are obviously influenced considerably by this work: as we discover more about them, there is a need to incorporate this knowledge into their classification and nomenclature. Of particular importance in this respect is the extensive amphibole synthesis that has been done in the past 10–15 yr. This work has indicated major new chemical fields in which the amphibole structure is stable. Although from the point of view of the formal definition of a mineral, such synthetic compounds are not minerals, it is our view that the classification of the amphiboles should be able to incorporate such information, as it will deepen our understanding of this group. Thus we have expanded the number of subgroups from four (IMA1997) to eight. Minerals from one of the new subgroups, the lithium amphiboles, have since been found to be reasonably common rock-forming minerals (e.g., Oberti et al. 2000, 2003, 2004, 2006; Caballero et al. 2002), and synthesis work (e.g., Iezzi et al. 2004, 2005a, 2005b, 2006; Maresch et al. 2009) has resulted in new compositions (Oberti et al. 2007). There have been several amphibole classifications produced in the last 50 yr, and the introduction of these new schemes has caused some irritation in the mineralogical and petrological communities. Here, we have tried to minimize such problems by introducing a scheme that can accommodate future compositional and structural discoveries in the amphiboles.

REFERENCES CITED

Bayliss, P., Kaesz, H.D., and Nickel, E.H. (2005) The use of chemical-element adjectival modifiers in mineral nomenclature. Canadian Mineralogist, 43, 1429–1433.

Burke, E.A.J. and Leake, B.E. (2004) "Named amphiboles": a new category of amphiboles recognized by the International Mineralogical Association (IMA), and the proper order of prefixes to be used in amphibole names. Canadian Mineralogist, 42, 1881–1883.

Caballero, J.M., Monge, A., La Iglesia, A., and Tornos, F. (1998) Ferriclinoferroholmquistite, $Li_2(Fe^{2+},Mg)_3Fe^{3+}_2Si_8O_{22}(OH)_2$, a new ^{B}Li clinoamphibole from the Pedriza Massif, Sierra de Guadarrama, Spanish Central System. American Mineralogist, 83, 167–171.

Caballero, J.M., Oberti, R., and Ottolini, L. (2002) Ferripedrizite, a new monoclinic ^{B}Li amphibole end-member from the Eastern Pedriza Massif, Sierra de Guadarrama, Spain, and improvements in the nomenclature of Mg-Fe-Mn-Li amphiboles. American Mineralogist, 87, 976–982.

Cámara, F., Oberti, R., Iezzi, G., and Della Ventura, G. (2003) The $P2_1/m \leftrightarrow C2/m$ phase transition in the synthetic amphibole Na NaMg Mg_5 Si_8 O_{22} $(OH)_2$: Thermodynamic and crystal-chemical evaluation. Physics and Chemistry of Minerals, 30, 570–581.

Cámara, F., Oberti, R., Della Ventura, G., Welch, M.D., and Maresch, W.V. (2004) The crystal-structure of synthetic $NaNa_2Mg_5Si_8O_{21}(OH)_3$, a triclinic $C\bar{1}$ amphibole with a triple-cell and excess hydrogen. American Mineralogist, 89, 1464–1473.

Deer, W.A., Howie, R.A., and Zussman, J. (1992) An Introduction to the Rock-forming Minerals, 2nd ed. Longman Group, Essex, U.K.

Enders, M., Speer, D., Maresch, M.V., and McCammon, C.A. (2000) Ferric/ferrous iron ratios in sodic amphiboles: Mössbauer analysis, stoichiometry-based model calculations and the high-resolution microanalytical flank method. Contributions to Mineralogy and Petrology, 140, 135–147.

Fialin, M., Bezos, A., Wagner, C., Magnien, V., and Humler, E. (2004) Quantitative electron microprobe analysis of $Fe^{3+}/\Sigma Fe$: Basic concepts and experimental protocol for glasses. American Mineralogist, 89, 654–662.

Hatert, F. and Burke, E.A.J. (2008) The IMA-CNMNC dominant-constituent rule revisited and extended. Canadian Mineralogist, 46, 717–728.

Hawthorne, F.C. (1983) The crystal chemistry of the amphiboles. Canadian Mineralogist, 21, 173–480.

——— (2002) The use of end-member charge arrangements in defining new mineral species and heterovalent substitutions in complex minerals. Canadian Mineralogist, 40, 699–710.

Hawthorne, F.C. and Oberti, R. (2006) On the classification of amphiboles. Canadian Mineralogist, 44, 1–21.

——— (2007) Amphiboles: crystal chemistry. In F. C. Hawthorne, R. Oberti, G. Della Ventura, A. Mottana, Eds., Amphiboles: Crystal Chemistry, Occurrence and Health Issues, 67, 1–54. Reviews in Mineralogy and Geochemistry, Mineralogical Society of America, Chantilly, Virginia.

Hawthorne, F.C., Ungaretti, L., Oberti, R., Cannillo, E., and Smelik, E.A. (1994) The mechanism of $^{[6]}$Li incorporation in amphibole. American Mineralogist, 79, 443–451.

Hawthorne, F.C., Oberti, R., Ungaretti, L., and Grice, J.D. (1996) A new hypercalcic amphibole with Ca at the A site: fluor-cannilloite from Pargas, Finland. American Mineralogist, 81, 995–1002.

Hawthorne, F.C., Oberti, R., Zanetti, A., and Czamanske, G.K. (1998) The role of Ti in hydrogen-deficient amphiboles: sodic-calcic and sodic amphiboles from Coyote Peak, California. Canadian Mineralogist, 36, 1253–1265.

Höfer, H.E., Brey, G.P., Schulz-Dobrick, B., and Oberhänsli, R. (1994) The determination of the iron oxidation state by the electron microprobe. European Journal of Mineralogy, 6, 407–418.

Iezzi, G., Della Ventura, G., Oberti, R., Cámara, F., and Holtz, F. (2004) Synthesis and crystal-chemistry of $Na(NaMg)Mg_5Si_8O_{22}(OH)_2$, a $P2_1/m$ amphibole. American Mineralogist, 89, 640–646.

Iezzi, G., Gatta, G.D., Kockelmann, W., Della Ventura, G., Rinaldi, R., Schäfer, W., Piccinini, M., and Gaillard, F. (2005a) Low-*T* neutron powder-diffraction and synchrotron-radiation IR study of synthetic amphibole $Na(NaMg)Mg_5Si_8O_{22}(OH)_2$. American Mineralogist, 90, 695–700.

Iezzi, G., Tribaudino, M., Della Ventura, G., Nestola, F., and Bellatreccia, R. (2005b) High-T phase transition of synthetic $^{A}Na^{B}(LiMg)^{C}Mg_5Si_8O_{22}(OH)_2$ amphibole: an X-ray synchrotron powder diffraction and FTIR spectroscopic study. Physics and Chemistry of Minerals, 32, 515–523.

Iezzi, G., Della Ventura, G., and Tribaudino, M. (2006) Synthetic $P2_1/m$ amphiboles in the system Li_2O-Na_2O-MgO-SiO_2-H_2O (LNMSH). American Mineralogist, 91, 426–429.

Kretz, R. (1983) Symbols for rock-forming minerals. American Mineralogist, 68, 277–279.

Lamb, W.M., Guillemette, R., Popp, R.K., Fritz, S.J., and Chmiel, G.J. (2012) Determination of Fe^{3+}/Fe using the electron microprobe: A calibration for amphiboles. American Mineralogist, 97, 951–961.

Leake, B.E. (1968) A catalog of analyzed calciferous and sub-calciferous amphiboles together with their nomenclature and associated minerals. Geological Society of America Special Paper, 98, 210p.

——— (1978) Nomenclature of amphiboles. Canadian Mineralogist, 16, 501–520.

Leake, B.E., Woolley, A.R., Arps, C.E.S., Birch, W.D., Gilbert, M.C., Grice, J.D., Hawthorne, F.C., Kato, A., Kisch, H.J., Krivovichev, V.G., Linthout, K., Laird, J., Mandarino, J.A., Maresch, W.V., Nickel, E.H., Rock, N.M.S., Schumacher, J.C., Smith, D.C., Stephenson, N.C.N., Ungaretti, L., Whittaker, E.J.W., and Guo, Y. (1997) Nomenclature of amphiboles: Report of the subcommittee on amphiboles of the International Mineralogical Association, Commission on New Minerals and Mineral Names. Canadian Mineralogist, 35, 219–246.

Leake, B.E., Woolley, A.R., Birch, W.D., Burke, E.A.J., Ferraris, G., Grice, J.D., Hawthorne, F.C., Kisch, H.J., Krivovichev, V.G., Schumacher, J.C., Stephenson, N.C.N., and Whittaker, E.J.W. (2003) Nomenclature of amphiboles: additions and revisions to the International Mineralogical Association's amphibole nomenclature. Canadian Mineralogist, 41, 1355–1370.

Maresch, W.V., Welch, M.D., Gottschalk, M., Ruthmann, W., Czank, M., and Ashbrook, S.E. (2009) Synthetic amphiboles and triple-chain silicates in the system Na_2O-MgO-SiO_2-H_2O: phase characterization, compositional relations

and excess H. Mineralogical Magazine, 73, 957–996.
Mills, S.J., Hatert, F., Nickel, E.H., and Ferraris, G. (2009) The standardisation of mineral group hierarchies: application to recent nomenclature proposals. European Journal of Mineralogy, 21, 1073–1080.
Moore, P.B., Davis, A.M., Van Derveer, D.G., and Sen Gupta, P.K. (1993) Joesmithite, a plumbous amphibole revisited and comments on bond valences. Mineralogy and Petrology, 48, 97–113.
Oberti, R. and Ghose, S. (1993) Crystal-chemistry of a complex Mn-bearing alkali amphibole on the verge of exsolution. European Journal of Mineralogy, 5, 1153–1160.
Oberti, R., Ungaretti, L., Cannillo, E., and Hawthorne, F.C. (1992) The behaviour of Ti in amphiboles. I. Four- and six-coordinated Ti in richterite. European Journal of Mineralogy, 3, 425–439.
Oberti, R., Hawthorne, F.C., Ungaretti, L., and Cannillo, E. (1995) $^{[6]}$Al disorder in amphiboles from mantle peridotite. Canadian Mineralogist, 33, 867–878.
Oberti, R., Caballero, J.M., Ottolini, L., Lopez-Andres, S., and Herreros, V. (2000) Sodic-ferripedrizite, a new monoclinic amphibole bridging the magnesium-iron-manganese-lithium and the sodium-calcium group. American Mineralogist, 85, 578–585.
Oberti, R., Cámara, F., Ottolini, L., and Caballero, J.M. (2003) Lithium in amphiboles: detection, quantification, and incorporation mechanisms in the compositional space bridging sodic and ^{B}Li amphiboles. European Journal of Mineralogy, 15, 309–319.
Oberti, R., Cámara, F., and Caballero, J.M. (2004) Ferri-ottoliniite and ferriwhittakerite, two new end-members of the new Group 5 for monoclinic amphiboles. American Mineralogist, 88, 888–893.
Oberti, R., Cámara, F., and Ottolini, L. (2005) Clinoholmquistite discredited: the new amphibole end-member fluoro-sodic-pedrizite. American Mineralogist, 90, 732–736.
Oberti, R., Cámara, F., Della Ventura, G., Iezzi, G., and Benimoff, A.I. (2006) Parvo-mangano-edenite and parvo-manganotremolite, two new Group 5 monoclinic amphiboles from Fowler, New York, and comments on the solid solution between Ca and Mn^{2+} at the M4 site. American Mineralogist, 91, 526–532.
Oberti, R., Della Ventura, G., and Cámara, F. (2007) New amphibole compositions: Natural and synthetic. In F. C. Hawthorne, R. Oberti, G. Della Ventura, A. Mottana, Eds., Amphiboles: Crystal Chemistry, Occurrence and Health Issues, 67, p. 89–123. Reviews in Mineralogy and Geochemistry, Mineralogical Society of America, Chantilly, Virginia.
Saxena, S.K. and Ekström, T.K. (1970) Statistical chemistry of calcic amphiboles. Contributions to Mineralogy and Petrology, 26, 276–284.
Schumacher, J.C. (1991) Empirical ferric iron corrections: necessity, assumptions, and effects on selected geothermobarometers. Mineralogical Magazine, 55, 3–18.
——— (1997) Appendix 2. The estimation of the proportion of ferric iron in the electron-microprobe analysis of amphiboles. Canadian Mineralogist, 35, 238–246.
——— (2007) Metamorphic amphiboles: composition and coexistence. In F.C. Hawthorne, R. Oberti, G. Della Ventura, A. Mottana, Eds., Amphiboles: Crystal Chemistry, Occurrence and Health Issues, 67, 359–416. Reviews in Mineralogy and Geochemistry, Mineralogical Society of America, Chantilly, Virginia.
Tiepolo, M., Zanetti, A., and Oberti, R. (1999) Detection, crystal-chemical mechanisms and petrological implications of $^{[6]}$Ti^{4+} partitioning in pargasite and kaersutite. European Journal of Mineralogy, 11, 345–354.

Manuscript received June 25, 2012
Manuscript accepted August 7, 2012
Manuscript handled by Andrew McDonald

Appendix I: The *C*2/*m* amphibole structure

A schematic representation of the *C*2/*m* structure type is shown in Appendix Figure 1 (below). There are two distinct *T* sites that are occupied by the T cations, *T*(1) and *T*(2), that are tetrahedrally coordinated and link to form one distinct type of double chain of tetrahedra. The *T*(1) and *T*(2) tetrahedra alternate along the length of the double chain, and the *T*(1) tetrahedra bridge across the double chain. There are three distinct octahedrally coordinated *M* sites that are occupied by the C cations. The *M*(1) site is coordinated by two O(1) and two O(2) O-atoms, and by two O(3) W anions (OH, F, Cl, O) in a *cis* arrangement, and the *M*(3) site is coordinated by four O(1) oxygen atoms and two O(3) W anions in a *trans* arrangement. The double chain of tetrahedra links to the strip of octahedra in the **b** direction through *T*(2)–*M*(2) linkage via common O(4) O-atoms, and in the **a** direction through *T*(1) and *T*(2) linkage to the strip via common O(1) and O(2) O-atoms. The *M*(4) site is situated at the periphery of the strip of octahedra and is occupied by B cations. Note that the cation occupancy of this site (1) is the primary feature on which the major subgroups of amphiboles are classified, and (2) correlates strongly with the space-group variations in amphiboles. The *A* site occurs at the center of a large cavity between the back-to-back double-chains of the structure. The center of the cavity has point symmetry 2/*m*, but the A cations actually occupy off-centered sites of point symmetry 2 or *m*, *A*(2), and *A*(*m*), respectively.

Appendix II: The role of Fe, H, and Li

Prior to the development of the electron microprobe, all major and minor constituents in amphiboles were analyzed as a matter of course, and compilations such as that of Leake (1968) are invaluable sources of complete results of chemical analysis. The advent of the electron microprobe completely changed the situation with regard to mineral analysis. It became relatively easy to make numerous chemical analyses at a very fine scale, making available chemical data on finely zoned materials. However, this step forward came at a cost: the concentration of some elements (e.g., H, Li) cannot be so established, and valence state is not accessible. For many minerals, these limitations are not relevant; for amphiboles, they are major disadvantages. Recent work has shown that (1) Li is a much more common constituent in amphiboles than had hitherto been realized (Hawthorne et al. 1994; Oberti et al. 2003), and (2) H, as (OH), can be a variable component in amphiboles unassociated with the process of oxidation-dehydrogenation (Hawthorne et al. 1998). Moreover, the role of Fe in amphiboles is very strongly a function of its valence state and site occupancy. Lack of knowledge of these constituents results in formulas that generally must be regarded as only semiquantitative. Of course, if Li and Fe^{3+} are not present and (OH + F) = 2 apfu, the resulting formula can be accurate. However, such a situation is uncommon [few amphiboles have Li = Fe^{3+} = 0 and (OH + F) = 2 apfu], resulting in formulas with significant systematic error.

All previous classifications have obscured this issue by not

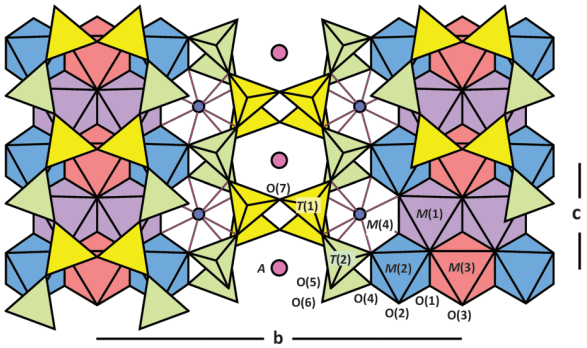

Appendix Figure 1. The crystal structure of a monoclinic *C*2/*m* amphibole projected onto (100). (Color online.)

incorporating C cations into the classification procedure, and thus the problem is not visually apparent in the classification diagrams. However, the problem is still present in that the formulas are still inaccurate, and the lack of H, Li, and Fe^{3+} seriously distorts the amounts of other constituents, particularly those that are distributed over two different groups of sites (e.g., ^{T}Al and ^{C}Al, ^{B}Na, and ^{A}Na). There are methods available to determine these components, and amphibole analysts should be acquiring or using these on a routine basis. For "small-laboratory" instrumentation, secondary-ion mass spectrometry (SIMS) can microbeam-analyze amphiboles for H and Li (using the appropriate methodology and standards); laser-ablation inductively coupled plasma mass spectrometry (LA-ICP-MS) can microbeam-analyze amphiboles for Li; single-crystal-structure refinement (SREF) can characterize the levels of Li, Fe^{2+} and Fe^{3+} at a scale of ≥30 μm, and with structure-based equations, one can estimate the amount of $^{W}O^{2-}$; electron energy-loss spectroscopy (EELS) can measure $Fe^{3+}/(Fe^{2+} + Fe^{3+})$ at a scale of ≥1 μm; electron microprobe (the Flank method, Höfer et al. 1994; the peak-shift method, Fialin et al. 2004) can measure $Fe^{3+}/(Fe^{2+} + Fe^{3+})$ at a scale of ≥1 μm where FeO_{tot} > ~6–8 wt% with reasonable accuracy in amphiboles (Enders et al. 2000; Lamb et al. 2012); milli-Mössbauer spectroscopy can measure $Fe^{3+}/(Fe^{2+} + Fe^{3+})$ at a scale of ≥50 μm. For "big-laboratory" instrumentation, usually involving a synchrotron light-source, single-crystal refinement of the structure can characterize Li, Fe^{2+} and Fe^{3+} at a scale of ≥2 μm, and milli-X-ray photoelectron spectroscopy (XPS) can measure $Fe^{3+}/(Fe^{2+} + Fe^{3+})$ at a scale of ≥40 μm. Where only small amounts of separate are available (a few milligrams), hydrogen-line extraction and Karl-Fischer titration can give accurate values for H (as H_2O) content. Values for $Fe^{3+}/(Fe^{2+} + Fe^{3+})$ can also be calculated using assumed site-occupancy limitations and the electroneutrality principle (Appendix III), and although the values obtained are not very accurate (Hawthorne 1983), they are in general better than assuming $Fe^{3+}/(Fe^{2+} + Fe^{3+}) = 0.0$ (Schumacher 1991, 1997). Values for $^{W}O^{2-}$ can be calculated also using Ti^{4+} as a proxy (Appendix III), although it is probable that the proxy relation does not always hold. As noted in the main text, if the $^{W}O^{2-}$ content is known from chemical or crystal-chemical analysis, it replaces use of the Ti content as a proxy. To give an example, analyses done by EMP, SIMS, SREF, and Mössbauer spectroscopy on a sample from Kaersut, Greenland (rather ironically, the type locality of kaersutite) gave ^{C}Ti 0.62–0.69 and $^{W}O^{2-}$ 0.88–0.95 apfu with half of the Ti ordered at *M*(2) (Oberti et al., in prep). In terms of attributing a name, the $^{W}O^{2-}$ content dominates over the Ti content, and this is an (OH, F, Cl)-dominant amphibole, despite the fact that Ti >0.50 apfu.

Hydrogen in excess of 2 apfu was long suspected in amphiboles, but was never considered as confirmed because of the difficulty in obtaining reliable and accurate analytical data for H in solids. Maresch et al. (2009) reviewed the synthesis and spectroscopic evidence for H > 2 apfu in synthetic amphibole in the system Na_2O–MgO–SiO_2–H_2O, and Cámara et al. (2004) solved the structure of a triclinic synthetic amphibole of composition $Na_3Mg_5Si_8O_{21}(OH)_3$. Thus the evidence is now incontrovertible that H > 2 apfu can occur in amphiboles. However, it is likely that the additional H is itinerant (i.e., not associated with a specific anion longer than a few picoseconds); if this is the case, then such an amphibole would have a high ionic conductivity relative to other amphiboles, and the formula should then be written as $Na_3Mg_5Si_8O_{22}(OH)_2H$. According to our principles of nomenclature, $Na_3Mg_5Si_8O_{22}(OH)_2H$ is a ^{W}(OH, F, Cl)-dominant amphibole and would require a new root name if found in Nature. Homovalent variants and new root compositions can be named according to our general rules.

Here, we make the case for basing amphibole classification on the contents of the A, B, and C cations, and hence the Fe^{3+} content of an amphibole plays a major role in the classification scheme. Thus use of some of the techniques outlined above, in addition to electron-microprobe analysis, is required to characterize the chemical formulas of amphiboles accurately. To make an analoguey with 40 yr ago, wet-chemical analysis was in widespread use and the electron microprobe was a novel instrument of limited availability. However, the ability of the electron microprobe to deal with heterogeneous material and obviate problems of sample contamination led to its current extensive use. We are in a similar situation today. The electron microprobe is in widespread use, but the techniques for the analysis of Fe^{3+}/Fe^{2+} and light lithophile elements outlined above are far less widespread. However, these techniques considerably increase our ability to analyze minerals accurately. To increase our knowledge of the chemistry of minerals in general (and amphiboles in particular), as a community we need to acquire this instrumentation so that in the near future, these other analytical techniques become as routine as electron-microprobe analysis.

Appendix III: Calculation of Fe^{3+} and (OH) in amphiboles

As discussed in Appendix II, Fe^{3+} and (OH) are significant and variable constituents in amphiboles but are generally not determined in most analytical work. This generally has the result of distorting the stoichiometry, e.g., indicating unusual site-occupancies: Ti^{4+} as a T-group cation, Na or Ca as a C-group cation, greater than 16 total cations, which in turn may affect the assignment of a name. This situation may be resolved by measuring one or more of these constituents, or somewhat alleviated by numerical modeling: calculating the Fe^{3+} content and/or calculating the formula using expressions for the (OH) content other than (OH + F + Cl) = 2.0 apfu. Although not a substitute for direct measurement, these different methods of normalization are a way of addressing missing constituents and the ensuing problems with stoichiometry.

Calculation of amphibole formulas and (OH) content

There are many papers on the calculation of amphibole formulas (Hawthorne and Oberti 2007, and references therein). It is usually recommended that amphibole formulas be normalized on the basis of 24(O, OH, F, Cl) with (OH, F, Cl) = 2 apfu where H_2O is not known. Although this is equivalent to the 23O calculation, it has the advantage of generating a calculated H_2O content and hence a more appropriate sum of constituent oxides.

One of the principal problems in the chemical characterization of amphiboles is the lack of determination of H_2O, and the general assumption that (OH, F, Cl) = 2 apfu is probably not correct in the majority of cases. It is well known (Leake 1968; Saxena and Ekström 1970; Hawthorne et al. 1998; Tiepolo et

al. 1999) that a deficiency of monovalent anions correlates with an increase in Ti in amphiboles. Although ^{C}Ti may occur at all three *M* sites, $^{M(3)}$Ti is very rare (Tiepolo et al. 1999), whereas Ti partition between *M*(1) and *M*(2) is common and depends on conditions of formation. Titanium is incorporated at the *M*(1) site according to the following local mechanism (Oberti et al. 1992):

$$^{M(1)}Ti^{4+} + 2^{W}O^{2-} \rightarrow {}^{M(1)}(Mg, Fe^{2+}) + 2^{W}(OH)^{-}.$$

This substitution will reduce the amount of (OH) at O(3) by twice the amount of Ti at *M*(1). In principle, one may use the Ti content of *M*(1) as a proxy for OH. We do not commonly know $^{M(1)}$Ti; however, Ti generally preferentially orders at *M*(1), and we may use the approximation $^{M(1)}$Ti = Ti. The correlations presented by Leake (1968) and Saxena and Ekström (1970) support the general applicability of the relations $^{M(1)}$Ti = Ti and $Ti^{4+} = 2 - 2(OH)$. Thus in the absence of a direct estimate of the (OH, F, Cl) content, we recommend that amphibole formulas be calculated on the basis of 24(O, OH, F, Cl) with (OH, F, Cl) = (2 – 2Ti) apfu (being aware that this choice will produce the maximum value of O^{2-}). However, the reader should also be aware that, in some cases, a significant fraction of Ti may occur at *M*(2) (Hawthorne et al. 1998; Tiepolo et al. 1999).

Calculation of amphibole formulas and Fe^{3+} content

The $Fe^{3+}/(Fe^{2+} + Fe^{3+})$ value in an amphibole can be calculated by constraining the sum of a set of cations to a particular value and adjusting $Fe^{3+}/(Fe^{2+} + Fe^{3+})$ for electroneutrality. The particular cation sums may be strictly adhered to (or may be "usually" adhered to) except for particular compositions or parageneses. Below, we note where there are exceptions to the criteria listed.

Above, we discuss the use of two different schemes of calculation for amphiboles: (1) 24(O, OH, F, Cl) with (OH, F, Cl) = 2 apfu and (2) 24(O, OH, F, Cl) with (OH, F, Cl) = (2 – 2Ti) apfu. The calculation of Fe^{3+} content described below is done on the basis of 24(O, OH, F, Cl) with (OH, F, Cl) = 2 apfu. The methods are the same if one uses the basis 24(O, OH, F, Cl) with (OH, F, Cl) = (2 – 2Ti) apfu (although the numbers are somewhat different).

General points

(1) Where not adjusting the $Fe^{3+}/(Fe^{2+} + Fe^{3+})$ value, the formula is normalized to 24(O, OH, F, Cl) with (OH, F, Cl) = 2 apfu [except where O^{2-} enters the O(3) site through the presence of Ti^{4+} at the *M*(1) site; in this case, the formula should be normalized to 24(O, OH, F, Cl) with (OH, F, Cl) = (2 – 2Ti) apfu, see above]. The advantage over the 23O calculation is that H_2O is also calculated and the total oxide sum is derived, giving another criterion for evaluation of the analytical results.

(2) Some constituents of amphiboles are not routinely measured, and their presence in the amphibole considered will invalidate the calculations that are done here. Thus major and variable Li occurs in certain types of amphiboles, and will invalidate the procedures discussed here if present and not quantified.

(3) In some (rare) cases, Fe^{3+} plays a similar role to Ti, i.e., is involved in (usually) post crystallization dehydrogenation, $^{M(1,3)}Fe^{3+} + {}^{O(3)}O^{2-} \rightarrow {}^{M(1,3)}Fe^{2+} + {}^{O(3)}(OH)^{-}$, and orders at the *M*(1) and *M*(3) sites. In those cases, calculations should be done based on (OH, F, Cl) = (2 – 2Ti – xFe^{3+}) apfu, where x is the amount of Fe^{3+} involved in dehydrogenation.

Calculation procedures

For the calculations shown here, we use a composition from Deer et al. (1992, page 678). The chemical composition and unit formula are given in Appendix Table 1 (below), analyses (1) [the original analysis calculated on the basis of 24(O,OH)] and (2) [the original analysis omitting H_2O and calculated on the basis of 24(O,OH) with (OH) = 2 apfu].

(*1) Calculate formula with Fe_2O_3 set to zero (all-ferrous calculation) and FeO set to zero (all-ferric calculation), both with (OH + F + Cl) = 2* apfu *and normalizing on 24 (O + OH + F + Cl) (analyses 3 and 4, Appendix Table 1).*

(i) The all-ferrous calculation gives the maximum amount of cations in the amphibole formula. Conversion of FeO into Fe_2O_3 in the analysis increases the amount of O and hence decreases the resulting amounts of normalized cations (compare analyses 3 and 4).

(ii) Because of (i), the sums of the A, B, C and T cations are at their maximum for the all-ferrous formula. If they exceed their maximum possible stoichiometric value(s), the sums may be reduced by conversion of FeO into Fe_2O_3.

(2) *Assign the cations in the all-ferrous formula to the* T-, C-, B-, *and* A-*cation groups as described in the main report.*

(3) *If the following criteria are violated, Fe^{3+} may be present in the formula:*

(i) Si ≤8 apfu.

(ii) Sum [Si + Al + Ti + Fe^{3+} + Fe^{2+} + Mn^{2+} + Mg + Ca + Na + K] ≤ 16 apfu.

(iii) Sum [Si + Al + Ti + Fe^{3+} + Fe^{2+} + Mn^{2+} + Mg + Ca] ≤ 15 apfu.

Appendix Table 1. Calculation of Fe^{3+} for an amphibole

	(1)	(2)	(3)	(4)	(5)	(6)	(7)
SiO_2 wt%	51.63	51.63	51.63	51.63	51.63	51.63	51.63
Al_2O_3	7.39	7.39	7.39	7.39	7.39	7.39	7.39
Fe_2O_3	2.50	2.50	0.00	8.30	1.26	6.25	6.07
FeO	5.30	5.30	7.55	0.00	6.42	1.93	2.08
MnO	0.17	0.17	0.17	0.17	0.17	0.17	0.17
MgO	18.09	18.09	18.09	18.09	18.09	18.09	18.09
CaO	12.32	12.32	12.32	12.32	12.32	12.32	12.32
Na_2O	0.61	0.61	0.61	0.61	0.61	0.61	0.61
H_2O	2.31	2.14	2.13	2.17	2.14	2.16	2.16
Total	100.32	100.15	99.89	100.68	100.02	100.55	100.53
Si apfu	7.196	7.220	7.261	7.128	7.240	7.158	7.161
Al	0.804	0.780	0.739	0.872	0.760	0.842	0.839
ΣT	8.000	8.000	8.000	8.000	8.000	8.000	8.000
Al	0.410	0.438	0.486	0.330	0.461	0.366	0.369
Fe^{3+}	0.262	0.263	–	0.862	0.132	0.652	0.634
Fe^{2+}	0.618	0.620	0.888	–	0.753	0.223	0.242
Mn	0.020	0.020	0.020	0.020	0.020	0.020	0.020
Mg	3.759	3.771	3.793	3.723	3.782	3.739	3.740
ΣC	5.069	5.112	5.187	4.935	5.148	5.000	5.005
Δ	0.069	0.112	0.187	–	0.148	–	0.005
Ca	1.840	1.846	1.856	1.822	1.851	1.830	1.831
Na	0.091	0.039	–	0.163	–	0.164	0.164
ΣB	2.000	2.000	2.043	1.985	1.999	1.994	2.000
Na	0.074	0.126	–	–	0.166	–	–
OH	2.148	2.000	2.000	2.000	2.000	2.000	2.000
$Fe^{3+}/(Fe^{2+} + Fe^{3+})$	0.298	0.298	0	1	0.149	0.745	0.724

(1) Original analysis; (2) original FeO and Fe_2O_3, H_2O set to OH = 2 apfu; (3) all FeO, OH = 2 apfu; (4) all Fe_2O_3, OH = 2 apfu; (5) sum (cations to Ca) = 15 apfu, Fe^{3+} calc, OH = 2 apfu; (6) sum (cations to Mg) = 13 apfu, Fe^{3+} calc, OH = 2 apfu; (7) sum (cations to Na) = 15 apfu, Fe^{3+} calc, OH = 2 apfu.

Criterion (i): This is rigorously fixed by the structure, i.e., Si cannot exceed 8 apfu as there are no other tetrahedrally coordinated sites in the amphibole structure for Si to occupy.

Criterion (ii): This is rigorously fixed by the structure, i.e., all cation sites are fully occupied at 16 apfu.

Criterion (iii): With this criterion, one assumes that Ca is not an A cation. This is not constrained by the structure and is not always correct; in amphiboles from marbles, Ca may be an A cation. However, in most rocks, this is not the case, and criterion iii may be applied (with caution).

(*4) The all-ferrous formula (analysis 3, Appendix Table 1) is inspected with regard to each of the above criteria:*

(i) Si = 7.261 < 8 apfu.

(ii) Sum [Si + Al + Ti + Fe^{3+} + Fe^{2+} + Mn^{2+} + Mg + Ca + Na] = 15.209 < 16 apfu.

(iii) Sum [Si + Al + Ti + Fe^{3+} + Fe^{2+} + Mn^{2+} + Mg + Ca] = 15.043 > 15 apfu.

(*5) Criterion (iii) is violated; this indicates the possible occurrence of Fe^{3+}; the formula is normalized on [Si + Al + Ti + Fe^{3+} + Fe^{2+} + Mn^{2+} + Mg + Ca] = 15* apfu *and $Fe^{3+}/(Fe^{2+} + Fe^{3+})$ is adjusted for electroneutrality (analysis 5, Appendix Table 1).*

(i) This normalization gives the minimum estimate for the Fe^{3+} content.

(ii) If more than one of the three criteria does not hold in analysis (3), then the calculation scheme used is that which gives a formula that accords with all of these criteria.

(*6) The following criteria limit the maximum possible amount of Fe^{3+} in the formula:*

(i) Si + Al = 8 apfu.

(ii) [Si + Al + Ti + Fe^{3+} + Fe^{2+} + Mn^{2+} + Mg + Ca + Na] = 15 apfu.

(iii) Sum [Si + Al + Ti + Fe^{3+} + Fe^{2+} + Mn^{2+} + Mg] = 13 apfu.

Criterion (i): This is not constrained by the structure and is not always correct. Richterite may contain Ti^{4+} as a T cation, and in these circumstances, criterion i should not be used. However, in most rocks, this is not the case and criterion i may be applied (with caution).

Criterion (ii): With this criterion, one assumes that K does not occur as a B cation. This is not always correct, as K can occur as a B cation in richterite.

Criterion (iii): This criterion can be wrong if there is Li in the structure, or if there is (Fe^{2+},Mn^{2+},Mg) as a B cation [e.g., calcium amphiboles commonly contain small but significant amounts of $^{B}(Fe^{2+} + Mn^{2+} + Mg)$].

(*7) The formula [analysis (5), Appendix Table 1] is then inspected with regard to each of the above criteria:*

(i) Si + Al = 8.461 ≥ 8 apfu.

(ii) Sum [Si + Al + Ti + Fe^{3+} + Fe^{2+} + Mn^{2+} + Mg + Ca + Na] = 15.165 > 15 apfu.

(iii) Sum [Si + Al + Ti + Fe^{3+} + Fe^{2+} + Mn^{2+} + Mg] = 13.148 > 13 apfu.

(*8) The formula is normalized on each of equalities (ii) and (iii) in section (6) and $Fe^{3+}/(Fe^{2+} + Fe^{3+})$ is adjusted for electroneutrality [analyses (6) and (7), Table A1].*

(i) Note that we cannot use equality (i) (Section 6) as the amount of Fe_2O_3 required for this constraint exceeds the maximum possible amount of Fe^{3+} in the analysis (see analysis 4).

(ii) In analysis 6, [Si + Al + Ti + Fe^{3+} + Fe^{2+} + Mn^{2+} + Mg + Ca + Na] = 14.994 < 15 apfu, indicating that this constraint cannot be used for this particular analysis.

(iii) In analysis 7, [Si + Al + Ti + Fe^{3+} + Fe^{2+} + Mn^{2+} + Mg + Ca + Na] = 15.000 apfu and all other aspects of the formula are well behaved. Hence analysis 7 gives the maximum estimate of Fe^{3+} in this amphibole.

The minimum and maximum values of $Fe^{3+}/(Fe^{2+} + Fe^{3+})$ are 0.149 (analysis 5) and 0.724 (analysis 7), respectively, and the mean value is 0.437, to be compared with the experimental value of 0.298 (analysis 2).

Where experimental and measured values of Fe^{3+} contents in amphiboles have been compared (e.g., Hawthorne 1983; Hawthorne and Oberti 2007), it can be seen that methods of estimation are not accurate. However, one must deal with this problem when calculating an amphibole formula. Even ignoring it means setting Fe^{3+} = 0.00 apfu and hence an estimate of $Fe^{3+}/(Fe^{2+} + Fe^{3+})$ is still made (i.e., 0.0). As $Fe^{3+}/(Fe^{2+} + Fe^{3+})$ varies between 0.0 and 1.0 in amphiboles, in general an estimate using the techniques outlined here will give a better (i.e., closer to the true) value of $Fe^{3+}/(Fe^{2+} + Fe^{3+})$ than setting $Fe^{3+}/(Fe^{2+} + Fe^{3+})$ = 0.0.

Appendix IV: Principal variables used in the classification procedure

In most scientific problems, one focuses on the variables that show the greatest degree of relative variation, as these are the most informative. In addition, IMA procedures concerning the definition of distinct minerals focus on the dominant species (cation or anion) at a site. Of the A, B, C, T cations, and W anions, all except T show various dominant cations or anions in the set of all amphibole compositions; T is invariably dominated by Si (i.e., ^{T}Al <4.0 apfu). These issues indicate that the T cations should *not* be used as a primary parameter in an amphibole classification (of course, this does not preclude the use of T cations in showing graphically the variation in amphibole composition).

The W anions

There is continuous variation in (OH,F,Cl) and O contents in amphiboles. Where $W_2 \approx (OH,F,Cl)_2$, the high-charge cations are ordered predominantly at the *M*(2) site, whereas where $W_2 \approx O_2^{2-}$, the high-charge cations are distributed over the *M*(1,2,3) sites, those at the *M*(1,3) sites being associated with $W = O^{2-}$. Thus the presence of a significant oxo component (i.e., $W_2 \approx O_2^{2-}$) is accompanied by different patterns of order of C cations relative to amphiboles with $W_2 \approx (OH,F,Cl)_2$. This consideration suggests that the W constituents be used initially to divide amphiboles into two broad classes: **(1) hydroxy-fluoro-chloro-amphiboles** with (OH,F,Cl) ≥ 1.00 apfu, and **(2) oxo-amphiboles** with (OH,F,Cl) < 1.00 apfu (we do not use the term oxy as this has too many associations with the process of oxidation-dehydrogenation). Within these two classes, the A, B and C constituents are used to classify the amphiboles further.

Hydroxy-fluoro-chloro-amphibole group

Hydroxy-fluoro-chloro-amphiboles are divided into subgroups according to the dominant B-cation or group of B cations. Let us write the sum of the small divalent cations as $\Sigma M^{2+} = {}^{B}Mg + {}^{B}Fe^{2+} + {}^{B}Mn^{2+}$, and the sum of the B cations as $\Sigma B = {}^{B}Li + {}^{B}Na$

$+ \Sigma M^{2+} + {}^{B}Ca$ (which generally is equal to 2.00 apfu). Thus the dominant B constituents may be represented as indicated in the main text of the report, giving rise to the following amphibole subgroups:

Magnesium-iron-manganese amphiboles
Calcium amphiboles
Sodium-calcium amphiboles
Sodium amphiboles
Lithium amphiboles
Sodium-(magnesium-iron-manganese) amphiboles
Lithium-(magnesium-iron-manganese) amphiboles
Lithium-calcium amphiboles.

The resulting supergroup-group-subgroup hierarchy is illustrated in Appendix Figure 2.

Problems with the previous amphibole classification

There were many problems with this stage of the previous amphibole classification; some of these issues are discussed next.

(1) The role of ^{B}Li. There is no good crystal-chemical or chemical reason for including Li amphiboles in the *magnesium-iron-manganese-lithium* group of IMA1997. Lithium is an alkali metal, is formally monovalent, and shows complete solid-solution with Na at the *M*(4) site in monoclinic amphiboles, e.g., leakeite – ferri-pedrizite: $NaNa_2(Mg_2Fe^{3+}_2Li)Si_8O_{22}(OH)_2$ – $NaLi_2(Mg_2Fe^{3+}_2Li)Si_8O_{22}(OH)_2$, Oberti et al. (2003); magnesio-riebeckite – clino-ferri-holmquistite: $Na_2(Mg_3Fe^{3+}_2)Si_8O_{22}(OH)_2$ – $Li_2(Mg_3Fe^{3+}_2)Si_8O_{22}(OH)_2$, Oberti et al. (2004).

These points indicate that amphiboles with Li dominant at *M*(4) should *not* be included as part of the magnesium-iron-manganese subgroup. There are two possible ways in which to treat such amphiboles: (1) recognize a separate subgroup of amphiboles with Li as the dominant B-cation (analogous to that with dominant ^{B}Na), or (2) include ^{B}Li with ^{B}Na as a principal constituent of an alkali-amphibole subgroup. However, ^{B}Li amphiboles have some features that are not shared with ^{B}Na amphiboles; for instance, ^{B}Li amphiboles may occur with orthorhombic *Pnma* symmetry (holmquistite) and are also expected to occur with monoclinic $P2_1/m$ symmetry ("clino-holmquistite"). Hence, the simpler solution is to define a distinct subgroup of ^{B}Li amphiboles. Intermediate compositions between ^{B}Li and $^{B}\Sigma M^{2+}$ amphiboles fall in the lithium-(magnesium-iron-manganese) subgroup and give rise to root compositions analogous to those of sodium-calcium amphiboles (likewise the lithium-calcium amphiboles).

(2) The names of the principal subgroups. Having recognized a separate subgroup with Li as the dominant B-cation, it is obvious that the term "lithic", in accord with "calcic" and "sodic", is not a suitable name for this subgroup. Moreover, the names of the current five subgroups (IMA2003) are rather inhomogeneous, using both nouns (e.g., magnesium), element symbols (e.g., Mg) and adjectives (e.g., calcic, sodic). Here, we will use nouns to name the subgroups. The other inhomogeneity with regard to the names of these subgroups is the use of element symbols: the magnesium-iron-manganese subgroup is frequently referred to as the Mg-Fe-Mn subgroup (indeed, this is done in IMA1997), whereas the calcium subgroup is not referred to as the Ca subgroup. Some sort of consistency is required in the use of these subgroup names; either element names or symbols may be used, but authors should maintain consistency of use in a single publication.

The new classification

(1) The role of the sodium-calcium, lithium-calcium, sodium-(magnesium-iron-manganese), and lithium-(magnesium-iron-manganese) subgroups. A significant source of complexity in the classification of amphiboles is the recognition of the intermediate subgroups: sodium-calcium, lithium-calcium, sodium-(magnesium-iron-manganese), and lithium-(magnesium-iron-manganese) amphiboles. Let us consider the reason for these intermediate subgroups, considering the sodium-calcium subgroup as an example. The sodium-calcium subgroup was defined by IMA1978 and redefined by IMA1997, but its use was not justified from a nomenclature perspective. As noted above, IMA procedures involving the definition of distinct minerals focus on the dominant species at a site. Using this criterion, the sodium-calcium subgroup of amphiboles would not be recognized: amphiboles with $2.00 > Ca \geq 1.00$ apfu would belong to the calcium subgroup, and amphiboles with $2.00 > Na > 1.00$ apfu would belong to the sodium subgroup. Using this criterion to reduce the number of primary subgroups would certainly reduce both the complexity of the nomenclature and the number of distinct amphiboles. However, following this course will result in a problem with richterite (and other amphiboles with the same root-charge arrangement). This issue is investigated in Appendix Figure 3, which shows A-B-C compositional space for amphiboles with only Ca and Na as B cations (note that this excludes magnesium-iron-manganese and lithium amphiboles). Compositions of previous "end-members" are shown as black squares and white circles. Note that the compositions represented

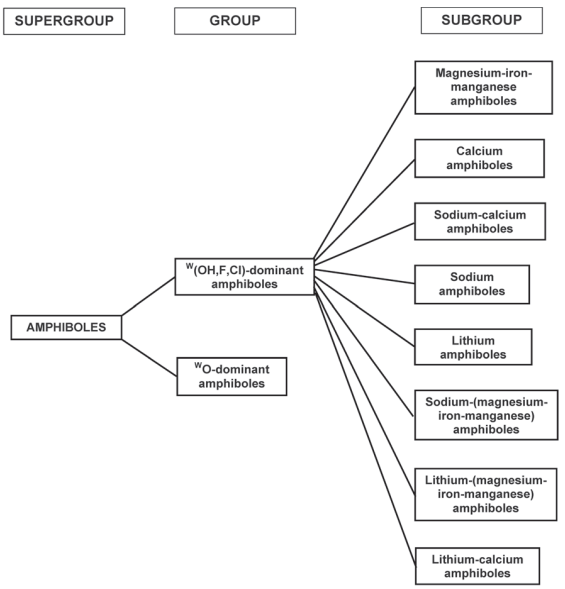

Appendix Figure 2. The supergroup-group-subgroup hierarchy of the amphiboles.

by white circles can always be represented as 50:50 mixtures of other "end-member" compositions. Thus magnesio-hornblende can be represented as 0.50 tremolite and 0.50 tschermakite, and barroisite can be represented as 0.50 tschermakite and 0.50 glaucophane. However, richterite cannot be represented by a combination of two end-members, as is apparent graphically from Appendix Figure 3; richterite is thus a true end-member according to the criteria of Hawthorne (2002). However, IMA criteria for the recognition of a valid mineral species do not involve its status as a valid end-member. The criteria include the dominance of a specific cation at a site or group of sites. This approach would definitely dispose of pargasite and magnesio-hornblende as distinct amphibole species. However, richterite cannot be resolved into a combination of two end-members; it is irreducible and hence a distinct species, and requires the existence of the sodium-calcium subgroup.

(2) Lithium-calcium, sodium-(magnesium-iron-manganese), and lithium-(magnesium-iron-manganese) subgroups. The above discussion concerning the sodium-calcium amphibole subgroup can be applied to all mixed-valence pairings of B cations. Thus B_2 = (Li Ca), (Li Mg), (Na Mg), and their $^{B}Fe^{2+}$ and $^{B}Mn^{2+}$ analogues will all result in end-member compositions of the type Na B_2 Mg_5 Si_8 O_{22} W_2 that cannot be decomposed into calcium-, lithium-, magnesium-iron-manganese-, or sodium-subgroup compositions. In this regard, consider the composition $^{A}(Na_{0.33}K_{0.03})_{\Sigma 0.36}$ $^{B}(Na_{0.82}Ca_{0.39}Mn_{0.57}Mg_{0.22})_{\Sigma 2.00}$ $^{C}(Mg_{3.83}Mn^{2+}_{0.37}Fe^{3+}_{0.73}Li_{0.07})_{\Sigma 5.00}$ $^{T}(Si_{7.86}Al_{0.11})_{\Sigma 7.97}$ O_{22} $(OH_{1.60}F_{0.40})$, reported from Tirodi, India, by Oberti and Ghose (1993). This amphibole is close to the root composition $^{A}\square$ $^{B}(Na\ Mn^{2+})$ $^{C}(Mg_4\ Fe^{3+})$ $^{T}Si_8$ O_{22} $(OH)_2$ and is named fluorian manganoan parvowinchite (IMA-CNMMN 2003-066), following IMA2003. This composition gives rise to a new root name, and hence requires definition of a new subgroup of ^{B}[Na (Mg,Fe,Mn)] amphiboles.

The ^{B}(Na Mg) and ^{B}(Li Mg) joins have been investigated by synthesis; intermediate compositions with a "richterite-like" charge-arrangement are stable and have $P2_1/m$ symmetry at room temperature (Cámara et al. 2003; Iezzi et al. 2004, 2005a, 2005b).

(3) The A cations. Having divided amphiboles with 1 < (OH,F,Cl) ≤ 2 apfu into eight subgroups based on the B cations, we have the A and C cations to classify within these subgroups and to assign specific names to specific compositional ranges and root compositions. For the A cations, the variation observed in Nature spans the complete range possible from a structural perspective: □, Na, and K can vary over the range 0–1 apfu (at present, the maximum content of ^{A}Ca observed only slightly exceeds 0.50 apfu). Thus we use the variable ^{A}(Na + K + 2Ca) in the classification graphs of this paper.

(4) The C cations. The situation for the C cations is more complicated, as these cations occur at three distinct sites in amphibole structures: *M*(1), *M*(2), and *M*(3) in all common amphibole structure-types (but not in the $P2/a$ and $C\bar{1}$ structures, where there are five and eight *M* sites, respectively, Hawthorne and Oberti 2007). Most heterovalent variations occur at the *M*(2) site, where there is complete solid-solution among Mg, Fe^{2+}, Al, Fe^{3+}, and Ti^{4+}. Some Al can disorder over *M*(2) and *M*(3) in Mg-rich calcium amphiboles (Oberti et al. 1995), and some Ti^{4+} and Fe^{3+} can occur at *M*(1) and at *M*(1,3), respectively, but trivalent

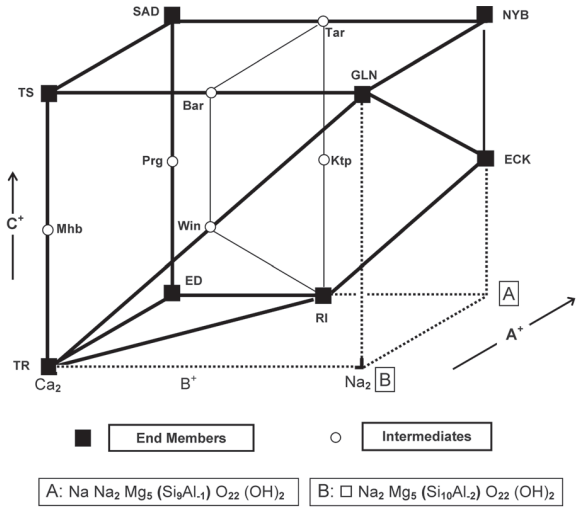

Appendix Figure 3. Compositional space for monoclinic Na-Ca-Mg-Al-Si amphiboles using ^{B}Na, ^{A}Na and ^{C}Al as proxies for the aggregate charges of the B, A and C groups of cations. The heavy solid black lines indicate the limits of possible amphibole compositions. Filled black squares are the locations of end-members at the corners of the compositional space; open circles are the locations of end-members on the edges of compositional space. Bar = barroisite; Eck = eckermannite; Ed = edenite; Gln = glaucophane; Mhb = magnesio-hornblende; Ktp = katophorite; Nyb = nybøite; Prg = pargasite; Ri = richterite; Sad = sadanagaite; Tar = taramite; Tr = tremolite; Ts = tschermakite; Win = winchite. We use the symbols of Kretz (1983) for the amphiboles, and introduce new symbols for amphiboles not included in the original list of symbols. The full list of symbols used here for amphiboles is given as Appendix VII.

cations are never dominant at *M*(1) or *M*(3) in amphiboles with (OH,F,Cl) ≥ 1.00 apfu. Lithium can become dominant at the *M*(3) site, normally being accompanied by Fe^{3+} at the *M*(2) site.

We need to be able to represent the variation in C cations by a single variable, which therefore must be some function of their aggregate formal charge. The most common variation in C involves divalent and trivalent cations. The root composition for tremolite has $C = Mg_5$, and it is convenient to represent variation in C by the additional formal charge introduced by incorporation of trivalent and tetravalent cations as C cations, as the additional charge corresponds arithmetically to the amount of trivalent and tetravalent C-cations in the amphibole ($Al + Fe^{3+} + 2Ti^{4+}$). If we consider C cations of formal charge greater than 2^+, i.e., Al, Fe^{3+}, Cr^{3+}, V^{3+}, Ti^{4+}, Sc, and Zr, we can express the additional C-cation charge as M^{3+} where $M^{3+} = Al + Fe^{3+} + Cr^{3+} + V^{3+} + Sc + 2Ti^{4+} + 2Zr$; in most amphiboles, this reduces to $M^{3+} = Al + Fe^{3+} + 2Ti^{4+}$. If we are dealing with amphiboles in which W = $(OH,F,Cl)_2$, all of these cations will occur at the *M*(2) site [except for some Al–Mg disorder over *M*(2) and *M*(3) in Mg-rich calcium amphiboles, which is immaterial to this argument], and thus the high-charge cations cannot exceed 2 apfu (i.e., the additional formal charge is at most 2^+).

However, note that M^{3+} can exceed 2.0 for some compositions. Where $^{O(3)}O^{2-}$ is not the dominant W anion, the behavior of $^{C}Ti^{4+}$ also affects M^{3+} because of the different roles that $^{C}Ti^{4+}$ can

play in amphiboles: (a) $^{C}Ti^{4+}$ may occur at the *M*(2) site where it contributes $2^{C}Ti^{4+}$ to M^{3+}; (b) $^{C}Ti^{4+}$ may occur at the *M*(1) site [coupled to the occurrence of O^{2-} at the O(3) site, i.e., as a W anion] where it does not contribute to M^{3+}: i.e., $M^{3+} = Al + Fe^{3+}$. The same is true for Fe^{3+} at the *M*(1) and *M*(3) sites in calcic oxo-amphiboles (from volcanic environments, where dehydrogenation is related to post-crystallization oxidation processes). If known, the oxo component in amphiboles must be accounted for by subtracting the appropriate amount of Ti^{4+} and Fe^{3+} from M^{3+} before classification. In addition, the same amount of Fe^{3+} must be subtracted from the total amount of Fe^{3+} in the formula with regard to the assignment of the prefix *ferri-*. Thus ferri- is assigned on the basis of $[^{C}Fe^{3+} - {}^{M(1,3)}Fe^{3+}]$ if $^{M(1,3)}Fe^{3+}$ is known.

A correction to M^{3+} is required also where Li is a C cation because ^{C}Li enters the amphibole structure via the substitution $^{M(3)}Li + {}^{M(2)}Fe^{3+} \rightarrow {}^{M(2,3)}Fe^{2+}_{2}$. As ^{C}Li is not incorporated into the A-B-C classification procedure but is considered separately, it is necessary to adjust the value of M^{3+} for the effect of the substitution $^{M(3)}Li + {}^{M(2)}Fe^{3+} = {}^{M(2,3)}Fe^{2+}_{2}$. This is done by subtracting an amount of trivalent cations equal to the amount of ^{C}Li.

We use the variable $^{C}(Al + Fe^{3+} + 2Ti^{4+})$ in the classification graphs of this paper. Note that this variable must be modified by adding $[Cr^{3+} + V^{3+} + Sc + 2Zr]$ and subtracting $[{}^{M(3)}Li + {}^{M(1,3)}Fe^{3+} + {}^{2M(1)}Ti^{4+}]$ where appropriate (see above discussion). Major differences between this classification and the classifications of IMA1997 and IMA2003 are outlined in Appendix V.

(5) Ti >0.50 apfu. The occurrence of titanium as a C cation is not related to a homovalent substitution, and hence there is no titano- prefix. Titanium may be incorporated into the amphibole structure by heterovalent-cation substitution (e.g., $^{C}Ti^{4+} + 2^{T}Al = {}^{C}Mg + 2^{T}Si$) or by oxo- substitution ($^{C}Ti^{4+} + 2^{W}O^{2-} = {}^{C}Mg + 2^{W}OH$). Both types of substitution lead to new charge arrangements and hence new root compositions, [e.g., $NaCa_2(Mg_4Ti)(Si_5Al_3)O_{22}(OH)_2$ and $NaCa_2(Mg_4Ti)(Si_7Al)O_{22}O_2$], both being derived from edenite by the substitutions $^{C}Ti^{4+} + 2^{T}Al = {}^{C}Mg + 2^{T}Si$ and $^{C}Ti^{4+} + 2^{W}O^{2-} = {}^{C}Mg + 2^{W}OH$]. Thus compositions with ^{C}Ti >0.5 apfu involve new names, both in (OH,F,Cl) amphiboles and in oxo-amphiboles (e.g., dellaventuraite, kaersutite, obertiite). The occurrence of significant ^{C}Ti, although less than 0.50 apfu in (OH,F,Cl) amphiboles, is important both for mineralogical and petrological reasons, and can be indicated using the modifier Ti-rich where $0.50 > {}^{C}Ti > 0.30$ apfu.

Appendix V: Major differences between the new classification and IMA1997 and IMA2003

(1) We have changed the criterion to identify the different subgroups, bringing it more into accord with the *dominant-cation* criterion of current IMA-CNMNC nomenclature. IMA1997 and IMA2003 referred to specific atom contents in the formula unit to define the boundary between subgroups. Thus an amphibole was assigned to the calcium subgroup where the following conditions apply: $^{B}(Mg,Fe^{2+},Mn^{2+}, Li) \leq 0.50$, $^{B}(Ca,Na) \geq 1.50$, and $^{B}Na \leq 0.50$ apfu. In the present classification, amphiboles are assigned to various subgroups based on the *dominant cation* (or group of cations) at a site (or group of sites).

(2) IMA1997 and IMA2003 considered ^{B}Li together with $^{B}(Mg,Fe^{2+},Mn^{2+})$. The crystal-chemical behavior of Li is very different from that of (Mg,Fe^{2+},Mn^{2+}) and Ca, and is more similar to that of Na. Moreover, extensive recent work (Caballero et al. 1998, 2002; Oberti et al. 2003, 2004) has shown complete solid-solution between ^{B}Li and ^{B}Na, behavior that is different from that of the $^{B}(Mg,Fe^{2+},Mn^{2+})$ amphiboles. The existence of ^{B}Li amphibole with orthorhombic and monoclinic primitive symmetries indicates that ^{B}Li-dominant amphiboles should be a distinct subgroup.

(3) IMA2003 defined a sodium-calcium-magnesium-iron-manganese-lithium group in which intermediate compositions require (1) a new root name if $^{B}Li > 0.50$ apfu, or (2) the prefixes *parvo* and *magno* if $^{B}Li \leq 0.50$ apfu. We have defined new subgroups: lithium-calcium, sodium-(magnesium-iron-manganese), and lithium-(magnesium-iron-manganese) amphiboles. These amphibole compositions have the same charge arrangement as richterite, and hence cannot be reduced to a combination of other end-members.

(4) IMA1997 AND IMA2003 used both nouns and adjectives to define the main groups (now subgroups) of amphiboles (e.g., magnesium-iron-manganese-lithium, calcic, sodic). Here we use nouns (e.g., magnesium-iron-manganese, calcium, sodium) or element or cation symbols in all cases.

(5) IMA1997 and IMA2003 used the A, B, and T cations for classification purposes. However, the dominant T-cation does not change: it is invariably Si, and hence compositional variation at T is not an appropriate variable to use for classification. All other groups show two or more cations as dominant, and hence the A, B, and C cations are more appropriate for classification purposes and accord with the dominant-cation principle currently used in IMA nomenclature. This point is the major difference between the two schemes. The use of C cations for classification has been implemented by considering the variation in $^{C}M^{3+}$ (the amount of highly charged C-cations not involved in the processes related to the oxo component) as a classification variable.

Three major crystal-chemical issues have been explored in detail since publication of the previous scheme of classification (IMA1997): (a) the behavior of ^{C}Li, (b) the behavior of ^{B}Li, and (c) the occurrence of dominant O^{2-} at W. For (a) and (c), electroneutrality is maintained by incorporation of "unusual" cations at sites containing "normal" C-cations: (a) $^{M(3)}Li$ is accompanied by $^{M(2)}Fe^{3+}$; (b) $^{W}O^{2-}$ is accompanied by $^{M(1)}Ti^{4+}$ or $^{M(1,3)}(Fe^{3+},Mn^{3+})$. For classification purposes, these components are dealt with by subtracting the relevant amounts of Fe^{3+} and Ti^{4+} from $^{C}M^{3+}$ before using the standard compositional diagrams.

(6) The present classification recognizes a distinct group of amphiboles with O^{2-} as the dominant W anion (oxo-amphiboles). These amphiboles contain high-charge C-cations, and have distinct root-names.

(7) We have adopted a different use of prefixes. Because some root compositions have been redefined as their magnesio-, alumino- analogues, the use of the prefixes *magnesio* and *alumino* has been restricted to a few root-names of petrological relevance (riebeckite, arfvedsonite, hastingsite, and hornblende), and the prefix *sodic* has been abolished. Appendix VI lists root-names that have been redefined in the present classification.

Appendix VII: Symbols for amphiboles*

Act Actinolite
Ath Anthophyllite
Arf Arfvedsonite
Bar Barroisite
Can Cannilloite
Cho Clino-holmquistite
Cum Cummingtonite
Del Dellaventuraite
Eck Eckermannite
Ed Edenite
Ged Gedrite
Gln Glaucophane
Gru Grunerite
Hs Hastingsite
Hol Holmquistite
Krs Kaersutite
Ktp Katophorite
Lkt Leakeite
Mhb Magnesio-hornblende
Nyb Nybøite
Ob Obertiite
Prg Pargasite
Ped Pedrizite
Ri Richterite
Rbk Riebeckite
Sad Sadanagaite
Tar Taramite
Tr Tremolite
Ts Tschermakite
Un Ungarettiite
Win Winchite.

Symbols in bold are from Kretz (1983); symbols in normal font are introduced here. Other lists of symbols have been published subsequent to that of Kretz (1983), but these are also incomplete with regard to amphibole names.

The Canadian Mineralogist
Vol. 35, pp. 1571-1606 (1997)

RECOMMENDED NOMENCLATURE FOR ZEOLITE MINERALS: REPORT OF THE SUBCOMMITTEE ON ZEOLITES OF THE INTERNATIONAL MINERALOGICAL ASSOCIATION, COMMISSION ON NEW MINERALS AND MINERAL NAMES

DOUGLAS S. COOMBS[1] (Chairman)
Geology Department, University of Otago, P.O. Box 56, Dunedin, New Zealand

ALBERTO ALBERTI
Istituto di Mineralogia, Università di Ferrara, Corso Ercole I° d'Este, 32, I-44100 Ferrara, Italy

THOMAS ARMBRUSTER
Laboratorium für chemische und mineralogische Kristallographie, Universität Bern, Freiestrasse 3, CH-3012 Bern, Switzerland

GILBERTO ARTIOLI
Dipartimento di Scienze della Terra, Università di Milano, via Botticelli, 23, I-20133 Milano, Italy

CARMINE COLELLA
Dipartimento di Ingegneria dei Materiali e della Produzione, Università Federico II di Napoli, Piazzale V. Tecchio, 80, I-80125 Napoli, Italy

ERMANNO GALLI
Dipartimento di Scienze della Terra, Università di Modena, via S. Eufemia, 19, I-41100 Modena, Italy

JOEL D. GRICE
Mineral Sciences Division, Canadian Museum of Nature, Ottawa, Ontario K1P 6P4, Canada

FRIEDRICH LIEBAU
Mineralogisch-Petrographisches Institut, Universität Kiel, Olshausenstrasse 40, D-24098 Kiel, Germany

JOSEPH A. MANDARINO (*retired from Subcommittee, December, 1994*)
Department of Mineralogy, Royal Ontario Museum, Toronto, Ontario M5S 2C6 Canada

HIDEO MINATO
5-37-17 Kugayama, Suginami-ku, Tokyo 168, Japan

ERNEST H. NICKEL
Division of Exploration and Mining, CSIRO, Private Bag, Wembley 6014, Western Australia, Australia

ELIO PASSAGLIA
Dipartimento di Scienze della Terra, Università di Modena, via S. Eufemia, 19, I-41100 Modena, Italy

DONALD R. PEACOR
Department of Geological Sciences, University of Michigan, Ann Arbor, Michigan 48109, U.S.A.

SIMONA QUARTIERI
Dipartimento di Scienze della Terra, Università di Modena, via S. Eufemia, 19, I-41100 Modena, Italy

ROMANO RINALDI
Dipartimento di Scienze della Terra, Università di Perugia, I-06100 Perugia, Italy

MALCOLM ROSS
U.S. Geological Survey, MS 954, Reston, Virginia 20192, U.S.A.

RICHARD A. SHEPPARD
U.S. Geological Survey, MS 939, Box 25046, Federal Center, Denver, Colorado 80225, U.S.A.

EKKEHART TILLMANNS
Institut für Mineralogie und Kristallographie, Universität Wien, Althanstrasse 14, A-1090 Vienna, Austria

GIOVANNA VEZZALINI
Dipartimento di Scienze della Terra, Università di Modena, via S. Eufemia, 19, I-41100 Modena Italy

[1] *E-mail address*: doug.coombs@stonebow.otago.ac.nz

Abstract

This report embodies recommendations on zeolite nomenclature approved by the International Mineralogical Association, Commission on New Minerals and Mineral Names. In a working definition of a zeolite mineral used for this review, structures containing an interrupted framework of tetrahedra are accepted where other zeolitic properties prevail, and complete substitution by elements other than Si and Al is allowed. Separate species are recognized in topologically distinctive compositional series in which different extra-framework cations are the most abundant in atomic proportions. To name these, the appropriate chemical symbol is attached by a hyphen to the series name as a suffix, except for the names harmotome, pollucite and wairakite in the phillipsite and analcime series. Differences in space-group symmetry and in order–disorder relationships in zeolites having the same topologically distinctive framework do not in general provide adequate grounds for recognition of separate species. Zeolite species are not to be distinguished solely on the ratio Si : Al except for heulandite (Si : Al < 4.0) and clinoptilolite (Si : Al ≥ 4.0). Dehydration, partial hydration, and overhydration are not sufficient grounds for the recognition of separate species of zeolites. Use of the term "ideal formula" should be avoided in referring to a simplified or averaged formula of a zeolite. Newly recognized species in compositional series are as follows: brewsterite-Sr, -Ba, chabazite-Ca, -Na, -K, clinoptilolite-K, -Na, -Ca, dachiardite-Ca, -Na, erionite-Na, -K, -Ca, faujasite-Na, -Ca, -Mg, ferrierite-Mg, -K, -Na, gmelinite-Na, -Ca, -K, heulandite-Ca, -Na, -K, -Sr, levyne-Ca, -Na, paulingite-K, -Ca, phillipsite-Na, -Ca, -K, and stilbite-Ca, -Na. Key references, type locality, origin of name, chemical data, IZA structure-type symbols, space-group symmetry, unit-cell dimensions, and comments on structure are listed for 13 compositional series, 82 accepted zeolite mineral species, and three of doubtful status. Herschelite, leonhardite, svetlozarite, and wellsite are discredited as mineral species names. Obsolete and discredited names are listed.

Keywords: zeolite nomenclature, herschelite, leonhardite, svetlozarite, wellsite, brewsterite, chabazite, clinoptilolite, dachiardite, erionite, faujasite, ferrierite, gmelinite, heulandite, levyne, paulingite, phillipsite, stilbite.

Sommaire

Ce rapport contient les recommandations à propos de la nomenclature des zéolites, telles qu'approuvées par l'Association minéralogique internationale, commission des nouveaux minéraux et des noms de minéraux. Dans la définition d'une zéolite retenue ici, les structures contenant une trame interrompue de tétraèdres sont acceptées dans les cas où les autres propriétés satisfont les critères de cette famille de minéraux. De plus, il peut y avoir remplacement complet de Si et Al par d'autres éléments. Des espèces distinctes font partie de séries de compositions dont l'agencement topologique est le même, le cation dominant ne faisant pas partie de la trame déterminant l'espèce. Pour en déterminer le nom, il s'agit de rattacher le symbole chimique approprié au nom de la série par un trait d'union, sauf dans les cas de harmotome, pollucite et wairakite, faisant partie des séries de la phillipsite et de l'analcime. Des différences en symétrie exprimées par le groupe spatial et en degré d'ordre Si–Al dans les zéolites ayant le même agencement topologique ne suffisent pas en général pour définir une espèce distincte. Le seul critère de rapport Si : Al ne suffit pas pour distinguer les espèces de zéolites, sauf pour la heulandite (Si : Al < 4.0) et clinoptilolite (Si : Al ≥ 4.0). L'état de déshydratation, d'hydratation partielle, et de sur-hydratation ne suffit pas pour reconnaître une espèce distincte de zéolite. On doit éviter d'utiliser le concept d'une "formule idéale" en parlant des formules simplifiées ou représentatives des zéolites. Les nouveaux noms d'espèces dans ces séries de compositions sont: brewsterite-Sr, -Ba, chabazite-Ca, -Na, -K, clinoptilolite-K, -Na, -Ca, dachiardite-Ca, -Na, érionite-Na, -K, -Ca, faujasite-Na, -Ca, -Mg, ferrierite-Mg, -K, -Na, gmelinite-Na, -Ca, -K, heulandite-Ca, -Na, -K, -Sr, lévyne-Ca, -Na, paulingite-K, -Ca, phillipsite-Na, -Ca, -K, et stilbite-Ca, -Na. Nous présentons les références-clés, la localité-type, l'origine du nom, des données chimiques, le symbole structural IZA, le groupe spatial et la symétrie, les paramètres réticulaires et des commentaires sur la structure de 13 séries compositionnelles, 82 espèces homologuées, et trois dont le statut est douteux. Herschelite, léonhardite, svetlozarite, et wellsite sont discréditées comme noms d'espèces minérales. Nous dressons une liste des noms obsolètes et discrédités.

(Traduit par la Rédaction)

Mots-clés: nomenclature des zéolites, herschelite, léonhardite, svetlozarite, wellsite, brewsterite, chabazite, clinoptilolite, dachiardite, érionite, faujasite, ferrierite, gmelinite, heulandite, lévyne, paulingite, phillipsite, stilbite.

Introduction

The name "zeolite" was introduced by the Swedish mineralogist Cronstedt in 1756 for certain silicate minerals in allusion to their behavior on heating in a borax bead (Greek *zeo* = boil; *lithos* = stone). Three such minerals were listed by Haüy (1801), namely stilbite, analcime, and harmotome, together with "mesotype", which has not survived. Chabazite and leucite had been named even earlier. Nineteen had been described with their present meaning by 1842. Forty-six zeolites were listed by Gottardi & Galli (1985), and new species continue to be described. The first crystal-structure determination of a zeolite was done on analcime (Taylor 1930); following this, Hey (1930) concluded that zeolites in general have aluminosilicate frameworks with loosely bonded alkali or alkali-earth cations, or both. Molecules of H_2O occupy extra-framework positions. He pointed out the consequential requirements that the molar ratio

Al_2O_3 : $(Ca,Sr,Ba,Na_2,K_2)O$ = 1 and that O : (Si + Al) = 2 in the empirical formula.

Zeolites have other highly characteristic features developed to varying degrees, notably the potential for reversible low-temperature dehydration, the ability of the dehydrated forms to reversibly absorb other molecules, a tendency toward more or less easy low-temperature exchange of extra-framework cations, and a lack of clear-cut, structurally controlled constraints on end-member compositions in terms of Si : Al ratios within the framework. In some cases, observed extra-framework compositions may be artefacts of cation exchange resulting from human activities in the laboratory or elsewhere, and furthermore, the compositions are not conveniently determined by traditional optical methods. Perhaps for a combination of such reasons, separate names have been given to few zeolites on the basis of the dominant extra-framework cation in solid-solution series. This conflicts with standard practice in most mineral groups and with guidelines of the Commission on New Minerals and Mineral Names (CNMMN) (Nickel & Mandarino 1987).

With intensification of research and the advent of the electron microprobe, a flood of information on compositions has become available, and with automated single-crystal X-ray diffractometers and other developments, many complexities have been investigated, including order–disorder relationships in the frameworks and associated changes in unit-cell parameters and symmetry. Thus in the case of analcime, Mazzi & Galli (1978), Teertstra *et al.* (1994), and others have demonstrated a wide range of space-group symmetries associated with different patterns of order in the framework and possible displacive transformations. Sites of extra-framework cations are commonly less well defined in an open, zeolitic structure than in most other minerals, and are variably occupied. Guidelines allowing recognition of separate species depending on the dominant ion occupying each structural site are thus compromised in the case of extra-framework sites in zeolites. Furthermore, changes in the occupancy of such sites can distort the framework to varying degrees, changing the space-group symmetry.

Some minerals meet traditional criteria for zeolites in all respects except that they contain P, Be, or other elements in tetrahedral sites, with consequent departure from the requirement of Hey (1930) that O : (Si + Al) = 2. Other structurally related minerals with zeolitic properties have all tetrahedral sites occupied by elements other than Si and Al. Certain other minerals displaying zeolitic properties depart from traditional requirements for a zeolite in having a framework that is interrupted by some (OH) groups. An example is parthéite, listed by Gottardi & Galli (1985) as a zeolite. Synthesis and structural analysis of materials having zeolitic properties have become major fields of research and have led to a voluminous literature, as has the industrial use of zeolitic materials.

The recommendations of an IMA CNMMN subcommittee set up to review zeolite nomenclature are set out below. These recommendations have been adopted by the Commission.

Definition of a Zeolite Mineral

In arriving at its working definition of a zeolite, the Subcommittee took the view that zeolites in the historical and mineralogical sense are naturally occurring minerals, irrespective of how the term may be applied to synthetic materials and in industry. In the light of advances in mineralogy, the Hey (1930) definition is found to be too restrictive. The Subcommittee gave particular consideration to the following questions. Is more than 50% substitution of elements other than Si and Al permissible in tetrahedral sites? Is the presence of H_2O and of extra-framework cations absolutely essential? Can "interrupted" framework structures qualify as zeolite minerals? These matters are further discussed in Appendix 1.

Definition

A zeolite mineral is a crystalline substance with a structure characterized by a framework of linked tetrahedra, each consisting of four O atoms surrounding a cation. This framework contains open cavities in the form of channels and cages. These are usually occupied by H_2O molecules and extra-framework cations that are commonly exchangeable. The channels are large enough to allow the passage of guest species. In the hydrated phases, dehydration occurs at temperatures mostly below about 400°C and is largely reversible. The framework may be interrupted by (OH,F) groups; these occupy a tetrahedron apex that is not shared with adjacent tetrahedra.

Application of the definition (see also Appendix 1)

Relatively easy exchange of extra-framework cations at relatively low temperature is a characteristic feature of zeolites and zeolitic behavior, but varies greatly from species to species. Its extent does not provide a convenient basis for the definition of zeolites. In practice, it appears that channels must have a minimum width greater than that of 6-membered rings (*i.e.,* rings consisting of six tetrahedra) in order to allow zeolitic behavior at normal temperatures and pressures. Framework structures such as in feldspars, nepheline, sodalites, scapolites, melanophlogite, and probably leifite, in which any channels are too restricted to allow typical zeolitic behavior such as reversible dehydration, molecular sieving, or cation exchange, are not regarded as zeolites.

Framework density, defined as the number of tetrahedral sites in 1000 $Å^3$, was used as the criterion for inclusion in the *Atlas of Zeolite Structure Types*

(Meier *et al.* 1996). However, this criterion provides no evidence that the channels necessary for diffusion are present, as well as cages, and it has not been adopted in the present definition.

In some minerals with a tetrahedral framework structure and other zeolitic characteristics as described, namely parthéite, roggianite, maricopaite, and chiavennite, one apex of some tetrahedra is occupied by an (OH) group or F atom instead of being occupied by an O atom. This (OH) group or F atom does not form a bridge with an adjacent tetrahedron. The framework is thus interrupted. Such minerals are here accepted as zeolites.

In terms of the definition adopted, minerals of the cancrinite group can arguably be considered as zeolites. This group has long been regarded by many or most mineralogists as distinct from the zeolites, in part, at least, because of the presence of large volatile anions (*e.g.,* Hassan 1997). They are not reviewed in the present report. Rather similarly, wenkite contains large cages and channels, but these are blocked by SO_4, Ca, and Ba ions (Wenk 1973, Merlino 1974), inhibiting zeolitic behavior. In addition, no water is lost below 500°C. Wenkite is not included as a zeolite in this report.

Leucite has seldom been regarded as a zeolite, as it does not display a full range of zeolitic behavior. Nevertheless, it has the same framework structure as analcime and conforms to the adopted definition. Ammonioleucite can be regarded as an analcime derivative, can be synthesized from analcime by cation exchange, and may have formed naturally by low-temperature replacement of analcime. Leucite and ammonioleucite are included in the list of zeolites, as is kalborsite, a derivative of the edingtonite structure.

Also conforming to the definition adopted are the beryllophosphates pahasapaite and weinebeneite. These contain neither Si nor Al and can be regarded as end-member examples of Si-free zeolites or zeolite phosphates.

Rules for Nomenclature of Zeolite Minerals

In presenting the following rules for nomenclature of zeolite minerals, the Subcommittee feels strongly that they should be viewed as guidelines rather than as being rigidly prescriptive. As stated by Nickel & Mandarino (1987): "It is probably not desirable to formulate rigid rules to define whether or not a compositional or crystallographic difference is sufficiently large to require a new mineral name, and each new mineral proposal must be considered on its own merits". Explanatory notes following the proposed rules or guidelines give examples of how the Subcommittee envisages that rule being applied, but like Nickel and Mandarino, the Subcommittee urges that each case be treated on its merits. In some cases, compelling reasons may exist on grounds of historical usage for retaining an existing name, or other grounds may exist for departing from the rules for giving a new name. Cases arising under Rule 2 are particularly difficult, and require individual consideration.

Rule 1

(a) One or more zeolite minerals having a topologically distinctive framework of tetrahedra, and a composition that is distinctive for zeolites having that framework, constitute separate *species*. (b) Zeolites having the same topologically distinctive framework of tetrahedra constitute a *series* when they display a substantial range in composition in which differing extra-framework cations may be the most abundant in atomic proportions. These cations may occupy different extra-framework sites. Such *series* consist of two or more *species* that are distinguished on the basis of the most abundant extra-framework cation.

Application of the rule

Laumontite, for example, has a topologically distinctive framework and a composition which, as far as is currently known, is distinctive in that Ca is always the dominant extra-framework cation. It is a separate zeolite species under Rule 1a. Natrolite, mesolite, and scolecite have the same topologically distinctive framework structure as each other, and have compositions that are distinctive. They also are separate species under Rule 1a.

Zeolites having the topologically distinctive chabazite structure have a range of compositions in which any one of Ca, Na, or K may be the most abundant extra-framework cation. Substantial Sr is in some cases present as well, but so far has never been reported as the most abundant in natural examples. Chabazite is a series consisting of three separate species under Rule 1b. It is known that near-end-member Na, K, Ca, and Sr compositions are readily obtainable by ion exchange from natural Ca-dominant chabazite at 110°C (Alberti *et al.* 1982a), but this is not the essential criterion for recognition of the natural series.

Mesolite may have either Na or Ca slightly in excess of the other, but the ratio Na : Ca is always close to 1 : 1. The range of its composition is not regarded as "substantial", and mesolite is not divided into more than one species on grounds of composition.

Several distinct structural sites for extra-framework cations are recognized in many zeolites, but in view of the relatively loose bonding and specialized problems in establishing the individual site-occupancies, only the total population of extra-framework cations should in general be used in defining zeolite species.

Rule 2

(a) Differences in space-group symmetry and in order–disorder relationships in zeolite minerals having the same topologically distinctive framework do not in

general provide adequate grounds for recognition of separate species, but each case should be treated on its merits. (b) In assessing such cases, other factors, such as relationship to chemical composition, should be taken into consideration.

Application of the rule

The Subcommittee found it to be impracticable to formulate quantified criteria for handling problems arising from this rule. Irrespective of decisions that have been made in the past, care should be taken that departures envisaged in Rule 2b from the principle enunciated in Rule 2a are based on grounds that are truly compelling.

Analcime and certain other zeolites exist with several different space-group symmetries, in some cases occurring on a very fine scale in the same hand specimen and with the same chemistry. Even though this may be related to Si,Al ordering, separate species names in these cases are in general not warranted.

Gismondine and garronite are examples of zeolites that have the same topologically distinctive framework. Both have Ca as the dominant extra-framework cation. Their differing space-group symmetry is associated with disordered Si,Al and the presence of significant Na in garronite. They are accepted as separate species. Gobbinsite and amicite have topologically the same framework structure as gismondine, but are alkali-dominant. Their different space-group symmetries appear to be related to Si,Al disorder in gobbinsite and possible chemical differences, and they are provisionally retained. Barrerite is topologically similar to stilbite and stellerite, but it has different symmetry correlated with the presence of extra cations that cause rotational displacements within the framework (Galli & Alberti 1975b); it is similarly retained.

Rule 3

Zeolite mineral species shall not be distinguished solely on the basis of the framework Si : Al ratio. An exception is made in the case of heulandite and clinoptilolite; heulandite is defined as the zeolite mineral series having the distinctive framework topology of heulandite and the ratio Si : Al < 4.0. Clinoptilolite is defined as the series with the same framework topology and Si : Al ≥ 4.0.

Application of the rule

Many zeolites have a widely variable Si : Al ratio, but this, in itself, is not regarded as providing adequate grounds for recognition of separate species. The exception is based on entrenched usage of the names *heulandite* and *clinoptilolite*, and their convenience for recognizing an important chemical feature. The cutoff value adopted (following Boles 1972) is arbitrary in a continuous range of compositions. The usual 50% compositional rule cannot be applied, as there are no clearly defined Si,Al end-member compositions for heulandite and clinoptilolite. Thermal stability has been used by some investigators to distinguish clinoptilolite from heulandite. This is a derivative property, however, suggested by Mumpton (1960) as an aid to identification, and it is not appropriate as the basis for definition. Alietti (1972) and Boles (1972) have shown that there is no gap in composition either in framework or extra-framework cation contents between heulandite and clinoptilolite, and that samples transitional in composition show intermediate properties in terms of thermal stability.

Rule 4

Dehydration, partial hydration, and overhydration, whether reversible or irreversible, are not sufficient grounds for the recognition of separate species of zeolite minerals.

Application of the rule

If a new topologically distinctive framework arises from overhydration or partial dehydration, separate species status would result from application of Rule 1. Leonhardite, a partially and in most cases reversibly dehydrated form of laumontite, is not accepted as a separate mineral species.

Rule 5

Individual species in a zeolite mineral series with varying extra-framework cations are named by attaching to the series name a suffix indicating the chemical symbol for the extra-framework element that is most abundant in atomic proportions, *e.g.,* chabazite-Ca.

The following exceptions are made: a) On grounds of historical precedence and long-established usage, the name *harmotome* is retained for the Ba-dominant member of the phillipsite series. b) On grounds of long-established usage, pollucite is retained as the Cs-dominant zeolite of the analcime structure-type. On grounds of established usage and markedly different space-group symmetry and Si,Al order related to the extra-framework cation content (Rule 2b), wairakite is retained as the Ca-dominant zeolite of the analcime structure-type. On the other hand, herschelite is suppressed in favor of chabazite-Na (Appendix 2).

Application of the rule

New species arising from Rule 5 that are well authenticated by published data are set out in Table 1. Future proposals for additional new species under this rule should be dealt with as for any other proposal for a new mineral name.

Adoption of a Levinson-style system of suffixes avoids the proliferation of a large number of new and potentially unrelated species names, and ensures that all members of a topologically identical compositional series are indexed together. It has the great advantage that where adequate chemical data are not required or are not available, a mineral can be referred to correctly by an unambiguous series name. The system adopted here is without the brackets (parentheses) used by Levinson (1966) in suffixes for rare-earth minerals.

Substantial amounts of extra-framework cations other than the dominant one may be indicated, if desired, by the use of adjectives such as calcian and sodian, *e.g.,* calcian clinoptilolite-K. Such adjectival modifiers are not part of the formal name of a species.

Informal use is often made of descriptive terms such as calcium chabazite and Ca chabazite, in which the name or symbol of an element is used adjectivally. In conformity with general IMA guidelines, these should not appear in print as mineral names or in hyphenated form. The correct name for the mineral species in this case is chabazite-Ca. Terms such as sodium-substituted chabazite-Ca are suggested for what in effect would be a synthetic chabazite-Na prepared by cation exchange from chabazite-Ca. Chabazite remains the correct name for a member of the chabazite series that is not specifically identified on compositional grounds.

TABLE 1. NEWLY PROPOSED ZEOLITE SPECIES WITHIN COMPOSITIONAL SERIES§

Series	Species name	Series	Species name
brewsterite	brewsterite-Sr	gmelinite	gmelinite-Na
	brewsterite-Ba		gmelinite-Ca
			gmelinite-K
chabazite	chabazite-Ca		
	chabazite-Na	heulandite	heulandite-Ca
	chabazite-K		heulandite-Na
			heulandite-K
clinoptilolite	clinoptilolite-K		heulandite-Sr
	clinoptilolite-Na		
	clinoptilolite-Ca	levyne	levyne-Ca
			levyne-Na
dachiardite	dachiardite-Ca		
	dachiardite-Na	paulingite	paulingite-K
			paulingite-Ca
erionite	erionite-Na		
	erionite-K	phillipsite	phillipsite-Na
	erionite-Ca		phillipsite-Ca
			phillipsite-K
faujasite	faujasite-Na		
	faujasite-Ca	stilbite	stilbite-Ca
	faujasite-Mg		stilbite-Na
ferrierite	ferrierite-Mg		
	ferrierite-K		
	ferrierite-Na		

§ The first-named member of each series is the one to which the original type-specimen for the series seems to belong.

Rule 6

(a) Space-group variants of zeolite mineral species may be indicated by placing the space-group symbol in round brackets (parentheses) after the mineral species name, *e.g.,* analcime (*Ibca*), heulandite-Ca (*C*2/*m*). (b) Levels of order may be indicated by adjectival use of words such as "disordered" or "fully ordered" before the mineral name.

Application of the rule

Modifiers as suggested here are not part of the formal name of the mineral.

Accepted Zeolite Series and Species

Zeolites to be elevated to series status and the consequential new species to be recognized on the basis of the most abundant extra-framework cation (Rule 5) are set out in Table 1.

An annotated list of accepted zeolite series and species follows below. In each entry for series, and for those species that are not members of compositional series, a simplified or generalized formula is given in the first line. This is followed by *Z*, the number of these formula units per unit cell, as given later in the entry. The simplified or generalized formula should be regarded as representative only, and should not be regarded as an "ideal" composition (see next paragraph). Users of the list should bear in mind that the Si : Al ratio, or, more generally, occupancy of tetrahedral sites by Si, Al, P, Be, Zn, and possibly other elements, varies widely in many zeolites. The total extra-framework cation charge varies accordingly. Major variation in more-or-less exchangeable, extra-framework cations is also a feature of many natural zeolites. Contents of H_2O tend to decrease with increasing number and size of extra-framework cations, as well as with increasing temperature and decreasing $P(H_2O)$. Such variations can be vital to petrological, geochemical, environmental, and experimental considerations.

Simplified or generalized formulae of zeolites, *e.g.,* $NaAlSi_2O_6 \cdot H_2O$ for analcime, have often been referred to as "ideal" formulae. However, the supposed ideality may be in writers' desire for simplicity, rather than in anything fundamental to the zeolites concerned, and can lead to false assumptions. There is much evidence that the composition of naturally occurring analcime is a function of the chemical environment in which it forms (*e.g.,* Coombs & Whetten 1967). In environments of low Si activity, as in altered strongly silica-deficient

alkaline rocks, natural analcime approaches a Si : Al ratio of 1.5. The composition in burial metamorphic rocks in equilibrium with quartz appears to be distinctly more Si-rich than the supposed "ideal" Si : Al value of 2. The evidently metastable equilibrium in natural environments containing siliceous volcanic glass or other source of silica yielding higher activity of Si than coexistence with quartz, leads to analcime with Si : Al approaching 3. Analogous observations apply to heulandite and other zeolites. If "ideal" is taken to imply equilibrium, it can therefore be concluded that this is a function of the chemical (and P–T) environment during crystallization, rather than simply being a function of crystal structure. Differing Si : Al ratios may in turn favor different patterns of order in the framework. Application of the term "ideal" to simplified or averaged formulae of zeolites should be avoided.

Also given in the first line of each entry is the structure-type code allocated by the Structure Commission of the International Zeolite Association (IZA) and listed in Meier *et al.* (1996). The code consists of three capital letters. A preceding hyphen indicates an interrupted framework of tetrahedra.

The second line of each relevant entry starts with the original reference in which the current name of the mineral, or a near variant of that name, is given, followed by the type locality, or, in the case of descriptions that predate the concept of type localities, the general region of origin of the material on which the name and original description are based, where this is known. The locality is followed by a note on the derivation of the name. Further information on these matters is given by Gottardi & Galli (1985), Clark (1993), and Blackburn & Dennen (1997), but in some cases the information is here revised.

Next is given information on the currently known range in composition of the mineral concerned. This includes known values, or range of values, for T_{Si}, the proportion of tetrahedron sites occupied by Si atoms, as reported in published results of acceptable analyses. For many zeolites, this value varies widely, and the values reported may not indicate the full range possible, especially in the case of the rarer zeolites.

Much information on zeolite compositions was given by Gottardi & Galli (1985). The present compilation incorporates results of further extensive searches of the literature. A widely used criterion for acceptability of zeolite compositions is that the value of the balance-error function of Passaglia (1970)

$$E\ (\%) = 100 \times \frac{(Al + Fe^{3+}) - (Li + Na + K) - 2(Mg + Ca + Sr + Ba)}{(Li + Na + K) + 2(Mg + Ca + Sr + Ba)}$$

should be less than 10%, a figure that is itself arguably excessive. The calculation of E% may be modified to allow for other suspected cations, such as Fe^{2+} and Cs^{+}. The role of Fe causes problems that may not be resolvable. Some Fe reported in zeolites is undoubtedly a contaminant, but there are reasons to suspect that both Fe^{2+} and Fe^{3+} may enter the structures of some zeolites in extra-framework or framework sites, or both.

Space-group symmetry and crystallographic parameters follow. Many accepted zeolite species exist with more than one known space-group symmetry, and these are listed. Variations in space-group symmetry and variations in order–disorder relationship of framework cations are not in themselves adequate evidence for establishing new species (Rule 2). Cell parameters given are as reported for material specified in key references. Cell dimensions of many species vary widely as a result of variable compositions, variable extent of order, and differing levels of hydration. Except for a few newly described species, details of structure, including size and orientation of channels, can be obtained for each structure type from Meier *et al.* (1996) and are discussed in Gottardi & Galli (1985).

The accepted series and species are as follows:

Amicite

$K_4Na_4[Al_8Si_8O_{32}]\bullet 10H_2O$ $Z = 1$ GIS

Alberti *et al.* (1979). Type locality: Höwenegg (a Tertiary melilite nephelinite volcano), Hegau, southwestern Germany. Named after Giovan Battista Amici (1786–1863), inventor of the Amici lens and microscope objectives with a hemispherical front lens.

Both type amicite and the only other known example (Khomyakov *et al.* 1982) include minor Ca. T_{Si} = 0.51, 0.49.

Monoclinic, *I*2, *a* 10.226(1), *b* 10.422(1), *c* 9.884(1) Å, ß 88.32(2)°.

The framework is characterized by double crankshaft chains as in gismondine (Alberti & Vezzalini 1979).

Amicite has the same framework topology as gismondine. Si,Al and Na,K distributions are ordered and lower the symmetry from topological $I4_1/amd$ to real symmetry *I*2.

Ammonioleucite

$(NH_4)[AlSi_2O_6]$ $Z = 16$ ANA

Hori *et al.* (1986). Type locality: Tatarazawa, Fujioka, Gunma Prefecture, Japan. The name reflects its composition and relationship to leucite.

Material from the only known locality contains significant K. T_{Si} = 0.70.

Tetragonal, $I4_1/a$, *a* 13.214(1), *c* 13.713(2) Å.

Analcime

$Na[AlSi_2O_6]\bullet H_2O$ $Z = 16$ ANA

Haüy (1797, p. 278). Type locality: near Catanes, Cyclopean Isles, Italy (Haüy, 1801, p. 180-185). Name from Greek roots meaning "without strength", in

allusion to the weak electrical effects induced by friction. In most analyzed specimens, Na is the only substantial extra-framework cation, but analcime forms a continuous series with pollucite and possibly with wairakite (Seki & Oki 1969, Seki 1971, Cho & Liou 1987). T_{Si} varies widely, 0.59–0.73 (*e.g.,* Coombs & Whetten 1967). As Si increases, NaAl decreases and H_2O increases.
Topological symmetry is cubic, *Ia*3*d*. Real symmetry variants include:
cubic, *Ia*3*d*, *a* 13.725 Å;
tetragonal, $I4_1/acd$, *a* 13.723(7), *c* 13.686(10) Å; *a* 13.721(1), *c* 13.735(1) Å (Mazzi & Galli 1978);
tetragonal, $I4_1/a$;
orthorhombic, *Ibca*, *a* 13.733(1), *b* 13.729(1), *c* 13.712(1) Å; *a* 13.727(2), *b* 113.714(2), *c* 13.740(2) Å (Mazzi & Galli 1978);
monoclinic with 2-fold axis parallel both to pseudo-cubic [100] and [110];
triclinic, *a* 13.6824(5), *b* 13.7044(6), *c* 13.7063(5) Å, α 90.158(3)°, ß 89.569(3)°, γ 89.543(3)° (Hazen & Finger 1979);
and probably trigonal with variable Si,Al order (*e.g.,* Hazen & Finger 1979, Teertstra *et al.* 1994).
The name applies to Na-dominant compositions with this framework structure regardless of the degree and patterns of order.

Barrerite

$Na_2[Al_2Si_7O_{18}]\bullet 6H_2O$ $Z = 8$ STI
Passaglia & Pongiluppi (1974, 1975). Type locality: Capo Pula, Sardinia, Italy. Named after Professor Richard M. Barrer (1910–1996) of Imperial College, London, for contributions to the chemistry of molecular sieves.
Also known from Kuiu Island, Alaska (Di Renzo & Gabelica 1997). T_{Si} = 0.77, 0.78. The type example has composition:
$(Na_{5.45}K_{1.06}Ca_{0.84}Mg_{0.17})[Al_{8.19}Fe_{0.01}Si_{27.72}O_{72}]\bullet 25.78H_2O$.
Orthorhombic, *Amma* or *Ammm*, *a* 13.643(2), *b* 18.200(3), *c* 17.842(3) Å (Passaglia & Pongiluppi 1974).
The structure is similar to that of stilbite and stellerite, but it has different symmetry as a result of extra cations, which cause rotational displacements within the framework (Galli & Alberti 1975b).

Bellbergite

$(K,Ba,Sr)_2Sr_2Ca_2(Ca,Na)_4[Al_{18}Si_{18}O_{72}]\bullet 30H_2O$
$Z = 1$ EAB
Rüdinger *et al.* (1993). Type and only known locality: Bellberg (or Bellerberg) volcano, near Mayen, Eifel, Germany. Named after the locality.
Ca is overall the dominant extra-framework cation. T_{Si} = 0.51.
Hexagonal, possible space-groups $P6_3/mmc$, $P\bar{6}2c$, and $P6_3mc$, *a* 13.244(1), *c* 15.988(2) Å.
The framework structure is as for synthetic zeolite TMA–EAB.

Bikitaite

$Li[AlSi_2O_6]\bullet H_2O$ $Z = 2$ BIK
Hurlbut (1957). Type locality: Bikita, Zimbabwe. Named after the type locality.
Two known localities, with the bikitaite having very similar compositions. T_{Si} = 0.67.
Monoclinic, $P2_1$, *a* 8.613(4), *b* 4.962(2), *c* 7.600(4) Å, ß 114.45(1)° (Kocman *et al.* 1974).
Also triclinic, *P*1, *a* 8.606(1), *b* 4.953(1), *c* 7.599(1) Å, α 89.89(2)°, ß 114.42(2)°, γ 89.96(2)° (Bissert & Liebau 1986).
The framework structure consists of 5-membered rings linked by additional tetrahedra. Its topological symmetry is $P2_1$. The monoclinic $P2_1$ variant of Kocman *et al.* has partly ordered Si,Al distribution; the triclinic *P*1 variant of Bissert and Liebau is highly ordered.

Boggsite

$Ca_8Na_3[Al_{19}Si_{77}O_{192}]\bullet 70H_2O$
$Z = 1$ BOG
Pluth *et al.* (1989) and Howard *et al.* (1990). Type locality: Basalt above cliff, Goble Creek, south side of the Neer Road, 0.2 km north of Goble, Columbia County, Oregon, U.S.A. Named after Robert Maxwell Boggs (father) and Russell Calvin Boggs (son), mineral collectors in the Pacific Northwest.
Type boggsite approximates the above formula, with minor Fe, Mg, and K. Boggsite from Mt. Adamson, Antarctica (Galli *et al.* 1995) approximates $Ca_6Na_5K[Al_{18}Si_{78}O_{192}]\bullet 70H_2O$, with minor Fe, Mg, Sr, Ba. T_{Si} = 0.81.
Orthorhombic, *Imma*, *a* 20.236(2), *b* 23.798(1), *c* 12.798(1) Å (Pluth & Smith 1990).
Si,Al highly disordered.

Brewsterite (series)

$(Sr,Ba)_2[Al_4Si_{12}O_{32}]\bullet 10H_2O$
$Z = 1$ BRE
Brooke (1822). Type locality: Strontian, Argyll, Scotland. Named after Sir David Brewster (1781–1868), Scottish natural philosopher who discovered laws of polarization of light in biaxial crystals.
Monoclinic, $P2_1/m$, $P2_1$, or triclinic (Akizuki 1987a, Akizuki *et al.* 1996).
The structure is sheet-like parallel to (010) (Perrotta & Smith 1964).

Brewsterite-Sr

New name for the original species of the series; Sr is the most abundant extra-framework cation. T_{Si} in the range 0.74–0.75.
Monoclinic, $P2_1/m$, *a* 6.793(2), *b* 17.573(6), *c* 7.759(2) Å, ß 94.54(3)°, for composition $(Sr_{1.42}Ba_{0.48}K_{0.02})$

$[Al_{4.12}Si_{11.95}O_{32}]•nH_2O$ (Schlenker *et al.* 1977a).
On optical grounds, possibly triclinic (Akizuki 1987a). Refined as triclinic in three separate growth-sectors by Akizuki *et al.* (1996).
Partly ordered Si,Al distribution.

Brewsterite-Ba

New name; Ba is the most abundant extra-framework cation.
Proposed type-example: the Gouverneur Talc Company's No. 4 wollastonite mine near Harrisville, Lewis County, New York, U.S.A. (Robinson & Grice 1993). Also Cerchiara mine, Liguria, Italy (Cabella *et al.* 1993, including structure refinement). T_{Si} = 0.73, 0.74.
Monoclinic, $P2_1/m$ or $P2_1$, *a* 6.780(3), *b* 17.599(9), *c* 7.733(2) Å, ß 94.47(3)° for type example, containing up to 0.85 Ba per 16 O atoms.

Chabazite (series)

$(Ca_{0.5},Na,K)_4[Al_4Si_8O_{24}]•12H_2O$
Z = 1 (trigonal) CHA
Bosc d'Antic (1792), as "chabazie". The source of the original specimen is unclear. The name is from a word "chabazion" used for an unknown substance in the story of Orpheus.
Ca-, Na-, and K-dominant species occur in that order of frequency, with Sr and Mg occasionally significant, Ba more minor. T_{Si} varies widely, 0.58 to 0.81.
Topological symmetry of the framework, trigonal ($R\bar{3}m$), where *a* ≈ 13.2, *c* ≈ 15.1 Å (pseudohexagonal cell). Significant deviations to triclinic, $P\bar{1}$, *a* ≈ 9.4, *b* ≈ 9.4, *c* ≈ 9.4 Å, α ≈ 94°, ß ≈ 94°, γ ≈ 94° (Smith *et al.* 1964, Mazzi & Galli 1983).
Partial ordering leads to the lower symmetry.

Chabazite-Ca

New name for the original and most common species; Ca is the most abundant single extra-framework cation. Other cations vary widely. T_{Si} in the range 0.58–0.80.
a 13.790(5), *c* 15.040(4) Å, for pseudo-hexagonal cell, with composition $(Ca_{1.86}Na_{0.03}K_{0.20}Mg_{0.02}Sr_{0.03})[Al_{3.94}Fe_{0.01}Si_{8.03}O_{24}]•13.16H_2O$, from Col de Lares, Val di Fassa, Italy (Passaglia 1970, #13).

Chabazite-Na

New name; Na is the most abundant single extra-framework cation. Other cations vary widely. T_{Si} in the range 0.62–0.79.
Suggested type-locality: biggest "Faraglione" facing Aci Trezza, Sicily, Italy (Passaglia 1970, #1). *a* 13.863(3), *c* 15.165(3) Å, for hexagonal cell, with composition $(Na_{3.11}K_{1.05}Ca_{0.19}Mg_{0.06}Sr_{0.05})[Al_{4.53}Fe_{0.01}Si_{7.40}O_{24}]•11.47H_2O$.

Although originally described as containing "silex, alumina, and potash" (Lévy 1825), the name *herschelite* has often been applied to chabazite minerals of tabular habit and high Na content. Herschelite should no longer be used as a species name.

Chabazite-K

New name; K is the most abundant single extra-framework cation. Other cations vary widely. T_{Si} in the range 0.60–0.74.
Suggested type-specimen: Tufo Ercolano, Ercolano, Naples, Italy (De Gennaro & Franco 1976), *a* 13.849(3), *c* 15.165(3) Å, for hexagonal cell, with composition $(K_{2.06}Na_{0.98}Ca_{0.46}Mg_{0.10}Sr_{0.01})[Al_{4.37}Fe_{0.08}Si_{7.60}O_{24}]•11.42H_2O$.

Chiavennite

$CaMn[Be_2Si_5O_{13}(OH)_2]•2H_2O$
Z = 4 –CHI
Bondi *et al.* (1983), Raade *et al.* (1983). Type locality: Chiavenna, Lombardy, Italy. Named after type locality.
The limited data available show up to 0.72 Al and 0.15 B in tetrahedral sites, and significant extra-framework Fe and Na (Raade *et al.* 1983, Langhof & Holstam 1994). T_{Si} in the range 0.63 to 0.68.
Orthorhombic, *Pnab*, *a* 8.729(5), *b* 31.326(11), *c* 4.903(2) Å (Tazzoli *et al.* 1995).
A Ca,Mn beryllosilicate with an interrupted framework of four-connected $[SiO_4]$ and three-connected $[BeO_4]$ tetrahedra.

Clinoptilolite (series)

$(Na,K,Ca_{0.5},Sr_{0.5},Ba_{0.5},Mg_{0.5})_6[Al_6Si_{30}O_{72}]•\sim 20H_2O$
Z = 1 HEU
Schaller (1923, 1932). Type locality: in decomposed basalt at a high point on ridge running east from Hoodoo Mountain, Wyoming, U.S.A. ("crystallized mordenite" of Pirsson 1891). The name reflects its inclined extinction and supposed similarity in composition to "ptilolite" (mordenite). Ptilo-, from Greek, alludes to the downy, finely fibrous nature of that mineral.
The cation content is highly variable. Ca-, Na-, and K-dominant compositions are known, and Sr, Ba, and Mg are in some cases substantial. Fe^{2+} and Fe^{3+} are possible constituents. In Pirsson's (1890) analysis, K is the most abundant single cation by a small margin. Clinoptilolite-K is therefore taken as the type species of the series. T_{Si} in the range 0.80–0.84.
Minerals with the same framework topology but with $T_{Si} < 0.80$, Si/Al < 4.0 are classified as heulandite, with which clinoptilolite forms a continuous series.
Monoclinic, *C*2/*m*, or *C*2, or *Cm*.
Structure refinements by Alberti (1975a) and Armbruster (1993) demonstrate variations in extra-

framework cation sites compared with heulandite and as a function of the extent of dehydration.

Clinoptilolite-K

New name for the original species; K is the most abundant single extra-framework cation. A moderately K-rich clinoptilolite-K was referred to as "potassium clinoptilolite" by Minato & Takano (1964). T_{Si} in the range 0.80–0.83.

Monoclinic, *C*2/*m, C*2, or *Cm*, *a* 17.688(16), *b* 17.902(9), *c* 7.409(7) Å, ß 116.50(7)°, for $(K_{4.72}Na_{0.85}Ca_{0.04}Sr_{0.37}Mg_{0.19}Fe_{0.03}Mn_{0.01})[Al_{6.52}Si_{29.38}O_{72}]\bullet nH_2O$, from an off-shore borehole, Japan (Ogihara & Iijima 1990).

Clinoptilolite-Na

New name; Na is the most abundant single extra-framework cation. Other cations vary widely. T_{Si} in the range 0.80–0.84.

Suggested type-example: Barstow Formation, about 1.6 km east of mouth of Owl Canyon, San Bernardino County, California, U.S.A., USGS Lab. no. D100594 (Sheppard & Gude 1969a).

Monoclinic, *C*2/*m, C*2, or *Cm*, *a* 17.627(4), *b* 17.955(4), *c* 7.399(4) Å, ß 116.29(2)° (Boles 1972), for type material of Sheppard & Gude (1969a), $(Na_{3.78}K_{1.31}Ca_{0.61}Ba_{0.09}Mg_{0.23}Mn_{0.01})[Al_{6.61}Fe_{0.16}Si_{29.19}O_{72}]\bullet 20.4H_2O$.

Clinoptilolite-Ca

New name; Ca is the most abundant single extra-framework cation. Other cations vary widely. T_{Si} in the range 0.80–0.84.

Suggested type-specimen: Kuruma Pass, Fukushima Prefecture, Japan (Koyama & Takéuchi 1977).

Monoclinic, *C*2/*m, C*2, or *Cm*, *a* 17.660(4), *b* 17.963(5), *c* 7.400(3) Å, ß 116.47(3)° based on *C*2/*m* (Koyama & Takéuchi 1977), for Kuruma Pass specimen, $(Na_{1.76}K_{1.05}Ca_{1.90}Mg_{0.17})[Al_{6.72}Si_{29.20}O_{72}]\bullet 23.7H_2O$.

Cowlesite

$Ca[Al_2Si_3O_{10}]\bullet 5.3H_2O$ $Z = 52$ (IZA code not assigned)

Wise & Tschernich (1975). Type locality: road cuts 0.65 km northwest of Goble, Columbia County, Oregon, U.S.A. Named after John Cowles of Rainier, Oregon, amateur mineralogist.

Minor substitution for Ca by Na and lesser K, Mg, Sr, Ba, Fe. T_{Si} in the range 0.60–0.62 (Vezzalini *et al.* 1992).

Orthorhombic, $P222_1$ or *Pmmm*, *Pmm*2, *P*2*mm*, *P*222 (Nawaz 1984), *a* 23.249(5), *b* 30.629(3), *c* 24.964(4) Å (Artioli *et al.* 1987).

Structure and degree of order of framework cations have not been determined.

Dachiardite (series)

$(Ca_{0.5},Na,K)_{4-5}[Al_{4-5}Si_{20-19}O_{48}]\bullet 13H_2O$

$Z = 1$ DAC

D'Achiardi (1906). Type locality: San Piero in Campo, Elba, Italy. Named by the author in memory of his father, Antonio D'Achiardi (1839–1902), first full professor of Mineralogy at the University of Pisa.

May contain minor Cs and Sr. T_{Si} in the range 0.78–0.86.

Monoclinic, topological symmetry *C*2/*m*, real symmetry *Cm*.

The structure consists of complex chains of 5-membered rings cross-linked by 4-membered rings (Gottardi & Meier 1963), but with complexities that commonly result in diffuse and streaked X-ray-diffraction maxima (Quartieri *et al.* 1990).

Dachiardite-Ca

New name for the original species of the series; Ca is the most abundant extra-framework cation. Dachiardite from the type locality contains 0.12 Cs atoms per formula unit (*apfu*) (Bonardi 1979). T_{Si} in the range 0.78–0.83.

Monoclinic, topological symmetry *C*2/*m*, real symmetry *Cm*. *a* 18.676, *b* 7.518, *c* 10.246 Å, ß 107.87°, for the composition $(Ca_{1.54}Na_{0.42}K_{0.92}Cs_{0.11}Sr_{0.12}Ba_{0.01})[Al_{4.86}Fe_{0.02}Si_{18.96}O_{48}]\bullet 12.56H_2O$ from the type locality (Vezzalini 1984).

Partly ordered distribution of Si,Al.

Dachiardite-Na

New name; Na is the most abundant extra-framework cation.

Suggested type-example: Alpe di Siusi, Bolzano, Italy (Alberti 1975b).

Available analytical results for material from seven localities, *e.g.,* Bonardi *et al.* (1981) show considerable variation in Na : K : Ca proportions. T_{Si} in the range 0.81–0.86.

Monoclinic, *a* 18.647(7), *b* 7.506(4), *c* 10.296(4) Å, ß 108.37(3)°, for $(Na_{2.59}K_{0.71}Ca_{0.53}Mg_{0.04}Ba_{0.01})[Al_{4.27}Fe_{0.11}Si_{19.61}O_{48}]\bullet 13.43H_2O$ from the type locality (Alberti 1975b).

Diffuse diffraction-spots indicate disorder.

Edingtonite

$Ba[Al_2Si_3O_{10}]\bullet 4H_2O$ $Z = 2$ EDI

Haidinger (1825). Type locality: Kilpatrick Hills, near Glasgow, Scotland. Named after a Mr. Edington of Glasgow, in whose collection Haidinger found the mineral.

Small amounts of K, Na, and Ca may replace Ba. T_{Si} in the range 0.59–0.61.

Orthorhombic, $P2_12_12_1$, *a* 9.550(10), *b* 9.665(10), *c* 6.523(5) Å (Böhlet mine, Westergotland, Sweden) (Galli 1976).

Also tetragonal, $P\bar{4}2_1m$, *a* 9.584(5), *c* 6.524(3) Å (Old Kilpatrick, near Glasgow, Scotland) (Mazzi *et al.* 1984).
From optical evidence, Akizuki (1986) suggested that a triclinic true symmetry also is possible.
The structure is similar to that of natrolite, but with a distinctive cross-linking of the chains (Taylor & Jackson 1933, Mazzi *et al.* 1984). Examples of orthorhombic edingtonite have nearly perfect (Si,Al) order. The tetragonal form is disordered, and available analytical results show that slightly more Ba has been replaced by other ions.

Epistilbite

$(Ca,Na_2)[Al_2Si_4O_{12}]\bullet 4H_2O$
$Z = 4$ EPI

Rose (1826). Type localities: "Iceland" and "Faröe Islands". Named from Greek *epi* in the sense of near, and stilbite, from its supposed similarity to the latter.
Na/(Na + Ca) varies from about 0.1 to 0.3, with minor K and Ba (*e.g.,* Galli & Rinaldi 1974). T_{Si} in the range 0.72–0.77.
Monoclinic, *C*2, *a* 9.101(2), *b* 17.741(1), *c* 10.226(1) Å, ß 124.66(2)° (Teigarhorn, Iceland: Alberti *et al.* 1985), or
triclinic, *C*1, *a* 9.083(1), *b* 17.738(3), *c* 10.209(1) Å, α 89.95(1)°, ß 124.58(1)°, γ 90.00(1)° (Gibelsbach, Valais, Switzerland: Yang & Armbruster 1996).
The structural framework belongs to the mordenite group (Gottardi & Galli 1985). Earlier work suggested space-group symmetry *C*2/*m* (Perrotta 1967). Alberti *et al.* (1985) proposed a domain structure involving acentric configurations of tetrahedra, and space group *C*2. Yang & Armbruster (1996) indicated that the proposed domains can be modeled by (010) disorder caused by a local mirror plane, and that increased partial order of Si,Al leads to triclinic symmetry.

Erionite (series)

$K_2(Na,Ca_{0.5})_8[Al_{10}Si_{26}O_{72}]\bullet 30H_2O$
$Z = 1$ ERI

Eakle (1898). Type locality: Durkee, Oregon, U.S.A., in rhyolitic, welded ash-flow tuff. Name from Greek root meaning wool, in reference to its appearance.
Substantial amounts of any or all of Ca, Na, and K, and subordinate Mg may be present, and there is evidence that trace Fe may enter tetrahedral and extra-framework sites. Eakle's (1898) analysis of type erionite shows Na as the most abundant extra-framework cation; Passaglia *et al.* (1998) found Ca to be the most abundant in a type-locality specimen. T_{Si} in the range 0.68–0.79.
Hexagonal, $P6_3/mmc$, *a* 13.15, *c* 15.02 Å (Kawahara & Curien 1969).
The structure is related to those of offretite, with which it may form intergrowths with stacking faults (Schlenker *et al.* 1977b), and levyne, on which it forms epitactic growths (Passaglia *et al.* 1998). The three minerals have 4-, 6- and 8-membered rings. They differ in the stacking of single and double 6-membered rings, resulting in different *c* dimensions and differently sized and shaped cages. Si,Al disordered.

Erionite-Na

New name; Na is the most abundant extra-framework cation.
Proposed type-example: Cady Mountains, California, U.S.A. (Sheppard *et al.* 1965). T_{Si} in the range 0.74–0.79.
For the type specimen, *a* 13.214(3), *c* 15.048(4) Å, composition $(Na_{5.59}K_{2.00}Ca_{0.11}Mg_{0.18}Fe_{0.02})[Al_{7.57}Si_{28.27}O_{72}]\bullet 24.60H_2O$ (Sheppard & Gude 1969b).

Erionite-K

New name; K is the most abundant extra-framework cation.
Proposed type-example: Rome, Oregon, U.S.A., in which K makes up 58% of extra-framework cations; significant Na, Ca, and Mg also are present (Eberly 1964). T_{Si} in the range 0.74–0.79.
For a specimen from Ortenberg, Germany, *a* 13.227(1), *c* 15.075(3) Å, $(K_{3.32}Na_{2.31}Ca_{0.99}Mg_{0.06}Ba_{0.02})[Al_{8.05}Si_{28.01}O_{72}]\bullet 31.99H_2O$ (Passaglia *et al.* 1998).

Erionite-Ca

New name; Ca is the most abundant extra-framework cation.
Proposed type-example: Mazé, Niigata Prefecture, Japan (Harada *et al.* 1967). T_{Si} in the range 0.68–0.79.
For the type example: *a* 13.333(1), *c* 15.091(2) Å; $(Ca_{2.28}K_{1.54}Na_{0.95}Mg_{0.86})[Al_{8.83}Si_{26.90}O_{72}]\bullet 31.35H_2O$ (Harada *et al.* 1967).

Faujasite (series)

$(Na,Ca_{0.5},Mg_{0.5},K)_x[Al_xSi_{12-x}O_{24}]\bullet 16H_2O$
$Z = 16$ FAU

Damour (1842). Type locality: Sasbach, Kaiserstuhl, Germany. Named after Barthélémy Faujas de Saint Fond, noted for his work on extinct volcanoes.
Major amounts of Na, Ca, and Mg are commonly present, and in some cases, K; minor Sr is also reported. The ratio Si : Al also varies; T_{Si} in the range 0.68–0.74, with one record of 0.64. In most samples analyzed, *x* in the above generalized formula is in the range 3.2–3.8, with one record of 4.4 (Rinaldi *et al.* 1975a, Wise 1982, Ibrahim & Hall 1995).
Cubic, $Fd\bar{3}m$, *a* 24.65 Å (material from Sasbach: Bergerhoff *et al.* 1958).
The framework structure is very open, with complete sodalite-type cages and with very large cavities having 12-membered ring openings. Up to 260 molecules of H_2O can be accommodated per unit cell (Bergerhoff *et al.* 1958, Baur 1964).

Faujasite-Na

New name; Na is the most abundant extra-framework cation, as it is in the original (incomplete) and most subsequent analyses of samples from the type locality, Sasbach, Kaiserstuhl, and some other localities. T_{Si} in the range 0.70–0.74, with one report of 0.64.
Reported values of *a* range from 24.638(3) Å (Wise 1982) to 24.728(2) Å (Ibrahim & Hall 1995).

Faujasite-Ca

New name; Ca is the most abundant extra-framework cation. Reported T_{Si} in the range 0.68–0.73. Proposed type-example: drill core from Haselborn near Ilbeshausen, Vogelsberg, Hessen, Germany (Wise 1982), composition $(Ca_{1.32}Na_{0.56}Mg_{0.26}K_{0.04})[Al_{3.83}Si_{8.19}O_{24}]$ $\bullet nH_2O$, $Z = 16$.
Reported values of *a*: 24.714(4) and 24.783(3) Å (Jabal Hanoun, Jordan: Ibrahim & Hall 1995).

Faujasite-Mg

New name; Mg is the most abundant extra-framework cation.
Proposed type (and only) example: "Old (museum) sample" (# 32, Genth Collection, Pennsylvania State University) from Sasbach, Kaiserstuhl, Germany (anal. #15, Rinaldi *et al.* 1975a), composition $(Mg_{15.3}Ca_{4.0}Na_{7.0}K_{6.4})[Al_{56}Si_{137}O_{384}]\bullet nH_2O$, $Z = 1$.

Ferrierite (series)

$(K,Na,Mg_{0.5},Ca_{0.5})_6[Al_6Si_{30}O_{72}]\bullet 8H_2O$
$Z = 1$ FER
Graham (1918). Type locality: Kamloops Lake, British Columbia, Canada. Named after Dr. Walter F. Ferrier, mineralogist, mining engineer, and one-time member of the Geological Survey of Canada, who first collected it. Substantial amounts of any or all of Mg, K, Na, and Ca, may be present, and smaller amounts of Fe, Ba, and Sr. T_{Si} in the range 0.80–0.88.
Statistical symmetry, orthorhombic, *Immm*; true symmetries orthorhombic, *Pnnm*, *a* 19.23, *b* 14.15, *c* 7.50 Å (Alberti & Sabelli 1987), and monoclinic, $P2_1/n$, *a* 18.89, *b* 14.18, *c* 7.47 Å, ß 90.0° (Gramlich-Meier *et al.* 1985).
The structure was first determined by Vaughan (1966). Framework Si,Al partially ordered (Alberti & Sabelli 1987).

Ferrierite-Mg

New name for the original member of the series; Mg is the most abundant single extra-framework cation.
Substantial extra-framework Na, K, and lesser Ca commonly present. T_{Si} in the range 0.80–0.84.
True symmetry orthorhombic, *Pnnm*, *a* 19.231(2), *b* 14.145(2), *c* 7.499(1) Å for specimen from Monastir, Sardinia, of composition $(Mg_{2.02}K_{1.19}Na_{0.56}Ca_{0.52}Sr_{0.14}Ba_{0.02})[Al_{6.89}Si_{29.04}O_{72}]\bullet 17.86H_2O$ (Alberti & Sabelli 1987).

Ferrierite-K

New name; K is the most abundant single extra-framework cation.
Proposed type-example: Santa Monica Mountains, California, U.S.A., composition $(K_{2.05}Na_{1.14}Mg_{0.74}Ca_{0.14})[Al_{5.00}Si_{31.01}O_{72}]\bullet nH_2O$ (Wise & Tschernich 1976, #3). T_{Si} in the range 0.81–0.87.
Orthorhombic, *a* 18.973(7), *b* 14.140(6), *c* 7.478(4) Å for type specimen.

Ferrierite-Na

New name; Na is the most abundant single extra-framework cation.
Proposed type-example: Altoona, Washington, U.S.A., composition $(Na_{3.06}K_{0.97}Mg_{0.38}Ca_{0.05}Sr_{0.03}Ba_{0.02})[Al_5Si_{31}O_{72}]\bullet 18H_2O$ (Wise & Tschernich 1976, #1). T_{Si} in the range 0.85–0.88.
Monoclinic, $P2_1/n$, *a* 18.886(9), *b* 14.182(6), *c* 7.470(5) Å, ß 90.0(1)° (Gramlich-Meier *et al.* 1985, for a specimen from Altoona, Washington).

Garronite

$NaCa_{2.5}[Al_6Si_{10}O_{32}]\bullet 14\ H_2O$
$Z = 1$ GIS
Walker (1962). Type locality: slopes of Glenariff Valley, County Antrim, Northern Ireland. Named after the Garron Plateau, where the type locality is sited.
Ca/(Na + K) is variable, but Ca predominates. Type-locality garronite has about 1.3 Na *apfu*, some others have (Na + K) < 0.2 *apfu*. H_2O in the range 13.0–14.0 molecules per formula unit. T_{Si} in the range 0.60–0.65.
The crystal structure has been refined in tetragonal symmetry, $I\bar{4}m2$, *a* 9.9266(2), *c* 10.3031(3) Å, by Artioli (1992), and Na-free synthetic garronite has been refined in $I4_1/a$, *a* 9.873(1), *c* 10.288(1) Å, by Schröpfer & Joswig (1997). Orthorhombic symmetry has been proposed on the basis of X-ray diffraction with twinned crystals (Nawaz 1983) and crystal morphology (Howard 1994).
The framework topology is the same as for gismondine, but Si and Al are essentially disordered. The different space-group symmetry (Artioli 1992) is associated with disorder and the presence of significant Na. Gottardi & Alberti (1974) proposed partial ordering subsequent to growth to explain twin domains.

Gaultite

$Na_4[Zn_2Si_7O_{18}]\bullet 5H_2O$ $Z = 8$ VSV
Ercit & Van Velthuizen (1994). Type locality: Mont Saint-Hilaire, Quebec, Canada. Named after Robert A.

Gault, (b. 1943), mineralogist at the Canadian Museum of Nature, Ottawa, Ontario, Canada.
No other elements detected in the one reported example; $T_{Si} = 0.78$.
Orthorhombic, *F*2*dd*, *a* 10.211(3), *b* 39.88(2), *c* 10.304(4) Å.
The zincosilicate framework of tetrahedra is characterized by stacked sheets of edge-sharing 4- and 8-membered rings. The sheets are cross-linked by tetrahedra. Gaultite is isostructural with synthetic zeolite VPI–7 and similar in structure to lovdarite (Ercit & Van Velthuizen 1994).

Gismondine

$Ca[Al_2Si_2O_8]\bullet 4.5H_2O$ $Z = 4$ GIS

von Leonhard (in footnote, 1817), renaming "zeagonite" of Gismondi (1817). Type locality: Capo di Bove, near Rome, Italy. Named after Carlo Giuseppe Gismondi (1762–1824), lecturer in Mineralogy in Rome.

(K + Na) does not exceed 0.12 *apfu* with K less than 0.08 *apfu*; analyses showing high K result from intergrown phillipsite. Minor Sr may be present; T_{Si} in the range 0.51–0.54 (Vezzalini & Oberti 1984). H_2O is slightly variable (4.4–4.5 molecules per formula unit) because of mixed 6- and 7-coordination of Ca (Artioli *et al.* 1986b).

Monoclinic, originally refined in $P2_1/a$ by Fischer & Schramm (1970); cell converted to standard $P2_1/c$ second setting is *a* 10.023(3), *b* 10.616(5), *c* 9.843(15) Å, ß 92.42(25)°. Also refined (two samples) by Rinaldi & Vezzalini (1985).

The framework topology is based on crankshaft chains of 4-membered rings as in feldspars, connected in UUDD configuration.
Si,Al are strictly ordered.

Gmelinite (series)

$(Na_2,Ca,K_2)_4[Al_8Si_{16}O_{48}]\bullet 22H_2O$
$Z = 1$ GME

Brewster (1825a). Type locality: the name was proposed for minerals occurring both at Little Deer Park, Glenarm, County Antrim, Northern Ireland, and at Montecchio Maggiore, Vicenza, Italy. Named after Christian Gottlob Gmelin, Professor of Chemistry, University of Tübingen.

Na-dominant members are the most common. T_{Si} in the range 0.65–0.72.
Hexagonal, $P6_3/mmc$, *a* 13.62–13.88, *c* 9.97–10.25 Å. The structure is similar to that of chabazite, with which it is commonly intergrown (Strunz 1956), but gmelinite has a different stacking of the double 6-membered rings (Fischer 1966). Si,Al are disordered.

Gmelinite-Na

New name for the most common species of the series. It occurs in at least one of the gmelinite type-localities (Montecchio Maggiore). The Ca content is commonly substantial, K is minor, and Sr is significant in a few samples analyzed. T_{Si} in the range 0.65–0.71.
Hexagonal, $P6_3/mmc$, *a* 13.756(5), *c* 10.048(5) Å (Galli *et al.* 1982), for near-end-member material from Queensland, Australia, of composition $(Na_{7.61}Ca_{0.03}K_{0.16})[Al_{7.41}Si_{16.49}O_{48}]\bullet 21.51H_2O$ (Passaglia *et al.* 1978a).

Gmelinite-Ca

New name for a species that also occurs in at least one of the type localities (Montecchio Maggiore). Ca is the most abundant single extra-framework cation. Significant to substantial Sr and Na, minor K. T_{Si} in the range 0.68–0.70.
Hexagonal, $P6_3/mmc$, *a* 13.800(5), *c* 9.964(5) Å (Galli *et al.* 1982), from Montecchio Maggiore, of composition $(Ca_{2.06}Sr_{1.35}Na_{0.78}K_{0.11})[Al_{7.82}Si_{16.21}O_{48}]\bullet 23.23H_2O$ (Passaglia *et al.* 1978a).

Gmelinite-K

New name; K is the most abundant single extra-framework cation. Proposed type-example: Fara Vicentina, Vicenza, Italy, composition $(K_{2.72}Ca_{1.67}Sr_{0.39}Na_{0.22}Mg_{0.13})[Al_{7.79}Si_{16.32}O_{48}]\bullet 23.52H_2O$ (Vezzalini *et al.* 1990). Also known from the Kola Peninsula (Malinovskii 1984).
Hexagonal, $P6_3/mmc$, *a* 13.621(3), *c* 10.254(1) Å.

Gobbinsite

$Na_5[Al_5Si_{11}O_{32}]\bullet 12H_2O$ $Z = 1$ GIS

Nawaz & Malone (1982). Type locality: basalt cliffs near Hills Port, south of the Gobbins area, County Antrim, Northern Ireland. Named after the locality.
Na : Ca : Mg : K variable, with Na greatly predominant, Ca < 0.6 *apfu*. Reports of high K are ascribed to intergrown phillipsite (Artioli & Foy 1994). T_{Si} in the range 0.62–0.68, substantially higher than in gismondine.
Orthorhombic, $Pmn2_1$, *a* 10.108(1), *b* 9.766(1), *c* 10.171(1) Å for the anhydrous composition $(Na_{2.50}K_{2.11}Ca_{0.59})[Al_{6.17}Si_{9.93}O_{32}]$ from Two-Mouth Cave, County Antrim, Northern Ireland (McCusker *et al.* 1985); *a* 10.1027(5), *b* 9.8016(5), *c* 10.1682(6) Å for $(Na_{4.3}Ca_{0.6})[Al_{5.6}Si_{10.4}O_{32}]\bullet 12H_2O$ from Magheramorne quarry, Larne, Northern Ireland (Artioli & Foy 1994).
The framework topology is the same as for gismondine and is based on crankshaft chains of 4-membered rings, as in feldspars. Distortion from tetragonal topological symmetry results from the arrangement of cations in the channels. Si,Al in the framework are disordered.

Gonnardite

$(Na,Ca)_{6–8}[(Al,Si)_{20}O_{40}]•12H_2O$
$Z = 1$ NAT

Lacroix (1896). Type locality: Chaux de Bergonne, Gignat, Puy-de-Dôme, France. Named after Ferdinand Gonnard, who had earlier described the material as "mesole" (= thomsonite).

Forms an extensive substitution series, commonly approximating $Na_{8–3x}Ca_{2x}[Al_{8+x}Si_{12–x}O_{40}]•12H_2O$ (after Ross *et al.* 1992), with minor Fe^{3+}, Mg, Ba, Sr, and K. T_{Si} in the range 0.52–0.59 (or 0.52–0.62 if tetranatrolite = gonnardite).

Tetragonal, $I\bar{4}2d$, *a* 13.21(1), *c* 6.622(4) Å for material from Tvedalen, Langesund, Norway, of composition $(Na_{6.42}K_{0.01}Ca_{1.50})[Al_{9.22}Si_{10.73}O_{40}]•12.37H_2O$ (Mazzi *et al.* 1986).

The structure is similar to that of natrolite, but with Si,Al disordered, and usually with significant to substantial Ca (Mazzi *et al.* 1986, Artioli & Torres Salvador 1991, Alberti *et al.* 1995).

Goosecreekite

$Ca[Al_2Si_6O_{16}]•5H_2O$ $Z = 2$ GOO

Dunn *et al.* (1980). Type locality: Goose Creek quarry, Loudoun County, Virginia, U.S.A. Named after the locality. Results of the single analysis available conform closely to the formula given, with no other elements detected. $T_{Si} = 0.75$.

Monoclinic, $P2_1$, *a* 7.401(3), *b* 17.439(6), *c* 7.293(3) Å, ß 105.44(4)° (Rouse & Peacor 1986).

The framework consists of 4-, 6-, and 8-membered rings that link to form layers parallel to (010), with some similarities to the brewsterite structure. Si,Al are nearly perfectly ordered (Rouse & Peacor 1986).

Gottardiite

$Na_3Mg_3Ca_5[Al_{19}Si_{117}O_{272}]•93H_2O$
$Z = 1$ NES

Alberti *et al.* (1996), Galli *et al.* (1996). Mt. Adamson, Victoria Land, Antarctica. Named after Professor Glauco Gottardi (1928–1988), University of Modena, in recognition of his pioneering work on the structure and crystal chemistry of natural zeolites.

Known from the type locality only, with composition approximating the above simplified formula; minor K, and very high Si. $T_{Si} = 0.86$.

Orthorhombic, topological symmetry *Fmmm*, real symmetry *Cmca*, *a* 13.698(2), *b* 25.213(3), *c* 22.660(2) Å (Alberti *et al.* 1996).

The framework topology is the same as for the synthetic zeolite NU–87, which, however, has monoclinic symmetry, $P2_1/c$. Some Si,Al order is probable.

Harmotome

$(Ba_{0.5},Ca_{0.5},K,Na)_5[Al_5Si_{11}O_{32}]•12H_2O$
$Z = 1$ PHI

Haüy (1801, p. 191-195), renaming andreasbergolite, also known as andréolite, of Delamétherie (1795, p. 393). Type locality: Andreasberg, Harz, Germany. Named from Greek words for a "joint" and "to cut", in allusion to a tendency to split along junctions (twin planes).

Ba is the most abundant extra-framework cation. Harmotome forms a continuous series with phillipsite-Ca. The name *harmotome* predates *phillipsite*; on grounds of history and usage, both are retained in spite of Rule 1 of the present report. T_{Si} in the range 0.68–0.71 (*e.g.,* Černý *et al.* 1977).

Monoclinic, refined in $P2_1/m$, but on piezoelectric and optical grounds, the true symmetry may be noncentrosymmetric and triclinic, *P*1 (*e.g.,* Akizuki 1985, Stuckenschmidt *et al.* 1990), *a* 9.879(2), *b* 14.139(2), *c* 8.693(2) Å, ß 124.81(1)° for $(Ba_{1.93}Ca_{0.46}K_{0.07})[Al_{4.66}Si_{11.29}O_{32}]•12H_2O$ from Andreasberg, Harz (Rinaldi *et al.* 1974).

The structure is the same as for phillipsite, with little or no Si,Al order.

Heulandite (series)

$(Ca_{0.5},Sr_{0.5},Ba_{0.5},Mg_{0.5},Na,K,)_9[Al_9Si_{27}O_{72}]•{\sim}24H_2O$
$Z = 1$ HEU

Brooke (1822). Type locality: none; the name was given to the more distinctly monoclinic minerals previously known as stilbite. Named after Henry Heuland, English mineral collector.

The cation content is highly variable. Ca-, Na-, K-, and Sr-dominant compositions are known, and Ba and Mg are in some cases substantial. T_{Si} in the range 0.71 to 0.80. Minerals with the same framework topology, but with $T_{Si} \geq 0.80$, $Si/Al \geq 4.0$, are distinguished as clinoptilolite.

Monoclinic, with highest possible topological symmetry $C2/m$ ($I2/m$). *Cm* and *C*2 also have been suggested.

The sheet-like structure was solved by Merkle & Slaughter (1968). There is partial order of Si,Al.

Heulandite-Ca

New name for the most common species of the series, and that deduced from results of most older analyses. Ca is the most abundant single extra-framework cation. T_{Si} in the range 0.71–0.80.

Monoclinic, $C2/m$, *Cm*, or *C*2, *a* 17.718(7), *b* 17.897(5), *c* 7.428(2) Å, ß 116.42(2)° from Faröe Islands, composition $(Ca_{3.57}Sr_{0.05}Ba_{0.06}Mg_{0.01}Na_{1.26}K_{0.43})[Al_{9.37}Si_{26.70}O_{72}]•26.02H_2O$ ($T_{Si} = 0.74$) (Alberti 1972).

Heulandite-Sr

New name; Sr is the most abundant single extra-framework cation.
One known example: Campegli, Eastern Ligurian ophiolites, Italy, of composition $(Sr_{2.10}Ca_{1.76}Ba_{0.14}Mg_{0.02}Na_{0.40}K_{0.22})[Al_{9.19}Si_{26.94}O_{72}]\bullet nH_2O$, T_{Si} = 0.75 (Lucchetti *et al*. 1982).
Monoclinic, *C*2/*m, Cm*, or *C*2, *a* 17.655(5), *b* 17.877(5), *c* 7.396(5) Å, ß 116.65°.

Heulandite-Na

New name; Na is the most abundant single extra-framework cation.
Proposed type-example: Challis, Idaho, U.S.A., U.S. National Museum #94512/3 (Ross & Shannon 1924, Boles 1972, #6).
Monoclinic, *C*2/*m*, *Cm*, or *C*2, *a* 17.670(4), *b* 17.982(4), *c* 7.404(2) Å, ß 116.40(2)° (Boles 1972) for the type example, of composition $(Na_{3.98}Ca_{1.77}K_{0.55})[Al_{7.84}Si_{28.00}O_{72}]\bullet 21.74H_2O$, T_{Si} = 0.78.

Heulandite-K

New name; K is the most abundant single extra-framework cation.
Proposed type-example: Albero Bassi, Vicenza, Italy (Passaglia 1969a), composition $(K_{2.40}Na_{0.96}Ca_{1.64}Mg_{0.64}Sr_{0.56}Ba_{0.12})[Al_{9.08}Fe_{0.56}Si_{26.48}O_{72}]\bullet 25.84H_2O$, T_{Si} = 0.73.
Monoclinic, *C*2/*m, Cm,* or *C*2, *a* 17.498, *b* 17.816, *c* 7.529 Å, ß 116.07°.
A close approach to end-member $K_9[Al_9Si_{27}O_{72}]\bullet nH_2O$ has been reported by Nørnberg (1990).

Hsianghualite

$Li_2Ca_3[Be_3Si_3O_{12}]F_2$ Z = 8 ANA

Huang *et al.* (1958). Type locality unclear, in metamorphosed Devonian limestone, Hunan Province, China. The name is from a Chinese word for fragrant flower.
Known from the original locality only. Minor Al, Fe, Mg, Na, and 1.28% loss on ignition reported (Beus 1960). T_{Si} = 0.48.
Cubic, $I2_13$, *a* 12.864(2) Å.
Has an analcime-type structure, with tetrahedral sites occupied alternately by Si and Be. Extra-framework Ca, Li, and F ions (Rastsvetaeva *et al.* 1991).

Kalborsite

$K_6[Al_4Si_6O_{20}]B(OH)_4Cl$
Z = 2 ?EDI

Khomyakov *et al.* (1980), Malinovskii & Belov (1980). Type locality: rischorrite pegmatite, Mt. Rasvumchorr, Khibina alkaline massif, Kola Peninsula, Russia. The name alludes to the composition.
Known from two localities in the Khibina massif, both with compositions close to the above formula (Pekov & Chukanov 1996). T_{Si} values are 0.59, 0.61.
Tetragonal, $P42_1c$, *a* 9.851(5), *c* 13.060(5) Å.
Framework of Si,Al tetrahedra, with channels along **c** containing $B(OH)_4$ tetrahedra and K, Cl (Malinovskii & Belov 1980). Considered by Smith (1988) to be an anhydrous analogue of the edingtonite structure-type EDI.

Laumontite

$Ca_4[Al_8Si_{16}O_{48}]\bullet 18H_2O$ Z = 1 LAU

As lomonite, Jameson (1805), who credits the name to Werner without specific reference; spelling changed to laumonite by Haüy (1809), and to laumontite by von Leonhard (1821). Named after Gillet de Laumont, who collected material described as "zéolithe efflorescente" by Haüy (1801, p. 410-412), from lead mines of Huelgoët, Brittany. The later spellings were applied to this material, and the Huelgoët mines are effectively the type locality.
Always Ca-dominant, with minor (K,Na). "Primary leonhardite" of Fersman (1908) is laumontite with approximately 1.5 Ca replaced by 3(K,Na) *apfu* and reduced H_2O. T_{Si} in the range 0.64–0.70.
Monoclinic, *C*2/*m* (although reported to be pyroelectric), *a* 14.845(9), *b* 13.167(2), *c* 7.5414(8) Å, ß 110.34(2)° (Nasik, India: Artioli & Ståhl 1993).
Except where unusually rich in (K,Na), reversibly loses *ca*. $4H_2O$ at low humidity at room temperature and pressure to form the variety termed "leonhardite" (*e.g.,* Fersman 1908, Armbruster & Kohler 1992); structure refined by Bartl (1970) and others. Si,Al in the framework is highly ordered.

Leucite

$K[AlSi_2O_6]$ Z = 16 ANA

Blumenbachs (1791), who attributed the name to Werner, who had previously described the mineral as "white garnet". Type locality: Vesuvius, Italy. Named from Greek, meaning white, in reference to color.
Minor substitution of Na for K at low temperatures, and Si in excess of that in the simplified formula, are commonly reported, also significant Fe^{3+}. T_{Si} in the range 0.66–0.69.
Tetragonal, $I4_1/a$, *a* 13.09, *c* 13.75 Å (Mazzi *et al.* 1976).
At ordinary temperatures, leucite is invariably finely twinned as a result of a displacive inversion from a cubic polymorph with the structure of analcime, space group $Ia3d$, apparently stable above 630°C (Wyart 1938, Peacor 1968). Heaney & Veblen (1990) noted that high leucite inverts to lower symmetry at temperatures between 600° and 750°C depending on the sample, and that there is a tetragonal, metrically cubic form intermediate between high (cubic) and low (tetragonal) forms.

Levyne (series)

$(Ca_{0.5},Na,K)_6[Al_6Si_{12}O_{36}]\bullet\sim 17H_2O$

$Z = 3$ LEV

Brewster (1825b). Type locality: Dalsnypen, Faröe Islands. Named after Armand Lévy (1794–1841), mathematician and crystallographer, Université de Paris.

Extra-framework cations range from strongly Ca-dominant to strongly Na-dominant, with minor K and, in some cases, minor Sr or Ba; Si:Al is also variable (Galli *et al.* 1981). T_{Si} in the range 0.62–0.70.

Trigonal, $R3\bar{m}$, *a* 13.32–13.43, *c* 22.66–23.01 Å.

The stacking of single and double 6-membered rings differs from that in the related structures of erionite and offretite (Merlino *et al.* 1975).

Levyne-Ca

New name for the original member of the series; Ca is the most abundant extra-framework cation. Type locality: Dalsnypen, Faröe Islands. Material closely approaching end-member $Ca_3[Al_6Si_{12}O_{36}]\bullet 17H_2O$ has been reported by England & Ostwald (1979) from near Merriwa, New South Wales, Australia. T_{Si} in the range 0.62–0.70.

Hexagonal, $R\bar{3}m$, *a* 13.338(4), *c* 23.014(9) Å for composition $(Ca_{2.73}Na_{0.65}K_{0.20})[Al_{6.31}Si_{11.69}O_{36}]\bullet 16.66H_2O$ from near the Nurri to Orroli road, Nuora, Sardinia (Passaglia *et al.* 1974, Merlino *et al.* 1975).

Levyne-Na

New name; Na is the most abundant extra-framework cation.

Proposed type-example: Chojabaru, Nagasaki Prefecture, Japan (Mizota *et al.* 1974). T_{Si} in the range 0.65–0.68.

Hexagonal, $R\bar{3}m$, *a* 13.380(5), *c* 22.684(9) Å for $(Na_{3.84}K_{0.38}Ca_{0.89}Mg_{0.08})[Al_{6.33}Si_{11.71}O_{36}]$ (Mizota *et al.* 1974).

Lovdarite

$K_4Na_{12}[Be_8Si_{28}O_{72}]\bullet 18H_2O$

$Z = 1$ LOV

Men'shikov *et al.* (1973). Type locality: alkaline pegmatites on Mt. Karnasurt, Lovozero alkaline massif, Kola Peninsula, Russia. Name means "a gift of Lovozero".

In the type and only known occurrence, approximately 1 Al atom substitutes for Si in the above structure-derived formula, with introduction of additional extra-framework Na and Ca. $T_{Si} = 0.75$.

Orthorhombic, *Pma*2, but contains *b*-centered domains in which *a* is doubled; *a* 39.576(1), *b* 6.9308(2), *c* 7.1526(3) Å (Merlino 1990).

The structure consists of a three-dimensional framework of Si (with minor Al) and Be tetrahedra. It contains three-membered rings, made possible by the presence of Be instead of Si in one of the tetrahedra.

Maricopaite

$(Pb_7Ca_2)[Al_{12}Si_{36}(O,OH)_{100}]\bullet n(H_2O,OH)$, $n \approx 32$

$Z = 1$ Structure closely related to MOR

Peacor *et al.* (1988). Type locality: Moon Anchor mine, near Tonopah, Maricopa County, Arizona, U.S.A. Named after the locality.

Only one known occurrence. $T_{Si} = 0.76$.

Orthorhombic, *Cm*2*m* (pseudo-*Cmcm*), *a* 19.434(2), *b* 19.702(2), *c* 7.538(1) Å (Rouse & Peacor 1994).

Has an interrupted, mordenite-like framework. Pb atoms form $Pb_4(O,OH)_4$ clusters with Pb_4 tetrahedra within channels (Rouse & Peacor 1994).

Mazzite

$(Mg_{2.5}K_2Ca_{1.5})[Al_{10}Si_{26}O_{72}]\bullet 30H_2O$

$Z = 1$ MAZ

Galli *et al.* (1974). Type locality: in olivine basalt near top of Mont Semiol, south slope, near Montbrison, Loire, France. Named after Fiorenzo Mazzi, Professor of Mineralogy at the University of Pavia, Italy.

A new chemical analysis from the type and only known locality (G. Vezzalini, pers. commun., 1996) gives the above formula (*cf.* Rinaldi *et al.* 1975b). $T_{Si} = 0.72$.

Hexagonal, $P6_3/mmc$, *a* 18.392 (8), *c* 7.646(2) Å.

The framework is characterized by stacked gmelinite-type cages (Galli 1975), with evidence for limited Si,Al order (Alberti & Vezzalini 1981b).

Merlinoite

$K_5Ca_2[Al_9Si_{23}O_{64}]\bullet 22H_2O$

$Z = 1$ MER

Passaglia *et al.* (1977). Type locality: Cupaello quarry in kalsilite melilitite, near Santa Rufina, Rieti, Italy. Named after Stefano Merlino, Professor of Crystallography at the University of Pisa.

The two available reliable analyses (Passaglia *et al.* 1977, Della Ventura *et al.* 1993) show strongly K-dominant compositions, with significant Ca, and less Na and Ba; $T_{Si} = 0.66, 0.71$.

Orthorhombic, *Immm*, *a* 14.116(7), *b* 14.229(6), *c* 9.946(6) Å (Passaglia *et al.* 1977).

The framework is built of double 8-membered rings linked with 4-membered rings (Galli *et al.* 1979). The structure is related to, but different from, that of phillipsite.

Mesolite

$Na_{16}Ca_{16}[Al_{48}Si_{72}O_{240}]•64H_2O$

$Z = 1$ NAT

Gehlen & Fuchs (1813), as mesolith, for some varieties of "mesotype" (mostly natrolite) of Haüy (1801). No type locality was given. Fuchs (1816) clarified the distinctions among natrolite, scolecite, and mesolite, and gave analytical data for mesolite from the Faröe Islands, Iceland and Tyrol. The name recognizes its compositional position between natrolite and scolecite. (Na + K)/(Mg + Ca + Sr + Ba) varies from 0.45 to 0.52, with K, Mg, Sr, Ba very minor (Alberti *et al.* 1982b). T_{Si} in the range 0.59– 0.62.

Orthorhombic, *Fdd*2, *a* 18.4049(8), *b* 56.655(6), *c* 6.5443(4) Å, for material from Poona, India (Artioli *et al.* 1986a).

Ordered Si,Al in the framework, with one natrolite-like layer alternating with two scolecite-like layers parallel to (010) (Artioli *et al.* 1986a, Ross *et al.* 1992).

Montesommaite

$K_9[Al_9Si_{23}O_{64}]•10H_2O$ $Z = 1$ MON

Rouse *et al.* (1990). Type locality: Pollena, Monte Somma, Vesuvius, Italy. Named after the locality.

Minor Na was detected in the one published analytical data-set. $T_{Si} = 0.70$.

Orthorhombic, *Fdd*2, *a* = *b* 10.099(1), *c* 17.307(3) Å (pseudotetragonal, $I4_1/amd$).

The framework can be constructed by linking (100) sheets of five- and eight-membered rings; it has similarities to those of merlinoite and the gismondine group (Rouse *et al.* 1990).

Mordenite

$(Na_2,Ca,K_2)_4[Al_8Si_{40}O_{96}]•28H_2O$

$Z = 1$ MOR

How (1864). Type locality: shore of Bay of Fundy, 3–5 km east of Morden, King's County, Nova Scotia, Canada. Named after the locality.

The cation content is variable, with Na/(Na + Ca) typically in the range 0.50–0.81. Some K, Mg, Fe, Ba, and Sr also may be present (Passaglia 1975, Passaglia *et al.* 1995). In some examples, K is reported as the dominant cation (Thugutt 1933, Lo *et al.* 1991, Lo & Hsieh 1991), potentially justifying the recognition of a mordenite series with Na- and K-dominant species. T_{Si} in the range 0.80–0.86.

Orthorhombic, *Cmcm*, *a* 18.052–18.168, *b* 20.404–20.527, *c* 7.501–7.537 Å (Passaglia 1975).

Structure determined by Meier (1961). Si,Al disorder in the framework is extensive, but not complete.

Mutinaite

$Na_3Ca_4[Al_{11}Si_{85}O_{192}]•60H_2O$

$Z = 1$ MFI

Galli *et al.* (1997b), Vezzalini *et al.* (1997b). Type locality: Mt. Adamson, Northern Victoria Land, Antarctica. The name is for Mutina, the ancient Latin name for Modena, Italy.

Electron-microprobe analyses of mutinaite from the type and only known locality show limited departure from the simplified formula, with minor Mg (~0.21 *apfu*) and K (~0.11 *apfu*). Very high Si, $T_{Si} = 0.88$.

Orthorhombic, *Pnma*, *a* 20.223(7), *b* 20.052(8), *c* 13.491(5) Å.

Mutinaite conforms closely in structure with synthetic zeolite ZSM–5.

Natrolite

$Na_2[Al_2Si_3O_{10}]•2H_2O$ $Z = 8$ NAT

Klaproth (1803). Type locality: Hohentwiel, Hegau, Baden-Württemberg, Germany. Name from *natro-* for sodium-bearing.

(Na + K)/(Mg + Ca + Sr + Ba) varies from 0.97 to 1.00, with K, Mg, Sr, and Ba very minor. T_{Si} in the range 0.59– 0.62 (Alberti *et al.* 1982b, Ross *et al.* 1992).

Orthorhombic, *Fdd*2, *a* 18.272, *b* 18.613, *c* 6.593 Å (Si,Al highly ordered, Dutoitspan, South Africa: Artioli *et al.* 1984); *a* 18.319(4), *b* 18.595(4), *c* 6.597(1) Å (~70% Si,Al order, Zeilberg, Germany: Hesse 1983).

Si,Al partly to highly ordered (Alberti & Vezzalini 1981a, Ross *et al.* 1992, Alberti *et al.* 1995).

Offretite

$CaKMg[Al_5Si_{13}O_{36}]•16H_2O$

$Z = 1$ OFF

Gonnard (1890) as offrétite. Type locality: Mont Simionse (Mont Semiol), Loire, France. Named after Albert J.J. Offret, professor in the Faculty of Sciences, Lyon, France.

Ca, Mg, and K substantial, commonly in proportions approaching 1 : 1 : 1; Na commonly trace or minor. Passaglia *et al.* (1998) and W. Birch (pers. commun., 1997) show that earlier published analytical data pertaining to apparently Ca- and Na-dominant variants are compromised by identification problems, including possible mixtures. T_{Si} in the range 0.69–0.74.

Hexagonal, $P\bar{6}m2$, *a* 13.307(2), *c* 7.592(2) Å for composition $(Mg_{1.06}Ca_{0.97}K_{0.88}Sr_{0.01}Ba_{0.01})[Al_{5.26}Si_{12.81}O_{36}]•16.85H_2O$ from the type locality (Passaglia & Tagliavini 1994).

The framework is related to those of erionite and levyne, but differs in the stacking of sheets of six-membered rings, resulting in different values for *c* and differently sized and shaped cages (Gard & Tait

1972). A high degree of Si,Al order is inferred. Offretite may contain intergrown macro- or crypto-domains of erionite (*e.g.,* Rinaldi 1976). It forms epitactic intergrowths with chabazite, but epitactic associations with levyne are questionable (Passaglia *et al.* 1998).

Pahasapaite

$(Ca_{5.5}Li_{3.6}K_{1.2}Na_{0.2}\square_{13.5})Li_8[Be_{24}P_{24}O_{96}]\bullet 38H_2O$
$Z = 1$ RHO

Rouse *et al.* (1987). Type locality: Tip Top mine, Black Hills, South Dakota, U.S.A. Named after Pahasapa, a Sioux Indian name for the Black Hills.
Known from the type locality only. $T_{Si} = 0$.
Cubic, *I*23, *a* 13.781(4) Å.
A beryllophosphate zeolite with ordered BeO_4 and PO_4 tetrahedra and a distorted synthetic zeolite RHO-type framework, structurally related to the faujasite series (Rouse *et al.* 1989).

Parthéite

$Ca_2[Al_4Si_4O_{15}(OH)_2]\bullet 4H_2O$
$Z = 4$ –PAR

Sarp *et al.* (1979). Type locality: in ophiolitic rocks, 7 km southeast of Doganbaba, Burdur province, Taurus Mountains, southwestern Turkey. Named after Erwin Parthé, Professor of Structural Crystallography, University of Geneva, Switzerland.
Minor Na and K. $T_{Si} = 0.52$ and 0.495 in the only two known occurrences.
Monoclinic, *C*2/*c*, *a* 21.553(3), *b* 8.761(1), *c* 9.304(2) Å, ß 91.55(2)° (type locality; Engel & Yvon 1984).
The framework contains various 4-, 6-, 8-, and 10-membered rings, and is interrupted at every second AlO_4 tetrahedron by hydroxyl groups. Si and Al are ordered.

Paulingite (series)

$(K,Ca_{0.5},Na,Ba_{0.5})_{10}[Al_{10}Si_{32}O_{84}]\bullet 27–44H_2O$
$Z = 16$ PAU

Kamb & Oke (1960). Type locality: Rock Island Dam, Columbia River, Wenatchee, Washington, U.S.A. Named after Linus C. Pauling, Nobel Prize winner and Professor of Chemistry, California Institute of Technology.
Electron-microprobe analyses show K as the most abundant cation at three known localities and Ca at two. Significant Ba and Na also are reported (Tschernich & Wise 1982, Lengauer *et al.* 1997). T_{Si} in the range 0.73–0.77.
Cubic, $Im\bar{3}m$, *a* 35.093(2) Å (Gordon *et al.* 1966).
The framework contains several kinds of large polyhedral cages (Gordon *et al.* 1966). The structure has been refined by Bieniok *et al.* (1996) and by Lengauer *et al.* (1997).

Paulingite-K

New name; K is the most abundant extra-framework cation.
Average composition from five analyses of samples from Rock Island Dam, Washington, U.S.A., the suggested type-example for paulingite-K: $(K_{4.44}Na_{0.95}Ca_{1.88}Ba_{0.18})[Al_{9.82}Si_{32.21}O_{84}]\bullet 44H_2O$ (Tschernich & Wise 1982); *a* 35.093(2) Å (Gordon *et al.* 1966).

Paulingite-Ca

New name; Ca is the most abundant extra-framework cation. Average result of four analyses, Ritter, Oregon, U.S.A., the suggested type-locality for paulingite-Ca: $(Ca_{3.70}K_{2.67}Na_{0.86}Ba_{0.10})[Al_{10.78}Si_{31.21}O_{84}]\bullet 34H_2O$; *a* 35.088(6) Å (Tschernich & Wise 1982).
Lengauer *et al.* (1997) found evidence of reduced H_2O content (27 H_2O for $Z = 16$) in barian paulingite-Ca from Vinarická Hora, Czech Republic.

Perlialite

$K_9Na(Ca,Sr)[Al_{12}Si_{24}O_{72}]\bullet 15H_2O$
$Z = 1$ LTL

Men'shikov (1984). Type locality: pegmatites of Mt. Eveslogchorr and Mt. Yukspor, Khibina alkaline massif, Kola Peninsula, Russia. Named after Lily Alekseevna Perekrest, instructor in mineralogy at Kirov Mining Technical School.
Minor substitution by Sr and Ba, but little other compositional variation in the two known occurrences. T_{Si} in the range 0.65–0.67.
Hexagonal, *P*6/*mmm*, *a* 18.49(3), *c* 7.51(1) Å (Men'shikov 1984).
Perlialite has the same framework topology as synthetic zeolite-L (Artioli & Kvick 1990). Structural columns have alternating cancrinite-type cages and double 6-membered rings. No Si,Al order has been detected.

Phillipsite (series)

$(K,Na,Ca_{0.5},Ba_{0.5})_x[Al_xSi_{16-x}O_{32}]\bullet 12H_2O$
$Z = 1$ PHI

Lévy (1825). Type locality as recorded by Lévy: Aci Reale, now Acireale, on the slopes of Etna, Sicily, Italy. Contemporary literature (see Di Franco 1942) and present-day exposures suggest that the occurrence was probably in basaltic lavas at Aci Castello, nearby. Named after William Phillips (1773–1828), author of geological and mineralogical treatises and a founder of the Geological Society of London.
Either K, Na, Ca, or Ba may be the most abundant extra-framework cation, but the name *harmotome* is retained for the Ba-dominant member of the series. Minor Mg and Sr may be present. In the generalized formula above, *x* ranges from about 4 to about 7. T_{Si}

varies from approximately 0.56 to 0.77.
Monoclinic, $P2_1$ or $P2_1/m$, *a* 9.865(2), *b* 14.300(4), *c* 8.668(2) Å, ß 124.20(3)° (phillipsite-K with substantial Ca from Casal Brunori, Rome, Italy: Rinaldi *et al.* 1974). A pseudo-orthorhombic cell has $a \approx 9.9$, $b \approx 14.2$, $c \approx 14.2$ Å, ß ≈ 90.0°, $Z = 2$.
Two cation sites have been identified, one, with two atoms per formula unit fully occupied by K in phillipsite-K and by Ba in harmotome, is surrounded by eight framework atoms of oxygen and four molecules of H_2O; the other is partly occupied by Ca and Na in distorted octahedral coordination with two framework atoms of oxygen and four molecules of H_2O (Rinaldi *et al.* 1974). Framework Si,Al largely disordered.

Phillipsite-Na

New name; Na is the most abundant extra-framework cation.
Na forms 81% of all extra-framework cations in material from Aci Castello, Sicily, Italy, suspected to be the original locality for phillipsite (#6 of Galli & Loschi Ghittoni 1972). Known range in T_{Si}: 0.64–0.77.
For pseudocell, *a* 9.931–10.003, *b* 14.142–14.286, *c* 14.159–14.338 Å, ß 90°, $Z = 2$ (*e.g.,* Galli & Loschi Ghittoni 1972, Sheppard & Fitzpatrick 1989).

Phillipsite-K

New name; K is the most abundant extra-framework cation. Proposed type-locality: Capo di Bove, Rome, Italy (Hintze 1897, #2 of Galli & Loschi Ghittoni 1972).
Known range in T_{Si}: 0.59–0.76.
For the pseudocell, *a* 9.871–10.007, *b* 14.124–14.332, *c* 14.198–14.415 Å, ß 90°, $Z = 2$ (*e.g.,* Galli & Loschi Ghittoni 1972, Sheppard *et al.* 1970).

Phillipsite-Ca

New name; Ca is the most abundant extra-framework cation. Proposed type-locality: Lower Salt Lake Tuff, Puuloa Road near Moanalua Road junction, Oahu, Hawaii (Iijima & Harada 1969).
Known range in T_{Si}: 0.57–0.74.
For the pseudocell, *a* 9.859–9.960, *b* 14.224–14.340, *c* 14.297–14.362 Å, ß 90°, $Z = 2$ (*e.g.,* Galli & Loschi Ghittoni 1972, Passaglia *et al.* 1990).

Pollucite

$(Cs,Na)[AlSi_2O_6]\bullet nH_2O$, where $(Cs + n) = 1$
$Z = 16$ ANA
Breithaupt (1846). Type locality: Elba, Italy. Named "pollux" with coexisting mineral "castor" (a variety of petalite) for twins Castor and Pollux, of Greek mythology; name modified to pollucite by Dana (1868). Forms a series with analcime (Černý 1974) reaching end-member compositions (Teertstra & Černý 1995). T_{Si} in the range 0.67–0.74. Minor Rb and Li may be present. Sodian pollucite commonly contains more Si than the simplified formula. The name *pollucite* applies where Cs exceeds Na in atomic proportions.
Cubic, *Ia3d*, *a* 13.69 Å for $(Cs_{11.7}Na_{3.1}Li_{0.25}K_{0.4})[Al_{15}Si_{33}O_{96.2}]\bullet H_2O$ (Beger 1969); *a* in the range 3.672(1)–13.674(1) Å for 0.114–0.173 Na *apfu*, $Z = 16$ (Černý & Simpson 1978).
Si,Al disordered.

Roggianite

$Ca_2[Be(OH)_2Al_2Si_4O_{13}]\bullet{<}2.5H_2O$
$Z = 8$ –ROG
Passaglia (1969b). Type locality: in albitite dike (E. Passaglia, pers. commun., 1998) at Alpe Rosso in Val Vigezzo about 1.5 km south of Orcesco, Novara Province, Italy. Named after Aldo G. Roggiani, a teacher of natural sciences, who first found the mineral.
Contains minor Na and K.
Tetragonal, *I*4/*mcm*, *a* 18.33(1), *c* 9.16(1) Å (Galli 1980).
Contains framework tetrahedrally coordinated Be (Passaglia & Vezzalini 1988) and framework-interrupting (OH) groups (Giuseppetti *et al.* 1991).

Scolecite

$Ca[Al_2Si_3O_{10}]\bullet 3H_2O$ $Z = 4$ or 8 NAT
Gehlen & Fuchs (1813), as skolezit. Clark (1993) gave the type locality as Berufjord, Iceland, but this is not apparent in the original reference. Fuchs (1816) clarified the distinctions among natrolite, scolecite, and mesolite. He listed occurrences of scolecite as Faröe Islands, Iceland and Staffa (Western Isles, Scotland), with analytical data for specimens from the Faröe Islands and Staffa. Named from Greek *skolex*, worm, for a tendency to curl when heated.
(Na + K)/(Mg + Ca) varies from 0 to 0.16, with very little K, Mg, or other elements. T_{Si} in the range 0.60– 0.62 (Alberti *et al.* 1982b).
Monoclinic, *Cc*, *a* 6.516(2), *b* 18.948(3), *c* 9.761(1) Å, ß 108.98(1)°, $Z = 4$ (Bombay, India: Kvick *et al.* 1985), or, by analogy with natrolite, pseudo-orthorhombic *Fd*, *e.g., a* 18.508(5), *b* 18.981(5) *c* 6.527(2) Å, ß 90.64(1)°, $Z = 8$ (Berufjord, Iceland: Joswig *et al.* 1984).
The structure is similar to that of natrolite, with a well-ordered Si,Al framework, Ca instead of Na_2, and an extra molecule of H_2O.

Stellerite

$Ca[Al_2Si_7O_{18}]\bullet 7H_2O$ $Z = 8$ STI
Morozewicz (1909). Type locality: Commander Island, Bering Sea. Named after Wilhelm Steller (1709–1746),

natural scientist and military doctor who made important observations on Commander Island.
Variations in composition include up to about 0.2 *apfu* Na and minor K, Mg, Fe. T_{Si} in the range 0.75–0.78.
Orthorhombic, *Fmmm*, *a* in the range 13.507–13.605, *b* in the range 18.198–18.270, *c* in the range 17.823–17.863 Å (Passaglia *et al.* 1978b).
The framework is topologically the same as for stilbite, but it has higher symmetry, correlated with fewer extra-framework cations. Only one independent extra-framework site is occupied, and the symmetry is *Fmmm* (Galli & Alberti 1975a). Na-exchanged stellerite retains the *Fmmm* symmetry, unlike the Na zeolite, barrerite, with which it is isostructural (Passaglia & Sacerdoti 1982).
Villarroel (1983) has suggested the occurrence of Na-dominant *Fmmm* stellerite from Roberts Island, South Shetland group.

Stilbite (series)

$(Ca_{0.5},Na,K)_9[Al_9Si_{27}O_{72}]\bullet 28H_2O$
$Z = 1$ STI

Haüy (1801, p. 161-166), for minerals, apparently including heulandite, that had previously been described with informal names. He mentioned occurrences in volcanic terranes, and named Iceland, Andreasberg in Harz, Alpes Dauphinoises, and Norway, but there is no clear type-locality. Named from Greek word for mirror, in allusion to its luster ("un certain éclat").
Ca is almost always the dominant extra-framework cation, accompanied by subordinate Na and minor K and Mg, approximating $Ca_4(Na,K)$ per formula unit, but Na-rich members also are known. T_{Si} in the range 0.71 to 0.78.
Monoclinic, *C*2/*m*, *a* 13.64(3), *b* 18.24(4), *c* 11.27(2) Å, ß 128.00(25)° (Galli & Gottardi 1966, Galli 1971); an alternative setting is pseudo-orthorhombic, *F*2/*m*, *Z* = 2.
Increasing departure from the topological symmetry of the orthorhombic framework, *Fmmm*, tends to correlate with increasing content of monovalent cations (Passaglia *et al.* 1978b), which causes the framework to rotate (Galli & Alberti 1975a, b). However, {001} growth sectors with appreciable Na and orthorhombic *Fmmm* symmetry have been observed in crystals in which other isochemical sectors are monoclinic, *C*2/*m* (Akizuki & Konno 1985, Akizuki *et al.* 1993). The centrosymmetric space-group depends on statistically complete Si,Al disorder, and the true space-group may be noncentrosymmetric (Galli 1971).

Stilbite-Ca

New name for common stilbite in which Ca is the most abundant extra-framework cation.
For the pseudo-orthorhombic cell, *F*2/*m*, *a* 13.595–13.657, *b* 8.201–18.291, *c* 17.775–17.842 Å, ß 90.06–90.91° (Passaglia *et al.* 1978b).

Stilbite-Na

New name; Na is the most abundant extra-framework cation.
Proposed type-locality: Capo Pula, Cagliari, Sardinia, Italy (Passaglia *et al.* 1978b, #21).
Known examples contain significant Ca and K, and minor Mg, as well as clearly predominant Na. T_{Si} in the range 0.73–0.78 (Passaglia *et al.* 1978b, Ueno & Hanada 1982, Di Renzo & Gabelica 1997).
Monoclinic, *C*2/*m*. Using the pseudo-orthorhombic *F*2/*m* setting, *a* 13.610, *b* 18.330, *c* 17.820 Å, ß 90.54° for type material, of composition $(Na_{8.18}K_{1.94}Ca_{3.45}Mg_{0.08})[Al_{16.62}Si_{55.25}O_{144}]\bullet 53.53H_2O$ (Quartieri & Vezzalini 1987).
In spite of the high Na content, the monoclinic *C*2/*m* symmetry of stilbite is retained, in contrast to stellerite, *Fmmm*, and barrerite, *Amma*.

Terranovaite

$NaCa[Al_3Si_{17}O_{40}]\bullet >7H_2O$
$Z = 4$ TER

Galli *et al.* (1997a). Type locality: Mt. Adamson, Northern Victoria Land, Antarctica. Named after the Italian Antarctic station at Terranova Bay.
Type material contains minor amounts of K and Mg. $T_{Si} = 0.85$.
Orthorhombic, *Cmcm*, *a* 9.747(1), *b* 23.880(2), *c* 20.068(2) Å.
The framework topology is not known in other natural or synthetic zeolites. It contains polyhedral units found in laumontite, heulandite, and boggsite.

Thomsonite

$Ca_2Na[Al_5Si_5O_{20}]\bullet 6H_2O$
$Z = 4$ THO

Brooke (1820). Type locality: Old Kilpatrick, near Dumbarton, Scotland. Named after Dr. Thomas Thomson (1773–1852), editor of the journal in which the name was published, and who contributed to the improvement of methods of chemical analysis.
Extensive variation in Na:(Ca + Sr) and Si : Al approximately according to the formula $Na_{4+x}(Ca,Sr)_{8-x}[Al_{20-x}Si_{20+x}O_{80}]\bullet 24H_2O$, where *x* varies from about 0 to 2; small amounts of Fe, Mg, Ba, and K also may be present (Ross *et al.* 1992). T_{Si} in the range 0.50–0.56.
Orthorhombic, *Pncn*, *a* l3.1043(14), *b* 13.0569(18), *c* 13.2463(30) Å (Ståhl *et al.* 1990).
Chains with a repeat unit of five tetrahedra occur as in the NAT structure type, but they are cross-linked in a different way; Si,Al are highly ordered, but disorder increases with increasing Si : Al (Alberti *et al.* 1981).

Tschernichite

$Ca[Al_2Si_6O_{16}]\bullet\sim 8H_2O$ $Z = 8$ BEA

Smith *et al.* (1991), Boggs *et al.* (1993). Type locality: Goble Creek, 0.2 km north of Goble, Columbia County, Oregon, U.S.A. Named after Rudy W. Tschernich, zeolite investigator of the American Pacific Northwest, who discovered the mineral.

Na, Mg, and K are minor but variable constituents in specimens from the one known locality. T_{Si} in the range 0.74–0.78 (0.73, 0.80 in a tschernichite-like mineral from Mt. Adamson, Antarctica: Galli *et al.* 1995).

Tetragonal, possible space-group $P4/mmm$, a 12.880(2), c 25.020(5) Å, but may consist of an intergrowth of a tetragonal enantiomorphic pair with space groups $P4_122$ and $P4_322$ and a triclinic polymorph $P1$. See also Galli *et al.* (1995).

This is a structural analogue of synthetic zeolite beta.

Tschörtnerite

$Ca_4(K_2,Ca,Sr,Ba)_3Cu_3(OH)_8[Al_{12}Si_{12}O_{48}]\bullet nH_2O$, $n \geqslant 20$ $Z = 16$ (IZA code not assigned)

Krause *et al.* (1997), Effenberger *et al.* (1998). Bellberg volcano, near Mayen, Eifel, Germany. Named after Jochen Tschörtner, mineral collector and finder of the mineral.

$T_{Si} = 0.50$ for the only known occurrence.

Cubic, $Fm\bar{3}m$, a 31.62(1) Å.

Cages in the framework include a large super-cage with 96 tetrahedra and 50 faces. A Cu,(OH)-bearing cluster occupies another cage. The framework density is the lowest known for a zeolite with a non-interrupted framework.

Wairakite

$Ca[Al_2Si_4O_{12}]\bullet 2H_2O$ $Z = 8$ ANA

Steiner (1955), Coombs (1955). Wairakei, Taupo Volcanic Zone, New Zealand. Named after the locality.

Most analyzed samples have Na/(Na + Ca) less than 0.3, but wairakite possibly forms a continuous solid-solution series with analcime (Seki & Oki 1969, Seki 1971, Cho & Liou 1987). Other reported substitutions are very minor. T_{Si} in the range 0.65–0.69.

Monoclinic (highly ordered), $I2/a$, a 13.692(3), b 13.643(3), c 13.560(3) Å, ß 90.5(1)° for $(Ca_{0.90}Na_{0.14})[Al_{1.92}Si_{4.07}O_{12}]\bullet 2H_2O$ (Takéuchi *et al.* 1979).

Tetragonal or near-tetragonal, $I4_1/acd$, a 13.72(4), c 13.66(4) Å for $(Ca_{0.92}Na_{0.10})[Al_{1.92}Si_{4.07}O_{12}]\bullet 2.11H_2O$ (Nakajima 1983).

The framework topology is similar to that of analcime, but Al is preferentially located in a pair of tetrahedral sites associated with Ca, and Ca is in one specific extra-framework site. Smaller departures from cubic symmetry are correlated with decreased Si,Al order. The name applies to zeolites of ANA structural type in which Ca is the most abundant extra-framework cation, irrespective of the degree of order or space-group symmetry.

Weinebeneite

$Ca[Be_3(PO_4)_2(OH)_2]\bullet 4H_2O$ $Z = 4$ WEI

Walter (1992). Type locality: vein of spodumene-bearing pegmatite 2 km west of Weinebene Pass, Koralpe, Carinthia, Austria. Named after the locality.

No elements other than those in the given formula were detected in the one known occurrence.

Monoclinic, Cc, a 11.897(2), b 9.707(1), c 9.633(1) Å, ß 95.76(1)°.

A calcium beryllophosphate zeolite with 3-, 4-, and 8-membered rings in the framework (Walter 1992).

Willhendersonite

$K_xCa_{(1.5-0.5x)}[Al_3Si_3O_{12}]\bullet 5H_2O$, where $0 < x < 1$ $Z = 2$ CHA

Peacor *et al.* (1984). Type locality: San Venanzo quarry, Terni, Umbria, Italy. Named after Dr. William A. Henderson, of Stamford, Connecticut, U.S.A., who noted this as an unusual mineral and provided it for study.

Type willhendersonite conforms closely to $KCa[Al_3Si_3O_{12}]\bullet 5H_2O$. End-member $Ca_{1.5}[Al_3Si_3O_{12}]\bullet 5H_2O$ and intermediate compositions are now known (Vezzalini *et al.* 1997a). $T_{Si} = 0.50, 0.51$.

Triclinic, $P1$, a 9.206(2), b 9.216(2), c 9.500(4) Å, α 92.34(3)°, ß 92.70(3)°, γ 90.12(3)° (Ettringer Bellerberg, near Mayen, Eifel, Germany: Tillmanns *et al.* 1984).

The framework is the same as for chabazite, which has idealized framework topological symmetry $R\bar{3}m$, but with much lower Si and with Si,Al fully ordered. This reduces the topochemical framework symmetry to $R\bar{3}$, and the nature and ordering of the extra-framework cations further reduce the framework symmetry to $P\bar{1}$. The low-K variants also have fully ordered Si,Al, but are less markedly triclinic (Vezzalini *et al.* 1996).

Yugawaralite

$Ca[Al_2Si_6O_{16}]\bullet 4H_2O$ $Z = 2$ YUG

Sakurai & Hayashi (1952). Type locality: Yugawara Hot Springs, Kanagawa Prefecture, Honshu, Japan. Named after the locality.

Reported compositions are close to the ideal stoichiometry, with up to 0.2 *apfu* of Na + K + Sr. T_{Si} in the range 0.74–0.76.

Monoclinic, Pc, a 6.700(1), b 13.972(2), c 10.039(5) Å, ß 111.07° (Kvick *et al.* 1986).

Triclinic, $P1$, by symmetry reduction ascribed to local Si,Al order, has been reported on the basis of optical measurements (Akizuki 1987b).

Si,Al are strictly ordered in samples from Iceland (Kerr & Williams 1969, Kvick *et al.* 1986). The partial order reported for the Yugawara sample (Leimer & Slaughter 1969) is doubtful (Gottardi & Galli 1985).

Zeolites of Doubtful Status and a Possible Zeolite

Further work is recommended to clarify the status of paranatrolite and tetranatrolite. Essential data for these minerals and for tvedalite, which is possibly a beryllosilicate zeolite, are as follows.

Paranatrolite

$Na_2[Al_2Si_3O_{10}]•3H_2O$ $Z = 8$ NAT
Chao (1980). Type locality, Mont Saint-Hilaire, Quebec, Canada. The name recognizes its association with and similarity in chemical composition to natrolite, $Na_2[Al_2Si_3O_{10}]•2H_2O$.
Contains additional H_2O relative to natrolite, also minor Ca and K.
Pseudo-orthorhombic, *F****, probably monoclinic, *a* 19.07(1), *b* 19.13(1), *c* 6.580(3) Å. Gives very diffuse diffraction-spots, and a powder pattern similar to that of gonnardite (Chao 1980).
Dehydrates to tetranatrolite and could be regarded as overhydrated natrolite, tetranatrolite or gonnardite. Without further justification, separate species status is debatable according to Rule 4.

Tetranatrolite

$(Na,Ca)_{16}[Al_{19}Si_{21}O_{80}]•16H_2O$
$Z = 0.5$ NAT
Chen & Chao (1980). Type locality: Mont Saint-Hilaire, Quebec, Canada. The name indicates a tetragonal analogue of natrolite. First described as "tetragonal natrolite", from Ilímaussaq, Greenland, by Krogh Andersen *et al.* (1969).
Extensive solid-solution approximating $Na_{16-x}Ca_xAl_{16+x}Si_{24-x}O_{80}•16H_2O$, where x varies from about 0.4 to 4, is reported by Ross *et al.* (1992). Small amounts of Fe^{3+}, Sr, Ba, and K may replace Na and Ca. T_{Si} in the range 0.50–0.59.
Tetragonal, $I\bar{4}2d$, *a* 13.141, *c* 6.617 Å (Mont Saint-Hilaire, Quebec, Canada: Ross *et al.* 1992).
The framework is of disordered natrolite type. Tetranatrolite is considered to be a product of dehydration of paranatrolite (Chen & Chao 1980, Ross *et al.* 1992). It differs from natrolite in CaAl substitution for NaSi, as well as in space-group symmetry. These, however, are also characteristics of gonnardite, to which its relationship is debatable.

Tvedalite

$(Ca,Mn)_4Be_3Si_6O_{17}(OH)_4•3H_2O$
$Z = 2$
Larsen *et al.* (1992). Type locality: Vevya quarry, Tvedalen, Vestfold County, Norway. Named after the locality.
Spot analyses show a range from $(Ca_{3.20}Mn_{0.72}Fe_{0.08})_{\Sigma 4}$ to $(Ca_{2.00}Mn_{1.86}Fe_{0.14})_{\Sigma 4}$ for $Be_3Si_6O_{17}(OH)_4•3H_2O$, with about 0.1 to 0.2 Al and minor Be substituting for Si in the generalized formula.
Orthorhombic (*c*-centered), *a* 8.724(6), *b* 23.14(1), *c* 4.923(4) Å.
Considered to be structurally related to chiavennite, but in the absence of an adequate determination of its structure, it has not been listed here as an accepted zeolite species.

Discredited, Obsolete, and Other Non-Approved Zeolite Names

Herschelite, **leonhardite**, **svetlozarite**, and **wellsite** are discredited as names of mineral species (Appendix 2).

Kehoeite was regarded by McConnell (1964) as a zinc phosphate analogue of analcime, but according to White & Erd (1992), type kehoeite is a heterogeneous mixture of quartz and sphalerite with other phases including gypsum and woodhouseite, or a very similar phase. No phase present bears any relationship to analcime. It is not accepted as a valid zeolite species.

Viséite is shown by Di Renzo & Gabelica (1995) not to be a zeolite, as had commonly been supposed. They regard it as a defective member of the crandallite group, with composition $CaAl_3(PO_4,SiO_4)_2(OH)_n•mH_2O$. Kim & Kirkpatrick (1996) showed that a specimen examined by them is very disordered, with a structure similar to that of crandallite, but contains other phases including opal. Viséite is excluded from the list of accepted zeolites.

Obsolete and discredited names are listed below, followed by the correct names or identifications. The list is based on one compiled by the late G. Gottardi, using the following references: Hintze (1897), Dana (1914), Cocco & Garavelli (1958), Davis (1958), Hey (1960, 1962), Merlino (1972), and Strunz (1978). Numerous additions and amendments have been made in the light of more recently published work and of the notes below, and of listings in Clark (1993), in which much information on the history and usages of these names can be found.

abrazite = gismondine, phillipsite
acadialite = chabazite
achiardite = dachiardite
adipite = chabazite?
aedelforsite = laumontite?, stilbite?
aedelite (of Kirwan), aedilite = natrolite
ameletite = mixtures of sodalite, analcime, phillipsite, and relict nepheline
amphigène = leucite

analcidite = analcime
analcite = analcime
analzim = analcime
andreasbergolite = harmotome
andreolite, andréolithe = harmotome
antiëdrite = edingtonite
apoanalcite = natrolite
arduinite = mordenite
aricite = gismondine
ashtonite = strontian mordenite
bagotite = thomsonite
barium-heulandite = barian heulandite (unless Ba is the most abundant cation)
barytkreuzstein = harmotome
beaumontite = heulandite
bergmannite = natrolite
blätterzeolith = heulandite, stilbite
brevicite = natrolite
cabasite = chabazite
caporcianite = laumontite
carphostilbite = thomsonite
chabasie, chabasite = chabazite
christianite (of des Cloizeaux) = phillipsite
cluthalite = analcime
comptonite = thomsonite
crocalite = natrolite
cubicite, cubizit = analcime
cubic zeolite = analcime?, chabazite
cuboite = analcime
cuboizite = chabazite
desmine = stilbite
diagonite = brewsterite
dollanite = analcime
doranite = analcime with thomsonite, natrolite, and Mg-rich clay minerals (Teertstra & Dyer 1994)
echellite = natrolite
efflorescing zeolite = laumontite
eisennatrolith = natrolite with other mineral inclusions
ellagite = a ferriferous natrolite or scolecite?
epidesmine = stellerite
epinatrolite = natrolite
ercinite = harmotome
eudnophite = analcime
euthalite, euthallite = analcime
euzeolith = heulandite
falkenstenite = probably plagioclase (Raade 1996)
fargite = natrolite
faröelite = thomsonite
fassaite (of Dolomieu) = probably stilbite
feugasite = faujasite
flokite, flockit = mordenite
foliated zeolite = heulandite, stilbite
foresite = stilbite + cookeite
galactite = natrolite
gibsonite = thomsonite
ginzburgite (of Voloshin *et al.*) = roggianite
gismondite = gismondine
glottalite = chabazite
granatite = leucite
grenatite (of Daubenton) = leucite
groddeckite = gmelinite?
hairzeolite (group name) = natrolite, thomsonite, mordenite
harmotomite = harmotome
harringtonite = thomsonite, mesolite mixture
haydenite = chabazite
hegauit (högauite) = natrolite
hercynite (of Zappe) = harmotome
herschelite = chabazite-Na
högauite = natrolite
hsiang-hua-shih = hsianghualite
hydrocastorite = stilbite, mica, petalite mixture
hydrolite (of Leman) = gmelinite
hydronatrolite = natrolite
hydronephelite = a mixture, probably containing natrolite
hypodesmine = stilbite
hypostilbite = stilbite or laumontite
idrocastorite (hydrocastorite) = stilbite, mica, petalite mixture
kali-harmotome, kalkharmotome = phillipsite
kalithomsonite = ashcroftine (not a zeolite)
kalkkreuzstein = phillipsite
karphostilbite = thomsonite
kehoeite = a mixture including quartz, sphalerite, gypsum, and ?woodhouseite
koodilite = thomsonite
krokalith = natrolite
kubizit = analcime
kuboite = analcime
laubanite = natrolite
laumonite = laumontite
ledererite, lederite (of Jackson) = gmelinite
lehuntite = natrolite
leonhardite = H_2O-poor laumontite
leuzit = leucite
levyine, levynite, levyite = levyne
lime-harmotome = phillipsite
lime-soda mesotype = mesolite
lincolnine, lincolnite = heulandite
lintonite = thomsonite
lomonite = laumontite
marburgite = phillipsite
mesole = thomsonite
mesoline = levyne? chabazite?
mesolitine = thomsonite
mesotype = natrolite, mesolite, scolecite
metachabazite = partially dehydrated chabazite
metadesmine = partially dehydrated stilbite
metaepistilbite = partially dehydrated epistilbite
metaheulandite = partially dehydrated heulandite
metalaumontite = partially dehydrated laumontite
metaleonhardite = dehydrated “leonhardite” (laumontite)
metaleucite = leucite
metamesolite = mesolite
metanatrolite = partially dehydrated natrolite

metascolecite, metaskolecit, metaskolezit = partially dehydrated scolecite
metathomsonite = partially dehydrated thomsonite
monophane = epistilbite
mooraboolite = natrolite
morvenite = harmotome
natrochabazite = gmelinite
natron-chabasit, natronchabazit (of Naumann) = gmelinite
natronite (in part) = natrolite
needle zeolite, needle stone = natrolite, mesolite, scolecite
normalin = phillipsite
orizite, oryzite = epistilbite
ozarkite = thomsonite
parastilbite = epistilbite
phacolite, phakolit(e) = chabazite
picranalcime = analcime
picrothomsonite = thomsonite
pollux = pollucite
poonahlite, poonalite = mesolite
portite = natrolite (Franzini & Perchiazzi 1994)
potassium clinoptilolite = clinoptilolite-K
pseudolaumontite = pseudomorphs after laumontite
pseudomesolite = mesolite
pseudonatrolite = mordenite
pseudophillipsite = phillipsite
ptilolite = mordenite
puflerite, pufflerite = stilbite
punahlite = mesolite
radiolite (of Esmark) = natrolite
ranite = gonnardite (Mason 1957)
reissite (of Fritsch) = epistilbite
retzite = stilbite?, laumontite?
sarcolite (of Vauquelin) = gmelinite
sasbachite, saspachite = phillipsite?
savite = natrolite
schabasit = chabazite
schneiderite = laumontite (Franzini & Perchiazzi 1994)
schorl blanc = leucite
scolesite, scolezit = scolecite
scoulerite = thomsonite
seebachite = chabazite
skolezit = scolecite
sloanite = laumontite?
snaiderite (schneiderite) = laumontite
soda-chabazite = gmelinite
soda mesotype = natrolite
sodium dachiardite = dachiardite-Na
sommaite = leucite
spangite = phillipsite
sphaerodesmine, sphaerostilbite = thomsonite
spreustein = natrolite (mostly)
staurobaryte = harmotome
steeleite, steelit = mordenite
stellerycie = stellerite
stilbite anamorphique = heulandite
stilbite (of many German authors) = heulandite
strontium-heulandite = strontian heulandite and heulandite-Sr
svetlozarite = dachiardite-Ca
syanhualite, syankhualite = hsianghualite
syhadrite, syhedrite = impure stilbite?
tetraedingtonite = edingtonite
tonsonite = thomsonite
triploclase, triploklase = thomsonite
vanadio-laumontite = vanadian laumontite
verrucite = mesolite
Vesuvian garnet = leucite
Vesuvian (of Kirwan) = leucite
viséite = disordered crandallite and other phases
weissian = scolecite
wellsite = barian phillipsite-Ca and calcian harmotome
white garnet = leucite
winchellite = thomsonite
Würfelzeolith = analcime, chabazite
zeagonite = gismondine, phillipsite
zeolite mimetica = dachiardite
zéolithe efflorescente = laumontite

Acknowledgements

Members of the present Subcommittee, which commenced work in 1993, are grateful to a previous Subcommittee, established in 1979 under the Chairmanship of Professor W.S. Wise of the University of California, Santa Barbara, California, for work contained in a draft report completed in 1987. Members of the 1979 Subcommittee included L. P. van Reeuwijk and the late G. Gottardi and M.H. Hey, as well as D.S.C. and H.M. of the present Subcommittee. J.V. Smith, W.M. Meier, R.W. Tschernich, and the late V.A. Frank-Kamenetskii were consultants. Although recommendations in the present report differ significantly from those in the 1987 report, the existence of that report has greatly facilitated our task. We thank J.V. Smith and L.B. McCusker for advice, C.E.S. Arps and W.D. Birch, successive secretaries of CNMMN, for much help, and many other colleagues for contributions of time, advice, and specimens. Staff of the Science Library, University of Otago, and others, helped trace obscure references.

References

Akizuki, M. (1985): The origin of sector twinning in harmotome. *Am. Mineral.* **70**, 822-828.

_____ (1986): Al–Si ordering and twinning in edingtonite. *Am. Mineral.* **71**, 1510-1514.

_____ (1987a): Crystal symmetry and order–disorder structure of brewsterite. *Am. Mineral.* **72**, 645-648.

_____ (1987b): An explanation of optical variation in yugawaralite. *Mineral. Mag.* **51**, 615-620.

_____ & Konno, H. (1985): Order–disorder structure and the internal texture of stilbite. *Am. Mineral.* **70**, 814-821.

_____, Kudoh, Y. & Kuribayashi, T. (1996): Crystal structures of the {011}, {610}, and {010} growth sectors in brewsterite. *Am. Mineral.* **81**, 1501-1506.

_____, _____ & Satoh, Y. (1993): Crystal structure of the orthorhombic {001} growth sector of stilbite. *Eur. J. Mineral.* **5**, 839-843.

Alberti, A. (1972): On the crystal structure of the zeolite heulandite. *Tschermaks Mineral. Petrogr. Mitt.* **18**, 129-146.

_____ (1975a): The crystal structure of two clinoptilolites. *Tschermaks Mineral. Petrogr. Mitt.* **22**, 25-37.

_____ (1975b): Sodium-rich dachiardite from Alpe di Siusi, Italy. *Contrib. Mineral. Petrol.* **49**, 63-66.

_____, Cruciani, G. & Dauru, I. (1995): Order–disorder in natrolite-group minerals. *Eur. J. Mineral.* **7**, 501-508.

_____, Galli, E. & Vezzalini, G. (1985): Epistilbite: an acentric zeolite with domain structure. *Z. Kristallogr.* **173**, 257-265.

_____, _____, _____, Passaglia, E. & Zanazzi, P.F. (1982a): Position of cations and water molecules in hydrated chabazite. Natural and Na-, Ca-, Sr- and K-exchanged chabazites. *Zeolites* **2**, 303-309.

_____, Hentschel, G. & Vezzalini, G. (1979): Amicite, a new natural zeolite. *Neues Jahrb. Mineral., Monatsh.*, 481-488.

_____, Pongiluppi, D. & Vezzalini, G. (1982b): The crystal chemistry of natrolite, mesolite and scolecite. *Neues Jahrb. Mineral., Abh.* **143**, 231-248.

_____ & Sabelli, C. (1987): Statistical and true symmetry of ferrierite: possible absence of straight T–O–T bridging bonds. *Z. Kristallogr.* **178**, 249-256.

_____ & Vezzalini, G. (1979): The crystal structure of amicite, a zeolite. *Acta Crystallogr.* **B35**, 2866-2869.

_____ & _____ (1981a): A partially disordered natrolite: relationships between cell parameters and Si–Al distribution. *Acta Crystallogr.* **B37**, 781-788.

_____ & _____ (1981b): Crystal energies and coordination of ions in partially occupied sites: dehydrated mazzite. *Bull. Minéral.* **104**, 5-9.

_____, _____, Galli, E. & Quartieri, S. (1996): The crystal structure of gottardiite, a new natural zeolite. *Eur. J. Mineral.* **8**, 69-75.

_____, _____ & Tazzoli, V. (1981): Thomsonite: a detailed refinement with cross checking by crystal energy calculations. *Zeolites* **1**, 91-97.

Alietti, A. (1972): Polymorphism and crystal-chemistry of heulandites and clinoptilolites. *Am. Mineral.* **57**, 1448-1462.

Armbruster, T. (1993): Dehydration mechanism of clinoptilolite and heulandite: single-crystal X-ray study of Na-poor, Ca-, K-, Mg-rich clinoptilolite at 100 K. *Am. Mineral.* **78**, 260-264.

_____ & Kohler, T. (1992): Re- and dehydration of laumontite: a single-crystal X-ray study at 100 K. *Neues Jahrb. Mineral., Monatsh.*, 385-397.

Artioli, G. (1992): The crystal structure of garronite. *Am. Mineral.* **77**, 189-196.

_____ & Foy, H. (1994): Gobbinsite from Magheramorne quarry, Northern Ireland. *Mineral. Mag.* **58**, 615-620.

_____, Gottardi, G., Rinaldi, R., Satow, Y., Horiuchi, H., Ye, J., Sawada, H., Tanaka, M. & Tokonami, M. (1987): A single crystal diffraction study of the natural zeolite cowlesite. *Photon Factory, National Laboratory for High Energy Physics, Activity Rep.* **1987**, 316.

_____ & Kvick, Å. (1990): Synchrotron X-ray Rietveld study of perlialite, the natural counterpart of synthetic zeolite-L. *Eur. J. Mineral.* **2**, 749-759.

_____, Rinaldi, R., Kvick, Å. & Smith, J.V. (1986b): Neutron diffraction structure refinement of the zeolite gismondine at 15 K. *Zeolites* **6**, 361-366.

_____, Smith, J.V. & Kvick, Å. (1984): Neutron diffraction study of natrolite, $Na_2Al_2Si_3O_{10}$•$2H_2O$, at 20 K. *Acta Crystallogr.* **C40**, 1658-1662.

_____, _____ & Pluth, J.J. (1986a): X-ray structure refinement of mesolite. *Acta Crystallogr.* **C42**, 937-942.

_____ & Ståhl, K. (1993): Fully hydrated laumontite: a structure study by flat-plate and capillary powder diffraction techniques. *Zeolites* **13**, 249-255.

_____ & Torres Salvador, M.R. (1991): Characterization of the natural zeolite gonnardite. Structure analysis of natural and cation exchanged species by the Rietveld method. *Material Science Forum* **79-82**, 845-850.

Bartl, H. (1970): Strukturverfeinerung von Leonhardit, $Ca[Al_2Si_4O_{12}]$•$3H_2O$, mittels Neutronenbeugung. *Neues Jahrb. Mineral., Monatsh.*, 298-310.

Baur, W.H. (1964): On the cation and water positions in faujasite. *Am. Mineral.* **49**, 697-704.

Beger, R.M. (1969): The crystal structure and chemical composition of pollucite. *Z. Kristallogr.* **129**, 280-302.

Bergerhoff, G., Baur, W.H. & Nowacki, W. (1958): Über die Kristallstruktur des Faujasits. *Neues Jahrb. Mineral., Monatsh.*, 193-200.

Beus, A.A. (1960): *Geochemistry of Beryllium and the Genetic Types of Beryllium Deposits*. Akademii Nauk, SSSR, Inst. mineral., geokhim., i kristallochim. redkikh elementov, 1-329 (in Russian). Abstract in *Am. Mineral.* **46**, 244.

Bieniok, A., Joswig, W. & Baur, W.H. (1996): A study of paulingites: pore filling by cations and water molecules. *Neues Jahrb. Mineral., Abh.* **171**, 119-134.

Bissert, G. & Liebau, F. (1986): The crystal structure of a triclinic bikitaite, $Li[AlSi_2O_6]•H_2O$, with ordered Al/Si distribution. *Neues Jahrb. Mineral., Monatsh.*, 241-252.

Blackburn, W.H. & Dennen, W.H. (1997): Encyclopedia of Minerals Names. *Can. Mineral., Spec. Publ.* **1**.

Blumenbachs, J.F. (1791): Auszuge und Kezensioneit bergmanischer und mineralogischer Schriften. *Bergmannisches J.* **2**, 489-500.

Boggs, R.C., Howard, D.G., Smith, J.V. & Klein, G.L. (1993): Tschernichite, a new zeolite from Goble, Columbia County, Oregon. *Am. Mineral.* **78**, 822-826.

Boles, J.R. (1972): Composition, optical properties, cell dimensions, and thermal stability of some heulandite group zeolites. *Am. Mineral.* **57**, 1463-1493.

Bonardi, M. (1979): Composition of type dachiardite from Elba: a re-examination. *Mineral. Mag.* **43**, 548-549.

_____, Roberts, A.C. & Sabina, A.P. (1981): Sodium-rich dachiardite from the Francon quarry, Montreal Island, Quebec. *Can. Mineral.* **19**, 285-289.

Bondi, M., Griffin, W.L., Mattioli, V. & Mottana, A. (1983): Chiavennite, $CaMnBe_2Si_5O_{13}(OH)_2•2H_2O$, a new mineral from Chiavenna (Italy). *Am. Mineral.* **68**, 623-627.

Bosc D'Antic, L. (1792): Mémoire sur la chabazie. *J. d'Histoire Naturelle* **2**, 181-184.

Breithaupt, A. (1846): Pollux. (*Poggendorff's*) *Annalen der Physik und Chemie* **69**, 439.

Brewster, D. (1825a): Description of gmelinite, a new mineral species. *Edinburgh J. Sci.* **2**, 262-267.

_____ (1825b): Description of levyne, a new mineral species. *Edinburgh J. Sci.* **2**, 332-334.

Brooke, H.J. (1820): On mesotype, needlestone, and thomsonite. *Annals of Philosophy* **16**, 193-194.

_____ (1822): On the comptonite of Vesuvius, the brewsterite of Scotland, the stilbite and the heulandite. *Edinburgh Philos. J.* **6**, 112-115.

Cabella, R., Lucchetti, G., Palenzona, A., Quartieri, S. & Vezzalini, G. (1993): First occurrence of a Ba-dominant brewsterite: structural features. *Eur. J. Mineral.* **5**, 353-360.

Černý, P. (1974): The present status of the analcime–pollucite series. *Can. Mineral.* **12**, 334-341.

_____, Rinaldi, R. & Surdam, R.C. (1977): Wellsite and its status in the phillipsite – harmotome group. *Neues Jahrb. Mineral., Abh.* **128**, 312-320.

_____ & Simpson, F.M. (1978): The Tanco pegmatite at Bernic Lake, Manitoba. X. Pollucite. *Can. Mineral.* **16**, 325-333.

Chao, G.Y. (1980): Paranatrolite, a new zeolite from Mont St-Hilaire, Québec. *Can. Mineral.* **18**, 85-88.

Chen, T.T. & Chao, G.Y. (1980): Tetranatrolite from Mont St-Hilaire, Québec. *Can. Mineral.* **18**, 77-84.

Cho, M. & Liou, J.G. (1987): Prehnite–pumpellyite to greenschist facies transition in the Karmutsen metabasites, Vancouver Island, B.C. *J. Petrol.* **28**, 417-443.

Clark, A.M. (1993): *Hey's Mineral Index*. Chapman & Hall, London, U.K.

Cocco, G. & Garavelli, C. (1958): Riesame di alcune zeoliti elbane. *Atti Soc. Toscana Sci. Naturali* **65**, 262-283.

Coombs, D.S. (1955): X-ray observations on wairakite and non-cubic analcime. *Mineral. Mag.* **30**, 699-708.

_____ & Whetten, J.T. (1967): Composition of analcime from sedimentary and burial metamorphic rocks. *Geol. Soc. Am., Bull.* **78**, 269-282.

Cronstedt, A.F. (1756): Observation and description of an unknown kind of rock to be named zeolites. *Kongl. Vetenskaps Acad. Handl. Stockholm* **17**, 120-123 (in Swedish).

D'Achiardi, G. (1906): Zeoliti del filone della Speranza presso S. Piero in Campo (Elba). *Atti Soc. Toscana Sci. Naturali* **22**, 150-165.

Damour, M. (1842): Description de la faujasite, nouvelle espèce minérale. *Annales des Mines*, *Sér.* **4**, **1**, 395-399.

Dana, E.S. (1914): *A System of Mineralogy of J.D. Dana* (6th ed., with Appendices I and II). John Wiley & Sons, New York, N.Y.

Dana, J.D. (1868): *A System of Mineralogy* (5th ed.). John Wiley & Sons, New York, N.Y.

Davis, R.J. (1958): Mordenite, ptilolite, flokite, and arduinite. *Mineral. Mag.* **31**, 887-888.

De Gennaro, M. & Franco, E. (1976): La K-chabazite di alcuni "Tufi del Vesuvio". *Rend. Accad. Naz. Lincei* **40**, 490-497.

Delamétherie, J.-C. (1795): *Théorie de la Terre* **1**. Chez Maradan, Paris, France.

Della Ventura, G., Parodi, G.C. & Burragato, F. (1993): New data on merlinoite and related zeolites. *Rend. Lincei Sci. Fisiche Naturali, Ser.* **9**, **4**, 303-312.

Di Franco, S. (1942): *Mineralogia Etnea*. Zuccarello & Izzi, Catania, Italy (158-161).

Di Renzo, F. & Gabelica, Z. (1995): New data on the structure and composition of the silicoaluminophosphate viséite and a discreditation of its status as a zeolite. *In* Natural Zeolites '93: Occurrence, Properties, Use (D.W. Ming & F.A. Mumpton, eds.). International Committee on Natural Zeolites, Brockport, New York, N.Y. (173-185).

_____ & _____ (1997): Barrerite and other zeolites from Kuiu and Kupreanof islands, Alaska. *Can. Mineral.* **35**, 691-698.

Dunn, P.J., Peacor, D.R., Newberry, N. & Ramik, R.A. (1980): Goosecreekite, a new calcium aluminum silicate hydrate possibly related to brewsterite and epistilbite. *Can. Mineral.* **18**, 323-327.

Eakle, A.S. (1898): Erionite, a new zeolite. *Am. J. Sci.* **156**, 66-68.

Eberly, P.E., Jr. (1964): Adsorption properties of naturally occurring erionite and its cationic-exchanged forms. *Am. Mineral.* **49**, 30-40.

Effenberger, H., Giester, G., Krause, W. & Bernhardt, H.-J. (1998): Tschörtnerite, a copper-bearing zeolite from the Bellberg volcano, Eifel, Germany. *Am. Mineral*. **83,** 607-617.

Engel, N. & Yvon, K. (1984): The crystal structure of parthéite. *Z. Kristallogr.* **169**, 165-175.

England, B.M. & Ostwald, J. (1979): Levyne – offretite intergrowths from Tertiary basalts in the Merriwa district, Hunter Valley, New South Wales, Australia. *Aust. Mineral.* **25**, 117-119.

Ercit, T.S. & Van Velthuizen, J. (1994): Gaultite, a new zeolite-like mineral species from Mont Saint-Hilaire, Quebec, and its crystal structure. *Can. Mineral.* **32**, 855-863.

Fersman, A.E. (1908): Materialien zur Untersuchung der Zeolithe Russlands. I. Leonhardit und Laumontit aus der Umgebung von Simferopol (Krim). *Trav. du Musée géol. Pierre le Grand pr. l'Acad. Imp. de Science St Pétersbourg* **2**, 103-150 (abstr. in *Z. Kristallogr.* **50**, 75-76).

Fischer, K. (1966): Untersuchung der Kristallstruktur von Gmelinit. *Neues Jahrb. Mineral., Monatsh.*, 1-13.

_____ & Schramm, V. (1970): Crystal structure of gismondite, a detailed refinement. *In* Molecular Sieve Zeolites. *Am. Chem. Soc., Adv. Chem. Ser.* **101**, 250-258.

Franzini, M. & Perchiazzi, N. (1994): Portite discredited = natrolite and new data on "schneiderite" (= laumontite). *Eur. J. Mineral.* **6**, 351-353.

Fuchs, J.N. (1816): Ueber die Zeolithe. (*Schweigger's*) *J. Chem. und Phys*. **18**, 1-29.

Galli, E. (1971): Refinement of the crystal structure of stilbite. *Acta Crystallogr.* **B27**, 833-841.

_____ (1975): Crystal structure refinement of mazzite. *Rend. Soc. It. Mineral. Petrol.* **31**, 599-612.

_____ (1976): Crystal structure refinement of edingtonite. *Acta Crystallogr.* **B32**, 1623-1627.

_____ (1980): The crystal structure of roggianite, a zeolite-like silicate. Proc. 5th Int. Conf. on Zeolites (L.V.C. Rees, ed.). Heyden, London, U.K. (205-213).

_____ & Alberti, A. (1975a): The crystal structure of stellerite. *Bull. Soc. fr. Minéral. Cristallogr.* **98**, 11-18.

_____ & _____ (1975b): The crystal structure of barrerite. *Bull. Soc. fr. Minéral. Cristallogr.* **98**, 331-340.

_____ & Gottardi, G. (1966): The crystal structure of stilbite. *Mineral. Petrogr. Acta* (*Bologna*) **12**, 1-10.

_____, _____ & Pongiluppi, D. (1979): The crystal structure of the zeolite merlinoite. *Neues Jahrb. Mineral., Monatsh.*, 1-9.

_____ & Loschi Ghittoni, A.G. (1972): The crystal chemistry of phillipsites. *Am. Mineral.* **57**, 1125-1145.

_____, Passaglia, E., Pongiluppi, D. & Rinaldi, R. (1974): Mazzite, a new mineral, the natural counterpart of the synthetic zeolite **Ω**. *Contrib. Mineral. Petrol.* **45**, 99-105.

_____, _____ & Zanazzi, P.F. (1982): Gmelinite: structural refinements of sodium-rich and calcium-rich natural crystals. *Neues Jahrb. Mineral., Monatsh.*, 145-155.

_____, Quartieri, S., Vezzalini, G. & Alberti, A. (1995): Boggsite and tschernichite-type zeolites from Mt. Adamson, Northern Victoria Land (Antarctica). *Eur. J. Mineral.* **7**, 1029-1032.

_____, _____, _____ & _____ (1996): Gottardiite, a new high-silica zeolite from Antarctica: the natural counterpart of synthetic NU-87. *Eur. J. Mineral.* **8**, 687-693.

_____, _____, _____, _____ & Franzini, M. (1997a): Terranovaite from Antarctica: a new 'pentasil' zeolite. *Am. Mineral.* **82**, 423-429.

_____ & Rinaldi, R. (1974): The crystal chemistry of epistilbites. *Am. Mineral.* **59**, 1055-1061.

_____, _____ & Modena, C. (1981): Crystal chemistry of levynes. *Zeolites* **1**, 157-160.

_____, Vezzalini, G., Quartieri, S., Alberti, A. & Franzini, M. (1997b): Mutinaite, a new zeolite from Antarctica: the natural counterpart of ZSM–5. *Zeolites* **19**, 318-322.

Gard, J.A. & Tait, J.M. (1972): The crystal structure of the zeolite offretite, $K_{1.1}Ca_{1.1}Mg_{0.7}[Si_{12.8}Al_{5.2}O_{36}]\bullet 15.2H_2O$. *Acta Crystallogr.* **B28**, 825-834.

Gehlen, A.F. & Fuchs, J.N. (1813): Ueber Werner's Zeolith, Haüy's Mesotype und Stilbite. (*Schweigger's*) *J. Chem. und Phys.* **8**, 353-366.

Gismondi, C.G. (1817): Osservazioni sopra alcuni fossili particolari de' contorni di Roma. *Giornale Enciclopedico di Napoli, Anno* **XI**, **2**, 3-15.

Giuseppetti, G., Mazzi, F., Tadini, C. & Galli, E. (1991): The revised crystal structure of roggianite: $Ca_2[Be(OH)_2Al_2Si_4O_{13}]<2.5H_2O$. *Neues Jahrb. Mineral., Monatsh.*, 307-314.

Gonnard, F. (1890): Sur l'offrétite, espèce minérale nouvelle. *C.R. Acad. Sci., Paris* **111**, 1002-1003.

Gordon, E.K., Samson, S. & Kamb, W.B. (1966): Crystal structure of the zeolite paulingite. *Science* **154**, 1004-1007.

Gottardi, G. & Alberti, A. (1974): Domain structure in garronite: a hypothesis. *Mineral. Mag.* **39**, 898-899.

_____ & Galli, E. (1985): *Natural Zeolites*. Springer-Verlag, Berlin, Germany.

_____ & Meier, W.M. (1963): The crystal structure of dachiardite. *Z. Kristallogr.* **119**, 53-64.

Graham, R.P.D. (1918): On ferrierite, a new zeolitic mineral, from British Columbia; with notes on some other Canadian minerals. *Trans. R. Soc. Can., Ser.* **3**, **12**, 185-201.

Gramlich-Meier, R., Gramlich, V. & Meier, W.M. (1985): The crystal structure of the monoclinic variety of ferrierite. *Am. Mineral.* **70**, 619-623.

Haidinger, W. (1825): Description of edingtonite, a new mineral species. *Edinburgh J. Sci.* **3**, 316-320.

Harada, K., Iwamoto, S. & Kihara, K. (1967): Erionite, phillipsite and gonnardite in the amygdales of altered basalt from Mazé, Niigata Prefecture, Japan. *Am. Mineral.* **52**, 1785-1794.

Hassan, I. (1997): Feldspathoids and their relationships to zeolites. *Kuwait J. Sci. Engineering* **24**, 163-187.

Haüy, R.-J. (1797): Analcime. *J. des Mines* **5**, 278-279.

_____ (1801): *Traité de minéralogie* **3**. Chez Louis, Paris, France.

_____ (1809): *Tableau Comparatif des Résultats de Cristallographie et de l'Analyse Chimique Relativement à la Classification des Minéraux.* Courcier, Paris, France.

Hazen, R.M. & Finger, L.W. (1979): Polyhedral tilting: a common type of pure displacive phase transition and its relationship to analcite at high pressure. *Phase Transitions* **1**, 1-22.

Heaney, P.J. & Veblen, D.R. (1990): A high-temperature study of the low–high leucite phase transition using the transmission electron microscope. *Am. Mineral.* **75**, 464-476.

Hesse, K.-F. (1983): Refinement of a partially disordered natrolite, $Na_2Al_2Si_3O_{10}•H_2O$. *Z. Kristallogr.* **163**, 69-74.

Hey, M.H. (1930): Studies on the zeolites. I. General review. *Mineral. Mag.* **22**, 422-437.

_____ (1960): Glottalite is chabazite. *Mineral. Mag.* **32**, 421-422.

_____ (1962): *An Index of Mineral Species and Varieties Arranged Chemically* (2nd ed., and Appendices, 1963 and 1974). British Museum, London, U.K.

Hintze, C. (1897): *Handbuch der Mineralogie* **2**. Von Veit, Leipzig, Germany.

Hori, H., Nagashima, K., Yamada, M., Miyawaki, R. & Marubashi, T. (1986): Ammonioleucite, a new mineral from Tatarazawa, Fujioka, Japan. *Am. Mineral.* **71**, 1022-1027.

How, H. (1864): On mordenite, a new mineral from the trap of Nova Scotia. *J. Chem. Soc.* **17** (*new ser.*), **17**, 100-104.

Howard, D.G. (1994): Crystal habit and twinning of garronite from Fara Vicentina, Vicenza (Italy). *Neues Jahrb. Mineral., Monatsh.*, 91-96.

_____, Tschernich, R.W., Smith, J.V. & Klein, G.L. (1990): Boggsite, a new high-silica zeolite from Goble, Columbia County, Oregon. *Am. Mineral.* **75**, 1200-1204.

Huang, Wen-Hui, Tu, Shao-Hua, Wang, K'ung-Hai, Chao, Chun-Lin & Yu, Cheng-Chih (1958): Hsiang-hua-shih, a new beryllium mineral. *Ti-chih-yueh-k'an* **7**, 35 (abstr. in *Am. Mineral.* **44**, 1327-1328; **46**, 244).

Hurlbut, C.S., Jr. (1957): Bikitaite, $LiAlSi_2O_6•H_2O$, a new mineral from Southern Rhodesia. *Am. Mineral.* **42**, 792-797.

Ibrahim, K. & Hall, A. (1995): New occurrences of diagenetic faujasite in the Quaternary tuffs of north-east Jordan. *Eur. J. Mineral.* **7**, 1129-1135.

Iijima, A. & Harada, K. (1969): Authigenic zeolites in zeolitic palagonite tuffs on Oahu, Hawaii. *Am. Mineral.* **54**, 182-197.

Jameson, R. (1805): *System of Mineralogy* **II**. Bell and Bradfute, Edinburgh, U.K. (539).

Joswig, W., Bartl, H. & Fuess, H. (1984): Structure refinement of scolecite by neutron diffraction. *Z. Kristallogr.* **166**, 219-223.

Kamb, W.B. & Oke, W.C. (1960): Paulingite, a new zeolite, in association with erionite and filiform pyrite. *Am. Mineral.* **45**, 79-91.

Kawahara, A. & Curien, H. (1969): La structure cristalline de l'érionite. *Bull. Soc. fr. Minéral. Cristallogr.* **92**, 250-256.

Kerr, I.S. & Williams, D.J. (1969): The crystal structure of yugawaralite. *Acta Crystallogr.* **B25**, 1183-1190.

KHOMYAKOV, A.P., CHEREPIVSKAYA, G.YE., KUROVA, T.A. & KAPTSOV, V.V. (1982): Amicite, $K_2Na_2Al_4Si_4O_{16}$•$5H_2O$, first find in the USSR. *Dokl. Akad. Nauk SSSR* **263**, 978-980 (in Russ.).

_____, SANDOMIRSKAYA, S.M. & MALINOVSKII, YU.A. (1980): Kalborsite, $K_6BAl_4Si_6O_{20}(OH)_4Cl$, a new mineral. *Dokl. Akad. Nauk SSSR* **252,** 1465-1468 (in Russ.).

KIM, Y. & KIRKPATRICK, R.J. (1996): Application of MAS NMR spectroscopy to poorly crystalline materials: viséite. *Mineral. Mag.* **60**, 957-962.

KLAPROTH, M.H. (1803): Chemische Untersuchung des Natroliths. *Ges. Naturforschender Freunde zu Berlin, Neue Schriften* **4**, 243-248.

KOCMAN, V., GAIT, R.I. & RUCKLIDGE, J. (1974): The crystal structure of bikitaite, $Li[AlSi_2O_6]$•H_2O. *Am. Mineral.* **59**, 71-78.

KOYAMA, K. & TAKÉUCHI, Y. (1977): Clinoptilolite: the distribution of potassium atoms and its role in thermal stability. *Z. Kristallogr.* **145**, 216-239.

KRAUSE, W., BERNHARDT, H.-J., EFFENBERGER, H. & GIESTER, G. (1997): Tschörtnerite, a copper-bearing zeolite from the Bellberg volcano, Eifel, Germany. *Ber. Deutsch. Mineral. Ges.* **1**, 205 (abstr.).

KROGH ANDERSEN, E., DANØ, M. & PETERSEN, O.V. (1969): A tetragonal natrolite. *Medd. om Grønland* **181**, 1-19.

KVICK, Å., ARTIOLI, G. & SMITH, J.V. (1986): Neutron diffraction study of the zeolite yugawaralite at 13 K. *Z. Kristallogr.* **174**, 265-281.

_____, STÅHL, K. & SMITH, J.V. (1985): A neutron diffraction study of the bonding of zeolitic water in scolecite at 20 K. *Z. Kristallogr.* **171**, 141-154.

LACROIX, A. (1896): Sur la gonnardite. *Bull. Soc. fr. Minéral.* **19**, 426-429.

LANGHOF, J. & HOLSTAM, D. (1994): Boron-bearing chiavennite and other late-stage minerals of the Proterozoic lithium-pegmatites of Utö, Stockholm, Sweden. *Int. Mineral. Assoc., 16th Gen. Meet. (Pisa), Abstr.*, 232.

LARSEN, A.O., ÅSHEIM, A., RAADE, G. & TAFTØ, J. (1992): Tvedalite, $(Ca,Mn)_4Be_3Si_6O_{17}(OH)_4$•$3H_2O$, a new mineral from syenite pegmatite in the Oslo region, Norway. *Am. Mineral.* **77**, 438-443.

LEIMER, H.W. & SLAUGHTER, M. (1969): The determination and refinement of the crystal structure of yugawaralite. *Z. Kristallogr.* **130**, 88-111.

LENGAUER, C.L., GIESTER, G. & TILLMANNS, E. (1997): Mineralogical characterization of paulingite from Vinarická Hora, Czech Republic. *Mineral. Mag.* **61**, 591-606.

VON LEONHARD, K.C. (1817): Die Zeagonit, ein neues Mineral vom Capo do Bove bei Rom. *Taschenbuch für die gesammte Mineralogie mit Hinsicht auf die neuesten Entdeckungen* **11**, 164-168 (extracted from Gismondi 1817).

_____ (1821): *Handbuch der Oryktognosie*. Mohr & Winter, Heidelberg, Germany (448).

LEVINSON, A.A. (1966): A system of nomenclature for rare-earth minerals. *Am. Mineral.* **51**, 152-158.

LÉVY, A. (1825): Descriptions of two new minerals. *Annals of Philosophy, new ser.* **10**, 361-363.

LO, H.-J. & HSIEH, Y.-L. (1991): High potassium natural mordenite and the chemical variation of mordenite. *Proc. Geol. Soc. China* (*Taiwan*) **34**, 305-312.

_____, SONG, S.-R. & WEN, S.-B. (1991): High potassium mordenite in the andesite from the Coastal Range, eastern Taiwan. *Proc. Geol. Soc. China* (*Taiwan*) **34**, 293-304.

LUCCHETTI, G., MASSA, B. & PENCO, A.M. (1982): Strontian heulandite from Campegli (eastern Ligurian ophiolites, Italy). *Neues Jahrb. Mineral., Monatsh.*, 541-550.

MALINOVSKII, YU.A. (1984): The crystal structure of K-gmelinite. *Kristallografiya* **29**, 426-430 (in Russ.).

_____ & BELOV, N.V. (1980): Crystal structure of kalborsite. *Dokl. Akad. Nauk SSSR* **252**, 611-615 (in Russ.).

MASON, B.H. (1957): Gonnardite (ranite) from Langesundsfjord. *Norsk geol. Tidsskr.* **37**, 435-437.

MAZZI, F. & GALLI, E. (1978): Is each analcime different? *Am. Mineral.* **63**, 448-460.

_____ & _____ (1983): The tetrahedral framework of chabazite. *Neues Jahrb. Mineral., Monatsh.*, 461-480.

_____, _____ & GOTTARDI, G. (1976): The crystal structure of tetragonal leucite. *Am. Mineral.* **61**, 108-115.

_____, _____ & _____ (1984): Crystal structure refinement of two tetragonal edingtonites. *Neues Jahrb. Mineral., Monatsh.*, 373-382.

_____, LARSEN, A.O., GOTTARDI, G. & GALLI, E. (1986): Gonnardite has the tetrahedral framework of natrolite: experimental proof with a sample from Norway. *Neues Jahrb. Mineral., Monatsh.*, 219-228.

MCCONNELL, D. (1964): A zinc phosphate analogue of analcime: kehoeite. *Mineral. Mag.* **33**, 799-803.

MCCUSKER, L.B., BAERLOCHER, C. & NAWAZ, R. (1985): Rietveld refinement of the crystal structure of the new zeolite mineral gobbinsite. *Z. Kristallogr.* **171**, 281-289.

MEIER, W.M. (1961): The crystal structure of mordenite (ptilolite). *Z. Kristallogr.* **115**, 439-450.

_____, OLSON, D.H. & BAERLOCHER, C. (1996): Atlas of zeolite structure types. *Zeolites* **17**, 1-230.

Men'shikov, Yu.P. (1984): Perlialite, $K_9Na(Ca,Sr)[Al_{12}Si_{24}O_{72}]•15H_2O$, a new potassian zeolite from the Khibina Massif. *Zap. Vses. Mineral. Obshchest.* **113**, 607-612.

_____, Denisov, A.P., Uspenskaya, E.I. & Lipatova, E.A. (1973): Lovdarite, a new hydrous beryllosilicate of alkalis. *Dokl. Akad. Nauk SSSR* **213**, 429-432 (in Russ.).

Merkle, A.B. & Slaughter, M. (1968): Determination and refinement of the structure of heulandite. *Am. Mineral.* **53**, 1120-1138.

Merlino, S. (1972): Orizite discredited (= epistilbite). *Am. Mineral.* **57**, 592-593.

_____ (1974): The crystal structure of wenkite. *Acta Crystallogr.* **B30**, 1262-1268.

_____ (1990): Lovdarite, $K_4Na_{12}(Be_8Si_{28}O_{72})•18H_2O$, a zeolite-like mineral: structural features and OD character. *Eur. J. Mineral.* **2**, 809-817.

_____, Galli, E. & Alberti, A. (1975): The crystal structure of levyne. *Tschermaks Mineral. Petrogr. Mitt.* **22**, 117-129.

Minato, H. & Takano, T. (1964): An occurrence of potassium clinoptilolite from Itaya, Yamagata Prefecture, Japan. *J. Clay Sci. Soc. Japan* **4**, 12-22 (in Japanese with English abstr.).

Mizota, T., Shibuya, G., Shimazu, M. & Takeshita, Y. (1974): Mineralogical studies on levyne and erionite from Japan. *Geol. Soc. Japan, Mem.* **11**, 283-290.

Morozewicz, J. (1909): Über Stellerit, ein neues Zeolithmineral. *Bull. International de l'Académie des Sciences de Cracovie*, 344-359.

Mumpton, F.A. (1960): Clinoptilolite redefined. *Am. Mineral.* **45**, 351-369.

Nakajima, W. (1983): Disordered wairakite from Hikihara, Haga Town, Hyōgo Prefecture. *Bull. Faculty of Education, Kobe Univ.* **70**, 39-46.

Nawaz, R. (1983): New data on gobbinsite and garronite. *Mineral. Mag.* **47**, 567-568.

_____ (1984): New data on cowlesite from Northern Ireland. *Mineral. Mag.* **48**, 565-566.

_____ & Malone, J.F. (1982): Gobbinsite, a new zeolite mineral from Co. Antrim, N. Ireland. *Mineral. Mag.* **46**, 365-369.

Nickel, E.H. & Mandarino, J.A. (1987): Procedures involving the IMA Commission on New Minerals and Mineral Names, and guidelines on mineral nomenclature. *Can. Mineral.* **25**, 353-377.

Nørnberg, P. (1990): A potassium-rich zeolite in soil development on Danian chert. *Mineral. Mag.* **54**, 91-94.

Ogihara, S. & Iijima, A. (1990): Exceptionally K-rich clinoptilolite – heulandite group zeolites from three offshore boreholes off northern Japan. *Eur. J. Mineral.* **2**, 819-826.

Passaglia, E. (1969a): Le zeoliti di Albero Bassi (Vicenza). *Per. Mineral.* **38**, 237-243.

_____ (1969b): Roggianite, a new silicate mineral. *Clay Minerals* **8**, 107-111.

_____ (1970): The crystal chemistry of chabazites. *Am. Mineral.* **55**, 1278-1301.

_____ (1975): The crystal chemistry of mordenites. *Contrib. Mineral. Petrol.* **50**, 65-77.

_____, Artioli, G. & Gualtieri, A. (1998): Crystal chemistry of the zeolites erionite and offretite. *Am. Mineral.* **83,** 577-589.

_____, _____, _____ & Carnevali, R. (1995): Diagenetic mordenite from Ponza, Italy. *Eur. J. Mineral.* **7**, 429-438.

_____, Galli, E., Leoni, L. & Rossi, G. (1978b): The crystal chemistry of stilbites and stellerites. *Bull. Minéral.* **101**, 368-375.

_____, _____ & Rinaldi, R. (1974): Levynes and erionites from Sardinia, Italy. *Contrib. Mineral. Petrol.* **43**, 253-259.

_____ & Pongiluppi, D. (1974): Sodian stellerite from Capo Pula, Sardegna. *Lithos* **7**, 69-73.

_____ & _____ (1975): Barrerite, a new natural zeolite. *Mineral. Mag.* **40**, 208.

_____, _____ & Rinaldi, R. (1977): Merlinoite, a new mineral of the zeolite group. *Neues Jahrb. Mineral., Monatsh.*, 355-364.

_____, _____ & Vezzalini, G. (1978a): The crystal chemistry of gmelinites. *Neues Jahrb. Mineral., Monatsh.*, 310-324.

_____ & Sacerdoti, M. (1982): Crystal structural refinement of Na-exchanged stellerite. *Bull. Minéral.* **105**, 338-342.

_____ & Tagliavini, A. (1994): Chabazite – offretite epitaxial overgrowths in cornubianite from Passo Forcel Rosso, Adamello, Italy. *Eur. J. Mineral.* **6**, 397-405.

_____ & Vezzalini, G. (1985): Crystal chemistry of diagenetic zeolites in volcanoclastic deposits of Italy. *Contrib. Mineral. Petrol.* **90**, 190-198.

_____ & _____ (1988): Roggianite: revised chemical formula and zeolitic properties. *Mineral. Mag.* **52**, 201-206.

_____, _____ & Carnevali, R. (1990): Diagenetic chabazites and phillipsites in Italy: crystal chemistry and genesis. *Eur. J. Mineral.* **2**, 827-839.

Peacor, D.R. (1968): A high temperature single crystal diffractometer study of leucite, $(K,Na)AlSi_2O_6$. *Z. Kristallogr.* **127**, 213-224.

_____, Dunn, P.J., Simmons, W.B., Tillmanns, E. & Fischer, R.X. (1984): Willhendersonite, a new zeolite isostructural with chabazite. *Am. Mineral.* **69**, 186-189.

_____, _____, _____, Wicks, F.J. & Raudsepp, M. (1988): Maricopaite, a new hydrated Ca–Pb, zeolite-like silicate from Arizona. *Can. Mineral.* **26**, 309-313.

Pekov, I.V. & Chukanov, N.V. (1996): New data on kalborsite. *Zap. Vses. Mineral. Obshchest.* **125**(4), 55-59 (in Russ.).

Perrotta, A.J. (1967): The crystal structure of epistilbite. *Mineral. Mag.* **36**, 480-490.
111
_____ & Smith, J.V. (1964): The crystal structure of brewsterite, $(Sr,Ba,Ca)_2(Al_4Si_{12}O_{32})•10H_2O$. *Acta Crystallogr.* **17**, 857-862.

Pirsson, L.V. (1890): On mordenite. *Am. J. Sci.* **140**, 232-237.

Pluth, J.J. & Smith, J.V. (1990): Crystal structure of boggsite, a new high-silica zeolite with the first three-dimensional channel system bounded by both 12- and 10-rings. *Am. Mineral.* **75**, 501-507.

_____, _____, Howard, D.G. & Tschernich, R.W. (1989): Boggsite; the first three-dimensional channel system with both 12-and 10-rings. *In* Zeolites for the Nineties, Recent Research Reports (J.C. Jansen, L. Moscou & M.F.M. Post, eds.). Eighth Int. Zeolite Conf. (Amsterdam), 111-112 (abstr.).

Quartieri, S. & Vezzalini, G. (1987): Crystal chemistry of stilbites: structure refinements of one normal and four chemically anomalous samples. *Zeolites* **7**, 163-170.

_____, _____ & Alberti, A. (1990): Dachiardite from Hokiya-dake: evidence of a new topology. *Eur. J. Mineral.* **2**, 187-193.

Raade, G. (1996): Minerals originally described from Norway. Including notes on type material. *Norsk Bergverksmuseums Skriftserie* **11**.

_____, Åmli, R., Mladeck, M.H., Din, V.K., Larsen, A.O. & Åsheim, A. (1983): Chiavennite from syenite pegmatites in the Oslo region, Norway. *Am. Mineral.* **68**, 628-633.

Rastsvetaeva, R.K., Rekhlova, O.Y., Andrianov, V.I. & Malinovskii, Yu.A. (1991): Crystal structure of hsianghualite. *Dokl. Akad. Nauk SSSR* **316**, 624-628 (in Russ.).

Rinaldi, R. (1976): Crystal chemistry and structural epitaxy of offretite – erionite from Sasbach, Kaiserstuhl. *Neues Jahrb. Mineral., Monatsh.*, 145-156.

_____, Pluth, J.J. & Smith, J.V. (1974): Zeolites of the phillipsite family. Refinement of the crystal structures of phillipsite and harmotome. *Acta Crystallogr.* **B30**, 2426-2433.

_____, _____ & _____ (1975b): Crystal structure of mazzite dehydrated at 600°C. *Acta Crystallogr.* **B31**, 1603-1608.

_____, Smith, J.V. & Jung, G. (1975a): Chemistry and paragenesis of faujasite, phillipsite and offretite from Sasbach, Kaiserstuhl, Germany. *Neues Jahrb. Mineral., Monatsh.*, 433-443.

_____ & Vezzalini, G. (1985): Gismondine; the detailed X-ray structure refinement of two natural samples. *In* Zeolites; Synthesis, Structure, Technology and Application (B. Držaj, S. Hočevar & S. Pejovnik, eds.). Elsevier, Amsterdam, The Netherlands (481-492).

Robinson, G.W. & Grice, J.D. (1993): The barium analog of brewsterite from Harrisville, New York. *Can. Mineral.* **31**, 687-690.

Rose, G. (1826): Ueber den Epistilbit, eine neue zur Familie der Zeolithe gehörige Mineralgattung. (*Poggendorff's*) *Annalen der Physik und Chemie* **6**, 183-190.

Ross, C.S. & Shannon, E.V. (1924): Mordenite and associated minerals from near Challis, Custer County, Idaho. *Proc. U.S. Nat. Museum* **64**(19), 1-19.

Ross, M., Flohr, M.J.K. & Ross, D.R. (1992): Crystalline solution series and order–disorder within the natrolite mineral group. *Am. Mineral.* **77**, 685-703.

Rouse, R.C., Dunn, P.J., Grice, J.D., Schlenker, J.L. & Higgins, J.B. (1990): Montesommaite, $(K,Na)_9Al_9Si_{23}O_{64}•10H_2O$, a new zeolite related to merlinoite and the gismondine group. *Am. Mineral.* **75**, 1415-1420.

_____ & Peacor, D.R. (1986): Crystal structure of the zeolite mineral goosecreekite, $CaAl_2Si_6O_{16}•5H_2O$. *Am. Mineral.* **71**, 1494-1501.

_____ & _____ (1994): Maricopaite, an unusual lead calcium zeolite with an interrupted mordenite-like framework and intrachannel Pb_4 tetrahedral clusters. *Am. Mineral.* **79**, 175-184.

_____, _____, Dunn, P.J., Campbell, T.J., Roberts, W.L., Wicks, F.J. & Newbury, D. (1987): Pahasapaite, a beryllophosphate zeolite related to synthetic zeolite rho, from the Tip Top pegmatite of South Dakota. *Neues Jahrb. Mineral., Monatsh.*, 433-440.

_____, _____ & Merlino, S. (1989): Crystal structure of pahasapaite, a beryllophosphate mineral with a distorted zeolite rho framework. *Am. Mineral.* **74**, 1195-1202.

Rüdinger, B., Tillmanns, E. & Hentschel, G. (1993): Bellbergite – a new mineral with the zeolite structure type EAB. *Mineral. Petrol.* **48**, 147-152.

Sakurai, K. & Hayashi, A. (1952): "Yugawaralite", a new zeolite. *Sci. Rep., Yokohama Nat. Univ., Ser.* **II**, **1**, 69-77.

Sarp, H., Deferne, J., Bizouard, H. & Liebich, B.W. (1979): La parthéite, $CaAl_2Si_2O_8•2H_2O$, un nouveau silicate naturel d'aluminium et de calcium. *Schweiz. Mineral. Petrogr. Mitt.* **59**, 5-13.

Schaller, W.T. (1923): Ptilolite and related zeolites. *In* Proc. Societies (E.T. Wherry, ed.). *Am. Mineral.* **8**, 93-94.

_____ (1932): The mordenite – ptilolite group; clinoptilolite, a new species. *Am. Mineral.* **17**, 128-134.

Schlenker, J.L., Pluth, J.J. & Smith, J.V. (1977a): Refinement of the crystal structure of brewsterite, $Ba_{0.5}Sr_{1.5}Al_4Si_{12}O_{32}•10H_2O$. *Acta Crystallogr.* **B33**, 2907-2910.

_____, _____ & _____ (1977b): Dehydrated natural erionite with stacking faults of the offretite type. *Acta Crystallogr.* **B33**, 3265-3268.

Schröpfer, L. & Joswig, W. (1997): Structure analyses of a partially dehydrated synthetic Ca-garronite single crystal under different T, pH_2O conditions. *Eur. J. Mineral.* **9**, 53-65.

Seki, Y. (1971): Wairakite – analcime solid solution as an indicator of water pressures in low-grade metamorphism. *J. Geol. Soc. Japan* **77**, 667-674.

_____ & Oki, Y. (1969): Wairakite – analcime solid solutions from low-grade metamorphic rocks of the Tanzawa Mountains, central Japan. *Mineral. J.* **6**, 36-45.

Sheppard, R.A. & Fitzpatrick, J.J. (1989): Phillipsite from silicic tuffs in saline, alkaline-lake deposits. *Clays Clay Minerals* **37**, 243-247.

_____ & Gude, A.J., III (1969a): Diagenesis of tuffs in the Barstow Formation, Mud Hills, San Bernardino County, California. *U.S. Geol. Surv., Prof. Pap.* **634**, 1-35.

_____ & _____ (1969b): Chemical composition and physical properties of the related zeolites offretite and erionite. *Am. Mineral.* **54**, 875-886.

_____, _____ & Griffin, J.J. (1970): Chemical composition and physical properties of phillipsite from the Pacific and Indian oceans. *Am. Mineral.* **55**, 2053-2062.

_____, _____ & Munson, E.L. (1965): Chemical composition of diagenetic zeolites from tuffaceous rocks of the Mojave Desert and vicinity, California. *Am. Mineral.* **50**, 244-249.

Smith, J.V. (1988): Topochemistry of zeolites and related materials. 1. Topology and geometry. *Chem. Rev.* **88**, 149-182.

_____, Knawels, C.R. & Rinaldi, R. (1964): Crystal structures with a chabazite framework. III. Hydrated Ca-chabazite at +20 and –150°C. *Acta Crystallogr.* **17**, 374-384.

_____, Pluth, J.J., Boggs, R.C. & Howard, D.G. (1991): Tschernichite, the mineral analogue of zeolite beta. *J. Chem. Soc., Chem. Commun.*, 363-364.

Ståhl, K., Kvick, Å. & Smith, J.V. (1990): Thomsonite, a neutron diffraction study at 13 K. *Acta Crystallogr.* **C46**, 1370-1373.

Steiner, A. (1955): Wairakite, the calcium analogue of analcime, a new zeolite mineral. *Mineral. Mag.* **30**, 691-698.

Strunz, H. (1956): Die Zeolithe Gmelinit, Chabasit, Levyn (Phakolith, Herschelit, Seebachit, Offretit). *Neues Jahrb. Mineral., Monatsh.*, 250-259.

_____ (1978): *Mineralogische Tabellen* (7th ed.). Akademische Verlagges., Leipzig, Germany.

Stuckenschmidt, E., Fuess, H. & Kvick, Å. (1990): Investigation of the structure of harmotome by X-ray (293 K, 100 K) and neutron diffraction (15 K). *Eur. J. Mineral.* **2**, 861-874.

Takéuchi, Y., Mazzi, F., Haga, N. & Galli, E. (1979): The crystal structure of wairakite. *Am. Mineral.* **64**, 993-1001.

Taylor, W.H. (1930): The structure of analcite ($NaAlSi_2O_6•H_2O$). *Z. Kristallogr.* **74**, 1-19.

_____ & Jackson, R. (1933): The structure of edingtonite. *Z. Kristallogr.* **86**, 53-64.

Tazzoli, V., Domeneghetti, M.C., Mazzi, F. & Cannillo, E. (1995): The crystal structure of chiavennite. *Eur. J. Mineral.* **7**, 1339-1344.

Teertstra, D.K. & Černý, P. (1995): First natural occurrences of end-member pollucite: a product of low-temperature reequilibration. *Eur. J. Mineral.* **7**, 1137-1148.

_____ & Dyer, A. (1994): The informal discreditation of "doranite" as the magnesium analogue of analcime. *Zeolites* **14**, 411-413.

_____, Sherriff, B.L., Xu, Zhi & Černý, P. (1994): MAS and DOR NMR study of Al–Si order in the analcime – pollucite series. *Can. Mineral.* **32**, 69-80.

Thugutt, S.J. (1933): O ptylocie z Mydzka na Wolyniu – Sur la ptilolite de Mydzk en Volhynie. *Arch. Minéral., Soc. Sci. Varsovie* **9**, 99-102 (Polish), 103-104 (French résumé). (*Mineral. Abstr.* **6**, 129).

Tillmanns, E., Fischer, R.X. & Baur, W.H. (1984): Chabazite-type framework in the new zeolite willhendersonite, $KCaAl_3Si_3O_{12}•5H_2O$. *Neues Jahrb. Mineral., Monatsh.*, 547-558.

Tschernich, R.D. & Wise, W.S. (1982): Paulingite: variations in composition. *Am. Mineral.* **67**, 799-803.

Ueno, T. & Hanada, K. (1982): Chemical compositions and geneses of zeolites from Tsuyazaki, Fukuoka Prefecture, Japan. *J. Mineral. Soc. Japan* **15**, 259-272 (in Japanese, with English abstr.).

VAUGHAN, P.A. (1966): The crystal structure of the zeolite ferrierite. *Acta Crystallogr.* **21**, 983-990.

VEZZALINI, G. (1984): A refinement of Elba dachiardite: opposite acentric domains simulating a centric structure. *Z. Kristallogr.* **166**, 63-71.

_____, ARTIOLI, G. & QUARTIERI, S. (1992): The crystal chemistry of cowlesite. *Mineral. Mag.* **56**, 575-579.

_____ & OBERTI, R. (1984): The crystal chemistry of gismondines: the non-existence of K-rich gismondines. *Bull. Minéral.* **107**, 805-812.

_____, QUARTIERI, S. & GALLI, E. (1996): Relazioni strutturali nelle zeoliti con topologia CHA alla luce del ritrovamento di una Ca-willhendersonite. *XXVI Congresso Nazionale della Associazione Italiana di Cristallografia* (*Alessandria*), 91 (abstr.).

_____, _____ & _____ (1997a): Occurrence and crystal structure of a Ca-pure willhendersonite. *Zeolites* **19**, 75-79.

_____, _____, _____, ALBERTI, A., CRUCIANI, G. & KVICK, Å. (1997b): Crystal structure of the zeolite mutinaite, the natural analogue of ZSM–5. *Zeolites* **19**, 323-325.

_____, _____ & PASSAGLIA, E. (1990): Crystal structure of a K-rich natural gmelinite and comparison with the other refined gmelinite samples. *Neues Jahrb. Mineral., Monatsh.*, 504-516.

VILLARROEL, H.S. (1983): Sobre la existencia de otras variedades de estellerita y una forma de reconocerlas. *Anais Academia Brasileira de Ciencias* **55**, 87-91.

WALKER, G.P.L. (1962): Garronite, a new zeolite, from Ireland and Iceland. *Mineral. Mag.* **33**, 173-186.

WALTER, F. (1992): Weinebeneite, $CaBe_3(PO_4)_2(OH)_2{\cdot}4H_2O$, a new mineral species: mineral data and crystal structure. *Eur. J. Mineral.* **4**, 1275-1283.

WENK, H.-R. (1973): The structure of wenkite. *Z. Kristallogr.* **137**, 113-126.

WHITE, J.S. & ERD, R.C. (1992): Kehoeite is *not* a valid species. *Mineral. Mag.* **56**, 256-258.

WISE, W.S. (1982): New occurrence of faujasite in southeastern California. *Am. Mineral.* **67**, 794-798.

_____ & TSCHERNICH, R.W. (1975): Cowlesite, a new Ca-zeolite. *Am. Mineral.* **60**, 951-956.

_____ & _____ (1976): Chemical composition of ferrierite. *Am. Mineral.* **61**, 60-66.

WYART, J. (1938): Étude sur la leucite. *Bull. Soc. fr. Minéral.* **61**, 228-238.

YANG, PING & ARMBRUSTER, T. (1996): (010) disorder, partial Si,Al ordering, and Ca distribution in triclinic (*C*1) epistilbite. *Eur. J. Mineral.* **8**, 263-271.

Received December 3, 1997.

Appendix 1. Notes on the Definition of a Zeolite

Is more than 50% substitution of elements other than Si and Al permissible in tetrahedral sites?

There was complete agreement in the Subcommittee that some substitution of elements such as P and Be for Si and Al in tetrahedral sites must be permitted in the definition. Discussion in this context focussed on whether a 50% rule should be applied. The so-called 50% rule (Nickel 1992) is normally applied to split a binary solid-solution series into two species at the half-way point according to the predominant cations concerned, but not to separate members of a solid-solution series into two separate classes of minerals, as could happen if applied in the present context. Proponents of a 50% rule argued that the definition of zeolites should be on grounds of both structure and composition, zeolites being aluminosilicates or possibly Al-free silicates. The contrary opinion is that where structures are topologically equivalent and other essentially identical zeolitic characteristics prevail, irrespective of Si and Al contents in tetrahedral sites, any restrictions based on specific Si and Al contents would be arbitrary and undesirable. The Subcommittee voted by a substantial majority for this view. The beryllosilicates lovdarite and chiavennite, like the zincosilicate gaultite, have more than 50% tetrahedral sites occupied by Si, and are here accepted as zeolites in spite of having little if any Al. Also included are the beryllophosphates pahasapaite and weinebeneite, which have neither Si nor Al, but have typically zeolitic structures and other zeolitic characteristics. They can be regarded as end-member examples of Si-free zeolites or zeolite phosphates.

A compositional factor is included in the adopted definition in that the framework consists essentially of oxygen atoms together with cations that enter into tetrahedral co-ordination with oxygen.

Is the presence of H_2O and of extra-framework cations essential?

Reversible dehydration is a characteristic feature of zeolitic behavior, but how much H_2O must be present for a mineral to be considered a zeolite? Pollucite forms a continuous series with analcime, the H_2O content declining progressively with increasing Cs content such that the Na-free, Cs member is essentially anhydrous. It seems unnecessary, impractical, and illogical to prescribe some arbitrary H_2O content below which pollucite (or other mineral) would be defined as anhydrous, and no longer a zeolite. Furthermore, it is not inconceivable that some typical zeolite might be reversibly dehydrated under natural conditions without essential loss of structure. If so, it has not ceased to be a zeolite. Although zeolites typically are hydrous, it is inexpedient to specify the presence of H_2O in the definition.

Natural zeolites are known with up to 88% of tetrahedral sites occupied by Si, as in mutinaite, and there is no theoretical reason why this figure cannot be exceeded. If the site occupancy of tetrahedra by Si approaches 100%, the extra-framework cation content will approach zero, even though the structure and other characteristics may remain typically zeolitic. It is again considered inexpedient to word the definition so as to exclude such a hypothetical end-member case from the zeolite category. Melanophlogite, a low-density SiO_2 phase with large cages in its framework, would be a possible example, but is otherwise excluded by the adopted definition because it lacks appropriate channels for the passage of guest species.

Reference

Nickel, E.H. (1992): Solid solutions in mineral nomenclature. *Can. Mineral.* **30**, 231-234.

Appendix 2. Discreditations

Herschelite is chabazite-Na

Herschelite, $Na[AlSi_2O_6]\bullet 3H_2O$, was named by Lévy (1825) from material brought to him by Herschel from "Aci Reale" (now Acireale), on the flanks of Mt. Etna in Sicily. Contemporary literature and present-day exposures suggest that the actual occurrence may have been in basaltic lavas at Aci Castello, nearby. Lévy described herschelite as tabular crystals of hexagonal outline that contain "silex, alumina, and potash". It was later identified with chabazite (*e.g.,* Hausmann 1847) and relegated to synonymy, although shown to be Na-rich, not K-rich. Strunz (1956) confirmed that herschelite and chabazite give essentially identical X-ray powder patterns. Mason (1962) proposed revalidation on the bases of a supposed compositional gap between herschelite and "normal" Ca-rich chabazite, the distinctive habit, and lower indices of refraction.

Passaglia (1970) demonstrated a continuum of compositions from Ca- to Na-dominant types, extending into the field of K-dominance in a ternary series; there is no discernible gap in composition. The lower indices of refraction reflect the Na-rich composition. Variant crystal habit is not an accepted basis for species status for minerals, and some examples of strongly Na-dominant chabazite have rhombohedral, not tabular habit, as in the case of micrometer-scale crystals aggregated into thin ragged plates, illustrated by Sheppard *et al.* (1978).

In view of its chequered history and the above considerations, the name herschelite is suppressed, and the name chabazite-Na is to be applied to those members of the chabazite series in which Na is the most abundant extra-framework cation. Herschelite may retain some use as a term for a distinctive habit.

Leonhardite is H_2O-poor laumontite

Leonhardite $Ca_4[Al_8Si_{16}O_{48}]$•~$14H_2O$ was described by Blum (1843) for a mineral closely related to laumontite $Ca_4[Al_8Si_{16}O_{48}]$•$18H_2O$, but with different morphology. The type locality was near Schemnitz, nowadays Banska Stiavnica, then in Hungary, now in Slovakia. Delffs (1843) showed that type-locality leonhardite has less H_2O (*ca*. 13 molecules of H_2O per formula unit) than laumontite. Doelter (1921) agreed that leonhardite is identical in composition to laumontite, apart from its lower content of H_2O. The name has continued to be used widely for a material that forms rapidly and reversibly by partial dehydration of laumontite under ambient conditions. This happens upon exposure in the field and in the laboratory as a function of H_2O vapor pressure or by soaking in water, giving a readily observable change in extinction angle and cell dimensions (*e.g.,* Coombs 1952, Armbruster & Kohler 1992).

Fersman (1908) introduced the term "primary leonhardite" for a variety from Kurtsy (nowadays Ukrainka), Crimea, with 14 molecules of H_2O, which neither dehydrates nor rehydrates under ambient conditions. In it, $(K,Na)_2$ substitutes for Ca, although Ca is still dominant (Pipping 1966).

Type leonhardite of Blum from Schemnitz catalogued in the Museum of Natural History, Vienna, in 1843 and type "primary leonhardite" of Fersman obtained from the Fersman Mineralogical Museum in Moscow are shown by Wuest & Armbruster (1997) and Stolz & Armbruster (1997), respectively, to have the same Si,Al ordered framework of tetrahedra as laumontite. The low H_2O content of "primary leonhardite" is attributed to space limitations resulting from the introduction of additional cations of larger size.

In conformity with Rule 4, leonhardite is discredited as the name of a separate species. It is an H_2O-poor variety of laumontite. "Primary leonhardite" is H_2O-poor sodian potassian laumontite.

Svetlozarite is dachiardite-Ca

Svetlozarite was described by Maleev (1976) as a high-silica zeolite occurring as spherulites in chalcedony veinlets in brecciated andesites west of Zvesdel, eastern Rhodopes, Bulgaria. Analysis showed Ca > Na > K, and minor Fe and Mg. From X-ray powder-diffraction studies, Maleev suggested an orthorhombic symmetry, with a *c*-axis repeat of 7.5 Å, which is characteristic of the mordenite group, to which he attributed the mineral.

Gellens *et al.* (1982) concluded from powder and single-crystal X-ray and transmission electron microscopy (TEM) studies, that svetlozarite, space group *Ccma* (?), is related to the ideal dachiardite structure by irregular periodic twinning and stacking faults, and that it is not a topologically distinct member of the mordenite family. Its composition is within the range of other samples of dachiardite. It is regarded as a multiply twinned and highly faulted dachiardite (dachiardite-Ca), and is discredited as a separate species.

Wellsite is barian phillipsite-Ca and calcian harmotome

The mineral named wellsite by Pratt & Foote (1897) has been shown by Galli (1972) and Galli & Loschi Ghittoni (1972) to be isostructural with phillipsite and harmotome, and Černý *et al.* (1977) have shown that zoning in crystals of wellsite covers most of the range from Ca-rich phillipsite to potassian calcian harmotome. Wellsite is discredited. Most examples of wellsite are barian phillipsite-Ca, and others are calcian harmotome.

References

Armbruster, T. & Kohler, T. (1992): Re- and dehydration of laumontite: a single-crystal X-ray study at 100 K. *Neues Jahrb. Mineral., Monatsh.*, 385-397.

Blum, J.R. (1843): Leonhardit, ein neues Mineral. (*Poggendorff's*) *Annalen der Physik und Chemie* **59**, 336-339.

Černý, P., Rinaldi, R. & Surdam, R.C. (1977): Wellsite and its status in the phillipsite–harmotome group. *Neues Jahrb. Mineral., Abh.* **128**, 312-320.

Coombs, D.S. (1952): Cell size, optical properties and chemical composition of laumontite and leonhardite. *Am. Mineral.* **37**, 812-830.

Delffs, W. (1843): Analyse des Leonhardits. (*Poggendorff's*) *Annalen der Physik und Chemie* **59**, 339-342.

Doelter, C. (1921): *Handbuch der Mineralchemie* **II**, **3**. Verlag Theodor Steinkopff, Dresden, Germany.

Fersman, A.E. (1908): Materialien zur Untersuchung der Zeolithe Russlands. I. Leonhardit und Laumontit aus der Umgebung von Simferopol (Krim). *Trav. du Musée géol. Pierre le Grand pr. l'Acad. Imp. de Science St Pétersbourg* **2**, 103-150 (abstr. in *Z. Kristallogr.* **50**, 75-76).

Galli, E. (1972): La phillipsite barifera ("wellsite") di M. Calvarina (Verona). *Per. Mineral.* **41**, 23-33.

_____ & Loschi Gittoni, A.G. (1972): The crystal chemistry of phillipsites. *Am. Mineral.* **57**, 1125-1145.

Gellens, R.L., Price, G.D. & Smith, J.V. (1982): The structural relation between svetlozarite and dachiardite. *Mineral. Mag.* **45**, 157-161.

HAUSMANN, J.F.L. (1847): *Handbuch der Mineralogie* (2nd ed.). **2**, 1600.

LÉVY, A. (1825): Descriptions of two new minerals. *Annals of Philosophy, new ser.* **10**, 361-363.

MALEEV, M.N. (1976): Svetlozarite, a new high-silica zeolite. *Zap. Vses. Mineral. Obshchest.* **105**, 449-453 (in Russ.).

MASON, B. (1962): Herschelite – a valid species? *Am. Mineral.* **47**, 985-987.

PASSAGLIA, E. (1970): The crystal chemistry of chabazites. *Am. Mineral.* **55**, 1278-1301.

PIPPING, F. (1966): The dehydration and chemical composition of laumontite. *Mineral. Soc. India, IMA Vol.*, 159-166.

PRATT, J.H. & FOOTE, H.W. (1897): On wellsite, a new mineral. *Am. J. Sci.* **153**, 443-448.

SHEPPARD, R.A., GUDE, A.J. & EDSON, G.M. (1978): Bowie zeolite deposit, Cochise and Graham Counties, Arizona. *In* Natural Zeolites – Occurrence, Properties and Use (L.B. Sand & F.A. Mumpton, eds.). Pergamon, Oxford, U.K. (319-328).

STOLZ, J. & ARMBRUSTER, T. (1997): X-ray single-crystal structure refinement of a Na,K-rich laumontite, originally designated "primary leonhardite". *Neues Jahrb. Mineral., Monatsh.* 131-134.

STRUNZ, H. (1956): Die Zeolithe Gmelinit, Chabasit, Levyn (Phakolith, Herschelit, Seebachit, Offretit). *Neues Jahrb. Mineral., Monatsh.*, 250-259.

WUEST, T. & ARMBRUSTER, T. (1997): Type locality leonhardite: a single-crystal X-ray study at 100 K. *Zeolite '97, 5th Int. Conf. on the Occurrence, Properties, and Utilization of Natural Zeolites* (*Ischia, Italy*), *Program Abstr.*, 327-328.

Eur. J. Mineral.
2008, **20**, 7–46
Published online February 2008

Sulfosalt systematics: a review. Report of the sulfosalt sub-committee of the IMA Commission on Ore Mineralogy

YVES MOËLO[1,*], Secretary, EMIL MAKOVICKY[2,**], Associate Secretary, NADEJDA N. MOZGOVA[3], past President of the Sulfosalt Sub-Committee, JOHN L. JAMBOR[4], NIGEL COOK[5], ALLAN PRING[6], WERNER PAAR[7], ERNEST H. NICKEL[8], STEPHAN GRAESER[9], SVEN KARUP-MØLLER[10], TONČI BALIC-ŽUNIC[2], WILLIAM G. MUMME[8], FILIPPO VURRO[11], DAN TOPA[7], LUCA BINDI[12], KLAUS BENTE[13] and MASAAKI SHIMIZU[14]

[1] Institut des Matériaux Jean Rouxel, UMR 6502 CNRS-Université de Nantes, 2, rue de la Houssinière, 44 322 Nantes Cedex 3, France
*Corresponding author, e-mail: Yves.Moelo@cnrs-imn.fr
[2] Department of Geography and Geology, University of Copenhagen, Østervoldgade 10, 1350 Copenhagen, Denmark
**Corresponding author, e-mail: emilm@ged.ku.dk
[3] IGEM, Russian Academy of Sciences, Staromonetny per. 35, Moscow 109017, Russia
[4] Leslie Research and Consulting, 316 Rosehill Wynd, Tsawwassen, B.C. V4M 3L9, Canada
[5] Natural History Museum (Geology), University of Oslo, Postboks 1172 Blindern, 0318 Oslo, Norway
[6] South Australian Museum, Department of Mineralogy, North Terrace, Adelaide, South Australia 5000, Australia
[7] Department of Materials Engineering and Physics, University of Salzburg, Hellbrunnerstraße 34, 5020 Salzburg, Austria
[8] CSIRO-Exploration & Mining, PO Box 5, Wembley, Western Australia 6913, Australia
[9] Naturhistorisches Museum, Augustinerstraße 2, 4001 Basel, Switzerland
[10] Institute of Mineral Industry, Danish Technical University, 2800 Lyngby, Denmark
[11] Dipartimento Geomineralogico, Università degli Studi di Bari, via E. Orabona 4, 70125 Bari, Italy
[12] Museo di Storia Naturale, Sezione di Mineralogia, Università degli Studi di Firenze, via La Pira 4, 50121 Firenze, Italy
[13] Institute of Mineralogy, Crystallography and Material Science, University of Leipzig, Scharnhorststraße 20, 04275 Leipzig, Germany
[14] Department of Earth Sciences, Faculty of Sciences, University of Toyama, Toyama 9308555, Japan

Abstract: This report deals with a general reexamination of the systematics of sulfosalts. It represents an update of the activity of the Sulfosalt Sub-Committee within the Commission on Ore Mineralogy of the International Mineralogical Association, in connection with the Commission on New Minerals, Nomenclature and Classification (CNMNC-IMA). Part I presents generalities of sulfosalt definition and nomenclature. After an extended chemical definition of sulfosalts, attention is focused on "classic" sulfosalts with As^{3+}, Sb^{3+}, Bi^{3+} or Te^{4+} as cations, corresponding to the general formula $(Me^{+}, Me'^{2+}, etc.)_x$ $[(Bi, Sb, As)^{3+}, Te^{4+}]_y$ $[(S, Se, Te)^{2-}]_z$ (*Me*, *Me'*: various metals). General aspects of their chemistry and classification principles are summarized, especially with regard to chemical substitutions and modular analysis of complex crystal structures. On this basis, Part II presents a review of sulfosalt systematics. Six main crystal-chemical sub-groups are distinguished (plus some unclassified species), concerning more than 220 valid mineral species. Among others whose status is questioned are those considered to be varieties of well-defined species; minerals with ill-defined X-ray data; those that are possibly identical species; and those that represent the potential revalidation of old species. More than 50 crystal structures still remain unsolved, among which about a half probably corresponds to new structure types.

Key-words: sulfosalt, nomenclature, crystal chemistry, systematics.

DOI: 10.1127/0935-1221/2008/0020-1778
0935-1221/08/0020-1778 $ 18.00

Preamble

Y. MOËLO and E. MAKOVICKY

The International Mineralogical Association (IMA) was founded in 1958. To coordinate its regular activity between general meetings (held every two years initially, and every four years since 1982), the IMA organized different specialized commissions, the best known being the Commission on New Minerals and Mineral Names (CNMMN – now Commission on New Minerals, Nomenclature and Classification, CNMNC). The Commission on Ore Microscopy (COM), since renamed the Commission on Ore Mineralogy, was originally created to establish quantitative data on the optical properties of opaque minerals. The data were subsequently published as *Quantitative Data File* volumes (see the Web-site of the IMA-COM). Within this Commission, the aim of the Sulfosalt Sub-Committee, under the direction of late Dr Roy Phillips, Chairman, was primarily to collect data for a complex group of ore minerals which, at the time, were poorly characterised. During the 13th General Meeting of IMA at Varna, Bulgaria (1982), Dr N. Mozgova succeeded R. Phillips as the new chair, with Dr. Y. Moëlo as secretary and the active collaboration of D.C. Harris (CANMET, Ottawa). Since the 15th IMA meeting at Beijing, China (1990), the activity of the Sulfosalt Sub-Committee has been carried on by us (Moëlo & Makovicky), primarily by compiling the internal reports and disseminating these among the committee members and specialists.

During the last four decades there has been a tremendous evolution of knowledge in the field of mineral systematics. More than 60 % of the mineral species known today were described since the foundation of the IMA-CNMMN. The percentage is even higher in the field of ore minerals, especially the complex groups of sulfosalts and the minerals of the platinum-group elements (Cabri, 1981, 2002). Together with the classic procedures to define the ore minerals, the increasing number of crystal-structure studies has permitted a general deciphering of the crystal chemistry of sulfosalts, which is the basis for a precise definition of mineral species and an understanding of their limits of validity.

This report is an update of the systematics of sulfosalts, reflecting a fruitful collaboration, past and present, of many specialists of sulfosalt mineralogy. Part I presents generalities concerning the definition and chemistry of sulfosalts, as well as some basic principles relevant to sulfosalt crystal-chemical classification. Part II is a detailed presentation of all known sulfosalts species, with selected references about their definition (if recent) and crystal structure (if solved). Problems concerning the definition and nomenclature of some species are discussed on the basis of published data.

The choice of the crystal-chemical scheme used for the classification in Part II is a development of the modular approach to crystal structures. This choice does not necessarily reflect that of all the contributors and committee members, who may have adopted other points of view; above all, the choice is intended to promote the use of crystal-structure analysis as a basis for understanding the complex chemistry of sulfosalts in nature.

A draft version of this report was presented by E. Makovicky during the 19th General Meeting of the IMA at Kobe, Japan (July 23–28, 2006). A copy of this internal report was sent to the national representatives of the COM and CNMNC, for information and critical reading. This circulation led to significant improvements in the preparation of the final manuscript. The report has been approved as a whole by the CNMNC, through the direction of its Secretary, W.D. Birch. Nevertheless, due to the complexity of the sulfosalt group, this final version may contain errors and imperfections, for which we (Y.M. & E.M.) accept sole responsibility. Above all, this report must be considered as a guide for specialists interested in the field of ore mineralogy, and as help for the discovery and description of new mineral species. Without any excessive pretention, we hope that the report will be considered as the "state of the art" in sulfosalt systematics; however, the details of the classification of these species are considered as a basis for further work rather than a definitive scheme. The review of sulfosalt systematics may also be useful in the field of solid-state chemistry and material sciences, as sulfosalts today have aroused increasing attention in the search for new materials with interesting physical properties, such as in thermoelectricity, photovoltaic conversions, and magnetism.

All participating members are sincerely thanked for their contribution. We mention especially Dr N. Mozgova, past President of the Sulfosalt Sub-Committee, as well as Drs J.L. Jambor, N. Cook (Chairman of the IMA-COM) and E.H. Nickel (former Vice-Chairman of the CNMMN), for their careful reading of the text. We also thank E.A.J. Burke and W.D. Birch (Chairman and Secretary of the CNMNC, respectively), and anonymous members of this commission, as well as Prof. Y. Takéuchi (University of Tokyo) and Dr. Y. Matsushita (National Institute for Materials Science), for their useful comments and corrections.

Part I. Revision of sulfosalt definition and nomenclature: generalities

Y. MOËLO and E. MAKOVICKY

1. Definition and general formula

1.1. What is a sulfosalt?

The term "sulfosalt" (or "thiosalt") was created by chemists during the XIXth century, by analogy to complex salts of oxygen, such as sulfate, phosphate, arsenate, antimonate, arsenite and antimonite. Oxysalts generally correspond to the combination of a simple cation with a complex anion $(MeO_m)^{n-}$; this has been confirmed by crystal-structure studies and bond-valence calculations. In sulfosalts, S is considered to play the role of oxygen to similarly form complex anions. Although the configurations found in most modern studies of sulfosalts are more complicated than those encountered in similar oxysalts (*e.g.*, oxyarsenites), the term "sulfosalt" has been preserved as a practical, working category in the field of ore mineralogy. The main reason is that sulfosalt minerals form a genetically well-defined group encountered in specific conditions of ore formation, usually referred to as hydrothermal processes.

1.2. Chemical nomenclature: an extended definition

In the literature, the definition of sulfosalts takes either formal chemistry or structural considerations as the starting point. According to the chemical definition, most sulfosalts are thioarsenites, thioantimonites, thiobismuthites and their combinations, *i.e.*, sulfosalts in which As, Sb and Bi have the same oxidation state +3. Goldfieldite is the only natural example of a thiotellurite (*i.e.*, with Te^{4+}).

Remark: In the chemical literature, elements of group 15 of the periodic system, P, As, Sb and Bi (but not N, chemically very different) are designated as "pnictogens" (like "chalcogens" for S, Se and Te). Compounds in which pnictogens act as anions correspond to pnictides (see "sulfosalt-pnictides" below).

If the bond-valence concept is accepted as a basis for classification, the sulfosalts of both the lower- or higher valence elements [with groups such as $(As^{3+}S_3)^{3-}$ or $(As^{5+}S_4)^{3-}$] represent classification categories equally well justified as those of oxyarsenites $(As^{3+}O_3)^{3-}$ or oxyarsenates $(As^{5+}O_4)^{3-}$. This aspect was first considered by Nowacki (1968, 1969). Any problem encountered for some sulfosalts using this concept will have a near-mirror image in the oxy-realm as well, with somewhat diminished covalence.

A very limited number of natural sulfosalts correspond to thioarsenates (As^{5+} – enargite, luzonite) or thioantimonates (Sb^{5+} – famatinite). There are about 15 thiostannates (Sn^{4+}), mainly related to the ZnS archetypes (sphalerite and wurtzite), and a few thiogermanates (Ge^{4+}). Similarly, sulvanite could be considered as a thiovanadate (V^{4+}), whereas thio tungstates (W^{6+}), and thio molybdates (Mo^{6+}) are exceptional. Thiophosphates (P^{5+}) are as yet unknown in nature. Minerals corresponding to selenio- and telluro-salts, with trivalent As, Sb or Bi, or, exceptionally, Sb^{5+} (permingeatite) are uncommon.

Table 1. Different chemical types of thiosalts/sulfosalts and related chalcogenides.

Anion	Cation	Chemical name	Example	Frequency in nature
S^{2-}	**As^{3+}**	**thioarsenite**	tennantite	numerous species
	Sb^{3+}	**thioantimonite**	boulangerite	numerous species
	Bi^{3+}	**thiobismuthite**	cosalite	numerous species
	Te^{4+}	**thiotellurite**	goldfieldite	exceptional
	(P^{5+})	thiophosphate	none	unknown in nature
	As^{5+}	thioarsenate	enargite	rare
	Sb^{5+}	thioantimonate	famatinite	very rare
	(Bi^{5+})	unknown with S		
	(Te^{6+})	unknown with S		
	Sn^{4+}	thiostannate	stannite	a few
	Ge^{4+}	thiogermanate	briartite	very rare
	V^{5+}	thiovanadate	sulvanite	very rare
	Mo^{6+}	thiomolybdate	hemusite	exceptional
	W^{6+}	thiotungstate	kiddcreekite	exceptional
Se^{2-}	**As^{3+}**	**selenio-arsenite**	giraudite	exceptional
	Sb^{3+}	**selenio-antimonite**	hakite	exceptional
	Bi^{3+}	**selenio-bismuthite**	bohdanowiczite	exceptional
	Sb^{5+}	selenio-antimonate	permingeatite	exceptional
Te^{2-}	**Bi^{3+}**	**telluro-bismuthite**	volynskite	exceptional

In bold type: chalcogeno-salts dealt with in the detailed report (Part II).

Table 1 enumerates these different types of chalcogeno-salts. The present report deals only with the definition and nomenclature of chalcogeno-salts with As^{3+}, Sb^{3+}, Bi^{3+} and Te^{4+}, having lone-pair electrons with generally a strong stereochemical activity, that enhances the complexity of crystal structures. However, Table 2 summarizes all mineral species corresponding to other chemical types of chalcogeno-salts.

In **morozeviczite**, $(Pb, Fe)_3Ge_{1-x}S_4$, **polkovicite**, $(Fe, Pb)_3Ge_{1-x}S_4$, and **florensovite**, $Cu(Cr, Sb)_2S_4$, structural data are insufficient to decide whether these minerals are sulfosalts.

In **cylindrite** and related compounds (its homeotype **lévyclaudite** and its homologue **franckeite**), the composite crystal structure is built on the regular alternation of two types of layers (Makovicky, 1976; Evain *et al.*, 2006a), one pseudo-tetragonal ("Q" type), probably containing the bulk of Sb^{3+} or Bi^{3+}, the other pseudo-hexagonal ("H" type), containing principally Sn^{4+}. This series is thus of the thioantimonite/stannate type.

In **schlemaite**, $(Cu,\nabla)_6(Pb,Bi)Se_4$ (∇ = vacancy), a crystal-structure study (Förster *et al.*, 2003) gave the

Table 2. List of minerals of the chalcogeno-salt types not considered in Part II.

Type	Species	Formula
Thioarsenates (As^{5+})	Billingsleyite	Ag_7AsS_6
	Enargite	Cu_3AsS_4
	Fangite	Tl_3AsS_4
	Luzonite	Cu_3AsS_4
Thioantimonates (Sb^{5+})	Famatinite	Cu_3SbS_4
Thiostannates (Sn^{4+})	Canfieldite	Ag_8SnS_6
	Černýite	Cu_2CdSnS_4
	Chatkalite	$Cu_6FeSn_2S_8$
	Ferrokesterite	$Cu_2(Fe,Zn)SnS_4$
	Hocartite	Ag_2FeSnS_4
	Kesterite	$Cu_2(Zn,Fe)SnS_4$
	Kuramite	Cu_3SnS_4
	Mawsonite	$Cu_6Fe_2SnS_8$
	Mohite	Cu_2SnS_3
	Petrukite	$(Cu,Ag)_2(Fe,Zn)(Sn,In)S_4$
	Pirquitasite	Ag_2ZnSnS_4
	Stannite	Cu_2FeSnS_4
	Stannoidite	$Cu_8(Fe,Zn)_3Sn_2S_{12}$
	Velikite	Cu_2HgSnS_4
Thioindates (In^{3+})	Cadmoindite	$CdIn_2S_4$
	Indite	$FeIn_2S_4$
Thiogermanates (Ge^{4+})	Argyrodite	Ag_8GeS_6
	Barquillite	$Cu_2(Cd,Zn)GeS_4$
	Briartite	$Cu_2(Fe,Zn)GeS_4$
	Calvertite	$Cu_5Ge_{0.5}S_4$
	Germanite	$Cu_{13}Fe_2Ge_2S_{16}$
	Putzite	$(Cu_{4.7}Ag_{3.3})_{\Sigma=8}GeS_6$
Thiovanadates (V^{5+})	Sulvanite	Cu_3VS_4
Thio-molybdate/stannate	Hemusite	Cu_6SnMoS_8
Thio-tungstate/stannate	Kiddcreekite	Cu_6SnWS_8
Thio-molybdate/germanate	Maikainite	$Cu_{20}(Fe,Cu)_6Mo_2Ge_6S_{32}$
Thio-tungstate/germanate	Catamarcaite	Cu_6GeWS_8
	Ovamboite	$Cu_{20}(Fe,Cu,Zn)_6W_2Ge_6S_{32}$
Other mixed types	Colusite	$(Cu_{12}V(Sb,As,Sn)_3)_{\Sigma=16}S_{16}$
	Germanocolusite	$Cu_{13}V(Ge,As)_3S_{16}$
	Nekrasovite	$Cu_{13}V(Sn,As,Sb)_3S_{16}$
	Renierite	$(Cu,Zn)_{11}Fe_4\,(Ge,As)_2S_{16}$
	Stibiocolusite	$Cu_{13}V(As,Sb,Sn)_3S_{16}$
	Vinciennite	$(Cu_{10}Fe_4SnAs)_{\Sigma=16}S_{16}$
Selenio-antimonate	Permingeatite	Cu_3SbSe_4

general formula $(Cu_{6-x}\nabla_x)(Pb_{1-x}Bi_x)Se_4$ (with x close to 0.4), with identical coordinates for Pb and Bi. This species ought to be considered as a Bi-rich selenide of Pb, whereas the Bi-dominant derivative ($x > 0.5$), if it exists, would be a selenio-salt.

1.3. General formula of the principal sulfosalt category with As^{3+}, Sb^{3+}, Bi^{3+} or Te^{4+}

1.3.1. Basic structural formula

As the bulk of natural thioarsenites, thiostannates, *etc*. corresponds structurally to homeotypes of simple sulfides, the term "sulfosalt" is usually limited to the vast group of chalcogeno-salts containing trivalent As, Sb or Bi, as well as (exceptionally) Te^{4+}. They correspond to complex sulfides (more generally chalcogenides) wherein one or more of the cations As^{3+}, Sb^{3+}, Bi^{3+} or Te^{4+} is associated with one or more metallic cation(s), *Me*, as essential (intrinsic) constituents. The S^{2-} anion may be replaced by Se^{2-} or Te^{2-} (chalcogeno-salts). Thus, the general chemical formula can be given as:

$$(Me^{+},\ Me'^{2+},\ etc.)_x\,[(\mathrm{Bi,\ Sb,\ As})^{3+},\ \mathrm{Te}^{4+}]_y \times [(S,\ Se,\ Te)^{2-}]_z. \quad (1)$$

From a structural point of view, atoms of the metals and atoms of the metalloids are not bonded to one another, and are bonded only to anions. Thus, compounds such as arsenopyrite, FeAsS, löllingite, $FeAs_2$, or gudmundite, FeSbS, are not sulfosalts, as As or Sb are directly bonded to Fe, and act as anions relative to the metal. In sulfosalts, it is the lone-electron-pair activity of As^{3+}, *etc*. and, as a consequence, a nearly universally present asymmetric coordination of these metalloids, that causes the structural complexity and specificity of these compounds, setting them apart from nearly all other chalcogenides.

1.3.2. Borderline compounds

Several mineral species combine the structural properties of sulfides (chalcogenides) with those of the other chemical groups, and can be considered as borderline cases.

Sulfur-excess compounds

Sulfur (chalcogen) excess corresponds to S–S bonds in the crystal structure. These occur alongside the metal–sulfur bonds. Such compounds may be qualified as "*persulfides*" ("*perchalcogenides*" – the words "*polysulfides*" and "*polychalcogenides*" are also convenient). A well-known example among sulfosalts is **livingstonite**, $HgSb_4S_6(S_2)$ (Srikrishnan & Nowacki, 1975). It is also the case for **moëloite**, $Pb_6Sb_6S_{14}(S_3)$ (Orlandi *et al.*, 2002), and of the synthetic sulfosalts $Cu_4Bi_4X_9$ (X = S, Se – Bente & Kupčik, 1984; Makovicky *et al.*, 2002). Another possible example is that of **museumite**, $Pb_2(Pb,Sb)_2S_8[Te,Au]_2$ (Bindi & Cipriani, 2004a).

Subsulfides/subchalcogenides

In this case, the compounds have a sulfur (chalcogen) deficiency relative to those with 'normal' valences. Cations in their crystal structure show metal–metal or metalloid–metalloid bonding alongside the metal–chalcogen bonding. The name of "subsulfides" ("subchalcogenides") has been used for such cases.

As the first example, within the tetradymite homologous series of layered structures, all compounds having a chalcogen deficit display pairs of Bi atomic layers, implying Bi–Bi bonding. Such is the case for the thiobismutite **babkinite**, $Pb_2Bi_2(S,Se)_3$.

In **gabrielite**, $Cu_2AgTl_2As_3S_7$, the valence balance is respected. Nevertheless, examination of the crystal structure (Balić-Žunić *et al.*, 2006) showed that Tl atoms form Tl–Tl pairs with a short distance (3.09 Å) corresponding to the sum of covalent radii, that indicates a metal–metal interaction. This is similar to the interaction in the Hg–Hg pairs (2.535 Å) in deanesmithite, $(Hg_2)Hg_3CrO_5S_2$ (Szymañski & Groat, 1997). In **stalderite**, $Cu(Zn,Fe,Hg)_2TlAs_2S_6$ (Graeser *et al.*, 1995),

and its isotype **routhierite**, $CuHg_2TlAs_2S_6$, Tl–Tl pairs, with a somewhat longer bond, are also present.

Dervillite, Ag_2AsS_2, **vaughanite**, $HgTlSb_4S_7$, and **fettelite**, $Ag_{24}HgAs_5S_{20}$, all with unknown crystal structures, apparently have a small excess of positive charges with respect to the charge balance, thus probably indicating some cation–cation bonding. The "excess" of positive charges is more pronounced in **criddleite**, $Ag_2Au_3TlSb_{10}S_{10}$, and **tvalchrelidzeite**, Hg_3SbAsS_3 (Yang *et al.*, accept.). In all of these structures either metalloid–metalloid or metal–metalloid bonds are probably present, or even entire antimonide portions exist. Analogies to these situations are pääkkonenite Sb_2AsS_2 (Bonazzi *et al.*, 1995) and chalcothallite (a sulfide–antimonide of Tl and Cu) (Makovicky *et al.*, 1980).

The same situation is encountered in two PGE (Platinum Group Elements)-bearing chalcogenides, **borovskite**, Pd_3SbTe_4, and **crerarite**, $(Pt,Pb)Bi_3(S,Se)_{4-x}$, for which the valence state of the metalloid is unknown.

Sulfosalt-pnictides

In the crystal structure of **hauchecornite**, $Ni_9Bi(Bi,Sb)S_8$, the pure Bi atom position is preferentially bound to four S atoms (together with two Ni atoms) and acts partly as a cation, whereas the mixed (Bi, Sb) atom is exclusively bound to Ni atoms, and acts as an anion (Kocman & Nuffield, 1974). The same duality can be observed in other species isotypic with hauchecornite: **arsenohauchecornite**, **bismutohauchecornite**, **tellurohauchecornite** and **tucekite**. All these minerals are transition compounds between sulfosalts and pnictides.

Halide-sulfides (or halogeno-sulfides)

Ardaite, $Pb_{17}Sb_{15}S_{35}Cl_9$, **dadsonite**, $Pb_{23}Sb_{25}S_{60}Cl$, and **playfairite**, $Pb_{16}(Sb,As)_{19}S_{44}Cl$, are three examples of natural chloro-sulfosalts. Only the crystal structure of dadsonite is known (Makovicky *et al.,* 2006b), but here, despite the very low Cl/S ratio, the Cl atom is fixed in a specific atomic position. Consequently Cl is essential for the formation of the mineral species.

Oxide (hydroxide)-sulfides

In **scainiite**, $Pb_{14}Sb_{30}S_{54}O_5$ (Moëlo *et al.*, 2000), the O atoms are bound preferentially to Sb atoms, in a way analogous to that in kermesite Sb_2S_2O. Scainiite can be considered as an oxy-sulfosalt.

In **cetineite**, $\sim NaK_5Sb_{14}S_6O_{18}(H_2O)_6$, both the SbS_3 and SbO_3groups are present, and K is bound almost exclusively, and Na completely, to O atoms (Sabelli *et al.*, 1988; Wang & Liebau, 1999), with additional H_2O molecules bound only to Na. This compound is thus a hydrated thio-oxysalt, like its Na-pure end-member, **attensite** (Sejkora & Hyrsl, 2007).

In **sarabauite**, $(Sb_4S_6)(CaSb_6O_{10})$, Sb atoms again bind both to S and O atoms, whereas Ca atoms are exclusively bound to O atoms (Nakai *et al.*, 1978). This compound could be considered to be a "thio-oxysalt".

Apuanite and **versiliaite** are two Sb-containing oxy-sulfides, derived from the oxide schafarzikite (Mellini & Merlino, 1979). In apuanite, ideally $Fe^{2+}Fe^{3+}_4Sb^{3+}_4O_{12}S$, the Sb is bound only to O; thus the mineral cannot be considered to be an oxy-sulfosalt. In versiliaite, $Fe^{2+}_2(Fe^{3+}_3Sb^{?+}_{0.5}Zn^{2+}_{0.5})_{\Sigma=4}Sb^{3+}_6O_{16}S$, the situation is more complicated, as some Sb partly replaces Fe in a tetrahedral site, coordinated by 1 S and 3 O atoms. The Sb should correspond to Sb^{5+}, which suggests that versiliaite is a combination of antimonite-antimonate with thio-antimonate.

Hydrated sulfosalts

In **gerstleyite**, $Na_2(Sb,As)_8S_{13}\cdot 2H_2O$ (Nakai & Appleman, 1981), Sb is bound only to S atoms, whereas Na is bound to S atoms and H_2O molecules; the mineral corresponds to a hydrated sulfosalt. Numerous synthetic hydrated sulfosalts have been synthesized.

Oxy-chloro-sulfides

Minor contents of O and Cl have been recently discovered in two new Pb–Sb sulfosalts, **pillaite**, $Pb_9Sb_{10}S_{23}ClO_{0.5}$, and **pellouxite**, $(Cu,Ag)_2Pb_{21}Sb_{23}S_{55}ClO$. Crystal-structure studies proved the O and Cl to be intrinsic components (Meerschaut *et al.*, 2001; Palvadeau *et al.*, 2004). These two minerals correspond to oxy-chloro-sulfosalts.

1.4. Conclusion

Taking into account the mineral species listed in Table 2 (more than 40 compounds) and those corresponding to the general formula [1] above (see the alphabetical index), as well as the borderline compounds, more than 260 mineral species belong to the "sulfosalt group" (sulfosalts and other chalcogeno-salts). There are also about 200 incompletely defined minerals (so-called "UM" – unnamed minerals) in the literature related to this vast group (Smith & Nickel, 2007), mainly because the chemical composition alone was determined by EPMA, which is generally easier to obtain than crystallographic data.

The "sulfosalt group" is as heterogeneous from a crystal-chemical point of view as, *e.g.*, the silicate group. Consequently, a rigorous classification and nomenclature of sulfosalts is much more complicated than that of more restricted mineral groups which have been reexamined in the past by specific committees of the IMA (amphiboles, micas, zeolites...). As already mentioned, some sulfosalts fit perfectly in specific sulfide groups; for instance, most of the sulfostannates belong structurally within the sphalerite group. Only the vast group of sulfosalts with As^{3+}, Sb^{3+}, Bi^{3+} or Te^{4+} stands structurally as an almost separate family – this group is the topic of the present report. At the present stage of research, some groups of these sulfosalts can already be neatly classified on a crystal-chemical basis, whereas others await further discoveries for achieving the same depth of classification. The latter are grouped on purely chemical principles. The intention of the report is to assist further development of mineralogical studies in the field of complex sulfides.

Table 3. Classification hierarchy within the present sulfosalt report.

Level of classification	Example
Class	Chalcogenides
Chemical sub-type	Sulfosalts
Large structural family (plesiotypic and merotypic series, other groups)	Boulangerite plesiotypic family
Homologous series	Lillianite homologous series
	Plagionite homologous series
Iso- and homeotypic series	Tetrahedrite isotypic series; aikinite homeotypic series
Species	
Sub-species: Polytypes	Pearceite and polybasite polytypes

2. Sulfosalts with As^{3+}, Sb^{3+}, Bi^{3+} or Te^{4+}: chemistry and classification principles

2.1. General outline

There are various ways of classifying minerals. Some classifications are extrinsic (*i.e.*, a paragenetic classification), but intrinsic ones are the best for development of the scientific field of mineralogy. Today, the deeper level of knowledge about minerals is that of their crystal structure (their "genetic code"); thus, the best classification ought to be a crystal-chemical classification. The first general crystal-chemical approach for sulfide minerals and related species was presented by Hellner (1958). Since the end of the 1960s, several mineralogical crystallographers have paid special attention to the sulfosalt group: Makovicky (1967), Nowacki (1969), Takéuchi & Sadanaga (1969), Povarennykh (1971), Wuensch (1974) and Edenharter (1976). In the following decade, some important aspects of the systematics of sulfosalts were emphasized: polymerization of complex anions and comparison with the classification of silicates (Ramdohr & Strunz, 1978; Kostov & Minčeva-Stefanova, 1981; Nakai & Nagashima, 1983), problems of non-stoichiometry (Mozgova, 1984), modular analysis of the crystal structures (Makovicky, 1981, 1985a, 1989). Noteworthy is also the more recent work of Takéuchi (1997) on tropochemical cell-twinning (Remark: 'cell-twinning', defined by Takéuchi *et al.* (1979), differs from ordinary twinning – see Nespolo *et al.*, 2004).

Table 3 presents the hierarchical structure of the system chosen for this review. Whenever possible, the system is based on the level of structural relationships among mineral species. Thus, for a large number of species the system is essentially a *modular* classification. The general definition of isotypic, homeotypic, and homologous series is given in "Nomenclature of Inorganic Structure Types" (Lima-de-Faria *et al.*, 1990). The best known example of homeotypic series is certainly the aikinite–bismuthinite series (Topa *et al.*, 2002a). A clear example of homologous series is that of the plagionite series, $Pb_{3+2n}Sb_8S_{15+2n}$ (with n = 0, 1, 2, or 3). The lillianite series is more complex, with numerous homeotypic and homologous phases. Dimorphism has been recognized in several, relatively rare cases, *e.g.* for proustite *versus* xanthoconite, Ag_3AsS_3, for pyrargyrite *versus* pyrostilpnite, Ag_3SbS_3, or for clerite *versus* synthetic monoclinic $MnSb_2S_4$.

The notion of family is less rigorous and corresponds to the "plesiotypic" and "merotypic" series of Makovicky (1997), or to more complex groups which may include such series. As detailed in Ferraris *et al.* (2004), within "plesiotypic" and "merotypic" series are grouped complex crystal structures showing a lower degree of topologic similarities than homologous series. For instance, in the zinkenite family, crystal structures consist of rods with simpler internal structure that are organized in different ways around pseudo-trigonal columns with Pb atoms in mono- or bicapped prismatic coordination. This zinkenite family belongs to the supergroup of Pb sulfosalts with rod-type building blocks.

Definition of many of these series is fortified by data for a number of synthetic sulfosalts that do not have natural equivalents (*e.g.*, especially in Makovicky 1989, 1997, and Ferraris *et al.*, 2004). The current presentation, which in many aspects is distinct from the general classification of Strunz & Nickel (2001), is not intended to be an overall crystal-chemical classification; rather, the presentation is a review of sulfosalt species, organized on the basis of chemistry and, where possible, on the basis of crystal chemistry. In the future, discovery of new sulfosalt species, as well as the resolution of up to now unknown crystal structures, will permit the development and improvement of this sulfosalt systematization.

2.2. Chemistry

The formula indicated is the ideal formula derived from a crystal-structure study or, if the species is poorly characterised, it is the simplified formula given for the type sample. For non-commensurate composite structures (for instance cylindrite), a reduced formula is given, which is always an approximation of the true formula.

Many sulfosalts have a complex chemistry, and frequently a minor chemical component appears to be essential for the stabilization of a mineral species (*e.g.*, Cu in natural meneghinite, Cl in dadsonite). For a given species, the choice of the structural formula must indicate such minor components, whereas other elements, which are verifiably not essential (solid solution), can be excluded from the ideal formula as much as possible.

For the derivation of simplified formulae, it is important to know the principal substitution rules encountered among sulfosalts. For instance, if there is minor As together with

major Sb, in many cases As can be totally substituted by Sb, and thus will disappear from the final structural formula. On the contrary, Cl even in low concentration (some tenths of a percent – see dadsonite), is expected to play a specific role and therefore, generally, must be retained in the formula. The avoidance or retention of a minor component necessitates a precise knowledge of the crystal structure, particularly of the specific atomic positions at which this minor component is located. Experimental studies are often the only way to obtain the compound without the minor component, and to verify that this pure compound has the same crystallographic characteristics. For instance, natural geocronite always contains minor amounts of As, but synthetic As-free geocronite is known (Jambor, 1968).

Table 4 presents a non-exhaustive list of various substitution rules encountered in sulfosalts. It represents a first step in the examination of new EPMA data, in order to correlate them more or less precisely with a chemical group of sulfosalts or a definite mineral species.

Remark: A one-for-one atom substitution does not necessarily imply that one element substitutes another on the same position in the crystal structure. Sometimes, it may imply distinct sub-sites within a polyhedron, or quite distinct sites. The mechanism may be more complex for heterovalent substitution rules.

The role of temperature can be important in controlling the substitution. Extended solid solutions at high temperature (in hydrothermal conditions: 300 to 400 °C) may be drastically restricted at low temperature (epithermal conditions). For instance this aspect is particularly important in the aikinite–bismuthinite series (Topa *et al.*, 2002a). The substitution rules in Table 4 generally correspond to solid solutions, but the rules may also describe the homeotypic derivation of a species of complex chemistry, from another species that has a very close structure but a simpler composition (*e.g.*, all Pb- and Cu-containing derivatives of bismuthinite in the aikinite–bismuthinite homeotypic series).

Careful EPMA of sulfosalts in routine conditions (for instance, 20 kV, 20 nA, counting time 10 s, compositionally close secondary standards) permits a very good mineral identification, if no minor element is omitted (down to 0.*n* wt.%). When such minor elements are present, and are not essential constituents (contrary to the 0.4 wt.% Cl in dadsonite, $Pb_{23}Sb_{25}S_{60}Cl$), their subtraction using the substitution rules from Table 4 gives a simplified chemical formula that generally results in only one mineral species.

Remark: Exceptionally, some sulfosalts have a very low content of oxygen (0.n wt.%), which is nevertheless essential for their stability, as their crystal structure reveals a specific position for oxygen atoms (pillaite, pellouxite). EPMA would not be sufficient to prove the presence of oxygen within the structure, due to the easy formation of an oxidation film at the polished surface of the sample.

The search for minor elements is important both for mineral identification and for ore geochemistry and regional metallogeny, as is well known especially for the tetrahedrite series. Another example is the andorite series, which contains small amounts of Sn, Cd, and In in the Potosi district (Bolivia), whereas in Romania the characteristic minor elements are Mn and Fe.

2.3. Crystal structure and modular analysis

Knowledge of the crystal structure is not necessary for the validation of a new mineral species by the CNMNC of the IMA. Nevertheless, for sulfosalts having a large unit cell (*e.g.*, most of the Pb sulfosalts), a solution of the crystal structure is today strongly recommended in order to prove the uniqueness of a new mineral species, and to reveal the role of minor components in the structure and composition. For these large structures it is also the only way to obtain a precise structural formula, and in some cases to decide whether a solid solution exceeds the 50 % limit in a characteristic site of the crystal structure, thereby giving a new isotypic mineral species.

Differences between the bonding strength and character of the metalloids (As, Sb, Bi) and metals, especially Pb, are less pronounced in sulfosalts than those between the bonding character in tetrahedral/triangular coordinations of Si, B, P, *etc*. and the associated cations in the relevant oxysalts. This difference, together with the variable types of coordination polyhedra of As, Sb and Bi and other crystal-chemical phenomena connected with the covalent character of bonding in the majority of sulfosalts, makes a polyhedral classification ineffective for most sulfosalt families. The approach at a higher level of organization in accordance with the principles of modular analysis seems to be the most efficient way to obtain a crystal-chemical classification of sulfosalts. Modular analysis of a crystal structure is based on the discrimination of sub-units called *building blocks*. This does not signify that interatomic bonding between constitutive building blocks is weaker than inside these blocks (they can be as strong, indeed stronger).

Typical for the combined arrays of metalloids and Pb and some other metals (*e.g.*, Ag), as well as for some fairly pure Bi or Sb arrays, are extensive building blocks. The blocks approximate the topology of the PbS structure (cases with low activity of lone electron pairs) or of the SnS structure (TlI, $TlSbS_2$ are also approximations) for arrays that have well-expressed activity of lone electron pairs. lone electron pairs of metalloids are accommodated by the archetypal motif (often congregating in common spaces, so-called "lone electron pair micelles") whereas the contact between blocks takes place via mutually noncommensurate surfaces or by means of unit-cell twinning (details in Makovicky 1989, 1997). Structures with low contents of metalloids tend to follow the topologies dictated by the principal metals, eventually modified to satisfy the metalloid requirements as well.

The structural principles outlined in the preceding paragraph commonly lead to the presence of homologous series differing in the size of blocks but not in the principles of their recombination into one structure, or to more general families of related structures when the simple homologous expansion is hindered on structural grounds. Increase in the block size alters the Pb(Sn)/metalloid ratio in favour of divalent metals; the same may happen in favour of combined AgBi or, rarely, even CuBi arrays. More extensive arrays and less expressed lone-electron-pair character may be favoured by elevated temperatures and by the substitution of S by Se or even Te.

Table 4. Principal chemical substitution rules observed in natural sulfosalts.

Anions	Comments/Examples
$S^{2-} \leftrightarrow Se^{2-}$	cannizzarite ↔ wittite (***e*** – see abbreviations at the bottom of the table)
$(Se, S)^{2-} \rightarrow Te^{2-}$	watkinsonite (***l***)
$Cl^{-} \leftrightarrow S^{2-}$	pellouxite, dadsonite (***l***), coupled with cation substitutions
Cations	**Comments/ Examples**
$Bi^{3+} \leftrightarrow Sb^{3+}$	easy and frequent
$Sb^{3+} \leftrightarrow As^{3+}$	easy and frequent (especially: tetrahedrite–tennantite isoseries)
$As^{3+} \rightarrow Bi^{3+}$	jordanite (***l***); tennantite (***e*** – but rare)
$Pb^{2+} \rightarrow Sn^{2+}$	cylindrite, franckeite (***e***)
$Pb^{2+} \rightarrow (Mn, Fe, Cd)^{2+}$	andorite series (***l***)
$Cd^{2+} \rightarrow Pb^{2+}$	kudriavite (***l***)
$3\ Pb^{2+} \rightarrow 2\ Bi^{3+} + \nabla$	easy in galena, but difficult to prove in Pb sulfosalts (Ag-free lillianite – ***l***)
$3\ Pb^{2+} \rightarrow 2\ Sb^{3+} + \nabla$	limited in galena, possible but not proved in Pb sulfosalts
$2\ Pb^{2+} \leftrightarrow Ag^{+} + Bi^{3+}$	lillianite series (***e***)
$2\ Pb^{2+} \leftrightarrow Ag^{+} + Sb^{3+}$	andorite series (***e***)
$2Pb^{2+} \rightarrow (Ag, Tl)^{+} + As^{3+}$	sartorite series
$Bi^{3+} + \nabla \leftrightarrow Pb^{2+} + Cu^{+}$	bismuthinite–aikinite series (***e*** – ordered compounds (homeotypes) with decreasing *T*); cosalite, nuffieldite (***l***)
$Sb^{3+} + \nabla \leftrightarrow Pb^{2+} + Cu^{+}$	rare (zinkenite – ***l***; meneghinite)
$Fe^{2+} + Pb^{2+} \rightarrow Cu^{+} + Bi^{3+}$	kobellite homologous series (***l***)
$Bi^{3+} \rightarrow 3\ Cu^{+}$ (distinct sites)	pavonite series (***l***). In this series and in some other sulfosalts, Cu may enter various interstitial sites, and the exact substitution rule needs accurate studies (first of all, precise crystal-structure data)
$2\ Bi^{3+} \rightarrow 2\ Ag^{+} + 4\ Cu^{+}$ (distinct sites)	angelaite
$Bi^{3+} \rightarrow In^{3+}$	kudriavite
$Sb^{3+} + Ag^{+} \leftrightarrow Pb^{2+} + Mn^{2+}$	at high temperature; ordering at low *T*: uchucchacuaite
$Tl^{+} \leftrightarrow Ag^{+}$	never in the same atomic position! Limited at low *T* (rathite?); in the sartorite homologous series, Tl and Ag are apparently distributed in distinct sites, or in distinct sulfosalts (Lengenbach deposit)
$Fe^{2+} \leftrightarrow Mn^{2+}$	jamesonite–benavidesite (***e***)
$Hg^{2+} \leftrightarrow Zn^{2+}, (Fe^{2+})$	routhierite–stalderite (***e***)
Mutual substitution among $Fe^{2+} \leftrightarrow Zn^{2+} \leftrightarrow Mn^{2+} \leftrightarrow Cd^{2+} \leftrightarrow Hg^{2+}$	easy, up to 2 metal atoms among 12 in the tetrahedrite series (some Sn or Pb also possible)
$Ag^{+} \leftrightarrow Cu^{+}$	tetrahedrite series (***e***); lengenbachite (***l***); pearceite–polybasite series (***l***)
$2\ Fe^{2+} \leftrightarrow Fe^{3+} + Cu^{+}$	tetrahedrite series (up to 1 atom in the structural formula)
$Fe^{3+} + Cu^{+} \leftrightarrow 2\ Cu^{2+}$	tetrahedrite series (remark: the presence of divalent Cu in sulfides *etc.* may be a purely formal expression of the true situation; this is discussed by the specialists of chalcogenide solid chemistry)
$(Fe^{2+}, Zn^{2+}...) + (As, Sb)^{3+} \leftrightarrow Cu^{+} + Te^{4+}$	tetrahedrite–goldfieldite series (up to 2 atoms in the structural formula)
$Cu^{+} + (Sb,As)^{3+} \leftrightarrow \nabla + Te^{4+}$	tetrahedrite–goldfieldite series (when Te > 2 atoms in the structural formula)
$Fe^{2+} \leftrightarrow 2\ Cu^{+}$	cylindrite–lévyclaudite (***e***)
$Cs^{+} \leftrightarrow Tl^{+}$	exceptional (galkhaite – ***e***)
$Cu^{+}\ (Ag^{+}?) \rightarrow Au^{+}$	exceptional (goldfieldite – ***l***; needs crystal-structure study)
$Ag^{+} \rightarrow Au^{+}$	exceptional (polybasite)
Solid solutions with unknown substitution rules	
$S^{2-} \rightarrow \nabla^{0}$	with increasing Ag content in freibergite (and decreasing unit cell)
In^{3+} in ramdohrite (***l***)	
Tl^{+} in owyheeite (***l***)	

Abbreviations: ***e*** = easy/extended substitution; ***l*** = limited; ∇ = vacancy; ↔ = reciprocal; → = unidirectional.

Blocks of these archetypal structures can be, according to the general vocabulary:

- 0-dimensional (0D): fragments; clusters; molecules
- 1D: chains, rods, ribbons, columns (= complex rods)
- 2D: layers (generally plane, sometimes undulated); sheets (= layers with weaker interlayer bonding); slabs (= thick, complex layers)
- 3D: cases where the entire structure approximates an archetype (= 3-dimensional; no blocks distinguished) are rarer.

Numerous Pb sulfosalts, among them the boulangerite plesiotypic series, have been described using an intermediate category between 2D- and 1D blocks. The intermediate category is the "*rod-layer*" type, which results from the connection of rods along one direction (Makovicky, 1993).

The description of the general organization of a crystal structure involves the discrimination of the constitutive building blocks, and how they are interconnected. The description thus permits definition of the type of architecture of the crystal structure. The main part of the architectural types is based on a single type of building block. A significant part results in the combination of two types of blocks, as in some homologous series. The most complex architectural type is the boxwork type, a combination of three distinct blocks, as exemplified by the crystal structure of neyite (Makovicky *et al.*, 2001a).

2.4. Non-stoichiometry in sulfosalts

The concept of non-stoichiometry in sulfosalts has been promoted especially by Mozgova (1984, 2000), and is discussed briefly here by using both a general approach and specific examples. The most common case of non-stoichiometry corresponds to various solid solutions, as presented in Table 4. Some substitution rules, isovalent or heterovalent, do not change the total number of atoms in the structural formula (= in the unit cell); other substitutions imply filling, or creating vacancies, which changes the total number of atoms present.

At the opposite end of the scale, syntactic intergrowths correspond to a mixture, at the (pseudo-)crystal level, of 3D domains of (at least) two species with similar crystal structures. Such intergrowths have various origins and present various textures (exsolution process, myrmekites by decomposition or substitution, simultaneous precipitation…). When the size of domains decreases to a micrometer scale, it becomes difficult to recognize the domains even at the highest magnification with a metallographic microscope, and microprobe analysis typically shows analytical dispersion around theoretical stoichiometric formulae; examples are the plagionite (Mozgova & Borodaev, 1972) and andorite–fizélyite (Moëlo *et al.*, 1989) homologous series.

Intergrowths of the aforementioned type may be present even at a nanometric scale, and are visible with high-resolution techniques such as electron microscopy. SEM may give good images, which generally reveal a strong geometrical anisotropy of intergrowths, towards 2D domains with more or less pronounced stacking disorder. One of the best approaches is HRTEM, which permits a precise crystallographic characterisation of associated sulfosalts. These species correspond to two closely related members of a homologous series (Pring *et al.*, 1999), exceptionally even to more distinct species (Pring & Etschmann, 2002; Ciobanu *et al.*, 2004).

The most complex cases encountered in the sulfosalt group are exsolution aggregates of the bismuthinite series, wherein some samples correspond to a nanometric association of two or three members, some of them with their own deviations from a simple stoichiometry, which are related to a solid-solution mechanism (Topa *et al.*, 2002b).

Of course, these various types of non-stoichiometric members will give different X-ray signatures in powder diagrams or by single-crystal study.

A special example of non-stoichiometry is that of sulfosalts with layered composite non-commensurate structure (cylindrite and related compounds – Makovicky & Hyde, 1981, 1992). In these sulfosalts, each of the two constituent layers may have a stoichiometric formula, but the non-commensurate (non-integer) ratio between one or two pairs of in-plane parameters results in a "non-stoichiometric" (*i.e.*, complex) structural formula.

Part II. Review of sulfosalt systematics

IMA-COM Sulfosalt Sub-Committee

Introduction: general presentation of sulfosalt species

This general presentation takes into account the sulfosalt species given by "Fleischer's Glossary of Mineral Species" (Mandarino & Back, 2004) (see also Blackburn & Dennen, 1997; Martin & Blackburn, 1999, 2001; Martin, 2003), plus the new species published or approved recently by the CNMNC-IMA (see its website). The presentation is concerned with more than 220 sulfosalt species, for which an alphabetical list is given at the end of the text, together with an appendix that lists discredited species.

As the crystal-chemical classification of sulfosalts is incomplete at present, the following general presentation of sulfosalt mineral species is subdivided into large chemical groups. Within each group, subdivisions are generally based on well-defined structure types.

Sulfosalt species whose specific crystal structure does not have a close relationship to those of other species are indicated separately as "*Single type*". If the crystal structure of a species is not known, this species is classified, as much as possible, with sulfosalts that have a similar chemistry.

About the references

To reduce as much as possible the number of references cited in this review, only the following have been included:

- systematically, the studies presenting the crystal structures of the sulfosalt species (noted "STR" afterwards), but also taking into account data obtained on synthetic compounds ("synth." afterwards);
- recent papers that define sulfosalt species (since 1990, or older, when necessary);
- all references needed for the presentation and discussion of problems of definition and nomenclature.

Crystallographic data (unit-cell parameters, symmetry, space group) have been avoided, except when a change in symmetry or space group appears crucial for the distinction between two very close species (*e.g.*, giessenite *versus* izoklakeite).

All other references and basic data are available in fundamental books on systematic mineralogy (*e.g.*, Strunz & Nickel, 2001; Mandarino & Back, 2004), as well as in PDF (JCPDF) or ICSD (FIZ – Karlsruhe) databases. Concerning the crystal structures, especially noteworthy is the extensive work of Dr Y. Matsushita, who has compiled systematically all chalcogenide and related structures, both of natural and synthetic phases. Access to the data-library is free at http://www.crystalmaker.co.uk/library/chalcogenides.html.

Where problems are present regarding the definition of a species, relevant comments are given after the presentation of each species or group. The aim is to present the current status of sulfosalt definition, nomenclature and classification for all specialists interested in this field of research, thereby pointing out various unsolved questions and facilitating the discovery of new mineral species.

1. Sulfosalts with atom ratio of cation/chalcogen = 1

1.1. Binary sulfosalts ($MPnCh_2$), where *M* = univalent cation (Cu, Ag, Tl); *Pn* = pnictogen (As, Sb, Bi); *Ch* = chalcogen

These sulfosalts are presented according to the organisation of pnictogen polyhedra.

1. Matildite isotypic series (trigonal derivatives of PbS, according to $(PbS)_{111}$ slices)

Matildite, $AgBiS_2$
STR (synth.): Geller & Wernick (1959).
Bohdanowiczite, $AgBiSe_2$
STR (synth.): Geller & Wernick (1959).
Volynskite, $AgBiTe_2$
STR (synth.): Pinsker & Imamov (1964).

All these structures could also be considered as derivatives of the CdI_2 archetype (single layer of $BiCh_6$ octahedra), with Ag atoms intercalated between the layers (so-called "intercalation compounds"). However, these old structure determinations appear to be (pseudo)cubic approximations, as it is unrealistic to consider regular $BiCh_6$ octahedra because of the lone-electron-pair of Bi^{3+}.

2. Aramayoite isotypes

Aramayoite, $Ag_3Sb_2(Bi,Sb)S_6$
Baumstarkite, $Ag_3Sb_3S_6$
Definition of baumstarkite and STR of aramayoite and baumstarkite are given by Effenberger *et al.* (2002).

3. (Single type)

Cuboargyrite, $AgSbS_2$
Defined by Walenta (1998).
STR (synth.): Geller & Wernick (1959).

4. (Single type) (sheared derivative of SnS archetype)

Miargyrite, $AgSbS_2$
STR: Smith *et al.* (1997).

5. (Single type)

Smithite, $AgAsS_2$
STR: Hellner & Burzlaff (1964). In the structure, As in triangular pyramidal coordination forms As_3S_6 trimers arranged in columns parallel to *b*.

6. (Single type) Cyclic trigonal

Trechmannite, $AgAsS_2$
STR: Matsumoto & Nowacki (1969). Arsenic in triangular pyramidal coordination forms As_3S_6 trimers that have trigonal symmetry.

7. Emplectite isotypic series

Emplectite, $CuBiS_2$
STR: Portheine & Nowacki (1975a).
Chalcostibite, $CuSbS_2$
STR: Razmara *et al.* (1997).

8. Weissbergite homeotypic pair

Weissbergite, $TlSbS_2$
STR: Rey *et al.* (1983).
Lorandite, $TlAsS_2$
STR: Balić-Žunić *et al.* (1995).
Weissbergite is a direct substitution derivative of the SnS archetype, whereas lorandite is a stacking variant related to this archetype with a double-layer periodicity.

1.2. Ternary sulfosalts ($M1^{+}M2^{2+}PnS_3$)

1. Freieslebenite family (3-dimensional PbS-like arrays)

Freieslebenite (isotypic) series
Freieslebenite, $AgPbSbS_3$
STR: Ito & Nowacki (1974a).
Marrite, $AgPbAsS_3$
STR: Wuensch & Nowacki (1967).
Related
Diaphorite, $Ag_3Pb_2Sb_3S_8$
STR: Armbruster *et al.* (2003).
Quadratite, $Ag(Cd,Pb)(As,Sb)S_3$
STR: Berlepsch *et al.* (1999).
Schapbachite, $Ag_{0.4}Pb_{0.2}Bi_{0.4}S$
Redefinition: Walenta *et al.* (2004).
Schirmerite **(Type 1)**, $Ag_4PbBi_4S_9$

Schapbachite and schirmerite (Type 1): the same compound?
Schapbachite, initially defined as the cubic form of $AgBiS_2$, was subsequently discredited because it is a high-temperature form that always decomposes at low T to its trigonal dimorph, matildite. Schapbachite, was recently redefined by Walenta *et al.* (2004) through the study of a sample containing a significant amount of Pb (~ 20 % of the cation sum). This Pb content seems necessary for the stabilization of schapbachite, and ought to appear in the chemical formula.

Previously, Bortnikov *et al.* (1987) discovered a mineral ("Phase I") that has the composition originally assigned to schirmerite (Type I), $Ag_4PbBi_4S_9$ (that is, strictly in the $AgBiS_2$–PbS pseudo-binary system), but without X-ray data. This schirmerite is very close to the stable form of schapbachite ($Ag_4PbBi_4S_9 = Ag_{0.445}Pb_{0.11}Bi_{0.445}S$); however, in the absence of crystallographic data, it is not possible to conclude whether schirmerite is equivalent to schapbachite or corresponds to an ordered dimorph.

2. Bournonite isotypic series

Bournonite, $CuPbSbS_3$
STR: Edenharter *et al.* (1970).
Seligmannite, $CuPbAsS_3$
STR: Edenharter *et al.* (1970).
Součekite, $CuPbBi(S,Se)_3$

3. Mückeite isotypic series

Mückeite, $CuNiBiS_3$
STR: Bente *et al.* (1990). Isolated BiS_{3+1} polyhedra.
Lapieite, $CuNiSbS_3$
Malyshevite, $CuPdBiS_3$
Def.: Chernikov *et al.* (2006).
IMA 2007-003, $CuPtBiS_3$

4. (Single type)

Christite, $HgTlAsS_3$
STR: Brown & Dickson (1976). It is a layered structure where a HgS mono-atomic layer alternates with a di-atomic layer ($TlAsS_2$) of the SnS archetype.

1.3. Quaternary sulfosalts ($M1^{+}M2^{+}M3^{2+}Pn_2S_5$)

Hatchite isotypes

Hatchite, $AgTlPbAs_2S_5$
STR: Marumo & Nowacki (1967a); Boiocchi & Callegari (2003).
Wallisite, $CuTlPbAs_2S_5$
STR: Takéuchi *et al.* (1968); Boiocchi & Callegari (2003).

2. Lead sulfosalts with a pronounced 2D architecture, their derivatives with a composite structure, and related compounds

2.1. Layered sulfosalts related to the tetradymite archetype

Tetradymite is the archetype of a complex group of chalcogenides, composed of numerous natural and synthetic compounds, of a great interest in the field of thermoelectrics. All crystal structures are derivatives of a NaCl distorted close packing, generally with trigonal symmetry. Within this group, minerals can be classified according to two complementary homologous series:

- the first homologous series results from the combination of (Bi_2) layers with tetradymite-type layers (Bi_2Ch_3) (Ch = Te, Se, S), giving the general formula $\boldsymbol{n}\mathbf{Bi_2}.\boldsymbol{m}\mathbf{Bi_2}\boldsymbol{Ch}_3$;
- the second homologous series ("aleksite series") corresponds to an expansion of the tetradymite layer, related to an incorporation of Pb in specific atom sheets, according to the general formula $\mathbf{Pb}_{(n-1)}\mathbf{Bi_2}\boldsymbol{Ch}_{(n+2)}$;
- an unique case (babkinite) results apparently from the combination of these two trends (see below).

Details concerning the crystal chemistry of minerals of this group, especially complex Pb–Te derivatives, are presented by Cook *et al.* (2007a, 2007b). These Pb derivatives relate to the chemical definition of sulfosalt; but one must point that, in all this group, Bi^{3+} ought to present a fairly its octahedral coordination, indicating a weak stereochemical activity of lone electron pair. Within this group are six Pb-Bi sulfosalts, among which five belong to the aleksite homologous series**.**

Aleksite homologous series, $Pb_{(n-1)}Bi_2Ch_{(n+2)}$

Kochkarite, $PbBi_4Te_7$ (c = 72.09 Å) (n = 1, 2)
STR (synth. – c = 23.6 Å): Petrov & Imamov (1970); Shelimova *et al.* (2004). The structure has a regular alternation, along c, of two layers, the first of which is five atoms thick (Te–Bi–Te–Bi–Te), and the second seven atoms thick (Te–Bi–Te–Pb–Te–Bi–Te). It can thus be modelled as a 1/1 intergrowth of tellurobismuthite Bi_2Te_3 with rucklidgeite.

Poubaite isotypic pair (n = 2)

In this series, the c periodicity corresponds to three seven-atoms-thick layers *Ch–Me–Ch–Me–Ch–Me–Ch*, with the central *Me* atom probably corresponding to Pb, and the two marginal ones to Bi.
Poubaite, $PbBi_2(Se,Te,S)_4$ (c = 40.09 Å)
STR (synth. – c = 39.20 Å): Agaev & Semiletov (1963). Only a simplified structural model, based on an electron-diffraction study, is available.
Rucklidgeite, $PbBi_2Te_4$ (c = 41.49 Å)
STR (synth. – c = 41.531 Å): Zhukova & Zaslavskii (1972). The structural model was proposed on the basis of X-ray powder diagrams (especially 00*l* reflections).

Aleksite, $PbBi_2S_2Te_2$ (c = 79.76 Å) (n = 2)
STR: unknown. The c periodicity corresponds to (14 × 3) atom layers, and may correspond ideally to the stacking sequence (Te–Bi–S–Pb–S–Bi–Te) (Z = 6).

Saddlebackite, $Pb_2Bi_2Te_2S_3$ (c = 33.43 Å) (n = 3)
Def.: Clarke (1997). c would correspond to an 18-atom sequence.
STR: unknown. Petrov & Imamov (1970) described the crystal structure of $Pb_2Bi_2Te_5$, with c = 17.5 Å, and a nine-atoms-thick layer with the sequence –(Te–Pb–Te–Bi–Te–Bi–Te–Pb–Te)–.

Complex derivative

Babkinite, $Pb_2Bi_2(S, Se)_3$ (c = 39.60 Å)
Def.: Bryzgalov *et al.* (1996). STR: unknown. The *Me*/*Ch* ratio is > 1, and the formula is unbalanced, indicating a transitional compound of the subchalcogenide type. It can be modeled as $2Bi_2.1Bi_2Ch_3.6PbCh$, and may be the chief-member of a complex homologous series, ***n*Bi$_2$.*m*Bi$_2$*Ch*$_3$.*p*PbCh** (Cook *et al.*, 2007b).

Remarks: 1. Higher or combined members of the aleksite series require detailed X-ray structure determinations. 2. Cannizzarite (see 2.3) is a composite structure with one of the two layers of the tetradymite type. 3. "Platynite", commonly given as $PbBi_2(Se, S)_7$ in the literature, has been discredited (Holstam & Söderhielm, 1999).

2.2. Composite structures from alternating pseudohexagonal and PbS/SnS-like tetragonal layers

1. Commensurate structures

Nagyágite homologous series

Buckhornite, $(Pb_2BiS_3)(AuTe_2)$ (N = 1)
STR: Effenberger *et al.* (2000).
Nagyágite, $[Pb_3(Pb, Sb)_3S_6](Te, Au)_3$ (N = 2)
STR: Effenberger *et al.* (1999).

Related
Museumite, $[Pb_2(Pb, Sb)_2S_8][Te, Au]_2$
Def.: Bindi & Cipriani (2004a).
Berryite, $Cu_3Ag_2Pb_3Bi_7S_{16}$
STR: Topa *et al.* (2006a).

Tentative assignment to this series
Watkinsonite, $Cu_2PbBi_4(Se, S)_8$
Def.: Johan *et al.* (1987).
STR: unknown. A structure model was recently proposed by Topa *et al.* (2006a), on the basis of crystallographic similarities with berryite.

2. Non-commensurate structures

Type 1: Cylindrite homologous series

Cylindrite type
Cylindrite, ~ $FePb_3Sn_4Sb_2S_{14}$
STR: Makovicky (1974) and Williams & Hyde (1988) (mean structure).
Lévyclaudite, ~ $Cu_3Pb_8Sn_7(Bi, Sb)_3S_{28}$
Def.: Moëlo *et al.* (1990).
STR: Evain *et al.* (2006a), for the synthetic Sb-pure isotype ("lévyclaudite-(Sb)").
IMA 2006-016, $Pb_2SnInBiS_7$

Franckeite type
Franckeite, ~ $Fe(Pb, Sn^{2+})_6Sn_2^{4+}Sb_2S_{14}$
STR: Williams & Hyde (1988) and Wang & Kuo (1991) (mean structure).
"*Potosiite*", ~ $FePb_6Sn_2^{4+}Sb_2S_{14}$
"*Incaite*", ~ $FePb_4Sn_2^{2+}Sn_2^{4+}Sb_2S_{14}$
Isotype
IMA 2005-024, $(Pb, Sn)_{12.5}As_3Sn_5FeS_{28}$

Potosiite and incaite: two varieties of franckeite

Franckeite has a composite layered structure, with in-plane non-commensurability (Makovicky & Hyde, 1981). One layer "H" is of the CdI_2 type, $(Sn, Fe, Sb)S_2$, like in cylindrite (Makovicky, 1974); the second one "Q" is of the SnS/TlI type, four atoms thick (twice that of cylindrite): $(Pb, Sn, Sb, Fe?)_4S_4$. Sn is tetravalent in H, divalent in Q, where it substitutes for divalent Pb. The synthetic composite compound $[(Pb, Sb)S]_{2.28}NbS_2$ (Lafond *et al.*, 1997) has the same Q layer as franckeite; here Sb is exclusively in the two central atomic planes of this layer. Wolf *et al.* (1981 – definition of potosiite) and Mozgova *et al.* (1976) pointed out that franckeite is crystallographically similar to potosiite and incaite (defined by Makovicky, 1974 and 1976). On the basis of the crystal-chemical model, potosiite is Sn^{2+}-poor franckeite (Makovicky & Hyde, 1992), and incaite is Sn^{2+}-rich franckeite, always with $Pb > Sn^{2+}$ in natural samples. Thus, potosiite and incaite correspond to varietal compositions in the franckeite solid-solution field (Mozgova *et al.*, 1976) and should be taken off the list of mineral species.

In synthetic samples, Sn/Pb can surpass 1 (up to Pb-free franckeite and cylindrite – Moh, 1987). The discovery of such samples in nature would permit redefinition of incaite as a new mineral species.

Type 2

Lengenbachite, $\sim Cu_2Ag_4Pb_{18}As_{12}S_{39}$
STR: Williams & Pring (1988) (structural model through HRTEM study).
Crystal chemistry revised by Makovicky *et al.* (1994).

Type 3: Cannizzarite isotypic pair

Cannizzarite, $\sim Pb_8Bi_{10}S_{23}$
STR: Matzat (1979).
Wittite, $\sim Pb_8Bi_{10}(S, Se)_{23}$

Remark: "Wittite B" of Large & Mumme (1975) corresponds to proudite (Mumme, 1976).

Wittite: original species, or Se-rich cannizzarite?

Wittite and cannizzarite obey the same crystal-chemical model of composite, non-commensurate structure: a $(Pb, Bi)_2(S, Se)_2$ layer "Q" alternating with a $(Bi, Pb)_2(S, Se)_3$ layer of the tetradymite type (*i.e.*, a double-octahedral layer). The main difference in the structural formula is the high Se/S ratio of wittite (Mumme, 1980a). This Se/S atomic ratio never exceeds 1, but the tetradymite-type layer is very probably enriched in Se relative to the Q layer (Mozgova *et al.*, 1992). Precise knowledge of the Se partitioning between the two layers is necessary to validate wittite as a species, if $Se/S > 1$ in the tetradymite-type layer.

On the contrary, if in natural compounds the Se/S atomic ratio is always below 1 in the tetradymite-type layer, wittite would correspond to a Se-rich variety of cannizzarite. The pure Se derivative of cannizzarite has been synthesized recently, and its structure solved (Zhang *et al.*, 2005). This complete Se-for-S substitution enhances the possibility of validating wittite.

2.3. Commensurate composite derivatives of cannizzarite

In this group, all structures show an alternation of two types of ribbons or stepped layers resulting from the fragmentation of the two layers comprising the cannizzarite-like structure (one pseudo-quadratic, of the PbS archetype, the other pseudo-hexagonal, of the CdI_2 archetype). Three factors govern structural variations: 1) the thickness of each layer/ribbon; 2) the widths between consecutive planes of slip/shear and the width of their interface (according to a mQ/nH ratio); and 3) the spatial offset of ribbons of each type around planes of step (relative to the original layer).

1. Cannizzarite plesiotypic derivatives

This sub-group is described by Makovicky (1997).

(a) Stepped layers

Homologous pair
Junoite, $3Q,{}^4/_2H - Cu_2Pb_3Bi_8(S, Se)_{16}$
Def./STR: Mumme (1975a); Large & Mumme (1975).
Felbertalite, $3Q,{}^4/_2H - Cu_2Pb_6Bi_8S_{19}$
Defined by Topa *et al.* (2001).
STR: Topa *et al.* (2000a).
Nordströmite, $4Q,{}^5/_2H - CuPb_3Bi_7(S, Se)_{14}$
STR: Mumme (1980b).
Proudite, $8Q, {}^9/_2H - Cu_2Pb_{16}Bi_{20}(S, Se)_{47}$
Def./STR: Mumme (1976, and unpublished new revision). First description as "wittite B" in Large & Mumme (1975).

(b) Sheared layers (chessboard type)

Galenobismutite, $^1/_2Q,{}^1/_2H - PbBi_2S_4$
STR: Iitaka & Nowacki (1962); Wulf (1990).
Angelaite, $Cu_2AgPbBiS_4$
(Remark: The *Me*/S ratio is > 1)
Def.: Brodtkorb & Paar (2004); (Topa *et al.*, in prep.).
STR: Topa *et al.* (2004 – abstract). It is a homeotype of galenobismutite.
Nuffieldite, $1Q,{}^2/_2H - Cu_{1.4}Pb_{2.4}Bi_{2.4}Sb_{0.2}S_7$
Redefinition: Moëlo (1989).
STR: Moëlo *et al.* (1997). The general structural formula is $Cu_{1+x}Pb_{2+x}Bi_{3-x-y}Sb_yS_7$.
Weibullite, $6Q,{}^7/_2H - Ag_{0.33}Pb_{5.33}Bi_{8.33}(S, Se)_{18}$
STR: Mumme (1980c).

2. Boxwork derivatives of cannizzarite

This boxwork type results from a combination of three types of building blocks. There are two types of ribbons (slab fragments) alternating to form complex slabs. These slabs are separated by a layer or ribbon-layer (here three atoms in thickness), giving the final boxwork architecture. One type of ribbons in the complex slabs and the latter layer (both with surfaces of pseudotetragonal character) form a boxwork system of partitions; the remaining type of fragments fills the boxes.

Neyite, $7Q, {}^9/_2H - Cu_6Ag_2Pb_{25}Bi_{26}S_{68}$
STR: Makovicky *et al.* (2001a).
Rouxelite, $5Q,{}^7/_2H - Cu_2HgPb_{22}Sb_{28}S_{64}(O, S)_2$

Def./STR: Orlandi *et al.* (2005).

Remark: Complex Pb/Sb oxy-(chloro)-sulfosalts (scainiite, pillaite and pellouxite) belonging to the zinkenite plesiotypic series can also be described by a similar boxwork architecture.

3. Lead sulfosalts based on large 2D fragments of PbS/SnS archetype

3.1. Lillianite homologous series (PbS archetype)

The definition and crystal chemistry of this homologous series were presented by Makovicky (1977), and Makovicky & Karup-Møller (1977a, 1977b). Additional data were given in Makovicky & Balić-Žunić (1993). All structures are based on PbS-like slabs of various thickness (number N of octahedra). Each homologue type is symbolized as ${}^{N}L$, or as ${}^{N1,N2}L$ (when there are two slabs of distinct thickness).

1. Lillianite homeotypic series (${}^{4}L$)

Bi-rich members
Lillianite, $Ag_xPb_{3-2x}Bi_{2+x}S_6$
STR: Takagi & Takéuchi (1972); Ohsumi *et al.* (1984).
Gustavite, $AgPbBi_3S_6$
STR (synth.): Bente *et al.* (1993).

Sb-rich members
General formula: $Ag_xPb_{3-2x}Sb_{2+x}S_6$ (And_n: $n = 100\ x$)
Andorite VI*, $AgPbSb_3S_6$ (And_{100})
*Named "senandorite" by Moëlo *et al.* (1984a).
STR: Sawada *et al.* (1987).
Nakaséite, $\sim (Ag_{0.93}Cu_{0.13})_{\Sigma=1.06}Pb_{0.88}Sb_{3.06}S_6$ ($\sim And_{106}$)
Andorite IV*, $Ag_{15}Pb_{18}Sb_{47}S_{96}$ ($And_{93.75}$)
*Named "quatrandorite" by Moëlo *et al.* (1984a).
Ramdohrite, $(Cd, Mn, Fe)Ag_{5.5}Pb_{12}Sb_{21.5}S_{48}$ ($And_{68.75}$)
STR: Makovicky & Mumme (1983).
Fizélyite, $Ag_5Pb_{14}Sb_{21}S_{48}$ ($And_{62.5}$)
Uchucchacuaite, $MnAgPb_3Sb_5S_{12}$ (And_{50})
Roshchinite, $(Ag, Cu)_{19}Pb_{10}Sb_{51}S_{96}$ ($And_{118.75}$)
Def.: Spiridonov *et al.* (1990).
STR: Petrova *et al.* (1986).

Lillianite dimorph (${}^{4,4}L$)
Xilingolite, $Pb_3Bi_2S_6$
STR: Berlepsch *et al.* (2001a). In comparison with lillianite, the cations in the crystal structure are ordered in a monoclinic fashion.

Doubtful
"*Bursaite*", $Pb_{3-3x}Bi_{2+2x}S_6$ (?)

Andorites IV and VI: two distinct species
These two minerals have distinct symmetry, with very close but distinct chemistry, without solid solution, as they are frequently observed in close epitactic intergrowth (Moëlo *et al.*, 1984a, 1989). Thus they correspond to two homeotypic species, with distinct superstructures (4*c* and 6*c*, respectively) and not to two polytypic forms of the same species. The study of Sawada *et al.* (1987) solved the true (6*c*) crystal structure of andorite VI (or "senandorite").

Nakaséite: a variety of andorite VI
Nakaséite, defined by Ito & Muraoka (1960) as a Cu-rich derivative of andorite with a superstructure of ($c \times 24$), was considered by Fleischer (1960) to be a polytypic variety of andorite (andorite XXIV). A later detailed examination of minerals of the andorite–fizélyite series (Moëlo *et al.*, 1989) confirmed that nakaséite is an oversubstituted, Cu-rich ($\sim$ 1 wt.%) variety of andorite VI, with a formula close to $(Ag_{0.93}Cu_{0.13})_{\Sigma=1.06}Pb_{0.88}Sb_{3.06}S_6$.

Ramdohrite: species, or variety of fizélyite?
Ramdohrite from the type deposit has a significant Cd content (Moëlo *et al.*, 1989) and is compositionally close to fizélyite (ideally $And_{68.75}$ and $And_{62.5}$, respectively), but it is not known if there is a solid solution (ramdohrite = Cd-rich variety of fizélyite?) or an immiscibility gap (ramdohrite = specific species?). Fizélyite from Kisbánya (Romania) shows exsolutions of a (Mn, Fe)-rich variety of ramdohrite; such exsolutions correspond to a specific species (same study). A crystal-structure study of fizélyite from the type deposit is necessary to confirm the distinction between these two species.

"Bursaite"
Bursaite from the type deposit corresponds to Ag-poor lillianite (Makovicky & Karup-Møller, 1977b). A new occurrence (Shumilovskoe, West Transbaikal) studied by Mozgova *et al.* (1988) was found by X-ray powder and electron-microdiffaction data to be an intergrowth of two lillianite-related phases, each with a distinct unit cell. The electron-microprobe composition, which represents a composite from the two phases, indicates a Pb deficit ($N \sim 3.83$). Bursaite would correspond to the Pb-poor phase, with cation vacancies.

(^{4,7}L) homologue

Vikingite, $Ag_5Pb_8Bi_{13}S_{30}$
STR: Makovicky *et al.* (1992).

(^{4,8}L) homologue

Treasurite, $Ag_7Pb_6Bi_{15}S_{30}$

Remark: Borodaevite (see 3.2) may correspond to a homeotypic derivative of treasurite (Ilinca & Makovicky, 1997).

2. Heyrovskýite homeotypic series (${}^{7}L$)

Orthorhombic, disordered (with minor Ag)
Heyrovskýite, $Pb_6Bi_2S_9$
STR: Otto & Strunz (1968 – synth.); Takéuchi & Takagi (1974). The structure of an (Ag, Bi)-rich derivative was solved by Makovicky *et al.* (1991). Its structural formula is $Pb_{3.36}Ag_{1.32}Bi_{3.32}S_9$, and one of the cation sites has major Ag (s.o.f. $\sim$ 0.657), that could justify (Ag, Bi)-rich heyrovskýite as a specific mineral species.
Homeotype (monoclinic, ordered)
Aschamalmite, $Pb_{6-3x}Bi_{2+x}S_9$
STR: Mumme *et al.* (1983).

Related ($^{5,9}L$ dimorph)
Eskimoite, $Ag_7Pb_{10}Bi_{15}S_{36}$

3. Ourayite homeotypic pair ($^{11,11}L$)

Ourayite (*B*-centered), $Ag_3Pb_4Bi_5S_{13}$
Ourayite-P (primitive unit cell), ~ $Ag_{3.6}Pb_{2.8}Bi_{5.6}S_{13}$ (empirical formula)

4. Disordered phase

"*Schirmerite*" (Type 2), $Ag_3Pb_3Bi_9S_{18}$ to $Ag_3Pb_6Bi_7S_{18}$

5. Related?

Ustarasite, $Pb(Bi, Sb)_6S_{10}$

Ourayite and ourayite-P: close, but distinct species
An exsolution pair of major ourayite with minor ourayite-*P* has been described by Makovicky & Karup-Møller (1984). Ourayite-*P*, poorer in Pb than ourayite, is clearly a distinct species (probably an ordering variant of ourayite), but it needs further data that include an exact chemical formula and crystal structure.

Schirmerite: two "schirmerites", and two questions
Reexamination of schirmerite (Type 2) from the type deposit (Karup-Møller, 1977; Makovicky & Karup-Møller, 1977b) proved it to be a disordered intergrowth of different proportions of slabs ^{4}L and ^{7}L, with a composition between those of gustavite and (Ag, Bi)-rich heyrovskýite. Such a disordered intergrowth is not a valid species.

On the other hand, in another deposit, Bortnikov *et al.* (1987) discovered a new phase (Type 1 – see schapbachite) with the original composition of schirmerite (that is, strictly in the $AgBiS_2$–PbS pseudo-binary system).

Ustarasite: needs unit-cell data
Ustarasite was defined by Sakharova (1955) on the basis of chemical analysis and X-ray powder data. The mineral is compositionally close to synthetic Phase V of Otto & Strunz (1968), which is ~ $PbBi_4S_7$ (lillianite–pavonite super-family). Unit-cell data are needed to validate ustarasite.

3.2. Pavonite homologous series

The pavonite homologous series was defined by Makovicky *et al.* (1977) (^NP = homologue number), and additional structural data were presented by Mumme (1990).

Grumiplucite, $HgBi_2S_4$ (^3P)
Def.: Orlandi *et al.* (1998).
STR (synth.): Mumme & Watts (1980).

Kudriavite, $(Cd, Pb)Bi_2S_4$ (^3P)
Def.: Chaplygin *et al.* (2005).
STR: Balić-Žunić & Makovicky (2007). About 1/10 Bi is substituted by In.

Makovickyite, $Cu_{1.12}Ag_{0.81}Pb_{0.27}Bi_{5.35}S_9$ (^4P)
Def.: Žák *et al.* (1994).
STR: Mumme (1990); Topa *et al.* (2007).

Homeotype
Cupromakovickyite, $Cu_4AgPb_2Bi_9S_{18}$ (^4P)
Def.: (Topa & Paar, accept.).
The name of this new species was first given in the definition paper of kupčíkite (Topa *et al.*, 2003a).
STR: Topa *et al.* (2007).

Pavonite, $AgBi_3S_5$ (^5P)
STR (synth.): Makovicky *et al.* (1977).
Homeotype
Cupropavonite, $Cu_{0.9}Ag_{0.5}Pb_{0.6}Bi_{2.5}S_5$ (^5P)

Benjaminite, $Ag_3Bi_7S_{12}$ (^7P)
STR: Makovicky & Mumme (1979).

Mummeite, $Cu_{0.58}Ag_{3.11}Pb_{1.10}Bi_{6.65}S_{13}$ (^8P)
Def.: Karup-Møller & Makovicky (1992).
STR: Mumme (1990).

Borodaevite, $Ag_{4.83}Fe_{0.21}Pb_{0.45}(Bi, Sb)_{8.84}S_{16}$ (^{11}P)
Def.: Nenasheva *et al.* (1992), who considered this species as ^{12}P. Borodaevite is questionable as a pavonite homologue (see treasurite (3.1.1) – Ilinca & Makovicky, 1997).
IMA 2005-036, $Cu_8Ag_3Pb_4Bi_{19}S_{38}$

Derivatives

Mozgovaite, $PbBi_4(S, Se)_7$
Def.: Vurro *et al.* (1999). According to the unit-cell parameter (with b = 37.4 Å, derived from powder data), this mineral probably corresponds to synthetic Phase V2 (Takéuchi, 1997), giving the ideal formula $Pb_{3.19}\nabla_{0.27}Bi_{12.54}S_{22}$ (∇ = cationic vacancy). The structure would be a composite of lillianite- and pavonite-type layers ($m\,^2P + n\,^2L$).

Livingstonite, $HgSb_4S_6(S_2)$
STR: Srikrishnan & Nowacki (1975). It is a composite structure formed of two rod-layers, one of which is equivalent to a component of the rod-layer structure of grumiplucite. Homeotype of ^2P.

3.3. Cuprobismutite homologous series

A general review of this series is given by Topa *et al.* (2003b).
Kupčíkite, $Cu_{3.4}Fe_{0.6}Bi_5S_{10}$ (Type 1,1,1)
Definition and STR: Topa *et al.* (2003a).
Hodrushite, $Cu_8Bi_{12}S_{22}$ (Type 1, 2, 1, 2)
STR: Topa *et al.* (2003b). It explains chemical shifts relative to the ideal formula given here, analogous to those in kupčíkite and cuprobismutite.
Cuprobismutite, $Cu_8AgBi_{13}S_{24}$ (Type 2, 2, 2)
STR: Topa *et al.* (2003b).

Related:

Pizgrischite, $(Cu, Fe)Cu_{14}PbBi_{17}S_{34}$
Definition and STR: Meisser *et al.* (2007).
It is further twinning of a kupčíkite-like structure.

Related (unit-cell-intergrowth derivative of kupčíkite)

Paděraite, $Cu_7[(Cu, Ag)_{0.33}Pb_{1.33}Bi_{11.33}]_{\Sigma 13}S_{22}$
STR: Mumme (1986); Topa & Makovicky (2006).

3.4. Meneghinite homologous series (SnS archetype)

This series, defined by Makovicky (1985a), was reexamined by Berlepsch *et al.* (2001b). It also includes the aikinite–bismuthinite homeotypic series (N = 2), placed in section 4.5 of the present report.

Meneghinite, $CuPb_{13}Sb_7S_{24}$ (N = 5)
STR: Euler & Hellner (1960). Moëlo *et al.* (2002) for a Cu-poor variety.

Jaskolskiite, $Cu_xPb_{2+x}(Sb, Bi)_{2-x}S_5$ (x close to 0.2) (N = 4)
STR: Makovicky & Nørrestam (1985).

3.5. Jordanite homologous series

1. Jordanite isotypic pair (N = 4)

Jordanite, $Pb_{14}(As, Sb)_6S_{23}$
STR: Ito & Nowacki (1974b).
Geocronite, $Pb_{14}(Sb, As)_6S_{23}$
STR: Birnie & Burnham (1976).
There is a continuous solid solution between jordanite and geocronite. In nature, geocronite always contains some As, but the pure Sb member has been synthesized (Jambor, 1968).

2. Kirkiite homologue (N = 3)

Kirkiite, $Pb_{10}Bi_3As_3S_{19}$
STR: Makovicky *et al.* (2006a).

3. Related?

Tsugaruite, $Pb_4As_2S_7$
Def.: Shimizu *et al.* (1998).
The crystal structure of tsugaruite is unknown, but is probably complex as is indicated by the large unit cell (V = 4678 Å^3).

3.6. (Single type) PbS hexagonal derivative

Gratonite, $Pb_9As_4S_{15}$
STR: Ribár & Nowacki (1969).

3.7. Plagionite homologous series

The crystal chemistry of this homologous series was characterised by Kohatsu & Wuensch (1974), and was reexamined by Takéuchi (1997). General formula: $Pb(Pb_NSb_4)_2S_{13+2N}$ (N = 1 to 4).

Fülöppite, $Pb_3Sb_8S_{15}$ (N = 1)
STR: Nuffield (1975), and Edenharter & Nowacki (1975).
Plagionite, $Pb_5Sb_8S_{17}$ (N = 2)
STR: Cho & Wuensch (1974).
Heteromorphite, $Pb_7Sb_8S_{19}$ (N = 3)
STR: Edenharter (1980).
Semseyite isotypic pair (N = 4)
Semseyite, $Pb_9Sb_8S_{21}$
STR: Kohatsu & Wuensch (1974); Matsushita *et al.* (1997).
Rayite, $(Ag,Tl)_2Pb_8Sb_8S_{21}$

Rayite: true unit cell?
Rayite (Basu *et al.*, 1983) was related to semseyite on the basis of the powder diagram, but this choice was disputed by Roy Choudury *et al.* (1989), who could only synthesize (Ag, Tl)-rich boulangerite with a composition close to that of rayite. This result was confirmed by Bente & Meier-Salimi (1991). Rayite needs a single-crystal study (X-ray or electron diffraction) of the type sample to confirm the unit cell and the relationship of rayite to the plagionite series.

3.8. Sartorite homologous series

General building principles for structures of this series were described by Le Bihan (1962); the homologous series itself was defined by Makovicky (1985a) and was completed by Berlepsch *et al.* (2001c). Only two types of homologous slabs are known (N = 3 or 4), and each homologue type corresponds to a regular stacking of these slabs.

1. Sartorite homeotypes (N = 3)

Sartorite, $PbAs_2S_4$ (or $Pb_{1+2x}As_{2-2x}S_{4-x}$?)
STR (subcell): Nowacki *et al.* (1961); Iitaka & Nowacki (1961).
Sartorite-9c, $Tl_{1.5}Pb_8As_{17.5}S_{35}$
STR: Berlepsch *et al.* (2003).
Twinnite, $Pb(Sb_{0.63}As_{0.37})_2S_4$
Guettardite, $Pb_8(Sb_{0.56}As_{0.44})_{16}S_{32}$

2. Baumhauerite homeotypes (N = 3, 4, 3, 4)

Baumhauerite, $Pb_{12}As_{16}S_{36}$
Baumhauerite-2*a*, ~ $Ag_{1.5}Pb_{22}As_{33.5}S_{72}$
Def.: Pring *et al.* (1990). Remark: The proposed chemical formula, which with a 2*a* periodicity is $Ag_{1.4}Pb_{22}(As, Sb)_{35.2}S_{72}$, is not charge balanced. A simplified formula is proposed above on the basis of EPMA by Laroussi *et al.* (1989).
STR: according to Laroussi *et al.* (1989), the crystal structure of "baumhauerite" published by Engel & Nowacki (1969) corresponds to baumhauerite-2*a*, and not to baumhauerite.
Baumhauerite-ψO3abc, $Ag_3Pb_{38.1}(As, Sb)_{52.8}S_{96}$
Def.: Pring & Graeser (1994).

3. Homologue N = 4, 3, 4

Liveingite, $Pb_{20}As_{24}S_{56}$
STR: Engel & Nowacki (1970) ("Rathit II").

4. Dufrénoysite homeotypes (N = 4)

Dufrénoysite, $Pb_2As_2S_5$

STR: Marumo & Nowacki (1967b).

Veenite, $Pb_2(Sb, As)_2S_5$

Rathite, $Ag_2Pb_{12-x}Tl_{x/2}As_{18+x/2}S_{40}$

STR: Marumo & Nowacki (1965); Berlepsch *et al.* (2002). The developed structural formula is $Pb_8Pb_{4-x}(Tl_2As_2)_x(Ag_2As_2)As_{16}S_{40}$.

5. Homologues with long-range periodicity

Marumoite (IMA 1998-004), $Pb_{32}As_{40}S_{92}$

This mineral species was approved by the CNMNC, but the description has not as yet been published. Preliminary data were given by Ozawa & Takéuchi (1983). The composition and unit-cell parameters indicate that the mineral belongs to the sartorite series. The long periodicity (115 Å) corresponds to 2 × (4, 3, 4, 3, 4) stacking sequences. Recently, the name marumoite was used in the study of another occurrence of the mineral (Shimizu *et al.*, 2005).

Rathite-IV (unknown formula)

This **rathite-IV** (Ozawa & Nowacki, 1974) is the renamed **rathite-V** of Nowacki *et al.* (1964); its periodicity of 138 Å corresponds to the stacking sequence (4, 3, 4, 3, 4, 4, 3, 4, 3, 4, 3, 4) (see Berlepsch *et al.*, 2003). The mineral is an insufficiently described homologue, more complicated and quantitatively different from liveingite. The chemical composition is unknown; without additional cations, the stacking sequence would give the formula $Pb_{19}As_{24}S_{55}$.

6. Unit-cell-intergrowth derivative of dufrénoysite

Chabournéite, $Tl_5(Sb, As)_{21}S_{34}$

Def.: Mantienne (1974); Johan *et al.* (1981).

STR: Nagl (1979).

The structural formula proposed by Nagl (1979) for a *b*/2 subcell is $Tl_8Pb_4Sb_{21}As_{19}S_{68}$. This formula is questioned by Johan *et al.* (1981), who proposed the formula $Tl_{21}(Sb, As)_{91}S_{147}$ for the unit cell of the Pb-free member, but this formula shows clearly a S excess, incompatible with the modular organisation of the crystal structure. According to the substitution $Tl^+ + (Sb, As)^{3+} \rightarrow 2\ Pb^{2+}$, demonstrated by Johan *et al.* (1981), the general simplified formula is $Tl_{5-x}Pb_{2x}(Sb, As)_{21-x}S_{34}$. The Pb-free pole ($x = 0$) corresponds to $Tl_5(Sb, As)_{21}S_{34}$, while the Pb-rich composition studied by Nagl ($x \sim 1$) is close to $Tl_4Pb_2(Sb, As)_{20}S_{34}$.

7. Pierrotite homeotypic pair (N = 3, 3)

Pierrotite, $Tl_2(Sb, As)_{10}S_{16}$ (ortho.)

STR: Engel *et al.* (1983).

Parapierrotite, $TlSb_5S_8$ (monocl.)

STR (synth.): Engel (1980).

Sartorite: chemical formula?

The crystal chemistry of sartorite is very complex, and has been recently reviewed by Berlepsch *et al.* (2003). Various supercells and non-commensurate superstructures seem common (Pring *et al.,* 1993). According to Berlepsch *et al.* (2003) different chemical and crystallographic varieties of sartorite ought to be considered as polytypoids, and not as distinct mineral species.

The classic stoichiometric formula, $PbAs_2S_4$, is doubtful, and has never been encountered in modern EPMA. There is always some Tl, which is up to 6.4 wt.% in sartorite-9*c*, whose structural formula is $Tl_{1.5}Pb_8As_{17.5}S_{35}$. A Tl-poor variety ("Mineral A" of Laroussi *et al.*, 1989) is close to $Tl_{0.02}Pb_{1.11}As_{1.87}S_{3.96}$ ($\Sigma_{cations}$ = 3 at.), but its crystal structure is unknown. Tentatively, Tl-free sartorite may correspond to the formula $Pb_{1+2x}As_{2-2x}S_{4-x}$, with x close to 0.07.

Twinnite and guettardite: one or two species?

Twinnite and guettardite, defined by Jambor (1967b), and reanalyzed by Jambor *et al.* (1982), are very close, chemically and structurally. Original twinnite has a slightly higher Sb/As ratio than guettardite (~ 1.7 against ~ 1.3, respectively), but this ratio may reach 3.1 (Moëlo *et al.*, 1983). Guettardite is defined as a monoclinic dimorph of twinnite, but Z. Johan (unpublished – see Mantienne, 1974), on the basis of the examination of twinnite from another deposit, considered twinnite and guettardite as identical. Reexamination of the type samples, including structure data, would be necessary to understand the exact structural relationships.

Baumhauerite varieties: polytypes or homeotypes?

Baumhauerite-2*a* and baumhauerite-*ψO3abc* were considered by Pring & Graeser (1994) as polytypes of baumhauerite, but they differ chemically because of the presence of Ag. Thus, it seems better to consider them as homeotypes. Whereas baumhauerite-2*a* is a well-defined species, approved by the IMA-CNMNC, the validation of baumhauerite-*ψO3abc* would need a crystal-structure study.

Baumhauerite II of Rösch & Hellner (1959) was first obtained by hydrothermal synthesis, and was subsequently recognized by those authors in a natural sample. Pring & Graeser (1994) considered baumhauerite II as identical to baumhauerite-2*a*. However, baumhauerite II does not contain Ag. See also Pring (2001).

Rathite varieties

Numerous rathite varieties from the deposit of Lengenbach, Switzerland, have been described. A critical review of these rathites has been given by Makovicky (1985a), and, more recently, by Berlepsch *et al.* (2002), through the reexamination of the crystal structure of rathite. According to these authors and some previous works, the following is concluded:

- ***"α-Rathite"*** = rathite;
- "***Rathite-I***" = rathite or dufrénoysite;
- "***Rathite-1a***" = dufrénoysite;
- "***Rathite II***" is liveingite (Nowacki, 1967);
- "***Rathite III***" is most probably a misidentified compound;
- ***"Rathite-IV"*** (of Nowacki *et al.*, 1964) = sartorite.

3.9. Unclassified

Mutnovskite, $Pb_2AsS_3(I, Cl, Br)$
Def./STR: Zelenski *et al.* (2006).
The crystal structure of this halogeno-sulfosalt is very specific, with a layered organisation, but there is no clear relationship with any other Pb sulfosalt.

4. Sulfosalts based on 1D derivatives of PbS/SnS archetype, *i.e.*, on rod-type building blocks

A general review of this vast group of Pb sulfosalts and related synthetic compounds has been presented by Makovicky (1993). The main geometric factors that are used for the description and comparison of the various crystal structures and their hierarchy are:

- the size of the rod component(s);
- the number of different rod-types coexisting in a structure (generally only one; exceptionally up to four);
- their general organisation, giving principally the "rod-layer", "cyclic" and "chessboard" sub-types.

4.1. Rod-layer sub-type (boulangerite plesiotypic family)

Cosalite, $Pb_2Bi_2S_5$
STR: Srikrishnan & Nowacki (1974).
Falkmanite, $Pb_3Sb_2S_6$ (or $Pb_{5.4}Sb_{3.6}S_{10.8}$?)
Redefinition: Mozgova *et al.* (1983).
Boulangerite, $Pb_5Sb_4S_{11}$
STR: Mumme (1989).
Plumosite, $Pb_2Sb_2S_5$
Redefinition: Mozgova *et al.* (1984).
Moëloite, $Pb_6Sb_6S_{14}(S_3)$
Definition & STR: Orlandi *et al.* (2002).
Dadsonite, $Pb_{23}Sb_{25}S_{60}Cl$
STR: Makovicky & Mumme (1984 – abstract); Makovicky *et al.* (2006b).
Robinsonite, $Pb_4Sb_6S_{13}$
STR: Skowron & Brown (1990 – synth.); Franzini *et al.* (1992); Makovicky *et al.* (2004).

Jamesonite isotypic series

Jamesonite, $FePb_4Sb_6S_{14}$
STR: Niizeki & Buerger (1957); Léone *et al.* (2003); Matsushita & Ueda (2003 – synth.)
Benavidesite, $MnPb_4Sb_6S_{14}$
STR: Léone *et al.* (2003 – synth.).
Sakharovaite, $FePb_4(Sb, Bi)_6S_{14}$
Def.: Kostov (1959).

Sakharovaite: species, or jamesonite variety?
In sakharovaite, the Bi-for-Sb substitution is close to the 50 % at. limit, but does not clearly exceed it (Sakharova, 1955; Kostov, 1959; Borodaev & Mozgova, 1975). Thus, unless there is strong partitioning in the substitution of Bi among the three Sb positions in the jamesonite crystal structure (see below for the example of garavellite), sakharovaite is a Bi-rich variety of jamesonite. Confirmation of sakharovaite needs a crystal-structure study.

Parajamesonite: reexamination of a specimen from the type deposit (Herja, Romania)
Parajamesonite was defined by Zsivny & Naray-Szabo (1947) as a dimorph of jamesonite, with a distinct X-ray powder diagram. The unit cell was not determined, but the elongate crystals were reported to be up to 8 mm long and 2.8 mm wide, and would have easily permitted a single-crystal study. It was thought that the type sample was destroyed by fire during the conflict in Budapest in 1956, but rediscovery of the original samples studied by Zsivny permitted the discreditation (Papp, 2004; Papp *et al.*, 2007).

Falkmanite: crystal structure relative to that of boulangerite?
The validity of falkmanite was questioned for a long time. Re-examination of falkmanite from the type locality led Mozgova *et al.* (1983) to suggest its close relationship with boulangerite but with a higher Pb/Sb ratio and a different degree of structural ordering. McQueen (1987) studied a second occurrence of falkmanite, with a chemical composition very close to the ideal one, $Pb_3Sb_2S_6$, and with crystal data (X-ray powder pattern; unit cell) almost identical to those of boulangerite. Without cation excess, its formula could be $Pb_{5.4}Sb_{3.6}S_{10.8}$. A solution of the crystal structure of falkmanite is necessary for its definite classification.

Plumosite: a specific, but incompletely defined mineral species
Many old museum samples labelled "plumosite", $Pb_2Sb_2S_5$, correspond to various Pb–Sb sulfosalts with a hair-like habit. Mozgova & Bortnikov (1980) identified a plumosite-type phase, ~ $Pb_2Sb_2S_5$, in symplectitic association with boulangerite. Later, Mozgova *et al.* (1984) and Vrublevskaya *et al.* (1985) described another occurrence of plumosite as lamellar exsolutions in boulangerite, with the same sub-cell, but with a distinct true unit cell. Like falkmanite, plumosite is considered as a homologous derivative of boulangerite (the term "homeotype" seems more appropriate). Mumme (1989) pointed out similarities between plumosite and jaskolskiite. Crystal-structure data are needed to classify this species.

Berthierite isotypic series

Berthierite, $FeSb_2S_4$
STR: Lemoine *et al.* (1991).
Garavellite, $FeSbBiS_4$
Def.: Gregorio *et al.* (1979).
STR: Bindi & Menchetti (2005).
Clerite, $MnSb_2S_4$
Def.: Murzin *et al.* (1996).
STR (synth.): Bente & Edenharter (1989).

Remark: A synthetic monoclinic dimorph of clerite is known; its crystal structure (Pfitzner & Kurowski, 2000) is isotypic with that of grumiplucite (Part III, § 3.2). Unnamed $MnSb_2S_4$ described by Harris (1989) in the Hemlo

gold deposit (Ontario) may correspond to this monoclinic dimorph.

Garavellite: a definite species
The recent study by Bindi & Menchetti (2005) of a new occurrence of garavellite has proved that Sb and Bi atoms, despite their close crystal-chemical affinity, are positioned on distinct sites in the crystal structure. As a consequence, garavellite is clearly a definite mineral species, and not a Bi-rich variety of berthierite. This aspect is considered for the discussion of the validity of sakharovaite.

4.2. "Cyclic" sub-type and chessboard derivatives (zinkenite family)

The fundamentals of the crystal chemistry of this family have been defined by Makovicky (1985b).

1. Zinkenite plesiotypic series (cyclic rod-type)

Zinkenite, $Pb_9Sb_{22}S_{42}$
STR: Portheine & Nowacki (1975b).
Pillaite, $Pb_9Sb_{10}S_{23}ClO_{0.5}$
Def.: Orlandi *et al.* (2001).
STR: Meerschaut *et al.* (2001).

Remark: An iodine derivative of pillaite was recently synthesized (Kryukowa et al., 2005).

Scainiite, $Pb_{14}Sb_{30}S_{54}O_5$
Def.: Orlandi *et al.* (1999).
STR: Moëlo *et al.* (2000).
Marrucciite, $Hg_3Pb_{16}Sb_{18}S_{46}$
Definition and STR: Orlandi *et al.* (2007); STR: Laufek *et al.* (2007).
Pellouxite, $(Cu, Ag)_2Pb_{21}Sb_{23}S_{55}ClO$
Def.: Orlandi *et al.* (2004).
STR: Palvadeau *et al.* (2004).
Vurroite, $Sn_2Pb_{20}(Bi, As)_{22}S_{54}Cl_6$
Def.: Garavelli *et al.* (2005).
STR: Pinto *et al.* (2004 – abstract; accept.).
Owyheeite, $Ag_3Pb_{10}Sb_{11}S_{28}$
The chemistry of owyheeite was reexamined by Moëlo *et al.* (1984b), giving the general structural formula: $Ag_{3+x}Pb_{10-2x}Sb_{11+x}S_{28}$ ($-0.13 < x < +0.20$).
STR: Laufek *et al.* (2007). The proposed structural formula, $Ag_{1.5}Pb_{4.43}Sb_{6.07}S_{14}$, is outside the compositional field established by Moëlo *et al.* (1984b).

Remark: Pillaite, scainiite and pellouxite can also be described according to a "boxwork" principle (see neyite and rouxelite in Sect. 2.3).

2. Chessboard derivatives (kobellite plesiotypic series)

Kobellite homologous series

The crystal chemistry of this series has been defined by Zakrzewski & Makovicky (1986) and Makovicky & Mumme (1986), and a general chemical formula was proposed by Moëlo *et al.* (1995).

Kobellite isotypic pair

Kobellite, $(Cu, Fe)_2Pb_{11}(Bi, Sb)_{15}S_{35}$
STR: Miehe (1971).
Tintinaite, $Cu_2Pb_{10}Sb_{16}S_{35}$
The composition was redefined by Moëlo *et al.* (1984c).

Giessenite homeotypic pair

Giessenite, $(Cu, Fe)_2Pb_{26.4}(Bi, Sb)_{19.6}S_{57}$
Izoklakeite, $(Cu, Fe)_2Pb_{26.4}(Sb, Bi)_{19.6}S_{57}$
STR: Makovicky & Mumme (1986); Armbruster & Hummel (1987), for a Bi-rich variety.

Giessenite and izoklakeite: from monoclinic to orthorhombic symmetry with increasing Sb content
There is apparently a quasi-continuous solid solution from giessenite to izoklakeite with increasing Sb/Bi ratio, which is nevertheless always < 1 except for izoklakeite of the type locality (~ 1.04). The main difference is that the monoclinic symmetry of giessenite (Bi-rich) changes to orthorhombic in izoklakeite (Sb-rich) (Makovicky & Karup-Møller, 1986). The exact Sb/Bi ratio at which the symmetry changes is unknown.

Related

Eclarite, $(Cu, Fe)Pb_9Bi_{12}S_{28}$
Def.: Paar *et al.* (1983).
STR: Kupčík (1984).

3. Related?

Zoubekite, $AgPb_4Sb_4S_{10}$

Zoubekite: needs single-crystal study
Zoubekite, defined by Megarskaya *et al.* (1986), was approved by the IMA-CNMNC, although the unit cell was calculated solely on the basis of a powder diagram with only six lines above 2.00 Å. Zoubekite is compositionally close to owyheeite; X-ray single-crystal study is needed to prove that the two are distinct species.

4.3. Aikinite–bismuthinite homeotypic series

This family constitutes the most complex and didactic series of homeotypes among the sulfosalts. The first sulfosalt member, aikinite, was defined by Chapman (1843), and the fundamental work of Johansson (1924) permitted definition of the series on the basis of the new descriptions of gladite, lindströmite and hammarite. Since the end of the 1960s, numerous papers have brought new chemical, crystallographic and crystal-structure data, and very recent works have presented a relatively advanced overview of this series.

Besides the end-member bismuthinite, there are ten homeotypic sulfosalt species. Three members, the two end-members bismuthinite (Bi_4S_6 = ***b***) and aikinite ($Cu_2Pb_2Bi_2S_6$ = ***a***), and the median one krupkaite ($CuPbBi_3S_6$ = ***k***), permit definition of structural formulae of the eight other members by a simple combination of ***b*** or ***a*** with ***k***. This also leads to the idealized classical formulae given below.

Nevertheless, careful examination of various samples indicates that chemical shifts from the ideal compositions (Mozgova *et al.*, 1990) are common because of Cu over- or undersubstitution (Topa *et al.*, 2002b), or because of the presence of very fine exsolution or intergrowth textures (Topa *et al.*, 2002a) that extend to the nanometer scale (Pring & Hyde, 1987). As a consequence, it is dangerous to assign specific mineral names (the end-members excepted) on the basis of EPMA data alone, and the best way is to use a chemical notation, as proposed by Makovicky & Makovicky (1978), indicating the "aikinite substitution percentage", n_{aik}, equal to [2Pb/(Pb + Bi)] × 100. For instance, ideal hammarite, $Cu_2Pb_2Bi_4S_9$, corresponds to $n_{aik} = 67$.

Remark: This homeotypic series is also the lowest known homologue of the meneghinite homologous series (see Part 3, Sect. 4).

In the following list, the idealized substitution percentage is followed by the observed analytical values (in italics), when different. All species probably have narrow solid-solution fields (see for instance krupkaite and gladite – Topa *et al.*, 2002b), but the fields are difficult to delimit, all the more because they may vary with crystallization temperature.

Aikinite, $CuPbBiS_3$ (***a*** = $Cu_2Pb_2Bi_2S_6$ – n_{aik}: 100)
STR: Ohmasa & Nowacki (1970).
Friedrichite, $Cu_5Pb_5Bi_7S_{18}$ (***2a*** + ***k*** – n_{aik}: 83; *80*)
Def.: Chen *et al.* (1978).
STR: unknown.
Hammarite, $Cu_2Pb_2Bi_4S_9$ (***a*** + ***2k*** – n_{aik}: 67; *68*)
STR: Horiuchi & Wuensch (1976).
Emilite, $Cu_{10.7}Pb_{10.7}Bi_{21.3}S_{48}$ (***a*** + ***3k*** – n_{aik}: 63; *67*)
Def.: Topa *et al.* (2006b).
STR: Balić-Žunić *et al.* (2002).
Lindströmite, $Cu_3Pb_3Bi_7S_{15}$ (***a*** + ***4k*** – n_{aik}: 60)
STR: Horiuchi & Wuensch (1977).
Krupkaite, $CuPbBi_3S_6$ (***k*** – n_{aik}: 50; *49* to *50* ?)
STR: Mumme (1975b), and Syneèek & Hybler (1975).
Paarite, $Cu_{1.7}Pb_{1.7}Bi_{6.3}S_{12}$ (***b*** + ***4k*** – n_{aik}: 40; *42*)
Def.: Topa *et al.* (2005).
STR: Makovicky *et al.* (2001b).
Salzburgite, $Cu_{1.6}Pb_{1.6}Bi_{6.4}S_{12}$ (***b*** + ***3 k*** – n_{aik}: 38; *41*)
Def.: Topa *et al.* (2005).
STR: Topa *et al.* (2000b).
Gladite, $CuPbBi_5S_9$ (***b*** + ***2 k*** – n_{aik}: 33; below *33*, up to *38*)
STR: Syneček & Hybler (1975), Kohatsu & Wuensch (1976), Topa *et al.* (2002b).
Pekoite, $CuPbBi_{11}S_{18}$ (***2b*** + ***k*** – n_{aik} : 17)
STR: Mumme & Watts (1976).
Bismuthinite, Bi_2S_3 (***b*** = Bi_4S_6 – n_{aik} : 0)
Ciobanu & Cook (2000) detected by ore microscopy and EPMA two new Bi-rich minerals, "Phase 70", close to $CuPbBi_7S_{12}$ (n_{aik} = 25), and "Phase 88.6", close to $Cu_{0.33}Pb_{0.33}Bi_{7.67}S_{12}$ (n_{aik} = 8), which could correspond to new homeotypes between gladite and pekoite (type "***b*** + ***k***"?), and between pekoite and bismuthinite (type "5***b*** + ***k***"?), respectively. Similar suggestions, with $n_{aik} \sim 22$ and 27, appear in Topa *et al.* (2002b). All of these possible minerals need further study.

4.4. Related sulfosalts?

The crystal structures of following species are unknown, which does not permit their classification among the groups within Sect. 4 (or in Sects. 2 or 3).

Ardaite, $Pb_{17}Sb_{15}S_{35}Cl_9$
Def.: Breskovska *et al.* (1982).

Launayite, $CuPb_{10}(Sb, As)_{13}S_{30}$
Madocite, $Pb_{19}(Sb, As)_{16}S_{43}$
Playfairite, $Pb_{16}(Sb, As)_{19}S_{44}Cl$
Sorbyite, $CuPb_9(Sb, As)_{11}S_{26}$
Sterryite, $(Ag, Cu)_2Pb_{10}(Sb, As)_{12}S_{29}$
These five species have been defined in the same deposit of Madoc, Ontario (Jambor, 1967a, 1967b).

IMA 2007-010, $PbHgAs_2S_6$
Considering As only at the trivalent state would indicate a S excess ("persulfosalt"?).

5. Specific Tl(Pb) and Hg sulfosalts: structures with SnS layers (with or without additional layers)

A first overview of the systematics of Tl sulfosalts has been presented by Balić-Žunić (1989).

5.1. Hutchinsonite merotypic series

The general outline of this series is given in Makovicky (1997 – Table 5). The series consists principally of Tl sulfosalts and related compounds (natural or synthetic) with large monovalent cations (Na^+, $(NH_4)^+$, Cs^+). All structures are based on the combination of two types of layers, one of which corresponds to an $(010)_{SnS}$ slab of variable width (with the exception of gerstleyite, derived from the PbS archetype).

1. Hutchinsonite–bernardite homologous pair

Hutchinsonite, $TlPbAs_5S_9$
STR: Takéuchi *et al.* (1965); Matsushita & Takéuchi (1994).
Bernardite, $TlAs_5S_8$
Definition and STR: Pasava *et al.* (1989).

2. Edenharterite–jentschite pair

A detailed structural comparison of edenharterite and jentschite was given by Berlepsch *et al.* (2000).
Edenharterite, $TlPbAs_3S_6$
Def.: Graeser & Schwander (1992).
STR: Balić-Žunić & Engel (1983 – synth.); Berlepsch (1996).
Jentschite, $TlPbAs_2SbS_6$
Def.: Graeser & Edenharter (1997).
STR: Berlepsch (1996).

3. Other members

Imhofite, $Tl_{5.8}As_{15.4}S_{26}$
STR: Divjakovic & Nowacki (1976); Balić-Žunić & Makovicky (1993).
Gillulyite, $Tl_2As_{7.5}Sb_{0.3}S_{13}$
Def.: Wilson *et al.* (1991).
STR: Foit *et al.* (1995); Makovicky & Balić-Žunić (1999).

4. PbS archetype

Gerstleyite, $Na_2(Sb, As)_8S_{13}{\cdot}2H_2O$
STR: Nakai & Appleman (1981).

5.2. Rebulite plesiotypic pair

A comparative modular analysis of the crystal structures of rebulite and jankovićite has been presented by Makovicky & Balić-Žunić (1998).
Rebulite, $Tl_5As_8Sb_5S_{22}$
Def.: a complete description required for a definition is lacking.
STR: Balić-Žunić *et al.* (1982).
Jankovićite, $Tl_5Sb_9(As, Sb)_4S_{22}$
Def.: Cvetkovic *et al.* (1995).
STR: Libowitsky *et al.* (1995).

5.3. Single type: sicherite

Sicherite, $Ag_2Tl(As, Sb)_3S_6$
Definition and STR: Graeser *et al.* (2001).

5.4. Unclassified

Erniggliite, $SnTl_2As_2S_6$
Definition and STR: Graeser *et al.* (1992).
Vrbaite, $Hg_3Tl_4As_8Sb_2S_{20}$
STR: Ohmasa & Nowacki (1971).
Simonite, $HgTlAs_3S_6$
Def.: a complete description required for a definition is lacking.
STR: Engel *et al.* (1982).
Vaughanite, $HgTlSb_4S_7$
Def.: Harris *et al.* (1989).
Gabrielite, $Cu_2AgTl_2As_3S_7$
Def.: Graeser *et al.* (2006).
STR: Balić-Žunić *et al.* (2006). A 3-slab structure, with one of the layers related to cyclic sulfosalts.

Rebulite: needs a mineralogical description
Rebulite was defined on the basis of its crystal-structure study (Balić-Žunić *et al.*, 1982), but without a proposal submitted to the IMA-CNMNC. A complete mineralogical description is needed.

Simonite: needs a mineralogical description
Like rebulite, simonite is known only by its crystal-structure study (Engel *et al.*, 1982). It has been approved by the IMA-CNMNC, but a mineralogical description is lacking.

6. Sulfosalts with an excess of small (univalent) cations (Ag, Cu) relative to (As, Sb, Bi)

In the majority of these sulfosalts the ratio (ΣMe)/S is > 1; however, in the presence of divalent metals (Zn, Hg, Fe), the ratio may equal 1 (galkhaite, laffittite, routhierite and stalderite).

6.1. Cu(Ag)-rich sulfosalts

1. Wittichenite homeotypic pair

Wittichenite, Cu_3BiS_3
STR: Kocman & Nuffield (1973).
Skinnerite, Cu_3SbS_3
STR: Makovicky & Balić-Žunić (1995).

2. Tetrahedrite isotypic series

Among sulfosalts, this is the most complex isotypic series, because of the multiplicity of iso- and heterovalent substitutions. Numerous crystal-structure studies have been performed since the early ones of Machatschki (1928) and Pauling & Neuman (1934). The simplified general formula is $A_6(B, C)_6X_4Y_{12}Z$, where A is Cu or Ag in triangular coordination, B is Cu or Ag in tetrahedral coordination, C is generally a divalent metal (typically Fe or Zn, but also Hg, Mn, Cd...) in the same tetrahedral coordination, X is Sb, As, Bi or Te in trigonal pyramidal coordination, Y is S or Se in tetrahedral coordination, and Z is S or Se in a special octahedral coordination. The presence of vacancies or interstitial atoms (*e.g.*, Cu), or heterovalent substitutions due to the incorporation of Fe^{3+} or Te^{4+}, have been confirmed by structural studies.

In tetrahedrite–tennantite, the amount of divalent metals is limited to 2 a.p.f.u. but, especially in synthetic samples, it may vary between 0 and 2, indicating the variable presence of (formal) Cu^{2+}.

There are seven well-defined species, but various data (EPMA, experimental studies, Mössbauer spectroscopy, X-ray) indicate that the crystal chemistry of this series is complex, and individual problems can require highly specialized research methods. As a consequence, limits between mineral species (for instance freibergite or goldfieldite relative to tetrahedrite) are still questionable.

Structural formulae presented below are simplified to ideal ones as much as possible (for instance, the B/C ratio is equal to 4/2, and C is restricted generally to Fe and Zn). In other cases, the formula of the type sample is also given (for very rare species).

Tetrahedrite, $Cu_6[Cu_4(Fe, Zn)_2]Sb_4S_{13}$
STR: Wuensch (1964); Peterson & Miller (1986); Makovicky & Skinner (1979) and Pfitzner *et al.* (1997) for Cu-pure synthetic varieties, $Cu_{12+x}Sb_4S_{13}$.
Tennantite, $Cu_6[Cu_4(Fe, Zn)_2]As_4S_{13}$
STR: Wuensch *et al.* (1966); Makovicky *et al.* (2005) for a Cu-rich unsubstituted composition, $Cu_{12.5}As_4S_{13}$.
Freibergite, $Ag_6[Cu_4Fe_2]Sb_4S_{13-x}$(?)
STR: Rozhdestvenskaya *et al.* (1993).
Argentotennantite, $Ag_6[Cu_4(Fe, Zn)_2]As_4S_{13}$
Type sample (Spiridonov *et al.*, 1986a):

$(Ag_{5.67}Cu_{4.48})_{\Sigma=10.15}(Zn_{1.52}Fe_{0.37})_{\Sigma=1.89}(As_{2.14}Sb_{1.89})_{\Sigma4.03}S_{12.90}$

Argentotetrahedrite, $Ag_{10}(Fe, Zn)_2Sb_4S_{13}$

Formula according to Zhdanov *et al.* (1992): $Ag_{10.9}(Fe, Zn, Hg)_{1.9}(Sb_{3.9}As_{0.1})_{4.0}S_{12.2}$.

Goldfieldite, $Cu_{10}Te_4S_{13}$

Relative to this ideal end-member, charge-balanced with Cu^+ and Te^{4+}, natural compositions of goldfieldite with decreasing Te content agree with the two complementary formulae (see comments below):

(1) $Cu_{12-x}[Te_{2+x}(Sb, As, Bi)_{2-x}]S_{13}$ ($2 > x > 0$), and

(2) $Cu_{10+y}(Fe, Zn...)_{2-y}[Te_y(Sb, As, Bi)_{4-y}]S_{13}$ ($y < 2$, and Te > Sb, As, Bi).

Numerous EPMA data are given by Kovalenker & Rusinov (1986).

STR: Kalbskopf (1974), on the synthetic, pure Te end-member; Dmitrieva & Bojik (1988).

Hakite, $Cu_6[Cu_4Hg_2]Sb_4Se_{13}$

Type sample (Johan & Kvaccek, 1971):

$(Cu_{10.2}Hg_{1.8})_{\Sigma12}(Sb_{3.1}As_{1.0})_{\Sigma4.1}(Se_{10.4}S_{2.6})_{\Sigma13.0}$

Giraudite, $Cu_6[Cu_4(Fe, Zn)_2]As_4Se_{13}$

Type sample (Johan *et al.*, 1982):

$(Cu_{10.6}Ag_{0.3}Zn_{1.0}Hg_{0.1})_{\Sigma12}$ $(As, Sb)_4$ $(Se, S)_{13}$

In giraudite (formal) Cu^{2+} is present.

"***Annivite***", $Cu_6[Cu_4(Fe, Zn)_2](Bi, Sb, As)_4S_{13}$.

Related

Galkhaite, $(Cs,Tl,\nabla)(Hg, Cu, Zn, Tl)_6(As, Sb)_4S_{12}$

This mineral species was initially defined as $HgAsS_2$ by Gruzdev *et al.* (1972). The structural role of Tl was determined by Divjakovic & Nowacki (1975), but Chen & Szymañski (1981, 1982) subsequently proved that Cs always exceeds Tl.

STR: Divjakovic & Nowacki (1975); Chen & Szymañski (1981).

Freibergite

The status of freibergite as a valid species is still discussed. The Ag-for-Cu substitution induces a regular increase of the parameter *a*, as exemplified by the tennantite–argentotennantite complete solid solution; this solid solution has been also observed to occur between tetrahedrite and its pure Ag derivative, argentotetrahedrite. However, when the Ag content is more than about 23 wt.% (~ 4 a.p.f.u.), an abnormal trend of decreasing **a** has been observed (Riley, 1974; Samusikov *et al.*, 1988; Balitskaya *et al.*, 1989). The decrease has been explained by Rozhdestvenskaya *et al.* (1993) as follows. In the metal site with planar triangular coordination, Cu is mainly or completely substituted by Ag. At the same time, the special S position (*Z*) with octahedral coordination is progressively emptied, thereby permitting the formation of Ag_6 octahedral metallic clusters. For the highest Ag content, the crystal structural formula is: $^{[3]}Ag_6^{[4]}[Cu_{4.44}(Fe, Zn)_{1.56}]_{\Sigma6}^{[3]}Sb_4^{[3]}S_{12}^{[6]}S_{0.09}$.

Thus, this abnormal trend may be considered as belonging to a specific species, freibergite, which is distinct from Ag-rich tetrahedrite (improperly called "freibergite"). For the time being, the structural formula of this freibergite trend may be idealised as: $(Ag_{4+2x}Cu_{2-2x})[(Cu, Ag)_4(Fe, Zn)_2]_{\Sigma6}Sb_4S_{12}S_{1-x}$ ($0 < x < 1$). Varieties with Ag below 4 a.p.f.u. should be called Ag-rich tetrahedrite. The problem definitely needs further study.

Argentotetrahedrite

This name was proposed by Spiridonov *et al.* (1986b) for a Sb-rich derivative of argentotennantite, on the basis of EPMA, but without X-ray data. Later, Zhdanov *et al.* (1992) analysed an Ag end-member without Cu, and gave the unit cell as 10.92 Å, but without submitting a formal proposal to the CNMNC. These data validate the existence in the tetrahedrite series of a mineral species with ideal formula $Ag_{10}(Fe, Zn)_2Sb_4S_{13}$, in accordance with the experimental data of Pattrick & Hall (1983). A (re)definition through a proposal to the CNMNC is highly desirable, with more complete data (X-ray powder pattern; reflectance data).

Goldfieldite nomenclature

In goldfieldite Te^{4+} substitutes for Sb^{3+} in the tetrahedrite structure. For compositions with up to 2 Te a.p.f.u., the valence balance is maintained by an equivalent substitution of the divalent metals (Fe, Zn...) by monovalent Cu, as in structural formula (2) above. When Te is > 2 a.p.f.u., there are no more divalent metals; hence, the excess of Te above 2 at. is balanced by an equal number of vacancies among Cu sites that have three-fold coordination (structural formula (1) above). In these two consecutive solid-solution fields, the name goldfieldite is to be used when Te is predominant over each of Sb, As and Bi. Conversely, if for instance Te is minor together with major Sb, one has Te-rich tetrahedrite, and not goldfieldite.

"Annivite": potential revalidation

"Annivite" from the type deposit of Einfisch or Anniviers valley (Wallis, Switzerland) corresponds to a Bi-rich (~ 5 wt.%) variety of tennantite, according to the original analysis of Fellenberg (1854). On the basis of a total of 16 cations, its structural formula is $(Cu_{9.93}Fe_{1.22}Zn_{0.55})_{\Sigma=11.70}(As_{2.60}Sb_{1.28}Bi_{0.42})_{\Sigma=4.30}S_{13.15}$. Since this time, microprobe analyses have revealed in some deposits compositions in which the Bi atom concentration exceeds those of Sb or As (Kieft & Eriksson, 1984; Bortnikov *et al.*, 1979; Spiridonov *et al.*, 1986a). X-ray data from one of these occurrences could permit the validation of annivite as the Bi pole relatively to tetrahedrite and tennantite.

3. Nowackiite isotypic series

Nowackiite, $Cu_6Zn_3As_4S_{12}$
STR: Marumo (1967).
Aktashite, $Cu_6Hg_3As_4S_{12}$
STR: Kaplunnik *et al.* (1980).
Gruzdevite, $Cu_6Hg_3Sb_4S_{12}$

Related
Sinnerite, $Cu_6As_4S_9$
STR: Makovicky & Skinner (1975).

Watanabeite, $Cu_4(As, Sb)_2S_5$
Def.: Shimizu *et al.* (1993).

Laffittite, $AgHgAsS_3$
STR: Nakai & Appleman (1983).

4. Routhierite isotypic pair

Routhierite, $CuHg_2TlAs_2S_6$
Stalderite, $Cu(Zn, Fe, Hg)_2TlAs_2S_6$
Definition and STR: Graeser *et al.* (1995).

Routhierite: new structural formula
The formula of routhierite (Johan *et al.*, 1974) was revised by Graeser *et al.* (1995), together with the definition of stalderite: routhierite is the Hg isotype of stalderite (Zn-rich end-member).

5. Unclassified Cu sulfosalts

Miharaite, $Cu_4FePbBiS_6$
STR: Petrova *et al.* (1988).
Isotypic pair
Petrovicite, $Cu_3HgPbBiSe_5$
Mazzettiite, $Ag_3HgPbSbTe_5$
Def.: Bindi & Cipriani (2004b).
Chaméanite, $(Cu, Fe)_4As(Se, S)_4$
Def.: Johan *et al.* (1982).
Mgriite, $(Cu, Fe)_3AsSe_3$
Def.: Dymkov *et al.* (1982).
Larosite, $(Cu, Ag)_{21}PbBiS_{13}$
Arcubisite, $CuAg_6BiS_4$

Chaméanite and mgriite: the same species?
Chaméanite (Johan *et al.*, 1982) and mgriite (Dymkov *et al.*, 1982) have very similar chemical compositions and X-ray powder diagrams; the *a* parameter of chaméanite is twice that of mgriite. They probably are the same species; in this case, chaméanite (IMA 1980-088) would have priority relatively to mgriite (IMA 1980-100), but reexamination of the type samples is needed.

In the Cu–As–Se ternary system (Cohen *et al.*, 1995), there are only two ternary phases, $CuAsSe_2$ and Cu_3AsSe_4. According to Golovej *et al.* (1985), Cu_3AsSe_4 has the same unit cell as mgriite (5.530 Å; chaméanite: 5.519 × 2), and its crystal structure is given. Thus, the discrepancy between Cu/As/Se ratios of these three close compounds is difficult to explain.

6.2. Ag-rich sulfosalts

1. (Single type)

Samsonite, $MnAg_4Sb_2S_6$
STR: Edenharter & Nowacki (1974); Bindi & Evain (2007).

2. Pyrargyrite family

Pyrargyrite isotypic pair
Pyrargyrite, Ag_3SbS_3
Proustite, Ag_3AsS_3
STR: the two structures were refined by Engel & Nowacki (1966).
Related
Ellisite, Tl_3AsS_3
STR: Gostojic (1980 – synth.).

3. Pyrostilpnite isotypic pair

Pyrostilpnite, Ag_3SbS_3
STR: Kutoglu (1968).
Xanthoconite, Ag_3AsS_3
STR: Engel & Nowacki (1968); Rosenstingl & Pertlik (1993).

4. Polybasite isotypic series

The nomenclature of this series has now been clarified through the resolution of the crystal structures of various polytypes. Details are given by Bindi *et al.* (2007a).
Polybasite, $Cu(Ag, Cu)_6Ag_9Sb_2S_{11}$
STR: Evain *et al.* (2006b). The structural formula is $[Ag_9CuS_4][(Ag, Cu)_6(Sb, As)_2S_7]$.
Pearceite, $Cu(Ag, Cu)_6Ag_9As_2S_{11}$
STR: Bindi *et al.* (2006). The structural formula is $[Ag_9CuS_4][(Ag, Cu)_6(As, Sb)_2S_7]$.
Correspondence between old mineral names and related unit-cell types and new polytype nomenclature is given in Table 5.
Selenopolybasite, $Cu(Ag, Cu)_6Ag_9Sb_2(S, Se)_9Se_2$
Def.: Bindi *et al.* (accept.). It is the Se-rich analogue of the polytype polybasite-*Tac*.
STR: Evain *et al.* (2006c). The structural formula is: $[(Ag, Cu)_6(Sb, As)_2(S, Se)_7]$ $[Ag_9Cu(S, Se)_2Se_2]$.

5. Stephanite isotypic pair

Stephanite, Ag_5SbS_4
STR: Ribár & Nowacki (1970).
Selenostephanite, $Ag_5Sb(Se, S)_4$
Related?
Fettelite, $Ag_{24}HgAs_5S_{20}$
Def.: Wang & Paniagua (1996).
STR: abstract by Pérez-Priede *et al.* (2005), who indicate similarities with laffittite althougt in this species the (Ag, Hg)/*Pn*/S ratio is quite distinct, and is identical to that of stephanite (5/1/4).

6. Unclassified Ag sulfosalts

Benleonardite, $Ag_8(Sb, As)Te_2S_3$
Tsnigriite, $Ag_9Sb(S, Se)_3Te_3$
Def.: Sandomirskaya *et al.* (1992). May be related to the argyrodite group.
Dervillite, Ag_2AsS_2
Redefinition: Bari *et al.* (1983).

Dervillite: As–As bonding? (subsulfosalt)
As in tvalchrelidzeite (see below), the redefinition of dervillite (Bari *et al.*, 1983) indicates a sulfur deficit that may correspond to As–As bonding, as in realgar. A crystal-structure determination is needed.

7. Unclassified sulfosalts

7.1. Oxysulfosalts

Sarabauite, $Sb_4S_6{\cdot}CaSb_6O_{10}$

Table 5. Polytype nomenclature in the polybasite-pearceite series (Bindi *et al.*, 2007a).

Name	As/Sb ratio	Unit-cell	Old name	Structure
Pearceite-*Tac*	As > Sb	Type 111	Pearceite	Bindi *et al.* (2006)
Pearceite-*T*2*ac*	As > Sb	Type 221	Arsenpolybasite	Bindi *et al.* (2007b)
Pearceite-*M*2*a*2*b*2*c*	As > Sb	Type 222	Arsenpolybasite	– – –
Polybasite-*Tac*	Sb > As	Type 111	Antimonpearceite	– – –
Polybasite-*T*2*ac*	Sb > As	Type 221	Polybasite	Evain *et al.* (2006b)
Polybasite-*M*2*a*2*b*2*c*	Sb > As	Type 222	Polybasite	– – –

STR: Nakai *et al.* (1978).
Cetineite, ~ $NaK_5Sb_{14}S_6O_{18}(H_2O)_6$
STR: Sabelli *et al.* (1988).
Isotype:
Ottensite, $Na_3(Sb_2O_3)_3(SbS_3)\cdot 3H_2O$
Def.: Sejkora & Hyrsl (2007).

7.2. "Subsulfosalts"

Tvalchrelidzeite, Hg_3SbAsS_3
STR: Yang *et al.* (2007).
Criddleite, $Ag_2Au_3TlSb_{10}S_{10}$
Jonassonite, $Au(Bi,Pb)_5S_4$
Def.: Paar *et al.* (2006). There are two varieties of jonassonite. One variety, including that from the type deposit (Nagybörzsöny, Hungary) is Pb-rich (between 5 and 8 wt.%); the second one, which is more common, is Pb-free. Without crystal-structure data, one cannot say if the incorporation of Pb just corresponds to a solid solution, or if it induces structural changes.

Sulfosalts, or not?
All these three minerals show a strong sulfur deficiency ("subsulfides"), indicating that As, Sb or Bi may also act as an anion (see also dervillite). Crystal-structure studies are needed to answer this question and to confirm that these minerals conform to the extended definition of a sulfosalt.

7.3. PGE sulfosalts?

Borovskite, Pd_3SbTe_4
Crerarite, $(Pt,Pb)Bi_3(S,Se)_{4-x}$
Def.: Cook *et al.* (1994).
Crystal-structure data are necessary to ascertain whether these minerals are sulfosalts.

8. Conclusion

This re-examination of sulfosalt systematics indicates that today there are more than 220 valid mineral species (see the alphabetical index). Together with the regular discovery of new species, as exemplified by the annual reports of the IMA-CNMNC and previous CNMMN, the progress in crystal-structure study will play a critical role for the resolution of some questions of systematics still in abeyance. More than 50 crystal structures remain unsolved, among which about half probably correspond to new structure types.

In addition to the sulfosalt minerals listed in this report, the published literature contains reports of about 200 unnamed minerals that can probably be regarded as sulfosalts, with compositions significantly different from those of known sulfosalt minerals. Data on these minerals are included in a report by the Sub-Committee for Unnamed Minerals of the IMA Commission on New Minerals, Nomenclature and Classification (Smith & Nickel, 2007).

The still-outstanding questions of systematics encountered in this report are summarized below. The questions mainly concern the status of about twenty species. As a complement, the final appendix is an extract of discredited names of sulfosalt species.

1. Valid minerals without specific published definitions

- Approved by the IMA-CNMNC, but unpublished: marumoite (IMA 1998-004);
- approved by the IMA-CNMNC, but only the crystal structure has been published: simonite (IMA 1982-052) (Engel *et al.*, 1982);
- without approval of the IMA-CNMNC, with publication of only the crystal structure: rebulite (Balić-Žunić *et al.*, 1982).

2. Identical, or distinct species?

- Fizélyite – ramdohrite pair;
- twinnite – guettardite pair;
- chaméanite – mgriite pair.

3. "Sulfosalt limbo"

3.1. Ill-defined or still questionable mineral species

- Falkmanite ($Pb_3Sb_2S_6$) and plumosite ($Pb_2Sb_2S_5$): relationship with boulangerite?
- Sakharovaite [$FePb_4(Sb,Bi)_6S_{14}$]: species, or Bi-rich jamesonite?
- Ustarasite [$Pb(Bi,Sb)_6S_{10}$]: no unit-cell determination.
- Wittite [$Pb_8Bi_{10}(S,Se)_{23}$]: species, or Se-rich variety of cannizzarite?
- Zoubekite ($AgPb_4Sb_4S_{10}$): doubtful unit-cell data.

3.2. Possible definition or redefinition as valid species

- *Annivite* [$Cu_6[Cu_4(Fe,Zn)_2](Bi,Sb,As)_4S_{13}$]: possible revalidation for Bi > Sb, As (unit-cell data lacking);
- *Baumhauerite-ψO3abc* [$Ag_3Pb_{38.1}(As,Sb)_{52.8}S_{96}$]: homeotype of baumhauerite and baumhauerite-2*a*?
- *Bursaite* [$Pb_{3-3x}Bi_{2+2x}S_6(?)$]: needs crystal-structure data;

– *Incaite* (~ $FePb_4Sn_2Sn_2Sb_2S_{14}$): possible revalidation if $Sn^{2+} > Pb^{2+}$ in a natural sample;
– *Ourayite-P* (~ $Ag_{3.6}Pb_{2.8}Bi_{5.6}S_{13}$): empirical formula;
– *Rathite*-IV: chemical formula unknown;
– *Schirmerite* (Type 1 – $Ag_4PbBi_4S_9$): identical with schapbachite, or a dimorph?

Beyond, and complementary to the definition of each individual mineral species, is the question of relative limits of neighbouring sulfosalts in complex crystal-chemical systems. Four examples have been presented in this report:

– the aikinite–bismuthinite homeotypic series. Here numerous intermediate homeotypes have been defined, but the narrow solid-solution fields of all species have to be defined;
– the sartorite homologous series. In this goup complex superstructures are present, especially for As-rich members, together with the presence of minor Tl or Ag. New resolutions of true structures in this system are necessary to understand the role of these chemical factors;
– tetrahedrite isotypic series. Contrary to the aikinite–bismuthinite series, in this series there are extended solid solutions, and the transitions between different poles must be defined (*e.g.*, the limits between tetrahedrite, freibergite and argentotetrahedrite);
– the lillianite–andorite homologous series. Here there are extended (but not complete) solid solutions on the one hand (*e.g.*, $Bi^{3+} \leftrightarrow Sb^{3+}$, or $2\ Pb^{2+} \leftrightarrow Ag^{+} + Bi^{3+}$), and, on the other hand, stabilization of discrete compounds by metals with minor content (Mn, Cd, Fe).

In the years to come, progress in the field of the systematics of sulfosalts will be more and more dependent on crystal structure studies, that requires the availability of well-ordered natural or synthetic crystals, as well as a combination of various methods, taking into account modern approaches (*e.g.*, single crystal and powder synchrotron X-ray diffraction; application of non-harmonic approach to atomic displacement parameters for Cu- and Ag-rich sulfosalts; *ab initio* structure determinations).

Alphabetical index of accepted species of sulfosalts with As^{3+}, Sb^{3+}, Bi^{3+} or Te^{4+}

CSU: Crystal structure unsolved. ∇: vacancy. Q: Validity questionable (see Sect. 3.1 of the final conclusion)

Species	Chapter	Formula	Remark
A			
Aikinite	4.3	$CuPbBiS_3$	
Aktashite	6.1.3	$Cu_6Hg_3As_4S_{12}$	
Aleksite	2.1	$PbBi_2S_2Te_2$	CSU
Andorite IV	3.1.1	$Ag_{15}Pb_{18}Sb_{47}S_{96}$	CSU – also named “quatrandorite”
Andorite VI	3.1.1	$AgPbSb_3S_6$	Also named “senandorite”
Angelaite	2.3.1	$Cu_2AgPbBiS_4$	
Aramayoite	1.1.2	$Ag_3Sb_2(Bi, Sb)S_6$	
Arcubisite	1.5	$CuAg_6BiS_4$	CSU
Ardaite	4.4	$Pb_{17}Sb_{15}S_{35}Cl_9$	CSU
Argentotennantite	6.1.2	$Ag_6[Cu_4(Fe, Zn)_2]As_4S_{13}$	CSU
Argentotetrahedrite	6.1.2	$Ag_{10}(Fe, Zn)_2Sb_4S_{13}$	CSU. Published without CNMNC approval
Aschamalmite	3.2	$Pb_{6-3x}Bi_{2+x}S_9$	
B			
Babkinite	2.1	$Pb_2Bi_2(S, Se)_3$	CSU
Baumhauerite	3.8.2	$Pb_{12}As_{16}S_{36}$	CSU
Baumhauerite-2*a*	3.8.2	~ $Ag_{1.5}Pb_{22}As_{33.5}S_{72}$	
Baumstarkite	1.1.2	$Ag_3Sb_3S_6$	
Benavidesite	4.1	$MnPb_4Sb_6S_{14}$	
Benjaminite	3.2	$Ag_3Bi_7S_{12}$	
Benleonardite	6.2.6	$Ag_8(Sb, As)Te_2S_3$	CSU
Bernardite	5.1.1	$TlAs_5S_8$	
Berryite	2.2.1	$Cu_3Ag_2Pb_3Bi_7S_{16}$	
Berthierite	4.1	$FeSb_2S_4$	
Bohdanowiczite	1.1.1	$AgBiSe_2$	True crystal-structure unknown
Borodaevite	3.2	$Ag_{4.83}Fe_{0.21}Pb_{0.45}(Bi, Sb)_{8.84}S_{16}$	CSU
Borovskite	7.3	Pd_3SbTe_4	CSU
Boulangerite	4.1	$Pb_5Sb_4S_{11}$	
Bournonite	1.2.2	$CuPbSbS_3$	
Buckhornite	2.2.1	$(Pb_2BiS_3)(AuTe_2)$	

Species	Chapter	Formula	Remark
C			
Cannizzarite	2.2.2	~ $Pb_8Bi_{10}S_{23}$	
Cetineite	7.1	$NaK_5Sb_{14}S_6O_{18}(H_2O)_6$	
Chabournéite	3.8.5	$Tl_5(Sb, As)_{21}S_{34}$	
Chalcostibite	1.1.7	$CuSbS_2$	
Chaméanite	6.1.5	$(Cu, Fe)_4As(Se, S)_4$	CSU – probably identical with mgriite
Christite	1.2.4	$HgTlAsS_3$	
Clerite	4.1	$MnSb_2S_4$	
Cosalite	4.1	$Pb_2Bi_2S_5$	
Crerarite	7.3	$(Pt,Pb)Bi_3(S, Se)_{4-x}$	CSU
Criddleite	7.2	$Ag_2Au_3TlSb_{10}S_{10}$	CSU
Cuboargyrite	1.1.3	$AgSbS_2$	
Cuprobismutite	3.3	$Cu_8AgBi_{13}S_{24}$	
Cupromakovickyite	3.2	$Cu_4AgPb_2Bi_9S_{18}$	
Cupropavonite	3.2	$Cu_{0.9}Ag_{0.5}Pb_{0.6}Bi_{2.5}S_5$	CSU
Cylindrite	2.2.2	~ $FePb_3Sn_4Sb_2S_{14}$	(mean structure only)
D			
Dadsonite	4.1	$Pb_{23}Sb_{25}S_{60}Cl$	
Dervillite	6.2.6	Ag_2AsS_2	CSU
Diaphorite	1.2.1	$Ag_3Pb_2Sb_3S_8$	
Dufrénoysite	3.8.6	$Pb_2As_2S_5$	
E			
Edenharterite	5.1.2	$TlPbAs_3S_6$	
Ellisite	6.2.2	Tl_3AsS_3	
Emilite	4.3	$Cu_{10.7}Pb_{10.7}Bi_{21.3}S_{48}$	
Eclarite	4.2.2	$(Cu, Fe)Pb_9Bi_{12}S_{28}$	
Emplectite	1.1.7	$CuBiS_2$	
Erniggliite	5.4	$SnTl_2As_2S_6$	
Eskimoite	3.1.2	$Ag_7Pb_{10}Bi_{15}S_{36}$	(CSU – structure model only)
F			
Falkmanite	4.1	$Pb_3Sb_2S_6$	Q – CSU. Relationship with boulangerite?
Felbertalite	2.3.1	$Cu_2Pb_6Bi_8S_{19}$	
Fettelite	6.2.5	$Ag_{24}HgAs_5S_{20}$	Crystal structure: abstract only
Fizélyite	3.1.1	$Ag_5Pb_{14}Sb_{21}S_{48}$	CSU
Franckeite	2.2.2	$Fe(Pb, Sn)_6Sn_2Sb_2S_{14}$	(mean structure only)
Freibergite	6.1.2	$Ag_6[Cu_4Fe_2]Sb_4S_{13-x}$(?)	Limit with Ag-rich tetrahedrite?
Freieslebenite	1.2.1	$AgPbSbS_3$	
Friedrichite	4.3	$Cu_5Pb_5Bi_7S_{18}$	CSU
Fülöppite	3.7	$Pb_3Sb_8S_{15}$	
G			
Gabrielite	5.4	$Cu_2AgTl_2As_3S_7$	
Galenobismutite	2.3.1	$PbBi_2S_4$	
Galkhaite	6.1.2	$(Cs, Tl, \nabla)(Hg, Cu, Zn, Tl)_6\ (As, Sb)_4S_{12}$	
Garavellite	4.1	$FeSbBiS_4$	
Geocronite	3.5.1	$Pb_{14}(Sb, As)_6S_{23}$	
Gerstleyite	5.1.4	$Na_2(Sb, As)_8S_{13}\cdot 2H_2O$	
Giessenite	4.2.2	$(Cu, Fe)_2Pb_{26.4}(Bi, Sb)_{19.6}S_{57}$	CSU
Gillulyite	5.1.3	$Tl_2As_{7.5}Sb_{0.3}S_{13}$	
Giraudite	6.1.2	$Cu_6[Cu_4(Fe, Zn)_2]As_4Se_{13}$	CSU
Gladite	4.3	$CuPbBi_5S_9$	
Goldfieldite	6.1.2	$Cu_{10}Te_4S_{13}$	
Gratonite	3.6	$Pb_9As_4S_{15}$	
Grumiplucite	3.2	$HgBi_2S_4$	
Gruzdevite	6.1.3	$Cu_6Hg_3Sb_4S_{12}$	CSU
Guettardite	3.8.1	$Pb_8(Sb_{0.56}As_{0.44})_{16}S_{32}$	CSU – difference with twinnite?
Gustavite	3.1.1	$AgPbBi_3S_6$	

Species	Chapter	Formula	Remark
Hakite	6.1.2	$Cu_6[Cu_4Hg_2]Sb_4Se_{13}$	CSU
Hammarite	4.3	$Cu_2Pb_2Bi_4S_9$	
Hatchite	1.3	$AgTlPbAs_2S_5$	
Heteromorphite	3.7	$Pb_7Sb_8S_{19}$	
Heyrovskýite	3.1.2	$Pb_6Bi_2S_9$	
Hodrushite	3.3	$Cu_8Bi_{12}S_{22}$	
Hutchinsonite	5.1.1	$TlPbAs_5S_9$	
I			
Imhofite	5.1.3	$Tl_{5.8}As_{15.4}S_{26}$	
Izoklakeite	4.2.2	$(Cu, Fe)_2Pb_{26.4}(Sb, Bi)_{19.6}S_{57}$	
J			
Jamesonite	4.1	$FePb_4Sb_6S_{14}$	
Jankovićite	5.2	$Tl_5Sb_9(As, Sb)_4S_{22}$	
Jaskólskiite	3.4	$Cu_xPb_{2+x}(Sb, Bi)_{2-x}S_5$	
Jentschite	5.1.2	$TlPbAs_2SbS_6$	
Jonassonite	7.2	$Au(Bi, Pb)_5S_4$	CSU
Jordanite	3.5.1	$Pb_{14}(As, Sb)_6S_{23}$	
Junoite	2.3.1	$Cu_2Pb_3Bi_8(S, Se)_{16}$	
K			
Kirkiite	3.5.2	$Pb_{10}Bi_3As_3S_{19}$	
Kobellite	4.2.2	$(Cu, Fe)_2Pb_{11}(Bi, Sb)_{15}S_{35}$	
Kochkarite	2.1	$PbBi_4Te_7$	
Krupkaite	4.3	$CuPbBi_3S_6$	
Kudriavite	3.2	$(Cd, Pb)Bi_2S_4$	
Kupčíkite	3.3	$Cu_{3.4}Fe_{0.6}Bi_5S_{10}$	
L			
Laffittite	6.1.3	$AgHgAsS_3$	
Lapieite	1.2.3	$CuNiSbS_3$	CSU
Larosite	6.1.5	$(Cu, Ag)_{21}PbBiS_{13}$	CSU
Launayite	4.4	$CuPb_{10}(Sb, As)_{13}S_{30}$	CSU
Lengenbachite	2.2.2	$\sim Cu_2Ag_4Pb_{18}As_{12}S_{39}$	CSU – structural model
Lévyclaudite	2.2.2	$\sim Cu_3Pb_8Sn_7(Bi, Sb)_3S_{28}$	
Lillianite	3.1.1	$Ag_xPb_{3-2x}Bi_{2+x}S_6$	
Lindströmite	4.3	$Cu_3Pb_3Bi_7S_{15}$	
Liveingite	3.8.3	$Pb_{20}As_{24}S_{56}$	
Livingstonite	3.2	$HgSb_4S_6(S_2)$	
Lorandite	1.1.7	$TlAsS_2$	
M			
Madocite	4.4	$Pb_{19}(Sb, As)_{16}S_{43}$	CSU
Makovickyite	3.2	$Cu_{1.12}Ag_{0.81}Pb_{0.27}Bi_{5.35}S_9$	
Malyshevite		$CuPdBiS_3$	CSU
Marrite	1.2.1	$AgPbAsS_3$	
Marumoite	3.8.5	$Pb_{32}As_{40}S_{92}$	CSU – no mineral description (IMA 1998-004)
Marrucciite	4.2.1	$Hg_3Pb_{16}Sb_{18}S_{46}$	
Matildite	1.1.1	$AgBiS_2$	True crystal-structure unknown
Mazzettiite	6.1.5	$Ag_3HgPbSbTe_5$	CSU
Meneghinite	3.4	$CuPb_{13}Sb_7S_{24}$	
Mgriite	6.1.5	$(Cu, Fe)_3AsSe_3$	CSU – probably identical with chaméanite
Miargyrite	1.1.4	$AgSbS_2$	
Miharaite	6.1.5	$Cu_4FePbBiS_6$	
Moëloite	4.1	$Pb_6Sb_6S_{14}(S_3)$	
Mozgovaite	3.2	$PbBi_4(S, Se)_7$	CSU
Mückeite	1.2.3	$CuNiBiS_3$	
Mummeite	3.2	$Cu_{0.58}Ag_{3.11}Pb_{1.10}Bi_{6.65}S_{13}$	
Museumite	2.2.1	$Pb_2(Pb, Sb)_2S_8[Te, Au]_2$	CSU
Mutnovskite	3.9	$Pb_2AsS_3(I, Cl, Br)$	

Species	Chapter	Formula	Remark
N			
Nagyágite	2.2.1	$[Pb_3(Pb, Sb)_3S_6](Te, Au)_3$	
Neyite	2.3.2	$Cu_6Ag_2Pb_{25}Bi_{26}S_{68}$	
Nordströmite	2.3.1	$CuPb_3Bi_7(S, Se)_{14}$	
Nowackiite	6.1.3	$Cu_6Zn_3As_4S_{12}$	
Nuffieldite	2.3.1	$Cu_{1.4}Pb_{2.4}Bi_{2.4}Sb_{0.2}S_7$	
O			
Ottensite	7.1	$Na_3(Sb_2O_3)_3(SbS_3)\cdot 3H_2O$	CSU
Ourayite	3.1.3	$Ag_3Pb_4Bi_5S_{13}$	CSU
Owyheeite	4.2.1	$Ag_3Pb_{10}Sb_{11}S_{28}$	
P			
Paarite	4.3	$Cu_{1.7}Pb_{1.7}Bi_{6.3}S_{12}$	
Paděraite	3.3	$Cu_7[(Cu, Ag)_{0.33}Pb_{1.33}Bi_{11.33}]_{\Sigma 13}S_{22}$	
Parapierrotite	3.8.7	$TlSb_5S_8$	
Pavonite	3.2	$AgBi_3S_5$	
Pearceite	6.2.4	$Cu(Ag, Cu)_6Ag_9As_2S_{11}$	
Pekoite	4.3	$CuPbBi_{11}S_{18}$	
Pellouxite	4.2.1	$(Cu, Ag)_2Pb_{21}Sb_{23}S_{55}ClO$	
Petrovicite	6.1.5	$Cu_3HgPbBiSe_5$	CSU
Pierrotite	3.8.7	$Tl_2(Sb, As)_{10}S_{16}$	
Pillaite	4.2.1	$Pb_9Sb_{10}S_{23}ClO_{0.5}$	
Pizgrischite	3.3	$(Cu, Fe)Cu_{14}PbBi_{17}S_{34}$	
Plagionite	3.7	$Pb_5Sb_8S_{17}$	
Playfairite	4.4	$Pb_{16}(Sb, As)_{19}S_{44}Cl$	CSU
Plumosite	4.1	$Pb_2Sb_2S_5$	Q – CSU. Relationship with boulangerite?
Polybasite	6.2.4	$Cu(Ag, Cu)_6Ag_9Sb_2S_{11}$	
Poubaite	2.1	$PbBi_2(Se,Te,S)_4$	
Proudite	2.3.1	$Cu_2Pb_{16}Bi_{20}(S, Se)_{47}$	
Proustite	6.2.2	Ag_3AsS_3	
Pyrargyrite	6.2.2	Ag_3SbS_3	
Pyrostilpnite	6.2.3	Ag_3SbS_3	
Q			
Quadratite	1.2.1	$Ag(Cd, Pb)(As, Sb)S_3$	
R			
Ramdohrite	3.1.1	$(Cd, Mn, Fe)Ag_{5.5}Pb_{12}Sb_{21.5}S_{48}$	Distinction from fizélyite?
Rathite	3.8.4	$Ag_2Pb_{12-x}Tl_{x/2}As_{18+x/2}S_{40}$	
Rayite	3.7	$(Ag,Tl)_2Pb_8Sb_8S_{21}$	CSU – needs an unit-cell redetermination
Rebulite	5.2	$Tl_5As_8Sb_5S_{22}$	No mineral description, nor CNMNC approval
Robinsonite	4.1	$Pb_4Sb_6S_{13}$	
Roshchinite	3.1.1	$(Ag, Cu)_{19}Pb_{10}Sb_{51}S_{96}$	
Routhierite	6.1.4	$CuHg_2TlAs_2S_6$	CSU
Rouxelite	2.3.2	$Cu_2HgPb_{22}Sb_{28}S_{64}(O, S)_2$	
Rucklidgeite	2.1	$PbBi_2Te_4$	
S			
Saddlebackite	2.1	$Pb_2Bi_2Te_2S_3$	CSU
Salzburgite	4.3	$Cu_{1.6}Pb_{1.6}Bi_{6.4}S_{12}$	
Sakharovaite	4.1	$FePb_4(Sb, Bi)_6S_{14}$	Q – CSU. unit cell not given
Samsonite	6.2.1	$MnAg_4Sb_2S_6$	
Sarabauite	7.1	$Sb_4S_6\cdot CaSb_6O_{10}$	
Sartorite	3.8.1	$PbAs_2S_4$	
Scainiite	4.2.1	$Pb_{14}Sb_{30}S_{54}O_5$	
Schapbachite	1.2.1	$Ag_{0.4}Pb_{0.2}Bi_{0.4}S$	Redefinition
Selenopolybasite	6.2.4	$Cu(Ag, Cu)_6Ag_9Sb_2(S, Se)_9Se_2$	
Selenostephanite	6.2.5	$Ag_5Sb(Se, S)_4$	CSU
Seligmannite	1.2.2	$CuPbAsS_3$	

Species	Chapter	Formula	Remark
Semseyite	3.7	$Pb_9Sb_8S_{21}$	
Sicherite	5.3	$Ag_2Tl(As, Sb)_3S_6$	
Simonite	5.4	$HgTlAs_3S_6$	No mineral description
Sinnerite	6.1.3	$Cu_6As_4S_9$	
Skinnerite	6.1.1	Cu_3SbS_3	
Smithite	1.1.5	$AgAsS_2$	
Sorbyite	4.4	$CuPb_9(Sb, As)_{11}S_{26}$	CSU
Součekite	1.2.2	$CuPbBi(S, Se)_3$	CSU
Stalderite	6.1.4	$Cu(Zn, Fe, Hg)_2TlAs_2S_6$	
Stephanite	6.2.5	Ag_5SbS_4	
Sterryite	4.4	$(Ag, Cu)_2Pb_{10}(Sb, As)_{12}S_{29}$	CSU
T			
Tennantite	6.1.2	$Cu_6[Cu_4(Fe, Zn)_2]As_4S_{13}$	
Tetrahedrite	6.1.2	$Cu_6[Cu_4(Fe, Zn)_2]Sb_4S_{13}$	
Tintinaite	4.2.2	$Cu_2Pb_{10}Sb_{16}S_{35}$	CSU
Treasurite	3.1.1	$Ag_7Pb_6Bi_{15}S_{30}$	CSU
Trechmannite	1.1.6	$AgAsS_2$	
Tsnigriite	6.2.6	$Ag_9Sb(S, Se)_3Te_3$	CSU
Tsugaruite	3.5.3	$Pb_4As_2S_7$	CSU
Tvalchrelidzeite	7.2	Hg_3SbAsS_3	
Twinnite	3.8.1	$Pb(Sb_{0.63}As_{0.37})_2S_4$	CSU – difference with guettardite?
U			
Uchucchacuaite	3.1.1	$MnAgPb_3Sb_5S_{12}$	CSU
Ustarasite	3.1.5	$Pb(Bi, Sb)_6S_{10}$	Q – CSU. No unit-cell data
V			
Vaughanite	5.4	$HgTlSb_4S_7$	CSU
Veenite	3.8.4	$Pb_2(Sb, As)_2S_5$	CSU
Vikingite	3.1.1	$Ag_5Pb_8Bi_{13}S_{30}$	
Volynskite	1.1.1	$AgBiTe_2$	True crystal structure unknown
Vrbaite	5.4	$Hg_3Tl_4As_8Sb_2S_{20}$	
Vurroite	4.2.1	$Sn_2Pb_{20}(Bi, As)_{22}S_{54}Cl_6$	
W			
Wallisite	1.3	$CuTlPbAs_2S_5$	
Watanabeite	6.1.3	$Cu_4(As, Sb)_2S_5$	CSU
Watkinsonite	2.2.1	$Cu_2PbBi_4(Se, S)_8$	CSU
Weibullite	2.3.1	$Ag_{0.33}Pb_{5.33}Bi_{8.33}(S, Se)_{18}$	
Weissbergite	1.1.7	$TlSbS_2$	
Wittichenite	6.1.1	Cu_3BiS_3	
Wittite	2.2.2	$Pb_8Bi_{10}(S, Se)_{23}$	Q
X			
Xanthoconite	6.2.3	Ag_3AsS_3	
Xilingolite	3.1.1	$Pb_3Bi_2S_6$	
Z			
Zinkenite	4.2.1	$Pb_9Sb_{22}S_{42}$	
Zoubekite	4.2.3	$AgPb_4Sb_4S_{10}$	Q
IMA approved*			
IMA 2005-024	2.2.2	$(Pb, Sn)_{12.5}As_3Sn_5FeS_{28}$	As-derivative of franckeite
IMA 2005-036	3.2	$Cu_8Ag_3Pb_4Bi_{19}S_{38}$	Pavonite series
IMA 2006-016	2.2.2	$Pb_2SnInBiS_7$	In-derivative of cylindrite
IMA 2007-003	1.2.3	$CuPtBiS_3$	Pt-isotype of lapieite
IMA 2007-010	4.4	$PbHgAs_2S_6$	

Total: 223 sulfosalt species. *Data source: IMA-CNMNC website.

Appendix: Additional list of discredited species

This list represents a selection of abandoned names, which are found in modern publications. The great majority of these discredited names (noted *) is compiled in the recent report on "Mass discreditation of GQN minerals" by E.A.J. Burke (2006), Chairman of the CNMNC-IMA. This report is of free access on the Net, at the CNMNC-IMA site.

**: Possible revalidation (see 3.1 in the final conclusion).

Alaskaite = a mixture of various Bi sulfosalts (Karup-Møller, 1972).

*Annivite*** = Bi-rich tennantite.

*Beegerite** = a mixture of "schirmerite" and matildite (Karup-Møller, 1973).

*Bonchevite**, $PbBi_4S_7$, defined by Kostov (1958), was formally discredited by the CNMNC (IMA 67-2a; Franz *et al.*, 1967; 1969), as a mixture of galenobismutite with a sulfosalt of the lillianite type. Through reexamination of new material from the type deposit, Birch & Mumme (1985) identified pekoite, and considered bonchevite as a mixture of pekoite and galenobismutite.

*Brongniardite/Brongniartite**, $PbAg_2Sb_2S_5$ (Pb-poor diaphorite – Mozgova *et al.*, 1989) (retained in Strunz & Nickel, 2001).

*Bursaite** = an intergrowth of two phases (Mozgova *et al.*, 1988).

Eichbergite = a mixture of jaskolskiite and Bi-bearing meneghinite (Paur *et al.*, in prep.)

*Goongarrite**, $Pb_6Bi_2S_9$ = a symplectitic mixture of galena and cosalite, from the decomposition of metastable heyrovskýite (Klominsky *et al.*, 1971). See also Rieder (1963).

*Gelnicite/Gelnicaite** = identical with marrucciite (Orlandi *et al.*, 2007).

*Incaite***: Sn^{2+}-rich franckeite (Mozgova *et al.*, 1976).

*Kitaibelite** = Pb-containing pavonite (Weiszburg *et al.*, 1992).

Nakaséite, $Ag_3CuPb_4Sb_{12}S_{24}$ (Fleischer, 1960) = a disordered precursor of andorites IV and VI (Moëlo *et al.*, 1989).

*Parajamesonite**, $FePb_4Sb_6S_{14}$ = a mixture of jamesonite and other sulfosalts (Papp, 2004; Papp *et al.*, 2007).

Platynite, $Pb_4Bi_7S_4Se_7$ = a mixture of laitakarite and galena (Holtstam & Söderhielm, 1999) (retained in Strunz & Nickel, 2001).

Potosiite = Sn^{2+}-poor franckeite (Makovicky & Hyde, 1992).

Rathite varieties: see details in this report.

Rézbányite = a mixture of aikinite derivatives, paděraite and other sulfosalts (Žák *et al.*, 1992).

Schirmerite (*Type I*)**, $Ag_4PbBi_4S_9$ = schaphachite.?

Schirmerite (*Type II*), ~ $AgPbBi_3S_6$ to $Ag_{1.5}Pb_3Bi_{3.5}S_9$ = a disordered member of the lillianite homologous series (Makovicky & Karup-Møller, 1977b).

Schulzite, $Pb_{14}Sb_6S_{23}$ (As-free geocronite).

Scleroclase, $PbAs_2S_4$ (old name for sartorite).

Teremkovite, $Pb_7Ag_2Sb_8S_{20}$ (CNMMN-IMA, 1971) (probable Ag-poor variety of owyheeite – Moëlo *et al.*, 1984b).

Wittite B = proudite (Mumme, 1976).

References

Agaev, K.A. & Semiletov, S.A. (1963): Electron-diffraction study of the structure of $PbBi_2Se_4$. *Sov. Phys. Crystallogr.,* **13**, 201-203.

Armbruster, T. & Hummel, W. (1987): (Sb, Bi, Pb) ordering in sulfosalts: Crystal-structure refinement of a Bi-rich izoklakeite. *Am. Mineral.,* **72**, 821-831.

Armbruster, T., Makovicky, E., Berlepsch, P., Sejkora, J. (2003): Crystal structure, cation ordering, and polytypic character of diaphorite, $Pb_2Ag_3Sb_3S_8$, a PbS-based structure. *Eur. J. Mineral.,* **15**, 137-146.

Balić-Žunić, T. (1989): Systematics of sulfosalts and the role of thallium in their crystal structure. *God. Jugosl. cent. kristalogr.*, **24**, 19-32.

Balić-Žunić, T. & Engel, P. (1983): Crystal structure of synthetic $PbTlAs_3S_6$. *Z. Kristallogr.,* **165**, 261-269.

Balić-Žunić, T. & Makovicky, E. (1993): Contributions to the crystal chemistry of thallium sulphosalts. I. The O-D nature of imhofite. *N. Jb. Miner. Abh.,* **165**, 317-330.

—, — (2007): The crystal structure of kudriavite, $(Cd, Pb)Bi_2S_4$. *Can. Mineral.*, **45**, 437-443.

Balić-Žunić, T., Scavnicar, S., Engel, P. (1982): The crystal structure of rebulite, $Tl_5As_8Sb_5S_{22}$. *Z. Kristallogr.,* **160**, 109-125.

Balić-Žunić, T., Makovicky, E., Moëlo, Y. (1995): Contributions to the crystal chemistry of thallium sulphosalts. III. The crystal structure of lorandite ($TlAsS_2$) and its relation to weissbergite ($TlSbS_2$). *N. Jb. Miner. Abh.,* **168**, 213-235.

Balić-Žunić, T., Topa, D., Makovicky, E. (2002): The crystal structure of emilite, $Cu_{10.7}Pb_{10.7}Bi_{21.3}S_{48}$, the second 45 Å derivative of the bismuthinite–aikinite solid-solution series. *Can. Mineral.,* **40**, 239-245.

Balić-Žunić, T., Makovicky, E., Karanović, L., Poleti, D., Graeser, S. (2006): The crystal structure of gabrielite, $Tl_2AgCu_2As_3S_7$, a new species of thallium sulfosalt from Lengenbach, Switzerland. *Can. Mineral.,* **44**, 141-158.

Balitskaya, O.V., Mozgova, N.N., Borodaev, Yu.S., Efimova, A.V., Tsepin, A.I. (1989): Evolution of the unit cell parameter of fahlores with their silver content. *Izv. Akad.. Nauk SSSR, Geol. Ser.,* **9**, 112-120 (in Russian).

Bari, H., Cesbron, F., Moëlo, Y., Permingeat, F., Picot, P., Pierrot, R., Schubnel, H.J., Weil, R. (1983): La dervillite, Ag_2AsS_2, nouvelle définition de l'espèce. *Bull. Minéral.,* **106**, 519-524.

Basu, K., Bortnikov, N.S., Mookherjee, A., Mozgova, N.N., Tsepin, A.I., Vyalsov, L.N. (1983): Rare minerals from Rajpura-Dariba, Rajasthan, India IV: a new Pb–Ag–Tl–Sb sulphosalt, rayite. *N. Jb. Miner. Mh.*, **1983** (7), 296-304.

Bente, K. & Edenharter, A. (1989): Roentgenographische Strukturanalyse von $MnSb_2S_4$ und Strukturverfeinerung von Berthierite, $FeSb_2S_4$. *Z. Kristallogr.*, **186**, 31-33.

Bente, K. & Kupčik, V. (1984): Redetermination and refinement of the structure of tetrabismuth tetracopper enneasulphide $Cu_4Bi_4S_9$. *Acta Cryst.*, **C40**, 1985-1986.

Bente, K. & Meier-Salimi, M. (1991): Substitution experiments and structure investigations on Ag–Tl-bearing boulangerites – a contribution to the rayite problem. *N. Jb. Miner. Abh.*, **163**, 212-216.

Bente, K., Doering, Th., Edenharter, A., Kupčik, V., Steins, M., Wendschuh-Josties, M. (1990): Structure of the new mineral mückeite, $BiCuNiS_3$. *Acta Cryst.,* **C46**, 127-128.

Bente, K., Engel, M., Steins, M. (1993): Crystal structure of lead bismuth silver sulfide. *Z. Kristallogr.,* **205**, 327-328.

Berlepsch, P. (1996): Crystal structure and crystal chemistry of the homeotypes edenharterite ($TlPbAs_3S_6$) and jentschite ($TlPbAs_2SbS_6$) from Lengenbach, Binntal (Switzerland). *Schweiz. Mineral. Petrogr. Mitt.,* **76**, 147-157.

Berlepsch, P., Balić-Žunić, T., Makovicky, E. (1999): The superposition structure of quadratite $Ag(Cd,Pb)AsS_3$. Danske Krystallografmøde, 20-21 May 1999, Forskningcenter Risoe, Abstr. 30.

Berlepsch, P., Makovicky, E., Balić-Žunić, T. (2000): Contribution to the crystal chemistry of Tl-sulfosalts. VI. Modular-level structure relationship between edenharterite $TlPbAs_3S_6$ and jentschite $TlPbAs_2SbS_6$. *N. Jb. Miner. Mh.*, **2000** (7), 315-332.

Berlepsch, P., Armbruster, T., Makovicky, E., Hejny, C., Topa, D., Graeser, S. (2001a): The crystal structure of (001) twinned xilingolite, $Pb_3Bi_2S_6$, from Mittal-Hohtenn, Valais, Swizerland. *Can. Mineral.,* **39**, 1653-1663.

Berlepsch, P., Makovicky, E., Balić-Žunić, T. (2001b): Crystal chemistry of meneghinite homologues and related sulfosalts. *N. Jb. Miner. Mh.,* **2001** (3), 115-135.

—, —, — (2001c): Crystal chemistry of sartorite homologues and related sulfosalts. *N. Jb. Miner. Abh.,* **176**, 45-66.

Berlepsch, P., Armbruster, T., Topa, D. (2002): Structural and chemical variations in rathite, $Pb_8Pb_{4-x}(Tl_2As_2)_x(Ag_2As_2)As_{16}S_{40}$: modulations of a parent structure. *Z. Kristallogr.,* **217**, 581-590.

Berlepsch, P., Armbruster, T., Makovicky, E., Topa, D. (2003): Another step toward understanding the true nature of sartorite: Determination and refinement of a ninefold superstructure. *Am. Mineral.,* **88**, 450-461.

Bindi, L. & Cipriani, C. (2004a): Museumite, $Pb_2(Pb,Sb)_2S_8[Te,Au]_2$, a new mineral from the gold telluride deposit of Sacarîmb, Metaliferi Mountains, western Romania. *Eur. J. Mineral.*, **16**, 835-838.

—, — (2004b): Mazzettiite, $Ag_3HgPbSbTe_5$, a new mineral species from Findley Gulch, Saguache County, Colorado, USA. *Can. Mineral.,* **42**, 1739-1743.

Bindi, L. & Evain, M. (2007): Gram-Charlier development of the atomic displacement factors into mineral structures: The case of samsonite, $Ag_4MnSb_2S_6$. *Am. Mineral.,* **92**, 886-891.

Bindi, L. & Menchetti, S. (2005): Garavellite, $FeSbBiS_4$, from the Caspari mine, North Rhine-Westphalia, Germany: composition, physical properties and determination of the crystal structure. *Mineral. Petrol.,* **85**, 131-139.

Bindi, L., Evain, M., Menchetti, S. (2006): Temperature dependence of the silver distribution in the crystal structure of natural pearceite, $(Ag,Cu)_{16}(As,Sb)_2S_{11}$. *Acta Cryst.,* **B62**, 212-219.

Bindi, L., Evain, M., Spry, P.G., Menchetti, S. (2007a): The pearceite–polybasite group of minerals: Crystal chemistry and new nomenclature rules. *Am. Mineral.,* **92**, 918-925.

Bindi, L., Evain, M., Menchetti, S. (2007b): Complex twinning, polytypism and disorder phenomena in the crystal structures of antimonpearceite and arsenpolybasite. *Can. Mineral.,* **45**, 321-333.

Bindi, L., Evain, M., Menchetti, S.: Selenopolybasite, $[(Ag,Cu)_6(Sb,As)_2(S,Se)_7]$-$[Ag_9Cu(S,Se)_2Se_2]$, a new member of the pearceite–polybasite group from the De Lamar mine, Owyhee County, Idaho, USA. *Can. Mineral.* (accept.).

Birch, W.D. & Mumme, W.G. (1985): Pekoite from Narechen, Bulgaria – a possible solution to the bonchevite problem. *Mineral. Mag.,* **49**, 135-137.

Birnie, R.W. & Burnham, C.W. (1976): The crystal structure and extent of solid solution of geocronite. *Am. Mineral.,* **61**, 963-970.

Blackburn, W.H. & Dennen, W.H. (1997): Encyclopedia of Mineral Names. Mineral. Assoc. Can. Special Publication **1**, 360 p.

Boiocchi, M. & Callegari, A. (2003): Crystal structure refinement of a wallisite-hatchite solid solution. *N. Jb. Miner. Mh.*, **2003** (9), 396-406.

Bonazzi, P., Borrini, D., Mazzi, F., Olmi, F. (1995): Crystal structure and twinning of Sb_2AsS_2, the synthetic analogue of pääkönenite. *Am. Mineral.*, **80**, 1054-1058.

Borodaev, Yu.S. & Mozgova, N.N. (1975): Bismuth-antimony sulfosalts of lead from the Pochekuev deposit (East Transbaikal). *Geol. Rudn. Mestorozh.,* **2**, 47-58 (in Russian).

Bortnikov, N.S., Kudryavtsev, A.S., Troneva, N.V. (1979): Bi-rich tetrahedrite from the Tary-Ekan deposit (East Karamazar, Central Asia). *Mineral. Zhurnal*, **198**, 61-64 (in Russian).

Bortnikov, N.S., Laputina, I.P., Safonov, Yu.G. (1987): A new group of minerals in the system Ag–Pb–Bi–S from the Kanimansursk ore field (Karamazar). *Dokl. Akad. Nauk SSSR,* **292**, 1235-1238 (in Russian).

Breskovska, V.V., Mozgova, N.N., Bortnikov, N.S., Gorshkov, A.I., Tsepin, A.I. (1982): Ardaite – a new lead-antimony chlorosulphosalt. *Mineral. Mag.*, **46**, 357-361.

Brodtkorb, M.K. & Paar, W. (2004): Angelaíta en la paragénesis del distrito Los Manantiales, provincia del Chubut: Una nueva especie mineral. *Revista de la Associacion Geologica Argentina*, **59** (4), 787-789.

Brown, K.L. & Dickson, F.W. (1976): The crystal structure of synthetic christite, $HgTlAsS_3$. *Z. Kristallogr.,* **144**, 367-376.

Bryzgalov, I.A., Spiridonov, E.M., Petrova, I.V., Sakharova, M.S. (1996): Babkinite $Pb_2Bi_2(S,Se)_3$ – a new mineral. *Dokl. Akad. Nauk SSSR*, **346**, 656-659 (in Russian).

Burke, E.A.J. (2006): A mass discreditation of GQN minerals. *Can. Mineral.,* **44**, 1557-1560.

Cabri, L.J. (1981): The platinum group minerals. *in* "Platinum-group elements: mineralogy, geology, recovery", L.J. Cabri, ed. Canadian Institute of Mining and Metallurgy, Special Vol. **23**, 136-138.

— (2002): The platinum-group minerals. *in* "The Geology, Geochemistry, Mineralogy and Mineral Beneficiation of Platinum Group Element". L.J. Cabri, ed. Canadian Institute of Mining, Metallurgy and Petroleum, Special Vol. **54**, 13-130.

Chaplygin, I.V., Mozgova, N.N., Magazina, L.O., Kuznetsova, O.Yu., Safonov, Yu.G., Bryzgalov, I.A., Makovicky, E., Balić-Žunić, T. (2005): Kudriavite, $(Cd,Pb)Bi_2S_4$, a new mineral species from Kudriavy volcano, Iturup island, Kurile arc, Russia. *Can. Mineral.,* **43**, 695-701.

Chapman, E.J. (1843): Practical mineralogy. London, Paris, and Leipzig (8 vol.).

Chen, T.T. & Szymański, J.T. (1981): The structure and chemistry of galkhaite, a mercury sulfosalt containing Cs and Tl. *Can. Mineral.,* **19**, 571-581.

—, — (1982): A comparison of galkhaite from Nevada and from the type locality, Khaydarkan, Kirgizia, U.S.S.R. *Can. Mineral.,* **20**, 575-577.

Chen, T.T., Kirchner, E., Paar, W. (1978) Friedrichite, $Cu_5Pb_5Bi_7S_{18}$, a new member of the aikinite-bismuthinite series. *Can. Mineral.*, **16**, 127-130.

Chernikov, A.A., Chistyakova, N.I., Uvarkina, O.M., Dubinchuk, V.T., Rassulov, V.A., Polekhovsky, Y.S. (2006): Malyshevite – A new mineral from Srednyaya Padma deposit in Southern Karelia. *New Data on Minerals*, **41**, 14-17.

Cho, Seung-Am & Wuensch, B.J. (1974): The crystal structure of plagionite, $Pb_5Sb_8S_{17}$, the second member in the homologous series $Pb_{3+2n}Sb_8S_{15+2n}$. *Z. Kristallogr.,* **139**, 351-378.

Ciobanu, C.L. & Cook, N.J. (2000): Intergrowths of bismuth sulphosalts from Ocna de Fier Fe-skarn deposit, Banat, Southwest Romania. *Eur. J. Mineral.,* **12**, 899-917.

Ciobanu, C.L., Pring, A., Cook, N.J. (2004): Micro- to nano-scale intergrowths among members of the cuprobismutite series and paděraite: HRTEM and microanalytical evidence. *Mineral. Mag.,* **68**, 279-300.

Clarke, R.M. (1997): Saddlebackite, $Pb_2Bi_2Te_2S_3$, a new mineral species from the Boddington gold deposit, Western Australia. *Austral. Mineral. J.,* **3**, 119-124.

CNMMN–IMA (1971): Report of the CNMMN of the IMA. *Mineral. Mag.*, **38**, 102-105.

Cohen, K., Rivet, J., Dugué, J. (1995): Description of the Cu–As–Se ternary system. *J. Alloys & Compounds,* **224**, 316-329.

Cook, N.J., Wood, S.A., Gebert, W., Bernhardt, H.-J., Medenbach, O. (1994): Crerarite, a new Pt–Bi–Pb–S mineral from the Cu–Ni–PGE deposit at Lac Sheen, Abitibi-Témiscaminque, Québec, Canada. *N. Jb. Miner. Mh.*, **1994** (12), 567-575.

Cook, N.J., Ciobanu, C.L., Stanley, C.J., Paar, W.H., Sundblad, K. (2007a): Compositional data for Bi–Pb tellurosulfides. *Can. Mineral.*, **45**, 417-435.

Cook, N.J., Ciobanu, C.L., Wagner, T., Stanley, C.J. (2007b): Minerals of the system Bi–Te–Se–S related to the tetradymite archetype: review of classification and compositional variation. *Can. Mineral.*, **45**, 665-708.

Cvetkovic, L., Boronikhin, V.A., Pavicevic, M.K., Krajnoviv, D., Grzetic, I., Libowitzky, E., Giester, G., Tillmanns, E. (1995): Jankovićite, $Tl_5Sb_9(As,Sb)_4S_{22}$, a new Tl-sulfosalt from Allchar, Macedonia. *Mineral. Petrol.,* **53**, 125-131.

Divjaković, V. & Nowacki, W. (1975): Die Kristallstruktur von Galchait $[Hg_{0,76}(Cu,Zn)_{0,24}]_{12}Tl_{0,96}(AsS_3)_8$. *Z. Kristallogr.,* **142**, 262-270.

—, — (1976): Die Kristallstruktur von Imhofit, $Tl_{5.6}As_{15}S_{25.3}$. *Z. Kristallogr.,* **144**, 323-333.

Dmitrieva, M.T. & Bojik, G.B. (1988): The crystallochemical mechanism of formation of vacancies in goldfieldite structure. *Z. Kristallogr.,* **185**, 601.

Dymkov, Yu.M., Loseva, T.I., Zavyalov, E.N., Ryjov, B.I., Bochek, L.I. (1982): Mgriite, $(Cu,Fe)_3AsSe_3$, a new mineral. *Zapiski Vsesoyuz. Mineral. Obshch.,* **111**, 215-219 (in Russian).

Edenharter, A. (1976): Progress in the field of crystal chemistry of sulfosalts. *Schweiz. Mineral. Petrogr. Mitt.*, **56**, 195-217.

— (1980): Die Kristallstruktur von Heteromorphit, $Pb_7Sb_8S_{19}$. *Z. Kristallogr.,* **151**, 193-202.

Edenharter, A. & Nowacki, W. (1974): Verfeinerung der Kristallstruktur von Samsonit $(SbS_3)_2Ag(III)_2Ag(IV)_2Mn(VI)$. *Z. Kristallogr.,* **140**, 87-89.

—, — (1975): Die Kristallstruktur von Fülöppit $(Sb_8S_{15}|Pb^{VIII}Pb_2^{VII})$. *Z. Kristallogr.,* **142**, 196-215.

Edenharter, A., Nowacki, W., Takéuchi, Y. (1970): Verfeinerung der Kristallstruktur von Bournonit $[(SbS_3)_2|Cu_2^{IV}Pb^{VII}Pb^{VIII}]$ und von Seligmannit $[(AsS_3)_2|Cu_2^{IV}Pb^{VII}Pb^{VIII}]$. *Z. Kristallogr.,* **131**, 397-417.

Effenberger, H., Paar, W.H., Topa, D., Culetto, F.J., Giester, G. (1999): Toward the crystal structure of nagyágite, $[Pb(Pb,Sb)S_2][(Au,Te)]$. *Am. Mineral.,* **84**, 669-676.

Effenberger, H., Culetto, F.J., Topa, D., Paar, W.H. (2000): The crystal structure of synthetic buckhornite, $[Pb_2BiS_3][AuTe_2]$. *Z. Kristallogr.,* **215**, 10-16.

Effenberger, H., Paar, W.H., Topa, D., Criddle, A.J., Fleck, M. (2002): The new mineral baumstarkite and a structural reinvestigation of aramayoite and miargyrite. *Am. Mineral.,* **87**, 753-764.

Engel, P. (1980): Die Kristallstruktur von synthetischem Parapierrotit, $TlSb_5S_8$. *Z. Kristallogr.,* **151**, 203-216.

Engel, P. & Nowacki, W. (1966): Die Verfeinerung der Kristallstruktur von Proustit, Ag_3AsS_3, und Pyrargyrit, Ag_3SbS_3. *N. Jb. Miner. Mh.,* **1966** (6), 181-184.

—, — (1968): Die Kristallstruktur von Xanthokon, Ag_3AsS_3. *Acta Cryst.,* **B24**, 77-81.

—, — (1969): Die Kristallstruktur von Baumhauerite. *Z. Kristallogr.,* **129**, 178-202.

—, — (1970): Die Kristallstruktur von Rathit-II. *Z. Kristallogr.,* **131**, 356-375.

Engel, P., Nowacki, W., Balić-Žunić, T., Scavnicar, S. (1982): The crystal structure of simonite, $TlHgAs_3S_6$. *Z. Kristallogr.,* **161**, 159-166.

Engel, P., Gostojic, M., Nowacki, W. (1983): The crystal structure of pierrotite, $Tl_2(Sb,As)_{10}S_{16}$. *Z. Kristallogr.*, **165**, 209-215.

Euler, R. & Hellner, E. (1960): Über komplex zusammengesetze sulfidische Erze. VI. Zur Kristallstruktur des Meneghinits, $CuPb_{13}Sb_7S_{24}$. *Z. Kristallogr.,* **113**, 345-372.

Evain, M., Petricek, V., Moëlo, Y., Maurel, C. (2006a): First (3+2)-dimensional superspace approach of the structure of lévyclaudite-(Sb), a member of the cylindrite-type minerals. *Acta Cryst.,* **B62**, 775-789.

Evain, M., Bindi, L., Menchetti, S. (2006b): Structural complexity in minerals: twinning, polytypism and disorder in the crystal structure of polybasite, $(Ag,Cu)_{16}(Sb,As)_2S_{11}$. *Acta Cryst.,* **B62**, 447-456.

—, —, — (2006c): Structure and phase transition in the Se-rich variety of antimonpearceite, $[(Ag,Cu)_6(Sb,As)_2(S,Se)_7][Ag_9Cu(S,Se)_2Se_2]$. *Acta Cryst.*, **B62**, 768-774.

Fellenberg (von), L.R. (1854): Über ein eigenthümliches Fahlerz aus dem Einfischthale im Kanton Wallis. *Mitt. Natur. Gesell. Bern*, **317**-**318**, 57-59.

Ferraris, G., Makovicky, E., Merlino, S. (2004): Crystallography of modular materials. IUCr Monographs on Crystallography, Oxford University Press, 400 p.

Fleischer, M. (1960): New mineral names. *Am. Mineral.*, **45**, 1314-1315.

Foit, F.F. Jr., Robinson, P.D., Wilson, J.R. (1995): The crystal structure of gillulyite, $Tl_2(As,Sb)_8S_{13}$, from the Mercury gold deposit, Tooele County, Utah, U.S.A. *Am. Mineral.,* **80**, 394-399.

Förster, H.-J., Cooper, M.A., Roberts, A.C., Stanley, C.J., Criddle, A.J., Hawthorne, F.C., Laflamme, J.H.G., Tischendorf, G. (2003): Schlemaite, $(Cu,\square)_6(Pb,Bi)Se_4$, a new mineral species from Niederschlema-Alberoda, Erzgebirge, Germany: description and crystal structure. *Can. Mineral.*, **41**, 1433-1444.

Franz, L., Kupčik, V., Makovicky, E. (1967): New data on lillianite and bonchevite. IMA proposal 67–2a (unpublished).

—, —, — (1969): Mineralogical data on a sulphosalt from the Rhodope Mts, Bulgaria. *Tschermaks Mineral. Petrogr. Mitt.,* **13**, 149-156.

Franzini, M., Orlandi, P., Pasero, M. (1992): Morphological, chemical and structural study of robinsonite ($Pb_4Sb_6S_{13}$) from Alpi apuane, Italy. *Acta Vulcanologica*, *Marinelli*, **2**, 231-235.

Garavelli, A., Mozgova, N.N., Orlandi, P., Bonaccorsi, E., Pinto, D., Moëlo, Y., Borodaev, Yu.S. (2005): Rare sulfosalts from Vulcano, Aeolian Islands, Italy. VI. Vurroite, $Pb_{20}Sn_2(Bi,As)_{22}S_{54}Cl_6$, a new mineral species. *Can. Mineral.,* **43**, 703-711.

Geller, S. & Wernick, J.H. (1959): Ternary semiconducting compounds with sodium chloride-like structures: $AgSbSe_2$, $AgSbTe_2$, $AgBiS_2$, $AgBiSe_2$. *Acta Cryst.,* **12**, 46-54.

Golovej, M.I., Voroshilov, Yu.V., Potorii, M.V. (1985): The ternary systems Cu(Ag,Tl)–*B*(5)–Se. *Izv. Vys. Uch. Zav., Khim. Khim. Tekhn.,* **28**, 7-11 (in Russian).

Gostojic, M. (1980): Die Kristallstruktur von synthetischem Ellisit, Tl_3AsS_3. *Z. Kristallogr.,* **151**, 249-254.

Graeser, S. & Edenharter, A. (1997): Jentschite ($TlPbAs_2SbS_6$) – a new sulphosalt from Lengenbach, Binntal (Switzerland). *Mineral. Mag.,* **61**, 131-137.

Graeser, S. & Schwander, H. (1992): Edenharterite ($TlPbAs_3S_6$): a new mineral from Lengenbach, Binntal (Switzerland). *Eur. J. Mineral.,* **4**, 1265-1270.

Graeser, S., Schwander, H., Wulf, R., Edenharter, A. (1992): Erniggliite ($Tl_2SnAs_2S_6$), a new mineral from Lengenbach, Binntal, Switzerland: description and crystal structure determination based on data from synchrotron radiation. *Schweiz. Mineral. Petrogr. Mitt.,* **72**, 293-305.

—, —, —, — (1995): Stalderite, $TlCu(Zn,Fe,Hg)_2As_2S_6$ – a new mineral related to routhierite: description and crystal structure determination. *Schweiz. Mineral. Petrogr. Mitt.,* **75**, 337-345.

Graeser, S., Berlepsch, P., Makovicky, E., Balić-Žunić, T. (2001): Sicherite, $TlAg(As,Sb)_3S_6$, a new sulfosalt mineral from Lengenbach (Binntal, Switzerland): Description and structure determination. *Am. Mineral.,* **86**, 1087-1093.

Graeser, S., Topa, D., Balić-Žunić, T., Makovicky, E. (2006): Gabrielite, $Tl_2AgCu_2As_3S_7$, a new species of thallium sulfosalt from Lengenbach, Binntal, Switzerland. *Can. Mineral.,* **44**, 135-140.

Gregorio, F., Lattanzi, P., Tanelli, G., Vurro, F. (1979): Garavellite, $FeSbBiS_4$, a new mineral from the Cu–Fe deposit of Valle del Frigido in the Apuane Alps, northern Tuscany, Italy. *Mineral. Mag.,* **43**, 99-102.

Gruzdev, V.S., Stepanov, V.I., Shumkova, N.G., Chernistova, N.M., Yudin, R.N., Bryzgalov, I.A. (1972): Galkhaite ($HgAsS_2$), a new mineral from arsenic-antimony-mercury deposits of the U.S.S.R. *Dokl. Akad. Nauk SSSR,* **205**, 1194-1197 (in Russian).

Harris, D.C. (1989): The mineralogy and geochemistry of the Hemlo gold deposit, Ontario. *Geol. Surv. Canada, Econ. Geol. Rep.* **38**, 88 p.

Harris, D.C., Roberts, A.C., Criddle, A.J. (1989): Vaughanite, $TlHgSb_4S_7$, a new mineral from Hemlo, Ontario, Canada. *Mineral. Mag.,* **53**, 79-83.

Hellner, E. (1958): A structural scheme for the sulphide minerals. *J. Geol.*, **66**, 503-525.

Hellner, E. & Burzlaff, H. (1964): Die Struktur des Smithits $AgAsS_2$. *Naturwiss.,* **51**, 35-36.

Holstam, D. & Söderhielm, J. (1999): The discreditation of platynite. *Can. Mineral.,* **37**, 1313-1315.

Horiuchi, H. & Wuensch, B.J. (1976): The ordering scheme for metal atoms in the crystal structure of hammarite, $Cu_2Pb_2Bi_4S_9$. *Can. Mineral.,* **14**, 536-539.

—, — (1977): Lindströmite, $Cu_3Pb_3Bi_7S_{15}$: its space group and ordering scheme for metal atoms in the crystal structure. *Can. Mineral.,* **15**, 527-535.

Iitaka, Y. & Nowacki, W. (1961): Refinement of the pseudo crystal structure of scleroclase, $PbAs_2S_4$. *Acta Cryst.,* **14**, 1291-1292.

—, — (1962): A redetermination of the crystal structure of galenobismutite, $PbBi_2S_4$. *Acta Cryst.,* **15**, 691-698.

Ilinca, G. & Makovicky, E. (1997): Note on the definition of borodayevite $[Ag_5(Fe,Pb)Bi_7]_{13}(Sb,Bi)_2S_{17}$. *N. Jb. Miner. Mh.*, **1997** (8), 337-353.

Ito, Tei & Muraoka, H. (1960): Nakaseite, an andorite-like new mineral. *Z. Kristallogr.*, **113**, 94-98.

Ito, Tetsu & Nowacki, W. (1974a): The crystal structure of freieslebenite, $PbAgSbS_3$. *Z. Kristallogr.,* **139**, 85-102.

—, — (1974b): The crystal structure of jordanite, $Pb_{28}As_{12}S_{46}$. *Z. Kristallogr.,* **139**, 161-185.

Jambor, J.L. (1967a): New lead sulfantimonides from Madoc, Ontario. Part 1. *Can. Mineral.,* **9**, 7-24.

— (1967b): New lead sulfantimonides from Madoc, Ontario. Part 2 – Mineral descriptions. *Can. Mineral.,* **9**, 191-213.

— (1968): New lead sulfantimonides from Madoc, Ontario. Part 3 – Syntheses, paragenesis, origin. *Can. Mineral.,* **9**, 505-521.

Jambor, J.L., Laflamme, J.H.G., Walker, D.A. (1982): A re-examination of the Madoc sulfosalts. *Mineral. Record*, **30**, 93-100.

Johan, Z. & Kvaček, M. (1971): La hakite, un nouveau minéral du groupe de la tétraèdrite. *Bull. Soc. fr. Minéral. Cristallogr.,* **94**, 45-48.

Johan, Z., Mantienne, J., Picot, P. (1974): La routhiérite, $TlHgAsS_3$, et la laffittite, $AgHgAsS_3$, deux nouvelles espèces minérales. *Bull. Soc. fr. Minéral. Cristallogr.,* **97**, 48-53.

—, —, — (1981): La chabournéite, un nouveau minéral thallifère. *Bull. Minéral.*, **104**, 10-15.

Johan, Z., Picot, P., Ruhlmann, F. (1982): Evolution paragénétique de la minéralisation uranifère de Chaméane (Puy-de-Dôme), France: chaméanite, geffroyite et giraudite, trois séléniures nouveaux de Cu, Fe, Ag et As. *Tschermaks Mineral. Petrogr. Mitt.,* **29**, 151-167.

—, —, — (1987): The ore mineralogy of the Otish Mountains uranium deposit, Quebec: skippenite, Bi_2Se_2Te, and watkinsonite, $Cu_2PbBi_4(Se,S)_8$, two new mineral species. *Can. Mineral.,* **25**, 625-638.

Johansson, K. (1924): Bidrag till Gladhammar-gruvornas mineralogi. *Ark. Kemi, Mineral. Geol.*, **9** (8), 1-22.

Kalbskopf, R. (1974): Synthese und Kristallstruktur von $Cu_{12-x}Te_4S_{13}$, dem Tellur-Endglied der Fahlerze. *Tschermaks Mineral. Petrogr. Mitt.*, **21**, 1-10.

Kaplunnik, L.N., Pobedimskaya, E.A., Belov, N.V. (1980): The crystal structure of aktashite, $Cu_6Hg_3As_4S_{12}$. *Dokl. Akad. Nauk SSSR*, **251**, 96-98 (in Russian).

Karup-Møller, S. (1972): New data on pavonite, gustavite and some related sulphosalt minerals. *N. Jb. Miner. Abh.,* **117**, 19-38.

— (1973): New data on schirmerite. *Can. Mineral.*, **11**, 952-957.

— (1977): Mineralogy of some Ag–(Cu)–Pb–Bi sulphide associations. *Bull. Geol. Soc. Denmark,* **26**, 41-68.

Karup-Møller, S. & Makovicky, E. (1992): Mummeite – A new member of the pavonite homologous series from Alaska Mine, Colorado. *N. Jb. Miner. Mh.*, **1992** (12), 555-576.

Kieft, K. & Eriksson, G. (1984): Regional zoning and metamorphic evolution of the Vindfall Pb–Zn ore, east central Sweden. *Geol. Fören. Stockholm Förh.*, **106**, 305-317.

Klomínský, J., Rieder, M., Kieft, C., Mraz, L. (1971): Heyrovskýite, $6(Pb_{0.86}Bi_{0.08}(Ag, Cu)_{0.04})S.Bi_2S_3$ from Hůrky, Czechoslovakia, a new mineral of genetic interest. *Miner. Depos.*, **6**, 133-147.

Kocman, V. & Nuffield, E.W. (1973): The crystal structure of wittichenite, Cu_3BiS_3. *Acta Cryst.*, **B29**, 2528-2536.

—, — (1974): Crystal structure of antimonian hauchecornite from Westphalia. *Can. Mineral.*, **12**, 269-274.

Kohatsu, J.J. & Wuensch, B.J. (1974): Semseyite, $Pb_9Sb_8S_{21}$, and the crystal chemistry of the plagionite group, $Pb_{3+2n}Sb_8S_{15+2n}$. *Acta Cryst.*, **B30**, 2935-2937.

—, — (1976): The crystal structure of gladite, $CuPbBi_5S_9$, a superstructure intermediate in the series Bi_2S_3–$CuPbBiS_3$ (bismuthinite–aikinite). *Acta Cryst.*, **B32**, 2401-2409.

Kostov, I. (1958): Bonchevite, $PbBi_4S_7$, a new mineral. *Mineral. Mag.*, **31**, 821-828.

— (1959): Bismuth jamesonite or sakharovaite – a new mineral species. *Trudy Mineral. Muz. Akad. Nauk SSSR*, **10**, 148-149 (in Russian).

Kostov, I. & Minćeva-Stefanova, J. (1981): Sulphide minerals: crystal chemistry, parageneses and systematics. Bulgarian Academy of Sciences, Sofia, 212 p.

Kovalenker, V.A. & Rusinov, V.L. (1986): Goldfieldite: Chemical composition, parageneses and conditions of formation. *Mineral. Zhurnal*, **8**, 57-70 (in Russian).

Kryukowa, G.N., Heuer, M., Wagner, G., Doering, Th., Bente, K. (2005): Synthetic $Cu_{0.5}Pb_{8.7}Sb_{8.2}I_{1.6}S_{20}$ nanowires. *J. Solid State Chem.,* **178**, 376-381.

Kupčík, V. (1984): Die Kristallstruktur des Minerals Eclarit, $(Cu, Fe)Pb_9Bi_{12}S_{28}$. *Tschermaks Mineral. Petrogr. Mitt.*, **32**, 259-269.

Kutoglu, A. (1968): Die Struktur des Pyrostilpnits (Feuerblende) Ag_3SbS_3. *N. Jb. Miner. Mh.*, **1968** (4), 145-160.

Lafond, A., Nader, A., Moëlo, Y., Meerschaut, A., Briggs, A., Perrin, S., Monceau, P., Rouxel, J. (1997): X-ray structure determination and superconductivity of a new layered misfit compound with a franckeite-like stacking, $[(Pb, Sb)S]_{2.28}NbS_2$. *J. Alloys Compd.*, **261**, 114-122.

Large, R.R. & Mumme, W.G. (1975): Junoite, "wittite", and related seleniferous bismuth sulfosalts from Juno mine, Northern Territory, Australia. *Econ. Geol.*, **70**, 369-383.

Laroussi, A., Moëlo, Y., Ohnenstetter, D., Ginderow, D. (1989): Argent et thallium dans les sulfosels de la série de la sartorite (gisement de Lengenbach, vallée de Binn, Suisse). *C. R. Acad. Sci. Paris*, **308**, Sér. II, 927-933.

Laufek, F., Pažout, R., Makovicky, E. (2007): Crystal structure of owyheeite, $Ag_{1.5}Pb_{4.43}Sb_{6.07}S_{14}$: refinement from powder synchrotron X-ray diffraction. *Eur. J. Mineral.*, **19**, 557-566.

Laufek, F., Sejkora, J., Fejfarová, K., Dusek, M., Ozdín, D. (2007): The mineral marrucciite monoclinic $Hg_3Pb_{16}Sb_{18}S_{46}$, *Acta Cryst.* E **63**, i190.

Le Bihan, M.-Th. (1962): Etude structurale de quelques sulfures de plomb et d'arsenic naturels du gisement de Binn. *Bull. Soc. fr. Minéral. Cristallogr.*, **85**, 15-47.

Lemoine, P., Carré, D., Robert, F. (1991): Structure du sulfure de fer et d'antimoine, $FeSb_2S_4$ (berthiérite). *Acta Cryst.*, **C47**, 938-940.

Léone, P., Le Leuch, L.-M., Palvadeau, P., Molinié, P., Moëlo, Y. (2003): Single crystal structures and magnetic properties of two iron or manganese-lead-antimony sulfides: $MPb_4Sb_6S_{14}$ (M: Fe, Mn). *Solid State Sciences*, **5** (5), 771-776.

Libowitzky, E., Giester, G., Tillmanns, E. (1995): The crystal structure of jankovićite, $Tl_5Sb_9(As, Sb)_4S_{22}$. *Eur. J. Mineral.*, **7**, 479-487.

Lima-de-Faria, J., Hellner, E., Liebau, F., Makovicky, E., Parthé, E. (1990): Nomenclature of inorganic structure types. Report of the International Union of Crystallography – Commission on Crystallographic Nomenclature Subcommittee. *Acta Cryst.*, **A46**, 1-11.

Machatschki, F. (1928): Präzisionsmessungen der Gitterkonstanten verschiedener Fahlerze Formel und Struktur desselben. *Z. Kristallogr.*, **68**, 204-222.

Makovicky, E. (1967): Bemerkungen zu der Systematik und Mineralogie der Sulfosalze der Metalle der 5. Gruppe. *Geologicky Sbornik*, **18**, 39-64.

— (1974): Mineralogical data on cylindrite and incaite. *N. Jb. Miner. Mh.,* **1974** (6), 235-256.

— (1976): Crystallography of cylindrite. Part I. Crystal lattices of cylindrite and incaite. *N. Jb. Miner. Abh.*, **126**, 304-326.

— (1977): Chemistry and crystallography of the lillianite homologous series. Part III: Crystal chemistry of lillianite homologues. Related phases. *N. Jb. Miner. Abh.*, **131**, 187-207.

— (1981): The building principles and classification of bismuth-lead sulphosalts and related compounds. *Fortschr. Mineral.*, **59**, 137-190.

— (1985a): The building principles and classification of sulphosalts based on the SnS archetype. *Fortschr. Mineral.*, **63**, 45-89.

— (1985b): Cyclically twinned sulphosalt structures and their approximate analogues. *Z. Kristallogr.*, **173**, 1-23.

— (1989): Modular classification of sulphosalts – current status. Definition and application of homologous series. *N. Jb. Miner. Abh.*, **160**, 269-297.

— (1993): Rod-based sulphosalt structures derived from the SnS and PbS archetypes. *Eur. J. Mineral.*, **5**, 545-591.

— (1997): Modular crystal chemistry of sulphosalts and other complex sulphides. *in* "Modular aspects of minerals", S. Merlino, ed. *EMU Notes in Mineralogy*, **1**, Eötvös University Press, 237-271.

Makovicky, E. & Balić-Žunić, T. (1993): Contribution to the crystal chemistry of thallium sulphosalts. II. $TlSb_3S_5$ – the missing link of the lillianite homologous series. *N. Jb. Miner. Abh.*, **165**, 331-344.

—, — (1995): Determination of the crystal structure of skinnerite, $P2_1/c$ – Cu_3SbS_3, from powder data. *Can. Mineral.*, **33**, 655-663.

—, — (1998): Contribution to the crystal chemistry of thallium sulfosalts. IV. Modular description of Tl–As–Sb sulfosalts rebulite and jankovićite. *N. Jb. Miner. Abh.*, **174**, 181-210.

—, — (1999): Gillulyite $Tl_2(As, Sb)_8S_{13}$: Reinterpretation of the crystal structure and order-disorder phenomena. *Am. Mineral.*, **84**, 400-406.

Makovicky, E. & Hyde, B.G. (1981): Non-commensurate (misfit) layer structures. *Structure and Bonding,* **46**, 101-170.

—, — (1992): Incommensurate, two-layer structures with complex crystal chemistry: Minerals and related synthetics. *Mat. Sci. Forum*, **100**, **101**, 1-100.

Makovicky, E. & Karup-Møller, S. (1977a): Chemistry and crystallography of the lillianite homologous series. Part I: General properties and definitions. *N. Jb. Miner. Abh.,* **130**, 264-287.

—, — (1977b): Chemistry and crystallography of the lillianite homologous series. Part II: Definition of new minerals: eskimoite, vikingite, ourayite and treasurite. Redefinition of schirmerite and new data on the lillianite–gustavite solid-solution series. *N. Jb. Miner. Abh.,* **131**, 56-82.

—, — (1984): Ourayite from Ivigtut, Greenland. *Can. Mineral.,* **22**, 565-575.

—, — (1986): New data on giessenite from the Bjørkåsen sulfide deposit at Otoften, Northern Norway. *Can. Mineral.,* **24**, 21-25.

Makovicky, E. & Makovicky, M. (1978): Representation of compositions in the bismuthinite–aikinite series. *Can. Mineral.*, **16**, 405-409.

Makovicky, E. & Mumme, W.G. (1979): The crystal structure of benjaminite $Cu_{0.50}Pb_{0.40}Ag_{2.30}Bi_{6.80}S_{12}$. *Can. Mineral*., **17**, 607-618.

—, — (1983): The crystal structure of ramdohrite, $Pb_6Sb_{11}Ag_3S_{24}$, and its implications for the andorite group and zinckenite. *N. Jb. Miner. Abh.,* **147**, 58-79.

—, — (1984): The crystal structures of izoklakeite, dadsonite and jaskólskiite. 13th Int. Congress of Crystallogr., Hamburg, 9-18 August, Collected Abstracts, C-246.

—, — (1986): The crystal structure of isoklakeite, $Pb_{51.3}Sb_{20.4}Bi_{19.5}Ag_{1.2}Cu_{2.9}Fe_{0.7}S_{114}$. The kobellite homologous series and its derivatives. *N. Jb. Miner. Abh.*, **153**, 121-145.

Makovicky, E. & Nørrestam, R. (1985): The crystal structure of jaskólskiite, $Cu_xPb_{2+x}(Sb, Bi)_{2-x}S_5$ ($x \approx 0.2$), a member of the meneghinite homologous series. *Z. Kristallogr.*, **171**, 179-194.

Makovicky, E. & Skinner, B. (1975): Studies of the sulfosalts of copper. IV. Structure and twinning of sinnerite, $Cu_6As_4S_9$. *Am. Mineral.*, **60**, 998-1012.

—, — (1979): Studies of the sulfosalts of copper. VII. Crystal structures of the exsolution products $Cu_{12.3}Sb_4S_{13}$ and $Cu_{13.8}Sb_4S_{13}$ of unsubstituted synthetic tetrahedrite. *Can. Mineral.,* **17**, 619-634.

Makovicky, E., Mumme, W.G., Watts, J.A. (1977): The crystal structure of synthetic pavonite, $AgBi_3S_5$, and the definition of the pavonite homologous series. *Can. Mineral.*, **15**, 339-348.

Makovicky, E., Johan, Z., Karup-Møller, S. (1980): New data on bukovite, thalcusite, chalcothallite and rohaite. *N. Jb. Miner. Abh.*, **138**, 122-146.

Makovicky, E., Mumme, W.G., Hoskins, B.F. (1991): The crystal structure of Ag–Bi-bearing heyrovskýite. *Can. Mineral.,* **29**, 553-559.

Makovicky, E., Mumme, W.G., Madsen, I.C. (1992): The crystal structure of vikingite. *N. Jb. Miner. Mh.*, **1992** (10), 454-468.

Makovicky, E., Leonardsen, E., Moëlo, Y. (1994): The crystallography of lengenbachite, a mineral with the non-commensurate layer structure. *N. Jb. Miner. Abh.*, **2**, 169-191.

Makovicky, E., Balić-Žunić, T., Topa, D. (2001a): The crystal structure of neyite, $Ag_2Cu_6Pb_{25}Bi_{26}S_{68}$. *Can. Mineral.,* **39**, 1365-1376.

Makovicky, E., Topa, D., Balić-Žunić, T. (2001b): The crystal structure of paarite, the newly discovered 56 Å derivative of the bismuthinite–aikinite solid-solution series. *Can. Mineral.,* **39**, 1377-1382.

Makovicky, E., Søtofte, I., Karup-Møller, S. (2002): The crystal structure of $Cu_4Bi_4Se_9$. *Z. Kristallogr.* **217**, 597-604.

Makovicky, E., Balić-Žunić, T., Karanović, L., Poleti, D. Prček, J. (2004): Structure refinement of natural robinsonite, $Pb_4Sb_6S_{13}$: cation distribution and modular analysis. *N. Jb. Miner. Mh.*, **2004** (2), 49-67.

Makovicky, E., Karanovi, L., Poleti, D., Balić-Žunić, T., Paar, W.H. (2005): Crystal structure of copper-rich unsubstituted tennantite, $Cu_{12.5}As_4S_{13}$. *Can. Mineral.*, **43**, 679-688.

Makovicky, E., Balić-Žunić, T., Karanović, L., Poleti, D. (2006a): The crystal structure of kirkiite, $Pb_{10}Bi_3As_3S_{19}$. *Can. Mineral.*, **44**, 177-188.

Makovicky, E., Topa, D., Mumme, W.G. (2006b): The crystal structure of dadsonite. *Can. Mineral.,* **44**, 1499-1512.

Mandarino, J.A. & Back, M.E. (2004): Fleischer's glossary of mineral species 2004. The Mineralogical Record Inc., Tucson, 309 p.

Mantienne, J. (1974): La minéralisation thallifère de Jas-Roux (Hautes-Alpes). Thesis, University of Paris, 153 p.

Martin, R.F. (2003): Encyclopedia of mineral names: third update. *Can. Mineral.,* **41**, 1075-1096.

Martin, R.F. & Blackburn, W.H. (1999): Encyclopedia of mineral names: first update. *Can. Mineral.,* **37**, 1045-1078.

—, — (2001): Encyclopedia of mineral names: second update. *Can. Mineral.,* **39**, 1199-1218.

Marumo, F. (1967): The crystal structure of nowackiite, $Cu_6Zn_3As_4S_{12}$. *Z. Kristallogr.,* **124**, 351-368.

Marumo, F. & Nowacki, W. (1965): The crystal structure of rathite-I. *Z. Kristallogr.,* **122**, 433-456.

—, — (1967a): The crystal structure of hatchite $PbTlAgAs_2S_5$. *Z. Kristallogr.,* **125**, 249-265.

—, — (1967b): The crystal structure of dufrénoysite, $Pb_{16}As_{16}S_{40}$. *Z. Kristallogr.,* **124**, 409-419.

Matsumoto, T. & Nowacki, W. (1969): The crystal structure of trechmannite, $AgAsS_2$. *Z. Kristallogr.,* **129**, 163-177.

Matsushita, Y. & Takéuchi, Y. (1994): Refinement of the crystal structure of hutchinsonite, $TlPbAs_5S_9$. *Z. Kristallogr.,* **209**, 475-478.

Matsushita, Y. & Ueda, Y. (2003): Structure and physical properties of 1D magnetic chalcogenide, jamesonite ($FePb_4Sb_6S_{14}$). *Inorg. Chem.*, **42**, 7830-7838.

Matsushita, Y., Takéuchi, Y., Nishi, F. (1997): The crystal structure of semseyite, $Pb_9Sb_8S_{21}$. *in* "Tropochemical cell-twinning: A Structure-Building Mechanism in Crystalline Solids". Terra Scientific Publishing Company, Tokyo, 288-293.

Matzat, E. (1979): Cannizzarite. *Acta Cryst.,* **B35**, 133-136.

McQueen, K.G. (1987): A second occurrence of falkmanite: Pinnacles mine, Broken Hill, New South Wales. *Can. Mineral.*, **25**, 15-19.

Meerschaut, A., Palvadeau, P., Moëlo, Y., Orlandi, P. (2001): Lead–antimony sulfosalts from Tuscany (Italy). IV. Crystal structure

of pillaite, $Pb_9Sb_{10}S_{23}ClO_{0.5}$, an expanded monoclinic derivative of hexagonal $Bi(Bi_2S_3)_9I_3$. *Eur. J. Mineral.,* **13**, 779-790.

Megarskaya, L., Rykl, D., Taborsky, Z. (1986): Zoubekite, $AgPb_4Sb_4S_{10}$, a new mineral from Příbram, Czechoslovakia. *N. Jb. Miner. Mh.,* **1986** (1), 1-7.

Meisser, N., Schenk, K., Berlepsch, P., Brugger, J., Bonin, M., Criddle, A.C., Thélin, P., Bussy, F. (2007): Pizgrischite, $(Cu, Fe)Cu_{14}PbBi_{17}S_{35}$, a new sulfosalt from the Swiss Alps: description, crystal structure and occurrence. *Can. Mineral.*, **45**, 1229-1245.

Mellini, M. & Merlino, S. (1979): Versiliaite and apuanite: Derivative structures related to schafarzikite. *Am. Mineral.*, **64**, 1235-1242.

Miehe, G. (1971): Crystal structure of kobellite. *Nature, Phys. Sci.,* **231**,133-134.

Moëlo, Y. (1989): Antimoine dans la nuffieldite associée à de la friedrichite (commune des Houches, Alpes de Haute-Savoie); redéfinition cristallochimique de la nuffieldite. *C. R. Acad. Sci. Paris*, **309**, Sér. II, 1659-1664.

Moëlo, Y., Borodaev, Yu.S., Mozgova, N.N. (1983): Association twinnite-zinkénite-plagionite du gisement complexe à Sb–Pb–Zn de Rujevac (Yougoslavie). *Bull. Minéral.*, **106**, 505-510.

Moëlo, Y., Makovicky, E., Karup-Møller, S. (1984a): New data on the minerals of the andorite series. *N. Jb. Miner. Mh.,* **1984** (4), 175-182.

Moëlo, Y., Mozgova, N., Picot, P., Bortnikov, N., Vrublevskaya, Z. (1984b): Cristallochimie de l'owyheeite: nouvelles données. *Tschermaks Mineral. Petrogr. Mitt.,* **32**, 271-284.

Moëlo, Y., Jambor, J.L., Harris, D.C. (1984c): Tintinaite et sulfosels associés de Tintina (Yukon): la cristallochimie de la série de la kobellite. *Can. Mineral.,* **22**, 219-226.

Moëlo, Y., Makovicky, E., Karup-Møller, S. (1989): Sulfures complexes plombo-argentifères : minéralogie et cristallochimie de la série andorite–fizélyite, $(Pb, Mn, Fe, Cd, Sn)_{3-2x}(Ag, Cu)_x(Sb, Bi, As)_{2+x}(S, Se)_6$. *Documents du BRGM*, **167**, BRGM éd., Orléans, 107 p.

Moëlo, Y., Makovicky, E., Karup-Møller, S., Cervelle, B., Maurel, C. (1990): La lévyclaudite, $Pb_8Sn_7Cu_3(Bi, Sb)_3S_{28}$, une nouvelle espèce minérale à structure incommensurable, de la série de la cylindrite. *Eur. J. Mineral.,* **2**, 711-723.

Moëlo, Y., Roger, G., Maurel-Palacin, D., Marcoux, E., Laroussi, A. (1995): Chemistry of Pb–(Cu, Fe)–(Sb, Bi)-sulfosalts from France and Portugal, and correlated substitutions in the Cu-poor part of the Pb_2S_2–Cu_2S–Sb_2S_3–Bi_2S_3 system. *Mineral. Petrol.,* **53**, 229-250.

Moëlo, Y., Meerschaut, A., Makovicky, E. (1997): Refinement of the crystal structure of nuffieldite, $Pb_2Cu_{1.4}(Pb_{0.4}Bi_{0.4}Sb_{0.2})Bi_2S_7$: structural relationships and genesis of complex lead sulfosalt structures. *Can. Mineral.,* **35**, 1497-1508.

Moëlo, Y., Meerschaut, A., Orlandi, P., Palvadeau, P. (2000): Lead–antimony sulfosalts from Tuscany (Italy): II – Crystal structure of scainiite, $Pb_{14}Sb_{30}S_{54}O_5$, an expanded monoclinic derivative of $Ba_{12}Bi_{24}S_{48}$ hexagonal sub-type (zinkenite series). *Eur. J. Mineral.,* **12**, 835-846.

Moëlo, Y., Palvadeau, P., Meisser, N., Meerschaut, A. (2002): Structure cristalline d'une ménéghinite naturelle pauvre en cuivre, $Cu_{0.58}Pb_{12,72}(Sb_{7,04}Bi_{0.24})S_{24}$. *C. R. Geoscience,* **334**, 529-536.

Moh, G. (1987): Mutual Pb^{2+}/Sn^{2+} substitution in sulfosalts. *Mineral. Petrol.,* **36**, 191-204.

Mozgova, N.N. (1984): Principles of classification of sulfosalts. *in* Proceedings of the 27th International Geological Congress, Moscow, August 4-14, Section **C10**, 53-65.

— (2000): Sulfosalt mineralogy today. *in* IMA COM short course "Modern approaches to ore and environmental mineralogy", Espoo, Finland, June 11–17, 4 p. (extended abstract).

Mozgova, N.N. & Borodaev, Yu.S. (1972): Homologies within the semseyite-plagionite series. *Zapiski Vsesoyuz. Mineral. Obshch.,* **3**, 299-312 (in Russian).

Mozgova, N.N. & Bortnikov, N.S. (1980): Non-stoichiometry of acicular lead sulfosalts. Geokh. Mineral., XXVIth Interm. Geol. Congr., Moscow, 126-138 (in Russian).

Mozgova, N.N., Organova, N.I., Gorshkov, A.I. (1976): Structural resemblance between incaite and franckeite. *Dokl. Acad. Nauk SSSR,* **228**, 110-113 (in Russian).

Mozgova, N.N., Bortnikov, N.S., Tsepin, A.I., Borodaev, Yu.S., Vrublevskaja, S.V., Vyalsov, L.N., Kuzmina, O.V., Sivtsov, A.V. (1983): Falkmanite, $Pb_{5.4}Sb_{3.6}S_{11}$, new data and relationship with sulphantimonites of lead (re-examination of type material from Bayerland Mine, Bavaria). *N. Jb. Miner. Abh.,* **147**, 80-98.

Mozgova, N.N., Vrublevskaya, Z.V., Sivtsov, A.V. (1984): New data on the boulangerite homologous series. *Dokl. Acad. Nauk SSSR,* **274**, 169-172 (in Russian).

Mozgova, N.N., Organova, N.I., Borodaev, Yu.S., Ryabeva, E.G., Sivtsov, A.V., Getmanskaya, T.I., Kuzmina, O.V. (1988): New data on cannizzarite and bursaite. *N. Jb. Miner. Abh.,* **158**, 293-309.

Mozgova, N.N., Efimov, A.V., Nenasheva, S.N., Golovanova, T.I., Sivtsov, A.V., Tsepin, A.I., Dobretsova, I.G. (1989): New data on diaphorite and brongniardite. *Zapiski Vsesoyuz. Mineral. Obshch.,* **5**, 47-63 (in Russian).

Mozgova, N.N., Nenasheva, S.N., Chistyakova, N.I., Mogilevkin, S.B., Sivtsov, A.V. (1990): Compositional fields of minerals in the bismuthinite-aikinite series. *N. Jb. Miner. Mh.,***1990** (1), 35-45.

Mozgova, N.N., Moëlo, Y., Borodaev, Yu.S., Nenasheva, S.N., Efimov, A.V. (1992): Wittite with Se-rich cosalite and bismuthinite from Nevskoe tin deposit (Magadan district, Russia). *Mineral. Petrol.,* **46**, 137-153.

Mumme, W.G. (1975a): Junoite, $Cu_2Pb_3Bi_8(S, Se)_{16}$, a new sulfosalt from Tennant Creek, Australia: its crystal structure and relationship with other bismuth sulfosalts. *Am. Mineral.,* **60**, 548-558.

— (1975b): The crystal structure of krupkaite, $CuPbBi_3S_6$, from the Juno Mine at Tennant Creek, Northern Territory, Australia. *Am. Mineral.,* **60**, 300-308.

— (1976): Proudite from Tennant Creek, Northern Territory, Australia: its crystal structure and relationship with weibullite and wittite. *Am. Mineral.,* **61**, 839-852.

— (1980a): Seleniferous lead–bismuth sulphosalts from Falun, Sweden: Weibullite, wittite, and nordströmite. *Am. Mineral.*, **65**, 789-796.

— (1980b): The crystal structure of nordströmite $CuPb_3Bi_7(S, Se)_{14}$, from Falun, Sweden: a member of the junoite homologous series. *Can. Mineral.,* **18**, 343-352.

— (1980c): Weibullite $Ag_{0.32}Pb_{5.09}Bi_{8.55}Se_{6.08}S_{11.92}$ from Falun, Sweden: a higher homologue of galenobismutite. *Can. Mineral.,* **18**, 1-12.

— (1986): The crystal structure of paděraite, a mineral of the cuprobismutite series. *Can. Mineral.*, **24**, 513-521.

— (1989): The crystal structure of $Pb_{5.05}(Sb_{3.75}Bi_{0.28})S_{10.72}Se_{0.28}$: boulangerite of near ideal composition. *N. Jb. Miner. Mh.*, **1989** (11), 498-512.

— (1990): A note on the occurrence, composition and crystal structures of pavonite homologous series members ^{4}P, ^{6}P, and ^{8}P. *N. Jb. Miner. Mh.,* **1990** (5), 193-204.

Mumme, W.G. & Watts, J.A. (1976): Pekoite, $CuPbBi_{11}S_{18}$, a new member of the bismuthinite–aikinite mineral series: its crystal structure and relationship with naturally- and synthetically-formed members. *Can. Mineral.,* **14**, 322-333.

—, — (1980): $HgBi_2S_4$: Crystal structure and relationship with the pavonite homologous series. *Acta Cryst.,* **B36**, 1300-1304.

Mumme, W.G., Niedermayr, G., Kelly, P.R., Paar, W.H. (1983): Aschamalmite, $Pb_{5.92}Bi_{2.06}S_9$, from Untersulzbach Valley in Salzburg, Austria – "monoclinic heyrovskýite". *N. Jb. Miner. Mh.,* **1983** (10), 433-444.

Murzin, V.V., Bushmakin, A.F., Sustavov, S.G., Shcherbachev, D.K. (1996): Clerite, $MnSb_2S_4$ – a new mineral from the Vorontsovskoye gold deposit in the Urals. *Zapiski Vsesoyuz. Mineral. Obshch.,* **124**, 95-101 (in Russian).

Nagl, A. (1979): The crystal structure of a thallium sulfosalt, $Tl_8Pb_4Sb_{21}As_{19}S_{68}$. *Z. Kristallogr.,* **150**, 85-106.

Nakai, I. & Appleman, D.E. (1981): The crystal structure of gerstleyite $Na_2(Sb,As)_8S_{13}{\cdot}2H_2O$: The first sulfosalt mineral of sodium. *Chem. Letters (Japan),* **10**, 1327-1330.

—, — (1983): Laffittite, $AgHgAsS_3$: crystal structure and second occurrence from the Getchell mine, Nevada. *Am. Mineral.,* **68**, 235-244.

Nakai, I. & Nagashima, K. (1983): crystal-chemical classification of sulfosalts – an approach towards complex inorganic compounds... *in* "Progress of Analytical Chemistry", S. Fujiwara, ed. Hirokawashoten, Tokyo, 163-184 (in Japanese).

Nakai, I., Nagashima, K., Koto, K., Morimoto, N. (1978): Crystal chemistry of oxide-chalcogenide. I. The crystal structure of sarabauite. *Acta Cryst.,* **B34**, 3569-3572.

Nenasheva, S.N., Efimov, A.V., Sivtzov, A.V., Mozgova, N.N. (1992): Borodaevite $[Ag_5(Fe,Pb)_1Bi_7]_{13}(Sb,Bi)_2S_{17}$ – a new mineral. *Zapiski Vsesoyuz. Mineral. Obshch.,* **121**, 113-120 (in Russian).

Nespolo, M., Ferraris, G., Ďurovič, S., Takéuchi, Y. (2004): Twins vs. modular crystal structures. *Z. Kristallogr.*, **219**, 773-778.

Niizeki, N. & Buerger, M.J. (1957): The crystal structure of jamesonite, $FePb_4Sb_6S_{14}$. *Z. Kristallogr.*, **109**, 161-183.

Nowacki, W. (1967): Über die mögliche Identität von "Liveingit" mit Rathit-II. *N. Jb. Miner. Mh.*, **1967** (11), 353-354.

— (1968): Kristallchemie der Sulfosalze aus dem Lengenbach. *Jb. Nat. Hist. Mus. Bern*, **1966-1968**, 63-78.

— (1969): Zur Klassifikation und Kristallchemie des Sulfosalze. *Schweiz. Mineral. Petrogr. Mitt.*, **49**, 109-156.

Nowacki, W., Iitaka, Y., Burki, H., Kunz, V. (1961): Structural investigations on sulfosalts from the Lengenbach, Binn Valley (Ct. Wallis). Part 2. *Schweiz. Mineral. Petrogr. Mitt.*, **41**, 103-116.

Nowacki, W., Marumo, F., Takeuchi, Y. (1964): Investigations on sulfides from Binntal (Canton Valais, Switzerland). *Schweiz. Mineral. Petrogr. Mitt.*, **44**, 5-9.

Nuffield, E.W. (1975): The crystal structure of fülöppite, $Pb_3Sb_8S_{15}$. *Acta Cryst.,* **B31**, 151-157.

Ohmasa, M. & Nowacki, W. (1970): A redetermination of the crystal structure of aikinite $[BiS_2|S|Cu^{IV}Pb^{VII}]$. *Z. Kristallogr.,* **132**, 71-86.

—, — (1971): The crystal structure of vrbaite $Hg_3Tl_4As_8Sb_2S_{20}$. *Z. Kristallogr.,* **134**, 360-380.

Ohsumi, K., Tsutsui, K., Takéuchi, Y., Tokonami, M. (1984): Reinvestigation of the lillianite structure... *in* "Photon Factory Activity Report 1983/1984", VI-23.

Orlandi, P., Dini, A., Olmi, F. (1998): Grumiplucite, a new mercury–bismuth sulfosalt species from the Levigliani mine, Apuan Alps, Tuscany, Italy. *Can. Mineral.,* **36**, 1321-1326.

Orlandi, P., Moëlo, Y., Meerschaut, A., Palvadeau, P. (1999): Lead–antimony sulfosalts from Tuscany (Italy): I. Scainiite, $Pb_{14}Sb_{30}S_{54}O_5$, the first Pb–Sb oxy-sulfosalt, from Buca della Vena mine. *Eur. J. Mineral.,* **11**, 949-954.

—, —, —, — (2001): Lead–antimony sulfosalts from Tuscany (Italy). III. Pillaite, $Pb_9Sb_{10}S_{23}ClO_{0.5}$, a new Pb–Sb chlorosulfosalt, from Buca della Vena mine. *Eur. J. Mineral.,* **13**, 605-610.

Orlandi, P., Meerschaut, A., Palvadeau, P., Merlino, S. (2002): Lead–antimony sulfosalts from Tuscany (Italy): Definition and crystal structure of moëloite, $Pb_6Sb_6S_{14}(S_3)$, a new mineral from the Ceragiola marble quarry. *Eur. J. Mineral.,* **14**, 599-606.

Orlandi, P., Moëlo, Y., Meerschaut, A., Palvadeau, P., Léone, P. (2004): Lead–antimony sulfosalts from Tuscany (Italy). VI. Pellouxite, ~ $(Cu,Ag)_2Pb_{21}Sb_{23}S_{55}ClO$, a new oxy-chlorosulfosalt, from Buca della Vena mine, Apuan Alps. *Eur. J. Mineral.,* **16**, 839-844.

—, —, —, —, — (2005): Lead–antimony sulfosalts from Tuscany (Italy). VIII. Rouxelite, $Cu_2HgPb_{22}Sb_{28}S_{64}(O,S)_2$, a new sulfosalt from Buca della Vena mine, Apuan Alps: definition and crystal structure. *Can. Mineral.,* **43**, 919-933.

Orlandi, P., Moëlo, Y., Campostrini, I., Meerschaut, A. (2007): Lead–antimony sulfosalts from Tuscany (Italy). IX. Marrucciite, $Hg_3Pb_{16}Sb_{18}S_{46}$, a new sulfosalt from Buca della Vena mine, Apuan Alps: Definition and crystal structure. *Eur. J. Mineral.,* **19**, 267-279.

Otto, H.H. & Strunz, H. (1968): Zur Kristallchemie synthetischer Blei–Wismut–Spiessglanze. *N. Jb. Miner. Abh.,* **108**, 1-19.

Ozawa, T. & Nowacki, W. (1974): Note on the mineral rathite-IV. *N. Jb. Miner. Mh.*, **1974** (11), 530-531.

Ozawa, T. & Takéuchi, Y. (1983): A new Pb–As sulfosalt, having a long periodicity, from Lengenbach. Annual Meeting Mineralogical Society Japan, 1983, Abstr., 92 (in Japanese).

Paar, W.H., Chen, T.T., Kupčik, V., Hanke, K. (1983): Eclarit, $(Cu,Fe)Pb_9Bi_{12}S_{28}$, ein neues Sulfosalz von Bärenbad, Hollersbachtal, Salzburg, Österreich. *Tschermaks Mineral. Petrogr. Mitt.*, **32**, 103-110.

Paar, W.H., Putz, H., Roberts, A.C., Stanley, C.J., Culetto, F.J. (2006): Jonassonite, $Au(Bi,Pb)_5S_4$, a new mineral species from Nagybörzsöny, Hungary. *Can. Mineral.,* **44** 1127-1136.

Palvadeau, P., Meerschaut, A., Orlandi, P., Moëlo, Y. (2004): Lead–antimony sulfosalts from Tuscany (Italy). VII. Crystal structure of pellouxite, ~ $(Cu,Ag)_2Pb_{21}Sb_{23}S_{55}ClO$, an expanded monoclinic derivative of $Ba_{12}Bi_{24}S_{48}$ hexagonal sub-type (zinkenite group). *Eur. J. Mineral.,* **16**, 845-855.

Papp, G. (2004): History of minerals, rocks and fossil resins discovered in the Carpatian region. Hungarian Natural History Museum, Budapest, 215 p.

Papp, G., Criddle, A.J., Stanley, C.J., Kriston, L., Nagy, G. (2008): Parajamesonite revisited: Background of the discreditation of an enigmatic mineral species. *Swiss J. Geosci.*, (online - DOI 10.1.1007/500015-007-1233-1).

Pasava, J., Pertlik, F., Stumpfl, E.F., Zemann, J. (1989): Bernardite, a new thallium arsenic sulphosalt from Allchar, Macedonia, with the determination of the crystal structure. *Mineral. Mag.,* **53**, 531-538.

Pattrick, R.A.D. & Hall, A.J. (1983): Silver substitution into synthetic zinc, cadmium and iron tetrahedrites. *Mineral. Mag.,* **47**, 441-451.

Pauling, L. & Neuman, E.W. (1934): The crystal structure of binnite, $(Cu, Fe)_{12}As_4S_{13}$, and the chemical composition and structure of minerals of the tetrahedrite group. *Z. Kristallogr.,* **88**, 54-62.

Pérez-Priede, M., Xolans-Huguet X., Moreiras-Blanco D., Garcia-Granda, S. (2005): Going inside fettelite, a Hg-sulfosalt mineral. XXth IUCr Congress, Florence, 23-31 August, abstract vol., 380.

Peterson, R.C. & Miller, I. (1986): Crystal structure and cation distribution in freibergite and tetrahedrite. *Mineral. Mag.,* **50**, 717-721.

Petrov, I.I. & Imamov, R.M. (1970): Electron-diffraction of PbTe–Bi_2Te_3 system phases. *Sov. Phys. Crystallogr.,* **14**, 593-595.

Petrova, I.V., Pobedimskaya, E.A., Spiridonov, E.M. (1986): Crystal structure of roshchinite. *Mater. X Vses. Sov. po Rentg. Miner. Sir.*, Tbilisi, 99-100 (in Russian).

Petrova, I.V., Pobedimskaya, E.A., Bryzgalov, I.A. (1988): Crystal structure of miharaite, $Cu_4FePbBiS_6$. *Dokl. Akad. Nauk SSSR,* **33**, 157-159 (in Russian).

Pfitzner, A. & Kurowski, D. (2000): A new modification of $MnSb_2S_4$ crystallizing in the $HgBi_2S_4$ structure type. *Z. Kristallogr.,* **215**, 373-376.

Pfitzner, A., Evain, M., Petricek, V. (1997): $Cu_{12}Sb_4S_{13}$: A temperature-dependent structure investigation. *Acta Cryst.*, **B53**, 337-345.

Pinsker, Z.G. & Imamov, R.M. (1964): Electron diffraction study of the compound $AgBiTe_2$. *Kristallografia,* **9**, 347-351.

Pinto, D., Balić-Žunić, T., Bonaccorsi, E., Makovicky, E. (2004): The crystal structure of the new mineral vurroite. 26th Nordic Geological Winter Meeting, Uppsala, Sweden, 106-107 (abstract).

Pinto, D., Bonaccorsi, E., Balić-Žunić, T., Makovicky, E.: The crystal structure of vurroite, $Pb_{20}Sn_2(Bi,As)_{22}S_{54}Cl_6$: OD-character, polytypism, twinning and moduter description. Am. Mineral. (accept.).

Portheine, J.C. & Nowacki, W. (1975a): Refinement of the crystal structure of emplectite, $CuBiS_2$. *Z. Kristallogr.,* **141**, 387-402.

—, — (1975b): Refinement of the crystal structure of zinckenite, $Pb_6Sb_{14}S_{27}$. *Z. Kristallogr.,* **141**, 79-96.

Povarennykh, A.S. (1971): Crystallochemistry of complex sulfides of arsenic, antimony and bismuth. *in* Proc. IMA–IAGOD Meetings'70, Joint Symposium Vol., Soc. Mining Geol. Japan Special Issue **2**, 42-46.

Pring, A. (2001): The crystal chemistry of the sartorite group minerals from Lengenbach, Binntal, Switzerland – a HRTEM study. *Schweiz. Mineral. Petrogr. Mitt.,* **81**, 69-87.

Pring, A. & Etschmann, B. (2002): HRTEM observations of structural and chemical modulations in cosalite and its relationship to the lillianite homologues. *Mineral. Mag.,* **66**, 451-458.

Pring, A. & Graeser, S. (1994): Polytypism in baumhauerite. *Am. Mineral.,* **79**, 302-307.

Pring, A. & Hyde, B.G. (1987): Structural disorder in lindströmite: a bismuthinite–aikinite derivative. *Can. Mineral.,* **25**, 393-399.

Pring, A., Birch, W.D., Sewell, D., Graeser, S., Edenharter, A., Criddle, A. (1990): Baumhauerite-2*a*: A silver-bearing mineral with a baumhauerite-like supercell from Lengenbach, Switzerland. *Am. Mineral.,* **75**, 915-922.

Pring, A., Williams, T.B., Withers R.L. (1993): Structural modulation in sartorite: an electron microscope study. *Am. Mineral.*, **78**, 619-626.

Pring, A., Jercher, M., Makovicky, E. (1999): Disorder and compositional variation in the lillianite homologous series. *Mineral. Mag.,* **63**, 917-926.

Ramdohr, P. & Strunz, H. (1978): Klockmanns Lehrbuch der Mineralogie, 16th edn. Ferdinand-Enke ed., Stuttgart, 876 p.

Razmara, M.F., Henderson, C.M.B., Pattrick, R.A.D., Bell, A.M.T., Charnock, J.M. (1997): The crystal chemistry of the solid solution series between chalcostibite ($CuSbS_2$) and emplectite ($CuBiS_2$). *Mineral. Mag.,* **61**, 79-88.

Rey, N., Jumas, J.C., Olivier-Fourcade, J., Philippot, E. (1983): Sur les composés III-V-VI: Etude structurale du disulfure d'antimoine et de thallium. *Acta Cryst.,* **C39**, 971-974.

Ribár, B. & Nowacki, W. (1969): Neubestimmung der Kristallstruktur von Gratonit, $Pb_9As_4S_{15}$. *Z. Kristallogr.,* **128**, 321-338.

—, — (1970): Die Kristallstruktur von Stephanit, $[SbS_3|S|Ag_5^{III}]$. *Acta Cryst.,* **B26**, 201-207.

Rieder, M. (1963): X-ray powder data for two discredited minerals "warthaite" and "goongarrite". *Acta Univ. Carolinae, Geol.*, **2**, 115-119.

Riley, J.F. (1974): The tetrahedrite–freibergite series, with reference to the Mount Isa Pb–Zn–Ag orebody. *Miner. Depos.,* **9**, 117-124.

Rösch, H. & Hellner, E. (1959): Hydrothermale Untersuchungen am System PbS-As_2S_3. *Naturwiss.*, **46**, 72.

Rosenstingl, J. & Pertlik, F. (1993): Neuberechnung der Kristallstruktur von natürlichem und synthetischem monoklinen Ag_3AsS_3 (=Xanthokon) nebst einer Diskussion zur Symmetrie. *Mitt. Öster. Mineral. Gesell.*, **138**, 9-15.

Roy Choudhury, K., Bente, K., Mookherjee, A. (1989): Chemical and structural correlation problems of rayite. *N. Jb. Miner. Abh.,* **160**, 30-33.

Rozhdestvenskaya, I.V., Zayakina, N.V., Samusikov, V.P. (1993): Crystal structure features of minerals from the tetrahedrite–freibergite series. *Mineral. Zhurnal,* **15**, 9-17 (in Russian).

Sabelli, C., Nakai, I., Katsura, S. (1988): Crystal structure of cetineite and its synthetic analogue $Na_{3.6}(Sb_2O_3)_3(SbS_3)(OH)_{0.6}\cdot 2.4H_2O$. *Am. Mineral.,* **73**, 398-404.

Sakharova, M.S. (1955): Bismuth sulfosalts from Ustarasai deposit. *Trudy Mineral. Muzeya,* **7**, 112-126 (in Russian).

Samusikov, V.P., Zayakina, N.V., Leskova, N.V. (1988): Dependence of unit-cell dimension of tetrahedrite–tennantite ores on silver content. *Dokl. Akad. Nauk SSSR,* **299**, 468-471 (in Russian).

Sandomirskaya, S.M., Arifulov, Ch.Kh., Botova, M.M., Mozgova, N.N., Nenasheva, S.N., Tsepin, A.I., Sivtsov, A.N. (1992): Tsnigriite – a new mineral. *Zapiski Vsesoyuz. Mineral. Obshch.,* **121**, 95-101 (in Russian).

Sawada, H., Kawada, I., Hellner, E., Tokonami, M. (1987): The crystal structure of senandorite (andorite VI): $PbAgSb_3S_6$. *Z. Kristallogr.,* **180**, 141-150.

Sejkora, J. & Hyrsl, J. (2007): Ottensite: a new mineral from Qinglong, Guizhou Province, China. *Mineral. Record*, **38**, 77-81.

Shelimova, L.E., Karpinskii, O.G., Svechnikova, T.E., Avilov, E.S., Kretova, M.A., Zemskov, V.S. (2004): Synthesis and structure

of layered compounds in the PbTe-Bi_2Te_3 and PbTe-Sb_2Te_3 systems. *Inorg. Mater.*, **40**, 1264-1270.

Shimizu, M., Kato, A., Matsubara, S., Criddle, A.J., Stanley, C.J. (1993): Watanabeite, $Cu_4(As,Sb)_2S_5$, a new mineral from the Teine mine, Sapporo, Hokkaido, Japan. *Mineral. Mag.,* **57**, 643-650.

Shimizu, M., Miyawaki, R., Kato, A., Matsubara, S., Matsuyama, F., Kiyota, K. (1998): Tsugaruite, $Pb_4As_2S_7$, a new mineral species from the Yunosawa, Aomori Prefecture, Japan. *Mineral. Mag.,* **62**, 793-799.

Shimizu, M., Ishizaki, Y., Honma, T., Matsubara, S., Miyawaki, R. (2005): Dufrenoysite and marumoite from the Okoppe mine, Japan. *in* "Mineral Deposit Research: Meeting the Global Challenge", J. Mao & F.P. Bierlein, ed. Springer-Verlag, Berlin, Vol. **1**, 695-697.

Skowron, A. & Brown, I.D. (1990): Refinement of the structure of robinsonite, $Pb_4Sb_6S_{13}$. *Acta Cryst.*, **C46**, 527-531.

Smith, D.G.W. & Nickel, E.H. (2007): A system of codification for unnamed minerals: report of the Subcommittee for Unnamed Minerals of the IMA Commission on New Minerals, Nomenclature and Classification. *Can. Mineral*., **45**, 983-1055.

Smith, J.V., Pluth, J.J., Han, S.-X. (1997): Crystal structure refinement of miargyrite, $AgSbS_2$. *Mineral. Mag.,* **61**, 671-675.

Spiridonov, E.M., Sokolova, N.F., Gapeyev, A.K., Dashevskaya, D.M., Yevstigneyeva, T.L., Chvileva, T.N., Demidov, V.G., Balashov, Ye.P., Shul'ga, V.I. (1986a): The new mineral argentotennantite. *Dokl. Akad. Nauk SSSR,* **290**, 206-210 (in Russian).

Spiridonov, E.M., Chvileva, T.N., Borodaev, Yu.S., Vinogradova, R.A., Kononov, O.V. (1986b): The influence of bismuth on optical properties of gray copper. *Dokl. Akad. Nauk SSSR,* **290**, 1475-1478 (in Russian).

Spiridonov, E.M., Petrova, I.V., Dashevskaya, D.M., Balashov, E.P., Klimova, L.M. (1990): Roshchinite, $Pb_{10}Ag_{19}Sb_{51}S_{96}$ – a new mineral. *Dokl. Akad. Nauk SSSR,* **312**, 197-200 (in Russian).

Srikrishnan, T. & Nowacki, W. (1974): A redetermination of the crystal structure of cosalite, $Pb_2Bi_2S_5$. *Z. Kristallogr.,* **140**, 114-136.

—, — (1975): A redetermination of the crystal structure of livingstonite $HgSb_4S_8$. *Z. Kristallogr.,* **141**, 174-192.

Strunz, H. & Nickel, E.H. (2001): Strunz mineralogical tables, 9th edn. Schweizerbart, Stuttgart, 869 p.

Syneček, V. & Hybler, J. (1975): The crystal structures of krupkaite, $CuPbBi_3S_6$, and of gladite, $CuPbBi_5S_9$, and the classification of superstructures in the bismuthinite–aikinite group. *N. Jb. Miner. Mh.*, **1975** (12), 541-560.

Szymański, J.T. & Groat, L.A. (1997): The crystal structure of deanesmithite, $Hg_2^{1+}Hg_3^{2+}Cr^{6+}O_5S_2$. *Can. Mineral.,* **35**, 765-772.

Takagi, J. & Takéuchi, Y. (1972): The crystal structure of lillianite. *Acta Cryst.,* **B28**, 649-651.

Takéuchi, Y. (1997): Tropochemical cell-twinning. A Structure-Building Mechanism in Crystalline Solids. Material Science of Minerals and Rocks, Terra Scientific Publishing Company, Tokyo, 319 p.

Takéuchi, Y. & Sadanaga, R. (1969): Structural principles and classification of sulfosalts. *Z. Kristallogr.*, **130**, 346-368.

Takéuchi, Y. & Takagi, J. (1974): The structure of heyrovskýite ($6PbS.Bi_2S_3$). *Proc. Japan. Acad. Sci.,* **50**, 76-79.

Takéuchi, Y., Ghose, S., Nowacki, W. (1965): The crystal structure of hutchinsonite, $(Tl,Pb)_2As_5S_9$. *Z. Kristallogr.*, **121**, 321-348.

Takéuchi, Y., Ohmasa, M., Nowacki, W. (1968): The crystal structure of wallisite, $PbTlAgAs_2S_5$, the Cu analogue of hatchite, $PbTlCuAs_2S_5$. *Z. Kristallogr.,* **127**, 349-365.

Takéuchi, Y., Ozawa, T., Tagaki, J. (1979): Tropochemical cell-twinning and the 60 Å structure of phase V in the PbS-Bi_2S_3 system. *Z. Kristallogr.*, **150**, 75-84.

Topa, D. & Makovicky, E. (2006): The crystal structure of paděraite, $Cu_7(X_{0.33}Pb_{1.33}Bi_{11.33})_{\Sigma 13}S_{22}$, with X = Cu or Ag: new data and interpretation. *Can. Mineral.,* **44**, 481-495.

Topa, D. & Paar, W.H.: Cupromakovickyite, $Cu_8Pb_4Ag_2Bi_{18}S_{36}$ a new mineral of the pavonite homologous series. *Can. Mineral.* (accept.).

Topa, D., Makovicky, E., Balić-Žunić, T., Berlepsch, P. (2000a): The crystal structure of $Cu_2Pb_6Bi_8S_{19}$. *Eur. J. Mineral.,* **12**, 825-833.

Topa, D., Balić-Žunić, T., Makovicky, E. (2000b): The crystal structure of $Cu_{1.6}Pb_{1.6}Bi_{6.4}S_{12}$, a new 44.8 Å derivative of the bismuthinite–aikinite solid-solution series. *Can. Mineral.,* **38**, 611-616.

Topa, D., Makovicky, E., Criddle, A., Paar, W.H., Balić-Žunić, T. (2001): Felbertalite, a new mineral species from Felbertal, Salzburg Province, Austria. *Eur. J. Mineral.,* **13**, 961-972.

Topa, D., Makovicky, E., Paar, W.H. (2002a): Composition ranges and exsolution pairs for the members of the bismuthinite–aikinite series from Felbertal, Austria. *Can. Mineral.,* **40**, 849-869.

Topa, D., Makovicky, E., Balić-Žunić, T. (2002b): The structural role of excess Cu and Pb in gladite and krupkaite based on new refinements of their structure. *Can. Mineral.,* **40**, 1147-1159.

Topa, D., Makovicky, E., Balić-Žunić, T., Paar, W.H. (2003a): Kupčíkite, $Cu_{3.4}Fe_{0.6}Bi_5S_{10}$, a new Cu–Bi sulfosalt from Felbertal, Austria, and its crystal structure. *Can. Mineral.,* **41**, 1155-1166.

Topa, D., Makovicky, E., Balić-Žunić, T. (2003b): Crystal structures and crystal chemistry of members of the cuprobismutite homologous series of sulfosalts. *Can. Mineral.,* **41**, 1481-1501.

Topa, D., Makovicky, E., Paar, W.H., Brodtkorb, M.K. de (2004): The crystal structure of angelaite, $Cu_2AgPbBiS_4$, a new mineral species from Angela mine, Province of Chubut, Argentina. 32nd IGC, Florence, 20–28 August (abstract).

Topa, D., Makovicky, E., Paar, W.H. (2005): Mineralogical data on salzburgite and paarite, two new members of the bismuthinite–aikinite series. *Can. Mineral.,* **43**, 909-917.

Topa, D., Makovicky, E., Putz, H., Mumme, W.G. (2006a): The crystal structure of berryite, $Cu_3Ag_2Pb_3Bi_7S_{16}$. *Can. Mineral.,* **44**, 465-480.

Topa, D., Paar, W.H., Balić-Žunić, T. (2006b): Emilite, $Cu_{10.72}Pb_{10.72}Bi_{21.28}S_{48}$, the last missing link of the bismuthinite–aikinite series? *Can. Mineral*., **44**, 459-464.

Topa, D., Makovicky, E., Balić-Žunić, T. (2007): What is the reason of the doubled unit-cell volumes of copper-lead-rich pavonite homologues? The crystal structures of cupromakovickyite and makovickyite. *Can. Mineral.*, **45** (in press).

Vrublevskaya, Z.V., Mozgova, N.N., Sivtsov, A.V. (1985): Structural characteristics of boulangerite homologues and their study with electron microdiffraction. *Izv. Akad. Nauk SSSR*, *Ser. Geol.*, **4**, 90-97 (in Russian).

Vurro, F., Garavelli, A., Garbarino, C., Moëlo, Y., Borodaev, Yu.S. (1999): Rare sulfosalts from Vulcano, Aeolian Islands, Italy. II. Mozgovaite, $PbBi_4(S,Se)_7$, a new mineral species. *Can. Mineral.,* **37**, 1499-1506.

Walenta, K. (1998): Cuboargyrit, ein neues Silbermineral aus dem Schwarzwald. *Lapis,* **23**, 11/89, 21-23.

Walenta, K., Bernhardt, H.-J., Theye, T. (2004): Cubic $AgBiS_2$ (schapbachite) from the Silberbrünnle mine near Gengenbach in the Central Black Forest, Germany. *N. Jb. Miner. Mh.*, **2004** (9), 425-432.

Wang, N. & Paniagua, A. (1996): Fettelite, a new Hg-sulfosalt mineral from Odenwald. *N. Jb. Miner. Mh.*, **1996** (7), 313-320.

Wang, S. & Kuo, K.H. (1991): Crystal lattices and crystal chemistry of cylindrite and franckeite. *Acta Cryst.,* **A47**, 381-392.

Wang, X. & Liebau, F. (1999): An investigation of microporous cetineite-type phases $A_6(B_{12}O_{18})(CX_3)_2(D_x(H_2O, OH, O)_{6-y})$ II. Crystal structures of cetineites, $A_6(Sb_{12}O_{18})(SbX_3)_2(D_xY_{(6-y)})$, and their changes with composition. *Z. Kristallogr.,* **214**, 820-834.

Weiszburg, T.G., Criddle, A.J., Stanley, C.J. (1992): Reexamination of the original "wehrlite" sample. *Joint Annual Meet. of Geol. Assoc. Can./Mineral. Assoc. Can., Abstr.* **17**, A116.

Williams, T.B. & Hyde, B.G. (1988): Electron microscopy of cylindrite and franckeite. *Phys. Chem. Miner.,* **15**, 521-544.

Williams, T.B. & Pring, A. (1988): Structure of lengenbachite: A high-resolution transmission electron microscope study. *Am. Mineral.*, **73**, 1426-1433.

Wilson, J.R., Robinson, P.D., Wilson, P.N., Stanger, L.W., Salmon, G.L. (1991): Gillulyite, $Tl_2(As, Sb)_8S_{13}$, a new thallium arsenic sulfosalt from the Mercury gold deposit, Utah. *Am. Mineral.,* **76**, 653-656.

Wolf, M., Hunger, H.-J., Bewilogua, K. (1981): Potosiit – ein neues Mineral der Kylindrit–Franckeit-Gruppe. *Freib. Forschung.,* **C364**, 113-133.

Wuensch, B.J. (1964): The crystal structure of tetrahedrite, $Cu_{12}Sb_4S_{13}$. *Z. Kristallogr.,* **119**, 437-453.

— (1974): Sulfide crystal chemistry. *in* "Sulfide mineralogy". *Mineral. Soc. Am. Short Course Notes*, **1**, 21-44.

Wuensch, B.J. & Nowacki, W. (1967): The crystal structure of marrite, $PbAgAsS_3$. *Z. Kristallogr.,* **125**, 1-6.

Wuensch, B.J., Takéuchi, Y., Nowacki, W. (1966): Refinement of the crystal structure of binnite, $Cu_{12}As_4S_{13}$. *Z. Kristallogr.,* **123**, 1-20.

Wulf, R. (1990): Experimental distinction of elements with similar atomic numbers using anomalous dispersion (δ synthesis): An application of synchrotron radiation in crystal structure analysis. *Acta Cryst.*, **A46**, 681-688.

Yang, H., Downs, R.T., Costin, G., Eichler, C.M. (2007): Crystal structure and revision of chemical formula of tvalchrelidzeite, Hg_3SbAsS_3. *Can. Mineral.*, **45** (in press).

Žák, L., Megarskaya, L., Mumme, W.G. (1992): Rézbányite from Ocna de fier (Vaskö): a mixture of bismuthinite derivatives and cosalite. *N. Jb. Miner. Mh.*, **1992** (2), 69-79.

Žák, L., Fryda, J., Mumme, W.G., Paar, W.H. (1994): Makovickyite, $Ag_{1.5}Bi_{5.5}S_9$, from Baita Bihorului, Romania: The ^{4}P natural member of the pavonite series. *N. Jb. Miner. Abh.,* **168**, 147-169.

Zakrzewski, M. & Makovicky, E. (1986): Izoklakeite from Vena, Sweden, and the kobellite homologous series. *Can. Mineral.,* **24**, 7-18.

Zelenski, M., Balić-Žunić, T., Bindi, L., Garavelli, A., Makovicky, E., Pinto, D., Vurro, F. (2006): First occurrence of iodine in natural sulfosalts: The case of mutnovskite, $Pb_2AsS_3(I, Cl, Br)$, a new mineral from the Mutnovsky volcano, Kamchatka Peninsula, Russian Federation. *Am. Mineral.,* **91**, 21-28.

Zhang, Y., Wilkinson, A.P., Lee, P.L., Shastri, S.D., Shu, D., Chung, D.-Y., Kanatzidis, M. (2005): Determining metal ion distributions using resonant scattering at very high-energy *K*-edges: Bi/Pb in $Pb_5Bi_6Se_{14}$. *J. Appl. Cryst.*, **38**, 433-441.

Zhdanov, Yu.Ya., Amuzinskii, V.A., Andrianov, N.G. (1992): Discovery of a natural Ag-rich fahlore with the highest parameter of the unit cell. *Dokl. Akad. Nauk SSSR,* **326**, 337-340 (in Russian).

Zsivny, V. & Náray-Szabó, I. (1947): Parajamesonit, ein neues Mineral von Kisbánya. *Schweiz. Mineral. Petrogr. Mitt.,* **27**, 183-189.

Zhukova, T.B. & Zaslavskii, A.I. (1972): Crystal structures of the compounds $PbBi_4Te_7$, $PbBi_2Te_4$, $SnBi_4Te_7$, $SnBi_2Te_4$, $SnSb_2Te_4$ and $GeBi_4Te_7$. *Sov. Phys. Crystallogr.*, **16**, 796-799.

Received 12 September 2007
Accepted 20 September 2007

Mineralogical Magazine, June 2017, Vol. 81(3), pp. 411–461

OPEN ACCESS

Review

Nomenclature of the perovskite supergroup: A hierarchical system of classification based on crystal structure and composition

Roger H. Mitchell[1,*], Mark D. Welch[2] and Anton R. Chakhmouradian[3]

[1] Department of Geology, Lakehead University, Thunder Bay, Ontario P7B 5E1, Canada,
[2] Department of Earth Sciences, The Natural History Museum, Cromwell Road, London SW7 5BD, UK
[3] Department of Geological Sciences, University of Manitoba, Winnipeg, Manitoba R3T 2N2, Canada

[*Received 10 July 2016; Accepted 3 October 2016; Associate Editor: Stuart Mills*]

ABSTRACT

On the basis of extensive studies of synthetic perovskite-structured compounds it is possible to derive a hierarchy of hettotype structures which are derivatives of the arisotypic cubic perovskite structure (ABX_3), exemplified by $SrTiO_3$ (tausonite) or $KMgF_3$ (parascandolaite) by: (1) tilting and distortion of the BX_6 octahedra; (2) ordering of *A*- and *B*-site cations; (3) formation of *A*-, *B*- or *X*-site vacancies. This hierarchical scheme can be applied to some naturally-occurring oxides, fluorides, hydroxides, chlorides, arsenides, intermetallic compounds and silicates which adopt such derivative crystal structures. Application of this hierarchical scheme to naturally-occurring minerals results in the recognition of a perovskite supergroup which is divided into stoichiometric and non-stoichiometric perovskite groups, with both groups further divided into single ABX_3 or double $A_2BB'X_6$ perovskites. Subgroups, and potential subgroups, of stoichiometric perovskites include: (1) silicate single perovskites of the bridgmanite subgroup; (2) oxide single perovskites of the perovskite subgroup (tausonite, perovskite, loparite, lueshite, isolueshite, lakargiite, megawite); (3) oxide single perovskites of the macedonite subgroup which exhibit second order Jahn-Teller distortions (macedonite, barioperovskite); (4) fluoride single perovskites of the neighborite subgroup (neighborite, parascandolaite); (5) chloride single perovskites of the chlorocalcite subgroup; (6) *B*-site cation ordered double fluoride perovskites of the cryolite subgroup (cryolite, elpasolite, simmonsite); (7) *B*-site cation ordered oxide double perovskites of the vapnikite subgroup [vapnikite, (?) latrappite]. Non-stoichiometric perovskites include: (1) *A*-site vacant double hydroxides, or hydroxide perovskites, belonging to the söhngeite, schoenfliesite and stottite subgroups; (2) Anion-deficient perovskites of the brownmillerite subgroup (srebrodolskite, shulamitite); (3) *A*-site vacant quadruple perovskites (skutterudite subgroup); (4) *B*-site vacant single perovskites of the oskarssonite subgroup [oskarssonite, waimirite-(Y)]; (5) *B*-site vacant inverse single perovskites of the cohenite and auricupride subgroups; (6) *B*-site vacant double perovskites of the diaboleite subgroup; (7) anion-deficient partly-inverse *B*-site quadruple perovskites of the hematophanite subgroup.

Keywords: perovskite, group theory, ordered perovskites, hydroxide perovskites, crystal structure, hierarchial classification.

Introduction

Since the last revision to the nomenclature of the perovskite group of minerals by Nickel and McAdam (1963) several new members of this structural group have been approved by the Commission on New Minerals, Nomenclature and Classification (CNMNC) of the International Mineralogical Association (IMA). These include the silicate perovskite, bridgmanite [$(Mg,Fe)SiO_3$], which is now considered to be the dominant mineral of the silicate mantle of the Earth.

*E-mail: rmitchel@lakeheadu.ca
https://doi.org/10.1180/minmag.2016.080.156

(Tschauner *et al*., 2014). The recognition of Mg and Ca-based silicate perovskites, although these are stable only at high pressures, has stimulated an extraordinary interest in the stability and phase transformations of silicate perovskites (Liu, 1976; Hirose, 2014) and their fluoride analogues, such as the $NaMgF_3$–$KMgF_3$ solid solution series (Zhao *et al*., 1994; Chakhmouradian *et al*., 2001). Contemporaneously, interest in perovskite as a petrogenetic indicator mineral resulted in numerous studies (see summary by Mitchell, 2002) of the paragenesis, composition and crystallography of minerals with the perovskite structure occurring in a wide variety of igneous and metamorphic rocks. Perovskite-group minerals have also gained importance in isotopic (Woodhead *et al*., 2009; Zurevinski *et al*., 2011) and geochronological (Smith *et al*., 1989; Wu *et al*., 2010) studies as it was recognized that their Sr and Nd isotopic compositions are sensitive indicators of the mantle sources of kimberlites, lamproites and melilitites. Perovskite-structured compounds of diverse composition are important constituents of slags produced by the aluminothermic reduction of pyrochlore (Mitchell and Mariano, 2016) and SYNROC-type nuclear waste forms (Ringwood, 1985; Lumpkin, 2014).

Simultaneously with renewed interest in naturally-occurring perovskites, studies of perovskites by the materials science and solid state chemistry communities have resulted in thousands of publications on the structure and properties of synthetic perovskites and related compounds. This work is driven by the actual, and potential, industrial uses of materials with the perovskite structure in applications ranging from ferroelectric ceramics through superconductivity and giant magnetoresistance devices to photovoltaic cells (Gallaso, 1990; Bruce *et al*., 2010; see also Table 1 of Chakhmouradian and Woodward, 2014). Much of this work was driven by the observation that the perovskite structure is extremely 'flexible' with regard to cationic and anionic replacements and tolerance to ionic defects. Unlike many other structural types, every element of the periodic table, including the noble gases (Shcheka and Keppler, 2012; Britvin *et al*., 2015; 2016), can be found in some variant of perovskite-structured compounds.

Of particular relevance to the mineralogical community were investigations of the *P-T-X*-driven distortions of the aristotypic cubic lattices of single (ABX_3) and ordered or double ($A_2BB'X_6$) perovskites. The application of group theory (Howard and Stokes, 1998, 2002, 2004, 2005; Stokes *et al*., 2002) resulted in the establishment of a hierarchy of space groups of perovskites with distorted crystal structures, termed hettotypes. Most perovskite supergroup minerals do not adopt the cubic space groups $Pm\bar{3}m$ or $Fm\bar{3}m$ and thus are considered as hettotypes of reduced symmetry.

Synthetic perovskites can be classified according to a hierarchy of structural types (Fig. 1) ranging from simple ABX_3 compounds and ordered variants through cation- and anion-deficient varieties to layered complex derivatives (Mitchell, 2002). This classification is in principle applicable to naturally-occurring perovskite supergroup minerals and can be used to explain why particular space groups are adopted and to predict the structural and compositional variants of perovskites that might be expected to occur in nature. Note that many of the more complex non-stoichiometric or layered derivatives of the ABX_3 aristotype structure, such as high temperature superconducting compounds, depart too far in topology to be considered as members of the perovskite supergroup as defined in this work.

Aristotype perovskite

The 'ideal' perovskite structure (Goldschmidt, 1926) from which the structures of all other compounds having the perovskite structure are derived is illustrated in Fig. 2. Ideal, or single, perovskites, where 'single' refers to the number of symmetrically non-equivalent *A* and *B* sites, have the general formula ABX_3, where the *A*-site cations are larger than the *B*-site cations and similar in size to the *X*-site anions. To a first approximation the structure consists of a cubic close-packed array of *X* anions with one quarter of these replaced by *A*-site cations in an ordered manner. The *A*-site cations are surrounded by 12 anions in twelve-fold cubo-octahedral coordination, and the *B*-cations are surrounded by 6 anions in octahedral coordination. The *X* anions are coordinated by two *B*-site cations and four *A*-site cations (Goldschmidt, 1926). Perovskites having the ideal structure adopt the cubic space group $Pm\bar{3}m$ ($P4/m\bar{3}2/m$; #221). The compound $SrTiO_3$ is commonly regarded as the archetypal cubic perovskite, although $KMgF_3$ is a better alternative as, unlike $SrTiO_3$, it remains cubic from 3.6 K to its melting point, and its structure is not affected by pressure up to 50 GPa (Mitchell *et al*., 2006; Aguado *et al*., 2008). Many naturally-occurring oxide and fluoride perovskites probably crystallized initially as cubic or tetragonal perovskites, and adopted their room temperature structure

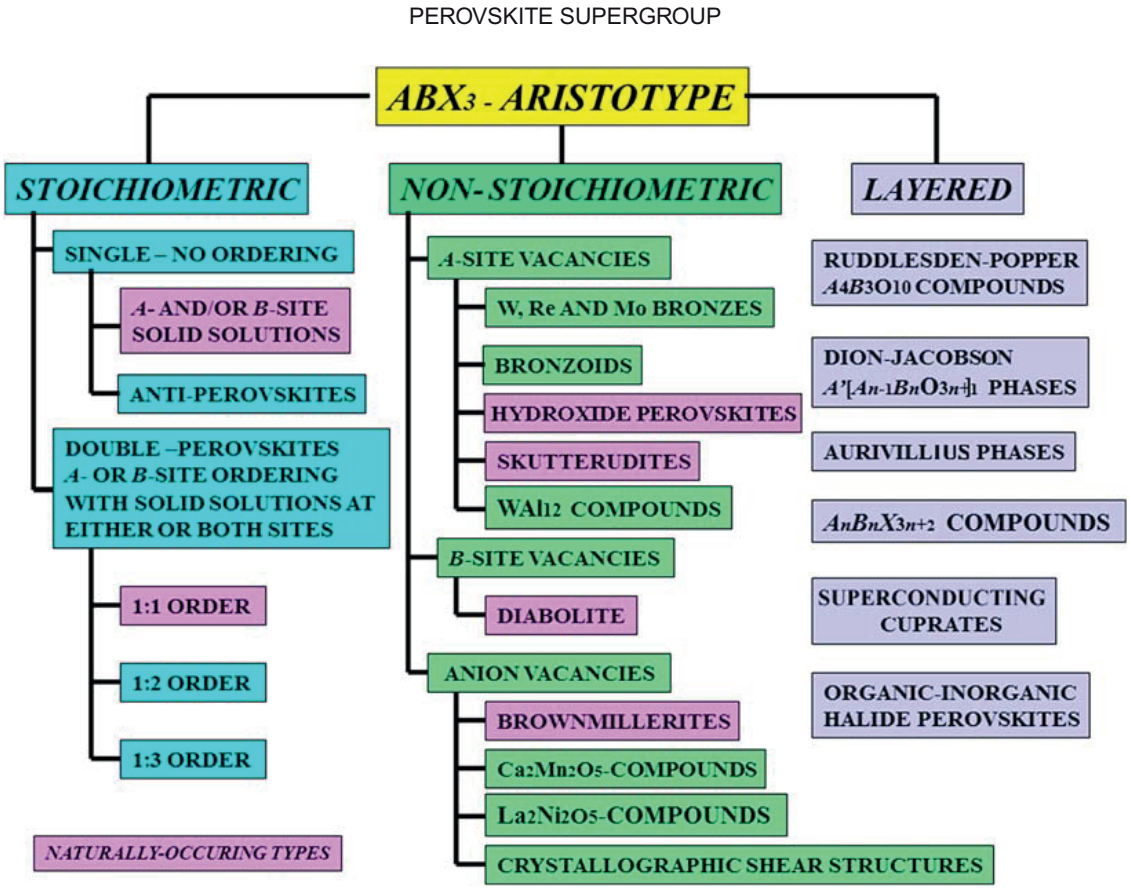

FIG. 1. Hierarchical classification of synthetic compounds with the perovskite structure and its derivatives.

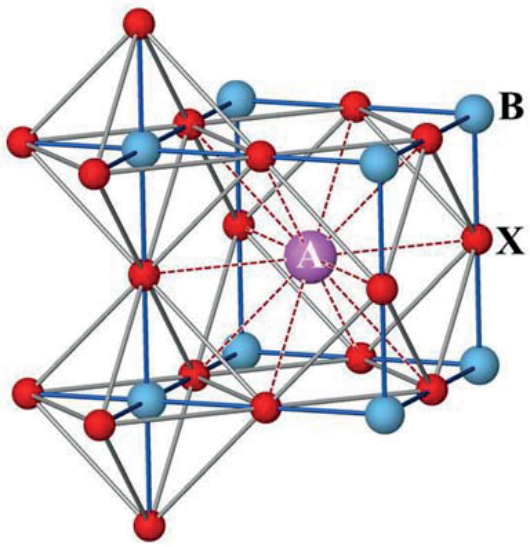

FIG. 2. The ideal ABX_3 perovskite structure showing the octahedral and icosahedral (12-fold) coordination of the *B*- and *A*-site cations, respectively.

as a consequence of distortion of these structures during cooling. Other perovskite-group minerals, including $CaTiO_3$ perovskite, typically crystallize at temperatures below the temperature required for phase transitions to a higher symmetry (e.g. located at >1100°C for synthetic $CaTiO_3$; Redfern, 1996; Carpenter *et al*., 2006). It is essentially unknown what the effect of composition is on the phase transition temperatures of complex naturally-occurring perovskite-group minerals. For example, the cubic-to-tetragonal transition can be reduced by several hundred degrees with the substitution of 25% Ca for Sr in synthetic $CaTiO_3$ (Carpenter *et al*., 2006). Hu *et al*. (1992) used transmission electron microscopy to examine several perovskite-group minerals, including cumulus loparite from igneous rocks, and found no evidence for transformation twinning in any of the samples investigated as many twins appear to be growth twins. Note that hydroxide perovskites, such as dzhalindite or stottite, which form in supergene environments are unlikely to have undergone phase transitions in

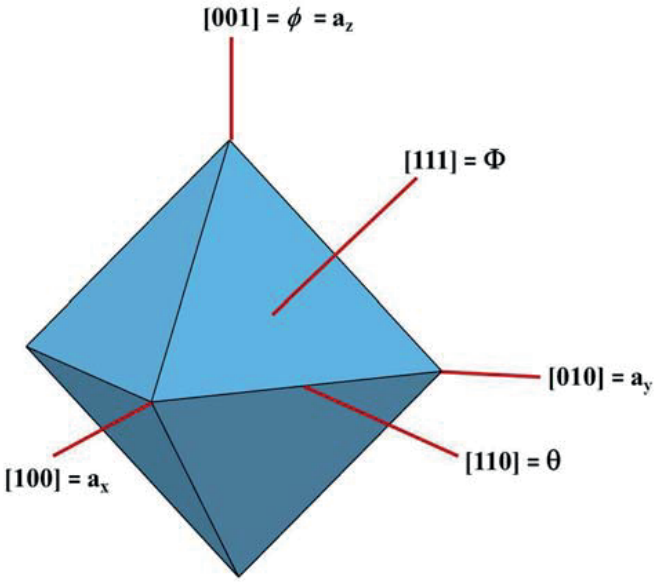

FIG. 3. Directions of rotation of the BX_6 octahedron relative to the pseudocubic cell axes. Glazer (1972) tilt axes are shown as a_x, a_y and a_z. Also shown is the commonly used notation (Zhao *et al*., 1994) for describing the magnitude of the tilts about the pseudocubic $[110]_p$, $[001]_p$ and $[111]_p$ axes as the rotation angles θ, φ and Φ. Note that the θ angle is the resultant of the Glazer a_x and a_y tilts.

nature, although these have been observed in some experimental studies (see below).

Distorted ABX_3 perovskites

The majority of simple synthetic and natural perovskites are distorted derivatives of the aristotypic perovskite structure resulting from: (1) tilting (i.e. rotation) of rigid BX_6 polyhedra; (2) first order Jahn-Teller distortion of BX_6 octahedra; (3) second order Jahn-Teller effects affecting the *A*- and *B*-cation polyhedra, and reflecting the mixing of molecular orbitals and/or lone-pair effects. Tilting of the BX_6 polyhedra is the commonest type of distortion found in naturally-occurring perovskites, although the other modes can be found in barioperovskite, macedonite and diaboleite.

BX_6 octahedron tilting

Octahedron tilting occurs when the size of the *A* cation is too small for the 12-fold site within the BX_6 polyhedral framework: e.g. Ca^{2+} in the synthetic $(Sr,Ca)TiO_3$ solid solution series (Yamanaka *et al*., 2002). To accommodate such cations, the octahedra tilt about the three axes of the pseudocubic precursor cubic cell (*x*, *y* and *z*), so as to achieve the lowest energy mode for the crystal. In most tilting models it is assumed that the BX_6 octahedra are rigid, but not necessarily ideal, and the rotation does not disrupt their corner-sharing connectivity. Tilting results in changes in the *A*–*X* bond lengths so that they are no longer equal. This changes the *A*-site coordination, with concomitant reduction in symmetry from space group $Pm\bar{3}m$ to that of a hettotype. Coordination of the *A*-site cation as determined from bond valence analysis of the first coordination sphere can range from 12 to 8, depending upon the style and magnitude of the octahedron tilt. Many naturally-occurring ABX_3 perovskite-group minerals, including $CaTiO_3$ (perovskite *sensu stricto*), adopt the orthorhombic *Pbnm* $GdFeO_3$ structure type with the *A*-site cations in 8-fold coordination.

Distorted perovskites are commonly described using the nomenclature devised by Glazer (1972). In this scheme BX_6 octahedron rotations are described in terms of three orthogonal Cartesian axes coincident with the three axes of the aristotype cubic unit cell (Fig. 3). In the general case of unequal rotation angles about the *x*, *y* and *z* axes, the rotation scheme is denoted as *a*, *b* and *c* degrees, with sense of the rotations (i.e. clockwise or anticlockwise) in successive layers of octahedra perpendicular to a specific rotation axis given as

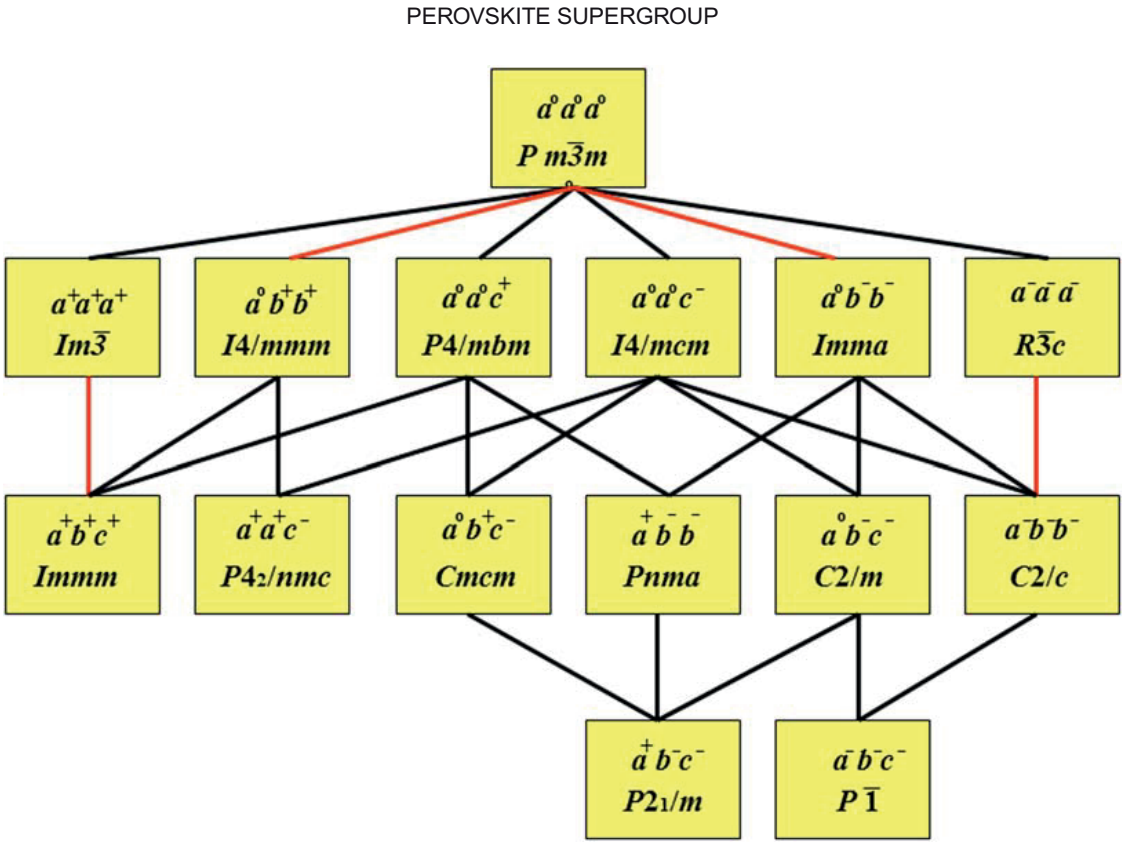

FIG. 4. Group–subgroup relations associated with particular tilt systems for ABX_3 single perovskites as evaluated by Howard and Stokes (1998, 2002) using group theoretical methods. Space group $Pm\bar{3}m$ is the aristotype from which all hettotypes are derived. Red and black lines indicate possible first and second order phase transitions, respectively.

superscripts. A positive superscript indicates tilt of octahedra in successive layers in the same direction (i.e. an in-phase tilt), whereas a negative superscript indicates rotation of consecutive octahedra along a specific rotation axis in the opposite sense (i.e. an anti-phase tilt). Thus, the symbol $a^+b^+c^+$ indicates three unequal angles of rotation about x, y and z with consecutive octahedra along the same axis (i.e. x, y or z) rotating in the same sense. For equal angles of rotation the notation would become $a^+a^+a^+$. A zero superscript is used for no rotations about a specific axis, e.g. the cubic aristotype lacking any octahedron tilting has the tilt symbol $a^0b^0c^0$ and space group $Pm\bar{3}m$.

Glazer (1972) used crystallographic principles to evaluate all possible combinations of tilting for single ABX_3 perovskites and identified 23 tilt systems corresponding to particular space groups. Howard and Stokes (1998) using group theory, confirmed Glazer's (1972) analysis, but reduced the number of tilt systems to 15, as some of Glazer's tilt systems were combinations of one or more of the basic fifteen. Such combinations and their associated space groups are possible in principle but have not been observed in real crystals. Certain tilting patterns, e.g. those combining in-phase rotations about x and/or y with an antiphase rotation about z, cannot maintain the connectivity of rigid octahedra and hence require polyhedral distortions (Woodward, 1997). Figure 4 illustrates the space-group relationships associated with particular tilt systems for ABX_3 perovskites and identifies possible first and second order phase transitions from the cubic aristotype. These relationships are directly applicable to the *P-T-X* space-group transitions possible for natural perovskite-group minerals.

Similar analyses of octahedron tilting have been subsequently provided for 1:1, 1:2, and 1:3 *B*-cation ordered perovskites by: Woodward (1997); Howard *et al*. (2003); Lufaso and Woodward (2004); Howard and Stokes (2004); and Lufaso *et al*. (2006). The tilt schemes and the hierarchy of phase transitions (Fig. 5) for 1:1 ordered (or double) perovskites are given by Howard *et al*. (2003) and are applicable

directly to fluoride-based ordered perovskite-group minerals such as simmonsite and cryolite (see below).

Perovskite nomenclature

Perovskite-supergroup minerals as defined here are those minerals whose structures consist of three-dimensional networks of corner-sharing octahedra and which adopt the aristotypic ABX_3 perovskite structure or those of its derivatives. The octahedra can be tilted and/or distorted without destroying the connectivity. Cations at the *B*-site can be distributed randomly and termed single perovskites or ordered and termed double perovskites. The *A*-site can be filled or vacant, in the latter case forming *A*-site deficient single or double perovskites such as the hydroxide perovskites. The *B*-site can be partially, or entirely, vacant as in the minerals **diaboleite** or **waimirite-(Y)**, respectively.

Naturally-occurring perovskite supergroup minerals occur as oxides, fluorides, chlorides, hydroxides, arsenides, antimonides, intermetallic compounds and silicates. Many of these have the ABX_3 perovskite structure and exhibit significant solid solution, coupled with the compositionally-driven space group changes which occur between potential ideal end-member compositions. Perovskite supergroup minerals can be also described as 'homeotypic' in that they have the same essential topology but not necessarily the same space group.

Tables 1–3 together with Figs 6 and 7, present a hierarchical classification of the currently named members of the perovskite supergroup together with their room temperature space group as determined from diffraction studies of natural crystals or by analogy with synthetic analogues. This classification has been approved by the IMA-CNMNC (Hålenius *et al*., 2016). The etymology of members of the supergroup is given in the Appendix to this paper (deposited with the Principal Editor of *Mineralogical Magazine* and available from http://www.minersoc.org/pages/e_journals/dep_mat_mm.html).

Two major groups are recognized in the perovskite supergroup: stoichiometric and non-stoichiometric groups. The former have ABX_3 or $A_2BB'X_6$ stoichiometry, and the latter include hydroxide- and arsenide-based minerals, which are also known as defect perovskites, characterized by *A*- and/or *B*-site vacancies together with the anion-deficient minerals of the brownmillerite and hematophanite subgroups. Note that many 'non-stoichiometric' perovskites have well-defined fixed ratios of *A*- or *B*-site cations or *X* anions but are considered here as non-stoichiometric relative to

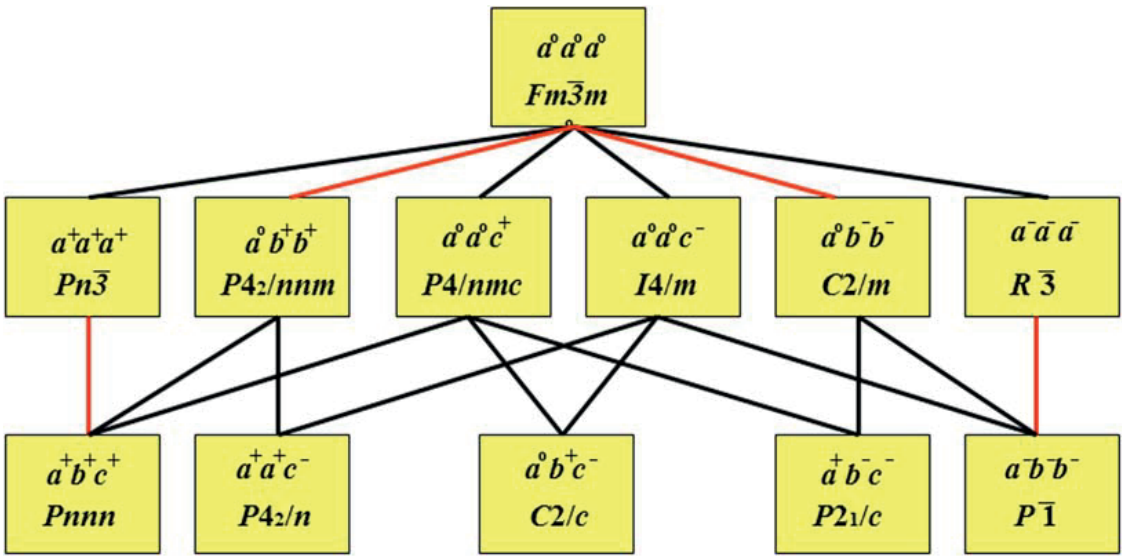

FIG. 5. Group–subgroup relations associated with particular tilt systems for 1:1 *B*-site ordered, or double perovskites, perovskites as evaluated by Howard *et al*. (2003) using group theoretical methods. Space group $Fm\bar{3}m$ is the aristotype from which all hettotypes are derived. Red and black lines indicate possible first and second order phase transitions, respectively.

PEROVSKITE SUPERGROUP

TABLE 1. Classification of stoichiometric perovskites ABX_3 and $A_2BB'X_6$.

Group/subgroup	Composition	Ideal	Sp. gp.	Tilt
Single perovskites ABX_3				
Bridgmanite subgroup				
Bridgmanite	$(Mg,Fe)SiO_3$	$MgSiO_3$	*Pbnm*	$a^-a^-c^+$
Unnamed	?	$CaSiO_3$	?	
Perovskite subgroup				
Barioperovskite	$BaTiO_3$	$BaTiO_3$	*Amm*2*	$a^oa^oa^o$
Isolueshite	$(Na,La,Ce)(Nb,Ti)O_3$	$(Na,La)NbO_3$	$Pm\bar{3}m$	$a^oa^oa^o$
Lakargiite	$(Ca)(Zr,Sn,Ti)O_3$	$CaZrO_3$	*Pbnm*	$a^-a^-c^+$
Loparite	$(Na,REE,Ca,Sr,Th)(Ti,Nb)O_3$	$(Na,REE)Ti_2O_6$	*Pbnm*	$a^-a^-c^+$
Lueshite	$(Na,REE,Ca)(Nb,Ti)O_3$	$NaNbO_3$	*Pmmn*	
Macedonite	$(Pb,Bi)TiO_3$	$PbTiO_3$	*P*4*mm**(?)	$a^oa^oa^o$
Megawite	$(Ca)(Sn,Zr,Ti)O_3$	$CaSnO_3$	*Pbnm*	$a^-a^-c^+$
Perovskite	$(Ca,REE,Na)(Ti,Nb)O_3$	$CaTiO_3$	*Pbnm*	$a^-a^-c^+$
Tausonite	$(Sr,Ca,REE,Na)(Ti,Nb)O_3$	$SrTiO\bar{3}$	$Pm\bar{3}m$	$a^oa^oa^o$
Neighborite subgroup				
Neighborite	$(Na,K)MgF_3$	$NaMgF_3$	*Pbnm*	$a^-a^-c^+$
Parascandolaite	$KMgF_3$	$KMgF_3$	$Pm\bar{3}m$	$a^oa^oa^o$
Chlorocalcite subgroup				
Chlorocalcite	$KCaCl_3$	$KCaCl_3$	*Pbnm*	$a^-a^-c^+$
Double perovskites $A_2BB'X_6$				
Elpasolite subgroup				
Elpasolite	K_2NaAlF_6	K_2NaAlF_6	$Fm\bar{3}m$	$a^oa^oa^o$
Cryolite	Na_2NaAlF_6	Na_2NaAlF_6	$P2_1/n$	$a^-a^-c^+$
Simmonsite	Na_2LiAlF_6	Na_2LiAlF_6	$P2_1/n$	$a^-a^-c^+$
Vapnikite subgroup				
Vapnikite	Ca_2CaUO_6	Ca_2CaUO_6	$P2_1/n$	$a^-a^-c^+$
Latrappite (?)	$(Ca,Na)(Nb,Fe^{3+},Ti)O_3$	$Ca_2NbFe^{3+}O_6$	$P2_1/n$	$a^-a^-c^+$
Double antiperovskites $B_2XX'A_6$				
Sulphohalite subgroup				
Sulphohalite	$Na_6FCl(SO_4)_2$	$Na_6FCl(SO_4)_2$	$Fm\bar{3}m$	$a^oa^oa^o$

* Octahedra in space groups *Amm*2 and *P*4*mm* are not tilted and the reduction in symmetry from $Pm\bar{3}m$ results from second order Jahn-Teller distortion.
Composition = compositional range of the mineral. Ideal = ideal composition of the end-member molecule. Sp.gp. = space group. Tilt = Glazer (1972) tilt scheme. *REE* = rare-earth element.

ABX_3 or $A_2BB'X_6$ perovskites. Within these groups following the dominant-constituent or dominant valency rules we recognize several compositional and structural subgroups depending on diverse combinations of the dominant *A*- or *B*-site cation or *X* anion. Together these constitute the perovskite supergroup.

We do not intend to use the modifying prefix 'keno' (from the Ancient Greek κενός = empty), as introduced by Atencio *et al*. (2010) for the *A*-site deficient minerals of the pyrochlore supergroup, as we consider this to be redundant for all *A*-site deficient perovskite structures. Moreover, the terms *A*-site deficiency, *A*-site vacancy, and defect perovskite are entrenched in the materials science and solid-state chemistry literature and thus have precedence; especially with regard to keyword search terms and potential interactions of mineralogists with those communities.

Although many compounds termed hexagonal perovskites have been synthesized (Mitchell, 2002) only a few are found in nature (Krivovichev, 2008). The structures of the majority of these are hexagonal antiperovskite polytypes characterized by combinations of face- and corner-sharing of octahedra rather than corner-sharing alone (Krivovichev, 2008). For this reason we do not consider such minerals as: 2*H*-nacaphite;

TABLE 2 Classification of non-stoichiometric perovskites.

	Composition	Ideal	Sp. gp.	Tilt
	***A*-site vacant hydroxide perovskites**			
Single hydroxide perovskites				
Söhngeite subgroup				
Dzhalindite	$(In,Fe)(OH)_6$	$In(OH)_3$	$Im\bar{3}$	$a^+a^+a^+$
Söhngeite	$(Ga,Al,Fe)(OH)_3{\cdot}xH_2O$	$Ga(OH)_3$	$P4_2/nmc$ or $P4_2/n$	$a^+a^+c^-$
Bernalite	$(Fe^{3+}_{0.93}Si_{0.06}Zn_{0.01})[(OH)_{2.95}O_{0.04}]$	$Fe(OH)_3$	$Pmmn$	$a^+b^+c^-$
Double hydroxyperovskites				
Schoenfliesite subgroup				
Schoenfliesite#	$(Mg_{0.94}Mn_{0.13})_{1.07}Sn_{0.97}(OH)_6$	$MgSn(OH)_6$	$Pn\bar{3}$	$a^+a^+a^+$
Burtite	$(Ca_{0.98}Mg_{0.02})Sn(OH)_6{\cdot}0.39H_2O$	$CaSn(OH)_6$	$Pn\bar{3}$	$a^+a^+a^+$
Jeanbandyite	$Fe^{3+}_xFe^{2+}_{(1-x)}Sn(OH)_{(6-x)}O_x (1\geq x\geq 0.5)$	$Fe^{3+}Sn(OH)_5O$	$Pn\bar{3}$	$a^+a^+a^+$
Mushistonite	$(Cu_{0.48}Zn_{0.39}Fe_{0.17})_{1.04}Sn(OH)_{5.95}$	$CuSn(OH)_6$	$Pn\bar{3}$	$a^+a^+a^+$
Natanite#	$(Fe_{0.46}Zn_{0.36}Cu_{0.28})Sn(OH)_{6.09}$	$FeSn(OH)_6$	$Pn\bar{3}$	$a^+a^+a^+$
Vismirnovite	$(Zn_{0.89}Fe_{0.08}Cu_{0.1})Sn(OH)_{6.04}$	$ZnSn(OH)_6$	$Pn\bar{3}$	$a^+a^+a^+$
Wickmanite#	$(Mn_{095}Mg_{0.03}Ca_{0.2})Sn(OH)_6$	$MnSn(OH)_6$	$Pn\bar{3}$	$a^+a^+a^+$
Stottite subgroup				
Stottite	$(Fe^{2+}_{1.15}Mg_{0.03}Mn_{0.03}Ca_{0.01})_{1.22}Ge_{0.95}(OH)_6$	$FeGe(OH)_6$	$P4_2/n$	$a^+a^+c^-$
Mopungite	$NaSb(OH)_6$	$NaSb(OH)_6$	$P4_2/n$	$a^+a^+c^-$
Tetrawickmanite	$[(Mn_{0.94}Fe_{0.05}Ca_{0.01})(Sn_{0.98}Si_{0.11}Al_{0.010}(OH)_6$	$MnSn(OH)_6$	$P4_2/n$	$a^+a^+c^-$

Extensive solid solution exists between natanite, schoenfliesite and wickmanite from Pitkäranta (Nefedov *et al*., 1977). Composition = compositional range of the mineral. Ideal = ideal composition of the end-member molecule. Sp. gp. = space group. Tilt = Glazer (1972) tilt scheme.

5*H*-galeite; 7*H*-schairerite; 9*R*-kogarkoite; and 9*R*-hatrurite, as members of the perovskite supergroup. Only **sulphohalite**, $Na_6FCl(SO_4)_2$, an ordered double antiperovskite which adopts a cubic ($Fm\bar{3}m$) anti-elpasolite 3*C* polytype structure, is considered here as a member of the perovskite supergroup, as corner-sharing of the FNa_6 and $ClNa_6$ octahedra is maintained. The minerals palmierite, a derivative of the 9*R* hexagonal perovskite structure type (Mitchell, 2002), and orthorhombic *Pnma* javoreite ($KFeCl_3$; Kodera *et al*., 2016) contain only face-sharing octahedra and thus are not a members of the perovskite supergroup.

Recently, McDonald *et al*. (2013) have noted that peatite-(Y) and ramikite-(Y), both complex Na-Li ± Zr phosphate carbonate minerals, can be described as cluster compounds based on simpler unit cells, and which are cation-deficient perovskite-related structures. Similar cluster compounds, such as $Cs_3Zr_6Br_{15}C$, are known as synthetic phases (Qi and Corbett, 1995) suggesting that there could exist a large number of perovskite-related cluster phases and minerals. In this work peatite-(Y) and ramikite-(Y) are not considered as members of the perovskite supergroup as their structures are far-removed from those of other members.

Stoichiometric perovskite group – single ABX_3 perovskites

Silicate single perovskites – bridgmanite subgroup

The presence of silicates having the perovskite structure in the Earth's mantle has long been postulated on the basis of experimental petrological studies of pyrolite and lherzolite at high pressures and temperatures (Ringwood, 1991; Jackson and Rigden, 1998; Hirose, 2014) together with circumstantial evidence based on the character of decompressed silicate inclusions in diamonds (Stachel *et al*., 2000). Recently, sub-micrometre crystals with the composition of $(Mg,Fe)SiO_3$ occurring in a four-phase mixture in shock-induced veins in the Tenham (L6) chondritic meteorite, were found by full profile refinement of X-ray diffraction (XRD) data to adopt space group *Pbnm*. This material with the perovskite structure was named bridgmanite by Tschauner *et al*. (2014). By analogy it is now

TABLE 3. Classification of *A*- and *B*-site vacant, and anion deficient perovskites.

	Composition	Ideal	Sp. gp.	Tilt
***A*-site vacant skutterudites**				
Skutterudite subgroup				
Skutterudite	$(Co,Fe,Ni)As_{2-3}$	$CoAs_3$	$Im\bar{3}$	$a^+a^+a^+$
Kieftite	$(Co,Ni,Fe,Cu)(Sb,Cl)_3$	$CoSb_3$	$Im\bar{3}$	$a^+a^+a^+$
Nickelskutterudite	$NiAs_{2-3}$	$NiAs_3$	$Im\bar{3}$	$a^+a^+a^+$
Ferroskutterudite	$(Fe,Co)As_3$	$FeAs_3$	$Im\bar{3}$	$a^+a^+a^+$
***B*-site vacant perovskites**				
Single perovskites				
Oskarssonite subgroup				
Oskarssonite	$Al(F_{2.62}(OH)_{0.49})$	AlF_3	$R\bar{3}c$	$a^-a^-c^-$
Waimirite-(Y)	$(Y_{0.69}, REE_{0.28}, Ca_{0.03})(F_{2.54}, \square_{0.25}, O_{0.21})$	YF_3	*Pbnm*	$a^-a^-c^+$
Single antiperovskites				
Cohenite subgroup				
Cohenite	$C(Fe,Ni,Co)_3$	CFe_3	*Pm*	$a^-a^-c^+$
Auricupride subgroup				
Auricupride	$(Au,Pd)Cu_3$	$AuCu_3$	$Pm\bar{3}m$	$a^oa^oa^o$
Atokite	$Sn(Pd,Pt)_3$	$SnPd_3$	$Fm\bar{3}m$	$a^oa^oa^o$
Awaruite	$Fe(Ni,Co)_3$	$FeNi_3$	$Pm\bar{3}m$	$a^oa^oa^o$
Chengdeite	$(Fe,Ni,Co,Cu)(Ir,Pt)$	$FeIr_3$	$Pm\bar{3}m$	$a^oa^oa^o$
Isoferroplatinum	$(Fe,Cu,Ni)Pt_3$	$FePt_3$	$Pm\bar{3}m$	$a^oa^oa^o$
Rustenburgite	$Sn(Pt,Pd)_3$	$SnPt_3$	$Fm\bar{3}m$	$a^oa^oa^o$
Yixunite	$InPt_3$	$InPt_3$	$Pm\bar{3}m$	$a^oa^oa^o$
Zvyagintsevite	$(Pb,Bi)(Pd,Pt)_3$	$PbPt_3$	$Pm\bar{3}m$	$a^oa^oa^o$
Double Perovskite				
Diaboleite	$[Pb_2Cu(OH)_4Cl_2]$	$[Pb_2Cu(OH)_4Cl_2]$	*P4mm*	$a^oa^oa^o$
Anion deficient perovskites				
Brownmillerite subgroup				
Brownmillerite	$Ca_2Fe^{3+}AlO_5$	$Ca_2Fe^{3+}AlO_5$	*Ibm*2	-
Srebrodolskite	$Ca_2(Fe,Mg,Mn)_2O_5$	$Ca_2Fe_2^{2+}O_5$	*Pcmn*	-
Shulamitite	$(Ca,Sr,REE)(Ti,Zr,Nb)(Fe^{3+},Mn,Mg)(Al,Fe^{3+},Si)O_8$	$Ca_3TiFe^{3+}AlO_8$	*Pmma*	-
Hematophanite subgroup				
Hematophanite	$Pb_4(Fe_3^{3+},\square)(Cl,OH)O_8$		*P4/mmm*	-

Composition = compositional range of the mineral. Ideal = ideal composition of the end-member molecule. Sp. gp. = space group. Tilt = Glazer (1972) tilt scheme.

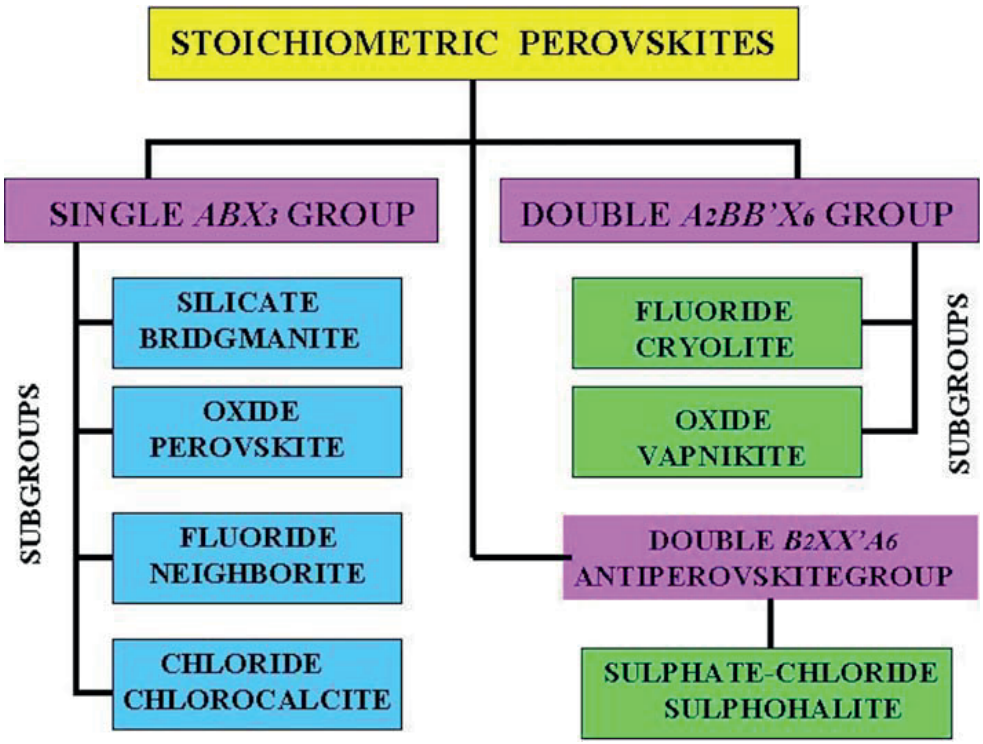

FIG. 6. Hierarchical classification of the stoichiometric perovskite supergroup minerals.

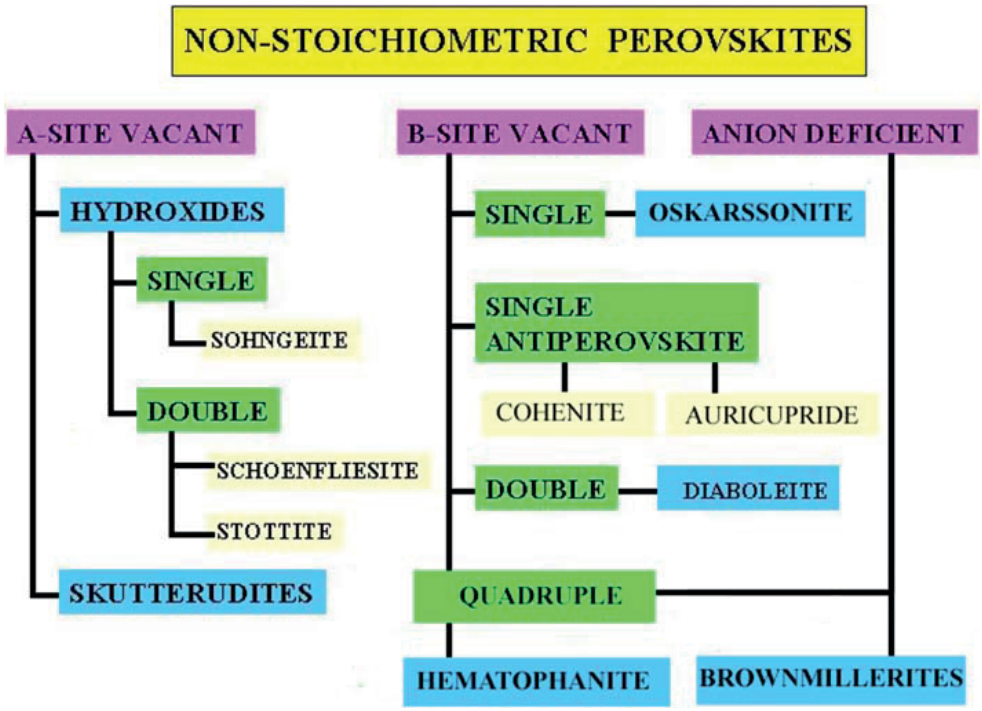

FIG. 7. Hierarchical classification of the non-stoichiometric perovskite supergroup minerals.

assumed that *Pbnm* bridgmanite is the most abundant mineral in the Earth and the dominant mineral in the lower mantle, i.e. from below ~700 km depth to near the core-mantle boundary where it probably transforms to a *Cmcm* $CaIrO_3$-type structure, commonly referred to as 'post-perovskite' by the geophysical community. This phase is stable above 120 GPa at 2500 K (Murakami *et al*., 2004; Oganov and Ono, 2004; Tsuchiya *et al*., 2004). These conditions correspond to a depth of ~2600 km and the location of the D" seismic discontinuity at the base of the lower mantle. The 'post-perovskite' $CaIrO_3$-type phase has a pseudo-two-dimensional layer structure (Sugahara *et al*., 2008) and is not a member of the perovskite supergroup.

Experimental studies of the phase relationships of $CaSiO_3$ at high pressures (Gasparik *et al*., 1994) coupled with observations on decompressed calcium silicate inclusions in diamonds (Stachel *et al*., 2000; Kaminsky *et al*., 2001), clearly indicate that bridgmanite must be accompanied by $CaSiO_3$ with the perovskite structure in the lower mantle. The symmetry of this phase, initially identified as cubic (Liu and Ringwood, 1975), has been debated by Akber-Knutson *et al*. (2002), Caracas and Wentzcovitch, (2005); and Fang and Ahuja (2006). *In situ* experimental diffraction data relevant to resolution of this question are limited. As yet, quenched examples of this phase have not been found and the mineral remains unnamed.

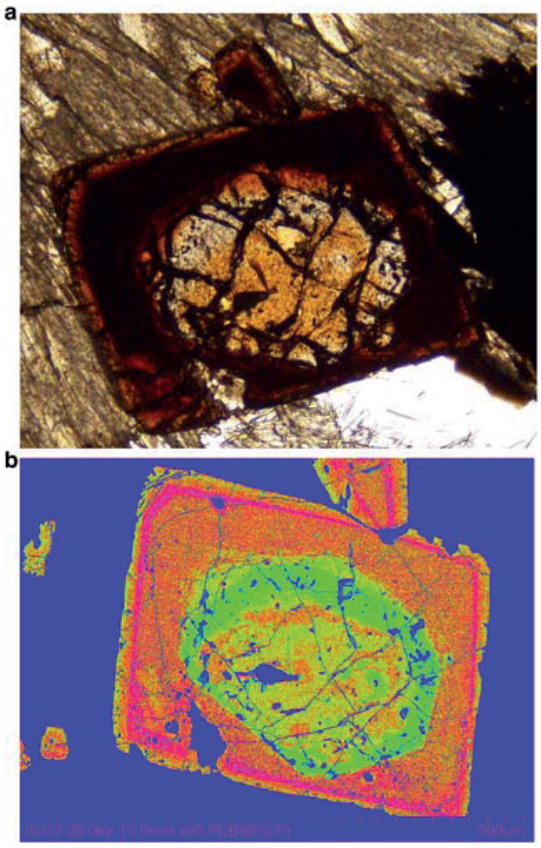

FIG. 8. Tausonite-strontian loparite from the Little Murun complex, Yakutia, Russia. Tausonite occurs in the core of this strongly-zoned crystal. (*a*) Plane polarized light optical image; (*b*) false coloured back-scattered electron image. See Mitchell and Vladykin (1993) for compositional data.

Oxide single perovskites – perovskite subgroup

Members of this group (Table 1; Fig. 6) are characterized by oxygen as the dominant anion. Many of these ABO_3 perovskites are titanates which typically exhibit extensive solid solution between potential end-member compositions, as diverse cations can occupy the *A* and *B* sites. These minerals are the commonest members of the perovskite supergroup in the Earth's crustal environment (Mitchell, 2002), and as calcium-aluminum-rich (CAI) inclusions in chondritic meteorites. The latter are considered to represent remnants of the earliest accretionary material in the Solar System (McPherson *et al*., 2005).

Tausonite ($SrTiO_3$)

Tausonite was described initially from the Little Murun potassic alkaline complex, Sakha (Russia) by Vorob'yev *et al*. (1984). Most tausonite from Little Murun is complexly zoned (Fig. 8) and contains significant amounts of Na and rare-earth elements (*REE*), representing a solid solution towards loparite (Vorob'yev *et al*., 1984; Mitchell and Vladykin, 1993). The material studied by Vorob'yev *et al*. (1984) represents an average composition in the tausonite–loparite series (~85 mol.% $SrTiO_3$), and thus is not that of pure $SrTiO_3$. In addition, silicate inclusions, represented by 2.2–5.0 wt.% SiO_2, were present in the material analysed by Vorob'yev *et al*. (1984). Calcium-bearing tausonite (2.1–2.5 wt.% CaO; 92–93 mol.% $SrTiO_3$) has been described from the P2-West lamproite, Wajrakurur (India) by Gurmeet Kaur and Mitchell (2013), where it occurs with baryte, pectolite and hydrogarnet as pseudomorphs after an unidentified primary phase. Tausonite with a composition close to that of pure $SrTiO_3$ (98 mol.%)

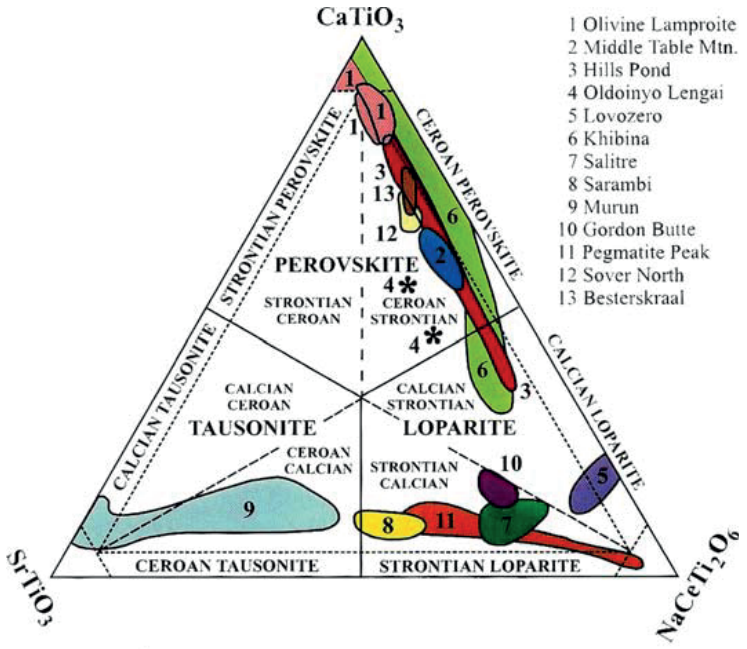

FIG. 9. Compositional variation (mol.%) of perovskite-group minerals from potassic and agpaitic syenites, rheomorphic fenites, lamproites and orangeites depicted in the ternary system $SrTiO_3$–$NaCeTi_2O_6$–$CaTiO_3$ (tausonite–loparite–perovskite) (after Mitchell, 2002). Note subdivisions of the compositional fields are used for the complete description of diverse compositions of these perovskite-supergroup minerals (Mitchell and Valdykin, 1993; Mitchell, 2002).

has also been found in Sr-rich metamorphic rocks of the Itoigawa-Ohmi District (Japan) by Miyajima *et al*. (2002). Tausonite with elevated levels of CaO (5–9 wt.%) and Na_2O (1.9–2.6 wt.%) has been described from several types of feldspathic hornfels xenoliths entrained in foyaite in the Khibiny alkaline complex (Kola Peninsula, Russia) by Yakovenchuk *et al*. (2005)

The crystal structures of tausonites from all of the above occurrences have not been determined. However, Vorob'yev *et al*. (1984) noted that as the powder XRD pattern (a = 3.9048 Å) of the holotype tausonite from Little Murun was similar to that of synthetic $SrTiO_3$ (a = 3.9050 Å; Hutton and Nelmes, 1981), it was assumed, by analogy, that the mineral must adopt space group $Pm\bar{3}m$. Synthetic compounds forming solid solutions in the binary system $SrTiO_3$–$NaNdTi_2O_6$ with >90 wt.% $SrTiO_3$ have cubic $Pm\bar{3}m$ structures (Ranjan *et al*. 2006; Mitchell and Tavener, unpublished data). Thus, although single-crystal determination of the structure of naturally-occurring pure tausonite has not been undertaken, it can be assumed reasonably that the end-member adopts space group $Pm\bar{3}m$. Stronitum-bearing perovskites exhibiting significant solid solution towards loparite most probably have tetragonal structures (Ranjan *et al*., 2006; Mitchell *et al*., 2000*a*) thus the strontian loparite described by Haggerty and Mariano (1983) as 'cubic Sr-tausonite' (*sic*), probably has an $I4/mcm$ structure (see below).

We recommend that **tausonite** be retained as the name for perovskite-supergroup minerals with the

FIG. 10. Perovskite crystals from the type locality, Akhmatovskaya Kop, in the Kusinskii Massif, Urals (Russia). Photo credit: A. A. Evseev, Fersman Museum, Moscow.

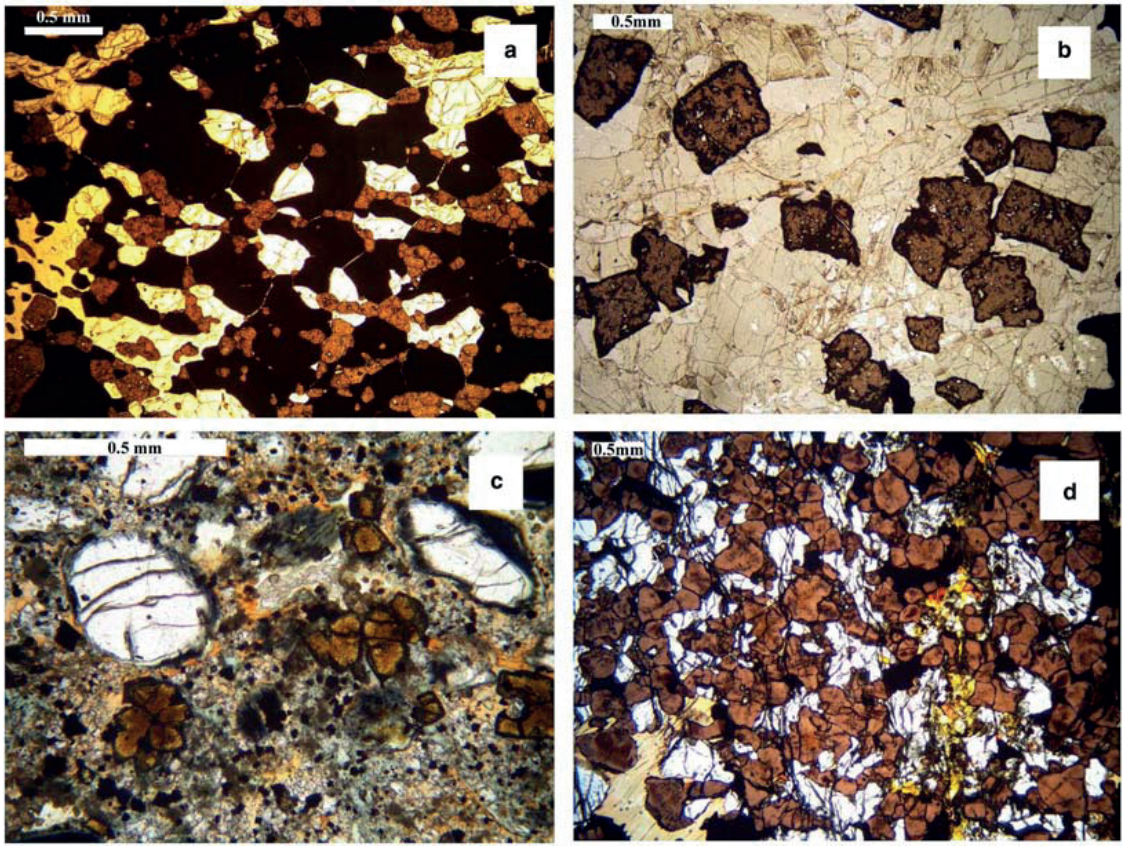

FIG. 11. Plane polarized light images of perovskite in: (*a*) afrikandite, Afrikanda complex, Kola (Russia); (*b*) uncomphagrite, Iron Hill, Colorado (USA); (*c*) kimberlite, Pipe 200, Lesotho; (*d*) perovskite pyroxenite, Tapira complex (Brazil).

general formula (Sr,Ca,*REE*,Na)(Ti,Nb)O_3 and no *A*- or *B*-site cation ordering, whose compositions (following the IMA dominant constituent/valency rules) are such that: (1) divalent cations predominate in the *A*-site with Sr as the dominant constituent; tetravalent cations predominate in the *B*-site with Ti as the dominant constituent. Compositions fall within the tausonite field in the ternary compositional (mol.%) system $SrTiO_3$–$CaTiO_3$ (Fig. 9).

Following IMA nomenclature protocols (Nickel and Grice, 1998; Hatert *et al*., 2013) 'impurity-stabilized' derivatives of tausonite, whose structures are topologically similar to, but depart from that of the cubic end-member, cannot be defined as distinct mineral species. We recommend that their relationship to tausonite be reflected in the root name, rather than an entirely new name to reduce the proliferation of mineral names that has plagued other mineral groups. Thus, the name of the tetragonal Na-*REE*-rich members of the tausonite–loparite series should indicate the true symmetry by means of a hyphenated suffix i.e. tausonite-*I*4/*mcm*. Although these minerals, following the recommendations of Nickel and Grice (1998), could be referred to as 'tausonite-Q', we consider this symbolism not to be informative, or useful, especially if the true symmetry has been determined.

Perovskite ($CaTiO_3$)

Perovskite (*sensu stricto*), was initially described by Rose (1839) in calc-silicate contact metamorphic rocks in the Ural Mountains, Russia (Fig. 10). Perovskite is a characteristic minor-to-accessory mineral in a wide variety of undersaturated alkaline rocks ranging from kimberlite through melilitolites to carbonatites (Fig. 11). Investigations of the crystal structure have been hampered by the ubiquitous twinning, and initially the mineral was considered to be: orthorhombic (Bowman, 1908);

cubic (Barth, 1925); monoclinic $P2_1/m$ (Náray-Szabó, 1943); orthorhombic or monoclinic (Megaw, 1946). Kay and Bailey (1957) recognized that the powder XRD patterns of synthetic and natural $CaTiO_3$ were identical and suggested by analogy that the mineral adopts the orthorhombic space group *Pcmn*; a non-standard setting of space group *Pnma* (#62).

The determination of the room-temperature crystal structure of natural near end-member $CaTiO_3$ perovskite by single-crystal methods was not undertaken until that of Beran *et al*. (1996) on twin-poor crystals from the Benitoite Gem mine (San Benito, California), followed by that of Arakcheeva *et al*.,(1997) using material from near the type locality (Akhmatovskaya Kop) in the Kusinskii Massif, Urals (Russia). These studies demonstrated conclusively that $CaTiO_3$ perovskite adopts the space group #62, with the structural data reported in the *Pnma* setting. However, the structure is now commonly described in terms of the *Pbnm* setting (Fig. 12; Glazer tilt system $a^-a^-c^+$), and considered to represent the $GdFeO_3$ structure type following the work of Geller (1956) and Sasaki *et al*. (1987).

We recommend that **perovskite** be retained as the name for a mineral in the perovskite supergroup with the general formula (Ca,*REE*,Na)(Ti,Nb)O_3 and no *A*- or *B*-site cation ordering, whose compositions are such that: (1) divalent cations predominate in the *A* site with Ca as the dominant constituent; (2) tetravalent cations predominate in the *B* site with Ti as the dominant constituent. Perovskite compositions fall within the perovskite field in the ternary compositional (mol.%) systems $NaNbO_3$–Na*REE*Ti_2O_6–$CaTiO_3$ (Fig. 13) and $SrTiO_3$–Na*REE*Ti_2O_6–$CaTiO_3$ (Fig. 9).

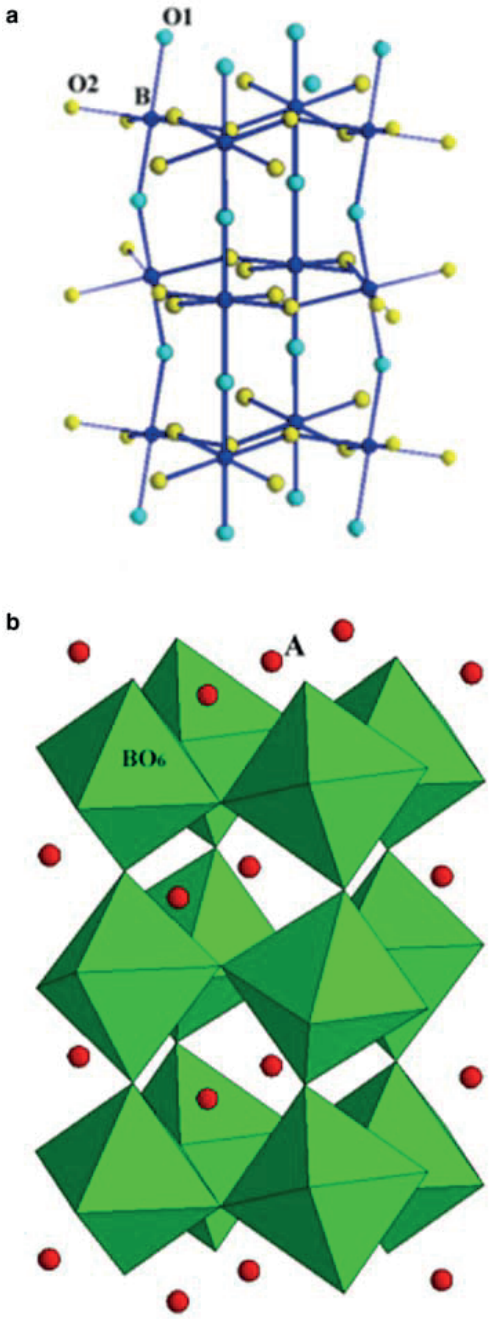

FIG. 12. Structure of $CaTiO_3$ and other ABX_3 stoichiometric oxide, silicate and fluoride perovskites adopting the $GdFeO_3$ structure with space group *Pbnm*. (*a*) Coordination of the BO_6 octahedra; (*b*) polyhedral model showing the location of the *A*-site cations relative to the BO_6 octahedra.

Loparite (Na,REE,Sr,Ca)(Ti,Nb)$_2O_6$

Loparite was the second oxide perovskite-structured mineral to be recognized and was described briefly from nepheline syenite of the Lovozero peralkaline complex (Kola Peninsula, Russia) as 'Mineral no.1' by Ramsay and Hackman (1894). Subsequently, the mineral was misinterpreted as being perovskite by Ramsay (1897). The first complete description of loparite as a member of the perovskite group was by Kuznetsov (1925) using material from a nepheline syenite pegmatite in the adjacent Khibiny alkaline complex (Fig. 14). The mineral is typically complexly-twinned both macroscopically and at the resolution of the transmission electron microscope (Hu *et al*., 1992). Loparite is, incorrectly, described in most glossaries of mineralogy as possessing cubic or pseudocubic symmetry. Loparite occurs principally

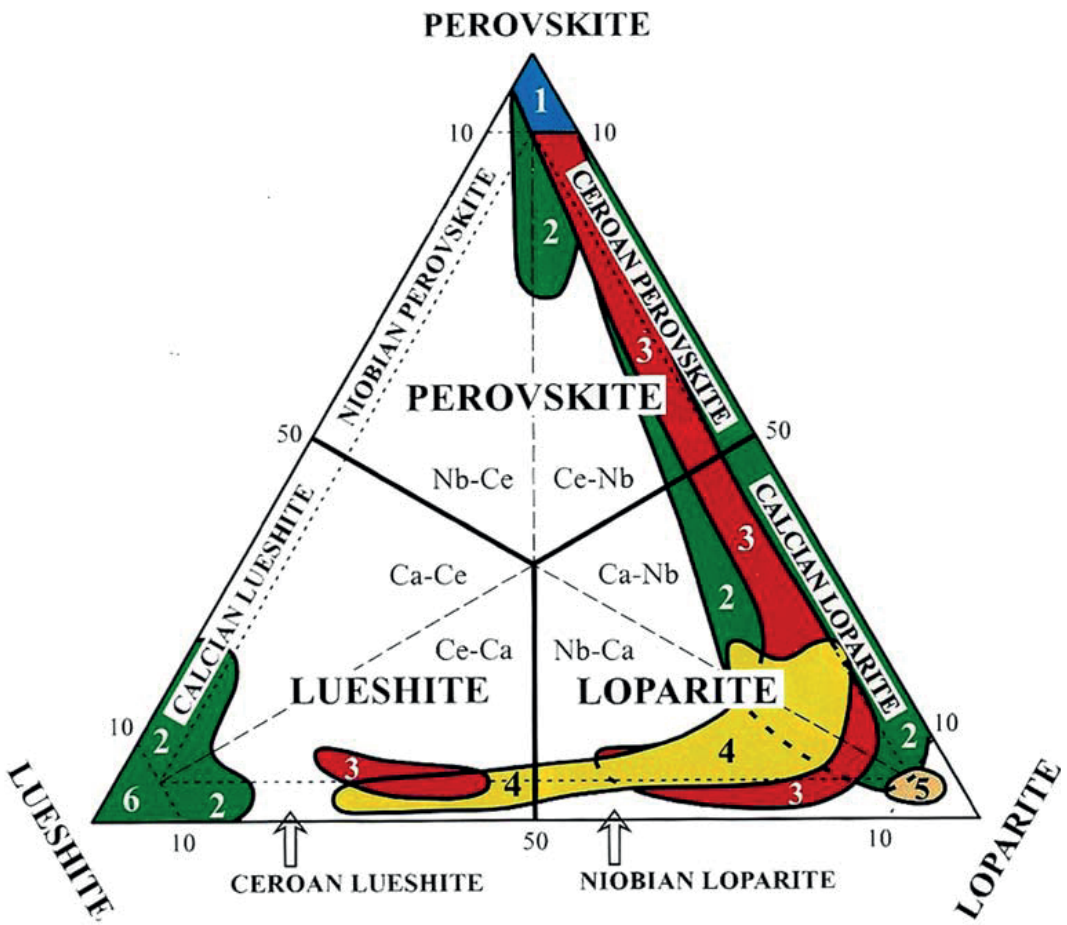

FIG. 13. Compositional variation (mol.%) of perovskite-group minerals from: (1) kimberlites; (2) alkaline ultramafic rocks and carbonatites; (3) Khibina nepheline syenites and ijolites; (4) Lovozero nepheline syenites and urtites; (5) Burpala albitites and aegirinites; (6) Lueshe carbonatite, depicted in the ternary system $NaNbO_3$–$NaCeTi_2O_6$–$CaTiO_3$ (lueshite–loparite–perovskite) (after Mitchell, 2002). Note subdivisions of the compositional fields are used for the complete description of diverse compositions of these perovskite-supergroup minerals (Mitchell and Valdykin, 1993; Mitchell, 2002).

in peralkaline nepheline syenites and carbonatites (Mitchell, 2002)

Importantly, none of the loparite samples analysed show the predominance of *REE* among the large cations present (Mitchell and Chakhmouradian, 1996, 1998; Chakhmouradian and Mitchell, 1997, 2002). As a consequence of the presence of Nb (±Ta) in this mineral, which requires the incorporation of monovalent cations for charge compensation, Na is invariably the predominant *A*-site cation in loparite, including material from the type locality (Chakhmouradian and Mitchell, 1997), and in samples investigated by X-ray diffraction from three different localities by Mitchell *et al*. (2000*b*). Given the disordered distribution of cations in the structure of this mineral (see below), the use of Levinson modifiers [e.g. loparite-(Ce)] to indicate the dominant *REE* species is clearly unwarranted. The ubiquitous presence of Nb, which can be assigned to the $NaNbO_3$ end-member, in natural loparite explains the predominance of Na over *REE* in its composition. The only exception is metamict loparite which has been affected to variable degrees by cation leaching. This primarily affects Na and produces a Na-deficient phase (or phases) of uncertain status, referred to in the literature as 'metaloparite' (Chakhmouradian *et al*., 1999).

Loparite (*sensu lato*) exhibits a very wide range in composition and is typically a quaternary solid solution. The space group adopted by any particular example is determined by whether the solid

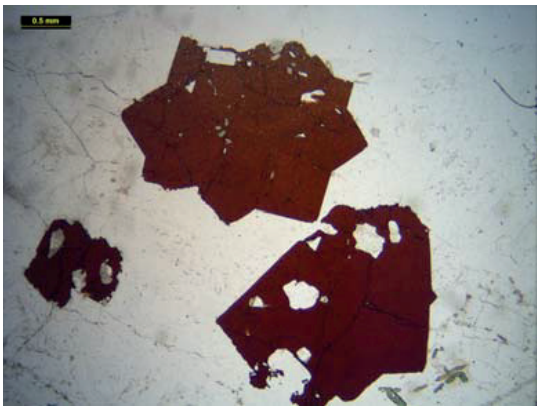

FIG. 14. Plane polarized light image of twinned loparite crystals from the type locality, the Khibiny peralkaline complex, Kola (Russia).

solution present is towards lueshite ($NaNbO_3$), tausonite ($SrTiO_3$) or perovskite ($CaTiO_3$). Very few single-crystal determinations of the structure of loparite have been undertaken, although the structures of synthetic analogues have been well-characterized by Rietveld methods. Mitchell *et al*. (2000*b*) determined the structures of three compositionally-distinct crystals by single-crystal methods and showed that depending on composition, loparite can adopt space groups *Pbnm* (#62) or *I*4/*mcm* (#140).

Stronium-poor niobian calcian loparite (mol.%: 3.4–3.5 $SrTiO_3$; 9.0–9.3 $CaTiO_3$; 24.0–25.4 $NaNbO_3$; 57.0–61.4 $Na_{0.5}REE_{0.5}TiO_3$: Mitchell *et al*., 2000*b*) similar in composition to the holotype material from Khibiny has a similar structure to *Pbnm* $CaTiO_3$, but with a smaller octahedron tilt angle resulting from the presence of the significant amounts of the large, relative to Ca, *A*-site disordered cations. This loparite is close to being metrically tetragonal as $a > b$, suggesting that a slight increase in Na or Sr content would result in adoption of the *I*4/*mcm* space group. Studies of synthetic $NaREETi_2O_6$ compounds containing individual *REE* (Shan *et al*., 1998; Sun *et al*., 1997; Chakhmouradian *et al*., 1999) have shown that, with the exception of $NaLaTi_2O_6$, all adopt the *Pbnm* $GdFeO_3$ structure. Depending upon the synthesis method $NaLaTi_2O_6$ can be rhombohedral $R\bar{3}c$ (Mitchell *et al*., 2000*a*), tetragonal *I*4/*mcm* (Feng *et al*., 2016) or orthorhombic *Pbnm* (Sun *et al*., 1997). Mitchell and Liferovich (2005) determined that light-*REE*-rich synthetic perovskites in the system $Na_{0.75}REE_{0.25}Ti_{0.5}Nb_{0.5}O_3$, apart from the La compound, adopt space group *Pbnm*. Chakhmouradian *et al*. (1999) considered that loparite from the Burpala complex (*c*. 81 mol.% $NaREETi_2O_6$) probably adopts the same structure, as determined by Rietveld methods, as the synthetic *Pbnm* compound $NaCeTi_2O_6$. Thus, given that the *REE* content of the majority of analysed loparite is dominated by Ce it is considered that the structures of synthetic *Pbnm* $NaCeTi_2O_6$ and Khibiny loparite as determined by single-crystal methods (Mitchell *et al*., 2000*b*) best reflects that of the natural material approaching the end-member composition.

Mitchell *et al*. (2000*b*) have determined by single-crystal methods that both calcian niobian loparite (mol.%: 4.3–4.8 $SrTiO_3$; 12.6–13.9 $CaTiO_3$; 10.7–15.7 $NaNbO_3$; 60.6–69.4 $Na_{0.5}REE_{0.5}TiO_3$) and strontian calcian loparite (mol.%: 7.2–8.2 $CaTiO_3$; 5.2–5.8 $NaNbO_3$; 27.1–32.0 $SrTiO_3$; 48.7–52.1 $Na_{0.5}REE_{0.5}TiO_3$) adopt the space group *I*4/*mcm* as a consequence of compositionally-driven space group changes in the quaternary solid solution series loparite–lueshite–tausonite–perovskite (Mitchell *et al*., 2000*b*). Thus, in common with tausonite (see above), without both structural and compositional data it is not possible to describe completely any particular loparite. Accordingly, we consider it is possible to recognize both *Pbnm* and *I*4/*mcm* varieties of loparite *sensu lato*.

We recommend that **loparite** be retained as the name for the mineral in the perovskite subgroup with the general formula (Na,*REE*,Ca,Sr,Th)(Ti,Nb)O_3 and no *A*- or *B*-site cation ordering, whose compositions are such that: (1) monovalent cations predominate in the *A*-site with Na as the dominant constituent; (2) tetravalent cations predominate in the *B*-site with Ti as the dominant constituent. Compositions fall within the loparite field in the ternary systems (mol.%) $SrTiO_3$–$NaREETi_2O_6$–$CaTiO_3$ (Fig. 9) or $NaNbO_3$–$NaREETi_2O_6$–$CaTiO_3$ (Fig 13). Specific structural varieties can be named as loparite-*Pbnm* or loparite-*I*4/*mcm*, etc. if their crystal structures have been determined by either Rietveld or single-crystal methods.

For the reasons discussed above, the Levinson modifier, loparite-(Ce), as previously used in descriptions of loparite should be discontinued. The hypothetical end-member loparite (*sensu stricto*) can be defined as *Pbnm* $NaREETi_2O_6$ for the purposes of calculation of end-member molecules from the compositions of natural loparite (*sensu lato*), where *REE* is the sum of the rare-earth elements present (atoms per formula unit, apfu) combined with an equivalent amount of Na (apfu). Any remaining Na is assigned with Nb to lueshite as $NaNbO_3$.

PEROVSKITE SUPERGROUP

Lueshite (Na,REE)(Nb,Ti)O_3

Lueshite (Fig. 15) was originally described by Safianikoff (1959) from the Lueshe carbonatite complex (North Kivu, Democratic Republic of the Congo). Simultaneously, Danø and Sørenson (1959) described a mineral of similar composition in agpaitic nepheline syenite from the Ilímaussaq complex (Greenland). This mineral was provisionally termed 'igdloite'. Because this mineral was inadequately characterized with respect to its composition and properties, the name was abandoned in favour of lueshite in the revision of perovskite-group nomenclature by Nickel and McAdam (1963).

Safianikoff (1959) noted that the powder XRD pattern of lueshite was 'similar' to that of synthetic $NaNbO_3$ studied by Vousden (1953), who claimed that the room temperature space group was orthorhombic $P22_12$ (#17). Safianikoff (1959) did not determine the actual crystal structure of lueshite and merely assumed this was identical to that determined by Vousden and reported the structure in the conventional setting $P222_1$. This space group has been assigned to lueshite in some glossaries of mineral names (Blackburn and Dennen, 1997). Other glossaries (Anthony *et al*., 1997) following the determination of the crystal structure of synthetic $NaNbO_3$ by Sakowski-Cowley *et al*. (1969) and Hewat (1974) consider by analogy that lueshite adopts space group *Pbma* (*#57*; a non-standard setting of *Pbcm*). Note that the many crystal structures of synthetic $NaNbO_3$ remain under active discussion (Johnson *et al*., 2010; Peel *et al*., 2012; Cheon *et al*., 2015)

No determinations of the actual structure of lueshite were undertaken until those of Mitchell *et al*. (2002; 2014) who showed that the XRD powder patterns of lueshite were not compatible with synthetic $NaNbO_3$ and that the mineral probably adopts the space group *Pbnm* (#62). Single-crystal X-ray determinations of the structure of lueshite from several localities by Mitchell *et al*. (2014) indicated that the mineral might adopt the space group *Pbnm*. However, conventional and time-of-flight powder neutron diffraction methods of structure determination were inconclusive, but indicated that lueshite at room temperature might consist of intergrown pinned metastable domains with orthorhombic (?*Pbnm* + *Cmcm*) and/or monoclinic (?$P2_1/n$) structures. Such structural changes are analogous to those observed for $NaTaO_3$ during cooling which shows phase coexistence of *Pbnm* + *Cmcm* structures at room temperature (Knight and Kennedy, 2015). Arulesan *et al*. (2016*a*,*b*) have demonstrated, using K- and $CaTiO_3$-doped

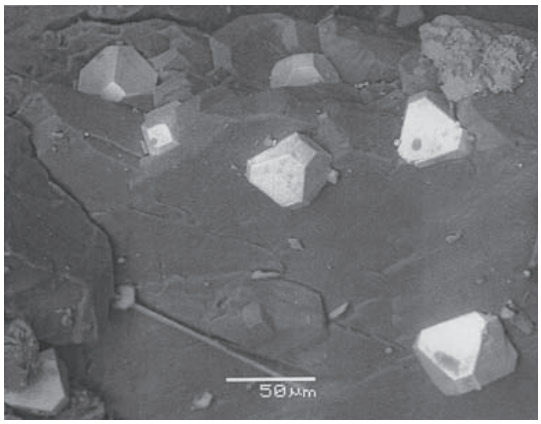

FIG. 15. Scanning electron micrograph of euhedral crystals of lueshite perched on aegirine from the St. Amable sill, Varennes Québec.

$NaTaO_3$, that the phase coexistence is not a function of hysteresis on cooling but is related to compositional heterogeneities or defects stabilizing the *Cmcm* phase. These data could explain why lueshite does not exhibit the same crystal structure as pure $NaNbO_3$. However, recently, we have reassessed the room-temperature structure of lueshite using time-of-flight high-resolution neutron diffraction data and concluded that a phase coexistence model is not appropriate (Mitchell, Kennedy and Knight, unpublished data). Instead we have determined that lueshite at room temperature adopts the space group *Pmmn* [$a = 7.8032(4)$ Å; $b = 7.8193(4)$ Å; $c = 15.6156(9)$ Å], analogous to that of phase S of synthetic $NaNbO_3$ at 480–510°C (Peel *et al*., 2012) with a $2a_p \times 2a_p \times 4a_p$ superlattice This structure cannot be described using the original Glazer tilt scheme as there are compound octahedron tilts along the *c* axis. Peel *et al*. (2012) describe the structure as resulting from combinations of zero (0), in-phase (C) and anti-phase tilts (A) along the *c* axis, with the compound tilt scheme being $a^+b^+c^*$ where *c**, represents a compound tilt system composed of three distinct contributions; ACAC, CCCC; A0C0.

We recommend that **lueshite** be retained as the name for perovskite-group minerals with the general formula (Na,*REE*,Ca)(Nb,Ti)O_3 and no *A*- or *B*-site cation ordering, whose compositions are such that: (1) monovalent cations predominate in the *A*-site with Na as the dominant constituent; (2) pentavalent cations predominate in the *B*-site with Nb as the dominant constituent. Compositions fall within the lueshite field in the ternary compositional system (mol.%) $NaNbO_3$–Na*REE*Ti_2O_6–$CaTiO_3$ (Fig. 13).

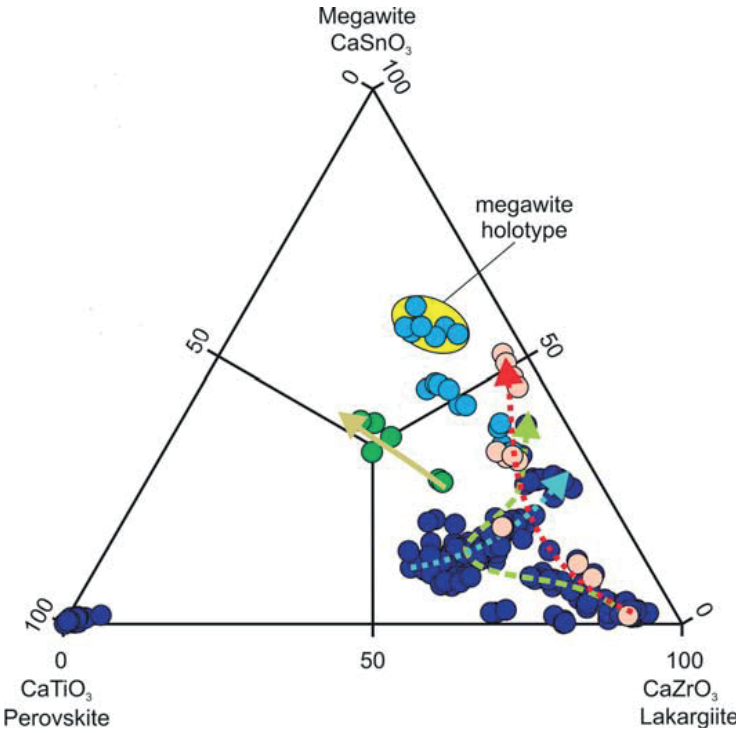

FIG. 16. Composition variation (mol.%) of megawite and lakargiite expressed in the ternary system $CaTiO_3$–$CaZrO_3$–$CaSnO_3$ (perovskite–lakargiite–megawite). Arrows indicate direction of composition change (after Galuskin *et al.*, 2011)

Recently, Menesez Filho *et al.* (2015) have described a polymorph of $NaNbO_3$ with a trigonal structure from the Jacupiranga carbonatite complex (Brazil). The mineral, named pauloabibite, adopts an ilmenite-type structure and is thus not a member of the perovskite supergroup.

Isolueshite (Na,La,Ce,Ca,Sr)(Nb,Ti,Ta)O_3

Isolueshite is found only in a hydrothermally-altered pegmatite vein in urtite-ijolite at the Khibiny alkaline complex (Chakhmouradian *et al.*, 1997). Isolueshite exhibits discontinuous compositional zoning with the La/Ce ratio, Nb, Th, Sr and Ca contents decreasing from the cores of cubo-dodecahedral crystals to their margin. The mineral in terms of its composition, but not structure, can be regarded as *REE*-rich (La-dominant) lueshite, and is approximately an intermediate member of the solid solution series between $NaNbO_3$ and $Na\mathit{REE}Ti_2O_6$. Isolueshite is not an end-member $NaNbO_3$ composition and is considered by Chakhmouradian *et al.* (1997) not to be a dimorph of lueshite, although the mineral is listed simply as $NaNbO_3$ in the current IMA list of mineral names. Krivovichev *et al.* (2000) have shown by single-crystal diffraction methods that the mineral is cubic $Pm\bar{3}m$ and, unlike other cubic perovskites, is characterized by a disordered arrangement of the oxygen atoms in the 12 *h* site. The *A*-site is cation deficient (0.05–0.07 apfu) and the presence of hydroxyl groups (0.1 apfu) replacing oxygen was confirmed by infrared spectrometry.

The status of isolueshite as a distinct mineral species rather than a higher-symmetry variety of lueshite is perhaps ambiguous. However, isolueshite is topologically distinct from lueshite in that the oxygen atoms are disordered (Krivovichev *et al.*, 2000), thus justifying a different root name (Nickel and Grice, 1998). Applying the dominant constituent rule, Na and Nb are the dominant cations in the *A*- and *B*-sites with *REE* occurring as subordinate *A*-site constituents. As **isolueshite** is an IMA approved mineral name we recommend retention of this name.

Lakargiite ($CaZrO_3$)

Lakargiite occurs in high-temperature skarns in calc-silicate rocks found as xenoliths in ignimbrites of the Upper-Chegem volcanic structure, North

Caucasus (Galuskin *et al*., 2008). Lakargiite is a member of the ternary solid solution series $CaZrO_3$–$CaTiO_3$–$CaSnO_3$. The maximum content of the $CaZrO_3$ component reaches 93 mol.%, whereas the minimum content is *c.* 50 mol.% (Fig. 16), with the remainder consisting of $CaTiO_3$, $CaSnO_3$, and in some examples, minor $Ca_2(Fe^{3+}Nb)O_6$. Galuskin *et al*. (2008) were unable to obtain structural data using single-crystal methods because of the complex twinning of all crystals examined. However, powder X-ray diffraction patterns could be refined by Rietveld methods in space group *Pbnm* in accord with the space group of synthetic $CaZrO_3$ (Koopmans *et al*., 1983). Note that all end-members of the ternary system $CaZrO_3$–$CaTiO_3$–$CaSnO_3$ (Fig. 15) are *Pbnm* $GdFeO_3$-structured compounds, thus it is reasonable to assume that all samples of lagarkiite are orthorhombic *Pbnm* minerals. Lakargiite has also been found as sub-micrometre crystals in a carbonaceous chondritic meteorite (Ma, 2011).

We recommend that **lakargiite** be retained as the name for perovskite-group minerals with the general formula $(Ca)(Zr,Sn,Ti)O_3$ and no *A*- or *B*-site cation ordering, whose compositions are such that: (1) divalent cations predominate in the *A*-site with Ca as the dominant constituent; (2) tetravalent cations predominate in the *B*-site with Zr as the dominant constituent. Compositions fall within the lakargiite field in the ternary compositional (mol.%) system $CaZrO_3$–$CaTiO_3$–$CaSnO_3$ (Fig. 16).

Megawite ($CaSnO_3$)

Megawite occurs in high-temperature skarns in calc-silicate rocks found as xenoliths in ignimbrites of the Upper-Chegem volcanic structure, North Caucasus (Galuskin *et al*., 2011). The mineral occurs in the same paragenetic association as lakargiite (see above) and is also a member of the ternary system $CaZrO_3$–$CaTiO_3$–$CaSnO_3$. The $CaSnO_3$ content of the holotype reaches 61 mol.%, and the mineral represents the limit of the compositional evolutionary trend of Sn-rich lakargiite (Fig. 16).

All megawite crystals so far found have been too small (<15 μm) for investigation by single-crystal diffraction methods and the structure was determined from electron back-scattered diffraction patterns. These data were compatible with structural data obtained for synthetic $Ca(Sn_{1-x}Zr_x)O_3$ perovskites (Tarrida *et al*., 2009) and indicated that the mineral adopts the orthorhombic space group *Pbnm.*

We recommend that **megawite** be retained as the name for perovskite-group minerals with the general formula $(Ca)(Sn,Zr,Ti)O_3$ and no *A*- or *B*-site cation ordering, whose compositions are such that: (1) divalent cations predominate in the *A*-site with Ca as the dominant constituent; (2) tetravalent cations predominate in the *B*-site with Sn as the dominant constituent. Compositions fall within the lakargiite field in the ternary compositional (mol.%) system $CaZrO_3$–$CaTiO_3$–$CaSnO_3$ (Fig. 16).

Oxide single perovskites with second order Jahn-Teller distortions

Second order Jahn-Teller distortions result from weak covalent bonding and/or lone-pair effects. Compounds having the perovskite structure exhibiting this style of distortion are characterized by displacements of the *A*- and *B*-site cations from the centres of coordination polyhedra with (e.g. $PbHfO_3$) or without (e.g. $PbTiO_3$) octahedron tilting. Megaw (1968, 1973) noted that three styles of Jahn-Teller distortion are possible for perovskite BX_6 polyhedra: (I) along the tetrad axis resulting in a tetragonal unit cell; (II) along a diad giving an orthorhombic unit cell; (III) along a triad giving a rhombohedral unit cell. Macedonite and barioperovskite are examples of types I and II distortion, respectively (see below).

Macedonite ($PbTiO_3$)

Macedonite was initially described from Crni Kamen (or Kara Kamen), near Prilep, south-central Republic of Macedonia (Radusinović and Markov, 1971). The holotype mineral consisted of small (<0.2 mm) crystals in amazonite quartz syenite veins emplaced in pyroxene amphibole schist. Subsequently, macedonite was found as small inclusions (<50 μm) within hematite and ganomalite from Mn-rich skarns at Långban and Jakobsberg, Värmland (Sweden) by Burke and Kieft (1971) and Dunn *et al*. (1985). Macedonite from Crni Kamen is the only natural perovskite mineral known to contain significant amounts of Bi_2O_3 (2.2 wt.%). The crystal structure has not been determined by single crystal or Rietveld methods, but is considered on the basis of the powder X-ray diffraction pattern to be isomorphous with synthetic tetragonal *P*4*mm* $PbTiO_3$ (Nelmes and Kuhs, 1985) and $BaTiO_3$ (Buttner and Maslen, 1992).

Macedonite, if analogous in structure to *P*4 *mm* $PbTiO_3$, is the only known example of a perovskite-group mineral whose structure is determined by

type I second order Jahn-Teller effects from the aristotype. For synthetic *P*4*mm* $PbTiO_3$, the Ti atoms are displaced 0.32 Å along the *c* axis of the TiO_6 polyhedra with the Pb cations displaced in the same sense, but with a different magnitude (0.48 Å), resulting in the adoption of tetragonal symmetry.

We recommend that **macedonite** be retained as the name for naturally-occurring $PbTiO_3$ whose compositions are such that: (1) divalent cations predominate in the *A*-site with Pb as the dominant constituent; (2) tetravalent cations predominate in the *B*-site with Ti as the dominant constituent.

Barioperovskite ($BaTiO_3$)

Barioperovskite occurs as micro-to-nanocrystals in a host of amorphous material within hollow tubular inclusions in benitoite at the Benitoite Gem mine, California (Ma and Rossman, 2008). Although Ma and Rossman (2008) report the presence of 0.89 wt.% SiO_2, this is considered to result from excitation of the host matrix. The crystals found were too small for single-crystal X-ray diffraction studies and the structure was determined from electron back-scattered diffraction patterns as compared to those of synthetic $BaTiO_3$. These patterns gave a best fit with the orthorhombic *Amm*2 structure, which is stable between 183 and 278 K. This orthorhombic polymorph of $BaTiO_3$ is an example of a type II second order Jahn-Teller distortion. Note that synthetic $BaTiO_3$ also adopts a *P*4*mm* structure between 278 and 393 K (Kwei *et al*., 1993) and that the material examined by Ma and Rossman (2008) could have inverted from this tetragonal precursor. Note also that structural studies of $BaTiO_3$ are hampered by the development of metastable monoclinic and rhombohedral domains in tetragonal and orthorhombic crystals (Cao *et al*., 2009; Tsuda *et al*., 2013). The only other report of a natural occurrence of $BaTiO_3$, in the matrix of the Allende meteorite (Tanaka and Okumura, 1977), was not confirmed by Ma and Rossman (2008).

We recommend that **barioperovskite** be retained as the name for naturally-occurring $BaTiO_3$ where the compositions are such that: (1) divalent cations predominate in the *A*-site with Ba as the dominant constituent; (2) tetravalent cations predominate in the *B*-site with Ti as the dominant constituent.

Fluoride single perovskites – neighborite subgroup

The fluoride single perovskites ABF_3 (Table 1; Fig. 6) are the fluoride analogues of the oxide single perovskites. The structures of minerals in this group can be described by the octahedron tilting schemes used for ABO_3 perovskites.

Neighborite ($(Na,K)(Mg,Ba)F_3$)

Neighborite, $NaMgF_3$, was initially described by Chao *et al*. (1961) from a dolomitic shale of the Eocene Green River Formation, South Ouray, Uintah County, Utah, USA. Subsequently, neighborite has been found in a variety of parageneses ranging from biotite albitite through alkaline granites to calcite carbonatites (see Mitchell, 2002). In all of these examples the mineral is essentially pure $NaMgF_3$. Only, the neighborite occurring in the natrocarbonatite lavas erupted by the volcano Oldoinyo Lengai (Tanzania) differs in containing 15.5–16.8 wt.% K and 8.0–15.2 wt.% Ba, thus exhibiting solid solution towards $KMgF_3$ and $KBaF_3$ (Mitchell, 1997).

Chao *et al*. (1961) were unable to determine the crystal structure of neighborite, and on the basis of the similarity of the powder XRD pattern with that of $CaTiO_3$, following Kay and Bailey (1957), assigned it to space group *Pcmn*. As the mineral is effectively pure $NaMgF_3$, and in keeping with the space group settings used for other members of the supergroup, neighborite is best described in the orthorhombic *Pbnm* setting (Zhao, 1998; Chakhmouradian *et al*., 2001).

We recommend that **neighborite** be retained as the name for naturally-occurring (Na,K)(Mg,Ba)F_3, whose compositions are such that: (1) monovalent cations predominate in the *A*-site with Na as the dominant constituent; (2) divalent cations predominate in the *B*-site with Mg as the dominant constituent.

Parascandolaite ($KMgF_3$)

Parascandolaite, $KMgF_3$, occurs as a volcanic sublimate in a fumarole developed on scoria produced by the 1944 eruption of Vesuvius (Demartin *et al*., 2014). Previously, a mineral with the probable composition of $KMgF_3$ had been reported in sublimates from Nyiragongo volcano (Democratic Republic of Congo) by Herman *et al.* (1960), although this was not recognised as a novel mineral species. Parascandolaite, has also been found as nano-inclusions in diamonds from Juina by Kaminsky *et al.* (2016).

Parascandolaite is pure $KMgF_3$, and single-crystal X-ray diffraction studies show conclusively that it adopts the cubic space group $Pm\bar{3}m$, in

common with the synthetic analogue (Zhao, 1998; Chakhmouradian *et al*., 2001).

The material from Oldoinyo Lengai shows that neighborite and parascanodolaite undoubtedly form a continuous solid solution series in agreement with studies of the synthetic system $NaMgF_3$–$KMgF_3$ (Zhao, 1998; Chakhmouradian *et al*., 2001). Note that intermediate members (35–55 mol.% $KMgF_3$) of this solid solution adopt the tetragonal space group *P*4/*mbm* (#127; Glazer tilt $a^oa^oc^+$). Thus, potassian neighborite and sodian parascanodolaite are probably tetragonal minerals. These fluoroperovskites provide a good illustration of how the room temperature structure of single ABX_3 perovskites change as a consequence of compositional changes not involving any variations in intensive parameters.

We recommend that **parascandolaite** be retained as the name for naturally-occurring (K,Na)(Mg,Ba)F_3, whose compositions are such that: (1) monovalent cations predominate in the *A*-site with K as the dominant constituent; (2) divalent cations predominate in the *B*-site with Mg as the dominant constituent

Chloride single perovskite – chlorocalcite subgroup

Chlorocalcite, $KCaCl_3$, was recognized in 1872 as a sublimate in fumaroles from Vesuvius volcano (Palache *et al*., 1951). No single-crystal X-ray diffraction studies of the mineral have apparently been undertaken although synthetic $KCaCl_3$ adopts the space group *Pbnm* (Midorikawa *et al*.,1979).

Stoichiometric double perovskites $A_2BB'X_6$,

Ordered members of the perovskite supergroup (Table 1; Fig. 6) are derivatives of the aristotype $Pm\bar{3}m$ structure formed when either or both of the *A*- and *B*-site cations are replaced by a combination of other cations located at a specific crystallographic site. If these cations are ordered at only one site the compounds are termed double perovskites, whereas if ordering occurs at both sites they are referred to as complex or quadruple perovskites.

The commonest of the *B*-site ordered perovskites have the general formula $A_2BB'X_6$, where *B* and *B*′ are different cations in octahedral coordination situated in crystallographically-distinct sites. The *A*-site ordered double perovskites $AA'BX_6$ and quadruple perovskites $AA'BB'X_6$ have not yet been found as minerals but are well-known as synthetic phases. Skutterudites can be considered as non-stoichiometric *A*-site vacant quadruple perovskites $\square\square BB'X_6$. The quadruple perovskite $KCa(NaXe)O_6$ with Na^+ and Xe^{8+} ordered on *B* and *B*′ sites synthesized by Britvin *et al*. (2015) is possibly important with respect to terrestrial noble gas geochemistry. Britvin *et al*. (2015) have suggested that the observed depletion in Xe in the Earth's atmosphere could result from trapping of Xe in lower mantle perovskites.

Compounds with equal proportions of *B* and *B*′ cations are termed 1:1 *B*-site ordered perovskites. In these, the *B* cations are ordered along $(111)_p$ planes (Fig. 17). Ideally, they exhibit long range order with no mixing of the cations over the two available crystallographic sites. However, site mixing is well-known in synthetic double perovskites and can be quantified by X-ray diffraction by calculation of a long range order parameter (Sleight, 1963; Mitchell, 2002). Such *B*-site mixing is present in vapnikite (see below). If the BO_6 and $B'O_6$ octahedra are not tilted, the compounds adopt the space group $Fm\bar{3}m$ (#225) with a $2a_p$ (~8 Å) unit cell. With octahedron tilting, eleven space groups (Fig. 5) of reduced symmetry are possible (Howard *et al*., 2003). The majority of natural minerals are fluorides of monovalent and trivalent cations with 1:1 *B*-site ordering (i.e. $A_2^+B^+B^{3+}F_6$), although a hydroxy-chloride (diaboleite) and an oxide (vapnikite) have also been recognized.

Double fluoride perovskites – cryolite subgroup

Cryolite (Na_2NaAlF_6)

Cryolite is the commonest mineral of the double fluoride perovskite subgroup. Cryolite was discovered during the latter part of the eighteenth century in pegmatites associated with F-rich albitized riebeckite granites at Ivigtut, West Greenland. The first description by Abilgaard (1799) predates that of $CaTiO_3$-perovskite by Rose (1839), making cryolite the earliest perovskite-supergroup mineral to be recognized. Cryolite occurs in a very wide range of parageneses (see Mitchell, 2002 for a summary).

Initial optical studies (Krenner, 1883; Böggild, 1912) indicating that cryolite adopts monoclinic symmetry were confirmed by Náray-Szabó and Sasvári (1938), who determined the space group to be monoclinic $P2_1/n$ (#14: an unconventional setting of $P2_1/c$). Subsequently, the crystal structure has been confirmed and refined using single-crystal (Hawthorne and Ferguson, 1975) and Rietveld (Ross *et al*., 2003) methods. Thus, cryolite is a 1:1 *B*-site ordered fluoride perovskite characterized by

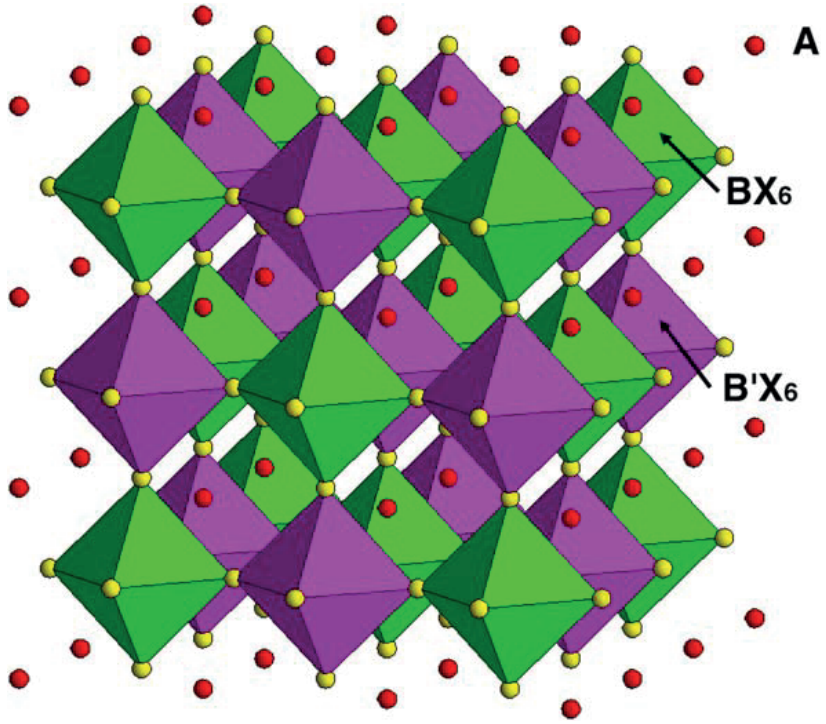

FIG. 17. Ideal 1:1 *B*-site ordering in $Fm\bar{3}m$ $A_2BB'X_6$ double perovskites illustrated by ordering of the BX_6 (green) and $B'X_6$ (purple) octahedra on rock-salt sublattices.

tilting of the NaF_6 and AlF_6 octahedra about three axes ($a^+b^-b^-$). The mineral is typically complexly twinned, possibly as a consequence of inversion from the high temperature $Fm\bar{3}m$ structure, via a first-order phase transition to a monoclinic $C2/m$ (#12; $a^0b^-b^-$) intermediate structure, with the transition from the latter to the room temperature monoclinic $P2_1/n$ structure being a second-order phase transition (Howard *et al*., 2003). Solid solution between cryolite and elpasolite has not been reported.

Elpasolite (K_2NaAlF_6)

Elpasolite, was described initially from quartz riebeckite microcline pegmatites of the Mount Rosa area of the St.Peter's Dome district, El Paso County, Colorado (Cross and Hillebrand, 1885). Subsequently, the mineral has been found in a wide variety of parageneses [see Mitchell (2002) for a summary].

Frondel (1948) on the basis of a powder XRD pattern of the holotype material concluded that elpasolite adopts the space group $Fm\bar{3}m$. Subsequently, Sabelli (1987), using single-crystal diffraction confirmed this hypothesis and determined that the mineral is a 1:1 *B*-site ordered perovskite. The NaF_6 and AlF_6 octahedra are neither tilted nor distorted. The presence of the large K^+ cations in the 12-fold coordinated *A*-site prevents tilting of the BF_6 octahedra.

Simmonsite (Na_2LiF_6)

Simmonsite was described initially from the Zapot pegmatite amazonite-topaz-zinnwaldite pegmatite, Hawthorne, New Mexico (Foord *et al*., 1999). Here the mineral occurs in a late-stage breccia pipe with cryolite, cryolithionite and elpasolite. Simmonsite has been reported, but not described, from the cryolite-bearing Katuginskoye peralkaline granite (Seltman *et al*., 2010), Transbaikalia, Eastern Siberia.

Foord *et al*. (2009) were unable to determine the crystal structure because of the ubiquitous twinning, although suggesting the mineral was monoclinic. Ross *et al*. (2003) have shown that synthetic Na_2LiF_6, in common with cryolite, adopts space group $P2_1/n$ and concluded that the natural material must adopt this space group.

In summary, we recommend retention of the mineral names **elpasolite**, **cryolite** and **simmonsite** and classify them as members of the cryolite

subgroup of 1:1 ordered double fluoride perovskites.

Oxide double perovskites – vapnikite subgroup

Vapnikite (Ca_2CaUO_6)

Although 1:1 *B*-site ordered double perovskites are one of the commonest structural types of synthetic perovskite (Mitchell, 2002), the only *bona fide* naturally-occurring example is vapnikite (Galuskin *et al*., 2014). Other minerals with this structure recognised in the future would be members of a potential vapnikite (or latrappite see below) subgroup. Vapnikite occurs as small (<10 μm) crystals in larnite-bearing pyrometasomatic rocks of the Hatrurim Formation at Jabel Harmun, Israel. Single-crystal structure determination showed that the mineral adopts the monoclinic space group $P2_1/n$ (#14), as a consequence of ordering and tilting of the CaO_6 and UO_6 octahedra. The mineral is the natural analogue of β-$Ca_2CaU^{6+}O_6$, a member of a large group of synthetic U-bearing double perovskites (Knyzazev *et al*., 2011). Numerous compounds with Te^{6+} instead of U^{6+}, including the Te-analogue of vapnikite have also been synthesized (Christy *et al*., 2016). Vapnikite differs from the synthetic compound in having a larger degree of Ca and U disorder at the octahedral sites and minor incorporation of U^{6+} at the *A* site coupled with splitting of the O3 site. The structural formula for vapnikite proposed by Galuskin *et al*. (2014) is $[(Ca_{1.96}U_{0.04})(Ca_{0.92}U_{0.08})(U_{0.83}Ca_{0.17})(O1_2O2_2O3_{1.85}O3A_{0.15}]$. Vapnikite does not exhibit any solid solution with any other elements but is hydrated (1.3–3.4 wt.% H_2O) at the margins of the crystals. We recommend retention of the name **vapinkite** and recognise a vapnikite subgroup, into which other oxide double perovskites could be placed upon their recognition.

Nb- and Fe-rich perovskites – The status of latrappite

The nomenclature of niobium- and iron-rich perovskites has not yet been satisfactorily resolved. In the older literature niobium-rich perovskite was termed 'knopite', 'nioboloparite' or 'dysanalyte'. Nickel and McAdam (1963) recommended that both knopite and dysanalyte be abandoned as these minerals are merely Nb-bearing perovskites and members of the loparite–perovskite solid solution series. However, 'dysanalyte' from the Kaiserstuhl and Oka carbonatite complexes contains significant amounts of Fe^{3+} and in this respect is not similar to other Nb-bearing perovskites (Mitchell *et al*., 1998). Following Bonshtedt-Kupletskaya (1946), Tikhnenkov and Kazakova (1957) recognized that $Ca_2Fe^{3+}NbO_6$ could be a significant, though not dominant component of 'dysanalyte'. This component was not given a specific name. Regardless of Nickel and McAdam's (1963) recommendations the term 'dysanalyte' remains in use as a varietal name for Nb-Fe-rich perovskites. The name nioboloparite was discredited by Mitchell *et al*. (1996) as this mineral was shown to be niobian calcian loparite and/or niobian loparite.

The name 'latrappite' was introduced by Nickel (1964) on the grounds that unlike $CaTiO_3$ perovskite, the Nb content was greater than the Ti content, although the significant Fe^{3+} content was not considered. It is important to note that the material investigated by Nickel (1964) and Nickel and McAdam (1963) is not a potential end-member composition, and is actually a complex quaternary solid solution involving the components $Ca_2Nb_2O_7$, $Ca_2Fe^{3+}NbO_6$, $CaTiO_3$ and $NaNbO_3$ (Fig. 18). The dominant components of this solid solution are $Ca_2Nb_2O_7$ and $Ca_2Fe^{3+}NbO_6$. The latter component was termed 'latrappite' by Mitchell *et al.* (1998) and Mitchell (2002), following Tikhnenkov and Kazakova (1957).

In this work, Na-poor, very Ca-Nb-Fe-rich perovskites are considered as unlikely to be a simple solid solution given that one of the three synthetic polymorphs of $Ca_2Nb_2O_7$ (Scheunemann and Müller-Buschbaum, 1974: Ishizawa *et al*., 1980; Lewandowski, *et al*., 1992; Levin and Bendersky, 1999) is an orthorhombic $Pbn2_1$ layered perovskite (Scheunemann and Müller-Buschbaum, 1974; Levin and Bendersky, 1999) belonging to the $A_nB_nX_{3n+2}$ structural group. The orthorhombic, and monoclinic $Ca_2Nb_2O_7$ compounds, are different in topology from 'true' perovskites in that the *B*-*X*-*B* links are broken and slabs of perovskite-like units are mutually displaced (see below). Note that if the $Ca_2Nb_2O_7$ component of Nb-rich perovskite is considered to have the same structural topology as ABX_3 perovskite it would be required to have *A*- and *B*-site vacancies i.e $(Ca_{1.714}\square_{0.286})(Nb_{1.714}\square_{0.286})O_3$.

Synthetic $Ca_2Fe^{3+}NbO_6$ is a 1:1 *B*-site ordered double perovskite which adopts the monoclinic space group $P2_1/n$ (tilt scheme $a^-a^-c^+$; Chakhmouradian and Mitchell, 1998; Barnes *et al*., 2009). In addition, synthetic $Ca_2Fe^{3+}NbO_6$ has also been shown by Chakhmouradian and

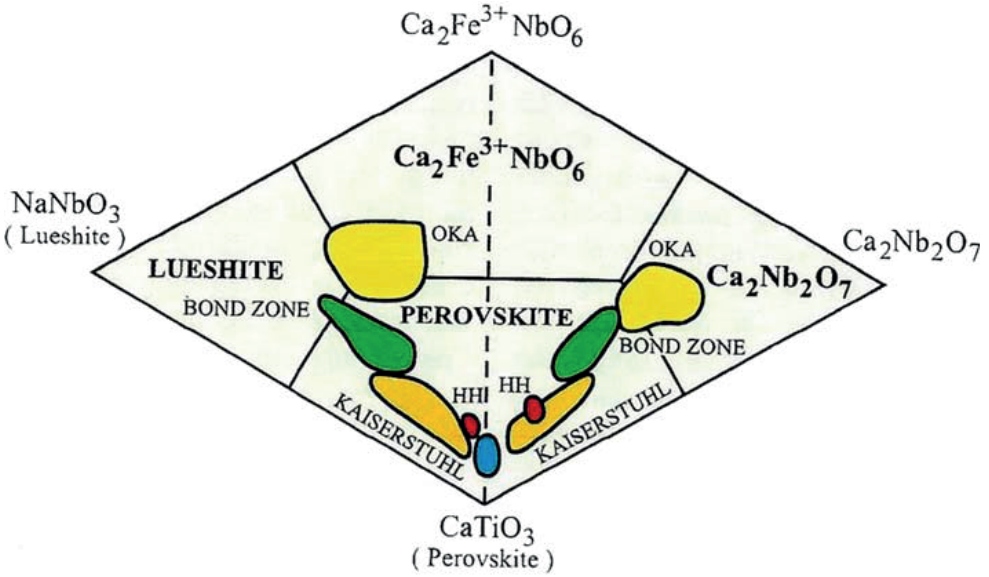

FIG. 18. Compositional variation (mol.%) of Nb-rich perovskites and latrappite from Oka (red, green and yellow fields), Kaiserstuhl (orange field) and Magnet Cove (blue field) carbonatite complexes, depicted in the quaternary system $NaNbO_3$–$CaTiO_3$–$Ca_2Nb_2O_7$–$Ca_2Fe^{3+}NbO_6$ (after Mitchell *et al*., 1998; Mitchell, 2002).

Mitchell (1998) to exhibit *B*-site mixing. Simple continuous solid solutions between these potential end-member compounds is extremely unlikely, except for examples in which $(Nb + Fe^{3+}) < Ti$ (apfu). Note that most natural *Pbnm* $CaTiO_3$ perovskites exhibit very limited substitution of Ti by Fe^{3+} (1–2 wt.% Fe_2O_3) even in Fe-rich parageneses (Mitchell, 2002). Kimura and Muan (1971*a*,*b*) have shown that under strongly reducing conditions in the system CaO–FeO–TiO_2 there is no appreciable solid solution of Fe in $CaTiO_3$, whereas in air, perovskite can contain up to 83 wt.% Fe substituting for Ti. Chakhmouradian and Mitchell (2001) have found some groundmass perovskite in kimberlites to contain up to 8.3 wt.% Fe_2O_3 which is present as an orthoferrite component (6–13 mol.% *REE*FeO_3).

Mitchell *et al*. (1998), on the basis of Rietveld refinement of the laboratory powder X-ray diffraction pattern, claimed that latrappite from Oka is an orthorhombic *Pbnm*-structured mineral. However, Barnes *et al*. (2009) and Lufaso and Woodward (2004) note that neutron and/or synchrotron diffraction methods are required for determination of the correct crystal structure of many single and double perovskites. Thus, it is highly probable that standard powder laboratory X-ray diffraction methods do not have the required resolution to distinguish between the *Pbnm*, $P2_1/n$ and $Pbn2_1$ space groups.

In their structural study of synthetic binary perovskites with compositions $CaTi_{2-x}Fe_xNb_xO_3$ ($0 \le x \le 0.5$), Chakmouradian and Mitchell (1998) found that all had the *Pbnm* structure with complete disorder of Fe^{3+},Ti^{3+} and Nb^{5+} at the *B*-site. Stachowicz, Welch and Mitchell (unpublished data) have determined the crystal structures of eleven natural Nb-rich $(Na, Ca)_2(Fe^{3+},Ti^{3+}, Nb^{5+})_2O_6$ perovskites having $Ca_2Fe^{3+}NbO_6$ (latrappite) contents of 25–62 mol.%, $Na_2Nb_2O_6$ contents of 25–48 mol% and $Ca_2Nb_2O_7$ contents of 8–24 mol.%. There is a clear negative correlation between $Ca_2Nb_2O_7$ and $Ca_2Fe^{3+}NbO_6$ contents. All of these perovskites have the *Pbnm* structure, with Nb^{5+}, Fe^{3+} and Ti^{4+} disordered at the *B*-site. Refinements in space group $P2_1/n$, which allows for ordering at two non-equivalent *B*-sites, indicated almost identical compositions (refined site-scattering values) for these two sites, demonstrating that the disordered *Pbnm* model is correct. No evidence for a 'defect' $Ca_2Nb_2O_7$-type structural component was found, e.g anomalous displacement parameters of oxygen atoms; superlattice reflections violating the *Pbnm* cell. Thus, any $Ca_2Nb_2O_7$ component in these perovskites would appear to be incorporated as a part of the general disorder at the *B*-sites and does not have a distinctive structural signature.

It remains to be shown if latrappites with higher $Ca_2Nb_2O_7$ and Ca_2FeNbO_6 contents can have a structural signature associated with

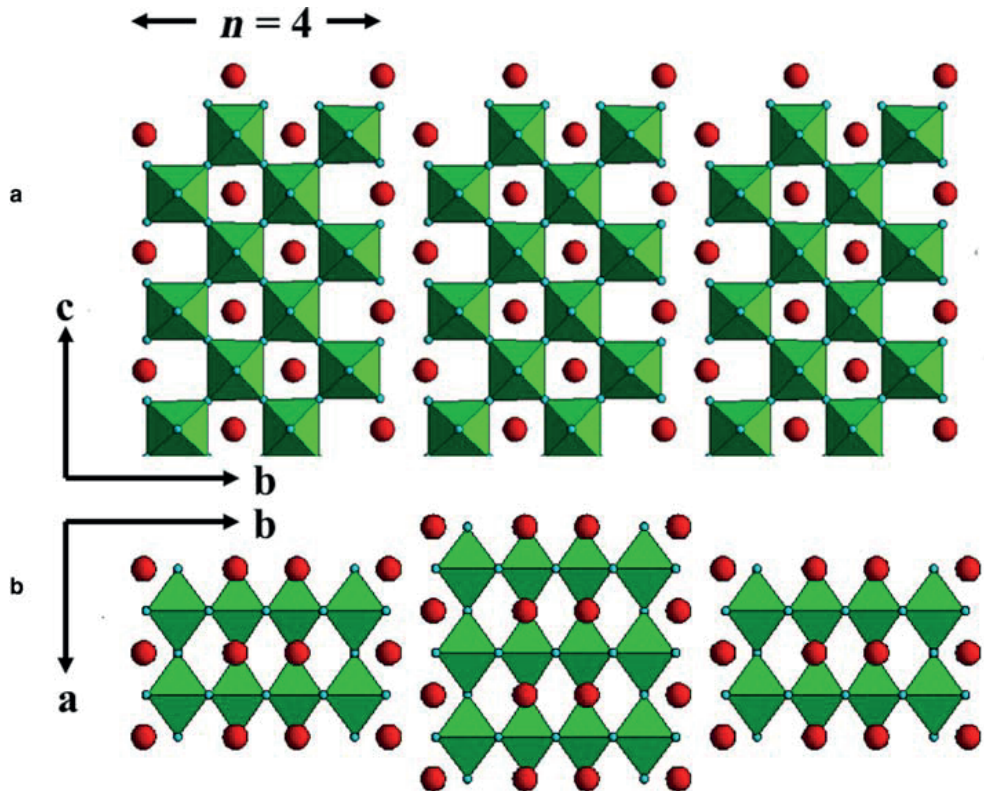

FIG. 19. The crystal structure of orthorhombic $Ca_4Nb_4O_{14}$ (or $Ca_2Nb_2O_7$) the $n = 4$ member of the $A_nB_nX_{3n+2}$ homologous series (Scheunemann and Müller-Buschbaum (1974) showing: (*a*) [100] projection; (*b*) [001] projection (after Mitchell, 2002).

vacancies, ordering, or $Ca_2Nb_2O_7$ polysomatic intergrowths (see below). The compositions of the latrappites chosen for structural studies undertaken so far confirm the dominance of the characteristic Ca_2FeNbO_6 component in solid solutions.

The orthorhombic compound $Ca_2Nb_2O_7$ (actually $Ca_4Nb_4O_{14}$) is the $n = 4$ member of the homologous $A_nB_nX_{3n+2}$ series (Levin and Bendersky, 1999). These compounds consist of perovskite-like slabs containing n layers of BO_6 octahedra (Fig. 19) The perovskite slabs are off-set from each other by crystallographic shear with a translation vector of about $(\sqrt{3}/2)a_p$. In effect extra oxygen is added to the vacancies in the BO_6 lattice created by the crystallographic shear. Of relevance to latrappite is that high resolution transmission electron microscopy (HRTEM) studies have revealed that many synthetic $A_nB_nX_{3n+2}$ compounds are actually composed of ordered intergrowths of different members of a homologous series, i.e. a polysomatic series. Portier *et al*. (1974) initially recognized that the $(NaCa)_nNb_nO_{3n+2}$ or, the $Ca_2Nb_2O_7$–$NaNbO_3$ solid solution series, with $n = 4.5$ were composed of slabs with 4 and 5 layers of octahedra which formed ordered intergrowths in the sequence 5-4-4-5-4-4-5 ($NaCa_{12}Nb_{13}O_{45}$) and 4-5-4-5 ($NaCa_8Nb_9O_{31}$). Other studies (Nanot *et al*., 1975; Williams *et al*., 1993; Levin *et al*., 2000) have reported blocks of 'normal' perovskite interspersed with slabs of layered perovskites. From these studies it is apparent that the homologous series of compounds between $Ca_2Nb_2O_7$ and $NaNbO_3$ (Portier *et al*.,1974) or $Ca_2Nb_2O_7$ and $CaTiO_3$ (Nanot *et al*., 1975) form a polysomatic series rather than atomic solid solutions. As applied to latrappite it is possible that increasing Nb contents are accommodated by the formation of slabs of layered perovskite between blocks of normal perovskite. Mitchell *et al*. (1998) attempted to obtain evidence for this hypothesis from HRTEM lattice images. However, high-resolution images did not reveal any intergrowths for any of the grains examined. Either these samples did not contain sufficient amounts of the $Ca_2Nb_2O_7$

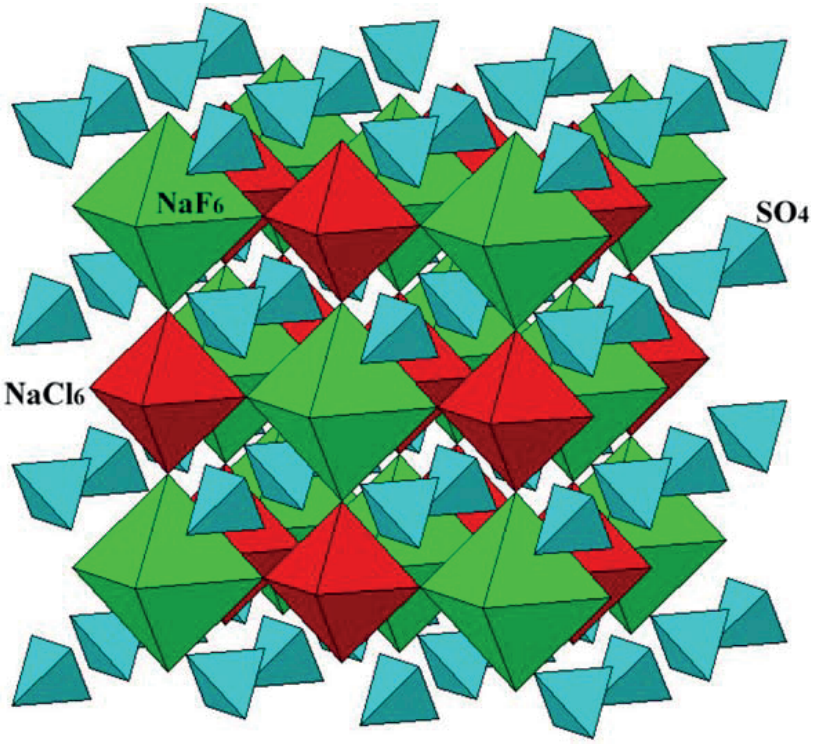

FIG. 20. The crystal structure of sulphohalite.

component to permit formation of discrete polysynthetic intergrowths, or such layers occurred in an orientation that was not visible in this preliminary study. In summary, the mechanism by which Fe^{3+} and Nb^{5+} are accommodated as either $Ca_2Fe^{3+}NbO_6$, $Ca_2Nb_2O_7$ or $Ca(Fe^{3+},Nb)O_3$ with or without lattice vacancies remains elusive. Further study of the crystal structure of $Ca_2Fe^{3+}NbO_6$–$Ca_2Nb_2O_7$-rich latrappite by HRTEM and synchrotron X-ray diffraction is desirable to determine whether cation ordering, cation vacancies, polysomatic intergrowths, or other compositional domains are present or not. The formation of discrete short-range ordered domains with cation vacancies is one possibility.

How is latrappite to be defined if the name is to be retained? The mineral is not merely a Nb-rich *Pbnm* $CaTiO_3$ perovskite and the original definition by Nickel (1964) ignores the Fe^{3+} content. Given the observation that the dominant molecules in very Nb-and Fe^{3+}-rich perovskites appear to be $Ca_2Nb_2O_7$ and $Ca_2Fe^{3+}NbO_6$, we suggest that the potential end-member latrappite be considered as analogous to synthetic 1:1 ordered $Ca_2Fe^{3+}NbO_6$. However, without further crystallographic data, and in order to retain the name latrappite, we recommend that Ca-rich, Nb- and Fe-rich perovskites $[(Ca,Na)_2(Nb,Fe^{3+},Ti)_2O_6]$ whose compositions are such that: (1) divalent cations prevail in the *A*-site with Ca dominant; and (2) pentavalent cations prevail in the *B*-site(s) with Nb dominant be termed **latrappite**. Compositions (mol.%) plotting within the $Ca_2Fe^{3+}NbO_6$ and $Ca_2Nb_2O_7$ fields in the quaternary compositional system $Ca_2Nb_2O_7$–$CaTiO_3$–$Ca_2Fe^{3+}NbO_6$–$NaNbO_3$ (Fig.18) can be termed **latrappite**. Note: $Ca_2Nb_2O_7$ is another potential naturally-occurring perovskite supergroup end-member composition for which a name would be desirable.

Double antiperovskite group $B_2XX'A_6$

Sulphohalite subgroup

Sulphohalite, $Na_6FCl(SO_4)_2$, was originally described from the Searles Lake (California) inter-montane evaporate deposits by Hidden and MacKintosh (1888), and its cubic structure determined by Pabst (1934). Sulphohalite has recently been identified by Kaldos *et al.* (2015) in carbonate-rich melt inclusions in jacupirangite from Kerimasi volcano (Tanzania). Krivovichev

(2008) has recognized that sulphohalite is an ordered double antiperovskite with the anti-elpasolite structure and the space group $Fm\bar{3}m$. Double antiperovskites have the general formula $B_2X\,X'A_6$ (Mitchell, 2002, Krivovichev, 2008). In sulphohalite the structure consists of a framework of alternating anion-centred [FNa_6] and [$ClNa_6$] octahedra with tetrahedral $(SO)_4$ units occupying the cavities in this framework (Fig. 20) We consider that **sulphohalite** is a member of the perovskite supergroup and recommend retention of the name.

Non-stoichiometric perovskites

Here we define 'non-stoichiometric' specifically in relation to the stoichiometry of ABX_3 perovskites in which all sites (cation and anion) are fully occupied, i.e. a non-stoichiometric perovskite has partial occupancy of cation (*A*,*B*) and/or anion (*X*) sites. Such perovskites (Tables 2 and 3; Fig. 7) include: (1) *A*-site vacant double hydroxides, or hydroxide perovskites, belonging to the söhngeite, schoenfliesite and stottite subgroups; (2) Anion-deficient perovskites of the brownmillerite subgroup (brownmillerite; srebrodolskite, shulamitite); (3) *A*-site vacant quadruple perovskites (skutterudite subgroup); (4) *B*-site vacant single perovskites (oskarssonite subgroup); (5) *B*-site vacant inverse single perovskites (cohenite and auricupride subgroups); (6) *B*-site vacant double perovskites (diaboleite subgroup); (7) Anion-deficient partly-inverse quadruple perovskites (hematophanite subgroup).

A-site vacant hydroxide perovskites

Natural and synthetic examples of both single and double perovskites are known for hydroxides lacking lacking *A*-cations and having the general stoichiometry $\square_2(BB')(OH)_6$. The octahedral framework sites can accommodate homovalent and heterovalent cations. The primary distinction made in this classification of hydroxide perovskites is between those with one or two different cations in their end-member formula. Following our hierarchical classification (Table 2; Fig. 7) we refer to these fundamentally different types as 'single' and 'double' hydroxide perovskites.

Paragenesis and current nomenclature

Detailed descriptions of the compositional variation and parageneses of hydroxide perovskite minerals can be found in Mitchell (2002). The currently IMA-approved nomenclature together with our hierarchical classification of these minerals is given in Table 2. Note that some of the components reported in published analyses may reflect the presence of impurities.

Hydroxide perovskites form as rare secondary minerals resulting from the alteration of primary minerals, especially zinc and tin-bearing minerals, in a very wide range of parageneses. The formation conditions (Eh, pH, f_{O_2} etc) of the hydroxide perovskites have not been determined, although the environment can range from sub-areal supergene to marine sub-aqueous.

Hydroxide perovskite aristotypes

The aristotype of single hydroxide perovskites (Fig. 21), as represented by synthetic $In(OH)_3$ (Mullica *et al*., 1979) and $Sc(OH)_3$ (Schubert and Seitz, 1948) has space group $Im\bar{3}$ (#204) and tilt system ($a^+a^+a^+$). The structure of natural $In(OH)_3$, the mineral dzhalindite, is unknown, but assumed to be $Im\bar{3}$ as powder XRD data indicate a cubic unit cell.

In double hydroxide perovskites (Fig. 22), the ordering of the *B* and *B*′ cations leads to the loss of *I*-centring and the aristotype has space group $Pn\bar{3}$ (#201), but with the same tilt system $a^+a^+a^+$. Numerous natural stannate hydroxide perovskites have this space group, including: schoenfliesite $MgSn(OH)_6$; wickmanite $MnSn(OH)_6$; and natanite $FeSn(OH)_6$.

Topological constraints on space groups

The presence of an O–H bond forces the *B*–O–*B*′ linkages to be non-linear, resulting in highly-tilted octahedra and rendering impossible the aristotypic tilt system $a^0a^0a^0$ (space group $Pm\bar{3}m$) of hydroxide perovskites. Hence, no hydroxide perovskite has a zero tilt. Furthermore, mirror symmetry is only possible for single hydroxide perovskites, such as söhngeite $Ga(OH)_3$ ($P4_2/nmc$, #137; or $P4_2/n$, #86) and $In(OH)_3$ ($Im\bar{3}$, #204), as the mirror planes pass through the oxygen atoms between octahedra. In contrast, while it is theoretically possible for double perovskites to have mirror planes, these must bisect octahedra and the resulting structures have gross distortions due to size mismatch between cations, as seen in the previously reported structures of natanite $FeSn(OH)_6$ ($Pn\bar{3}m$; Strunz and Contag, 1960) and

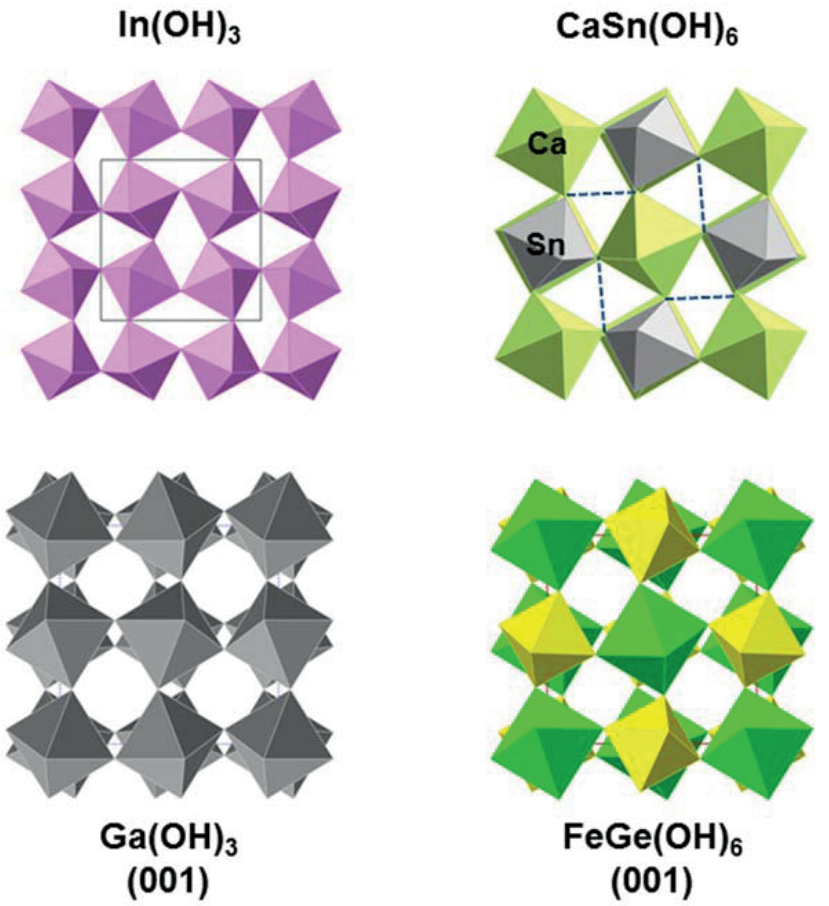

FIG. 21. Examples of framework motifs of single and double hydroxide perovskites. $In(OH)_3$, a single hydroxide perovskite, is cubic $Im\bar{3}$ with a single *In* site. Burtite $CaSn(OH)_6$, a double perovskite, is cubic $Pn\bar{3}$ with single *Ca* and *Sn* sites. The cubic phases have tilts of $a^+a^+a^+$. Söhngeite $Ga(OH)_3$, a single hydroxide perovskite, is tetragonal $P4_2/nmc$ ($a^+a^+c^-$). Four O–(H)···O bridges across the shorter O···O distances (2.8 and 3.0 Å) are shown for the $CaSn(OH)_6$ structure.

$CuSn(OH)_5$ ($P4_2/nnm$, Morganstern-Badarau, 1976) which are clearly incorrect.

Figure 22 shows the hydrogen-bonded arrangement of burtite $CaSn(OH)_6$ ($Pn\bar{3}$; #201) in which an isolated ring of four O–H···O linkages occurs. There are two non-equivalent H atoms, H(1) and H(2), each half-occupied. This isolated ring configuration is characteristic of all cubic hydroxide perovskites. The H(1)···H(1) and H(2)···H(2) distances are ~1 and ~1.4 Å (Basciano *et al.*, 1998). Thus, in the cubic structures ($Pn\bar{3}$ and $Im\bar{3}$) each oxygen atom is both a donor and an acceptor. The two local ring configurations are also shown in Fig. 21. Isolated rings also occur in combination with other O–H···O configurations in some non-cubic space groups. The dual donor-acceptor role of oxygen is a characteristic feature of hydroxide perovskites.

Single hydroxide perovskites

Three natural homovalent, or single, hydroxide perovskites have been found: bernalite [$Fe(OH)_3$] (Birch *et al.*, 1993; Welch *et al.*, 2005); dzhalindite [$In(OH)_3$] (Mullica *et al.*, 1979; Genkin and Mura'eva, 1964); and söhngeite [$Ga(OH)_3$] (Scott, 1971). In addition, a synthetic single hydroxide perovskite, δ-$Al(OD)_3$ (Matsui *et al.*, 2011), has been synthesized which is orthorhombic with space group $P2_12_12_1$ (tilt system $a^-a^-c^+$). Dzhalindite is the only single hydroxide perovskite having a cubic structure (space group $Im\bar{3}$) at ambient conditions.

A definitive structure for bernalite has yet to be reported. Originally, the structure of bernalite was determined in space group *Immm* (#71; tilt scheme $a^+b^+c^+$) by Birch *et al.* (1993). Subsequently, space

group *Pmmn* (#71; tilt scheme $a^+b^+c^-$) was proposed by McCammon *et al*. (1995) and Welch *et al*. (2005), as numerous strong reflections violating *I*-centring were observed.

The original reported structure of söhngeite, $Ga(OH)_3$, from Tsumeb (Scott, 1971) was orthorhombic with the non-centrosymmetric space group $Pmn2_1$ (#31; tilt scheme $a^-b^-c^+$). A recent structure determination of söhngeite using single-crystal XRD (Welch and Kleppe, 2016) found that it adopts either space group $P4_2/nmc$ (#137) or $P4_2/n$ (#86) with a very different tilt system ($a^+a^+c^-$), and on heating to 423 K transforms to an $Im\bar{3}$ structure ($a^+a^+a^+$).

Double hydroxide perovskites

All heterovalent double hydroxide perovskites $\square_2BB'(OH)_6$ have ordered frameworks in which different cations alternate on crystallographically non-equivalent *B*-sites e.g. schoenfliesite [$MgSn(OH)_6$]; burtite [$CaSn(OH)_6$]; stottite [$FeGe(OH)_6$]; and mopungite $NaSb(OH)_6$. Complete ordering of heterovalent cations in double hydroxide perovskites is required to satisfy bond-valence constraints of bridging O atoms, each of which is bonded to an H atom as OH. Disorder in heterovalent structures is prohibited by under- or over-bonding of these O atoms, e.g. Mg–O–Mg + O–H = 1.67 valence units (vu), Sn–O(H)–Sn + O–H = 2.33 vu, compared with Mg–O–Sn + O–H = 0.33 + 0.67 + 1 = 2 vu. The motifs of burtite and stottite are shown in Fig. 21.

Most double hydroxide perovskites reported to date are stannates and, with the exception of tetrawickmanite $MnSn(OH)_6$ and synthetic $CuSn(OH)_6$, are cubic (reported space groups $Pn\bar{3}$ or $Pn\bar{3}m$). Of the non-stannates, stottite $FeGe(OH)_6$ (Strunz *et al*., 1958; Strunz and Giglio, 1961; Ross II *et al*., 1988) and mopungite $NaSb(OH)_6$ (Williams, 1985) are reported as tetragonal with space group $P4_2/n$ (#86). $CuSn(OH)_6$ was reported as having space group $P4_2/nnm$ (Morgenstern-Badarau, 1976), but this is almost certainly incorrect as the mirror planes of this structure bisect octahedra (see above).

Jeanbandyite $Fe^{3+}Sn(OH)_5O$

Kampf (1982) refined unit-cell parameters of type jeanbandyite from Llallagua, Bolivia, from powder X-ray diffraction data as $a = c = 7.648(7)$ Å, recognizing that while this cell is metrically cubic, the mineral is optically uniaxial and, therefore, probably

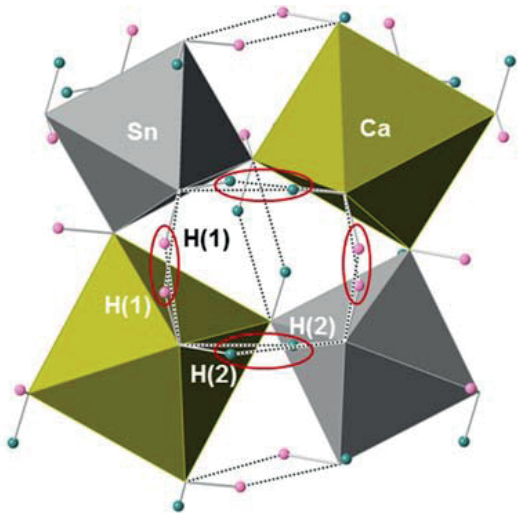

FIG. 22. The hydrogen-bonding topology of burtite, $CaSn(OH)_6$. The isolated ring comprises four O–H···O bridges, having O···O distances of 2.8 and 3.0 Å. H···H distances are indicated. Isolated four-membered rings are characteristic of all cubic hydroxide perovskites. The lower diagrams illustrate the two local ring configurations of cubic hydroxide perovskites that are averaged in the cubic space groups $Pn\bar{3}$ and $Im\bar{3}$ which require ½ occupancy of each H site in the average structures.

tetragonal. The identification of jeanbandyite as a hydroxide perovskite was based upon the similarity of its unit-cell parameters, powder diffraction pattern and general stoichiometry to stottite-group minerals. The empirical formula of jeanbandyite from the type locality Llallagua, Bolivia, originally reported by Kampf (1982) is $(Fe^{3+}_{0.71}Mn^{2+}_{0.21}Mg_{0.04})(Sn^{4+}_{0.84}Si_{0.03})(OH)_6$, which is not charge-balanced (an excess charge of +0.11), but was preferred over a charge-balanced formula requiring O^{2-} replacing some OH. The +0.11 excess charge was inferred to be due to some minor undetermined amount of Fe^{2+}. Kampf (1982) gave a general formula $(Fe^{3+}_{1-x},\square_x)(Sn_{1-y},\square_y)$

$(OH)_6$, in which vacancies are a potentially significant component.

Jeanbandyite was re-examined by Betterton *et al*. (1998) from Hingston Down Quarry, Cornwall (UK), who noted that the empirical formula of Kampf (1982) did not consider the presence of divalent cations and was not charge-balanced. They proposed a revised empirical formula $(Fe^{3+}_{0.46}Fe^{2+}_{0.24}Mn^{2+}_{0.14}Mg_{0.03})(Sn^{4+}_{0.90}Si_{0.05})(OH)_6$, which is charge-balanced. However, this revised formula also implies 13% vacancies at *B*-sites (and 5% vacancies at *B*′-sites).

In view of the uncertainties in the formula of jeanbandyite and the absence of a structure determination, Welch and Kampf (2017) re-examined samples from Llallagua (Kampf, 1982) and Hingston Down (Betterton *et al*., 1998), and determined the structures of crystals from both localities. All crystals are cubic with space group $Pn\bar{3}$ and have fully-occupied *B*- and *B*′-sites (Fe and Sn, respectively). Welch and Kampf (2017) emphasize that $Pn\bar{3}$ and $P4_2/n$ structures have significantly different octahedral tilt systems ($a^+a^+a^+$ and $a^+a^+c^-$, respectively) that lead to different oxygen arrays which can be distinguished by single-crystal XRD. Bond-valence sums and octahedral volumes of the *B*-sites show clearly that Fe is predominantly in the ferric state. For example, the volume of the $Fe(OH)_6$ octahedron of Hingston jeanbandyite is 11.15 Å^3. This value compares with 10.80 Å^3 for $Fe^{3+}(OH)_6$ in bernalite $Fe(OH)_3$ (Birch *et al*., 1993), and 13.13 Å^3 for $Fe^{2+}(OH)_6$ in stottite $Fe^{2+}Ge(OH)_6$ (Kleppe *et al*., 2012). Assuming a linear variation in octahedral volume with composition, then the value observed for Hingston jeanbandyite implies 85% Fe^{3+} and 15% Fe^{2+} at this site. This calculation for Llallagua jeanbandyite gives 78% Fe^{3+} and 22% Fe^{2+}. Bond-valence sums for the *B*-sites of these two crystals are 2.93 vu and 2.82 vu, respectively. Welch and Kampf (2017) confirm that jeanbandyite is a *bona fide* mineral species and revise its end-member formula to $Fe^{3+}Sn(OH)_5O$. As such, jeanbandyite corresponds compositionally to oxidized natanite; it is an example of a stoichiometric partially-protonated hydroxide perovskite. What appears to be an analogous synthetic phase was reported by Nakayama *et al*. (1977) using powder XRD. The reader is referred to Welch and Kampf (2017) for a full discussion of the crystal chemistry of jeanbandyite.

Wunder *et al*. (2011) reported that the synthetic high-pressure '3.65Å-phase', $MgSi(OH)_6$, is also a hydroxide perovskite. Originally, the space group was determined as orthorhombic *Pnam* (#62), but has been shown subsequently to be monoclinic with a space group that is either $P2_1$ (#4) by density-functional theory (Wunder *et al*., 2012) or $P2_1/n$ (#14) by single-crystal XRD (Welch and Wunder, 2013).

Synthetic hydroxide perovskites

The synthesis of stannate hydroxide perovskites has been investigated extensively by the materials science community in the search for non-spherical hollow nanostructures. Synthesis methods typically involve fast stoichiometric precipitation from alkaline solution (Kramer *et al*., 2010; Wang *et al*., 2013) or sonochemical (Cheng *et al*., 2013) methods at ambient conditions. Numerous synthetic analogues of stannate hydroxide perovskites have been produced by diverse hydrolysis reaction involving metal chlorides and either stannous chloride ($SnCl_4$) with sodium citrate (Wang *et al*., 2013), or alkali hexa-hydroxide stannates under alkaline conditions (NH_4OH or NaOH), e.g.

$$CaCl_2 + K_2Sn(OH)_6.3H_2O \rightarrow CaSn(OH)_6 + 2KCl + 6H_2O$$

The hydroxide perovskites formed in these reactions are very insoluble in water and precipitate immediately on mixing of the reagents. Rinsed products are usually pure and well-crystallized with no amorphous residue. Studies of synthetic hydroxide perovskites should be particularly useful for understanding the structures and potential solid solutions of natural examples e.g. the schoenfliesite–wickmanite–natanite solid solution series (see below). For example, Neilson *et al*. (2011), in contrast to natural hydroxide perovskites, have shown that precipitation can yield ordered compounds only when the *B* cation is Mn^{2+} or Co^{2+} and not when it is any other transition metal or Zn^{2+}.

Solid solutions

Most natural hydroxide perovskites exhibit very limited solid solution and occur as near end-member compositions. It appears that the framework does not tolerate large differences in atomic radii of divalent cations at the *B*-sites, suggesting that next-nearest-neighbour interactions between homovalent cations are important.

The only examples of significant solid solution found so far are: mushistonite (Cu, Mn^{2+}, Fe^{2+})Sn$(OH)_6$ (Marshukova *et al*.,1978, 1984); natural and

synthetic $CuSn(OH)_6$–$ZnSn(OH)_6$ hydroxide perovskites (Marshukova *et al*., 1984; $(Mn^{2+}, Fe^{2+}, Mg)Sn(OH)_6$ in schoenfliesite–wickmanite (Nefedov *et al*., 1977) and $(In, Fe)(OH)_3$ in dzhalindite (Kiseleva *et al*., 2008).

The type-locality mushistonite, from the Mushiston tin deposit (Tadzhkistan) is reported by (Marshukova *et al*., 1978) to exhibit a wide range of composition, i.e. $(Cu_{0.68–0.41}Zn_{0.14–0.41}Fe_{0.23–0.40})Sn_{0.82–1.25}(OH)_{5.69–6.0}$. Natural mushistonite, defined generally as $(Cu,Zn,Fe^{2+})Sn(OH)_6$, has been reported as cubic $Pn\bar{3}m$. However, the synthetic end-member $CuSn(OH)_6$ has a metrically tetragonal unit cell and its structure has been refined in space group $P4_2/nnm$ (Morganstern-Badarau, 1976), corresponding to tilts of $a^0b^+b^+$. However, as noted above, the reported structure is improbable as it requires extremely distorted $Cu(OH)_6$ and $Sn(OH)_6$ octahedra. In addition, a zero tilt is very unlikely on account of the strong hydrogen-bonded bridges and an empty *A*-site. The structure of mushistonite and synthetic $CuSn(OH)_6$ requires re-evaluation and investigation of potential Jahn-Teller effects.

Synthetic vismirnovite $ZnSn(OH)_6$ adopts space group $Pn\bar{3}$ (Cohen-Addad, 1968). For solid solutions between $ZnSn(OH)_6$ and $CuSn(OH)_6$, the cubic ($Pn\bar{3}$) structure extends from vismirnovite $ZnSn(OH)_6$ to $(Cu_{0.4}Zn_{0.6})Sn(OH)_6$. Bulk compositions from $Cu_{50}Zn_{50}$ to $Cu_{80}Zn_{20}$ produce mixtures of tetragonal ($P4_2/n$?) and cubic phases. There is very limited solid solution in the tetragonal phase ($Cu_{90}Zn_{10}$–Cu_{100}). The Raman spectrum of synthetic $CuSn(OH)_6$ contains six peaks and is consistent with space group $P4_2/n$. Vismirnovite from the type locality, the Trudovoe tin deposit (Kyrgyzstan) has the composition $(Zn_{0.89}Cu_{0.1}Fe_{0.08})Sn_{1.0}(OH)_{6.04}$ (Marshukova *et al*., 1981) and presumably adopts space group $Pn\bar{3}$.

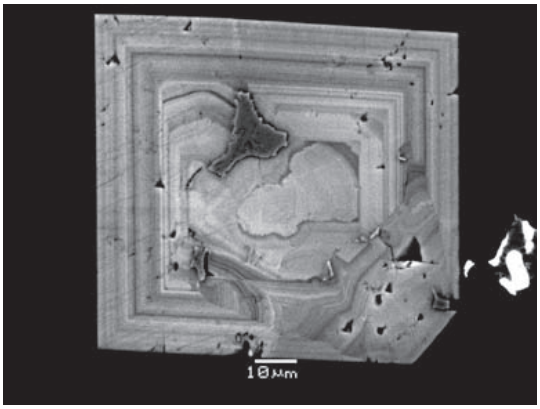

FIG. 23. Back-scattered elctron image of complexly-zoned dzhalindite from the Bugdaya Au-Mo-(W)-porphyry deposit, Eastern Transbaikalia (Russia).

In a study of hydrothermally-mineralized skarns at Pitkäranta, Nefedov *et al*. (1977) showed that minerals of the schoenfliesite–wickmanite series exhibited a wide range in composition ranging from Mn-rich schoenfliesite (up to 55 atomic % wickmanite) to Fe-rich wickmanite (up to 50 atomic % natanite). The minerals were found to be compositionally heterogeneous on a scale of micrometres and did not represent any regular core-to-rim zoning. Nefedov *et al*. (1977) concluded that there is undoubtedly a continuous solid solution series between schoenfliesite, wickmanite and natanite. Further study is required to verify this hypothesis.

Kiseleva *et al*. (2008) have described optically- and compositionally-zoned dzhalindite from the Bugdaya Au-Mo-W deposit (E. Transbaikalia, Russia). The 30–94 µm oscillatory-zoned cubic crystals (Fig. 23) consist of colourless zones with 0.6–1.1 wt.% Fe and light brown zones with up to 3.6 wt.% Fe. Kiseleva *et al*. (2008) have suggested that the Fe is present as microinclusions of Fe^{3+} compounds and that Fe does not replace In at the lattice site. Further study is required to verify this hypothesis.

Hydrogen-bonding topologies of hydroxide perovskites

The octahedra of hydroxide perovskites are corner-linked and there is no *A*-site cation. Thus, hydrogen-bonded linkages can assume a potentially significant role in controlling the degrees of rotation of octahedra, and prevent zero tilts; they may also drive phase transitions.

Hydrogen positions have been determined using powder neutron diffraction for schoenfliesite, burtite (Basciano *et al*., 1998) and synthetic $In(OH)_3$ (Mullica *et al*., 1979). The hydrogen-bonding connectivity of the framework of octahedra as defined by O–H···O donor-acceptor bridges, can be inferred. These bridges form across the shorter O···O distance (2.5–2.7 Å) in each quartet of octahedra; the other O···O distance is far too long (>4 Å) for such bridges to form. Different tilt systems lead to different hydrogen-bonding topologies. Knowing the tilt system permits inference of the hydrogen-bonding connectivity and thereby evaluation of plausible H positions in difference-Fourier maps.

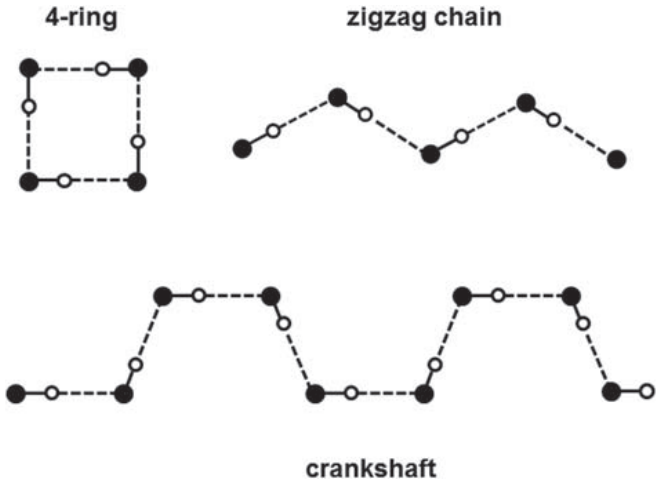

FIG. 24. The three different components of hydrogen-bonding topologies of hydroxide perovskites: isolated ring; crankshaft; and zigzag chain. The inferred local occupancy of hydrogen sites is shown. Hydrogen positions have been located in the cubic phases dzhalindite, schoenfliesite, wickmanite and burtite, all of which have only isolated rings. In these three phases there are two ½-occupied H sites.

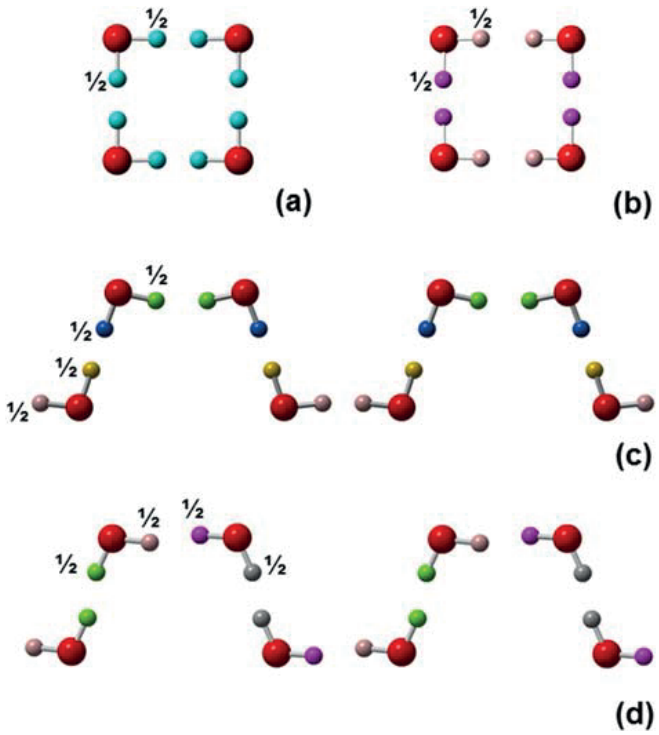

FIG. 25. Hydrogen bonding topologies of hydroxide perovskites determined by single-crystal XRD. Isolated 4-membered rings in (*a*) söhngeite $Ga(OH)_3$ ($P4_2/nmc$) and (*b*) burtite ($Pn\bar{3}$). Crankshafts in (*c*) söhngeite $Ga(OH)_3$ and (*d*) stottite $FeGe(OH)_6$ ($P4_2/n$). All H sites are half-occupied in the averaged structure determined by diffraction methods. The number of non-equivalent OH groups in söhngeite (five) and stottite (six) have been confirmed by Raman spectroscopy. In the ring of söhngeite the pairs of H sites are mirror-related, whereas they are non-equivalent in stottite which being a double-perovskite lacks mirror symmetry.

Very recent single-crystal XRD studies of hydroxide perovskites with space groups $Pn\bar{3}$ and $P4_2/n$ have found that [110] merohedral twinning is common (Lafuente *et al*., 2015; Welch and Kleppe, 2016). Merohedral twinning has been recognized in all $Pn\bar{3}$ and $P4_2/n$ hydroxide perovskites including Mn-schoenfliesite, wickmannite, tetrawickmanite and stottite. Once merohedral twinning has been refined a key aspect of the crystal structure emerges in difference-Fourier maps: the presence of half-occupied H sites, as discussed in detail below. It is, perhaps, surprising that it is possible to assign ½ electron to a plausible half-occupied H site, but the close correspondence between approximate H positions found by single-crystal XRD in wickmannite–schoenfliesite and those determined by neutron diffraction for schoenfliesite, burtite and $In(OH)_3$ leaves little room for doubt.

Once H sites have been located, it is possible to make sense of vibrational (infrared and Raman) spectra in the OH-stretching region which, for non-cubic species, seem to be at variance *prima facie* with the determined space group. The presence of such half-occupied H sites increases the number of OH peaks in spectra beyond that expected for full occupancy. For example, the O–H spectrum of tetrawickmanite (Lafuente *et al*., 2015) has five resolved peaks, which is incompatible with $P4_2/n$ symmetry if all H sites are full (three non-equivalent OH). The tetrawickmanite structure determined by Lafuente *et al*. (2015) has four half-occupied H sites and a fifth fully-occupied H site in a very different type of location from those of the other four H sites. Analogous features have now been recognized in stottite and synthetic $MgSi(OH)_6$.

Three different components of the hydrogen-bonding connectivities of hydroxide perovskites have been identified: (1) isolated four-membered rings; (2) crankshafts; (3) zigzag chains. Figure 24 shows the local configurations of OH groups associated with each component. Figure 25 shows the hydrogen bonding topologies of söhngeite and stottite determined by single-crystal XRD. In stottite and tetrawickmanite (both $P4_2/n$) pairs of half-occupied H sites lie along the O–(H)–O crankshaft and there is only a single fully-occupied H site in the 4-membered ring, giving five non-equivalent H sites in all. In söhngeite ($P4_2/nmc$) there are again four non-equivalent half-occupied H sites in the crankshaft, but the {100} mirror planes produce four pairs of half-occupied equivalent sites in the four-membered ring.

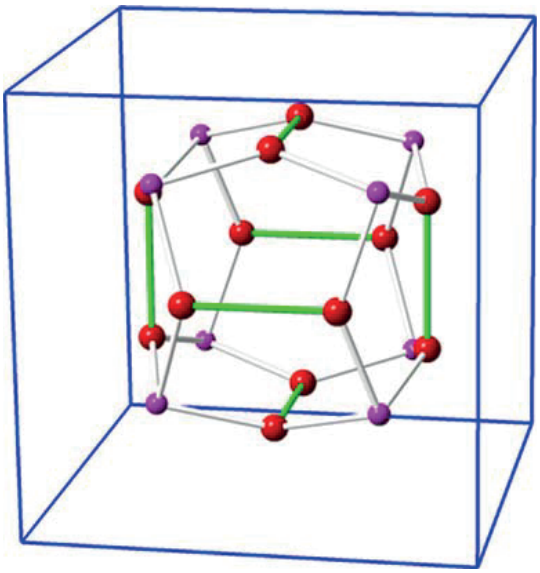

FIG. 26. Cubic hydroxide perovskites have a large empty dodecahedral cage site defined by 12 oxygen and 8 cation sites, as shown here for the single perovskite dzhalindite $In(OH)_3$ ($Im\bar{3}$). There are two dodecahedral cages per unit cell. Six of the O–O edges of the dodecahedron are O–H···O bridges (shown in blue). All other O–O edges (shown in green) are shared with octahedra. Adjacent cages are connected via single octahedra.

Tilt systems of hydroxide perovskites

The tilt systems of hydroxide perovskites are shown in Table 2. As with other perovskites, the tilt notation is based upon the orientation of the rotation axes of the cubic aristotype (Glazer, 1972). Natural hydroxide perovskites studied so far have tilt systems $a^+a^+a^+$ ($Pn\bar{3}$ and $Im\bar{3}$), $a^+a^+c^-$ ($P4_2/nmc$, $P4_2/n$, $P2/n$), $a^+b^+c^-$ ($Pmmn$), $a^-a^-b^+$ ($P2_1/n$), $a^-b^-b^+$ ($P2_1$) and $a^+b^-b^-$ ($Pnma$ and $P2_12_12_1$) have been reported for synthetic hydroxide perovskites. Each tilt system is associated with a distinctive hydrogen-bonding connectivity, as described below.

The two cubic space groups of hydroxide perovskites, $Im\bar{3}$ and $Pn\bar{3}$, with the tilt system $a^+a^+a^+$ are the aristotypes of the single and double perovskites, respectively. Both have a unique large vacant cage site located at a centre of symmetry and defined by twelve oxygen atoms at the apices of an icosahedron (Fig. 26). Each pentagonal face of this icosahedron consists of three oxygen and two cation sites. Six O···O distances bounding this cage are O–H···O bridges associated with one of the two non-equivalent H atoms. The hydrogen-bonding connectivity consists only of isolated 4-membered rings.

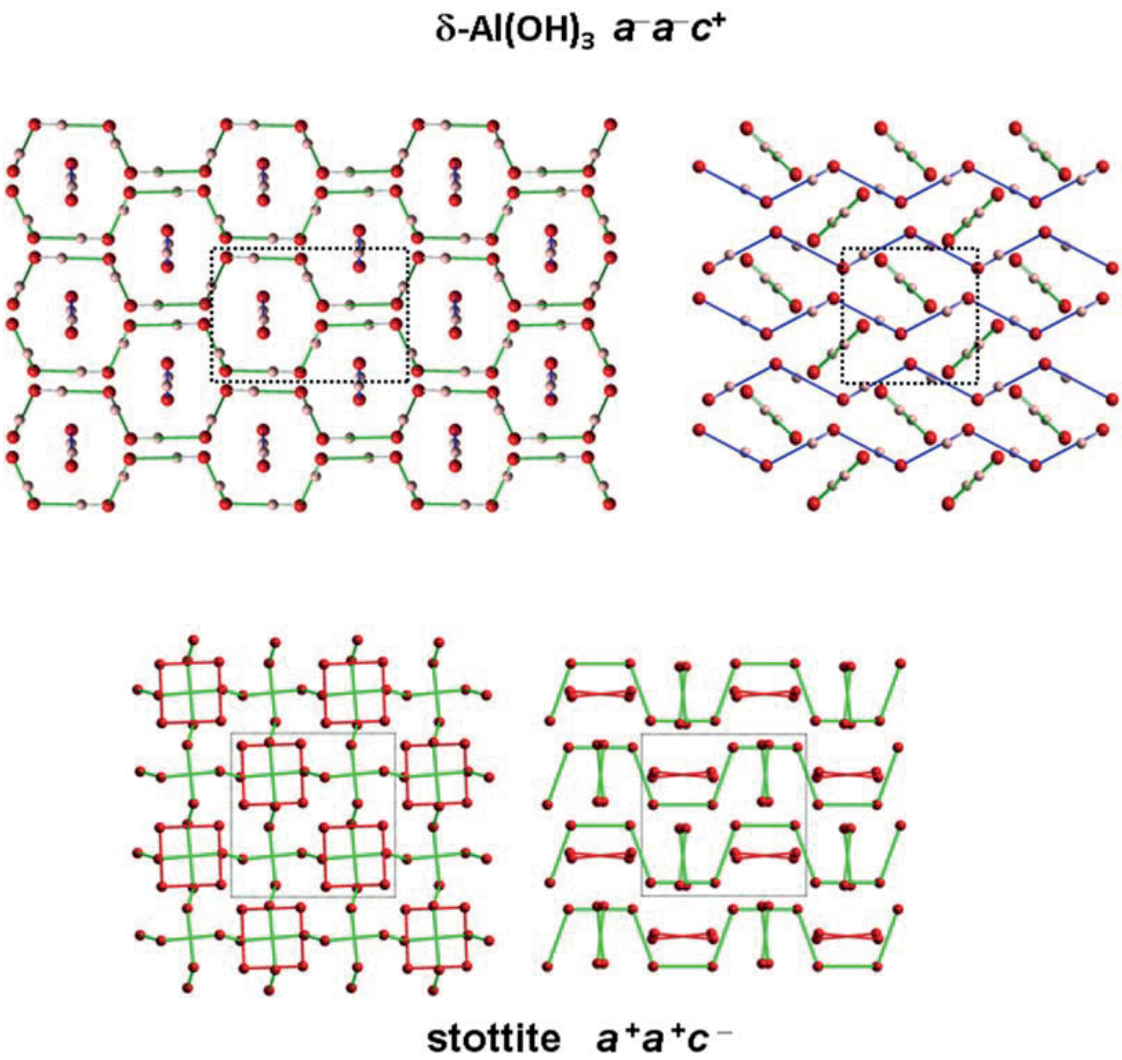

FIG. 27. The hydrogen-bonding topologies of orthorhombic δ-$Al(OH)_3$ and tetragonal $FeGe(OH)_6$. Each line connects the two oxygen atoms of a O–H···O bridge. Isolated 4-membered rings are shown in red, crankshafts in green and zigzag chains in blue. The δ-$Al(OH)_3$ structure has two sets of crankshafts extending ||[010] oriented interleaved with zigzag chains running ||[100]. The hydrogen-bonding topology of stottite $FeGe(OH)_6$ consists of two sets of crankshafts running <100> and interposed 4-membered rings within planes ||(001). There are no hydrogen-bonded connections between chains, crankshafts or rings.

It has been suggested that the icosahedral cage site might host H_2O (Birch *et al*., 1993), but there is no clear evidence so far to support this suggestion. For example, no significant residual electron density within the cage site cavity has been found by diffraction methods. However, it is conceivable that H_2O could be disordered over several partially-occupied sites within this large cavity.

The second type of non-framework 'cavity' in these cubic structures is much more restricted in volume and is defined by eight cation and eight oxygen sites, with pentagonal bounding faces. A 4-membered ring lies at the centre of this volume.

Hydroxide perovskites with space groups *Pmmn* ($a^+b^+c^-$), $P4_2/nmc$, $P4_2/n$ ($a^+a^+c^-$) and $P2/n$ ($a^+b^+c^-$) are characterized by one antiphase tilt and two in-phase tilts. The hydrogen bonding connectivity consists of alternating layers of crankshafts and isolated 4-membered rings. The example of stottite is shown in Fig. 27.

Hydroxide perovskites with space groups *Pnma* ($a^+b^-b^-$), $P2_1/n$ ($a^-a^-c^+$), $P2_12_12_1$ ($a^-a^-c^+$) and

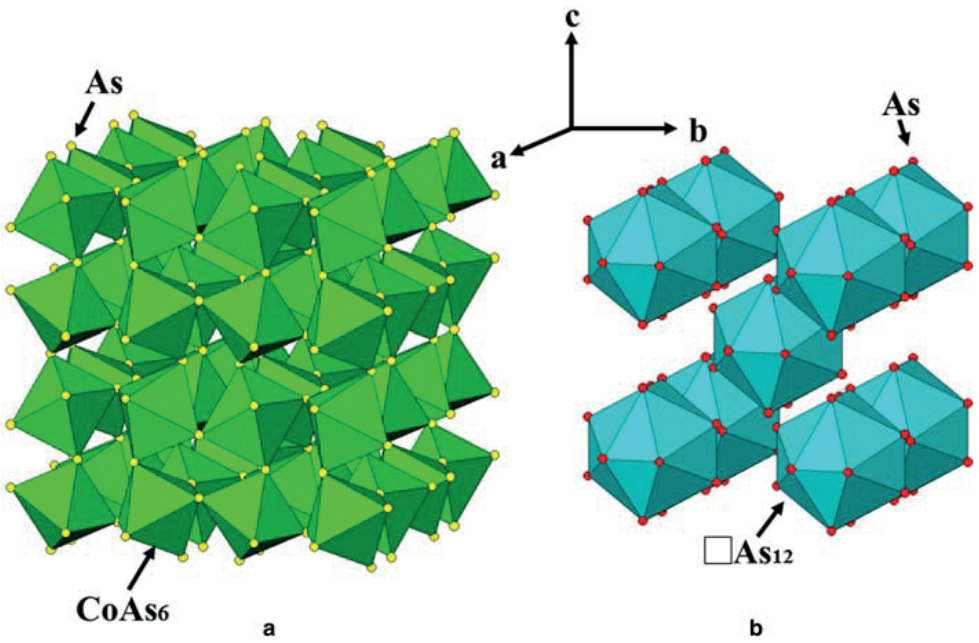

FIG. 28. The crystal structure of skutterudite ($CoAs_3$) showing: (*a*) The framework of tilted $CoAs_6$ octahedra; (*b*) The icosahedral polyhedra defined by the As anions around the empty *A* sites.

$P2_1$ ($a^-a^-c^+$), are characterized by having two anti-phase and one in-phase tilt. Their hydrogen-bonding connectivity consists of interleaved crankshafts and zigzag chains. The example of synthetic δ-$Al(OH)_3$ (Matsui *et al*., 2011), space group *Pnma*, is shown in Fig. 27.

Phase transformations of hydroxide perovskites

Compared to oxide and fluoroperovskites, very few investigations of phase transitions of hydroxide perovskites have been undertaken. Possible continuous transitions can, in principle, be postulated using a group theoretical approach. However, account must be taken of the potential effects of strong hydrogen bonding, which might inhibit tilting-related transitions. As such hydroxide perovskites are very suitable structures for evaluating the role of hydrogen bonding in phase transitions. Examination of group-subgroup relations for known hydroxide perovskite space groups suggests that continuous transitions might be rare, due to the avoidance of structures with zero tilts i.e. due to strong hydrogen bonds.

A further constraint on phase transitions relates to the absence of mirror symmetry in double hydroxide perovskites. Only single hydroxide perovskites can have mirror symmetry, as these planes must pass through shared oxygen atoms. As discussed above this is not possible for double hydroxide perovskites as adjacent octahedra are occupied by different cations, and mirror planes bisecting octahedra result in implausible distortions.

In the absence of continuous phase transitions in double hydroxide perovskites involving the creation of mirror symmetry and/or zero tilts, the options seem to be limited. The most obvious possibilities are $P2/n \leftrightarrow P4_2/n \leftrightarrow P4_2/nmc$ in single hydroxide perovskites and $P2/n \leftrightarrow P4_2/n$ in double hydroxide perovskites. Transitions involving loss or gain of centrosymmetry might also be possible i.e., $P2_1/n \rightarrow P2_1$ or $P2_1/n \rightarrow Pn$. Evidence, from Raman spectra, for a pressure induced transition $P2/n \leftrightarrow P4_2/n$ at ~11 GPa in stottite, was reported by Kleppe *et al*. (2012). This transition is reversible but shows clear hysteresis on decompression.

Polymorphism involving structures with different tilt systems can occur in hydroxide perovskites. However, as far as we are aware, the only example of polymorphism in hydroxide perovskites is that of $MnSn(OH)_6$ for which the polymorphs are wickmanite (cubic $Pn\bar{3}$) and tetrawickmanite (tetragonal $P4_2/n$). Following our comments above on space group nomenclature for polymorphs note that tetrawickmanite could also be termed wickmanite-$P4_2/n$. The cubic polymorph has a cell volume (489 $Å^3$) that is 2% larger than that of tetrawickmanite

(480 Å^3); evidently, the change in tilt system permits a marked contraction of the framework. Welch and Kleppe (2016) report a temperature-induced structural transformation in söhngeite $Ga(OH)_3$ from the ambient $P4_2/nmc$ (or $P4_2/n$) structure to cubic $Im\bar{3}$ at ~150°C. This transition has considerable hysteresis and the cubic polymorph is preserved metastably on cooling to room temperature.

Classification of hydroxide perovskites

The hierarchical classification of hydroxide perovskites is given in Table 2 and is based upon composition and symmetry. It highlights the major distinctions and similarities between these phases. In developing this classification we intend to provide a basis for predicting further possible structures, and to allow for the incorporation of future discoveries of new stoichiometries.

The classification of hydroxide perovskites follows that proposed above for ABX_3 and $A_2BB'X_6$ perovskites. Thus, the fundamental distinction is between 'single hydroxide perovskites' and 'double hydroxide perovskites'. This classification of hydroxide perovskites leads to the recognition of three subgroups: the single hydroxides of the söhngeite subgroup; and the double hydroxide perovskites of the cubic schoenfliesite and the tetragonal stottite subgroups. Table 2; Fig. 7).

Finally, it is evident that there are several interesting avenues of research for future study of hydroxide perovskites namely: (1) What are the correct space groups of hydroxide perovskites? (2) What phase transitions occur in hydroxide perovskites? (3) What is the interplay between composition and tilt system? (4) What is the physical significance of the different hydrogen-bonding topologies, e.g. upon compressional behaviour?

A-site vacant quadruple perovskites

Skutterudite subgroup

The skutterudite group (Table 3; Fig. 7) are derivatives of ordered quadruple perovskites $[AA'_3B_4X_{12}]$ characterized by vacant *A*-sites i.e. $\square\square_3B_4X_{12}$ (*B* = Fe, Co, Ni, Ru, Rh, Ir, Os; *X* = As, Sb, P). Many synthetic skutterudite-group compounds have been synthesized but only four minerals have been recognized, namely: skutterudite ($CoAs_{3-x}$; Haidinger, 1845); ferroskutterudite [$(Fe,Co)As_3$; Spiridonov *et al*., 2007)]; nickelskutterudite ($NiAs_{3-x}$; Spirodov and Gritsenko, 2007); and kieftite [$CoSb_3$; Dobbe *et al*., 1994). Other synthetic skutterudites are known with the large *A*-site filled partially e.g. $A\square_3B_4X_{12}$ (*A* = La–Yb, U, Th), such as $La\square_3Fe_4P_{12}$ (Jeitscho and Braun, 1977), but are as yet unknown as minerals.

All skutterudites adopt the space group $Im\bar{3}$ with the tilt system $a^+a^+a^+$. The structure consists of a framework of corner-sharing $CoAs_6$ or $CoSb_6$ octahedra (Fig. 28). The As and Sb anions in the skutterudite subgroup are bonded to form square planar tetramers $[X_4]^{4-}$, making them also good examples of Zintl compounds (Luo *et al*., 2014). To date *B*-site ordered derivatives have not been recognized. The structure of the skutterudites is nearly identical to that of the single hydroxide perovskite dzhalindite [$In(OH)_6$], except that in the latter the anion bonds are asymmetrical O–H···O rather than the symmetrical *X*–*X* bonds of the skutterudites. Dzhalindite could be also considered as an *A*-site vacant quadruple perovskite.

B-site vacant perovskites

B-site vacant single perovskites $A\square X_3$

Oskarssonite subgroup

Two *B*-site vacant single fluoride perovskites (Table 3; Fig. 7), oskarssonite (ideally AlF_3) and waimirite-(Y) [ideally YF_3], have been approved as valid members of the perovskite supergroup (Table 3; Fig. 7). Both are derivative structures of the cubic ReO_3 aristotype formed by tilting of AlF_6 or YF_6 octahedra. In common with ReO_3 no cations occupy the *B* site of the octahedron framework.

Although Al-fluorides had been recognized in fumaroles from the Hekla (Oskarsson, 1981) and Mount Erebus (Rosenberg, 1988) volcanoes, a complete structural characterization was not available until material from fumaroles of the Eldfell volcano (Iceland) was undertaken by Jacobsen *et al*. (2014). A mineral with the composition of oskarssonite, together with parascandolaite, has also been found as nano-inclusions in diamonds from Juina by Kaminsky *et al*. (2016). Oskarssonite [$Al(F_{2.62}(OH)_{0.49})$] adopts the rhombohedral space group $R\bar{3}c$ (#167) in common with the synthetic analogue α-AlF_3 (Le Bail and Calvayrac, 2006). Oskarssonite is the only known natural perovskite-supergroup mineral with the $a^-a^-a^-$ tilt scheme resulting in an anticlockwise rotation angle (ω) of 10.65° about $[111]_p$ of the AlF_6 octahedra (Fig. 29). Oskarssonite transforms to the cubic ReO_3 structure above 450°C (Jacobsen *et al*., 2014).

PEROVSKITE SUPERGROUP

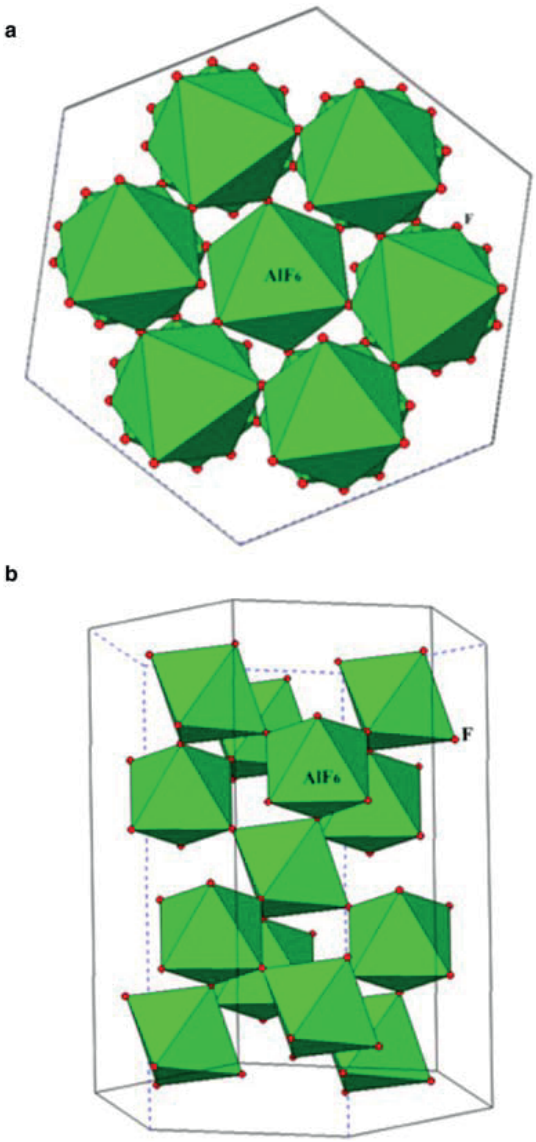

FIG. 29. Polyhederal representation of the crystal structure of oskarssonite. (*a*) Projection along the c_H axis. (*b*) Projection perpendicular to the c_H axis showing the 6 layers of fluorine atoms (red) in the unit cell.

The *B*-site vacant single perovskite, waimirite-(Y), [(Y,*REE*)(F,O)$_3$], has been recognized from A-type granitic rocks occurring at Pitinga (Brazil) and Jabal Tawlah (Saudi Arabia) by Atencio *et al*. (2015), and as a hydrothermal mineral in *REE*-enriched granites from Myanmar (Sanematsu *et al*., 2016). Single-crystal XRD studies of the material from Jabal Tawlah show that the mineral adopts space group *Pbnm* and is the natural analogue of synthetic β-YF_3 (O'Keefe and Hyde, 1977; Galashina *et al*., 1980). The *A* site is dominated by Y coupled with substantial amounts of the heavy *REE* ($Y_{0.69–0.79}REE_{0.21–0.28}$), and the *X* site contains significant O and vacancies ($F_{2.54}$,$\square_{0.25}$, $O_{0.21}$).

B-site vacant single antiperovskites X□A$_3$

Stoichiometric antiperovskites (Table 3; Fig.7) have the composition A_3BX or XBA_3 e.g. K_3OBr; Ca_3NAs (Mitchell, 2002, Krivovichev, 2008). When the *B*-site is vacant, as in $X\square A_3$, derivative synthetic compounds such as Au□Cu_3 (auricupride) and C□Fe_3 are formed (ÒKeefe and Hyde, 1977) Note synthetic auride antiperovkites containing Au^{-1} anions e.g. $AuOK_3$, have been synthesized by Feldmann and Jansen (1995).

Cohenite Subgroup

Cohenite, C(Fe,Ni,Co)$_3$ is a *B*-site vacant carbide antiperovskite which adopts the space group *Pbnm*. The mineral was initially found in the Magura meteorite (Slovakia) and is a common constituent of other iron meteorites. Other occurrences are in highly reducing environments produced when high temperature basaltic lavas have invaded coal deposits e.g. Qeqertasuaq (Disko) Island, Greenland (Pauly, 1969). Kaminsky *et al*. (2015) have reported the presence of a N-bearing mineral similar to cohenite as nano-inclusions in Juina diamonds.

Auricupride subgroup

Auricupride is a *B*-site vacant intermetallic antiperovskite (Au□Cu_3) formed in serpentinites by the low-temperature unmixing of Au-Cu alloys. Palladium-bearing varieties were formerly described by the now discredited name rozhokovite. Auricupride and the synthetic analogue adopt the space group $Pm\bar{3}m$ (Megaw, 1973), although a tetragonal *P*4/*mmm* polymorph is also known (Bayliss, 1990). Although many intermetallic antiperovskites have been synthesized the only varieties which occur as minerals in a wide variety of serpentinites and platinum-group element ore deposits include: $Pm\bar{3}m$ awaruite (Fe□Ni_3); chengdeite (Fe□Ir_3); isoferroplatinum (Fe□Pt_3); yixunite (In□Pt_3); and zvyagintsevite (Pb□Pt_3); together with $Fm\bar{3}m$ rustenburgite (Sn□Pt_3); and atokite (Sn□Pd_3). Rustenburgite and atokite form a complete solid solution series. The reduction in symmetry from $Pm\bar{3}m$ in the synthetic analogues to

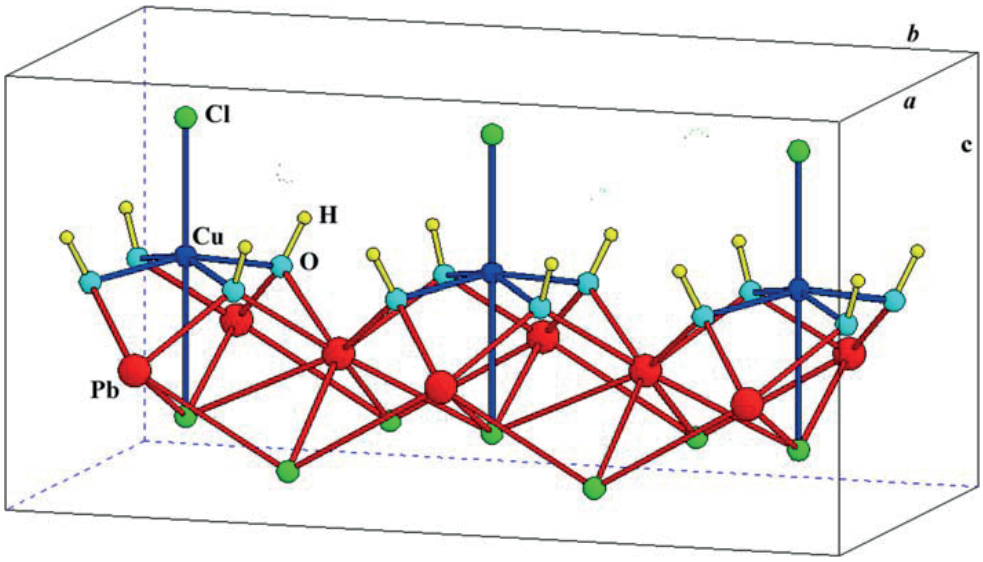

FIG. 30. Crystal structure of diaboleite (after Cooper and Hawthorne, 1995) showing the coordination of Cu and Pb.

$Fm\bar{3}m$ is considered to result from strain induced during mineral processing (Mihalik *et al*., 1975).

B-site vacant ordered double perovskites

Diaboleite subgroup

The chloro-hydroxy double perovskite **diaboleite** ($Pb_2Cu\square Cl_2(OH)_4$; *P*4*mm*) is unusual in that in addition to having vacancies at one octahedral site, its structure exhibits both first order Jahn-Teller and lone-pair effects arising from the presence of Cu and Pb, respectively. Diaboleite was described originally from the iron ore mine located at Higher Pitts Quarry, Mendip Hills, Somerset (UK) by Spencer and Mountain (1923), and has been found subsequently in a variety of parageneses, particularly as a secondary phase in oxidized Ag-Pb veins and chemically-weathered metallurgical slags.

The crystal structure was initially determined by Byström and Wilhelmi (1950) and refined by Rouse (1971) who recognized the mineral is a tetragonal *P*4 *mm* (#99) defect perovskite. Subsequent work by Cooper and Hawthorne (1995) confirmed the structure as a *B*-site defect perovskite of the type $Pb_2(Cu\square)X_6$ in which half of the octahedra are not occupied by cations. In diaboleite the Pb coordination is highly asymmetric as it is surrounded on one side by four OH^- anions (Pb–OH = 2.46 Å), and on the other by four Cl^- anions (3.22 Å and 3.40 Å) in square antiprismatic coordination (Fig. 30). The lone pair electrons project towards the Cl^- anions. The Cu^{2+} site exhibits strong [4+2] first order Jahn-Teller distortion and is surrounded by four equatorial OH^- anions (Pb–OH = 1.97 Å) and two apical Cl^- anions (Pb–Cl 2.55 Å and 2.95 Å) with Cu^{2+} displaced 0.34 Å from the centre of the polyhedron (Fig. 30). The coordination can be considered as intermediate between octahedral and square pyramidal.

Anion-deficient or defect oxide perovskite subgroups

Anion-deficient, non-stoichiometric perovskites (Table 3; Fig. 7) typically range in composition from ABO_3 to $ABO_{2.5}$, and have the general formula $ABO_{3-\delta}$ ($0 < \delta \leq 0.5$). The anion deficiency reflects the replacement of cations by other ions in a lower oxidation state (e.g. Ti^{4+} by Fe^{3+} in $CaTiO_3$; Becerro *et al*., 1999). The vacancies created can be ordered or random. In the ordered structures the vacancies are arranged in parallel rows along $[101]_p$ of the original cubic cell forming layers on either side of a layer of tilted corner-sharing perovskite BO_6 octahedra. Within the oxygen-deficient layers cations occur as pairs of corner-sharing tetrahedra (Fig. 31). The original perovskite stoichiometry is thus modified to $A_2BTX_5\square$, where T represents a tetrahedral coordinated cation. The compounds with the maximum oxygen vacancy are termed brownmillerites in the materials science literature, after the compound $Ca_2Fe^{3+}AlO_5$, occurring as a

mineral and a major component of Portland cement (Colville and Geller, 1971).

Brownmillerite-subgroup

Brownmillerite [$(Ca_2(Fe^{3+}Al)O_5$]

Brownmillerite was recognized, and named (without IMA approval), as a constituent of Portland cement (Hansen *et al*., 1928; Bogue, 1955) prior to its discovery as a mineral. Natural brownmillerite was recognized subsequently in spurrite- and larnite-bearing metamorphosed argillaceous limestones of the Hatrurim Formation (Israel) and thermally-metamorphosed limestone xenoliths in the lavas of the Ettringer Bellerberg volcano, Eifel District (Germany) by Bentor *et al*. (1963) and Hentschel (1964), respectively. Although, the proposal of Hentschel (1964) to name the material from Bellerberg 'brownmillerite' appeared after the publication of Bentor *et al*. (1963), the latter report did not actually contain any analytical information about the new mineral, and hence, Bellerberg should be considered as the type locality. Compositional data obtained by electron microprobe analysis indicates that the Hatrurim material ranges from Fe-dominant compositions with ~20 mol.% $Ca_2Al_2O_5$ (Sharygin *et al*., 2008) to varieties with Al > Fe (up to 54 mol.% $Ca_2Al_2O_5$: Gross, 1977; Sokol *et al*., 2011). Minor constituents exceeding 0.12 apfu are Mg, Ti and Cr. The crystal structure of neither Hatrurim or Bellerberg samples was determined and, on the basis of the powder XRD patterns, was assumed to be identical to that of synthetic orthorhombic *Ibm*2 (#46) $Ca_2(Fe^{3+}Al)O_5$. Note, however that compositions with < 28 mol.% $Ca_2Al_2O_5$ (e.g. samples M5–31 and H–201 in Table 2 of Sharygin *et al*. (2008) probably adopt space group *Pnma* (see below).

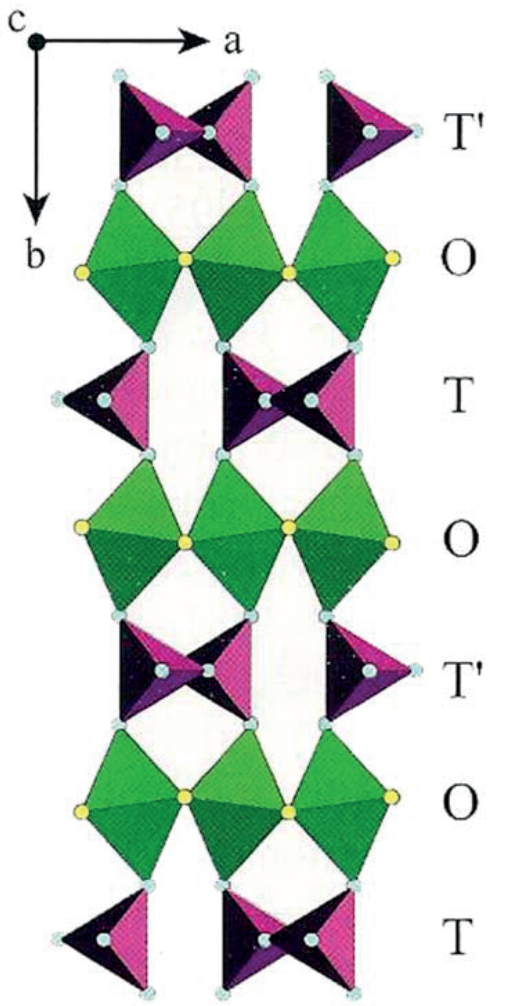

FIG. 31. The crystal structure of *Ibm*2 brownmillerite (Colville and Geller 1971) projected along [001] illustrating the stacking sequence of the octahedral (O) and tetrahedral (T, T′) layers.

Srebrodolskite ($Ca_2Fe_2^{3+}O_5$)

Srebrodolskite, $Ca_2Fe_2^{3+}O_5$, was initially described from petrified wood 'baked' by burning coal in mines at Kopeisk in the Chelabynsk coal basin, Urals (Chesnokov and Bazhenova, 1985). Note that the mineral and name were approved prior to the IMA decision not to approve technogenic phases as new species. The type material contains 0.08 apfu Mg and 0.03 apfu Mn and is devoid of detectable Al. Subsequently, srebrodolskite has been found in the Clearwater impact crater (Rosa and Martin, 2010), the Bellerberg volcano, the Hatrurim Formation (Sharygin *et al*., 2008), Lakargi Mountain (Galuskin *et al*., 2008), and several other less well-characterized localities.

The crystal structure has not been determined by single-crystal methods for any of these examples but is assumed (Chesnokov and Bazhenova, 1985), on the basis of the powder XRD pattern, to be that of synthetic $Ca_2Fe_2^{3+}O_5$ i.e. *Pnma* (#62: Berggren, 1971). Note that the structural data for synthetic srebrodolskite are also reported in the *Pcmn* (#62: cba) setting (Bertaut *et al*., 1959).

Brownmillerite and srebrodolskite adopt different space groups as the orientation of the TO_4 tetrahedra in the two structure types differ. In brownmillerite, all tetrahedra point in the same

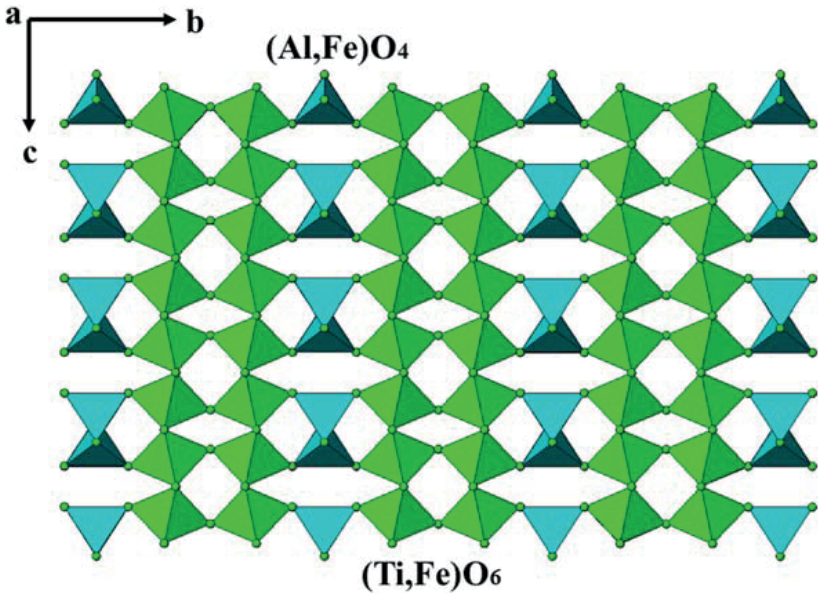

FIG. 32. The crystal structure of shulamitite (Sharygin *et al*., 2013).

direction, to form the sequence $T_{up}OT'_{up}O$ (Fig. 31), whereas in srebrodolskite the sequence is $T_{up}OT'_{down}O$. Regardless of this structural difference, studies of synthetic compounds show there is continuous solid solution between brownmillerite and the ferric end-member with the transition from *Ibm*2 to *Pcmn* occurring at $Ca_2Fe^{3+}_{1.43}Al_{0.56}O_5$ (Collville and Geller, 1972; Redhammer *et al*., 2004). The $Ca_2Al_2O_5$ end-member exists only as a quenchable high-pressure phase (P = 2.5 GPa) isostructural with brownmillerite (Kahlenberg *et al*., 2000). At ambient pressure, Al-dominant compositions with as much as 70 mol.% $Ca_2Al_2O_5$ can be prepared (Taylor, 1997).

Pure $Ca_2Fe^{3+}_2O_5$ and compositions in the solid solution series $Ca_2Fe^{3+}_{2-x}Al_xO_5$ with x up to 0.56 adopt space group *Pnma*, whereas compounds with $x > 0.56$ have *Ibm*2 symmetry (Redhammer *et al*., 2004).Thus, synthetic stoichiometric brownmillerite ($Ca_2Fe^{3+}AlO_5$), and Al-dominant phases adopt space group *Ibm*2. If naturally-occurring phases conform to the same structural principles as their synthetic counterparts, the name brownmillerite should be applied to all intermediate members of the $Ca_2Al_2O_5$–$Ca_2Fe^{3+}_2O_5$ series which adopt space group *Ibm*2 and those adopting space group *Pnma* should be termed srebrodolskite. However because of preferential partitioning of Al into the *T*-site further structural complexities can arise. Thus, brownmillerites could be defined as minerals/compounds having a preponderance of Al in the *T*-site, regardless of the Fe/Al ratio. This is because Al is partitioned strongly into the *T* site until about 2/3 of this site is occupied (Redhammer *et al*., 2004). However, any Al exceeding 2/3 *T*-site occupancy is distributed equally between the tetrahedrally and octahedrally coordinated sites (Redhammer *et al*., 2004). Clearly, in addition to brownmillerite *sensu stricto*, where Al is the dominant cation in the *T*-site and Fe^{3+} in the *B* site, compositions with Al as the dominant species in both sites could possibly exist in nature (including high-pressure phases approaching $Ca_2Al_2O_5$ in their composition). These hypothetical phases will represent a mineral species distinct from brownmillerite and hence require a different name. If naturally-occurring brownmillerite-type phases exhibit the same pattern of cation distribution as their synthetic counterparts, at least ~25 wt.% Al_2O_3 is required from Al to be the dominant cation in both the *T*- and *B*-sites. The greatest Al_2O_3 reported to date (23.2 wt.%; Sokol *et al*., 2011) falls short of that value. A possible high-pressure $Ca_2Al_2O_5$ brownmillerite-type phase was reported by Rappenglück *et al*. (2013) as inclusions in Fe-silicides from the Holocene Chiemgau impact strewnfield in southern Germany, but no structural data to support this interpretation were presented.

In, summary, recognizing the complexities of Al distribution in this solid solution series we recommend that brownmillerite and srebrodolskite be retained as valid names and that: (1)

PEROVSKITE SUPERGROUP

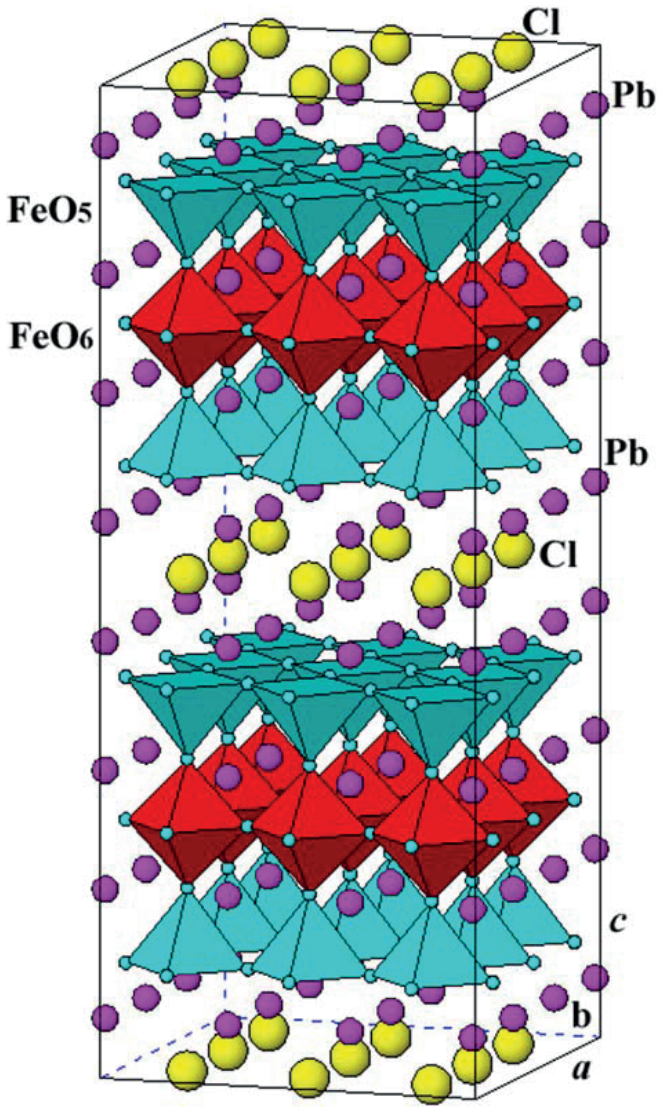

FIG. 33. Polyhedral representation of the crystal structure of hematophanite.

brownmillerites are minerals in the solid solution series $Ca_2Fe^{3+}_{2-x}Al_xO_5$ with $x > 0.56$ which adopt space group *Ibm*2; (2) **srebrodolskites** are minerals in the solid solution series $Ca_2Fe^{3+}_{2-x}Al_xO_5$ with $x < 0.56$ which adopt space group *Pnma*.

Shulamitite *($Ca_3TiFe^{3+}AlO_8$)*

Shulamitite, occurs as a major to accessory mineral in high-temperature metacarbonate larnite rock of the Hatrurim Basin, Israel (Sharygin *et al*., 2013). The mineral can be considered as an intermediate compound between $CaTiO_3$ perovskite and $Ca_2(Fe^{3+},Al)O_5$ bownmillerite and is the natural analogue of synthetic orthorhombic $Pcm2_1$ $Ca_3TiFe^{3+}_2O_8$ (Rodrígues-Carvajal *et al*., 1989). The holotype mineral has the composition $Ca_3TiFe^{3+}(Al_{0.7}Fe^{3+}_{0.3})O_8$. Sharygin *et al*. (2013) recognize other examples for which $Fe^{3+} > Al$ i.e. an unnamed Fe-analogue $[Ca_3(TiFe^{3+})Fe^{3+}O_8]$ of shulamitite assuming the existence of a solid solution between $Ca_3TiFeAlO_8$ and $Ca_3TiFeFeO_8$. Single-crystal structure determination shows that shulamitite adopts the orthorhombic space group *Pmma*, that there is no preferred octahedral site occupancy for Ti or Fe^{3+}, and that the majority of the Al (with some Fe) is in tetrahedral coordination. The crystal structure of shulamitite consists of double layers of tilted $(Ti,Fe)O_6$ octahedra separated by single layers of paired $(Al,Fe)O_4$

tetrahedra. The latter have different orientations between each octahedral double layer (Fig. 32).

Partially vacant *B*-site quadruple perovskites – hematophanite subgroup

Hematophanite was initially recognized from Jakobsberg and Långban, Värmland, Sweden (Johansson, 1928). It is also occurs in slag from Reichelsdorf, Hesse, Germany and at the Kombat Cu-Pb-Ag mine, Namibia.

Rouse (1973) recognized that hematophanite, ideally $Pb_4(Fe_3^{3+}\square)(Cl,OH)(O_8\square_4)$ (or $Pb_4Fe_3^{3+}O_8Cl$), was a derivative of the perovskite structure produced by the stacking of four $PbFeO_3$ perovskite-like cells leading to the hypothetical quadruple perovskite $Pb_4Fe_4O_{12}$. In order to achieve charge balance every fourth Fe^{3+} cation must be replaced by Cl^- (and/or Br^- and OH^-) leading to the introduction of *B*-site vacancies. The *X*-sites that are adjacent to the Cl anion are vacant resulting in partial occupation by oxygen anions.

Thus, the structure of *P*4/*mmm* hematophanite consists of incomplete perovskite $Pb_4Fe_3O_8$ blocks separated by layers of (Cl,OH) anions. Each perovskite block consists of a corner-sharing FeO_6 octahedral layer that is sandwiched between two FeO_5 square pyramids. Lead atoms occur at sites within this framework (Fig. 33). Batuk *et al*. (2013) have shown hematophanite is actually the $n = 3$ member of a homologous series of layered synthetic perovskites with the general formula $A_{3n+1}B_nO_{3n-1}Cl$.

No other minerals with this structure have been found. We recommend that the name be retained and **hematophanite** be recognised as a *bona fide* member of the perovskite supergroup.

Acknowledgements

This study is supported by the Natural Sciences and Engineering Research Council of Canada (RHM, ARC), Lakehead University (RHM), and the University of Manitoba (ARC). MDW thanks Roy Kristiansen (Norway) for support of his work on hydroxide perovskites by the generous donation of rare samples. Anthony Kampf is thanked for cooperation with the determinations of the crystal structure of jeanbandyite. Galina Kiseleva is thanked for information on, and images, of dzhalindite. Members of the IMA-CNMNC and Andy Christy are thanked for constructive comments on the mineralogy and classification of the perovskite supergroup minerals. Peter Williams is thanked for editorial handling of the manuscript.

References

Abilgaard, H. (1799) Cryolith, Thonerde mit Flussäure. *Allgemeines Journal der Chemie*, **2**, 502–000.

Aguado, F., Rodriguez, F., Hirai, S., Walsh, J.N., Lennie, A. and Redfern, S.A.T. (2008) High-pressure behaviour of KMF_3 perovskite. *High Pressure Research*, **28**, 539–544.

Akber-Knutson, S., Bukowinski, M.S.T. and Matas, J. (2002) On the structure and compressibility of $CaSiO_3$ perovskite. *Geophysical Research Letters*, **29**, 4-1–4-4.

Anthony, J.W., Bideaux, R.A., Bladh, K.W. and Nicholls, M.C. (1997). *Handbook of Mineralogy. Volume III. Halides, Hydroxides, Oxides.* Mineral Data Publishing, Tucson, Arizona, USA.

Arakcheeva, A.V., Lubman, G.U., Pisharovski, D.U., Gekimyants, V.M. and Popov, G.U. (1997) Crystal structure of micro-twinned natural orthorhombic perovskite $CaTiO_3$. *Crystallography Reports*, **42**, 46–54.

Arulesan, S.W., Kayser, P., Kennedy, B.J. and Knight, K. S. (2016*a*) The impact of room temperature polymorphism in K doped $NaTaO_3$ on structural phase transition behaviour. *Journal of Solid State Chemistry*, **238**, 109–122.

Arulesan, S.W., Kayser, P., Kennedy, B.J., Kimpton, J.A. and Knight, K.S. (2016*b*) Phase separation in $NaTaO_3$. Impact of temperature and doping. *Solid State Sciences*, **52**, 149–153.

Atencio, D., Andrade, M.B., Christy, A.G., Gieré, R. and Kartashov, P.M. (2010) The pyrochlore supergroup of minerals: nomenclature. *The Canadian Mineralogist*, **48**, 673–698.

Atencio, D., Bastos Neto, A.C., Pereiria, V.P., Ferron, J.T. M.M., Hoshino, M., Moriyama, T., Watanabe, Y., Miyawaki, R., Continho, J.M.V., Andrade, M.B., Domanik, K., Chukanov, M.V., Momma, K., Hirano, H. and Tsunematso, M. (2015) Waimirite-(Y), orthorhombic YF_3, a new mineral from the Pitinga Mine, Presidente Figueiredo, Amazonas, Brasil, and from Jabal Tawlah, Saudi Arabia: Descritption and crystal structure. *Mineralogical Magazine*, **79**, 767–780.

Barnes, P.W., Lufaso, M.W. and Woodward, P.M. (2009) Structure determination of $A_2M^{3+}TaO_6$ and $A_2M^{3+}NbO_6$ ordered perovskites: octahedral tilting and pseudosymmetry. *Acta Crystallographica*, **B62**, 384–396.

Barth, T. (1925) Die Kristallstruktur von Perovskit und verwandten Verbindugen. *Norsk Geologisk Tidskrift*, **8**, 201–216.

Basciano, L.C., Peterson, R.C. and Roeder, P.L. (1998) Description of schoenfliesite, $MgSn(OH)_6$ and roxbyite, $Cu_{1.72}S$, from a 1375 BC shipwreck, and Rietveld neutron-diffraction refinement of synthetic schoenfliesite, wickmanite, $MnSn(OH)_6$ and burtite, $CaSn(OH)_6$. *The Canadian Mineralogist*, **36**, 1203–1210.

Batuk, M., Batuk, D., Tsirlin, A.A., Rozova, M.G., Antipov, E.V., Hadermann, J. and Van Tendeloo, G.

(2013) Homologous series of layered perovskites $A_{n+1}B_nO_{3n-1}Cl$: Crystal and magnetic structure of the oxychloride $Pb_4BiFe_4O_{11}Cl$. *Inorganic Chemistry*, **52**, 2208–2218.

Bayliss, P. (1990) Revized unit-cell dimensions, space group, and chemical formula of some metallic minerals. *The Canadian Mineralogist*, **28**, 751–755.

Becerro, A.J., Lauterbach, S., McCammon, C.A., Langhorst, F., Angel, R. and Seifert, F. (1999). Oxygen defect clustering in $CaTiO_3$–$CaFeO_{2.5}$ perovskites: a model for the lower mantle. *European Journal of Mineralogy*, **11**, Supplement 1, p. 27.

Bentor, Y.K., Grass, S. and Heller, L. (1963) High temperature minerals in non-metamorphosed sediments in Israel. *Nature*, **199**, 478–479.

Beran, A., Libowitzky, E. and Armbruster, T.A. (1996) Single crystal infra-red spectroscopic and X-ray diffraction study of untwinned San Benito perovskite containing OH groups. *The Canadian Mineralogist*, **34**, 803–809.

Berggren, J. (1971) Refinement of the crystal structure of dicalcium ferrite $Ca_2Fe_2O_5$. *Acta Chemica Scandinavica*, **25**, 3616–3624.

Bertaut, E.F., Blum, P. and Sagnières, P. (1959) Structure du barite bicalcique et de la brownmillerite. *Acta Crystallographica*, **12**, 149–159.

Betterton, J., Green, D.L., Jewson, C., Spratt, J. and Tandy, P. (1998) The composition and structure of jeanbandyite and natanite. *Mineralogical Magazine*, **62**, 707–712.

Birch, W.D., Pring, A., Reller, A. and Schmalle, H.W. (1993) Bernalite, $Fe(OH)_3$, a new mineral from Broken Hill, New South Wales: Description and structure. *American Mineralogist*, **78**, 827–834.

Blackburn, W.H. and Dennen, W.H. (1997) *Encylopedia of Mineral Names.* The Canadian Mineralogist Special Publication **1**. Mineralogical Association of Canada Québec, Canada.

Böggild, O.B. (1912) Krystallform und Zwillingsbildungen des Kryoliths, des Perowskits und des Baracits. *Zeischrift für Kristallographie*, **50**, 439–429.

Bogue, R.H. (1955) *The Chemistry of Portland Cement.* Reinhold, New York.

Bonshtedt-Kupletskaya, E.M. (1946) New observations on minerals of the perovskite group. *Problems in Mineralogy, Geochemistry and Petrography.* Nauka Press, Moscow.

Bowman, H.L. (1908) On the structure of perovskite from the Bergumer Alp, Pfitschtal, Tyrol. *Mineralogical Magazine*, **15**, 156–176.

Britvin, S.A., Kashtanov, M.G., Krzhizhanovskaya, A., Gurinov, O.V., Glumov, S., Strekopytov, S., Kretser, L. Y., Zaitsev, A.N., Chukanov, N.V. and Krivovichev, S. V. (2015) Perovskites with framework-forming xenon. *Angewandte Chemie*, **54**, 14340–14344.

Britvin, S.A., Kashtanov, S.A., Krivovichev, S.V. and Chukanov, N.V. (2016) Xenon in rigid oxide frameworks: Structure, bonding and explosive properties of layered perovskite $K_4Xe_3O_{12}$. *Journal of the American Chemical Society*, **138**, 13838–13841.

Bruce, D.W., O'Hare, D. and Walton, R.L. (2010) *Functional Oxides.* John Wiley & Sons, London, 304 pp.

Burke, E.A.J. and Kieft, C. (1971) Second occurrence of macedonite, $PbTiO_3$, Långban, Sweden. *Lithos*, **4**, 101–104.

Buttner, R.H. and Maslen, E.N. (1992) Structural parameters and electron difference density in $BaTiO_3$. *Acta Crystallograpica*, **B48**, 764–769.

Byström, A. and Wilhelmi, K.A. (1950) The crystal structure of diaboleite $Pb_2Cu(OH)_4Cl_2$. *Arkiv Kemi*, **2**, 397–404.

Cao, H., Devreugd, C.P., Ge, W., Li, J., Viehland, D., Luo, H. and Zhao, X. (2009) Monoclinic *Mc* phase in (001) field-cooled $BaTiO_3$ single crystals. *Applied Physics Letters*, **94**, 032901.

Caracas, R. and Wentzcovitch, R.M. (2005) Equation of state and stability of $CaSiO_3$ under pressure. *Geophysical Research Letters*, **32**, L06303.

Carpenter, M.A., Sondergeld, P., Li, B., Liebermann, R. C., Walsh, J.W., Schreuer, J. and Darling, T.W. (2006) Structural evolution, strain and elasticity of perovskites at high pressures and temperatures. *Journal of Mineralogical and Petrological Sciences IMA issue 1*, **101**, 95–109.

Chakhmouradian, A.R. and Mitchell, R.H. (1997) Compositional variation of perovskite-group minerals from carbonatite complexes of the Kola alkaline province, Russia. *The Canadian Mineralogist*, **35**, 1293–1310.

Chakhmouradian, A.R. and Mitchell, R.H. (1998) A structural study of the perovskite series $CaTi_{2-x}Fe_xNb_xO_3$. *Journal of Solid State Chemistry*, **138**, 272–277.

Chakhmouradian, A.R. and Mitchell, R.H. (2001) Three compositional varieties of perovskite from kimberlites of the Lac de Gras field (Northwest Territories, Canada). *Mineralogical Magazine*, **65**, 133–148.

Chakhmouradian, A.R. and Mitchell, R.H. (2002) New data on pyrochlore- and perovskite-group minerals from the Lovozero alkaline complex, Russia. *European Journal of Mineralogy*, **14**, 821–836.

Chakhmouradian, A.R. and Woodward, P.M. (2014) Celebrating 175 years of perovskite research: a tribute to Roger H. Mitchell. *Physics and Chemistry of Minerals*, **41**, 387–391.

Chakhmouradian, A.R., Yakovenchuk, V., Mitchell, R.H. and Bogdanova, A. (1997) Isolueshite: a new mineral of the perovskite group from the Khibina alkaline complex. *European Journal of Mineralogy*, **9**, 483–490.

Chakhmouradian, A.R., Mitchell, R.H., Pankov, A.V. and Chukanov, N.V. (1999) Loparite and "metaloparite" from the Burpala alkaline complex, Baikal Alkaline Province (Russia). *Mineralogical Magazine*, **63**, 519–534.

Chakhmouradian, A.R., Ross, K., Mitchell, R.H. and Swainson, I. (2001) The crystal chemistry of synthetic potassium-bearing neighborite $Na_{1-x}Mg_xF_3$. *Physics and Chemistry of Minerals*, **28**, 277–284.

Chao, E.C.T., Evans, H.T., Skinner, B.J. and Milton, C. (1961) Neighborite, $NaMgF_3$, a new mineral from the Green River Formation, South Ouray, Utah. *American Mineralogist*, **46**, 379–393.

Cheng, P., Yongsheng, N., Yuan, K. and Hong, J. (2013) Fast sonochemical synthesis of $CoSn(OH)_6$ nanocubes, conversion towards shape-preserved SnO_2–Co_3O_4 hybrids and their photodegradation properties. *Materials Letters*, **90**, 19–22.

Cheon, C.L., Joo, H.W., Chae, K.W., Kim, J.S., Lee, S.H., Torii, S. and Kamiyama, T. (2015) Monoclinic ferroelectric $NaNbO_3$ at room temperature: Crystal structure solved by using super high resolution neutron powder diffraction. *Materials Letters*, **156**, 214–219.

Chesnokov, B.V. and Bazhenova, L.F. (1985) Srebrodolskite, $Ca_2Fe_2O_5$, a new mineral. *Zapiski Vses Mineralogii Obshchestvo*, **114**, 195–199.

Christy, A.G., Mills, S.J. and Kampf, A.R. (2016) A review of the structural architecture of tellurium oxycompounds. *Mineralogical Magazine*, **80**, 415–545.

Cohen-Addad, C. (1968) Étude structurale des hydroxystannates $CaSn(OH)_6$ et $ZnSn(OH)_6$ par diffraction neutronique, absorption infrarouge et resonance magnetique nucleaire. *Bulletin Sociéte de France Mineralogie et Crystallographie*, **91**, 315–324.

Colville, A.A. and Geller, S. (1971) The crystal structure of brownmillerite Ca_2FeAlO_5. *Acta Crystallographica*, **B27**, 2311–2315.

Colville, A.A. and Geller, S. (1972) Crystal structures of $Ca_2Fe_{1.43}Al_{0.57}O_5$ and $Ca_2Fe_{1.28}Al_{0.72}O_5$. *Acta Crystallographica*, **B28**, 3196–3200.

Cooper, M.A. and Hawthorne, F.C. (1995) Diaboleite, $Pb_2Cu(OH)_4Cl_2$, a defect perovskite structure with lone pair behaviour of Pb^{2+}. *The Canadian Mineralogist*, **33**, 1125–129.

Cross, E.B. and Hillebrand, W.F. (1885) Minerals from the neighbourhood of Pikes Peak. *U.S. Geological Survey Bulletin*, **20**, 40–68.

Danø, M. and Sørenson, H. (1959) An examination of some rare minerals from the nepheline syenites of southwest Greenland. *Meddelelser om Grønland*, **162**, 1–35.

Demartin, F., Campostrini, I., Castellano, C. and Russo, M. (2014) Parascandolaite, $KMgF_3$, a new perovskite-type fluoride. *Physics and Chemistry of Minerals*, **41**, 403–407.

Dobbe, R.T.M., Lustenhouwer, W. and Zakrzewski, M.A. (1994) Kieftite, $CoSb_3$, a new member of the skutterudite group from Tunaberg, Sweden. *The Canadian Mineralogist*, **32**, 179–183.

Dunn, P.J., Peacor, D.R., Valley, J.W. and Randell, C.A. (1985) Ganomalite from Franklin, New Jersey, and Jakobsberg, Sweden: new chemical and crystallographic data. *Mineralogical Magazine*, **49**, 579–582.

Fang, C.M. and Ahuja, R. (2006) Structures and stability of ABO_3 orthorhombic perovskites at the Earth's mantle conditions from first-principles theory. *Physics of the Earth and Planetary Interiors*, **157**, 1–7.

Feldman, C. and Jansen, M. (1995) Ternary oxides containing anionic gold. *Zeitschrifte für Anorganische und Allegemeine Chemie*, **621**, 201–206.

Feng, D., Shivaramaiah, R. and Navrotsky, A. (2016) Rare earth perovskite along the join $CaTiO_3$–$Na_{0.5}La_{0.5}TiO_3$ join: Phase transformations, formation enthalpies, and implications for loparite minerals. *American Mineralogist*, **101**, 2051–2016.

Foord, E.E., O'Conner, J.T., Hughes, J.M., Sutley, S.J., Falster, A.V., Soregaroli, A.E., Lichte, F. and Kile, D. E. (1999) Simmonsite, Na_2LiAlF_6, a new mineral from the Zapot amazonite-topaz-zinnwaldite pegmatite, Hawthorne, Nevada, USA. *American Mineralogist*, **84**, 769–772.

Frondel, C. (1948) New data on elpasolite and hagemannite. *American Mineralogist*, **33**, 84–87.

Galasso, F.S. (1990) *Perovskites and High T_c Superconductors.* Gordon & Breach Science Publications, New York.

Galuskin, E.V., Gazeev, V.M., Armbruster, T., Zadov, A. E., Galuskina, I.O., Pertsev, N.N., Dzierzanowski, P., Kadiyski, M., Gurbanov, A.G., Wrzalik, R. and Winiarski, A. (2008) Lakargiite, $CaZrO_3$: A new mineral of the perovskite group from the North Caucasus, Kabardino-Balkaria, Russia. *American Mineralogist*, **93**, 1903–1910.

Galuskin, E.V. Galuskina, I.O., Gazeev, V.M., Dzierzanowski, P., Prusik, K., Pertsev, N.N., Zadov, A.E., Bailau, R. and Gubanov, A.G. (2011) Megawite, $CaSnO_3$: A new perovskite-group mineral from skarns of the Upper Chegem-caldera, Kabardino-Balkaria, Northern Caucasus, Russia. *Mineralogical Magazine*, **75**, 2563–2572.

Galuskin, E.V., Galuskina, I.O., Kusz, J., Armbruster, T., Marzec, K., Dzierzanowski, P. and Murasko, M. (2014) Vapnikite Ca_3UO_6 – a new double perovskite mineral from pyrometamorphic larnite rocks of the Jebel Harum, Palestine Autonomy, Israel. *Mineralogical Magazine*, **78**, 571–581.

Galashina, L.S., Sobolev, B.P., Aleksandrov, V.B. and Vishnyakov, Y.S. (1980) Crystal chemistry of rare

earth fluorides. *Soviet Physics Crystallography*, **25**, 171–174.

Gasparik, T., Wolf, K. and Smith, C.M. (1994) Experimental determinations of phase relations in the $CaSiO_3$ system from 8 to 15 GPa. *American Mineralogist*, **79**, 1219–1222.

Geller, S. (1956) Crystal structure of gadolinium orthoferrite, $GdFeO_3$. *Journal of Chemical Physics*, **24**, 1236–1239.

Genkin, A.D. and Murav'eva, L.V. (1964) Indite and dzhalindite: new indium minerals. *American Mineralogist*, **49**, 439.

Glazer, A.M. (1972) The classification of tilted octahedra in perovskites. *Acta Crystallographica*, **B28**, 3384–3392.

Goldschmidt, V.M. (1926) Geochemische Verteilungssgesetze der Elementer VII. *Skrifter der Norske Videnskaps Akademi Klasse 1. Matematisk Naurvidenskaplig Klasse.* Oslo, Norway.

Gross, S. (1977) The mineralogy of the Hatrurim Formation, Israel. *Geological Survey of Israel Bulletin*, **70**, 1–80.

Gurmeet Kaur and Mitchell, R.H. (2013) Mineralogy of the P2-West "kimberlite", Wajrakarur kimberlite field, Andra Pradesh, India: kimberlite or lamproite? *Mineralogical Magazine*, **77**, 3175–3196.

Haggerty, S.E. and Mariano, A.N. (1983) Srontianloparite and strontio-chevkinite: Two new minerals in rheomorphic fenites from the Paraná Basin carbonatites. *Contributions to Mineralogy and Petrology*, **84**, 365–381.

Haidinger, W. (1845) *Handbuch der bestimmenden Mineralogie, enthaltend die Terminologie, Systematik, Nomenklatur und Charakteristik der Naturgeschischte des Mineralreiches.* Braumuller & Seidel, Vienna, 550 pp.

Hålenius, U., Hatert, T., Pasero, M. and Mills, S.J. (2016) CNMNC Newsletter No. 30, April 2016, page 413. *Mineralogical Magazine*, **80**, 407–413.

Hansen, W.C., Brownmiller, L.T. and Bogue, R.H. (1928) Studies on the system calcium oxide–alumina–ferric oxide. *Journal of the American Chemical Society*, **50**, 396–406.

Hatert, F., Mills, S.J., Pasero, M. and Williams, P.A. (2013) CNMNC guidelines for the use of suffixes and prefixes in mineral nomenclature, and the preservation of mineral names. *European Journal of Minealogy*, **25**, 113–115.

Hawthorne, F.C. and Ferguson, R.B. (1975) Refinement of the crystal structure of cryolite. *The Canadian Mineralogist*, **13**, 377–382.

Hentschel, G.M. (1964) Myerit, $12Ca_{O.7}Al_2O_3$ und Brown milllerit, $2CaO{\cdot}(Al,Fe)_2O_3$, zwei neue Minerale in der Lavas des Ettinger Bellerberges. *Neues Jahrbuch für Mineralogie Monatshefte*, **1964**, 22–29.

Hermann, P., Vandenstetten, R. and Hubaux, A. (1960) Sublimés du Nyiragongo (Kivu). *Bulletin des Séances de l'Academie Royal des Sciences d'Outr-mer*, **6**, 961–971.

Hewat, A.W. (1974) Neutron powder profile refinement of ferroelectric and antiferroelectric crystal structures – sodium niobate at 22°C. *Ferroelectrics*, **7**, 83–85.

Hidden, W.E. and MacKintosh, A. (1888) Sulphohalite, a new sodian sulphato-chloride. *American Journal of Science, 3rd Series*, **36**, 463.

Hirose, K. (2014) Deep Earth mineralogy revealed by ultrahigh-pressure experiments. *Mineralogical Magazine*, **78**, 437–446.

Howard, C.J. and Stokes, H.T. (1998) Group theoretical analysis of octahedral tilting in perovskites. *Acta Crystallographica*, **B54**, 782–789.

Howard, C.J. and Stokes, H.T. (2002) Group theoretical analysis of octahedral tilting in perovskites. Erratum. *Acta Crystallographica*, **B58**, 565.

Howard, C.J. and Stokes, H.T. (2004) Octahedral tilting in cation-ordered perovskites – a group-theoretical analysis. *Acta Crystallographica*, **B60**, 674–684.

Howard, C.J. and Stokes, H.T. (2005) Structures and phase transitions in perovskites a group theoretical approach. *Acta Crystallographica*, **A61**, 93–111.

Howard, C.J., Kennedy, B.J. and Woodward, P.M. (2003) Ordered double perovskites – a group theoretical analysis. *Acta Crystallographica*, **B59**, 463–471.

Hu, M., Wenk, H.R. and Sinitsyna, D. (1992) Microstructures in natural perovskites. *American Mineralogist*, **77**, 359–373.

Hutton, J. and Nelmes, R.J. (1981) High resolution studies of cubic perovskite by elastic neutron diffraction. *Acta Crystallographica*, **A37**, 916–920.

Ishizawa, N., Marumo, F., Iwai, S., Kimura, M. and Kawamura, T. (1980) Compounds with perovskite-like slabs III. The structure of a monoclinic modification of $Ca_2Nb_2O_7$. *Acta Crystallographica*, **B36**, 763–766.

Jackson, I. and Rigden, S.M. (1998) Composition and temperature of the Earth's mantle: seismological models interpreted through experimental studies of Earth Materials. Pp. 404–460 in: *The Earth's Mantle: Composition, Structure and Evolution* (I. Jackson, editor). Cambridge University Press, UK.

Jacobsen, M.J., Balić-Žunić, T., Mitolo, D., Katerinopoulou, A., Garavelli, A. and Jakobsson, S. P. (2014) Oskarssonite, AlF_3, a new fumarolic mineral from Eldfell volcano, Heimaey, Iceland. *Mineralogical Magazine*, **78**, 215–222.

Jeitschko, W. and Braun, D.J. (1977) $LaFe_4P_{12}$ filled with $CoAs_3$-type structure and isotypic lanthanoid-transition metal polyphosphides. *Acta Crystallographica*, **B33**, 3401–3406.

Johansson, K. (1928) Hematophanite. *Zeitschrifte fur Kristallographie*, **18**, 87–118.

Johnson, K.E. Tang, C.C., Parker, J.E., Knight, K.S., Lightfoot, P. and Ashbrook, S.E. (2010) The polar phase of $NaNbO_3$: a combined study by powder diffraction, solid state NMR and first principles calculations. *Journal of the American Chemical Society*, **132**, 8732–8746.

Kahlenberg, V., Fischer, R.X. and Shaw, C.S.J. (2000) Rietveld analysis of dicalcium aluminate ($Ca_2Al_2O_5$) – a new high-pressure phase with brownmillerite-type structure. *European Journal of Mineralogy*, **85**, 1061–1065.

Kaldos, R., Guzmics, T., Mitchell, R.H., Dawson, J.B., Milke, R. and Szabo, C. (2015) A melt evolution model for Kerimasi volcano, Tanzania: Evidence from carbonate melt inclusions in jacupirangite. *Lithos*, **238**, 101–119.

Kaminsky, F.V., Zakarchenko, O.D., Davies, R., Griffin, W.L., Khachtryan-Blinova, G.K. and Shiryaev, A.A. (2001) Super-deep diamonds from the Juina area, Mato Grosso State, Brazil. *Contributions to Mineralogy and Petrology*, **140**, 734–753.

Kaminsky, F.V., Wirth, R. and Schreiber, A. (2015) A microinclusion of lower-mantle rock and other minerals and nitrogen lower mantle inclusions in a diamond. *The Canadian Mineralogist*, **53**, 83–104.

Kaminsky, V., Ryabchikov, I.D. and Wirth, R. (2016) A primary natrocarbonatitic association in the Deep Earth. *Mineralogy and Petrology*, **110**, 387–398.

Kampf, A.R. (1982) Jeanbandyite, a new member of the stottite group from Llallagua, Bolivia. *Mineralogical Record*, **13**, 235–239.

Kay, H.F. and Bailey, P.C. (1957) Structure and properties of $CaTiO_3$. *Acta Crystallographica*, **A10**, 219–226.

Kimura, S. and Muan, A. (1971*a*) Phase relationships in the system CaO-iron oxide-TiO_2 in air. *American Mineralogist*, **56**, 1333–1346.

Kimura, S. and Muan, A. (1971*b*) Phase relationships in the system CaO–iron oxide–TiO_2 under strongly reducing conditions. *American Mineralogist*, **56**, 1347–1358.

Kiseleva, G.D., Kovalenko, V.A., Trubkin, N.V., Borisovsky, S.E. and Mokhov, A.V. (2008) Rare minerals of In, Cd, Mo, and W in gold-base metal veins of the Bugdaya Au-Mo(W)-porphyry deposit, Eastern Transbaikalia, Russia. *Russian Academy of Sciences Fersman Mineralogical Museum New Data on Minerals*, **43**, 13–22.

Kleppe, A.K., Welch, M.D., Crichton, W.A. and Jephcoat, A.P. (2012) Phase transitions in hydroxide perovskites: a Raman study of $FeGe(OH)_6$ stottite to 21 GPa. *Mineralogical Magazine*, **76**, 949–962.

Knight, K.S. and Kennedy, B.J. (2015) Phase coexistence in $NaTaO_3$ at room temperature: a high resolution neutron powder diffraction study. *Solid State Sciences*, **43**, 15–21.

Koděra, P., Takács, Á., Racek, M., Šhimko, F., Lupatáková, J., Váczi, T. and Antal, P. (2016) Javorieite. IMA 2016-020 CNMNC Newsletter No. 32, August 2016, page 917. *Mineralogical Magazine*, **80**, 915–922.

Koopmans, H.J.A., van de Velde, G.M.H. and Gellings, P. J. (1983) Powder neutron diffraction study of the perovskites $CaTiO_3$ and $CaZrO_3$. *Acta Crystallographica*, **C39**, 1323–1325.

Knyzazev, A.V. Chernorukov, N.G., Dashkina, Z.S., Bulanov, E.N. and Ladenkov, I.V. (2011) Synthesis, structures, physicochemical properties, and crystal-chemical systematics of $M^{II}_2A^{II}UO_6$ (M^{II} = Pb, Ba, Sr; A^{II} = Mg, Ca, Sr, Ba, Mn, Fe, Co, Ni, Cu, Zn, Cs, Pb) compounds. *Russian Journal of Inorganic Chemistry*, **56**, 888–898.

Kramer, J.W., Kelly, B. and Manivannan, V. (2010) Synthesis of $MSn(OH)_6$ (where M = Mg, Ca, Zn, Mn, or Cu) materials at room temperature. *Central European Journal of Chemistry*, **8**, 65–69.

Krenner, J.A. (1883) Die Gronlandischen minerale der kryolithgruppe. *Mathematisk Naturwissenschaften Berichten aus Ungarn*, **1**, 151–172.

Krivovichev, S.V. (2008) Minerals with the antiperovskite structure: a review. *Zeitschrift für Kristallographie*, **223**, 109–115.

Krivovichev, S.V., Chakhmouradian, A.R., Mitchell, R. H., Filatov, S.K. and Chukanov, N.V. (2000) Crystal structure of isolueshite and its synthetic compositional analogue. *European Journal of Mineralogy*, **12**, 597–607.

Kuznetsov, I.G. (1925) Loparite a new rare earth mineral from the Khibina Tundra. *Izvestia Geologicheskogo Komiteta*, **44**, 663–682 [in Russian].

Kwei, G.H., Lawson, A.C., Billings, S.J.L. and Cheong, S.W. (1993) Structures of the ferroelectric phases of barium titanate. *Journal of Physical Chemistry*, **97**, 2368–2377.

Lafuente, B., Yang, H. and Downes, R.T. (2015) Crystal structure of tetrawickmanite $Mn^{2+}Sn^{4+}(OH)_6$. *Acta Crystallographica*, **E71**, 234–237.

Le Bail, A. and Calvayrac, F. (2006) Hypothetical AlF_3 crystal structures. *Journal of Solid State Chemistry*, **179**, 3159–3166.

Levin, I. and Bendersky, L.A. (1999) Symmetry classification of the layered perovskite-derived $A_nB_nX_{3n+2}$ structures. *Acta Crystallographica*, **B55**, 853–866.

Levin, I., Bendersky, L.A. and Vanderah, T.A. (2000) A structural study of the layered perovskite-derived $Sr_n(NbTi)_nO_{3n+2}$ compounds by TEM. *Philosophical Magazine*, **80**, 411–446.

Lewandowski, J.T., Pickering, I.J. and Jacobson, A.J. (1992) Hydrothermal synthesis of calcium-niobium and tantalum oxides with the pyrochlore structure. *Materials Research Bulletin*, **27**, 981–988.

Liu, L.G. (1976) Orthorhombic perovskite phases observed in olivine, pyroxene and garnet at high pressures and temperatures. *Physics of the Earth and Planetary Interiors*, **11**, 289–298.

Liu, L.G. and Ringwood, A.E. (1975) Synthesis of a perovskite-type polymorph of $CaSiO_3$. *Earth and Planetary Science Letters*, **28**, 209–211.

Lufaso, M.W. and Woodward, P.M. (2004) Jahn-Teller distortions, cation ordering and octahedral tilting in perovskites. *Acta Crystallographica*, **B60**, 10–20.

Lufaso, M.W., Barnes, P.W. and Woodward, P.M. (2006) Structure prediction of ordered perovskites and disordered multiple octahedral cation perovskites using *SPuDs*. *Acta Crystallographica*, **B62**, 397–410.

Lumpkin, G.R. (2014) The role of Th-U minerals in assessing the performance of nuclear waste forms. *Mineralogical Magazine*, **78**, 1071–1095.

Luo, H., Krizan, J.W., Muechler, L., Haldolaarachige, N., Klimczuk, T., Xie, W., Fucillo, M.K., Felser, K. and Cava, R.J. (2014) A large family of filled skutterudites stabilized by electron count. *Nature Communications*, **6**, Article 6489.

Ma, C. (2011) Discovery of meteoritic lakargiite ($CaZrO_3$); a new ultra refractory mineral from the ACFER 094 carbonaceous chondrite. *Meteoritical Society 74th Annual Meeting*, abstract 5169.

Ma, C. and Rossman, G.R. (2008) Barioperovskite, $BaTiO_3$, a new mineral from the Benitoite Mine, California. *American Mineralogist*, **93**, 154–157.

Marshukova, N.K., Sidorenko, G.A. and Chistyakova, N.I. (1978) New data on hydrostannates. *Russian Academy of Science Fersman Mineralogical Museum New Data on Minerals of the U.S.S.R.*, **27**, 89–95.

Marshukova, N.K., Pavlovskii, A.B. and Sidorenko, G.A. and Chistyakova, N.I. (1981) Vismirnovite, $ZnSn(OH)_6$ and natanite $FeSn(OH)_6$, new tin minerals. *Zapiski Vsesoyusnogo Mineralogicheskogo Obshchestva*, **110**, 492–500.

Marshukova, N.K., Pavlovskii, A.B., and Sidorenko, G.A. (1984) Mushistonite $(Cu,Zn,Fe)Sn(OH)_6$ – a new tin mineral. *Zapiski Vsesoyusnogo Mineralogicheskogo Obshchestva*, **113**, 612–617.

Matsui, M., Komatsu, K., Ikeda, E., Sano-Furukawa, A., Gotou, H. and Yagi, T. (2011) The crystal structure of δ-$Al(OH)_3$: Neutron diffraction measurements and *ab initio* calculations. *American Mineralogist*, **96**, 854–859.

McCammon, C.A., Pring, A., Keppler, H. and Sharp, T.A. (1995) A study of bernalite, $Fe(OH)_3$, using Mössbauer spectroscopy, optical spectroscopy, and transmission electron microscopy. *Physics and Chemistry of Minerals*, **22**, 11–20.

McDonald, A.M., Back, M.E., Gault, R.A. and Horváth, L. (2013) Peatite-(Y) and ramikite-(Y), two new Na-Li-Y±Zr phosphate-carbonate minerals from the Poudrette Pegmatite, Mont Saint-Hilaire, Quèbec. *The Canadian Mineralogist*, **51**, 569–596.

McPherson, G.J., Simon, S.B., Davis, A.M., Grossman, L. and Krot, A.N. (2005) Calcium aluminum-rich inclusions: Major unanswered questions. Pp. 225–250, in *Chondrites and the Protoplanetary Disk* (A.N. Krot, A.N. Scott and B. Reipurth, editors). Astronomical Society of the Pacific Conference Papers, **341**.

Megaw, H.D. (1946) Crystal structures of double oxides of the perovskite type. *Proceedings of the Philosophical Society of London*, **58**, 133–152.

Megaw, H.D. (1968) A simple theory of the off-centre displacements of cations in octahedral environments. *Acta Crystallographica*, **B24**, 149–153.

Megaw, H.D. (1973) *Crystal structures: A working approach.* W.B. Saunders Co., Philadelphia, USA.

Menezes Filho, L.A.D., Atencio, D., Andrade, M.B., Downs, R.T., Chaves, M.L.S.C., Romano, A.W., Scholz, R. and Persiano, A.I.C. (2015) Pauloabibite, trigonal $NaNbO_3$, isostructural with ilmenite, from the Jacupiranga carbonatite, Cajati, São Paulo, Brazil. *American Mineralogist*, **100**, 442–446.

Midorikawa, M., Ishibashi, Y. and Takagi, M. (1979) Optical and dilatometric studies of $KCaCl_3$ and $RbCaCl_3$. *Journal of the Physics Society of Japan*, **46**, 1240–1244.

Mihalik, P. Hienstra, S.A. and de Villiers, J.P.R. (1975) Two new platinum group minerals from the Merensky Reef, Bushveld igneous complex. *The Canadian Mineralogist*, **13**, 146–150.

Mitchell, R.H. (1997) Carbonate-carbonate immiscibility, neighborite and potassium iron sulphide in Oldoinyo Lengai natrocarbonatite. *Mineralogical Magazine*, **61**, 779–789.

Mitchell, R.H. (2002) *Perovskites: Modern and Ancient.* Almaz Press, Thunder Bay (www.almazpress.com)

Mitchell, R.H. and Chakhmouradian, A.R. (1996) Compositional variation of loparite from the Lovozero alkaline complex, Russia. *The Canadian Mineralogist*, **34**, 977–990.

Mitchell, R.H. and Chakhmouradian, A.R. (1998) Th-rich loparite from the Khibina complex, Kola Peninsula: Isomorphism and paragenesis. *Mineralogical Magazine*, **62**, 341–353.

Mitchell, R.H. and Liferovich, R.P. (2005) A structural study of the perovskite series $Na_{0.75}Ln_{0.25}Ti_{0.5}Nb_{0.5}O_3$. *Journal of Solid State Chemistry*, **178**, 2586–2593.

Mitchell, R.H. and Mariano, A.N. (2016) Primary phases in alumious slags produced by the aluminothermic reduction of pyrochlore. *Mineralogical Magazine*, **80**, 383–397.

Mitchell, R.H. and Vladykin, N.V. (1993) Rare earth element-bearing tausonite and potassium barium titanites from the Little Murun potassic alkaline

complex, Yakutia, Russia. *Mineralogical Magazine*, **57**, 651–664.

Mitchell, R.H., Chakhmouradian, A.R. and Yakovenchuk, V.N. (1996) Nioboloparite: a re-investigation and discreditation. *The Canadian Mineralogist*, **34**, 991–999.

Mitchell, R.H., Choi, J.B., Hawthorne, F.C., McCammon, C.A. and Burns, P.C. (1998) Latrappite: a re-investigation. *The Canadian Mineralogist*, **36**, 107–116.

Mitchell, R.H., Chakhmouradian, A.R. and Woodward, P. M. (2000*a*) Crystal chemistry of perovskite-compounds in the tausonite loparite series $(Sr_{1-x}Na_xLa_x)TiO_3$. *Physics and Chemistry of Minerals*, **27**, 583–589.

Mitchell, R.H., Burns, P.C. and Chakhmouradian, A.R. (2000*b*) The crystal structures of loparite-(Ce). *The Canadian Mineralogist*, **38**, 145–152.

Mitchell, R.H., Burns, P.C., Chakhmouradian, A.R. and Levin, I. (2002) The crystal structures of lueshite and $NaNbO_3$. *International Mineralogical Association Meeting*, Edinburgh, Scotland, Abstract A9–5.

Mitchell, R.H., Cranswick, L.M.D. and Swainson, I. (2006) Neutron diffraction determination of the cell dimensions and thermal expansion of the fluoro-perovskite $KMgF_3$ from 293 to 3.6 K. *Physics and Chemistry of Minerals*, **33**, 587–591.

Mitchell, R.H., Burns, P.C., Knight, K.S., Howard, C.J. and Chakhmouradian, A.R. (2014) Observations on the crystal structures of lueshite. *Physics and Chemistry of Minerals*, **41**, 393–401.

Miyajima, H., Miyawaki, R. and Ito, K. (2002) Matsubaraite, $Sr_4Ti_5(Si_2O_7)_2O_8$, a new mineral, the Sr-Ti analogue of perrierite from the Itoigawa-Ohmi district, Niigata Prefecture, Japan. *European Journal of Mineralogy*, **14**, 1119–1128.

Morgenstern-Badarau, I. (1976) Effet Jahn-Teller et structure cristalline de l'hydroxyde $CuSn(OH)_6$. *Journal of Solid State Chemistry*, **17**, 399–400.

Mullica, D.F., Beall, G.W. and Milligan, W.O. (1979) The crystal structure of cubic $In(OH)_3$ by X-ray and neutron diffraction methods. *Journal of Inorganic and Nuclear Chemistry*, **41**, 277–282.

Murakami, M., Hirose, K., Kawamura, K., Sata, N. and Ohishi, Y. (2004) Post-perovskite phase transition in $MgSiO_3$. *Science*, **304**, 855–858.

Nakayama, N., Kosuge, K. and Kachi, S. (1977) Magnetic properties of $FeSn(OH)_6$ and its oxidation product $FeSnO(OH)_5$. *Materials Research Bulletin*, **13**, 17–22.

Nanot, M., Queyroux, F., Gilles, J.C., Portier, R. and Fayard, M. (1975) Étude par diffraction X et microscopie electronique de composés inedits de formule $A_nB_nO_{3n+2}$ dans les systems $La_2Ti_2O_7$–$CaTiO_3$, $Nd_2Ti_2O_7$–$CaTiO_3$ et $Ca_2Nb_2O_7$–$CaTiO_3$. *Materials Research Bulletin*, **10**, 313–318.

Náray-Szabó, S.V. (1943) Der strukturtyp des Perowskites ($CaTiO_3$). *Naturwissenschaften*, **31**, 202–203.

Náray-Szabó, S.V. and Sasvari, K. (1938) Die struktur des Kryoliths Na_3AlF_6. *Zeitschrift für Kristallographie*, **99**, 27–31.

Nefedov, E.I., Griffin, W.L. and Kristiansen, R. (1977) Minerals of the schoenfliesite wickmanite series from Pitkäranta, Karelia, USSR. *The Canadian Mineralogist*, **15**, 437–445.

Nelmes, R.J. and Kuhs, W.F. (1985) The crystal structure of tetragonal PbTiO3 at room temperature and at 700 K. *Solid State Communications*, **54**, 721–723.

Nickel, E.H. (1964) Latrappite – a proposed new mineral name for the perovskite-type calcium niobate mineral from the Oka area of Québec. *The Canadian Mineralogist*, **8**, 121–122.

Nickel, E.H. and McAdam, R.C. (1963) Niobian perovskite from the Oka, Québec, a new classification for minerals of the perovskite group. *The Canadian Mineralogist*, **7**, 683–697.

Nickel, E.H. and Grice, J. (1998) The IMA Commission on New Minerals and Mineral Names: Procedures and guidelines on mineral nomenclature, 1998. *The Canadian Mineralogist*, **36**, 913–926.

Nielson, J.R., Kurzman, J.A., Seshadri, R. and Morse, D. E. (2011) Ordering double perovskite hydroxides by kinetically controlled aqueous hydrolysis. *Inorganic Chemistry*, **50**, 3003–3009.

Oganov, A.R. and Ono, S. (2004) Theoretical and experimental evidence for a post-perovskite phase of $MgSiO_3$ in Earth's D″ layer. *Nature*, **430**, 445–448.

O'Keefe, M. and Hyde, B.G. (1977) Some structures topologically related to cubic perovskite ($E2_1$), ReO_3 (DO_9) and Cu_3Au ($L1_2$). *Acta Crystallographica B*, **33**, 3802–3813.

Oskarsson, N. (1981) The chemistry of Icelandic lava incrustations and the latest stages of degassing. *Journal of Volcanology and Geothermal Research*, **10**, 93–111.

Pabst, A. (1934) The crystal structure of sulphohalite. *Zeitscrift fur Kristallographie*, **89**, 514–517.

Palache, C., Berman, H. and Frondel, F. (1951) *The System of Mineralogy of James Dwight Dana and Edward Salisbury Dana.* Volume II, 7th edition, pp. 91–92. John Wiley and Sons, New York.

Pauly, H. (1969) White cast iron with cohenite schreibersite and sulphides from Tertiary basalts on Disko. *Meddeleser fra Dansk Geologisk Forening*, **19**, 26–28.

Peel, M.D., Thompson, S.P., Daoud-Aladine, A., Ashbrook, S.E. and Lightfoot, P. (2012) New twists on the perovskite theme: Crystal structures of the elusive phases R and S of $NaNbO_3$. *Inorganic Chemistry*, **51**, 6876–6889.

Portier, R., Fayard, M., Carpy, A. and Galy, J. (1974) Étude par microscopie électronique de quelques termes de la serie $(Na,Ca)_nNb_nO_{3n+2}$. *Materials Research Bulletin*, **9**, 371–378.

Qi, R.Y. and Corbett, J.D. (1995) $Cs_3Zr_6Br_{15}Z$ (Z = C,B): a stuffed rhombohedral perovskite structure of linked clusters. *Inorganic Chemistry*, **34**, 1657–1662.

Radusinović, D. and Makov, C. (1971) Macedonite – lead titanate: A new mineral. *American Mineralogist*, **56**, 387–394.

Ramsay, W. (1897) Das Nephelinesyenitgebiet auf der Halbinsel Kola II. *Fennia*, **15**, 1–15.

Ramsay, W. and Hackman, V. (1894) Das Nephelinesyenitgebiet auf der Halbinsel Kola I. *Fennia*, **11**, 1–225.

Ranjan, R., Agrawal, A. Senyshyn, A. and Boysen, H. (2006) Phases in the system $Na_{½}Nd_{½}TiO_3$– $SrTiO_3$: a powder neutron diffraction study. *Journal of Physics: Condensed Matter*, **18**, 9679–9689.

Rappenglück, M.A., Bauer, F., Hiltl, M., Neumair, A. and Ernstson, K. (2013) Calcium-aluminum-rich inclusions (CAIs) in iron silicide (xifengite, gupeite, hapkeite) matter: evidence of a cosmic origin. *Meteoritics and Planetary Science*, **48** issue s1, abstract #5055.

Redfern, S.A.T. (1996) High-temperature phase transitions in perovskite ($CaTiO_3$). *Journal of Physics of Condensed Matter*, **8**, 8267–8275.

Redhammer, G.J., Tippelt, G., Roth, G. and Amthauer, G. (2004) Structural variations in the brownmillerite series $Ca_2(Fe_{2-x}Al_x)O_5$: Single-crystal X-ray diffraction at 25°C and high-temperature X-ray powder diffraction (25°C ≤ *T* ≤ 1000°C). *American Mineralogist*, **89**, 405–420.

Ringwod, A.E. (1985) Disposal of high level nuclear wastes: Geological perspectives. *Mineralogical Magazine*, **49**, 159–176.

Ringwood, A.E. (1991) Phase transformations and their bearing on the constitution and dynamics of the mantle. *Geochimica et Cosmochimica Acta*, **55**, 2083–2110.

Rodrígues-Carvajal, J., Valett-Regí, M. and González-Calbert, J.M. (1989) Perovskite three-fold superlattices: a structure determination of the $A_3M_3O_8$ phase. *Materials Research Bulletin*, **24**, 423–430.

Rosa, D. and Martin, R.F. (2010) A spurrite-, merwinite- and srebrodolskite-bearing skarn assemblage, West Clearwater Lake impact crater, northern Quebec. *The Canadian Mineralogist*, **48**, 1519–1532.

Rose, G. (1839) Beschreibung einiger neuer Mineralien vom Ural. *Pogendorff Annalen der Physik und Chemie*, **48**, 551–572.

Rosenberg, P.E. (1988) Aluminum fluoride hydrates, volcanogenic salts from Mount Erebus, Antarctica. *American Mineralogist*, **73**, 855–860.

Ross II, C.R., Bernstein, L.R. and Waychunas, G.A. (1988) Crystal structure refinement of stottite FeGe $(OH)_6$. *American Mineralogist*, **73**, 657–661.

Ross, K.C., Mitchell, R.H. and Chakhmouradian, A.R. (2003) The crystal structure of synthetic simmonsite, Na_2LiAlF_6. *Journal of Solid State Chemistry*, **172**, 95–101.

Rouse, R.C. (1971) The crystal chemistry of diaboleite. *Zeitschrift für Kristallographie*, **134**, 69–80.

Rouse, R.C. (1973) Hematophanite, a derivative of the perovskite structure. *Mineralogical Magazine*, **39**, 49–53.

Sabelli, C. (1987) Structure refinement of elpasolite from Cetrine Mine, Tuscany, Italy. *Neues Jahrbuch für Mineralogie*, **1987**, 481–487.

Safianikoff, A. (1959) Un nouveau minéral de niobium. *Academe des Seances Royale de l'Outre-mer Bulletin*, **5**, 1251–1255.

Sakowski-Cowley, A.C., Lukaszewicz, K. and Megaw, H. D. (1969) The structure of sodium niobate at room temperature, and the problem of reliability in pseudo-symmetric structure. *Acta Crystallographica*, **25**, 851–865.

Sanematsu, K., Ehma, T., Kon, Y., Manaka, T., Zaw, K., Morita, S. and Seo, Y., (2016) Fractionation of rare-earth elements during magmatic differentiation and weathering of calc-alkaline granites in southern Myanmar. *Mineralogical Magazine*, **80**, 77–102.

Sasaki, S., Prewitt, C.T. and Liebermann, R.C. (1987) The crystal structure of $CaGeO_3$ perovskite and the crystal chemistry of $GdFeO_3$-type perovskites. *American Mineralogist*, **68**, 1189–1198.

Scheunemann, K. and Müller-Buschbaum, H.K. (1974) Zur Kristallstruktur von $Ca_2Nb_2O_7$. *Journal of Inorganic and Nuclear Chemistry*, **36**, 1965–1970.

Schubert, K. and Seitz, A. (1948) Kristallstruktur von Sc $(OH)_3$ and $In(OH)_3$. *Zeitschrifte für Anorganische und Allegemeine Chemie*, **256**, 226–238.

Scott, J,D. (1971) Crystal structure of a new mineral, söhngeite. *American Mineralogist*, **56**, 355.

Seltman, R., Soloviev, S., Shatov, V., Piranjo, F., Naumov, E. and Cerkasov, S. (2010) Metallogeny of Siberia: tectonic, geologic and metallogenic settings of selected significant deposits. *Australian Journal of Earth Sciences*, **57**, 655–706.

Shan, Y.J., Nakamura, T., Inaguma, Y. and Itoh, M. (1998) Preparation and dielectric properties of the novel perovskite-type oxides $(Ln_{/2}Na_{1/2})TiO_3$ (Ln = Dy, Ho, Er, Tm, Yb, Lu). *Solid State Ionics*, **108**, 123–128.

Sharygin, V.V., Sokol, E.V. and Vapnik, Y. (2008) Minerals of the pseudobinary perovskite-brownmillerite series from combustion metamorphic larnite-rocks of the Hatrurim Formation (Israel). *Russian Geology and Geophysics*, **49**, 709–726.

Sharygin, V.V., Lazic, B., Armbruster, T.M., Murashko, M.N., Wirth, R., Galuskina, I.O., Galuskin, E.V., Vapnik, Y., Britvin, S.N. and Logvinova, A.M. (2013) Shulamitite $Ca_3TiFe^{3+}AlO_8$ – a new perovskite-related mineral from the Hatrurim Basin, Israel. *European Journal of Mineralogy*, **25**, 97–111.

Shcheka, S.S. and Keppler, H. (2012) The origin of the terrestrial noble gas signature. *Nature*, **490**, 531–535.

Sleight, A.W. (1963) *A study of the incidence of the ordered perovskite structure*. PhD Thesis, University of Connecticut, USA.

Sokol, E.V., Gaskova, O.L., Kokh, S.N., Kozmenko, O.A., Seryotkin, Y.S., Vapnik, Y. and Murashko, M.N. (2011) Chromatite and its Cr^{3+}- and Cr^{6+}-bearing precursor minerals from the Nabi Musa Mottled Zone Complex. Judean Desert. *American Mineralogist*, **96**, 659–674

Spencer, L.J. and Mountain, E.D. (1923) Diaboleite. *Mineralogical Magazine*, **20**, 76–80.

Smith, C.B., Allsopp, H.L., Gravie, O.G., Kramers, J.D., Jackson, F.S. and Clement, C.R.C. (1989) Note on the U-Pb perovskite method for dating kimberlites: Examples from the Wesselton and De Beers mines, South Africa and Somerset Island, Canada. *Chemical Geology*, **79**, 137–145.

Spiridonov, E.M. and Gritsenko, Y.D. (2007) Ferroskutterudite, nickelskutterudite and skutterudite from the Norilsk Ore Field. *Russian Academy of Science Fersman Mineralogical Museum, New data on Minerals*, **42**, 16–27.

Spiridonov, E.M., Gritsenko, Y.D. and Kulikova, I.M. (2007) Ferroskutterudite (Fe,Co)As_3: A new mineral species from the dolomite-calcite veins of the Norilsk Ore Field. *Doklady Akademi Nauk Earth Sciences Section*, **417**, 242–244.

Stachel, T., Harris, J.W., Brey, G.P. and Joswig, W. (2000) Kankan diamonds (Guinea) II: lower mantle inclusion parageneses. *Contributions to Mineralogy and Petrology*, **140**, 16–27.

Stokes, H.T., Kisi, E.H., Hatch, D.M. and Howard, C.J. (2002) Group theoretical analysis of octahedral tilting in ferroelectric perovskites. *Acta Crystallographica*, **B58**, 934–936.

Strunz, H. and Contag, B. (1960) Hexahydroxystannate [Fe, Mn, Co, Mg, Ca,]$Sn(OH)_6$ und deren Kristallstruktur. *Acta Crystallographica*, **13**, 601–603.

Strunz, H. and Giglio, M. (1961) Die Kristallstructur von Sottit Fe[$Ge(OH)_6$]. *Acta Crystallographica*, **14**, 205–208.

Strunz, H., Söhnge, G. and Geier, B.H. (1958) Stottit, ein neues Germanium-Mineral und seine Paragenese in Tsumeb. *Neues Jahrbuch für Mineralogie Monatshefte*, **1958**, 85–96.

Sugahara, M., Yoshiasa, A., Yoneda, A., Hashimoto, T., Sakai, S., Okube, M., Nakatsuka, A. and Ohtaka, O. (2008) Single-crystal X-ray diffraction study of $CaIrO_3$. *American Mineralogist*, **93**, 1148–1152.

Sun, P.H., Nakamura, T., Shan, Y.J., Inaguma, Y. and Itoh, M. (1997) High temperature quantum paraelectricity in perovskite-type titanates $Ln_{1/2}Na_{1/2}TiO_3$. (Ln = La, Pr, Nd, Sm, Eu, Gd, and Tb). *Ferroelectrics*, **200**, 93–107.

Tanaka, T. and Okumara, K. (1977) Ultrafine barium titanate particles in the Allende meteorite. *Geochemical Journal*, **11**, 137–145.

Tarrida, M., Larguem, H. and Madon, M. (2009) Structural investigations of (Ca,Sr)ZrO_3 and Ca(Sn, Zr)O_3 perovskite compounds. *Physics and Chemistry of Minerals*, **36**, 403–413.

Taylor, H.F.W. (1977) *Cement Chemistry.* Thomas Telford, London, 459 pp.

Tikhnenkov, I.P. and Kazakova, M.E. (1957) Nioboloparite – a new mineral of the perovskite group. *Zapiski Vsesoyusnogo Mineralogicheskogo Obshchestva*, **86**, 641–644.

Tschauner, O., Ma, C., Beckett, J.R., Prescher, C., Prakapenka, V.B. and Rossman, G.R. (2014) Discovery of bridgmanite, the most abundant mineral in the Earth, in a shocked meteorite. *Science*, **346**, 1100–1102.

Tsuchiya, T., Tsuchiya, J., Umemoto, K. and Wentzcovitch, R.M. (2004) Phase transitions of $MgSiO_3$ perovskite in the earth's lower mantle. *Earth and Planetary Science Letters*, **224**, 241–248.

Tsuda, K., Yasuhara, A. and Tanaka, M. (2013) Two-dimensional mapping of polarizations of rhombohedral nanostructures in the tetragonal phase of $BaTiO_3$ by the combined use of scanning transmission electron microscopy and convergent-beam electron diffraction methods. *Applied Physics Letters*, **103**, 082908.

Vorobyev, E.I., Konev, A.A., Malyshonok, Y.V., Afonina, G.F. and Sapozhnikov, A.N. (1984) Tausonite $SrTiO_3$. A new mineral of the perovskite group. *Zapiski Vsesoyusnogo Mineralogicheskogo Obshchestva*, **113**, 86–89.

Vousden, P. (1953) The structure of the ferroelectric sodium niobate at room temperature. *Acta Crystallographica*, **4**, 545–551.

Wang, Z.Y., Wang, Z.C., Wu, Z.Y. and Lou, X.W.D. (2013) Mesoporous single crystal $CoSn(OH)_6$ hollow structures with multilevel interiors. *Nature Scientific Reports*, **3**, srep 01391.

Welch, M.D. and Kampf, A.R. (2017) Stoichiometric partially-protonated states in hydroxide perovskites: the jeanbandyite enigma revisited. *Mineralogical Magazine*, **81**, 297–303.

Welch, M.D. and Kleppe, A.K. (2016) Polymorphism of the hydroxide perovskite $Ga(OH)_3$ and possible proton-driven transformational behaviour. *Physics and Chemistry of Minerals*, **43**, 515–536.

Welch, M.D. and Wunder, B. (2013) A single crystal X-ray diffraction study of the 3.65Å-phase MgSi$(OH)_6$, a high-pressure hydroxide perovskite. *Physics and Chemistry of Minerals*, **39**, 693–697.

Welch, M.D., Crichton, W.A. and Ross, N.L. (2005) Compression of the perovskite-related mineral bernalite $Fe(OH)_3$ to 9 GPa and a re-appraisal of its structure. *Mineralogical Magazine*, **69**, 309–315.

Williams, S.A. (1985) Mopungite, a new mineral from Nevada. *Mineralogical Record*, **16**, 73–74.

Williams, T., Lichtenberg, F., Widmer, D., Bednorz, G.and Reller, A. (1993) Layered perovskitic structures in pure and doped $LaTiO_{3.5-x}$ and $SrNbO_{3.5-x}$. *Journal of Solid State Chemistry*, **103**, 375–386.

Woodhead, J.D., Phillips, D., Hergt, J.M. and Paton, C. (2009) African kimberlites revisited: In situ Sr-isotope analysis of groundmass perovskite. *Lithos*, **112**, 311–317.

Woodward, P. (1997) Octahedral tilting in perovskites. I. Geometrical considerations. *Acta Crystallographica*, **B53**, 32–43.

Wu, F., Yang, Y.H., Mitchell, R.H., Li, Q.L., Yang, J.H. and Zhang, Y.B. (2010) In situ U-Pb age determination and Nd isotopic analysis of perovskites from kimberlites in southern Africa and Somerset Island, Canada. *Lithos*, **155**, 205–222.

Wunder, B., Wirth, R. and Koch-Müller, M. (2011) The 3.65 Å phase in the system $MgO–SiO_2–H_2O$: Synthesis, structure and composition. *American Mineralogist*, **96**, 1207–1214.

Wunder, B., Jhan, S., Koch-Müller, M. and Speziale, S. (2012) The 3.65 Å phase, $MgSi(OH)_6$: structural insights from DFT-calculations and T-dependent IR spectroscopy. *American Mineralogist*, **97**, 1043–1048.

Yakovenchuk, V., Ivanyuk, G., Pakhpmovsky, Y. and Men'shikov, Y. (2005) *Khibiny.* Laplandia Minerals, Apatity, Russia, 468 pp.

Yanamaka, T., Hirai, N. and Komatsu, Y. (2002) Structural changes of $Ca_{1-x}Sr_xTiO_3$ perovskite with composition and pressure. *The American Mineralogist*, **87**, 1183–1189.

Zhao, Y. (1998) Crystal chemistry and phase transitions of perovskites in P-T-X space: Data for $(K_xNa_{1-x})F_3$. *Journal of Solid State Chemistry*, **141**, 121–132.

Zhao, Y., Weidner, D.J., Leinenweber, K., Liu, X., Li, B., Meng, Y., Pacalo, E.G., Vaughan, M.T., Wang, Y. and Yaganeh-Haeri, A. (1994) Perovskite at high P-T conditions: In situ synchrotron X-ray diffraction study of $NaMgF_3$ perovskite. *Journal of Geophysical Research*, **99 B2**, 2871–2885.

Zurevinski, S.E., Heaman, L.M. and Creaser, R.A. (2011) The origin of Triassic/Jurassic kimberlite magmatism, Canada: Two mantle sources revealed from the Sr-Nd isotopic composition of groundmass perovskite. *G3: Geochemistry Geophysics Geosystems*, **12**, https://doi.org/10.1029/2011GC003659

ADDENDUM

Popova *et al*. (2017) have recently described a non-centrosymmetric variety of loparite from the Khibiny complex with space group *Imma*2 [$a = 5.51292(2)$; $b = 5.5129(2)$; $c = 7.7874(5)$ Å]. This loparite adopts this space group and the tilt scheme $a^0b^-b^-$ as result of being richer in the $Na_{0.5}Ce_{0.5}TiO_3$ component than the *Pbnm* loparite described by Mitchell *et al*. (2000*b*) from the same locality.

Popova, E.A., Lushnikov, S..G., Yakovenchuk, V.N. and Krivovichev, S.V. (2017). The crystal structure of loparite; a new acentric variety. *Mineralogy and Petrology*, DOI 10.1007/s00710-017-0498-y.

673

The Canadian Mineralogist
Vol. 48, pp. 673-698 (2010)
DOI: 10.3749/canmin.48.3.673

THE PYROCHLORE SUPERGROUP OF MINERALS: NOMENCLATURE

DANIEL ATENCIO[§]

Instituto de Geociências, Universidade de São Paulo, Rua do Lago, 562, 05508-080, São Paulo, SP, Brazil

MARCELO B. ANDRADE

Instituto de Física de São Carlos, Universidade de São Paulo, 13560–970, São Carlos, SP, Brazil

ANDREW G. CHRISTY

Research School of Earth Sciences, Australian National University, Canberra, ACT 0200, Australia

RETO GIERÉ

Institut für Geowissenschaften, Albert-Ludwigs-Universität, Albertstrasse 23b, D–79104 Freiburg, Germany

PAVEL M. KARTASHOV

Institute of Geology, Ore Deposits, Petrography, Mineralogy and Geochemistry (IGEM), Russian Academy of Sciences, Staromonetnyi pereulok 35, 109017, Moscow, Russia

ABSTRACT

A new scheme of nomenclature for the pyrochlore supergroup, approved by the CNMNC–IMA, is based on the ions at the *A*, *B* and *Y* sites. What has been referred to until now as the pyrochlore group should be referred to as the pyrochlore supergroup, and the subgroups should be changed to groups. Five groups are recommended, based on the atomic proportions of the *B* atoms Nb, Ta, Sb, Ti, and W. The recommended groups are pyrochlore, microlite, roméite, betafite, and elsmoreite, respectively. The new names are composed of two prefixes and one root name (identical to the name of the group). The first prefix refers to the dominant anion (or cation) of the dominant valence [or H_2O or □] at the *Y* site. The second prefix refers to the dominant cation of the dominant valence [or H_2O or □] at the *A* site. The prefix "keno-" represents "vacancy". Where the first and second prefixes are equal, then only one prefix is applied. Complete descriptions are missing for the majority of the pyrochlore-supergroup species. Only seven names refer to valid species on the grounds of their complete descriptions: oxycalciopyrochlore, hydropyrochlore, hydroxykenomicrolite, oxystannomicrolite, oxystibiomicrolite, hydroxycalcioroméite, and hydrokenoelsmoreite. Fluornatromicrolite is an IMA-approved mineral, but the complete description has not yet been published. The following 20 names refer to minerals that need to be completely described in order to be approved as valid species: hydroxycalciopyrochlore, fluornatropyrochlore, fluorcalciopyrochlore, fluorstrontiopyrochlore, fluorkenopyrochlore, oxynatropyrochlore, oxyplumbopyrochlore, oxyyttropyrochlore-(Y), kenoplumbopyrochlore, fluorcalciomicrolite, oxycalciomicrolite, kenoplumbomicrolite, hydromicrolite, hydrokenomicrolite, oxycalciobetafite, oxyuranobetafite, fluornatroroméite, fluorcalcioroméite, oxycalcioroméite, and oxyplumboroméite. For these, there are only chemical or crystal-structure data. Type specimens need to be defined. Potential candidates for several other species exist, but are not sufficiently well characterized to grant them any official status. Ancient chemical data refer to wet-chemical analyses and commonly represent a mixture of minerals. These data were not used here. All data used represent results of electron-microprobe analyses or were obtained by crystal-structure refinement. We also verified the scarcity of crystal-chemical data in the literature. There are crystal-structure determinations published for only nine pyrochlore-supergroup minerals: hydropyrochlore, hydroxykenomicrolite, hydroxycalcioroméite, hydrokenoelsmoreite, hydroxycalciopyrochlore, fluorcalciopyrochlore, kenoplumbomicrolite, oxycalciobetafite, and fluornatroroméite. The following mineral names are now discarded: alumotungstite, bariomicrolite, bariopyrochlore, bindheimite, bismutomicrolite, bismutopyrochlore, bismutostibiconite, calciobetafite, ceriopyrochlore-(Ce), cesstibtantite, ferritungstite, jixianite, kalipyrochlore, monimolite, natrobistantite, partzite, plumbobetafite, plumbomicrolite,

§ *E-mail address*: datencio@usp.br

plumbopyrochlore, stannomicrolite, stetefeldtite, stibiconite, stibiobetafite, stibiomicrolite, strontiopyrochlore, uranmicrolite, uranpyrochlore, yttrobetafite-(Y), and yttropyrochlore-(Y).

Keywords: pyrochlore supergroup, nomenclature, pyrochlore group, microlite group, betafite group, roméite group, elsmoreite group.

Sommaire

Nous proposons un nouveau système de nomenclature pour les minéraux du supergroupe du pyrochlore, sanctionné par le Comité des Noms de Minéraux, de Nomenclature et de Classification de l'Association internationale de Minéralogie, et fondé sur les ions se trouvant aux sites *A*, *B* et *Y*. Ce qui a déjà été considéré le groupe du pyrochlore devient le supergroupe du pyrochlore, et les sous-groupes deviennent dorénavant des groupes. Cinq groupes sont maintenant recommandés, selon la proportion des atomes Nb, Ta, Sb, Ti, et W au site *B*. Les groupes recommandés sont nommés pyrochlore, microlite, roméite, bétafite, et elsmoreïte, respectivement. Les nouveaux noms contiennent jusqu'à deux préfixes et un nom-racine, qui est identique au nom du groupe. Le premier préfixe fait allusion à l'anion prédominant (ou cation) de la valence dominante [ou H_2O ou □] au site *Y*. Le second se rapporte au cation prédominant de la valence dominante [ou H_2O ou □] au site *A*. Le préfix "kéno-" représente "lacune". Dans les cas où le premier et le second préfixe sont les mêmes, seul un préfixe suffira. Des descriptions complètes ne sont pas disponibles pour la majorité des espèces du supergroupe du pyrochlore. Seuls sept noms font référence à des espèces considérées valides à cause de leur description complète: oxycalciopyrochlore, hydropyrochlore, hydroxykénomicrolite, oxystannomicrolite, oxystibiomicrolite, hydroxycalcioroméite, et hydroknoelsmoreïte. La fluornatromicrolite est une espèce approuvée, mais la description complète de cette espèce n'a pas encore été publiée. Les vingt noms suivants se rapportent à des espèces dont la description doit être complétée pour être considérées valides: hydroxycalciopyrochlore, fluornatropyrochlore, fluorcalciopyrochlore, fluorstrontiopyrochlore, fluorkénopyrochlore, oxynatropyrochlore, oxyplumbopyrochlore, oxyyttropyrochlore-(Y), kénoplumbopyrochlore, fluorcalciomicrolite, oxycalciomicrolite, kénoplumbomicrolite, hydromicrolite, hydrokénomicrolite, oxycalciobetafite, oxyuranobétafite, fluornatroroméite, fluorcalcioroméite, oxycalcioroméite, et oxyplumboroméite. Dans ces cas, il n'y a que des données chimiques ou des données sur la structure cristalline. On doit définir des échantillons-types. Dans plusieurs autres cas, des candidats potentiels existent, mais ils ne sont pas suffisamment bien caractérisés pour leur attribuer un statut officiel. Les données chimiques plus anciennes reposent sur des analyses par voie humide, et représenteraient en général des mélanges. De telles données n'ont pas été utilisées ici. Toutes les données représentent donc des résultats d'analyses obtenues avec une microsonde électronique ou bien des données établies par analyse de la structure cristalline. Nous avons aussi vérifié la rareté des données cristallochimiques dans la littérature. Nous avons trouvé des déterminations de la structure cristalline pour seulement neuf minéraux du supergroupe du pyrochlore: hydropyrochlore, hydroxykénomicrolite, hydroxycalcioroméite, hydroknoelsmoreïte, hydroxycalciopyrochlore, fluorcalciopyrochlore, kénoplumbomicrolite, oxycalciobetafite, et fluornatroroméite. Les noms suivants deviennent désuets: alumotungstite, bariomicrolite, bariopyrochlore, bindheimite, bismutomicrolite, bismutopyrochlore, bismutostibiconite, calciobétafite, cériopyrochlore-(Ce), cesstibtantite, ferritungstite, jixianite, kalipyrochlore, monimolite, natrobistantite, partzite, plumbobétafite, plumbomicrolite, plumbopyrochlore, stannomicrolite, stetefeldtite, stibiconite, stibiobétafite, stibiomicrolite, strontiopyrochlore, uranmicrolite, uranpyrochlore, yttrobétafite-(Y), et yttropyrochlore-(Y).

(Traduit par la Rédaction)

Mots-clés: supergroupe du pyrochlore, nomenclature, groupe du pyrochlore, groupe du microlite, groupe de la bétafite, groupe de la roméite, groupe de l'elsmoreïte.

Introduction

In 1977, Hogarth presented a comprehensive classification and nomenclature for the pyrochlore supergroup, which represented the then-current body of knowledge on pyrochlore-supergroup minerals. The study produced a concise classification, and reduced the proliferation of synonyms to a handful of names. The IMA CNMMN (now CNMNC) has recently received a series of submissions for potentially new members of the pyrochlore supergroup. Some of the submissions invoked new interpretations or extensions of the approach of Hogarth (1977). In addition, some Commission members expressed concern about Hogarth's species and group divisions, which do not conform to current IMA criteria (Nickel 1992).

The official pyrochlore-supergroup system of classification (Hogarth 1977) does not follow the current IMA rules of mineralogical nomenclature, although that system is currently still approved by IMA. Hogarth (1977) assigned species prefixes according to the chemical composition of the *A* position of the pyrochlore formula. Species in which an exotic cation (*i.e.*, anything other than Ca or Na) made up more than 20% of the total number of *A* cations were assigned a special prefix indicating the presence of the cation. In such cases, the prefix was to apply to the dominant exotic cation. For example, a member of the pyrochlore group with 25% Pb and 20% Sr would be named plumbopyrochlore, with "strontian", as an optional (varietal) adjectival modifier. At the *A* site, Hogarth's (1977) system does not differentiate between occupancy

by Ca and Na. In spite of this, the species *fluornatromicrolite* was approved on the basis of predominance of Na at the *A* site. The *natro-* prefix is also present in the name *natrobistantite*. The prefix *calcio-* was used for calciobetafite (Mazzi & Munno 1983). Regarding the *B*-site occupancy, the division among the groups is not made with a tripartite symmetrical classification (as suggested by Zurevinski & Mitchell 2004), nor is it based on the dominant-valence rule (as adopted in this proposal). The species with Nb + Ta > 2Ti and Nb > Ta are considered as pyrochlore-group minerals; if Nb + Ta > 2Ti and Ta ≥ Nb, the mineral is considered to belong to the microlite group, and if 2Ti ≥ Nb + Ta, the mineral belongs to the betafite group. Isostructural species with other predominant cations at the *B* site were not included in the pyrochlore supergroup (for example, roméite, with dominant Sb, and elsmoreite, with dominant W). The anions are not taken into account in the classification, but the predominance of fluorine was used for the approval of the species *fluornatromicrolite*. Other names that disagree with IMA recommendations, such as cesstibtantite and natrobistantite, were also introduced with IMA approval.

Many problematic features of pyrochlore-supergroup minerals and synthetic pyrochlores have been resolved since Hogarth (1977). The structural role of H_2O, very large cations (K, Cs, Rb), atypical *B* cations (Fe^{3+}, Zr, W), and cations with stereoactive lone-pair electrons (Sb^{3+}, Sn^{2+}) are now understood. In addition, modern electron-probe microanalysis (EPMA) permits routine determination of F, providing better-quality data on the anion content.

A new CNMMN subcommittee on pyrochlore (Chairman: Scott Ercit. Members: Petr Černý, Greg Lumpkin, Ernie Nickel, Milan Novák, and Roland Rouse) was established in 1998. One interim report was issued in 1999, but no additional report was presented formally to the Commission since then. This subcommittee was terminated in June 2008. An unofficial report prepared in 2003 by Scott Ercit was provided to the new subcommittee and served as a basis for the preparation of this report.

The following represents a modernization of Hogarth's (1977) system, in which we have taken into account the ideas presented in the paper by Hatert & Burke (2008). We believe that the new names being proposed are more rational, and their use should be preferred.

In order to make this report consistent with the recently approved definitions of group nomenclature by Mills *et al*. (2009), what is up to now referred to as the pyrochlore group should be referred to as the pyrochlore supergroup, and the subgroups should be changed to groups.

The Formula

The pyrochlore-supergroup minerals crystallize in the isometric crystal system (space group $Fd\bar{3}m$ or its subgroups) and exhibit a unit cell characterized by a ≈ 10.4 Å and Z = 8 (Rouse *et al*. 1998). They conform to the general formula:

$$\boldsymbol{A}_{2-m}\,\mathbf{B}_2\,\boldsymbol{X}_{6-w}\,\mathbf{Y}_{1-n}.$$

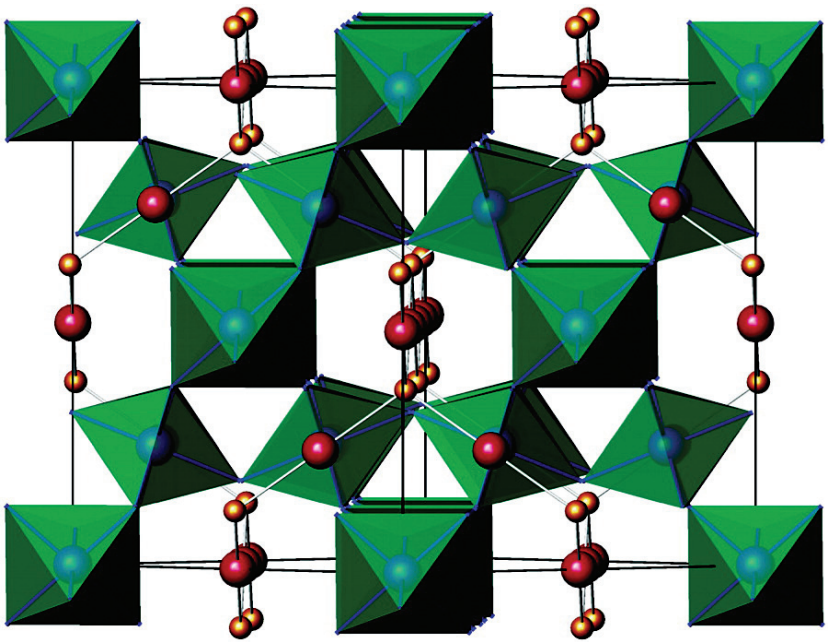

FIG. 1. Ideal pyrochlore crystal structure viewed along the [110] axis (*A* red, *Y* orange and BO_6 octahedra in green) (Henderson *et al*. 2007).

In this formula, ***A*** typically is a large [8]-coordinated cation with a radius of ~1.0 Å or a vacancy (□), but can also be H_2O (includes ions with or without lone-pair electrons on sites 16*d* or 96*g* in $Fd\bar{3}m$). The *A* site therefore may host **Na, Ca,** Ag, Mn, **Sr,** Ba, Fe^{2+}, **Pb^{2+}, Sn^{2+}, Sb^{3+},** Bi^{3+}, **Y**, Ce (and other REE), Sc, **U**, Th, □, **or H_2O**. The main constituents are shown in **bold**.

B is a [6]-coordinated cation (site 16*c*), typically of high field-strength. This site thus may contain **Ta, Nb, Ti, Sb^{5+}, W**, but also V^{5+}, Sn^{4+}, Zr, Hf, Fe^{3+}, Mg, Al and Si.

X typically is **O**, but can include subordinate OH and F (site 48*f*).

Y typically is an anion, but can also be a vacancy, H_2O, or a very large (>> 1.0 Å) monovalent cation (site 8*b*). Examples are **OH^-, F, O**, □, **H_2O**, K, Cs, Rb. Displacements to 96*g*, 32*e* and 192*i* positions were also located.

The symbols *m, w,* and *n* represent parameters that indicate incomplete occupancy of the *A*, *X* and *Y* sites, respectively. Vacancies have not been found to occur at the *B* site (Borodin & Nazarenko 1957, van Wambeke 1970). Compositions with a substantial concentration of vacancies at the *A* site have been described as "defect pyrochlores". However, it is undesirable to give this term official status in this context, since it is non-specific, and likely to be used to describe other deviations from the ideal structure and stoichiometry. Lumpkin & Ewing (1992, 1995), Ercit & Robinson (1994), Brugger *et al*. (1997), and Nasraoui & Waerenborgh (2001) noted vacancies at the *X* site in some extreme cases of secondary alteration. According to Lumpkin & Ewing (1995), the following ranges are encountered: $m = 0$ to 1.7, $w = 0$ to 0.7, and $n = 0$ to 1. Actually, *m* can range up to 2 (Ercit *et al*. 1994, Brugger *et al*. 1997).

Hogarth *et al*. (2000), among others, discussed the distribution of cations at the structural sites of pyrochlore-supergroup minerals. Synthetic pyrochlores have a much more variable chemical composition than natural examples (Subramanian *et al*. 1983).

For structural reasons, *A* can be subdivided into constituents without lone-pair electrons (*e.g*., Na, Ca), which occupy 16*d*, and stereoactive cations (*e.g*., Sb^{3+}), which occupy less symmetrical positions displaced slightly from 16*d*, *e.g*., 96*g*. For the purpose of this nomenclature, no subdivision is made. This approach has its analogues in the nomenclature of silicate minerals. For instance, the *A* site of the amphibole formula represents general or special positions, and the *C* "site" consists of the combination of the crystal-chemically similar *M*l to *M*3 sites.

The pyrochlore structure (Fig. 1) is an essential building block for other minerals and mineral groups, such as alunite (Goreaud & Raveau 1980) or pittongite (Grey *et al*. 2006).

The New Scheme of Nomenclature

In the present work, a new scheme of nomenclature based on the ions at the *A*, *B* and *Y* sites is presented. The new names are composed of two prefixes and one root name (identical to the name of the group). Five groups are recommended, on the basis of the atomic proportions of the *B*-site atoms Nb, Ta, Sb, Ti, and W. The recommended groups are **pyrochlore, microlite, roméite, betafite**, and **elsmoreite**, respectively. According to this new scheme, the pyrochlore supergroup now also includes mineral species with W or Sb^{5+} as the dominant cation at the *B* site. These species were once regarded as tungstates or antimonates rather than conventional oxides, but they contain W^{6+} or Sb^{5+} in octahedral coordination with oxygen, and the resulting octahedra are polymerized to form the framework of the pyrochlore structure. Furthermore, the W and Sb species show various degrees of solid solution with "conventional" members of the supergroup (Brugger & Gieré 1999). The determination of a proper group is made by the dominant valence at *B*, not by a single, dominant ion. That is, the numbers of all tetravalent cations are summed to give a total number of M^{4+}, the numbers of all pentavalent cations to give a sum M^{5+}, and so on. For this purpose, a group of atoms with the same valence state are considered to be a single constituent (Hatert & Burke 2008).

If $M^{4+} > M^{5+}$ and $M^{4+} > M^{6+}$, then the group is:
Betafite, if Ti is the dominant M^{4+} cation.

If $M^{5+} > M^{4+}$ and $M^{5+} > M^{6+}$, then the group is:
Pyrochlore, if Nb is the dominant M^{5+} cation,
Microlite, if Ta is the dominant M^{5+} cation,
Roméite, if Sb is the dominant M^{5+} cation.

If $M^{6+} > M^{4+}$ and $M^{6+} > M^{5+}$, then the group is:
Elsmoreite, if W is the dominant M^{6+} cation.

New root names were required for the new W- and Sb^{5+}-dominant pyrochlore groups. In accordance with Hogarth (1977), roméite will be the root name for species of the Sb^{5+}-dominant pyrochlore group because this is the name of the Ca–Na-dominant species. However, as no Ca–Na member has been established for the W-dominant pyrochlore group, we had to choose a root name among the four species that were considered valid: ferritungstite, alumotungstite, elsmoreite, and jixianite. The three first names are defined and distinguished on the basis of minor constituents at the *A* and *B* sites (*cf*. Ercit & Robinson 1994, Williams *et al*. 2005). In all three, vacancies are dominant at *A*, and W is the dominant species of the dominant valence at *B*, so by the criteria proposed here, these names refer to the same species. Ferritungstite would have historical precedence, as it was described in 1911 by Schaller.

Jixianite, described in 1979 by Liu Jianchang, refers to the mineral with Pb dominant at *A* and W at *B*. However, there is a problem with "ferritungstite" as the root name for a species of the W-dominant pyrochlore group: the name erroneously implies distinct crystallographic roles for W and Fe^{3+} in the structure of ferritungstite. In fact, Fe^{3+} is merely a subordinate cation at the W-dominant *B* site of the ferritungstite structure (Ercit & Robinson 1994), as is Al in the alumotungstite structure (≡ ferritungstite with subordinate Al: Ercit & Robinson 1994). The name could be jixianite, but in absence of a crystal-structure study, it is not possible to know the dominant anion of the dominant valence at the *Y* site of this mineral. Consequently, the name for this group, and the root name for all species of this group, will be **elsmoreite**. As a mineral group consists of two or more minerals (Mills *et al*. 2009), elsmoreite cannot really be considered, for now, as a mineral group. Hydrokenoelsmoreite should be designated as an unassigned member of the pyrochlore supergroup, because there is no other member to allow a group to be established.

Extensive solid-solution exists among Nb-, Ta-, and Ti-dominant pyrochlores. Hogarth (1977) delimited the betafite group from the Nb and Ta groups at the 33% mark in order to place more compositions in the sparsely populated field of betafite. We propose here that all group divisions be rearranged in accordance with the dominant valence at *B*, not by a single, dominant ion (see Fig. 2). Figures 2 and 3 were extracted from a preliminary version of this proposal made by the previous committee. Certainly, they include results of both microprobe and wet-chemical analyses. The two points near the Ti corner belong to betafite- and roméite-group minerals. Their apparent position in the far apex of the triangle is a projection artefact due to the absence of a Sb^{5+} corner in the diagram: Ti and Sb in nearly equal proportions are the dominant *B*-site cations in these minerals, with Nb and Ta almost completely absent. For example, one of the oxycalciobetafite compositions is $(Ca_{0.872}Ce_{0.609}Mn_{0.415}Na_{0.051}\square_{0.053})_{\Sigma 2.000}(Ti_{1.126}Sb_{0.783}Nb_{0.037}W_{0.033}Fe_{0.013}V_{0.008})_{\Sigma 2.000}O_6(O_{0.634}F_{0.068}\square_{0.053})$ (Brugger & Gieré 1999). Pyrochlore-type phases with *ca*. 2Ti are well known synthetically [*e.g*., $CaUTi_2O_7$ (Dickson *et al*. 1989), $Y_2Ti_2O_7$ (Matteucci *et al*. 2007)], but the clustering of natural compositions near (Nb, Sb):Ti = 1:1 suggests entropy stabilization at the middle of the solid-solution series. Relative lack of Ti–Ta solid solution is an important and interesting difference between Ta and Nb.

The new scheme of nomenclature based on two prefixes and a root name allows one to use the root names without prefixes, or with only one prefix [*e.g*.,"plumboelsmoreite"] to specify at least a group for minerals that have not been fully analyzed. The first prefix will refer to the dominant anion (or cation) of the dominant valence [or H_2O or □] at the *Y* site. The second prefix will refer to the dominant cation of the dominant valence [or H_2O or □] at the *A* site. Given the Classical Greek derivation of "oxy-", "hydro-" and "hydroxy-", we suggest "keno-" to represent "vacancy", from the Greek κενος, meaning "empty". The term *keno-* has been previously suggested by Permingeat (in van Wambeke 1971) as a prefix modifier for cation-deficient members of the pyrochlore supergroup. Where the first and second prefixes are equal, then only one prefix is applied ("hydropyrochlore", not "hydrohydropyrochlore"). The only problem is that we might want to use "hydropyrochlore" to mean any pyrochlore in the group of species with H_2O at the *Y* sites and unspecified *A*-site occupancies.

Hogarth (1977) assigned species names incorporating prefixes that were determined by the *A*-site composition of the pyrochlore formula. These prefixes were used to define names of new species where a cation other than Ca or Na made up more than 20% of the total number of *A*-site cations. The prefix specified the dominant cation that is not Na or Ca. For example, a member of the pyrochlore group with 25% Pb would be named plumbopyrochlore. This approach has been modified in the new system of nomenclature to reflect current knowledge of the crystal chemistry of pyrochlore-supergroup minerals, and also to bring pyrochlore nomenclature into better consistency with current best practice for complex solid-solutions (Hatert & Burke 2008). Like the *B* sites, the *A* sites of pyrochlores can contain species of several different charges. They can also contain a neutral molecular species, H_2O, and vacancies. Consistent with the procedure for the *B* site, it is possible to group *A*-site species into valence groups M^{1+}, M^{2+} and so on, and a zero-charge group for H_2O and vacant sites. The second prefix is then determined by the dominant species of the dominant-valence group, as follows.

The zero-charge group

The occupancy of the *A* position in pyrochlore-supergroup minerals by cations is in some cases very low (<50%). Where the zero-charge group exceeds any valence group of the *A* site, the second prefix "keno" is proposed for species in which □ exceeds H_2O, and the second prefix "hydro" is proposed for species in which H_2O exceeds □.

The dominant valence rule

The Hogarth (1977) rules of nomenclature that reflect the chemical composition at the *A* position have been modified to conform to the **dominant-valence rule**. Consequently, where neutral species are not the largest valence-based group at the *A* position, a second prefix is now to be applied for the dominant cation of the dominant valence. There is a natural clustering of compositions near Na = Ca = 1 *apfu* (Fig. 3), a charge-balancing requirement for members of the B^{5+} groups.

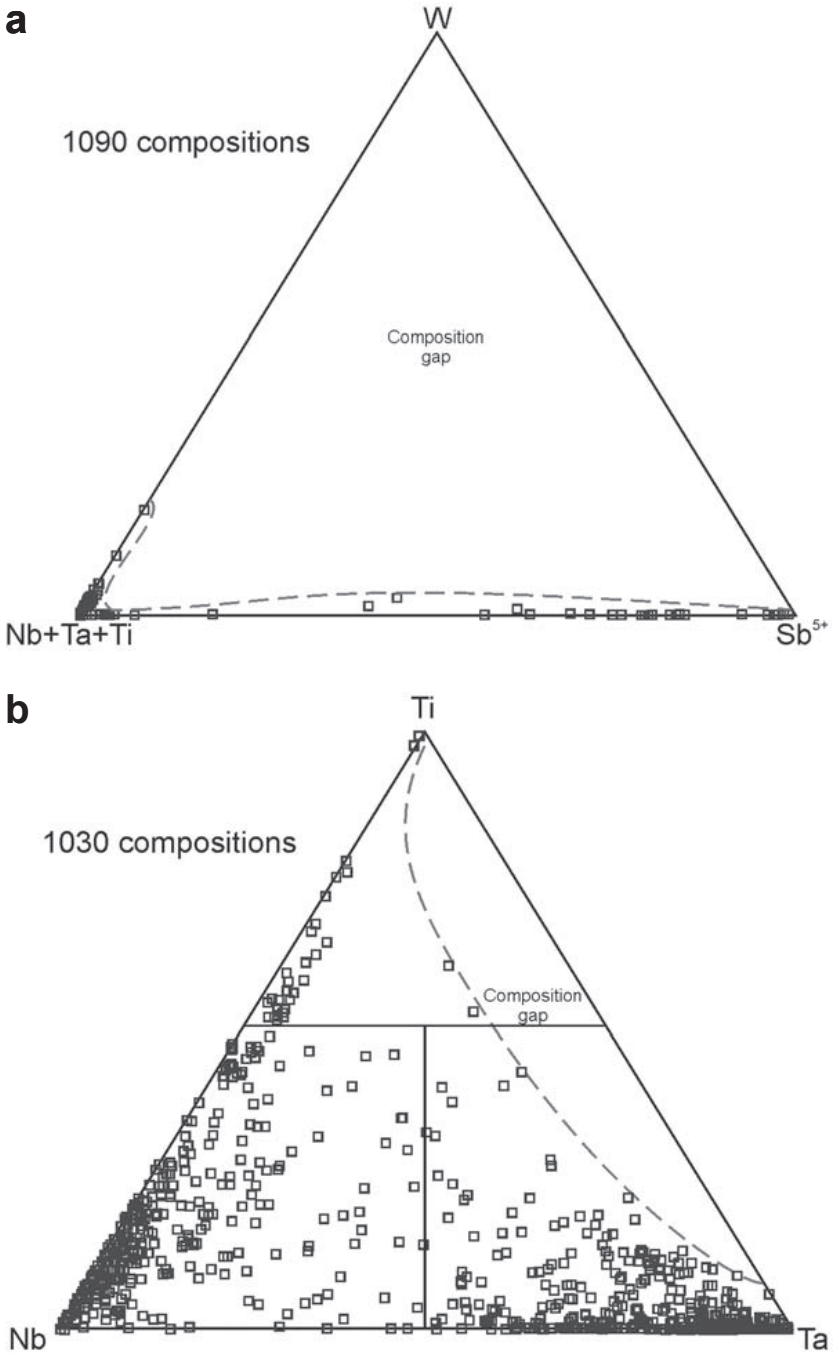

FIG. 2. Pyrochlore-supergroup minerals, *B*-site composition.

Hence, in Hogarth (1977), if the dominant cation was either Ca or Na, no prefix was used, and dominance of either of these cations was not indicated. Prefixes were only used to indicate substantial amounts of other cations. In order to regain consistency, it is proposed here to use second prefixes from now on in order to indicate Ca and Na predominance.

The pyrochlore supergroup presents complexities in the specification of end-member formulae, and also whether single-species names should correspond to single chemical end-members. For some species, a single unambiguous charge-balanced end-member formula cannot exist. For example, the fluornatromicrolite of Witzke *et al*. (IMA#98–018) exists with composition $(Na_{1.15}Ca_{0.70}Bi_{0.15})_{\Sigma 2}Ta_2O_6F$. Use of only dominant species at each site suggests the ideal "end-member" formula $Na_2Ta_2O_6F$, which is not electrostatically neutral and hence is physically impossible. In the real mineral, the heterovalent substitution $2Ca^{2+} = Bi^{3+} + Na^+$ takes place, so it is intermediate between the two charge-balanced end-members $NaCaTa_2O_6F$ and $Na_{1.5}Bi_{0.5}Ta_2O_6F$. These compositions have components of more than one valence on only one site, and thus are end-members in the sense of Hawthorne (2002). The boundary between these two end members is located at 50 mol.%, and corresponds to the composition $Na_{1.25}Ca_{0.5}Bi_{0.25}Ta_2O_6F$. The example above is close to this boundary, but has $NaCaTa_2O_6F$ predominant. Given the strong clustering of pyrochlore compositions near this end member, it is tempting to find a way to define this end member as corresponding to one species despite the 50:50 mixed occupancy of the *A* sites, in which case fluornatromicrolite would be a Bi-rich example of this species. We agree that it is unfortunate that a single composition field, with no major change in properties or paragenesis and with compositions clustering around the 50:50 mark, should be broken into Na-dominant and Ca-dominant halves. However, the division of the composition field does not really present a new nomenclatural difficulty. As the *A*-site and *Y*-site content of pyrochlore cannot be established without analysis, second prefixes can only be used with confidence for analyzed specimens. Compositions that are near the 50:50 composition can be explicitly flagged as being "near the 50:50 mark". Root names without prefixes are recommended for incompletely analyzed material.

Rigorous adherence to the principle of using a single dominant species in a dominant-valence group produces a mismatch between species and end members in pyrochlores. The charge-balanced end-member $NaCaTa_2O_6F$ is not at the center of the composition field of a species, but marks the boundary between fluornatromicrolite and fluorcalciomicrolite. Conversely, neither of these species names can be associated with a unique charge-balanced end-member. The formula $(Na_{1.5}Bi_{0.5})Ta_2O_6F$ is an example of one possible end-member for fluornatromicrolite, with neutrality maintained by the subordinate Bi^{3+} at the *A* site. The minor substituent need not be Bi: $(Na_{1.5}Y_{0.5})Ta_2O_6F$ and $(Na_{1.667}U_{0.333})Ta_2O_6F$ are examples of end members that would share

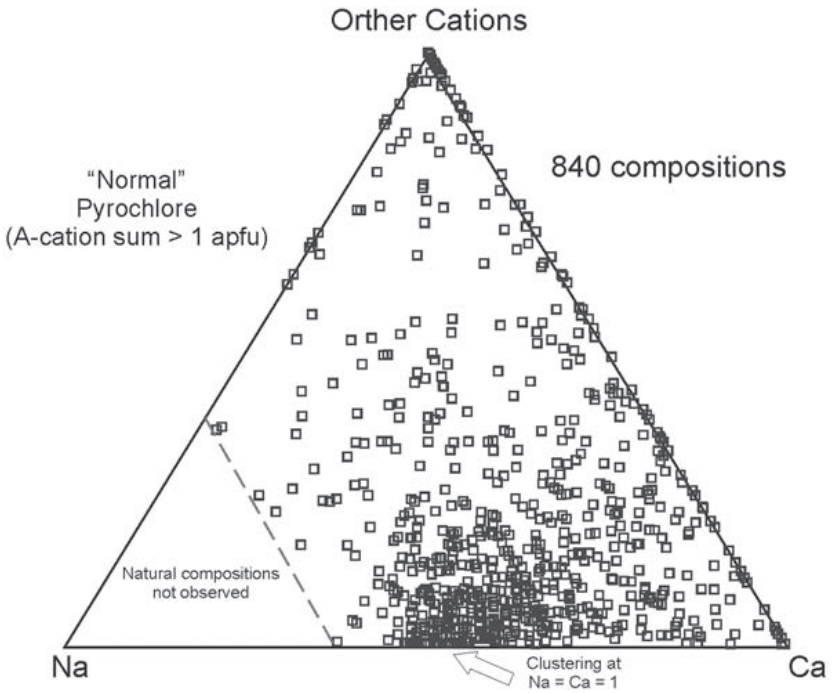

FIG. 3. Pyrochlore-supergroup minerals, *A*-site composition.

the same name in our scheme. In order to maintain simplicity and avoid proliferation of names, only the predominant Na is used to determine species, and we have a "one-to-many" mapping between names and some end members. These end members can collectively be represented as $(Na,\#)_2Ta_2O_6F$, where "#" is understood to mean a subordinate amount of an unspecified charge-balancing component. The situation is analogous for fluorcalciomicrolite, although the "#" components for that species would have a charge less than +1 rather than in excess of +2. In this scheme, the "fluornatromicrolite" composition above clearly pertains to fluornatromicrolite, with Ca and Bi as minor charge-balancing components. Mismatch of species and end members arises because the multiplicity of the *A* site (Na, Ca, *etc.*) is twice the multiplicity of the non-framework anion site (F, OH, O, H_2O), and the most common *B*-site and *Y*-site components require 50:50 occupancy of *A* by two different valences. This problem arises in many complex solid-solutions, and our solution for the pyrochlores may provide a template for the nomenclature of other mineral groups.

Nomenclature based on the dominant element in a dominant-valence group is simple and reproducible. This is not true for the alternative scheme of one end member is equal to one name, which is another reason for rejecting that model. In multidimensional coupled solutions, particularly where there are several different valence-groups at more than one site, it is not easy to define a rigorous, reproducible way of extracting a unique dominant end-member. An example is shown below.

Consider a formula such as $(Na_{1.1}Ca_{0.4}Y_{0.2}U_{0.2}\square_{0.1})(Nb_{1.7}Ti_{0.3})O_6(OH)$. Our rules quickly lead to the name "hydroxynatropyrochlore". However, it is possible to partition the various cations so as to find a great many end-members within it, for example:

0.08 $(\square_{1.25}U_{0.75})Nb_2O_6(OH)$
+ 0.14 $(NaU)Ti_2O_6(OH)$
+ 0.02 $Ca_2(NbTi)O_6(OH)$
+ 0.40 $(Na_{1.5}Y_{0.5})Nb_2O_6(OH)$
+ 0.36 $(NaCa)Nb_2O_6(OH)$

but this is not a unique decomposition of the formula into "Hawthornian" end-members. The following decomposition also corresponds to the same overall formula:

0.10 $(\square Y)Nb_2O_6(OH)$
+ 0.60 $(Na_{1.67}U_{0.33})Nb_2O_6(OH)$
+ 0.10 $(CaY)Ti_2O_6(OH)$
+ 0.10 $Ca_2(NbTi)O_6(OH)$
+ 0.10 $(NaCa)Nb_2O_6(OH)$

in which only two out of five end-members are the same, but their proportions are quite different! Even identifying the single dominant end-member unambiguously is not possible without careful definition of an elaborate procedure. The simplicity and reliability of our current scheme make it preferable.

Variability at the Y site

Pyrochlore-supergroup minerals show a variable *Y*-site composition. In the past, variations in *Y*-site occupancy were not reflected in species nomenclature, in part owing to a lack of knowledge of the structural chemistry of pyrochlore, but also owing to difficulties with the determination of some *Y* species. As the dominant constituent at the *Y* position can now commonly be established *via* EPMA and structure analysis, it is reasonable to indicate the composition of this site in the nomenclature. Rouse *et al.* (1998) demonstrated the presence of structural (OH) groups by infrared spectroscopy. The dominant-valence rule is also valid for anionic sites (Hatert & Burke 2008). Hence, a set of prefixes is to be used to indicate the dominant species of the dominant-valence group at the *Y* site. According to Lumpkin *et al.* (1986), a major difficulty is the determination of whether the "water" is present as OH or molecular H_2O. Borodin & Nazarenko (1957) assumed a total of seven anions and calculated the amount of OH necessary to achieve charge balance. Excess "water" was allocated as H_2O. In general, this procedure will not always be valid because of anion vacancies at the *Y* site (Pyatenko 1959, Aleshin & Roy 1962, Subramanian *et al.* 1983, Chakoumakos 1984). Assumptions involved in calculating structural formulae mainly affect O, OH, H_2O, and *Y*-site vacancies. The reader should be aware of these uncertainties in the following discussion. Some cases may be analyzed:

1) If the sum of cation valences is greater than 13.5, O will necessarily be the dominant species at the *Y* site, for reasons of charge balance.

2) If F exceeds 0.5 *apfu*, F will be considered as the dominant species at the *Y* site. The underlying assumption is that F orders at *Y*, which may not be correct in every case. A subset of data consisting of 32 oxyfluoride pyrochlores was considered separately by Chakoumakos (1984) to determine if any one of three possible anion configurations would yield better calculated values of the cell edge as compared with the observed values. The three anion configurations considered were: (1) $A_2B_2(O_6F)$, O and F disordered over *X* and *Y*; (2) $A_2B_2(O_5F)O$, O and F disordered over *X*, and O at *Y*, and (3) $A_2B_2X_6Y$, fully ordered with O at *X* and F at *Y*.

The regression statistics for the calculated *versus* the observed cell-edge for these three cases were not significantly different. Although arguments of electrostatic neutrality and calculations of Madelung energy rank the fully ordered case as the most likely distribution of anions, the cell edge does not appear to be sensitive

enough to distinguish among the three configurations of anions.

3) If the sum of cation valences is less than 13.5 and F is less than 0.5 *apfu*, O, OH, F, H_2O or □ can be the dominant species at the *Y* site. For example, an Na-dominant microlite sample with a valence sum of cations equal to 12.72 may have a formula ending with $\ldots O_{6.00}(\square_{0.45}F_{0.37}O_{0.17})_{\Sigma 1.00}$, $\ldots O_{6.00}[(H_2O)_{0.45}F_{0.37}O_{0.17}]_{\Sigma 1.00}$, $\ldots O_{6.00}[F_{0.37}(OH)_{0.35}\square_{0.28}]_{\Sigma 1.00}$, or $\ldots [O_{5.72}(OH)_{0.28}]_{\Sigma 6.00}[(OH)_{0.63}F_{0.37}]_{\Sigma 1.00}$. The name of this species would be kenonatromicrolite, hydronatromicrolite, fluornatromicrolite, or hydroxynatromicrolite, respectively. All these options may be equally correct without additional information. If, for some reason, it is not possible to know the dominant species of the dominant valence at the *Y* site, we suggest that a name with the anion prefix suppressed, such as "natromicrolite" be applied.

The new nomenclature system, therefore, results in mineral names of the type:

yaroot

where **root** is the name of the group, determined by the dominant species of the dominant-valence group at the *B* site, **y** indicates the dominant species of the dominant-valence group at the *Y* site, and **a** indicates the dominant species of the dominant-valence group at the *A* site.

Calculation of the Formula

Basis for formula calculation

Vacancies can occur at any of the *A*, *X* and *Y* sites, but have not been found to occur at the *B* site. Consequently, pyrochlore formulae should be calculated on the basis of an ideal number of *B* cations (2 *apfu*). See the section entitled "The formula" for a list of typical *B*-site cations to be used in the normalization.

The Si content

Pyrochlore-supergroup minerals that exhibit high Si contents are fairly common in geochemically evolved parageneses. The presence and structural role of Si in the structure of pyrochlore-supergroup minerals have been long debated but have been only partially resolved. Different explanations have been invoked to clarify the way in which Si is incorporated into natural pyrochlores, including the presence of Si as a dispersed crystalline or amorphous silicate phase (Hogarth 1977, Hogarth & Horne 1989, Voloshin *et al*. 1989), and its presence as an essential part of the structure. Despite the absence of tetrahedral sites suitable for Si incorporation in the pyrochlore structure, octahedral Si is possible: $Si(OH)_6^{2-}$ is stable at low pressure and temperature in thaumasite, $Ca_3[Si(OH)_6][SO_4][CO_3]\bullet 12H_2O$ (Edge & Taylor 1971). The real restriction on the occurrence of $^{[6]}Si$ in crystal structures is the crowding of cations around oxygen ions (O'Keeffe & Hyde 1981). Using TEM–EDX investigations combined with crystal-chemical considerations, Bonazzi *et al*. (2006) showed that a significant fraction (30–50%) of the Si detected by EMPA does in fact occupy the octahedral sites of the pyrochlore structure, whereas a larger fraction (50–70%) of Si is concentrated in radiation-damaged portions of the sample. On the basis of this observation, we could perhaps recommend that in the calculation of a formula, no more than 50% Si be attributed to *B*. Nevertheless, we prefer no recommendation on how to allot Si. The incorporation or not of Si into the pyrochlore-supergroup mineral structure should be investigated, but low Si contents can be included as a *B*-site cation or assumed to be due to contaminant phases, and this probably will not modify the name of the mineral. Synthetic pyrochlore-like phases have also been shown to contain Si at the *B* site (Reid *et al*. 1977). Results of two chemical analyses of pyrochlore-supergroup minerals presented by Uher *et al*. (1998) show Si as the dominant cation of the dominant valence at *B*. If it is proved that all the analyzed Si is really at this site, then a new pyrochlore group will exist and a new root name will have to be created.

The content of Cs, Rb and K

For stereochemical reasons, the very large Cs, Rb and K cations prefer the 8*b* (*Y*) site. They should not be assigned to the *A* position of the formula. Chemists refer to pyrochlore-supergroup minerals with very high numbers of vacancies at *A* and abundant Cs, Rb and K at *Y* as "inverse pyrochlores" (Ercit *et al*. 1993). No mineral with a predominance of these cations at *Y* has been described.

The content of F, OH and H_2O

The maximum amount of H_2O in the pyrochlore structure is controlled by the cation occupancy of the *A* site; the maximum content of H_2O ranges from 1.00 H_2O *pfu* for ideal pyrochlores (two *A* cations *pfu, i.e., m* = 0) to 1.75 H_2O *pfu* for *A*-deficient pyrochlores (no *A* cations, *i.e.*, *m* = 2; Ercit *et al*. 1994). Low *A*-site cation content, high displacement-parameters for the *Y*-site constituents, and the site splitting observed in some cases for the *Y* site indicate that the "O" at the *Y* sites can be H_2O. Ercit *et al*. (1994) found that H_2O molecules were actually displaced away from the ideal 8*b Y* sites, and partially occupied higher-multiplicity positions nearby. Displacements attained 0.57 Å along approximate <112> directions to 96*g Y*', or a similar distance along <111> to 32*e Y*" positions. A 192*i* position (*Y*"') very close to *Y*' was also located by Philippo *et al*.

(1995). Such displacements allow optimal distances between *A*- and *Y*-site species to be maintained.

For a normal pyrochlore AB_2X_6Y, in which *A* and *B* are cations, and *X* and *Y* are anions, there are no stereochemical constraints on the maximum occupancies of the *A* and *Y* sites. However, for pyrochlore-supergroup minerals with H_2O at both the *A* and *Y* sites, the maximum occupancies of both sites are limited owing to the short separation between the ideal *A* and *Y* sites, which is in the neighborhood of 2.3 Å (Ercit *et al*. 1994). Partial occupancy of the *A* site and positional disorder of H_2O at *A* and *Y* sites permit stable O...O separations for neighboring H_2O groups in pyrochlore. Ercit *et al*. (1994) found that positional disorder resulted in eight fractionally occupied *A'* sites around each *A* site, displaced from the ideal site by about 0.11 Å along <111> directions. Five of the eight are too close to the offset *Y*' and *Y*" positions to represent stable O...O separations for H_2O groups; however, three of the eight are sufficiently distant to represent stable intermolecular distances (averaging 2.74 Å). Philippo *et al*. (1995) reported a different scheme of displacement, in which H_2O partially occupies *A*" sites displaced from *A* by 0.75 Å along <100>. For synthetic *A*-cation-free pyrochlore, the maximum H_2O content *pfu* may be limited by the need to avoid close H_2O ... H_2O distances: if there is one H_2O group *pfu* at the *Y* site, then there can be only 3/8 H_2O groups at the *A* site. This constraint translates to a maximum of 1.75 H_2O *pfu* for *A*-cation-free pyrochlore. Previous refinements of the structures of H_2O-bearing pyrochlore have shown H_2O only in the vicinity of the *Y* site (*e.g.*, Groult *et al*. 1982). As no synthetic or natural pyrochlore has been found with all H_2O ordered at *A*, we presume that the *Y* site and its displaced variants are the preferred locations for H_2O, and that H_2O only enters the *A* sites if *Y* cannot accommodate more H_2O. The maximum amount of H_2O *pfu* in the pyrochlore structure is thus given as $1 + (3m/8)$. For an ideal pyrochlore with full *A*-site occupancies ($m = 0$), there can be no more than 1 H_2O *pfu*; as described above, the limit for *A*-deficient pyrochlore ($m = 2$) is 1.75 H_2O *pfu* (Ercit *et al*. 1994).

If there is a large deficit of cations at *A* and the analytical total is very low, we could suspect the presence of H_2O at *A* sites of the mineral. We can calculate the maximum possible amount of structural H_2O in the mineral and compare it with the analytical deficits in EPMA data. But one should neither assume that all H_2O in actinide-bearing, radiation-damaged pyrochlore-supergroup minerals is structural, nor that analytical deficits in EPMA data for pyrochlore-supergroup minerals are attributable to structural H_2O. Much of the H_2O in metamict or semi-metamict pyrochlore-supergroup minerals is adsorbed, and thus not structural. In this regard, it is interesting to note that chemical data on geologically young, non-metamict U-rich pyrochlore (Hogarth & Horne 1989) indicate low H_2O contents. If the H_2O content has been established directly and accurately, *e.g.*, by TGA, then it may indeed be shown that some H_2O must occupy the *A* sites. Unfortunately, we cannot monitor the content of a neutral species other than by density measurements, or from determination of the electron density in a structure, neither of which would be very accurate in the presence of significant heavy atoms. For nomenclature purposes, it will be important to know the H_2O content in *A* only if the total number of any valence group of *A*-site cations is exceeded by the zero-charge group. Two possibilities exist: (1) the cation deficit is comprised mainly of H_2O, and (2) the deficit mainly involves actual site-vacancies. If it is not possible to prove which of the two scenarios is correct, the expression "zero-valence-dominant species" can be used.

Names of Pyrochlore-Supergroup Species

The new names are presented below, in groups distinguished by the dominant *B* cation. For each group, a table is shown indicating the combinations of dominant species of the dominant-valence group at the *A* site and dominant species of the dominant-valence group at the *Y* site for which there is evidence of a mineral. With each table, a series of references is given for the corresponding species or potential species. Complete descriptions are missing for the majority of the pyrochlore-supergroup species. The seven names marked with an asterisk (*) refer to valid mineral species because of their complete descriptions. Fluornatromicrolite is an IMA-approved mineral, but the complete description has not yet been published. The other 20 names refer to minerals that need to be completely described in order to be approved as valid species. For these, there are only chemical or crystal-structure data. Type specimens need to be defined and deposited in public mineralogical museums. Potential candidates for several other species exist, but are not characterized well enough for any official status. Ancient chemical data derived by wet-chemical analyses commonly represent a mixture of minerals. These data were not used here. All data used were acquired by electron-microprobe analysis or were obtained by crystal-structure refinements. We also verified the scarcity of crystal-chemical data in the literature. Crystal-structure determination were made for only nine pyrochlore-supergroup minerals. The names of these species are marked with a dagger (†) in the tables. A serious problem is identified with the roméite-group minerals, because of an erroneous assumption that all the Sb is pentavalent.

Minerals of the pyrochlore group (Table 1)

In the listings that follow, the name attributed by the author or authors is shown is square brackets.

TABLE 1. PRESENT MEMBERS OF THE PYROCHLORE GROUP

Dominant at *A* site	Dominant species of the dominant-valence group at the *Y* site				
	OH	F	O	H_2O	□
Na		fluornatropyrochlore	oxynatropyrochlore		
Ca	hydroxycalciopyrochlore†	fluorcalciopyrochlore†	oxycalciopyrochlore*		
Sn^{2+}					
Sr		fluorstrontiopyrochlore			
Pb^{2+}			oxyplumbopyrochlore		kenoplumbopyrochlore
Sb^{3+}					
Y			oxyyttropyrochlore-(Y)		
U^{4+}					
H_2O				hydropyrochlore*†	
□		fluorkenopyrochlore			

In the left column are shown the dominant species of the dominant-valence group at the *A* site. An asterisk indicates a fully described species, and a dagger indicates that a structure refinement has been published.

fluornatropyrochlore

P.M. Kartashov (unpublished data)

oxynatropyrochlore

Hogarth & Horne (1989): anal. 3 [uranpyrochlore] is oxynatropyrochlore; anal. 1, 2 and 4 [uranpyrochlore], 5 and 6 [uranoan pyrochlore] are "natropyrochlore".
Knudsen (1989): at least three reported compositions are oxynatropyrochlore [pyrochlore].
Chukanov *et al*. (1999): the formula on page 41 [bismutopyrochlore].

hydroxycalciopyrochlore

Bonazzi *et al*. (2006) [pyrochlore]: only by crystal-structure study was it possible to confirm a hydroxycalciopyrochlore composition.

fluorcalciopyrochlore

There are several examples of analyzed fluorcalciopyrochlore [pyrochlore] in the literature, *e.g*., Hogarth (1961), Ohnenstetter & Piantone (1992), Nasraoui *et al*. (1999), Nasraoui & Bilal (2000), Seifert *et al*. (2000), Thompson *et al*. (2002), Lee *et al*. (2006). The crystal structure of fluorcalciopyrochlore was determined by Bonazzi *et al*. (2006).

oxycalciopyrochlore

There are several examples of analyzed oxycalciopyrochlore in the literature, *e.g*., Hogarth (1961), Černý *et al*. (1979) [the type "stibiobetafite"], Williams (1996), Chukanov *et al*. (1999) [formula on page 40], Mokhov *et al*. (2008) [Moon]. The type specimen of "stibiobetafite" described by Černý *et al*. (1979) should be considered as the type specimen of oxycalciopyrochlore.

fluorstrontiopyrochlore

Franchini *et al*. (2005): The "strontiopyrochlore" Ja–13 (first point) is fluorstrontiopyrochlore.

oxyplumbopyrochlore

Voloshin & Pakhomovskiy (1986), their anal. 1, Table 3.1.

kenoplumbopyrochlore

Voloshin & Pakhomovskiy (1986), their anal. 20, Table 3.1.

oxyyttropyrochlore-(Y)

Tindle & Breaks (1998): sample 96–29.

fluorkenopyrochlore

Kartashov *et al*. (1998): "strontiopyrochlore" 4, and "ceriopyrochlore" 8.
Schmitt *et al*. (2002): AM206 Pcl g1–s2 rim.

hydropyrochlore

The type sample of "kalipyrochlore" of van Wambeke (1978) and that of Ercit *et al*. (1994) [crystal structure determined] are hydropyrochlore. The type specimen of "kalipyrochlore" described by van Wambeke (1978) should be considered as the type specimen of hydropyrochlore.

Note that potential candidates for "fluorhydropyrochlore" exist [Nasraoui & Bilal (2000), the first "kalipyrochlore" and the first "ceriopyrochlore" samples of their Table 4; Xie *et al*. (2006), grain 1 Pyc–I and grain 3 Pyc–I)]

Minerals of the microlite group (Table 2)

TABLE 2. PRESENT MEMBERS OF THE MICROLITE GROUP

Dominant at *A* site	Dominant species of the dominant-valence group at the *Y* site				
	OH	F	O	H_2O	□
Na		fluornatromicrolite			
Ca		fluorcalciomicrolite	oxycalciomicrolite		
Sn^{2+}			oxystannomicrolite*		
Sr					
Pb^{2+}					kenoplumbomicrolite†
Sb^{3+}			oxystibiomicrolite*		
Y					
U^{4+}					
H_2O				hydromicrolite	
□	hydroxykenomicrolite*†			hydrokenomicrolite	

In the left column are shown the dominant species of the dominant-valence group at the *A* site. An asterisk indicates a fully described species, and a dagger indicates that a structure refinement has been published.

fluornatromicrolite

The IMA proposal 98–018 for fluornatromicrolite (Witzke *et al*. 1998) was approved, but the complete paper is only now in press. Some data were published by Atencio (2000). Chemical compositions that correspond to fluornatromicrolite from other occurrences are available in the papers by Ohnenstetter & Piantone (1992), Belkasmi *et al*. (2000), Huang *et al*. (2002) and Baldwin *et al*. (2005).

fluorcalciomicrolite

There are several compositions of fluorcalciomicrolite in the literature, *e.g*., Lumpkin *et al*. (1986), Baldwin (1989), Ohnenstetter & Piantone (1992), Tindle & Breaks (1998), Huang *et al*. (2002), Geisler *et al*. (2004), Tindle *et al*. (2005).

oxycalciomicrolite

Černý *et al*. (2004) [stibiomicrolite]; Guastoni *et al*. (2008) [microlite].

oxystannomicrolite

Vorma & Siivola (1967) [sukulaite]; Ercit *et al*. (1987) [stannomicrolite]. The type specimen of "sukulaite" described by Vorma & Siivola (1967) should be considered as the type for oxystannomicrolite.

kenoplumbomicrolite

Bindi *et al*. (2006b): crystal-structure study of kenoplumbomicrolite.

oxystibiomicrolite

Groat *et al*. (1987): the type sample of "stibiomicrolite"; Novák & Černý (1998). The type specimen of "stibiomicrolite" described by Groat *et al*. (1987) should be considered as the type specimen of oxystibiomicrolite.

hydrokenomicrolite

M.B. Andrade & D. Atencio (unpublished data).

hydromicrolite

M.B. Andrade & D. Atencio (unpublished data).

hydroxykenomicrolite

Ercit *et al*. (1993): crystal-structure study of "cesstibtantite". The type specimen of "cesstibtantite" described by Voloshin *et al*. (1981) should be considered as the type specimen of hydroxykenomicrolite.

Minerals of the betafite group (Table 3)

TABLE 3. PRESENT MEMBERS OF THE BETAFITE GROUP

Dominant at *A* site	Dominant species of the dominant-valence group at the *Y* site				
	OH	F	O	H_2O	□
Na					
Ca			oxycalciobetafite†		
Sn^{2+}					
Sr					
Pb^{2+}					
Sb^{3+}					
Y					
U^{4+}			oxyuranobetafite		
H_2O					
□					

In the left column are shown the dominant species of the dominant-valence group at the *A* site. A dagger indicates that a structure refinement has been published.

oxycalciobetafite

Meyer & Yang (1988) [yttrobetafite-(Y)]: no H_2O reported in the analytical results, as this is a lunar mineral; Brugger & Gieré (1999); Cámara *et al*. (2004): crystal structure determined.

oxyuranobetafite

Mokhov *et al*. (2008), from the Moon.

Minerals of the roméite group (Table 4)

TABLE 4. PRESENT MEMBERS OF THE ROMÉITE GROUP

Dominant at *A* site	Dominant species of the dominant-valence group at the *Y* site				
	OH	F	O	H_2O	□
Na		fluornatroroméite†			
Ca	hydroxycalcioroméite*†	fluorcalcioroméite	oxycalcioroméite		
Sn^{2+}					
Sr					
Pb^{2+}			oxyplumboroméite		
Sb^{3+}					
Y					
U^{4+}					
H_2O					
□					

In the left column are shown the dominant species of the dominant-valence group at the *A* site. An asterisk indicates a fully described species, and a dagger indicates that a structure refinement has been published.

fluornatroroméite

Matsubara *et al*. (1996): crystal structure determined.

hydroxycalcioroméite

Rouse *et al*. (1998) and Zubkova *et al*. (2000): crystal structure determined ["lewisite"]. The type specimen of "lewisite" described by Hussak & Prior (1895) should be considered as the type specimen of hydroxycalcioroméite.

fluorcalcioroméite

Brugger *et al*. (1997), Uher *et al*. (1998), Brugger & Gieré (1999).

oxycalcioroméite

Christy & Gatedal (2005).

oxyplumboroméite

Christy & Gatedal (2005) [bindheimite].

Minerals of the elsmoreite group (Table 5)

TABLE 5. PRESENT MEMBER OF THE ELSMOREITE GROUP

Dominant at *A* site	Dominant species of the dominant-valence group at the *Y* site				
	OH	F	O	H_2O	□
Na					
Ca					
Sn^{2+}					
Sr					
Pb^{2+}					
Sb^{3+}					
Y					
U^{4+}					
H_2O					
□				hydrokenoelsmoreite*†	

In the left column are shown the dominant species of the dominant-valence group at the *A* site. An asterisk indicates a fully described species, and a dagger indicates that a structure refinement has been published.

hydrokenoelsmoreite

Schaller (1911) ["ferritungstite"]; Sahama (1981) ["alumotungstite"]; Ercit & Robinson (1994) ["ferritungstite"]: crystal structure determined; Williams *et al*. (2005) ["elsmoreite"]. The type specimen of "elsmoreite" described by Williams *et al*. (2005) should be considered as the type specimen of hydrokenoelsmoreite.

Correspondence Between Old and New Names

All the following mineral names shown in italics should be discarded, as they do not correspond to distinct species in the new classification. Note that there is not a one-to-one correlation between the new names and the traditional names in the literature.

Kalipyrochlore

Kalipyrochlore of van Wambeke (1978) is insufficiently K-rich to warrant the name "kalipyrochlore". The type sample and that of Ercit *et al*. (1994) are examples of hydropyrochlore, with H_2O dominant at both the *A* and *Y* sites. Additional data for samples from the type occurrence are given by Wall *et al*. (1996).

Strontiopyrochlore

Strontiopyrochlore of Lapin *et al*. (1986), Lottermoser & England (1988), Voloshin *et al*. (1989), Wall *et al*. (1996), Kartashov *et al*. (1998), Chakhmouradian & Mitchell (1998, 2002), and Franchini *et al*. (2005) [except fluorstrontiopyrochlore] are Ca- or zero-valent-dominant pyrochlore.

Bariopyrochlore

Bariopyrochlore of Jäger *et al*. (1959) ["pandaite"], Knudsen (1989), Wall *et al*. (1996), Williams *et al*. (1997), Subbotin & Subbotina (2000), and Bindi *et al*. (2006a) are all zero-valent-dominant pyrochlore.

Plumbopyrochlore

Plumbopyrochlore of Skorobogatova *et al*. (1966), Kartashov *et al*. (1992), Voloshin *et al*. (1993), Kovalenko *et al*. (1995), and Xie *et al*. (2006) is "plumbopyrochlore". Plumbopyrochlore of Chakhmouradian & Mitchell (2002), Wang *et al*. (2003), and Beurlen *et al*. (2005) is zero-valent-dominant pyrochlore. Plumbopyrochlore of Voloshin & Pakhomovskiy (1986) corresponds to oxyplumbopyrochlore [their anal. 1, Table 3.1], kenoplumbopyrochlore [their anal. 20, Table 3.1] and "plumbopyrochlore" [several compositions].

Bismutopyrochlore

Bismutopyrochlore of Chukanov *et al*. (1999) and Ercit *et al*. (2003) is zero-valent-dominant pyrochlore.

Ceriopyrochlore-(Ce)

Ceriopyrochlore-(Ce) of Weidmann & Lenher (1907), van Wambeke (1980), Wall *et al*. (1996), Chakhmouradian (1996), and Zurevinski & Mitchell (2004) is Ca- or zero-valent-dominant pyrochlore.

Yttropyrochlore-(Y)

Yttropyrochlore-(Y) of Kalita (1957) ["obruchevite"], and Ercit *et al*. (2003) is a zero-valent-dominant mineral. Yttropyrochlore-(Y) of Tindle & Breaks (1998) is oxyyttropyrochlore-(Y).

Uranpyrochlore

For all recorded cases of uranpyrochlore, U is not the dominant cation of the dominant valence at *A*, except for sample 9 from Khibina studied by Chakhmouradian & Mitchell (2002). Nevertheless, it is not possible to know the dominant anion of the dominant valence at the *Y* site of this mineral. It should be referred as "uranopyrochlore". Uranpyrochlore of Hogarth & Horne (1989) is "natropyrochlore".

Stannomicrolite

The stannomicrolite species of Ercit *et al*. (1987) ["sukulaite" of Vorma & Siivola (1967)] is oxystannomicrolite. The stannomicrolite of Uher *et al*. (2008) is Ca- or zero-valent-dominant microlite.

Plumbomicrolite

The plumbomicrolite of Safiannikoff & van Wambeke (1961), Beurlen *et al*. (2005) and Uher *et al*. (2008) is zero-valent-dominant microlite. The plumbomicrolite of Bindi *et al*. (2006b) is, by crystal-structure refinement, kenoplumbomicrolite.

Stibiomicrolite

The type sample for stibiomicrolite (Groat *et al*. 1987) and also the sample of Novák & Černý (1998) are now to be classified as oxystibiomicrolite. Two compositions by Černý *et al*. (2004) are oxycalciomicrolite, and one is "calciomicrolite". The stibiomicrolite of Beurlen *et al*. (2005) is zero-valent-dominant microlite.

Bismutomicrolite

The composition claimed for the original bismutomicrolite ["westgrenite"] (von Knorring & Mrose 1963) probably refers to a mixture. The bismutomicrolite studied by Erichsen de Oliveira *et al*. (1970) and Tindle & Breaks (1998) is zero-valent-dominant microlite.

Bariomicrolite

The bariomicrolite species of Hogarth (1977), the "rijkeboerite" of van der Veen (1963), is too poor in Ba to warrant this name. The type sample apparently has □ dominant at the *A* position and H_2O at the *Y* position, and as such is probably hydrokenomicrolite. The bariomicrolite studied by Beurlen *et al*. (2005) is probably also hydrokenomicrolite.

Uranmicrolite

No samples described as uranmicrolite ("djalmaite" of Guimarães 1939) (*e.g*., Baldwin 1989, Rub *et al*. 1998, Tindle & Breaks 1998, Novák & Černý 1998, Zhang *et al*. 2004, Breiter *et al*. 2007, van Lichtervelde *et al*. 2007, Uher *et al*. 2007) are rich enough in U to warrant a status as a separate species.

Cesstibtantite

Cesstibtantite was described originally at Vasin Myl'k Mountain in Voronie Tundry, the Kola Peninsula, Russia, by Voloshin *et al*. (1981). Other occurrences were described in Manitoba, Canada, by Ercit *et al*. (1985), at Mt. Holland, Australia, by Nickel & Robinson (1985), and at Utö, Sweden, by Smeds *et al*. (1999). The crystal structure of cesstibtantite from Vasin Myl'k Mountain and Manitoba was solved by Ercit *et al*. (1993). Both are now to be classified as hydroxykenomicrolite. The two other samples are also zero-valent-dominant microlite, but it is not possible prove that they are hydroxykenomicrolite.

Natrobistantite

Natrobistantite studied by Voloshin *et al*. (1983) and by Beurlen *et al*. (2005) are both zero-valent-dominant microlite.

Calciobetafite

Hogarth (1977) defined betafite as a uranium-rich Ti-dominant pyrochlore, hence the origin of calciobetafite, a calcium-dominant Ti-rich pyrochlore (Mazzi & Munno 1983). However, all published analytical data on (non-defect) betafite have Ca in excess of U [except the mineral from the Moon studied by Mokhov *et al*. (2008) (oxyuranobetafite)]; consequently, by current standards, betafite is defined as a calcium-rich and Ti-dominant pyrochlore. This renders the name

calciobetafite redundant, and has the added effect of bringing members of the betafite group in line with the other groups (furthermore, type calciobetafite is Nb-dominant, not Ti-dominant, and belongs to the pyrochlore group).

Stibiobetafite

Černý *et al*. (1979) defined stibiobetafite as the Sb^{3+} analogue of betafite; however, the type sample has Nb + Ta > Ti *apfu*, and Ca is the dominant species of the dominant-valence group at the *A* site. The type sample is now to be classified as oxycalciopyrochlore. It is not possible to calculate the formula of stibiobetafite studied by Tindle & Breaks (1998) owing to errors in the table of analytical data.

Plumbobetafite

Plumbobetafite of Ganzeev *et al*. (1969) is zero-valent-dominant pyrochlore. Plumbobetafite of Voloshin *et al*. (1993) is "plumbobetafite".

Yttrobetafite-(Y)

Yttrobetafite-(Y) of Kalita (1959) and Liferovich & Mitchell (2005) are zero-valent-dominant pyrochlore. Yttrobetafite-(Y) from the Moon (Meyer & Yang 1988) is oxycalciobetafite.

Lewisite

Crystal-structure studies (Rouse *et al*. 1998, Zubkova *et al*. 2000) proved "lewisite" to be hydroxycalcioroméite.

Stetefeldtite

Very old references (Riotte 1867, Mason & Vitaliano 1953). Probably "argento-roméite". This material needs to be examined chemically and structurally.

Stibiconite

Original material described by Beudant (1837). Probably "stibioroméite". No electron-microprobe data are available. This material needs to be examined chemically and structurally.

Bindheimite

Original material described by Dana (1868). Only with the data of Christy & Gatedal (2005) is it possible to correlate this mineral with oxyplumboroméite.

Monimolite

The problematical species monimolite (Igelström 1865, Mason & Vitaliano 1953) is almost certainly identical with oxyplumboroméite, but needs re-examination.

Bismutostibiconite

The mineral was described by Walenta (1983). The chemical data are considered inadequate owing to a standardless energy-dispersion spectroscopy (EDS), with all Sb assumed to be 5+, and results of the analysis normalized to 100%. It probably is "bismutoroméite". Needs a chemical and structural investigation.

Partzite

Arents (1867). Probably "cuproroméite". No electron-microprobe data. This material needs to be examined chemically and structurally.

Ferritungstite and alumotungstite

Ferritungstite (Schaller 1911, Ercit & Robinson 1994) and alumotungstite (Sahama 1981) are hydrokenoelsmoreite.

Jixianite

Jixianite (Liu 1979) is "plumboelsmoreite". In the absence of a crystal-structure study, it is not possible to know the dominant anion of the dominant valence at the *Y* site of jixianite.

The Formula of Selected Species

Formulae are given in Table 6 for all 28 pyrochlore species for which we have analytical evidence. Note that subordinate components at the *A*, *B*, *X* or *Y* sites have no nomenclatural significance. We show specific examples here that are typical of the minor components observed, but any of these could be replaced by "#", indicating an unspecified heterovalent species required for charge balance.

TABLE 6. FORMULAE OF ALL 28 PYROCHLORE SPECIES FOR WHICH ANALYTICAL EVIDENCE IS DEEMED ADEQUATE

1	oxycalciopyrochlore*	$Ca_2Nb_2O_6O$
2	hydropyrochlore*†	$(H_2O,\square)_2Nb_2(O,OH)_6(H_2O)$
3	hydroxykenomicrolite*†	$(\square,Na,Sb^{3+})_2Ta_2O_5(OH)$
4	oxystannomicrolite*	$Sn_2Ta_2O_6O$
5	oxystibiomicrolite*	$(Sb^{3+},Ca)_2Ta_2O_6O$
6	hydroxycalcioroméite*†	$(Ca,Sb^{3+})_2(Sb^{5+},Ti)_2O_6(OH)$
7	hydrokenoelsmoreite*†	$\square_2W_2O_6(H_2O)$
8	fluornatromicrolite	$(Na,Ca,Bi)_2Ta_2O_6F$
9	hydroxycalciopyrochlore†	$(Ca,\square)_2Nb_2(O,OH)_6(OH)$
10	fluorcalciopyrochlore†	$(Ca,\square)_2Nb_2(O,OH)_6F$
11	kenoplumbopyrochlore†	$(Pb,\square)_2Nb_2O_5(\square,O)$
12	oxycalciobetafite†	$Ca_2(Ti,Nb)_2O_6O$
13	fluornatroroméite†	$(Na,Ca)_2Sb_2(O,OH)_6F$
14	fluornatropyrochlore	$(Na,REE,Ca)_2Nb_2(O,OH)_6F$
15	oxynatropyrochlore	$(Na,Ca,U)_2Nb_2O_6(O,OH)$
16	fluorstrontiopyrochlore	$(Sr,\square)_2Nb_2(O,OH)_6F$
17	oxyplumbopyrochlore	$Pb_2Nb_2O_6O$
18	oxyyttropyrochlore-(Y)	$(Y,\square)_2Nb_2O_6O$
19	fluorkenopyrochlore	$(\square,Na,Ce,Ca)_2(Nb,Ti)_2O_6F$
20	fluorcalciomicrolite	$(Ca,Na)_2Ta_2O_6F$
21	oxycalciomicrolite	$Ca_2Ta_2O_6O$
22	kenoplumbomicrolite	$(Pb,\square)_2Ta_2O_6(\square,O,OH)$
23	hydromicrolite	$(H_2O,\square)_2Ta_2(O,OH)_6(H_2O)$
24	hydrokenomicrolite	$(\square,H_2O)_2Ta_2(O,OH)_6(H_2O)$
25	oxyuranobetafite	$(U,Ca,\square)_2(Ti,Nb)_2O_6O$
26	fluorcalcioroméite	$(Ca,Sb^{3+})_2(Sb^{5+},Ti)_2O_6F$
27	oxycalcioroméite	$Ca_2Sb_2O_6O$
28	oxyplumboroméite	$Pb_2Sb_2O_6O$

An asterisk indicates a fully described species, and a dagger indicates that a structure refinement has been published, as indicated in Tables 1 to 5.

Index of Mineral Names

We show in Table 7 the correspondence between published names (with references) and the new names proposed, with an indication of the recommended fate of the old name.

Acknowledgements

We acknowledge Stuart Mills, Dana Griffen, Bill Birch, Frédéric Hatert, Ernst Burke, Robert F. Martin, Andrey Bulakh and all members of the IMA Commission on New Minerals, Nomenclature and Classification for their helpful suggestions and comments, and FAPESP (Fundação de Amparo à Pesquisa do Estado de São Paulo) for financial support (processes 2008/04984–7 and 2009/09125–5).

References

Aleshin, E. & Roy, R. (1962): Crystal chemistry of pyrochlore. *American Ceramic Society Journal* **45**, 18-25.

Arents, A. (1867): Partzite, a new mineral. *American Journal of Science* **93**, 362.

Atencio, D. (2000): *Type Mineralogy of Brazil* (first ed.). Museu de Geociências, Universidade de São Paulo, São Paulo, Brazil.

Baldwin, J.R. (1989): Replacement phenomena in tantalum minerals from rare-metal pegmatites in South Africa and Namibia. *Mineralogical Magazine* **53**, 571-581.

Baldwin, J.R., Hill, P.G., Finch, A.A., von Knorring, O. & Oliver, G.J.H. (2005): Microlite–manganotantalite exsolution lamellae: evidence from rare-metal pegmatite, Karibib, Namibia. *Mineralogical Magazine* **69**, 917-935.

Belkasmi, M., Cuney, M., Pollard, P.J. & Bastoul, A. (2000): Chemistry of the Ta–Nb–Sn–W oxide minerals from the Yichun rare metal granite (SE China): genetic implications and comparison with Moroccan and French Hercynian examples. *Mineralogical Magazine* **64**, 507-523.

Beudant, F.S. (1837): *Traité élémentaire de Minéralogie* (deuxième édition). Carilian Jeune, Libraire, Paris, France.

Beurlen, H., Soares, D.R., Thomas, R., Prado-Borges, L.E. & Castro, C. (2005): Mineral chemistry of tantalate species new in the Borborema Pegmatitic Province, northeast Brazil. *Anais da Academia Brasileira de Ciências* **77**, 169-182.

Bindi, L., Petříček, V., Withers, R.L., Zoppi, M. & Bonazzi, P. (2006a): A novel high-temperature commensurate superstructure in a natural bariopyrochlore: a structural study by

TABLE 7. THE CORRESPONDENCE BETWEEN PUBLISHED NAMES AND THE NEW NAMES PROPOSED

Current name	New name	Discredit, redefine, new species	References
–	"fluornatropyrochlore"	possible new species	P.M. Kartashov (unpublished data)
–	"hydromicrolite"	possible new species	Andrade & Atencio (unpublished data)
–	"hydrokenomicrolite"	possible new species	Andrade & Atencio (unpublished data)
alumotungstite	= hydrokenoelsmoreite	discredited	Sahama (1981)
bariomicrolite	probably "hydrokenomicrolite"	discredited	van der Veen (1963), Beurlen *et al.* (2005)
bariopyrochlore	= zero-valent-dominant pyrochlore	discredited	Jager *et al.* (1959), Knudsen (1989), Wall *et al.* (1996), Williams *et al.* (1997), Subbotin & Subbotina (2000), Bindi *et al.* (2006a)
betafite	"oxycalciobetafite"	possible new species	Brugger & Gieré (1999), Cámara *et al.* (2004)
betafite	"oxyuranobetafite"	possible new species	Mokhov *et al.* (2008)
bindheimite	"oxyplumboroméite"	possible new species	Christy & Gatedal (2005)
bindheimite	probably "plumboroméite"	discredited	Dana (1868)
bismutomicrolite	probably a mixture	discredited	Von Knorring & Mrose (1963)
bismutomicrolite	= zero-valent-dominant microlite	discredited	Erichsen de Oliveira *et al.* (1970), Tindle & Breaks (1998)
bismutopyrochlore	"oxynatropyrochlore"	possible new species	Chukanov *et al.* (1999)
bismutopyrochlore	= zero-valent-dominant pyrochlore	discredited	Chukanov *et al.* (1999), Ercit *et al.* (2003)
bismutostibiconite	probably "bismutoroméite".	discredited	Walenta (1983)
calciobetafite	a pyrochlore-group mineral	discredited	Mazzi & Munno (1983)
ceriopyrochlore-(Ce)	"fluorkenopyrochlore"	possible new species	Kartashov *et al.* (1998)
ceriopyrochlore-(Ce)	= Ca- or zero-valent-dominant pyrochlore	discredited	Weidmann & Lenher (1907), van Wambeke (1980), Wall *et al.* (1996), Chakhmouradian (1996), Zurevinski & Mitchell (2004)
cesstibtantite	hydroxykenomicrolite	redefined	Voloshin *et al.* (1981), Ercit *et al.* (1993)
cesstibtantite	= zero-valent-dominant microlite	discredited	Nickel & Robinson (1985), Smeds *et al.* (1999)
elsmoreite	hydrokenoelsmoreite	redefined	Williams *et al.* (2005)
ferritungstite	= hydrokenoelsmoreite	discredited	Schaller (1911), Ercit & Robinson (1994)
fluornatromicrolite	"fluornatromicrolite"	approved (IMA#98-018)	Witzke *et al.* (1998), Ohnenstetter & Piantone (1992), Belkasmi *et al.* (2000), Huang *et al.* (2002), Baldwin *et al.* (2005)
jixianite	"plumboelsmoreite".	discredited	Liu (1979)
kalipyrochlore	hydropyrochlore	redefined	van Wambeke (1978), Ercit *et al.* (1994)
lewisite	hydroxycalcioroméite	redefined	Hussak & Prior (1895), Rouse *et al.* (1998), Zubkova *et al.* (2000)
microlite	"fluorcalciomicrolite"	possible new species	Lumpkin *et al.* (1986), Baldwin (1989), Ohnenstetter & Piantone (1992), Tindle & Breaks (1998), Huang *et al.* (2002), Geisler *et al.* (2004), Tindle *et al.* (2005).
microlite	"oxycalciomicrolite"	possible new species	Guastoni *et al.* (2008)
monimolite	probably "oxyplumboroméite"	discredited	Igelström (1865), Mason & Vitaliano (1953)
natrobistantite	= zero-valent-dominant microlite	discredited	Voloshin *et al.* (1983), Beurlen *et al.* (2005)
partzite	probably "cuproroméite"	discredited	Arents (1867)
plumbobetafite	= zero-valent-dominant pyrochlore	discredited	Ganzeev *et al.* (1969)
plumbobetafite	= "plumbobetafite"	discredited	Voloshin *et al.* (1993)
plumbomicrolite	"kenoplumbomicrolite"	possible new species	Bindi *et al.* (2006b)
plumbomicrolite	zero-valent-dominant microlite	discredited	Safiannikoff & van Wambeke (1961), Beurlen *et al.* (2005), Uher *et al.* (2008)
plumbopyrochlore	"oxyplumbopyrochlore"	possible new species	Voloshin & Pakhomovskiy (1986)
plumbopyrochlore	"kenoplumbopyrochlore"	possible new species	Voloshin & Pakhomovskiy (1986)
plumbopyrochlore	= "plumbopyrochlore".	discredited	Skorobogatova *et al.* (1966), Voloshin & Pakhomovskiy (1986), Kartashov *et al.* (1992), Voloshin *et al.* (1993), Kovalenko *et al.* (1995), Xie *et al.* (2006)
plumbopyrochlore	= zero-valent-dominant pyrochlore	discredited	Chakhmouradian & Mitchell (2002), Wang *et al.* (2003), Beurlen *et al.* (2005)
pyrochlore	"oxynatropyrochlore"	possible new species	Knudsen (1989)
pyrochlore	"hydroxycalciopyrochlore"	possible new species	Bonazzi *et al.* (2006)
pyrochlore	"fluorcalciopyrochlore"	possible new species	Hogarth (1961), Ohnenstetter & Piantone (1992), Nasraoui *et al.* (1999), Nasraoui & Bilal (2000), Seifert *et al.* (2000), Thompson *et al.* (2002), Lee *et al.* (2006), Bonazzi *et al.* (2006)
pyrochlore	"fluorkenopyrochlore"	possible new species	Schmitt *et al.* (2002)
roméite	"fluornatroroméite"	possible new species	Matsubara *et al.* (1996)

TABLE 7 (cont'd). THE CORRESPONDENCE BETWEEN PUBLISHED NAMES AND THE NEW NAMES PROPOSED

Current name	New name	Discredit, redefine, new species	References
roméite	"fluorcalcioroméite"	possible new species	Brugger *et al.* (1997), Uher *et al.* (1998), Brugger & Gieré (1999)
roméite	"oxycalcioroméite"	possible new species	Christy & Gatedal (2005)
stannomicrolite	oxystannomicrolite	redefined	Vorma & Siivola (1967), Ercit *et al.* (1987)
stannomicrolite	= Ca- or zero-valent-dominant microlite	discredited	Uher *et al.* (2008)
stetefeldtite	probably "argentoroméite"	discredited	Riotte (1867), Mason & Vitaliano (1953)
stibiconite	probably "stibioroméite"	discredited	Beudant (1837)
stibiobetafite	oxycalciopyrochlore	redefined	Černý *et al.* (1979)
stibiobetafite	? (errors in the table of analyses)	discredited	Tindle & Breaks (1998)
stibiomicrolite	"oxycalciomicrolite"	possible new species	Černý *et al.* (2004)
stibiomicrolite	oxystibiomicrolite	redefined	Groat *et al.* (1987), Novák & Černý (1998)
stibiomicrolite	calciomicrolite	discredited	Černý *et al.* (2004)
stibiomicrolite	= zero-valent-dominant microlite	discredited	Beurlen *et al.* (2005)
strontiopyrochlore	"fluorstrontiopyrochlore"	possible new species	Franchini *et al.* (2005)
strontiopyrochlore	"fluorkenopyrochlore"	possible new species	Kartashov *et al.* (1998)
strontiopyrochlore	= Ca or zero-valent pyrochlore	discredited	Lapin *et al.* (1986), Lottermoser & England (1988), Voloshin *et al.* (1989), Wall *et al.* (1996), Kartashov *et al.* (1998), Chakhmouradian & Mitchell (1998 and 2002), Franchini *et al.* (2005)
uranmicrolite	not sufficiently rich in U	discredited	Guimarães (1939), Baldwin (1989), Rub *et al.* (1998), Tindle & Breaks (1998), Novák & Černý (1998), Zhang *et al.* (2004), Breiter *et al.* (2007), van Lichtervelde *et al.* (2007), Uher *et al.* (2007)
uranpyrochlore	"oxynatropyrochlore"	possible new species	Hogarth & Horne (1989)
uranpyrochlore	= "uranopyrochlore"	discredited	Chakhamouradian & Mitchell (2002)
uranpyrochlore	natropyrochlore	discredited	Hogarth & Horne (1989)
yttrobetafite-(Y)	"oxycalciobetafite"	possible new species	Meyer & Yang (1988)
yttrobetafite-(Y)	= zero-valent-dominant pyrochlore	discredited	Kalita (1959), Liferovich & Mitchell (2005)
yttropyrochlore-(Y)	"oxyyttropyrochlore-(Y)"	possible new species	Tindle & Breaks (1998)
yttropyrochlore-(Y)	= zero-valent-dominant minerals	discredited	Kalita (1957), Ercit *et al.* (2003)

means of a multiphase crystal structure refinement. *Journal of Solid State Chemistry* **179**, 729-738.

Bindi, L., Zoppi, M. & Bonazzi, P. (2006b): Plumbomicrolite from the Ploskaya Mountain, Keivy Massif, Kola Peninsula, Russia: composition and crystal structure. *Periodico di Mineralogia* **75**, 51-58.

Bonazzi, P., Bindi, L., Zoppi, M., Capitani, G.C. & Olmi, F. (2006): Single-crystal diffraction and transmission electron microscopy studies of "silicified" pyrochlore from Narssârssuk, Julianehaab district, Greenland. *American Mineralogist* **91**, 794-801.

Borodin, L.S. & Nazarenko, I.I. (1957): Chemical composition of pyrochlore and diadochic substitution in the $A_2B_2X_7$ molecule. *Geokhimiya* **4**, 386-400 (in Russian; transl. *Geochemistry International* **4**, 330-349, 1957).

Breiter, K., Škoda, R. & Uher, P. (2007): Nb–Ta–Ti–W–Sn-oxide minerals as indicators of a peraluminous P- and F-rich granitic system evolution: Podlesí, Czech Republic. *Mineralogy and Petrology* **91**, 225-248.

Brugger, J. & Gieré, R. (1999): As, Sb, Be and Ce enrichment in minerals from metamorphosed Fe–Mn deposit, Val Ferrera, Eastern Swiss Alps. *Canadian Mineralogist* **37**, 37-52.

Brugger, J., Gieré, R., Graeser, S. & Meisser, N. (1997): The crystal chemistry of roméite. *Contributions to Mineralogy and Petrology* **127**, 136-146.

Cámara, F., Williams, C.T., Della Ventura, G., Oberti, R. & Caprilli, E. (2004): Non-metamict betafite from Le Carcarelle (Vico volcanic complex, Italy): occurrence and crystal structure. *Mineralogical Magazine* **68**, 939-950.

Černý, P., Chapman, R., Ferreira, K. & Smeds, S.-A. (2004): Geochemistry of oxide minerals of Nb, Ta, Sn, and Sb in the Varuträsk granitic pegmatite, Sweden: the case of an "anomalous" columbite–tantalite trend. *American Mineralogist* **89**, 505-518.

Černý, P., Hawthorne, F.C., Laflamme, J.H.G. & Hinthorne, J.R. (1979): Stibiobetafite, a new member of the pyrochlore group from Vežná, Czechoslovakia. *Canadian Mineralogist* **17**, 583-588.

Chakoumakos, B.C. (1984): Systematics of the pyrochlore structure type, ideal $A_2B_2X_6Y$. *Journal of Solid State Chemistry* **53**, 120-129.

CHAKHMOURADIAN, A.R. (1996): On the development of niobium and rare-earth minerals in monticellite–calcite carbonatite of the Oka Complex, Quebec. *Canadian Mineralogist* **34**, 479-484.

CHAKHMOURADIAN, A.R. & MITCHELL, R.H. (1998): Lueshite, pyrochlore and monazite-(Ce) from apatite–dolomite carbonatite, Lesnaya Varaka complex, Kola Peninsula, Russia. *Mineralogical Magazine* **62**, 769-782.

CHAKHMOURADIAN, A.R. & MITCHELL, R.H. (2002): New data on pyrochlore- and perovskite-group minerals from the Lovozero alkaline complex, Russia. *European Journal of Mineralogy* **14**, 821-836.

CHRISTY, A.G. & GATEDAL, K. (2005): Extremely Pb-rich rock-forming silicates including a beryllian scapolite and associated minerals in a skarn from Långban, Värmland, Sweden. *Mineralogical Magazine* **69**, 995-1018.

CHUKANOV, N.V., SKRIGITIL, A.M., KUZMINA, O.V. & ZADOV, A.E. (1999): Bismutopyrochlore (Bi, U, Ca, Pb)$_{1+x}$(Nb,Ta)$_2$O$_6$(OH)•*n*H$_2$O – a new mineral from the Mika pegmatite vein (eastern Pamirs). *Zapiski Vsesoyuznoye Mineralogichestogo Obshchestvo* **128**(4), 36-41 (in Russian).

DANA, J.D. (1868): *A System of Mineralogy* (5th ed.). John Wiley and Son, New York, N.Y.

DICKSON, F.J., HAWKINS, H.D. & WHITE, T.J. (1989): Calcium uranium titanate – a new pyrochlore. *Journal of Solid State Chemistry* **82**, 146-150.

EDGE, R.A. & TAYLOR, H.F.W. (1971): Crystal structure of thaumasite, [Ca$_3$Si(OH)$_6$•12H$_2$O](SO$_4$)(CO$_3$). *Acta Crystallographica* **B27**, 594-601.

ERCIT, T.S., ČERNÝ, P. & HAWTHORNE, F.C. (1985): Normal and inverse pyrochlore group minerals. *Geological Association of Canada – Mineralogical Association of Canada, Program with Abstracts* **10**, A17.

ERCIT, T.S., ČERNÝ, P. & HAWTHORNE, F.C. (1993): Cesstibtantite – a geologic introduction to the inverse pyrochlores. *Mineralogy and Petrology* **48**, 235-255.

ERCIT, T.S., ČERNÝ, P. & SIIVOLA, J. (1987): The composition of stannomicrolite. *Neues Jahrbuch für Mineralogie, Monatshefte,* 249-252.

ERCIT, T.S., GROAT, L.A. & GAULT, R.A. (2003): Granitic pegmatites of the O'Grady batholith, N.W.T., Canada: a case study of the evolution of the elbaite subtype of rare-element granitic pegmatite. *Canadian Mineralogist* **41**, 117-137.

ERCIT, T.S., HAWTHORNE, F.C. & ČERNÝ, P. (1994): The structural chemistry of kalipyrochlore, a "hydropyrochlore". *Canadian Mineralogist* **32**, 415-420.

ERCIT, T.S. & ROBINSON, G.W. (1994): A refinement of the structure of ferritungstite from Kalzas Mountain, Yukon, and observations on the tungsten pyrochlores. *Canadian Mineralogist* **32**, 567-574.

ERICHSEN DE OLIVEIRA, O., ROCHA BAPTISTA, N. & BAPTISTA, A. (1970): Westgrenita no pegmatito de Tromba, Estado de Goiás. *Anais da Academia Brasileira de Ciências* **42**, 41-44.

FRANCHINI, M., LIRA, R., MEINERT, L, RÍOS, F.J., POKLEPOVIC, M.F., IMPICCINI, A. & MILLONE, H.A. (2005): Na–Fe–Ca alteration and LREE (Th–Nb): mineralization in marble and granitoids of Sierra de Sumampa, Santiago del Estero, Argentina. *Economic Geology* **100**, 733-764.

GANZEEV, A.A., EFIMOV, A.F. & LYUBOMILOVA, G.V. (1969): Plumbobetafite – a new mineral variety of the pyrochlore group. *Trudy Mineralogiches Muzeya, Akademiya Nauk SSSR* **19**, 135-137 (in Russian).

GEISLER, T., BERNDT, J., MEYER, H.-W., POLLOK, K. & PUTNIS, A. (2004): Low-temperature aqueous alteration of crystalline pyrochlore: correspondence between nature and experiment. *Mineralogical Magazine* **68**, 905-922.

GOREAUD, M. & RAVEAU, B. (1980): Alunite and crandallite: a structure derived from that of pyrochlore. *American Mineralogist* **65**, 953-956.

GREY, I.E., BIRCH, W.D., BOUGEROL, C. & MILLS, S.J. (2006): Unit-cell intergrowth of pyrochlore and hexagonal tungsten bronze structures in secondary tungsten minerals. *Journal of Solid State Chemistry* **179**, 3860-3869.

GROAT, L.A., ČERNÝ, P. & ERCIT, T.S. (1987): Reinstatement of stibiomicrolite as a valid species. *Geoliska Föreningens i Stockholm Förhandlingar* **109**, 105-109.

GROULT, D., PANNETIER, J. & RAVEAU, B. (1982): Neutron diffraction study of the defect pyrochlores TaWO$_{5.5}$, HTaWO$_6$, H$_2$Ta$_2$O$_6$, and HTaWO$_6$•H$_2$O. *Journal of Solid State Chemistry* **41**, 277-285.

GUASTONI, A., DIELA, V. & PEZZOTTA, F. (2008): Vigezzite and associated oxides of Nb–Ta from emerald-bearing pegmatites of the Vigezzo Valley, Western Alps, Italy. *Canadian Mineralogist* **46**, 619-633.

GUIMARÃES, C.P. (1939): Djalmaita, um novo mineral radioativo. *Annaes da Academia Brasileira de Sciencias* **11**, 347-350.

HATERT, F. & BURKE, E.A.J. (2008): The IMA–CNMNC dominant-constituent rule revisited and extended. *Canadian Mineralogist* **46**, 717-728.

HAWTHORNE, F.C. (2002): The use of end-member charge-arrangements in defining new mineral species and heterovalent substitutions in complex minerals. *Canadian Mineralogist* **40**, 699-710.

HENDERSON, S.J., SHEBANOVA, O., HECTOR, A.L., MCMILLAN, P.F. & WELLER, M.T. (2007): Structural variations in pyrochlore-structured Bi$_2$Hf$_2$O$_7$, Bi$_2$Ti$_2$O$_7$ and Bi$_2$Hf$_{2-x}$Ti$_x$O$_7$ solid solutions as a function of composition and

temperature by neutron and x-ray diffraction and raman spectroscopy. *Chemistry of Materials* **19**, 1712-1722.

HOGARTH, D.D. (1961): A study of pyrochlore and betafite. *Canadian Mineralogist* **6**, 610-633.

HOGARTH, D.D. (1977): Classification and nomenclature of the pyrochlore group. *American Mineralogist* **62**, 403-410.

HOGARTH, D.D. & HORNE, J.E.T. (1989): Non-metamict uranoan pyrochlore and uranpyrochlore from tuff near Ndale, Fort Portal area, Uganda. *Mineralogical Magazine* **53**, 257-262.

HOGARTH, D.D., WILLIAMS, C.T. & JONES, P. (2000): Primary zoning in pyrochlore group minerals from carbonatites. *Mineralogical Magazine* **64**, 683-697.

HUANG, XIAO LONG, WANG, RU CHENG, CHEN, XIAO MING, HU, HUAN & LIU, CHANG SHI (2002): Vertical variations in the mineralogy of the Yichun topaz–lepidolite granite, Jiangxi Province, southern China. *Canadian Mineralogist* **40**, 1047-1068.

HUSSAK, E. & PRIOR, G.T. (1895): Lewisite and zirkelite, two new Brazilian minerals. *Mineralogical Magazine* **11**, 80-88.

IGELSTRÖM, L.J. (1865): Nya och sällsynta mineralier från Vermland. *Öfversigt af Kongl. Vetenskaps-Akademiens Förhandlingar* **22**, 227-229.

JÄGER, E., NIGGLI, E. & VAN DER VEEN, A.H. (1959): A hydrated barium–strontium pyrochlore in a biotite rock from Panda Hill, Tanganyika. *Mineralogical Magazine* **32**, 10-25.

KALITA, A.P. (1957): On the composition of obruchevite – a hydrated uranium–yttrium variety of pyrochlore. *Doklady Akademii Nauk SSSR* **117**, 117-120 (in Russian).

KALITA, A.P. (1959): New data on some minerals of the Alakurtti veins. *Trudy Inst. Mineral. Geokhimii Kristallokhimii Redkikh Elementov* **2**, 164-172 (in Russian).

KARTASHOV, P.M., MOKHOV, A.V. & KOVALENKO, V.I. (1998): Rare earth Sr-pyrochlore from Western Mongolia: the first find in association with alkalic granites. *Doklady Earth Sciences* **359**, 510-513.

KARTASHOV P.M., VOLOSHIN A.V. & PAKHOMOVSKY YA.A. (1992): On plumbopyrochlore from Western Mongolia. *Doklady Akademii Nauk SSSR* **322**, 1137-1140 (in Russian).

KNUDSEN, C. (1989): Pyrochlore group minerals from the Qaqarssuk carbonatite complex. *In* Lanthanides, Tantalum and Niobium (P. Möller, P. Černý & F. Saupé, eds.). Springer-Verlag, Berlin, Germany (80-99).

KOVALENKO, V.I., TSARYEVA, G.M., GOREGLYAD, A.V., YARMOLYUK, V.V., TROITSKY, V.A., HERVIG, R.L. & FARMER, G.L. (1995): The peralkaline granite-related Khaldzan–Buregtey rare metal (Zr, Nb, REE) deposit, western Mongolia. *Economic Geology* **90**, 530-547.

LAPIN, A.V., MALYSHEV, A.A., PLOSHKO, V.V. & CHEREPIVSKAYA, G.YE. (1986): Strontiopyrochlore from lateritic crusts of weathering of carbonatites. *Doklady Akademii Nauk SSSR* **290**, 1212-1217 (in Russian).

LEE, MI JUNG, LEE, JONG IK, GARCIA, D., MOUTTE, J., WILLIAMS, C.T., WALL, F. & KIM, YEADONG (2006): Pyrochlore chemistry from the Sokli phoscorite–carbonatite complex, Finland: implications for the genesis of phoscorite and carbonatite association. *Geochemical Journal* **40**, 1-13.

LIFEROVICH, R.P. & MITCHELL, R.H. (2005*):* Composition and paragenesis of Na-, Nb- and Zr-bearing titanite from Khibina, Russia, and crystal-structure data for synthetic analogues. *Canadian Mineralogist* **43**, 795-812.

LIU JIANCHANG (1979): Jixianite $Pb(W,Fe^{3+})_2(O,OH)_7$ – a new tungsten mineral. *Acta Geologica Sinica* **53**, 46-49 (in Chinese).

LOTTERMOSER, B.G. & ENGLAND, B.M. (1988): Compositional variation in pyrochlores from the Mt. Weld carbonatite laterite, Western Australia. *Mineralogy and Petrology* **38**, 37-51.

LUMPKIN, G.R., CHAKOUMAKOS, B.C. & EWING, R.C. (1986): Mineralogy and radiation effects of microlite from the Harding pegmatite, Taos County, New Mexico. *American Mineralogist* **71**, 569-588.

LUMPKIN, G.R. & EWING, R.C. (1992): Geochemical alteration of pyrochlore group minerals: microlite subgroup. *American Mineralogist* **77**, 179-188.

LUMPKIN, G.R. & EWING, R.C. (1995*):* Geochemical alteration of pyrochlore group minerals: pyrochlore subgroup. *American Mineralogist* **80**, 732-743.

MASON, B. & VITALIANO, C.J. (1953): The mineralogy of the antimony oxides and antimonates. *Mineralogical Magazine* **30**, 100-112.

MATSUBARA, S., KATO, A., SHIMIZU, M., SEKIUCHI, K. & SUZUKI, Y. (1996): Romeite from Gozaisho mine, Iwaki, Japan. *Mineralogical Journal* **18**(4), 155-160.

MATTEUCCI, F., CRUCIANI, G., DONDI, M., BALDI, G. & BARZANTI, A. (2007): Crystal structural and optical properties of Cr-doped $Y_2Ti_2O_7$ and $Y_2Sn_2O_7$ pyrochlores. *Acta Materialia* **55**, 2229-2238.

MAZZI, F. & MUNNO, R. (1983): Calciobetafite (new mineral of the pyrochlore group) and related minerals from Campi Flegrei, Italy; crystal structures of polymignyte and zirkelite: comparison with pyrochlore and zirconolite. *American Mineralogist* **68**, 262-276.

MEYER, C. & YANG, S.V. (1988): Tungsten-bearing yttrobetafite in lunar granophyre. *American Mineralogist* **73**, 1420-1425.

MILLS, S.J., HATERT, F., NICKEL, E.H. & FERRARIS, G. (2009): The standardisation of mineral group hierarchies: application to recent nomenclature proposals. *European Journal of Mineralogy* **21**, 1073-1080.

MOKHOV, A.V., KARTASHOV, P.M., BOGATIKOV, O.A., ASHIKHMINA, N.A., MAGAZINA, L.O. & KOPORULINA, E.V. (2008): Fluorite, hatchettolite, calcium sulfate, and bastnasite-(Ce) in the lunar regolith from Mare Crisium. *Doklady Earth Sciences* **422**(1), 1178-1180.

NASRAOUI, M. & BILAL, E. (2000): Pyrochlores from the Lueshe carbonatite complex (Democratic Republic of Congo): a geochemical record of different alteration stages. *Journal of Asian Earth Sciences* **18**, 237-251.

NASRAOUI, M., BILAL, E. & GIBERT, R. (1999): Fresh and weathered pyrochlore studies by Fourier transform infrared spectroscopy coupled with thermal analysis. *Mineralogical Magazine* **63**, 567-578.

NASRAOUI, M. & WAERENBORGH, J.C. (2001): Fe speciation in weathered pyrochlore-group minerals from the Lueshe and Araxá (Barreiro) carbonatites by ^{57}Fe Mössbauer spectroscopy. *Canadian Mineralogist* **39**, 1073-1080.

NICKEL, E.H. (1992): Solid solutions in mineral nomenclature. *Canadian Mineralogist* **30**, 231-234.

NICKEL, E.H. & ROBINSON, B.W. (1985): Kimrobinsonite, a new tantalum mineral from Western Australia, and its association with cesstibtantite. *Canadian Mineralogist* **23**, 573-576.

NOVÁK, M. & ČERNÝ, P. (1998): Niobium–tantalum oxide minerals from complex granitic pegmatites in the Moldanubicum, Czech Republic: primary *versus* secondary compositional trends. *Canadian Mineralogist* **36**, 659-672.

OHNENSTETTER, D. & PIANTONE, P. (1992): Pyrochlore-group minerals in the Beauvoir peraluminous leucogranite, Massif Central. France. *Canadian Mineralogist* **30**, 771-784.

O'KEEFFE, M. & HYDE, B.G. (1981). The role of nonbonded forces in crystals. *In* Structure and Bonding in Crystals (M. O'Keeffe & A. Navrotsky, eds.). John Wiley & Sons, New York, N.Y. (227-254).

PHILIPPO, S., NAUD, J., DECLERQ, J.P. & FENEAU-DUPONT, J. (1995): Structure refinement and X-ray powder diffraction data for kalipyrochlore $(K,Sr,Na,Ca,H_2O)_{2-m}(Nb,Ti)_{2-x}O_{6-w}Y_{1-n}$ with ($0 < m < 0.8$, $x \sim 0.2$, $w = 0$ and $0.2 < n < 1$). *Powder Diffraction* **10**, 180-184.

PYATENKO, YU.A. (1959): Some aspects of the chemical crystallography of the pyrochlore-group minerals. *Kristallografiya* **4**, 204-208 (in Russian, transl. *Soviet Physics – Crystallography* **4**, 184-186, 1960).

REID, A.F., LI, C. & RINGWOOD, A.E. (1977): High-pressure silicate pyrochlores, $Sc_2Si_2O_7$ and $In_2Si_2O_7$ *Journal of Solid State Chemistry* **20**, 219-226.

RIOTTE, E.N. (1867): Stetefeldtit, ein neues Mineral. *Berg- und HuettenmÆnnische Zeitung* **26**, 253-254.

ROUSE, R.C., DUNN, P.J., PEACOR, D.R. & WANG LIPING (1998): Structural studies of the natural antimonian pyrochlores. I. Mixed valency, cation site splitting, and symmetry reduction in lewisite. *Journal of Solid State Chemistry* **141**, 562-569.

RUB, A.K., STEMPROK, M. & RUB, M.G. (1998): Tantalum mineralization in the apical part of the Cínovec (Zinnwald) granite stock. *Mineralogy and Petrology* **63**, 199-222.

SAFIANNIKOFF, A. & VAN WAMBEKE, L. (1961): Sur une terme plombifère du groupe pyrochlore–microlite. *Bulletin de la Société française de Minéralogie et de Cristallographie* **84**, 382-384.

SAHAMA, T.G. (1981): The secondary tungsten minerals, a review. *Mineralogical Record* **12**, 81-83.

SCHALLER, W.T. (1911): Ferritungstite, a new mineral. *American Journal of Sciences* **182**, 161-162.

SCHMITT, A.K., TRUMBULL, R.B., DULSKI, P. & EMMERMANN, R. (2002): Zr–Nb–REE Mineralization in peralkaline granites from the Amis Complex, Brandberg (Namibia): evidence for magmatic pre-enrichment from melt inclusions. *Economic Geology* **97**, 399-413.

SEIFERT, W., KÄMPF, H. & WASTERNACK, J. (2000): Compositional variation in apatite, phlogopite and other accessory minerals of the ultramafic Delitzsch complex, Germany: implication for cooling history of carbonatites. *Lithos* **53**, 81-100.

SKOROBOGATOVA, N.V., SIDORENKO, G.A., DOROFEEVA, K.A. & STOLYAROVA, T.I. (1966): Plumbopyrochlore. *Geologiya Mestorozhdenii Redkikh Elementov* **30**, 84-95 (in Russian).

SMEDS, S.-A., ČERNÝ, P. & CHAPMAN, R. (1999): Niobian calciotantite and plumboan–stannoan cesstibtantite from the island of Utö, Stockholm Archipelago, Sweden. *Canadian Mineralogist* **37**, 665-672.

SUBRAMANIAN, M.A., ARAVAMUDAN, G., & RAO SUBBA, G.V. (1983): Oxide pyrochlores – a review. *Progress in Solid State Chemistry* **15**, 55-143.

SUBBOTIN, V.V. & SUBBOTINA, G.F. (2000): Pyrochlore-group minerals from phoscorites and carbonatites of the Kola Peninsula. *Vestnik Moscow State University* **3**, 273-284 (in Russian).

THOMPSON, R.N., SMITH, P.M., GIBSON, S.A., MATTEY, D.P. & DICKIN, A.P. (2002): Ankerite carbonatite from Swartbooisdrif, Namibia: the first evidence for magmatic ferrocarbonatite. *Contributions to Mineralogy and Petrology* **143**, 377-395.

TINDLE, A.G. & BREAKS, F.W. (1998): Oxide minerals of the Separation Rapids rare-element granitic pegmatite group, northwestern Ontario. *Canadian Mineralogist* **36**, 609-635.

TINDLE, A.G., SELWAY, J.B. & BREAKS, F.W. (2005): Liddicoatite and associated species from the McCombe spodumene-subtype rare-element granitic pegmatite, northwestern Ontario, Canada. *Canadian Mineralogist* **43**, 769-793.

UHER, P., ČERNÝ, P. & CHAPMAN, R. (2008): Foordite–thoreaulite, $Sn^{2+}Nb_2O_6$– $Sn^{2+}Ta_2O_6$: compositional variations and alteration products. *European Journal of Mineralogy* **20**, 501-516.

UHER, P., ČERNÝ, P., CHAPMAN, R., HATÁR, J. & MIKO, O. (1998): Evolution of Nb,Ta-oxide minerals in the Prašivá granitic pegmatites, Slovakia. II. External hydrothermal Pb,Sb overprint. *Canadian Mineralogist* **36**, 535-545.

UHER, P., ŽITŇAN, P. & OZDÍN, D. (2007): Pegmatitic Nb–Ta oxide minerals in alluvial placers from Limbach, Bratislava Massif, western Carpathians, Slovakia: compositional variations and evolutionary trend. *Journal of Geosciences* **52**, 133-141.

VAN DER VEEN, A.H. (1963): A study of pyrochlore. *Verhandelingen van het Koninklijk Nederlands geologisch mijnbouwkundig genootschap, Geologische serie* **22**, 1-188.

VAN LICHTERVELDE, M., SALVI, S., BÉZIAT, D. & LINNEN, R.L. (2007): Textural features and chemical evolution in tantalum oxides: magmatic versus hydrothermal origins for Ta mineralization in the Tanco Lower Pegmatite, Manitoba, Canada. *Economic Geology* **102**, 257-276.

VAN WAMBEKE, L. (1970): The alteration processes of the complex titano-niobo-tantalates and their consequences. *Neues Jahrbuch für Mineralogie, Abhandlungen* **112**, 117-149.

VAN WAMBEKE, L. (1971): The problem of cation deficiencies in some phosphates due to alteration processes. *American Mineralogist* **56**, 1366-1384.

VAN WAMBEKE, L. (1978): Kalipyrochlore, a new mineral of the pyrochlore group. *American Mineralogist* **63**, 528-530.

VAN WAMBEKE, L. (1980): Lattrapite and ceriopyrochlore, new minerals for the Federal Republic of Germany. *Neues Jahrbuch für Mineralogie, Monatshefte,* 171-174.

VOLOSHIN, A.V., MEN'SHIKOV, YU.P., PAKHOMOVSKIY, YA.A. & POLEZHAEVA, L.I. (1981): Cesstibtantite, (Cs,Na) $SbTa_4O_{12}$ – a new mineral from granitic pegmatites. *Zapiski Vsesoyuznoye Mineralogichestogo Obshchestvo* **110**, 345-351 (in Russian).

VOLOSHIN, A.V. & PAKHOMOVSKIY, YA.A. (1986): *Minerals and Evolution of Mineral Formation in Amazonite Pegmatites of Kola Peninsula*. Nauka, Leningrad, Russia.

VOLOSHIN, A.V., PAKHOMOVSKIY, YA.A. & BAKHCHISARAYTSEV, A.Y. (1993): Plumbobetafite in amazonite pegmatites of western Keyv (Kola Peninsula). *Mineralogicheskiy Zhurnal* **15**(2), 76-80 (in Russian).

VOLOSHIN, A.V., PAKHOMOVSKIY, YA.A., PUSHCHAROVSKIY, L.YU., NADEZHINA, T.N., BAKHCHISARAYTSEV, A.Y. & KOBYASHEV, YU.S. (1989): Strontium pyrochlore: composition and structure. *Novye Dannye Mineral. SSSR* **36**, 12-24 (in Russian).

VOLOSHIN, A.V., PAKHOMOVSKIY, YA.A., STEPANOV, V.I. & TYUSHEVA, F.N. (1983): Natrobistantite (Na,Cs) $Bi(Ta,Nb,Sb)_4O_{12}$ – a new mineral from granitic pegmatites. *Mineralogicheskiy Zhurnal* **5**(2), 82-86 (in Russian).

VON KNORRING, O. & MROSE, M.E. (1963): Westgrenite and waylandite, two new bismuth minerals from Uganda. *Geological Society of America, Special Paper* **73**, 256-257 (abstr.).

VORMA, A. & SIIVOLA, J. (1967): Sukulaite – $Ta_2Sn_2O_7$ – and wodginite as inclusions in cassiterite in the granite pegmatite in Sukula, Tammela, in SW Finland. *Bulletin de la Commission géologique de Finlande* **229**, 173-187.

XIE, L., WANG, R.C., WANG, D.Z. & QIU, J.S. (2006): A survey of accessory mineral assemblages in peralkaline and more aluminous A-type granites of the southeast coastal area of China. *Mineralogical Magazine* **70**, 709-729.

WALENTA, K. (1983): Bismutostibiconit, ein neues Mineral der Stibiconitgruppe aus dem Schwarzwald. *Chemie der Erde* **42**, 77-81.

WALL, F., WILLIAMS, C.T., WOOLLEY, A.R. & NASRAOUI, M. (1996): Pyrochlore from weathered carbonatite at Lueshe, Zaire. *Mineralogical Magazine* **60**, 731-750.

WANG, RU CHENG, FONTAN, F., CHEN, XIAO MING, HU, HUAN, LIU, CHANG SHI, XU, SHI JIN & DE PARSEVAL, P. (2003): Accessory minerals in the Xihuashan Y-enriched granitic complex, southern China: a record of magmatic and hydrothermal stages of evolution. *Canadian Mineralogist* **41**, 727-748.

WEIDMANN, S. & LENHER, V. (1907): Marignacite, a new variety of pyrochlore from Wausau, Wisconsin. *American Journal of Science* **173**, 287-292.

WILLIAMS, C.T. (1996): The occurrence of niobian zirconolite, pyrochlore and baddeleyite in the Kovdor carbonatite complex, Kola Peninsula, Russia. *Mineralogical Magazine* **60**, 639-646.

WILLIAMS, C.T., WALL, F., WOOLLEY, A.R., & PHILLIPO, S. (1997): Compositional variation in pyrochlore from the Bingo carbonatite, Zaire. *Journal of African Earth Sciences* **25**, 137-145.

WILLIAMS, P.A., LEVERETT, P., SHARPE, J.L., COLCHESTER, D.M. & RANKIN, J. (2005): Elsmoreite, cubic $WO_3 \bullet 0.5H_2O$, a new mineral species from Elsmore, New South Wales, Australia. *Canadian Mineralogist* **43**, 1061-1064.

WITZKE, T., STEINS, M. DORING, T., SCHUCKMANN, W., WEGNER, R. & POLLMANN, H. (1998): Fluornatromicrolite. IMA CNMMN Submission 98–018. Now in press (*Can. Mineral.* **48**).

ZHANG, A.C., WANG, R.C., HU, H., ZHANG, H., ZHU, J.C. & CHEN, X.M. (2004): Chemical evolution of Nb–Ta oxides

and zircon from the Koktokay No. 3 granitic pegmatite, Altai, northwestern China. *Mineralogical Magazine* **68**, 739-756.

ZUBKOVA, N.V., PUSHCHAROVSKY, D.YU., ATENCIO, D., ARAKCHEEVA, A.V. & MATIOLI, P.A. (2000): The crystal structure of lewisite, $(Ca,Sb^{3+},Fe^{3+},Al,Na,Mn,\square)_2(Sb^{5+},Ti)_2O_6(OH)$. *Journal of Alloys and Compounds* **296**, 75-79.

ZUREVINSKI, S.E. & MITCHELL, R.H. (2004*):* Extreme compositional variation of pyrochlore-group minerals at the Oka Carbonatite Complex, Quebec: evidence of magma mixing? *Canadian Mineralogist* **42**, 1159-1168.

Received June 12, 2010.

Mineralogical Magazine, February 2013, Vol. 77(1), pp. 13–20

Letter

Clarification of status of species in the pyrochlore supergroup

A. G. Christy[1,*] and D. Atencio[2]

[1] Centre for Advanced Microscopy, Australian National University, Canberra, ACT 0200, Australia
[2] Instituto de Geociências, Universidade de São Paulo, Rua do Lago, 562, 05508-080, São Paulo, Brazil

[*Received 29 October 2012; Accepted 8 November 2012; Associate Editor: Peter Leverett*]

ABSTRACT

After careful consideration of the semantics of status categories for mineral species names, minor corrections and disambiguations are presented for a recent report on the nomenclature of the pyrochlore supergroup. The names betafite, elsmoreite, microlite, pyrochlore and roméite are allocated as group names within the pyrochlore supergroup. The status of the names bindheimite, bismutostibiconite, jixianite, monimolite, partzite, stetefeldtite and stibiconite is changed from 'discredited' to 'questionable' pending further research.

Keywords: pyrochlore, betafite, elsmoreite, microlite, roméite, bindheimite, partzite, stetefeldtite, stibiconite, mineral species status, mineral nomenclature.

Introduction

The aims of this letter are to correct minor errors and resolve ambiguities in the recent Commission on New Minerals, Nomenclature and Classification (CNMNC) report on the classification and nomenclature of the pyrochlore supergroup (Atencio *et al*., 2010). These issues are primarily the result of the complex one-to-many and many-to-many mapping of older names onto new names. This has led to some uncertainty in the correspondence between old names and new names, and in the status of some old names and of type material. The discreditation of several old names appears to have been premature. To fully clarify the situation it should be stated explicitly that the 'status' applies to a species name, not to the population of specimens that physically represents the species. The status categories used here are defined as follows:

'A' (approved): the name has been approved by the CNMNC or its predecessor commission as a valid name for the mineral species.

'D' (discredited): the name is no longer the official name for a mineral species, it is now regarded as a synonym or varietal name, or was so poorly defined in the first place that it cannot be used in a reproducible fashion.

'G' (grandfathered): the name is an old one that pre-dates the requirement for approval by the CNMNC or its predecessors, and is generally accepted as valid.

'Group': the name refers to a group within the pyrochlore supergroup, defined on the basis of *B*-site occupancy. In the case of the pyrochlores, all such names are no longer valid as species names, and hence have the status 'D + Group'.

'N' (not approved): the name has been published without the approval of the CNMNC or its predecessors.

'Q' (questionable): the name refers to one or more mineral species which are probably valid, but type material was not well enough characterized for species to be unambiguously identified using current criteria. Further study is required for classification of the name into the 'A', 'D' or 'Rd' categories.

'Rd' (redefined): the current valid name now describes a chemical or structural variation for a species that is narrower, broader or otherwise different from that before the redefinition.

* E-mail: andrew.christy@anu.edu.au
DOI: 10.1180/minmag.2013.077.1.02

TABLE 1. Status of old names for pyrochlore-supergroup minerals. Abbreviations are as defined in the text.

Mineral name	Status of name, Nickel and Nichols (2009)	Status of name, Atencio *et al.* (2010) Table 7	Correct status of name (2012)	Corresponding species names in the scheme of Atencio *et al.* (2010)
Alumotungstite	A	D	D	= Hydrokenoelsmoreite
Bariomicrolite	A	D	D	Probably hydrokenomicrolite
Bariopyrochlore	A	D	D	Zero-valent-dominant pyrochlore
Betafite	Rd	Possible new species	D + Group	Analysed instances = possible new species oxycalciobetafite, oxyuranobetafite
Bindheimite	G	D / Possible new species	Q	Analysed instance = possible new species oxyplumboroméite
Bismutomicrolite	A	D	D	Analysed instances = zero-valent-dominant microlite, or probable mixture.
Bismutopyrochlore	A	D / Possible new species	D	Analysed instances = possible new species oxynatropyrochlore,
zero-valent-dominant pyrochlore				
Bismutostibiconite	A	D	Q	Probably a Bi-dominant roméite species
Calciobetafite	A	D	D	Type material is Ca-dominant pyrochlore
Ceriopyrochlore-(Ce)	Rn	D / Possible new species	D	Analysed instances = possible new species fluorkenopyrochlore,
Ca- or zero-valent-dominant pyrochlore				
Cesstibtanite	A	Rd	D	Type material is now type hydroxykenomicrolite. Other occurrences may be other zero-valent-dominant microlite species
Elsemoreite	A	Rd	D + Group	Type material is now type hydrokenoelsmoreite
Ferritungstite	A	D	D	Hydrokenoelsmoreite
Fluornatromicrolite	-	A	A	IMA1998-018; full description published after delay as Witzke *et al.* (2011)
Jixianite	A	D	Q	Pb-dominant elsmoreite species.
Kalipyrochlore	A	Rd	D	Type material is now type hydropyrochlore
Lewisite	D	Rd	D	Type material is now type hydroxycalcioroméite
Microlite	A	Possible new species	D + Group	Analysed instances = possible new species fluorcalciomicrolite, oxycalciomicrolite
Monimolite	Q	D	Q	Probably "oxyplumboroméite"
Natrobistantite	A	D	D	Zero-valent-dominant microlite species
Partzite	G	D	Q	May be Cu-dominant roméite species
Plumbobetafite	A	D	D	Analysed instances = Pb-dominant betafite or zero-valent-dominant pyrochlore species

Plumbomicrolite	A	D/Possible new species	D	Analysed instances = possible new species kenoplumbomicrolite or zero-valent-dominant microlite species
Plumbopyrochlore	A	D/Possible new species	D	Analysed instances = possible new species oxyplumbopyrochlore, kenoplumbopyrochlore, unspecified Pb-dominant or zero-valent-dominant pyrochlore species
Pyrochlore	A	Possible new species	D + Group + Supergroup	Analysed instances = possible new species oxynatropyrochlore, hydroxycalciopyrochlore, fluorcalciopyrochlore, fluorkenopyrochlore
Roméite	G	Possible new species	D + Group	Analysed instances = possible new species fluornatroroméite, fluorcalcioroméite, oxycalcioroméite
Stannomicrolite	Rn	D / Rd	D	Type material of sukulaite is now type oxystannomicrolite. Other instances are Ca- or zero-valent-dominant microlite species
Stetefeldtite	Q	D	Q	May be Ag-dominant roméite species
Stibiconite	G	D	Q	May be Sb-dominant or other roméite species
Stibiobetafite	A	D / Rd	D	Type material is now type oxycalciopyrochlore
Stibiomicrolite	Rd	D / Rd / Possible new species	D	Type material is now type oxystibiomicrolite. Other analysed instances are possible new species oxycalciomicrolite, Ca- or zero-valent-dominant microlite species
Strontiopyrochlore	N	D / Possible new species	D	Analysed instances = possible new species fluorstrontiopyrochlore, fluorkenopyrochlore, or Ca- or zero-valent-dominant pyrochlore species
Uranmicrolite	Rn	D	D	Other microlite species
Uranpyrochlore	Rn	D / Possible new species	D	Analysed instances = possible new species oxynatropyrochlore, Na-dominant or U-dominant pyrochlore species
Yttrobetafite-(Y)	A	D / Possible new species	D	Analysed instances = possible new species oxycalciobetafite or zer-valent-dominant pyrochlore
Yttropyrochlore-(Y)	Rn	D / Possible new species	D	Analysed instances = possible new species oxyyttropyrochlore-(Y) or zero-valent-dominant pyrochlore

'Rn' (renamed): the current valid name replaced an earlier name without any change in species definition.

'Supergroup': the name now refers to the supergroup.

Note that 'Rn' and 'Rd' are special cases of 'A'. They are useful in that they highlight recent changes in status.

The pyrochlore-supergroup species names that were extant prior to the revision of Atencio *et al*. (2010), their status in the IMA–CNMNC list of mineral names compiled in October 2008 by E.H. Nickel and M.C. Nichols (which has been deposited with *Mineralogical Magazine* and can be downloaded from http://www.minersoc.org/pages/e_journals/dep_mat_mm.html), the status in Atencio *et al*. (2010) and the status as at November 2012, are listed in Table 1. If chemical analyses published for a particular mineral name allow identification of a species name or set of names that are consistent with the new nomenclature scheme, those names are also given.

The principal additions and changes to the scheme described by Atencio *et al*. (2010) are listed in the following text.

(1) The names betafite, elsmoreite, microlite, pyrochlore and roméite are reallocated as group names; these are defined on the basis of their *B*-site occupancy as described in Atencio *et al*. (2010). All except the elsmoreite group contain more than one approved species. Minerals that were formerly described using one of the group names require characterization of their *A*- and *Y*-site occupancies to be named to species level.

(2) If an old species name can be mapped unambiguously onto a new species name, and the structure and composition of the type material has been characterized to an appropriate standard, the old type specimen or specimens can be redefined to be types for the new species. Examples include type elsmoreite, which now corresponds to type hydrokenoelsmoreite; type cesstibtantite which now corresponds to type hydroxykenomicrolite; and type kalipyrochlore which now corresponds to type hydropyrochlore. None of the old pyrochlore-supergroup species names are valid in the new nomenclature scheme, and all are therefore discredited. The case of lewisite is unusual in that the name had been discredited prior to the creation of the pyrochlore supergroup as it was found to be synonymous with Ti-rich roméite (Burke, 2006), but the type material now serves as the type for hydroxycalcioroméite. However, it should be noted that other material with the same old species name may map onto a different new species.

(3) More than one old species may map onto the same new species. For example, alumotungstite and ferritungstite are no longer valid mineral names, both are synonyms of hydrokenoelsmoreite. All such redundant names are discredited.

(4) Some old names, including bindheimite, bismutostibiconite, jixianite, monimolite, partzite, stetefeldtite and stibiconite, probably correspond to one or more names in the new scheme, but the data available are insufficient to pinpoint the new species. In these cases, type material for the old names, if extant, cannot be redefined as type material for a specific new species name without further study. Many bindheimite specimens, for example, are probably the as yet unconfirmed mineral oxyplumboroméite, but further research is required to show that this is the case for the type specimen of bindheimite, or for all bindheimite specimens. The Sb-rich mineral stibiconite requires careful quantification of the oxidation state of its Sb for full characterization as although it may correspond to one or more Sb^{3+}-dominant roméite-group species; synthetic $Sb_2O_5{\cdot}1{-}3H_2O$ phases with the pyrochlore structure that contain no Sb^{3+} have also been reported (Natta and Baccaredda, 1936; England *et al*., 1980). Note that the Sb_2O_5 hydrate formulae can be rewritten to emphasize the pyrochlore structure as $\square_2Sb_2O_4(OH)_2\square$, $(H_2O\square)Sb_2O_4(OH)_2H_2O$ or $(H_3O\square)Sb_2O_6(OH)$. A structure refinement for $(Sb^{3+}\square)Sb_2^{5+}O_6(OH)$ was reported in a very early study by Dihlstroem and Westgren (1937) but the presence of significant Sb^{3+} remains to be demonstrated unequivocally in natural roméite-group minerals (P.A. Williams, pers. comm.). Partzite is complex in that some specimens may be multiphase mixtures, whereas others may contain one or more Cu-dominant roméite-group species. It is noteworthy that neither pyrochlore cation site is stereochemically favourable for occupation by Cu^{2+}, and that no synthetic Cu antimonates with the pyrochlore structure are known (Roper *et al*., 2012 and references therein). Artificial $CuSb_2O_6$ has the trirutile structure or a slight distortion thereof (Gieré *et al*., 1997). Stetefeldite is another interesting case. Synthetic $Ag_2Sb_2O_6$ with a pyrochlore structure is known (Mizoguchi *et al*., 2004) suggesting that phases that corresponding to one or more Ag-dominant roméite-group species might occur in nature. Natural and synthetic solid solutions with various Ag:Sb ratios that give pyrochlore-like

powder X-ray diffraction patterns have been described by Mason and Vitaliano (1953) and Stewart and Knop (1970), respectively. However, the existence of polymorphs of $Ag_2Sb_2O_6$ which do not have the pyrochlore structure (Hong *et al*., 1974), allows for the possibility that some old descriptions in this category, which were identified on the basis of their composition, may not be members of the pyrochlore supergroup.

The minerals described using the names in the foregoing paragraph require further study. If they are members of the pyrochlore supergroup, the nomenclature system of Atencio *et al*. (2010) prevents the old names being used either as species

TABLE 2. Species names in the pyrochlore supergroup according to Atencio *et al*. (2010) and new mineral descriptions published subsequently, with current status of species: 'A' = approved, 'P' = possible new species, 'T' = type material of an old name has been transferred to a new name (this is a special case of 'A'). References are given in Atencio *et al*. (2010), if not otherwise stated.

Mineral name	Best evidence for existence	Current status (October 2012)
Fluorcalciomicrolite	Andrade *et al*. (2012*b*); IMA2012-036	A
Fluorcalciopyrochlore	Published analyses	P
Fluorcalcioroméite	Published analyses	P
Fluorhydropyrochlore	Published analyses*	P
Fluorkenopyrochlore	Published analyses	P
Fluornatromicrolite	Witzke *et al*. (2011)	A
Fluornatropyrochlore	Unpublished analyses	P
Fluornatroroméite	Published structure determination	P
Fluorstrontiopyrochlore	Published analyses	P
Hydrokenoelsmoreite	Type specimen of former species elsmoreite transferred to new name	T
Hydrokenomicrolite	Andrade *et al*. (2012*a*); IMA2011-103	A
Hydromicrolite	Unpublished analyses	P
Hydropyrochlore	Type specimen of former species kalipyrochlore transferred to new name	T
Hydroxycalciopyrochlore	Yang *et al*. (2011); IMA2011-026	A
Hydroxycalcioroméite	Type specimen of former species lewisite transferred to new name	T
Hydroxykenomicrolite	Type specimen of former species cesstibtantite transferred to new name	T
Hydroxymanganopyrochlore	Chukanov *et al*. (2012); IMA2012-005	A
Kenoplumbomicrolite	Published structure determination	P
Kenoplumbopyrochlore	Published analyses	P
Oxycalciobetafite	Published analyses and structure	P
Oxycalciomicrolite	Published analyses	P
Oxycalciopyrochlore	Type specimen of former species stibiobetafite transferred to new name	T
Oxycalcioroméite	Biagioni and Orlandi (2012); IMA2012-022	A
Oxynatropyrochlore	Published analyses	P
Oxyplumbopyrochlore	Published analyses	P
Oxyplumboroméite	Published analyses	P
Oxystannomicrolite	Type specimen of former species sukulaite (= stannomicrolite) transferred to new name	T
Oxystibiomicrolite	Type specimen of former species stibiomicrolite transferred to new name	T
Oxyuranobetafite	Published analyses	P
Oxyyttropyrochlore-(Y)	Published analyses	P

* See discussion in text of Atencio *et al*. (2010)

names or root names, and it is for this reason that Atencio *et al*. (2010) classified them as discredited. However, the possibility remains that a future study might result in one or more of the old names being redefined as a species that does not belong to the pyrochlore supergroup. Unfortunately, the discreditation of the old names leaves extant specimens of compositionally distinctive material with no acceptable name, or forces the use of discredited names, which the CNMNC wishes to discourage. Therefore, it is preferable to amend the classification of the old names to 'questionable', which gives CNMNC sanction to their continued usage until sufficient data is available to either fully discredit them and replace their names by one or more pyrochlore supergroup names that are consistent with Atencio *et al*. (2010), or redefine them as a species that is not a member of the pyrochlore supergroup.

(5) One pre-2010 mineral species, fluornatromicrolite, is defined and named consistently with the 2010 scheme. Therefore, the name is listed in Table 1 as 'approved'.

(6) As the species names of Atencio *et al*. (2010) correspond to compositional ranges that are different from those of older schemes, all other names in the new scheme require explicit validation by the CNMNC. This was achieved for oxycalciopyrochlore, hydropyrochlore, hydroxykenomicrolite, oxystannomicrolite, oxystibiomicrolite, hydroxycalcioroméite and hydrokenoelsmoreite by reassigning the type material for well described former species to a new name (Atencio *et al*., 2010). As of November 2012, the new species, hydroxycalciopyrochlore (IMA 2011-026) and hydrokenomicrolite (IMA 2011-103), have also been approved by the CNMNC. Fluornatromicrolite was approved by the CNMNCs predecessor, the CNMMN (as IMA 1998-018), but controversies about its species status and the nomenclature of the pyrochlore supergroup delayed full publication. When the description of fluornatromicrolite was submitted for the first time, in 1998, problems arose as (although it was approved by the CNMMN–IMA) the name fluornatromicrolite was not in accord with the nomenclature of Hogarth (1977), which was then still *de rigueur*. The name fluornatromicrolite is, however, perfectly in line with the newly approved system

TABLE 3. Status of the names of Table 2, summarized in matrix form. Rows are ordered by *A*-site prefix, then *Y*-site prefix. Status symbols 'A','P' and 'T' are 'A' = approved, 'P' = possible new species, 'T' = type material of an old name has been transferred to a new name (this is a special case of 'A')..

Y-site prefix	*A*-site prefix	Betafite group (Ti^{4+} on *B*)	Elsmoreite group (W^{6+} on *B*)	Microlite group (Ta^{5+} on *B*)	Pyrochlore group (Nb^{5+} on *B*)	Roméite group (Sb^{5+} on *B*)
Fluor-	-calcio-			A	P	P
Hydroxy-	-calcio-				A	T
Oxy-	-calcio-	P		P	T	A
Fluor-	-hydro-				P	
Hydro-	(-hydro-)*			P	T	
Fluor-	-keno-				P	
Hydro-	-keno-		T			
Hydroxy-	-keno-			T		
Hydroxy-	-mangano-				A	
Fluor-	-natro-			A	P	P
Oxy-	-natro-				P	
Keno-	-plumbo-			P	P	
Oxy-	-plumbo-				P	P
Oxy-	-stanno-			T		
Oxy-	-stibio-			T		
Fluor-	-strontio-				P	
Oxy-	-urano-	P				
Oxy-	-yttro-...-(Y)				P	

* Omitted to avoid repetition.

TABLE 4. Composition ranges with inadequately analysed *Y*-site occupancies where there is evidence for additional new species are indicated by '×'.

A-site prefix	*A*-site species	Betafite group (Ti^{4+} on *B*)	Elsmoreite group (W^{6+} on *B*)	Microlite group (Ta^{5+} on *B*)	Pyrochlore group (Nb^{5+} on *B*)	Roméite group (Sb^{5+} on *B*)
-argento-	Ag^{+}					×
-bismuto-	Bi^{3+}					×
-calcio-	Ca^{2+}			×	×	
-cupro-	Cu^{2+}					×
-hydro- or -keno-	$H_2O/\square$			×	×	
-natro-	Na^{+}				×	
-plumbo-	Pb^{2+}	×	×		×	×
-stibio-	Sb^{3+}					×
-urano-	U^{4+}				×	

of nomenclature and the mineral description has been published recently (Witzke *et al*., 2011).

New species names discussed in Atencio *et al*. (2010) for which examples appear to exist, on the basis of analyses or crystal structure determinations, are listed in Table 2. Species that have been approved by the CNMNC since that report are also included. The status of the names is indicated as 'A' if the new species has already been approved by the CNMNC. To clarify the various status changes, two new categories have been created. The code 'T' (type transferred) is used if type material of a former species has been reassigned to be type material for a new species. In other words, if the type specimen has been transferred from an old discredited name to a valid new name. Note that this is quite distinct from the redefinition of a *name* as defined above. The category 'T' is not 'Rd', but a distinct special case of 'A'. The category 'P' (probable new species), is used if material exists that appears to correspond to a new species name, but no proposal has yet been made to the CNMNC. Note that this category is not equivalent to 'Q' as defined above. The category 'P' indicates that the name is currently *not* valid but would become so if a proposal was to be approved. The list of Table 2 is summarized by mineral groups in a more compact two-dimensional matrix form in Table 3; this complements Tables 1–5 of Atencio *et al*. (2010) but indicates the current status explicitly.

It is very probable that further new species exist, but they are not included in Tables 2–3 as their current state of chemical/structural characterization does not allow specification of the exact species name according to the new scheme. Atencio *et al*. (2010) require two prefixes in pyrochlore-supergroup species names, the first indicating the dominant species of the dominant valence in the *Y* sites, and the second indicating the dominant species of the dominant valency in the *A* site; in these cases, only the latter is known. On the basis of the names labelled 'Q' and comments on other names in Table 1, the composition fields in which such new species are likely to be found are summarized in Table 4. Material with such compositions includes the questionable species bismutostibiconite, bindheimite, jixianite, monimolite, partzite, stetefeldtite and stibiconite, and many other incomplete analyses of the betafite, microlite and pyrochlore groups.

References

Andrade, M.B., Atencio, D., Chukanov, N.V. and Ellena, J. (2012*a*) Hydrokenomicrolite, IMA 2011-103. CNMNC Newsletter No. 13, June 2012, page 809; *Mineralogical Magazine*, **76**, 807–817.

Andrade, M.B., Atencio, D., Yang, H., Downs, R.T., Persiano, A.I.C. and Ellena, J. (2012*b*) Fluorcalciomicrolite, IMA 2012-036. CNMNC Newsletter No. 14, October 2012, page 1286; *Mineralogical Magazine*, **76**, 1281–1288.

Atencio, D., Andrade, M.B., Christy, A.G., Gieré, R. and Kartashov, P.M. (2010) The pyrochlore supergroup of minerals: nomenclature. *The Canadian Mineralogist*, **48**, 673–698.

Biagioni, C. and Orlandi, P. (2012) Oxycalcioroméite,

IMA 2012-022. CNMNC Newsletter No. 14, October 2012, page 1283; *Mineralogical Magazine*, **76**, 1281–1288.

Burke, E.A.J. (2006) A mass discreditation of GQN minerals. *The Canadian Mineralogist*, **44**, 1557–1560.

Chukanov, N.V., Blass, G., Zubkova, N.V., Pekov, I.V., Pushcharovsky, D.Y. and Prinz, H. (2012) Hydroxymanganopyrochlore, IMA 2012-005. CNMNC Newsletter No. 13, June 2012, page 813; *Mineralogical Magazine*, **76**, 807–817.

Dihlstroem, K. and Westgren, A. (1937) Über den Bau des sogenannten Antimontetroxyds und der damit isomorphen Verbindung $BiTa_2O_6F$. *Zeitschrift für Anorganische und Allgemeine Chemie*, **235**, 153–160.

England, W.A., Cross, M.G., Hamnett, A., Wiseman, P.J. and Goodenough, J.B. (1980) Fast proton conduction in inorganic ion-exchange compounds. *Solid State Ionics*, **1**, 231–249.

Gieré, E.O., Brahimi, A., Dieseroth, H.J. and Reinen, D. (1997) The geometry and electronic structure of the Cu^{2+} polyhedra in trirutile-type compounds $Zn(Mg)_{1-x}Cu_xSb_2O_6$ and the dimorphism of $CuSb_2O_6$: a solid state and EPR study. *Journal of Solid State Chemistry*, **131**, 263–274.

Hogarth, D.D. (1977) Classification and nomenclature of the pyrochlore group. *American Mineralogist*, **62**, 403–410.

Hong, H.Y.-P., Kafalas, J.A. and Goodenough, J.B. (1974) Crystal chemistry in the system $MSbO_3$. *Journal of Solid State Chemistry*, **9**, 345–351.

Mason, B. and Vitaliano, C.J. (1953) The mineralogy of the antimony oxides and antimonates. *Mineralogical Magazine*, **30**, 100–112.

Mizoguchi, H., Eng, H.W. and Woodward, P.M. (2004) Probing the electronic structures of ternary perovskite and pyrochlore oxides containing Sn^{4+} or Sb^{5+}. *Inorganic Chemistry*, **43**, 1667–1680.

Natta, G. and Baccaredda, M. (1936) Composti chimici interstiziali. Struttura del pentossido di antimonio idrato e di alcuni antimoniati. *Gazzetta Chimica Italiana*, **66**, 308–316.

Roper, A.J., Williams, P.A. and Filella, M. (2012) Secondary antimony minerals: phases that control the dispersion of antimony in the supergene zone. *Chemie der Erde – Geochemistry*, **72** supplement **4**, 9–14.

Stewart, D.J. and Knop, O. (1970) Pyrochlores. VI. Preparative chemistry of sodium and silver antimonates and related compounds. *Canadian Journal of Chemistry*, **48**, 1323–1332.

Witzke, T., Steins, M., Doering, T., Schuckmann, W., Wegner, R. and Pöllmann, H. (2011) Fluornatromicrolite, $(Na,Ca,Bi)_2Ta_2O_6F$, a new mineral species from Quixaba, Paraíba, Brazil. *The Canadian Mineralogist*, **49**, 1105–1110.

Yang, G., Li, G., Xiong, M., Pan, B. and Yan, C. (2011) Hydroxycalciopyrochlore, IMA 2011-026. CNMNC Newsletter No. 10, October 2011, page 2554; *Mineralogical Magazine*, **75**,. 2549–2561.

Mineralogical Magazine, October 2012, Vol. 76(5), pp. 1289–1336

Nomenclature of the hydrotalcite supergroup: natural layered double hydroxides

S. J. Mills[1,*,†], A. G. Christy[2,‡], J.-M. R. Génin[3], T. Kameda[4] and F. Colombo[5]

[1] Geosciences, Museum Victoria, GPO Box 666, Melbourne 3001, Victoria, Australia
[2] Centre for Advanced Microscopy, Sullivans Creek Road, Australian National University, Canberra 0200, ACT, Australia
[3] Institut Jean Barriol FR2843, CNRS-Université de Lorraine, ESSTIN, 2 rue Jean Lamour, F-54500 Vandoeuvre-Lès-Nancy, France
[4] Graduate School of Environmental Studies, Tohoku University, 6-6-07 Aoba, Aramaki, Aoba-ku, Sendai 980-8579, Japan
[5] Cátedra de Geología General, Facultad de Ciencias Exactas, Físicas y Naturales, Universidad Nacional de Córdoba, Vélez Sarsfield 1611, Córdoba, Argentina

[*Received 23 August 2012; Accepted 2 October 2012; Associate Editor: G. Diego Gatta*]

ABSTRACT

Layered double hydroxide (LDH) compounds are characterized by structures in which layers with a brucite-like structure carry a net positive charge, usually due to the partial substitution of trivalent octahedrally coordinated cations for divalent cations, giving a general layer formula $[(M^{2+}_{1-x}M^{3+}_{x})(OH)_2]^{x+}$. This positive charge is balanced by anions which are intercalated between the layers. Intercalated molecular water typically provides hydrogen bonding between the brucite layers. In addition to synthetic compounds, some of which have significant industrial applications, more than 40 mineral species conform to this description. Hydrotalcite, $Mg_6Al_2(OH)_{16}[CO_3]\cdot 4H_2O$, as the longest-known example, is the archetype of this supergroup of minerals. We review the history, chemistry, crystal structure, polytypic variation and status of all hydrotalcite-supergroup species reported to date. The dominant divalent cations, M^{2+}, that have been reported in hydrotalcite supergroup minerals are Mg, Ca, Mn, Fe, Ni, Cu and Zn; the dominant trivalent cations, M^{3+}, are Al, Mn, Fe, Co and Ni. The most common intercalated anions are $(CO_3)^{2-}$, $(SO_4)^{2-}$ and Cl^-; and OH^-, S^{2-} and $[Sb(OH)_6]^-$ have also been reported. Some species contain intercalated cationic or neutral complexes such as $[Na(H_2O)_6]^+$ or $[MgSO_4]^0$. We define eight groups within the supergroup on the basis of a combination of criteria. These are (1) the hydrotalcite group, with M^{2+}:M^{3+} = 3:1 (layer spacing ~7.8 Å); (2) the quintinite group, with M^{2+}:M^{3+} = 2:1 (layer spacing ~7.8 Å); (3) the fougèrite group, with $M^{2+} = Fe^{2+}$, $M^{3+} = Fe^{3+}$ in a range of ratios, and with O^{2-} replacing OH^- in the brucite module to maintain charge balance (layer spacing ~7.8 Å); (4) the woodwardite group, with variable M^{2+}:M^{3+} and interlayer $[SO_4]^{2-}$, leading to an expanded layer spacing of ~8.9 Å; (5) the cualstibite group, with interlayer $[Sb(OH)_6]^-$ and a layer spacing of ~9.7 Å; (6) the glaucocerinite group, with interlayer $[SO_4]^{2-}$ as in the woodwardite group, and with additional interlayer H_2O molecules that further expand the layer spacing to ~11 Å; (7) the wermlandite group, with a layer spacing of ~11 Å, in which cationic complexes occur with anions between the brucite-like layers; and (8) the hydrocalumite group, with $M^{2+} = Ca^{2+}$ and M^{3+} = Al, which contains brucite-like layers in which the Ca:Al ratio is 2:1 and the large cation, Ca^{2+}, is coordinated to a seventh ligand of 'interlayer' water.

* E-mail: smills@museum.vic.gov.au
† Chair of CNMNC sub-commission on hydrotalcite group nomenclature
‡ Vice-chair of CNMNC sub-commission on hydrotalcite group nomenclature
DOI: 10.1180/minmag.2012.076.5.10

The principal mineral status changes are as follows. (1) The names manasseite, sjögrenite and barbertonite are discredited; these minerals are the 2*H* polytypes of hydrotalcite, pyroaurite and stichtite, respectively. Cyanophyllite is discredited as it is the 1*M* polytype of cualstibite. (2) The mineral formerly described as fougèrite has been found to be an intimate intergrowth of two phases with distinct Fe^{2+}:Fe^{3+} ratios. The phase with Fe^{2+}:Fe^{3+} = 2:1 retains the name fougèrite; that with Fe^{2+}:Fe^{3+} = 1:2 is defined as the new species trébeurdenite. (3) The new minerals omsite (IMA2012-025), $Ni_2Fe^{3+}(OH)_6[Sb(OH)_6]$, and mössbauerite (IMA2012-049), $Fe^{3+}_6O_4(OH)_8[CO_3]\cdot 3H_2O$, which are both in the hydrotalcite supergroup are included in the discussion. (4) Jamborite, carrboydite, zincaluminite, motukoreaite, natroglaucocerinite, brugnatellite and muskoxite are identified as questionable species which need further investigation in order to verify their structure and composition. (5) The ranges of compositions currently ascribed to motukoreaite and muskoxite may each represent more than one species. The same applies to the approved species hydrowoodwardite and hydrocalumite. (6) Several unnamed minerals have been reported which are likely to represent additional species within the supergroup.

This report has been approved by the Commission on New Minerals, Nomenclature and Classification (CNMNC) of the International Mineralogical Association, voting proposal 12-B.

We also propose a compact notation for identifying synthetic LDH phases, for use by chemists as a preferred alternative to the current widespread misuse of mineral names.

Keywords: LDH, layered double hydroxide, hydrotalcite, hydrotalcite supergroup, brucite, nomenclature, manasseite, sjögrenite, barbertonite, cyanophyllite, fougèrite, trébeurdenite.

Introduction

The layered double hydroxides (LDHs) are a large class of natural and synthetic compounds whose layered structure is derived from that of brucite, $Mg(OH)_2$. In LDHs, two cations of different charge substitute on the sites corresponding to the Mg of brucite to give an overall positive charge to the hydroxide layer. The positive charge is balanced by monatomic or small complex anions which are intercalated between the layers. The interlayer species are loosely bound and can be exchanged readily (e.g. Meyn *et al*., 1990). This ability to exchange anions between the positively charged structural layers contrasts with the exchange of interlayer cations in silicate clays and channel cations in zeolites (Amphlett, 1958; Carroll, 1959; Barrer, 1978) and many other classes of microporous materials with heteropolyhedral polyhedral frameworks (cf. Ferraris *et al*., 2004; Ferraris and Merlino, 2005), which have negatively charged structural frameworks. All synthetic and many natural examples of the LDHs occur as clay-sized crystals with large surface area to volume ratios (Meyn *et al*., 1990). They have therefore become important to industry, and have found uses as catalysts, drug delivery media, and sequestering agents for organic polymers and CO_2 (Duan and Evans, 2006; Kameda *et al*., 2011*a*,*b*). Oxyanion adsorption and other properties of LDH compounds are reviewed by Goh *et al*. (2008). Organically modified LDH phases prepared by the intercalation of organic anions into the interlayer of the LDH can absorb heavy metal ions and non-ionic organic compounds from aqueous solutions (Kameda and Yoshioka, 2011). Other potential applications of organically modified LDHs lie in the fields of catalysis, photochemistry and electrochemistry (Newman and Jones, 1998). Deprotonation of OH^- ions in so-called Fe^{2+}–Fe^{3+} 'green rust' phases is also of interest in the reduction of oxidized pollutants such as nitrates (Génin *et al*., 2006*c*, 2008).

To date, 44 minerals have been described as natural examples of LDH phases; they are commonly known to mineralogists as the 'hydrotalcites' or 'hydrotalcite group' of minerals. These phases are commonly polytypic, and there are a number of examples where distinct names have been established for different polytypes of the same compound. As a result, a sub-commission was set up to make recommendations on the future naming of these phases, to provide a group taxonomy and to suggest a nomenclature that would be useful for synthetic analogues. The findings of this commission appear in the following text, and have been approved by the Commission on New Minerals, Nomenclature and Classification (CNMNC) of the International Mineralogical Association, voting proposal 12-B.

Crystal chemistry of the hydrotalcite supergroup

The minerals considered here all contain a structural layer based on that of brucite. The brucite structure consists of two adjacent hexagonal eutactic (geometrically 'close-packed') arrays of hydroxide anions, with Mg^{2+} cations filling all of the octahedral spaces between them (Fig. 1). The OH groups are oriented normal to the layers, with the H atoms on the opposite side of the oxygen to the Mg atoms, so that each O is coordinated approximately tetrahedrally by 3Mg + 1H. Layers stack so that each H atom in one layer points into one of the interstices between three H atoms in an adjacent layer. It is important to note that there is no significant H-bonding between layers at ambient pressure. If we

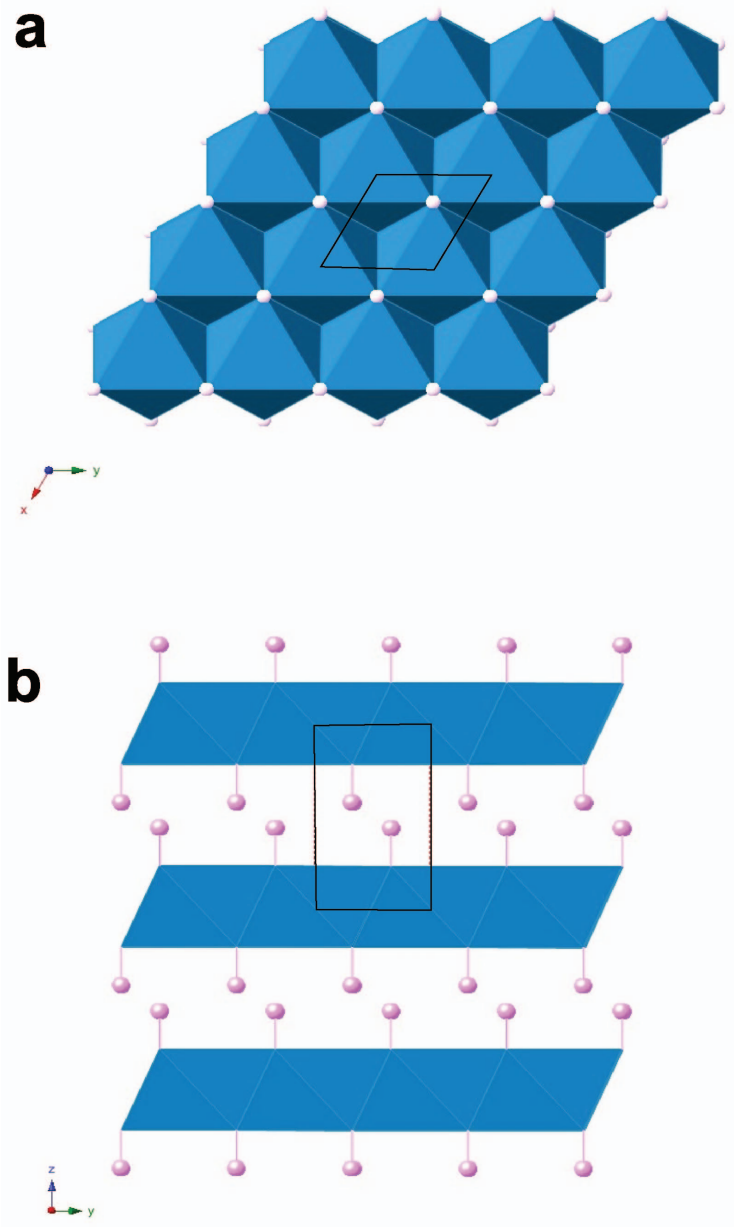

FIG. 1. Brucite structure viewed (*a*) down the *z* axis and (*b*) down the *x* axis. The MgO_6 octahedra are shown as polyhedra, H is shown as small spheres. The unit cell is indicated by the black outline.

represent the possible *xy* offsets of close-packed layers as *A*, *B*, *C* for the oxygens and α, β, γ for the magnesium atoms, the overall stacking sequence can be described as ...*C*α*B*−*C*α*B*−*C*α*B*..., giving a one-layer trigonal structure, with space group $P\bar{3}m1$, and unit-cell dimensions of a = 3.147 and c = 4.769 Å, with Z = 1 (e.g. Zigan and Rothbauer, 1967). Isostructural hydroxides include amakinite (Wyckoff, 1963: p. 239–444), portlandite (Henderson and Gutowsky, 1962), pyrochroite (Parise *et al.*, 1998) and theophrastite (Ramesh *et al.*, 2006), which are the Fe^{2+}, Ca^{2+}, Mn^{2+} and Ni^{2+} analogues, respectively.

The layers in brucite are electrostatically neutral. The LDH phases differ in that some of the octahedral M^{2+} cations are replaced by M^{3+} cations, producing layers with a net positive charge. This is balanced by negatively charged species in an expanded interlayer space, which can also accommodate water molecules and a resultant network of hydrogen bonds between layers. A distinctive feature of the expanded layers in the least structurally complex members of the supergroup, which have interlayer carbonate, is that the OH groups of adjacent brucite layers are aligned directly over one another rather than being offset. The O–H bonds are not necessarily aligned parallel to *c* (cf. Krivovichev *et al.*, 2010*a*). This arrangement presumably optimizes hydrogen bonding to the interlayer species.

Maximum degree of order (MDO) stacking sequences were defined by Dornberger-Schiff (1982) as those in which all layer pairs, triplets and *n*-tuples are geometrically equivalent. For the LDH structures considered here, these are …*C*α*B*–*X*–*B*α*C*–*X*–*C*α*B*–*X*–*B*α*C*… and …*C*α*B*–*X*–*B*γ*A*–*X*–*A*β*C*–*X*–*C*α*B*…, giving 2-layer hexagonal and 3-layer rhombohedral structures, with maximum possible space-group symmetries of $P6_3/mmc$ and $R\bar{3}m$, respectively (Fig. 2). In this scheme, *X* is defined as the interlayer ions and water.

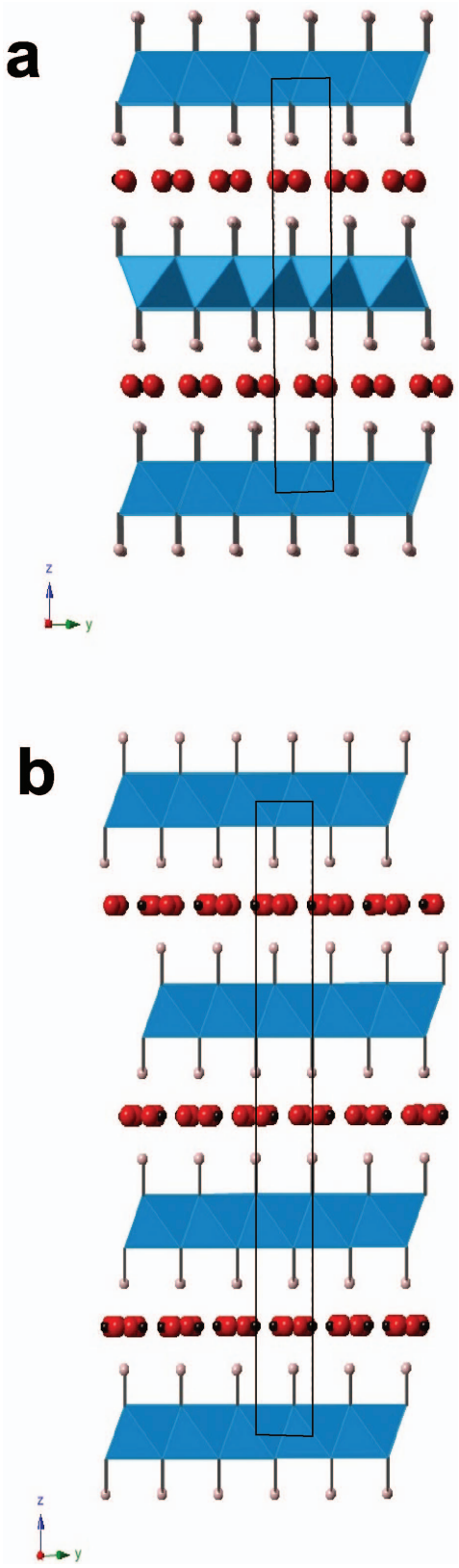

FIG. 2. Hydrotalcite structure viewed down the *x* axis for (*a*) $2H_1$ polytype with *c* ~16 Å and (*b*) $3R_1$ polytype with *c* ~24 Å. Disordered interlayer carbonate and water is indicated by sheets of carbonate groups (red spheres = oxygen, black = carbon). Note that offset of H atoms across the interlayer is different from that in brucite and that alternate brucite layers are rotated relative to one another about *z* by 180º in (*a*), but are translationally equivalent in (*b*).

HYDROTALCITE SUPERGROUP NOMENCLATURE

Hydrotalcite-supergroup minerals and LDHs are well known for the wide range of polytypism which they exhibit. The nature of this polytypism was discussed by Bookin and Drits (1993) and Bookin *et al.* (1993*a*,*b*), with a more recent summary by Evans and Slade (2006). Polytypism in the hydrotalcite structure-type is complex, but in the first instance arises due to the different possible ways the brucite-like layer can stack. Bookin and Drits (1993) discussed several theoretical polytypes and described the X-ray diffraction intensity criteria for distinguishing between them. These included one single-layer polytype, three 2-layer polytypes, nine 3-layer polytypes and a large number of 6-layer polytypes. The stacking sequences of Bookin and Drits (1993) include those with OH groups offset across the interlayer, as in brucite (Fig. 1), and those with OH juxtaposed across interlayers, as in the structures shown in Fig. 2; they referred to these two interlayer geometries as '*O* type' and '*P* type', respectively. A survey of X-ray diffraction data by Bookin *et al*. (1993*a*) showed that although the two MDO *P*-type structures of Fig. 2 were by far the most common, and were the only stacking sequences confirmed for the hydrotalcite group *sensu stricto*, other arrangements with *O*-type interlayers were present in members of the supergroup with expanded interlayers containing sulfate anions. The greater chemical and structural complexity of the interlayer appears to allow more variability in the hydrogen-bonding pattern in such cases. The stacking sequences of Bookin and Drits (1993) with three layers or less are summarized in Table 1. The polytype notation has been revised slightly to distinguish trigonal and hexagonal crystal systems, in accord with the nomenclature scheme of Guinier *et al*. (1984).

The interlayer spacing of hydrotalcite supergroup minerals and LDHs depends on the nature of the interlayer species. The brucite spacing of ~4.7 Å increases to ~7.8 Å in minerals with interlayer hydroxide, halide or carbonate groups, and to 8.5–9 Å in minerals with interlayer sulfate tetrahedra. Spacings of ~11 Å are observed if the interlayer contains additional H_2O coordinated to sulfate (e.g. the glaucocerinite group) or large, low-charge cations such as Na^+ and Ca^{2+} (e.g. the wermlandite group).

In hydrotalcite-supergroup minerals and LDHs, the M^{2+}:M^{3+} ratio is generally constant, and the minerals have a strong preference for a M^{2+}:M^{3+} ratio of either 3:1 or 2:1. Cation ratios greater than 3:1 are known, particularly in synthetic LDHs, but are less commonly observed in minerals (although brugnatellite appears to be an example). Cation ratios of less than 2:1 are uncommon for good crystal-chemical reasons. Three M^{3+} cations around a single OH in the trioctahedral sheet of

TABLE 1. Possible hydrotalcite stacking sequences with periods of 3 layers or less. Symbols {*A*,*B*,*C*} indicate offsets of hydroxide sublayers, {α,β,γ} offsets of octahedral cations, – indicates an *O*-type interlayer and = a *P*-type interlayer.

Symbol	Layer sequence	Interlayer type	OH sublayers all equivalent	Cation sublayers all equivalent	Maximum possible space group
1*T*	*A*β*C*–*A*β*C*	*O*	Yes	Yes	$P\bar{3}m1$
$2H_1$	*A*β*C*=*C*β*A*=*A*β*C*	*P*	Yes	Yes	$P6_3/mmc$
$2H_2$	*A*β*C*–*A*γ*B*–*A*β*C*	*O*	No	Yes	$P6_3mc$
2*T**	*A*β*C*–*B*γ*A*=*A*β*C*	*O* + *P*	No	Yes	$P\bar{3}m1$
$3R_1$	*A*β*C*=*C*α*B*=*B*γ*A*=*A*β*C*	*P*	Yes	Yes	$R\bar{3}m$
$3R_2$	*A*β*C*–*B*γ*A*–*C*α*B*–*A*β*C*	*O*	Yes	Yes	$R\bar{3}m$
$3T_1$	*A*β*C*–*A*γ*B*–*A*γ*B*–*A*β*C*	*O*	No	No	$P3m1$
$3T_2$	*A*β*C*–*A*γ*B*–*C*α*B*–*A*β*C*	*O*	No	No	$P\bar{3}m1$
$3T_3$	*A*β*C*–*A*γ*B*=*B*γ*A*=*A*β*C*	*O* + *P*	No	No	$P3m1$
$3T_4$	*A*β*C*–*A*β*C*=*C*β*A*=*A*β*C*	*O* + *P*	No	No	$P\bar{3}m1$
$3T_5$	*A*β*C*–*A*γ*B*=*B*α*C*–*A*β*C*	*O* + *P*	No	No	$P\bar{3}m1$
$3T_6$	*A*β*C*–*A*γ*B*–*C*β*A*=*A*β*C*	*O* + *P*	No	No	$P3m1$
$3T_7$	*A*β*C*–*A*β*C*–*B*γ*A*=*A*β*C*	*O* + *P*	No	No	$P3m1$

* 2*T* was labelled "$2H_3$" by Bookin and Drits (1993).

a hydrotalcite-type mineral will lead to over-bonding of the oxygen unless the M–O bonds are severely lengthened. The coordination polyhedra of these three highly-charged cations would also be sharing edges with one another, which is not favoured electrostatically. It seems likely that local ordering of M^{2+} and M^{3+} occurs to prevent the formation of such M^{3+} clusters. This is, in effect, an 'aluminium avoidance principle' analogous to that invoked by Loewenstein (1954) to account for tetrahedral cation order in aluminosilicates. Triangular clusters of edge-sharing M^{3+} cations can be avoided at M^{2+}:M^{3+} ratios of 2:1 if the M^{2+} are ordered in a honeycomb pattern within the layer, giving a $\sqrt{3}\times\sqrt{3}$ superlattice in the plane of the layer (Fig. 3). For ratios of 3:1, M^{3+} avoidance can be achieved without long-range order.

Within-layer ordering of M^{2+} and M^{3+} cations has been verified in some cases by infrared spectroscopy (e.g. Richardson and Braterman, 2007), ^{1}H and ^{25}Mg NMR spectroscopy (e.g. Sideris *et al*., 2008) and electron diffraction (e.g. Steeds and Morniroli, 1992). However, if the resulting superlattices of successive layers are offset in a disordered fashion, the local ordering may not be reflected in the unit cell determined by X-ray methods. The data available to date suggests that some LDH phases show no long-range stacking order of any *xy* superlattices; some show short-range order, giving rise to rods of diffuse scattering parallel to **c*** in X-ray diffraction patterns; and others show a high degree of long-range order. Examples of all three cases have recently been reported for the mineral quintinite (Krivovichev *et al*., 2010*a*,*b*,*c*). Long-range order in some hydrotalcite-supergroup minerals has produced *xy* superstructures with (pseudo)hexagonal unit nets (in multiples of the brucite *a* parameter) including the following: $\sqrt{3}\times\sqrt{3}$ [brugnatellite (Fenoglio, 1938), pyroaurite/sjögrenite (Ingram and Taylor, 1967), stichtite (Mills *et al*., 2011), chlormagaluminite (Kashaev *et al*., 1982), zincowoodwardite (Witzke and Raade, 2000), quintinite (Arakcheeva *et al*., 1996; Krivovichev *et al*., 2010*a*), zincalstibite (Bonaccorsi *et al*., 2007)]; 2×2 [pyroaurite (Ingram and Taylor, 1967), hydrotalcite (Allman and Jepsen, 1969), reevesite (White *et al*., 1967; De Waal and Viljoen, 1971)]; 3×3 [carrboydite (Nickel and Clarke, 1976), motukoreaite (Rodgers *et al*., 1977, Zamarreño *et al*., 1989), cualstibite (Walenta, 1984), wermlandite (Rius and Allmann, 1984), shigaite (Cooper and Hawthorne, 1996), nikischerite (Huminicki and Hawthorne, 2003)]; $\sqrt{12}\times\sqrt{12}$ [mountkeithite (Hudson and Bussell, 1981), quintinite, charmarite and caresite (Chao and Gault, 1997)]; $\sqrt{13}\times\sqrt{13}$ [pyroaurite/sjögrenite (Ingram and Taylor, 1967)]; and even $\sqrt{27}\times\sqrt{27}$ [karchevskyite (Britvin *et al*., 2008)]. Offsets of $\sqrt{3}\times\sqrt{3}$ layers in some cases result in a lowering of the symmetry to monoclinic and rectangular unit meshes of $\sqrt{3}\times2$ [hydrocalumite (Sacerdoti and Passaglia, 1988)] or $\sqrt{3}\times3$ times that of brucite [cyanophyllite (Kolitsch and Giester, 2007; Kolitsch *et al*., in press); quintinite (Krivovichev *et al*., 2010*b*)]. The unit meshes in

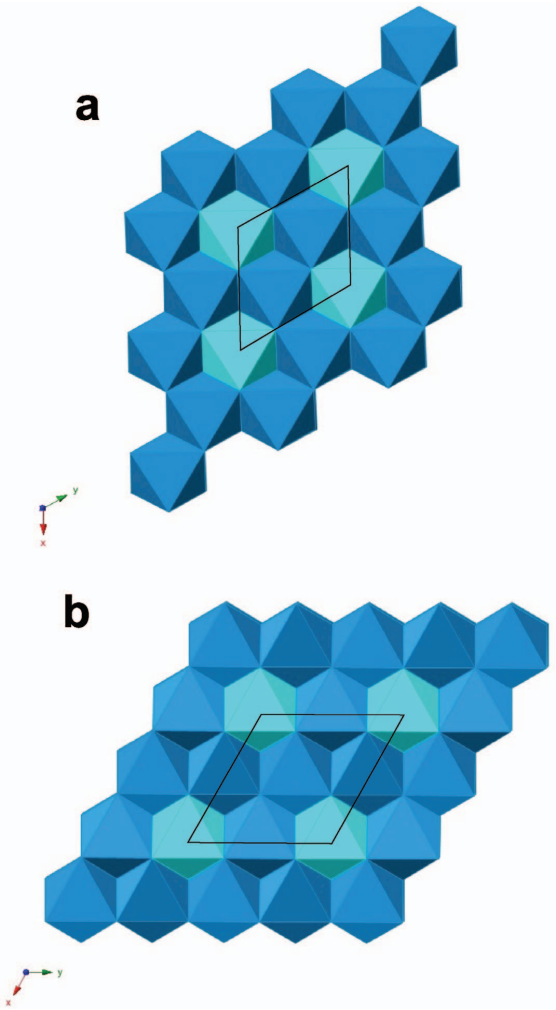

FIG. 3. Most symmetrical ordering patterns of two different types of octahedra in a brucite layer for (*a*) 2:1 ratio of the two species and (*b*) 3:1 ratio. In both cases, edge-sharing between two octahedra of the minority species is avoided.

the *xy* plane of the known superstructures are shown in Fig. 4. It should be noted that the polytype labelling scheme of Table 1 applies only for stacking of layers with *a* ~3 Å (1 × 1 mesh); if the true *a* and *b* repeats are larger: (1) a much wider range of stacking vectors are possible and (2) the structural significance of a stacking vector such as [⅔, ⅓, ⅓] may be quite different. For $\sqrt{3}\times\sqrt{3}$, 3×3, $\sqrt{12}\times\sqrt{12}$ and $\sqrt{27}\times\sqrt{27}$ supercells, this vector will juxtapose a cation or hydroxide sublayer in the '*A*/α' position against another *A*/α, rather than against *B*/β or *C*/γ.

The *c* repeat of the structure can be further modulated by long-range order of octahedral cations. For example, 'quinitinite-2*H*-3*c*' of Krivovichev *et al.* (2010*a*) has an overall formula $[Mg_4Al_2(OH)_{12}](CO_3)\cdot3H_2O$, and a well-defined 6-layer structure, in which the full periodicity along *z* is determined by factors other than stacking of the brucite layers alone. The unit mesh of one layer contains $[Mg_2Al(OH)_6]$, with 3 anions per unit mesh in each hydroxide sublayer (Krivovichev *et al.*, 2010*a*). If Mg and Al are not distinguished, the stacking pattern is $2H_1$. However, as the Mg and Al are ordered to produce a 3×3 superstructure in the *xy* plane, the Al positions are systematically offset so as to triple the repeat. Each charge-balancing interlayer contains $0.5(CO_3) + 1.5(H_2O)$, giving a total of 3 oxygens per unit mesh, but the partial occupancies and smearing of electron density in difference-Fourier maps both imply that the carbonate and water positions are not ordered in these minerals.

Strong positional and orientational ordering of interlayer species is present in some species such as wermlandite and shigaite (which are described in the following text), and this can also lead to increased periodicity along *z*. In these species, it is the offset and orientation of the *interlayers* that defines the polytypic stacking, rather than that of the octahedral layers. It is also possible for two different types of interlayers to interstratify regularly, as exemplified by coalingite (which is also discussed in the following text).

Minerals with the hydrotalcite structure type

The members of the hydrotalcite supergroup all have brucite-like structural layers with interlayer anions and water. Some of these minerals contain hydrated cations that are connected to the brucite layers only through hydrogen bonds. Layered calcium aluminate hydrate phases have been included as the hydrocalumite group, although they are anomalous in that the Ca of the layer makes a seventh bond to an 'interlayer' water. Phases in which hydroxides of the brucite layer are replaced by halides or by the oxygen atoms of complex anions such as sulfate are excluded; these include minerals such as spangolite, $Cu_6Al(OH)_{12}Cl(SO_4)\cdot3H_2O$ (Hawthorne *et al.*,

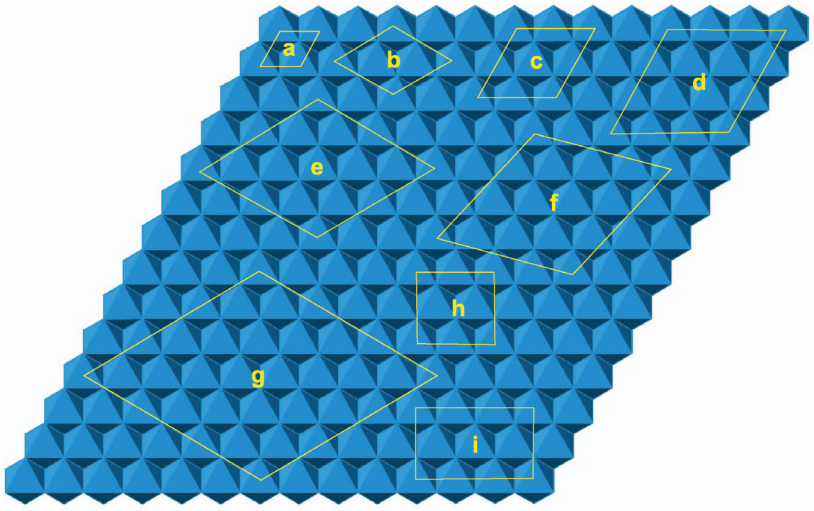

FIG. 4. A brucite-type octahedral layer showing the meshes of the known superstructures in the hydrotalcite supergroup in the *xy* plane. The (pseudo)hexagonal meshes are (*a*) 1 × 1 mesh of brucite; (*b*) $\sqrt{3}\times\sqrt{3}$; (*c*) 2×2; (*d*) 3×3; (*e*) $\sqrt{12}\times\sqrt{12}$; (*f*) $\sqrt{13}\times\sqrt{13}$; (*g*) $\sqrt{27}\times\sqrt{27}$. Orthogonal meshes are (*h*) $\sqrt{3}\times2$; (*i*) $\sqrt{3}\times3$.

1993). Species with essential vacancies in the layer or with direct linkages through OH to interlayer cations, as in mooreite, $Mg_9Zn_4Mn^{2+}_2(OH)_{26}(SO_4)_2{\cdot}8H_2O$ (Hill, 1980) are also excluded. Similarly, exclusions apply to minerals with vacancies in the octahedral layers such as chalcoalumite, $CuAl_4(OH)_{12}(SO_4){\cdot}3H_2O$, the Ni analogue 'nickelaumite', Zn analogue kyrgyzstanite and probable nitrate analogues mbobomkulite and hydrombobomkulite (Uvarova *et al.* 2005), and also to alvanite, $ZnAl_4(OH)_{12}(VO_3)_2{\cdot}2H_2O$, and its Ni analogue ankinovichite, which have inovanadate chains in the interlayers (Pertlik and Dunn, 1990). Cyanotrichite, $Cu_4Al_2(OH)_{12}(SO_4){\cdot}2H_2O$, and related species such as the antimonate camerolaite and the fluoride khaidarkanite, are compositionally similar, but do not possess a continuous edge-sharing layer of octahedra (Hager *et al.*, 2009). It is worthwhile noting that the term 'hydrotalcite group' has been applied loosely in the past, so as to include many of these excluded species (cf. Lozano *et al*., 2012).

Hydrotalcite and manasseite

Hydrotalcite and manasseite are both ideally $Mg_6Al_2(OH)_{16}[CO_3]{\cdot}4H_2O$. Hydrotalcite was the first LDH phase to be discovered (Hochstetter, 1842) as contorted, lamellar-to-fibrous white masses of waxy or pearly lustre in serpentinite from Snarum, Norway. It should be noted, however, that Hochstetter regarded the CO_2 content in his analyses as due to alteration. The early history of hydrotalcite is convoluted, as is that of the related minerals described below; it is well reviewed by Frondel (1941). Various occurrences were described under synonyms such as 'voelknerite' or 'houghite', and some authors believed hydrotalcite to be a mixture. Hydrotalcite became generally accepted as a valid species only after the optical, thermal and analytical characterization study of Manasse (1915), who derived the currently accepted formula, which was later confirmed by Foshag (1920).

Frondel (1941) performed an X-ray study on hydrotalcite from the type locality and three other occurrences, and found that all contained a mixture of hexagonal and rhombohedral phases, except for the hydrotalcite from Somerville, New York, which was exclusively rhombohedral. The rhombohedral phase gave patterns corresponding to a unit cell with a = 3.065 and c = 23.07 Å, similar to those of pyroaurite and stichtite, whereas the hexagonal phase had a = 3.06 and c = 15.34 Å, similar to those of sjögrenite and barbertonite. The name manasseite was proposed for the hexagonal phase, hydrotalcite being reserved for the rhombohedral phase, and this usage has persisted. The c parameters correspond to 3 brucite layers (23 Å repeat of hydrotalcite-3*R*) and 2 layers (15 Å repeat of manasseite-2*H*) per unit cell, respectively. It has been known, however, since the study of Ingram and Taylor (1967), that the two minerals are polytypic modifications. Pausch *et al*. (1986) noted that they commonly intergrow to form compound crystals, with manasseite (2*H* polytype) at the core and hydrotalcite (3*R* polytype) at the rim. The stacking sequences were verified as $2H_1$ and $3R_1$ by Bookin *et al*. (1993*a*).

As the a parameters listed above are approximately the same as that of brucite, these minerals have no long-range ordering of Mg and Al, and their unit cells contain 3 or 2 ($M^{2+} + M^{3+}$) and ⅜ or ¼ $[CO_3]^{2-}$, respectively. Such fractional unit-cell contents are unusual for phases of apparently fixed stoichiometry. It is perhaps not surprising that Allman and Jepsen (1969) reported a $R\bar{3}m$ cell with doubled a and c parameters (a = 6.13, c = 46.15 Å and Z = 3) for hydrotalcite.

Analyses of 'hydrotalcite' from the type locality with Mg:Al = 2:1 and 2.30:1 (Stanimirova, 2001) suggest that quintinite may also be present (as discussed in the following text) as well as intergrowths of the two phases.

Pyroaurite and sjögrenite

Pyroaurite was described with analyses from Långban, Värmland, Sweden, by Igelström (1865), however, the essential carbonate content and correct formula $Mg_6Fe^{3+}_2(OH)_{16}[CO_3]{\cdot}4H_2O$, were not confirmed until the study of Manasse (1915). The morphological crystallographic studies of Sjögren (1894) and Flink (1901) suggested rhombohedral symmetry for at least some of the golden-brown platy hexagonal material. The type material was found to contain coexisting hexagonal and rhombohedral phases in the X-ray study of Aminoff and Broomé (1931). These phases had cell parameters of a = 3.097 and c =15.56 Å; and a = 3.089 and c = 23.23 Å, respectively. Frondel (1941) reserved the name pyroaurite for the rhombohedral phase, and proposed sjögrenite for the hexagonal phase. Allmann (1968) noted that as with the Al analogues hydrotalcite and manasseite, these

polytypes can occur in a single crystal, with the higher temperature 2*H* phase at the core and the 3*R* phase at the rim. The stacking sequences were verified as $2H_1$ and $3R_1$ by Bookin *et al*. (1993*a*).

As is the case for hydrotalcite/manasseite, the unit cells may represent substructures. Ingram and Taylor (1967) reported a cell with a = 6.19 and c = 46.54 Å, with Z = 3 in $R\bar{3}m$ for pyroaurite, although their cell for sjögrenite (a = 3.113 and c = 15.61 Å in $P6_3/mmc$) is similar to that of Frondel (1941). Taylor (1969, 1973) observed diffraction corresponding to $\sqrt{3}\times\sqrt{3}$ and $\sqrt{13}\times\sqrt{13}$ *xy* superstructures in pyroaurite and sjögrenite.

The mineral 'igelströmite' was reported from Haaf Grunay, Shetland, Scotland by Heddle (1879) as the hydroxide analogue of pyroaurite. However, re-examination of material from the 'type locality' by Rouxhet and Taylor (1969) showed that although some interlayer OH^- replaced $[CO_3]^{2-}$, carbonate was dominant. However, they did not discount the possibility that a hydroxide-dominant phase might exist.

Stichtite and barbertonite

Stichtite was described as massive to fibrous material of a strong lilac colour, associated with serpentine minerals and chromite, from Dundas, Tasmania, Australia, by Petterd (1910: pp. 167–169). Foshag (1920) was the first to suggest the formula $Mg_6Cr_2^{3+}(OH)_{16}[CO_3]\cdot 4H_2O$, which is analogous to that of hydrotalcite, but the existence of two phases with unit cells similar to those of hydrotalcite and manasseite was not confirmed until the X-ray study of Frondel (1941). The hexagonal phase, which was found in specimens from Dundas and from Barberton, Transvaal, South Africa was named barbertonite by Frondel (1941); it has unit-cell parameters a = 3.085 and c =15.52 Å, whereas rhombohedral stichtite *sensu stricto*, has a = 3.09 and c = 23.19 Å. Mills *et al.* (2011) refined the structures of both minerals by the Rietveld technique for type barbertonite from the Kaapsehoop asbestos mine, Barberton district, South Africa and stichtite from Stichtite Hill, Dundas, Tasmania. Cell parameters were a = 3.096–3.097, c = 15.619–15.627 Å, with Z = ¼; and a = 3.096, c = 23.507 Å, with Z = ⅜, respectively, and the 2*H*–3*R* polytypic relationship was confirmed. Therefore, both minerals are polytypic varieties of stichtite. A 1*T* polytype was reported from the Terektinsky ridge, Altai Republic, Russia by Tatarinov *et al.* (1985) and mentioned by Bookin *et al.* (1993*b*). Bookin *et al.* (1993*b*) discussed the transformation of Terektinsky ridge stichtite on exposure to light or X-rays from pink material with the $3R_1$ structure of Bookin and Drits (1993) to green material with a = 5.30 and c = 7.36 Å, corresponding to the 1*T* polytype with a $\sqrt{3}\times\sqrt{3}$ superstructure in the *xy* plane, and stacking disorder indicated by diffuse *hk*0 reflections.

Meixnerite

Meixnerite was described in association with talc from fractures in a serpentinite at Ybbs-Persenberg, Niederösterreich, Austria by Koritnig and Süsse (1975). The formula, $Mg_6Al_2(OH)_{18}.4H_2O$, is derived from that of hydrotalcite if the $[CO_3]^{2-}$ group is replaced by $2[OH]^-$. Thus, the hydroxide anion plays two distinct roles in the structure and the formula is better written as $[Mg_6Al_2(OH)_{16}](OH)_2\cdot 4H_2O$. Only the 3*R* polytype has been reported, with space group $R\bar{3}m$, and unit-cell parameters a = 3.046, c = 22.93 Å, with Z = ⅜.

Iowaite

Iowaite was described by Kohls and Rodda (1967), using material from a borehole core from Sioux County, Iowa. Only a small quantity of material was available, and they reported the formula as $[Mg_4Fe^{3+}(OH)_8]OCl\cdot 2-4H_2O$. Allmann and Donnay (1969) reviewed the data of Kohls and Rodda (1967) and noted their similarity with those of the pyroaurite group. Braithwaite *et al*. (1994) re-investigated iowaite from the Palabora open pit mine, South Africa, and concluded that the correct formula was $[Mg_6Fe_2^{3+}(OH)_{16}]Cl_2\cdot 4H_2O$, indicating that iowaite is the Fe^{3+} analogue of woodallite and the Cl analogue of pyroaurite/sjögrenite. Crystal structure analyses reported by Braithwaite *et al*. (1994) gave a cell with the space group $R\bar{3}m$, and the parameters a = 3.1183 and c = 24.113 Å, with Z = ⅜, indicating the 3*R* polytype.

Droninoite

Droninoite, was described by Chukanov *et al*. (2009) as the Ni analogue of iowaite and reevesite from the Dronino meteorite (Dronino, Kasimov district, Ryazan Oblast', Russia). The mineral forms dark green to brown fine-grained crusts, with individual crystals less than a micrometre

across. The empirical formula, based on $Z = 6$ is $Ni_{2.16}Fe^{2+}_{0.75}Fe^{3+}_{0.97}Cl_{1.62}(OH)_{7.10}\cdot 2.28H_2O$, which corresponds to an ideal formula $[Ni_6Fe^{3+}_2(OH)_{16}]Cl_2\cdot 4H_2O$, grouping Ni and Fe^{2+}. Chukanov *et al*. (2009) gave the lattice type as trigonal *R*, with unit-cell parameters a = 6.206 and c = 46.184 Å; i.e. a $\sqrt{13}\times\sqrt{13}$ *xy* supercell and 6*R* stacking sequence. Based on the unit cell for pyroaurite given by Ingram and Taylor (1967), droninoite is likely to crystallize in the space group $R\bar{3}m$. It is noteworthy that IR spectroscopy showed the complete absence of carbonate and sulfate in the structure.

Woodallite

Woodallite, the Cl analogue of stichtite/barbertonite, was described by Grguric *et al*. (2001) from the Mount Keith nickel mine, which is also the type locality for mountkeithite. Woodallite forms lilac masses of platelets <100 μm across which are visually similar to stichtite and mountkeithite. The ideal formula, $[Mg_6Cr_2(OH)_{16}]Cl_2\cdot 4H_2O$, is consistent with other Cl-rich members of the hydrotalcite supergroup, and the space group and unit cell are $R\bar{3}m$ and a = 3.102, c = 24.111 Å, with Z = ⅜, indicating the 3*R* polytype.

At Mount Keith, a complete solid-solution series was shown to exist between woodallite and stichtite (e.g. Woodhouse, 2006; Mills *et al*., 2012*c*), and Rietveld analysis was employed to model the 3*R* structure at various points in the series (Whitfield *et al*., 2010; Mills *et al*., 2012*c*).

Desautelsite

Desautelsite, $Mg_6Mn^{3+}_2(OH)_{16}[CO_3]\cdot 4H_2O$, is the Mn^{3+} analogue of hydrotalcite. It has been reported from several localities in the USA (Dunn *et al*., 1979) and in Japan (Matsubara *et al*., 1984), as bright orange hexagonal crystals. The space group and unit-cell parameters are $R\bar{3}m$, and a = 3.114, c = 24.39 Å, with Z = ⅜, indicating the 3*R* polytype. No superstructure reflections were observed, implying no long-range order in the structure. Experiments (e.g. Hansen and Taylor, 1991) show that desautelsite forms at low temperatures (~35ºC), in slightly alkaline (pH ~9) solutions.

Takovite

Takovite was first described by Maksimović (1957) as $Ni_5Al_4O_2(OH)_{18}\cdot 4H_2O$, from Takovo, Serbia; its properties and genesis were described in further papers (Maksimović, 1958, 1959). As takovite was originally reported to be carbonate-deficient, and in view of its similarities with LDH phases, Bish and Brindley (1977) investigated samples from Serbia, Australia and France. In these samples CO_3 was found to range from 0.80 to 0.95 a.p.f.u. Cation M^{2+}:M^{3+} ratios of 5.87:2.12 and 5.73:2.28 were reported leading to the ideal formula $Ni_6Al^{3+}_2(OH)_{16}[CO_3]\cdot 4H_2O$, which is consistent with a hydrotalcite-group mineral.

Bish and Brindley (1977) reported a rhombohedral unit cell with parameters a = 3.0250 and c = 22.595 Å, which is consistent with the 3*R* polytype, and Bookin *et al*. (1993*a*) verified the $3R_1$ stacking sequence. Mills *et al.* (2012*c*) confirmed the $R\bar{3}m$ space group with unit-cell parameters a = 3.0290(2) and c = 22.5995(15) Å, on crystals from the Agoudal mine, Bou Azzer, Tazenakht, Morocco.

Bish (1980) exchanged the interlayer carbonate of takovite with sulfate to produce the Al analogue of honessite with c = 26.74 = 3 × 8.91 Å and carrboydite with c = 32.47–32.50 = 3 × 10.82–10.83 Å. Bookin *et al*. (1993*a*) deduced the $3R_1$ stacking sequence for carrboydite, and reported the unusual $3R_2$ structure for the Al analogue of honessite. Their work implies that anion exchange in the interlayer can cause displacement of the brucite layers and a concomitant change in the polytype.

Reevesite

Reevesite was described by White *et al.* (1967) as fine-grained bright yellow cavity infillings in meteorites from Wolf Creek, Western Australia. They noted a strong resemblance between its X-ray powder data and those of pyroaurite, and from qualitative chemical analysis deduced that it must be the Ni^{2+} analogue, ideally $Ni_6Fe^{3+}_2(OH)_{16}(CO_3)\cdot 4H_2O$. They estimated the unit-cell parameters as a = 6.15 and c = 45.61 Å. A more detailed description was published by De Waal and Viljoen (1971) from material that formed minute greenish yellow hexagonal platelets in nickel ore in the Bon Accord area of the Barberton Mountain Land, South Africa. They gave its formula as $(Ni_{16.69}Fe^{2+}_{0.83}Mg_{0.41}Co_{0.07})Fe^{3+}_{6.00}(OH)_{48}(CO_3)_3\cdot 12H_2O$, which is in accord with the ideal endmember formula suggested by White *et al.* (1967). The unit cell parameters are a = 6.164 and c = 45.54 Å. The data from both of these sets of authors suggest a 6-layer polytype

with a 2×2 superlattice in the *xy* plane. However, the diffraction data of De Wall and Viljoen (1971) were reinterpreted by Bookin *et al.* (1993*b*) as corresponding to an intergrowth of a $3R_1$ structure with a = 3.082 and c = 22.770 Å and a 1*T* structure with a $\sqrt{3} \times \sqrt{3}$ superstructure in the *xy* plane, with a somewhat contracted layer spacing of a = 5.337 and c = 21.608 Å.

Jamborite

Morandi and Dalrio (1973) described jamborite as green fibrous-lamellar pseudomorphs after millerite from ophiolites at Ca' dei Ladri and Monteacuto Ragazza near Bologna and Castelluccio di Moscheda near Modena, Italy. The X-ray powder patterns indicated a hexagonal cell (more probably rhombohedral in actuality) with a = 3.07 and c = 23.3 Å. Nickel was the dominant cation, and small but consistent amounts of Co and Fe were present. The S content was consistently found to be 3.5 wt.%, but this was not thought to be due to interlayer sulfate as dissolution in HCl did not give a precipitate with a $BaCl_2$ solution. The S was therefore reported to be present as interlayer sulfide anions, which is unique amongst the LDH minerals. There is about one sulfide ion per 7−8 octahedral cations. The general formula of Morandi and Dalrio, amended to include Co^{3+}, is $[(Ni,Co,Fe)^{2+}_{1-x}(Ni,Co,Fe)^{3+}_{x}(OH)_2][(OH)_2,S_{x/2}] \cdot 1-{}^{x}/_{2}H_2O$. If we assume that Co and Fe are fully oxidized, the analytical data are consistent with the formula $[(Ni^{2+}_{0.94-x}Ni^{3+}{}_{x}Co^{3+}_{0.04}Fe^{3+}_{0.02})(OH)_2]S_{0.14}(OH)_{x-0.22} \cdot yH_2O$, in which $y \sim 1$. Note that x must be $\geqslant 0.22$. At the minimum value of x, 0.28 of the octahedral cations are trivalent, which is close to the ideal hydrotalcite ratio of ¼, and $S^{2-} >> OH^-$. It is tempting to speculate that the ideal endmember formula might be $[(Ni^{2+}_6Ni^{3+}_2)(OH)_{16}]S^{2-} \cdot 4H_2O$, but at the same time it must be noted that the coexistence of oxidized Ni^{3+} and reduced S^{2-} in an oxycompound is unusual, and that the pale green colour of jamborite is not consistent with charge transfer between Ni^{2+} and Ni^{3+}.

Quintinite

Quintinite was initially described from Mont Saint-Hilaire, Québec, Canada, as a 3*T* polytype of $Mg_4Al_2(OH)_{12}[CO_3] \cdot 3H_2O$, by Chao and Gault (1997). The space group given was $P3_112$, with unit-cell parameters a = 10.751 and c = 22.71 Å, and Z = 6. Although the c parameter is similar to that of hydrotalcite, the a repeat is about $\sqrt{12}$ times that of brucite, implying the existence of long-range order within the layers. The Mg:Al ratio is higher than that of hydrotalcite, as Al occupies ⅓ of the octahedral sites rather than ¼. The carbonate content is correspondingly higher (one $[CO_3]^{2-}$ per 6 octahedra, rather than one per 8 octahedra), but the water content is effectively the same as that of hydrotalcite (one H_2O per two octahedra). Chao and Gault (1997) also re-examined a well-crystallized gemmy yellow mineral occurring in cavities in dolomite from the Jacupiranga carbonatite, Brazil, originally reported as manasseite by Menezes and Martins (1984), and found it to be a 2*H* polytype of quintinite, with space group $P6_322$ and unit-cell parameters a = 10.571 and c = 15.171 Å, with Z = 4. Chao and Gault (1997) reported several other instances in which phases with a quintinite-like composition had been wrongly described as either hydrotalcite or manasseite. The 3*T* and 2*H* polytypes were initially described as distinct mineral species and were assigned separate IMA proposal numbers; they are now regarded as polytypes of a single species.

Arakcheeva *et al*. (1996) had previously examined the 2*H* polytype from Jacupiranga without describing it as a new mineral; however, they reported a different space group ($P\bar{6}2m$) and unit-cell parameters a = 5.283 and c = 15.150 Å, with Z = 1. Nevertheless, they described strong long-range order of Mg and Al within the brucite layers.

Recently, quintinite from the Kovdor alkaline massif, Kola peninsula, Russia, was examined by Krivovichev *et al.* (2010*a*,*b*,*c*). Their single-crystal X-ray study confirmed that quintinite occurs in several structural varieties, with different stacking sequences and different degrees of long-range order. They published structure solutions for three new varieties of quintinite. One is related to the structure of Arakcheeva *et al*. (1996), but has the repeat in the c direction tripled due to [⅔,⅓,0] layer displacements every second layer. Thus, the data for quintinite are space group $R32$, with unit-cell parameters a = 5.275 and c = 45.36 Å, and Z = 3 (Krivovichev *et al*., 2010*a*). The authors proposed the designation 'quintinite-2*H*-3*c*' for this modification, to indicate that the stacking of the brucite layers is 2*H* if Mg−Al order is ignored, but that said, ordering introduces an additional tripling of *c*. A disadvantage of the notation proposed by

Krivovichev *et al.* (2010*a*) is that it does not make explicit the *R* lattice of the overall structure. There is a strong c = 15.12 Å subcell, and reflections with $l \neq 3n$ are weak and diffusely streaked, implying substantial stacking disorder. Their second quintinite variant (Krivovichev *et al*., 2010*b*) displayed monoclinic symmetry for the first time in natural LDH phases other than those of the cualstibite and hydrocalumite groups. They reported the space group as *C*2/*m*, with the unit-cell dimensions a = 5.266, b = 9.114 (which is $\sim\sqrt{3}a$), c = 7.766 Å and β = 103.17º, with Z = 1, giving $c\sin\beta$ = 7.562 Å and $-c\cos\beta$ = 1.769 Å = $a/3$. Again, reflections due to Mg−Al order within layers were weak and diffuse. In the structure, all layers are equivalent, and the structure is a cation-ordered superstructure of the conventional 3*R* polytype. The third quintinite variant (Krivovichev *et al*., 2010*c*) was disordered quinitinite-2*H*, with the space group $P6_3/mmc$ (corrected from $P6_3/mcm$ as published) and unit-cell parameters a = 3.045 and c = 15.12−15.18 Å, with Z = ⅙. Note that cation ordering may or may not be preserved within a layer; however, it is certain that registration between layers is absent in this phase.

Charmarite and caresite

Charmarite, $Mn_4Al_2(OH)_{12}[CO_3]\cdot 3H_2O$, and caresite, $Fe_4Al_2(OH)_{12}[CO_3]\cdot 3H_2O$, are the Mn^{2+} and Fe^{2+} analogues of quintinite, respectively. They were described along with quintinite by Chao and Gault (1997) from Mont Saint-Hilaire. Charmarite occurs as 2*H* and 3*T* polytypes, with the following space groups and unit-cell data: $P6_322$, a = 10.985 and c = 15.10 Å, with Z = 4 (2*H*); and $P3_112$, a = 10.985 and c = 22.63 Å, with Z = 6 (3*T*). As with quintinite, the 3*T* and 2*H* polytypes were initially described as distinct mineral species and were assigned separate IMA proposal numbers, but they are now considered to be polytypes of a single species. Caresite is known only as the 3*T* polytype, with the space group $P3_112$ and unit-cell parameters a = 10.805 and c = 22.48 Å, with Z = 6.

Zaccagnaite

Zaccagnaite, ideally $Zn_4Al_2(OH)_{12}[CO_3]\cdot 3H_2O$, the Zn analogue of quintinite, was described from the Carrara marble of Calagio Quarry, Tuscany, Italy, by Merlino and Orlandi (2001). The space group and unit-cell parameters correspond to the disordered 2*H* polytype, with the space group $P6_3/mmc$ and unit-cell parameters a = 3.073 and c = 15.114 Å, with Z = ⅙. Diffuse streaks parallel to **c*** were observed at (⅓,⅓,*l*)* and equivalent loci, and interpreted to imply strong Zn−Al ordering in two dimensions, albeit with no interlayer correlation. Witzke and Raade (2000) noted that a second occurrence of zaccagnaite, from Lavrion, Greece, occurred as the 3*R* polytype, but the unit cell was not refined due to intergrowth with related phases. A 3*R* polytype was described from the El Soplao cave, Cantabria, Spain by Lozano *et al*. (2012). This material has space group $R\bar{3}m$, and unit-cell parameters a = 3.0662 and c = 22.6164 Å, with a formula $(Zn_{0.593}Fe_{0.004}Mg_{0.015}Mn_{0.008}Al_{0.380})(OH)_2\ (CO_3)_{0.19}\cdot 0.19H_2O$. Thus, the M^{2+}:M^{3+} ratio is 1.63:1 rather than 2.00:1, and the high Al content is charge-balanced by a higher than normal carbonate content (≡ 1.14 per 12[OH]) in the interlayer. Note that a variable M^{2+}:M^{3+} ratio, with a tendency toward high contents of M^{3+}, is a common feature of minerals in the woodwardite and glaucocerinite groups containing the small divalent cations Zn^{2+}, Cu^{2+} and Ni^{2+} (as noted in the following discussion).

Chlormagaluminite

Chlormagaluminite was described from a magnetite−chlorite skarn in the Kapaevskaya explosion pipe, Irkutsk Oblast', Russia, by Kashaev *et al.* (1982). Analysis of the type material gave a formula $(Mg_{3.55}Fe^{2+}_{0.27}Na_{0.05})_{\Sigma 3.87}(Al_{1.93}Fe^{3+}_{0.07}Ti_{0.01})_{\Sigma 2.01}(OH)_{12}[CO_3]_{0.12}Cl_{1.48}\cdot 2.42H_2O$, which strongly suggests an ideal endmember formula $Mg_4Al_2(OH)_{12}Cl_2\cdot 3H_2O$, and hence that chlormagaluminite is, in terms of its composition, the chloride analogue of quintinite. The space group was reported to be $P6_3/mcm$, $P6_3cm$ or $P\bar{6}c2$, with unit-cell parameters a = 5.29 and c = 15.46 Å, and Z = ¾. These data correspond to the 2*H* polytype with $\sqrt{3}\times\sqrt{3}$ superstructure in *xy* plane. The mineral was previously reported under the name 'chlormanasseite' by Feoktistov *et al.* (1978).

Comblainite

Comblainite was described as turquoise cryptocrystalline crusts from the Shinkolobwe mine, Katanga, Democratic Republic of the Congo, with a formula $(Ni^{2+}_xCo^{3+}_{1-x})(OH)_2(CO_3)_{(1-x)/2}\cdot yH_2O$ by Piret and Deliens (1980). The unit cell is

rhombohedral, and the parameters recalculate to give axes of a = 3.038 and c = 22.79 Å. The two formulae reported by Piret and Deliens (1980) can be recast on the basis of $6[M^{2+} + M^{3+}]$ as: $[(Ni^{2+}_{4.07}Co^{3+}_{1.93}(OH)_{12}](CO_3)_{0.88}(OH)_{0.18}\cdot 4.47H_2O$ and $[(Ni^{2+}_{4.07}Co^{3+}_{1.93}(OH)_{12}](CO_3)_{0.68}(OH)_{0.56}\cdot 6.61H_2O$. Possession of R translational symmetry for the 3-layer polytype is more typical of the pyroaurite group than the quintinite group; however, the M^{2+}:M^{3+} ratio is consistently 2:1 rather than 3:1, so comblainite can be considered to be the $Ni^{2+}-Co^{3+}$ analogue of quintinite.

Fougèrite

There is a very special case in the hydrotalcite supergroup where the two cations in the octahedral layer are the same chemical element in different oxidation states, namely Fe^{2+} and Fe^{3+} in the mineral fougèrite (and possibly also Ni^{2+} and Ni^{3+} in jamborite). Vysostskii (1905) first described the bluish green colour of so-called gleysols from below the water table ('gley' is transliterated from the Russian 'глей' = 'clay'); this colour was attributed by Arden (1950) to a mixed-valence Fe mineral which was described as 'ferrosic hydroxide' with Fe^{2+} dominant and the formula $Fe(OH)_{2+x}$ (see also Taylor, 1980; Herbillon, 2006). The phase was never properly characterized because of the low concentration of Fe that is usually found in waterlogged soils (about 5%). However, it was possible, using Mössbauer spectroscopy, (an Fe-oxidation state selective technique) to attribute the Fe^{2+} content to a chemical compound which is commonly described as 'green rust', because it is an intermediate $Fe^{2+}-Fe^{3+}$ compound which forms during the corrosion of Fe-based materials and steels (Génin *et al.*, 1986, 1996, 1998, 2002; Drissi *et al.*, 1995; Trolard *et al*., 1997, 2007; Refait *et al*., 2003). Green rust was first identified by Girard and Chaudron (1935). It is an LDH type compound, with Fe^{2+} and Fe^{3+} in the octahedral layer (cf. Simon *et al.*, 2003; Aïssa *et al.*, 2006). The symmetry depends on the shape of the intercalated anion, being $R\bar{3}m$ ($3R$ polytype) for a phase described as 'green rust I' with spherical or planar intercalated anions such as F^-, Cl^-, I^-, CO_3^{2-}, CH_3COO^- or $C_2O_4^{2-}$; or $P\bar{3}m1$ ($1T$ polytype) for 'green rust II' with tetrahedral anions such as SO_4^{2-} or SeO_4^{2-} (Bernal *et al*., 1959). The $3R$ phases have unit-cell dimensions a = 3.17–3.18 and c = 22.7–22.9 Å if the intercalated anions are CO_3^{2-}. The intercalated anion in natural material was not initially known, and it took some time before it was shown to be CO_3^{2-}. This carbonate-bearing material is the most thermodynamically stable green rust phase, and has been produced in the laboratory by bacterial reduction of γ-FeOOH in anoxic conditions similar to those found in aquifers (Ona-Nguema *et al*., 2002). In nature, the CO_3^{2-} is produced by the oxidation of organic matter as part of a redox couple in which Fe-reducing bacteria reduce Fe^{3+} in the absence of oxygen (Ruby *et al*., 2006).

Characterization of the natural material was complicated by the fact that the Fe^{3+} molar fraction x = (Fe^{3+}/Fe_{tot}), as determined by Mössbauer spectroscopy, was always found to be greater than ⅓ (e.g. Génin *et al.*, 1998, 2005; Féder *et al.*, 2005; Rodionov *et al.*, 2006). In contrast, synthetic samples produced by co-precipitation always had x = ¼–⅓, as in any other LDH (Génin *et al.*, 2006*b*; Génin and Ruby, 2008), and compositions such as $Fe^{2+}_6Fe^{3+}_2(OH)_{16}CO_3\cdot 3H_2O$ and $Fe^{2+}_4Fe^{3+}_2(OH)_{12}CO_3\cdot 3H_2O$ (Génin *et al.*, 2005). This inconsistency was resolved when it was shown that green rust oxidizes by one of two mechanisms. In the most common mechanism the green rust dissolves, with subsequent precipitation of ferric oxyhydroxides such as ferrihydrite, lepidocrocite and finally goethite (Drissi *et al.*, 1995; Benali *et al.*, 2001). The less common mechanism involves oxidation accompanied by *in situ* deprotonation to produce the compound $Fe^{2+}_{6(1-x)}Fe^{3+}_{6x}O_{12}H_{14-6x}CO_3\cdot 3H_2O$, with x > ⅓ and hence some O^{2-} replacing OH^- in the hydroxide layer (Génin *et al.* 2005, 2006*a*). The existence of this phase might be taken to indicate the existence of a continuous solid solution, with x ranging from 0 to 1. However, studies of the variation of x in synthetic samples with electrode potential E_h and the derived chemical potential indicate that for x values in the range ⅓–⅔, the compositions are mixtures of two endmember phases with x = ⅓ and x = ⅔. Furthermore, it was found that for x in the range ⅔–1, the compositions are mixtures of endmember phases with x = ⅔ and x = 1, and an additional endmember exists at x = 0 (Ruby *et al.*, 2010). Low-temperature Mössbauer spectroscopy and magnetic susceptibility measurements support this conclusion (Rusch *et al*., 2008), and show that these four different compounds have distinct magnetic properties arising from long-range ordering of Fe^{2+} and Fe^{3+} within the layers. If x = 0 [i.e. in $Fe^{2+}_6(OH)_{10}(H_2O)_2CO_3\cdot 3H_2O$], all of

the cations are Fe^{2+}; if x = ⅓ [i.e. in $Fe^{2+}_4Fe^{3+}_2(OH)_{12}CO_3{\cdot}3H_2O$], the Fe^{3+} cations are all surrounded by six Fe^{2+} cations in the pattern shown in Fig. 3*a*, to minimize electrostatic repulsion; if x = ⅔ [i.e. in $Fe^{2+}_2Fe^{3+}_4O_2(OH)_{10}CO_3{\cdot}3H_2O$], the Fe^{2+} cations are surrounded by six Fe^{3+} cations; and if x = 1 [i.e. in $Fe^{3+}_6O_4(OH)_8CO_3{\cdot}3H_2O$], all of the cations are Fe^{3+} (Rusch *et al*., 2008). This unusual redox flexibility has a major role in determining gleysol properties.

Samples of 'fougèrite' collected from below the permanent water table display experimental average values of x in the range ⅓–⅔, which indicates that they contain a mixture of domains with x = ⅓ and x = ⅔, intergrown in a topotactic relationship, with an overall composition derived from the relative proportions of the two phases according to the lever rule (Génin *et al.*, 2012*a*). Type fougèrite, as described by Trolard *et al.* (2007), has such a range and therefore contains two distinct mineral species (which are discussed in the following text). Gleys recently found in maritime marshes (Génin *et al.*, 2012*b*) have x values in the range ⅔–1, indicating that they are a mixture of domains with x = ⅔ and x = 1 in topotactic intergrowth. The x = 1 phase corresponds to the new mineral mössbauerite.

Mössbauerite

Mössbauerite, (IMA2012–049), ideally $Fe^{3+}_6O_4(OH)_8CO_3{\cdot}3H_2O$, is the fully oxidized Fe^{3+} analogue of the mixed valence Fe^{2+}–Fe^{3+} green rust minerals fougèrite (described in the foregoing text; see also Trolard *et al*., 2007) and trébeurdenite (described in the following text). The type locality is Mont Saint-Michel Bay, France. Mössbauerite crystallizes in space group $R\bar{3}m$, and the unit-cell parameters are a = 3.079 and c = 22.253 Å, with Z = ½, implying a 3R polytype with no superstructure in the xy plane. Further details of the identification of mössbauerite by Mössbauer spectroscopy are included in the following text (see also the redefinition of fougèrite) and in Génin *et al.* (2012*b*).

Woodwardite

Woodwardite is a grandfathered species from an unknown type locality in Cornwall, UK (Dana, 1892). The formula was given by Palache *et al.* (1951) as "probably $[Cu_4Al_2(OH)_{12}](SO_4){\cdot}2–4H_2O$". A sample from Cornwall in the Natural History Museum, London (specimen BM 40035), studied by Nickel (1976), was difficult to analyse due to decomposition under the electron beam, but showed variability in the Cu:Al atomic ratio (1.73–2.03, with one anomalously low value of 1.21). Weak and diffuse powder X-ray data were obtained, corresponding to a rhombohedral cell with a = 3.00 and $c = 3 \times 9.1$ = 27.3 Å (Raade *et al*., 1985). Nickel (1976) noted that dehydration occurred readily with increasing temperature, causing a steady decrease in layer spacing from 9.1 Å at room temperature to 8.1 Å at 120ºC. For consistency with more recently described members of the group, such as reevesite, the formula may be better expressed $[Cu_{1-x}Al_x(OH)_2](SO_4)_{x/2}{\cdot}nH_2O$, in which x = 0.33–0.37 and $n \leqslant 0.5$. The lower water content differentiates this species from hydrowoodwardite.

Zincowoodwardite

Witzke and Raade (2000) described zincowoodwardite from Naturhistorisches Museum (Vienna) samples H 858 and G 2172, from Lavrion, Greece, which were previously examined by Raade *et al.* (1985). Witzke and Raade (2000) also reported data from additional natural material from the Hilarion Mine at Lavrion and synthetic samples, initially described in Witzke (1995). They expressed the formula as $(Zn_{1-x}Al_x)(OH)_2(SO_4)_{x/2}{\cdot}nH_2O$. Diffraction indicated the existence of two polytypes, 1T and 3R, with probable space groups $P\bar{3}$ and $R\bar{3}m$, respectively, and cell contents Z = 1 and Z = 3. Cell parameters were a = 3.063 and c = 8.91 Å for 1T; and a = 3.065 and $c = 25.42 = 3 \times 8.47$ Å for 3R. Raade *et al.* (1985) had previously reported $a = 5.306 = \sqrt{3} \times 3.063$ Å and c = 26.77 Å for sample H858, suggesting that a $\sqrt{3} \times \sqrt{3}$ superstructure can occur in the xy plane. The composition was, however, variable. The ratio $M^{3+}/(M^{2+} + M^{3+})$ ranged from 0.32–0.33 in the 1T polytype, and from 0.35–0.50 in the 3R polytype. In the natural 3R polytype, some Zn was reported to be replaced by Cu, with Cu/(Zn + Cu) in the range 0.22–0.24; this ratio ranged from 0–0.47 in synthetic samples. The analysis reported for material from sample H858 by Raade *et al.* (1985) can be recalculated to produce the formula $[(Zn_{4.38}Cu_{0.94}Al_{2.68})(OH)_{16}]Na_{0.33}(SO_4)_{1.33}(CO_3)_{0.56}.8.98H_2O$; the Na content and high water content suggest an admixture with natroglaucocerinite. The best simplified formula is probably $[Zn_{1-x}Al_x(OH)_2](SO_4)_{x/2}{\cdot}nH_2O$, in which x = 0.32–0.50 and n < 3x/2.

HYDROTALCITE SUPERGROUP NOMENCLATURE

Honessite

Honessite was described as an oxidation product of Ni-Fe sulfides from Linden, Iowa County, Wisconsin, USA, by Heyl *et al.* (1959). Bish (1980), studying anion exchange in LDH phases, concluded that honessite was $[Ni_6Fe_2^{3+}(OH)_{16}](SO_4)\cdot 4H_2O$, and therefore the sulfate analogue of reevesite. Additional data was reported by Bish and Livingstone (1981), who reported a rhombohedral cell with $a = 3.083$ and $c = 3 \times 8.90 = 25.8$ Å. Bookin *et al*. (1993*a*) deduced a $3R_1$ stacking sequence from X-ray intensity data. Honessite, and the similar but more hydrous phase hydrohonessite, $[Ni_6Fe_2^{3+}(OH)_{16}](SO_4)\cdot\sim 7H_2O$, which has a larger interlayer spacing of ~11 Å (see following text), interconvert readily depending on temperature and humidity (Bish, 1980). Given the compositional variability shown by other members of this group, it is safest to assume that the 3:1 Ni:Fe ratio is not fixed, and that the best simplified formula for honessite is probably $[Ni_{1-x}Fe^{3+}_x(OH)_2](SO_4)_{x/2}\cdot nH_2O$ in which $x < 0.5$ and $n < 3x/2$.

Glaucocerinite

Glaucocerinite was originally described as a waxy material of uneven blue colour by Dittler and Koechlin (1932) on specimens in the collection of the Naturhistorisches Museum (Vienna) from Lavrion, Greece. These specimens were re-examined by Raade *et al.* (1985), who regarded those with catalogue numbers G1377 and G1378 to be the true type material. Powder X-ray diffraction indicated that glaucocerinite coexists with a woodwardite-like mineral on sample G2172, and only the latter mineral was found on samples G2173 and H858. The analyses of Raade *et al.* (1985) indicated that this woodwardite-like phase was zincowoodwardite, and this was confirmed by Witze and Raade (2000). Historically, there has been much confusion between glaucocerinite- and woodwardite-like phases, as evidenced by the JCPDS card 17-132 for 'woodwardite' from Caernarvonshire, Wales, which has powder data corresponding to a glaucocerinite-like cell and is in fact hydrowoodwardite (Witzke, 1999). The same is true for the Cornish 'woodwardite' of Nickel (1976). The unit-cell data of Raade *et al.* (1985) for glaucocerinite correspond to a rhombohedral cell with $a = 3.057-3.070$ and $c = 32.52-32.65$ Å, although two weak additional lines in one diffraction pattern suggested that the true symmetry may be lower. Raade *et al.* (1985) calculated a formula based on their own analyses of $[(Zn,Cu)_{4.98}Al_{3.02}(OH)_{16}](SO_4)_{1.47}(OH)_{0.08}\cdot 9.10H_2O$. Witzke (1999) presented analytical data for a range of natural and synthetic glaucocerinites for comparison with hydrowoodwardite. The Al/(Zn + Cu + Al) ratios were 0.38−0.43 in natural samples and 0.32−0.50 in synthetic material and the Cu/(Zn + Cu) ratios were 0.26−0.29 in natural samples and 0.00−0.47 in synthetic material. Hence, there appears to be a complete solid solution from the Zn endmember towards the Cu analogue hydrowoodwardite, and a M^{3+} content ranging from values comparable to those of the quintinite group to M^{2+}:M^{3+} = 1:1.

Witzke (1999) noted that the maximum sulfate content that is sterically permissible in glaucocerinite is one sulfate for every three *M* cations, and that the expanded interlayer accommodates three water molecules per sulfate ion in addition to those that are present in the woodwardite group; these form hydrogen bonds to the apical oxygens of the sulfate tetrahedron. Therefore, the total water content is $n > 3x/2$. The most general simplified formula for glaucocerinite is thus $[Zn_{1-x}Al_x(OH)_2](SO_4)_{x/2}\cdot nH_2O$, in which $x = 0.32-0.50$ and $n > 3x/2$, which is similar to zincowoodwardite, but with a higher water content.

Hydrowoodwardite

Hydrowoodwardite was described as a porous blue botryoidal coating from the St Briccius mine, Königswalde, Saxony, Germany, by Witzke (1999). Its formula was given as $[Cu_{1-x}Al_x(OH)_2](SO_4)_{x/2}\cdot nH_2O$, with x ranging from 0.23−0.62 in natural samples, and a postulated minimum of $n = 3x/2$ water molecules. It is worthwhile noting that a value of $x > 0.50$ (i.e. Al > Cu) may justify the definition of a new species. Some Cu was replaced by Zn, the range of Cu/(Cu + Zn) being between 0.82 and 1.00 in the analysed natural samples, and 0.54−1.00 in synthetic material, showing that the solid-solution series to glaucocerinite is complete. Witzke (1999) also stated that the 'woodwardites' from the collection of the National Museum of Wales (specimen number NMW 27.111 GR 443 from Simdde Dylluan and number NMW 27.111 GR 464 from the Ffriddgoch mine) examined by Nickel (1976) and Raade *et al.* (1985) were hydrowoodwardite. This material gave weak and diffuse diffraction patterns similar to those of JCPDS 17-132, corresponding to a rhombohedral

cell with a = 3.066 and c = 3 × 10.93 = 32.80 Å. The partial analysis of Raade *et al.* (1985) gave a Cu:Zn:Al cation ratio of 57.0:0.5:42.5 for this sample, so that Cu/Al = 1.34, which contrasts with earlier analyses reported in Nickel (1976), which have Cu/Al ratios of 0.62−0.82. Witzke (1999) noted that hydrowoodwardite dehydrates to woodwardite in dry air over a period of weeks and can be rehydrated by immersion in water.

Witzke (1999) also reported a variety of hydrowoodwardite from the St Christoph mine, Bärenhecke, Germany, with $[CO_3]^{2-}$ substitution for $[SO_4]^{2-}$ accompanied by minor uranyl ions, which he presumed to reside in the interlayer, and gave the formula $[Cu_{0.49}Zn_{0.01}Al_{0.50}(OH)_2](SO_4)_{1.6}(CO_3)_{0.09}(UO_2)_{0.01}.nH_2O$.

Carrboydite

Carrboydite was described with a mean formula $(Ni,Cu)_{6.90}Al_{4.48}(SO_4,CO_3)_{2.78}(OH)_{21.69}\cdot 3.67H_2O$, from lateritized komatiites at the Carr Boyd Rocks mine, Western Australia, by Nickel and Clarke (1976). The reported Ni:Al ratio ranges between 1.05 and 1.80. Electron microscopy showed carrboydite spherulites to consist of aggregates of thin platy crystals, and an X-ray and electron diffraction study indicated a metrically hexagonal unit cell with a = 9.14 and c = 10.34 Å. A second phase with a larger layer spacing of ~11 Å was intimately associated. This was initially interpreted as a more highly hydrated relative of carrboydite, and was considered to be an unnamed nickel analogue of glaucocerinite by Nickel (1976) and Raade *et al.* (1985). It has a rhombohedral unit cell with a = 3.022 and c = 32.45 = 3 × 10.82 Å.

The mineral with c = 10.34 Å is the 1T polytype of carrboydite. Bookin *et al.* (1993*a*) identified the polytype with the 3-layer structure as $3R_1$, which is the same as the synthetic carrboydite of Bish (1980), which was synthesized from takovite by anion exchange.

The a repeat of carrboydite *sensu stricto* is typical of a 3 × 3 superstructure in the xy plane. Nickel and Clarke (1976) explained the unusual c repeat as possibly arising from the presence of a double brucite layer (i.e. and ...*XMXMX*... sandwich rather than ...*XMX*...); however, even with occupancy of the octahedral sites reduced to 75% to obtain the correct stoichiometry, this structure has an implausibly high coordination number for the central layer hydroxide ions. It is more probable that conventional MX_2 layers are present, and the interlayer spacing increases from 8 Å due to the presence of additional intercalated octahedral cations. Recalculating the formula on the basis of 18(OH) gives $[(Ni,Cu)_{5.28}Al_{3.72}(OH)_{18}]Ni_{0.44}(SO_4,CO_3)_{2.31}\cdot 3.04H_2O$.

Given the reversible hydration and dehydration properties of these minerals, there does not appear to be any justification for making a species-level distinction between carrboydite and the '11 Å phase'. Disregarding the superstructures in the xy plane and minor changes in the hydration state and M^{2+}:M^{3+} ratio, they can be regarded as the 1T and 3R polytypes of a more broadly defined carrboydite, with a general formula $[(Ni,Cu)_{1-x}Al_x(OH)_2]Ni_y(SO_4,CO_3)_{x/2+y}\cdot nH_2O$, which can be simplified to $[Ni_{1-x}Al_x(OH)_2](SO_4)_{x/2}\cdot nH_2O$, with x ~0.40 and n ~0.33. Regardless of the details of its superstructure, polytypic modification and interlayer content, carrboydite is the Ni analogue of glaucocerinite and the Al analogue of hydrohonessite.

Hydrohonessite

Hydrohonessite occurs as microscopic yellow flakes and was originally found in 1971 at Otter Shoot, Kambalda, Western Australia, in amounts that were too small for a full characterization (Nickel and Wildman, 1981). Its nature was finally determined by Nickel and Wildman (1981) by comparison with carrboydite, mountkeithite and motukoreaite. Bish and Livingstone (1981) reported another occurrence of hydrohonessite on the island of Unst, Shetland, Scotland. The hydrohonessite of Nickel and Wildman (1981) was described with a metrically hexagonal cell with a = 3.09 and c = 10.80 Å, indicating the 1T polytype, whereas that of Bish and Livingstone (1981) had c = 33.4 = 3 × 11.13 Å. An analysis of diffraction intensities led Bookin *et al*. (1993*a*) to suggest the unusual stacking sequence $3R_2$ for this latter polytype. The empirical formula reported by Nickel and Wildman (1981) was $[Ni_{5.43}Fe^{3+}_{2.57}(OH)_{16}]Ni_{0.98}(SO_4)_{2.26}\cdot 6.95H_2O$, which is close to honessite but with additional water. The excess of octahedral cations over hydroxide indicates the presence of interlayer octahedra, although the excess Ni in the structure does not appear to be as readily exchangeable as the excess Mg of mountkeithite (Nickel and Wildman, 1981). The formula given for Unst hydrohonessite by Bish and Livingstone (1981), $[Ni_{5.55}Mg_{0.10}Fe^{3+}_{2.35}(OH)_{16}](SO_4)_{1.18}\cdot xH_2O$, has less sulfate and no

interlayer Ni, suggesting either that the intercalated octahedral cation may not be essential or that the nickel content was overestimated by Nickel and Wildman (1981). The expansion of the layer spacing to ~11 Å may be a result of the presence of additional water, additional sulfate, additional octahedral cations of type similar to those of the brucite layers, or some combination of the above. Regardless of these details, hydrohonessite is considered to be the Fe^{3+} analogue of carrboydite.

Mountkeithite

Mountkeithite was described as a white flaky alteration product of stichtite from the Mount Keith nickel deposit, 400 km north-northwest of Kalgoorlie, Western Australia (Hudson and Bussell, 1981). The mineral has intercalated octahedral cations as in the wermlandite group, but a distinctive feature of its chemistry is that these are Mg^{2+}, and constitute an exchangeable $MgSO_4$ component. This component is lost so readily that mountkeithite reacts with water to produce a pyroaurite-like phase with a 7.8 Å layer spacing. This reaction can be fully reversed by immersion in a 1 M $MgSO_4$ solution. The powder data were best fitted by a hexagonal unit cell with a = 10.698 and c = 22.545 Å, corresponding to a $\sqrt{12} \times \sqrt{12}$ superstructure in the xy plane, a 2-layer structure with less than full occupancy of the interlayer sites for a formula with 24(OH) in the brucite layer, and Z = 2. The structural formula hypothesized by Hudson and Bussell (1981), with minor omissions, is $[(Mg_{8.15}Ni_{0.85}Cu_{0.02})(Fe^{3+}_{1.31}Cr_{1.02}Al_{0.65})(OH)_{24}](Mg_{1.94}Ni_{0.18})(SO_4)_{2.32}(CO_3)_{1.11}\cdot 9.39H_2O$, suggesting an ideal formula close to $[(Mg_9Fe^{3+}_3)(OH)_{24}]Mg_2(SO_4)_{3.5}\cdot 9H_2O$. No information about the ordering or interconnection of the interlayer Mg^{2+}, SO_4^{2-} and H_2O is currently available. However, regardless of its superstructure, polytypic modifications and exact interlayer composition (particularly the loosely held additional cations), mountkeithite is considered to be the Mg analogue of hydrohonessite, with a simplified formula $[Mg_{1-x}Fe^{3+}_x(OH)_2][SO_4]_{x/2}\cdot nH_2O$, in which x ~0.25 and n ~3x.

Zincaluminite

Zincaluminite is a grandfathered mineral species that is not described to modern standards and is therefore questionable. It occurs at the Kamariza mine, Lavrion, Greece (Bertrand and Damour, 1881; Palache *et al*., 1951) as small hexagonal or pseudohexagonal plates. The formula is commonly reported to be $Zn_6Al_6[SO_4]_2(OH)_{26}\cdot 5H_2O$, but no structural data are available. The formula can be recast as $[Zn_3Al_3(OH)_{12}][SO_4](OH)\cdot 2.5H_2O$, which suggests a hydrotalcite-like mineral. The M^{2+}:M^{3+} ratio of 1:1 is very high in comparison to most LDH compounds, but has been reported in synthetic Cu-free glaucocerinite (Witzke, 1999), which is almost identical in composition to zincaluminite. The mineral urgently needs further study; it is not obvious that it merits distinction from Cu-free glaucocerinite or zincowoodwardite.

Wermlandite

Wermlandite is the prototype for a group of LDH minerals which contain both anions and hydrated cations as intercalated species. Wermlandite was described by Moore (1971) as green-grey platy crystals with magnetite and drusy calcite in dolomitic marble from Långban, Värmland, Sweden. The interlayer anion was originally reported to be carbonate, but was later shown to be sulfate by Rius and Allmann (1984) who expressed the formula as $[Mg_7(Al_{0.57}Fe_{0.43})_2(OH)_{18}]^{2+}[(Ca_{0.6}Mg_{0.4})(SO_4)_2(H_2O)_{12}]^{2-}$ with half of the H_2O forming a coordination octahedron around the interlayer (Ca,Mg) and the remaining H_2O molecules being hydrogen-bonded to this octahedron, the sulfate and the hydroxide layers. The ideal formula is therefore $[Mg_7Al_2(OH)_{18}][Ca(H_2O)_6][SO_4]_2\cdot 6H_2O$. The space group and unit-cell parameters are $P\bar{3}c1$, and a = 9.303, c = 22.57 Å, with Z = 2, which are consistent with a 2-layer structure. It is important to note that Bookin *et al*. (1993*a*) showed that the stacking of the brucite-like layers is actually 1T, and the doubling of the period along z arises from orientational ordering of the interlayer sulfate and water groups. This complex but well-ordered interlayer, which contains large species, results in an increase of the layer periodicity in wermlandite to ~11 Å; the 3 × 3 superstructure in the xy plane allows ordering of the 7M^{2+} and 2M^{3+} in each layer. The wermlandite structure of Rius and Allmann (1984) is shown schematically in Fig. 5. The 7:2 ordering pattern of Mg and Al in the octahedral layer is shown in Fig. 6, along with the two differently oriented interlayers of the unit cell, which are related by a c-glide. By analogy with 'quintinite-2H-3c' (which is described in the

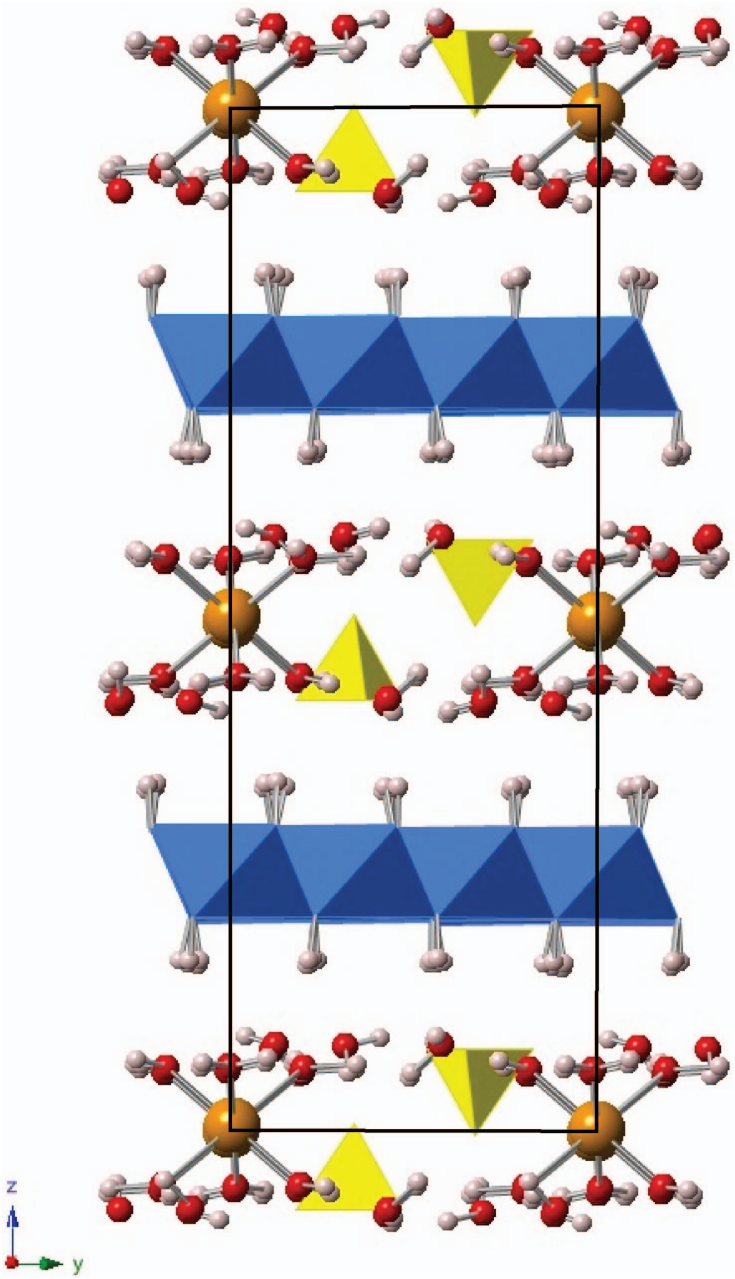

FIG. 5. View of the wermlandite structure down the *x* axis. The (Mg,Al) octahedra are blue, interlayer $[SO_4]^{2-}$ tetrahedra are yellow, Ca^{2+} are large orange spheres, H^{+} are small pink spheres and the O^{2-} of H_2O molecules are medium-sized red spheres. Note that the two octahedral layers are not offset but the sulfate tetrahedra of successive interlayers are differently oriented.

previous text), the wermlandite polytype could be described as 'wermlandite-1*T*-2*c*' rather than 'wermlandite-1*T*', to emphasize the fact that the two brucite layers are not oriented differently; however, this notation is problematic and is not adopted herein. For the wermlandite group, the standard polytype symbols proposed by Guinier *et al*. (1984) are probably sufficient, but the fact that the structural principle behind the stacking variation differs from that in the groups with simpler interlayers should be borne in mind: it is based on the offset and orientation of the

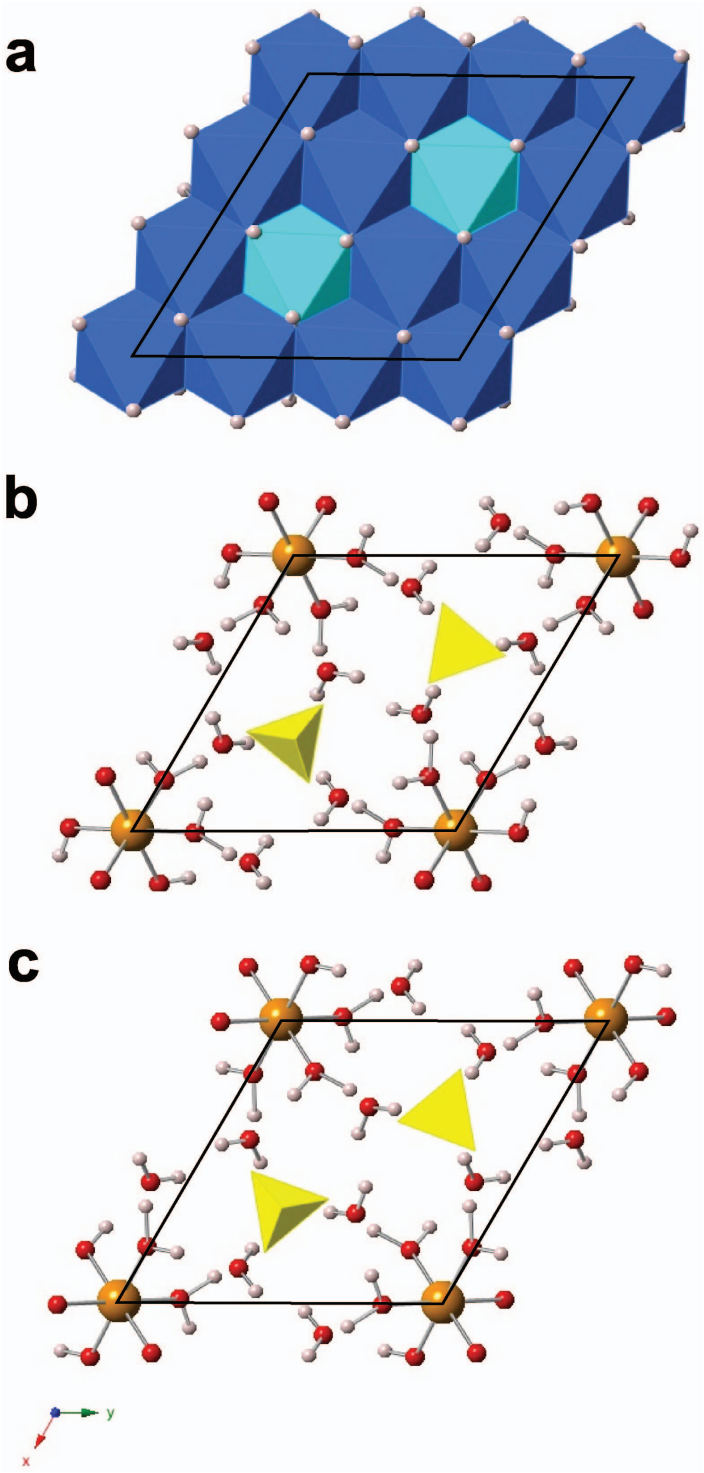

FIG. 6. Slices of the wermlandite structure parallel to (001). (*a*) The ordering pattern of 7 Mg (dark) and 2 Al (light) octahedra in the brucite layer at $0.1 < z < 0.4$; (*b*) the interlayer at $-0.1 < z < 0.1$, showing $[SO_4]^{2-}$ tetrahedra, $[Ca(H_2O)_6]^{2+}$ octahedra and additional H_2O; (*c*) the interlayer at $0.4 < z < 0.6$, reflected relative to that of (*b*) by a *c*-glide. The (Mg,Al) octahedra are blue, interlayer $[SO_4]^{2-}$ tetrahedra are yellow, Ca^{2+} are large orange spheres, H^+ are small pink spheres and the O^{2-} of H_2O molecules are medium-sized red spheres.

interlayer components rather than that of the octahedral layers.

Brindley (1979) and Rius and Allmann (1984) noted that expanded 11 Å layer structures are fragile, and are readily destroyed or converted into more compact layers by ion exchange, mild heating, grinding or dehydration. The resulting intergrowths of phases and their decomposition products may complicate characterizations of minerals in this group.

Shigaite

Shigaite was described as yellow hexagonal plates from the Ioi mine, Shiga Prefecture, Japan by Peacor *et al.* (1985) and has subsequently been reported from several other metamorphosed manganese deposits. It has the formula $[Mn_6Al_3(OH)_{18}][Na(H_2O)_6][SO_4]_2{\cdot}6H_2O$, which is analogous to that of wermlandite, but with a greater proportion of M^{3+} in the brucite-like sheets and Na^+ instead of Ca^{2+} in the interlayer. The structure was refined by Cooper and Hawthorne (1996) using a crystal from the N'Chwaning mine, South Africa. The space group and unit-cell parameters are $R\bar{3}$ and a = 9.512, c = 33.074 Å, with Z = 3. The 3×3 superstructure in the plane of the layers is similar to that of wermlandite. The $6M^{2+}$ and $3M^{3+}$ in each layer are well ordered, with M^{3+} occupying both of the sites in the wermlandite structure and one additional site, and M^{2+} forming a honeycomb net around M^{3+} such that no two M^{3+} octahedra share edges (as shown in Fig. 2*b*). The 3×3 *xy* unit mesh contains three Al atoms at vectors <⅔,⅓,0> relative to one another, so the 3-layer rhombohedral cell cannot be generated by displacements of the brucite sheets. Instead, the 3-layer periodicity is defined by shifts of the interlayer $[Na(H_2O)_6]^+$ and $[SO_4]^{2-}$ groups. Note that labelling the polytype '1*T*-3*c*' would fail to express the translational symmetry of the rhombohedral lattice, as is also the case for 'quintinite-2*H*-3*c*' (as discussed in the foregoing text). However, in common with wermlandite, it should be borne in mind that the standard polytype label '3*R*' does not have the same stacking implications for shigaite as it does, for example, in minerals of the hydrotalcite group.

Nikischerite

Nikischerite, $[Fe^{2+}_6Al_3(OH)_{18}][Na(H_2O)_6][SO_4]_2{\cdot}6H_2O$, is the Fe^{2+} analogue of shigaite. It was described from the Huanuni tin mine, Dalence Province, Oruro Department, Bolivia by Huminicki *et al.* (2003) as large euhedral green crystals; the structure was refined by Huminicki and Hawthorne (2003). The space group and unit-cell parameters for the 3*R* polytype are $R\bar{3}$ and a = 9.347, c = 33.000 Å, with Z = 3.

Motukoreaite

Motukoreaite was described from Motukorea (Brown's Island), Auckland, New Zealand, by Rodgers *et al.* (1977), as a white, clay-like cement phase in tuffs and beach rocks. Electron microscopy by Brindley (1979), Ramanaidou and Noack (1987) and Bryner *et al.* (1991) has confirmed a thin platy hexagonal habit at a micrometre scale. Various formulae have been given for the mineral. If the empirical formula of Rodgers *et al.* (1977) is recalculated to 9*M*, it becomes $(Na_{0.22}K_{0.02})_{\Sigma 0.24}(Mg_{5.47}Mn_{0.10}Zn_{0.06}Al_{3.37})_{\Sigma 9.00}(OH)_{15.45}[CO_3]_{1.88}[SO_4]_{1.20}{\cdot}8.21H_2O$, which can be rearranged to approximate a mineral of the wermlandite group as $[(Mg,Mn,Zn)_{5.63}Al_{3.37}(OH)_{17.33}(H_2O)_{0.67}][(Na,K)_{0.24}\square_{0.76}(H_2O)_6][HCO_3]_{1.88}[SO_4]_{1.20}{\cdot}0.63H_2O$. Note the extreme deficiency of alkalis and water, and the dominance of (bi)carbonate. The formula $NaMg_{19}Al_{12}(CO_3)_{6.5}(SO_4)_4(OH)_{54}{\cdot}28H_2O$ used by Bryner *et al.* (1991) is too low in water to provide a complete hydroxide layer and interlayer cation hydration sphere. The formula of motukoreaite departs from that expected for the wermlandite group due to dehydration and contamination by other phases (Brindley, 1979; Rius and Plana, 1986). Nevertheless, it has been accepted as the Mg analogue of shigaite and nikischerite (e.g. Rius and Plana, 1986; Huminicki and Hawthorne, 2003). The model formula used by Rius and Plana (1986) for their structure determination was $[Mg_6Al_3(OH)_{18}][(Na_{0.67}\square_{0.33})(H_2O)_6][SO_4]_{1.33}{\cdot}6H_2O$, which is not charge balanced. Huminicki and Hawthorne (2003), however, used an electrostatically neutral formula which can be rewritten $[Mg_{5.6}Al_{3.4}(OH)_{18}][(Na_{0.6}\square_{0.4})(H_2O)_6][SO_4]_{1.3}[CO_3]_{0.7}{\cdot}6H_2O$. This suggests the following: (1) there is some variability in the Mg:Al ratio; (2) the Na site is partially occupied, and the occupancy may be more or less than 50%; (3) carbonate (or possibly bicarbonate) or sulfate may predominate as the interlayer anion; and therefore (4) analyses may have been undertaken on more than one phase.

Structural data show that motukoreaite belongs to the wermlandite group. Rodgers *et al.* (1977) reported the unit cell to be hexagonal with a = 9.336 and c = 44.72 Å. The c repeat suggests that Z should be 4 for this formula unit. According to Zamarreño *et al.* (1989), motukoreaite is a common alteration product of submarine basaltic glasses. Their X-ray diffraction data suggest space group $R\bar{3}$ with a = 9.172 and c = 33.51 Å, implying Z = 3 and structure similar to that of shigaite. They note, however, that data for motukoreaite from different sources varies: Brindley (1979) give a = 3.062 and c = 33.51 Å, and report one moderately strong diffraction peak corresponding to a $\sqrt{3}\times\sqrt{3}$ superstructure; Alker *et al.* (1981) report c = 11.216 Å; and Ramanaidou and Noack (1987) report a = 3.065 and c = 33.47 Å. The data of Rad (1974) for an unnamed phase that appears to be motukoreaite are a = 3.057 and c = 11.18 Å. Ramanaidou and Noack (1987) report the coexistence of motukoreaite with a related but sulfate- and carbonate-free Mg-Al hydroxide, with the unit cell a = 3.045 and c = 22.68 Å in a palagonite. It appears that a 3×3 or $\sqrt{3}\times\sqrt{3}$ superstructure in the xy plane may or may not be present, and that 1, 2, 3 and 4-layer polytypes may exist.

It is not apparent why motukoreaite is so much more variable in composition and structure, and so poorly crystallized in comparison to wermlandite, shigaite and nikischerite. The compositional variability of motukoreaite suggests that careful chemical characterization might lead to its division into several species on the basis of the dominance of carbonate or sulfate as the interlayer anion, and occupancy of the Na site (greater or less than 50%). The type material may represent the $[Mg_6Al_3(OH)_{18}][\square(H_2O)_6][HCO_3][SO_4]\cdot6H_2O$ endmember, whereas the Humicki and Hawthorne (2003) formula is nearer to a $[Mg_6Al_3(OH)_{18}][Na(H_2O)_6][SO_4]_2\cdot6H_2O$ endmember. However, the available data are not yet sufficient to reliably list the species that have been observed or to nominate type localities.

Natroglaucocerinite

Natroglaucocerinite occurs at several mines in the Lavrion District of Greece. It was approved by the IMA in 1995 (IMA1995−025), but a full description remains to be published. An abstract by Witzke *et al.* (1995) gives the formula, $[Zn_5Al_3(OH)_{16}]Na_{1.5}(SO_4)_{2.25}\cdot9H_2O$, which is close to that of glaucocerinite, but with additional interlayer Na^+ and $[SO_4]^{2-}$. Given the Na content, natroglaucocerinite can be considered to be member of the wermlandite group, and the formula can be recalculated on the basis of 18(OH) as $[Zn_{5.63}Al_{3.37}(OH)_{18}]Na_{1.68}(SO_4)_{2.53}\cdot9.13H_2O$, which is comparable to $[Zn_6Al_3(OH)_{18}][Na(H_2O)_6][SO_4]_2\cdot6H_2O$, the hypothetical Zn analogue of shigaite, nikischerite and motukoreaite, but with a higher interlayer Na^+ and $[SO_4]^{2-}$ content and less water than in the rest of the group. Clearly, natroglaucocerinite is not the Na analogue of glaucocerinite *sensu stricto*, as the name might be taken to imply.

Karchevskyite

Karchevskyite was described by Britvin *et al.* (2008) as pearly white spherulites from the Zheleznyi mine, Kovdor carbonatite massif, Kola Peninsula, Russia. The empirical formula $[Mg_{18}Al_9(OH)_{54}](Sr_{1.79}Mg_{0.48}Ca_{0.09})_{\Sigma2.36}(CO_3)_{8.26}(PO_4)_{0.46}(H_2O)_{6.54}(H_3O)_{4.18}$, can be simplified to produce the endmember formula $[Mg_{18}Al_9(OH)_{54}]Sr_2(CO_3)_9(H_2O)_6(H_3O)_5$. The high degree of protonation of the interlayer water molecules, replacement of carbonate by phosphate, dominance of Sr^{2+} as the large interlayer cation (although at a very low occupancy of 2 per 27 octahedral cations) are all distinctive. The unit cell is trigonal P, with dimensions a = 16.0556, c = 25.66 Å and Z = 3. Karchevskyite has a 2T polytype, but it has an unusually large $\sqrt{27}\times\sqrt{27}$ superstructure in the xy plane, presumably due to ordering of the interlayer species.

Cualstibite

Cualstibite, ideally $Cu_2Al(OH)_6[Sb(OH)_6]$, was described from the Clara mine, Oberwolfach, Germany by Walenta (1984), and is the archetype of a small group of LDH phases in which the M^{2+}:M^{3+} ratio is 2:1 as in the quintinite group, but the intercalated anion is hexahydroxyantimonate, $[Sb^{5+}(OH)_6]^-$ without additional water. The space group is $P\bar{3}$, and unit-cell parameters are a = 9.15, c = 9.745 Å, with Z = 3, which implies a 1T polytype with a 3×3 superstructure in the xy plane. Whereas the layer periodicity of hydrotalcite and quintinite group minerals is 7.5−8 Å, the larger octahedral anion of cualstibite increases the periodicity to 9.7 Å.

Cyanophyllite

Cyanophyllite was described from the Clara mine by Walenta (1981). It has a different Cu:Al:Sb ratio to cualstibite, contains trivalent Sb, and has a relatively low water content. A re-examination by Kolitsch and Giester (2007) and Kolitsch *et al*. (in press) reported the same composition as cualstibite, with a monoclinic $P2_1/c$ cell with a = 9.941, b = 8.899 (which is ~$\sqrt{3}c$), c = 5.498 Å, β = 102.88º and Z = 2. The brucite-like layers are parallel to (100) (Kolitsch *et al*., in press). The layer spacing, $a\sin\beta$, is 9.691 Å, and the layer offset $-a\cos\beta$ is 2.216 Å which is 0.40c. Cyanophyllite and cualstibite therefore are 1M and 1T stacking variants of the same species. Although the name cyanophyllite has historical priority over cualstibite, the poorer quality of the original data means that the name cualstibite is preferred (as discussed in the following text).

Zincalstibite

Zincalstibite, $Zn_2Al(OH)_6[Sb(OH)_6]$, the Zn analogue of cualstibite, was described from the Fantiscritti quarry, Carrara, Tuscany, Italy by Bonaccorsi *et al.* (2007). The space group $P\bar{3}$, and the unit-cell parameters a = 5.327 and c = 9.792 Å, with Z = 1, correspond to a 1T polytype with $\sqrt{3}\times\sqrt{3}$ superstructure in the xy plane. Recently, Mills *et al.* (2012*a*) described a 9-layer polytype, which has the longest periodicity of an LDH mineral reported to date. This 9R polytype crystallizes in space group $R\bar{3}$, its unit-cell parameters are a = 5.340(2) and c = 88.01(2) Å, with Z = 9; it has a $\sqrt{3}\times\sqrt{3}$ superstructure in the xy plane.

Omsite

Omsite (IMA2012-025), ideally $(Ni,Cu)_2Fe(OH)_6[Sb(OH)_6]$, is the Ni−Fe analogue of cualstibite and zincalstibite; the type locality is Correc d'en Llinassos, Oms, Pyrénées-Orientales département, France (Mills *et al*., 2012*b*). Omsite crystallizes in space group $P\bar{3}$, and its unit cell parameters are a = 5.351 and c = 19.5802 = 2 × 9.7901 Å, with Z = 2, which corresponds to a 2T polytype with $\sqrt{3}\times\sqrt{3}$ superstructure in the xy plane.

Hydrocalumite

Hydrocalumite provides the prototype for the calcium aluminate LDH phases. Although rare as minerals, a wide range of synthetic examples of these substances have been studied and they are important constituents of Portland cements. The divalent cation in the layers of these materials is Ca, the trivalent cation is typically Al (although Fe^{3+} is present in some synthetic analogues). The divalent and trivalent cations are strongly ordered and the Ca:Al ratio is always 2:1. Due to the larger size of Ca^{2+} in comparison to Mg^{2+}, the distance between atoms in the brucite-like xy plane increases, and the Ca cation acts as a seventh ligand to one of the interlayer water molecules. Hydrocalumite was first described from the skarn at Scawt Hill, County Antrim, Northern Ireland by Tilley *et al.* (1934), with an approximate formula $[Ca_4Al_2(OH)_{12}](OH)_{1.56}(CO_3)_{0.22}\cdot 4.76H_2O$ [the formula has been normalized to 6(Ca + Al) for comparative purposes]. Passaglia and Sacerdoti (1988) reviewed published compositions of hydrocalumite from various localities and concluded that they lay in a ternary solid solution with endmember formulae $[Ca_4Al_2(OH)_{12}]Cl_2\cdot 4H_2O - [Ca_4Al_2(OH)_{12}](OH)_2\cdot 6H_2O - [Ca_4Al_2(OH)_{12}](CO_3)\cdot 6H_2O$. The original specimens from Scawt Hill correspond to the hydroxide endmember. However, the analyses collated by Passaglia and Sacerdoti (1988) revealed a chloride-dominant endmember [e.g. at Bellerberg in Germany, where material described by Fischer *et al.* (1980) corresponds to $[Ca_4Al_2(OH)_{12}]Cl_{1.90}(OH)_{0.10}\cdot 4H_2O$]. The carbonate endmember was not dominant in any of the collated analyses. Due to the larger size of the Ca^{2+} ion, the pseudohexagonal repeat a_{psh} in the $(Ca,Al)(OH)_2$ sheet is ~5.7 Å rather than ~3.1 Å as in the Mg-rich phases. Cation ordering and interlayer offsets result in a monoclinic cell for most hydrocalumite-related phases, the orthogonal net of the hydroxide layer having $a \sim \sqrt{3}a_{psh}$ = 9.953 Å (Cl-rich, Bellerberg) or 10.047 Å (OH- and CO_3-rich, Montalto di Castro, Viterbo, Italy) and $b \sim 2a_{psh}$ = 11.466 Å (Bellerberg) or 11.523 Å (Montalto di Castro). The c repeats are 16.292 and 16.271 Å, respectively, with β = 104.46º and 104.31º and Z = 4 for the formulae given above. The layer spacing is thus ½$c\sin\beta$ = 7.89 Å, which is similar to those of the hydrotalcite and quintinite groups. The space group is $P2/c$, but there is a strong $C2/c$ subcell with $b_{subcell} = b_{cell}/2$ (Sacerdoti and Passaglia, 1988). A second specimen from Bellerberg with a formula $[Ca_4Al_2(OH)_{12}]Cl_{1.60}(OH)_{0.40}\cdot\sim 4H_2O$ has been reported as rhombohedral, with space group $R\bar{3}c$, and unit-cell

dimensions of a = 5.765 and $c = 6 \times 7.630$ = 46.978 Å (Fischer *et al*., 1980). Thus, both 2*M* and 6*T* polytypes, with similar compositions, coexist at Bellerberg. Sacerdoti and Passaglia (1988) refined the structure of hydrocalumite from Montalto di Castro and found that the CO_3 has long-range ordering; they reported the structural formula $[Ca_8Al_4(OH)_{24}](CO_3)Cl_2(H_2O)_{1.6}\cdot 8H_2O$. They found that the doubling of b is due to ordering of the interlayer anions and does not occur for the $C2/c$ synthetic Cl endmember. Sacerdoti and Passaglia (1988) noted that various ordering schemes which maintain a continuous hydrogen-bonding network are possible, and also discussed the polytypic behaviour of various hydrocalumite analogues. A case can be made for the division of the OH- and Cl-dominant hydrocalumites into separate species. Species divisions on the basis of subsidiary quantities of carbonate can also be justified if long-range order is present.

Kuzelite

Kuzelite, $[Ca_4Al_2(OH)_{12}][(SO_4)\cdot 6H_2O$, was described from carbonaceous xenoliths found at Zeilberg quarry, Bavaria, Germany by Pollmann *et al.* (1997). It forms colourless to white platy microcrystals which crystallize in space group $R\bar{3}$, and has a unit cell with a = 5.76, $c = 6 \times 8.943$ = 53.66 Å and Z = 3. Kuzelite is the sulfate analogue of hydrocalumite. Spectroscopic data indicate that carbonate is absent from the structure. The increase in layer spacing from 7.6 to 8.9 Å, due to substitution of sulfate for carbonate, is very similar to that between the hydrotalcite and woodwardite groups. However, due the small number of Ca-rich hydrotalcite-supergroup species, the increase in layer spacing has not been proposed as a criterion for group separation.

Coalingite

Coalingite, $Mg_{10}Fe^{3+}_2(OH)_{24}[CO_3]\cdot 2H_2O$, forms red-brown to golden-brown crusts of microscopic platelets, and was originally reported from the New Idria Serpentinite, San Benito and Fresno Counties, California, USA by Mumpton *et al.* (1965). The material had previously been described as 'ferrobrucite'. Coalingite is almost always of endmember composition, and has ⅙ of the cations trivalent rather than ¼ as in pyroaurite. It is thus very close in composition to brugnatellite, but with a much lower water content. The structure reported by Pastor-Rodriguez and Taylor (1971) has a unit cell with a = 3.12, $c = 3 \times 12.47$ = 37.4 Å and Z = ½, in space group $R\bar{3}2m$, which indicates that there is no long-range Mg−Fe order within sheets or CO_3-H_2O order in the interlayer. Broadened reflections and streaking parallel to **c*** indicate stacking disorder. In particular, the (0003) reflection was reported to lie on a streak extending from about 0.04 to 0.14 $Å^{-1}$, with a diffuse maximum corresponding to 13.5 Å rather than the expected 12.5 Å. A distinctive feature of the structure is that only every second interlayer is occupied, giving alternating spacings between (Mg/Fe) planes along c of about 7.8 Å and 4.7 Å, which are similar to those of pyroaurite and brucite, respectively. In effect, coalingite is a 1:1 interstratification of these minerals.

Brugnatellite

Brugnatellite was described from Val Malenco, Sondrio, Lombardy, Italy, by Artini (1909). His calculated formula, $Mg_6Fe^{3+}(OH)_{13}[CO_3]\cdot 4H_2O$, includes carbonate, and is still quoted today. The X-ray study of Fenoglio (1938) reported a primitive trigonal symmetry with a = 5.47 Å and c = 15.97 Å. If these observations are valid, the mineral can be distinguished from pyroaurite/sjögrenite by having only ⅐ of the octahedral cations trivalent, rather than ⅓, having a $\sqrt{3} \times \sqrt{3}$ superstructure in the xy plane, and a distinctive space group symmetry. The c repeat indicates that the low M^{3+} content cannot be due to alternation of pyroaurite- and brucite-like stacking as in coalingite. Frondel (1941) noted that the same composition was reported for brugnatellite from four different Italian localities, but that his own examination of material from Val Malenco and Val Ramazzo showed samples labelled "brugnatellite" to consist largely of mixtures pyroaurite and brucite with additional minor phases. Nevertheless, Frondel (1941) concluded that brugnatellite was probably a distinct phase that coexisted with pyroaurite at these localities.

In common with carrboydite and mountkeithite, brugnatellite has $(M^{2+} + M^{3+}):(OH)^- > 1:2$. However, the c spacing is similar to that of a 2-layer member of the hydrotalcite or quintinite groups, so interlayer octahedral cations are unlikely to be present. Rewriting the formula as $Mg_6Fe^{3+}(OH)_{14}[HCO_3]\cdot 3H_2O$ would eliminate this anomaly. Note also that the formula with 7

octahedral cations is not compatible with the 3-fold superstructure in the *xy* plane, and a reformulation as $Mg_{5.14}Fe^{3+}_{0.86}(OH)_{12}[HCO_3]_{0.86}\cdot 2.57H_2O$ may be even more appropriate. Brugnatellite requires re-examination to determine its true stoichiometry and interlayer speciation.

Muskoxite

Muskoxite was described as red-brown fine-grained crystals in a drill core from the Muskox intrusion, Kitikmeot Region, Nunavut, Canada by Jambor (1969*b*). Precession X-ray photographs revealed $P\bar{3}m1$ symmetry with a strong a = 3.07 and c = 4.6 Å subcell. However, numerous closely spaced reflections along **c*** indicated that the true periodicity or periodicities were much longer. Chemical analysis of 200 mg of hand-picked material gave the overall formula (based on 8 cations) $Mg_{5.04}Fe^{3+}_{2.96}O_{9.48}\cdot 7.54H_2O$, with <1% CO_2 and all Fe assumed to be trivalent. This analysis has insufficient water to fit into a hydrotalcite-group template, as M:[O + OH + H_2O] = 1:2.13 rather than 1:2.75 (8:22) as would be expected for a hydroxide member of the hydrotalcite group or 1:2.83 (6:17) for a quintinite-like phase. The 4.6 Å subperiodicity along c, which is close to the layer spacing of brucite, and the low water content, suggest that muskoxite may not be the hydroxide analogue of sjögrenite. Microprobe analyses of veinlet material gave Mg:Fe:Mn atomic ratios of 38.2:57.5:4.3 and 22.6:71.8:5.6, implying a wide range of Mg:Fe:Mn compositions and probably a range of Fe oxidation states. In the absence of constraints on the latter, it is not possible to determine whether the solid solution spans Mg-dominant and Fe^{2+}-dominant species. Further investigation is required.

Status of the minerals in the hydrotalcite supergroup

Discreditations and questionable species

According to Nickel and Grice (1998): "Polytypes and polytypoids are not regarded as separate species and, like topologically similar polymorphs, they can be distinguished by the addition of a crystallographic suffix to the mineral name, as indicated in a later section." As such, the well established polytypes of the hydrotalcite supergroup can no longer be considered to be separate species. Considering only the stacking of layers (and neglecting any differences in the layer superstructures), the following mineral names are invalid (see also Table 2): manasseite (= hydrotalcite-2*H*), sjögrenite (= pyroaurite-2*H*), barbertonite (= stichtite-2*H*) and cyanophyllite (= cualstibite-1*M*). Hydrotalcite, pyroaurite and stichtite are preferred on the basis of historical precedence. In the case of cyanophyllite and cualstibite, cualstibite is preferred, despite being described later (1984 *vs*. 1981), because the chemistry, valence states and crystallography were initially described incorrectly for cyanophyllite. A complete description of the cyanophyllite structure is provided by Kolitsch *et al*. (in press).

Jamborite, carrboydite, zincaluminite, motukoreaite, natroglaucocerinite, muskoxite and brugnatellite are all considered to be questionable species on the basis of their poorly defined chemical compositions. In each case, the chemistry is not sufficiently well defined to associate the name with a unique formula which is distinct from all others; however, each of the species is probably valid and a member of the hydrotalcite supergroup. Fougèrite is redefined as two distinct species, fougèrite and trébeurdenite (see below). The current status of all of the members of the hydrotalcite supergroup is summarized in Table 2. We emphasize that the status is that of a name, not of a composition range. There has been ambiguity and inconsistency in the usage and interpretation of status categories in the past; in order to avoid this with the hydrotalcite group, they are defined here as follows:

'A' (approved): the name has been approved by the CNMNC or its predecessor Commission as a valid name for the mineral species.

'D' (discredited): the name is no longer the official name for a mineral species, as it is now regarded as a synonym, a varietal name, or was so poorly defined in the first place that it cannot be applied in a reproducible fashion.

'G' (grandfathered): the name is an old one that pre-dates the Commissions, but is generally accepted as valid.

'Group': the name now refers to a group within the supergroup. Names of groups may coincide with names of valid species, giving the status 'A + Group'. The groups are discussed in detail in the following text.

'Q' (questionable): the name refers to one or more mineral species, which are probably valid, but type material was not well enough characterized for species to be unambiguously identified by current criteria. Further study will allow reclassification of the name as 'A' or 'D'.

HYDROTALCITE SUPERGROUP NOMENCLATURE

TABLE 2. The minerals of the hydrotalcite supergroup as at March 2009, the current status of the names (this report), and their new status as approved by the CNMNC in 2012.

Mineral name	IMA status (2009)	IMA status (2012)	Comment
Hydrotalcite	G	G/Rd + Group + Supergroup	incorporates former manasseite
Manasseite	G	D	= hydrotalcite
Pyroaurite	G	G/Rd	incorporates former sjögrenite
Sjögrenite	G	D	= pyroaurite
Stichtite	G	G/Rd	incorporates former barbertonite
Barbertonite	Q	D	= stichtite
Meixnerite	A	A	
Iowaite	A	A	
Droninoite	A	A	
Woodallite	A	A	
Desautelsite	A	A	
Takovite	A	A	
Reevesite	A	A	
Jamborite	A	Q	
Quintinite	A	A + Group	
Charmarite	A	A	
Caresite	A	A	
Zaccagnaite	A	A	
Chlormagaluminite	A	A	
Comblainite	A	A	
Fougèrite	A	A/Rd + Group	= fougèrite + trébeurdenite
Woodwardite	G	A + Group	
Zincowoodwardite	A	A	
Honessite	A	A	
Glaucocerinite	G	A + Group	
Hydrowoodwardite	A	A	some may be new species with Al > Cu
Carrboydite	A	Q	
Hydrohonessite	A	A	
Mountkeithite	A	A	
Zincaluminite	Q	Q	= glaucocerinite?
Wermlandite	A	A + Group	
Shigaite	A	A	
Nikischerite	A	A	
Motukoreaite	A	Q	may correspond to >1 species
Natroglaucocerinite	A	Q	
Karchevskyite	A	A	
Cualstibite	A	A/Rd + Group	incorporates former cyanophyllite
Cyanophyllite	A	D	= cualstibite
Zincalstibite	A	A	
Hydrocalumite	G	G + Group	may correspond to >1 species
Kuzelite	A	A	
Coalingite	A	A	
Brugnatellite	G	Q	
Muskoxite	A	Q	may correspond to >1 species

'Rd' (redefined): the currently valid name now refers to a range of chemical or structural variation for the species that is narrower, broader or otherwise different from that before the redefinition. This is a temporary category highlighting that there is a discredited older name

referring to the same mineral as a result of recent changes; 'Rd' status is thus additional to 'A/G' status.

'Rn' (renamed): the currently valid name replaced an earlier name without any change in the scope. This is also a temporary category that is supplemental to 'A/G' status and flags a recent change. 'Rn' emphasizes that some specimens that used to carry the current name may no longer do so, whereas other specimens that used to be named differently may now carry the current name.

'Supergroup': the name now refers to the supergroup.

Redefinition of fougèrite

Mössbauer spectroscopy is the most reliable technique for quantitatively determining the proportions of Fe^{2+} and Fe^{3+} in green rust. As the Mössbauer spectra of the natural samples must be compared to those of the corresponding synthetic compounds measured at 78 K, we review the procedure for preparing the synthetic reference samples (cf. Génin *et al.*, 2005; Aïssa *et al.*, 2006), which is as follows: (1) $Fe_4^{2+}Fe_2^{3+}(OH)_{12}CO_3{\cdot}3H_2O$ (x = ½) is co-precipitated by mixing ferrous and ferric sulfates in a 2:1 $[Fe^{2+}]/[Fe^{3+}]$ ratio in the presence of $NaHCO_3$; (2) Hydrogen peroxide is introduced using a peristaltic pump into the $Fe_4^{2+}Fe_2^{3+}(OH)_{12}CO_3{\cdot}3H_2O$ solution, and the electrode potential E_h is recorded as the H_2O_2 is added. In addition to the initial $Fe_4^{2+}Fe_2^{3+}(OH)_{12}CO_3{\cdot}3H_2O$, four oxidation products have been characterized by transmission Mössbauer spectroscopy at 78 K, at compositions x = ½, 0.63, 0.78 and 1.

Mössbauer spectra can be fitted in two ways: by directly superimposing Lorentzian-shaped lines, or by deconvoluting Lorentzian-shaped lines with Gaussian distributions. The first method is usually adequate, but there are cases where the second method is more appropriate. The *in situ* deprotonation of the Fe^{2+}–Fe^{3+} oxyhydroxycarbonate by H_2O_2 is one of these, and this procedure was used initially. The fitted parameters are listed in Table 3, and spectra with fits are shown in Fig. 7. The intensity variation of the doublet intensities (D_1 + D_2), D_3 and D_4 as a function of composition are summarized in Fig. 8.

The spectrum of the initial precipitate with x = ⅓ (i.e. $Fe_4^{2+}Fe_2^{3+}(OH)_{12}CO_3{\cdot}3H_2O$) contains three quadrupole doublets (Fig. 7*a*,*b*); two of them, D_{1f} and D_{2f}, have a large quadrupolar splitting of about 2.9 and 2.6 mm s^{-1} and a 3:1 intensity ratio; these are attributed to Fe^{2+} and constitute 50 and 16.7% of the total octahedral cations, respectively. The D_{1f} profile is interpreted to correspond to Fe^{2+} in vertical registry with interlayer H_2O molecules, whereas D_{2f} is interpreted to correspond to Fe^{2+} in registry with the centre of a CO_3^{2-} anion. The third doublet, D_{3f}, with a small splitting of about 0.5 mm s^{-1}, corresponds to a unique Fe^{3+} site in registry with a CO_3^{2-} anion. The cations are ordered within each layer so that each Fe^{3+} cation is surrounded by six Fe^{2+} cations; this cation ordering induces interlayer anion ordering to minimize local charge imbalance. This composition corresponds to the mineral fougèrite as redefined herein, so these doublets are labelled with an 'f' subscript.

The spectra evolve progressively as H_2O_2 is added to the initial precipitate. As *in situ* oxidation proceeds, the two quadrupole doublets with large splitting (D_1 and D_2) decrease in intensity, and a second quadrupole doublet with smaller splitting appears. This shows that Fe^{2+} cations are oxidizing to Fe^{3+}. At x ~⅔, which corresponds to the mineral trébeurdenite $[Fe_2^{2+}Fe_4^{3+}O_2(OH)_{10}CO_3{\cdot}3H_2O]$ two quadrupole doublets with large splitting in a 3:1 intensity ratio are present (these are labelled D_{1t} and D_{2t}, where 't' stands for 'trébeurdenite') at abundances of 25 and 8.3%, respectively. There are also two distinct Fe^{3+} doublets, D_{3t} and D_{4t}, of equal intensity (i.e. 33.3 and 33.3%) (Fig. 7*e*,*f*). The Mössbauer parameters of the D_{3t} doublet are quite similar to those of the homologous D_{3f} doublet in fougèrite, but whereas the Fe^{3+} giving rise to D_{3f} is necessarily coordinated to 6[OH^-] in the octahedral layer, the new Fe^{3+} environment associated with D_{4t} contains O^{2-} ligands that replace OH^- due to deprotonation. The Gaussian distribution of quadrupole splitting parameters most probably results from the local distortions of the octahedra surrounding Fe cations when OH^- ions are partially replaced by O^{2-} anions. For an average value of x in the range ⅓–⅔, the mechanical mixture of fougérite and trébeurdenite gives rise to four doublets D_1, D_2, D_3 and D_4 with broadened Gaussian distributions, which are not further resolved (Fig. 7*c*,*d*).

The ferric green rust mössbauerite (which is actually orange in colour) contains no Fe^{2+} and has an ideal formula $Fe_6^{3+}O_4(OH)_8CO_3{\cdot}3H_2O$. It produces a spectrum with two Fe^{3+} doublets of small quadrupolar splitting, D_{3m} and D_{4m} ('m' for

TABLE 3. Mössbauer parameters for 'green rusts' with $x = [Fe^{3+}]/[Fe_{tot}]$ in the range ⅓–1.

	Quadrupole doublets	Δ (mm s^{-1})	<Δ> (mm s^{-1})	<ρΔ> (mm s^{-1})	*RA* (%)	*F* (%)	T (%)	M (%)
x = 0.33						100		
Fe^{2+}	D_{1f}	1.25	2.92	0	50			
	D_{2f}	1.25	2.63	0	17			
Fe^{3+}	D_{3f}	0.48	0.47	0	33			
x ~ ½						50	50	
Fe^{2+}	$D_{1f} + D_{1t}$	1.21	2.98	0.14	38			
	$D_{2f} + D_{2t}$	1.21	2.72	0.16	12.5			
Fe^{3+}	$D_{3f} + D_{3t}$	0.49	0.40	0.15	33			
	D_{4t}	0.49	0.70	0.28	16.5			
x ~ 0.63						9	91	
Fe^{2+}	D_{1t}	1.24	2.80	0.15	28			
	D_{2t}	1.24	3.05	0.05	9			
Fe^{3+}	D_{3t}	0.48	0.49	0.20	32			
	D_{4t}	0.48	0.90	0.21	31			
x ~ 0.78							66	34
Fe^{2+}	$D_{1t} + D_{2t}$	1.21	2.89	0.31	22			
Fe^{3+}	$D_{3t} + D_{3m}$	0.47	0.45	0.32	35			
	$D_{4t} + D_{4m}$	0.47	0.95	0.34	43			
x = 1								100
Fe^{3+}	D_{3m}	0.47	0.60	0.30	33			
	D_{4m}	0.47	0.88	0.41	67			

Values of x experimentally obtained are approximately ½, 0.63 and 0.78 and precisely 0.33 and 1. Spectra are measured at 78 K (Fig. 7) and fitted using a Voigt profile; columns are δ: isomer shift in mm s^{-1} (reference is α-iron at ambient temperature), <Δ>: mean value of quadrupole splitting in mm s^{-1} and <ρΔ>: its standard deviation; *RA* (%): relative area of peak doublets as a percentage of total intensity. The variables *F*, *T* and *M* indicate the molar percentages of fougèrite, trébeurdenite and mössbauerite, respectively, in the mixture, deduced from bulk composition according to the lever rule.

'mössbauerite'), in a 1:2 intensity ratio, which therefore account for 33.3% and 66.7% of the total intensity, respectively (Fig. 7*i*,*j*). These two doublets are produced by Fe^{3+} cations that are surrounded by six Fe^{3+} ions. The D_{3m} doublet is produced by those Fe^{3+} cations that initially balanced the charge on the CO_3^{2-} anions, D_{4m} is produced by Fe^{3+} ions associated with deprotonation. The widths of the Gaussian distributions for quadrupole splitting are much increased, particularly for D_{4m} (0.41 mm s^{-1}), as local lattice distortions are now due to $2[O^{2-}]$ and $4[OH^-]$ anions at the apices of the octahedrons surrounding Fe^{3+} ions. For an average x value in the range ⅔–1, the mechanical mixture of trébeurdenite and mössbauerite gives rise to only three Gaussian distributions of quadrupole doublets ($D_1 + D_2$), D_3 and D_4 (Fig. 7*g*,*h*). The two ferrous contributions can no longer be resolved, and merge into a single broader distribution.

Despite the change in x, the structure of the green rusts remains constant, in space group $R\bar{3}m$ (Fig. 9), as shown by their X-ray diffraction patterns (Fig. 10). The measured unit-cell parameters are a = 3.182 Å and c = 22.896 = 3 × 7.632 Å at x = ⅓; and a = 3.173 Å and c = 22.695 = 3 × 7.565 Å at x = ⅔. At x = 1, the unit-cell parameters are a = 3.079 Å and c = 22.253 = 3 × 7.418 Å. The absence of a supercell in the xy plane (a ~3 Å) shows that the 3-layer repeat arises from offsets of octahedral layers across the interlayers rather than from long-range order of Fe^{2+} and Fe^{3+} or of the interlayer contents. Although low-temperature Mössbauer and

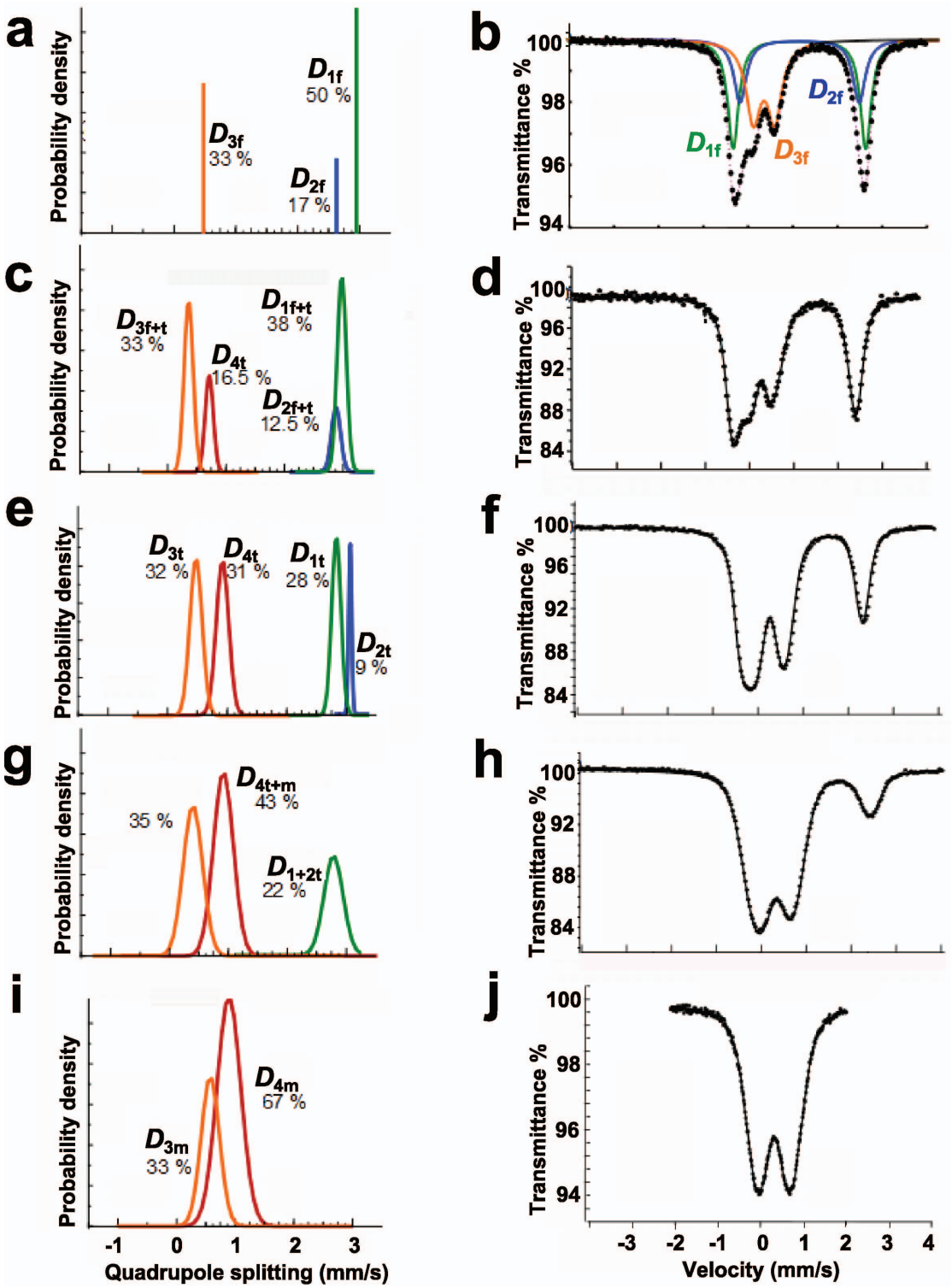

FIG. 7. Mössbauer spectra measured at 78 K of synthetic green rust samples for values of $x = [Fe^{3+}]/[Fe_{tot}]$ in the range ⅓–1. (*a*) Probability density for Gaussian distributions of quadrupole splittings fitted using Voigt-function profiles, and (*b*) total spectrum showing fitted doublets for x = ⅓; (*c*) and (*d*) are corresponding data for x = ½; (*e*) and (*f*) for x = 0.63; (*g*) and (*h*) for x = 0.78; (*i*) and (*j*) for x = 1.

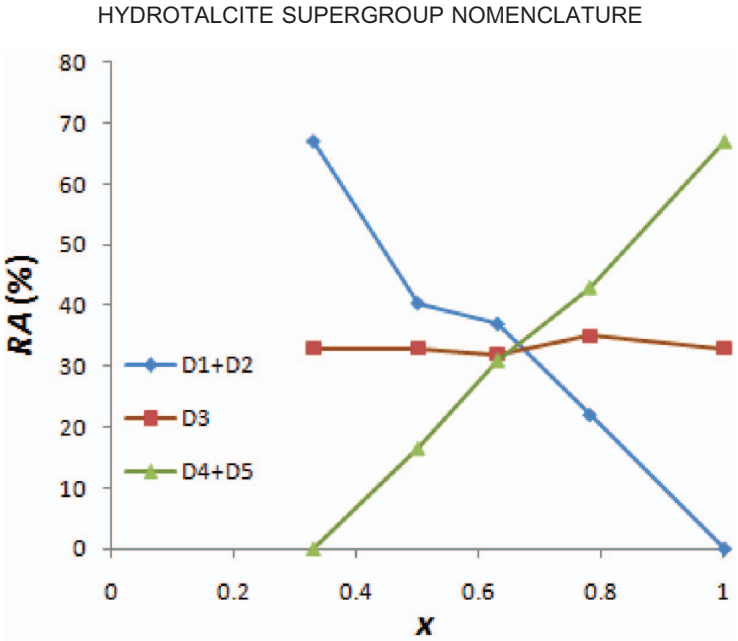

FIG. 8. Relative areas of the Mössbauer doublets D_{1f+t} + D_{2f+t}, D_{3f+t+m} and D_{4t+m} from Table 3 as a function of composition x.

magnetic susceptibility data show strong cation order *within* layers, there is clearly no strong coupling *between* layers.

As x increases, OH^- ions surrounding the octahedral cations are deprotonated. The consequent shortening of bond distances causes a lattice contraction which shifts the diffraction lines towards higher angles, and also results in distortion of the octahedra (Génin *et al.*, 2006*c*). These changes are well illustrated by the behaviour of the main d_{003} diffraction peak as x increases, although this peak is very hard to distinguish in mössbauerite (x = 1), due to broadening and decrease in intensity caused by local strain (Fig. 10). In synthetic samples with x = 1, the d_{101} reflection becomes dominant, however d_{003} remains the diagnostic reflection (Génin *et al.*, 2012*b*). In contrast, there is no change with oxidation in the external morphology of the hexagonal crystals as observed by transmission electron microscopy (Fig. 11), although the x = 1 sample of Fig. 11*c* has rings rather than spots in its electron diffraction pattern, produced by severe rotational disorder (Génin *et al.*, 2006*c*). The occurrence of a carbonated green

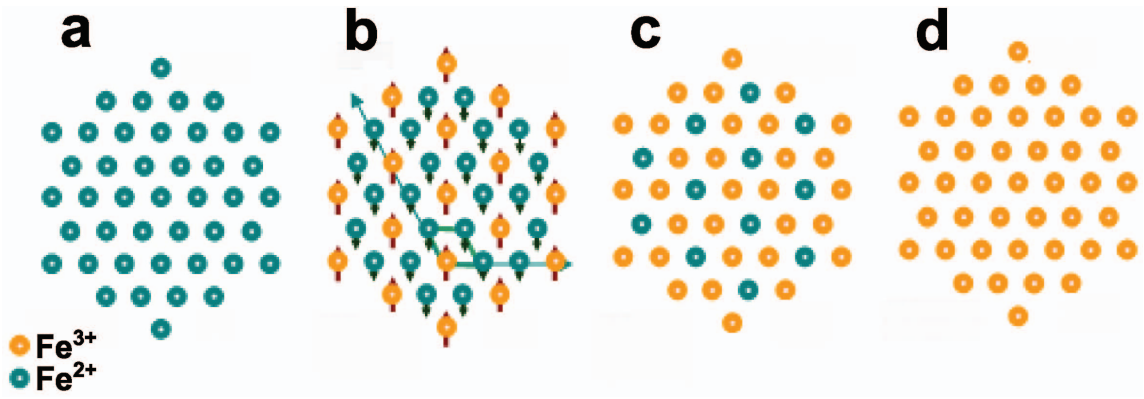

FIG. 9. Ordering of Fe^{2+} and Fe^{3+} cations within the octahedral layer, which leads to various magnetic properties: (*a*) $Fe^{2+}_6(OH)_{10}(H_2O)_2CO_3{\cdot}3H_2O$; (*b*) $Fe^{2+}_4Fe^{3+}_2(OH)_{12}CO_3{\cdot}3H_2O$, showing antiferromagnetic coupling of spins of Fe^{2+} and Fe^{3+} cations; (*c*) $Fe^{2+}_2Fe^{3+}_4O_2(OH)_{10}CO_3{\cdot}3H_2O$; (*d*) $Fe^{3+}_6O_4(OH)_8CO_3{\cdot}3H_2O$. Modified after Genin *et al.* (2012*a*).

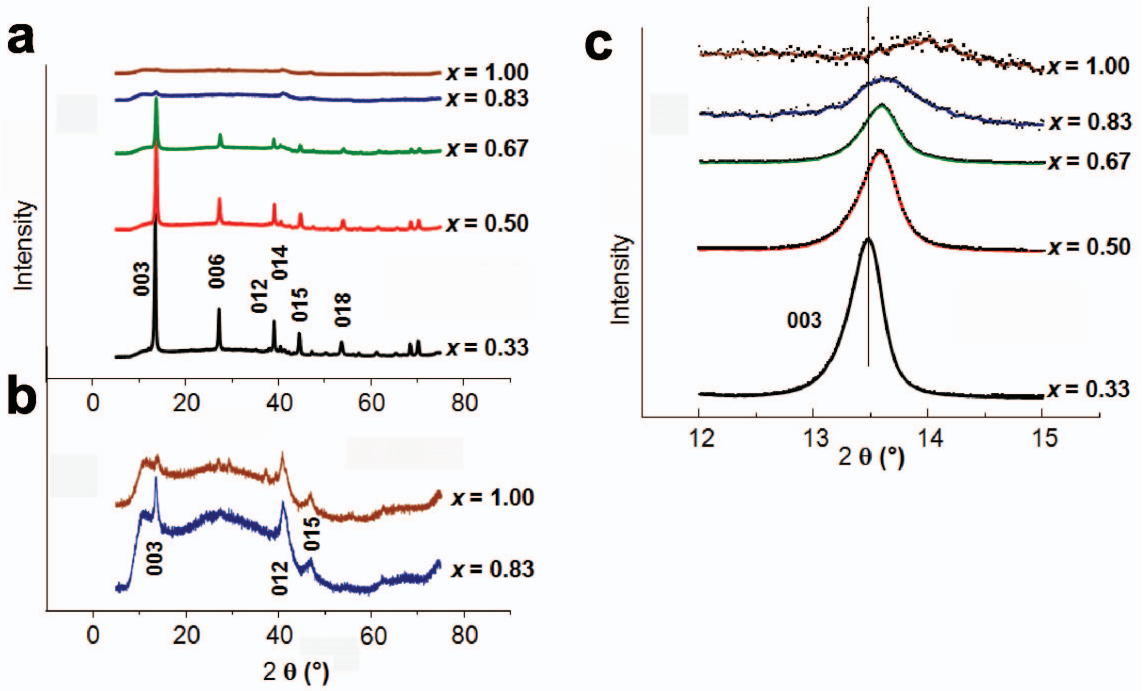

FIG. 10. The X-ray diffraction patterns of green rust samples during deprotonation, for $x = [Fe^{3+}]/[Fe_{tot}]$ ranging from ⅓–1. (*a*) All patterns using the same scale for intensity using Co*K*α radiation (λ = 1.7889 Å); (*b*) details for $x = 0.83$ and 1; and (*c*) the (003) lines only, demonstrating the contraction of the lattice with x and broadening due to the strain resulting from progressive deprotonation. Modified after Genin *et al.* (2012*a*).

rust related mineral was confirmed recently using XRD patterns of samples collected from groundwater from Bornholm, Denmark and Äspö, Sweden. The layer spacings (d_{003} in space group $R\bar{3}m$), were measured as 7.594 and 7.605 Å, which is consistent with synthetic samples with $x = 0.47–0.52$; i.e. fougèrite and trébeurdenite (Christiansen *et al.*, 2009).

The magnetic properties of the fougèrite-group minerals arise from strong ordering of Fe^{3+} cations within individual layers for the specific values of x = ⅓, ⅔ and 1 (Rusch *et al.*, 2008; Fig. 9). The two sublattices of Fe^{2+} and Fe^{3+} ions in the octahedral layer display an antiparallel coupling for x = ⅓ and ⅔, resulting in ferrimagnetic behaviour with Néel temperatures

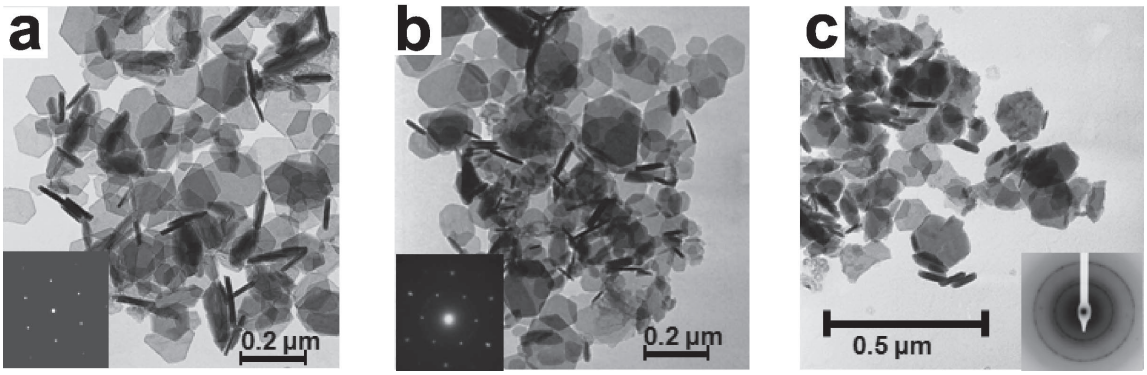

FIG. 11. Transmission electron micrographs of synthetic samples (*a*) $Fe_4^{2+}Fe_2^{3+}(OH)_{12}CO_3{\cdot}3H_2O$ green rust with x = ⅓, (*b*) x = ½ and (*c*) $Fe_6^{3+}O_4(OH)_8CO_3{\cdot}3H_2O$ with $x = 1$. Modified after Ruby *et al.* (2009).

of 5 K and ~20 K, respectively. In contrast, material with $x = 1$ is ferromagnetic with a Curie temperature ~80 K, and a broad range of transition. Although ordering of Fe^{2+} and Fe^{3+} restricts the composition of a given microscopic domain to $x = ⅓$, $x = ⅔$ and $x = 1$, the topotactic intergrowth of such domains allows any intermediate value of x, as observed in natural and synthetic samples.

Figure 12 shows Mössbauer spectra obtained from natural gley samples fitted using Lorentzian line shapes. Figure 12*a* displays the spectrum of a

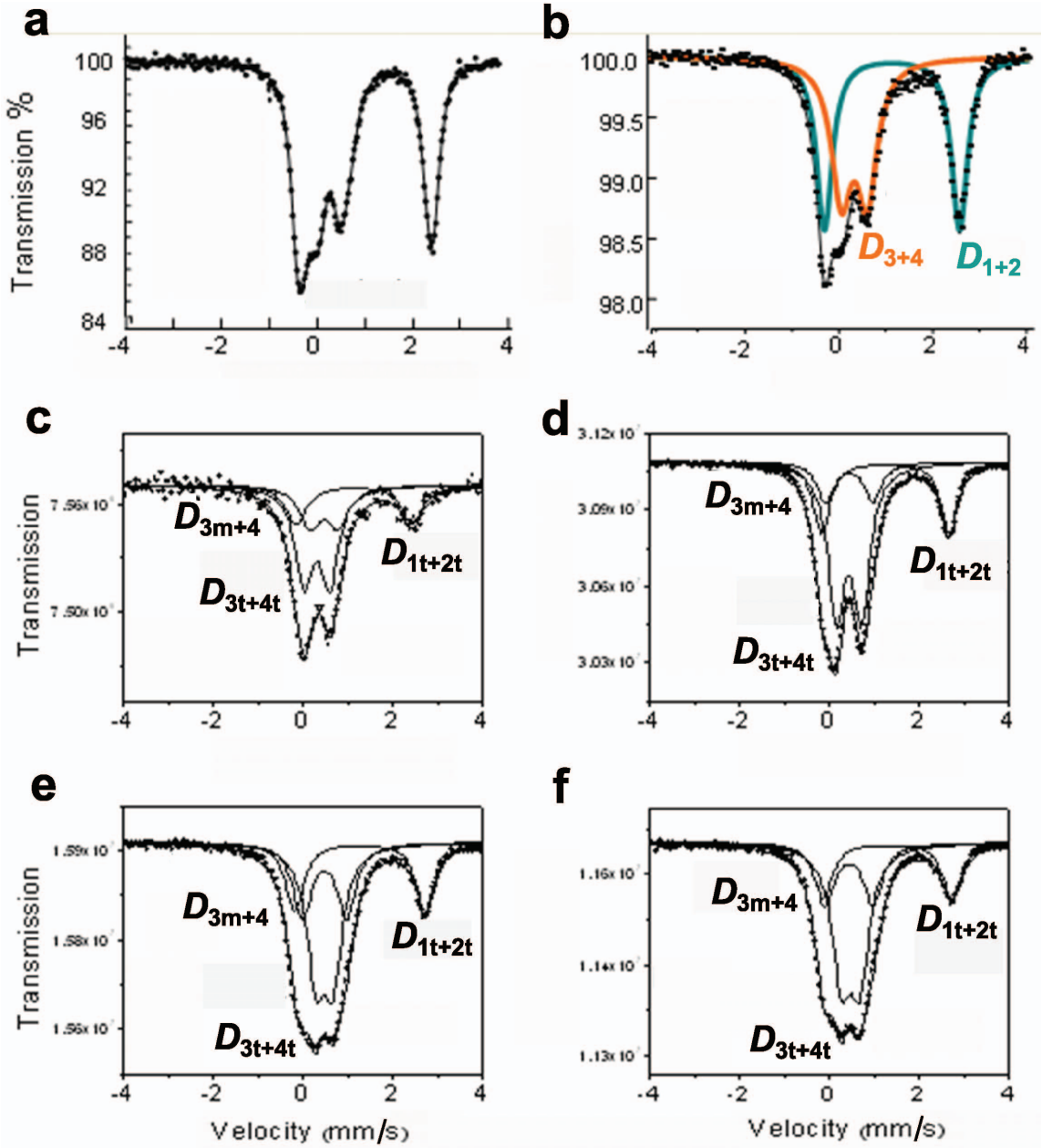

FIG. 12. Transmission Mössbauer spectra measured at 78 K of (*a*) a synthetic sample of green rust with $x = 0.50$; (*b*) a sample of gley extracted from the aquifer at the forest of Fougères with $x = 0.50$; (*c*) room-temperature spectrum of a gley sample extracted from the shore of a salt marsh in Trébeurden with $x = 0.75$; and (*d–f*) spectra measured at 78 K of samples extracted from widely scattered locations in the Bay of Mont Saint-Michel with $x = 0.72$, 0.74 and 0.77, respectively. Modified after Genin *et al*. (2012*a*).

synthetic sample with $x = ½$, for comparison, and Fig. 12*b* shows that of a sample collected from below the water table in the forest of Fougères; the spectra are nearly identical and, in both cases, only two quadrupole doublets are resolved. Figure 12*c*–*f* displays the spectra of four samples extracted from maritime marshes; the first one from Trébeurden was measured at room temperature (Fig. 12*c*) and the three others extracted from the Bay of Mont Saint-Michel (Fig. 12*d*–*f*) at 78 K. These spectra are qualitatively quite different from Fig. 12*a*,*b*. The Trébeurden spectrum shown in Fig. 12*c* clearly resembles those of Fig. 12*d*–*f* rather than Fig. 12*a*,*b*, despite the higher temperature of experimental measurement. The spectral resolution is somewhat poorer for natural samples compared to their synthetic counterparts, so a simpler method for fitting was employed, using a finite number of Lorentzian-shaped lines rather than Gaussian distributions of Lorentzians. In the range ⅓–⅔, it was sufficient to use one broadened Fe^{2+} doublet as D_{1f}, D_{2f}, D_{1t} and D_{2t} could hardly be distinguished. In contrast, in the range ⅔–1, three doublets were used: one Fe^{2+} doublet ($D_{1t} + D_{2t}$), an Fe^{3+} doublet with a larger intensity representing ($D_{3t} + D_{4t}$), and a doublet representing ($D_{3m} + D_{4m}$), with a larger quadrupole splitting and broader linewidth. This simplified fitting procedure gave excellent results for spectra measured at 78 K. Mössbauer parameters for spectra in Fig. 12*c*–*f* are listed in Table 4.

The difference between the spectra of Fig. 12*a*,*b* and Fig. 12*c*–*f* arises because gleys from below the water table such as that of Fig. 12*b* have x in the ⅓–⅔ range, whereas those from salt marshes have $x > ⅔$. The salt marshes are covered by water only at high tide, so the gley is partially oxidized and reaches a steady-state x value higher than that in permanently waterlogged aquifers. The samples extracted from Trébeurden and the Bay of Mont Saint- Michel all have $x = 0.72–0.77$ according to the data of Table 4. The linear variation of intensities with composition is consistent with a mechanical mixture of different proportions of trébeurdenite and mössbauerite (Fig. 13).

It is possible to further decompose the partially resolved experimental doublet intensities into components that correspond to all the distinct Fe^{2+} and Fe^{3+} environments that are discussed above, if we note, consistent with the data of Tables 3 and 4, that: (1) total $D_{3t} + D_{3m}$ is always 33.33%; (2) the intensities of D_{1f}:D_{2f} and D_{1t}:D_{2t} are always in a 3:1 ratio; (3) the intensity ratio D_{2f}:D_{3f} = 1:4 and hence ($D_{1f} + D_{2f}$) = D_{3f} = D_{4f}; and (4) D_{3m} and D_{4m} are in a 1:2 ratio.

TABLE 4. Mössbauer parameters for quadrupole doublets in gley samples extracted from maritime marshes.

Quadrupole doublet		$D_1 + D_2$ Fe^{2+}(T)	$D_{3t} + D_{4t}$ Fe^{3+}(T)	$D_{3m} + D_{4m}$ Fe^{3+}(M)
Trébeurden room temperature				
	δ (mm s^{-1})	1.294	0.301	0.307
$x = 0.75$	Δ (mm s^{-1})	2.66	0.549	0.972
	RA (%)	25	50	25
	Γ (mm s^{-1})	0.56	0.45	0.49
Mont Saint-Michel Bay 78 K				
No.1	δ (mm s^{-1})	1.245	0.429	0.441
$x = 0.72$	Δ (mm s^{-1})	2.842	0.560	1.059
	RA (%)	28	56	16
	Γ (mm s^{-1})	0.45	0.49	0.50
No. 2	δ (mm s^{-1})	1.263	0.471	0.470
$x = 0.74$	Δ (mm s^{-1})	2.908	0.381	0.986
	RA (%)	26	52	22
	Γ (mm s^{-1})	0.45	0.49	0.50
No. 3	δ (mm s^{-1})	1.292	0.466	0.434
$x = 0.77$	Δ (mm s^{-1})	2.877	0.405	1.073
	RA (%)	23	46	31
	Γ (mm s^{-1})	0.45	0.49	0.50

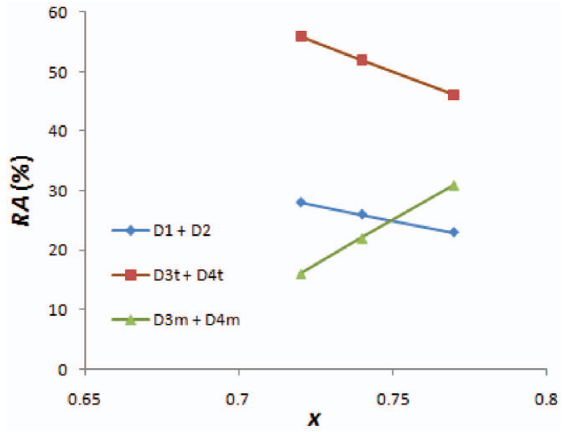

FIG. 13. Variation of relative areas for Mössbauer doublets D_1 + D_2, D_{3t}+ D_{4t} and D_{3m} + D_{4m} as a function of composition x for the data of Table 4.

Table 5 shows the results of this partitioning for the spectra of Fig. 12*c*–*f* and Table 4, compared with the sample with the most similar composition from Fig. 7*h* and Table 3. In the bottom four rows, the D_3 and D_4 peaks have been recombined according to the assignment schemes for both Table 3 and Table 4. It can be seen that the expected relative areas for the synthetic sample are within 2% of those given in Table 3, demonstrating that the site environment model, combined with the two doublet assignment schemes, applies to datasets from both the synthetic and natural samples, despite the use of different peak-fitting methodologies. Figure 14 shows the relative proportions for D_1–D_4 sites as a function of bulk composition for x in the range ⅓–1.

As there are distinct variants of D_1 and D_2 for fougèrite and trébeurdenite, and similarly, three versions of D_3 and two of D_4, there are nine Fe environments in total in the three minerals. The cation ordering patterns of Fig. 9 allow us to determine the identities of edge-sharing neighbour cations. As discussed above, the D_3 Fe^{3+} of fougèrite, i.e. D_{3f}, are obviously situated above and below interlayer carbonate anions, to facilitate charge balance. The constant proportion of D_3 cations in all three minerals confirms that this situation is maintained in each species, in which case the ordering patterns of Fig. 15 can be deduced for the site types D_1–D_4. If the O^{2-} anions in the hydroxide sublayer, produced by dehydroxylation, are required to be bonded to D_4 cations, the local environments around the Fe sites can be characterized as in Table 6. The distributions of these sites between the three species are summarized in Table 7.

Given that intermediate compositions are intergrowths of the phases with x = ⅓, ⅔ or 1, any sample in the range ⅓–⅔ is a mixture of fougèrite (F) and trébeurdenite (T), with proportions obtained by the lever rule $(2-3x)F + (3x-1)T$, whereas compositions in the range ⅔–1 are

TABLE 5. Expected relative abundances of distinct Fe cation environments corresponding to the Mössbauer spectra of Fig. 12*c*–*f* and Table 4, with the x = 0.78 synthetic specimen of Fig. 7*h* and Table 3 for comparison.

	Trébeurden	Mont St Michel no.1	Mont St Michel no.2	Mont St Michel no.3	Synthetic
x	0.75	0.72	0.74	0.77	0.78
T (mol.%)	75	84	78	69	66
M (mol.%)	25	16	22	31	34
D_{1t} (%)	18.75	21	19.5	17.25	16.5
D_{2t} (%)	6.25	7	6.5	5.75	5.5
D_{3t} (%)	25	28	26	23	22
D_{4t} (%)	25	28	26	23	22
D_{3m} (%)	8.33	5.33	7.33	10.33	11.33
D_{4m} (%)	16.67	10.67	14.67	20.67	22.67
D_{3t} + D_{3m}	33.33	33.33	33.33	33.33	33.33
D_{4t} + D_{4m}	33.33	38.67	40.67	43.67	44.67
D_{3t} + D_{4t}	50	56	52	46	44
D_{3m} + D_{4m}	25	16	22	31	34

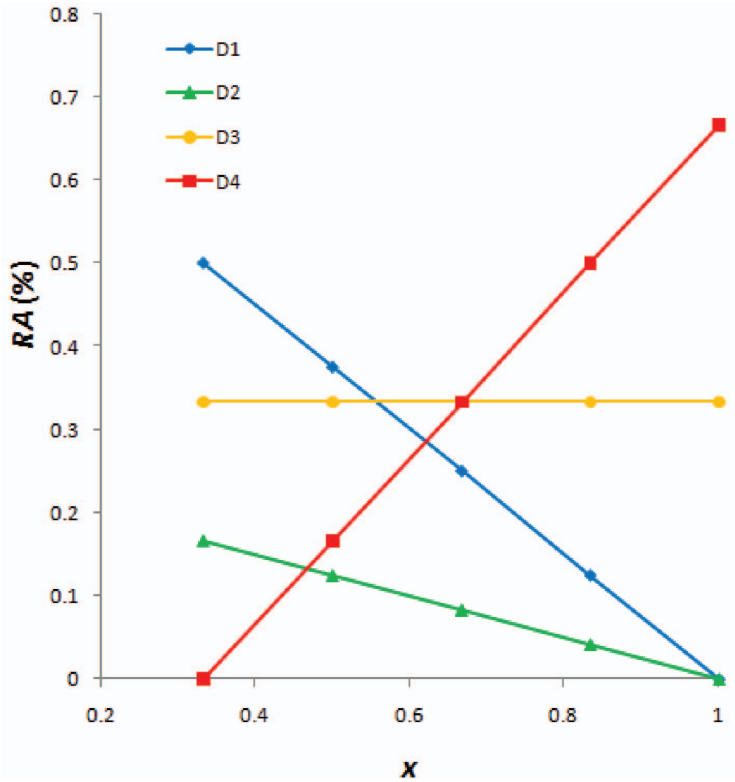

FIG. 14. Relative abundance of Fe cation environments D_1–D_4 as a function of bulk composition.

mixtures of T and mössbauerite (M) with the proportions $3(1-x)T + (3x-2)M$. To date, occurrences of gleys extracted from continental aquifers as at Fougères only have compositions in the range x = ⅓–⅔, whereas those from salt marsh environments such as Trébeurden or Mont

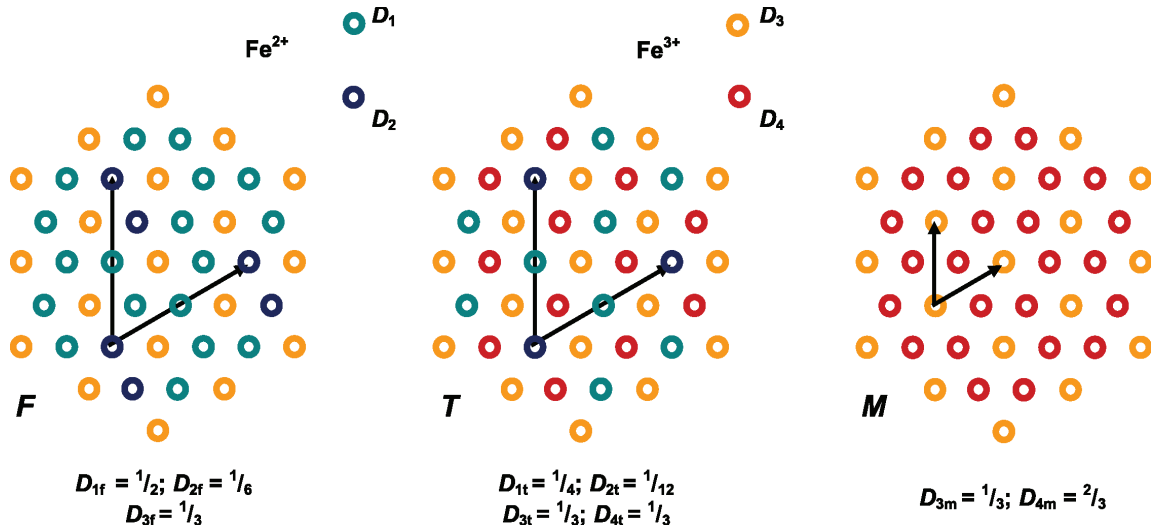

FIG. 15. Cations in the octahedral layer of fougèrite (F), trébeurdenite (T) and mössbauerite (M), showing the two-dimensional superstructures that arise if Fe^{2+} and Fe^{3+} order as in Fig. 9 and D_2 and D_3 environments which are clustered near interlayer carbonate. Arrows indicate vectors between equivalent Fe sites.

TABLE 6. Details of the local environments for Fe cations.

Local environment type	Cation	Edge-sharing octahedral neighbours	Interlayer species in vertical registry	Ligands in octahedral layer
D_{1f}	Fe^{2+}	$3Fe^{2+} + 3Fe^{3+}$	H_2O	$(OH)_6$
D_{2f}	Fe^{2+}	$3Fe^{2+} + 3Fe^{3+}$	CO_3^{2-}	$(OH)_6$
D_{3f}	Fe^{3+}	$6Fe^{2+}$	CO_3^{2-}	$(OH)_6$
D_{1t}	Fe^{2+}	$6Fe^{3+}$	H_2O	$(OH)_6$
D_{2t}	Fe^{2+}	$6Fe^{3+}$	CO_3^{2-}	$(OH)_6$
D_{3t}	Fe^{3+}	$3Fe^{2+} + 3Fe^{3+}$	CO_3^{2-}	$(OH)_5O$
D_{4t}	Fe^{3+}	$3Fe^{2+} + 3Fe^{3+}$	H_2O	$(OH)_4O_2$
D_{3m}	Fe^{3+}	$6Fe^{3+}$	CO_3^{2-}	$(OH)_4O_2$
D_{4m}	Fe^{3+}	$6Fe^{3+}$	H_2O	$(OH)_4O_2$

Saint-Michel Bay only have compositions in the range $x = ⅔–1$.

Based on the data and analysis outlined in the foregoing text:

(1) We redefine the former 'fougèrite', which was named for its occurrence in forest of Fougères by Trolard *et al.* (2007), as a $Fe^{2+}–Fe^{3+}$ hydroxycarbonate with the formula $Fe_4^{2+}Fe_2^{3+}(OH)_{12}CO_3{\cdot}3H_2O$, and with $x = ⅓$; it is the common $Fe^{2+}–Fe^{3+}$ LDH, and is commonly described as 'green rust' or 'carbonated green rust.' Note that the artificial equivalent of carbonated green rust commonly forms during the corrosion of Fe-based materials and steels (e.g. Drissi *et al.*, 1995).

(2) We define the $Fe^{2+}–Fe^{3+}$ oxyhydroxycarbonate with $x = ⅔$, and with the formula $Fe_2^{2+}Fe_4^{3+}O_2(OH)_{10}CO_3{\cdot}3H_2O$, as trébeurdenite; it is named for the township of Trébeurden, near the maritime marsh where the mineral was first found. The holotype specimen M52133 is accessioned in the collections of Museum Victoria in Melbourne, and is from l'Île d'Aval, near Penvern, Trébeurden, Brittany, France.

(3) The ferric oxyhydroxycarbonate with $x = 1$ and the formula $Fe_6^{3+}O_4(OH)_8CO_3{\cdot}3H_2O$ is named mössbauerite, after Professor Rudolf Mössbauer (1928–2011) who discovered the resonance of γ rays that bears his name, for which he was awarded the 1961 Nobel Prize in physics. The full type description of mössbauerite is reported in Génin *et al.* (2012*b*).

Group nomenclature

Group nomenclature for the hydrotalcite supergroup follows the CNMNC guidelines outlined by Mills *et al.* (2009). The group nomenclature scheme discussed here can be considered as a hybrid, in that the groups are defined firstly by the interlayer spacing and secondly by the M^{2+}:M^{3+} ratios in the brucite layers. The restricted ranges found for those ratios in many members of the supergroup suggest that they correlate with cation ordering patterns within layers, which may or may not correlate between layers, as evidenced by diffraction behaviour. The dominant M^{2+} and M^{3+} cations are important for defining individual species based on the dominant-constituent and dominant-valency rules (Hatert and Burke, 2008). Due to the differences in the ionic radii of the M^{2+} and M^{3+} cations in some of the minerals (e.g. in

TABLE 7. Abundance of different local Fe environments in the green rust minerals.

	— D_1 —		— D_2 —		——— D_3 ———			— D_4 —	
	D_{1f}	D_{1t}	D_{2f}	D_{2t}	D_{3f}	D_{3t}	D_{3m}	D_{4t}	D_{4m}
Fougèrite	50%		16.7%		33.3%				
Trébeurdenite		25%		8.3%		33.3%		33.3%	
Mössbauerite							33.3%		66.7%

the hydrotalcite group), specific M^{2+}:M^{3+} ratios are strongly favoured (e.g. 2:1). In other groups, where the ionic radii are very similar (e.g. in the woodwardite group), there may be wide variation in M^{2+}:M^{3+} ratios within and between species.

The following groups (in order of the smallest to largest interlayer periodicity) can be defined:

(1) Hydrotalcite group: hydrotalcite group members have an M^{2+}:M^{3+} ratio of 3:1, they contain interlayer carbonate, chloride or hydroxide and water, and have a layer spacing of ~7.8 Å.

(2) Quintinite group: quintinite group members have an M^{2+}:M^{3+} ratio of 2:1, they contain interlayer carbonate or chloride and water, and have a layer spacing of ~7.8 Å.

(3) Fougèrite group: the 'green rusts' of the fougèrite group have a layer spacing of ~7.8 Å; they are not included in either of the groups listed above because the dominant octahedral cations, either Fe^{2+} or Fe^{3+}, are readily interconverted by redox processes. Two members of the group, trébeurdenite and mössbauerite, provide the only examples of M^{3+} dominance in the hydrotalcite supergroup, and contain some O^{2-} in replacement of OH^{-}.

(4) Woodwardite group: minerals of the woodwardite group are characterized by the presence of interlayer sulfate and water, and have a layer spacing of ~8.9 Å. The M^{2+}:M^{3+} ratio is variable in members of the group and no evidence of cation ordering has been reported. The layer spacing is greater than hydrotalcite and quintinite due to the size of the sulfate tetrahedra. These compounds also differ from the hydrotalcite and quintinite groups in showing a marked preference for the small M^{2+} cations Ni, Cu and Zn rather than Mg, Mn and Fe. Furthermore, the woodwardite group minerals readily and reversibly undergo transformations to the more highly hydrated minerals of the glaucocerinite group by intercalation of additional interlayer water molecules.

(5) Cualstibite group: members of the cualstibite group are characterized by (M^{2+}, M^{3+})$(OH)_2$ brucite-type sheets, in which M^{2+} = Cu^{2+}, Ni^{2+} or Zn^{2+}, M^{3+} = Al^{3+} or Fe^{3+}, and the interlayer species is $[Sb(OH)_6]^{-}$. The layer spacing is ~9.7 Å.

(6) Glaucocerinite group: glaucocerinite group members are characterized by the presence of interlayer sulfate and water, and less commonly non-essential intercalated M^{2+} cations where M^{2+} = Mg^{2+} or Ni^{2+}. The layer spacing is ~11 Å, and the interlayers contain additional water in comparison to members of the woodwardite group. The M^{2+}:M^{3+} ratios are variable.

(7) Wermlandite group: wermlandite group members are characterized by the presence of interlayer sulfate, water and essential $[A(H_2O)_6]$ groups, where A = Na^{+}, Ca^{2+}, Sr^{2+}, or similarly large cations. The layer spacing is ~11 Å and M^{2+}:M^{3+} ratios are variable.

(8) Hydrocalumite group: hydrocalumite group members contain $(Ca,Al)(OH)_2$ sheets in which the Ca:Al ratio is always 2:1; Ca^{2+} is coordinated to a seventh ligand of 'interlayer' water. They may contain interlayer hydroxyl, carbonate, chloride or sulfate and water.

The members of these groups are listed in Table 8. Table 9 includes the ideal simplified formulae for the species listed in Table 8, as derived earlier in the discussion of individual species. These formulae are compared with those given in the 2009 IMA mineral list, which are available at http://pubsites.uws.edu.au/ima-cnmnc/IMA2009-01 UPDATE 160309.pdf.

Unnamed minerals

Unnamed Co^{3+} analogue of reevesite

Song and Moon (1998) reported 'reevesite' from serpentinized ultramafic rocks of the Kwangcheon area in Korea, which showed solid solution almost all the way to the Co^{3+} endmember, and verified the completeness of the solid solution by syntheses. The Co-dominant synthetic material is dark green in colour in comparison to the yellow-brown of synthetic reevesite. The $Ni^{2+}/(Fe^{3+} + Co^{3+})$ ratio was reported to be close to 3:1, which is typical of the hydrotalcite group and contrasts with the 2:1 ratio reported for comblainite (Piret and Deliens, 1980). The new mineral has not yet been fully described or submitted to the IMA for approval. The phase was given the unnamed mineral code UM1998-10-CO:CoHNi by Smith and Nickel (2007).

Unnamed Mg-Al analogue of honessite

Lisitsina *et al*. (1985) described a Mg-Al sulfate from a North Atlantic seamount with a = 3.05 and c = 26.50 = 3 × 8.83 Å. Bookin *et al.* (1993*a*) discussed attempts to fit the X-ray intensity data, and concluded that the phase had the unusual $3T_2$ stacking sequence. An intergrown 2-layer structure was also detected, but the diffraction data were not sufficient for more detailed characterization. In contrast, the synthetic

HYDROTALCITE SUPERGROUP NOMENCLATURE

TABLE 8. Group hierarchy of the hydrotalcite supergroup.

HYDROTALCITE SUPERGROUP
Hydrotalcite group
Hydrotalcite, Pyroaurite, Stichtite, Meixnerite, Iowaite, Droninoite, Woodallite, Desautelsite, Takovite, Reevesite, Jamborite*
Quintinite group
Quintinite, Charmarite, Caresite, Zaccagnaite, Chlormagaluminite, Comblainite
Fougèrite group
Fougèrite, Trébeurdenite, Mössbauerite
Woodwardite group
Woodwardite, Zincowoodwardite, Honessite
Glaucocerinite group
Glaucocerinite, Hydrowoodwardite, Carrboydite*, Hydrohonessite, Mountkeithite, Zincaluminite*
Wermlandite group
Wermlandite, Shigaite, Nikischerite, Motukoreaite*, Natroglaucocerinite*, Karchevskyite
Cualstibite group
Cualstibite, Zincalstibite, Omsite
Hydrocalumite group
Hydrocalumite, Kuzelite
Unclassified
Coalingite, Brugnatellite*, Muskoxite*

* Questionable species which need further study.

$Mg_6Al_2(OH)_{16}(SO_4)\cdot nH_2O$ of Miyata and Okada (1977) with $a = 3.05$ and $c = 25.97$ Å, has the $3R_1$ structure according to Bookin *et al.* (1993*a*).

Unnamed Mg analogue of carrboydite or Al analogue of mountkeithite

Lisitsina *et al*. (1985) reported a second Mg-Al sulfate from the North Atlantic seamount described in the foregoing text, with $c = 32.4 = 3 \times 10.8$ Å, for which Bookin *et al*. (1993*a*) deduced the $3R_1$ stacking sequence. Drits *et al*. (1987) described a similar phase with the formula $Mg_4Al_2(OH)_{12}(SO_4)\cdot nH_2O$ from Gaurdak, Turkmenistan, but this has $c = 11.16$ Å, and hence is the 1*T* polytype.

Unnamed Mg–Al interstratified sulfate–carbonate

Drits *et al*. (1987) described a phase with the formula $Mg_4Al_2(OH)_{12}(CO_3)_{0.5}(SO_4)_{0.5}\cdot nH_2O$, from the Inder salt dome, Caspian Depression, Kazakhstan. It has a unit cell with $a = 3.05$ and $c = 55.62 = 3 \times 18.54$ Å. Bookin *et al*. (1993*a*) interpreted the 18.54 Å spacing as the sum of a narrow 6.56 Å layer spacing corresponding to interlayer carbonate, and a wide 9.98 Å spacing corresponding to interlayer sulfate, implying a regular alternation of two types of interlayer in the structure. They suggested that the narrow interlayers were *P*-type and the wide ones *O*-type, corresponding to the unusual $6R_4$ stacking sequence overall.

Unnamed hydroxide analogue of coalingite

The 'coalingite' from the Muskox Intrusion, Canada, described by Jambor (1969*a*) was reported to have a very low carbonate content, and a formula (based on 12 cations) $[(Mg_{9.67}Fe^{3+}_{2.33}(OH)_{24}](CO_3)_{0.33}(OH)_{1.67}\cdot 1.75H_2O$. This was discussed further by Pastor-Rodriguez and Taylor (1971). The material is trigonal with $a = 3.1$ Å; c is uncertain but >30 Å. This phase may be the hydroxide analogue of coalingite, but requires further investigation.

TABLE 9. Formulae for minerals of Table 8 as given in 2009 IMA mineral list, and ideal formulae recommended on the basis of the current report.

Mineral	Group	Formula (IMA list 2009)	Recommended ideal formula
Brugnatellite	ungrouped	$Mg_6Fe^{3+}CO_3(OH)_{13}\cdot 4H_2O$	Needs reinvestigation
Caresite	Quintinite	$(Fe^{2+})_4Al_2(OH)_{12}CO_3\cdot 3H_2O$	$Fe^{2+}_4Al_2(OH)_{12}[CO_3]\cdot 3H_2O$
Carrboydite	Glaucocerinite	$(Ni,Al)_9(SO_4)_2(OH)_{18}\cdot .10H_2O$	$(Ni_{1-x}Al_x)(OH)_2][SO_4]_{x/2}\cdot nH_2O$ ($x < 0.5$, $n > 3x/2$)
Charmarite	Quintinite	$Mn_4Al_2(OH)_{12}CO_3\cdot 3H_2O$	$Mn_4Al_2(OH)_{12}[CO_3]\cdot 3H_2O$
Chlormagalumite	Quintinite	$Mg_4Al_2(OH)_{12}Cl_2\cdot 2H_2O$	$Mg_4Al_2(OH)_{12}Cl_2\cdot 3H_2O$
Coalingite	ungrouped	$Mg_{10}(Fe^{3+})_2CO_3(OH)_{24}\cdot 2H_2O$	$Mg_{10}Fe^{3+}_2(OH)_{24}[CO_3]\cdot 2H_2O$
Comblainite	Quintinite	$Ni_6(Co^{3+})_2CO_3(OH)_{16}\cdot 4H_2O$	$Ni_4Co^{3+}_2(OH)_{12}[CO_3]\cdot 3H_2O$
Cualstibite	Cualstibite	$Cu_2AlSb(OH)_{12}$	$Cu_2Al(OH)_6[Sb(OH)_6]$
Desautelsite	Hydrotalcite	$Mg_6(Mn^{3+})_2CO_3(OH)_{16}\cdot 4H_2O$	$Mg_6Mn^{3+}_2(OH)_{16}[CO_3]\cdot 4H_2O$
Droninoite	Hydrotalcite	$Ni_3Fe^{3+}Cl(OH)_8\cdot 2H_2O$	$Ni_6Fe^{3+}_2(OH)_{16}Cl_2\cdot 4H_2O$
Fougèrite	Fougèrite	$(Fe^{2+},Mg)_6(Fe^{3+})_2(OH)_{18}\cdot 4H_2O$	$Fe^{2+}_4Fe^{3+}_2(OH)_{12}[CO_3]\cdot 3H_2O$
Glaucocerinite	Glaucocerinite	$(Zn_{1-x}Al_x)(SO_4)_{x/2}(OH)_2\cdot nH_2O$	$(Zn_{1-x}Al_x)(OH)_2[SO_4]_{x/2}\cdot nH_2O$ ($x < 0.5$, $n > 3x/2$)
Honessite	Woodwardite	$(Ni,Fe^{3+})_8(SO_4)_{1.2}(OH)_{16}\cdot nH_2O$	$(Ni_{1-x}Fe^{3+}{}_x)(OH)_2[SO_4]_{x/2}\cdot nH_2O$ ($x < 0.5$, $n < 3x/2$)
Hydrocalumite	Hydrocalumite	$Ca_4Al_2(OH)_{12}(Cl,CO_3,OH)_{2-x}\cdot 4H_2O$	Possibly multiple species with formulae such as: $Ca_4Al_2(OH)_{12}Cl_2\cdot 4H_2O$, $Ca_4Al_2(OH)_{12}(OH)_2\cdot 4H_2O$ and $Ca_8Al_4(OH)_{24}[CO_3]Cl_2(H_2O)_{1.6}\cdot 8H_2O$
Hydrohonessite	Glaucocerinite	$(Ni,Fe^{3+})_9(SO_4)_2(OH)_{18}\cdot 7H_2O$	$(Ni_{1-x}\ Fe^{3+}{}_x)(OH)_2[SO_4]_{x/2}\cdot nH_2O$ ($x < 0.5$, $n > 3x/2$)
Hydrotalcite	Hydrotalcite	$Mg_6Al_2CO_3(OH)_{16}\cdot 4H_2O$	$Mg_6Al_2(OH)_{16}[CO_3]\cdot 4H_2O$
Hydrowoodwardite	Glaucocerinite	$(Cu,Al)_9(SO_4)_2(OH)_{18}.nH_2O$	$(Cu_{1-x}Al_x)(OH)_2[SO_4]_{x/2}\cdot nH_2O$ ($x < 0.5$, $n > 3x/2$)
Iowaite	Hydrotalcite	$Mg_6(Fe^{3+})_2\ (OH)_{16}Cl_2\cdot 4H_2O$	$Mg_6Fe^{3+}_2(OH)_{16}Cl_2\cdot 4H_2O$
Jamborite	Hydrotalcite	$Ni(OH,S,O)_2.nH_2O$ (?)	Needs reinvestigation: may be $Ni^{2+}_6Ni^{3+}_2(OH)_{16}S\cdot 4H_2O$
Karchevskyite	Wermlandite	$[Mg_{18}Al_9(OH)_{54}][Sr_2(CO_3,PO_4)_9(H_2O,-H_3O)_{11}]$	$Mg_{18}Al_9(OH)_{54}Sr_2(CO_3)_9(H_2O)_6(H_3O)_5$
Kuzelite	Hydrocalumite	$Ca_4Al_2(OH)_{12}(SO_4)\cdot 6H_2O$	$Ca_4Al_2(OH)_{12}[SO_4]\cdot 6H_2O$
Meixnerite	Hydrotalcite	$Mg_6Al_2(OH)_{18}\cdot 4H_2O$	$Mg_6Al_2(OH)_{16}(OH)_2\cdot 4H_2O$
Mössbauerite	Fougèrite	n/a	$Fe^{3+}_6O_4(OH)_8[CO_3]\cdot 3H_2O$
Motukoreaite	Wermlandite	$[Mg_6Al_3(OH)_{18}][Na(SO_4)_2\cdot 7H_2O]$	Needs reinvestigation: $Mg_6Al_3(OH)_{18}[Na(H_2O)_6][SO_4]_2\cdot 6H_2O$ possibly other species.

HYDROTALCITE SUPERGROUP NOMENCLATURE

Mountkeithite	Glaucocerinite	$Mg_{11}(Fe^{3+})_3(SO_4)_{3.5}(OH)_{24}{\cdot}11H_2O$	$(Mg_{1-x}\ Fe^{3+}{}_x)(OH)_2][SO_4]_{x/2}{\cdot}nH_2O$ ($x < 0.5$, $n > 3x/2$)
Muskoxite	ungrouped	$Mg_7(Fe^{3+})_4(OH)_{26}{\cdot}H_2O$ (?)	Needs reinvestigation, possibly more than one species.
Natroglaucocerinite	Wermlandite	$Zn_{8-x}Al_x(OH)_{16}(SO_4)_{x/2+y/2}Na_y(H_2O)_6$	Needs reinvestigation: may be $Zn_6Al_3(OH)_{18\ [Na(H_2O)_6]}[SO_4]_2{\cdot}6H_2O$
Nikischerite	Wermlandite	$Na(Fe^{2+})_6Al_3(SO_4)_2(OH)_{18}(H_2O)_{12}$	$Fe^{2+}_6Al_3(OH)_{18}[Na(H_2O)_6][SO_4]_2{\cdot}6H_2O$
Omsite	Cualstibite	n/a	$Ni_2Fe^{3+}(OH)_6[Sb(OH)_6]$
Pyroaurite	Hydrotalcite	$Mg_6(Fe^{3+})_2CO_3(OH)_{16}{\cdot}4H_2O$	$Mg_6Fe^{3+}_2(OH)_{16}[CO_3]{\cdot}4H_2O$
Quintinite	Quintinite	$Mg_4Al_2CO_3(OH)_{12}{\cdot}3H_2O$	$Mg_4Al_2(OH)_{12}[CO_3]{\cdot}3H_2O$,
Reevesite	Hydrotalcite	$Ni_6(Fe^{3+})_2CO_3(OH)_{16}{\cdot}4H_2O$	$Ni_6Fe^{3+}_2(OH)_{16}(CO_3){\cdot}4H_2O$
Shigaite	Wermlandite	$NaAl_3(Mn^{2+})_6(SO_4)_2(OH)_{18}.12H_2O$	$Mn_6Al_3(OH)_{18}[Na(H_2O)_6][SO_4]_2{\cdot}6H_2O$
Stichtite	Hydrotalcite	$Mg_6Cr_2CO_3(OH)_{16}{\cdot}4H_2O$	$Mg_6Cr_2(OH)_{16}[CO_3]{\cdot}4H_2O$
Takovite	Hydrotalcite	$Ni_6Al_2CO_3(OH)_{16}{\cdot}4H_2O$	$Ni_6Al_2(OH)_{16}[CO_3]{\cdot}4H_2O$
Trébeurdenite	Fougèrite	n/a	$Fe^{2+}_2Fe^{3+}_4O_2(OH)_{10}[CO_3]{\cdot}3H_2O$
Wermlandite	Wermlandite	$Mg_8Al_2(OH)_{18}(SO_4)_2{\cdot}12H_2O$	$Mg_7Al_2(OH)_{18}[Ca(H_2O)_6][SO_4]_2{\cdot}6H_2O$
Woodallite	Hydrotalcite	$Mg_6Cr_2\ (OH)_{16}Cl_2{\cdot}4H_2O$	$Mg_6Cr_2(OH)_{16}Cl_2{\cdot}4H_2O$
Woodwardite	Woodwardite	$(Cu,Al)_9(SO_4)_2(OH)_{18}.nH_2O$	$Cu_{1-x}Al_x(OH)_2[SO_4]_{x/2}{\cdot}nH_2O$ ($x < 0.5$, $n < 3x/2$)
Zaccagnaite	Quintinite	$Zn_4Al_2\ (OH)_{12}(CO_3){\cdot}3H_2O$	$Zn_4Al_2(OH)_{12}[CO_3]{\cdot}3H_2O$
Zincalstibite	Cualstibite	$Zn_2AlSb(OH)_{12}$	$Zn_2Al(OH)_6[Sb(OH)_6]$
Zincaluminite	Glaucocerinite	$(Zn,Al)_9(SO_4)_2(OH)_{18}.nH_2O$ (?)	Needs reinvestigation: may be same as glaucocerinite.
Zincowoodwardite	Woodwardite	$Zn_{1-x}Al_x(OH)_{12}(SO_4)_{x/2}.nH_2O$ ($x = 0.32-0.50$)	$Zn_{1-x}Al_x(OH)_2[SO_4]_{x/2}{\cdot}nH_2O$ ($x < 0.5$, $n < 3x/2$)

'Coalingite-K'

Mumpton *et al.* (1965) reported a second phase occurring in parallel intergrowth with coalingite, which was different in its optical and diffraction properties. This material was re-examined by Pastor-Rodriguez and Taylor (1971), who interpreted strong diffraction features at 5.72 and 4.38 Å as (0003) and (0004) reflections corresponding to a 17.2 Å *c* repeat, and hypothesized that the phase was an interstratification of three brucite layers and one interlayer, forming a polysomatic series with brucite, coalingite and pyroaurite. The ideal formula, in this case, would be $[Mg_{16}Fe^{3+}_2(OH)_{36}]$ $(CO_3)\cdot 2H_2O$, but this has not been verified, and the mineral has not been studied further or submitted for approval by the IMA.

Unnamed Mg^{2+}–Ni^{3+} hydroxide

A mineral described by Lapham (1965) from the Cedar Hill serpentinite quarry, Lancaster County, Pennsylvania is rhombohedral with a = 3.12 and c = 23.19 Å, which suggests a 3*R* polytype related to the hydrotalcite and quintinite groups. Carbonate is low or absent. The atomic Mg:Ni:Fe ratio was reported to be 80.8:15.0:4.2, implying that, at most, 1/5.3 of the octahedral cations is trivalent (Ni + Fe). This incompletely described phase may be a Mg^{2+}-Ni^{3+}-hydroxide analogue of brugnatellite. The phase was given the unnamed mineral code UM1965-08-OH:FeMgNi by Smith and Nickel (2007).

Unnamed Ni^{2+}–Ni^{3+} hydroxide

A nickel-rich mineral described by Jambor and Boyle (1964) from Rock Creek, British Columbia, Canada is rhombohedral with a = 3.07 and c = 22.74 Å, indicating that it is a 3*R* polytype related to the hydrotalcite and quintinite groups. Carbonate is low or absent and the Mg content is also negligible. The phase was compared by Lapham (1965) with his Mg-rich phase and to various synthetic compounds. This incompletely described phase may be a Ni^{2+}-Ni^{3+}-hydroxide analogue of hydrotalcite, quintinite or brugnatellite.

Nomenclature for synthetic LDH phases

Many synthetic LDH phases have a similar crystallography and chemistry to natural phases; however, a much wider range of octahedral cations and intercalcated anions have been incorporated in synthetic LDH compounds. Unfortunately, some chemists have tended to use mineral names incorrectly in referring to synthetic analogues of minerals and their structural relatives. As a result of this, and due to the inconsistencies in reporting and naming synthetic LDH phases, we propose a simple but flexible nomenclature scheme which can be applied to synthetic phases; it provides information about the chemistry and crystallography of the phase and also clearly identifies it as a synthetic compound. Such a scheme would only become best practice among chemists if it was adopted by the International Union for Pure and Applied Chemistry, but as informal nomenclature schemes are already being used in the synthetic LDH literature, we can at least offer a consistent and rational alternative to the misuse of mineral names.

Hydrotalcite-like Mg-Al LDHs can be prepared by mixing aqueous solutions of alkalis such as NaOH with Mg−Al solutions such as $MgCl_2-AlCl_3$ and $Mg(NO_3)_2-Al(NO_3)_3$ (e.g. Ross and Kodama, 1967; Miyata, 1975; Miyata and Okada, 1977). The stoichiometric equation describing the precipitation of synthetic Mg−Al LDHs, for example, can be written:

$$(1-x)Mg^{2+} + xAl^{3+} + 2OH^- + (x/n)A^{n-} \rightarrow Mg_{1-x}Al_x(OH)_2(A)_{x/n}$$

where $0.20 \leqslant x \leqslant 0.33$ and A^{n-} is an n-valent anion. The Mg/Al molar ratio x and anion A^{n-} can be controlled during preparation of the LDH and need to be specified in the nomenclature scheme. Our proposal for a nomenclature system for synthetic LDH phases uses the following formula: LDH $xM^{2+}yM^{3+}\cdot A[B]$-C, where x and y are the proportions of M^{2+} and M^{3+}; M^{2+} is the divalent cation in the octahedral layer; M^{3+} is the trivalent cation in the octahedral layer; A is the intercalated anion; B is an interlayer cation; and C is the polytype symbol.

If this scheme is adopted the following guidelines can usefully be applied:

(1) If there are no interlayer B cations, the associated brackets '[ ]' can be omitted.

(2) It is the ratio x:y which is important rather than the absolute values of x and y themselves, as is the case for any empirical formula. Thus, '6Mg2Al' is equivalent to '75Mg25Al' in this scheme; however, '1' is optional, as in chemical formulae, so '3Mg1Al' could be shortened to '3MgAl'.

(3) The different hydration states of the analogues of woodwardite- and glaucocerinite-group minerals are not explicitly distinguished, but such phases are likely to be rapidly and reversibly convertible.

(4) The polytype symbol *C* conveys the overall number of brucite layers in the repeat, and the overall crystal system/lattice type. If one of the precise stacking sequences for brucite layers of Table 1 is known and needs to be specified, numerical subscripts can be added. If a distinction between types of stacking that arise by different structural mechanisms (cf. discussion of quintinite and wermlandite) is required, extensions to the notation will be needed.

(5) It is assumed that there is only one type of interlayer. Interstratified structures such as that of coalingite are not provided for in the basic notation, although Bookin *et al*. (1993*a*) suggest a notation for encoding this information.

Given the fast crystallization kinetics of synthetic LDH phases, it is likely that the octahedral cation site or interlayer site occupancy patterns will not display long-range order of the types considered in points (3) and (4) above, so more complex notation is probably not necessary.

As examples of the notation, the mineral pyroaurite has the formula $Mg_6Fe_2(OH)_{16}CO_3 \cdot 4H_2O$. In this system, synthetic pyroaurite can be described as LDH 6Mg2Fe·CO_3-3*R*; synthetic takovite, $Ni_6Al_2(OH)_{16}CO_3 \cdot 4H_2O$, is LDH 6Ni2Al·$CO_3$-3*R*. Synthetic LDH phases with no mineralogical equivalent, such as $Mg_{0.80}Al_{0.20}(OH)_2(CO_3)_{0.10} \cdot 0.78H_2O$ (Kameda *et al*., 2003), can easily be represented in this system (in this case, as LDH 8Mg2Al·CO_3-3*R*). More exotic examples are provided by synthetic zincalstibite, $Zn_2Al(OH)_6[Sb(OH)_6]$, which is LDH 2ZnAl·[Sb(OH)$_6$]-1*T*; kuzelite, $[Ca_4Al_2(OH)_{12}][SO_4] \cdot 6H_2O$, which is LDH 4Ca2Al·$SO_4$-6*R*; and wermlandite, $[Mg_7Al_2(OH)_{18}][Ca(H_2O)_6][SO_4]_2 \cdot 6H_2O$, which is LDH 7Mg2Al·$SO_4$[Ca($H_2O$)$_6$]-1*T*.

Green rust phases have commonly been identified using notation such as '$GR(CO_3^{2-})$' (e.g. Génin *et al*., 2006*a*), which similarly only conveys part of the information about the phase. The four green rust phases with CO_3 in the interlayer are: $Fe_6^{2+}(OH)_{10}(H_2O)_2CO_3 \cdot 3H_2O$, $Fe_4^{2+}Fe_2^{3+}(OH)_{12}CO_3 \cdot 3H_2O$, $Fe_2^{2+}Fe_4^{3+}O_2(OH)_{10}CO_3 \cdot 3H_2O$ and $Fe_6^{3+}O_4(OH)_8CO_3 \cdot 3H_2O$. These can thus be described as LDH $6Fe^{2+}0Fe^{3+}\cdot CO_3$-3*R*; LDH $4Fe^{2+}2Fe^{3+}\cdot CO_3$-3*R* (fougèrite); LDH $2Fe^{2+}4Fe^{3+}\cdot CO_3$-3*R* (trébeurdenite); and LDH $0Fe^{2+}6Fe^{3+}\cdot CO_3$-3*R* (mössabuerite), respectively. This notation can also easily be adapted for the green rust phases with different interlayer species such as those described by Bernal *et al.* (1959). However, green rusts are a special case in the supergroup in that (1) the divalent and trivalent cations are the same element; (2) known compositions include ones with only one valency state in the octahedral layer; and (3) examples are known with predominantly trivalent octahedral cations, for which charge balance requires that some hydroxide anions are replaced by oxide. We recommend that the valence state for octahedral cations be included in the notation for these minerals, and that the stoichiometric number "0" be used to indicate the absent species explicitly in compositions in which the octahedral cations are all divalent or all trivalent.

Terms such as 'hydrotalcite-like' or 'quinitinite-like' do not contain precise information about the structure or the composition of the phase, and are commonly misleading. The alternative scheme proposed by Drits *et al.* (1987) suggests names such as '8.85-Å SO_4-hydrotalcite-2*H*', which include the layer spacing explicitly, but it is mineralogically misleading as such a phase is closer to a woodwardite-group mineral than a member of the hydrotalcite group. In addition, the M^{2+}:M^{3+} ratio and hence the charge on the brucite layer are not apparent in this name. Our proposed system conveys the M^{2+}:M^{3+} ratio and in consequence places quantitative constraints on the interlayer anion content. Therefore, it allows an empirical formula ($\pm H_2O$) to be written, that captures the data of most importance in describing the chemical properties of synthetic LDH phases.

Acknowledgements

We thank members of the CNMNC for their comments during the submission process and Tony Kampf for comments on the submitted manuscript.

References

Aïssa, R., François, M., Ruby, C., Fauth, F., Medjahdi, G., Abdelmoula, M. and Génin, J.-M. R. (2006) Formation and crystallographical structure of hydroxysulphate and hydroxycarbonate green rusts synthesized by coprecipitation. *Journal of Physical Chemistry of Solids*, **67**, 1016–1019.

Alker, A., Colob, P., Postl, W. and Waltinger, H. (1981)

Hydrotalkit, Nordstrandit und Motukoreait vom Stradner Kogel, südlich Gleichenberg, Steiermark. *Mitteilungen der Abteilung für Mineralogie des Landesmuseum Joanneum*, **49**, 1–13.

Allmann, R. (1968) The crystal structure of pyroaurite. *Acta Crystallographica*, **B24**, 972–979.

Allmann, R. and Donnay, J.D.H. (1969) About the structure of iowaite. *American Mineralogist*, **54**, 296–299.

Allmann, R. and Jepsen, H.P. (1969) Die struktur des hydrotalkits. *Neues Jahrbuch für Mineralogie Monatshefte*, **1969**, 544–551.

Aminoff, G. and Broomé, B. (1931) Contributions to the mineralogy of Långban. III. Contributions to the knowledge of the mineral pyroaurite. *Kungliga Svenska vetenskapsakademiens handlingar*, **9**, 23–48.

Amphlett, C.B. (1958) Ion exchange in clay minerals. *Endeavour*, **17**, 149–155.

Arakcheeva, A.V., Pushcharovskiy, D.Yu., Rastsvetaeva, R.K., Atencio, D. and Lubman, D.U. (1996) Crystal structure and comparative crystal chemistry of $Al_2Mg_4(OH)_{12}(CO_3)\cdot 3H_2O$, a new mineral from the hydrotalcite–manasseite group. *Crystallography Reports*, **41**, 972–981.

Arden, T.V. (1950) The solubility products of ferrous and ferrosic hydroxides. *Journal of the Chemical Society*, **1950**, 882–885.

Artini, E. (1909) Brugnatellite; nuova specie minerale trovata in Val Malenco. *Rendiconti della Regia Accademia Nazionale dei Lincei*, **18**, 3–6.

Barrer, R.M. (1978) Cation-exchange equilibria in zeolites and feldspathoids. Pp. 385–395 in: *Natural Zeolites: Occurrence, Properties, Use* (L.B. Sand and F.A. Mumpton, editors). Pergamon Press, New York.

Benali, O., Abdelmoula, M., Refait, Ph. and Génin, J.-M.R. (2001) Effect of orthophosphate on the oxidation products of Fe(II)-Fe(III) hydroxycarbonate: the transformation of green rust to ferrihydrite. *Geochimica et Cosmochimica Acta*, **65**, 1715–1726.

Bernal, J.D., Dasgupta, D.R. and Mackay, A.L. (1959) The oxides and hydroxides of iron and their structural inter-relationships. *Clay Minerals Bulletin*, **4**, 15–30.

Bertrand, E. and Damour, A. (1881) Zinc-aluminite, nouvelle espèce minérale du Laurium. *Bulletin de la Société Française de Minéralogie*, **4**, 135–136.

Bish, D.L. (1980) Anion-exchange in takovite: applications to other hydroxide minerals. *Bulletin de Minéralogie*, **103**, 170–175.

Bish, D.L. and Brindley, G.W. (1977) Reinvestigation of takovite, a nickel aluminum hydroxy-carbonate of the pyroaurite group. *American Mineralogist*, **62**, 458–464.

Bish, D.L. and Livingstone, A. (1981) The crystal chemistry and paragenesis of honessite and hydrohonessite. *Mineralogical Magazine*, **44**, 339–343.

Bonaccorsi, E., Merlino, S. and Orlandi, P. (2007) Zincalstibite, a new mineral, and cualstibite: crystal chemical and structural relationships. *American Mineralogist*, **92**, 198–203.

Bookin, A.S. and Drits, V.A. (1993) Polytype diversity of the hydrotalcite-like minerals. I. Possible polytypes and their diffraction features. *Clays and Clay Minerals*, **41**, 551–557.

Bookin, A.S., Cherkashin, V.I. and Drits, V.A. (1993*a*) Polytype diversity of the hydrotalcite-like minerals. II. Determination of the polytypes of experimentally studied varieties. *Clays and Clay Minerals*, **41**, 558–564.

Bookin, A.S., Cherkashin, V.I. and Drits, V.A. (1993*b*) Reinterpretation of the X-ray diffraction patterns of stichtite and reevesite. *Clays and Clay Minerals*, **41**, 631–634.

Braithwaite, R.S.W., Dunn, P.J., Pritchard, R.G. and Paar, W.H. (1994) Iowaite, a re-investigation. *Mineralogical Magazine*, **58**, 79–85.

Brindley, G.W. (1979) Motukoreaite – additional data and comparison with related minerals. *Mineralogical Magazine*, **43**, 337–340.

Britvin, S.N., Chukanov, N.V., Bekenova, G.K., Tagovkina, M.A., Antonov, A.V., Bogdanova, A.N. and Krasnova, N.I. (2008) Karchevskyite, $[Mg_{18}Al_9(OH)_{54}][Sr_2(CO_3,PO_4)_9(H_2O,H_3O)_{11}]$, a new mineral species of the layered double hydroxide family. *Geology of Ore Deposits*, **50**, 556–564.

Bryner, V., Rodgers, K.A., Courtney, S.F. and Postl, L. (1991) Motukoreaite from Brown Island, New Zealand, and Stradnerkögel, Austria – a scanning electron microscopic study. *Neues Jahrbuch für Mineralogie Abhandlung*, **163**, 291–304.

Carroll, D. (1959) Ion exchange in clays and other minerals. *Geological Society of America Bulletin*, **70**, 749–779.

Chao, G.Y. and Gault, R.A. (1997) Quintinite-2*H*, quintinite-3*T*, charmarite-2*H*, charmarite-3*T* and caresite-3*T*, a new group of carbonate minerals related to the hydrotalcite/manasseite group. *The Canadian Mineralogist*, **35**, 1541–1549.

Christiansen, B.C., Balic-Zunic, T., Dideriksen, K. and Stipp, S.L.S. (2009) Identification of green rust in groundwater. *Environmental Science and Technology*, **43**, 3436–3441.

Chukanov, N.V., Pekov, I.V., Levitskaya, L.A. and Zadov, A.E. (2009) Droninoite, $Ni_3Fe^{3+}Cl(OH)_8\cdot 2H_2O$, a new hydrotalcite-group mineral species from the weathered Dronino meteorite. *Geology of Ore Deposits*, **51**, 767–773.

Cooper, M.A. and Hawthorne, F.C. (1996) The crystal structure of shigaite, $[AlMn_2(OH)_6]_3(SO_4)_2Na(H_2O)_6\{H_2O\}_6$, a hydrotalcite-group mineral.

The Canadian Mineralogist, **34**, 91–97.

Dana, E.S. (1892) *The System of Mineralogy*, sixth edition. Wiley, New York, 962 pp.

De Waal, S.A. and Viljoen, E.A. (1971) Nickel minerals from Barberton, South Africa: IV. Reevesite, a member of the hydrotalcite group. *American Mineralogist*, **56**, 1077–1081.

Dittler, E. and Koechlin, R. (1932) Über Glaukokerinit, ein neues Mineral von Laurion. *Centralblatt für Mineralogie, Geologie und Paläontologie*, **A**, 13–17.

Dornberger-Schiff, K. (1982) Geometrical properties of MDO polytypes and procedures for their derivation. I. General concept and applications to polytype families consisting of OD layers all of the same kind. *Acta Crystallographica*, **A38**, 438–491.

Drissi, S.H., Refait, Ph., Abdelmoula, M. and Génin, J.-M.R. (1995) The preparation and thermodynamic properties of Fe(II)-Fe(III) hydroxycarbonate (green rust 1); Pourbaix diagram of iron in carbonate-containing aqueous media. *Corrosion Science*, **37**, 2025–2041.

Drits, V.A., Sokolova, T.N., Sokolova, G.V. and Cherkashin, V.I. (1987) New members of the hydrotalcite–manasseite group. *Clays and Clay Minerals*, **35**, 401–417.

Duan, X. and Evans, G.D. (2006) *Layered Double Hydroxides*. Springer, Berlin, 218 pp.

Dunn, P.J., Peacor, D.R. and Palmer, T.D. (1979) Desautelsite, a new mineral of the pyroaurite group. *American Mineralogist*, **64**, 127–130.

Evans, D.G. and Slade, R.C.T. (2006) Structural aspects of layered double hydroxides. Pp. 1–87 in: *Layered Double Hydroxides* (X. Duan and D.G. Evans, editors). Structure and Bonding, **119**. Springer, Berlin, 218 pp.

Féder, F., Trolard, F., Klingelhöfer, G. and Bourrié, G. (2005) *In situ* Mössbauer spectroscopy evidence for green rust (fougerite) in a gleysol and its mineralogical transformations with time and depth. *Geochimica et Cosmochimica Acta*, **69**, 4463–4483.

Feoktistov, G.D., Ivanov, S.I., Kashaev, A.A., Klyuchanskii, L.N., Taskina, N.G. and Ushchapovskaya, Z.F. (1978) The occurrence of chlormanasseite [= chlormagaluminite] in the USSR. *Zapiski Rossiiskogo Mineralogicheskogo Obshchestva*, **107**, 321–325, [in Russian].

Fenoglio, M. (1938) Ricerche sulla brugnatellite. *Periodico di Mineralogia*, **9**, 1–13.

Ferraris, G. and Merlino, S. (editors) (2005) *Micro- and Mesoporous Mineral Phases*. Reviews in Mineralogy and Geochemistry, **57**. Mineralogical Society of America, Washington DC and the Geochemical Society, St Louis, Missouri, USA, 448 pp.

Ferraris, G., Makovicky, E. and Merlino, S. (2004) *Crystallography of Modular Materials*. IUCr Monographs on Crystallography, **15**. Oxford University Press, Oxford, UK, 370 pp.

Fischer, R., Kuzel, H.-J. and Schellhorn, H. (1980) Hydrocalumit: Mischkristalle von "Friedelschem Salz" $3CaO{\cdot}Al_2O_3{\cdot}CaCl_2{\cdot}10H_2O$ und tetracalciumaluminathydrat $3CaO{\cdot}Al_2O_3{\cdot}Ca(OH)_2{\cdot}12H_2O$. *Neues Jahrbuch für Mineralogie Monatshefte*, **1980**, 322–334.

Flink, G. (1901) Mineralogische Notizen. *Bulletin of the Geological Institutions of the University of Uppsala*, **5**, 81–95.

Foshag, W.F. (1920) The chemical composition of hydrotalcite and the hydrotalcite minerals. *Proceedings of the United States National Museum*, **58**, 147–153.

Frondel, C. (1941) Constitution and polymorphism of the pyroaurite and sjögrenite groups. *American Mineralogist*, **26**, 295–316.

Génin, J.-M.R. and Ruby, C. (2008) Structure of some Fe^{II-III} hydroxysalt green rusts (carbonate, oxalate, methanoate) from Mössbauer spectroscopy. *Hyperfine Interactions*, **185**, 191–196.

Génin, J.-M.R., Bauer, Ph., Olowe, A.A. and Rézel, D. (1986) Mössbauer study of the kinetics of simulated corrosion process of iron in chlorinated aqueous solution around room temperature: the hyperfine structure of ferrous hydroxides and green rust I. *Hyperfine Interactions*, **29**, 1355–1360.

Génin, J.-M.R., Olowe, A.A., Refait, Ph. and Simon, L. (1996) On the stoichiometry and Pourbaix diagram of Fe(II)–Fe(III) hydroxysulphate or sulphate-containing green rust 2: An electrochemical and Mössbauer spectroscopy study. *Corrosion Science*, **38**, 1751–1762.

Génin, J.-M.R., Bourrié, G., Trolard, F., Abdelmoula, M., Jaffrezic, A., Refait, Ph., Maître, V., Humbert, B. and Herbillon, A.J. (1998) Thermodynamic equilibria in aqueous suspensions of synthetic and natural Fe^{II}–Fe^{III} green rusts: occurrences of the mineral in hydromorphic soils. *Environmental Science and Technology*, **32**, 1058–1068.

Génin, J.-M.R., Refait, Ph. and Abdelmoula, M. (2002) Green rusts and their relationship to iron corrosion; a key role in microbially influenced corrosion. *Hyperfine Interactions*, **139/140**, 119–131.

Génin, J.-M.R., Aïssa, R. Géhin, A., Abdelmoula, M., Benali, O., Ernstsen, V., Ona-Nguema, G., Upadhyay, C. and Ruby, C. (2005) Fougèrite and Fe^{II-III} hydroxycarbonate green rust; ordering, deprotonation and/or cation substitution; structure of hydrotalcite-like compounds and mythic ferrosic hydroxide $Fe(OH)_{(2+x)}$. *Solid State Science*, **7**, 545–572.

Génin, J.-M.R., Abdelmoula, M., Ruby, C. and Upadhyay, C. (2006*a*) Speciation of iron; characterisation and structure of green rusts and Fe^{II-III}

hydroxycarbonate fougerite. *Comptes Rendus Geosciences*, **338**, 402–419.

Génin, J.-M.R., Ruby, C., Géhin, A. and Refait, Ph. (2006*b*) Synthesis of green rusts by oxidation of $Fe(OH)_2$, their products of oxidation and reduction of ferric oxyhydroxides; E_h–pH Pourbaix diagrams. *Comptes Rendus Geosciences*, **338**, 433–446.

Génin, J.-M.R., Ruby, C. and Upadhyay, C. (2006*c*) Structure and thermodynamics of ferrous, stoichiometric and ferric oxyhydroxycarbonate green rusts; redox flexibility and fougerite mineral. *Solid State Science*, **8**, 1330–1343.

Génin, J.-M.R., Renard, A. and Ruby, C. (2008) Fougèrite Fe^{II-III} oxyhydroxycarbonate in environmental chemistry and nitrate reduction. *Hyperfine Interactions*, **186**, 31–37.

Génin, J.-M.R., Guérin, O., Herbillon, A.J., Kuzman, E., Mills, S.J., Morin, G., Ona-Nguema, G., Ruby, C. and Upadhyay, C. (2012*a*) Redox topotactic reactions in Fe^{II-III} (oxy)-hydroxycarbonate new minerals related to fougerite in gleysols; "trébeurdenite" and "mössbauerite". *Hyperfine Interactions*, **204**, 71–81.

Génin, J.-M.R., Mills, S.J., Christy, A.G., Guérin, O., Herbillon, A.J., Kuzman, E., Morin, G., Ona-Nguema, G., Ruby, C. and Upadhyay, C. (2012*b*) Mössbauerite, $Fe_6^{3+}O_4(OH)_8CO_3{\cdot}3H_2O$, the first fully oxidized 'green rust' mineral from Mont Saint-Michel Bay, France. *Mineralogical Magazine*, **76**, (in press).

Girard, A. and Chaudron, G. (1935) Sur la constitution de la rouille. *Comptes Rendus Académie des Sciences, Paris*, **200**, 127–129.

Goh, K.-H., Lim, T.-T. and Dong, Z. (2008) Application of layered double hydroxides for removal of oxyanions: a review. *Water Research*, **42**, 1343–1368.

Grguric, B.A., Madsen, I.C. and Pring, A. (2001) Woodallite, a new chromium analogue of iowaite from the Mount Keith nickel deposit, Western Australia. *Mineralogical Magazine*, **65**, 427–435.

Guinier, A., Bokij, G.B., Boll-Dornberger, K., Cowley, J.M., Durovič, S., Jagodzinski, H., Krishna, P., de Wolff, P.M., Zvyagin, B.B., Cox, D.E., Goodman, P., Hahn, Th., Kuchitsu, K. and Abrahams, S.C. (1984) Report of the International union of Crystallography ad hoc committee on the nomenclature of disordered, modulated and polytypic structures. *Acta Crystallographica*, **A40**, 399–404.

Hager, S.L., Leverett, P. and Williams, P.A. (2009) Possible structural and chemical relationships in the cyanotrichite group. *The Canadian Mineralogist*, **47**, 635–648.

Hansen, H.C.B. and Taylor, R.M. (1991) Formation of synthetic analogues of double metal-hydroxy carbonate minerals under controlled pH conditions. II. The synthesis of desautelsite. *Clay Minerals*, **26**, 507–525.

Hatert, F. and Burke, E.A.J. (2008) The IMA–CNMNC dominant-constituent rule revisited and extended. *The Canadian Mineralogist*, **46**, 717–728.

Hawthorne, F.C., Kimata, M. and Eby, R.K. (1993) The crystal structure of spangolite, a complex copper sulfate sheet mineral. *American Mineralogist*, **78**, 649–652.

Heddle, M.F. (1879) Geognosy and mineralogy of Scotland. *Mineralogical Magazine*, **2**, 106–133.

Henderson, D.M. and Gutowsky, H.S. (1962) A nuclear magnetic resonance determination of the hydrogen positions in $Ca(OH)_2$. *American Mineralogist*, **47**, 1231–1251.

Herbillon, A.J. (2006) Ferrosic hydroxides, green rusts and fougerite in the biogeochemical cycle of iron. *Comptes Rendus Geosciences*, **338**, 393–401.

Heyl, A.V., Milton, C. and Axelrod, J.M. (1959) Nickel minerals from near Linden, Iowa County, Wisconsin. *American Mineralogist*, **44**, 995–1009.

Hill, R.J. (1980) The crystal structure of mooreite. *Acta Crystallographica*, **B36**, 1304–1311.

Hochstetter, C. (1842) Untersuchung über die Zusammensetzung einiger Mineralien. *Journal für Praktische Chemie*, **27**, 375–378.

Hudson, D.R. and Bussel, M. (1981) Mountkeithite, a new pyroaurite-related mineral with an interlayer containing exchangeable $MgSO_4$. *Mineralogical Magazine*, **44**, 345–350.

Huminicki, D.M.C. and Hawthorne, F.C. (2003) The crystal structure of nikischerite, $NaFeAl_3(SO_4)_2(OH)_{18}(H_2O)_{12}$, a mineral of the shigaite group. *The Canadian Mineralogist*, **41**, 79–82.

Huminicki, D.M.C., Hawthorne, F.C., Grice, J.D., Roberts, A.C. and Jambor, J.L. (2003) Nikischerite, a new mineral from the Huanuni tin mine, Dalence Province, Oruro Department, Bolivia. *Mineralogical Record*, **34**, 155–158.

Igelström, L.J. (1865) Nya och sällsynta mineralier från Vermlands och Örebro län. *Öfversigt af Kongliga Vetenskaps-Akademiens Förhandlingar*, **16**, 399–400.

Ingram, L. and Taylor, H.F.W. (1967) The crystal structures of sjögrenite and pyroaurite. *Mineralogical Magazine*, **36**, 465–479.

Jambor, J.L. (1969*a*) Coalingite from the Muskox Intrusion, Northwest Territories. *American Mineralogist*, **54**, 437–447.

Jambor, J.L. (1969*b*) Muskoxite, a new hydrous magnesium-ferric iron hydroxide from the Muskox Intrusion, Northwest Territories, Canada. *American Mineralogist*, **54**, 684–696.

Jambor, J.L. and Boyle, R.W. (1964) A nickel hydroxide mineral from Rock Creek, British Columbia. *The Canadian Mineralogist*, **8**, 116–120.

Kameda, T. and Yoshioka, T. (2011) Hybrid inorganic/organic composites of layered double hydroxides intercalated with organic acid anions for the uptake of hazardous substances from aqueous solution. Pp. 123–148 in: *Metal, ceramic and polymeric composites for various uses* (J. Cuppoletti, editor). Intech, Croatia.

Kameda, T., Yoshioka, T., Mitsuhashi, T., Uchida, M. and Okuwaki, A. (2003) The simultaneous removal of calcium and chloride ions from calcium chloride solution using magnesium–aluminum oxide. *Water Research*, **37**, 4045–4050.

Kameda, T., Fubasami, Y. and Yoshioka, T. (2011*a*) Kinetics and equilibrium studies on the treatment of nitric acid with Mg–Al oxide obtained by thermal decomposition of NO_3^--intercalated Mg–Al layered double hydroxide. *Journal of Colloid and Interface Science*, **362**, 497–502.

Kameda, T., Uchiyama, N. and Yoshioka, T. (2011*b*) Removal of HCl, SO_2, and NO by treatment of acid gas with Mg–Al oxide slurry. *Chemosphere*, **82**, 587–591.

Kashaev, A.A., Feoktistov, G.D. and Petrova, S.V. (1982) Chlormagaluminite, $(Mg,Fe^{2+})_4Al_2(OH)_{12}(Cl,½CO_3)_2{\cdot}2H_2O$ – a new mineral of the manasseite–sjögrenite group. *Zapiski Rossiiskogo Mineralogicheskogo Obshchestva*, **111**, 121–127, [in Russian].

Kohls, D.W. and Rodda, J.L. (1967) Iowaite, a new hydrous magnesium hydroxide-ferric oxychloride from the Precambrian of Iowa. *American Mineralogist*, **52**, 1261–1271.

Kolitsch, U. and Giester, G. (2007) A preliminary determination of the crystal structure of cyanophyllite and revision of its chemical formula. *Mitteilungen der Österreichischen Mineralogischen Gesellschaft*, **153**, 66, [abstract].

Kolitsch, U., Giester, G. and Pippinger, T. (in press) The crystal structure of cualstibite-1*M* (formerly cyanophyllite), its revised chemical formula and its relation to cualstibite-1*T*. *Mineralogy and Petrology*.

Koritnig, S. and Süsse, P. (1975) Meixnerit, $Mg_6Al_2(OH)_{18}{\cdot}4H_2O$, ein neues Magnesium-Aluminium-Hydroxid-Mineral. *Tschermaks Mineralogische und Petrographische Mitteilungen*, **22**, 79–87.

Krivovichev, S.V., Yakovenchuk, V.N., Zhitova, E.S., Zolotarev, A.A., Pakhomovsky, Y.A. and Ivanyuk, G.Yu. (2010*a*) Crystal chemistry of natural layered double hydroxides. 1. Quintinite-2*H*-3*c* from the Kovdor alkaline massif, Kola peninsula, Russia. *Mineralogical Magazine*, **74**, 821–832.

Krivovichev, S.V., Yakovenchuk, V.N., Zhitova, E.S., Zolotarev, A.A., Pakhomovsky, Y.A. and Ivanyuk, G.Yu. (2010*b*) Crystal chemistry of natural layered double hydroxides. 2. Quintinite-1*M*. First evidence of a monoclinic polytype in M^{2+}–M^{3+} layered double hydroxides. *Mineralogical Magazine*, **74**, 833–840.

Krivovichev, S.V., Yakovenchuk, V.N., Zhitova, E.S., Zolotarev, A.A., Pakhomovsky, Y.A. and Ivanyuk, G.Yu. (2010*c*) Crystal chemistry of natural layered double hydroxides. 3. The crystal structure of Mg,Al-disordered quintinite-2*H*. *Mineralogical Magazine*, **74**, 841–848.

Lapham, D.M. (1965) A new nickeliferous magnesium hydroxide from Lancaster County, Pennsylvania. *American Mineralogist*, **50**, 1708–1716.

Lisitsina, N.A., Drits, V.A., Sokolova, G.V. and Aleksandrova, V.A. (1985) New complex secondary minerals – products of low temperature alteration of sedimentary rocks. *Litologia i Poleznie Iskopaemie*, **1985**, 20–38, [in Russian].

Loewenstein, W. (1954) The distribution of aluminum in the tetrahedra of silicates and aluminates. *American Mineralogist*, **39**, 92–96.

Lozano, R.P., Rossi, C., La Iglesia, A. and Matesanz, E. (2012) Zaccagnaite-3*R*, a new Zn-Al hydrotalcite polytype from El Soplao cave (Cantabria, Spain). *American Mineralogist*, **97**, 513–523.

Maksimović, Z. (1957) Takovite, hydrous nickel aluminate, a new mineral. *Zapisnici Srpskog geološkog društva*, **1955**, 219–224.

Maksimović, Z. (1958) An essay on the synthesis of nickel hydroaluminate and nickel hydrosilicate under normal conditions. *Bulletin of the Scientific Council of the Academy of Sciences of Yugoslavia*, **4**, 50 pp.

Maksimović, Z. (1959) The use of spectrochemical analysis for estimation of exchangable cations in clay minerals. *Bulletin Classe des Sciences Mathematiques et Natturalles*, **7**, 163–165.

Manasse, E. (1915) Rocce eritree e di Aden della collezione Issel. *Atti della Società Toscana di Scienze Naturali, Processi Verbali*, **24**, 92.

Matsubara, S., Kato, A. and Nagashima, K. (1984) Desautelsite from Konomori, Kochi City, Japan. *Bulletin of the National Science Museum*, **10**, 81–86.

Menezes, L.A.D. and Martins, J.M. (1984) The Jacupiranga mine, São Paulo, Brazil. *Mineralogical Record*, **15**, 261–270.

Merlino, S. and Orlandi, P. (2001) Carraraite and zaccagnaite, two new minerals from the Carrara marble quarries: their chemical compositions, physical properties and structural features. *American Mineralogist*, **86**, 1293–1301.

Meyn, M., Beneke, K. and Lagaly, G. (1990) Anion-exchange reactions of layered double hydroxides. *Inorganic Chemistry*, **29**, 5201–5207.

Mills, S.J., Hatert, F., Nickel, E.H. and Ferraris, G. (2009) The standardisation of mineral group hierarchies: application to recent nomenclature proposals. *European Journal of Mineralogy*, **21**,

1073–1080.

Mills, S.J., Whitfield, P.S., Wilson, S.A., Woodhouse, J.N., Dipple, G.M., Raudsepp, M. and Francis, C.A. (2011) The crystal structure of stichtite, re-examination of barbertonite and the nature of polytypism in MgCr hydrotalcites. *American Mineralogist*, **96**, 179–187.

Mills, S.J., Christy, A.G., Kampf, A.R., Housley, R.M., Favreau, G., Boulliard, J.-C. and Bourgoin, V. (2012*a*) Zincalstibite-9*R*: the first 9-layer polytype with the layered double hydroxide structure-type. *Mineralogical Magazine*, **76**, 1337–1345.

Mills, S.J., Kampf, A.R., Housely, R.M., Favreau, G., Pasero, M., Biagioni, C., Merlino, S., Berbain, C. and Orlandi, P. (2012*b*) Omsite, $(Ni,Cu)_2Fe^{3+}(OH)_6[Sb(OH)_6]$, a new member of the cualstibite group from Oms, France. *Mineralogical Magazine*, **76**, 1347–1354.

Mills, S.J., Whitfield, P.S., Kampf, A.R., Wilson, S.A., Dipple, G.M., Raudsepp, M. and Favreau, G. (2012*c*) Contribution to the crystallography of hydrotalcites: the crystal structure of woodallite and takovite. *Journal of Geosciences*, (in press).

Miyata, S. (1975) Synthesis of hydrotalcite-like compounds and their structures and physicochemical properties. I. The systems $Mg^{2+}–Al^{3+}–NO_3^-$, $Mg^{2+}–Al^{3+}–Cl^-$, $Mg^{2+}–Al^{3+}–ClO_4^-$, $Ni^{2+}–Al^{3+}–Cl^-$ and $Zn^{2+}–Al^{3+}–Cl^-$. *Clays and Clay Minerals*, **23**, 369–375.

Miyata, S. and Okada, A. (1977) Synthesis of hydrotalcite-like compounds and their physico-chemical properties – the systems $Mg^{2+}–Al^{3+}–SO_4^{2-}$ and $Mg^{2+}–Al^{3+}–CrO_4^{2-}$. *Clays and Clay Minerals*, **25**, 14–18.

Moore, P.B. (1971) Wermlandite, a new mineral from Långban, Sweden. *Lithos*, **4**, 213–217.

Morandi, N. and Dalrio, G. (1973) Jamborite: a new nickel hydroxide mineral from the northern Appenines, Italy. *American Mineralogist*, **58**, 835–839.

Mumpton, F.A., Jaffe, H.W. and Thompson, C.S. (1965) Coalingite, a new mineral from the New Idria serpentinite, Fresno and San Benito Counties, California. *American Mineralogist*, **50**, 1893–1913.

Newman, S.P. and Jones, W. (1998) Synthesis, characterization and applications of layered double hydroxides containing organic guests. *New Journal of Chemistry*, **22**, 105–115.

Nickel, E.H. (1976) New data on woodwardite. *Mineralogical Magazine*, **43**, 644–647.

Nickel, E.H. and Clarke, R.M. (1976) Carrboydite, a hydrated sulfate of nickel and aluminum: a new mineral from Western Australia. *American Mineralogist*, **61**, 366–372.

Nickel, E.H. and Grice, J.D. (1998) The IMA Commission on New Minerals and Mineral Names: procedures and guidelines on mineral nomenclature, 1998. *The Canadian Mineralogist*, **36**, 913–926.

Nickel, E.H. and Wildman, J.E. (1981) Hydrohonessite – a new hydrated Ni–Fe hydroxy-sulphate mineral; its relationship to honessite, carrboydite, and minerals of the pyroaurite group. *Mineralogical Magazine*, **44**, 333–337.

Ona-Nguema, G., Abdelmoula, M., Jorand, F., Benali, O., Géhin, A., Block, J.C. and Génin, J.-M.R. (2002) Iron (II,III) hydroxycarbonate green rust formation and stabilization from lepidocrocite bioreduction *Environmental Science and Technology*, **36**, 16–20.

Palache, C., Berman, H. and Frondel, C. (1951) *Dana's System of Mineralogy*, seventh edition. Wiley, New York.

Parise, J.B., Theroux, B., Li, R., Loveday, J.S., Marshall, W.G. and Klotz, S. (1998) Pressure dependence of hydrogen bonding in metal deuteroxides: a neutron powder diffraction study of $Mn(OD)_2$ and beta-$Co(OD)_2$. *Physics and Chemistry of Minerals*, **25**, 130–137.

Passaglia, E. and Sacerdoti, M. (1988) Hydrocalumite from Montalto di Castro, Viterbo, Italy. *Neues Jahrbuch für Mineralogie Monatshefte*, **1988**, 454–461.

Pastor-Rodriguez, J. and Taylor, H.F.W. (1971) Crystal structure of coalingite. *Mineralogical Magazine*, **38**, 286–294.

Pausch, I., Lohse, H.-H., Schürmann, K. and Allmann, R. (1986) Synthesis of disordered and Al-rich hydrotalcite-like compounds. *Clays and Clay Minerals*, **34**, 507–510.

Peacor, D.R., Dunn, P.J., Kato, A. and Wicks, F.J. (1985) Shigaite, a new manganese aluminum sulphate mineral from the Ioi mine, Shiga, Japan. *Neues Jahrbuch für Mineralogie Monatshefte*, **1985**, 453–457.

Pertlik, F. and Dunn, P.J. (1990) Crystal structure of alvanite, $(Zn,Ni)Al_4(VO_3)_2(OH)_{12}·2H_2O$, the first example of an unbranched zweier-single chain vanadate in nature. *Neues Jahrbuch für Mineralogie Monatshefte*, **1990**, 385–392.

Petterd, W.F. (1910) *Catalog of the minerals of Tasmania*. Mines Department Publication Hobart, Tasmania, Australia.

Piret, P. and Deliens, M. (1980) La comblainite, $(Ni_x^{2+}Co_{1-x}^{3+})(OH)_2(CO_3)_{(1-x)/2}·yH_2O$, noveau minéral du groupe de la pyroaurite. *Bulletin de Minéralogie*, **103**, 113–117.

Pollmann, H., Witzke, T. and Kohler, H. (1997) Kuzelite, $[Ca_4Al_2(OH)_{12}][(SO_4)·6H_2O]$, a new mineral from Maroldsweisach/Bavaria, Germany. *Neues Jahrbuch für Mineralogie Monatshefte*, **1997**, 423–432.

Raade, G., Elliott, C.J. and Din, V.K. (1985) New data on glaucocerinite. *Mineralogical Magazine*, **49**,

583–590.

Rad, U. (1974) Great Meteor and Josephine Seamounts (eastern North Atlantic): Composition and origin of bioclastic sands, carbonate and pyroclastic rocks. "Meteor" Forschungergebnisse I, **9**, 1–6.

Ramanaidou, E. and Noack, Y. (1987) Palagonites of the Red Sea: a new occurrence of hydroxysulphate. *Mineralogical Magazine*, **51**, 139–143.

Ramesh, T.N., Kamath, P.V. and Shivakumara, C. (2006) Classification of stacking faults and their stepwise elemination during the disorder → order transformation of nickel hydroxide. *Acta Crystallographica*, **B62**, 530–536.

Refait, Ph., Memet, J.B., Bon, C., Sabot, R. and Génin, J.-M.R. (2003) Formation of the Fe(II)–Fe(III) hydroxysulphate green rust during marine corrosion of steel. *Corrosion Science*, **45**, 833–845.

Richardson, M.C. and Braterman, P.S. (2007) Infrared spectra of oriented and nonoriented layered double hydroxides in the range from 4000 to 250 cm^{-1}, with evidence for regular short-range order in a synthetic magnesium-aluminum LDH with Mg:Al = 2:1 but not with Mg:Al = 3:1. *Journal of Physical Chemistry*, **C111**, 4209–4215.

Rius, J. and Allmann, R. (1984) The superstructure of the double layer mineral wermlandite $[Mg_7(Al_{0.57}Fe^{3+}_{0.43})_2(OH)_{18}]^{2+}[(Ca_{0.6}Mg_{0.4})(SO_4)_2(H_2O)_{12}]^{2-}$. *Zeitschrift für Kristallographie*, **168**, 133–144.

Rius, J. and Plana, F. (1986) Contribution to the superstructure resolution of the double layer mineral motukoreaite. *Neues Jahrbuch für Mineralogie Monatshefte*, **1986**, 263–272.

Rodgers, K.A., Chisholm, J.E., David, R.J. and Nelson, C.S. (1977) Motukoreaite, a new hydrated carbonate, sulphate, and hydroxide of Mg and Al from Auckland, New Zealand. *Mineralogical Magazine*, **41**, 389–390.

Rodionov, D., Klingelhöfer, G., Bernhardt, B., Schroder, C., Blumers, M., Kane, S., Trolard, F., Bourrié, G. and Génin, J.-M.R. (2006) Automated Mössbauer spectroscopy in the field and monitoring of fougerite. *Hyperfine Interactions*, **167**, 869–873.

Ross, G.J. and Kodama, H. (1967) Properties of a synthetic magnesium-aluminum carbonate hydroxide and its relationship to magnesium-aluminum double hydroxide, manasseite and hydrotalcite. *American Mineralogist*, **52**, 1036–1047.

Rouxhet, P.G. and Taylor, H.F.W. (1969) Thermal decomposition of sjögrenite and pyroaurite. *Chimia*, **23**, 480–485.

Ruby, C., Upadhyay, C., Géhin, A., Ona-Nguema, G. and Génin, J.-M.R. (2006) *In situ* redox flexibility of Fe^{II-III} oxyhydroxycarbonate green rust and fougerite. *Environmental Science and Technology*, **40**, 4696–4702.

Ruby, C., Abdelmoula, M., Naille, S., Renard, A., Khare, V., Ona-Nguema, G., Morin, G. and Génin, J.-M.R. (2010) Oxidation modes and thermodynamics of Fe^{II-III} oxyhydroxycarbonate green rust: dissolution-precipitation versus *in-situ* deprotonation. *Geochimica et Cosmochimica Acta*, **74**, 953–966.

Rusch, B., Génin, J.-M.R., Ruby, C., Abdelmoula, M. and Bonville, P. (2008) Ferrimagnetic properties in Fe^{II}–Fe^{III} (oxy)hydroxycarbonate green rusts. *Solid State Sciences*, **10**, 40–49.

Sacerdoti, M. and Passaglia, E. (1988) Hydrocalumite from Latium, Italy – its crystal structure and relationship with related synthetic phases. *Neues Jahrbuch für Mineralogie Monatshefte*, **1988**, 462–475.

Sideris, P.J., Nielsen, U.G., Gan, Z.H. and Grey, C.P. (2008) Mg/Al ordering in layered double hydroxides revealed by multinuclear NMR spectroscopy. *Science*, **321**, 113–117.

Simon, L., François, M., Refait, Ph., Renaudin, G., Lelaurain, M. and Génin, J.-M.R. (2003) Structure of the $Fe^{(II-III)}$ layered double hydroxysulphate green rust two from Rietveld analysis. *Solid State Sciences*, **5**, 327–334.

Sjögren, H. (1894) Contributions to Swedish Mineralogy. Part II. *Bulletin of the Geological Institutions of the University of Uppsala*, **2**, 39–74.

Smith, D.G.W. and Nickel, E.H. (2007) A system of codification for unnamed minerals: report of the subcommittee for unnamed minerals of the IMA Commission on New Minerals, Nomenclature and Classification. *The Canadian Mineralogist*, **45**, 983–1055.

Song, Y. and Moon, H.S. (1998) Additional data on reevesite and its Co-analogue, as a new member of the hydrotalcite group. *Clay Minerals*, **33**, 285–296.

Stanimirova, T. (2001) Hydrotalcite polytypes from Snarum, Norway. *Annual of the University of Sofia, Faculty of Geology*, **94**, 73–80.

Steeds, J.W. and Morniroli, J.P. (1992) Selected area electron diffraction (SAED) and convergent beam diffraction (CBED). Pp. 37–84 in: *Minerals and Reactions at the Atomic Scale: Transmission Electron Microscopy* (P.R. Buseck, editor). Reviews in Mineralogy, **27**. Mineralogical Society of America, Washington DC.

Tatarinov, A.V., Sapozhnikov, A.N., Prokudin, S. and Frolova, L.P. (1985) Stichtite in serpentinites of the Terekinsky Ridge (Gornyi Altai). *Zapiski Rossiiskogo Mineralogicheskogo Obshchestva*, **114**, 575–581, [in Russian].

Taylor, H.F.W. (1969) Segregation and cation-ordering in sjögrenite and pyroaurite. *Mineralogical Magazine*, **37**, 338–342.

Taylor, H.F.W. (1973) Crystal structures of some double

hydroxide minerals. *Mineralogical Magazine*, **39**, 377–389.

Taylor, R.M. (1980) Formation and properties of Fe(II) Fe(III) hydroxycarbonate and its possible significance in soil formation. *Clay Minerals*, **15**, 369–372.

Tilley, C.E., Megaw, H.D. and Hey, M.H. (1934) Hydrocalumite ($4CaO{\cdot}Al_2O_3{\cdot}12H_2O$). A new mineral from Scawt Hill, County Antrim. *Mineralogical Magazine*, **23**, 607–615.

Trolard, F., Génin, J.-M.R., Abdelmoula, M., Bourrié, G., Humbert, B. and Herbillon, A.J. (1997) Identification of a green rust mineral in a reductomorphic soil by Mössbauer and Raman spectroscopies. *Geochimica et Cosmochimica Acta*, **61**, 1107–1111.

Trolard, F., Bourrié, G., Abdelmoula, M., Refait, Ph. and Féder, F. (2007) Fougerite, a new mineral of the pyroaurite–iowaite group: description and crystal structure. *Clays and Clay Minerals*, **55**, 323–334.

Uvarova, Y.A., Sokolova, E., Hawthorne, F.C., Karpenko, V.V., Agakhanov, A. and Pautov, L.A. (2005) The crystal chemistry of the "nickelalumite"-group minerals. *The Canadian Mineralogist* **43**, 1511–1519.

Vysostskii, G.N. (1905) Gley. *Eurasian Soil Science (Pochvovedenie)*, **4**, 291–327.

Walenta, K. (1981) Cyanophyllit, ein neues Mineral aus der Grube Clara bei Oberwolfach im mittleren Schwarzwald. *Chemie der Erde*, **40**, 195–200.

Walenta, K. (1984) Cualstibit, ein neues Sekundärmineral aus der Grube Clara im mittleren Schwarzwald (BRD). *Chemie der Erde*, **43**, 255–260.

White, J.S. Jr, Henderson, E.P. and Mason, B. (1967) Secondary minerals produced by weathering of the Wolf Creek meteorite. *American Mineralogist*, **52**, 1190–1197.

Whitfield, P.S., Davidson, I.J., Mitchell, L.D., Wilson, S.A. and Mills, S.J. (2010) Problem solving with the *TOPAS* macro language: corrections and constraints in simulated annealing and Rietveld refinement. *Materials Science Forum*, **651**, 11–25.

Witzke, T. (1995) *Untersuchung natürlicher sulfathaltiger hybrider Schichtstrukturen: Charakterisierung, Systematik, Strukturmodellierung und Rietveld-Verfeinerung*. PhD Thesis, Martin-Luther-Universität Halle, Germany.

Witzke, T. (1999) Hydrowoodwardite, a new mineral of the hydrotalcite group from Königswalde near Annaberg, Saxony/Germany and other localities. *Neues Jahrbuch für Mineralogie Monatshefte*, **1999**, 75–86.

Witzke, T. and Raade, G. (2000) Zincowoodwardite, $[Zn_{1-x}Al_x(OH)_2][(SO_4)_{x/2}(H_2O)_n]$, a new mineral of the hydrotalcite group. *Neues Jahrbuch für Mineralogie Monatshefte*, **2000**, 455–465.

Witzke, T., Pöllmann, H. and Vogel, A. (1995) Struktur und Synthese von $[Zn_{8-x}AlOH)_{16}][(SO_4)_{X/2+Y/2}$ $Na_Y(H_2O)_6]$. *Zeitschrift für Kristallographie*, *Supplemental Issue*, **9**, 252.

Woodhouse, J.N. (2006) *The characterization of hydrotalcite-group minerals and their anion exchange capabilities at Mount Keith Nickel mine, Western Australia*. Unpublished BSc. Thesis, The University of British Columbia, Vancouver, Canada.

Wyckoff, R.W.G. (1963) *Crystal Structures*, second edition. Interscience Publishers, New York.

Zamarreño, I., Plana, F., Vasquez, A. and Clague, D.A. (1989) Motukoreaite: a common alteration product in submarine basalts. *American Mineralogist*, **74**, 1054–1058.

Zigan, F. and Rothbauer, R. (1967) Neutronenbeugungsmessungen am Brucit. *Neues Jahrbuch für Mineralogie Monatshefte*, **1967**, 137–143.

Eur. J. Mineral.
2010, **22**, 163–179
Published online March 2010

Nomenclature of the apatite supergroup minerals

MARCO PASERO[1,*] (Chairman), ANTHONY R. KAMPF[2] (Co-Chairman),
CRISTIANO FERRARIS[3], IGOR V. PEKOV[4], JOHN RAKOVAN[5] and TIMOTHY J. WHITE[6]

[1] Dipartimento di Scienze della Terra, Università di Pisa, Via S. Maria 53, 56126 Pisa, Italy
*Corresponding author, e-mail: pasero@dst.unipi.it
[2] Natural History Museum of Los Angeles County, 900 Exposition Blvd., Los Angeles, CA 90007, USA
[3] Muséum National d'Histoire Naturelle, UMR-CNRS 7202, LMCM, CP52, 61 rue Buffon, 75005 Paris, France
[4] Faculty of Geology, Moscow State University, Vorobievy Gory, 119992 Moscow, Russia
[5] Department of Geology, Miami University, 114 Shideler Hall, Oxford, OH 45056, USA
[6] Centre for Advanced Microscopy, Australian National University, GPO Box 475, Canberra, ACT 2601, Australia

Abstract: The apatite supergroup includes minerals with a generic chemical formula $^{IX}M1_2{}^{VII}M2_3(^{IV}TO_4)_3X$ ($Z = 2$); chemically they can be phosphates, arsenates, vanadates, silicates, and sulphates. The maximum space group symmetry is $P6_3/m$, but several members of the supergroup have a lower symmetry due to cation ordering and deviations from the ideal topology, which may result in an increase of the number of the independent sites. The apatite supergroup can be formally divided into five groups, based on crystal-chemical arguments: apatite group, hedyphane group, belovite group, britholite group, and ellestadite group. The abundance of distinct ions which may be hosted at the key-sites [M = Ca^{2+}, Pb^{2+}, Ba^{2+}, Sr^{2+}, Mn^{2+}, Na^{+}, Ce^{3+}, La^{3+}, Y^{3+}, Bi^{3+}; T = P^{5+}, As^{5+}, V^{5+}, Si^{4+}, S^{6+}, B^{3+}; X = F^{-}, $(OH)^{-}$, Cl^{-}] result in a large number of compositions which may have the status of distinct mineral species. Naming of apatite supergroup minerals in the past has resulted in nomenclature inconsistencies and problems. Therefore, an *ad hoc* IMA-CNMNC Subcommittee was established with the aim of rationalizing the nomenclature within the apatite supergroup and making some order among existing and potentially new mineral species. In addition to general recommendations for the handling of chemical (EPMA) data and for the allocation of ions within the various sites, the main recommendations of this subcommittee are the following:

1. Nomenclature changes to existing minerals. The use of adjectival prefixes for anions is to be preferred instead of modified Levinson suffixes; accordingly, six minerals should be renamed as follows: apatite-(CaF) to *fluorapatite*, apatite-(CaOH) to *hydroxylapatite*, apatite-(CaCl) to *chlorapatite*, ellestadite-(F) to *fluorellestadite*, ellestadite-(OH) to *hydroxylellestadite*, phosphohedyphane-(F) to *fluorphosphohedyphane*. For the apatite group species these changes return the names that have been used in thousands of scientific paper, treatises and museum catalogues over the last 150 years. The new mineral IMA 2008-009, approved without a name, is here named *stronadelphite*. Apatite-(SrOH) is renamed *fluorstrophite*. Deloneite-(Ce) is renamed *deloneite*. The new mineral IMA 2009-005 is approved with the name *fluorbritholite-(Y)*.

2. Potentially new mineral species. The following end-member compositions are eligible for status as distinct mineral species; the approved name, if any, is given in parentheses: $Ca_2Pb_3(AsO_4)_3(OH)$ (hydroxylhedyphane); $Ca_2Pb_3(PO_4)_3(OH)$ (hydroxylphosphohedyphane). $Ca_2Sr_3(PO_4)_3F$ (new root name); $Mn_2Ca_3(PO_4)_3Cl$ (new root name); $Pb_5(SiO_4)_{1.5}(SO_4)_{1.5}(OH)$ (hydroxylmattheddleite).

3. Minerals and mineral names which could be discredited. The mineral ellestadite-(Cl) is not thought to exist and should be discredited; the name melanocerite-(Ce) should be discontinued [= tritomite-(Ce)].

4. Changes of status from distinct species to polymorphic variants. Fermorite is the monoclinic polymorph of johnbaumite (= johnbaumite-*M*); clinohydroxylapatite is the monoclinic polymorph of hydroxylapatite (= hydroxylapatite-*M*); clinomimetite is the monoclinic polymorph of mimetite (= mimetite-*M*).

5. Recognition of a new polymorphic variant. A new monoclinic polymorph of apatite is recognized (chlorapatite-*M*).

6. Changes to end-member formulae. The ideal chemical formula of morelandite is $Ca_2Ba_3(AsO_4)_3Cl$ instead of $Ba_5(AsO_4)_3Cl$; the ideal chemical formula of deloneite is $(Na_{0.5}REE_{0.25}Ca_{0.25})$ $(Ca_{0.75}REE_{0.25})$ $Sr_{1.5}$ $(CaNa_{0.25}REE_{0.25})$ $(PO_4)_3$ $F_{0.5}(OH)_{0.5}$.

Key-words: nomenclature, apatite supergroup, apatite group, hedyphane group, belovite group, britholite group, ellestadite group.

1. Introduction

Apatite is a generic name, first introduced in the mineralogical literature by Werner (1786), and used to describe calcium phosphates with simplified formula $Ca_5(PO_4)_3X$ (X = F, Cl, OH). The name originates from the Greek $\alpha\pi\alpha\tau\acute{\alpha}\omega$, which means ''to deceive'', because the mineral was often mistaken for other species (Fig. 1). Since 1856–1860, these minerals

DOI: 10.1127/0935-1221/2010/0022-2022
0935-1221/10/0022-2022 $ 7.65

Fig. 1. Fluorapatite crystal exhibiting the common forms {001}, {100} and {101} on a matrix of albite and muscovite, from a granitic pegmatite in the Nagar area, Gilgit district, Northern Areas, Pakistan (Jeff Scovil photograph).

have been named fluorapatite, chlorapatite, and hydroxylapatite, depending on the dominant X^- anion. As the number of new species increased over the years, several comprehensive reviews on the crystal chemistry of the ''apatite group'' were published (*e.g.*, McConnell, 1938 and 1973; Nriagu & Moore, 1984; Elliott, 1994; Kohn *et al.*, 2002). Recently, in the context of a revision of the mineralogical nomenclature initiated by then chairman of the IMA Commission on New Minerals, Nomenclature and Classification E.A.J. Burke, and aimed at adopting, as far as possible, modified Levinson suffixes instead of adjectival prefixes such as ''fluor-'', ''chlor-'', and ''hydroxyl-'', the above minerals were renamed apatite-(CaF), apatite-(CaCl), and apatite-(CaOH), respectively (Burke, 2008). One of the rationales for that change was the benefit of having the names of these minerals appear consecutively in alphabetical listings and databases.

The changes introduced by Burke (2008) to the nomenclature of these and other minerals with the apatite structure, *e.g.* strontium-apatite and ''ellestadites'', did not fully consider the structural complexities of these minerals. The apatite structure type is flexible enough to allow a wide degree of substitutions among cations (*cf.* White & Dong, 2003; White *et al.*, 2005), and this fact, coupled with the possible lowering of symmetry related to ordering of cations and anions, dramatically increases the number of end-members which are potentially eligible as individual mineral species.

The recently approved nomenclature scheme of Burke (2008) could logically be extended to the renaming of other apatite group minerals, changing, *e.g.*, pyromorphite into apatite-(PbCl), or alforsite into apatite-(BaCl). And one could be tempted to include also the various tetrahedral cations (P, As, or V), into the extended suffix [*e.g.*, apatite-(PbAsCl) instead of mimetite, apatite-(CaAsOH) instead of johnbaumite]. The result would be mineral names that are more similar to chemical formulae. The limit of such an approach would be to adopt chemical formulae throughout, instead of mineral names. However, a nomenclature based extensively upon modified Levinson-style suffixes is likely to be rejected by the mineralogical community, since many would argue that multiple suffixes are difficult to be read, almost impossible to be spoken, not immediately self-explanatory, and unpleasant to the eye. Furthermore, such naming replaces many traditional names given to honour worthy individuals.

A specific example of a nomenclature problem resulting from ordering in the apatite structure is presented by the recently approved Sr end-member of apatite *lato sensu*, $Sr_5(PO_4)_3F$ (IMA 2008-009). While ''strontioapatite'' would have been an appropriate name for this species, a mineral with essentially the same name already exists, strontium-apatite [which has just been renamed apatite-(SrOH) after Burke (2008)]. Furthermore, the latter mineral has a cation-ordered structure, and it is actually F-dominant, with the ideal formula $SrCaSr_3(PO_4)_3F$ (Efimov *et al.*, 1962; Klevtsova, 1964; Pushcharovsky *et al.*, 1987); therefore, its renaming as apatite-(SrOH) is incorrect. To make the issue even more complicated, there is also another cation-ordered member along the join $Ca_5(PO_4)_3F \Leftrightarrow Sr_5(PO_4)_3F$, namely fluorcaphite, $SrCaCa_3(PO_4)_3F$.

For the above reasons the former chairman of the IMA CNMNC, E.A.J. Burke, asked us (MP & ARK) to convene a subcommittee to re-evaluate the nomenclature of minerals belonging to the ''apatite group'', to propose a new consistent nomenclature and to rationalize all existing mineral names in this group.

The ''apatite group'' traditionally includes phosphate, arsenate and vanadate minerals. Other minerals belonging to different chemical classes, namely silicates (*e.g.*, britholite), silicate-sulphates (*e.g.*, ellestadite), and sulphates (*e.g.*, cesanite) display the structural topology of apatite. In accordance with the newly approved standardisation of mineral group hierarchies (Mills *et al.*, 2009), all of these minerals can be included in the broader apatite supergroup. Because the same nomenclature questions are relevant for all members of the supergroup, they will all be considered in this report. All valid species within the apatite supergroup are listed in Table 1. Their ideal chemical formulae are also given, as they should appear in the official IMA List of Minerals. The minerals have here been divided into five groups on the basis of their crystallographic and/or chemical similarities. This report has been approved by the IMA Commission on New Minerals, Nomenclature and Classification.

2. Crystal-chemistry of apatite supergroup minerals

The archetype structure of apatite is hexagonal with space group $P6_3/m$ and unit-cell parameters $a = 9.3 - 9.6$, $c = 6.7 - 6.9$ Å. The generic crystal-chemical formula may be also written in its doubled form, which corresponds to the unit cell content, as follows: $^{IX}M1_4{}^{VII}M2_6(^{IV}TO_4)_6X_2$ ($Z = 1$),

Table 1. Existing names (after the IMA List of Minerals), approved names and end-member formulae for minerals within the apatite supergroup. The approved changes are set in bold. Names in quotes are the most appropriate names we would recommend for potential new minerals.

Existing name (IMA list of minerals)	Approved name (this subcommittee)	End-member formula
Apatite group		
Apatite-(CaF)	**Fluorapatite**	$Ca_5(PO_4)_3F$
Apatite-(CaCl)	**Chlorapatite**[a]	$Ca_5(PO_4)_3Cl$
—	**Chlorapatite-*M***[b]	$Ca_5(PO_4)_3Cl$
Apatite-(CaOH)	**Hydroxylapatite**[a]	$Ca_5(PO_4)_3OH$
Apatite-(CaOH)-*M*	**hydroxylapatite-*M***[b]	$Ca_5(PO_4)_3OH$
Svabite	Svabite	$Ca_5(AsO_4)_3F$
Turneaureite	Turneaureite	$Ca_5(AsO_4)_3Cl$
Johnbaumite	Johnbaumite[a]	$Ca_5(AsO_4)_3OH$
Fermorite	**Johnbaumite-*M***[b]	$Ca_5(AsO_4)_3OH$
2008-009[c]	**Stronadelphite**	$Sr_5(PO_4)_3F$
Pyromorphite	Pyromorphite	$Pb_5(PO_4)_3Cl$
Mimetite	Mimetite[a]	$Pb_5(AsO_4)_3Cl$
Clinomimetite	**Mimetite-*M***[b]	$Pb_5(AsO_4)_3Cl$
Alforsite	Alforsite	$Ba_5(PO_4)_3Cl$
Vanadinite	Vanadinite	$Pb_5(VO_4)_3Cl$
Hedyphane group		
Hedyphane	Hedyphane	$Ca_2Pb_3(AsO_4)_3Cl$
—	**"Hydroxylhedyphane"**[d]	$Ca_2Pb_3(AsO_4)_3OH$
Phosphohedyphane[e]	Phosphohedyphane	$Ca_2Pb_3(PO_4)_3Cl$
Phosphohedyphane-(F)	**Fluorphosphohedyphane**	$Ca_2Pb_3(PO_4)_3F$
—	**"Hydroxylphosphohedyphane"**[d]	$Ca_2Pb_3(PO_4)_3OH$
—	**New root name**[d]	$Ca_2Sr_3(PO_4)_3F$
Morelandite	Morelandite	$\mathbf{Ca_2Ba_3(AsO_4)_3Cl}$
—	**New root name**[d]	$Mn_2Ca_3(PO_4)_3Cl$
Cesanite	Cesanite	$Ca_2Na_3(SO_4)_3OH$
Caracolite	Caracolite	$Na_2(Pb_2Na)(SO_4)_3Cl$
Aiolosite	Aiolosite	$Na_2(Na_2Bi)(SO_4)_3Cl$
Belovite group		
Fluorcaphite	Fluorcaphite	$SrCaCa_3(PO_4)_3F$
Apatite-(SrOH)	**Fluorstrophite**	$SrCaSr_3(PO_4)_3F$[f]
Deloneite-(Ce)	**Deloneite**	$\mathbf{(Na_{0.5}\mathit{REE}_{0.25}Ca_{0.25})(Ca_{0.75}\mathit{REE}_{0.25})Sr_{1.5}}$ $\mathbf{(CaNa_{0.25}\mathit{REE}_{0.25})(PO_4)_3F_{0.5}(OH)_{0.5}}$
Belovite-(Ce)	Belovite-(Ce)	$NaCeSr_3(PO_4)_3F$
Belovite-(La)	Belovite-(La)	$NaLaSr_3(PO_4)_3F$
Kuannersuite-(Ce)	Kuannersuite-(Ce)	$NaCeBa_3(PO_4)_3F_{0.5}Cl_{0.5}$
Britholite group		
Britholite-(Ce)	Britholite-(Ce)	$(Ce,Ca)_5(SiO_4)_3OH$
Britholite-(Y)	Britholite-(Y)	$(Y,Ca)_5(SiO_4)_3OH$
Fluorbritholite-(Ce)	Fluorbritholite-(Ce)	$(Ce,Ca)_5(SiO_4)_3F$
2009-005[g]	**Fluorbritholite-(Y)**	$(Y,Ca)_5(SiO_4)_3F$
Fluorcalciobritholite	Fluorcalciobritholite	$(Ca,\mathit{REE})_5(SiO_4,PO_4)_3F$
Melanocerite-(Ce)	—[h]	
Tritomite-(Ce)	Tritomite-(Ce)	$Ce_5(SiO_4,BO_4)_3(OH,O)$
Tritomite-(Y)	Tritomite-(Y)	$Y_5(SiO_4,BO_4)_3(O,OH,F)$
Ellestadite group		
Ellestadite-(OH)	**Hydroxylellestadite**	$Ca_5(SiO_4)_{1.5}(SO_4)_{1.5}OH$
Ellestadite-(F)	**Fluorellestadite**	$Ca_5(SiO_4)_{1.5}(SO_4)_{1.5}F$
Ellestadite-(Cl)	—[i]	
Mattheddleite	Mattheddleite	$Pb_5(SiO_4)_{1.5}(SO_4)_{1.5}Cl$
—	**"Hydroxylmattheddleite"**[d]	$Pb_5(SiO_4)_{1.5}(SO_4)_{1.5}OH$

[a]Whenever necessary and convenient, the suffix *-H* could be used to denote the hexagonal polymorph.
[b]Name for the monoclinic polymorph. It should no longer be considered a distinct species.
[c]Mineral approved by the IMA CNMNC without a name.
[d]A potentially new mineral species.
[e]The change of the name into phosphohedyphane-(Cl) has been approved by the IMA CNMNC, but this is not yet of public domain. In the IMA List of Minerals the original name phosphohedyphane is still reported.
[f]There is a mistake in the IMA List of minerals. The mineral with ideal formula $Sr_5(PO_4)_3(OH)$ is named apatite-(SrOH) and is marked as Rn (renamed); the given reference is Burke (2008). Clearly, the above entry refers to the old strontium-apatite, which has the formula $SrCaSr_3(PO_4)_3F$, and was incorrectly renamed apatite-(SrOH) by Burke (2008), and not to the newly approved IMA 2008-009, which has the formula $Sr_5(PO_4)_3F$, and is the true strontium end-member (see text for more detail).
[g]Mineral and name approved by the IMA CNMNC; publication delayed.
[h]To be potentially discredited [= tritomite-(Ce)].
[i]To be discredited (a mineral with ideal end-member formula $Ca_5(SiO_4)_{1.5}(SO_4)_{1.5}Cl$ is assumed not to exist).

where the left superscripts indicate the ideal coordination numbers. In this report we will generally use the reduced formula with $Z = 2$, which is commonly adopted in the mineralogical literature. Despite the rather simple formula, with only four key sites (M1, M2, T, and X) besides those (O1, O2, and O3) which are known to be occupied by O^{2-} only, the number of distinct species based on cationic and anionic substitutions is quite large. This number increases further, because in some cases the M1 sites are split into pairs of non-equivalent sites with corresponding lowering of the space group symmetry. Concerning the coordination numbers, M1 has nine-fold (6 + 3) coordination with the innermost six ligands forming a polyhedron that is often referred to as a metaprism (White & Dong, 2003; Dong & White, 2004a and b; Mercier *et al.*, 2005). When the three more distant ligands are included, the M1 coordination polyhedron is often described as a tri-capped trigonal prism. The M2 site is considered to be seven-fold coordinated whenever Ca is the central cation; such a polyhedron can be described as a distorted pentagonal bipyramid (Dolivo-Dobrovolsky, 2006); in other cases, *e.g.*, when the site is occupied by Pb and/or the X site is occupied by Cl, the coordination of M2 sites may be more irregular and the central cation may be considered to be eight- or nine-fold coordinated. A drawing of the apatite structure-type is shown in Fig. 2. The relationships among ionic sites and multiplicity and Wyckoff positions in all known space groups of apatite supergroup minerals are shown in Table 2.

Species-forming M and T cations thus far known among minerals are: M = Ca^{2+}, Pb^{2+}, Ba^{2+}, Sr^{2+}, Mn^{2+}, Na^{+}, Ce^{3+}, La^{3+}, Y^{3+}, Bi^{3+}; T = P^{5+}, As^{5+}, V^{5+}, Si^{4+}, S^{6+}, B^{3+}. Species-forming substitutions at the X anionic site are limited to the monovalent anions F^{-}, Cl^{-}, and $(OH)^{-}$. This implies – for all minerals known thus far – a total of 50 negative charges per unit cell throughout [*i.e.*, 24 O^{2-} + 2 $(F, Cl, OH)^{-}$]. In addition, many studies of synthetic compounds with the apatite structure have demonstrated that the X site can be occupied by O^{2-} (which would increase the total negative charges) as well as vacancies and H_2O molecules (which would decrease the total negative charges), that the M site can be occupied by Cd, Co, K, and almost all *REE* and that the T site can be occupied by Be, Cr, Ge, and Mn^{5+}.

Even though in the present report we limit ourselves to natural compounds, the presence of M cations with charge 1+, 2+, and 3+, and of T cations with charge 4+, 5+, and 6+, implies a great number of possible combinations of different atoms, and thus of potentially different species.

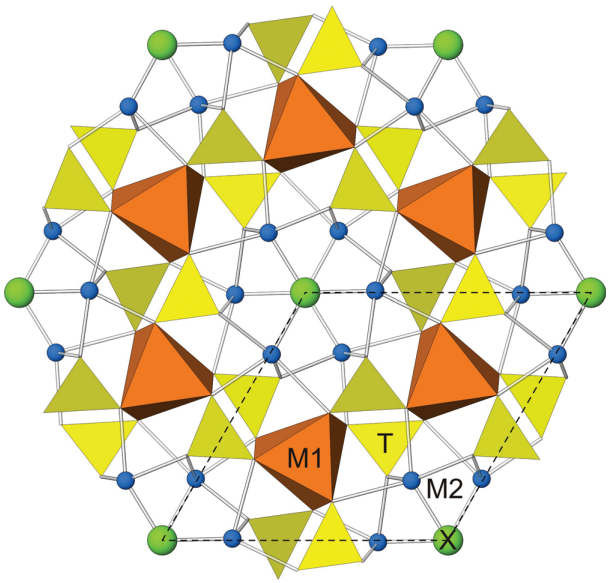

Fig. 2. The crystal structure of apatite, as seen along *c*. The unit cell is outlined. The M1-centred polyhedra are represented as six-fold coordinated metaprisms (the bonded O3 ligands are not included in this polyhedral representation). Two out of the seven bonds to M2 overlap in this projection, therefore only five are visible in the figure.

3. Minerals of the apatite supergroup: state of the art

The valid, IMA-accepted mineral species within the apatite supergroup can be divided into five groups. Although we are aware that different groupings could be chosen, *e.g.* based upon purely chemical grounds, we prefer for our purposes a subdivision based on a combination of crystallographic and chemical criteria. Our five groups are as follows:

(1) *Apatite group*: hexagonal and pseudo-hexagonal phosphates, arsenates, and vanadates containing the same prevailing (species-defining) cation at both the M1 and M2 sites.

(2) *Hedyphane group*: hexagonal and pseudo-hexagonal phosphates, arsenates and sulphates containing different prevailing (species-defining) cations at the M1 and M2 sites.

(3) *Belovite group*: hexagonal and trigonal phosphates with the M1 site split into the M1 and M1′ sites containing different prevailing (species-defining) cations.

(4) *Britholite group*: hexagonal and pseudo-hexagonal silicates, typically with partially ordered M1 and M2 cations.

(5) *Ellestadite group*: hexagonal and pseudo-hexagonal sulphato-silicates with the ideal ratio $(SiO_4)^{4-}$: $(SO_4)^{2-}$ = 1: 1.

3.1. Apatite group

3.1.1. Apatite-(CaF), apatite-(CaOH), apatite-(CaCl)

These three minerals have ideal formulas $Ca_5(PO_4)_3F$, $Ca_5(PO_4)_3OH$, and $Ca_5(PO_4)_3Cl$, respectively. They were formerly known as fluorapatite, hydroxylapatite, and chlorapatite and were recently renamed as apatite-(CaF), apatite-(CaOH), apatite-(CaCl) (Burke, 2008). The birth of the three distinct names to denote the F-, OH-, and Cl-dominant variants, and their distinction with respect to the original ‘‘apatite’’ *sensu lato* is uncertain, but is generally ascribed to Damour (1856) for ‘‘hydroxylapatite’’ and

Table 2. Structure site multiplicities and Wyckoff positions for all known space groups of apatite supergroup minerals.

Site	$P6_3/m$	$P6_3$	$P\bar{6}$	$P\bar{3}$	$P3$	$P2_1/m$	$P2_1$
M1	4*f*	2 × 2*b*	2*i*, 2*h*	2 × 2*d*	2 × 1*b*, 2 × 1*c*	4*f*	2 × 2*a*
M2	6*h*	6*c*	3*k*, 3*j*	6*g*	2 × 3*d*	2*a*, 2 × 2*e*	3 × 2*a*
T	6*h*	6*c*	3*k*, 3*j*	6*g*	2 × 3*d*	3 × 2*e*	3 × 2*a*
O	2 × 6*h*, 12*i*	4 × 6*c*	2 × 3*k*, 2 × 3*j*, 2 × 6*l*	4 × 6*g*	8 × 3*d*	6 × 2*e*, 3 × 4*f*	12 × 2*a*
X	2*a* or 2*b* or 4*e* (× 0.5)	2*a*	1*a*, 1*b* or 2*g*	1*a*, 1*b*	2 × 1*a*	2*a* or 2*e*	2*a*

Rammelsberg (1860) for ''fluorapatite'' and ''chlorapatite''. The crystal structure of ''apatite'' was first solved by Mehmel (1930) and Náray-Szabó (1930) in the space group $P6_3/m$, and typically all apatites crystallize in that space group. However, crystal structure refinement in lower symmetry space groups have been carried out on synthetic $Ca_5(PO_4)_3Cl$ (Mackie *et al.*, 1972), $Ca_5(PO_4)_3OH$ (Elliott *et al.*, 1973) and natural apatite-(CaCl) (Hughes *et al.*, 1990). This latter mineral, a monoclinic chlorapatite from Jackson Peak, Gunkock, Washington Co., Utah, USA is structurally identical (space group $P2_1/b$, with a doubled *b*-axis, and $\gamma \approx 120°$;) to apatite-(CaOH)-*M* (see below), of which it represents the Cl-dominant analogue.

3.1.2. Apatite-(CaOH)-M

The mineral was referred to as clinohydroxylapatite by Chakhmouradian & Medici (2006), and subsequently renamed apatite-(CaOH)-*M* (Burke, 2008). Its monoclinic symmetry (non standard space group $P2_1/b$, evidently chosen so as to maintain the typical axial setting of apatites) probably results from orientational ordering of $(OH)^-$ anions within [00*z*] anionic columns, with consequent doubling of the periodicity along [010]. The following unit-cell parameters are given: *a* 9.445(2), *b* 18.853(4) *c* 6.8783(6) Å, γ 120.00(2)°. All chemical analyses point to the ideal formula $Ca_5(PO_4)_3(OH)$. A coupled substitution of Ca^{2+} by Na^+ and of $(PO_4)^{3-}$ by $(SO_4)^{2-}$ has been reported. The formula of the most Na- and S-rich apatite-(CaOH)-*M* is ca. $(Ca_{4.4}Na_{0.6})(PO_4)_{2.4}(SO_4)_{0.6}(OH)$.

3.1.3. Svabite

Svabite, $Ca_5(AsO_4)_3F$, was first described by Sjögren (1892) from the Hartsigen mine, Värmland, Sweden. It is the arsenate analogue of apatite-(CaF). In the mineralogical literature svabite is commonly reported as hexagonal, $P6_3/m$. However, a crystal structure refinement of natural svabite is lacking. The structure of the synthetic analogue of svabite has been recently refined in the triclinic space group $P\bar{1}$ (Baikie *et al.*, 2007).

3.1.4. Johnbaumite

The hydroxyl analogue of svabite was observed as early as 1944 at the Franklin mine, New Jersey, USA, but was not formally described as a new mineral until 36 years later (Dunn *et al.*, 1980). Its chemical composition is not far from the end-member formula $Ca_5(AsO_4)_3(OH)$. Johnbaumite has the cell parameters *a* 9.70, *c* 6.93 Å. With the lack of a crystal structure refinement, the space group is speculated to be either $P6_3/m$ or $P6_3$. Because of its similarity to other related compounds, $P6_3/m$ is most likely the correct space group.

3.1.5. Turneaureite

This is the chlorine analogue of svabite, discovered at Långban, Sweden, Franklin, New Jersey, USA, and Balmat, New York, USA (Dunn *et al.*, 1985a). The chemical analysis for turneaureite from Långban, which is considered the type locality, yields the following formula: $(Ca_{4.88}Mn_{0.17}Pb_{0.02})(As_{2.44}P_{0.54})O_{12.04}Cl_{0.56}F_{0.40}$. Turneaureite has the cell parameters *a* 9.810, *c* 6.868 Å, and the space group $P6_3/m$ is inferred by analogy with the other members of the apatite group.

3.1.6. Fermorite

Fermorite was first described as a Sr-bearing calcium phosphate-arsenate, with hexagonal symmetry (Smith & Prior, 1911). The original chemical analysis by Smith & Prior (1911) carried out on a sample from the Sitapar manganese ore deposit (Chhindwara district, Madhya Pradesh state, India) yields the following chemical formula, conventionally recalculated on the basis of 13 total anions: $(Ca_{4.75}Sr_{0.58})(P_{1.70}As_{1.32})O_{12.74}F_{0.26}$. This formula has an excess of M cations, very low fluorine, and P > As. The anion content is a bit problematic. H_2O was analytically determined and is given as ''trace'' in the chemical analysis, and it is explicitly stated that no chlorine was detected in the mineral. If the above figures are correct, the analysis would indicate an ''oxy-apatite'', *i.e.* a mineral with O^{2-} as the dominant anion at the X site. A more recent chemical analysis (electron microprobe data) by Hughes & Drexler (1991), carried out on the type material, gave the formula: $(Ca_{4.21}Sr_{0.80})(As_{1.48}P_{1.45})O_{12}(OH_{0.65}F_{0.35})$, with the hydroxyl content calculated by difference. There is a slight dominance of As over P. A crystal structure analysis showed the mineral to have monoclinic symmetry (space group $P2_1/m$, *a* 9.594, *b* 6.975, *c* 9.597 Å, β 119.97°; Hughes & Drexler, 1991) and provided clear evidence that $(OH)^-$ and not O^{2-} is the dominant anion at the X site; therefore, fermorite should be considered the monoclinic polymorph of johnbaumite. The deviations from the hexagonal symmetry are admittedly small, given ''the three non equivalent monoclinic tetrahedral sites are similar in their chemical composition and bond lengths'' (Hughes & Drexler, 1991).

3.1.7. IMA 2008-009

A Sr-dominant analogue of apatite-(CaF), close to the Sr end-member of the series $Ca_5(PO_4)_3F$ – $Sr_5(PO_4)_3F$, with space group $P6_3/m$, was studied in detail by Pekov *et al.* (Pekov, pers. comm.) and recently approved by the CNMNC (IMA 2008-009) without a name.

As mentioned above, the existence of the ordered (on M1 and M1′) Sr-Ca apatite mineral with formula $SrCaSr_3(PO_4)_3F$ bearing the original name strontium-apatite makes the choice of a name for the new Sr apatite with formula $Sr_5(PO_4)_3F$ problematic.

3.1.8. Pyromorphite

Pyromorphite is the lead phosphate, with ideal formula $Pb_5(PO_4)_3Cl$, widespread in nature. The mineral was named by Hausmann (1813). A crystal structure refinement of pyromorphite was carried out in the space group $P6_3/m$ by Dai & Hughes (1989). In pyromorphite, the dominant X anion is typically chlorine. This may be related to the presence of lead as the dominant cation at both the M1 and M2 sites, which results in larger unit-cell dimensions and makes chlorine (whose ionic radius is markedly greater than those of fluorine and hydroxyl) the best candidate to occupy the X site. Similar reasons are also valid for alforsite, the barium-dominant member of the apatite group (see below).

Stalder & Rozendaal (2002) presented EPMA data of a mineral from the Gamsberg Pb-Zn deposit, Namaqua province, South Africa. It is described as a ''calcian pyromorphite'', but has a very low Cl + F content (and presumably ordering of Ca and Pb in the M1 and M2 sites, respectively).

3.1.9. Mimetite

Mimetite is the lead arsenate, with ideal formula $Pb_5(AsO_4)_3Cl$. The mineral was named by von Haidinger (1845). The crystal structure of mimetite was solved in the space group $P6_3/m$ by Sokolova *et al.* (1982) and refined by Dai *et al.* (1991). In the structure of mimetite, the special position of chlorine at (0, 0, ½) results in two equidistant Cl ions around Pb (M2 site) and in an eightfold coordination for the cation.

3.1.10. Clinomimetite

Clinomimetite is the monoclinic polymorph of mimetite. It was formally described as a mineral species by Dai *et al.* (1991), although it was already known as both a synthetic and natural phase. It crystallizes in the space group $P2_1/b$, with *a* 10.189(3) *b* 20.372(8), *c* 7.456 (1) Å, γ 119.88(3)°. Unit-cell parameters and space group are consistent with those of the other accepted apatite group mineral with monoclinic symmetry, apatite-(CaOH)-*M*.

3.1.11. Alforsite

Alforsite was described as the barium analogue of ''apatite'' (Newberry *et al.*, 1981). The single crystal X-ray diffraction study was carried out on synthetic material: long-exposure Weissenberg and precession photographs indicated the $P6_3/m$ space group and did not reveal any superstructure reflections. All known chemical analyses of alforsite point to the ideal end-member formula $Ba_5(PO_4)_3Cl$.

3.1.12. Vanadinite

Vanadinite, ideally $Pb_5(VO_4)Cl$, is the only vanadium-dominant member of the apatite group. Known for more than two centuries (the type locality is Zimapán, Hidalgo, Mexico), it was first given its present name by von Kobell (1838). Crystal structure studies for vanadinite have been published, all in the space group $P6_3/m$, by Trotter & Barnes (1958), Dai & Hughes (1989), and Laufek *et al.* (2006).

3.2. Hedyphane group

3.2.1. Hedyphane

Hedyphane was originally described from Långban, Sweden (Breithaupt, 1830). Another important occurrence for the mineral is the Franklin mine, New Jersey, USA (Foshag & Gage, 1925). Rouse *et al.* (1984) carried out a careful crystal-chemical study of hedyphane from both occurrences, which showed that Ca and Pb are ordered at M1 and M2, respectively This led to the redefinition of the ideal formula of the mineral as $Ca_2Pb_3(AsO_4)_3Cl$. Shortly thereafter, Dunn *et al.* (1985b) described another halogen-deficient hedyphane sample from the type locality, which contained 0.34 wt. H_2O (determined by Penfield method). The empirical formula of that sample is $(Ca_{1.69}Ba_{0.28})Pb_{3.01}(As_{2.69}P_{0.20}Si_{0.15})O_{12}[(OH)_{0.44}Cl_{0.42}F_{0.12}O_{0.02}]$. Although very close to the compositional boundary, and despite some analytical uncertainties, *e.g.* the somewhat high total of T cations, this mineral has OH > Cl and should, therefore, be considered a separate species, the hydroxyl analogue of hedyphane.

3.2.2. Phosphohedyphane

The new mineral was described by Kampf *et al.* (2006) from the Capitana mine, Atacama Province, Chile. New EDS analyses on numerous samples from world-wide localities and examination of earlier reported analyses for ''calcium-rich pyromorphite'' revealed that phosphohedyphane occurs at numerous other localities. The ideal end-member formula is $Ca_2Pb_3(PO_4)_3Cl$. Single crystal X-ray diffraction data confirmed that Ca and Pb are ordered at the M1 and M2 sites, respectively. The mineral was approved with the name phosphohedyphane, and then changed into phosphohedyphane-(Cl) after the discovery of phosphohedyphane-(F) (see below) and the concurrent recognition of ''phosphohedyphane'' as a series name. This change has been approved by IMA, but is not yet of public domain, since the publication of the paper with the description of phosphohedyphane-(F) is being delayed pending the outcome of this report.

3.2.3. Phosphohedyphane-(F)

The F-dominant analogue of phosphohedyphane from the Blue Bell claims, San Bernardino County, California, USA

was recently approved by the CNMNC (IMA 2008-068; Kampf & Housley, 2008). Chemical analysis showed the X site to be entirely occupied by F and structure analysis confirmed the ordering of Ca and Pb as well as the shorter Pb–F bonds of 2.867 Å in contrast with the Pb–Cl bond lengths of 3.068 Å in phosphohedyphane-(Cl).

3.2.4. Morelandite

This mineral is a bit problematic, because of the unknown partitioning of cations among the M1 and M2 sites. First described by Dunn & Rouse (1978), the original chemical analysis yields the formula $(Ba_{2.25}Ca_{1.65}Pb_{1.16}Fe_{0.06}Mn_{0.06})[(AsO_4)_{2.56}(PO_4)_{0.30}]Cl_{1.09}$.

In that paper, as well as in the IMA list of minerals, the ideal formula is given as $Ba_5(AsO_4)_3Cl$, but this would imply that barium is the dominant cation at both the M1 and M2 sites, which is impossible given the above stoichiometric ratios and the characteristics of the apatite structure. Assuming that the space group is $P6_3/m$, the most likely ideal formula is $Ca_2Ba_3(AsO_4)_3Cl$, resulting from a cation allocation as described in § 4.1. (see below).

3.2.5. Mn-rich apatite

Pieczka (2007) recently described a sample of ''Mn-rich apatite'' from the Szklary granitic pegmatite, Lower Silesia, Poland, which has the highest manganese content ever reported for an apatite (31.5 wt%, corresponding to 2.43 apfu). The chemical formula provided for that sample is $(Mn_{2.43}Ca_{2.29}Fe^{2+}_{0.23}Mg_{0.04}Na_{0.01})(PO_4)_{3.00}(Cl_{0.48}F_{0.32}OH_{0.20})$. In the absence of a structural study, this potentially new mineral species is tentatively included in the hedyphane group, under the assumption that Ca and Mn are ordered between the two M sites. This assumption is based on several studies that show a marked preference for the M1 site by Mn^{2+} in Mn-rich apatites (Suitch *et al.*, 1985; Hughes *et al.*, 2004). Mn^{5+} has also been identified in apatite, substituting for P on the T site, however at very low concentrations (Johnson *et al.*, 1963; Dardenne *et al.*, 1999; Hughes *et al.*, 2004).

3.2.6. Cesanite

First described by Cavarretta *et al.* (1981) and named after the type locality (the Cesano geothermal field, Latium, Italy), cesanite is a sulphate with the apatite structure. It is related to apatite by the coupled heterovalent substitution $Na_1(SO_4)_1Ca_{-1}(PO_4)_{-1}$. The only available chemical analysis points to the empirical formula $(Na_{3.42}Ca_{1.53}Sr_{0.03}K_{0.02})S_{2.99}O_{12}[(OH)_{0.44}F_{0.06}Cl_{0.06}(H_2O)_{0.44}]$. Cavarretta *et al.* (1981) proposed revision of the general formula of apatites to allow substantial incorporation of H_2O at the X anionic sites in order to allow for the reduced positive charge associated with cations, due to the presence of Na^+ as a major element. An initial crystal structure refinement was carried out in the space group $P6_3/m$ by Tazzoli (1983), and seemed to support this proposal, resulting in the structural formula $(Na_{3.51}Ca_{1.49})S_3O_{12}[(OH)_{0.49}(H_2O)_{0.45}]$. A more recent refinement of both natural and synthetic cesanite was carried out in the space group $P\bar{6}$ (Piotrowski *et al.*, 2002). In this latter space group, each of the M1 and M2 sites are split into two because of the lower symmetry. The refinement in $P\bar{6}$ determined Ca > Na at the M1′ site only (Wyckoff 3*j*), whereas M1″, M2′ and M2″ (Wyckoff 3*k*, 2*h*, and 2*l*, respectively) have Na > Ca. The resulting formula is similar to that obtained by Tazzoli (1983), and requires that the X site is occupied in equal parts by hydroxyls and water molecules $Na_4(Na_3Ca_3)(SO_4)_6(OH)(H_2O)$.

3.2.7. Caracolite

The mineral was first described by Websky (1886). According to a crystal structure refinement (Schneider, 1967), the ideal formula of caracolite is $Na_3Pb_2(SO_4)_3Cl$. However, the distribution of M cations in the basic $P6_3/m$ structure type is as follows: $4Na^+$ in the M1 site, $4Pb^{2+} + 2Na^+$ in the M2 site, yielding the formula $Na_2(Pb_2Na)(SO_4)_3Cl$. A second refinement carried out in the monoclinic $P2_1/m$ space group is characterized by the ordering of Pb (eight atoms per unit cell: $4 \times 2e$) and Na (12 atoms per unit cell: $2 \times 4f + 2 \times 2e$) and the concurrent doubling of the *a*-axis (Schneider, 1969).

3.2.8. Aiolosite

Aiolosite was recently approved as a new mineral from Vulcano, Aeolian Islands, Italy (Demartin *et al.*, 2010). Its ideal formula is $Na_2(Na_2Bi)(SO_4)_3Cl$. Aiolosite crystallizes in the space group $P6_3/m$, with *a* 9.626, *c* 6.880 Å. Similarly to caracolite, Na enters the M1 site, whereas Na and Bi occupy the M2 site.

3.3. Belovite group

3.3.1. Fluorcaphite

Fluorcaphite was originally described from Mt. Koashva, Khibiny, Kola peninsula, Russia (Khomyakov *et al.*, 1997). A crystal structure analysis carried out in the space group $P6_3$ (Rastsvetaeva & Khomyakov, 1996a) points to the formula $(Sr_{0.52}Na_{0.32})\ Ca(Ca_{2.16}Sr_{0.64}LREE_{0.33})(P_{2.96}Si_{0.06})O_{12}F_{0.66}(OH)_{0.34}$, ideally $SrCaCa_3(PO_4)_3F$.

More recently, Chakhmouradian *et al.* (2005) described a second occurrence of '' fluorcaphite'' from Lovozero, Kola peninsula, Russia. Their refinement, again in space group $P6_3$, provided the structural formula $(Ca_{0.48}Na_{0.29}Sr_{0.12}Ce_{0.11}La_{0.05})(Ca_{0.58}Na_{0.29}Ce_{0.11}Nd_{0.02})(Sr_{1.48}Ca_{1.39}La_{0.13})(PO_4)_3F$. Moreover, they also performed a further refinement for a ''fluorcaphite'' sample from Khibiny for comparative purposes, yielding $(Ca_{0.59}Sr_{0.21}Na_{0.19}La_{0.01})(Ca_{0.88}Ce_{0.07}Pr_{0.04}Nd_{0.01})(Ca_{1.83}Sr_{0.84}La_{0.16}\ Ce_{0.12}Nd_{0.05})(PO_4)_3F$.

Neither of these formulae match the presently accepted formula for fluorcaphite. The ideal composition of the crystal from Lovozero is $CaCaSr_3(PO_4)_3F$ (a potentially new end-member), that of the crystal from Khibiny is $CaCaCa_3(PO_4)_3F$ (chemically a fluorapatite in which the symmetry is lowered due to selected occupancy by subordinate cations).

3.3.2. Apatite-(SrOH)

The mineral was first described from the Inagli alkaline complex, South Yakutia, Siberia, Russia. The given name was strontium-apatite. Initially, it was considered to be the Sr-dominant analogue of fluorapatite, with the simplified formula $(Sr,Ca)_5(PO_4)_3(F,OH)$, and this was the rationale for its name (Efimov *et al.*, 1962). However, a structural study of the holotype specimen demonstrated its cation-ordered structure and, consequently, the space group symmetry $P6_3$ (Klevtsova, 1964). In strontium-apatite, the M1 site, of multiplicity 4 in space group $P6_3/m$, is transformed into two sites, M1 and M1′, each of multiplicity 2. The M1 site is mainly occupied by Sr and the M1′ site is mostly occupied by Ca; in the M2 site, Sr prevails over Ca. The crystal-chemical formula of the holotype specimen of strontium-apatite is $^{M1}[(Sr,Ba)]^{M1'}[Ca]^{M2}[Sr,Ca,\mathit{REE},Na]_3(PO_4)_3(F,OH)$.

Later, the crystal structure of strontium-apatite from Mt. Rasvumchorr, Khibiny, was studied. The same space group $P6_3$ and the same type of cation arrangement were found. The crystal-chemical formula of this latter sample is $^{M1}[Sr_{0.75}Ca_{0.25}]^{M1'}[Ca_{0.7}Sr_{0.3}]^{M2}[Sr_{2.6}Ca_{0.4}](PO_4)_3F$ (Pushcharovsky *et al.*, 1987). Thus, the idealized (end-member) formula of the mineral is $SrCaSr_3(PO_4)_3F$.

Recently, the mineral was renamed apatite-(SrOH) (Burke, 2008). However, the name should have been changed to apatite-(SrF) given that fluorine is the dominant X^- anion.

3.3.3. Belovite-(Ce), belovite-(La)

Belovites have the ideal formula $Na\mathit{REE}Sr_3(PO_4)_3F$. Belovite-(Ce) was first described from Mt. Malyi Punkaruaiv, Lovozero, Kola Peninsula, Russia, with formula $(Sr,Ce,Na,Ca)_5(P_3O_{12})(OH,O)$ (Borodin & Kazakova, 1954). Fluorine was not determined in this sample. Klevtsova & Borisov (1964) studied its structure and found ordering of Sr, Na and *REE* and space group $P\bar{3}$. Nadezhina *et al.* (1987) studied the structure of belovite-(Ce) from Mt. Karnasurt, Lovozero, confirmed the model found by Klevtsova & Borisov (1964) with space group $P\bar{3}$, and suggested the idealized formula $NaCeSr_3(P_3O_{12})OH$ (despite the fact that $F > 0.5$ *apfu*). The results of a detailed study of belovite-(Ce) from different localities, including the reinvestigation of the holotype from Mt. Malyi Pukaruaiv, Lovozero, established its idealized end-member formula as $NaCeSr_3(PO_4)_3F$ and confirmed the space group $P\bar{3}$ (Pekov *et al.*, 1995). These results were confirmed by Rakovan & Hughes (2000). Belovite-(La) was described as a new species by Pekov *et al.* (1996) from Mounts Kukisvumchorr and Eveslogchorr, Khibiny, Russia. A structural study of a crystal from the type specimen (Kabalov *et al.*, 1997) showed that belovite-(La) is isostructural with belovite-(Ce).

In belovites, Sr substitutes for Ca in the M2 site, and Na + *REE* substitute for Ca in the M1 site. The strict ordering of Na and *REE* at the M1 site lowers the symmetry from $P6_3/m$ to $P\bar{3}$. In this latter space group there are two independent sites (M1 and M1′, occupied by *REE* and Na, respectively) which correspond to the unique M1 site in the archetype apatite structure. Another consequence of the reduced space group symmetry is the splitting of O3 sites into a pair of non-equivalent sites (O3 and O4). These atoms represent the capping anions in the tri-capped trigonal prism coordination around M1 and M1′ sites. The M1-O3 and M1′-O4 distances (which are equivalent in the $P6_3/m$ structure) are markedly different in the $P\bar{3}$ structure, and reflect the different occupancy by *REE* and Na. Therefore the reduced symmetry results not only in the selected occupancy of M1 and M1′ sites by *REE* and Na, but also in a significant variation in the dimensions of the corresponding coordination polyhedra.

3.3.4. Kuannersuite-(Ce)

Kuannersuite-(Ce) is the Ba analogue of belovite-(Ce). As in belovite-(Ce), the ordering of *REE* and Na in kuannersuite-(Ce) lowers the symmetry from $P6_3/m$ to $P\bar{3}$; however, there is another difference. F and Cl are ordered at distinct anionic sites ($F_{1.00}$ and $Cl_{0.59}F_{0.41}$, respectively). Consequently, the ideal formula should be written (in its doubled form with $Z = 1$) as $Ce_2Na_2Ba_6(PO_4)_6FCl$ (Friis *et al.*, 2004).

3.3.5. Deloneite-(Ce)

Deloneite-(Ce) was described as a new mineral from Mt. Koashva, Khibiny, in syntactic intergrowths with fluorcaphite and belovite-(Ce). Its simplified formula was given as $NaCa_2SrCe(PO_4)_3F$ (Khomyakov *et al.*, 1996); however, this formula reflects only the rough cation ratios and not the cation arrangement. According to Rastsvetaeva & Khomyakov (1996b), deloneite-(Ce), with space group $P3$, is the most cation-ordered apatite-like mineral. In its structure, which is a derivative of the belovite structure type, the M1 and M1′ sites are split into two pairs: (1) $M1^1$ and $M1^2$, and (2) $M1'^1$ and $M1'^2$, respectively. Unlike other apatite group members, the M2 and T sites are also split into corresponding pairs: (1) M2 and M2′, and (2) T and T′. The X site is also split, similar to kuannersuite-(Ce), into X and X′. The crystal-chemical formula of the mineral based on 26 total anions is thus $^{M11}[Na_{0.5}\mathit{REE}_{0.3}Ca_{0.2}]\ ^{M12}[Na_{0.5}\mathit{REE}_{0.25}Ca_{0.25}]\ ^{M1'1}[Ca_{0.7}\mathit{REE}_{0.3}]\ ^{M1'2}[Ca_{0.7}\mathit{REE}_{0.3}]\ ^{M2}[Sr_{2.3}Ca_{0.7}]^{M2'}\ [Ca_{1.0}Na_{1.0}\mathit{REE}_{1.0}]\ ^{T}[P_3]^{T'}[(P,Si)_3]O_{24}\ ^{X}[F]\ ^{X'}[(OH),F]$ (Rastsvetaeva & Khomyakov, 1996b).The simplified form of this formula is $^{M1}[Na,\mathit{REE},Ca]_2^{M1'}\ [Ca,\mathit{REE}]_2\ ^{M2}[Sr,Ca]_3^{M2'}[Ca,Na,\mathit{REE}]_3(P_6O_{24})\ ^{X}[F]^{X'}\ [OH]$, or $(Na,\mathit{REE},Ca)_2\ (Ca,\mathit{REE})_2Sr_3(Ca,Na,\mathit{REE})_3(PO_4)_6F(OH)$.

The crystal-chemical formula shows that no sites exist with *REE* prevailing over other cations; therefore, the -(Ce) suffix is incorrect and the mineral should be renamed deloneite.

3.4. Britholite group

3.4.1. Britholite-(Ce)

Britholite-(Ce) was first described from Ilimaussaq complex, Narsaq, Kitaa, West Greenland, by Winther (1901). Its formula is $(\mathit{REE},Ca)_5[(Si,P)O_4]_3(OH,F)$ or, in simplified form, $(Ce,Ca)_5(SiO_4)_3(OH)$, or, assuming cation

ordering, $(Ce_3Ca_2)(SiO_4)_3(OH)$. This mineral is typically Th-bearing and metamict. Some crystalline samples are hexagonal with space group $P6_3/m$ or $P6_3$ (Gay, 1957; Kalsbeek *et al.*, 1990; Genkina *et al.*, 1991; Noe *et al.*, 1993), or monoclinic pseudo-hexagonal with space group $P2_1$ (Noe *et al.*, 1993). *REE* prevail over Ca generally, but the M cations can be disordered or partially ordered in the M1 and M2 sites. For instance, structurally studied samples demonstrate two major types of cation arrangements, $(REE,Ca)_2(REE,Ca)_3[(Si,P)O_4]_3(OH,F)$ (Genkina *et al.*, 1991; Noe *et al.*, 1993) or $(Ca,REE)_2(REE,Ca)_3[(Si,P)O_4]_3(OH,F)$ (Noe *et al.*, 1993).

3.4.2. *Britholite-(Y)*

Britholite with a predominance of Y among the M cations and OH > F was first described under the name abukumalite by Hata (1938) from the Suishoyama pegmatite, Abukuma massif, Fukushima Prefecture, Japan. Later, it was reinvestigated in detail by Omori & Hasegawa (1953) who confirmed the predominance of Y among the M cations and of OH over F. Then, abukumalite was renamed britholite-(Y) as part of the general changes in the nomenclature of rare-earth minerals (Levinson, 1966). Although the mineral is typically metamict, studies of crystal structures of rare crystalline samples show monoclinic pseudo-hexagonal symmetry with space group $P2_1$ and partial cation ordering at the M1 and M2 sites (Zhang *et al.*, 1992; Noe *et al.*, 1993). The simplified formula can be presented as $(Y,Ca,Ln)_5[(Si,P)O_4]_3(OH)$ or, considering the cation ordering, as $(Y_3Ca_2)(SiO_4)_3(OH)$.

3.4.3. *Fluorbritholite-(Ce)*

Fluorbritholite-(Ce) was described as a new mineral from Mont Saint-Hilaire, Québec, Canada (Gu *et al.*, 1994). It is considered the F-dominant analogue of britholite-(Ce). In the original paper, Gu *et al.* (1994) proposed the concurrent renaming of britholite-(Ce) and britholite-(Y) into hydroxylbritholite-(Ce) and hydroxylbritholite-(Y), respectively. The proposal has been ignored; however, it must be observed that a number of chemical analyses of minerals referred to as ''britholites'' actually have F > OH (*e.g.*, Oberti *et al.*, 2001) and, therefore, should be considered ''fluorbritholites''.

3.4.4. *IMA 2009-005*

The F-dominant analogue of britholite-(Y) was studied recently in detail by Pekov *et al.* (Pekov, pers. comm.) and a proposal for its approval as a new mineral was submitted to the CNMNC, IMA 2009-005. The mineral and its name were approved, and the authors have agreed to postpone publication of the description of the new mineral pending completion of the present nomenclature report. A crystalline sample from Lagmannsvik, Hamarøy, Nordland, Norway, is considered the holotype material for IMA 2009-005 and all important characteristics, namely chemical composition, X-ray single-crystal and powder data, crystal structure, IR spectrum and optical data, were obtained from this specimen. Note that britholite with Y dominant among the M cations and F > OH was first described from Mt. Vyuntspakhk, Western Keivy, Kola Peninsula, Russia, by Lunts (1962). This metamict sample was re-studied using electron probe and IR spectroscopy, its Y- and F-dominant character was confirmed, and it was included in the IMA 2009-005 proposal as the cotype. The mineral IMA 2009-005 has the simplified formula $(Y,Ca,Ln)_5[(Si,P)O_4]_3F$, or, ideally, $(Y_3Ca_2)(SiO_4)_3F$. The holotype from Lagmannsvik has the archetype space group $P6_3/m$, with predominance of $(Y + Ln)$ over Ca in both the M1 and M2 sites.

3.4.5. *Fluorcalciobritholite*

This mineral was defined as a distinct species by Pekov *et al.* (2007) with a unique combination of dominant cations at *M* and *T* sites in the space group $P6_3/m$. In fact, fluorcalciobritholite has the T site occupancy $(T^{4+}{}_2T^{5+})$, *i.e.* Si_2P, and thus differs from both ''britholite'' and ''apatite''. Britholite has $T^{4+}{}_3$, *i.e.* Si_3, must have at least 3 trivalent cations in M, and actually is a *REE*-dominant mineral. Apatite has $T^{5+}{}_3$, *i.e.* P_3, with only divalent cations at the M sites. The ideal chemical formula for fluorcalciobritholite may be written as $(Ca_3REE_2)[(SiO_4)_2(PO_4)]F$. In view of the coupled heterovalent substitutions occurring at the M and T sites in the series apatite – calciobritholite – britholite, it is more practical in this case for nomenclature purposes to consider the total abundance of M cations as a single, composite site (Fig. 3).

3.5. Ellestadite group

3.5.1. *Ellestadite-(OH), ellestadite-(F), ellestadite-(Cl)*

Ellestadites *lato sensu* are sulphato-silicates. For stoichiometric reasons, the incorporation of the sulphate anion $(SO_4)^{2-}$ in the structure of apatite in the place of $(PO_4)^{3-}$ or $(AsO_4)^{3-}$ must be coupled with a concurrent substitution by silicate anions $(SiO_4)^{4-}$. This holds in all cases in which the M sites are occupied by divalent cations. Pure sulphates with the apatite structure may occur only by reducing the overall positive charge associated with the M cations, as is the case in cesanite and caracolite.

Ellestadite was first described from Crestmore, Riverside County, California, USA (McConnell, 1937). Based on the original chemical analysis, the type specimen

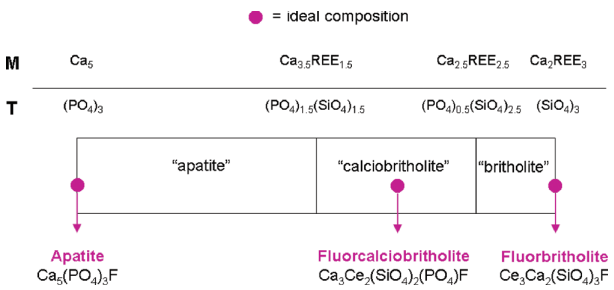

Fig. 3. Coupled heterovalent substitutions at the M and T sites in the series apatite – calciobritholite – britholite.

should be considered ellestadite-(OH). Later, Harada *et al.* (1971) redefined ellestadite from Chichibu mine, Saitama Prefecture, Japan as the OH-dominant calcium silicate-sulphate, and called it hydroxylellestadite, based on the wrong assumption that type ellestadite from Crestmore had Cl > (OH),F. Although analyses of natural ellestadite-(F) are known (*e.g.*, Rouse & Dunn, 1982), the Cl-dominant analogue, which has been synthesized (Pliego-Cuervo & Glasser, 1978), has never been found in nature (as far as we know); therefore, it should not be considered a mineral. Ellestadite-(F) was formally described as a new mineral species from Kopeisk, South Urals, Russia (Chesnokov *et al.*, 1987). The given name was fluorellestadite. The crystal structure of ellestadite-(OH) was refined in the space group $P2_1/m$ by Sudarsanan (1980) and by Hughes & Drexler (1991), and later in the space group $P6_3/m$ by Onac *et al.* (2006).

The names hydroxylellestadite, fluorellestadite, and chlorellestadite were changed into the suffixed names ellestadite-(OH), ellestadite-(F), ellestadite-(Cl) by Burke (2008).

3.5.2. Mattheddleite

This mineral was first described from Leadhills Dod, Strathclyde region, Scotland, UK (Livingstone *et al.*, 1987). The original chemical analyses are a bit odd in that they display a marked excess of lead and, hence, a Si/S ration greater than 1, and point to the chemical formula $Pb_{5.49}(SiO_4)_{1.87}(SO_4)_{1.09}O_{0.16}Cl_{0.99}$. Nevertheless, new electron microprobe data and a single-crystal structure refinement (Steele *et al.*, 2000) confirmed that mattheddleite can be ascribed to the apatite group, with the structural formula $Pb_5(SiO_4)_{1.5}(SO_4)_{1.5}Cl_{0.57}(OH)_{0.43}$, space group $P6_3/m$, $a = 10.006$, $c = 7.496$ Å.

More recently, another set of electron microprobe data on samples from the type locality (Essene *et al.*, 2006) confirmed the excess of Si over S in mattheddleite. The resulting charge imbalance is adjusted assuming small vacancies at the O sites, leading to an average formula $Pb_5(Si_{1.8}S_{1.2}O_{11.7}\square_{0.3})(Cl,OH)$. Moreover, the possible existence of an (OH)-dominant analogue of mattheddleite is mentioned.

3.6. Other minerals with the apatite structure

3.6.1. Tritomite-(Ce), melanocerite-(Ce), tritomite-(Y)

The three minerals tritomite-(Ce), melanocerite-(Ce), and tritomite-(Y) (Frondel, 1961) are listed as valid species in the IMA list of minerals. Tritomite-(Y) has been renamed, its original name being spencite (Jaffe & Molinski, 1962). All of these minerals are metamict; X-ray powder diffraction patterns were recorded on annealed material. Their chemical compositions are: tritomite-(Ce), $Ce_5(SiO_4,BO_4)_3(OH,O)$; melanocerite, $(Ce,Ca)_5(SiO_4,BO_4)_3(OH,F)\cdot nH_2O$; tritomite-(Y), $Y_5(SiO_4,BO_4)_3(O,OH,F)$. Therefore, these minerals can be considered borosilicates, with *REE*s strongly prevalent over calcium in the M sites for stoichiometric reasons. Clearly melanocerite-(Ce) and tritomite-(Ce) are probably the same mineral, and tritomite-(Y) could be the Y-dominant analogue. According to Dana (Gaines *et al.*, 1997), type localities and year of discovery are as follows: tritomite-(Ce)–Låven Island, Langesundfjord, Norway (1849); melanocerite-(Ce) – Kjeøy Island, Langesundfjord, Norway (1887); tritomite-(Y) – Cranberry Lake, Sussex, Co., New Jersey, USA (1962). Although commonly ascribed to the apatite group, the available chemical analyses (Engstrom, 1877; Jaffe & Molinski, 1962) do not conform to the usual M/T stoichiometric ratio, indicating either conspicuous vacancies at the M sites or, more likely, analytical inaccuracies and admixtures with other phases. Formally, tritomite-(Ce), melanocerite-(Ce) and tritomite-(Y) could be included, as *REE* silicates in the britholite subgroup. The relationships and the possible identity of tritomite-(Ce) and tritomite-(Y) with britholite-(Ce) and britholite-(Y), respectively, deserve further study.

3.6.2. Carbonate-fluorapatite, carbonate-hydroxylapatite

Although the above names are extensively used in literature, *e.g.*, to denote the mineral portion of bones and teeth of vertebrates, their validity as distinct mineral species belonging to the apatite group has always been under question. $(CO_3)^{2-}$ anion is known to occur as a subordinate component in members of the apatite group (*e.g.*, Knudsen & Gunter, 2002; Pan & Fleet, 2002). A paper by Baumer *et al.* (1990) reports infrared absorption spectra of a natural ''carbonate-fluorapatite''; however, neither chemical nor X-ray diffraction data are given. Ivanova *et al.* (2001), Fleet *et al.* (2004) and Fleet & Liu (2008) presented Rietveld and single-crystal X-ray diffraction data describing a possible substitution mechanism of (PO_4) by (CO_3) in synthetic fluorapatite and hydroxylapatite. After Burke (2008), both ''carbonate-fluorapatite'' and ''carbonate-hydroxylapatite'' have been discredited.

4. Chemical composition of apatite supergroup minerals

4.1. Calculation of crystal-chemical formulae

Determining the correct placement of a mineral within the apatite supergroup can be a difficult task, requiring a high-quality crystal structure refinement, mainly in those cases where ordering may occur. In most cases, the available analytical data consist of electron microprobe chemical analyses without any direct determination of the H_2O content (which may play a crucial role in some apatites). Hence, although the unequivocal identification of some existing apatite group minerals (or the recognition of potential new end-members) is impossible without structural information, we think it is useful to provide a series of suggestions for the handling of EMPA data, which can be used in most straightforward cases.

Given a set of chemical analyses within a group of minerals with similar crystal-chemical features, the

formula calculation basis may be more or less arbitrarily chosen; in the cases of apatites, for example, the following criteria may be selected:

(a) Calculation on the basis of 13 total anions. If the analytical value for H_2O is available, this will not result in exactly 12 O and 1 (F + Cl + OH). Typically, the total amounts of O and (F + Cl + OH) should not dramatically shift from the above values; however, in some cases, depending on the overall positive charges associated with cations, it could also be that some O^{2-} substitutes for monovalent anions at the X crystallographic site. If the analytical value for H_2O is lacking, it is reasonable to assume a calculated wt% H_2O so as to give 13 total anions (O + F + Cl + OH), with O = 12 and (F + Cl + OH) = 1, unless (F + Cl) $\geq$ 1 (in those cases H_2O_{calc} can be omitted).

(b) Calculation on the basis of 8 total (M + T) cations.

(c) Calculation on the basis of 3 T cations (*i.e.*, P + As + V + Si + S).

In principle, criterion (a) is preferable to criteria (b) and (c). In fact, calculation based on any subset of all atoms does not affect the stoichiometric ratios between them, but automatically shifts any analytical error to the atoms not belonging to that subset. Criteria (b) and (c) would be best to use in cases in which structural vacancies are possible at some sites, but this does not seem to be the case for any apatite supergroup mineral.

For cation allocation, P^{5+}, As^{5+}, V^{5+}, Si^{4+} and S^{6+} can be assumed to be in tetrahedral coordination and assigned to the T site, where they should sum up to 3. In cases of a marked deviation from the ideal value of 3 apfu (say more than 3 %), it may be inferred that the analysis is in error, or unreliable due to admixture with other phases or another such issue.

All remaining cations will enter the M1 and M2 sites. Elucidation of partitioning between these two sites (or more, in cases of split sites) is almost impossible without an accurate evaluation of the electron density at each of them, which makes a structural study mandatory. On the basis of both the historical appraisal of all available structural studies within the apatite supergroup and general crystal-chemical considerations, for cases where structural data are not available, we suggest allocation of M cations in order of increasing ionic radius, filling M1 sites (Wyckoff positions 4*f* in the $P6_3/m$ structure) with smaller cations (in particular Ca), and putting larger cations (Ba, Pb, etc.) in M2 sites (Wyckoff positions 6*h* in the $P6_3/m$ structure). This should result in correct allocations of cations in most cases, which can be used for identification or naming; however, this approach is not infallible in that some doubts remain regarding cation partitioning trends in apatite (*sensu lato*), mainly in the partitioning of Ca and *REE* between M1 and M2.

4.2. Effect of charge compensation on the idealized formulae

Cations with charges of +4, +5 and +6 can occupy the T site in the apatite structure and cations with charges of +1, +2 and +3 can occupy the M sites. Given the basic stoichiometry of apatite supergroup minerals, $M1_2M2_3(TO_4)_3X$ (or $M1M1'M2_3(TO_4)_3X$), and assuming, for the sake of simplicity, that the overall charge associated with anions is –25 [*i.e.*, 12 O^{2-} + 1 $(F, Cl, OH)^-$], charge compensation dictates the combinations of T and M site occupancies provided in Table 3.

Due to the symmetry of apatites, and to the existence of a single independent T site, the overall charge associated with T cations is, as a rule, a multiple of 3. The only exception to this rule is fluorcalciobritholite.

5. General nomenclature rules for apatite supergroup minerals

The crystal chemistry of apatites has important implications on nomenclature. After careful consideration of the intricacies of apatite crystal chemistry as described above, we propose the following basic guidelines for the nomenclature of apatite supergroup minerals:

(1) As a rule, each combination of M1, M2, and T dominant cations deserves a specific root name.

(2) Adjectival prefixes for the X anions are to be preferred over modified Levinson suffixes for two main reasons:

(i) Historical – Most minerals within the apatite group were originally named using the adjectival prefixes and some of these (esp. chlorapatite, fluorapatite and hydroxylapatite) have long histories of usage in the scientific literature. Renaming them at this point creates needless disruption in historical continuity, which is certainly not outweighed by issues of convenience, *e.g.* alphabetical listing.

(ii) Practical – There are members of the apatite supergroup which are *REE*-dominant minerals and in those cases, according to general nomenclature rules, the root name must be followed by the Levinson suffix denoting the most abundant among *REE*s [*e.g.*, belovite-(La), britholite-(Ce)]. The adoption of the suffix nomenclature for

Table 3. Possible combinations of cation site occupancies based upon cation charge.

T site occupancy	T charge	M1, M2 sites occupancy	M charge
$T^{4+}{}_3$	12	$M^{2+}{}_2\,M^{3+}{}_3$	13
$T^{4+}{}_2T^{5+}$	13	$M^{2+}{}_3\,M^{3+}{}_2$	12
$T^{5+}{}_3$	15	$M^{2+}{}_2\,M^{2+}{}_3$ or $(M^{1+}M^{3+})\,M^{2+}{}_3$	10
$T^{4+}{}_{1.5}T^{6+}{}_{1.5}$	15	$M^{2+}{}_2\,M^{2+}{}_3$	10
$T^{6+}{}_3$	18	$M^{1+}{}_2\,(M^{2+}{}_2M^{1+})$ or $M^{1+}{}_2\,(M^{1+}{}_2M^{3+})$	7

X-dominant anions would require a double Levinson suffix in some cases [*e.g.*, britholite (YF), instead of fluorbritholite-(Y)] and we believe that such mixed cation-anion suffixes are awkward.

Aiming to avoid unnecessary changes in the existing nomenclature, the use of adjectival prefixes should not be applied retroactively; in other words, it is not recommended to rename pyromorphite, $Pb_5(PO_4)_3Cl$, as chlorpyromorphite. If in the future the F analogue of pyromorphite, $Pb_5(PO_4)_3F$, is described, the name ''fluorpyromorphite'' could be logically adopted for it. There are plenty of examples of pairs of mineralogical names, in which only one has the adjectival prefix, *e.g.*, phlogopite – fluorophlogopite, clinohumite – hydroxylclinohumite, bartonite – chlorbartonite, etc. In general, a given mineral name is not meant to reveal the details of the chemical composition.

Neither is it recommended to adopt a prefix-based nomenclature for the calcium arsenates svabite, johnbaumite, and turneaureite, although the two latter minerals would have been better named hydroxylsvabite and chlorsvabite, respectively.

(3) Minerals with the same ideal chemical composition and different space group symmetries should be denoted with the same name, and with italicized suffixes denoting the crystalline system (*e.g.*, mimetite-*H*, mimetite-*M*). Thus far, among all known minerals of the apatite supergroup, there are only three such cases, and a fourth one has been recognized (see § 6.4. and 6.5.). According to the general IMA-CNMNC guidelines on nomenclature (Nickel & Grice, 1998), these are cases of polymorphic minerals with essentially the same structural topologies and should not be regarded as separate species. As happens with similar cases (*e.g.*, analcime, muscovite, sapphirine) for which topologically identical polymorphs (or polytypes) with different crystal systems are known, in the IMA List of Minerals only the basic, unsuffixed name need be used and this will be considered the official name for the mineral. The ''*–H*'' or ''*–M*'' will only be used in cases where there is a need to distinguish or identify the specific polymorph, *e.g.*, in papers discussing the crystallographic variants of a given mineral. We are aware that the pronunciation of such names may be a bit clumsy, but we anticipate that in verbal form most people will choose to use only the root name, *i.e.* mimetite, and when referring specifically to monoclinic polymorph, can preface the root name with ''monoclinic'', *i.e.* ''monoclinic mimetite''.

(4) In addition to monovalent anions (F, Cl, OH), O^{2-} may also enter the X site. For example, a structural model for a synthetic compound $Ca_{10}(PO_4)_6O$, obtained by dehydration of $Ca_{10}(PO_4)_6(OH)_2$ under electron microscope conditions, has been designed on the basis of simulated high resolution lattice images (Henning *et al.*, 1999). For the definition of a potential new mineral with O^{2-} as the dominant anion, it is required that the fraction of $^{X}O^{2-}$ is > 50 %. Here we refer to the concept of ''charge compensating anion'', according to which monovalent anions may be considered as a whole. In other words, for nomenclature purposes, if $^{X}O^{2-} > (F + Cl + OH)^{-}$, the mineral will have the adjectival prefix ''oxy'' (sometimes in literature the hypothetical ''oxyapatite'' component is mentioned for natural compounds, whereas synthetic end-members are well known; *e.g.*, Ito, 1968); if $(F + Cl + OH)^{-} > {}^{X}O^{2-}$ the mineral could have the adjectival prefix corresponding to the dominating anion of the dominant valency state (Hatert & Burke, 2008). As far as we are aware, as yet no reliable analyses of apatite supergroup minerals have been reported in the literature with $^{X}O^{2-} > (F + Cl + OH)^{-}$.

(5) Similar arguments may be valid for the possible substitution of monovalent anions by water molecules (the hypothetical ''hydroapatite'' component). Although the structural role of water molecules within the framework of apatite is yet to be clarified, in a single case, that of cesanite (Cavarretta *et al.*, 1981), the water content points to a formula which has substantial H_2O entering the X site. However, the reported formula still has $(OH + F + Cl) > H_2O$.

6. Approved changes

With the intent of rationalizing the nomenclature of minerals within the apatite supergroup, we propose a number of changes, which are listed in detail below and are also summarized in Table 1. In this endeavour, our two guiding principles have been: (1) to make a completely self-consistent nomenclature system, and (2) to reduce, as much as possible, changes to existing mineral names. Clearly, these two principles are not fully reconcilable with one another, and our final product represents the best compromise we could find between them. Overall, within the broad apatite supergroup, we have made six types of recommendations: (1) nomenclature changes to existing minerals, (2) potentially new mineral species, (3) minerals and mineral names which could be discredited, (4) changes of status from distinct species to polymorphic variants, (5) recognition of a new polymorphic variant, and (6) changes to end-member formulae.

6.1. Nomenclature changes to existing minerals

(1) In keeping with our suggestion to use adjectival prefixes instead of modified Levinson suffixes for the dominant X anion, a number of mineral names should be changed as follows: apatite-(CaF) to **fluorapatite**; apatite-(CaOH) to **hydroxylapatite**; apatite-(CaCl) to **chlorapatite**; ellestadite-(F) to **fluorellestadite**; ellestadite-(OH) to **hydroxylellestadite**; phosphohedyphane-(F) to **fluorphosphohedyphane**. Therefore, for ''apatites'' the historical names, adopted in the XIX century and occurring in thousands of mineralogical and non-mineralogical publications, should be reintroduced. The same holds for ''ellestadites'', although these minerals have a more recent history and are not as widespread as apatites.

Phosphohedyphane, which was renamed phosphohedyphane-(Cl) after the description of phosphohedyphane-(F), should be re-assigned its original name, with neither ''chlor-'' prefix nor ''-(Cl)'' suffix.

(2) **Stronadelphite** (given name for IMA 2008-009): The new mineral IMA 2008-009, $Sr_5(PO_4)_3F$, was approved without a name. Now we (MP & IP), being among the authors of the IMA 2008-009 proposal and of this nomenclature report, in agreement with the whole apatite subcommittee herewith propose for this mineral a new root name, namely stronadelphite. It is a compound word after the chemical element *stron*tium and αδελφός, Greek for ''brother''; the mineral is the full strontium analogue of fluorapatite, the most widespread member of the apatite group. We wish to avoid the constructions strontioadelphite or strontio-adelphite, because of the inconvenient fragment *oa* or *o-a*, and strontiadelphite because of the possibility that it might be misspelled as strontiodelphite by somebody unfamiliar with Greek roots.

(3) **Fluorstrophite** instead of apatite-(SrOH): To have a mineral named either apatite-(SrOH) (the new name) or ''strontium-apatite'' (the old name) after the discovery of a mineral (IMA 2008-009) which is more Sr-rich than strontium-apatite itself is clearly misleading. The original name strontium-apatite was given before the structural study of the mineral and incorrectly reflects its relationship with apatite; therefore, we propose to change its name to fluorstrophite. This seems a proper name for a mineral with ideal composition $SrCaSr_3(PO_4)_3F$, due to its parallelism, in both the name and the ideal formula, with the related mineral fluorcaphite, $SrCaCa_3(PO_4)_3F$. The root name originates from the combination of elements: *fluor*ine, *stron*tium (at the M2 site), and *ph*osphorus. Fluorcaphite is a similar acronym, with *ca*lcium instead of *stron*tium.

(4) **Deloneite** instead of deloneite-(Ce): The detailed structural analysis carried out by Rastsvetaeva & Khomyakov (1996b) showed that none of the four independent M sites has REE as the dominant cation, therefore deloneite should not be considered a REE mineral, and the Levinson suffix should be omitted.

(5) For the newly approved mineral IMA 2009-005, the originally proposed name, **fluorbritholite-(Y)**, perfectly fits with our nomenclature scheme; therefore, we recommend its adoption for the mineral with composition $(Y_3Ca_2)(SiO_4)_3F$, which is actually the F-dominant analogue of britholite-(Y) and the Y-dominant analogue of fluorbritholite-(Ce).

6.2. Potentially new mineral species

(1) Hedyphane has ideal formula $Ca_2Pb_3(AsO_4)_3Cl$. Dunn *et al.* (1985b) described a mineral, which was called ''hydroxyl-bearing hedyphane'', that has (OH) as the dominant anion at the X site. This mineral deserves distinct species status, with ideal formula $Ca_2Pb_3(AsO_4)_3(OH)$. The most logical name for it would be ''hydroxylhedyphane''. Aiming at reducing, as far as possible, the changes to existing names, we do not see any need for the concurrent renaming of hedyphane to chlorhedyphane, if this potentially new mineral is approved.

(2) Stalder & Rozendaal (2002) report a ''calcian pyromorphite'' with a very low content of Cl and F. Assuming ordering of Pb and Ca in the two M sites, one of their analyses (#5 in their Table 4) is consistent with this being close to the OH end-member of phosphohedyphane, $Ca_2Pb_3(PO_4)_3(OH)$. According to the naming approach recommended herein, the most logical name for this potentially new species would be ''hydroxylphosphohedyphane''.

(3) The mineral studied structurally by Chakhmouradian *et al.* (2005) and reported as the second occurrence of fluorcaphite has the ideal chemical formula $CaCaSr_3(PO_4)_3F$, or more simply $Ca_2Sr_3(PO_4)_3F$. This mineral is different from both fluorcaphite, $SrCaCa_3(PO_4)_3F$, and fluorstrophite, $SrCaSr_3(PO_4)_3F$, and deserves distinct species status and a new root name.

4) The ''Mn-rich apatite'' described by Pieczka (2007) deserves distinct species status. This would be the only mineral within the entire apatite supergroup having Mn as an essential element, but more significantly, it would be the only mineral in which a normally octahedrally-coordinated cation is an essential element. Although the ordering of Mn and Ca between the M1 and M2 sites cannot be confirmed without a structural study, one might expect Mn to go into the M1 site (*cf.* also § 4.1.). If this were the case, this mineral would have the ideal formula $Mn_2Ca_3(PO_4)_3Cl$.

(5) Mattheddleite has ideal formula $Pb_5(SiO_4)_{1.5}(SO_4)_{1.5}Cl$. Essene *et al.* (2006) re-analyzed samples from the type locality and found zones in some crystals with (OH) > Cl, although (OH) was admittedly calculated as 1 – Cl. This would represent a potentially new mineral, the OH-analogue of mattheddleite, for which the most logical name would be ''hydroxylmattheddleite''. As for hedyphane, also in the case that ''hydroxylmattheddleite'' will be approved as a valid species, we do not see any need to rename mattheddleite into ''chlormattheddleite''.

6.3. Minerals and mineral names which could be discredited

(1) Ellestadite-(Cl): As far as we are aware, no reliable chemical analyses were ever published for any ''ellestadite'' mineral having Cl^- as the dominant X^- anion; therefore, ellestadite-(Cl), formerly known as ''chlorellestadite'', is not thought to exist and we herewith propose to discredit the mineral and its name.

(2) Melanocerite-(Ce): Both the ''melanocerite'' and ''tritomite'' root names indicate *REE*-rich silicoborate minerals within the apatite supergroup. Although all these minerals are inadequately characterized, the existence of two distinct root names seems unnecessary. For priority reasons, the root name ''tritomite'' should be maintained; therefore, the name melanocerite-(Ce) for an apatite-like silicoborate having cerium as the dominant *REE*, could be potentially discredited, once its identity with tritomite-(Ce) is ascertained.

6.4. Changes of status from distinct species to polymorphic variants

(1) Fermorite is the monoclinic polymorph of johnbaumite, $Ca_5(AsO_4)_3(OH)$, but the two structures are topologically

equivalent. Therefore, according to existing IMA-CNMNC guidelines (Nickel & Grice, 1998), johnbaumite and fermorite should not be considered two distinct species. It could be a matter of discussion which of the above names has priority. In strictly chronological terms, the name fermorite (1911) existed before johnbaumite (1980); however, the original characterization of fermorite (Smith & Prior, 1911) was incorrect in two critical respects: the mineral was described as hexagonal (like johnbaumite) and the given chemical formula did not correspond to that of a calcium arsenate mineral. A complete characterization of fermorite as the monoclinic polymorph of $Ca_5(AsO_4)_3(OH)$ was presented by Hughes & Drexler (1991) after the description of hexagonal johnbaumite by Dunn *et al.* (1980). Within the entire apatite supergroup, the hexagonal structures can be generally considered as ''parents'' upon which the lower symmetry polymorphic structures are based. Moreover, in this specific case, the deviations from hexagonal symmetry are very limited (Hughes & Drexler, 1991). Therefore, we propose to maintain ''johnbaumite'' as the root name for the calcium arsenate, and to rename fermorite as johnbaumite-*M*. Concurrently, the hexagonal polymorph of johnbaumite should be renamed johnbaumite-*H*.

(2) Clinohydroxylapatite was described by Chakhmouradian & Medici (2006) as the monoclinic polymorph of $Ca_5(PO_4)_3(OH)$. According to existing IMA-CNMNC guidelines (Nickel & Grice, 1998), hydroxylapatite and clinohydroxylapatite should not be considered two distinct minerals, but two polymorphic variants of the same species. It is therefore recommended that clinohydroxylapatite be renamed hydroxylapatite-*M*. Concurrently, the hexagonal polymorph of hydroxylapatite should be renamed hydroxylapatite-*H*.

(3) Clinomimetite was described by Dai *et al.* (1991) as the monoclinic polymorph of mimetite. According to existing IMA-CNMNC guidelines (Nickel & Grice, 1998), mimetite and clinomimetite should not be considered two distinct minerals, but two polymorphic variants of the same species. It is, therefore, recommended that clinomimetite be renamed as mimetite-*M*. Concurrently, the hexagonal polymorph of mimetite should be renamed mimetite-*H*.

For the sake of convenience, the suffix -*H* will be generally omitted in the name of the hexagonal polymorphs, by far more common in nature than the monoclinic polymorphs.

6.5. Recognition of a new polymorphic variant

Hughes *et al.* (1990) refined the structure of a sample of monoclinic chlorapatite from Jackson Peak, Gunkock, Washington Co., Utah, USA, which is analogous to the monoclinic hydroxylapatite described by Chakhmouradian & Medici (2006). Therefore, as in the case of hydroxylapatite, the hexagonal and the monoclinic forms of chlorapatite are to be considered as polymorphs. The sample from Jackson Peak should be named chlorapatite-*M*. Concurrently, the hexagonal polymorph of chlorapatite should be renamed chlorapatite-*H* (see also § 6.4.).

6.6. Changes to end-member formulae

(1) Morelandite. The only available chemical analysis for morelandite yields the empirical formula $(Ba_{2.25}Ca_{1.65}Pb_{1.16}Fe_{0.06}Mn_{0.06})[(AsO_4)_{2.56}(PO_4)_{0.30}]Cl_{1.09}$ (Dunn & Rouse, 1978). In the IMA List of Minerals, morelandite is given the formula $Ba_5(AsO_4)_3Cl$. To conform with this ideal, ''end-member'' formula $[^{M1}Ba_2{}^{M2}Ba_3(AsO_4)_3Cl]$, barium would have to be the dominant cation at both the M1 and M2 sites (Ba $>$ 2.50 apfu), but it is not. Therefore, the ideal chemical formula of morelandite should be rewritten as $Ca_2Ba_3(AsO_4)_3Cl$, instead of $Ba_5(AsO_4)_3Cl$.

(2) Deloneite. The following charge-balanced formula better reflects the nature of deloneite, in which there are no *REE*-dominant sites: $(Na_{0.5}REE_{0.25}Ca_{0.25})$ $(Ca_{0.75}REE_{0.25})$ $Sr_{1.5}$ $(CaNa_{0.25}REE_{0.25})$ $(PO_4)_3$ $F_{0.5}(OH)_{0.5}$. This is in keeping with the approved removal of the Levinson suffix from its name.

Acknowledgements: We are grateful to all the members of the IMA Commission on New Minerals, Nomenclature and Classification who provided with suggestion and criticism, and to the CNMNC secretary, Stuart Mills, for handling the whole procedure.

References

Baikie, T., Mercier, P.H.J., Elcombe, M.M., Kim, J.Y., Le Page, Y., Mitchell, L.D., White, T.J., Whitfield, P.S. (2007): Triclinic apatites. *Acta Crystallogr.*, **B63**, 251–256.

Baumer, A., Caruba, R., Ganteaume, M. (1990): Carbonate-fluorapatite: mise en evidence de la substitution $2PO_4^{3-} \rightarrow SiO_4^{4-} + SO_4^{2-}$ par spectrométrie infrarouge. *Eur. J. Mineral.*, **2**, 297–304.

Borodin, L.S. & Kazakova, M.E. (1954): Belovite, a new mineral from alkaline pegmatites. *Dokl. Akad. Nauk SSSR*, **96**, 613–616 [in Russian].

Breithaupt, A. (1830): Bestimmung neuer Mineral-Specien, 2. Hedyphan. *J. Chem. Phys.*, **60**, 308–316.

Burke, E.A.J. (2008): Tidying up mineral names: an IMA-CNMNC scheme for suffixes, hyphens and diacritical marks. *Mineral. Rec.*, **39**, 131–135.

Cavarretta, G., Mottana, A., Tecce, F. (1981): Cesanite, $Ca_2Na_3[(OH)(SO4)_3]$, a sulphate isotypic to apatite, from the Cesano geothermal field (Latium, Italy). *Mineral. Mag.*, **44**, 269–273.

Chakhmouradian, A.R. & Medici, L. (2006): Clinohydroxylapatite: a new apatite-group mineral from northwestern Ontario (Canada), and new data on the extent of Na-S substitution in natural apatites. *Eur. J. Mineral.*, **18**, 105–112.

Chakhmouradian, A.R., Hughes, J.M., Rakovan, J. (2005): Fluorcaphite, a second occurrence and detailed structural analysis: simultaneous accommodation of Ca, Sr, Na, and LREE in the apatite atomic arrangement. *Can. Mineral.*, **43**, 735–746.

Chesnokov, B.V., Bazhenova, L.F., Bushmakin, A.F. (1987): Fluorellestadite, $Ca_{10}[(SO_4),(SiO_4)]_6F_2$ – a new mineral. *Zap. Vsers. Mineral. Obshchest.*, **116**(6), 743–746 [in Russian].

Dai, Y. & Hughes, J.M. (1989): Crystal structure refinements of vanadinite and pyromorphite. *Can. Mineral.*, **27**, 189–192.

Dai, Y., Hughes, J.M., Moore, P.B. (1991): The crystal structures of mimetite and clinomimetite, $Pb_5(AsO_4)_3Cl$. *Can. Mineral.*, **29**, 369–376.

Damour, A.A. (1856): Sur l'hydro-apatite, espèce minérale. *Ann. Mines*, **10**, 65–68.

Dardenne, K., Vivien, D., Huguenin, D. (1999): Color of Mn(V)-substituted apatites $A_{10}((B,Mn)O_4)_6F_2$, A = Ba, Sr, Ca; B = P, V. *J. Solid State Chem.*, **146**, 464–472.

Demartin, F., Gramaccioli, C.M., Campostrini, I., Pilati, T. (2010): Aiolosite, $Na_2(Na_2Bi)(SO_4)_3Cl$, a new sulfate isotypic to apatite from La Fossa Crater, Vulcano, Aeolian Islands, Italy. *Am. Mineral.*, **95**, 382–385.

Dolivo-Dobrovolsky, V.V. (2006): About a common mistake in treating the crystal structure of apatite. *Zap. Ross. Mineral. Obshchest.*, **3**, 123–125 [in Russian].

Dong, Z.-L. & White, T.J. (2004a): Calcium-lead fluoro-vanadinite apatites. I. Disequilibrium structures. *Acta Crystallogr.*, **B60**, 138–145.

—, — (2004b): Calcium-lead fluoro-vanadinite apatites. II. Equilibrium structures. *Acta Crystallogr.*, **B60**, 146–154.

Dunn, P.J. & Rouse, R.C. (1978): Morelandite, a new barium arsenate chloride member of the apatite group. *Can. Mineral.*, **16**, 601–604.

Dunn, P.J., Peacor, D.R., Newberry, N. (1980): Johnbaumite, a new member of the apatite group from Franklin, New Jersey. *Am. Mineral.*, **65**, 1143–1145.

Dunn, P.J., Peterson, E.U., Peacor, D.R. (1985a): Turneaureite, a new member of the apatite group from Franklin, New Jersey, Balmat, New York and Långban, Sweden. *Can. Mineral.*, **23**, 251–254.

Dunn, P.J., Rouse, R.C., Nelen, J.A. (1985b): Hydroxyl-bearing hedyphane from Långban, Sweden. *Geol. Fören. Stockholm Förhandl.*, **107**, 325–327.

Efimov, A.F., Kravchenko, S.M., Vasil'eva, Z.V. (1962): Strontium-apatite, a new mineral. *Dokl. Akad. Nauk SSSR*, **142**, 439–442 [in Russian].

Elliott, J.C. (1994): Structure and chemistry of the apatites and other calcium orthophosphates. Elsevier, Amsterdam, 389 p.

Elliott, J.C., Mackie, P.E., Young, R.A. (1973): Monoclinic hydroxyapatite. *Science*, **180**, 1055–1057.

Engstrom, N. (1877): Undersöknung of några mineral. Inaug. Diss. Upsala, 1877.

Essene, E.J., Henderson, C.E., Livingstone, A. (2006): The missing sulphur in mattheddleite, sulphur analysis of sulphates, and paragenetic relations at Leadhills, Scotland. *Mineral. Mag.*, **70**, 265–280.

Fleet, M.E. & Liu, X. (2008): Accommodation of the carbonate ion in fluorapatite synthesized at high pressure. *Am. Mineral.*, **93**, 1460–1469.

Fleet, M.E., Liu, X., King, P.L. (2004): Accommodation of the carbonate ion in apatite: an FTIR and X-ray structure study of crystals synthesized at 2–4 GPa. *Am. Mineral.*, **89**, 1422–1432.

Foshag, W.F. & Gage, R.B. (1925): Hedyphane from Franklin Furnace, New Jersey. *Am. Mineral.*, **10**, 351–353.

Friis, H., Balić-Žunić, T., Pekov, I.V., Petersen, O.V. (2004): Kuannersuite-(Ce), $Ba_6Na_2REE_2(PO_4)_6FCl$, a new member of the apatite group, from the Ilímaussaq alkaline complex, South Greenland: description and crystal chemistry. *Can. Mineral.*, **42**, 95–106.

Frondel, C. (1961): Two yttrium minerals: spencite and rowlandite. *Can. Mineral.*, **6**, 576–581.

Gaines, R.V., Skinner, H.C.W., Foord, E.E., Mason, B., Rosenzweig, A. (1997): Dana's New Mineralogy. Wiley, New York, 1819 p.

Gay, P. (1957): An X-ray investigation of some rare-earth silicates: cerite, lessingite, beckelite, britholite and stillwellite. *Mineral. Mag.*, **31**, 455–468.

Genkina, E.A., Malinovskii, Yu.A., Khomyakov, A.P. (1991): Crystal structure of Sr-containing britholith. *Sov. Phys. Crystallogr.*, **36**, 19–21.

Gu, J., Chao, G.Y., Tang, S. (1994): A new mineral – fluorbritholite-(Ce). *J. Wuhan Univ. Technol.*, **9**, 1855–1866.

Harada, K., Nagashima, K., Nakao, K., Kato, A. (1971): Hydroxylellestadite, a new apatite from Chichibu mine, Saitama Prefecture, Japan. *Am. Mineral.*, **56**, 1507–l518.

Hata, S. (1938): Abukumalite, a new mineral from pegmatites of Isaka, Fukushima prefecture. *Sci. Pap. Inst. Phys. Chem. Res. Tokyo*, **34**, 1018–1023.

Hatert, F. & Burke, E.A.J. (2008): The IMA-CNMNC dominant-constituent rule revisited and extended. *Can. Mineral.*, **46**, 717–728.

Hausmann, J.F.L. (1813): Handbuch der Mineralogie. Vandenhoek & Ruprecht, Göttingen, 1158 p.

Henning, P.A., Landa Cánovas, A.R., Larsson, A.K., Lidin, S. (1999): Elucidation of the crystal structure of oxyapatite by high-resolution electron microscopy. *Acta Crystallogr.*, **B55**, 170–176.

Hughes, J.M. & Drexler, J.W. (1991): Cation substitution in the apatite tetrahedral site: crystal structures of type hydroxylellestadtite and type fermorite, locality: Crestmore, California, USA. *N. Jb. Mineral. Mh.*, **1991**, 327–336.

Hughes, J.M., Cameron, M., Crowley, K.D. (1990): Crystal structures of natural ternary apatites: solid solution in the $Ca_5(PO_4)_3X$ (X = F, Cl, OH) system. *Am. Mineral.*, **75**, 295–304.

Hughes, J.M., Ertl, A., Bernhardt, H.J., Rossman, G.R., Rakovan, J. (2004): Mn-rich fluorapatite from Austria: crystal structure, chemical analysis and spectroscopic investigations. *Am. Mineral.*, **89**, 629–632.

Ito, J. (1968): Silicate apatites and oxyapatites. *Am. Mineral.*, **53**, 890–907.

Ivanova, T.I., Frank-Kamenetskaya, O.V., Kol'tsov, A.B., Ugolkov, V.L. (2001): Crystal structure of calcium-deficient carbonated hydroxyapatite. Thermal decomposition. *J. Solid State Chem.*, **160**, 340–349.

Jaffe, H.W. & Molinski, V.J. (1962): Spencite, the yttrium analogue of tritomite from Sussex County, New Jersey. *Am. Mineral.*, **47**, 9–25.

Johnson, P.D., Prener, J.S., Kingsley, J.D. (1963): Apatite: origin of blue color. *Science*, **141**, 1179–1180.

Kabalov, Yu.K., Sokolova, E.V., Pekov, I.V. (1997): Crystal structure of belovite-(La). *Dokl. Phys.*, **355**, 344–348.

Kalsbeek, N., Larsen, S., Rønsbo, J.G. (1990): Crystal structures of rare earth elements rich apatite analogues. *Z. Kristallogr.*, **191**, 249–263.

Kampf, A.R. & Housley, R.M. (2008): Phosphohedyphane-(F). New mineral proposal IMA 2008-068 – confidential document.

Kampf, A.R., Steele, I.M., Jenkins, R.A. (2006): Phosphohedyphane, $Ca_2Pb_3(PO_4)_3Cl$, the phosphate analog of hedyphane: description and crystal structure. *Am. Mineral.*, **91**, 1909–1917.

Khomyakov, A.P., Lisitsyn, D.V., Kulikova, I.M., Rastsvetaeva, R.K. (1996): Deloneite-(Ce), $NaCa_2SrCe(PO_4)_3F$, a new mineral with belovite-like structure. *Zap. Vser. Mineral. Obshchest.*, **5**, 83–94 [in Russian].

Khomyakov, A.P., Kulikova, I.M., Rastsvetaeva, R.K. (1997): Fluorcaphite, $Ca(Sr,Na,Ca)(Ca,Sr,Ce)_3(PO_4)_3F$, a new mineral with the apatite structural motif. *Zap. Ross. Mineral. Obshchest.*, 3, 87–97 [in Russian].

Klevtsova, R.F. (1964): About the crystal structure of strontium-apatite. *Zhurn. Strukt. Khimii*, **5**, 318–320 [in Russian].

Klevtsova, R.F. & Borisov, S.V. (1964): Crystal structure of belovite. *Zhurn. Strukt. Khimii*, **5**, 151–153 [in Russian].

Knudsen, A.C. & Gunter, M.E. (2002): Sedimentary phosphorites – an example: phosphoria formation, Southeastern Idaho, U.S.A. *in* ''Phosphates – Geochemical, Geobiological, and Materials Importance'', M.J. Kohn, J. Rakovan, J.M. Hughes, eds. *Rev. Mineral. Geochem.*, **48**, 363–389.

Kohn, M.J., Rakovan, J., Hughes, J.M. (2002): Phosphates – Geochemical, Geobiological, and Materials Importance. *Rev. Mineral. Geochem.*, **48**, p. 742.

Laufek, F., Skála, R., Haloda, J., Císařová, I. (2006): Crystal structure of vanadinite: refinement of anisotropic displacement parameters. *J. Czech Geol. Soc.*, **51**, 271–275.

Levinson, A.A. (1966): A system of nomenclature for rare-earth minerals. *Am. Mineral.*, **51**, 152–158.

Livingstone, A., Ryback, G., Fejer, E.E., Stanley, C.J. (1987): Mattheddleite, a new mineral of the apatite group from Leadhills, Strathclyde region. *Scott. J. Geol.*, **23**, 1–8.

Lunts, A.Y. (1962): Abukumalite from rare-earth pegmatites of North-West of the USSR. *Izv. Akad. Nauk Latv. SSR*, **4**, 67–76 [in Russian].

Mackie , P.E., Elliott, J.C., Young, P.A. (1972): Monoclinic structure of synthetic $Ca_5(PO_4)_3$ C1, chlorapatite. *Acta Crystallogr.,* **B28**, 1840–1848.

McConnell, D. (1937): The substitution of SiO_4- and SO_4-groups for PO_4-groups in the apatite structure: ellestadite, the end member. *Am. Mineral.*, **22**, 977–986.

— (1938): A structural investigation of the isomorphism of the apatite group. *Am. Mineral.*, **23**, 1–19.

— (1973): Apatite: its crystal chemistry, mineralogy, utilization, and geologic and biologic occurrences. Springer-Verlag, New York, 111 p.

Mehmel, M. (1930): Uber die Struktur des Apatits. I. *Z. Kristallogr.*, **75**, 323–331.

Mercier, P.H.J., Le Page, Y., Whitfield, P.S., Mitchell, L.D., Davidson, I.J., White, T.J. (2005): Geometrical parameterization of the crystal chemistry of $P6_3/m$ apatites: comparison with experimental data and *ab initio* results. *Acta Crystallogr.*, **B61**, 635–655.

Mills, S.J., Hatert, F., Nickel, E.H., Ferraris, G. (2009): The standardisation of mineral group hierarchies: application to recent nomenclature proposals. *Eur. J. Mineral.*, **21**, 1073–1080.

Nadezhina, T.N., Pushcharovsky, D.Yu., Khomyakov, A.P. (1987): Refinement of crystal structure of belovite. *Mineral. Zhurn.*, **9**, 45–48 [in Russian].

Náray-Szabó, S. (1930): The structure of apatite $(CaF)Ca_4(PO_4)_3$. *Z. Kristallogr.*, **75**, 387–398.

Newberry, N.G., Essene, E.J., Peacor, D.R. (1981): Alforsite, a new member of the apatite group: the barium analogue of chlorapatite. *Am. Mineral.*, **66**, 1050–1053.

Nickel, E.H. & Grice, J.D. (1998): The IMA commission on new minerals and mineral names: procedures and guidelines on mineral nomenclature, 1998. *Can. Mineral.*, **36**, 913–926.

Noe, D.C., Hughes, J.M., Mariano, A.M., Drexler, J.W., Kato, A. (1993): The crystal structure of monoclinic britholite-(Ce) and britholite-(Y). *Z. Kristallogr.*, **206**, 233–246.

Nriagu, J.O. & Moore, P.B. (1984): Phosphate Minerals. Springer, New York, 442 p.

Oberti, R., Ottolini, L., Della Ventura, G., Parodi, G.C. (2001): On the symmetry and crystal chemistry of britholite: new structural and microanalytical data. *Am. Mineral.*, **86**, 1066–1075.

Omori, K. & Hasegawa, S. (1953): Yttrialite and abukumalite from pegmatite of Suishoyama, Iisaka village, Fukushima, Japan. *J. Jap. Ass. Mineral. Petrol. Econ. Geol.*, **37**, 21–29.

Onac, B.P., Effenberger, H., Ettinger, K., Panzaru, S.C. (2006): Hydroxylellestadite from Cioclovina Cave (Romania): microanalytical, structural, and vibrational spectroscopy data. *Am. Mineral.*, **91**, 1927–1931.

Pan, Y. & Fleet, M.E. (2002): Compositions of the apatite-group minerals: substitution mechanisms and controlling factors. in ''Phosphates – Geochemical, Geobiological, and Materials Importance'', M.J. Kohn, J. Rakovan, J.M. Hughes, eds. *Rev. Mineral. Geochem.*, **48**, 13–49.

Pekov, I.V., Chukanov, N.V., Eletskaya, O.V., Khomyakov, A.P., Men'shikov, Yu.P. (1995): Belovite-(Ce): a new data, refined formula, and relationship with other apatite group minerals. *Zap. Vser. Mineral. Obshchest.*, 2, 98–110 [in Russian].

Pekov, I.V., Kulikova, I.M., Kabalov, Yu.K., Eletskaya, O.V., Chukanov, N.V., Menshikov, Yu.P., Khomyakov, A.P. (1996): Belovite-(La), $Sr_3Na(La,Ce)[PO_4]_3(F,OH)$ – a new rare-earth mineral of the apatite group. *Zap. Vser. Mineral. Obshchest.*, 3, 101–109 [in Russian].

Pekov, I.V., Pasero, M., Yaskovskaya, A.N., Chukanov, N.V., Pushcharovsky, D.Yu., Merlino, S., Zubkova, N.V., Kononkova, N.N., Men'shikov, Yu.P., Zadov, A.E. (2007): Fluorcalciobritholite, $(Ca,REE)_5[(Si,P)O_4]_3F$, a new mineral: description and crystal chemistry. *Eur. J. Mineral.*, **19**, 95–103.

Pieczka, A. (2007): Beusite and an unusual Mn-rich apatite from the Szklary granitic pegmatite, Lower Silesia, Southwestern Poland. *Can. Mineral.*, **45**, 901–914.

Piotrowski, A., Kahlenberg, V., Fischer, R.X., Lee, Y., Parise, J.B. (2002): The crystal structures of cesanite and its synthetic analogue – a comparison. *Am. Mineral.*, **87**, 715–720.

Pliego-Cuervo, Y. & Glasser, F.P. (1978): Phase relations and crystal chemistry of apatite and silicocarnotite solid solutions. *Cement Concrete Res.*, **8**, 519–524.

Pushcharovsky, D.Yu., Nadezhina, T.N., Khomyakov, A.P. (1987): Crystal structure of strontium apatite from Khibiny. *Sov. Phys. Crystallogr.*, **32**, 524–526.

Rakovan, J.F. & Hughes, J.M. (2000): Strontium in the apatite structure: strontian fluorapatite and belovite-(Ce). *Can. Mineral.*, **38**, 839–845.

Rammelsberg, C.F. (1860): Handbuch der Mineralchemie. Engelmann, Leipzig, 1038 p.

Rastsvetaeva, R.K. & Khomyakov, A.P. (1996a): Structural features of a new naturally occurring representative of the fluorapatite-deloneite series. *Crystallogr. Rep.*, **41**, 789–792.

— & — (1996b): Crystal structure of deloneite-(Ce), the highly ordered Ca analog of belovite. *Dokl. Russ. Akad. Nauk*, **349**, 354–357 [in Russian].

Rouse, R.C. & Dunn, P.J. (1982): A contribution to the crystal chemistry of ellestadite and the silicate sulfate apatites. *Am. Mineral.*, **67**, 90–96.

Rouse, R.C., Dunn, P.J., Peacor, D.R. (1984): Hedyphane from Franklin, New Jersey and Långban, Sweden: cation ordering in an arsenate apatite. *Am. Mineral.*, **69**, 920–927.

Schneider, W. (1967): Caracolit, das $Na_3Pb_2(SO_4)_3Cl$ mit Apatitstruktur. *N. Jb. Mineral. Mh.*, **1967**, 284–289.

— (1969): Bestimmung einer Überstruktur am Caracolit. *N. Jb. Mineral. Mh.*, **1969**, 58–64.

Sjögren, H. (1892): Svabite a new-member of the apatite group. *Bull. Geol. Inst. Upsala*, **1**, 50–56.

Smith, G.F.H. & Prior, G.T. (1911): On fermorite, a new arsenate and phosphate of lime and strontia, and tilasite, from the manganese-ore deposits of India. *Mineral. Mag.*, **16**, 84–96.

Sokolova, E.V., Egorov-Tismenko, Yu.K., Yakhontova, L.K. (1982): Crystal structure of rare arsenates – duftite and mimetite. *Vestn. Mosk. Univ., Ser. 4: Geol.*, 50–56.

Stalder, M. & Rozendaal, A. (2002): Graftonite in phosphatic iron formations associated with the mid-Proterozoic Zn-Pb deposit, Namaqua province, South Africa. *Mineral. Mag.*, **66**, 915–927.

Steele, I.M., Pluth, J.J., Livingstone, A. (2000): Crystal structure of mattheddleite; a Pb, S, Si phase with the apatite structure. *Mineral. Mag.*, **64**, 915–921.

Sudarsanan, K. (1980): Structure of hydroxylellestadite. *Acta Crystallogr.*, **B36**, 1636–1639.

Suitch, P.R., Lacout, J.L., Hewat, A.W., Young, R.A. (1985): The structural location and role of Mn^{2+} partially substituted for Ca^{2+} in fluorapatite. *Acta Crystallogr.*, **B41**, 173–179.

Tazzoli, V. (1983): The crystal structure of cesanite, $Ca_{1+x}Na_{4-x}(SO_4)_3(OH)_x \cdot (1-x)H_2O$, a sulphate isotypic to apatite. *Mineral. Mag.*, **47**, 59–63.

Trotter, J. & Barnes, W.H. (1958): The structure of vanadinite. *Can. Mineral.*, **6**, 161–173.

von Haidinger, W. (1845): Handbuch der bestimmenden Mineralogie. Braumuller & Seidel, Wien, 625 p.

von Kobell, F. (1838): Grundzüge der Mineralogie. Schrag, Nürnberg, 348 p.

Websky, M. (1886): Über Caracolit und Percylit. *Sitz. Akad. Wiss. Berlin*, 1045.

Werner, A.G. (1786): Kurze Klassification und Beschreibung der verschiedenen Gebirgsarten. *Abh. Böhmischen Gesell. Wissen.*, **1**, 272–297.

White, T.J. & Dong, Z.-L. (2003): Structural derivation and crystal chemistry of apatites. *Acta Crystallogr.*, **B59**, 1–16.

White, T., Ferraris, C., Kim, J., Srinivasan, M. (2005): Apatite – an adaptive framework structure. in ''Micro- and Mesoporous Mineral Phases'', G. Ferraris & S. Merlino, eds. *Rev. Mineral. Geochem.*, **57**, 307–402.

Winther, C. (1901): Britholith, a new mineral. *Medd. Grønl.*, **24**, 190–196.

Zhang, J., Fang, Z., Liao, L. (1992): A study of crystal structure of britholite-Y. *Acta Mineral. Sin.*, **12**, 131–142.

Received 25 January 2010
Accepted 25 January 2010